

MOLECULAR PHYSICS

VOLUME 8

Printed and Published by

TAYLOR & FRANCIS LTD

RED LION COURT, FLEET STREET, LONDON, E.C.4



Digitized by the Internet Archive
in 2024

CONTENTS OF VOLUME 8

NUMBER 1

	Page
Molecular orbital theory of nuclear spin coupling constants. J. A. POPLE and D. P. SANTRY	1
¹⁴ N chemical shifts in organic compounds. D. HERBISON-EVANS and R. E. RICHARDS	19
Interactions spin-spin nucléaires [1] II. Couplages spin-spin dans des époxydes substitués. JEAN-MARIE LEHN et JEAN-JACQUES RIEHL ..	33
A variational solution of the time-dependent Schrodinger equation. A. D. McLACHLAN	39
The negative ions of tetraphenylene and 1,2: 5,6-dibenzcyclooctatetraene. A. CARRINGTON, H. C. LONGUET-HIGGINS and P. F. TODD	45
H-D isotope effects in the decomposition of acetylene by electron impact. P. C. HAARHOFF	49
Mean lifetimes of active molecules and oscillator models of unimolecular reactions. E. E. NIKITIN	65
The line shapes of the E.S.R. spectrum of a system of interacting triplets. RUTH M. LYNDEN-BELL	71
The rotational-torsional wavefunctions of molecules that have two identical co-axial rotors. P. R. BUNKER	81

RESEARCH NOTES

Long-range couplings in the N.M.R. spectra of alkyl formates. DORA G. DE KOWALEWSKI and VALDEMAR J. KOWALEWSKI	93
Proton magnetic resonance of Würster's blue perchlorate. ASAKO KAWAMORI and KEISUKE SUZUKI	95
Association between pyrazine anions and sodium ions. N. M. ATHERTON and A. E. GOGGINS	99

NUMBER 2

An electron spin resonance study of proton transfer equilibria involving the pyrogallol semiquinone radical. A. CARRINGTON and I. C. P. SMITH	101
The statistical mechanics of systems with steep intermolecular potentials. J. S. ROWLINSON	107

CONTENTS OF VOLUME 8

	Page
Solvent effects in the electron spin resonance spectrum of fluorenone ketyl. G. R. LUCKHURST and L. E. ORGEL	117
Electron spin resonance line widths of transition metal ions in solution. Relaxation through zero-field splitting. A. CARRINGTON and G. R. LUCKHURST	125
The effects of π -electron distribution and intramolecular electric fields on the ^{19}F N.M.R. shielding in substituted perfluorobenzenes. N. BODEN, J. W. EMSLEY, J. FEENEY and L. H. SUTCLIFFE	133
Alternant molecular orbital treatment of the allyl cation, radical and anion. D. P. CHONG and J. W. LINNETT	151
Ein neues Programm zur quantentheoretischen Berechnung von Molekülen und Atomsystemen. I. Grundlagen. H. PREUSS	157
Transient nuclear magnetic resonance signals for liquids with exchanging nuclei. J. G. POWLES and J. H. STRANGE	169

RESEARCH NOTES

An heuristic estimate of correlation energies in many-electron atoms. CHR. KLIXBÜLL JØRGENSEN	191
Electron spin resonance of the SeO_2^- radical ion. R. J. COOK, J. R. ROWLANDS and D. H. WHIFFEN	195
Effect of intramolecular Van der Waals forces on N.M.R. spectra. V. M. S. GIL and W. A. GIBBONS	199

NUMBER 3

Low-energy states of the CH_2 radical. R. N. DIXON	201
Theory of the isotropic g value of 4.27 found for some high-spin ferric ions. J. S. GRIFFITH	213
Intermediate symmetry. J. S. GRIFFITH	217
Electron spin resonance absorption spectrum of CO_2^- molecule-ions in single crystal calcite. S. A. MARSHALL, A. R. REINBERG, R. A. SERWAY and J. A. HODGES	225
Die $^1\Sigma^-$ - und $^3\Sigma^-$ -Energiekurven von zweiatomigen Systemen mit zwei Elektronen. H. PREUSS	233
The electron spin resonance spectrum of the NF_2 radical trapped in inert matrices at 4.2° K. J. B. FARMER, M. C. L. GERRY and C. A. McDOWELL	253
Electronic spectra of p -benzosemiquinone ions. YOSHIYA HARADA and HIROO INOKUCHI	265

CONTENTS OF VOLUME 8

	Page
Electronic structure of <i>p</i> -benzosemiquinone ion. YOSHIYA HARADA ..	273

Hypersensitive pseudoquadrupole transitions in lanthanides. CHR. KLIXBÜLL JØRGENSEN and B. R. JUDD	281
--	-----

RESEARCH NOTES

Conformational interconversion in the monovalent ions of 1,2,3,6,7,8-hexahydropyrene. E. DE BOER and A. P. PRAAT	291
--	-----

Scheibe's rule and the SCF theory. U. H. KOLLAARD and J. P. COLPA ..	295
--	-----

Restricted rotation of alkyl groups in alkyl cyclooctatetraene anions. A. CARRINGTON and P. F. TODD	299
---	-----

NUMBER 4

Zero-field splitting of the lowest triplet state of some aromatic hydrocarbons: Calculation and comparison with experiment. J. H. VAN DER WAALS and G. TER MATEN	301
--	-----

Theory of optical rotatory power. W. J. A. MAASKANT and L. J. OOSTERHOFF	319
--	-----

Intermolecular vibrations of solid carbon dioxide. S. H. WALMSLEY and J. A. POPLÉ	345
---	-----

The electron spin resonance spectrum of the radical anion of 1, 3, 5-trinitrobenzene. P. H. H. FISCHER and C. A. MCDOWELL	357
---	-----

Raman selection rules for vibration-rotation transitions in symmetric top molecules. IAN M. MILLS	363
---	-----

Excitons in molecular crystals. G. N. FOWLER	375
--	-----

On the theory of hypochromism. G. N. FOWLER	383
---	-----

Dye sensitized photo-response in organic semiconductors. V. MYLNIKOV and A. TEREININ	387
--	-----

RESEARCH NOTES

The electron resonance spectra of free radicals dissolved in liquid crystals. A. CARRINGTON and G. R. LUCKHURST	401
---	-----

Conformation of the <i>EXO</i> -methylene ketone group in α -methylene cycloketones. R. KAISER and D. L. HOOPER	403
--	-----

Hyperfine coupling in $>\dot{\text{C}}\text{OH}$ containing radicals. D. E. HENN and D. H. WHIFFEN	407
--	-----

CONTENTS OF VOLUME 8

	Page
NUMBER 5	
Resonance transfer of molecular excitation energy. A. D. McLACHLAN	409
Proton magnetic resonance of symmetrical molecules: II. The analysis of A_2B_2 spectra by perturbation methods: the A_2X_2 and the $(AX)_2$ approximations. BO GESTBLOM, RAGNAR A. HOFFMAN and SÖREN RODMAR	425
Die Berechnung der Potentialflächen von mehratomigen Systemen nach der Methode der Ladungsentwicklungen. H. PREUSS	441
The electronic structure and spectrum of nitrobenzene. O. MATSUOKA and Y. I'HAYA	455
The N.M.R. spectrum and configuration of decafluorobiphenyl. N. BODEN, J. W. EMSLEY, J. FEENEY and L. H. SUTCLIFFE	467
The compound-molecule model in the theory of chemical reactions. E. E. NIKITIN	473
The orbital penetration term in aromatic substituent effects. D. P. CRAIG and G. DOGGETT	485
Regular models for solid hydrogen: III. G. M. BELL and W. M. FAIRBAIRN	497
The effect of relaxation on the symmetry of N.M.R. spectra. JAY MARTIN ANDERSON	505

RESEARCH NOTES

On the proof of an identity. G. DAS	513
Note on the theory of dissociation pressures of gas hydrates. ROBERT M. MAZO	515

NUMBER 6

Semi-classical analysis of weakly inelastic molecular collisions. M. S. CHILD	517
Integral equations in ionic solution theory. A. R. ALLNATT	533
Alternant molecular orbital treatment of trimethylenemethyl, $C(CH_2)_3$ and its ions. D. P. CHONG and J. W. LINNETT	541
A rigid sphere model for the melting of argon. H. C. LONGUET-HIGGINS and B. WIDOM	549
Nitroxides [1]. IV. Le <i>t</i> -butyl isopropyl nitroxyde. H. LEMAIRE, R. RAMASSEUL et A. RASSAT	557

CONTENTS OF VOLUME 8

	Page
The theory of the temperature dependence of N.M.R. spectra of paramagnetic octahedral complexes. R. M. GOLDING	561
Proton-proton double resonance studies of formamide- ¹⁵ N and N-methylformamide- ¹⁵ N. A. J. R. BOURN and E. W. RANDALL ..	567
Hypochromism and optical rotation in helical polymers. A. D. MCLACHLAN and M. A. BALL	581
Fluorescence self-quenching in aromatic vapours. The effect of fluorescence reabsorption. B. STEVENS and P. J. MCCARTIN ..	597
Proton spin-lattice relaxation in aqueous ionic solutions. G. T. JONES and J. G. POWLES	607
RESEARCH NOTES	
The composition of the nematic mesophase of p-azoxyanisole. H. C. LONGUET-HIGGINS and G. R. LUCKHURST	613
Index of Authors (with the Titles of Papers)	617

Molecular orbital theory of nuclear spin coupling constants

by J. A. POPLE and D. P. SANTRY

Basic Physics Division, National Physical Laboratory, Teddington

(Received 26 September 1963)

Molecular orbital theory in the LCAO form is used in a study of the indirect coupling between nuclear spins through the electronic environment. By retaining only the largest one-centre integrals, approximate formulae involving the LCAO coefficients are derived for the three contributions due to (1) the electron orbital effect, (2) the dipolar interaction between nuclear and electron spins and (3) the Fermi contact effect. The theory is then applied in detail to the coupling between directly bonded atoms, when the contact term is usually dominant. Approximate calculations indicate that the reduced coupling constant K_{AB} (defined as $(2\pi/\hbar\gamma_A\gamma_B)J_{AB}$, where γ_A and γ_B are the nuclear magnetogyric ratios and J_{AB} is the usual constant in cycles/second) is negative if one of the atoms is fluorine. Broad agreement is obtained with the available experimental data for atoms up to fluorine connected by single bonds and a tentative pattern for signs and magnitudes is suggested.

1. INTRODUCTION

In addition to direct dipolar interaction, nuclear spins in a molecule are coupled indirectly by polarization of the electronic environment. This coupling is observed experimentally in high resolution nuclear magnetic resonance spectroscopy of fluids, where the direct dipolar effect averages to zero and the residual interaction energy between nuclei A and B takes the form

$$E_{AB} = \hbar J_{AB} \mathbf{I}_A \cdot \mathbf{I}_B, \quad (1.1)$$

\mathbf{I}_A and \mathbf{I}_B being the nuclear spin angular momenta (in units of \hbar) and J_{AB} the coupling constant in cycles/second.

A complete general theory of these interactions was first given by Ramsey [1] who showed that they arose by three distinct mechanisms. In the first of these, one nuclear magnetic moment induces orbital electronic currents which in turn produce magnetic fields at the site of a second nucleus. Secondly, the dipole interaction between the magnetic moment of one nucleus and the electron spins produces an 'electron spin polarization' so that there are non-vanishing magnetic fields which act on other nuclei. Finally there is a coupling involving the Fermi contact interaction between nuclear moments and electron spins in *s*-orbitals, which also leads to electron spin polarization. Ramsey developed general formulae for these three contributions to the spin coupling constant using quantum-mechanical perturbation theory.

An important step towards the application of these formulae to large molecules was taken by McConnell [2], who used molecular orbital wave functions in conjunction with a 'mean excitation energy' approximation in which perturbation theory is simplified by replacing the electronic energies of all triplet

states interacting with the ground state by an appropriate average. Combining this with LCAO (linear combination of atomic orbital) approximations for molecular orbitals, McConnell was able to derive tractable formulae for the coupling constants between nuclei separated by several bonds and to make estimates of the magnitudes of the various parts. The present paper is concerned with the further development and refinement of this molecular orbital approach and particularly with its application to the coupling between the nuclei of directly bonded atoms.

2. GENERAL THEORY

To facilitate the comparison of nuclear spin coupling constants in different molecules, it is convenient to introduce a *reduced coupling constant* K_{AB} which is independent of the nuclear moments of A and B and only depends on the electronic environment†. This will be defined as

$$K_{AB} = (2\pi/\hbar\gamma_A\gamma_B)J_{AB}, \quad (2.1)$$

where γ_A, γ_B are the nuclear magnetogyric ratios; its units are cm^{-3} . It should be noted that K_{AB} and J_{AB} will have different signs if one of γ_A and γ_B is negative. Among the nuclei considered in this paper, this would apply to ^{15}N and ^{17}O .

K_{AB} is the mean value of a *reduced coupling tensor* $(K_{AB})_{\alpha\beta}$ which is such that the energy perturbation caused by fixed nuclear magnetic moments $\mu_{A\alpha}$ and $\mu_{B\beta}$ includes a cross term

$$E_{AB} = (K_{AB})_{\alpha\beta}\mu_{A\alpha}\mu_{B\beta} \quad (2.2)$$

using the summation convention for the tensor suffixes α and β . These fixed nuclear moments must be treated as if they produce a dipolar magnetic field:

$$F_{\alpha}^{(\text{dip})} = (3r_{\alpha}r_{\beta} - r^2\delta_{\alpha\beta})r^{-5}\mu_{\beta}, \quad (2.3)$$

together with a 'contact field':

$$F_{\alpha}^{(\text{cont})} = (8\pi/3)\delta(\mathbf{r})\mu_{\alpha}, \quad (2.4)$$

the latter acting only on the electron spins.

The three contributions to the total coupling constant K referred to in the introduction arise respectively from the orbital effects of $F_{\alpha}^{(\text{dip})}$, the action of $F_{\alpha}^{(\text{dip})}$ on electron spins and the corresponding action of $F_{\alpha}^{(\text{cont})}$. Ramsey [1] showed that there were no cross-terms between these effects in E_{AB} , so that each reduced coupling constant may be written in terms of three separate contributions:

$$K_{AB} = K_{AB}^{(1)} + K_{AB}^{(2)} + K_{AB}^{(3)}. \quad (2.5)$$

Ramsey's perturbation theory formulae for these three parts may be written :
Orbital :

$$K_{AB}^{(1)} = (2e^2/3mc^2) \left(0 \left| \sum_p \mathbf{r}_{pA} \cdot \mathbf{r}_{pB} r_{pA}^{-3} r_{pB}^{-3} \right| 0 \right) \\ - \frac{8}{3}\beta^2 \sum_n (E_n - E_0)^{-1} \left(0 \left| \sum_p r_{pA}^{-3} \mathbf{M}_{pA} \right| n \right) \cdot \left(n \left| \sum_q r_{qB}^{-3} \mathbf{M}_{qB} \right| 0 \right). \quad (2.6)$$

† A similar suggestion has been made by Lynden-Bell and Sheppard [3].

Spin dipolar :

$$K_{AB}^{(2)} = -\frac{8}{3}\beta^2 \sum_n (E_n - E_0)^{-1} \left(0 \left| \sum_p \{ 3(\mathbf{S}_p \cdot \mathbf{r}_{pA}) \mathbf{r}_{pA} r_{pA}^{-5} - \mathbf{S}_p r_{pA}^{-3} \} \right| n \right) \\ \times \left(n \left| \sum_q \{ 3(\mathbf{S}_q \cdot \mathbf{r}_{qB}) \mathbf{r}_{qB} r_{qB}^{-5} - \mathbf{S}_q r_{qB}^{-3} \} \right| 0 \right). \quad (2.7)$$

Spin contact :

$$K_{AB}^{(3)} = - (8\pi/3) \frac{2}{3} \beta^2 \sum_q (E_n - E_0)^{-1} \\ \times \left(0 \left| \sum_p \delta(\mathbf{r}_{pA}) \mathbf{S}_p \right| n \right) \cdot \left(n \left| \sum_q \delta(\mathbf{r}_{qB}) \mathbf{S}_q \right| 0 \right). \quad (2.8)$$

In these formulae, β is the Bohr magneton, \sum_n is a summation over the electronic excited states of the molecule, \mathbf{M}_{pA} is the orbital angular momentum of electron p about nucleus A (in units of \hbar) and \mathbf{S}_p is the spin angular momentum of electron p (also in units of \hbar). All matrix elements in (2.6)–(2.8) refer, of course, to many-electron wave functions.

In the next three sections we shall develop these general formulae in terms of molecular orbital theory, along similar lines to the treatment of McConnell [2]. However, we shall not make the mean excitation energy approximation until the final stage, so that detailed calculations without this can be considered in later sections. This modification turns out to be of some importance for the contact term $K_{AB}^{(3)}$.

According to the molecular orbital theory of closed shell molecules (with $2N$ electrons), the ground state many-electron wave function may be approximated by a determinant of one-electron orthonormal orbitals $\psi_1, \psi_2, \dots, \psi_N$, each associated with both α and β spin functions :

$$\Psi_0 = [(2N)!]^{-1/2} \begin{vmatrix} \psi_1(1)\alpha(1) & \psi_1(1)\beta(1) & \psi_2(1)\alpha(1) & \dots & \dots & \dots \\ \psi_1(2)\alpha(2) & \dots & \dots & \dots & \dots & \dots \\ \vdots & \vdots & \vdots & \vdots & \vdots & \vdots \\ \psi_N(2N)\alpha(2N) & \dots & \dots & \dots & \dots & \dots \\ \psi_N(2N)\beta(2N) & \dots & \dots & \dots & \dots & \dots \end{vmatrix} \quad (2.9)$$

We shall use the shorter notation :

$$\Psi_0 = |\psi_1 \bar{\psi}_1 \psi_2 \bar{\psi}_2 \dots \psi_N \bar{\psi}_N|. \quad (2.10)$$

In addition to $\psi_1 \dots \psi_N$, there will be further unoccupied molecular orbitals $\psi_{N+1}, \psi_{N+2}, \dots$ which can be used to construct approximate wave functions for electronic excited states. The lowest of these, and indeed the only ones that contribute to the perturbation formulae (2.6)–(2.8) are formed by the excitation of a single electron from an occupied MO ψ_i into an unoccupied one ψ_j . There are four such states for each excitation, leading to a singlet and a triplet with wave functions:

$$\left. \begin{aligned} {}^1\Psi_{i \rightarrow j} &= \{ |\psi_1 \dots \psi_i \bar{\psi}_j \dots| + |\psi_1 \dots \psi_j \bar{\psi}_i \dots| \} / \sqrt{2}, \\ {}^3\Psi_{i \rightarrow j} &= \left\{ \begin{aligned} &|\psi_1 \dots \bar{\psi}_i \bar{\psi}_j \dots| \\ &\{ |\psi_1 \dots \psi_i \bar{\psi}_j \dots| - |\psi_1 \dots \psi_j \bar{\psi}_i \dots| \} / \sqrt{2}. \end{aligned} \right\} \end{aligned} \right\} \quad (2.11)$$

The corresponding excitation energies will be written ${}^1\Delta_{i \rightarrow j}$ and ${}^3\Delta_{i \rightarrow j}$. In

the further development of the theory, we shall also use the LCAO approximation in which each molecular orbital is written as a linear combination of a set of atomic orbitals ϕ_μ :

$$\psi_i = \sum_{\mu} c_{i\mu} \phi_{\mu}. \quad (2.12)$$

(Throughout this paper, all unperturbed orbitals and all coefficients $c_{i\mu}$ will be real.) For a finite set of M atomic orbitals, there will be only the same number of molecular orbitals. Further, if the atomic orbitals are orthogonal to each other, or if the overlap integrals $\int \phi_{\mu} \phi_{\nu} d\tau$ ($\mu \neq \nu$) are neglected, the matrix $c_{i\mu}$ will be orthogonal. It is then useful to define a molecular orbital charge-density and bond-order matrix :

$$P_{\mu\nu} = 2 \sum_{i=1}^N c_{i\mu} c_{i\nu}. \quad (2.13)$$

$P_{\mu\mu}$ is a measure of the total electron density in the atomic orbital ϕ_{μ} and $P_{\mu\nu}$ ($\mu \neq \nu$) is the MO bond order between ϕ_{μ} and ϕ_{ν} if these are on neighbouring atoms.

By substituting these molecular orbital wave functions in the general Ramsey formulae, explicit expressions are obtained for the coupling constants in terms of one-electron integrals which can then be evaluated either fully, or with further approximations.

3. MOLECULAR ORBITAL THEORY FOR THE CONTACT CONTRIBUTION

We shall consider the contact contribution as it turns out to be the most important in the systems we shall consider explicitly in later sections. The only excited states which mix with the ground state in equation (2.8) are the triplets, for which molecular orbital wave functions ${}^3\Psi_{i \rightarrow j}$ are given by (2.11). On reduction of the many-electron matrix elements, we obtain the following molecular orbital expression for $K_{AB}^{(3)}$:

$$K_{AB}^{(3)} = - (256\pi^2/9)\beta^2 \sum_i^{\text{occ}} \sum_j^{\text{unocc}} ({}^3\Delta E_{i \rightarrow j})^{-1} (\psi_i | \delta(\mathbf{r}_A) | \psi_j) (\psi_j | \delta(\mathbf{r}_B) | \psi_i) \quad (3.1)$$

where the elements $(\psi_i | \delta(\mathbf{r}_A) | \psi_j)$ $(\psi_j | \delta(\mathbf{r}_B) | \psi_i)$ are now one-electron integrals and i and j are summed over occupied and unoccupied molecular orbitals respectively.

If the LCAO approximation is used, (3.1) can be written in terms of integrals involving atomic orbitals. Thus :

$$\begin{aligned} K_{AB}^{(3)} = & - (256\pi^2/9)\beta^2 \sum_i^{\text{occ}} \sum_j^{\text{unocc}} ({}^3\Delta E_{i \rightarrow j})^{-1} \\ & \times \sum_{\lambda\mu\nu\sigma} c_{i\lambda} c_{j\mu} c_{j\nu} c_{i\sigma} (\phi_{\lambda} | \delta(\mathbf{r}_A) | \phi_{\mu}) (\phi_{\nu} | \delta(\mathbf{r}_B) | \phi_{\sigma}). \end{aligned} \quad (3.2)$$

Many of these integrals will be small because some pairs of orbitals will only have a small product in the neighbourhood of the nuclei A and B. This will be so, for example, if ϕ_{λ} and ϕ_{μ} are on different atoms or both on the same atom other than A. To get an idea of the magnitudes of the dominant terms, it is

useful to consider an approximate form of the theory in which *only one-centre integrals are retained*. For the contact terms, this means that ϕ_λ , ϕ_μ must both be s -orbitals on atom A and ϕ_ν , ϕ_σ must be s -orbitals on atom B. Further, since inner-shells take little part in the formation of bonding molecular orbitals, the most important terms will be those involving the valence-shell s -functions (1s for hydrogen and 2s for boron, carbon, nitrogen, oxygen and fluorine, etc.). We shall write these s_A and s_B and then :

$$K_{AB}^{(3)} = -(256\pi^2/9)\beta^2(s_A|\delta(\mathbf{r}_A)|s_A)(s_B|\delta(\mathbf{r}_B)|s_B) \\ \times \sum_i^{\text{occ}} \sum_j^{\text{unocc}} ({}^3\Delta E_{i \rightarrow j})^{-1} c_{is_A} c_{js_A} c_{js_B} c_{is_B}. \quad (3.3)$$

If an independent-electron molecular orbital model is used (in which the MO's are determined as eigenfunctions of a one-electron Hamiltonian), the excitation energy ${}^3\Delta E_{i \rightarrow j}$ is given by the difference of one-electron energies ($\epsilon_j - \epsilon_i$). (3.3) may then be written in the form :

$$K_{AB}^{(3)} = (64\pi^2/9)\beta^2(s_A|\delta(\mathbf{r}_A)|s_A)(s_B|\delta(\mathbf{r}_B)|s_B) \pi_{s_A s_B}, \quad (3.4)$$

where $\pi_{\mu, \nu}$ is written for a 'mutual polarizability' of the orbitals ϕ_μ , ϕ_ν as introduced by Coulson and Longuet-Higgins [4] :

$$\pi_{\mu, \nu} = 4 \sum_i^{\text{occ}} \sum_j^{\text{unocc}} (\epsilon_i - \epsilon_j)^{-1} c_{i\mu} c_{i\nu} c_{j\mu} c_{j\nu}. \quad (3.5)$$

Finally, if the mean excitation energy approximation is made, replacing all ${}^3\Delta E_{i \rightarrow j}$ by an average value ${}^3\Delta E$, (3.3) can be expressed in terms of the s_A - s_B bond order :

$$K_{AB}^{(3)} = (64\pi^2/9)\beta^2({}^3\Delta E)^{-1}(s_A|\delta(\mathbf{r}_A)|s_A)(s_B|\delta(\mathbf{r}_B)|s_B) P_{s_A s_B}^2. \quad (3.6)$$

Equation (3.6) was derived by McConnell [2], making the mean excitation energy approximation at an earlier stage. According to (3.6), $K_{AB}^{(3)}$ is always positive. However, this cannot be proved from the more accurate formula (3.3) and we shall find in later sections that negative contact contributions may indeed occur.

4. MOLECULAR ORBITAL THEORY FOR THE SPIN-DIPOLAR CONTRIBUTION

The molecular orbital development of the formula (2.7) for the spin-dipole part can be carried through a similar series of steps. Again, triplet wave functions ${}^3\Psi_{i \rightarrow j}$ are mixed with the ground-state wave function and reduction of the many-electron matrix elements gives :

$$K_{AB}^{(2)} = -(\frac{4}{3})\beta^2 \sum_i^{\text{occ}} \sum_j^{\text{unocc}} ({}^3\Delta E_{i \rightarrow j})^{-1} \\ \times (\psi_i|r_A^{-5}(3r_{A\alpha}r_{A\beta} - r_A^2\delta_{\alpha\beta})|\psi_j)(\psi_j|r_B^{-5}(3r_{B\alpha}r_{B\beta} - r_B^2\delta_{\alpha\beta})|\psi_i), \quad (4.1)$$

using a summation convention for the tensor suffixes α and β .

In the LCAO approximation, this becomes :

$$K_{AB}^{(2)} = -\left(\frac{4}{3}\right)\beta^2 \sum_i^{\text{occ}} \sum_j^{\text{unocc}} ({}^3\Delta E_{i \rightarrow j})^{-1} \sum_{\lambda\mu\nu\sigma} c_{i\lambda} c_{j\mu} c_{j\nu} c_{i\sigma} \\ \times (\phi_\lambda | r_A^{-5} (3r_{A\alpha} r_{A\beta} - r_A^2 \delta_{\alpha\beta}) | \phi_\mu) (\phi_\nu | r_B^{-5} (3r_{B\alpha} r_{B\beta} - r_B^2 \delta_{\alpha\beta}) | \phi_\sigma). \quad (4.2)$$

If we now make the approximation of retaining only one-centre integrals and limit the discussion to atomic orbitals up to $2p$, then ϕ_λ, ϕ_μ must be $2p$ orbitals on atom A and ϕ_ν, ϕ_σ must be $2p$ orbitals on B, all other one-centre terms vanishing. It follows that at this level of approximation, there will be no contribution $K_{AB}^{(2)}$ if either A or B is hydrogen.

If A and B both have $2p$ atomic orbitals in their valence shells, all one-electron matrix elements are easily evaluated. For example :

$$\left. \begin{aligned} (2px_A | r_A^{-5} (3r_{Ax}^2 - r_A^2) | 2px_A) &= \frac{4}{5} \langle r^{-3} \rangle_A, \\ (2px_A | r_A^{-5} (3r_{Ay}^2 - r_A^2) | 2px_A) &= -\frac{2}{5} \langle r^{-3} \rangle_A, \\ (2px_A | r_A^{-5} (3r_{Ax} r_{Ay}) | 2py_A) &= \frac{3}{5} \langle r^{-3} \rangle_A, \end{aligned} \right\} \quad (4.3)$$

where $\langle r^{-3} \rangle_A$ is the mean value of r^{-3} for the $2p$ orbitals of atom A. Substituting all possible integrals of this type in (4.2), and making the mean excitation approximation, we obtain :

$$K_{AB}^{(2)} = (4/25)\beta^2 \langle r^{-3} \rangle_A \langle r^{-3} \rangle_B ({}^3\Delta E)^{-1} \\ \times \{2(P_{x_A x_B}^2 + P_{y_A y_B}^2 + P_{z_A z_B}^2) + 3(P_{x_A x_B} P_{y_A y_B} + P_{y_A y_B} P_{z_A z_B} + P_{z_A z_B} P_{x_A x_B}) \\ - (P_{x_A y_B}^2 + P_{y_A x_B}^2 + P_{y_A z_B}^2 + P_{z_A y_B}^2 + P_{z_A x_B}^2 + P_{x_A z_B}^2) \\ + 3(P_{x_A y_B} P_{y_A x_B} + P_{y_A z_B} P_{z_A y_B} + P_{z_A x_B} P_{x_A z_B})\}. \quad (4.4)$$

If one axis is chosen along the AB bond, cross terms such as $P_{x_A y_B}$ will be zero or small. Equation (4.4) can then be written in terms of a $p\sigma$ -bond order P_σ and two π -bond orders P_π, P_π' :

$$K_{AB}^{(2)} = (4/25)\beta^2 \langle r^{-3} \rangle_A \langle r^{-3} \rangle_B ({}^3\Delta E)^{-1} \\ \times \{2(P_\sigma^2 + P_\pi^2 + P_\pi'^2) + 3(P_\sigma P_\pi + P_\sigma P_\pi' + P_\pi P_\pi')\}. \quad (4.5)$$

Numerical values for $K_{AB}^{(2)}$ given by this formula are, in fact, small compared with experimental coupling constants for directly bonded atoms (except possibly for F_2) and we shall not discuss them in detail. Some approximate calculations demonstrating this are summarized in table 1. In these carbon is supposed to utilize sp^3 , sp^2 and sp hybrids respectively in single, double and triple bonds, while fluorine uses a pure p -function.

5. MOLECULAR ORBITAL THEORY FOR THE ORBITAL CONTRIBUTION

Following McConnell [2], the two parts of $K_{AB}^{(1)}$ (equation (2.6)) may be considered separately. The first part, which does not involve molecular excited states, leads to :

$$K_{AB}^{(1a)} = (4e^2/3mc^2) \sum_i^{\text{occ}} (\psi_i | \mathbf{r}_A \cdot \mathbf{r}_B r_A^{-3} r_B^{-3} | \psi_i). \quad (5.1)$$

Bond	$\langle r^{-3} \rangle_A \langle r^{-3} \rangle_B$ (A.U.) ⁻⁶	P_σ	P_π	P_π'	$10^{-20} K^{(2)}$ (cm ⁻³)	$10^{-20} K^{(\text{expt})}$ (cm ⁻³)	Ref.
C—C	2.863	$-\frac{3}{4}$	—	—	+1.3	45.6	C ₂ H ₆ [3]
C=C	2.863	$-\frac{1}{3}$	1	—	+1.0	89.0	C ₂ H ₄ [3]
C≡C	2.863	$-\frac{1}{2}$	1	1	+5.0	225.9	C ₂ H ₂ [3]
C—F	12.768	$-\sqrt{\frac{3}{2}}$	—	—	+7.5	90.5	CF ₄ [3]
F—F	56.942	-1	—	—	+44.6	—	—

Table 1. Calculated $K^{(2)}$ contributions for directly bonded atoms (${}^3\Delta E = 10$ ev).

The second part involves the mixing of the ground-state function and the excited singlet function ${}^1\Psi_{i \rightarrow j}$ (equation (2.11)), leading to :

$$K_{AB}^{(1b)} = -(16/3)\beta^2 \sum_i^{\text{occ}} \sum_j^{\text{unocc}} ({}^1\Delta E_{i \rightarrow j})^{-1} \times (\psi_i | r_A^{-3} \mathbf{M}_A | \psi_j) \cdot (\psi_j | r_B^{-3} \mathbf{M}_B | \psi_i). \quad (5.2)$$

In the LCAO approximation, these formulae become :

$$K_{AB}^{(1a)} = (4e^2/3mc^2) \sum_i^{\text{occ}} \sum_{\lambda\mu} c_{i\lambda} c_{i\mu} (\phi_\lambda | \mathbf{r}_A \cdot \mathbf{r}_B r_A^{-3} r_B^{-3} | \phi_\mu) \quad (5.3)$$

and

$$K_{AB}^{(1b)} = -(16/3)\beta^2 \sum_i^{\text{occ}} \sum_j^{\text{unocc}} ({}^1\Delta E_{i \rightarrow j})^{-1} \times \sum_{\lambda\mu\nu\sigma} c_{i\lambda} c_{j\mu} c_{j\nu} c_{i\sigma} (\phi_\lambda | r_A^{-3} \mathbf{M}_A | \phi_\mu) \cdot (\phi_\nu | r_B^{-3} \mathbf{M}_B | \phi_\sigma). \quad (5.4)$$

If only one-centre integrals are retained, no terms in $K_{AB}^{(1a)}$ survive, for even if ϕ_λ and ϕ_μ are both on atom A, the matrix element will be small because of the factor r_B^{-3} . In $K_{AB}^{(1b)}$ (if we consider only atoms up to fluorine), the only non-vanishing terms are those in which ϕ_λ, ϕ_μ are both $2p$ -functions on A and ϕ_ν, ϕ_σ are $2p$ -functions on B. There are then a number of non-vanishing one-centre integrals such as :

$$(2px_A | r_A^{-3} M_{Az} | 2py_A) = -i \langle r^{-3} \rangle_A. \quad (5.5)$$

Collecting these terms and replacing ${}^1\Delta E_{i \rightarrow j}$ by a mean singlet excitation energy ${}^1\Delta E$ gives :

$$K_{AB}^{(1)} = (8/3)\beta^2 \langle r^{-3} \rangle_A \langle r^{-3} \rangle_B ({}^1\Delta E)^{-1} \times \{ P_{x_A x_B} P_{y_A y_B} + P_{y_A y_B} P_{z_A z_B} + P_{z_A z_B} P_{x_A x_B} - P_{x_A y_B} P_{y_A x_B} - P_{y_A z_B} P_{z_A y_B} - P_{z_A x_B} P_{x_A z_B} \}. \quad (5.6)$$

From this result, it follows that, at this level of approximation, the orbital contribution will be zero if either atom is hydrogen. Further (5.6) is non-zero for directly bonded atoms only *if there is multiple bonding between A and B*. For if one of the axes (say the x -axis) is taken along the AB bond, the cross-term in (5.6) will either be zero in molecules with high symmetry or small elsewhere, so $K_{AB}^{(1)}$ will vanish unless one of the π -bond orders $P_{y_A y_B}$ or $P_{z_A z_B}$ is non-zero.

Numerical values of $K^{(1)}$ are again rather small. Thus for C=C, use of the parameters given in table 1 leads to $K^{(1)} = -12.5 \times 10^{20}$, still substantially less than experimental magnitudes for K .

6. DIRECTLY BONDED X-H COUPLING CONSTANTS

In the next two sections we shall use the theory to make a comparative study of the coupling constants for directly bonded atoms up to fluorine. The analysis of §§ 4 and 5 suggests that the spin-dipolar and orbital contributions are small in almost all such cases, so only the contact part will be considered. The formulae for $K^{(3)}$ involve the magnitudes of the valence s -atomic orbitals at the nuclei. A set of values for these is given in table 2. These are taken from reference [6] except for hydrogen, for which a Slater orbital with $Z = 1.2$ is used. (It is generally found that the most appropriate hydrogen atomic orbitals in molecules are more contracted than free atoms.)

Atom	$(s \delta(r) s)$	Atom	$(s \delta(r) s)$
H	0.5500	N	4.770
B	1.408	O	7.638
C	2.767	F	11.966

Table 2. Atomic orbital constants in atomic units (reference [6]).

Let us first examine XH coupling constants in tetrahedral XH_4 molecules (BH_4^- , CH_4 , NH_4^+), already considered by Karplus and Grant [7]. In the present theory, the simplest theoretical expression for K_{XH} is given by (3.4) and is proportional to the mutual polarizability π_{s_X, s_H} between the $2s$ orbital of X and the $1s$ orbital of one of the hydrogen atoms. If valence molecular orbitals are constructed from the atomic orbitals $1s_H$, $2s_X$ and $2p_X$, only two will involve $2s_X$. These will be totally symmetric (symmetry A_1 in the group T_d) and have the form:

$$\left. \begin{aligned} \psi_1 &= a2s_X + b(1s_H + 1s_{H'} + 1s_{H''} + 1s_{H'''}) \\ \psi_2 &= c2s_X + d(1s_H + 1s_{H'} + 1s_{H''} + 1s_{H'''}) \end{aligned} \right\} \quad (6.1)$$

The first of these will be bonding and doubly occupied in the molecular ground state, while the second is anti-bonding and empty. If overlap integrals between atomic orbitals are neglected, orthonormality requires that $a^2 + 4b^2 = 1$, $c = -2b$, $d = \frac{1}{2}a$. Substitution in (3.3) then gives:

$$K_{XH}^{(3)} = (256\pi^2/9)\beta^2(^3\Delta E_{1 \rightarrow 2})^{-1}(2s_X|\delta|2s_X)(1s_H|\delta|1s_H)a^2b^2. \quad (6.2)$$

This is positive and has a maximum when $a = 1/\sqrt{2}$, $b = 1/2\sqrt{2}$, corresponding to a non-polar distribution of charge. This is reasonable for CH_4 ; in BH_4^- and NH_4^+ a/b may alter but the product ab will not change much from $(\frac{1}{4})$. The excitation

energy ${}^3\Delta E_{1\rightarrow 2}$ corresponds to excitation from the molecular orbital below the highest occupied, so a value greater than that corresponding to the main absorption is indicated; 15 eV seems a reasonable estimate. The calculated coupling constants using these values are given in table 3 together with the experimental data. The agreement of magnitudes is clearly satisfactory although this would be somewhat effected by a different choice of ${}^3\Delta E_{1\rightarrow 2}$. The signs of the coupling constants are not known experimentally, but there is indirect evidence that K_{CH} is positive. It is known that the long-range coupling between ortho protons in paranitrotoluene is positive [11] and that vicinal H-H and C-H constants have the same sign in cisdichloroethylene [12], implying $K_{\text{CH}} > 0$ in the latter molecule at least. The positive sign is clearly supported by the theory.

Molecule	$10^{-20}K_{\text{XH}} \text{ (cm}^{-3}\text{)}$		Reference
	Calc.	Expt.	
BH_4^-	+22	21.3	[8]
CH_4	+44	41.8	[9]
NH_4^+	+75	59	[10]

Table 3. Calculated and experimental coupling constants for XH_4 molecules.

These calculations may be compared with those on C-H couplings by Muller and Pritchard [9], who did an MO calculation using only the pair of electrons in a localized bonding orbital. This gives a result identical with (6.2) with $ab = \frac{1}{4}$ and with ${}^3\Delta E_{1\rightarrow 2}$ replaced by a mean excitation energy ΔE . Extending this method to other C-H bonds, they were able to establish an important correlation between the magnitude of K_{CH} and the s -character of the bonding hybrid orbital. This procedure can be justified from our more general theory (which treats all valence electrons) if the various excitation energies ${}^3\Delta E_{i\rightarrow j}$ are close enough to be replaced by an average. For then the McConnell formula (3.6) holds and the bond order $P_{s_A s_B}$ may be evaluated either from the delocalized molecular orbitals, or from a transformed set of localized orbitals (equivalent orbitals in the sense of Lennard-Jones [13]), only one of which will probably be important. But if the excitation energies are more widely spread, a fuller treatment based on (3.3) or (3.4) may be necessary.

Let us now examine the theory for hydrogen fluoride, where the $2s$ fluorine electrons are very tightly bound and the use of the mean excitation energy approximation is suspect. Here it is possible to show that if the $2s_{\text{F}}$ atomic energy level is sufficiently far below those for $2p_{\text{F}}$ and $1s_{\text{H}}$, then the coupling constant K_{FH} will *change sign and become negative*. To demonstrate this in a simple manner consider the three σ -molecular orbitals that may be constructed from the atomic orbitals $2s_{\text{F}}$, $2p_{\sigma_{\text{F}}}$ and $1s_{\text{H}}$ (π -type orbitals will not contribute to the contact contribution). The LCAO coefficients can be calculated approximately using an independent-electron model. If overlap integrals are neglected, they will be the eigenvectors of a Hamiltonian matrix:

$$H = \begin{pmatrix} \alpha & 0 & \beta_{sh} \\ 0 & \alpha_p & \beta_{ph} \\ \beta_{sh} & \beta_{ph} & \alpha_h \end{pmatrix}, \quad (6.3)$$

where suffixes s, p, h are used for $2s_F$, $2p\sigma_F$ and $1s_H$ respectively. The diagonal elements $\alpha_s, \alpha_p, \alpha_h$ are the energies of the separate atomic orbitals and β_{sh} and β_{ph} are bonding or resonance integrals between pairs of orbitals. If $2s_F$ is positive in its outer regions and the positive lobe of $2p\sigma_F$ is in the direction of the hydrogen atom, both β_{sh} and β_{ph} will be negative. No element β_{sp} is included as $2s_F$ and $2p\sigma_F$ are atomic orbitals of different symmetry on the same atom.

If the $2s_F$ orbital is sufficiently far down the energy scale, there will be little mixing between it and the other two functions. This mixing (due to the bonding resonance integral β_{sh}) may be treated as a perturbation. If $\beta_{sh}=0$ in the unperturbed situation and if we take $\alpha_p=\alpha_h=0$, the wave functions are s for the lone pair ψ_1 and $(p+h)/\sqrt{2}$, $(p-h)/\sqrt{2}$ for the bonding and anti-bonding molecular orbitals ψ_2 and ψ_3 respectively. In fact, the resonance integral β_{sh}

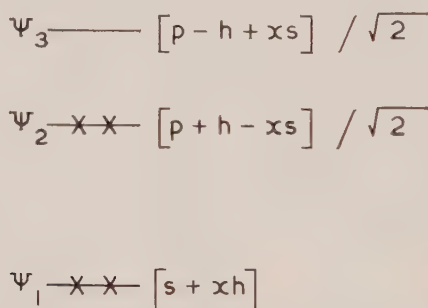


Figure 1. Energy level diagram and approximate molecular orbitals for HF.

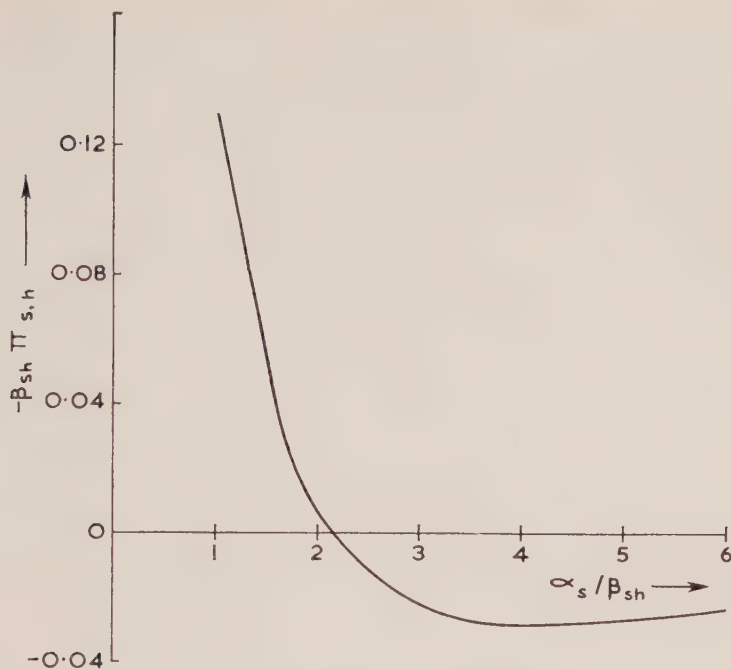
will lead to some bonding character between s and h in the *lowest* molecular orbital ψ_1 and hence to corresponding anti-bonding character in ψ_2 and ψ_3 . If the LCAO coefficients are expanded in powers of $x=\beta_{sh}/\alpha_s$ (>0), the leading terms are as shown in figure 1. The mutual polarizability $\pi_{s,h}$ has contributions from the two excitations $\psi_1 \rightarrow \psi_3$ and $\psi_2 \rightarrow \psi_3$. If α_s is sufficiently negative, the latter dominates because of the smaller excitation energy and

$$\pi_{s,h} \sim \frac{x^2}{\epsilon_2 - \epsilon_3} < 0, \quad (6.4)$$

corresponding to a negative coupling constant K_{FH} .

Although $\pi_{s,h}$ is negative for low α_s , the contribution of the transition $\psi_1 \rightarrow \psi_3$ to $\pi_{s,h}$ is positive and it becomes the larger if $(-\alpha_s)$ is smaller. Figure 2 shows the full variation of $\pi_{s,h}$ with α_s/β_{sh} if we take $\alpha_p=\alpha_h=0$, $\beta_{ph}=\sqrt{3}\beta_{sh}$ as a rough approximation. For these parameters the change of sign occurs when $\alpha_s/\beta_{sh}=2.2$. Estimates for HF might be $\alpha_s=-20$ eV, $\beta_{sh}=-4$ eV giving $\pi_{s,h}=-0.00067$ (eV) $^{-1}$ and $K_{HF}=-7.6 \times 10^{20}$ cm $^{-3}$. The experimental value is 46.1×10^{20} cm $^{-3}$ with unknown sign [14]. Thus this form of the theory predicts a negative sign but is unable to reproduce the observed magnitude.

Rather similar arguments can be developed for the N-H and O-H coupling constants in NH_3 and H_2O . For both these molecules, only totally symmetric (A_1) molecular orbitals contribute to $\pi_{s,h}$. Apart from the inner shells there are three such MO's. ψ_1, ψ_2, ψ_3 (two occupied as for HF), constructed in LCAO form from the $2s$ function, the $2p$ function directed along the symmetry axis of the molecule and the symmetrical combination of hydrogen $1s$ functions. In an

Figure 2. Variation of $\pi_{s,h}$ with α_s for hydrogen fluoride.

independent electron model using tetrahedral valence angles, the Hamiltonian matrices take the form

$$\begin{aligned} \text{NH}_3: & \begin{bmatrix} \alpha_s & 0 & \sqrt{3}\beta_{sh} \\ 0 & \alpha_p & \beta_{ph}/\sqrt{3} \\ \sqrt{3}\beta_{sh} & \beta_{ph}/\sqrt{3} & \alpha_h \end{bmatrix} \\ \text{H}_2\text{O}: & \begin{bmatrix} \alpha_s & 0 & \sqrt{2}\beta_{sh} \\ 0 & \alpha_p & \sqrt{(2/3)}\beta_{ph} \\ \sqrt{2}\beta_{sh} & \sqrt{(2/3)}\beta_{ph} & \alpha_h \end{bmatrix}, \end{aligned} \quad (6.5)$$

β_{ph} being the resonance integral between a hydrogen $1s$ orbital and a heavy atom $2p$ function along the bond. Again $\pi_{s,h}$ will be negative if α_s is sufficiently low and the full variation will be given by curves similar to that shown for HF in figure 2. However, the energy differences between atomic $2s$ and $2p$ orbitals increase along the series C, N, O, F so that there should be a change from positive to negative coupling constants somewhere along the series CH_4 , NH_3 , H_2O and HF.

As these approximate calculations depend rather sensitively on a partial cancellation between the contributions of opposite sign for the transitions $\psi_2 \rightarrow \psi_3$ and $\psi_1 \rightarrow \psi_3$ it is desirable to make as careful a calculation as possible of their relative sizes. This has been done by returning to the basic MO formula (3.1) which can be written:

$$K_{AB} = -(256\pi^2/9)\beta^2 \left\{ \frac{(\psi_1\psi_3)_X(\psi_1\psi_3)_H}{\Delta E_{1 \rightarrow 3}} + \frac{(\psi_2\psi_3)_X(\psi_2\psi_3)_H}{\Delta E_{2 \rightarrow 3}} \right\}, \quad (6.6)$$

where $(\psi_i\psi_j)_X$ is the value of $\psi_i\psi_j$ at the X nucleus. These can be evaluated in full

Molecule	$\Delta E_{1 \rightarrow 3}$ ev	$\Delta E_{2 \rightarrow 3}$ ev	$a_0 \frac{\langle \psi_1 \psi_3 \rangle_X \langle \psi_1 \psi_3 \rangle_H}{\frac{\Delta E_{1 \rightarrow 3}}{(\text{ev})^{-1}}}$	$a_0 \frac{\langle \psi_2 \psi_3 \rangle_X \langle \psi_2 \psi_3 \rangle_H}{\frac{\Delta E_{2 \rightarrow 3}}{(\text{ev})^{-1}}}$	$10^{20} K$ (calc) cm^{-3}	$10^{20} K$ (obs) cm^{-3}
CH ₄	15	—	—0.00634	—	+44	+41.8 (Ref. [9])
NH ₃	20	8	—0.00834	+0.00402	+30	±53.0 (Ref. [18])
H ₂ O	25	12	—0.00838	+0.00762	+5	±45.1 (Ref. [19])
HF	30	15	—0.02211	+0.03482	—87	±54.4 (Ref. [14])

Table 4. Calculated and observed coupling constants for simple hydrides.

from LCAO functions tabulated by Ransil [15] for HF (best limited LCAOMO), by Ellison and Shull [16] for H₂O and by Duncan [17] for NH₃. The results are summarized in table 4, together with the calculation of table 3 for CH₄. (The important excitation in methane is analogous to 1→3 for the other molecules, although it was previously labelled differently because of the higher symmetry.)

These calculations are subject to a number of rather uncertain errors. In the first place, the excitation energies (which should be those for vertical excitation to triplet states) can only be estimated very roughly. The values given should be approximately correct and reproduce the general trends along the series. Secondly, the calculations are based on different sets of atomic orbitals. In particular, those for NH₃ and H₂O use hydrogen 1s functions with Slater screening constants $Z_H=1$ which underestimate the orbital amplitudes at the hydrogen nuclei. If optimum values were used (~ 1.2 or 1.3) as for HF, calculated NH and OH coupling constants would probably be increased by a factor of nearly two.

The signs of the experimental coupling constants are unknown, apart from the indirect evidence that K_{CH} is positive as mentioned previously. The theoretical calculations of table 4 suggest that K_{CH} and K_{NH} are both positive, but that K_{HF} is negative for the qualitative reasons described above. For K_{OH} , the positive and negative contributions nearly cancel and no valid prediction of the sign can be made.

7. DIRECTLY BONDED X-Y COUPLING CONSTANTS

We now turn to the theory of coupling constants between directly bonded atoms, both of which are in the series B, C, N, O, F. Although there are fewer satisfactory MO wave functions for molecules with such bonds, it is possible to make some predictions using the same principles as in the calculations on hydrides.

Consider first the coupling between neighbouring carbon atoms in hydrocarbons. Here the energies of 2s atomic orbitals are not all that far below the 2p levels so the mean excitation energy approximation should be reasonably satisfactory. Equation (3.6) then gives:

$$K_{CC} = (64\pi^2/9)\beta^2(^3\Delta E)^{-1}(2s_c|\delta|2s_c)^2P_{s_c s_c'}^2, \quad (7.1)$$

where $P_{s_c s_c'}$ is the bond order between the 2s orbitals of the two carbon atoms. If the carbon-carbon localized bonding orbital is a non-polar linear combination of sp hybrids and if a, a' are the 2s coefficients in these hybrids ($\frac{1}{2}, 1/\sqrt{3}, 1/\sqrt{2}$ for tetrahedral, trigonal and digonal hybrids respectively), then:

$$P_{s_c, s_c'} = aa', \quad (7.2)$$

all overlap integrals being neglected. This result was derived by Frei and Bernstein [20], who found an excellent correlation between experimental data and the product of s-characters as predicted by the theory. There is no experimental evidence on the sign of K_{CC} but all values calculated from (7.1) are positive. If $^3\Delta E$ is chosen as 15 eV (as for methane) and $(2s_c|\delta|2s_c)$ is taken from table 2, then for single C-C bonds in saturated molecules ($a=a'=\frac{1}{2}$) the calculated value is

$K_{CC} = +55 \times 10^{20} \text{ cm}^{-3}$, which is in reasonable agreement with the experimental value of 45.6×10^{20} for ethane [3].

Next let us turn to carbon-fluorine coupling where there is a considerable amount of experimental data [5] and some evidence that K_{CF} has the opposite sign to K_{CH} [21]. The simplest molecule to consider is CF_4 which is tetrahedral (symmetry T_d) so that only molecular orbitals of A_1 symmetry contribute. In the valence shell LCAO approximation, these are constructed from the three basic symmetry functions:

$$\left. \begin{aligned} [s_F] &= \frac{1}{2}(2s_F + 2s_F' + 2s_F'' + 2s_F'''), \\ [\sigma_F] &= \frac{1}{2}(2p\sigma_F + 2p\sigma_F' + 2p\sigma_F'' + 2p\sigma_F'''), \\ [s_C] &= 2s_C, \end{aligned} \right\} \quad (7.3)$$

where each $2p\sigma_F$ orbital is directed along the F-C bond with its positive lobe pointing towards the carbon atom and the factors $\frac{1}{2}$ are included for normalization (in the overlap-neglected approximation). In an independent-electron model, the LCAO coefficients for the basis-functions (7.3) can be determined from the Hamiltonian matrix which takes the form:

$$\begin{bmatrix} \alpha_s^F & 0 & 2\beta_{ss} \\ 0 & \alpha_\sigma^F & 2\beta_{s\sigma} \\ 2\beta_{ss} & 2\beta_{s\sigma} & \alpha_s^C \end{bmatrix}, \quad (7.4)$$

the α and β elements being defined with respect to the atomic orbitals in the usual manner.

Since α_s^F will be substantially below both α_σ^F and α_s^C , the matrix (7.4) is closely analogous to that for hydrogen fluoride (equation (6.3)) and can be handled in a similar perturbation manner. To elaborate the previous treatment slightly, if the $[s_F]$ function is not mixed with the others at all ($\beta_{ss}=0$), the molecular orbitals are $[s_F]$, $\lambda[\sigma_F] + \mu[s_C]$, $-\mu[\sigma_F] + \lambda[s_C]$, where λ , μ are coefficients (with $\lambda^2 + \mu^2 = 1$) determining the distribution of the electrons between C and F.

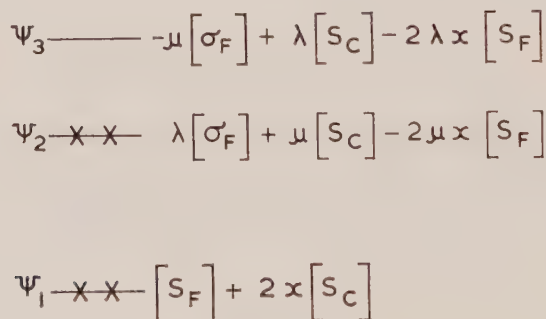


Figure 3. Energy level diagram and approximate molecular orbitals for CF_4 .

If mixing with the $[s_F]$ function is now introduced in powers of the positive parameter $x = \beta_{ss}/\alpha_s^F$ (α_σ^F and α_s^C being chosen near zero), the coefficients are approximately as shown in figure 3. If the fluorine $2s$ orbital is sufficiently low

in energy the mutual polarizability between $2s_F$ and $2s_C$ will be dominated by the $\psi_2 \rightarrow \psi_3$ contribution and will have the limiting form:

$$\pi_{s_C, s_F} \sim \frac{4\lambda^2 \mu^2 x^2}{\epsilon_2 - \epsilon_3} < 0. \quad (7.5)$$

However, this will be partially cancelled by a contribution of opposite sign from the excited state $\psi_1 \rightarrow \psi_3$.

There are no suitable wave functions for detailed calculations on CF coupling constants, but we may make some very rough estimates in comparison with hydrogen fluoride. As the electronegativities of carbon and hydrogen are much the same, it is reasonable to suppose that the λ/μ ratio and the relative contributions of the $\psi_2 \rightarrow \psi_3$ and $\psi_1 \rightarrow \psi_3$ transitions are the same in both calculations. If this is so, we expect K_{CF} and K_{HF} both to be negative and that

$$\frac{K_{CF}}{K_{HF}} \sim \frac{(2s_C|\delta|2s_C)}{(1s_H|\delta|1s_H)} \times \left(\frac{\beta_{s_C s_F}}{\beta_{s_H s_F}} \right)^2. \quad (7.6)$$

The ratio of atomic orbital amplitudes is about five from table 2. On the other hand the ratio of β -elements will be less than unity because of the longer bond. Experimentally $K_{CF} = \pm 90.5 \times 10^{20} \text{ cm}^{-1}$ in CF_4 [5] compared with $K_{HF} = \pm 54.4 \times 10^{20} \text{ cm}^{-1}$ in HF [14] which seems reasonable. The sign of K_{CF} in CF_4 is unknown but Tiers [21] has established that in the molecule CHFCl_2 , it is opposite to K_{CH} , so both experiment and theory favour $K_{CF} < 0$.

Pritchard (quoted in reference [5]) has measured the boron-fluorine coupling constant in BF_4^- which is isoelectronic with CF_4 . He found $K_{BF} = \pm 1.1 \times 10^{20} \text{ cm}^{-1}$, very much smaller than for CF_4 . In the theory, it should be possible to calculate K_{BF} from a set of molecular orbitals similar to those shown in figure 3, [s_C] being replaced by the boron $2s$ function. The main difference between BF_4^- and CF_4 is that the bonds will be more polar in the former, corresponding to a smaller value of the coefficient μ . The contribution from the excitation $\psi_2 \rightarrow \psi_3$ which tends to make K negative is proportional to $\lambda^2 \mu^2$, whereas the partly compensating positive contribution from $\psi_1 \rightarrow \psi_3$ is proportional only to λ^2 . Hence if K_{CF} is negative, as seems probable, the cancellation will be more complete for K_{BF} which is consistent with the low observed numerical value. A similar situation arises with BF_3 , where $K_{BF} = \pm 4.1 \times 10^{20} \text{ cm}^{-1}$ [5]. This is planar (symmetry D_{3h}) so that the totally symmetric molecular orbitals and energies are comparable to those shown in figure 3.

Another system worth examining is the fluorine molecule F_2 , even though the experimental coupling constant is inaccessible. The contributing molecular orbitals may be classified as σ_g or σ_u and, in the overlap-neglected LCAO approximation, are constructed from the symmetry combinations:

$$\left. \begin{aligned} [S_g] &= (s + s')/\sqrt{2} & [S_u] &= (s - s')/\sqrt{2}, \\ [P_g] &= (p + p')/\sqrt{2} & [P_u] &= (p - p')/\sqrt{2}, \end{aligned} \right\} \quad (7.7)$$

where s, s', p, p' are written for the $2s_F$ and $2p\sigma_F$ atomic orbitals on the two atoms. The positive lobes of both $2p\sigma_F$ are taken to be pointing inwards. Since the $2s_F$ energies are far below those of the $2p_F$ orbitals, the molecular orbitals and energies are approximately as shown in figure 4. x and y being small quantities.

The lowest excitation $\psi_3 \rightarrow \psi_4$ gives a positive contribution to the coupling constant (as does any $g \leftrightarrow u$ transition). However, this is not necessarily dominant

for it is proportional to x^2y^2 , while the contributions of $\psi_2 \rightarrow \psi_4$ and $\psi_1 \rightarrow \psi_4$ are proportional to y^2 . In the independent electron model, the MO coefficients of the functions (7.7) are determined from Hamiltonian matrices:

$$\left. \begin{aligned} \sigma_g : & \begin{bmatrix} \alpha_s + \beta_{ss'} & +\beta_{sp'} \\ +\beta_{sp'} & \alpha_p + \beta_{pp'} \end{bmatrix}, \\ \sigma_u : & \begin{bmatrix} \alpha_s - \beta_{ss'} & -\beta_{sp'} \\ -\beta_{sp'} & \alpha_p - \beta_{pp'} \end{bmatrix}. \end{aligned} \right\} \quad (7.8)$$

If α_p is taken as zero, an expansion in powers of $(1/\alpha_s)$, which will not be reproduced in detail, gives for the limiting form of the mutual polarizability:

$$\pi_{s,s'} \sim (\beta_{sp'}^2/2\beta_{pp'}\alpha_s^4)(-\beta_{ss'}^2 + 4\beta_{pp'}\beta_{ss'}). \quad (7.9)$$

Since the relevant signs are $\beta_{pp'} < 0$, $\beta_{ss'} < 0$ and since $\beta_{sp'}$ should presumably be intermediate in magnitude between $\beta_{pp'}$ and $\beta_{ss'}$, it follows that $\pi_{s,s'}$ is negative in this limit, corresponding to a negative value for $K_{\text{FF}}^{(3)}$. This means that the combined effect of transitions $\psi_1 \rightarrow \psi_4$ and $\psi_2 \rightarrow \psi_4$ dominates the contribution from $\psi_3 \rightarrow \psi_4$.

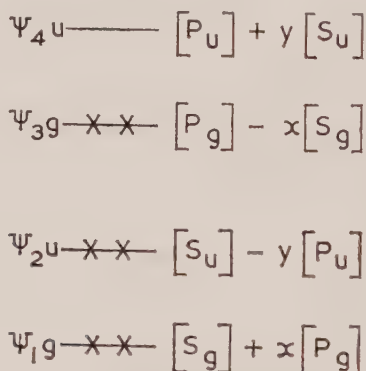


Figure 4. Energy level diagram and approximate molecular orbitals for F_2 .

We may also make a more direct calculation of K_{FF} in F_2 using Ransil's LCAOSCF functions (best limited LCAOMO). From a formula analogous to (6.6) we obtain:

$$K_{\text{FF}}^{(3)} = -(256\pi^2/9)\beta^2a_0^{-6} \left\{ -\frac{2\cdot500}{\Delta E_{1 \rightarrow 1}} + \frac{2\cdot935}{\Delta E_{2 \rightarrow 1}} - \frac{0\cdot133}{\Delta E_{3 \rightarrow 1}} \right\}. \quad (7.10)$$

Using energies of 35 eV, 30 eV and 10 eV for $\Delta E_{1 \rightarrow 1}$, $\Delta E_{2 \rightarrow 1}$ and $\Delta E_{3 \rightarrow 1}$ respectively, this gives $K_{\text{FF}}^{(3)} = -90 \times 10^{20} \text{ cm}^{-3}$, again a negative value. For this molecule, the spin-dipole contribution $K^{(2)}$ is comparable in magnitude. Using the value given in table 1, we obtain a total coupling constant $K_{\text{FF}} = -45 \times 10^{20} \text{ cm}^{-3}$. However, it should be emphasized that this figure is the result of cancellation of larger terms of opposite sign in (7.10) and is therefore subject to considerable error.

8. CONCLUSIONS

Three main conclusions may be drawn from the discussion of the nuclear spin coupling constants between directly bonded atoms given in the last two sections. In the first place, it has become clear that the large values are dominated by the contact term. Secondly, it has been shown that molecular orbital theory can lead to constants of either sign, provided that the relative energy levels are properly taken into account. The mean excitation energy approximation (which gives only positive coupling constants) is very unsatisfactory for bonds to fluorine where the $2s$ electrons have low energies and where a fuller molecular orbital treatment suggests that coupling constants are usually negative.

H H + 23.3	B + 21.3	C + 41.8	N + 53.0	O ± 45.1	F - 54.4
B	+	+	+	+	± 1.1
C		+ 44.8	+	\pm	- 90.5
N			+	\pm	- 190
O				\pm	—
F					—

Table 5. Experimental magnitudes of reduced coupling constants in single bonds (NF_3 value due to Randall and Baldeschwieler (quoted in reference [22] ; other references given earlier in the text)) and suggested sign distribution (\pm) indicating a small value of uncertain sign.

Thirdly, the theory may be of some value in indicating a general pattern of signs and magnitudes of coupling constants when comparing one type of bond with another. Table 5 gives the experimental magnitudes of constants for single bonds where available, together with a tentative pattern of signs suggested by the theory. This is based on the detailed discussion for the hydrides, CC, CF, BF and F_2 together with some interpolation. For example, it seems likely that the series CC, CN, CO, CF parallel the hydride series HC, HN, HO, HF. As mentioned previously, there is experimental evidence in favour of the proposed signs for CH and CF. Also, the small value for BF is consistent with the pattern. On the other hand, the value for OH is not as small as might be expected if there is a sign change along the hydride series. Clearly some further experimental entries in this table would help to elucidate its general features.

This work forms part of the programme of the Basic Physics Division of the National Physical Laboratory and is published by permission of the Director.

REFERENCES

- [1] RAMSEY, N. F., 1953, *Phys. Rev.*, **91**, 303.
- [2] MCCONNELL, H. M., 1956, *J. chem. Phys.*, **24**, 460.
- [3] LYNDEN-BELL, R. M., and SHEPPARD, N., 1962, *Proc. roy. Soc. A*, **269**, 385.
- [4] COULSON, C. A., and LONGUET-HIGGINS, H. C., 1947, *Proc. roy. Soc. A*, **191**, 39.

- [5] MULLER, N., and CARR, D. T., 1963, *J. phys. Chem.*, **67**, 112.
- [6] MORTON, J. R., ROWLANDS, J. R., and WHIFFEN, D. H., 1962, National Physical Laboratory Report BPR 13.
- [7] KARPLUS, M., and GRANT, D. M., 1959, *Proc. nat. Acad. Sci., Wash.*, **45**, 1269.
- [8] OGG, R. A., 1954, *J. chem. Phys.*, **22**, 1933.
- [9] MULLER, N., and PRITCHARD, D. E., 1959, *J. chem. Phys.*, **31**, 768.
- [10] OGG, R. A., and RAY, J. D., 1957, *J. chem. Phys.*, **26**, 1339.
- [11] BUCKINGHAM, A. D., and McLAUCHLAN, K. A., 1963, *Proc. chem. Soc.*, p. 144.
- [12] LAUTERBUR, P. C., and KURLAND, R. J., 1962, *J. Amer. chem. Soc.*, **84**, 3405.
- [13] LENNARD-JONES, J. E., 1949, *Proc. roy. Soc. A*, **198**, 1.
- [14] MACLEAN, C., and MACKOR, E. L., 1962, *Proc. XIth Colloque Ampere* (North-Holland Publishing Company), p. 571.
- [15] RANSIL, B. J., 1960, *Rev. mod. Phys.*, **32**, 239.
- [16] ELLISON, F. O., and SHULL, H., 1955, *J. chem. Phys.*, **23**, 2348.
- [17] DUNCAN, A. B. F., 1957, *J. chem. Phys.*, **27**, 423.
- [18] OGG, R. A., and RAY, J. D., 1957, *J. chem. Phys.*, **26**, 1515.
- [19] REUBEN, J., TZALMONE, A., and SAMUEL, D., 1962, *Proc. chem. Soc.*, p. 353.
- [20] FREI, K., and BERNSTEIN, H. J., 1963, *J. chem. Phys.*, **38**, 1216.
- [21] TIERS, G. V. D., 1962, *J. Amer. chem. Soc.*, **84**, 3972.
- [22] NOGGLE, J. H., BALDESCHWIELER, J. D., and COLBURN, C. B., 1962, *J. chem. Phys.*, **37**, 182.

¹⁴N chemical shifts in organic compounds

by D. HERBISON-EVANS and R. E. RICHARDS

Physical Chemistry Laboratory, South Parks Road, Oxford

(Received 8 October 1963)

Quadrupole broadening of nitrogen nuclear resonances can be minimized by using solvents of low viscosity. An extensive survey is presented of ¹⁴N chemical shifts in organic compounds.

1. INTRODUCTION

The study of the chemical shifts of nitrogen nuclear resonances has been relatively neglected. The reason for this is that the ¹⁴N nucleus has an electric quadrupole moment, and in many nitrogen compounds quadrupole relaxation causes the nuclear resonance to be very broad and to yield a poor signal to noise ratio. This quadrupole broadening can often be minimized by using dilute solutions in solvents of low viscosity such as ether or acetone; the results of a survey of ¹⁴N chemical shifts are given below.

2. EXPERIMENTAL

The ¹⁴N resonances were observed with a modified Varian 4300B wide line spectrometer at 3.940 Mc/s [1]. The chemical shifts were obtained by sample replacement methods using a reference sample; the shifts are expressed as δ , where

$$\delta = \frac{H_{(\text{sample})} - H_{(\text{NO}_3^-)}}{H_{(\text{NO}_3^-)}} \times 10^6.$$

The reference was a 4.5 M solution of Analar ammonium nitrate in 3 N aqueous hydrochloric acid. The nitrate resonance was used as it is a single narrow line with a shorter spin lattice relaxation time than that of the quintuplet nitrogen resonance of the ammonium ion. In the reference solution the shift between the NH_4^+ and NO_3^- resonances is 353.5 ± 0.5 p.p.m. The nitrogen resonance of CH_3NO_2 was used occasionally as a secondary standard; it is slightly broader than that of the NO_3^- resonance but much stronger.

3. RESULTS

The ¹⁴N resonance chemical shifts are listed in tables 1–5. For completeness, the results of other work are also included. The errors quoted are approximate 60% confidence limits.

The accuracy of the chemical shift measurements is not high enough to make corrections for bulk susceptibility worth while.

Some of the compounds were examined in several solvents, and the results are shown in table 6.

Pyridines

The ^{14}N shifts in a number of pyridine derivatives are given in table 7.

4. DISCUSSION

From the results in tables 1-5, a number of general comments can be made immediately. Thus, whereas most of ^{14}N shifts fall into the groups :

Amines	340 p.p.m.
Amides	270
Cyanides	100
Nitrocompounds	0

the shifts of nitrogen atoms in aromatic rings are spread over the whole range of shifts.

In the groups, low field shifts appear to be associated with an increasing electronegativity of substituents, e.g.

NH_3	376 p.p.m.
$(\text{NH}_2)_2\text{CO}$	298
$\text{NH}_2 \cdot \text{CO} \cdot \text{CH}_3$	267
Barbitone	230
Succinimide	199

An exception is found in the symmetric ammonium ions :

NH_4^+	353 p.p.m.
NMe_4^+	332
NEt_4^+	312

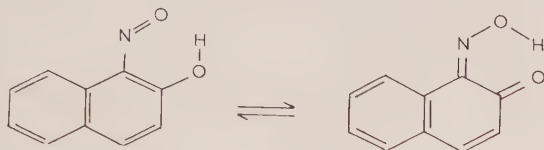
The group of nitrocompounds can perhaps be regarded as the lower limit of the NR_3 group with R very electronegative. Although there seems to be a clear correlation with electronegativity, the shifts are much too great to be accounted for by changes in the diamagnetic term alone. There must also be an important variation in the paramagnetic term (see below).

The normal shift of the CN groups in $\text{Cr}(\text{CN})_5\text{NO}^{--}$ is remarkable for a paramagnetic complex. It shows, as does the E.S.R. spectrum [24], that the odd electron is localized to a greater extent on the NO group than on the CN group.

The effect of quaternization is seen to be small generally, but conjugation and delocalization of the inert pair are associated with a shift to low field.

The difference between the shifts of the NO groups of α -nitroso- β -naphthol and para-nitroso-N-dimethylaniline is probably due to tautomerization of the

naphthol to the pseudo-oxime [25] :



Rapid proton exchange gives rise to a single resonance at the weighted mean of the shifts of the tautomers. Further measurements on this and similar compounds in various solvents may give valuable information on the tautomerizations which are so common in the organic chemistry of nitrogen.

Further insight into the values of the chemical shifts can be gained from the theory of Saika and Slichter [26], in which the value of σ , the shift with respect to the isolated nucleus, is regarded as composed of three parts, σ_D , the diamagnetic effect of the electrons on the atom concerned, σ_P , the paramagnetic shift due to the paramagnetic electronic excited states of the atom mixed with the ground state by the applied magnetic field, and σ_A , the long-range effect of other atoms in the molecule :

$$\sigma = \sigma_D + \sigma_P + \sigma_A. \quad (1)$$

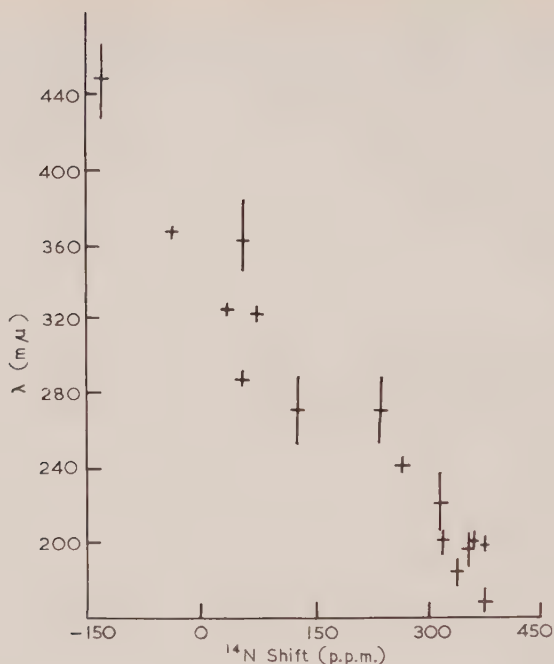
For one electron on ^{14}N , $\sigma_D(1s) = +124$ p.p.m. and $\sigma_D(2s, \text{ep}) = +31$ p.p.m., but this estimate takes no account of the electrical shielding of the nucleus by the 1s electron.

σ_P has been given by Ramsay [14] and involves matrix elements between the electronic ground state and excited states of the molecule. For nitrogen the most important terms arise from $n \rightarrow \pi^*$ and $n \rightarrow \sigma^*$ transitions of the inert pair electrons of the observed atom [13]. If the chemical shift is dominated by σ_P , one could then expect an approximately linear relation between the shift σ and $1/\Delta E$, where ΔE is the energy of excitation from the electronic ground state to excited states which are important in σ_P .

$n \rightarrow \pi^*$ transitions are normally weak and difficult to assign with certainty. Having assigned an $n \rightarrow \pi^*$ transition another difficulty remains, as in many compounds it is not clear on which atom the transition of one of the pair of non-bonding electrons occurs. Except in the cases where a full vibrational analysis has been made of the gas spectrum, there is uncertainty also due to the unknown difference between the position of the maximum of the spectral envelope and the position of the $o-o'$ transition.

Table 8 shows a collection of suspected $n(\text{N}) \rightarrow \pi^*$ or $n \rightarrow \sigma^*$ transition wavelengths which where possible refer to the $o-o'$ transition observed in the gas phase ; also listed are the corresponding ^{14}N shifts. The figure shows the graph of the wavelengths versus the ^{14}N shifts.

For the compounds considered there is an approximately linear relationship, as expected if the values of the matrix elements do not vary much from one compound to another. This is not unreasonable in this case, as for most compounds the nitrogen is not bonded to another atom with an unshared pair.



Pyridines

The most striking effect is the 120 p.p.m. shift to high field that occurs on the protonation of pyridine. The proton effectively fixes the non-bonding electrons of the nitrogen and reduces the contribution to σ_p of the $n \rightarrow \pi^*$ transition to one of a much greater energy: $\sigma \rightarrow \pi^*$.

The pyridinium ion may be compared with the N-oxide where the same stabilization of the non-bonding electrons occurs.

Pyridine	60 p.p.m.
Pyridine-N-oxide	100
1-Hydroxy-pyridinium	150
Pyridinium	180

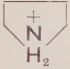
These figures can be explained in terms of the two $n(0) \rightarrow \pi^*$ transitions of the N-oxide, the one of the protonated N-oxide, and the absence of such transitions in pyridinium. These transitions contribute approximately equally to the paramagnetic part of σ_A .

The α and γ hydroxy pyridines in neutral aqueous solution are shifted to high field compared with both themselves in acid solution and the β compound in neutral solution. This shows that tautomerism to the amide forms occurs for the α and γ compounds.

The lack of shift between picolinic acid in neutral and acidic solution confirms that the stable neutral form is the zwitterion [22].

From the Saika-Slichter equation correlations may be expected between the shifts and the wavelengths of the $n \rightarrow \pi^*$ transitions. The wavelengths of the $n \rightarrow \pi^*$ transitions that have been identified are listed in table 9. There are as yet insufficient data to see any experimental correlation.

NR₄

Compound	Solvent	Shift	Error (±)	Reference
Co(NH ₃) ₆ ⁺⁺⁺	H ₂ O(Cl ⁻)	425 p.p.m.	10 p.p.m.	
Co(NH ₃) ₅ Cl ⁺⁺	H ₂ O(Cl ⁻)	420	20	
Co(NH ₃) ₅ (H ₂ O) ⁺⁺⁺	H ₂ O(Cl ⁻)	414	20	
Pt(NH ₃) ₄ ⁺⁺	H ₂ O(Cl ⁻)	408	10	
H ₂ Na ₂ EDTA	H ₂ O	400	15	
trans Coen ₂ Cl ₂ ⁺	H ₂ O(Cl ⁻)	390	10	
Ag(NH ₃) ₂ ⁺	H ₂ O ?	384	6	[2]
Zn(NH ₃) ₃ ⁺⁺	H ₂ O ?	374	6	[2]
Ca(NH ₃) ₃ ⁺⁺	H ₂ O ?	374	10	[2]
H ₃ N ⁺ . CH ₂ . CO ₂ H	CF ₃ COOH	365	10	
NH ₄ ⁺	H ₂ O(NO ₃ ⁻)	353	1	
H ₃ N ⁺ . CH ₂ . CO ₂ ⁻	H ₂ O	352	5	[3]
Me ₃ NH ⁺	H ₂ O + HCl	350	5	[4]
Me ₃ N . BF ₃	H ₂ O	345	10	
H ₃ N ⁻ . CHMe . CO ₂ ⁻	H ₂ O	342	5	[3]
MeNH ₃ ⁺	H ₂ O + HCl	342	1	[4]
Me ₂ NH ₂ ⁺	H ₂ O + HCl	336	5	[4]
PhNH ₃ ⁺	H ₂ O(Cl ⁻)	336	10	
	conc HCl	329	2	
C ₆ H ₁₁ . NH ₃ ⁺	H ₂ O(Cl ⁻)	329	2	
C ₁₆ H ₃₃ . NMe ₃ ⁺	H ₂ O(Br ⁻)	329	2	
PhCH ₂ . NMe ₃ ⁺	H ₂ O + HCl	326	1	[4]
NMe ₄ ⁺	H ₂ O(Br ⁻)	332	2	
NEt ₄ ⁺	H ₂ O(Br ⁻)	312	2	
H ₃ N ⁺ . SO ₃ ⁻	H ₂ O + HCl	285	2	
H ₃ NOH	H ₂ O(Cl ⁻)	276	20	[5]
Me ₃ NOH	H ₂ O(Cl ⁻)	269	3	
Me ₃ N ⁺ . O	NaOH aq	264	10	

EDTA = ethylene diamine tetraacetic acid.

en = ethylene diamine.

Table 1. Nitrogen resonance shifts.

NR₃

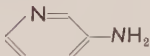


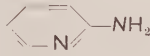
Compound	Solvent	Shift	Error (±)	Reference
NH ₃	Liqu	376 p.p.m.	1 p.p.m.	[4]
Me ₃ N	Et ₂ O	356	3	
(H ₂ NCH ₂) ₂ · H ₂ O	Liqu	364	25	[6]
Me ₂ NH	NaOH aq	355	2	
MeNH ₂	NaOH aq	353	1	[6]
OP(NMe ₂) ₃	Liqu	351	8	
Pyrrolidine	Et ₂ O	340	5	[6]
EtNH ₂	NaOH aq	338	1	
ⁿ Bu ₃ N	Et ₂ O	337	15	[6]
PhNMe ₂	Et ₂ O	337	4	
(Me ₂ N) ₂ CNH	Et ₂ O	332	2	[6]
PhNH ₂	Et ₂ O	330	3	
Et ₃ N	Liqu	329	20	[6]
PhNHMe	Et ₂ O	328	4	
	Et ₂ O	328	4	[6]
Me ₂ N-  -NO	Me ₂ CO	325	5	
Et ₂ NH	NaOH aq	323	2	[6]
N-  -NH ₂	Me ₂ CO	321	7	
ⁿ BuNH ₂	?	314	1	[6]
	Et ₂ O	313	10	
H ₄ N ₂	Liqu	312	20	[5]
(H ₂ N) ₂ CO	H ₂ O	298	3	
(H ₂ N) ₃ C ⁺	H ₂ O(CO ₃ ⁻⁻⁻)	293	10	[5]
H ₂ N · SO ₃ ⁻	NaOH aq	293	2	
(H ₂ N) ₂ COH ⁺	conc HCl	288	10	[5]
PhCONH ₂	Me ₂ CO	283	3	
(MeN · BEt) ₃	Et ₂ O	279	4	[5]
Me ₂ NCHO	Liqu	271	2	
(H ₂ N) ₂ CS	H ₂ O	266	7	[5]

Table 2.

Table 2 (continued)

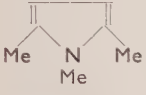
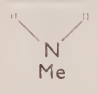
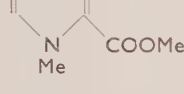
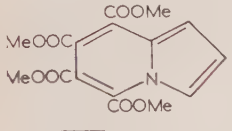

Compound	Solvent	Shift	Error (\pm)	Reference
$\text{H}_2\text{N} \cdot \text{COMe}$	H_2O	267 p.p.m.	8 p.p.m.	[5]
$\text{Me}_2\text{NCHOH}^+$	$\text{CF}_3\text{CO}_2\text{H}$	263	4	
H_2NCHO	Liqu	262	3	
Et_2NCHO	Liqu	259	7	[7]
Et_2NCOCI	Liqu	259	2	
$\text{Et}_2\text{N-CN}$	Liqu	258	2	
Indole	Et_2O	251	4	[6]
Barbitone	$\text{Me}_2\text{SO}/\text{Me}_2\text{CO}$	230	15	
Pyrrole	Liqu	230	2	
	Liqu	230	3	
	Liqu	227	2	
	Liqu	225	2	
	Me_2CO	217	10	
	Conc HCl	199	10	
Succinimide	H_2O	199	4	
Pyridinium	Conc HCl	176	5	
1,2, dimethyl pyridinium	$\text{H}_2\text{O}(\text{I}^-)$	173	5	
1-hydroxy-2 methyl pyridinium	Conc HCl	146	10	
$\text{Me}_2\text{N} \cdot \text{NO}$	Liqu	141	5	
2-Methyl pyridine N-oxide	CHCl_3	91	3	

Table 2. Nitrogen resonance shifts.

RNO₂

Compound	Solvent	Shift	Error (±)	Reference
CH ₂ NO ₂ ⁻	NaOH aq	60 p.p.m.	10 p.p.m.	[8]
HNO ₃	100 per cent	50	10	
C(NO ₂) ₄	Liqu	46	20	
C ₂ (NO ₂) ₆	Liqu	46	20	
Et . NH . NO ₂	Et ₂ O	32	2	[9]
<i>p</i> -nitrobenzoate	KOH aq	27	5	[9]
1,3,5, trichloro-2,4 dinitro-benzene	Me ₂ CO	16	2	
1 hydroxy-4 nitro-pyridinium	Conc HCl	13	2	
H ₂ N . NO ₂	Et ₂ O	12	2	
<i>p</i> -cyano-nitrobenzene	CHCl ₃	11	3	
<i>p</i> -nitrobenzoic acid	Me ₂ CO	10	15	
4-nitro-pyridine-N-oxide	CHCl ₃	10	4	
PhNO ₂	Liqu	5	2	
UO ₂ (NO ₃) ₂	MeOH	4	1	
<i>m</i> -nitro-phenoxide	KOH aq	4	4	
<i>o</i> -nitro-phenoxide	KOH aq	4	4	
NO ₃ ⁻	H ₂ O(NH ₄ ⁺)	0	0	
MeNO ₂	Liqu	- 5	2	
¹²⁵ Pr . NO ₂	Liqu	-28	20	

Table 3. Nitrogen resonance shifts.

NR₂


Compound	Solvent	Shift	Error (±)	Reference
Ph . NCO	Liqu	330 p.p.m.	5 p.p.m.	[7]
Et . NCS	Liqu	271	2	
Me . NC	Liqu	240	2	
(C ₆ H ₁₁ . N:) ₂ C	Liqu ?	240	3	
(Me ₂ N) ₂ C : NH	Et ₂ O	203	2	[7]
<i>p</i> -chloro-benzene isonitrile	EtOH/MeOH	201	5	
<i>p</i> -di-isocyano-benzene	EtOH/MeOH	200	5	
N ₃ ⁻ (centre)	H ₂ O(Na ⁺)	130	2	
NO ₂ ⁺	H ₂ SO ₄ /SO ₃	125	10	[10]
2,5, diphenyl oxazole	Et ₂ O	125	10	[9]
2- <i>n</i> -butanone oxime	CHCl ₃	80	60	
Iso-thiazole	?	79	1	[6]
Pyrimidine	Et ₂ O	78	2	
Benzthiazole	Et ₂ O	59	5	[11]
Pyridine	Liqu	57	2	
Ph-CH = N-Ph	Et ₂ O	55	5	
Pyrazine	Et ₂ O	41	2	
1, nitroso,-2, hydroxy naphthalene	Me ₂ CO	- 12	12	
Pyridazine	Et ₂ O	- 31	2	
Ph-N = N-Ph	Et ₂ O	-129	6	
Me ₂ N-NO	Liqu	-163	5	
NO ₂ ⁻	H ₂ O(Na ⁺)	-247	20	
Me ₃ N-  -NO	Me ₂ CO	-404	20	

Table 4. Nitrogen resonance shifts.

N-R

Compound	Solvent	Shift	Error (\pm)	Reference
NCO^-	$\text{H}_2\text{O}(\text{K}^+)$	304 p.p.m.	5 p.p.m.	
N_3^- (ends)	$\text{H}_2\text{O}(\text{Na}^+)$	280	3	[10]
$\text{Pt}(\text{SCN})_4^{--}$	$\text{H}_2\text{O}(\text{K}^+)$	168	3	
NCS^-	$\text{H}_2\text{O}(\text{NH}_4^+)$	166	1	[12]
$\text{Et}_2\text{N-CN}$	Liqu	149	2	[7]
MeCN	Liqu	135	2	
$\text{CH}_2=\text{CHCN}$	Liqu	130	5	
$(\text{CN})_2$	EtOH	129	3	
$\text{EtOOC} \cdot \text{CH}_2 \cdot \text{CN}$	Liqu	129	10	
2-cyano-pyridine	Et_2O	126	10	
4-cyano-pyridine	Et_2O	120	10	
$\text{CCl}_3 \cdot \text{CN}$	Liqu	120	2	
$\text{Ph} \cdot \text{CN}$	Me_2CO	119	3	
3-cyano-pyridine	Et_2O	115	10	
$\text{Fe}(\text{CN})_6^{4-}$	$\text{H}_2\text{O}(\text{K}^+)$	111	15	
$\text{Cr}(\text{CN})_5\text{NO}^{--}$	$\text{H}_2\text{O}(\text{K}^+)$	102	5	
EtSCN	Liqu	99	3	
CN^-	$\text{H}_2\text{O}(\text{K}^+)$	96	2	
$\text{Co}(\text{CN})_6^{3-}$	$\text{H}_2\text{O}(\text{K}^+)$	94	12	
N_2	?	14	20	[5]
$\text{Fe}(\text{CN})_6^{3-}$	$\text{H}_2\text{O}(\text{K}^+)$	-690	15	[13]

Table 5. Nitrogen resonance shifts.

	Uranyl nitrate	Nitro methane	Ammonia	Acetonitrile	Dimethyl Formamide	Aniline	2-amino pyridine	Pyridine	2-methyl pyridine-N-oxide	3-methyl pyridine-N-oxide	4-methyl pyridine-N-oxide
Neat	—	-5 ± 2	376 ± 1†	134 ± 2	270 ± 2	330 ± 2	—	57 ± 2	—	—	—
Et ₂ O	—	—	—	—	275 ± 2	330 ± 2	310 ± 10	60 ± 2	—	—	—
CF ₃ CO ₂ H	—	-5 ± 2	—	—	—	—	—	60 ± 2	90 ± 2	—	—
CHCl ₃	—	—	—	131 ± 2	—	—	308 ± 8	—	86 ± 2	104 ± 3	86 ± 3
Me ₂ NCHO	—	—	—	135 ± 2	—	—	—	—	102 ± 2	94 ± 3	103 ± 3
MeOH	4 ± 1	—	—	137 ± 2	—	—	—	—	—	—	—
1-methyl naphthalene	—	—	—	—	280 ± 5	—	—	—	—	—	—
H ₂ O	0 ± 1	—	375 ± 2†	—	—	—	—	—	91 ± 2	—	111 ± 5
PhNO ₂	—	—	—	—	—	—	—	—	89 ± 2	—	—
Me ₂ SO	—	—	—	—	—	—	—	—	96 ± 2	—	—
HCO ₂ Me	—	—	—	—	—	—	—	—	—	—	—
EtOH	—	—	364 ± 3†	—	—	—	—	—	—	—	—

† Reference [2].

Table 6. ¹⁴N chemical shifts.

Substance	Solvent	Shift
Pyridine	Et ₂ O	60 ± 2 p.p.m.
Pyridinium	Conc HCl	176 ± 5
Quinoline	Et ₂ O	72 ± 2
Iso-quinoline	Et ₂ O	64 ± 4

Pyridines	Solvent	α	β	γ
— Cl	Et ₂ O	75 ± 2	60 ± 2	72 ± 2 p.p.m.
— Br	Et ₂ O	72 ± 3	53 ± 5	65 ± 5
— CHO	Et ₂ O	66 ± 5	67 ± 2	61 ± 5
— CMeO	Et ₂ O	68 ± 8	67 ± 3	71 ± 5
— Me	Et ₂ O	64 ± 3	60 ± 3	67 ± 3
— OMe	Et ₂ O	117 ± 2		
— NH ₂	Et ₂ O	115 ± 10	78 ± 10	105 ± 7
— CN	Et ₂ O	64 ± 10	63 ± 10	71 ± 10
— OH	H ₂ O	205 ± 4	126 ± 8	222 ± 3
— OH	Conc HCl	194 ± 4	180 ± 10	199 ± 2
— OH	KOH aq			125 ± 50
— CO ₂ Et	Et ₂ O		70 ± 2	
— CO ₂ H	H ₂ O	168 ± 3		
— CO ₂ H	KOH aq	82 ± 10		

Pyridine-N-Oxides	Solvent	α	β	γ
— Me	MeOH	102 ± 3	94 ± 3	103 ± 3 p.p.m.
— Me	Conc HCl	146 ± 5		149 ± 10
— Me	KOH aq	107 ± 10		
— NO ₂	CHCl ₃			65 ± 3
— OMe	CHCl ₃			108 ± 4
— CN	CHCl ₃		83 ± 3	

Table 7. ¹⁴N chemical shifts, δ.

Substance	Lowest transition of the inert pair	Reference	δ
NH ₃	166 m μ	[16]	377 p.p.m.
MeNH ₂	198	[16]	353
Me ₂ NH	218	[16]	359
Me ₃ N	199	[16]	367
EtNH ₂	178	[16]	338
Et ₃ N	212	[16]	321
Pyrrolidine	233 \pm 30	[17]	340
Pyrrole	240 \pm 30	[18]	330
(EtN) ₂ C	270 \pm 30	[19]	240
(CN) ₂	270 \pm 30	[20]	129
Pyrimidine	322	[21]	78
Pyridine	288	[21]	60
Pyrazine	324	[21]	41
Pyridazine	365	[21]	- 31
Ph . CH : N . Ph	310 \pm 30	[17]	55
Ph . N : N . Ph	445 \pm 30	[17]	- 129

Table 8.

$$\lambda(n(\text{N}) \rightarrow \pi^*)$$

Compound	λ o'-o (gas)	Reference	λ Max (soln)	Reference	δ
Pyridine	288 m μ	[21]	270 m μ	[23]	60 \pm 2 p.p.m.
2CN "			278	[23]	64 \pm 10
3CN "			279	[23]	63 \pm 10
4CN "			270	[23]	71 \pm 10
2Me "	288	[27]			64 \pm 3
3Me "	289	[27]			60 \pm 3
4Me "	285	[27]			67 \pm 3
3Cl "	286	[27]			75 \pm 2
3Br "	287	[27]			53 \pm 5

Table 9.

We thank the Department of Scientific and Industrial Research for a Maintenance Grant for one of us (D. H.-E.). We are also grateful to the Department of Scientific and Industrial Research and to the Hydrocarbon Research Group of the Institute of Petroleum for financial assistance.

REFERENCES

- [1] HERBISON-EVANS, D., and RICHARDS, R. E., 1964, *Mol. Phys.*, **7**, 515.
- [2] SCHMIDT, B. M., BROWN, L. C., and WILLIAMS, D., 1958, *J. mol. Spectrosc.*, **2**, 539.
- [3] SCHMIDT, B. M., BROWN, L. C., and WILLIAMS, D., 1959, *J. mol. Spectrosc.*, **3**, 30.
- [4] OGG, R. A., and RAY, J. D., 1957, *J. chem. Phys.*, **26**, 1339.
- [5] HOLDER, B. E., and KLEIN, M. P., 1955, *J. chem. Phys.*, **23**, 1950.
- [6] TURNER, D. W. (private communication).
- [7] RAY, J. D., PIETTE, L. H., and HOLLIS, D. P., 1958, *J. chem. Phys.*, **29**, 1022.
- [8] MASUDA, Y., and KANDA, T., 1953, *J. phys. Soc., Japan*, **8**, 432.
- [9] RAY, J. D., and OGG, R. A., 1957, *J. chem. Phys.*, **26**, 1452.
- [10] KANDA, T., SAITO, Y., and KAWAMURA, K., 1962, *Bull. chem. Soc., Japan*, **35**, 172.
- [11] SCHMIDT, B. M., BROWN, L. C., and WILLIAMS, D., 1958, *J. mol. Spectrosc.*, **2**, 551.
- [12] HOWARTH, O. W., 1963, Thesis, Oxford.
- [13] BALDESCHWIELER, J. D., and RANDALL, E. W., 1961, *Proc. chem. Soc.*, p. 303.
- [14] RAMSAY, N. F., 1950, *Phys. Rev.*, **78**, 699.
- [15] TOWNES, C. H., and SCHAWLOW, A. L., 1955, *Microwave Spectroscopy* (McGraw-Hill), p. 225.
- [16] TANNENBAUM, E., COFFIN, E. M., and HARRISON, A. J., 1953, *J. chem. Phys.*, **21**, 311.
- [17] JAFFE, H. H., and ORCHIN, M., 1962, *Theory and Application of U.V. Spectroscopy* (Wiley).
- [18] MENCZEL, S., 1927, *Z. Phys.*, **125**, 161.
- [19] RAO, C. N. R., 1961, *U.V. and Visible Spectroscopy* (Butterworths).
- [20] PEARSE, R. W. B., and GAYDON, A. G., 1941, *Identification of Molecular Spectra* (Chapman & Hall).
- [21] MASON, S. F., 1959, *J. chem. Soc.*, p. 1240.
- [22] GREEN, R. W., and TONG, H. K., 1956, *J. Amer. chem. Soc.*, **78**, 4896.
- [23] MASON, S. F., 1959, *J. chem. Soc.*, p. 1247.
- [24] BERNAL, I., and HARRISON, S. E., 1961, *J. chem. Phys.*, **34**, 102.
- [25] SIDGWICK, N. V., TAYLOR, H. S., and BAKER, W., 1937, *Organic Chemistry of Nitrogen* (Clarendon Press), p. 221.
- [26] SAIKA, A., and SLICHTER, C. P., 1954, *J. chem. Phys.*, **22**, 26.
- [27] STEPHENSON, H. P., 1954, *J. chem. Phys.*, **22**, 1077.

Interactions spin-spin nucléaires [1]

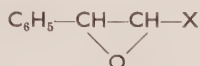
II. Couplages spin-spin dans des époxydes substitués

par JEAN-MARIE LEHN† et JEAN-JACQUES RIEHL‡

Institut de Chimie, 2 rue Goethe, Strasbourg

(Manuscrit reçu le 19 novembre 1963)

Les spectres de Résonance Magnétique Nucléaire (R.M.N.) d'une série d'époxydes disubstitués



ont été étudiés. Les constantes de couplage vicinales J^{cis} et J^{trans} varient linéairement avec l'électronégativité des substituants X. Dans ces composés les coefficients de l'équation de Karplus sur la dépendance angulaire des constantes de couplage sont dans l'ordre inverse ($k_{0^\circ} > k_{180^\circ}$) de celui généralement rencontré.

1. INTRODUCTION

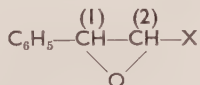
Le mécanisme du couplage indirect entre spins nucléaires consiste en une transmission des états de spin d'un noyau vers un autre noyau à travers les électrons des liaisons séparant les deux noyaux couplés. Pour des noyaux d'un type donné, l'intensité de ce couplage doit de ce fait être influencée par la structure électronique de ces liaisons.

Les travaux théoriques de Karplus et Grant [2] et d'Hiroike [3] ont établi que le couplage spin-spin dépend de la polarité des liaisons séparant les noyaux couplés. Par suite, l'introduction d'un substituant nouveau, en modifiant la distribution de charge électronique dans ces liaisons, modifie aussi le couplage entre les noyaux.

Plusieurs études expérimentales ont montré qu'il existe une relation linéaire entre les constantes de couplage des protons d'un système donné et l'électronégativité des substituants portés par ce système. Il en est ainsi dans des composés aliphatiques [4], vinyliques [5-7], aromatiques [8] et bicycliques [9, 10].

2. RESULTATS

Nous avons examiné les spectres de R.M.N. d'une série d'époxydes disubstitués du type



et nous avons constaté que la constante de couplage $J_{\text{H}_1\text{H}_2}$ dépend de l'électronégativité du groupe X. $J_{\text{H}_1\text{H}_2}$ varie de 2,5 c.p.s. pour $\text{X}=\text{H}$ [11] à 0,5 c.p.s.

† Adresse actuelle : Department of Chemistry, Harvard University, Cambridge 38, Mass., U.S.A.

‡ Adresse actuelle : Department of Chemistry, Massachusetts Institute of Technology, Cambridge 39, Mass., U.S.A.

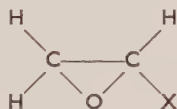
pour $X = \text{OAc}$ dans la série des époxydes *trans*, et de 4,1 c.p.s. pour $X = \text{H}$ [11] à 2,5 c.p.s. pour $X = \text{OAc}$ dans la série des époxydes *cis*. Ces variations, surtout dans le cas des époxydes *trans*, ne peuvent s'expliquer par une distorsion d'origine stérique du cycle époxydique. La nature *cis* ou *trans* des époxydes résulte de données chimiques [12], de leur méthode de préparation et du fait que le couplage $J_{\text{H}_1\text{H}_2}$ est toujours plus faible en *trans* qu'en *cis* [12–14].

Les valeurs de l'électronégativité des substituants ont été tirées de l'expression obtenue par Cavanaugh et Dailey [15] :

$$E = 0,0114\Delta\delta + 1,78$$

où $\Delta\delta$ est la différence de déplacement chimique en c.p.s. à 60 Mc entre les protons des groupes CH_3 et CH_2 dans une série de dérivés $\text{CH}_3 - \text{CH}_2 - X$. L'emploi de cette expression, qui peut inclure une contribution à $\Delta\delta$ provenant de l'anisotropie diamagnétique des substituants, est justifiée par la similitude entre les valeurs de l'électronégativité E ainsi obtenues et les électronégativités orbitales de Hinze *et al.* [16]. Les protons couplés formant un système AB, les constantes de couplage ont été mesurées directement sur le spectre.

Le tableau 1 donne les valeurs observées pour $J_{\text{H}_1\text{H}_2}$ en fonction de la somme $\sum E$ des électronégativités des substituants X et Y : $\sum E = E_X + E_Y$ avec $E_{\text{C}_6\text{H}_5} = 2,75$ et $E_{\text{H}} = 2,2$. Les valeurs des constantes de couplage obtenues par Reilly et Swalen [13, 17] pour les composés



(avec $X = \text{COOH}$, CN et CH_2Cl), ont été ajoutées à nos résultats. La figure 1 représente les variations de $J_{\text{H}_1\text{H}_2}^{\text{trans}}$ et de $J_{\text{H}_1\text{H}_2}^{\text{cis}}$ en fonction de $\sum E$. La figure 2 donne $(J_{\text{H}_1\text{H}_2}^{\text{trans}} + J_{\text{H}_1\text{H}_2}^{\text{cis}})$ en fonction de $\sum E$.

X	Y	E_X	$\sum E = E_X + E_Y$	J^{trans}	J^{cis}	$J^{\text{trans}} + J^{\text{cis}}$
H	C_6H_5	2,2†	4,95	2,52 c.p.s.	4,06 c.p.s.	6,58 c.p.s.
Me	C_6H_5	2,34‡§	5,09	2,0		
Et	C_6H_5	2,34‡§	5,09	2,0		
iPr	C_6H_5	2,34‡§	5,09	2,1		
CN	C_6H_5	2,49	5,24	1,8	3,9	5,7
COOEt	C_6H_5	2,60	5,35	1,7		
OCH ₃	C_6H_5	3,31	6,06	0,8		
OAc	C_6H_5	3,80	6,55	0,5	2,5	3,0
CN	H	2,49	4,69	2,5	4,25	6,74
COOH	H	2,60	4,80	1,7	5,1	6,8
CH_2Cl	H	2,47‡	4,67	2,4	4,0	6,4

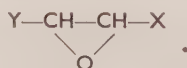
† M. L. Huggins, *J. Amer. chem. Soc.*, 1953, **75**, 4123.

‡ Réf. [16].

§ R. E. Kagarise, *J. Amer. chem. Soc.*, 1955, **77**, 1377.

|| Réf. [11].

Tableau 1. Constantes de couplage J^{trans} et J^{cis} dans des époxydes du type



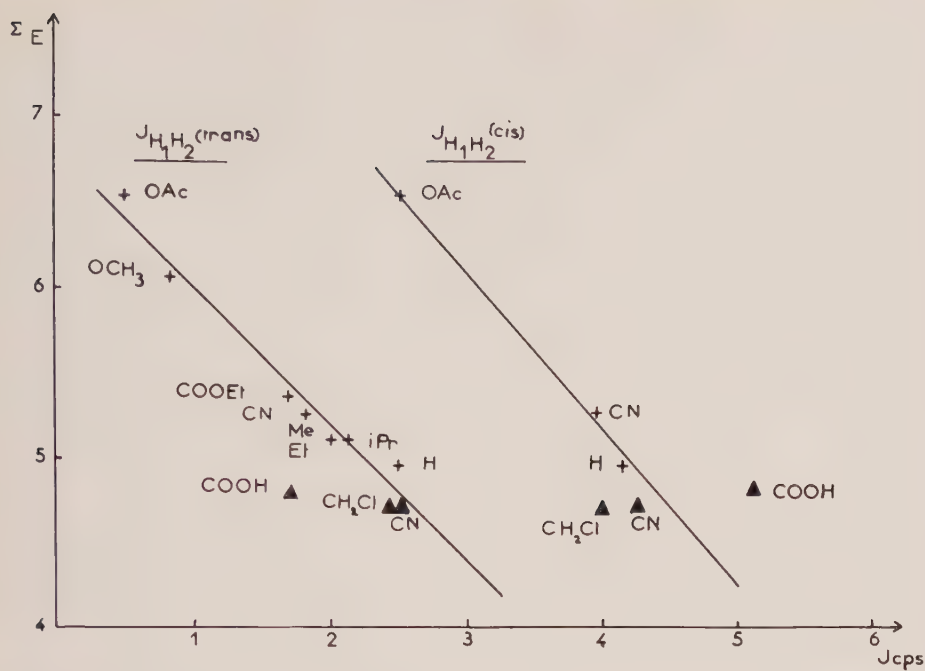


Figure 1. Variation de $J_{H_1H_2}^{cis}$ et de $J_{H_1H_2}^{trans}$ en fonction de l'électronégativité ΣE .

+ époxydes disubstitués (tableau 1 : $Y = C_6H_5$).
 ▲ époxydes monosubstitués (tableau 1 : $Y = H$).

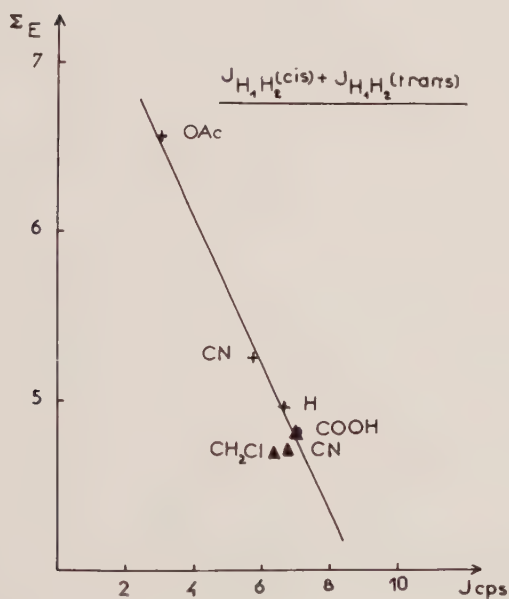


Figure 2. Variation de $J_{H_1H_2}^{cis} + J_{H_1H_2}^{trans}$ en fonction de l'électronégativité ΣE .

+ époxydes disubstitués (tableau 1 : $Y = C_6H_5$).
 ▲ époxydes monosubstitués (tableau 1 : $Y = H$).

3. DISCUSSION

La diminution de la constante de couplage entre protons vicinaux lorsque l'électronégativité des substituants augmente, est en accord avec les résultats théoriques [2, 3, 18] et avec les données expérimentales dans les autres séries de composés citées ci-dessus. En effet un substituant très électronégatif augmente la polarité des liaisons et diminue la densité électronique autour des protons couplés. Il en résulte un affaiblissement de l'interaction de contact spins nucléaires-spins électroniques, d'où une diminution de la constante de couplage.

Pour $X = \text{CN}$ et CH_2Cl (avec $Y = \text{H}$), l'accord entre les résultats de Reilly et Swalen [13, 17] et les nôtres est satisfaisant. Par contre pour $X = \text{COOH}$ ($Y = \text{H}$), seule la somme ($J^{\text{trans}} + J^{\text{cis}}$) est en accord avec nos résultats (figure 2) ; les valeurs individuelles de J^{trans} et de J^{cis} tombent loin en dehors des courbes (figure 1). Ce désaccord pourrait indiquer qu'il est nécessaire de réexaminer ces valeurs. Il semble en être de même pour les constantes de couplages signalées pour $X = \text{COCH}_3$ [13] et $X = \text{CHO}$ [14].

Les constantes de couplage J^{cis} sont dans tous les cas plus élevées que les constantes J^{trans} (tableau 1 ; réf. [11, 13, 14, 17]). Les travaux théoriques de Karplus [19] sur la dépendance angulaire des couplages entre protons vicinaux ont montré que cette dépendance peut être représentée approximativement par une relation de la forme :

$$J_1 = k_1 \cos^2 \phi - c, \quad 0^\circ \leq \phi \leq 90^\circ$$

$$J_2 = k_2 \cos^2 \phi - c, \quad 90^\circ \leq \phi \leq 180^\circ \quad (c = 0,28 \text{ c.p.s.})$$

où k_2 est supérieur à k_1 .

Tous les résultats expérimentaux obtenus à ce jour ont conduit au même résultat : $k_2 > k_1$, pour les systèmes les plus variés (voir par ex. réf. [7, 9, 20]) bien que les valeurs de k_2 et de k_1 soient très différentes suivant les systèmes considérés. Cependant, les époxydes, où J^{cis} et J^{trans} correspondent respectivement à $\phi = 0^\circ$ et à $\phi = 155^\circ$ †, représentent le premier cas dont nous ayons connaissance où k_1 est toujours supérieur à k_2 . En effet, puisque J^{trans} correspond à $\phi = 155^\circ$ on a

$$k_2 = \frac{J^{\text{trans}}}{\cos^2(155^\circ)} = \frac{J^{\text{trans}}}{0,82} \ddagger.$$

Le tableau 2 donne les valeurs de k_1 et de k_2 pour les composés $X = \text{H}, \text{CN}, \text{OAc}$ ($Y = \text{C}_6\text{H}_5$) et $X = \text{CN}, \text{CH}_2\text{Cl}$ ($Y = \text{H}$) du tableau 1.

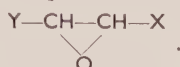
Dans tous les cas k_1 est supérieur à k_2 . Une explication de cette inversion est difficile à donner à l'heure actuelle ; les couplages entre spins nucléaires dépendent en effet de nombreux facteurs à la fois électroniques et géométriques [21, 22]. Cependant on peut faire remarquer que les dérivés cyclopropaniques [23], où le couplage vicinal J^{trans} correspond à $\phi = 147^\circ$ §, représentent un cas

† Cet angle dièdre a été calculé à partir des données géométriques publiées pour l'oxyde d'éthylène (G. L. Cunningham, A. W. Boyd, R. J. Myers, W. D. Gwinn et W. I. LeVan, *J. chem. Phys.*, 1951, **19**, 676) et pour l'oxyde de propylène et l'épichlorhydrine (M. Igarashi, *Bull. chem. Soc. Japan*, 1955, **28**, 58).

‡ Dans ces relations nous négligeons le coefficient c dont des déterminations expérimentales ont montré qu'il est pratiquement nul [27].

§ Calculé d'après les données géométriques publiées pour le cyclopropane (O. Hassel et H. Viervoll, *Acta chem. scand.*, 1947, **1**, 149).

X	Y	k_1	k_2
H	C ₆ H ₅	4,06 c.p.s.	3,07 c.p.s.
CN	C ₆ H ₅	3,9	2,2
OAc	C ₆ H ₅	2,5	0,6
CN	H	4,25	3,0
CH ₂ Cl	H	4,0	2,9

Tableau 2. Coefficients k_1 et k_2 de l'équation de Karplus pour des époxydes du type

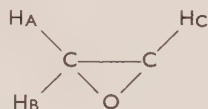
intermédiaire. On a $k_1 = J^{\text{cis}}$ et

$$k_2 = \frac{J^{\text{trans}}}{\cos^2(147^\circ)} = \frac{J^{\text{trans}}}{0,70}.$$

Les constantes de couplage J^{cis} et J^{trans} données par Wiberg et Nist [23] donnent soit $k_1 > k_2$, soit $k_1 < k_2$ selon les composés, J^{cis} étant cependant toujours supérieur à J^{trans} .

Les époxydes présentent une autre particularité, qui cette fois-ci les différencie nettement des composés cyclopropaniques.

Les trois constantes de couplage J_{AB} , J_{BC} et J_{AC} sont de même signe dans les époxydes monosubstitués



[11, 14].

Dans les composés cyclopropaniques [23] et dans pratiquement tous les systèmes étudiés (cf. par ex. [24-26]), J_{AB} est de signe opposé à J_{BC} et à J_{AC} et sans doute négative.

De plus, sur la base de résultats antérieurs [6, 7, 9], la décroissance de J^{cis} et de J^{trans} en valeur absolue lorsque l'électronégativité du substituant augmente (figures 1 et 2) indique que ces constantes de couplage, et donc aussi $J_{\text{AB}}^{\text{gem}}$, sont toutes *positives*, en accord avec les résultats antérieurs [11, 14].

Les propriétés spéciales des époxydes dans le domaine des interactions spin-spin nucléaires semblent donc provenir d'une part de la présence d'un cycle à trois chaînons comme dans les composés cyclopropaniques, d'autre part du remplacement d'un atome de carbone du cycle par un atome d'oxygène, conduisant à des modifications géométriques et électroniques du système.

Les spectres de R.M.N. ont été mesurés à l'aide d'un appareil Varian A-60 à la fréquence de 60 Mc sur des solutions dans le tétrachlorure de carbone. La préparation des composés utilisés a été décrite dans la littérature. Les valeurs des constantes de couplage sont mesurées à $\pm 0,1$ c.p.s. près.

Nous remercions M. F. Hemmert pour la mesure de la plupart des spectres.

BIBLIOGRAPHIE

- [1] FRANCK-NEUMANN, M., et LEHN, J. M., 1963-64, *Mol. Phys.*, **7**, 197.
- [2] KARPLUS, M., et GRANT, D. M., 1959, *Proc. nat. Acad. Sci., Wash.*, **45**, 1269.
- [3] HIROIKE, E., 1962, *J. phys. Soc., Japan*, **17**, 538.
- [4] GLICK, R. E., et BOTHNER-BY, A. A., 1956, *J. chem. Phys.*, **25**, 362.
- [5] BRUEGEL, W., ANKEL, TH., et KRUECKEBERG, F., 1960, *Z. Elektrochem.*, **64**, 1121.
- [6] BANWELL, C. N., SHEPPARD, N., et TURNER, J. J., 1960, *Spectrochim. acta*, **16**, 794.
- [7] SCHAEFER, T., 1962, *Canad. J. Chem.*, **40**, 1.
- [8] COX, P. F., 1963, *J. Amer. chem. Soc.*, **85**, 380.
- [9] WILLIAMSON, K. L., 1963, *J. Amer. chem. Soc.*, **85**, 516.
- [10] LASZLO, P., et VON R. SCHLEYER, P., 1963, *J. Amer. chem. Soc.*, **85**, 2709.
- [11] ELLEMAN, D. D., et MANATT, S. L., 1962, *J. mol. Spectrosc.*, **9**, 477.
- [12] HOUSE, H. O., et BLAKER, J. W., 1958, *J. Amer. chem. Soc.*, **80**, 6389.
- [13] REILLY, C. A., et SWALEN, J. D., 1960, *J. chem. Phys.*, **32**, 1378.
- [14] REILLY, C. A., et SWALEN, J. D., 1961, *J. chem. Phys.*, **34**, 980.
- [15] CAVANAUGH, J. R., et DAILEY, B. P., 1961, *J. chem. Phys.*, **34**, 1099.
- [16] HINZE, J., WHITEHEAD, M. A., et JAFFE, H. H., 1963, *J. Amer. chem. Soc.*, **85**, 148.
- [17] REILLY, C. A., et SWALEN, J. D., 1961, *J. chem. Phys.*, **35**, 1522.
- [18] RANFT, J., 1962, *Ann. Phys., Lpz.*, 7. Folge, **9**, 279.
- [19] KARPLUS, M., 1959, *J. chem. Phys.*, **30**, 11.
- [20] ABRAHAM, R. J., et HOLKER, J. S. E., 1963, *J. chem. Soc.*, p. 906.
- [21] LEHN, J. M. (résultats non publiés).
- [22] KARPLUS, M., 1963, *J. Amer. chem. Soc.*, **85**, 2870.
- [23] WIBERG, K. B., et NIST, B. J., 1963, *J. Amer. chem. Soc.*, **85**, 2788.
- [24] BERNSTEIN, H. J., et SHEPPARD, N., 1962, *J. chem. Phys.*, **37**, 3012.
- [25] FREEMAN, R., et BHACCA, N. S., 1963, *J. chem. Phys.*, **38**, 1088.
- [26] RAO, B. D. N., BALDESCHWIELER, J. D., et MUSER, J. I., 1962, *J. chem. Phys.*, **27**, 2480.
- [27] ABRAHAM, R. J., et McLAUCHLAN, K. A., 1962, *Mol. Phys.*, **5**, 513.

A variational solution of the time-dependent Schrodinger equation

by A. D. McLACHLAN

Department of Theoretical Chemistry,
University Chemical Laboratory, Lensfield Road, Cambridge

(Received 28 November 1963)

A variational method is described for finding approximate solutions of the time-dependent Schrodinger equation. It is closely related to Frenkel's, but better in some respects because it always leads to a true minimum of the error. For several interacting systems it leads to the time-dependent Hartree equations; for a system in an oscillating electric or magnetic field it gives a variational principle for calculating the susceptibility at any frequency.

1. VARIATIONAL PRINCIPLE FOR THE WAVE FUNCTION

It is well known that the Schrodinger equation for stationary states in quantum mechanics can be derived from the condition that the expectation value of the Hamiltonian is stationary for small variations of the wave function. Variational methods for the approximate solution of time-dependent problems are less familiar, but have been known for a long time. The earliest seems to be due to Dirac and Frenkel [1], and was used by Frenkel to derive the time-dependent Hartree-Fock equations for electrons [1-3]. Apart from a variational approach to scattering problems [4], little had been done since then, until Mavroyannis and Stephen [5] and Karplus and Kolker [6, 7] used a variational method to find the perturbed wave function of an atom in a small oscillating electric field. This approach is a very accurate and convenient way to calculate the electrical polarizability and the refractive index of a gas.

The object of this paper is to present a new version of Frenkel's principle and then show how it leads on the one hand to the time-dependent self-consistent field method, and on the other to a variational method for small oscillations. There are some difficulties in Frenkel's original formulation and these are removed in our version.

The problem to be solved is this, to find approximate solutions of the Schrodinger equation:

$$i\hbar \frac{\partial \Psi}{\partial t} = H\Psi \quad (1.1)$$

when the wave function $\Psi(t)$ is restricted to take some fairly simple form. In the variational principle we fix attention on a particular time t , and suppose that $\Psi(t)$ is known, but its rate of change is not. Thus if τ is small, the wave function at time $(t + \tau)$ is assumed to be

$$\Psi(t + \tau) = \Psi(t) - \frac{i}{\hbar} \Theta(t)\tau \quad (1.2)$$

with $\Theta = i\hbar \partial \Psi(t) / \partial t$ an unknown function. If Ψ is an exact solution of (1.1), then of course $\Theta = H\Psi$. For an approximate solution we form the 'remainder' $X = \Theta - H\Psi$ and demand that the quantity

$$I = \int |H\Psi - \Theta|^2 dv = \int |X|^2 dv \quad (1.3)$$

should be a minimum for all allowed variations of the function Θ . In this way one finds values of $\partial \Psi / \partial t$ at successive instants of time and constructs the time variation of Ψ . Since I is always positive the variational principle always leads to a definite minimum rather than a saddle point, and I vanishes only for the exact solution of (1.1). On varying Θ we have the condition that

$$\delta I = \int \delta \Theta^* (H\Psi - \Theta) dv + \int (H\Psi - \Theta)^* \delta \Theta dv = 0 \quad (1.4)$$

for all variations of Θ . In equation (1.4) one is tempted to treat $\delta \Theta$ and its complex conjugate as independent variables and conclude that both terms vanish separately. But I is not a homogeneous quadratic form in Θ and one cannot draw this conclusion. The sum vanishes, but not each separate part.

Frenkel's variational principle states that

$$\int \delta \Psi^*(t) [H - i\hbar \partial / \partial t] \Psi(t) dv = 0 \quad (1.5)$$

is stationary for small variations of the time-dependent wave function $\Psi(t)$. There are three important differences between his principle and ours. First we distinguish sharply between varying $\partial \Psi / \partial t$ at a certain instant and keeping $\Psi(t)$ itself fixed. Second, Frenkel's condition does not imply a true minimum for any quantity, and may lead to divergent solutions. Third, in contrast to (1.4) he would seem to treat $\delta \Psi^*$ and $\delta \Psi$ as independent variables. Although in the applications treated below (1.4) and (1.5) lead to the same results, it is likely that Frenkel's method could go wrong in other cases.

2. APPLICATIONS

2.1. Variation of constants

In the method of variation of constants one supposes that $\Psi(t)$ is a linear combination of a limited number of orthogonal fixed functions Φ_n , so that

$$\Psi(t) = \sum_n C_n(t) \Phi_n, \quad \Theta(t) = \sum_n D_n(t) \Phi_n. \quad (2.1)$$

One can also add in a further set of functions Φ_α so that Φ_n and Φ_α together form a complete set. One finds that

$$X = \sum_n \left(D_n - \sum_m H_{nm} C_m \right) \Phi_n - \sum_{m, \alpha} H_{\alpha m} C_m \Phi_\alpha, \quad (2.2)$$

$$\delta I = \sum_n \delta D_n^* \left(D_n - \sum_m H_{nm} C_m \right) + \text{complex conjugate}, \quad (2.3)$$

and since the variations of the D_n are completely unrestricted it is permissible to treat δD_n and δD_n^* as independent quantities. Thus the usual equations

$$i\hbar \frac{\partial C_n}{\partial t} = \sum_m H_{nm} C_m \quad (2.4)$$

follow from the variational principle.

2.2. Variation of parameters

The approximate wave function Ψ may be defined by the values of a number of parameters u_1, u_2, \dots . Then (1.4) leads to the condition that the real part

$$\operatorname{Re} \int \frac{\partial \Theta^*}{\partial u} (H\Psi - \Theta) dv = 0 \quad (2.5)$$

vanishes for each parameter u .

2.3. Time-dependent self-consistent field

We consider an approximate time-dependent wave function for n quantum-mechanical systems which interact with one another. The systems are supposed to be distinguishable and not necessarily identical. The wave function is taken to be a product

$$\Psi(t) = \psi_1(q_1, t) \psi_2(q_2, t) \dots \psi_n(q_n, t) \quad (2.6)$$

at all times, where q_i stands for the coordinates of system i and where the Hamiltonian is

$$H = \sum_i H_i(q_i) + \sum_{i < j} V_{ij}(q_i, q_j). \quad (2.7)$$

Each function ψ_i has a time variation θ_i , and so the total time variation is

$$\Theta = \sum_i \{\psi_1(q_1) \dots \theta_i(q_i) \dots \psi_n(q_n)\}. \quad (2.8)$$

The remainder is therefore

$$X = \sum_i \{\psi_1 \dots (\theta_i - H_i \psi_i) \dots \psi_n\} - \sum_{i < j} \{\psi_1 \dots (V_{ij} \psi_i \psi_j) \dots \psi_n\} \quad (2.8a)$$

and the variational principle leads to the equations

$$i\hbar \frac{\partial \psi_i}{\partial t} = (H_i + G_i + \lambda_i) \psi_i. \quad (2.9)$$

Here G_i is an average potential :

$$G_i(q_i) = \sum_{j \neq i} \int \psi_j^*(q_j) V_{ji}(q_j, q_i) \psi(q_j) dq_j \quad (2.10)$$

and λ_i is a number. Both G_i and λ_i vary with time and

$$\lambda_i = \sum_{k \neq i} \langle H_k - \epsilon_k \rangle + \sum_{(k < j) \neq i} \langle V_{kj} \rangle, \quad (2.11)$$

where the brackets stand for average values, and ϵ_i is defined as

$$\epsilon_i = i\hbar \int \psi_i^* \frac{\partial \psi_i}{\partial t} dq_i. \quad (2.12)$$

From (2.9), (2.11) and (2.12) it follows also that

$$\epsilon_i = \langle H_i + G_i + \lambda_i \rangle, \quad \sum_i \epsilon_i = \langle H \rangle, \quad \sum_i \lambda_i = -\langle V \rangle. \quad (2.13)$$

The time-dependent equations (2.9) are not very convenient because they contain the parameters λ_i . Furthermore, the λ_i are highly arbitrary. For

example, one may change any pair so that the sum $\sum_i \lambda_i$ remains constant ; and the transformation

$$\begin{aligned} \lambda_i &\rightarrow \lambda_i + \lambda, & \lambda_j &\rightarrow \lambda_j - \lambda, \\ \psi_i &\rightarrow \psi_i \exp(-is/\hbar), & \psi_j &\rightarrow \psi_j \exp(is/\hbar), \\ s(t) &= \int \lambda(t) dt \end{aligned} \quad (2.14)$$

gives an equivalent solution of (2.9), in the sense that the total wave function (2.6) is unchanged. Instead it is useful to take new individual functions $\phi_i(q_i, t)$ which satisfy the *time-dependent self-consistent field* equations

$$i\hbar \frac{\partial \phi_i}{\partial t} = (H_i + G_i)\phi_i, \quad (2.15)$$

and then one can show that the total wave function is

$$\Psi(t) = \phi_1(q_1, t) \dots \phi_n(q_n, t) \exp[-iS(t)/\hbar], \quad (2.16)$$

$$S(t) = - \int \langle V(t) \rangle dt. \quad (2.17)$$

As Dirac [2] has shown, (2.15) conserves the normalization and orthogonality of the wave functions, and for a time-independent Hamiltonian the expectation value $\langle H \rangle$ is conserved throughout the motion. From (2.16), (2.12) and (2.17) one finds also that

$$i\hbar \int \Psi^* \frac{\partial \Psi}{\partial t} dq = \sum_i \epsilon_i(t) - \langle V(t) \rangle = \langle H \rangle. \quad (2.18)$$

The equations of motion (2.15) hold for identical but distinguishable *particles*, as well as for separate *systems*. For electrons however the wave function (2.6) is a determinant instead of a product, and a similar proof leads to time-dependent Hartree-Fock equations with exchange terms [1].

2.4. Small oscillations

Suppose that a system in its ground state Ψ_0 is acted on by a small periodic force of frequency ω . The Hamiltonian and the wave function become :

$$H(t) = H_0 + F \exp(-i\omega t) + G \exp(i\omega^* t), \quad (2.19)$$

$$\psi(t) = [\psi_0 + f \exp(-i\omega t) + g \exp(i\omega^* t)] \exp(-iE_0 t/\hbar), \quad (2.20)$$

to first order in the perturbation. Since $H(t)$ must be Hermitian one has $G = F^\dagger$. Generally the frequency is real, but it is often useful to treat a complex frequency $\omega = \nu + i\lambda$ where the force is switched on in the remote past, and the perturbation varies as

$$\exp(\lambda t)[F \exp(-i\nu t) + F^\dagger \exp(+i\nu t)]. \quad (2.21)$$

To apply the variational principle we evaluate X up to first order only :

$$\begin{aligned} -X \exp(iE_0 t/\hbar) &= [(H_0 - E_0 - \hbar\omega)f + F\psi_0] \exp(-i\omega t) \\ &\quad + [(H_0 - E_0 + \hbar\omega^*)g + G\psi_0] \exp(i\omega^* t). \end{aligned} \quad (2.22)$$

The integral I now contains steady terms and oscillatory terms. We ignore the oscillatory terms, since their time average is zero, and minimize the steady

part only, retaining terms up to the second order in the perturbation. This requires that we minimize

$$I = \int |(H_0 - E_0 - \hbar\omega)f + F\psi_0|^2 dv + \int |(H_0 - E_0 + \hbar\omega^*)g + G\psi_0|^2 dv. \quad (2.23)$$

Thus in the lowest order of perturbation theory f and g are independent of one another. I has value zero only if f satisfies

$$(H_0 - E_0 - \hbar\omega)f + F\psi_0 = 0 \quad (2.24)$$

and g satisfies a similar equation. In the oscillation problem the ordinary Schrodinger equation and the variational principle lead to precisely the same equation (2.24) for f .

For calculating dispersion forces [5, 8-10] it is important to know the electrical polarizability of atoms at imaginary frequencies $\omega = -\omega^* = i\xi$. In this case the two terms F and G coincide :

$$H(t) = H_0 + F \exp(\xi t), \quad \psi(t) = [\psi_0 + f \exp(\xi t)] \exp(-iE_0 t/\hbar) \quad (2.25)$$

and f is chosen to minimize

$$I = \int |(H_0 - E_0 - i\hbar\xi)f + F\psi_0|^2 dv. \quad (2.26)$$

Karplus' variational principle [6, 7] looks for stationary values of the two quantities :

$$\left. \begin{aligned} L^- &= \int [f^*(H_0 - E_0 - \hbar\omega)f + f^*F\psi_0 + \psi_0^*F^\dagger f] dv, \\ L^+ &= \int [g^*(H_0 - E_0 + \hbar\omega^*)g + g^*G\psi_0 + \psi_0^*G^\dagger g] dv. \end{aligned} \right\} \quad (2.27)$$

The Euler equations for L also lead to (2.24), but care must be taken with L^- because it does not always have a true minimum, and this causes trouble, especially when ω is near an absorption frequency of the molecule.

To illustrate our method we calculate the electric polarizability of the hydrogen atom at imaginary frequency, taking $F = -eEx$ as the perturbation, and assuming that the perturbed wave function has the form $f = eE\lambda x\psi_0$. λ is an unknown parameter, chosen to make

$$I = e^2 E^2 \int [(\lambda(H_0 - E_0 - i\hbar\xi) - 1)x\psi_0]^2 dv \quad (2.28)$$

a minimum. One finds

$$\lambda = \frac{A}{B^2 + X^2 \xi^2}, \quad (2.29)$$

$$\alpha(i\xi) = 2\lambda e^2 X^2 = \frac{e^2}{m(\omega_0^2 + \xi^2)}. \quad (2.30)$$

Here the constants are given by :

$$\begin{aligned} A &= \langle x(H_0 - E_0)x \rangle / \hbar^2 = 1/2m, \\ B^2 &= \langle x(H_0 - E_0)^2 x \rangle / \hbar^2 = \langle p_x^2 \rangle / m^2 = e^2/3ma_0, \\ X^2 &= \langle x^2 \rangle = a_0^2, \\ \omega_0^2 &= B^2/X^2 = e^2/3ma_0^3, \end{aligned} \quad (2.31)$$

and a_0 is the Bohr radius. The expressions for A and B follow from the operator identity $\hbar p_x = im[H_0, x]$ and the oscillator strength sum rule. The exact polarizability is

$$\alpha(i\xi) = \sum_n \frac{e^2 f_{0n}}{m(\omega_{0n}^2 + \xi^2)}, \quad (2.32)$$

where ω_{0n} and f_{0n} are the frequencies and oscillator strengths of the transitions. The crude approximation (2.30) therefore gives the correct behaviour at high frequencies, but makes the static polarizability too small: $3a_0^3$ instead of $4\frac{1}{2}a_0^3$.

3. DISCUSSION

The variation principle for the wave function is useful in a variety of time-dependent problems. It is reliable because the quantity varied must always have a true minimum, and it is simple to use. It would be useful also to have a similar method for the time variation of the density matrix. The equation of motion is:

$$\sigma \equiv \hbar \frac{\partial \rho}{\partial t} = i[\rho, H], \quad (3.1)$$

so by analogy with (1.3) we could form the Hermitian matrix χ and seek to minimize the positive quantity

$$J = \text{Tr}\{\chi^2\}, \quad \chi = \sigma - i[\rho, H]. \quad (3.2)$$

The condition for a stationary value is that

$$\text{Tr}\{\delta\sigma(\sigma - i[\rho, H])\} = 0 \quad (3.3)$$

for all allowed variations of σ .

Unfortunately this procedure leads to unreasonable results. For example, in the Hartree approximation for two coupled systems one takes a product $\rho = \rho_1 \rho_2$. Then (3.3) leads to equations of motion for ρ_1 and ρ_2 which do not conserve the mean value of the energy.

REFERENCES

- [1] FRENKEL, J., 1934, *Wave Mechanics, Advanced General Theory* (Oxford: Clarendon Press), p. 435.
- [2] DIRAC, P. A. M., 1930, *Proc. Camb. phil. Soc.*, **26**, 376.
- [3] THOULESS, D. J., 1961, *The Quantum Mechanics of Many-body Systems* (New York: Academic Press), p. 88.
- [4] LIPPMAN, B. A., and SCHWINGER, J., 1950, *Phys. Rev.*, **79**, 469.
- [5] MAVROYANNIS, C., and STEPHEN, M. J., 1962, *Mol. Phys.*, **5**, 629.
- [6] KARPLUS, M., 1962, *J. chem. Phys.*, **37**, 2723.
- [7] KARPLUS, M., and KOLKER, H. J., 1963, *J. chem. Phys.*, **39**, 1493.
- [8] McLACHLAN, A. D., GREGORY, R. D., and BALL, M. A., 1963-64, *Mol. Phys.*, **7**, 119.
- [9] McLACHLAN, A. D., 1963, *Proc. roy. Soc. A*, **271**, 387.
- [10] SALEM, L., 1960, *Mol. Phys.*, **3**, 441.

The negative ions of tetraphenylene and 1,2 : 5,6-dibenzcyclooctatetraene

by A. CARRINGTON, H. C. LONGUET-HIGGINS and P. F. TODD

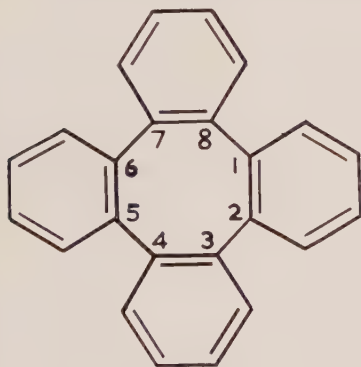
Department of Theoretical Chemistry, University of Cambridge

(Received 7 January 1964)

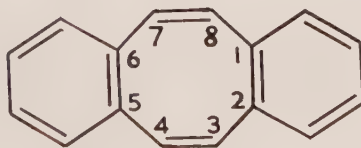
Electron spin resonance measurements are reported for the anions of tetraphenylene and 1,2 : 5,6-dibenzcyclooctatetraene. The proton hyperfine coupling constants obtained are in good agreement with those calculated theoretically by regarding the orbital of the unpaired electron as a linear combination of the molecular orbitals of the component parts of the molecule.

1. INTRODUCTION

The tetraphenylene molecule (I), which is formally a derivative of cyclooctatetraene, is far from planar; the centres of its four rings lie approximately at the vertices of a regular tetrahedron [1]. Likewise in 1,2 : 5,6-dibenzcyclooctatetraene (II) there must be a considerable angle of twist about the 'single' bonds in the eight-membered ring, so that conjugation across these bonds is largely inhibited. The addition of an electron to (I) or (II) would not be expected to make any great difference to the molecular geometry, so that it might be possible to interpret the electron spin resonance spectra of the corresponding negative ions in terms of weak coupling between the four unsaturated components. We here report an investigation designed to test this hypothesis.



(I)



(II)

2. EXPERIMENTAL

(a) Tetraphenylene (I) was prepared by the method of Rapson *et al.* [2]. A small amount of the material was dissolved in a mixture of one part of 1,2-dimethoxyethane and two parts of tetrahydrofuran. Treatment with metallic potassium *in vacuo* gave a violet solution, whose electron resonance spectrum was recorded at -90°C . The spectrum (see figure 1) consisted of nine main lines with a

binomial distribution of intensity and a separation of 1.4 gauss. Each of these lines was further split into a partially resolved multiplet with a splitting constant of 0.2 gauss.

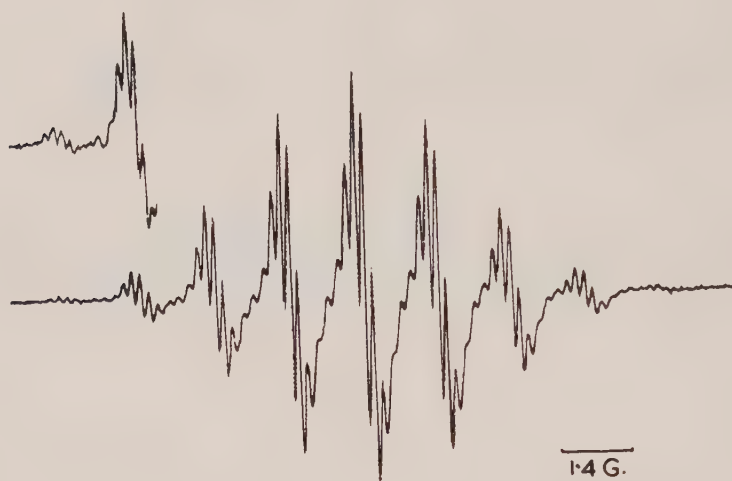


Figure 1. Tetraphenylene anion.



Figure 2. 1,2:5,6-dibenzcyclooctatetraene anion.

(b) 1,2:5,6-dibenzcyclooctatetraene (II) was prepared by the method of Fieser and Pechet [3], as modified by Cope and Fenton [4]. Reduction with lithium metal in tetrahydrofuran gave a red-brown solution whose electron spin resonance spectrum was recorded at room temperature. The hyperfine pattern, which is shown in figure 2, is the product of three 1:4:6:4:1 quintets with

splitting constants of 2.6, 1.8 and 0.2 gauss. The reconstruction is based on these values.

3. THEORY

If there were no coupling between the four benzene rings in I, or the benzene rings and the ethylenic fragments in II, the lowest anti-bonding orbital of I would be 8-fold degenerate and that of II would be 6-fold degenerate. This is because (in the Hückel theory) the lowest anti-bonding orbital of benzene is two-fold degenerate and has the same energy as the anti-bonding orbital of ethylene. If now a small resonance integral is introduced across each 'single' bond in the eight-membered ring, the degeneracy of the lowest anti-bonding orbital will be lifted, and the odd electron will go into the anti-bonding orbital of lowest energy. One may thus regard the orbital of the odd electron as a linear combination of the *molecular* orbitals of the component parts of the molecule, a point of view which was advocated by Dewar as long ago as 1949 [5].

One could determine the anti-bonding orbital of lowest energy by setting up an 8×8 secular equation for I, or a 6×6 secular equation for II. This, however, is unnecessary because it is easy to construct the desired orbital by inspection. To obtain a molecular orbital of low energy one requires the component orbitals to overlap as far as possible in phase, and with maximal amplitudes at the points of overlap. Now the atomic orbital coefficients in the degenerate anti-bonding orbitals of benzene are, in real form:

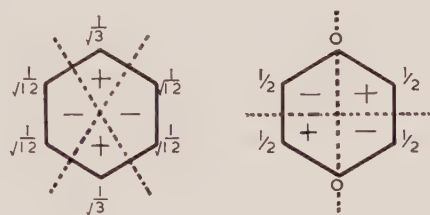


Figure 3.

For I, therefore, the lowest energy combination of benzene anti-bonding orbitals is that shown in figure 4; across each single bond the adjacent ring

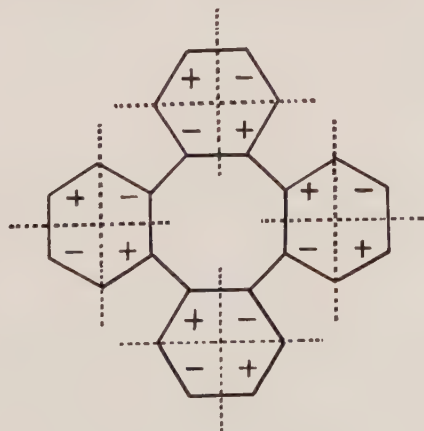


Figure 4.

orbitals overlap in phase and as much as possible. An electron in this molecular orbital is evenly distributed over the eight innermost and eight outermost carbon atoms, and avoids the others altogether. To calculate the proton splitting constants we use McConnell's relation $a_H = Q\rho_C$, where a_H is the proton splitting constant, ρ_C is the amount of unpaired spin on the neighbouring carbon atom and Q has the value 22.5 gauss, obtained from the electron resonance spectrum of the benzene negative ion. The calculated splitting constants therefore are $22.5/16 = 1.41$ gauss and 0.0 gauss, in excellent agreement with the experimental values 1.4 gauss and 0.2 gauss. These results leave no reasonable doubt that the larger splitting constant is due to the outermost protons.

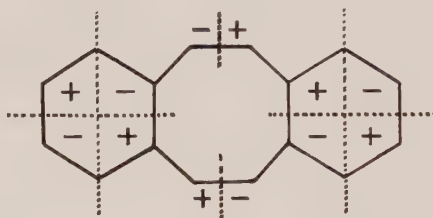


Figure 5.

Similar arguments may be used for identifying the orbital of the odd electron in II. The most effective in phase overlap between anti-bonding orbitals of the fragments is obtained by combining them in the manner shown in figure 5. An electron in this molecular orbital will divide itself equally between the four fragments, so that the spin density on an ethylenic carbon atom should be $1/8$ and the spin distribution in each benzene ring should be the same as in I. Using McConnell's relation, we arrive at the following splitting constants:

- 2.8 gauss for the ethylenic protons,
- 1.4 gauss for the outermost protons of the benzene rings, and
- 0.0 gauss for the remaining protons.

These values agree very well with the experimental values, namely 2.6 gauss, 1.8 gauss and 0.2 gauss, leaving little doubt as to which splitting constants are due to which sets of equivalent protons.

The good agreement between the calculated and observed splitting constants of the ions of I and II indicates that there is relatively weak conjugation across the bonds connecting the four unsaturated fragments, though it does not prove beyond question that the ions are non-planar.

We wish to acknowledge financial support from the D.S.I.R., General Electric, U.S.A. and the Shell International Petroleum Company. P. F. T. thanks I.C.I. Ltd., Petrochemical and Polymer Laboratory, for leave of absence.

REFERENCES

- [1] KARLE, I. L., and BROCKWAY, L. O., 1944, *J. Amer. chem. Soc.*, **66**, 1974.
- [2] RAPSON, W. S., SHUTTLEWORTH, R. G., and VAN NIEKERK, J. N., 1943, *J. chem. Soc.*, **3**, 326.
- [3] FIESER, L. F., and PECHET, M. M., 1946, *J. Amer. chem. Soc.*, **68**, 577.
- [4] COPE, A. C., and FENTON, S. W., 1951, *J. Amer. chem. Soc.*, **73**, 1668.
- [5] DEWAR, M. J. S., 1949, *Proc. Camb. phil. Soc.*, **45**, 638.

H-D isotope effects in the decomposition of acetylene by electron impact

by P. C. HAARHOFF†

Department of Theoretical Chemistry, University Chemical Laboratory,
Lensfield Road, Cambridge

(Received 16 October 1963; revision received 21 January 1964)

In an attempt to gain a better insight into the decomposition of small polyatomic molecules by irradiation, H-D isotope effects in the mass spectrum of acetylene are predicted by means of the quasi-equilibrium theory of mass spectra, and are compared with observed effects. The qualitative agreement between calculated and experimental isotope effects for fragment ions is good, and the quantitative agreement is fair in view of the uncertainty in several quantities, especially in the excitation energy distribution for molecular ions. It is concluded that the quasi-equilibrium theory provides a satisfactory account of the main phenomena which determine the decomposition pattern. There are however several indications that excitation energy is not completely randomly distributed in ions, and this might have to be taken into account in more refined treatments.

1. INTRODUCTION

Although all details of the quasi-equilibrium theory of mass spectra [1, 2] have not yet been fully vindicated by experiment, it is a valuable aid to the understanding of the decomposition of relatively large polyatomic molecules by irradiation [2]. The theory assumes that excitation energy of an ion is first randomly distributed by radiationless electronic transitions and vibrational anharmonicity, and that decomposition then takes place by competing unimolecular reactions.

Decomposition of small polyatomic molecules by irradiation is not well understood at present [3], although the quasi-equilibrium theory has for example been fitted empirically to the mass spectrum of methanol [4]. The number of intersections of potential energy surfaces of small polyatomic molecules may be insufficient to ensure randomization of electronic energy, and the quasi-equilibrium theory may therefore prove unsatisfactory or even fail completely in some cases. It is also possible that rupture of some bonds effectively takes place in one vibration and is determined by the potential energy stored in the bond immediately after ionization [5, 6]. This picture however seems too simplified to yield a realistic description of all decomposition processes.

The investigation described below has been undertaken to gain a better insight into the processes which take place when small polyatomic molecules are decomposed by irradiation. Decomposition of acetylene by electron impact

† Senior Research Officer, Atomic Energy Board, Pelindaba, Republic of South Africa.

is considered, since this molecule has only four atoms, and the mass spectra of the isotopic molecules C_2H_2 , C_2HD and C_2D_2 have been determined [7]. The quasi-equilibrium theory is used to obtain an approximate description of the reaction kinetics, which is modified to yield exact agreement between the calculated and observed mass spectrum of C_2H_2 . Isotope effects in the mass spectrum of acetylene are then predicted and compared with observed effects. Experimental data obtained for acetylene by Melton *et al.* [8] and by Monahan and Stanton [9], which have been interpreted as being in disagreement with the quasi-equilibrium theory, are also discussed.

2. REACTION SCHEME

Figure 1 gives the reaction scheme which is used to interpret the mass spectrum of C_2H_2 obtained by irradiation with 70 volt electrons. This scheme has been constructed on the basis of steric, energetic and other considerations, and is in accord with the observed appearance potentials. It is not difficult to show that processes which are not taken into account in figure 1 are probably only of minor importance, with the possible exception of the reaction $C_2H^+ \rightarrow C_2 + H^+$. The reaction scheme has been simplified by omitting this reaction, since isotopic changes in the relative abundance of H^+ and D^+ have not been determined for acetylene [7], and the data in figure 1 and in Appendix 1 show that reaction (4) is at least partly responsible for H^+ ions. It is concluded in § 5 that formation of H^+ from C_2H^+ does not have a marked effect on isotopic changes that have been observed.

All reactions in figure 1 except reactions (8) and (9) are considered in the quantitative treatment below. The complex mechanism of reaction (9) makes treatment thereof speculative. Reaction (8) is a more simple process, but the relative abundance of $C_2H_2^{++}$ and $C_2D_2^{++}$ has not been directly determined by Mohler *et al.* [7] and was taken as equal to that of C_2HD^{++} .

3. RATE THEORY

The following simplified form of the rate expression given by the quasi-equilibrium theory [1, 13] is used to determine the rate of a reaction r :

$$K_r = \frac{\sigma_r I_r^\ddagger(\epsilon - \epsilon_r)}{h\rho(\epsilon)}, \quad (1)$$

where the excitation energy ϵ is the total energy of the decomposing ion (excluding translational energy) as measured from the minimum energy of the lowest electronic state; the activation energy ϵ_r is the minimum excitation energy required for dissociation by reaction r ; $\rho(\epsilon)d\epsilon$ is the number of vibrational/rotational states of the lowest electronic state of the ion with excitation energy between ϵ and $\epsilon + d\epsilon$, and angular momentum equal to that with which the ion was formed (neglecting vibrational anharmonicity, identity of nuclei and electronic degeneracy); $\rho_r^\ddagger(\epsilon')d\epsilon'$ is a corresponding quantity for the activated complex, determined by regarding the reaction coordinate as fixed and by measuring energy from the activation energy; $I_r^\ddagger(\epsilon')$ is the integral of $\rho_r^\ddagger(\epsilon')$ with respect to ϵ' ; the symmetry number σ_r is the number of equivalent ways in which the reactant can decompose by reaction r . Equation (1) is obtained

by considering only the contributions of the lowest electronic states of the ion and of the activated complex to ρ and I_r^\ddagger , respectively. (This approximation is usually employed [1, 13] and is reasonable [4].) Vibrational anharmonicity and degeneracy of electronic states are, furthermore, neglected.

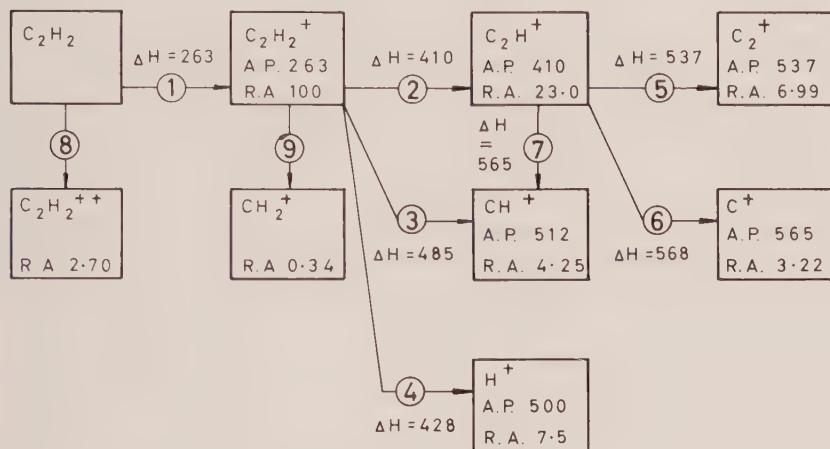


Figure 1. Reaction scheme for 70 volt mass spectrum of C_2H_2 . The relative abundance (R.A.) of H^+ [10] and of other ions [7] is their observed amounts normalized to 100 for $C_2H_2^+$. Appearance potentials (A.P.) of $C_2H_2^+$ [11], C_2H^+ and C_2^+ [12], and CH^+ , C^+ and H^+ [10] are given in kcal/mole. The heats of reaction ΔH , i.e., the minimum total energies required on thermodynamical grounds for reactions (1)–(7), are obtained (in kcal/mole) from the data in Appendix 1. Some ΔH values are accurate only to within about 10 kcal/mole and some A.P. values may be in error by about 20 kcal/mole.

The decomposition of C_2H_2 is now considered, and the results which are obtained are directly applicable to C_2D_2 , while only obvious extensions are required for C_2HD .

The ground state of $C_2H_2^+$ is linear [14] and the scheme given by Walsh [15] suggests that the ground state of C_2H^+ has a similar structure. It is assumed that this is true, and that the activated complexes for reactions (2)–(7) are linear. Alternative assumptions have also been considered and do not lead to any major changes in the calculations.

The angular momentum of $C_2H_2^+$ will usually be comparatively small, and is taken as zero to evaluate the rates of reactions (2)–(4). $\rho(\epsilon)$ is then the density of vibrational states of $C_2H_2^+$ for which the angular momentum J_z along the internuclear axis is zero, and the I_r^\ddagger are similarly defined. (Expressions for the above functions and for related quantities required in the present work are given in Appendix 2, and it is shown that angular momentum restrictions effectively reduce the number of vibrational degrees of freedom of $C_2H_2^+$ by one.) Calculations based on data in the following section show that negligibly few $C_2H_2^+$ and (C_2H^+) ions with sufficient energy to dissociate do not do so in 10^{-6} sec, which is about the time spent by an ion in the ion chamber of a mass

spectrometer [11]. The probability that a $C_2H_2^+$ ion with excitation energy ϵ_α decomposes by reaction r ($r=2, 3, 4$) is therefore taken as :

$$\theta_r(\epsilon_\alpha) = \frac{K_r(\epsilon_\alpha)}{\sum_{s=1}^3 K_s(\epsilon_\alpha)}, \quad \epsilon_\alpha \geq \epsilon_2, \quad (2)$$

and the average probability is found by integrating over the excitation energy distribution for $C_2H_2^+$.

When $C_2H_2^+$ ions decompose by reaction (2), excess energy will effectively be distributed only between six degrees of freedom of the system $C_2H^+ + H$, as a result of the conservation of momentum and angular momentum. It is assumed that after a $C_2H_2^+$ ion passes through the activated complex, its excitation energy in excess of ϵ_2 is randomly distributed between the four vibrations of C_2H^+ and two unspecified translations and/or rotations. As is shown in Appendix 3, the probability $w_\beta(\epsilon_\beta) d\epsilon_\beta$ that the vibrational energy of a C_2H^+ ion lies between ϵ_β and $\epsilon_\beta + d\epsilon_\beta$ is then given by :

$$w_\beta(\epsilon_\beta) = \frac{\rho(\epsilon_\beta)}{I(\epsilon_\alpha - \epsilon_2)}, \quad \epsilon_\beta \leq \epsilon_\alpha - \epsilon_2 \quad (3)$$

for dissociation of $C_2H_2^+$ ions with excitation energy ϵ_α . In the above equation $\rho(\epsilon_\beta)$ is the density of vibrational states of the C_2H^+ ion and $I(\epsilon_\alpha - \epsilon_2)$ is the number of vibrational states of the C_2H^+ ion with energy less than $\epsilon_\alpha - \epsilon_2$. The average probability $W_\beta(\epsilon_\beta) d\epsilon_\beta$ that a $C_2H_2^+$ ion will react, and yield a C_2H^+ ion with vibrational energy between ϵ_β and $\epsilon_\beta + d\epsilon_\beta$, is given from equation (3) by :

$$W_\beta(\epsilon_\beta) = \rho(\epsilon_\beta) \int_{\epsilon_\alpha - \epsilon_2}^{\epsilon_m} \frac{\theta_2(\epsilon_\alpha) W(\epsilon_\alpha) d\epsilon_\alpha}{I(\epsilon_\alpha - \epsilon_2)}. \quad (4)$$

$W(\epsilon_\alpha) d\epsilon_\alpha$ is the probability that the excitation energy of a $C_2H_2^+$ ion lies between ϵ_α and $\epsilon_\alpha + d\epsilon_\alpha$, and ϵ_m is the maximum value of ϵ_α .

The total angular momentum J_β of C_2H^+ ions (which may be comparatively large) is conserved during dissociation by reactions (5)–(7), but the angular momentum component $J_{\beta z}$ along the internuclear axis need not necessarily be conserved. Since $J_{\beta z}$ will be relatively small in comparison with J_β , it is assumed that only the angular momentum component perpendicular to the internuclear axis is approximately conserved. The rates of reactions (5)–(7) are therefore determined from equation (1) by neglecting rotation of C_2H^+ , and ρ is taken as the density of all vibrational states of C_2H^+ , while I_r^+ is taken as the number of vibrational states of the activated complex r with less than the specified energy. The probability that a C_2H^+ ion does not decompose, or decomposes by reaction (5), (6) or (7), is obtained from calculations similar to those for $C_2H_2^+$.

4. EVALUATION OF MASS SPECTRA

Vibrational frequencies which are used in the present work are estimated in Appendix 4, and the activation energies which are chosen for reactions are discussed in Appendix 5 and summarized in table 1. The only additional data required for the calculations are the excitation energy distribution functions for $C_2H_2^+$, C_2HD^+ and $C_2D_2^+$.

Reaction	C_2H_2		C_2HD		C_2D_2		C_r
	ν_r (10^{13} sec^{-1})	ϵ_r (kcal/mole)	ν_r (10^{13} sec^{-1})	ϵ_r (kcal/mole)	ν_r (10^{13} sec^{-1})	ϵ_r (kcal/mole)	
2 Product C_2H^+ C_2D^+	12.3	147	4.47 6.19	148.24 146.96	8.97	148.22	0.510
3 CH^+ CD^+	11.9	222	5.89 5.89	222.17 222.17	11.6	222.37	0.709
4 H^+ D^+	72.1	237	36.4 26.3	236.96 238.24	52.7	238.22	3
5 Reactant C_2H^+ C_2D^+	2.82	127	2.82 2.03	127 128.28	2.03	128.28	0.275
6 C_2H^+ C_2D^+	17.6	158	17.6 17.2	158 158.22	17.2	158.22	3
7 C_2H^+ C_2D^+	9.55	155	9.55 9.38	155 155.22	9.38	155.22	1.63

Table 1. Activation energies (ϵ_r) for reactions, and frequency factors (ν_r) and correction factors (C_r) for their rates. (The symmetry number σ_r for decomposition of C_2H_2 and C_2D_2 by reactions (2), (3) and (4) is equal to 2, and $\sigma_r = 1$ in all other cases.)

Although some information [3, 16, 17] is available about the distribution $W(\epsilon_\alpha)$ for $C_2H_2^+$, a detailed excitation function for $C_2H_2^+$ ions with sufficient energy to dissociate cannot be constructed at present. The mass spectrum of C_2H_2 is therefore interpreted by using a simplified function, i.e. it is assumed that $W(\epsilon_\alpha)$ is constant for $\epsilon_2' \leq \epsilon_\alpha \leq \epsilon_m$, where ϵ_2' is a few kcal/mole less than the activation energy for reaction (2), and ϵ_m is a maximum excitation energy. Similar functions have been employed in related investigations [1, 4].

The Franck-Condon principle [11] suggests that an excitation 'band' (resulting from transitions to a given electronic state) should in general have a different width, but about the same average energy, for isotopic molecules. It is therefore assumed that the excitation energy distributions for $C_2H_2^+$, C_2HD^+ and $C_2D_2^+$ are identical. (Thermal energy of acetylene is not of much importance at typical ion source temperatures and is neglected.)

The approximations in the preceding treatment render it unsuitable for the prediction of absolute amounts of reaction products. The rates of reactions (2)–(7) are therefore multiplied by empirical constants C_r , and the values of these and of ϵ_m are adjusted to yield exact agreement between the calculated† and experimental mass spectra of C_2H_2 . It is assumed that the values of the C_r are invariant for isotopic molecules, i.e. isotopic changes in reaction rates are found from the theory. Since only the relative (and not the absolute) rates of reactions (2), (3) and (4) and of reactions (5), (6) and (7) are of importance, five empirical parameters are effectively introduced, including ϵ_m . These are determined from the amounts of C_2^+ , CH^+ , C^+ and H^+ relative to that of C_2H^+ , and from the percentage of CH^+ formed by reaction (3). The latter was taken as 50 per cent to obtain approximate agreement between the calculated and observed CD^+/CH^+ ratio in the mass spectrum of C_2HD ; no other experimental results for C_2HD and C_2D_2 have been used to determine parameters.

Numerical integration has been employed to calculate the mass spectrum of C_2H_2 , and parameters were adjusted until predicted and experimental quantities agreed to within about 1 per cent. The mass spectra of C_2HD and C_2D_2 were subsequently evaluated. Correction factors for the rates of reactions (2)–(7) are given in table 1, assuming that the correction factors for reactions (4) and (6) are equal to 3, and it was found that $\epsilon_m = 459$ kcal/mole. The correction factors are reasonable in view of the approximations in the treatment, but their values do not provide a reliable test of the theory. If ϵ_m is defined as an energy beyond which $W(\epsilon_\alpha)$ is small, rough limits to its magnitude may be found from figures given by Tate *et al.* [10] and by Stevenson and Schissler [3], which show that the calculated value may be about 50 kcal/mole too large. A discrepancy of this magnitude should introduce less error than does the simplified shape of the function $W(\epsilon_\alpha)$.

The calculated and experimental mass spectra of C_2DH and C_2H_2 are compared by considering first isotopic changes in the amounts of the fragment ions relative to one another, and then changes in the probability that dissociation of the molecular ion takes place. All mass spectra are therefore normalized to a total intensity of 100 for the C_2X^+ , C_2^+ , CX^+ and C^+ ions (X denotes H or D), and experimental mass spectra [7] are shown in table 2. The term 'relative amount' is used for the intensity of an ion normalized as above; the 'isotope

† As the distribution function $W(\epsilon)_\alpha$ has not yet been defined for $\epsilon_\alpha \leq \epsilon_2'$, it may be chosen to yield the correct amount of $C_2H_2^+$.

C_2H_2		C_2HD		C_2D_2	
$C_2H_2^+$	267	C_2HD^+	281	$C_2D_2^+$	292
C_2H^+	61.4	C_2H^+ C_2D^+	21.5 41.3	C_2D^+	58.1
C_2^+	18.7	C_2^+	16.9	C_2^+	16.0
CH^+	(11.3)	CH^+ CD^+	5.22 6.40	CD^+	(16.8)
C^+	8.60	C^+	8.67	C^+	9.16
H^+	20	H^+ D^+	— —	D^+	—
CH_2^+	0.91	CHD^+	0.79	CD_2^+	0.73
$C_2H_2^{++}$	(7.21)	C_2HD^{++}	7.58	$C_2D_2^{++}$	(7.88)

Table 2. Mass spectra of C_2H_2 , C_2HD and C_2D_2 [7], normalized to a total intensity of 100 for the C_2X^+ , C_2^+ , CX^+ and C^+ ions. The relative amount of H^+ formed from C_2H_2 is obtained from figure 1. Values in parentheses have been estimated by Mohler *et al.* [7] by assuming that the ratios (of amounts of ions) $C_2H_2^{++}/C_2H_2^+$, C_2HD^{++}/C_2HD^+ and $C_2D_2^{++}/C_2D_2^+$ are equal.

C_2HD			C_2D_2		
	Observed	Calculated		Observed	Calculated
$C_2H^+ + C_2D^+$ C_2D^+/C_2H^+	1.02 1.92	1.00 1.44	C_2D^+	0.95	1.00
C_2^+	0.90	0.95	C_2^+	0.86	0.91
$CH^+ + CD^+$ CD^+/CH^+	1.03 1.23	1.07 1.22†	CD^+	1.49	1.15
C^+	1.01	1.02	C^+	1.07	1.03
$H^+ + D^+$ H^+/D^+	— —	0.97 1.39	D^+	—	0.94

† This value has been treated as an empirical parameter (§ 4).

Table 3. Calculated and observed isotope effects for fragment ions in the mass spectra of C_2HD and C_2D_2 . All quantities except C_2D^+/C_2H^+ , CD^+/CH^+ and H^+/D^+ are isotope ratios. Ratios such as C_2D^+/C_2H^+ refer to amounts of the ions formed from C_2HD .

ratio' for an ion in the mass spectrum of C_2HD or C_2D_2 is defined as the ratio of the relative amount of the ion to the relative amount obtained from the mass spectrum of C_2H_2 by neglecting mass effects. Isotope ratios determined from the calculated mass spectra are compared in table 3 with experimental isotope ratios found from table 2, for all fragment ions of C_2HD and C_2D_2 except CHD^+ and CD_2^+ . (Comparison of the data in table 2 with earlier data [18] suggests that the uncertainty in the experimental isotope ratios is at least 2 per cent. The isotope ratios for CH^+ and CD^+ are less accurate since these have been determined by estimating the contributions of doubly charged ions.)

Interpretation of the above data is facilitated by the construction of a 'break-down curve' for C_2H_2 . The probability that reaction of a $C_2H_2^+$ ion with given excitation energy will yield a certain fragment ion may be determined by means of the theory in § 3, and is shown in figure 2. Since the distribution function $W(\epsilon_\alpha)$ has been taken as constant for $\epsilon_2' \leq \epsilon_\alpha \leq \epsilon_m$, figure 2 also gives the amounts of the ions formed at various excitation energies.

'Frequency factors' ν_r for the various reactions, defined as their (formal) rates at infinite excitation energy, may furthermore be readily obtained and

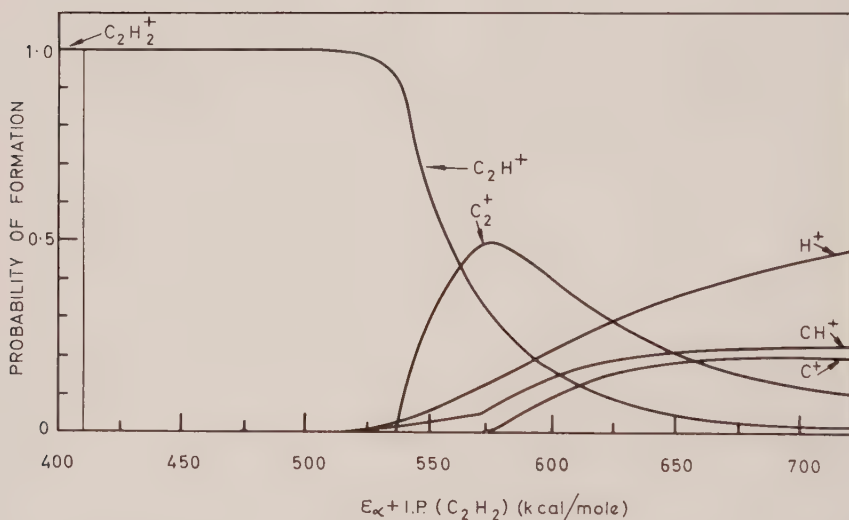


Figure 2. Probabilities for the formation of various ions from $C_2H_2^+$ ions with given excitation energy ϵ_α . The probabilities are shown as functions of the excitation energy ϵ_α plus the ionization potential of C_2H_2 , to facilitate comparison with figure 1.

are shown in table 1. Similar frequency factors occur in a drastically simplified version [1] of equation (1), i.e.

$$K_r = \nu_r \left(\frac{\epsilon - \epsilon_r}{\epsilon} \right)^{N-1}, \quad (5)$$

where N is equal to, or approximately equal to, the number of vibrations of the reactant.

5. GENERAL DISCUSSION

The qualitative agreement between the predicted and experimental isotope effects, as judged from the signs and orders of magnitude of the logarithms of the various ratios, is very satisfactory on the whole. This agreement strongly suggests that the general features of the fragmentation processes have been correctly described.

The isotope effects may be explained by means of the data in figure 2 and in table 1. According to figure 2, most C_2X^+ ions are formed at excitation energies where reaction (2) is the only important process, while other fragment ions mainly originate in another energy region. The total relative amount of the ions formed in each region should therefore remain approximately constant on isotopic substitution†. The results in table 1 show that reactions in which H or H^+ is lost are more rapid than corresponding reactions in which D or D^+ is lost, for two reasons: the frequency factor for H or H^+ loss is greater than that for D or D^+ loss, and the activation energy for the former is less than that for the latter as a result of zero point energy effects. Although the rates of reactions in which C-C bonds are broken are not affected much when D is substituted for H, such processes become relatively more important. Application of the preceding rules to C_2^+ shows for example that the relative amount of C_2^+ should decrease as the number of D atoms in the molecule is increased, since the ion is formed by two successive C-X bond breaking reactions. Other isotope effects may be similarly interpreted.

The discrepancy between the two results for $C_2H^+ + C_2D^+$ formed from C_2HD may be due to experimental error, but the isotope ratio for C_2D^+ in the mass spectrum of C_2D_2 is significantly less than unity, and the theory fails to predict this effect.

Although the CD^+/CH^+ ratio in the mass spectrum of C_2HD has been treated as an empirical parameter, it may readily be shown that this ratio should be greater than unity. Reaction (9) was neglected in the calculations, but it may be concluded that its rate is probably determined by migration of an H or D atom, since less CHD^+ and CD_2^+ than CH_2^+ is observed (table 2).

The calculated isotope ratios depend to some extent on estimates of various quantities, of which the excitation energy distribution of the molecular ion is the most important. The use of an exact energy distribution should not lead to any important qualitative changes in the results, but may have a marked effect on the values of the predicted ratios. In view of this, and possible experimental inaccuracy, the quantitative agreement between the two sets of results in table 3 is fair, and much better agreement could not be expected from the present treatment. Approximations other than that discussed above, e.g. the values assigned to activation energies and frequencies, the assumption that all activated complexes are linear and the assumption that all H^+ and D^+ is formed by reaction (4), should have a comparatively small effect on the agreement between theory and experiment. It was found by means of simple models of the reaction kinetics that omission of the reaction $C_2X^+ \rightarrow C_2 + X^+$ affects

† If the calculated relative amounts of H^+ and D^+ and the experimental relative amounts of CH_2^+ , CHD^+ and CD_2^+ are taken into account, it is clear that the sum of the relative amounts of all fragment ions remains approximately constant as the number of D atoms is increased.

only the results for H^+ and D^+ by more than a few per cent, even if the fraction of H^+ formed directly from $C_2H_2^+$ is taken as $\frac{1}{2}$ instead of 1.

On the basis of the results which have been obtained above the following may be concluded. The qualitative agreement between the predicted and experimental isotope effects for the fragment ions is a strong argument in favour of the postulated nature of the fragmentation processes. Quantitative agreement between the results for the fragment ions is sufficiently good to strengthen this argument. The results in particular support the view that fragment ions are formed by competitive unimolecular reactions, after the energy of the reactant has been randomized to a considerable extent. (For example, C_2H^+ and C_2D^+ are very clearly formed from C_2HD^+ by two *competitive* processes, since the relative amount of $C_2H^+ + C_2D^+$ is not affected much by deuterium substitution, even though the C_2D^+/C_2H^+ ratio for C_2HD^+ is considerably larger than unity.) Relative amounts of the fragment ions are apparently determined by the vibrational motion of decomposing ions on various potential energy surfaces, rather than by the rates of transitions between electronic states. Detailed features of the rate theory are not verified by the comparison in table 3. For example, it is difficult to estimate the precise extent to which electronic energy is distributed in ions, and it cannot be concluded that dissociation usually takes place on the lowest potential surface of an ion.

The preceding discussion has dealt with the amounts of the fragment ions relative to one another, and isotopic changes in the amount of fragmentation of the molecular ion are now considered.

The ratio F of the amount of the fragment ions to that of the molecular ion is given, according to the present treatment, by the probability that the excitation energy ϵ_e exceeds the activation energy ϵ_2 for reaction (2). Values of F calculated for C_2H_2 , C_2HD and C_2D_2 consequently do not differ by more than 0.6 per cent. This result is in disagreement with the data in table 2, and experimental values† of F for C_2HD and C_2D_2 are respectively equal to 0.95 and 0.91 of the value for C_2H_2 . A possible explanation for the decrease in F on deuterium substitution is the following. An ion in an attractive electronic state will require a certain minimum vibrational energy before a radiationless transition (or dissociation on the same potential surface) can take place. Some molecular ions for which $\epsilon_\alpha \geq \epsilon_2$ will thus not dissociate, and analogous results for diatomic molecules [11], make it plausible that fewer C_2HD^+ and $C_2D_2^+$ than $C_2H_2^+$ ions in excited electronic states will have sufficient vibrational energy to react. If deuteration decreases the amount of fragmentation for excited electronic states spread over the whole energy range $\epsilon_2 \leq \epsilon_\alpha \leq \epsilon_m$, the relative amounts of the fragment ions should be affected less strongly than is their absolute amount.

There are also other indications that electronic excitation energy of ions is not completely randomly distributed. The metastable peak corresponding to the reaction $C_2H^+ \rightarrow C_2^+ + H$, observed by Melton *et al.* [8], indicates that some C_2H^+ ions dissociate about 10^{-8} sec after the molecular ion is formed. Estimates based on the data in this paper show that the metastable peak is incompatible with rapid distribution of electronic energy, as we also concluded by Melton *et al.* [8]. Some $C_2H_2^+$ and C_2H^+ ions therefore probably dissociate via a relatively slow electronic transition, although the number of such ions

† These values are determined by ignoring H^+ and D^+ ions, but the calculated intensities of H^+ and D^+ show that the approximation should not affect the discussion.

may be small. The large excess energy of 72 kcal/mole required for the formation of H^+ (Appendix 5) may also be due to incomplete distribution of excitation energy. It is possible that no transitions take place from electronic states in which C_2H_2^+ is formed to the lowest potential surface on which H^+ may be produced.

Monahan and Stanton [9] have investigated the dependence of the mass spectrum of C_2H_2 on the energy of the ionizing electrons at high ionizing potentials. The results show that C_2H_2^+ , C_2H^+ , C_2^+ and $\text{CH}^+ + \text{C}^+$ ions are produced by different excitation processes, and Monahan and Stanton [9] concluded that excitation energy is therefore not randomly distributed in the molecular ion. According to figure 2, C_2H_2^+ , C_2H^+ , C_2^+ and $\text{CH}^+ + \text{C}^+$ ions however originate essentially in different excitation energy regions, and the above conclusion is therefore not justified.

6. CONCLUSION

Isotope effects yield valuable information about the decomposition of acetylene by electron impact. The present study of such effects has shown that the quasi-equilibrium theory of mass spectra provides a satisfactory description of the main processes which determine the decomposition pattern. Most molecular ions appear to dissociate by competing reactions, which are in many respects similar to thermal unimolecular reactions, after sufficient time has elapsed for the distribution of excitation energy between some vibronic degrees of freedom. However, it is probable that excitation energy of ions is not completely randomly distributed. This conclusion is not entirely unexpected since, as has been discussed in the introduction, the number of intersecting potential surfaces for a small ion may not be sufficient to ensure complete energy distribution.

The results which have been obtained suggest that the decomposition of small polyatomic molecules by irradiation may well be understood, ultimately, in terms of mechanisms which are similar to those postulated in the quasi-equilibrium theory. Further investigations along the lines of the present treatment, in which incomplete distribution of electronic energy is taken into account, should therefore be worth while. Such investigations would be greatly facilitated by extensive experimental data on the mass spectra of a few small polyatomic molecules, and data on H-D isotope effects at various ionizing voltages would be especially useful.

I wish to thank Professor H. C. Longuet-Higgins, F.R.S., and Professor C. A. McDowell for helpful discussions, and the Director of the South African Atomic Energy Board for permission to publish this paper.

APPENDIX 1

Heats of formation

The heats of reaction in figure 1 are determined from the heats of formation at 0°K given in table 4. All ΔH_f^0 values except those for C_2H^+ and C_2^+ are readily obtained from results in the references which have been quoted, and are not based on electron impact data. The preferred heats of formation of

C_2H^+ and C_2^+ are found from the appearance potentials of these ions in the mass spectrum of C_2H_2 [12], by assuming that no energy in excess of the heat of reaction is required for the processes $C_2H_2 + e \rightarrow C_2H^+ + H + 2e$ and $C_2H_2 + e \rightarrow C_2^+ + 2H + 2e$. The heats of formation of C_2H^+ which are obtained from the appearance potentials of the reactions $CH_3 - C_2H + e \rightarrow CH_3 + C_2H^+ + 2e$ [23] and $C_2H_4 + e \rightarrow C_2H^+ + H_2 + H + 2e$ [24] however agree within 10 kcal/mole with the value in table 4. It is also found from the ionization potential [11] of C_2 that $\Delta H_f^0 = 460 \pm 28$ kcal/mole for C_2^+ .

	Molecule/Radical		Positive ion	
	ΔH_f^0 (kcal/mole)	Reference	ΔH_f^0 (kcal/mole)	Reference
C_2H_2	54.3	[19]	317.4	[11]
C_2H	117	[20]	413	[12]
C_2	195	[21]	488	[12]
CH	141	[20]	398	[11]
C	169.6	[22]	429.3	[11]
H	51.6	[19]	365.1	[19]

Table 4. Heats of formation at 0°K.

APPENDIX 2

Densities of vibrational energy levels

Densities of vibrational energy levels and related quantities required in §3 are obtained as follows. For the present purpose, the density of energy levels for n harmonic oscillators is accurately given by [25, 26] :

$$\rho(\epsilon) = \frac{(\epsilon + \epsilon_z)^{n-1}}{(n-1)! \prod_i (h\nu_i)} \left[1 - A \left(\frac{\epsilon_z}{\epsilon + \epsilon_z} \right)^2 + B \left(\frac{\epsilon_z}{\epsilon + \epsilon_z} \right)^4 \right], \quad \epsilon \geq 0, \quad (A1)$$

where ϵ is the total energy in excess of the zero point energy ϵ_z , ν_i is the frequency of the i th vibration,

$$A = (n-1)(n-2)\alpha_2/6n, \quad B = (n-1)(n-2)(n-3)(n-4)\gamma_4/n^2, \quad \alpha_m = \overline{\nu_i^m}/(\overline{\nu_i})^m$$

and

$$\gamma_4 = (5\alpha_2^2 + 2\alpha_4/n)/360.$$

The number of states with energy less than ϵ is :

$$I(\epsilon) = \frac{(\epsilon + \epsilon_z)^n}{n! \prod_i (h\nu_i)} \left[1 - A' \left(\frac{\epsilon_z}{\epsilon + \epsilon_z} \right)^2 + B' \left(\frac{\epsilon_z}{\epsilon + \epsilon_z} \right)^4 \right], \quad \epsilon \geq 0 \quad (A2)$$

where $A' = (n-1)\alpha_2/6$ and $B' = (n-1)(n-2)(n-3)\gamma_4/n$. Equations (A1) and (A2) are used to obtain ρ and I for C_2H^+ and C_2D^+ , and to evaluate the rates of reactions (5)–(7).

The vibrational states of a linear four-atomic molecule (or activated complex) may be classified according to J_z , the angular momentum component along the internuclear axis, by means of the discussion given by Herzberg [28].

The following partition function may be obtained for energy levels of the bending vibrations for which $J_z = 0$:

$$Z = \frac{[1 + \exp\{-h(\nu_1^b + \nu_2^b)/kT\}]}{[1 - \exp\{-2h\nu_1^b/kT\}][1 - \exp\{-h(\nu_1^b + \nu_2^b)/kT\}][1 - \exp\{-2h\nu_2^b/kT\}]}, \quad (\text{A } 3)$$

where the temperature is equal to T , the frequencies of the four bending vibrations are given by ν_1^b , ν_1^b , ν_2^b and ν_2^b , and energy is measured from the zero-point energy of the vibrations. Examination of equation (A 3) shows that the density of vibrational energy levels with $J_z = 0$, for a four-atomic linear molecule or activated complex, is given by :

$$[\rho(\epsilon)]_{J_z=0} = \rho'(\epsilon) + \rho'(\epsilon - h(\nu_1^b + \nu_2^b)). \quad (\text{A } 4)$$

$\rho'(\epsilon)$ is the density of energy levels for a system of harmonic oscillators with frequencies given by $2\nu_1^b$, $\nu_1^b + \nu_2^b$, $2\nu_2^b$ and the stretching frequencies of the linear molecule or activated complex. The condition $J_z = 0$ therefore effectively reduces the number of vibrations by one. Equation (A 4) and a similar expression for the integral of $[\rho(\epsilon)]_{J_z=0}$ may be used to evaluate the rates of reactions (2)–(4).

APPENDIX 3

Partition of excess energy

Equation (3) is derived as follows. The four vibrations of C_2H^+ are denoted by V and two translational and/or rotational degrees of freedom by T. Assume that the energy of the combined system V + T lies between ϵ_{VT} and $\epsilon_{VT} + d\epsilon_{VT}$, and assign the same weight to each energy level of V + T in this range. The probability that the energy of V lies between ϵ_V and $\epsilon_V + d\epsilon_V$ is then proportional to the number of energy levels of V + T which satisfy the above two energy conditions. This number is given by $\rho(\epsilon_V)d\epsilon_V\rho_T(\epsilon_{VT} - \epsilon_V)d\epsilon_{VT}$, where ρ and ρ_T are the densities of energy levels for V and T respectively. It may be shown by methods which have been discussed elsewhere [26] that ρ_T is constant in the classical mechanical approximation, which is adequate for the purpose of this discussion. When an energy ϵ_{VT} is distributed randomly between V and T, the probability that the energy of V lies between ϵ_V and $\epsilon_V + d\epsilon_V$ is therefore proportional to $\rho(\epsilon_V)d\epsilon_V$, and equation (3) is obtained.

APPENDIX 4

Vibrational frequencies

The assignment of vibrational frequencies to the various ions and to the activated complexes for reactions (2)–(7) is necessarily very approximate. However, for the present purpose percentage changes in frequencies on isotopic substitution are more important than their absolute magnitudes. Reasonable estimates of such changes can be obtained.

The bending frequencies of a given activated complex are taken as those of the reactant and the stretching frequencies as those of the products. Frequencies are assigned to molecules and radicals as shown in table 5, and it is assumed that the frequencies of an ion are equal to those of the corresponding neutral

species. The data for C_2XY are taken from the literature [27] while those for C_2X and C_2X^+ have been obtained from estimated force constants and bond lengths.

Species	Stretching	Bending
C_2H_2 , $C_2H_2^+$	3374, 3287, 1974	729(2), 612(2)
C_2HD , C_2HD^+	3335, 2584, 1851	683(2), 519(2)
C_2D_2 , $C_2D_2^+$	2701, 2427, 1762	539(2), 505(2)
C_2H , C_2H^+	3333, 1639	678(2)
C_2D , C_2D^+	2502, 1575	540(2)
CH , CH^+	2800	
CD , CD^+	2056	
C_2^+	1600	

Table 5. Assignment of frequencies (cm^{-1}).

APPENDIX 5

Activation energies

The activation energies in table 1 are estimated by means of the following considerations.

There is no evidence from the data in figure 1 and in Appendix 1 that 'excess' energy, i.e. excitation energy in excess of the heat of reaction, is required for reactions (2) and (5)–(7). According to figure 1 the excess energy for reaction (3) is 27 kcal/mole, but reaction (2) strongly affects the rate of reaction (3) at excitation energies near the activation energy for the latter, as may be seen from figure 2. The activation energies for reactions (2), (3) and (5)–(7) are therefore directly determined from the heats of reaction in figure 1. An excess energy of 72 kcal/mole is required for decomposition of C_2H_2 by reaction (4), and the activation energy is estimated from figure 1 as $(500-263)$ kcal/mole = 237 kcal/mole. (This value has not been corrected for the possible effect of reaction (2), since the appearance potential for H^+ obtained by Tate *et al.* [10] is about 25 kcal/mole less than the 'apparent' value found from a figure in the paper.) A possible explanation for the large excess energy above is given in § 5.

Isotopic changes in activation energies are determined from the equation :

$$(\epsilon_r)_a - (\epsilon_r)_b = \{(\epsilon_z^\ddagger)_a - (\epsilon_z^\ddagger)_b\} - \{(\epsilon_z)_a - (\epsilon_z)_b\}, \quad (A5)$$

where ϵ_r is the activation energy for a reaction and ϵ_z^\ddagger and ϵ_z are the zero point energies of the activated complex and the reactant, respectively. Isotopic species are denoted by a and b. (Strictly speaking, it is not assumed that no excess energy is required for decomposition of C_2H_2 by reactions (2), (3) and (5)–(7), but that only a small amount is required. Isotopic changes in activation energies are therefore not determined from corresponding changes in heats of reaction.)

REFERENCES

- [1] ROSENSTOCK, H. M., WALLENSTEIN, M. B., WAHRHAFTIG, A. L., and EYRING, H., 1952, *Proc. nat. Acad. Sci., Wash.*, **38**, 667.
- [2] ROSENSTOCK, H. M., and KRAUSS, M., 1963, *Mass Spectrometry of Organic Ions*, edited by F. W. McLafferty (London: Academic Press), p. 1.
- [3] STEVENSON, D. P., and SCHISSLER, D. O., 1961, *The Chemical and Biological Action of Radiations*, Vol. 5, edited by M. Haissinsky (London: Academic Press), p. 167.
- [4] FRIEDMAN, L., LONG, F. A., and WOLFSBERG, M., 1957, *J. chem. Phys.*, **27**, 613.
- [5] SCHAEFFER, O. A., 1950, *J. chem. Phys.*, **18**, 1501.
- [6] SCHAEFFER, O. A., 1955, *J. chem. Phys.*, **23**, 1309.
- [7] MOHLER, F. L., DIBELER, V. H., WILLIAMSON, L., and DEAN, H. M., 1952, *J. Res. nat. Bur. Stand.*, **48**, 188.
- [8] MELTON, C. E., BRETSCHER, M. M., and BALDOCK, R., 1957, *J. chem. Phys.*, **26**, 1302.
- [9] MONAHAN, J. E., and STANTON, H. E., 1962, *J. chem. Phys.*, **37**, 2654.
- [10] TATE, J. T., SMITH, P. T., and VAUGHAN, A. L., 1935, *Phys. Rev.*, **48**, 525.
- [11] FIELD, F. H., and FRANKLIN, J. L., 1957, *Electron Impact Phenomena and the Properties of Gaseous Ions* (New York: Academic Press).
- [12] COATS, F. H., and ANDERSON, R. C., 1955, *J. Amer. chem. Soc.*, **77**, 895.
- [13] VESTAL, M., WAHRHAFTIG, A. L., and JOHNSTON, W. H., 1962, *J. chem. Phys.*, **37**, 1276.
- [14] WILKINSON, P. G., 1961, *J. mol. Spectrosc.*, **6**, 1.
- [15] WALSH, A. D., 1952, *J. chem. Soc.*, p. 2288.
- [16] MORRISON, J. D., 1954, *J. chem. Phys.*, **22**, 1219.
- [17] COLLIN, J. E., 1962, *Bull. Soc. chim. Belg.*, **71**, 15.
- [18] MOHLER, F. L., and DIBELER, V. H., 1947, *Phys. Rev.*, **72**, 158.
- [19] ROSSINI, F. D., WAGMAN, D. D., EVANS, W. H., LEVINE, S., and JAFFE, I., 1952, *Selected Values of Chemical Thermodynamic Properties*, Nat. Bureau of Standards, Circular 500.
- [20] KNOX, B. E., and PALMER, H. B., 1961, *Chem. Rev.*, **61**, 247.
- [21] BREWER, L., HICKS, W. T., and KRIKORIAN, O. H., 1962, *J. chem. Phys.*, **36**, 182.
- [22] LEWIS, G. N., and RANDALL, M., 1961, *Thermodynamics*, 2nd edn. (New York: McGraw-Hill Book Co.), p. 680.
- [23] COATS, F. H., and ANDERSON, R. C., 1957, *J. Amer. chem. Soc.*, **79**, 1340.
- [24] KUSCH, P., HUSTRULID, A., and TATE, J. T., 1937, *Phys. Rev.*, **52**, 843.
- [25] HAARHOFF, P. C., 1963, *Mol. Phys.*, **6**, 337.
- [26] HAARHOFF, P. C., 1963-64, *Mol. Phys.*, **7**, 101.
- [27] HERZBERG, G., 1945, *Infrared and Raman Spectra of Polyatomic Molecules* (New York: D. van Nostrand Co.).
- [28] REFERENCE [27], p. 81.

Mean lifetimes of active molecules and oscillator models of unimolecular reactions

by E. E. NIKITIN

Institute of Chemical Physics, Academy of Sciences, Moscow, USSR

(Received 11 October 1963)

The Kassel and Slater approaches to oscillator models of unimolecular reactions are discussed. The Slater quantum theory is shown to overestimate the contribution of tunnelling to the reaction rate. An alternative approach is suggested, based on consideration of the beating in a system of quantum oscillators.

There are at present two basic approaches to calculation of rate constants for thermal unimolecular reactions. The first is based on statistical considerations about intramolecular energy exchange. The corresponding theory—the so-called quasi-equilibrium theory of unimolecular reactions—considers that non-linear coupling (e.g. anharmonicity) in vibrationally excited molecules is sufficient to ensure equipartition of internal energy among various modes during the characteristic reaction time [1]. On the other hand, this coupling should be weak enough, in order that its effect on the dynamic behaviour of the molecule for small periods of time and on the density of vibrational states may be neglected. The other theory, developed mainly by Slater [2], involves a model of strictly harmonic vibrations, and connects the occurrence of reaction with some critical value q_0 of the internal coordinate q (the so-called critical configuration). The latter condition may, evidently, be formulated also within the principal concepts of the quasi-equilibrium theory. Due to the energy condition the attainment of the q_0 value is relatively rare, so that the frequency of transition of the critical configuration should be calculated allowing for the behaviour of $q(t)$ over long periods of time. This is the actual reason for very low anharmonicity leading to a principally new effect of equipartition, as compared to the harmonic approximation. Although qualitative and quantitative estimations of the effect of anharmonicity show [3, 4] that a strictly harmonic model can hardly be considered as reliable, it represents a very important limiting case of non-interacting normal modes. It seems to be of interest in this connection to calculate the mean lifetime $\tau(E)$ of an active molecule (capable of spontaneous transformation) on the basis of oscillator models of unimolecular reactions. A quantity such as $\tau(E)$ would be of prime interest for the theory of mass-spectra, for instance.

Rate constants of thermal unimolecular reactions for the limiting cases of high and low pressures may be conceived as [5]:

$$k_{\infty} = \int_{E_0}^{\infty} \frac{\sigma^*}{F} \exp(-\beta E) dE, \quad (1)$$

$$k_0 = Z_0 \int_{E_0}^{\infty} \tau(E) \frac{\sigma^*}{F} \exp(-\beta E) dE. \quad (2)$$

These equations suggest that classical mechanics may be used for describing intramolecular energy transfer, and that all vibrational quanta $\hbar\omega_i$ are small compared to kT . Here $\beta = 1/kT$, Z_0 is the collision number for deactivation, F is the vibrational partition function of the molecule, $\sigma^* = \int d\sigma^*$, $d\sigma^*$ being an element of hypersurface projected on the plane normal to the reaction coordinate q . For high pressures, when intramolecular energy exchange is not essential compared to the intermolecular one, both theories—the statistical and Slater's—are known to give identical results for k :

$$k_\infty = \tilde{\nu} \exp(-\beta E_0), \quad (3)$$

where the frequency factor is:

$$\tilde{\nu}^2 = \sum \mu_i^2 \nu_i^2, \quad (4)$$

μ_i are normalized amplitude factors and ν_i molecular frequencies. Taking into account that in the classical region $F \sim \beta^s$ and applying the inverse Laplace transformation to (1), we find:

$$\frac{\sigma^*}{F} = \frac{(E - E_0)^{s-1}}{(s-1)!} \beta^s. \quad (5)$$

To calculate $\tau(E)$ by inversion of (2) we may use the known expressions for $k_0(T)$ from both theories. (In what follows the subscripts 1 and 2 denote the statistical and the Slater theories, respectively.) Thus we obtain:

$$\tau_1 = \tilde{\nu}^{-1} \left(\frac{E_0}{E - E_0} \right)^{s-1}; \quad E - E_0 \gg \hbar\omega_{\max}s, \quad (6)$$

$$E - E_0 \ll E_0,$$

$$\mu_i^2 \gg \left(\frac{4\pi E_0}{E - E_0} \right)^{-1},$$

$$\tau_2 = \tilde{\nu}^{-1} \left(\frac{4\pi E_0}{E - E_0} \right)^{(s-1)/2} \frac{(s-1)!}{((s-1)/2)!}. \quad (7)$$

At the right side of (6) and (7) are the conditions under which the expressions for τ are valid. These indicate that the energy should be rather high above the threshold, and the coupling of the reaction coordinate to normal vibrations should be efficient. When the harmonic coupling is weak and

$$\mu_i^2 < (E - E_0)/4\pi E_0,$$

corresponding coefficients μ_i should be omitted from (7) and the number of oscillators s be decreased.

Knowledge of rate constants of thermal reactions for the quantum case is necessary for attempting to follow this procedure in deriving the mean lifetime near the threshold. Then, one of the basic questions would be whether it is still possible to use the energy E_0 as threshold for the lower limits in (1) and (2). E_0 is a well-defined value of the ordinary statistical theory, as all types of tunnel transition are neglected. Let us consider a system of s weakly coupled oscillators with nearly equal frequencies, the essential spectrum width $\Delta\nu$ being small compared to the mean frequency ν_0 . (It does not mean, of course, that the normal modes are localized.) The high pressure limit k_∞ for this model, calculated from the quasi-equilibrium theory, coincides with (3), the frequency factor being equal to ν_0 with an error of the order of $\Delta\nu$. For the quantum case integrals in (1) and (2) are in fact sums, and on condition that $\beta\hbar\omega_i \gg 1$ and $\beta\hbar\Delta\omega \ll 1$ only the first

term of the series is essential. Thus, from (1) and (2) we obtain $\sigma^*/F = \nu_0$ and

$$\tau_1 = \nu_0^{-1} \left(\frac{E_0}{\hbar\omega_0} \right)^{s-1} / (s-1)! \quad (8)$$

This is valid near the threshold, when

$$E - E_0 < \hbar\omega_0, \quad \frac{E_0}{\hbar\omega_0} \gg s.$$

To calculate $\tau_2(E)$ for the harmonic model, one should first note that the occurrence of reaction with q attaining the critical q_0 value is not unambiguous for the quantum case. This is because the Hamiltonian and the q operator do not commute, so that q_0 does not define the threshold energy E_0 . This could be overcome by assuming, for instance, that tunnelling from levels E below a certain value E_0 does not contribute to the reaction rate. This was, in fact, assumed in deriving (8). On the other hand, one could assume that the condition $q = q_0$ is valid whatever the energy, thus taking into account the contribution due to tunnelling. Slater actually adopted the latter suggestion, though he recognized the rather vague physical sense of this assumption (see, for example, the last chapter of his book [2]).

The Slater expression for k_∞ is:

$$k_\infty = \nu_0 \exp[-q_0^2/2\sigma^2], \quad \sigma^2 = \frac{1}{2\beta} \sum \alpha_i^2 \frac{\theta_i}{2} \coth \frac{\theta_i}{2} \approx \frac{1}{2\beta} \frac{\theta_0}{2} \coth \frac{\theta_0}{2}. \quad (9)$$

When $\theta_0 = \hbar\omega_0\beta \lesssim 1$, (9) exhibits an essentially non-Arrhenius temperature dependence. Now let us consider the model for which (9) is in a sense exact. When a reaction involves the transition of a molecule from one potential well to another which is the mirror image of the first, the reaction may be thought to proceed at low temperatures via tunnelling through the potential hump dividing these wells (the most simple example would be the inversion of NH_3). The specific rate $K(E)$ of tunnelling may be related then to the shift of frequency $\delta\nu$ caused by under-barrier transition†. On the other hand, in calculating the level shift $\delta E = \hbar\delta\nu$ we may follow the method described for the one-dimensional case in the book of reference [6]. The splitting, twice as high as the shift δE , is related to the derivative of the vibrational wave function by the equation:

$$2\delta E = 2\hbar\delta\nu = \frac{2\hbar^2}{M} \int \psi_E^* \frac{\partial}{\partial q} \psi_E d\tau \sim 2\hbar\nu_0 \int |\Psi_E(q=q_0)|^2 d\tau, \quad (10)$$

where integration is carried out over all normal coordinates on condition that $q = q_0$. It may be seen from (10) that the rate of tunnelling can be defined in terms of attaining the critical configuration $q = q_0$. This formulation is very near to Slater's approach, so that the averaging of (10) over all harmonic levels would be expected to yield equation (9). It will be noted that (10) is valid only far below the threshold E_0 , so that, strictly speaking, (9) is a sort of interpolation formula valid for the limiting cases $\theta \gg 1$ and $\theta \ll 1$.

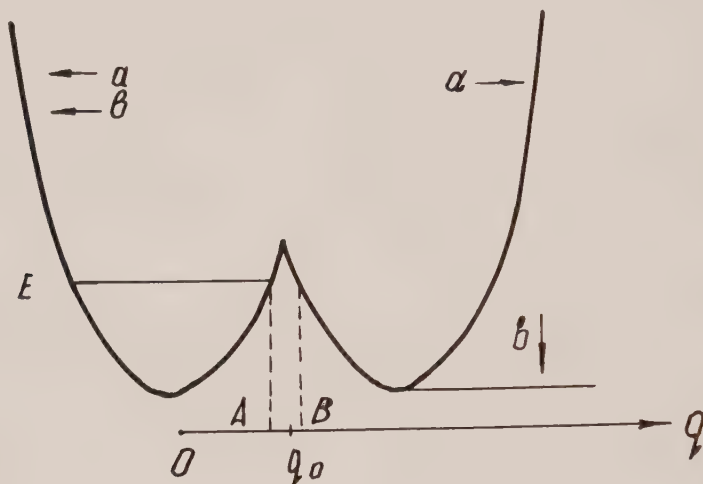
A model potential of this type is shown in the figure (curve 'a'). It will be seen that the critical value q_0 corresponds to half-way between the minima, but the calculated rate constant for the model should be somewhat lower than that for a more real potential without a cusp.

† Of course, some sort of relaxation mechanism should be operating to ensure the irreversible behaviour of the system. Derivation of the corresponding relaxation equation is a difficult task and we shall not consider it here. We shall assume the usual approximation for the high-pressure rate of tunnelling (cf., for example, [7]).

It has been shown by Slater [2] that equation (9), when fitted to the Arrhenius formula with an activation energy

$$E_{\text{act}} = kT^2 \frac{d \ln k_{\infty}}{dT},$$

exhibits an abnormally low frequency factor. This conclusion seems to be of interest, as some cases of isomerization involve low frequency factors that are believed to be due to a non-adiabatic process [8].



It will be noted that the identity of the wells or exact resonance between two levels of zero order are very essential. Let us consider for a moment a one-dimensional oscillator with a potential corresponding to curve 'b'.

The exponential factor of the transmission coefficient $\chi(E)$ may be estimated using the WKB method:

$$\chi(E) \sim \exp \left(-2 \int_A^B |\bar{p}/\hbar| dx \right) \sim |\Psi(q=q_0)|^4. \quad (11)$$

It follows that the rate constant $K(E) = \nu_0 \chi(E)$ cannot be formulated in terms of the probability of attaining the critical q_0 value.

The tunnelling correction near the cusp for high temperatures may be found for the Slater formula from (9) by expanding σ^2 in terms of θ . Thus, we obtain:

$$k_{\infty} \sim \exp(-\beta E_0) \exp(\beta E_0 \theta^2/12). \quad (12)$$

On the other hand, the exact transmission coefficient value for curve 'b' may be calculated by approximating wave functions near the cusp, using Airy functions [9]. Averaging over all energy states gives then the expression:

$$k_{\infty} \sim \exp(-\beta E_0) \exp[(\beta \epsilon)^3/12], \quad (13)$$

where $\epsilon = (\hbar F_1 F_2 / \Delta F \sqrt{(2M)})^{2/3}$, F_1 and F_2 are forces at $q = q_0$, $\Delta F = |F_1 - F_2|$, and M is the effective mass. Introducing into (13) the parameters appropriate to potential 'b' (figure), we obtain:

$$k_{\infty} \sim \exp(-\beta E_0) \exp(\beta E_0 \theta^2/48). \quad (14)$$

Thus, as would be anticipated, Slater's expression (12) gives excess contribution to tunnelling for a potential of type 'b'.

Consequently, it will be expected that for the decomposition of molecules it would be more appropriate to accept complete absence of tunnelling rather than overestimate it in accordance with Slater's formula. Then, the mean lifetime near the threshold will be calculated considering the energy flow between the oscillators, on condition that the total energy be approximately equal to E_0 . To do this for our model of weakly (harmonically) coupled oscillators we should first construct a wave packet localized at $t=0$ on the oscillator with coordinate q and approximating the n th wave function of this oscillator supposed to be isolated (evidently $n = E_0/\hbar\omega_0$). The probability amplitude A_n of this state will change with time due to harmonic coupling of oscillators (this coupling, in fact, results in delocalization of normal modes in molecules). It may be shown [10] that $A(t)$ is:

$$A_n(t) = \left[\sum_k \mu_k^2 \exp(i\Delta\omega_k t) \right]^n, \quad (15)$$

where $\Delta\omega_k$ is the difference in the frequency of an isolated q -oscillator and the frequency of the k th normal mode. Evidently, the average probability $\langle |A_n|^2 \rangle$ over a long period of time is inversely proportional to the mean lifetime, so that we may put:

$$\langle |A_n|^2 \rangle = [\nu\tau_2(E_0)]^{-1}. \quad (16)$$

Calculation of $\langle |A_n|^2 \rangle$, on condition that $n \gg 1$ and $\mu_i^2 \gg n^{-1}$, may be carried out using the method of steepest descent, which gives for non-degenerate cases:

$$\tau_2(E_0) = \nu_0^{-1} \left(\frac{4\pi E_0}{\hbar\omega_0} \right)^{(s-1)/2} \mu_1 \dots \mu_s. \quad (17)$$

The statistical theory and Slater's theory give the upper and lower limits for the mean lifetimes of the system of weakly coupled oscillators.

Thus, the true value of τ for such a model should be somewhere between (6) and (7) for energies far above the threshold, and between (8) and (17) for energy at the threshold. The separation between these limits cannot be narrowed without thorough examination of the dynamical effect of anharmonicity.

From (17) we derive the expression for the rate constant k_0 :

$$k_0 = Z_0 \left(\frac{4\pi E_0}{\hbar\omega_0} \right)^{(s-1)/2} \mu_1 \dots \mu_s \exp(-\beta E_0). \quad (18)$$

It will be remembered that a harmonic system cannot completely 'forget' its initial state. This problem of correlating the lifetime and the condition of 'preparation' of the vibrationally excited system is very important for the theory of mass-spectra [11]. Let us consider, for instance, an initial state approximating the n th vibrational function on the oscillator with coordinate q' . Then the probability amplitude for finding the q -oscillator on the n th level would be:

$$A_n(t) = [\sum_k \mu_k \mu_k' \exp(i\Delta\omega_k t)]^n, \quad (19)$$

where μ_k and μ_k' are normalized amplitude factors connecting q and q' -oscillators with the k th normal mode. The mean lifetime will then be:

$$\tau_2' = \nu_0^{-1} \left(\sum_k |\mu_k \mu_k'| \right)^{-n} |\mu_1 \mu_1'|^{1/2} \dots |\mu_s \mu_s'|^{1/2} \left(\frac{4\pi E_0}{\hbar\omega_0} \right)^{(s-1)/2}, \quad (20)$$

which is much larger, in general, than τ_2 , because of the inequality $\sum_k |\mu_k \mu_k'| < 1$.

It should be noted in conclusion that elimination of the contribution of the zero-point vibration to dispersion σ^2 of coordinate q , which is a necessary procedure to bridge the experimental results and the Slater quantum model [12], is, in fact, the elimination of an excess tunnelling contribution to the reaction rate.

The author is greatly indebted to Professor N. D. Sokolov for helpful discussions.

REFERENCES

- [1] KONDRATIEV, V. N., 1964, *Chemical Kinetics of Gas Reactions* (Pergamon Press) (to be published).
- [2] SLATER, N. B., 1959, *Theory of Unimolecular Reactions* (Cornell University Press).
- [3] NIKITIN, E. E., 1959, *C. R. Acad. Sci. U.R.S.S.*, **129**, 1957.
- [4] SLATER, N. B., 1962, *The Transition State*, Chemical Society, Special Publication No. 16.
- [5] THIELE, E., 1962, *J. chem. Phys.*, **36**, 1466.
- [6] LANDAU, L., and LIFSHITZ, E., 1958, *Quantum Mechanics* (Pergamon Press).
- [7] MAGEE, J. H., SHAND, W., and EYRING, H., 1941, *J. Amer. chem. Soc.*, **63**, 677.
- [8] GLASSSTONE, S., LAIDLER, K. J., and EYRING, H., 1941, *The Theory of Rate Processes* (Princeton University).
- [9] NIKITIN, E. E., 1964, *Mol. Phys.* (to be published).
- [10] NIKITIN, E. E., 1963, *C. R. Acad. Sci. U.R.S.S.*, **152**, 1395.
- [11] ROSENSTOCK, H. M., and KRAUSS, M., 1963, *Advanc. Mass-Spectromet.*, **2**, 251.
- [12] SLATER, N. B., 1961, *J. chem. Soc.*, p. 606.

The line shapes of the E.S.R. spectrum of a system of interacting triplets

by RUTH M. LYNDEN-BELL

University Chemical Laboratory, Lensfield Road,
Cambridge

(Received 5 December 1963)

The system considered is one in which the spectral lines are broadened by collisions between triplets. During a collision a pair of triplets interacts with the coupling $J\mathbf{S}_1 \cdot \mathbf{S}_2$. It is found that the lines of the zero field spectrum are shifted and broadened; the direction of the shift depends on the magnitude of the coupling J , and on the life-time of the collision. Similar results are predicted for the high field spectrum, although in this case eventually the two lines collapse into a single exchange narrowed line.

1. INTRODUCTION

Triplet exciton spectra have been observed in charge transfer salts [1] and in the crystals of Wurster's Blue Perchlorate at low temperatures [2]. In these crystals the ground state of each site is a singlet, but a low-lying triplet state is thermally accessible. The corresponding crystal states are, to a first approximation, triplet exciton states on a one-dimensional lattice [3, 4]. These can be observed by E.S.R. at low temperatures when the number of excitons is small. As the number increases the line shapes are affected by coupling between the excitons. Jones and Chesnut [5] have observed in detail the line broadening of the high field spectrum of some TCNQ salts, leading to a single exchange narrowed line at high temperatures†. They showed that the usual line broadening theory (valid for spin $\frac{1}{2}$ species) is inconsistent with the observations.

In this paper the line shapes of a model system appropriate to diffusional excitons are discussed. In a static lattice the stationary exciton states would be wave-like, and each exciton would interact with every other one. In a real system an exciton has only a finite life-time, and interacts with the phonons [9]. As a result the wave-like stationary states may never be achieved; each excitation is localized and diffused through the lattice. In this model each triplet state is assumed to be isolated for most of the time, but occasionally 'collides' with another randomly chosen triplet. During the collision the spins of the two triplets are coupled with an interaction energy $J\mathbf{S}_1 \cdot \mathbf{S}_2$. The concentration of triplets is assumed to be small enough that collisions of three triplets are very unlikely; the duration of a collision is much shorter than the time between collisions made by any one triplet.

It should be noticed that this model is not confined to a one-dimensional system of diffusional excitons, but is also appropriate for a three-dimensional crystal system. A similar analysis could be applied to the line broadening observed in solutions of free radicals as the temperature is raised [6].

† In Wurster's Blue Perchlorate the situation is complicated by a phase transition at high temperatures.

2. GENERAL METHOD

At any moment the system contains isolated triplets and colliding pairs or dimers. These will be considered as two different species which exchange with each other in a similar way to chemical exchange in N.M.R. The density matrix methods used for the latter problems are suitable here [7]. For a general discussion of the density matrix the reader is referred to books by Slichter and Abragam [8].

The isolated triplets are described by the 3×3 density matrix ρ which in the absence of 'exchange' with the dimer species would have the equation of motion:

$$i\dot{\rho} = [\mathcal{H}_T, \rho] - i\Gamma_T(\rho - \rho_0), \quad (1)$$

where \mathcal{H}_T is the spin Hamiltonian of the isolated triplet and $\Gamma_T(\rho - \rho_0)$ is a matrix representing the thermal relaxation of the system. As we shall be interested only in the broadening due to exchange we shall neglect Γ_T in the following.

The dimers are also described by a density matrix, σ' , which is a 9×9 matrix with the equation of motion in the absence of 'exchange':

$$i\dot{\sigma}' = [\mathcal{H}_T^1 + \mathcal{H}_T^2 + \mathcal{H}_J, \sigma'], \quad (2)$$

where $\mathcal{H}_J = J\mathbf{S}_1 \cdot \mathbf{S}_2$. The effect of 'exchange' is that terms representing the formation and break up of dimers must be added to (3). When a dimer is first formed it has the density matrix $\rho \times \rho$. If η is the rate of formation of dimers the rate of increase in σ' from new collisions is $\eta\rho \times \rho$ and as the rate of break-up must also be η , the equation for σ' is:

$$i\dot{\sigma}' = [\mathcal{H}_T^1 + \mathcal{H}_T^2 + \mathcal{H}_J, \sigma'] - i\eta\sigma' + i\eta\rho \times \rho. \quad (3)$$

Similarly equation (1) must also be corrected for the effects of 'exchange'. When a dimer breaks up the density matrices of the two monomers formed will be $\text{tr}_1 \sigma'$, where tr_1 means trace with respect to the states of either component of the dimer. If $2\gamma^{-1}$ is the mean time between successive collisions made by a triplet

$$i\dot{\rho} = [\mathcal{H}_T, \rho] + i\gamma \text{tr}_1 \sigma' - i\gamma\rho. \quad (4)$$

It is convenient to put $\sigma' = \rho \times \rho + \sigma$, so that σ is the change in the dimer density matrix due to J . The equations for σ and ρ are then:

$$i\dot{\rho} = [\mathcal{H}_T, \rho] + i\gamma \text{tr}_1 \sigma, \quad (5)$$

$$i\dot{\sigma} = [\mathcal{H}_T^1 + \mathcal{H}_T^2 + \mathcal{H}_J, \sigma] + [\mathcal{H}_J, \rho \times \rho] - i\eta\sigma - i\gamma(\rho \times (\text{tr}_1 \sigma) + (\text{tr}_1 \sigma) \times \rho). \quad (6)$$

Equations (5) and (6) may be now solved for ρ and σ , and the expectation value of any observable found by taking the trace of the corresponding operator with ρ .

3. THE ZERO-FIELD SPECTRUM

3.1. Calculation of the line-shape function

The Hamiltonian for an isolated triplet in the absence of an external field is

$$\mathcal{H}_T = DS_z^2 + E(S_x^2 - S_y^2) + \tilde{\mathbf{R}} \cdot \mathbf{S}, \quad (7)$$

where D and E are the zero-field splitting parameters and $\tilde{\mathbf{R}}$ is the product of the

r.f. field and the magnitude of the magnetic moment of the triplet. R is a small quantity. Using the linear combinations of $|m_s\rangle$ states

$$|A\rangle = 2^{-1/2}(|1\rangle + |-1\rangle),$$

$$|B\rangle = 2^{-1/2}(|1\rangle - |-1\rangle),$$

$$|C\rangle = |0\rangle.$$

as basis states, \mathcal{H}_T is diagonal except for the perturbation $\tilde{\mathbf{R}}$.

$$\mathcal{H}_T = \begin{bmatrix} D+E & \tilde{\mathbf{R}}_z & \tilde{\mathbf{R}}_x \\ \tilde{\mathbf{R}}_z & D-E & -i\tilde{\mathbf{R}}_y \\ \tilde{\mathbf{R}}_x & i\tilde{\mathbf{R}}_y & 0 \end{bmatrix}.$$

In the absence of exchange the spectrum consists of three lines at $D+E$, $D-E$ and $2E$. For convenience we will label the elements of the density matrix in this representation by the letters:

$$\rho = \begin{bmatrix} A & Z & X \\ \bar{Z} & B & -iY \\ \bar{X} & i\bar{Y} & C \end{bmatrix}.$$

The z component of magnetization is then $(Z + \bar{Z})$ and the x component $(X + \bar{X})$, etc.

The density matrix of the dimer will be written in the representation in which each basis state is the product of two of the monomer states $|A\rangle$, $|B\rangle$ and $|C\rangle$. Each element of the density matrix $\rho \times \rho$ will then be labelled by two capital letters, and the corresponding element of σ will be denoted by the same two letters in lower case.

We shall solve equation (6) for certain elements of σ in terms of ρ in order to substitute in equation (5) to find the z magnetization. To first order in R , equation (6) gives the following series of equations for the elements az , etc:

$$\left. \begin{aligned} ia\dot{z} &= (\nu - i\eta)az - J(az - b\bar{z}) - \frac{i\gamma}{3}z - \frac{1}{3}(Z - \bar{Z}), \\ ib\dot{z} &= (\nu - i\eta)bz + J(bz - a\bar{z}) - \frac{i\gamma}{3}z + \frac{1}{3}J(Z - \bar{Z}), \\ ic\dot{z} &= (\nu - i\eta)c\bar{z} - \frac{i\gamma}{3}\bar{z}, \\ i\dot{a}\bar{z} &= (-\nu - i\eta)a\bar{z} + J(a\bar{z} - bz) - \frac{i\gamma}{3}\bar{z} - \frac{1}{3}J(Z - \bar{Z}), \\ i\dot{b}\bar{z} &= (-\nu - i\eta)b\bar{z} + J(az - b\bar{z}) - \frac{i\gamma}{3}\bar{z} + \frac{1}{3}J(Z - \bar{Z}), \\ i\dot{c}\bar{z} &= (-\nu - i\eta)c\bar{z} - \frac{i\gamma}{3}\bar{z}. \end{aligned} \right\} \quad (8)$$

In these equations $z = az + bz + cz$, $\bar{z} = a\bar{z} + b\bar{z} + c\bar{z}$ and ν is the frequency of the z transition in the absence of collisions. In these equations elements involving z are not mixed with x or y elements. This implies that the three zero-field lines corresponding to the x , y and z transitions are not mixed with one another by these

collisions. Each behaves independently, and, as the labelling of the axes is arbitrary, they behave in the same way.

We wish to calculate the response to an r.f. field $\mathbf{R} \cos \omega t$. Putting $\tilde{\mathbf{R}} = \mathbf{R} \exp(i\omega t)$ we find that x, y and z are (to first order in R), of the form $a \exp(i\omega t)$ where a may be complex. From the equations (8) the elements az , etc. must be of the same form. Hence substituting $-\omega az$ for iaz , etc., we obtain (neglecting terms of order $\gamma\eta^{-1}$):

$$\begin{cases} z + \bar{z} = -\nu\eta^{-1}(Z - \bar{Z})f, \\ z - \bar{z} = q\eta^{-1}(Z - \bar{Z})f, \end{cases} \quad (9)$$

where f is the dimensionless function:

$$f = \frac{8J^2\eta q}{3[(q^2 - \nu^2)^2 - 4J^2q^2]}, \quad (10)$$

and

$$q = \omega - i\eta.$$

When these values for $\text{tr}_1 \sigma$ are substituted in equation (5), the z component of the magnetization of the triplets in the presence of an r.f. field $\mathbf{R} \cos \omega t$ is found to be:

$$Z + \bar{Z} = -\frac{2\nu(1 - icf)R_z(A - B) \exp(i\omega t)}{\omega^2(1 + icf) - \nu^2(1 - icf) + \eta\omega cf} + \text{C.C.} \quad (11)$$

where $c = \gamma\eta^{-1}$ is the relative number of dimers and isolated triplets. The real part of the coefficient of $\exp(i\omega t)$ in (11) gives the dispersion and the imaginary part the absorption of the system when the angular frequency of the r.f. field is ω . This coefficient is the line shape function.

3.2. Predicted line shapes

3.2.1. Displacement of lines

The zero of the dispersion, which corresponds closely to the maximum of the absorption, occurs when the real part of the line-shape function in (11) is zero. Writing $f = f_r + if_i$, this is when

$$g(\omega) = \omega^2 - \nu^2 - c(f_i(\omega^2 + \nu^2) - \eta\omega f_r) = 0. \quad (12)$$

The direction of the shift can be deduced from the sign of $g(\nu)$, for as $g(0)$ is negative, if $g(\nu)$ is still negative the line has shifted to high frequencies. This occurs if

$$2\nu f_i(\omega = \nu) > \eta f_r(\omega = \nu); \quad (13)$$

that is when

$$\eta^2 > 4J^2 \frac{(\eta^2 + \nu^2)}{(\eta^2 + 4\nu^2)}. \quad (14)$$

Thus the line shifts to high frequencies if $\eta > 2J$ and to low frequencies if $\eta < J$. In real situations η is probably always greater than ν . Under these conditions the position of the zero is easily found to be at the point ω , where

$$\omega^2 = \nu^2 \left(1 + \frac{8J^2c(\eta^2 - 4J^2)}{3(\eta^2 + 4J^2)^2} \right). \quad (15)$$

3.2.2. Line broadening

In general the line-shape function (11) is a complicated function of ω , η , J and ν . If $\nu \ll \eta$ or $\nu, \eta \ll J$ the expression (10) for f simplifies and the line-shape function can be written in the form (when c is small):

$$\frac{\nu R_z(A-B)}{\omega^2 - \nu^2(1+ca) - 2ibc\omega}. \quad (16)$$

This expression represents a Lorentz line of width bc and with a maximum at the point $\omega^2 = \nu^2(1+ca)$. The line widths found are given in table 1.

	Width	Shift
$\eta \gg \nu$	$\frac{4J^2\eta c}{3(\eta^2 + 4J^2)}$	$\frac{4J^2c(\eta^2 - 4J^2)\nu}{3(\eta^2 + 4J^2)^2}$
$\eta \gg J, \nu$	$\frac{4J^2c}{3\eta}$	$\frac{4J^2c\nu}{3\eta^2}$
$J \gg \eta, \nu$	$\frac{c\eta(\eta^2 + 2\nu^2)}{3(\eta^2 + \nu^2)}$	$-\frac{c\eta^2\nu}{3(\nu^2 + \eta^2)}$
$J \gg \eta > \nu$	$\frac{c\eta}{3} = \frac{\gamma}{3}$	$-\frac{c}{3}\nu$

Table 1. Summary of line widths and shifts of zero field lines.

4. THE HIGH-FIELD SPECTRUM

4.1. Calculation of the line-shape function

The Hamiltonian for an isolated triplet in the presence of a large magnetic field in the z direction is:

$$\mathcal{H}_T = \nu_0 S_z + D S_z^2 + \tilde{\mathbf{R}} S_x, \quad (17)$$

where ν_0 is the Zeeman energy, D depends on the zero field parameters and the orientation of the crystal and $\tilde{\mathbf{R}}$ has the same meaning as before. In the absence of exchange there are two lines at $\nu_0 \pm D$. In the representation with the three states $|m_s\rangle$ as basis states \mathcal{H}_T is diagonal except for the perturbation R . For convenience we shall label the elements of ρ by the letters:

$$\rho = \begin{bmatrix} A & K \\ \bar{K} & B & L \\ & \bar{L} & C \end{bmatrix},$$

and the elements of σ will each be denoted by two lower-case letters as before. The magnetization in the x direction is then $(K + \bar{K} + L + \bar{L})$. Again assuming that the relaxation time of a dimer is much longer than its life-time, equation (6) can be solved for the elements of σ in terms of the elements of ρ . We obtain the

series of simultaneous equations for the elements ak , etc.:

$$\left. \begin{aligned} i\dot{a}k &= (\nu_0 + D - i\eta)ak - \frac{i\gamma}{3}k, \\ i\dot{b}k &= (\nu_0 + D - i\eta)bk - \frac{i\gamma}{3}k + J(bk - al) + \frac{1}{3}J(K - L), \\ i\dot{c}k &= (\nu_0 + D - i\eta)ck - \frac{i\gamma}{3}k - J(ck - bl) - \frac{1}{3}J(K - L), \\ i\dot{a}l &= (\nu_0 - D - i\eta)al - \frac{i\gamma}{3}l + J(al - bk) - \frac{1}{3}J(K - L), \\ i\dot{b}l &= (\nu_0 - D - i\eta)bl - \frac{i\gamma}{3}l - J(bl - ck) + \frac{1}{3}J(K - L), \\ i\dot{c}l &= (\nu_0 - D - i\eta)cl - \frac{i\gamma}{3}l. \end{aligned} \right\} \quad (18)$$

In this case J mixes the k and l terms, showing that the two lines do not behave independently, but are mixed. Equations (18) are identical with equations (8) for zero field if the origin of the frequency ω is shifted to ν_0 , k and l are written for \bar{z} and \bar{z} and D is written for ν . Thus k and l are given by equations (9), and substituting in (5) we find:

$$K + L = \frac{2\tilde{R}(A - B)[\omega(1 + icf) + \eta cf] \exp(i\omega t)}{\omega^2(1 + icf) - \nu^2(1 - icf) + \eta\omega cf}. \quad (19)$$

The line-shape function is the coefficient of $\exp(i\omega t)$ in this expression. Its denominator is identical with that of the zero-field case, but the numerator is different.

4.2. Predicted line shapes

4.2.1. Initial behaviour

When the broadening is small compared to the line separation D , the line shapes are determined by the denominator of the line shape-function (19). Under these circumstances the shifts and breadths are given in table 1. If $\eta > 2J$ the lines initially move apart. As D is decreased by rotating the crystal, or c is increased by raising the temperature, the numerator causes a different behaviour, and the lines shift towards each other until they coalesce.

4.2.2. Line shifts

The real part of the line-shape function is zero when

$$g(\omega) = \omega(\omega^2 - \nu^2) - c[2f_i\omega^3 - (2\omega^2 - \nu^2)f_r] + c^2\omega(\omega^2 + \nu^2 + \eta^2)|f|^2 = 0. \quad (20)$$

As ω is a factor of f_r it is a factor of $g(\omega)$ and the dispersion is always zero at the Zeeman frequency ν_0 . Apart from this factor g depends on ω^2 , so the spectrum is symmetrical about ν_0 . The condition for the lines to be shifted away from each other is found from (20) to be:

$$c \frac{8J^2}{3} (2\nu^2 + \eta^2) (\nu^2 + \eta^2) < \nu^2 [\eta^2(\eta^2 + 4\nu^2) - 4J^2(\eta^2 + \nu^2)]. \quad (21)$$

When $\eta \gg \nu$ (as is probably true in practice) this condition becomes:

$$c < \frac{3\nu}{8J^2} \left(1 - \frac{4J^2}{\eta^2} \right). \quad (22)$$

Condition (22) shows that if ν is decreased by rotating the crystal the lines eventually move together even if they initially move apart. Finally the lines coalesce, and the absorption curve shows a maximum at ν_0 . The condition for this is that equation (20) has only one real root, or

$$\nu \leq \frac{8J^2\eta c}{3(\eta^2 + 4J^2)}. \quad (23)$$

When the absorption curve has two maxima these are situated at the points

$$\omega^2 = \nu^2 \left[1 + \frac{8J^2c(\eta^2 - 4J^2)}{3(\eta^2 + 4J^2)^2} \right] - \left[\frac{8J^2c\eta}{3(\eta^2 + 4J^2)} \right]^2 \quad (24)$$

if $\eta \gg \nu$. Under these conditions the maximum displacement of the lines away from each other when $\eta > J$ is:

$$\Delta\omega_{\max} = \frac{8J^2\nu^2}{3\eta^4} \nu. \quad (25)$$

In favourable circumstances such a shift should be observable.

4.2.3. The exchange narrowed line

When condition (23) is satisfied the absorption spectrum has a single maximum, and as ν is decreased or c increased the line narrows and its shape approaches that of a Lorentz line. Under these circumstances it is found that in the vicinity of the line the numerator of the line-shape function (19) is dominated by the imaginary part of the term ηcf . Dividing the denominator by the numerator we obtain the line-shape function:

$$\frac{2R(A - B)}{\omega + i\nu^2(1 + cf_i)/\eta cf_i}. \quad (26)$$

This represents a Lorentz line centred at ν_0 and of width

$$\frac{3\nu^2(\eta^2 + 4J^2)}{8\eta cJ^2}. \quad (27)$$

5. DISCUSSION

The behaviour of this model in the zero-field case, as summarized in table 1, depends on the value of $J\eta^{-1}$. This parameter represents the extent of the coupling in each collision. When J is large compared to η the state of a triplet after a collision is completely uncorrelated with its state before. The effective lifetime of each state is $\frac{2}{3}$ the time between collisions or $3\gamma^{-1}$. This gives rise to the observed width of $\frac{1}{3}\gamma$. If $J\eta^{-1}$ is less the probability of the state of the triplet being altered by a collision is smaller, and the line width less, as shown in table 1.

The shifts shown in table 1 are perhaps less easy to understand than the line widths. The explanation probably lies in the fact that this is not a normal relaxation process which is completely random. When $J\eta^{-1}$ is small a triplet will undergo several collisions without changing its state. Under these conditions the effect of the perturbation is primarily to change the energy of each of the triplet states and the lines are shifted to higher frequencies. When $J\eta^{-1}$ is larger the effect of the perturbation in mixing the states is more important. A process which averages the states leads to a shift of the lines towards zero frequency.

	Predicted by spin $\frac{1}{2}$ theory	This model	Observed values of β (ref. [5]) assuming spin $\frac{1}{2}$ theory	
			$\phi_3\text{AsMeTCNQ}$	$\text{Cs}_2(\text{TCNQ})_3$
Shift ($\omega^2 - \nu^2$)	$-2\beta^2$	$\frac{8J^2c\nu^2(\eta^2 - 4J^2)}{3(\eta^2 + 4J^2)^2} - \left[\frac{8J^2c\eta}{3(\eta^2 + 4J^2)} \right]^2$	$3 \times 10^{10} \exp(-0.05/kT)$	$10^{10} \exp(-0.054/kT)$
Width	β	$\frac{4J^2\eta c}{3(\eta^2 + 4J^2)}$	$3 \times 10^{12} \exp(-0.11/kT)$	$2 \times 10^{13} \exp(-0.22/kT)$
Width of narrowed line	$\frac{\nu^2}{2\beta}$	$\frac{3\nu^2(\eta^2 + 4J^2)}{8\eta cJ^2}$	$3 \times 10^{13} \exp(-0.16/kT)$	$4 \times 10^{13} \exp(-0.22/kT)$
c			$\exp(-0.065/kT)$	$\exp(-0.16/kT)$

Table 2. Line-shape parameters of high field spectra.

6. COMPARISON WITH EXPERIMENTAL OBSERVATIONS

6.1. *Approximations inherent in the model*

Before comparing the predicted line shapes with those observed for some triplet exciton systems the approximations made are summarized.

(1) Firstly the thermal relaxation of both the isolated triplets and the dimers has been neglected. This was unnecessary; if the transverse relaxation time, T_2 , of the triplets is taken to be β^{-1} , it can easily be shown that ω in all the equations should be replaced by $\omega - i\beta$. The total line width is then the sum of the natural line width and the broadening due to collisions. Under conditions where a line shift is observed β is negligible. It is necessary to assume that the relaxation of the dimer is negligible during its lifetime. Otherwise the growth of the off-diagonal matrix elements of σ such as $z\bar{z}$ must be taken into account.

(2) Successive collisions have been assumed to be completely uncorrelated. This is a particularly bad assumption for a one-dimensional system. However, the effect of successive collisions between the same two triplets is the same as a single longer collision. Even if the time of a single collision is assumed to be independent of temperature such effects would lead to an apparent temperature dependence of η .

(3) The concept of collisions used in the model will only be valid if the excitons are not spread out. The shape of the excitons is probably temperature dependent, leading again to a temperature dependence of J , η and ν .

(4) The ratio of the number of dimers to isolated pairs, which is proportional to the concentration of triplets, has always been assumed to be small. In particular equation (27) for the width of the exchange narrowed line must not be applied at high temperatures, or at temperatures where $kT < J$ when dimers with paired spins tend to stick together.

6.2. *Observations of the TCNQ free radical ions*

Jones and Chesnut [5] observed the high field spectrum of various TCNQ salts as a function of temperature at an arbitrary orientation of the crystal (ν fixed). Table 2 contains some of their observations together with the line shape parameters predicted by the theory for exchanging spin $\frac{1}{2}$ species, and by this model (assuming $\eta > \nu$). The observed values of β are of the form $a \exp(-E/kT)$, but the three measurements give different values of a and E . If the collision model is applicable the measurements of line widths should give consistent results; this is found for the caesium salt but not for the other salts. It may be that the observations of the exchange narrowed line are at too high a temperature for the theory to be valid.

In every case the value of β derived from the line shift is very different from the values obtained from the line width measurements as predicted by our model. As the shift is observed to be steadily in one direction, and as the temperature dependence is expressible in terms of a single exponential, only the first term of the line shift given in table 2 can be important, and $J > \eta$. If we assume that $4J^2 \gg \eta^2$ the line width is found to be $\frac{1}{3}\eta c$, and the line shift $\omega^2 - \nu^2 = -\frac{2}{3}\nu^2 c$. Although the simplest hypothesis would be that only c is temperature dependent, in which case the experimental data do not fit the theory very well, it is likely that η has a considerable temperature dependence.

7. CONCLUSIONS

There is a fundamental difference between the two line spectra of a triplet state and of two doublet states in different environments. It has been demonstrated here that the line broadening will not follow the same pattern in the two cases. More experimental evidence is needed before it can be decided whether the specific model discussed here is applicable to the TCNQ salts. Where it is applicable values of the parameters J , η and c can be found:

REFERENCES

- [1] CHESNUT, D. B., and PHILLIPS, W. D., 1961, *J. chem. Phys.*, **35**, 1002.
- [2] McCONNELL, H. M., POOLEY, D., and BRADBURY, A., 1962, *Proc. nat. Acad. Sci., Wash.*, **48**, 1480. THOMAS, D. D., KELLER, H., and McCONNELL, H. M., 1963, *J. chem. Phys.*, **39**, 2321.
- [3] McCONNELL, H. M., and LYNDEN-BELL, R. M., 1962, *J. chem. Phys.*, **36**, 2393.
- [4] LYNDEN-BELL, R. M., and McCONNELL, H. M., 1962, *J. chem. Phys.*, **37**, 794.
- [5] JONES, M. T., and CHESNUT, D. B., 1963, *J. chem. Phys.*, **38**, 1311.
- [6] PAKE, G. E., and TUTTLE, T. R., 1962, *Phys. Rev. Letters*, **3**, 423.
- [7] ALEXANDER, S., 1962, *J. chem. Phys.*, **37**, 967, 974.
- [8] SLICHTER, C. P., 1963, *Principles of Magnetic Resonance* (Harper & Row). ABRAGAM, A., 1961, *The Principles of Nuclear Magnetism* (Oxford University Press).
- [9] McCONNELL, H. M., and SOOS, Z., 1964, *J. chem. Phys.* (in press).

The rotational-torsional wavefunctions of molecules that have two identical co-axial rotors

by P. R. BUNKER

University Chemical Laboratory,
Lensfield Road, Cambridge

(Received 6 December 1963)

An expression is obtained for the rotational-torsional energy levels of a molecule that has two identical co-axial internal rotors, and the effect of introducing a torsional barrier is determined. The statistical weights of the rotational-torsional levels of dimethylacetylene and ferrocene are calculated.

1. INTRODUCTION

In a recent paper [1] Longuet-Higgins has defined the symmetry groups of non-rigid molecules, and shown how these groups may be used for classifying rotorsional (rotational-torsional) states and for determining statistical weights. In this paper we obtain an expression for the rotorsional energy levels of a molecule with two identical co-axial internal rotors, and find how the energies are affected by the introduction of a torsional barrier. We also determine, for dimethylacetylene and ferrocene, the statistical weights of the rotorsional levels, and correlate the high- and low-barrier cases.

2. SYMMETRY GROUPS

The molecular symmetry group of a molecule that has two co-axial methyl groups is a group of 36 elements, and the character table of this group is shown in table 1†[1]. The atoms are numbered as in figure 1. Table 2 shows the

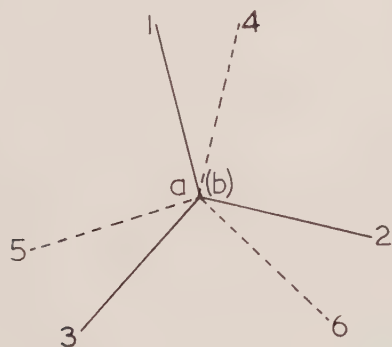


Figure 1. Labelling convention adopted for molecules having two co-axial methyl groups.

† For convenience all the tables are grouped together at the end of the paper.

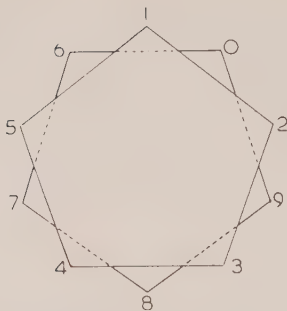


Figure 2. Labelling convention adopted for ferrocene.

character table of G_{100} , the molecular symmetry group of a dicyclopentadienyl compound like ferrocene. The permutation (ij) is the permutation of C_i with C_j and H_i with H_j and the labelling convention adopted is shown in figure 2.

Longuet-Higgins has shown how G_{36} factorizes into the product of a torsional and a rotational factor group, each of which is isomorphous with the point group C_{3v} . Similarly G_{100} factorizes into the product of a torsional and a rotational factor group, each of which is isomorphous with point group C_{5v} . It is tempting to give a simple geometrical interpretation of this factorization into groups that are isomorphous with the point group of the rotors. The error in doing this is demonstrated by the fact that the symmetry groups of molecules that have two identical co-axial rotors of C_{nv} symmetry, where n is *even*, do not factorize in this manner.

3. ROTORSIONAL WAVEFUNCTIONS AND ENERGIES WHEN THE TORSIONAL BARRIER IS LOW

The rotorsional wavefunction of a molecule that has two identical co-axial internal rotors and no torsional barrier is a combination of functions of the type :

$$\psi_{\text{RT}} = S_{JKM}(\theta, \phi) \exp(iK_a \chi_a) \exp(iK_b \chi_b),$$

where (θ, ϕ, χ_a) and (θ, ϕ, χ_b) are the Eulerian angles of the rotor groups and $S_{JKM}(\theta, \phi)$ is the (θ, ϕ) part of a symmetric top wavefunction. We can rewrite this wavefunction as :

$$\psi_{\text{RT}} = S_{JKM}(\theta, \phi) \exp\left(iK_s \frac{\chi}{2}\right) \exp\left(iL_s \frac{\tau}{2}\right),$$

where $\chi = \chi_a + \chi_b$, $\tau = \chi_b - \chi_a$, $K_s = K_a + K_b$ and $L_s = K_b - K_a$. The absolute values of K_s and L_s are the quantum numbers K and L respectively. In general the torsional wavefunction, $\exp[iL_s(\tau/2)]$, is the Mathieu function $\mathcal{M}(3\tau/2)$ which becomes $\exp[iL_s(\tau/2)]$ when the torsional barrier is zero [2]. Note that L_s is an integer having the same parity as K_s [3].

The species of the rotorsional wavefunctions of dimethylacetylene have been obtained by Longuet-Higgins and are the product of the separate 'rotational' and 'torsional' species shown in table 3. Similarly, as a result of the factorizations of G_{100} , we are able to determine separate rotational and torsional species in G_{100} for ferrocene which multiply to give the species of the rotorsional wavefunctions; these are shown in table 4.

When there is no torsional barrier the energies of the rotorsional states are given by :

$$E_{\text{RT}}(J, K, L) = hc\{BJ(J+1) - BK^2 + 2A(K_a^2 + K_b^2)\} \\ = hc\{BJ(J+1) + (A-B)K^2 + AL^2\},$$

where A and B are the usual rotational constants. We will now determine the effect of a low torsional barrier on the rotorsional energy levels of dimethylacetylene and infer the result for ferrocene.

The torsional barrier can be represented by a Fourier series in the torsional angle τ , that is as :

$$\sum_{n=1}^{\infty} V_{3n} [\exp(3ni\tau) + \exp(-3ni\tau)].$$

The constants V_{3n} for $n > 1$ are believed to be very small compared with V_3 and these terms are neglected. This is equivalent assuming that the torsional barrier is of the form :

$$2V_3 \cos 3\tau = V(\tau), \quad \text{say,}$$

where $4V_3$ is the difference in potential energy between staggered and eclipsed molecules.

The matrix element of $V(\tau)$ between the rotorsional states

$$|J', K_s', M', L_s'\rangle \quad \text{and} \quad |J'', K_s'', M'', L_s''\rangle$$

is V_3 if $J' = J''$, $K_s' = K_s''$, $M' = M''$, and $L_s' = L_s'' \pm 6$, but zero otherwise. Using second-order perturbation theory we deduce that for a rotorsional state in which $L \neq 3$ the effect of $V(\tau)$ on the energy E_0 is to shift to E' , where

$$E' = E_0 + \frac{V_3^2}{A[L^2 - (L-6)^2]} + \frac{V_3^2}{A[L^2 - (L+6)^2]} = E_0 + \frac{V_3^2}{2A(L^2 - 9)}.$$

The four-fold degenerate rotorsional states that have $L=3$ are resolved into two-fold degenerate states by the torsional barrier. This is because the two $L_s=3$ states are coupled with the two $L_s=-3$ states by the torsional barrier since they have L_s values that differ by six. Their perturbed energies, given as a function of their unperturbed energies E_0 , are :

$$E_+ = E_0 + V_3 - \frac{V_3^2}{A[9^2 - 3^2]} = E_0 + V_3 - \frac{V_3^2}{72A}, \\ E_- = E_0 - V_3 - \frac{V_3^2}{72A}.$$

Note that a state for which $L=3n$ ($n=2, 3, 4, \dots$) will be resolved into two states by the torsional barrier since the $L_s=3n$ and $L_s=-3n$ will be coupled in the n th order. The neglected terms that have $n > 1$ in the Fourier series expansions of the torsional barrier will also contribute to the splitting of these $L=3n$ states.

Figure 3 shows the effect of increasing V_3 on some of the rotorsional energy levels. An analogous treatment can be carried through with ferrocene using a torsional potential involving 5τ . All levels with $L=5n$ ($n=1, 2, 3, \dots$) will be split by the barrier.

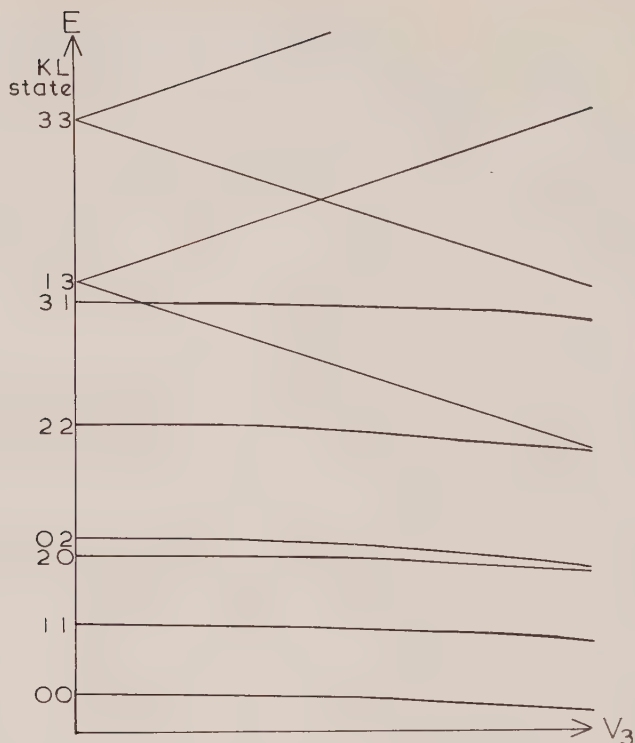


Figure 3. Effect of increasing the torsional barrier on some rotorsional energy levels of dimethylacetylene.

4. ENERGY LEVELS WHEN THE TORSIONAL BARRIER IS HIGH

When the torsional barrier is very high internal torsional motion of the molecule is a vibration about, say, a staggered configuration. Thus in ethane we can distinguish three conformers as shown in figure 4.

If torsional tunnelling is neglected the molecular symmetry group of each conformer is the point group D_{3d} which is of lower order than G_{36} . The symmetry groups G_A , G_B and G_C of the three conformers are isomorphous, but comprise different elements of G_{36} , as shown in table 5.

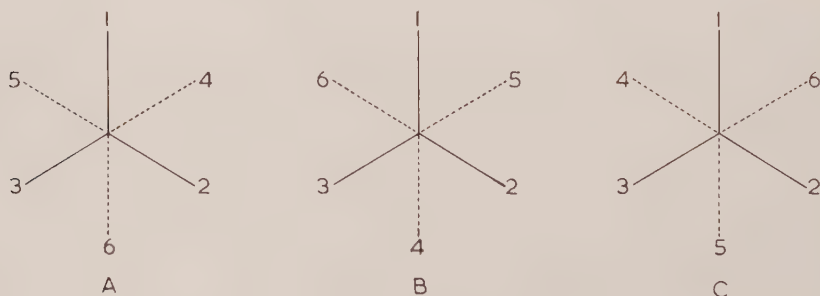


Figure 4. The three conformers of ethane.

The rotorsional wavefunctions of each conformer can be classified in its conformer symmetry group using the results of Hougen [4]. The torsional wavefunction is of species A_{1u} when the torsional quantum number n_t is odd and of species A_{1g} when it is even, as is well known. The species of the rotorsional wavefunction is simply the product of the rotational and torsional species. These results are shown in table 6.

When torsional tunnelling is allowed for, the molecular symmetry group becomes G_{36} . Tunnelling mixes conformer wavefunctions that have the same J , K , M and n_t values. The species in G_{36} of a set of conformer wavefunctions that are mixed by tunnelling follows directly from their species in their conformer symmetry groups, since these are sub-groups of G_{36} . The character of a particular element in G_{36} is the sum of the characters of that element in G_A , G_B and G_C on the understanding that if the element does not occur in G_A , G_B or G_C the character in that sub-group is taken to be zero. The species of the rotorsional wavefunctions when tunnelling occurs are shown in table 7. We see that the species of the rotorsional wavefunctions can be written as the product of a rotational species (the species in table 5 for n_t even) and a torsional species (A_1 for n_t even and A_3 for n_t odd).

Table 8 shows the results obtained for ferrocene in which the conformer groups are isomorphous with point group D_{5d} .

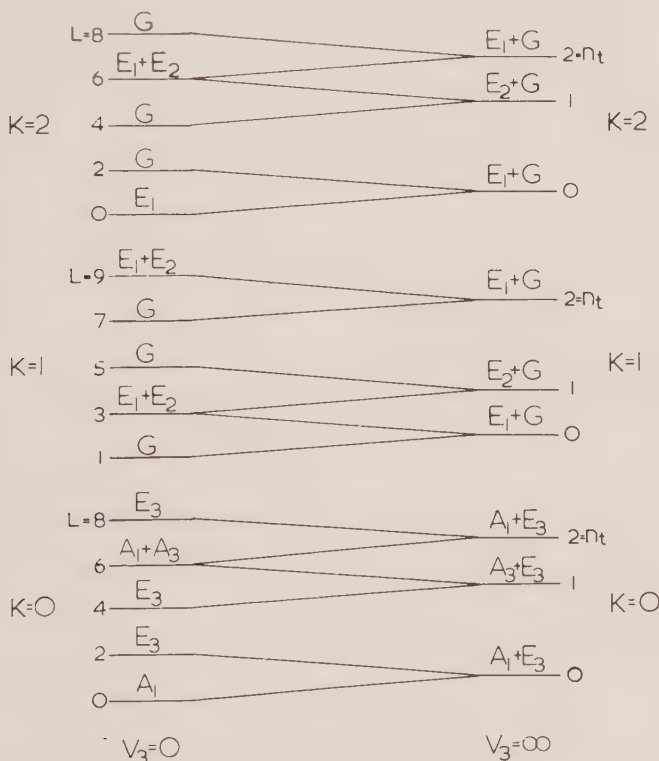


Figure 5. The correlation of the rotorsional energy levels of dimethylacetylene between high and low barrier situations.

In figures 5 and 6 the energy levels for the high barrier case are correlated with those of the free internal rotor for dimethylacetylene and ferrocene respectively. The species of the levels for intermediate barrier height can be inferred. No attempt is made to give quantitative energy separations and, for clarity, we have separated the sets of levels for each K -value. In both diagrams it is assumed that J is given for the purpose of classifying the $K=0$ levels in G_{36} and G_{100} .

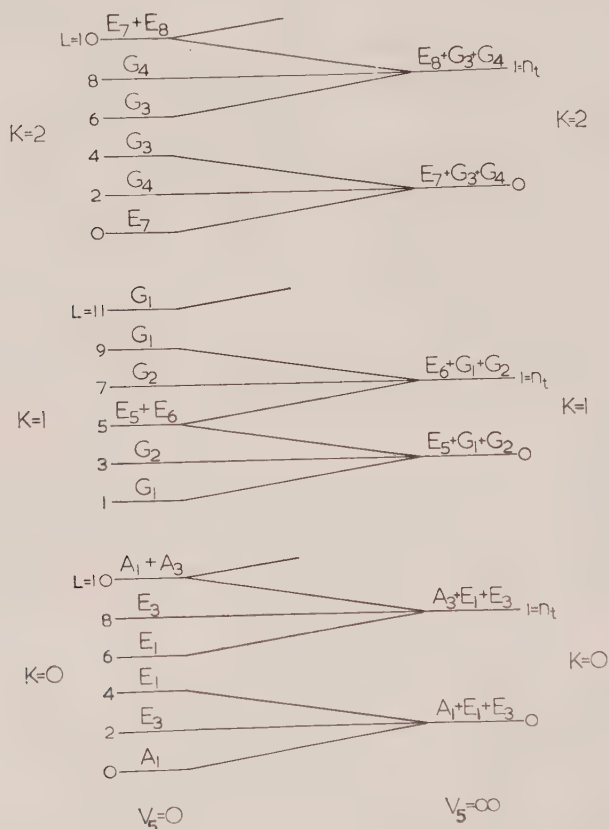


Figure 6. The correlation of the rotorsional energy levels of ferrocene between high and low torsional barrier situations.

5. STATISTICAL WEIGHTS OF THE ROTORSIONAL ENERGY LEVELS

Using the method described by Longuet-Higgins we determine the possible proton-spin states of dimethylacetylene to be :

$${}^7A_1; {}^5A_4 {}^5G; {}^3A_1 {}^3E_1 {}^3E_3 {}^3G; {}^1A_4 {}^1E_2 {}^1E_4$$

and by the exclusion principle the symmetry of the overall wavefunction must be A_2 or A_4 . The possible proton-spin states of ferrocene are :

$$\begin{aligned} &{}^{11}A_1; \\ &{}^9A_4 {}^9G_1 {}^9G_4; \\ &2^7A_1 {}^7A_4 {}^7G_1 {}^7G_2 {}^7G_3 {}^7G_4; \\ &{}^5A_1 {}^2^5A_4 {}^2^5E_1 {}^2^5E_2 {}^2^5E_3 {}^2^5E_4 {}^2^5E_5 {}^2^5E_6 {}^2^5E_7 {}^2^5E_8 {}^3^5G_1 {}^3^5G_2 {}^3^5G_3 {}^3^5G_4; \\ &{}^2^3A_1 {}^3^3E_1 {}^3^3E_2 {}^3^3E_3 {}^3^3E_4 {}^3^3E_5 {}^3^3E_6 {}^3^3E_7 {}^3^3E_8 {}^3^3G_1 {}^4^3G_2 {}^4^3G_3 {}^3^3G_4; \\ &2^1A_4 {}^2^1E_2 {}^2^1E_4 {}^2^1E_6 {}^2^1E_8 {}^1G_1 {}^2^1G_2 {}^2^1G_3 {}^1G_4. \end{aligned}$$

The symmetry of the overall wavefunction is A_2 or A_4 . The statistical weights of the rotorsional states of dimethylacetylene and ferrocene are determined from these results and shown in tables 9 and 10 respectively.

The statistical weights of the free rotor levels of dimethylacetylene are the same as those obtained by Wilson [5] who used a sub-group of G_{36} having 18 elements to classify the proton-spin states. When the splitting due to torsional tunnelling is not resolved we see that the statistical weight of each level is the sum of the statistical weights of the sub-levels into which it would be split; these statistical weights can be determined by considering only one equilibrium position and using standard rigid-molecule theory.

The results here obtained for dimethylacetylene can be directly applied to molecules such as dimethyl mercury, dimethyl zinc, dimethyl cadmium and perfluoro dimethylacetylene whilst those of ferrocene can be applied to any co-axial dicyclopentadienyl type of molecule.

I would like to thank Professor H. C. Longuet-Higgins, F.R.S., for suggesting this problem and for much valuable advice. I also wish to acknowledge a D.S.I.R. studentship.

REFERENCES

- [1] LONGUET-HIGGINS, H. C., 1963, *Mol. Phys.*, **6**, 445.
- [2] NIELSEN, H. H., 1932, *Phys. Rev.*, **40**, 445.
- [3] HOWARD, J. B., 1937, *J. chem. Phys.*, **5**, 442.
- [4] HOUGEN, J. T., 1962, *J. chem. Phys.*, **37**, 1433.
- [5] WILSON, JR., E. B., 1938, *J. chem. Phys.*, **6**, 740.

	1 E	2(123)(456)	3(14)(26)(35)(ab)	2(123)(465)	4(123)	6(142635)(ab)*	3(14)(25)(36)(ab)	6(142536)(ab)	9(12)(45)*
A_1	1	1	1	1	1	1	1	1	1
A_2	1	1	1	1	1	1	-1	-1	-1
A_3	1	1	-1	1	1	-1	1	1	-1
A_4	1	1	-1	1	1	-1	-1	-1	1
E_1	2	2	2	-1	-1	-1	0	0	0
E_2	2	2	-2	-1	-1	1	0	0	0
E_3	2	-1	0	2	-1	0	2	-1	0
E_4	2	-1	0	2	-1	0	-2	1	0
G	4	-2	0	-2	1	0	0	0	0

Table 1. The symmetry group of dimethylacetylene, G_{36} .

	<i>E</i>														
	1	2	2	5	2	4	4	10	2	4	4	10	5	10	10
		(12345)(67890)	(132524)(68079)	(16)(20)(39)(48)(57)*	(12345)(60987)	(13524)	(14253)(67890)	(1038562947)*	(13524)(69708)	(14253)(60987)	(15432)	(1950463728)*	(16)(27)(38)(49)(50)	(1739562840)	(1857463029)
<i>A</i> ₁	1	1	1	1	1	1	1	1	1	1	1	1	1	1	1
<i>A</i> ₂	1	1	1	1	1	1	1	1	1	1	1	1	-1	-1	-1
<i>A</i> ₃	1	1	1	-1	1	1	1	-1	1	1	1	-1	1	1	1
<i>A</i> ₄	1	1	1	-1	1	1	1	-1	1	1	1	-1	-1	-1	-1
<i>E</i> ₁	2	2 <i>a</i>	2 <i>b</i>	0	2	2 <i>a</i>	2 <i>b</i>	0	2	2 <i>a</i>	2 <i>b</i>	0	2	2 <i>a</i>	2 <i>b</i>
<i>E</i> ₂	2	2 <i>a</i>	2 <i>b</i>	0	2	2 <i>a</i>	2 <i>b</i>	0	2	2 <i>a</i>	2 <i>b</i>	0	-2	-2 <i>a</i>	-2 <i>b</i>
<i>E</i> ₃	2	2 <i>b</i>	2 <i>a</i>	0	2	2 <i>b</i>	2 <i>a</i>	0	2	2 <i>b</i>	2 <i>a</i>	0	2	2 <i>b</i>	2 <i>a</i>
<i>E</i> ₄	2	2 <i>b</i>	2 <i>a</i>	0	2	2 <i>b</i>	2 <i>a</i>	0	2	2 <i>b</i>	2 <i>a</i>	0	-2	-2 <i>b</i>	-2 <i>a</i>
<i>E</i> ₅	2	2	2	2	2 <i>a</i>	2 <i>a</i>	2 <i>a</i>	2 <i>a</i>	2 <i>b</i>	2 <i>b</i>	2 <i>b</i>	2 <i>b</i>	0	0	0
<i>E</i> ₆	2	2	2	-2	2 <i>a</i>	2 <i>a</i>	2 <i>a</i>	-2 <i>a</i>	2 <i>b</i>	2 <i>b</i>	2 <i>b</i>	-2 <i>b</i>	0	0	0
<i>E</i> ₇	2	2	2	2	2 <i>b</i>	2 <i>b</i>	2 <i>b</i>	2 <i>b</i>	2 <i>a</i>	2 <i>a</i>	2 <i>a</i>	2 <i>a</i>	0	0	0
<i>E</i> ₈	2	2	2	-2	2 <i>b</i>	2 <i>b</i>	2 <i>b</i>	-2 <i>b</i>	2 <i>a</i>	2 <i>a</i>	2 <i>a</i>	-2 <i>a</i>	0	0	0
<i>G</i> ₁	4	4 <i>a</i>	4 <i>b</i>	0	4 <i>a</i>	4 <i>a</i> ²	-1	0	4 <i>b</i>	-1	4 <i>b</i> ²	0	0	0	0
<i>G</i> ₂	4	4 <i>b</i>	4 <i>a</i>	0	4 <i>a</i>	-1	4 <i>a</i> ²	0	4 <i>b</i>	4 <i>b</i> ²	-1	0	0	0	0
<i>G</i> ₃	4	4 <i>a</i>	4 <i>b</i>	0	4 <i>b</i>	-1	4 <i>b</i> ²	0	4 <i>a</i>	4 <i>a</i> ²	-1	0	0	0	0
<i>G</i> ₄	4	4 <i>b</i>	4 <i>a</i>	0	4 <i>b</i>	4 <i>b</i> ²	-1	0	4 <i>a</i>	-1	4 <i>a</i> ²	0	0	0	0

$$a = \frac{\sqrt{(5)-1}}{4}; \quad b = -\frac{\sqrt{(5)+1}}{4},$$

Table 2. The symmetry group of ferrocene, *G*₁₀₀.

Value of <i>K</i>	0	1	2	3	4	5	6
Rotational species	<i>A</i> ₁ (<i>J</i> even) <i>A</i> ₂ (<i>J</i> odd)	<i>E</i> ₁	<i>E</i> ₁	<i>A</i> ₁ + <i>A</i> ₂	<i>E</i> ₁	<i>E</i> ₁	<i>A</i> ₁ + <i>A</i> ₂
Value of <i>L</i>	0	1	2	3	4	5	6
Torsional species	<i>A</i> ₁	<i>E</i> ₃	<i>E</i> ₃	<i>A</i> ₁ + <i>A</i> ₃	<i>E</i> ₃	<i>E</i> ₃	<i>A</i> ₁ + <i>A</i> ₃

Table 3. The rotational and torsional species of the rotorsional wavefunctions of dimethylacetylene.

<i>K</i>	Species	<i>L</i>	Species
0 (<i>J</i> even)	<i>A</i> ₁	0	<i>A</i> ₁
0 (<i>J</i> odd)	<i>A</i> ₂	5 <i>n</i> ± 1	<i>E</i> ₁
5 <i>n</i> ± 1	<i>E</i> ₅	5 <i>n</i> ± 2	<i>E</i> ₃
5 <i>n</i> ± 2	<i>E</i> ₇	5 <i>n</i>	<i>A</i> ₁ + <i>A</i> ₃
5 <i>n</i>	<i>A</i> ₁ + <i>A</i> ₂		

Rotational species.

Torsional species.

Table 4. The rotational and torsional species of the rotorsional wavefunctions of ferrocene.

D_{3d}	E	$2C_3$	$3C_2$	i	$2S_6$	3σ
G_A	E	(123)(465) (132)(456)	(14)(25)(36)(ab) (15)(26)(34)(ab) (16)(24)(35)(ab)	(16)(25)(34)(ab)*	(153624)(ab)* (142635)(ab)*	(12)(56)* (23)(45)* (31)(64)*
	E	(123)(465) (132)(456)	(15)(26)(34)(ab) (16)(24)(35)(ab) (14)(25)(36)(ab)	(14)(26)(35)(ab)*	(163425)(ab)* (152436)(ab)*	(12)(64)* (23)(56)* (31)(45)*
G_C	E	(123)(465) (132)(456)	(16)(24)(35)(ab) (14)(25)(36)(ab) (15)(26)(34)(ab)	(15)(24)(36)(ab)*	(143526)(ab)* (162534)(ab)*	(12)(45)* (23)(64)* (31)(56)*
A_{1g}	1	1	1	1	1	1
A_{1u}	1	1	1	-1	-1	-1
A_{2g}	1	1	-1	1	1	-1
A_{2u}	1	1	-1	-1	-1	1
E_g	2	-1	0	2	-1	0
E_u	2	-1	0	-2	1	0

Table 5. The conformer symmetry groups of ethane.

n_t	K	Species in D_{3d}
Even	$0 J_{\text{even}}$ J_{odd} $3n \pm 1$ $3n$	A_{1g} A_{2g} E_g $A_{1g} + A_{2g}$
Odd	$0 J_{\text{even}}$ J_{odd} $3n \pm 1$ $3n$	A_{1u} A_{2u} E_u $A_{1u} + A_{2u}$

Table 6. The species in D_{3d} of the rotorsional wavefunctions of ethane.

n_t	K	Species in G_{36}
Even	$0 J_{\text{even}}$ J_{odd} $3n \pm 1$ $3n$	$A_1 + E_3$ $A_2 + E_4$ $E_1 + G$ $A_1 + A_2 + E_3 + E_4$
Odd	$0 J_{\text{even}}$ J_{odd} $3n \pm 1$ $3n$	$A_3 + E_3$ $A_4 + E_4$ $E_2 + G$ $A_3 + A_4 + E_3 + E_4$

Table 7. The species in G_{36} of the rotorsional wavefunctions of ethane.

n_t	K	D_{5d} species	G_{100} species
Even	$0 J_{\text{even}}$ J_{odd} $5n \pm 1$ $5n \pm 2$ $5n$	A_{1g} A_{2g} E_{1g} E_{2g} $A_{1g} + A_{2g}$	$A_1 + E_1 + E_3$ $A_2 + E_2 + E_4$ $E_5 + G_1 + G_2$ $E_7 + G_3 + G_4$ $A_1 + A_2 + E_1 + E_2 + E_3 + E_4$
Odd	$0 J_{\text{even}}$ J_{odd} $5n \pm 1$ $5n \pm 2$ $5n$	A_{1u} A_{2u} E_{1u} E_{2u} $A_{1u} + A_{2u}$	$A_3 + E_1 + E_3$ $A_4 + E_2 + E_4$ $E_6 + G_1 + G_2$ $E_8 + G_3 + G_4$ $A_3 + A_4 + E_1 + E_2 + E_3 + E_4$

Table 8. The species of the rotorsional wavefunctions of ferrocene assuming there to be a high torsional barrier.

Rotorsional species	Proton spin state	Species of overall wavefunctions	Statistical weight
A_1	— ; ${}^5A_4, {}^1A_4$	$A_2 ; A_4$	6
A_2	${}^7A_1, {}^3A_1$; —	$A_2 ; A_4$	10
A_3	${}^5A_4, {}^1A_4$; —	$A_2 ; A_4$	6
A_4	— ; ${}^7A_1, {}^3A_1$	$A_2 ; A_4$	10
E_1	3E_1 ; 1E_2	$A_2 ; A_4$	4
E_2	1E_2 ; 3E_1	$A_2 ; A_4$	4
E_3	1E_4 ; 1E_4	$A_2 ; A_4$	2
E_4	3E_3 ; 3E_3	$A_2 ; A_4$	6
G	${}^5G, {}^3G$; ${}^5G, {}^3G$	$A_2 ; A_4$	16

Table 9. The statistical weights of the rotorsional states of dimethylacetylene.

Rotor. species	Proton spin states	Overall species	Stat. weight
A_1	— ; ${}^9A_4, {}^7A_4, 2{}^5A_4, 2{}^1A_4$	$A_2 ; A_4$	28
A_2	${}^{11}A_1, 2{}^7A_1, {}^5A_1, 2{}^3A_1$; —	$A_2 ; A_4$	36
A_3	${}^9A_4, {}^7A_4, 2{}^5A_4, 2{}^1A_4$; —	$A_2 ; A_4$	28
A_4	— ; ${}^{11}A_1, 2{}^7A_1, {}^5A_1, 2{}^3A_1$	$A_2 ; A_4$	36
E_1	$2{}^5E_2, {}^3E_2, 2{}^1E_2$; $2{}^5E_2, {}^3E_2, 2{}^1E_2$	$A_2 ; A_4$	30
E_2	$2{}^5E_1, 3{}^3E_1$; $2{}^5E_1, 3{}^3E_1$	$A_2 ; A_4$	38
E_3	$2{}^5E_4, {}^3E_4, 2{}^1E_4$; $2{}^5E_4, {}^3E_4, 2{}^1E_4$	$A_2 ; A_4$	30
E_4	$2{}^5E_5, 3{}^3E_3$; $2{}^5E_5, 3{}^3E_3$	$A_2 ; A_4$	38
E_5	$2{}^5E_5, 3{}^3E_5$; $2{}^5E_6, {}^3E_6, 2{}^1E_6$	$A_2 ; A_4$	34
E_6	$2{}^5E_6, {}^3E_6, 2{}^1E_6$; $2{}^5E_5, 3{}^3E_5$	$A_2 ; A_4$	34
E_7	$2{}^5E_7, 3{}^3E_7$; $2{}^5E_8, {}^3E_8, 2{}^1E_8$	$A_2 ; A_4$	34
E_8	$2{}^5E_8, {}^3E_8, 2{}^1E_8$; $2{}^5E_7, 3{}^3E_7$	$A_2 ; A_4$	34
G_1	${}^9G_1, 2{}^7G_1, 3{}^5G_1, 3{}^3G_1, {}^1G_1$; ${}^9G_1, 2{}^7G_1, 3{}^5G_1, 3{}^3G_1, {}^1G_1$	$A_2 ; A_4$	96
G_2	${}^7G_2, {}^5G_2, 4{}^3G_2, 2{}^1G_2$; ${}^7G_2, 3{}^5G_2, 4{}^3G_2, 2{}^1G_2$	$A_2 ; A_4$	72
G_3	${}^7G_3, 3{}^5G_3, 4{}^3G_3, 2{}^1G_3$; ${}^7G_3, 3{}^5G_3, 4{}^3G_3, 2{}^1G_3$	$A_2 ; A_4$	72
G_4	${}^9G_4, 2{}^7G_4, 3{}^5G_4, 3{}^3G_4, {}^1G_4$; ${}^9G_4, 2{}^7G_4, 3{}^5G_4, 3{}^3G_4, {}^1G_4$	$A_2 ; A_4$	96

Table 10. The statistical weights of the rotorsional states of ferrocene.

RESEARCH NOTES

Long-range couplings in the N.M.R. spectra of alkyl formates

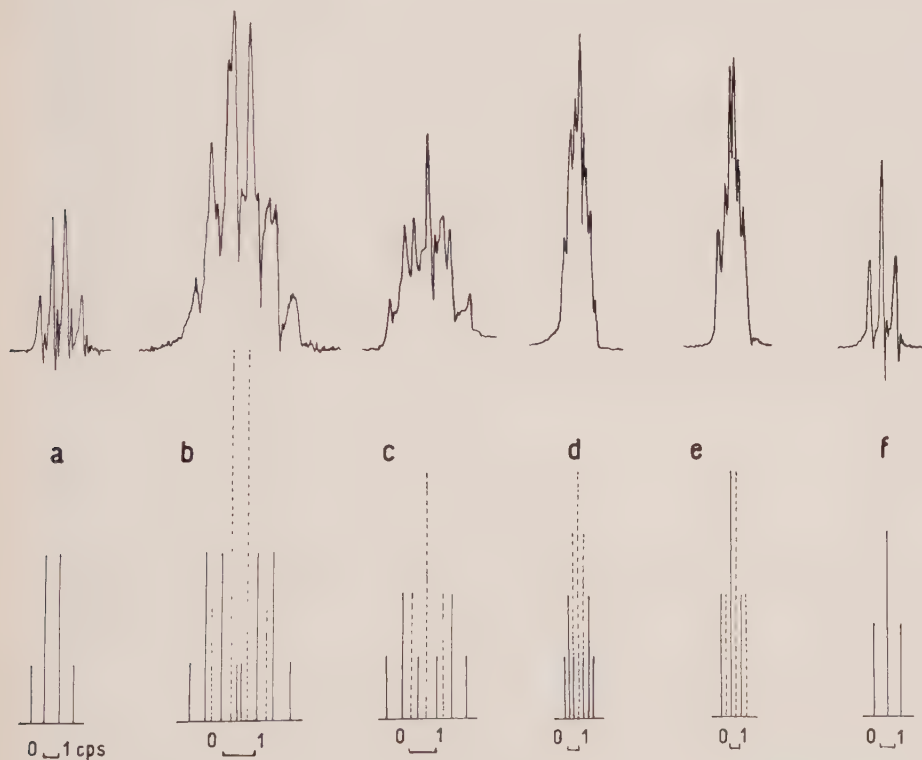
by DORA G. DE KOWALEWSKI and VALDEMAR J. KOWALEWSKI

Department of Physics, Faculty of Sciences, University of Buenos Aires,
Argentina

(Received 4 December 1963)

There are in the literature several reports on long-range spin-spin couplings across four and five bonds which are related to the chemical environment of the interacting nuclei [1]. A group of substances in which the long-range interaction involves the carboxyl group includes benzaldehydes [2], pyridine [3], thiophene [4] and furan aldehydes [5], methyl formamides [6] and vinyl formate [7]. It is the purpose of the present work to report the existence of similar long-range couplings in acyclic saturated compounds involving also the formyl group: the alkyl formates.

As can be seen from the accompanying figure, the proton N.M.R. signal of the formyl group in the formates is a multiplet of more or less complicated structure. Nevertheless, all observed splittings can be accounted for by spin-spin couplings across the C-O bond which reach even the β protons in the alkyl chain. The spectra were taken at two different frequencies: 60



60 Mc/sec N.M.R. signals of the OCH proton of saturated formates showing splittings due to the long-range spin-spin coupling across the C-O bond. (a) methyl; (b) ethyl; (c) propyl; (d) *n*-butyl; (e) *iso*-butyl; (f) benzyl formates.

and 19.25 Mc/s. Excepting small intensity changes, the spectra remained unaltered, showing that first-order theory is applicable. Whenever possible the spectrum of the alkyl chain was calculated with a Ferranti Mercury computer (programmes up to five spins were available). The ethyl group of the ethyl formate matches a theoretical A_2B_3 spectrum with $J/\delta = 0.048$ with all the lines doubled due to interaction with the formyl proton. The CH_2-CH_3 spectrum of propyl formate matches closely a similar one of the propyl group of butyronitrile [8] except for the extra doubling. The spectra of higher esters cannot be analysed at 60 Mc/s due to overlapping of the resonances of the several CH_2 groups, but in all of them the pattern of the formyl proton signal can be easily accounted for by the assumed interactions. The accompanying table gives the average values of the observed splittings (couplings), with a probable error of about 0.05 c.p.s.

<i>R</i>	J_{OCH-OR_1} c/s ($R_1 = CH_3\alpha, CH_2\alpha$)	J_{OCH-R_2} c/s ($R_2 = CH_3\beta, CH_2\beta, CH\beta$)
CH_3	0.85	—
C_2H_5	0.85	0.57
<i>n</i> - C_3H_7	0.88	0.62
<i>n</i> - C_4H_9	0.80	0.46
<i>iso</i> - C_4H_9	0.93	0.47
Benzyl	0.96	—

H-H couplings in saturated formates.

No long-range interaction across the C-O bond was observed in other alkyl esters, viz. acetates, propionates, acrylates and succinates (methyl, ethyl, *n*-propyl, isopropyl, *n*-butyl, isobutyl, vinyl and benzyl derivatives) in the whole range of temperatures between the freezing and boiling point of these substances. No significant change in the spectra with temperature was observed, in agreement with the assumed rigid structures of the alkyl esters [9-11]. (Though in contradiction with sound absorption measurements [12, 13] which correlate the observed relaxation processes with the presence of rotational isomers.) All these results, which point to the formyl group as responsible for the long-range interaction in some alkyl esters, can be probably related to the partially double bond character of the C-O bond [14, 15].

Useful remarks by the referee are dutifully acknowledged.

REFERENCES

- [1] BANWELL, C. N., and SHEPPARD, N., 1962, *Disc. Faraday Soc.*, **34**, 115.
- [2] KOWALEWSKI, D. G., and KOWALEWSKI, V. J., 1962, *J. chem. Phys.*, **37**, 1009.
- [3] KOWALEWSKI, V. J., and KOWALEWSKI, D. G., 1962, *J. chem. Phys.*, **36**, 266.
- [4] GRONOWITZ, S., and HOFFMAN, R. A., 1959, *Acta chem. scand.*, **13**, 1687.
- [5] LEANE, J. B., and RICHARDS, R. E., 1959, *Trans. Faraday Soc.*, **55**, 518.
- [6] KOWALEWSKI, D. G., 1962, *J. Phys. Radium*, **23**, 255.
- [7] SCHAEFFER, T., 1962, *J. chem. Phys.*, **36**, 2235.
- [8] CAVANAUGH, J. R., and DAILEY, B. P., 1961, *J. chem. Phys.*, **34**, 1094.
- [9] WILMSHURST, J. K., 1957, *J. mol. Spectrosc.*, **1**, 201.
- [10] MARDSEN, R. J. B., and SUTTON, L. E., 1936, *J. chem. Soc.*, p. 1383.
- [11] MIYAZAWA, T., 1961, *Bull. chem. Soc., Japan*, **34**, 691.
- [12] KARPOVICH, J., 1954, *J. chem. Phys.*, **28**, 1767.
- [13] TABUCHI, D., 1958, *J. chem. Phys.*, **28**, 1014.
- [14] CURL, R. F., 1959, *J. chem. Phys.*, **30**, 1529.
- [15] FRAENKEL, G., 1961, *J. chem. Phys.*, **34**, 1466.

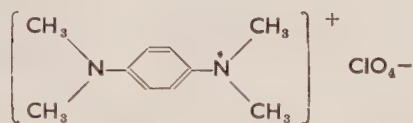
Proton magnetic resonance of Würster's blue perchlorate

by ASAKO KAWAMORI and KEISUKE SUZUKI

Faculty of Science, Kwansei Gakuin University, Nishinomiya,
Japan

(Received 4 January 1964)

Würster's blue perchlorate



has a phase transition as shown by measurement of paramagnetic susceptibility [1] and electron spin resonance [2]. Recently, McConnell *et al.* [3] have observed electron spin resonance of a single crystal of this substance, and shown that below the transition temperature Würster's blue cations form dimers and the observed spectra are due to triplet excitons. In addition, the change of crystal structure was observed by California group [4] and an anomaly in specific heat was also observed [5].

In this note, proton magnetic resonance of powdered Würster's blue perchlorate will be reported which was measured between the room temperature and the liquid nitrogen temperature at the field of 8000 oe. The change of derivative curve of proton resonance with increasing temperature is shown in figure 1 (a) to (c) together with an integrated curve shown in figure 1 (d) corresponding to figure 1 (c). Considering the ratio of areas under the two dotted lines in figure 1 (d), the one at the lower field is to be due to the methyl protons and the other at the higher field to the ring protons.

Then the displacement of the resonance peak can be expressed by:

$$\Delta H = H^* - H_0 = -a(\gamma_e/\gamma_p)\chi_m H_0, \quad (1)$$

where H^* is the observed field, H_0 the one for the reference substance†, and a the hyperfine constant of the proton under consideration. γ_e and γ_p are the gyro-magnetic ratios of an electron and proton, respectively, and χ_m is the paramagnetic susceptibility in e.m.u./mole of this substance.

Using $a_{\text{CH}_3} = +6.76$ gauss and $a_{\text{ring H}} = -1.97$ gauss by Bolton *et al.* [6] and $H_0 = 8000$ oe, the splitting of two lines is given by

$$H_{\text{sp}} = 4.12 \times 10^3 \chi_m. \quad (2)$$

Using equation (2) and the values of χ_m obtained by Okumura [1], the values of H_{sp} were calculated at various temperatures and are shown in figure 2 together

† Strictly speaking, protons in benzene should be used as reference, but any other substance may be used for the measurement of the relative splitting. So we used protons in water to which a small amount of copper sulphate had been added.

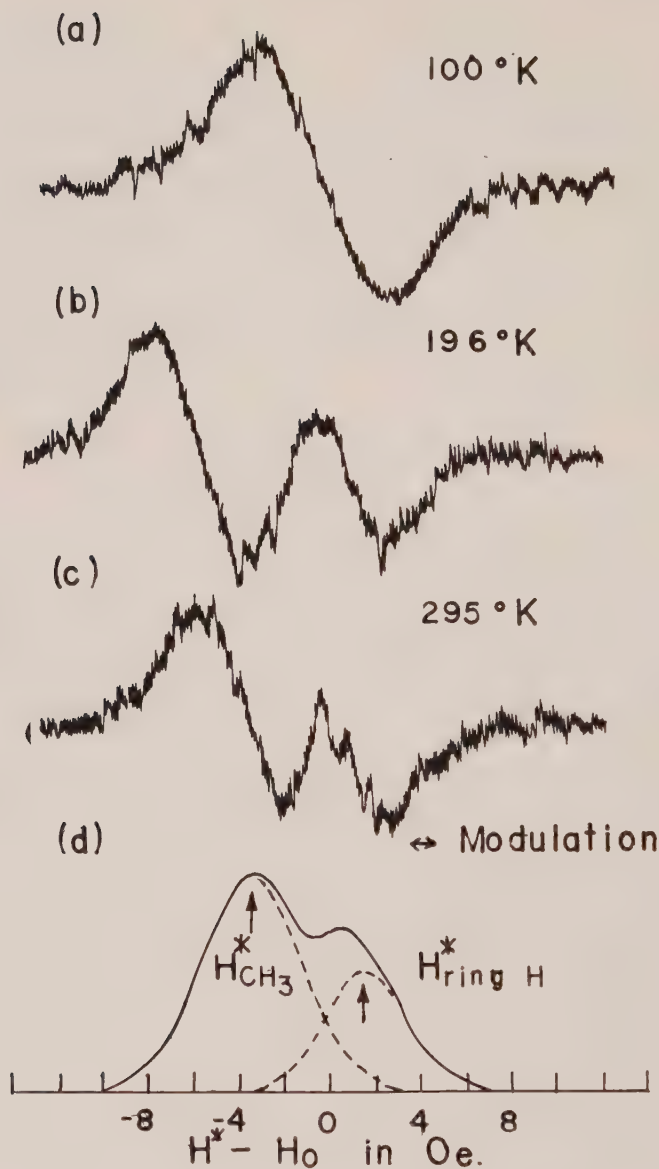


Figure 1. The temperature variation of the line shape. (a) At 100°K only one line is observed. (b) At the transition temperature 196°K the splitting is maximum. (c) At room temperature the splitting decreases a little. (d) The integrated curve corresponds to (c).

with experimental ones. The agreement with the present experiment is fairly good. This shows that the spin density at the protons decreases below the transition temperature. The assumption of the singlet ground state and thermally accessible triplet state postulated by McConnell [3] is confirmed by the present resonance experiments though the temperature range is different.

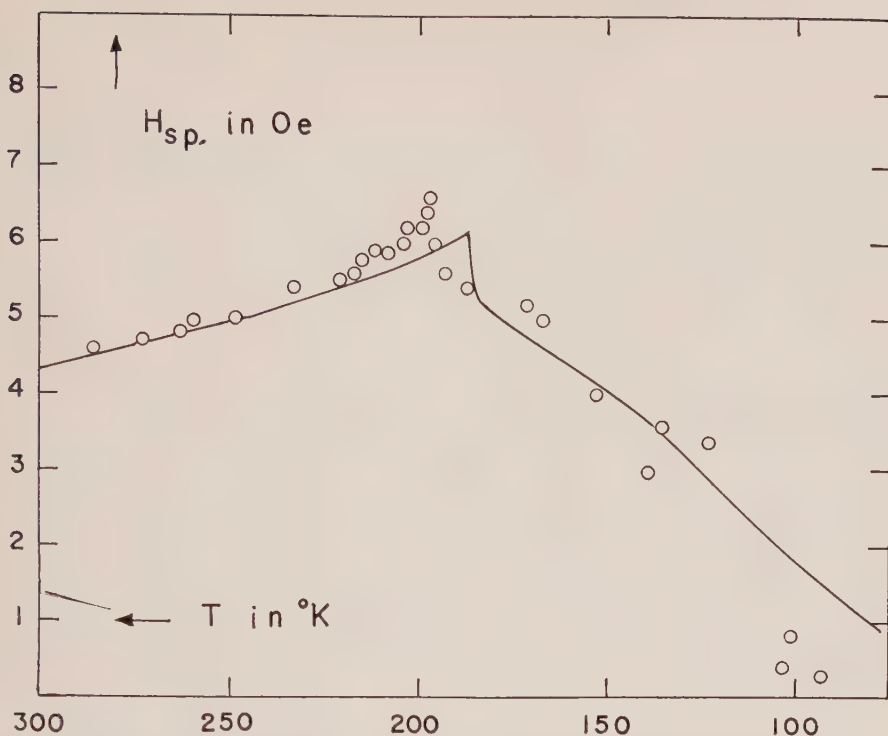


Figure 2. The temperature dependence of the splitting of proton magnetic resonance lines. Solid curve shows calculated values by equation (2) and circles represent experimental values.

Spin-lattice relaxation times have been measured at various temperatures. It is almost constant down to the transition temperature, where it shows a discontinuity, and then gradually increases. The observed result above the transition temperature is consistent with the assumption that the spin-lattice relaxation occurs through hyperfine interaction. Further work is now in progress and will be published elsewhere.

The authors wish to express their thanks to Professor Y. Ooshika at this Faculty for useful discussions and also to Professor J. Itoh at Osaka University for his continuous encouragement of this work.

REFERENCES

- [1] DUFFY, W., Jr., 1962, *J. chem. Phys.*, **36**, 490. OKUMURA, K., 1963, *J. phys. Soc., Japan*, **18**, 69.
- [2] RHODES, R. S., BURGESS, J. H., and EDELSTEIN, A. S., 1961, *Phys. Rev. Letters*, **6**, 462.
- [3] MCCONNELL, H. M., POOLEY, D., and BRADBURY, A., 1962, *Proc. nat. Acad. Sci., Wash.*, **48**, 1480. THOMAS, D. D., KELLER, H., and MCCONNELL, H. M., 1963, *J. chem. Phys.*, **39**, 2321.
- [4] Room temperature structure by Turner and Albrecht, and low temperature structure by Hughes and Kamb (unpublished works) cited in reference [3].
- [5] SUZUKI, K., KAWAMORI, A., and MITSUDO, H., Annual Meeting of Chemical Society, Japan, April 1963.
- [6] BOLTON, J. R., CARRINGTON, A., and DOS SANTOS-VEIGA, J., 1962, *Mol. Phys.*, **5**, 615.

Association between pyrazine anions and sodium ions

by N. M. ATHERTON and A. E. GOGGINS

Department of Chemistry, The University, Sheffield, 10

(Received 3 February 1964)

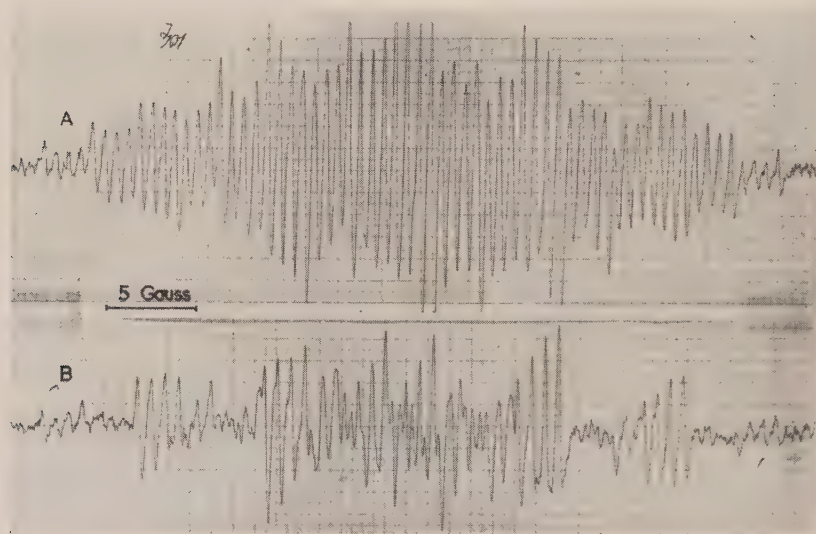
It is well known that when the anions of some aromatic compounds are prepared by reaction with alkali metals in solvents such as tetrahydrofuran the E.S.R. spectra show a hyperfine splitting arising from hyperfine interaction with the metal nucleus, and this extra splitting is accepted as evidence of ion-pair formation. Several observations of this phenomenon have been recorded in the literature, although few cases have been studied in detail. It seemed to us reasonable that the structure of such ion-pairs would be largely determined by the charge distribution in the anion, and that the cation would be located near regions of high negative charge density. Seeking evidence to support this view we have examined the E.S.R. spectra of the pyrazine-sodium-tetrahydrofuran system over a range of temperature.

Pyrazine was chosen for study because it was known to form ion-pairs [1] and the Hückel orbitals (with $\alpha_N = \alpha_C + 0.75\beta$), which are adequate for explaining the E.S.R. spectrum of the 'free' anion [1], predict negative charge densities of 0.45 on each nitrogen atom. The figure (A) shows the spectrum of the ion-pair at -30°C : the quartet structure from hyperfine interaction with ^{23}Na ($I=3/2$) is clearly visible. On cooling the sample the spectrum shows a marked 'line-width alternation' effect, illustrated in the figure (B) for -68°C . The ^{23}Na hyperfine splitting remains constant at 0.68 gauss between room-temperature and -68°C , in contrast to other ion-pairs [2, 3]. At still lower temperatures the spectrum begins to sharpen up again but becomes very complex.

The appearance of the spectrum at -68°C is readily understood in terms of an intramolecular exchange analogous to that postulated by de Boer and Mackor for pyracene-sodium ion pairs [3]. In pyrazine the line width alternation is consistent with the sodium ion 'hopping' from the vicinity of one nitrogen atom to that of the other. Such a process gives rise to the effect provided that the nuclear spins do not relax during an exchange and that the presence of a sodium ion, near a nitrogen atom in the 1 position for example, perturbs the spin distribution sufficiently for the ^{14}N hyperfine couplings to become different, and for the coupling to the protons in the 2,6-positions to become different from that to the 3,5-protons. The breadth of a hyperfine component will then be sensitive to the rate of the exchange if the radical from which it derives is taken into a different nuclear spin state by the exchange. Formal theories of this result have been given by Carrington [4], and by Freed and Fraenkel [5].

If the foregoing view of the situation is correct the spectrum at very low temperatures should show hyperfine splitting from two non-equivalent ^{14}N nuclei, two pairs of protons and a ^{23}Na nucleus. The spectra we obtain appear

to be complicated by the superposition of the 'free' anion spectrum and as yet we have not achieved a satisfactory interpretation.



A: E.S.R. spectrum of pyrazine anion, prepared with sodium in tetrahydrofuran, -30°C ;
B: spectrum at -68°C .

It is clear that a proper quantitative analysis of this sort of observation will yield some explicit information about the structure of ion-pairs and such knowledge will be of value in testing theoretical models. We are at present engaged on a thorough analysis of this and similar systems and will report our results in due course.

We thank the D.S.I.R. for providing the Varian E.S.R. spectrometer on which the spectra were obtained, and for a Research Studentship to A. E. G.

REFERENCES

- [1] CARRINGTON, A., and SANTOS-VEIGA, J. DOS, 1962, *Mol. Phys.*, **5**, 21.
- [2] ATHERTON, N. M., and WEISSMAN, S. I., 1961, *J. Amer. chem. Soc.*, **83**, 1330.
- [3] DE BOER, E., and MACKOR, E. L., 1963, *Proc. chem. Soc.*, p. 23.
- [4] CARRINGTON, A., 1962, *Mol. Phys.*, **5**, 425.
- [5] FREED, J. H., and FRAENKEL, G. K., 1963, *J. chem. Phys.*, **39**, 326.

An electron spin resonance study of proton transfer equilibria involving the pyrogallol semiquinone radical

by A. CARRINGTON and I. C. P. SMITH

Department of Theoretical Chemistry, University of Cambridge

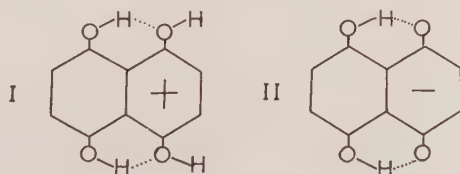
(Received 13 January 1964)

The electron spin resonance spectrum of the pyrogallol semiquinone radical has been measured in aqueous solutions of varying pH, a rapid flow system being employed for production of the radicals. Distinct spectra are obtained from species possessing two, one and zero hydroxyl protons and the first and second acid dissociation constants of the pyrogallol radical cation are estimated. It is possible to set upper limits on the rate of hydroxyl proton exchange between the radical species and the solvent.

1. INTRODUCTION

Semiquinone free radicals have been studied extensively by electron spin resonance. In strongly alkaline solution they exist as anion radicals, are quite stable, and give intense well-resolved spectra [1-3]. Many semiquinones are equally stable in concentrated sulphuric acid and again give well-resolved spectra but with additional hyperfine splitting from protons attached to the oxygen atoms [4, 5]. Until very recently, however, no studies in neutral or near-neutral solution have been reported. The simple para and ortho semiquinone radicals presumably exist largely as uncharged species and their lifetimes in solution are very much reduced. The introduction of rapid flow techniques makes their detection possible, however, and Piette [6] has indeed managed to obtain a resolved spectrum from the *p*-benzosemiquinone neutral radical.

Our interest in ortho semiquinones has been stimulated by earlier studies of the semiquinone radical derived from naphthazarin [7]. If naphthazarin is dissolved in concentrated sulphuric acid the radical cation (I) is formed and its electron resonance spectrum at room temperature shows hyperfine splitting from four equivalent ring protons and two distinct pairs of hydroxyl protons. Two separate hydroxyl proton splittings are observed because of the opportunity for internal hydrogen bonding as indicated in (I). At higher temperatures the four hydroxyl protons give equal splittings and from a study of the temperature dependence of the spectrum it was found possible to estimate the hydrogen bond energy.



In alkaline solution the radical anion (II) is evidently the predominant species since the electron resonance spectrum shows hyperfine splitting from four equivalent ring protons and just two equivalent hydroxyl protons [8]. The interpretations of the spectra in both acid and alkaline solutions were confirmed by appropriate deuterium substitution experiments.

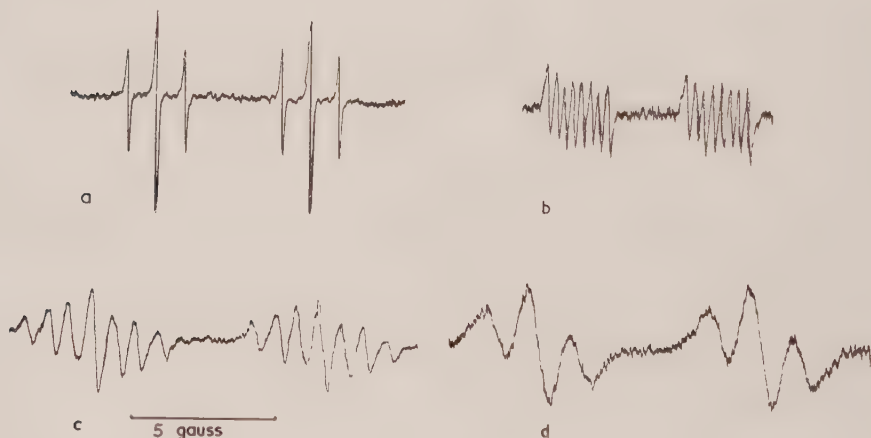
The results described in this paper are quite closely related to those described for the naphthazarin radical ions. We have studied the semiquinone radical produced by one-electron oxidation of pyrogallol (1,2,3-trihydroxybenzene) in aqueous solution. By using a flow technique for radical generation we have been able to vary the pH of the solution at will and study the corresponding changes in the spectra.

2. EXPERIMENTAL METHOD

We have made use of the technique developed by Dixon and Norman [9], two aqueous solutions being mixed and flowed through a cell similar to the one they describe. One solution contained titanous ion at a concentration of 10^{-3} M, the other containing hydrogen peroxide (10^{-3} M) and pyrogallol (0.02 M). Varying amounts of sulphuric acid were added to the solution and a flow rate of 5 ml per second was used. The electron resonance spectra were recorded using a Varian 100 kc E.P.R. spectrometer in conjunction with a Varian 6 in. magnet.

3. ANALYSIS AND INTERPRETATION OF THE SPECTRA

Four quite distinct spectra are observed depending on the acidity of the solution. In strongly alkaline solution ($\text{pH} \sim 14$) the spectrum shown in the figure (a) is obtained and is due to the radical dianion (III). This spectrum has been studied before and is readily analysed in terms of a doublet splitting due to the proton attached at position 5 and a triplet splitting from the two equivalent ring protons at positions 4 and 6.

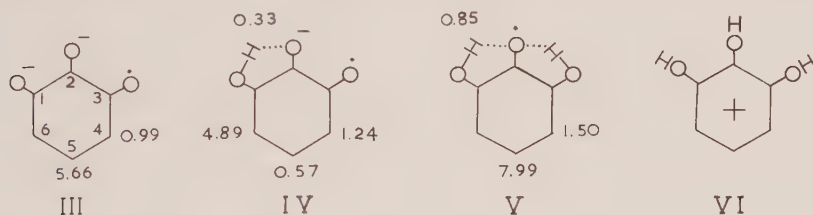


In the pH range 6.5–8.0 the spectrum shown in the figure (b) is observed. It consists of 16 equally intense lines, divided into two groups, which clearly arise from hyperfine interaction involving four inequivalent protons. If the pH is further lowered below 6.5 a quite different spectrum is observed; this is

shown in the figure (*c*) and arises from a large doublet splitting (7.99 gauss) and two smaller triplet splittings (1.50 and 0.85 gauss). As the concentration of sulphuric acid is increased still further, spectrum (*c*) becomes less well-resolved and eventually consists of only six lines (*d*), arising from a doublet (8.05 gauss) and a triplet (1.52 gauss) splitting.

We interpret the spectra (*a*, *b*, *c*) in terms of the radical structures (III), (IV) and (V) respectively, assigning the proton coupling constants as shown. In the case of radical (III) the assignment is unambiguous, in case (V) there are strong reasons for the assignment proposed which we will discuss a little later; in case (IV), however, the assignment is very uncertain.

It is usually possible to successfully interpret the splitting constants of aromatic radicals in terms of molecular orbital theory. The radical studied here is, however, somewhat exceptional in being an odd-alternant radical for which the simple theory is unlikely to be adequate. Indeed, Vincow and Fraenkel [10] in an exhaustive theoretical study of semiquinone anions were unable to account for the splitting constants of radical (III), although they were quite successful with all other simple para and ortho semiquinones. An adequate molecular orbital treatment of the pyrogallol anion would have to include configuration interaction and in view of the large number of parameters involved, we have not attempted such a calculation. Valence bond theory suffers from similar complications but lends itself more readily to qualitative discussion, in which we shall engage later.

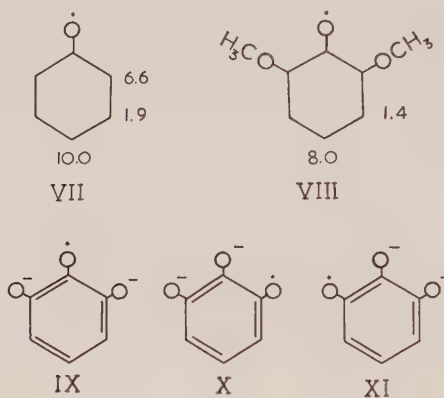


Let us first consider radical (V). The electron resonance spectrum shows that the two hydroxyl protons are equivalent, indicating that the radical possesses a two-fold symmetry axis, unlike species (IV). Moreover the ring proton splitting constants observed for (V) appear quite reasonable in the light of other data. We cite the phenoxy radical (VII) and the 2,6-dimethoxyphenoxy radical (VIII), the proton hyperfine splittings for which are shown below [11]. The comparison between (V) and (VIII) is particularly relevant since the hydroxy and methoxy groups are likely to have rather similar effects on the spin density distribution within the aromatic ring.

The change in spectrum passing from (*c*) to (*d*), brought about by further increasing the acidity, is readily understood. The fact that we observe hydroxyl proton structure from (V) means that the rate of proton exchange with the solvent is relatively slow. This in turn suggests that hydrogen bonding is important since, in other cases where internal hydrogen bonding is not possible, we have been unable to observe such hyperfine structure (see below). However, on further lowering of the pH the rate of hydroxyl proton exchange between (V) and the solvent becomes greater than the hyperfine splitting interval ($2.38 \times 10^6 \text{ sec}^{-1}$). Hence the triplet structure due to the hydroxyl protons is lost; the ring proton splittings however remain essentially the same. The spectrum observed at high acid

concentrations must depend upon the position of equilibrium between radicals (V) and (VI). Thus spectrum (*d*) very likely corresponds to the situation in which the equilibrium strongly favours radical (V), especially since the ring proton splittings are only slightly changed. The matter would be settled if one could observe the spectrum of (VI), complete with hydroxyl proton splitting. With this in mind we have examined the spectrum in concentrated sulphuric acid; unfortunately only a single broad unresolved line was obtained.

The spectrum shown in the figure (*b*) is in many ways the most interesting. There can be little doubt about the interpretation in terms of radical (IV), although the assignment of the four splitting constants is open to question; however we have our reasons for assigning the largest splitting to the proton at position 6. Suppose we were interpreting the results for radical (III) in terms of valence bond theory, using only resonance structures without long bonds. Assuming we further confine ourselves to structures in which the two negative charges are located on oxygen atoms, three different types of structure, shown below, are possible, there being five of each.



In the case of radical (III) each type of structure makes important contributions to the ground state resonance hybrid. However, addition of one proton at the O_1 position will lower the energy of structure (X), relative to (IX), so that its contribution to the ground state is increased. Hence, by analogy with the results for the phenoxy radical, one would expect to find the largest ring spin density para to the oxygen atom not involved in hydrogen bonding, i.e. position 4. Similar considerations are involved for a proton attached to O_3 .

By noting the precise pH at which spectrum (*c*) changes to (*b*) we are able to determine the second acid dissociation constant of the pyrogallol radical cation quite accurately. For the reasons given earlier we can only obtain an approximate estimate for the first dissociation constant. The values are given below and are compared with the corresponding dissociation constants measured for pyrogallol itself by Abichandani and Jatkar [12]. As one would expect the radical is a considerably stronger acid:

pyrogallol	$K_1 = 9.68 \times 10^{-10}$,	$K_2 = 2.30 \times 10^{-12}$,
pyrogallol radical cation	$K_1 \sim 10^{-2}$,	$K_2 = 4 \pm 2 \times 10^{-7}$.

We have studied a number of other radicals formed by oxidation of polyhydroxybenzenes and in each case the electron resonance spectrum is markedly

pH dependent. In all other cases examined so far, however, we do not observe hyperfine splitting from hydroxyl protons. With catechol anomalous line width variations are observed and we are in the process of analysing these changes to obtain the equilibrium constants for the various proton dissociation equilibria. It is already clear that internal hydrogen bonding is much less important, so that hydroxyl proton exchange with the solvent is fast enough to broaden the spectrum.

I. C. P. Smith gratefully acknowledges the award of a Shell International Post-Graduate Studentship. We thank the D.S.I.R. for financial assistance towards the purchase of equipment.

REFERENCES

- [1] VENKATARAMAN, B., and FRAENKEL, G. K., 1955, *J. Amer. chem. Soc.*, **77**, 2707.
- [2] WERTZ, J. E., and VIVO, J., 1956, *J. chem. Phys.*, **24**, 479.
- [3] HOSKINS, R., 1955, *J. chem. Phys.*, **23**, 1975, 2461.
- [4] BOLTON, J. R., and CARRINGTON, A., 1961, *Proc. chem. Soc.*, p. 385.
- [5] BOLTON, J. R., CARRINGTON, A., and VEIGA, J. S., 1962, *Mol. Phys.*, **5**, 285.
- [6] PIETTE, L. H., 1963 (personal communication).
- [7] BOLTON, J. R., CARRINGTON, A., and TODD, P. F., 1963, *Mol. Phys.*, **6**, 169.
- [8] FREED, J. H., and FRAENKEL, G. K., 1963, *J. chem. Phys.*, **38**, 2040.
- [9] DIXON, W. T., and NORMAN, R. O. C., 1963, *J. chem. Soc.*, p. 3119.
- [10] VINCOW, G., and FRAENKEL, G. K., 1961, *J. chem. Phys.*, **34**, 1333.
- [11] KOLKER, P. L., STONE, T. J., and WATERS, W. A., 1963, Proceedings of the Sixth International Symposium on Free Radicals, Cambridge.
- [12] ABICHANDANI, C. T., and JATKAR, S. K. K., 1938, *J. Indian Inst. Sci. A*, **21**, 417.

The statistical mechanics of systems with steep intermolecular potentials

by J. S. ROWLINSON

Department of Chemical Engineering and Chemical Technology, Imperial College of Science and Technology, London, S.W.7

(Received 17 February 1964)

The classical configurational free-energy of a system of molecules with steep intermolecular potentials is obtained from that of a system of hard spheres by an expansion in powers of n^{-1} , where n is a measure of the steepness of the potential. It is shown that the free energy can be obtained explicitly and exactly to the order of n^{-1} . Higher terms have non-thermodynamic coefficients. The first-order term yields an excellent equation of state for gases at high temperatures and densities. It can also be used to calculate the course of the melting line of monatomic close-packed solids at high pressures in terms of the parameters of the repulsive potential. It is shown, subject only to the neglect of terms of the order of n^{-2} , that there is no solid-fluid critical point for molecules with continuous but steep repulsive potentials.

1. INTRODUCTION

The equilibrium properties of a classical system of hard spherical molecules are now well-known, and the information available can be summarized, as follows. The first four coefficients of the virial expansion of the pressure are known exactly [1], the fifth coefficient has been obtained by direct calculation [2, 3], and the sixth by a Monte Carlo calculation [4]. Computers have been used to determine the pressures at higher densities and these calculations have shown that there is a first-order transition to an ordered or solid state at a high density [5, 6]. The asymptotic form of the equation of state of the solid phase at high pressure is almost certainly the simple free-volume equation [7].

The purpose of this paper is to use these known results as the starting-point for a calculation of the properties of a system in which the intermolecular potentials vary rapidly but continuously with separation. The partition function of the unknown assembly of soft spheres is obtained by a Taylor expansion from that of the known assembly of hard spheres. The expansion is made with respect to the reciprocal of a parameter that measures the steepness of the potential. The method resembles that by which Longuet-Higgins [8] obtained the partition function of a mixture of similar molecules from the presumed-known partition function of one of the pure components.

2. THE INTERMOLECULAR POTENTIALS

This treatment is not restricted to any particular class of potential, except by the incidental difficulties of calculating integrals. Four are used here, namely:

(1) The Lennard-Jones ($n, \frac{1}{2}n$) potential:

$$u(R) = \epsilon(R/R_m)^{-n} - 2\epsilon(R/R_m)^{-n/2}. \quad (2.1)$$

(2) The inverse-power potential:

$$u(R) = \epsilon (R/R_m)^{-n}. \quad (2.2)$$

(3) The exponential potential:

$$u(R) = \epsilon \exp \left[n \left(1 - \frac{R}{R_m} \right) \right]. \quad (2.3)$$

(4) A logarithmic potential:

$$\left. \begin{aligned} u(R) &= \epsilon \ln (R/R_m)^{-n}, & R < R_m, \\ u(R) &= 0, & R > R_m, \end{aligned} \right\} \quad (2.4)$$

where ϵ and R_m are characteristic energies and distances. The first three potentials call for no comment; the fourth has been chosen since it is everywhere positive or zero and yet can be made to fit (2.1) for values of R equal to and slightly less than the collision diameter σ , where $u(\sigma) = 0$ in (2.1), and where R_m of (2.4) is hence taken to be equal to σ of (2.1).

All these potentials reduce to that of a hard sphere as n becomes infinite, but there is no unique diameter of this sphere for two of the potentials. That is, it is possible to vary both ϵ and R_m in (2.2)–(2.3) in such a way as to leave the soft potential unchanged, whilst changing the hard potential, which is determined by R_m only. The results obtained below are independent of the individual values of ϵ and R_m , and depend only on the combinations that enter into (2.2)–(2.3).

The reduced variables:

$$r = R/R_m, \quad (2.5)$$

$$x = \tau^{-1} = \epsilon/kT, \quad (2.6)$$

are used throughout.

3. THE PARTITION FUNCTION

The configurational partition function of a classical assembly of N molecules between which there are pair potentials is:

$$Q = \frac{1}{N!} \int \dots \int \exp \left[- \sum_{i>j} u(R_{ij})/kT \right] d\mathbf{R}_1 \dots d\mathbf{R}_N. \quad (3.1)$$

Let $u(R_{ij})$ be given by (2.1) and differentiate Q with respect to n^{-1} . The integrand of (3.1) is the product of $N(N-1)/2$ identical factors. Hence

$$\begin{aligned} \left(\frac{\partial Q}{\partial n^{-1}} \right)_{N, V, T} &= \frac{-n^2 x}{2(N-2)!} \int \dots \int \ln r_{12} (r_{12}^{-n} - r_{12}^{-n/2}) \\ &\quad \times \exp \left[- \sum_{i>j} u_{ij}/kT \right] d\mathbf{R}_1 \dots d\mathbf{R}_N. \end{aligned} \quad (3.2)$$

Introduce the radial distribution function $g(r_{12})$:

$$g(r_{12}) = \frac{V^2}{QN^2(N-2)!} \int \dots \int \exp \left[- \sum_{i>j} u_{ij}/kT \right] d\mathbf{R}_3 \dots d\mathbf{R}_N \quad (3.3)$$

and integrate over $d\mathbf{R}_2$ to give:

$$\frac{\partial \ln Q}{\partial n^{-1}} = - \frac{2\pi N R_m^3}{V} n^2 x N \int_0^\infty \ln r (r^{-n} - r^{-n/2}) g(r) r^2 dr. \quad (3.4)$$

This integral vanishes as n^{-2} when n^{-1} approaches zero. The integrand is everywhere zero for large n except for $r \approx 1$. Now $g(r)$ has a discontinuity at $r = 1$,

for $n^{-1}=0$, but this can be removed by taking out a factor of $\exp[-u(r)/kT]$. That is, a function $y(r)$ defined by:

$$g(r) = y(r) \exp[-u(r)/kT], \quad (3.5)$$

is a smooth function of r , V and T even at $r=1$. Explicit expressions for $y(r)$ can be obtained by expansion in powers of the density [9], or, in principle, $y(r)$ can be written as a polynomial in r^2 [10]. Substitute (3.5) into (3.4), remove $y(1)$ from the integral and change the variable of integration from r to $r^{-n}=z$:

$$\frac{\partial \ln Q}{\partial n^{-1}} = \frac{2\pi N R_m^3}{V} N x y(1) \int_0^\infty z^{-3/n} \ln z (1 - z^{-1/2}) \exp(-xz) \exp(+2xz^{1/2}) dz. \quad (3.6)$$

The factor $z^{-3/n}$ becomes unity on letting n^{-1} become zero. The integral can be evaluated by expanding the second exponential factor to give:

$$\sum_{j=0}^{\infty} \frac{(2x)^j}{j!} \int_0^\infty z^{j/2} \exp(-xz) \ln z (1 - z^{-1/2}) dz. \quad (3.7)$$

Now

$$\int_0^\infty z^l \exp(-xz) \ln z dz = \frac{d}{dl} \int_0^\infty z^l \exp(-xz) dz, \quad (3.8)$$

$$= \frac{d}{dl} [x^{-l-1} l!], \quad (3.9)$$

$$= x^{-l-1} l! [\Psi'(l) - \ln x], \quad (3.10)$$

where $\Psi'(l)$ is the logarithmic derivative of the factorial function [11, 12]. Hence (3.7) becomes:

$$\sum_{j=0}^{\infty} 2^j x^{j/2-1} \frac{(j/2)!}{j!} \left[\Psi' \left(\frac{j}{2} \right) - \ln x \right] - \sum_{j=0}^{\infty} 2^j x^{j/2-1/2} \frac{(j/2-\frac{1}{2})!}{j!} \left[\Psi' \left(\frac{j}{2} - \frac{1}{2} \right) - \ln x \right]. \quad (3.11)$$

All but the first term in $\ln x$ can be cancelled by re-grouping the two sums so that the terms with $j=i+1$ in the first are taken with $j=i$ in the second. The two sums can now be combined by using the initial value and recurrence relation for Ψ' [11]:

$$\Psi'(0) = -\gamma, \quad \Psi'(l) = \Psi'(l-1) + l^{-1}, \quad (3.12)$$

where γ is Euler's constant. The result is:

$$-\frac{1}{x} \left[\ln x + \gamma - \sum_{k=1}^{\infty} \frac{(\frac{1}{2}k-1)! (2x^{1/2})^k}{k!} \right] = -\frac{1}{x} [\ln x + F(x)], \quad (3.13)$$

where $F(x)$, defined by (3.13), is a function previously used and tabulated in a discussion of the equation of state of Percus and Yevick for a system of Lennard-Jones molecules [13]. Hence, from (3.6):

$$\left(\frac{\partial \ln Q}{\partial n^{-1}} \right)_{n=\infty} = -\frac{2\pi N R_m^3}{V} N y(1) [\ln x + F(x)]. \quad (3.14)$$

The function $y(1)$ is related directly to the pressure in an assembly of hard spheres:

$$(pV)_{n=\infty} = RT + \left(\frac{2\pi N R_m^3}{3V} \right) RT y(1). \quad (3.15)$$

Hence

$$\left(\frac{\partial A}{\partial n^{-1}} \right)_{\infty} = -kT \left(\frac{\partial \ln Q}{\partial n^{-1}} \right)_{\infty} = 3[\ln x + F(x)] (pV - RT)_{\infty}, \quad (3.16)$$

where A is the molar configurational Helmholtz free-energy. Taylor's expansion now gives:

$$A_n\{V, T\} = A_\infty\{V, T\} + \frac{3}{n} [\ln x + F(x)](pV - RT)_\infty + O(n^{-2}). \quad (3.17)$$

This equation can be written in a neater form by introducing the reduced length:

$$\rho = x^{1/n} [1 + n^{-1}F(x)], \quad (\text{for (2.1)}), \quad (3.18)$$

when (3.17) can be expressed:

$$A_n\{V, T\} = A_\infty\{V\rho^{-3}, T\} - 3RT \ln \rho. \quad (3.19)$$

This equation is, of course, valid only to terms of the order of $(\rho - 1)$ on expansion around $\rho = 1$. Its form is the same as that of the equation that represents the effect of a change of molecular size on the free energy of a conformal assembly; for example, (4.15) of the paper by Longuet-Higgins [8], in which g^{-1} is equivalent to ρ in (3.19). The physical consequences of the two equations are very different since g is a true molecular constant whilst ρ is a function of temperature.

This result can now be extended to the potentials (2.2)–(2.4). The potential (2.2) is a special case of (2.1):

$$\rho = x^{1/n} [1 + n^{-1}F(0)] = x^{1/n} (1 + \gamma/n), \quad (\text{for 2.2 and 2.3}). \quad (3.20)$$

This equation is obtained again on repeating the analysis for (2.3), whilst the fourth potential yields the simple result:

$$\rho = \left(1 - \frac{1}{nx}\right), \quad (\text{for 2.4}). \quad (3.21)$$

Higher terms in the Taylor expansion could be obtained by repeated differentiation of Q with respect to n^{-1} , but these terms include averages over multi-body distribution functions (3- and 4-body for n^{-2}) which cannot be expressed in terms of thermodynamic functions. Again the position resembles that in the theory of conformal solutions where the second-order terms include averages over the 3- and 4-body distribution functions [14].

4. THE EQUATION OF STATE

The equation of state follows from (3.19):

$$p_n\{V, T\} = \rho^{-3} p_\infty\{V\rho^{-3}, T\}, \quad (4.1)$$

or

$$(pV)_n\{V, T\} = (pV)_\infty\{V\rho^{-3}, T\}. \quad (4.2)$$

The q th virial coefficient, L_q , is given by:

$$(L_q)_n\{T\} = \rho^{3(q-1)} (L_q)_\infty. \quad (4.3)$$

Thus these equations extend to the exact equation of state the results previously obtained [13] for the approximation of Percus and Yevick. Their approximation includes only a selection of the complete set of Mayer's cluster integrals and (4.3) was obtained previously by considering the structure of the selected integrals. The derivation above shows that (4.3) is valid for the whole set of cluster integrals.

The approximation that leads to (3.18), (3.19), (4.1), (4.2) and (4.3) for the potential (2.1) is useful only at high temperatures. It is formally correct to terms in n^{-1} at all temperatures but the higher terms are not small unless x , and so $|F(x)|$, are small. It was found previously that the useful temperature range in the gas

of low density is $x < 0.08$. It is shown below that this can be extended to $x < 0.3$ at densities near the solid-fluid transition.

The numerical comparisons with direct calculations and with experimental results on gases that were made previously [13] are virtually unaltered by the improvement effected in this paper, since the Percus-Yevick approximation yields an excellent equation of state for the gas of hard spheres. However the results of this paper allow these comparisons for the gas phase to be extended to potentials other than (2.1). Moreover the Percus-Yevick approximation has not yet yielded a solution for the solid phase that is found by the machine calculations. This phase is within the scope of this new treatment†.

5. THE MELTING LINE

A system of hard spheres has a transition from gas to solid at a pressure given by:

$$p_{\infty}(\frac{2}{3}\pi R_m^3) = 18 kT, \quad (5.1)$$

in which the number 18 ± 1 is obtained from the machine calculations [5, 6]. For the soft spheres the melting pressure is, from (3.19):

$$p_n\{T\} = \rho^{-3} p_{\infty}\{T\}. \quad (5.2)$$

The energy U_n can be found by differentiating (3.19) and has been tabulated for the potential (2.1) [13]. It is of the order n^{-1} since U_{∞} is zero. It has a simple form for the monotonic potentials (2.2)–(2.4):

$$U_n = \frac{3}{n} (pV - RT)_{\infty} > 0. \quad (5.3)$$

This is correct to n^{-1} but can be improved for (2.2) for which, alone, there is the exact result:

$$U_n = \frac{3}{n} (pV - RT)_n. \quad (5.4)$$

These results suffice to determine the slope of the melting line for (2.2)–(2.4):

$$\frac{d \ln p}{d \ln T} = 1 + \frac{\Delta U}{p \Delta V} = 1 + \frac{3}{n}. \quad (5.5)$$

This slope must lie between 1 and 2 since n must be greater than 3 in a system of central forces. Domb [15] showed that the form of this equation is consistent with the limiting form at high pressure of the widely used empirical equation of Simon [16]:

$$(p/p_*) = (T/T_t)^c - 1, \quad (5.6)$$

where T_t is the temperature of the triple point, and where the pressure p_* and the index c are empirical parameters. The experimental values of c generally lie between 1.2 and 1.5 for pressures up to 10^3 atm, but this pressure is not high enough for a quantitative comparison of (5.5) and (5.6).

† The derivation of the difference $(A_n - A_{\infty})$ in § 3 is given, for simplicity, in a form appropriate to a fluid. The distribution function g is a function of six variables in a crystal, for example, $(\mathbf{R}_1 - \mathbf{R}_2)$ and \mathbf{R}_2 . The integration over R_{12} can be made, as in (3.5) to (3.13), but those over the orientation of the vector $(\mathbf{R}_1 - \mathbf{R}_2)$ and over the position of \mathbf{R}_2 must be deferred from (3.4) to (3.15). The difference $(pV - RT)_{\infty}$ is now given by an integral of $y(r_{12} = 1)$ over these five variables (this follows from equation (30.19) of Hill [23]) and so (3.17) is obtained again, although p , V and T are different in the two phases.

Melting pressures calculated from (5.2) can be compared with those observed for the rare gases. They can be expected to be accurate only at high temperatures since the attractive forces are either neglected completely, as in (3.20) and (3.21), or else are treated only as a weak modification of the repulsive forces, as in (3.18). The logarithmic potential, (2.4), can be fitted to (2.1) for separations just less than the collision diameter by choosing R_m of (2.4) to be equal to σ or $(2^{-2/n}R_m)$ of (2.1), and ϵ of (2.4) to be (2ϵ) of (2.1). This choice gives both potentials the same slope at the point where they become zero, and is made in each of the calculations below.

The following Lennard-Jones potentials are taken from recent reviews [17, 18]:

Helium	$R_m = 2.88 \text{ \AA}$,	$\epsilon/k = 10.8^\circ\text{K}$,	$n = 12$,
Neon	$R_m = 3.09 \text{ \AA}$,	$\epsilon/k = 35.8^\circ\text{K}$,	$n = 12$,
Argon	$R_m = 3.83 \text{ \AA}$,	$\epsilon/k = 119^\circ\text{K}$,	$n = 12$.

Exponential repulsive potentials, (2.3), with parameters from the same source were also tried but were found to yield melting pressures that were very close to those obtained with (2.2) and the parameters above, and are not considered further.

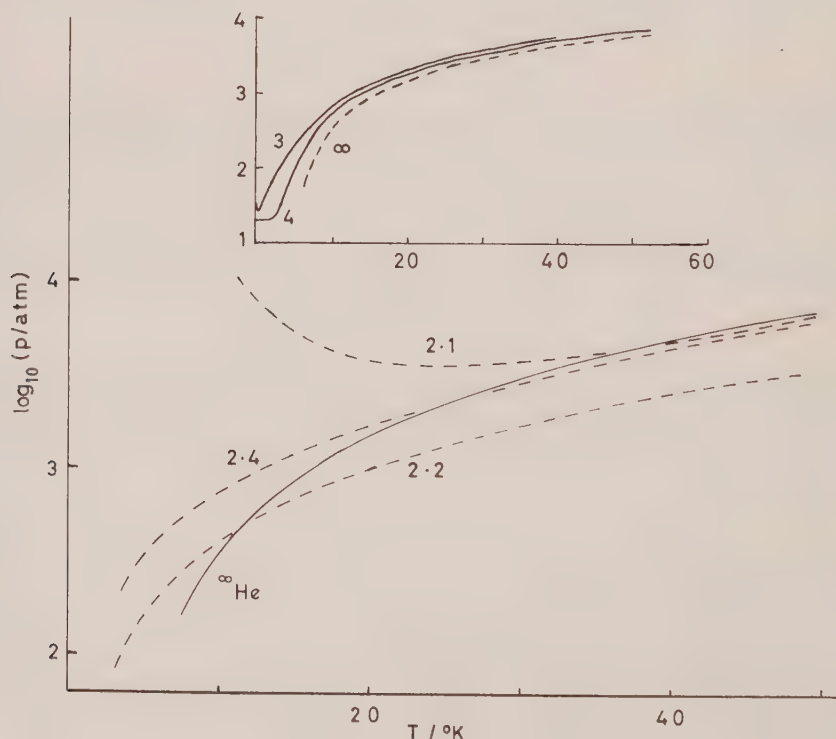


Figure 1. The melting line of helium. The inset shows the experimental results for ^3He and ^4He and the extrapolated curve for helium of infinite mass. The main diagram is a comparison of this extrapolated line with the curves calculated for the potentials (2.1), (2.2) and (2.4).

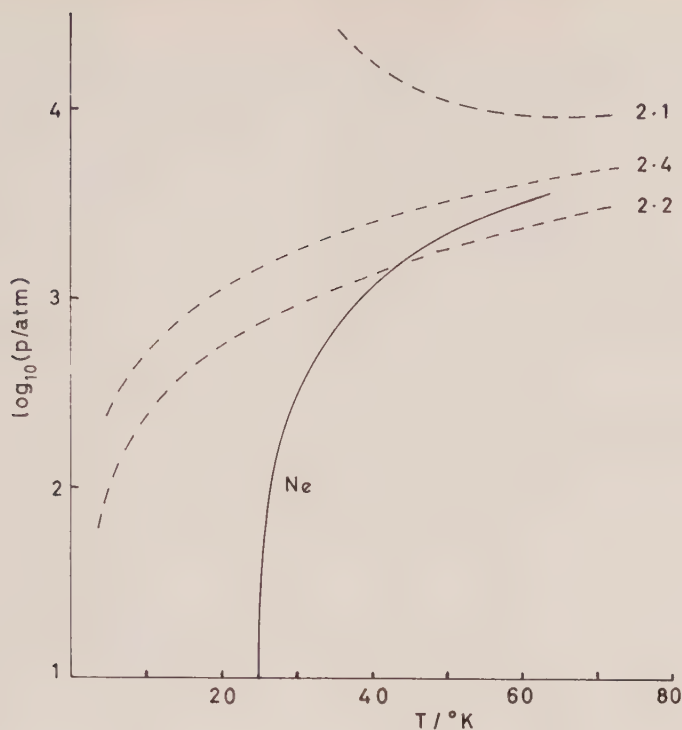


Figure 2. The melting line of neon. The experimental curve is compared with those calculated for the potentials (2.1), (2.2) and (2.4).

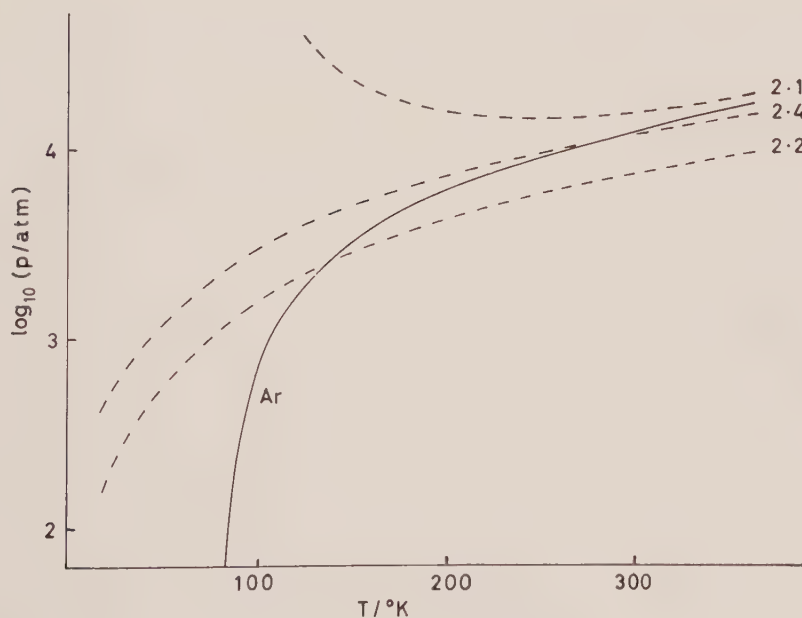


Figure 3. The melting line of argon. The experimental curve is compared with those calculated for the potentials (2.1), (2.2) and (2.4).

Classical statistical mechanics are used in this paper and so the results cannot be applied directly to helium. Fortunately quantal effects produce relatively little change in the melting pressure. The measurements of Mills and Grilly [19] on H_2 , D_2 and T_2 show that $(\ln p)$ is linear in m^{-1} , where m is the molecular mass. They have measured also the melting pressures of ^3He and ^4He and so it is possible to obtain an approximate pressure for He of infinite mass by extrapolation to $m^{-1} = 0$. The melting pressure of ^4He was measured also by Holland *et al.* [20], that of neon has been measured by Mills and Grilly [19] and that of argon by Robinson [21] and by Lahr and Eversole [22].

Figures 1–3 show the comparison of the observed melting lines and those calculated from (2.1), (2.2) and (2.4) with the parameters above. The separation of molecules in the crystal at pressures between 10^3 and 10^4 atm is close to the collision diameter and so it is not surprising that (2.4), which was chosen to fit this region of the potential, gives the best numerical fit with experiment at moderate pressures. The potential (2.2) overestimates the energy at these separations, and so underestimates the pressure, whilst (2.1) deals adequately with the attractive forces only for $x < 0.3$. This is a consequence of the unsatisfactory convergence of the Taylor expansion in n^{-1} when x is not small. The potentials (2.1) and (2.2) must, of course, lead to asymptotically approaching curves as p and T increase. Any one of the potentials (2.1), (2.2) or (2.3) should yield moderately satisfactory melting lines over a range of pressure of 10^4 – 10^6 atm, and hence over a wide range of temperature. Probably (2.1) would be the most accurate in spite of the known imperfections of Lennard–Jones potentials. Above 10^6 atm it is probable that a model based upon additive pair potentials would be inadequate.

6. CONCLUSIONS

The three principal conclusions to which this work leads are, as follows.

(1) The first-order deviation of Q from its value for an assembly of hard spheres is sufficiently complete to yield an excellent equation of state for gases at high pressures and temperatures.

(2) The course of the melting line of a monatomic close-packed solid is determined primarily by the nature and range of the repulsive forces. The attractive forces affect profoundly the shape of the line near the triple point, but the shape at pressures above 5×10^3 atm can be related quantitatively to the parameters of the repulsion potential only.

(3) There is no solid-fluid critical point for an inverse-power or exponential repulsive potential. An assembly of hard spheres has no critical point since its equation of state is of the form $p/T = f(V)$ and hence ΔV remains constant as p and T increase. ΔV will decrease as ρ^3 for an assembly of soft spheres and so becomes zero only at infinite temperature ($x=0$) when ρ is defined by (3.18) or (3.20). The logarithmic potential leads to (3.21) which would give $\Delta V = 0$ at $x = n^{-1}$, but this potential is unrealistic at small separations and hence as x tends to zero.

The validity of this demonstration of the absence of a critical point for potentials (2.1), (2.2) and (2.3) is subject only to the limitations that classical statistical mechanics are adequate and that terms of the order of n^{-2} can be neglected. No other assumption is made. The higher the temperature the better is the first condition satisfied, but there must remain some small uncertainty about the effect of the higher-order terms.

REFERENCES

- [1] VAN LAAR, J. J., 1899, *Proc. Acad. Sci. Amst.*, **1**, 273. BOLTZMANN, L., 1899, *Proc. Acad. Sci. Amst.*, **1**, 398.
- [2] KATSURA, S., and ABE, Y., 1963, *J. chem. Phys.*, **39**, 2068.
- [3] ROWLINSON, J. S., 1964, *Proc. roy. Soc. A*, (in the press).
- [4] REE, F. H., and HOOVER, W. G., 1964, *J. chem. Phys.*, **40**, 939.
- [5] WOOD, W. W., and JACOBSON, J. D., 1957, *J. chem. Phys.*, **27**, 1207.
- [6] ALDER, B. J., and WAINWRIGHT, T. E., 1960, *J. chem. Phys.*, **33**, 1439.
- [7] SALSBERG, Z. W., and WOOD, W. W., 1962, *J. chem. Phys.*, **37**, 798.
- [8] LONGUET-HIGGINS, H. C., 1951, *Proc. roy. Soc. A*, **205**, 247.
- [9] UHLENBECK, G. E., and FORD, G. W., 1962, *Studies in Statistical Mechanics* (Amsterdam: North-Holland Co.), Vol. 1, p. 160.
- [10] WIDOM, B., 1963, *J. chem. Phys.*, **39**, 2808.
- [11] JEFFREYS, H., and JEFFREYS, B. S., 1956, *Methods of Mathematical Physics*, 3rd ed. (Cambridge: University Press), p. 465.
- [12] JAHNKE, E., and EMDE, F., 1945, *Tables of Functions*, 4th ed. (New York: Dover), p. 81.
- [13] ROWLINSON, J. S., 1964, *Mol. Phys.*, **7**, 349.
- [14] BROWN, W. B., 1957, *Proc. roy. Soc. A*, **240**, 561.
- [15] DOMB, C., 1951, *Phil. Mag.*, **42**, 1316.
- [16] SIMON, F., RUHEMANN, M., and EDWARDS, W. A. M., 1929, *Z. phys. Chem.*, **B2**, 340.
- [17] KIHARA, T., 1958, *Adv. Chem. Phys.*, **1**, 267.
- [18] ROWLINSON, J. S., 1959, *Ann. Rep. Prog. Chem.*, **56**, 22.
- [19] MILLS, R. L., and GRILLY, E. R., 1955, *Phys. Rev.*, **99**, 480; 1956, *Ibid.*, **101**, 1246.
- [20] HOLLAND, F. A., HUGGILL, J. A. W., and JONES, G. O., 1951, *Proc. roy. Soc. A*, **207**, 268.
- [21] ROBINSON, D. W., 1954, *Proc. roy. Soc. A*, **225**, 393.
- [22] LAHR, P. H., and EVERSOLE, W. G., 1962, *J. chem. Eng. Data*, **7**, 42.
- [23] HILL, T. L., 1956, *Statistical Mechanics* (New York: McGraw-Hill).

Solvent effects in the electron spin resonance spectrum of fluorenone ketyl

by G. R. LUCKHURST and L. E. ORGEL

Department of Theoretical Chemistry, University Chemical Laboratory,
Lensfield Road, Cambridge

(Received 5 February 1964)

The electron spin resonance spectrum of the fluorenone anion has been measured in mixtures of an alcohol with dimethylformamide. The main dependence of the proton coupling constants on the concentration of alcohol may be understood in terms of an equilibrium between the solvated ketyl and a ketyl-alcohol hydrogen-bonded complex, but a secondary solvent effect must be postulated to account completely for the variation. The changes in spin density in the ketyl on formation of the ketyl-alcohol complex *cannot* be understood using simple Hückel molecular-orbital theory.

1. INTRODUCTION

The electron spin resonance spectra of non-polar radicals are insensitive to the nature of the solvent [1]; in contrast the nuclear hyperfine-coupling constants for polar radicals are often strongly solvent-dependent [2]. The cause of this difference is understood qualitatively [3], but no detailed quantitative studies of the variation of the resonance spectrum with the composition of the solvent have been published. Here we report the solvent-dependence of the electron spin resonance spectrum of the fluorenone anion which we have generated photochemically in binary solvent mixtures of an alcohol and dimethylformamide.

2. ANALYSIS OF THE ELECTRON SPIN RESONANCE SPECTRUM

Unfiltered ultra-violet irradiation of a dilute solution of fluorenone and sodium methoxide in methyl alcohol [4] gave the spectrum (a) shown in figure 1. This spectrum differs drastically from that obtained from a solution of the ketyl prepared by electrolytic reduction in dimethylformamide [5]. The proton hyperfine-coupling constants are very different for the two solutions and, in addition, the spectrum in methyl alcohol solution reveals a triplet separation which is not resolved in the spectrum in dimethylformamide solution (a reconstruction of the latter spectrum is included in figure 1). The spectrum of the ketyl in methyl alcohol differs also from that in ethyl alcohol [4], but the hyperfine-coupling constants are quite similar for the two spectra.

We have now measured the spectrum of the fluorenone anion at 20°C in binary solvent mixtures of methyl or ethyl alcohol with dimethylformamide. In figure 1 we give a selection of the spectra of the ketyl in methyl alcohol-dimethylformamide mixtures; they show how critically the overall appearance of the spectrum depends on the composition of the solvent. Each spectrum is

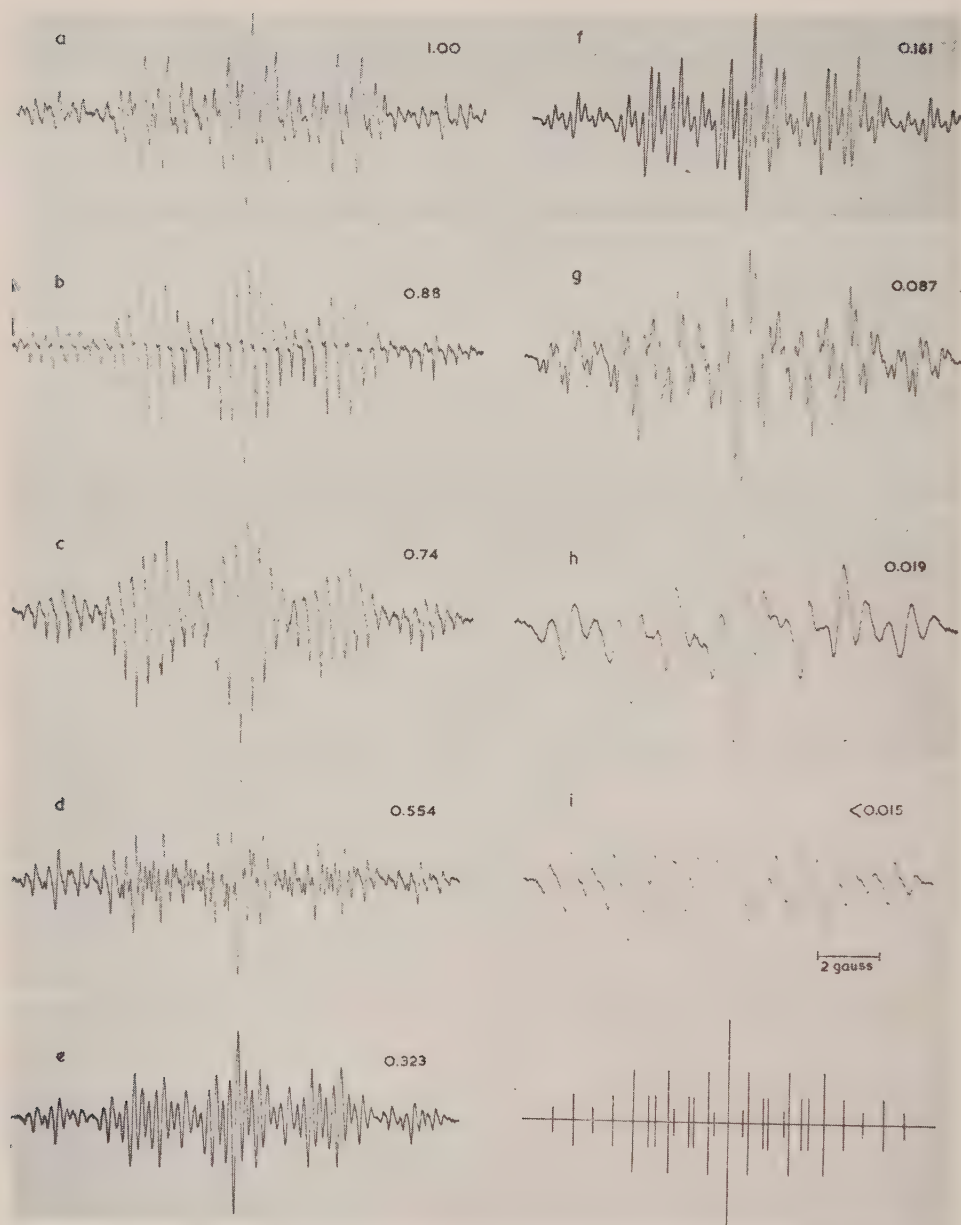


Figure 1. The electron spin resonance spectra of fluorenone ketyl in mixtures of methyl alcohol and dimethylformamide.

readily analysed in terms of four triplet splittings ; the magnitude of each splitting constant varies continuously as the proportion of dimethylformamide in the solvent is changed. The behaviour of the hyperfine coupling constants is similar for ethyl alcohol-dimethylformamide solutions. Our measurements of the spectrum of the ketyl in pure ethyl alcohol agree with those of Ayscough and Wilson [4].

The variation of the coupling constants with the mole fraction of methyl alcohol in the solvent is illustrated in figure 2. It should be noted that the addition of small amounts of methyl alcohol to the dimethylformamide solution causes relatively large increases in three of the four coupling constants. After about 0.1 mole of alcohol has been added the further change in the coupling constants is much more gradual. Our results for ethyl alcohol-dimethylformamide mixtures are very similar.

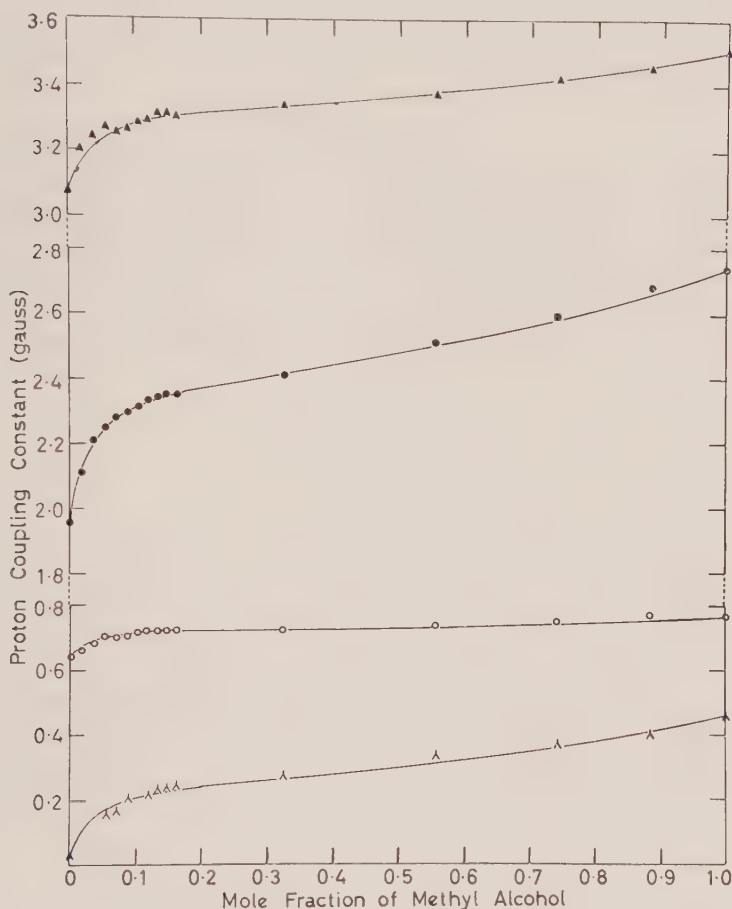


Figure 2. The variation of the proton coupling constants in fluorenone as a function of the mole fraction of methyl alcohol.

3. INTERPRETATION

In accordance with the simple theory [3] we shall suppose that in mixed solvents there is an equilibrium involving solvated ketyl molecules and hydrogen-bonded ketyl-alcohol adducts. To account for the variation of the coupling constants in the range of alcohol concentration 0–0.1 we must suppose that the two species have different hyperfine-coupling constants and that exchange of alcohol is sufficiently rapid to give an averaged spectrum. The variation of the spectrum as the alcohol concentration is increased beyond 0.2 can only be understood if

we postulate that the spectrum of the ketyl-alcohol adduct is solvent dependent, either on account of the formation of a 1:2 adduct or because of some more general solvent effect.

We write the equilibrium constant K as :

$$K = \frac{[XA]}{[XB]} \frac{1-x}{x}, \quad (1)$$

where $[XA]$ and $[XB]$ denote the concentrations of the ketyl-alcohol complex and solvated ketyl respectively and x is the mole fraction of methyl alcohol. Strictly we should use activities throughout but these, unfortunately, are not known. The coupling constants may now be expressed in the form :

$$\bar{a}_i = \frac{(1-x)a_i^s + Kxa_i^c}{1-x+Kx} \quad (2)$$

where a_i^s is the hyperfine coupling constant for the i th proton in the solvated species and a_i^c has the same significance for the hydrogen-bonded complex.

Both a_i^s and a_i^c are solvent-dependent. However, in the small but important range of methyl alcohol concentrations below a mole fraction of 0.1 we may neglect this general solvent dependence and replace a_i^s and a_i^c by the values A_i^s and A_i^c corresponding to solutions in pure dimethylformamide. Thus if we define δ by

$$\delta = \frac{2\bar{a}_i - (A_i^s + A_i^c)}{A_i^s - A_i^c} \quad (3)$$

we have :

$$\delta = \frac{1-x(K+1)}{1+x(K+1)} \quad (4)$$

for sufficiently small x .

Position (assignment due to Dehl and Fraenkel [5])	Coupling constant (gauss) in dimethyl formamide A_i^s	Methyl alcohol		Ethyl alcohol	Concentration equilibrium constant K
		A_i^c (gauss)	$S^i A_i^c$	$S^i A_i^c$	
1	1.96	2.42	0.32	0.26	30.1
2	0.03	0.26	0.20	0.16	
3	3.08	3.34	0.16	0.10	
4	0.65	0.73	0.03	0.03	

We have fitted our results for solutions containing little methyl alcohol to equation (4) using Dehl's values for the hyperfine-coupling constants in pure dimethylformamide [5]. In the table we give the values of A_i^c and the equilibrium constant K . In figure 3 we have plotted δ against the mole-fraction of methyl alcohol; since we have four independent measures of δ at each concentration this is in principle a rigorous test of our assumption of a single equilibrium. In fact only three of the coupling constants are relevant here since the variation to the fourth is too small compared with the experimental errors (for example,

± 3 per cent for the proton coupling constants) in our measurements. Agreement is quite satisfactory provided the points for this last proton (represented by open circles in figure 3) are neglected.

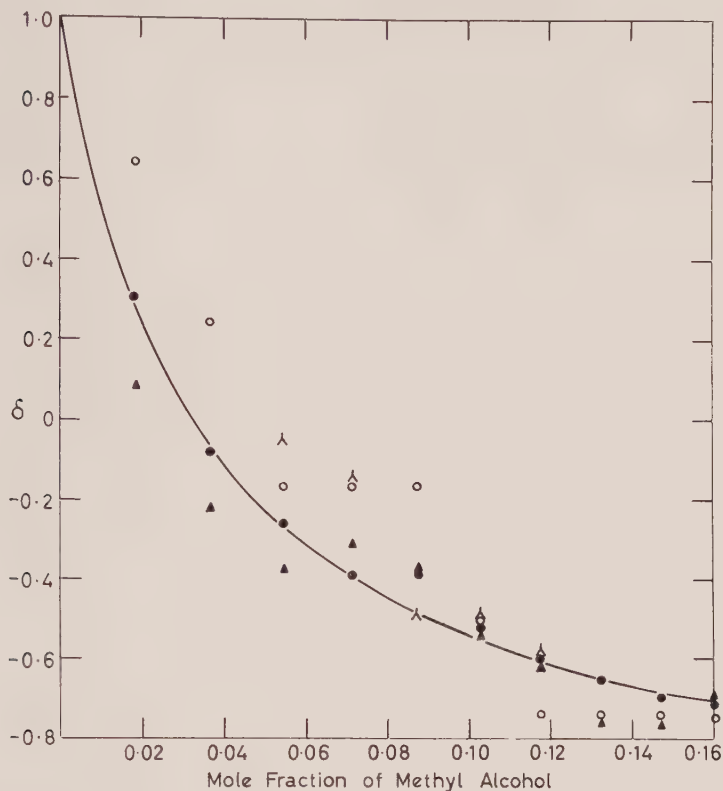


Figure 3. The variation of δ at low concentrations of methyl alcohol.

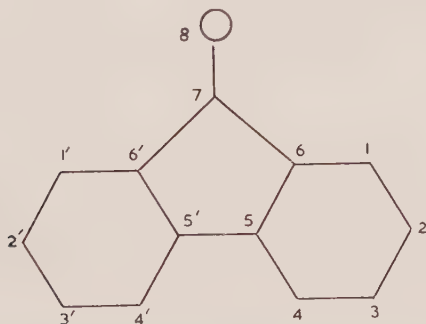


Figure 4. The numbering system in fluorenone.

We must next consider our results for solvents containing much methyl alcohol. Here we have been able to fit the observed coupling constants using the relation :

$$a_i^c = A_i^c(1 + S^2x^2). \quad (5)$$

This relation has no theoretical justification but is convenient since it permits us to write the coupling constant over the whole range of solvent compositions in the form :

$$\bar{a}_i = \frac{(1-x)A_i^s + xKA_i^c(1+S^ix^2)}{1-x+Kx} \quad (6)$$

The values of S^i are obtained from the coupling constants in pure methyl alcohol ; they are given in the table. The full curves in figure 2 have been obtained from equation (6). The excellent agreement with experiment should not be taken too seriously since we have been able to adjust two independent parameters.

Our results for solutions of the ketyl in ethyl alcohol-dimethylformamide mixtures are very similar to those described above. They may be fitted to equation (6) using the same values for A_i^c , A_i^s and K , but different values for the S^i . These are given in the table. It is not unreasonable that the equilibrium between solvated and hydrogen-bonded ketyl molecules should be similar for the two alcohols but that the generalized solvent effect should be different.

An equilibrium constant of 30 at 20°C corresponds to a Gibbs free energy change, ΔG , of about -2 kcal/mole. If we suppose that only a small fraction of this change is due to entropy effects we conclude that, for solutions containing little methyl or ethyl alcohol, the hydrogen bond to the ketyl anion is about 2 kcal/mole stronger than that to dimethylformamide. This value is quite reasonable since strong hydrogen bonds to 'keto' oxygen atoms often have heats of formation a little in excess of 5 kcal/mole.

The absorption lines in the spectra of the ketyl in the pure solvents and in most solvent mixtures are sharp. However, the spectra of solutions in methyl alcohol-dimethylformamide mixtures containing little alcohol (mole fractions less than 0.07) are broad. Part of the effect is undoubtedly due to an unresolved triplet splitting, but we have the impression that this alone cannot account for the poor quality of the spectra. We believe that these observations may indicate that the broadening is not due to electron exchange [6] or to the anisotropy of the g tensor [7, 8], but to fluctuations in spin-density due to formation and dissociation of the hydrogen-bonded complex. We intend to investigate this matter further in simpler systems in the hope that it may provide a way of measuring the rate of formation of hydrogen-bonded complexes.

4. MOLECULAR-ORBITAL CALCULATIONS

In attempting to account for observed spin-densities most authors have used Hückel molecular-orbital theory. In this theory there are a number of parameters, the α 's and β 's for atoms other than carbon, which can be adjusted more or less freely. These are varied systematically until the best fit is obtained [9]. However, Dehl and Fraenkel [5] in their treatment of the fluorenone ketyl used a more complete theory which included some configuration interaction [10]. The assignment adopted in the table is based on their calculations.

We have used simple Hückel theory to calculate the spin-densities in the fluorenone ketyl. The resonance integral for the 5-5' carbon-carbon bond was calculated by the method of Longuet-Higgins and Salem [11] to be 0.8β . The resonance integral for the carbon-oxygen bond was taken as 1.5β and that for the 6-7 carbon bond as 0.9β , values that have frequently been used for ketones [12]. The Coulomb integral α_0 for the oxygen atom was allowed to vary from

α to $\alpha + 2\beta$. In figure 5 we have plotted the spin densities at the different carbon atoms against α_0 ; we write $\alpha_0 = \alpha + \tau\beta$ and plot our calculated spin densities as a function of τ .

It is clear that no assumed pair of values for α_0 in the solvated ketyl and in the ketyl-alcohol complex can account for our experimental findings. All of the hyperfine coupling constants are larger for alcohol solutions while there is no value of α_0 for which the slopes of all of the spin-density curves have the same

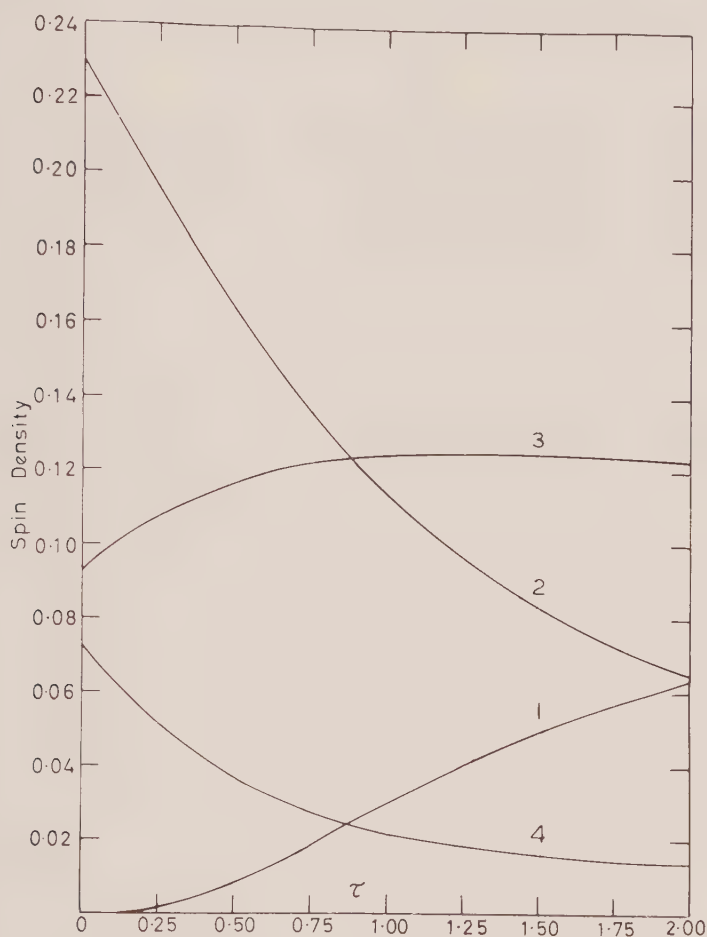


Figure 5. The variation of spin density at positions 1, 2, 3 and 4 in fluorenone as a function of τ .

sign. It is perhaps worth noting that Hückel molecular-orbital calculations do not lead unambiguously to Dehl's assignments, although they are consistent with them. The failure of the simple theory in this case is surprising in view of its success elsewhere; perhaps the non-alternant character of fluorenone is relevant here. The general features of the changes in spin density are also predicted by a configuration interaction calculation of the type described by McLachlan [10, 5].

5. CONCLUSION

We have shown that the variation of the spectrum of the fluorenone ketyl with solvent composition can be understood in terms of the formation of a 1 : 1 hydrogen-bonded complex if a further generalized solvent effect is assumed. Hückel molecular-orbital theory does not account for our observations, perhaps because we are dealing with a non-alternant system.

We are grateful to the B.P. Research Centre at Sunbury-on-Thames for help with the calculations. One of us (G. R. L.) wishes to acknowledge the assistance of a D.S.I.R. studentship.

REFERENCES

- [1] ATHERTON, N. M., and WEISSMAN, S. I., 1961, *J. Amer. chem. Soc.*, **83**, 1330.
- [2] PIETTE, L. H., LUDWIG, P., and ADAMS, R. N., 1962, *J. Amer. chem. Soc.*, **84**, 4212.
- [3] GENDELL, J., FREED, J. H., and FRAENKEL, G. K., 1962, *J. chem. Phys.*, **37**, 2832.
- [4] AYSCOUGH, P. B., and WILSON, R., 1963, *J. chem. Soc.*, p. 5412 ; RUSSELL, G. A., and GEELS, E. J., 1963, *Tet. Lett.*, **20**, 1333.
- [5] DEHL, R., and FRAENKEL, G. K., 1963, *J. chem. Phys.*, **39**, 1793.
- [6] WARD, R. L., and WEISSMAN, S. I., 1954, *J. Amer. chem. Soc.*, **76**, 3612 ; 1957, *Ibid.*, **79**, 2086.
- [7] CARRINGTON, A., and LONGUET-HIGGINS, H. C., 1962, *Mol. Phys.*, **5**, 447.
- [8] FREED, J. H., and FRAENKEL, G. K., 1963, *J. chem. Phys.*, **39**, 326.
- [9] VINCOW, G. A., and FRAENKEL, G. K., 1961, *J. chem. Phys.*, **34**, 1333.
- [10] McLACHLAN, A. D., 1960, *Mol. Phys.*, **3**, 233.
- [11] LONGUET-HIGGINS, H. C., and SALEM, L., 1959, *Proc. roy. Soc. A*, **251**, 172.
- [12] REIGER, P. H., and FRAENKEL, G. K., 1962, *J. chem. Phys.*, **37**, 2811.

Electron spin resonance line widths of transition metal ions in solution. Relaxation through zero-field splitting

by A. CARRINGTON and G. R. LUCKHURST

Department of Theoretical Chemistry, University of Cambridge

(Received 10 January 1964)

The factors which determine the electron resonance line widths of transition metal complexes in solution are considered. For complex ions possessing two or more unpaired electrons the dominant relaxation mechanism arises from coupling of the zero-field splitting of the spin multiplet with the random tumbling of the molecules in fluid solution. The theory of this effect is re-examined using the time-dependent density matrix methods of Redfield.

1. INTRODUCTION

The electron spin resonance absorption of a paramagnetic transition metal ion in fluid solution is frequently too broad to be detectable. Various factors are important in determining the widths of the resonance absorption lines, but a clear distinction can be made between ions with spin doublet ground states and those of higher spin multiplicity. Complexes containing one unpaired d electron can be divided into three categories for the purpose of this discussion. A resolved spectrum is obtained only if the ground state is sufficiently separated from the lower excited states for spin-orbit coupling to be unimportant. Examples of this situation are the $\text{Mo}(\text{CN})_8^{3-}$ and $\text{Cr}(\text{C}_6\text{H}_6)_2^+$ ions [1, 2] where the resolution in solution at room temperature is adequate to permit the observation of ligand hyperfine structure.

In other instances spin-orbit coupling leads to spin-lattice relaxation which, for the ion in a crystal, is so rapid that narrow lines are obtained only at very low temperatures. Among many examples are the $\text{Mn}(\text{CN})_6^{4-}$ [3], $\text{Fe}(\text{CN})_6^{3-}$ [4] and MnO_4^{2-} [5] ions; these complexes do not give observable spectra in fluid solutions.

The third category is somewhat restricted and concerns ions in which spin-orbit coupling is important enough to give rise to anisotropy in the hyperfine and g tensors, but does not significantly shorten the lifetime of the electron spin, so that narrow resonance lines are obtained from crystals at room temperature. Nearly all Cu^{II} complexes exhibit these features [6], principal g values between 2.1 and 2.4 being very common. In fluid solutions this anisotropy is, in principle, averaged to zero by the random tumbling motion of the molecules. In practice the tumbling rate is usually slow enough that the anisotropy, whilst not affecting the positions of absorption lines, does influence their shape and width. The theory of this effect was first treated by McConnell [7] (following the earlier methods of Bloembergen *et al.* [8]) in a paper of increasing significance in the light of more recent work on organic free radicals. McConnell starts with

the spin Hamiltonian appropriate for a tetragonally distorted $\text{Cu}(\text{H}_2\text{O})_6^{2+}$ complex in a crystal, namely,

$$\mathcal{H} = \beta \{ g_{\parallel} H_{\xi} S_{\xi} + g_{\perp} (H_{\eta} S_{\eta} + H_{\zeta} S_{\zeta}) + A S_{\xi} I_{\xi} + B (S_{\eta} I_{\eta} + S_{\zeta} I_{\zeta}) \}, \quad (1)$$

which we re-write in the form:

$$\mathcal{H} = \beta H_{\alpha} g_{\alpha\beta} S_{\beta} + I_{\alpha} T_{\alpha\beta} S_{\beta}. \quad (2)$$

Here and elsewhere in this paper S and I are the electron and nuclear spin vectors, g and T are the g and nuclear hyperfine tensors and we use the tensor convention of automatically summing over every Greek subscript which occurs twice in a term or product of terms. The reader may find it convenient to think of the Greek subscripts as referring to molecule-fixed axes.

The spin Hamiltonian (2) may be decomposed into the sum of an isotropic part:

$$\mathcal{H}_0 = \beta g H_{\alpha} S_{\alpha} + T I_{\alpha} S_{\alpha}, \quad (3)$$

in which $g = \frac{1}{3} g_{\alpha\alpha}$, $T = \frac{1}{3} T_{\alpha\alpha}$,

and an anisotropic part:

$$\mathcal{H}' = \beta H_{\alpha} g'_{\alpha\beta} S_{\beta} + I_{\alpha} t_{\alpha\beta} S_{\beta}, \quad (4)$$

in which

$$g'_{\alpha\beta} = g_{\alpha\beta} - g \delta_{\alpha\beta}, \quad t_{\alpha\beta} = T_{\alpha\beta} - T \delta_{\alpha\beta}.$$

The positions of the absorption lines in a solution spectrum are determined by microwave-induced transitions between the (stationary) eigenstates of \mathcal{H}_0 . \mathcal{H}' , combined with the tumbling motion, represents a time-dependent perturbation which both modulates the energies of the spin levels and induces transitions between them. Thus \mathcal{H}' affects the widths of the absorption lines, its effectiveness being determined by the tumbling rate. The essential feature of McConnell's theory is that the immediate environment of the copper ion is similar in the crystal and in solution, so that the same spin Hamiltonian is appropriate in both cases. Clearly this assumption will not always be valid, but we will leave this point until later.

In the case of an ion possessing two or more unpaired electrons the situation is rather different. As is well known, the degeneracy of the spin multiplet is at least partially lifted, even in the absence of a magnetic field, because of spin-orbit and spin-spin coupling forces. For an ion with lower than cubic symmetry the molecular tumbling in solution combined with the zero-field splitting constitutes the dominant relaxation mechanism, as was first pointed out by McGarvey [9]. He used the theory of McConnell to calculate the widths of the absorption lines for Cr^{III} , Fe^{III} and Mn^{II} ions in solution. Subsequent developments in the general theory of magnetic relaxation make it possible to apply more rigorous methods to the problem and certain aspects have already been considered by Bloembergen and Morgan [10]. They estimated the electron spin relaxation times for various metal ions in solution in order to understand proton nuclear resonance relaxation effects but did not explicitly consider the shape and width of the electron resonance absorptions.

Various questions remain to be answered. To see what these are, let us be more explicit and consider the case of the Cr^{III} ion with a quartet ($S=3/2$) ground state. If there was no zero-field splitting, either in the crystal or in solution, the four spin levels ($m_s = -3/2, -1/2, +1/2, +3/2$) would be evenly spaced and the three allowed transitions ($-3/2 \leftrightarrow -1/2$, $-1/2 \leftrightarrow +1/2$,

$+1/2 \leftrightarrow +3/2$) would, for a fixed microwave quantum, occur at the same external magnetic field strength. Now the zero-field splitting tensor is traceless so that for the ion in solution the time-averaged spacings between the four levels are still equal. The three transitions give, however, lines of different widths. Under what conditions is the single resonance line usually observed due to three separate transitions and is there any truth in the statement frequently made that only the $-1/2 \leftrightarrow +1/2$ transition is observed because it is 'less anisotropic'? McGarvey concluded, on the basis of experiment, that for the Cr^{3+} , Fe^{3+} and Mn^{2+} ions in water one does indeed observe all possible allowed transitions. On the other hand Mishra and Symons [11], for example, have concluded that the resonance line obtained from Mn^{IV} ($S=3/2$) in oleum arises from the $-1/2 \leftrightarrow +1/2$ transition only. It is clearly necessary to investigate the matter more fully and in this paper we consider complexes with triplet and quartet spin ground states.

2. RELAXATION THEORY

The basic theory required to solve our problem has been developed by Wangness and Bloch [12] and, in particular, Redfield [13]. We will therefore explain the method rather briefly and refer the reader to the excellent account given by Slichter [14], whose notation we shall adopt. The theory is more readily appreciated in terms of a specific example and we choose the quartet spin state for this purpose.

2.1. Quartet spin state relaxation

We will adopt the model of McConnell, treating the case of an ion in a quartet state with a static zero-field splitting, tumbling rapidly in fluid solution. We start with the usual spin Hamiltonian :

$$\mathcal{H} = g\beta H_z S_z + D[S_x^2 - \frac{1}{3}S(S+1)] + E(S_y^2 - S_z^2), \quad (5)$$

which we re-write in the form :

$$\mathcal{H} = g\beta H_\alpha S_\alpha + S_\alpha D_{\alpha\beta} S_\beta, \quad (6)$$

assuming, for convenience, that the g tensor is isotropic. In fluid solution and in the presence of an external magnetic field H_z , the four unperturbed energy levels are the eigenstates of the time-independent Hamiltonian :

$$\mathcal{H}_0 = g\beta H_z S_z, \quad (7)$$

whilst relaxation effects are produced by the time-dependent perturbing Hamiltonian :

$$\begin{aligned} \mathcal{H}'(t) = D_z(1/6)(2S_z^2 - S_x^2 - S_y^2) + D_{x^2-y^2}(1/2)(S_x^2 - S_y^2) \\ + D_{xy}(S_x S_y + S_y S_x) \\ + D_{xz}(S_x S_z + S_z S_x) + D_{yz}(S_y S_z + S_z S_y). \end{aligned} \quad (8)$$

The x, y, z in equations (8) and (7) refer to laboratory-fixed axes. The spin operators in (8) are time-independent; the various constants D_z^2 , etc., fluctuate with time because of the molecular tumbling but their instantaneous values may be expressed in terms of the original elements of the zero-field splitting tensor $D_{\alpha\beta}$ in equation (6).

We seek an equation for the shape of the electron resonance absorption induced by an appropriate microwave field applied in the x direction, the latter

causing transitions between the eigenstates of (7). The line shape function is obtained from the imaginary part of the equation for the susceptibility χ . Recalling that χ is defined by the expression $\langle M_x(t) \rangle = \text{Re}[\chi H_x \exp(i\omega t)]$, where H_x is the intensity of the microwave field with angular frequency ω , the problem reduces to that of determining $\langle M_x(t) \rangle$, the average value of the time-dependent component of magnetization along the x direction.

We now make use of the relationship :

$$\langle M_x \rangle = \sum_{\kappa\kappa'} \rho_{\kappa\kappa'} \langle \kappa' | M_x | \kappa \rangle, \quad (9)$$

where the $\rho_{\kappa\kappa'}$ are off-diagonal elements of a 4×4 density matrix, the summation being over the four eigenstates of the operator S_z . We consider only matrix elements between states which differ in energy by one microwave quantum and under these conditions Redfield has shown that such elements obey a set of linear differential equations of the form :

$$\frac{d}{dt} \rho_{\kappa\kappa'} = \sum_{\lambda\lambda'} R_{\kappa\kappa'\lambda\lambda'} \rho_{\lambda\lambda'}. \quad (10)$$

The right-hand side of equation (10) is now expanded as follows :

$$\begin{aligned} \sum_{\lambda\lambda'} R_{\kappa\kappa'\lambda\lambda'} \rho_{\lambda\lambda'} = & 2 \sum_{\lambda\lambda'q} \langle \kappa | S_q | \lambda \rangle \langle \lambda' | S_q | \kappa' \rangle k_q(\kappa - \lambda) \rho_{\lambda\lambda'} \\ & - \rho_{\kappa\kappa'} \sum_{\gamma q} \{ \langle \gamma | S_q | \kappa \rangle \langle \kappa | S_q | \gamma \rangle k_q(\gamma - \kappa) \\ & + \langle \gamma | S_q | \kappa' \rangle \langle \kappa' | S_q | \gamma \rangle k_q(\gamma - \kappa') \}. \end{aligned} \quad (11)$$

In order to evaluate this expression we consider each term in equation (8) in turn. The S_q are the five composite spin operators of equation (8); each $k_q(\omega)$ gives the spectral density of the q -component of the fluctuating field at frequency ω and is defined by :

$$k_q(\omega) = \frac{1}{2} \int_{-\infty}^{+\infty} \langle D_q(t) D_q(t+\tau) \rangle \exp(-i\omega\tau) d\tau. \quad (12)$$

We make the usual assumption that the five components D_q fluctuate independently.

The resulting differential equations for the relaxation of the off-diagonal elements of the density matrix are

$$\dot{\rho}_{\frac{1}{2}\frac{1}{2}} = -\rho_{\frac{1}{2}\frac{1}{2}} [\tau_1^{-1} + \tau_2^{-1} + \tau_3^{-1}] + \rho_{-\frac{1}{2}-\frac{1}{2}} \tau_1^{-1}, \quad (13)$$

$$\dot{\rho}_{\frac{1}{2}-\frac{1}{2}} = -\rho_{\frac{1}{2}-\frac{1}{2}} [\tau_1^{-1} + \tau_3^{-1}], \quad (14)$$

$$\dot{\rho}_{-\frac{1}{2}-\frac{1}{2}} = -\rho_{-\frac{1}{2}-\frac{1}{2}} [\tau_1^{-1} + \tau_2^{-1} + \tau_3^{-1}] + \rho_{\frac{1}{2}\frac{1}{2}} \tau_1^{-1}, \quad (15)$$

where

$$\tau_1^{-1} = 6k_{xy}(2\omega) + (3/2)k_{x^2-y^2}(2\omega), \quad (16)$$

$$\tau_2^{-1} = k_z(0), \quad (17)$$

$$\tau_3^{-1} = 6k_{xz}(\omega) + 6k_{yz}(\omega). \quad (18)$$

After solving the differential equations (13-15) and substituting in equation (9) we obtain the following absorption line shape equation :

$$g(\omega) = \frac{3\omega_0}{4kTm} \left\{ \frac{1}{1 + (\omega - \omega_0)^2 m^{-2}} \right\} + \frac{2\omega_0}{4kTn} \left\{ \frac{1}{1 + (\omega - \omega_0)^2 n^{-2}} \right\}, \quad (19)$$

where $m = \tau_2^{-1} + \tau_3^{-1}$ and $n = \tau_1^{-1} + \tau_3^{-1}$. In order to derive equation (19) we make use of the usual high temperature approximation [14] in deriving

the partition function and we also assume that the microwave power level is low enough to avoid saturation.

We have now to express each of the relaxation times τ_1 , τ_2 and τ_3 in terms of the molecular tumbling rate and the elements of the zero-field splitting tensor. The integrals k_{ij} are evaluated using the assumption that each component of the random perturbation fluctuates with a simple exponential autocorrelation function, with the same correlation time τ_0 , i.e.

$$\langle D_q(t)D_q(t+\tau) \rangle = \langle D_q^2(0) \rangle \exp(-|\tau|/\tau_0). \quad (20)$$

Thus the final stage is to evaluate the various quantities $\langle D_q^2 \rangle$ and this is readily performed using standard tensor averaging procedures [15, 16]. One finds that :

$$\begin{aligned} \text{(i)} \quad \langle D_{xz}^2 \rangle &= \langle D_{yz}^2 \rangle = \langle D_{xu}^2 \rangle \\ &= D_{\alpha\beta} D_{\mu\nu} \langle l_{x\alpha} l_{\beta y} l_{x\mu} l_{\nu y} \rangle \\ &= D_{\alpha\beta} D_{\mu\nu} [(2/15)\delta_{\alpha\mu}\delta_{\beta\nu} - (1/30)\delta_{\alpha\beta}\delta_{\mu\nu} - (1/30)\delta_{\alpha\nu}\delta_{\beta\mu}] \\ &= (1/10)D_{\alpha\beta}D_{\alpha\beta}. \\ \text{(ii)} \quad \langle D_{zz}^2 \rangle &= 9\langle D_{zz}^2 \rangle \\ &= 9D_{\alpha\beta}D_{\mu\nu}(1/15)[\delta_{\alpha\beta}\delta_{\mu\nu} + \delta_{\alpha\mu}\delta_{\beta\nu} + \delta_{\alpha\nu}\delta_{\beta\mu}] \\ &= (18/15)D_{\alpha\beta}D_{\alpha\beta}. \\ \text{(iii)} \quad \langle D_{xx}^2 \rangle &= \langle D_{yy}^2 \rangle = 2\langle D_{xx}D_{yy} \rangle + \langle D_{zz}^2 \rangle \\ \langle D_{xx}D_{yy} \rangle &= D_{\alpha\beta}D_{\mu\nu}[(2/15)\delta_{\alpha\beta}\delta_{\mu\nu} - (1/30)\delta_{\alpha\mu}\delta_{\beta\nu} - (1/30)\delta_{\alpha\nu}\delta_{\beta\mu}] \\ &= -(1/15)D_{\alpha\beta}D_{\alpha\beta}. \end{aligned}$$

Hence

$$\langle D_{x^2-y^2}^2 \rangle = (6/15)D_{\alpha\beta}D_{\alpha\beta}.$$

Substituting for m and n in equation (19) and replacing ω by $2\pi\nu$ we see that the resonance absorption is, in fact, the sum of two Lorentzian lines, the first arising from the $+1/2 \leftrightarrow -1/2$ transition and the second being itself the sum of two equal Lorentzians arising from the $+1/2 \leftrightarrow +3/2$ and $-1/2 \leftrightarrow -3/2$ transitions. The widths of the two superimposed Lorentzians are, respectively :

$$(T_2^{-1})_{\frac{1}{2}-\frac{1}{2}} = (6/5)D_{\alpha\beta}D_{\alpha\beta} \left[\frac{\tau_0}{1+4\pi^2\nu^2\tau_0^2} + \frac{\tau_0}{1+16\pi^2\nu^2\tau_0^2} \right], \quad (21)$$

$$(T_2^{-1})_{\frac{1}{2}\frac{3}{2}} = (6/5)D_{\alpha\beta}D_{\alpha\beta} \left[\tau_0 + \frac{\tau_0}{1+4\pi^2\nu^2\tau_0^2} \right]. \quad (22)$$

In terms of the original spin Hamiltonian (5), $D_{\alpha\beta}D_{\alpha\beta}$ is equal to $(2/3)D^2 + 2E^2$. Independent verification of the above expressions has been provided by McLachlan [17] who uses an operator method different from the more standard technique employed in this paper.

2.2. Triplet spin state relaxation

If we again adopt the spin Hamiltonian (6) with $S=1$, the relaxation problem is mathematically identical with that of the quadrupole relaxation in solution of a nucleus with spin 1 ; this situation has been discussed by Abragam [18]. The result is that any electron resonance absorption line observed in solution is the sum of two equivalent Lorentzians (corresponding to the two allowed transitions $+1 \leftrightarrow 0$, $0 \leftrightarrow -1$) with a width T_2^{-1} given by :

$$T_2^{-1} = (1/60)D_{\alpha\beta}D_{\alpha\beta} \left[18\tau_0 + \frac{30\tau_0}{1+4\pi^2\nu^2\tau_0^2} + \frac{12\tau_0}{1+16\pi^2\nu^2\tau_0^2} \right]. \quad (23)$$

2.3. Sextet spin state relaxation

One could treat the relaxation of a sextet spin state in solution by again using the spin Hamiltonian (6) with $S=5/2$. McLachlan has calculated the relaxation matrix for this system and we have independently confirmed his results using the methods described in this paper. However, in view of the presence of quartic terms [19] in the spin Hamiltonian this treatment may not be realistic. There are, indeed, several examples [20] of Mn^{II} and Fe^{III} complexes where the zero-field spin Hamiltonian contains *only* quartic terms. We have therefore decided to deal with this problem separately and discuss it elsewhere.

3. DISCUSSION

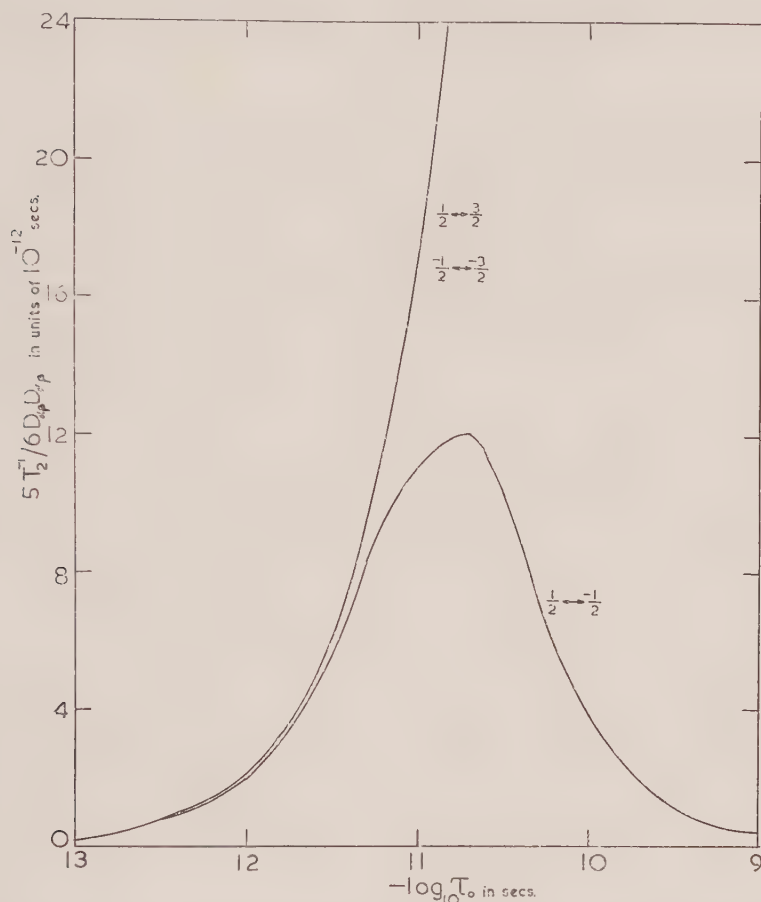
We now turn to consider the experimental information which is available. So far as triplet states are concerned, we have found no report of resonance studies in fluid solution. Among the transition metal ions with triplet ground states, octahedral Ni^{II} (d^8) complexes are the most common. Crystal studies indicate, however, that the zero-field splitting parameter D in equation (5) is usually rather large. The FeO_4^{2-} ion, which also possesses a triplet ground state, shows a fairly small zero-field splitting [5] but its relative instability in solution precludes the possibility of reliable line width studies. The situation is far more satisfactory in the case of quartet states, many Cr^{III} complexes being available for study.

In the figure we show a plot of the widths of the absorptions due to the two allowed transitions for the quartet state, as a function of the rotational correlation time τ_0 . The theory is, of course, valid only for the range of τ_0 values smaller than $\sim 10^{-10}$ sec. It *may* be true that only the $m_s=1/2 \leftrightarrow -1/2$ transition will be observable in very viscous solutions, as suggested by Mishra and Symons. However, in a preliminary study of some chromic complexes in water/glycerol mixtures, we have not been able to confirm this hypothesis. Clearly with increase in viscosity the width of the resonance line must approach the limiting value observed in a rigid glass.

One can be sure that, for any metal complex in aqueous solution at normal temperatures, the resonance line observed arises from all possible allowed transitions. This is a prediction of the theory which we have verified by comparing the integrated intensities of the lines obtained from $\text{TiF}_2(\text{H}_2\text{O})_4^+(S=1/2)$, $\text{Cr}(\text{NH}_3)_6^{3+}(S=3/2)$ and $\text{Mn}(\text{H}_2\text{O})_6^{2+}(S=5/2)$ in aqueous solution. The relative intensities for equal concentrations should be proportional to the relative values of $S(S+1)$, i.e. $3/4 : 15/4 : 35/4$; the experimental ratios agree with these values to within ± 10 per cent.

In applying the relaxation theory we have assumed that the zero-field splitting tensor varies only in orientation, not in its principal values, as the complex tumbles in solution; one might also wish to assume that for a given complex the magnitude of the zero-field splitting in fluid solution is similar to that in a crystalline environment. These assumptions are probably justified for a complex such as Cr^{III} tris-ethylene-diamine where the large zero-field splitting measured in the crystal [21] is an inherent consequence of the D_3 trigonal symmetry of the complex, and indeed this ion gives a very broad resonance line in solution. However, the situation for a hexahydrate, $\text{Cr}(\text{H}_2\text{O})_6^{3+}$ for example, is rather different. In the crystal the site symmetry of the ion is usually lower than cubic and the resulting zero-field splitting is quite large. However, the $\text{Cr}(\text{H}_2\text{O})_6^{3+}$

complex in the absence of any environmental effect would be expected to have nearly regular octahedral symmetry. If this were also true in aqueous solution we might expect to observe a narrow resonance line, which is not the case. On the other hand, the $\text{Cr}(\text{NH}_3)_6^{3+}$ complex does give a narrow line. Clearly there is no reason to suppose that the instantaneous symmetry of the complex in aqueous solution is the same as in a crystal.



Theoretical line widths for the allowed resonance transitions of a quartet state in solution, plotted as a function of the rotational correlation time. A microwave frequency of 9000 Mc/s has been assumed.

There are at least two other possible sources of line broadening. The first is exchange of ligands with the solvent; the line width will depend on the rate of exchange and the nature of the transition state. This effect might well be important for many hydrate complexes but in the particular case of Cr^{III} , ligand exchange is known to be rather slow [22]. A second source of line broadening arises from fluctuations in the shape of the complex, perhaps brought about by molecular collisions in solution. The line width is then determined by either the rate of such fluctuations or the rate of tumbling, or both. This mechanism has been examined by Al'tshuler and Valiev [23] and may well be of primary importance for complexes with cubic symmetry.

We therefore come to two main conclusions. The first is that in solutions of low viscosity the integrated signal intensity is proportional to $S(S+1)$ and that this must be taken into account in comparing the relative concentrations of different metal ions in different solutions. The second is that the width of the resonance depends on the symmetry of the immediate environment of the paramagnetic ion, and the rate at which the complex is tumbling; this fact has been exploited by McGarvey [9] in determining some ligand exchange equilibrium constants. Neither of these conclusions is new, but we have perhaps placed them on firmer theoretical foundations.

We would like to thank Professor H. C. Longuet-Higgins, F.R.S., and Dr. A. D. McLachlan for several helpful discussions during the course of this work. G. R. L. acknowledges a D.S.I.R. studentship.

REFERENCES

- [1] WEISSMAN, S. I., and COHN, M., 1957, *J. chem. Phys.*, **27**, 1440.
- [2] FELTHAM, R., 1961, *J. Inorg. nuclear chem.*, **16**, 197.
- [3] BAKER, J. M., BLEANEY, B., and BOWERS, K. D., 1956, *Proc. phys. Soc., Lond. B*, **69**, 1205.
- [4] BLEANEY, B., and O'BRIEN, M. C. M., 1956, *Proc. phys. Soc., Lond. B*, **69**, 1216.
- [5] CARRINGTON, A., INGRAM, D. J. E., LOTT, K. A. K., SCHONLAND, D. S., and SYMONS, M. C. R., 1960, *Proc. roy. Soc. A*, **254**, 101.
- [6] BOWERS, K. D., and OWEN, J., 1955, *Rep. Progr. Phys.*, **18**, 304.
- [7] MCCONNELL, H. M., 1956, *J. chem. Phys.*, **25**, 709.
- [8] BLOEMBERGEN, N., PURCELL, E. M., and POUND, R. V., 1948, *Phys. Rev.*, **73**, 679.
- [9] MCGARVEY, B. R., 1957, *J. phys. Chem.*, **61**, 1232.
- [10] BLOEMBERGEN, N., and MORGAN, L. O., 1961, *J. chem. Phys.*, **34**, 842.
- [11] MISHRA, H. C., and SYMONS, M. C. R., 1963, *J. chem. Soc.*, p. 4490.
- [12] WANGSNES, R. K., and BLOCH, F., 1953, *Phys. Rev.*, **89**, 728.
- [13] REDFIELD, A. G., 1957, *I.B.M. J. Res. Develop.*, **1**, 19.
- [14] SLICHTER, C. P., 1963, *Principles of Magnetic Resonance* (New York: Harper & Row), p. 127.
- [15] CARRINGTON, A., and LONGUET-HIGGINS, H. C., 1962, *Mol. Phys.*, **5**, 447.
- [16] ANDREWS, A. L., and BUCKINGHAM, A. D., 1959, *Mol. Phys.*, **3**, 183.
- [17] MCLACHLAN, A. D., 1964, *Proc. roy. Soc.* (to be published).
- [18] ABRAGAM, A., 1961, *The Principles of Nuclear Magnetism* (Oxford University Press).
- [19] BLEANEY, B., and STEVENS, K. W. H., 1953, *Rep. Progr. Phys.*, **16**, 108.
- [20] LOW, W., 1960, *Solid State Physics*, Supplement 2, p. 118.
- [21] SINGER, L. S., 1955, *J. chem. Phys.*, **23**, 379.
- [22] TAUBE, H., 1959, *Advanc. Inorg. Chem. Radiochem.*, **1**, 1.
- [23] AL'TSHULER, S. A., and VALIEV, K. A., 1958, *J. exp. theor. Phys.*, **35**, 947.

The effects of π -electron distribution and intramolecular electric fields on the ^{19}F N.M.R. shielding in substituted perfluorobenzenes

by N. BODEN, J. W. EMSLEY†, J. FEENEY and L. H. SUTCLIFFE
Donnan Chemical Laboratories, The University, Liverpool

(Received 16 December 1963)

Several workers have attempted to correlate ^{19}F chemical shifts in fluorinated benzene derivatives with the π -electron charge densities and bond orders as calculated by the Hückel molecular orbital method. In all cases chemical shifts of the fluorine nuclei in meta and para positions to substituents could be predicted successfully, but for fluorine nuclei at ortho positions large deviations were encountered. We have shown that such ortho effects in haloperfluorobenzenes can be accounted for satisfactorily in terms of intramolecular electric field contributions.

1. INTRODUCTION

Ramsey [1] derived an expression for the shielding constant σ_{N} of a nucleus in a molecule, and this may be summarized conveniently as the sum of two terms having opposite signs, namely :

$$\sigma_{\text{N}} = \sigma_{\text{N}}^{\text{dia}} + \sigma_{\text{N}}^{\text{para}}. \quad (1)$$

Saika and Slichter [2] have shown that the shielding of the ^{19}F nucleus in various compounds arises almost entirely from variations in the magnitude of $\sigma_{\text{N}}^{\text{para}}$. Ramsey [1] has shown that this contribution to the total shielding can be expressed in terms involving ground-state wave functions and an average excitation energy ΔE :

$$\sigma_{\text{N}}^{\text{para}} = \frac{e^2 \hbar^2}{m^2 c^2} \cdot \frac{1}{\Delta E} \left\langle 0 \left| \sum_{j,k} \frac{m_z k m_{-j}}{r_k^3} \right| 0 \right\rangle. \quad (2)$$

There have been several attempts to apply equation (2) to the calculation of ^{19}F chemical shifts : Karplus and Das [3] assumed that the calculation could be restricted to p electrons centred on the fluorine nucleus in question. They showed that in fluoro-aromatic molecules, the difference in the shielding constants between two fluorine nuclei, $\Delta\sigma$, is governed by the difference in ionic character ΔI , and in double-bond order Δp , of the C-F bonds. They derived the equation :

$$\sigma = \sigma_0 (a\Delta I + b\Delta p) = \delta/10^6, \quad (3)$$

where a and b are constants. σ_0 involves the nuclear constants and the average excitation energy ΔE . Because of the uncertainty in ΔE , σ_0 is difficult to calculate, hence Karplus and Das have derived an empirical value by comparing the

† Chemistry Department, South Road, The University, Durham City.

observed chemical shift difference between fluorine gas and monofluorobenzene with the theoretical values predicted from values of ΔI and Δp . In this way, they have found that :

$$\text{and} \quad \left. \begin{aligned} \sigma_0 &= 0.863 \times 10^{-3} \\ \delta &= 765\Delta I - 777\Delta p, \end{aligned} \right\} \quad (4)$$

where

$$\delta = \frac{(H_{\text{ref}} - H_{\text{sample}})}{H_{\text{ref}}} \times 10^6 \text{ p.p.m.}$$

The main drawback in using equation (4) for chemical shift calculation lies in the difficulty of calculating to the required accuracy values of the ionic character of the bonds. In order to determine ΔI values for a series of fluorobenzenes, Karplus and Das used equation (4) together with the observed shifts measured relative to the reference compound monofluorobenzene; the π -bond orders were calculated by the Hückel molecular orbital technique. The values of ΔI obtained were of the expected order of magnitude, except when the fluorine nucleus has a fluorine neighbour in the ortho position. This ortho effect causes fluorine nuclei to be more shielded than equation (4) predicts. The magnitude of this excess ortho shift is 16.8 p.p.m. It is worth emphasizing at this point that the empirical nature of equation (4) means that the direction of the anomalous ortho effect is determined by the choice of monofluorobenzene as the reference compound. If hexafluorobenzene were chosen as the reference for calculating σ_0 , then the ortho effect would be apparent whenever a fluorine has a hydrogen atom as a neighbour, and it would cause a shift to lower applied fields. Karplus and Das found that the ortho effect depends on both ortho neighbours and is additive.

Prosser and Goodman [4] have also applied equation (2) to the calculation of ^{19}F chemical shifts in fluoro-aromatic compounds. Their approach was very similar to that of Karplus and Das except that they included in the summation the contributions of electrons centred on the bonded carbon atom as well as on the fluorine atom. They obtained the chemical shift difference between two fluorine nuclei in terms of $q(\text{C}_z)$, $q(\text{F}_z)$ and $p(\text{C}_z\text{F}_z)$, the π -electron densities at carbon and fluorine atoms and the π -bond order respectively. For a series of molecules in which ΔE can be assumed to be constant they showed that the chemical shift from a reference compound is given by :

$$\delta = 488(\Delta E)^{-1}[0.1\Delta_q(\text{C}_z) + 11.9\Delta_q(\text{F}_z) + 3.9\Delta_p(\text{C}_z\text{F}_z)] \times 10^{-6}, \quad (5)$$

where $\Delta_q(\text{C}_z)$, $\Delta_q(\text{F}_z)$ and $\Delta_p(\text{C}_z\text{F}_z)$ are the differences between the π -electron parameters of the reference nucleus and those of a sample nucleus. ΔE is best obtained empirically by applying equation (5) to a case with known charge densities and bond orders. Apart from the difficulty of evaluating ΔE , equation (5) is preferable to equation (4) because all the quantities are calculable by molecular orbital theory. In the case of $\text{C}_6\text{H}_4\text{FX}$ para-substituted compounds, where X is a first row element, Taft *et al.* [5] have shown that equations (4) and (5) are equivalent.

The ortho effect observed in ^{19}F chemical shifts of fluorochlorobenzenes and in other fluorobenzenes seems to be general. Buckingham *et al.* [6] suggested that its origin lies in an increased paramagnetic term in equation (1) arising from

smaller values of ΔE associated with a fluorine atom at a position ortho to a substituent. This idea is in accord with the increasing magnitude of the ortho effect as the substituent becomes larger in size, and particularly when the substituent is a transition metal atom since suitable low lying excited states are then available. However, because of the experimental inaccessibility of ΔE values, explanations based on this suggestion are of necessity speculative. Another likely origin of the ortho effect is the presence of permanent and time-dependent electric fields in the molecule. For a nucleus X in a C-X bond, the shielding constant σ_x depends upon E_z , the electric field component along the C-X bond direction, and E^2 , the square of the electric field intensity at X such that [7] :

$$\sigma_x = -AE_z - BE^2, \quad (6)$$

where the constants A and B depend upon the ease of distortion of the electronic charge distribution along the bond direction and perpendicular to it respectively ; they vary in sign and magnitude according to the nature of X. There has not been a theoretical estimate of A and B for the case when X is a fluorine atom but Petrakis and Bernstein [8, 9] have determined these constants experimentally by observing the pressure dependence of chemical shifts of gaseous samples of fluorine-containing compounds. They find that A is negative and has the value of $(-9.9 \pm 3.6) \times 10^{-12}$ e.s.u. for the molecule CHF_3 ; whereas B is positive and varies from $(15.1 \pm 3.0) \times 10^{-18}$ in CHF_3 to $(43.5 \pm 5.1) \times 10^{-18}$ e.s.u. in SiF_4 . They suggest that the B values for X-F bonds depend upon the double-bond character.

The electric field at X can arise from the presence of neighbouring polar bonds in the molecule, but also a non-zero time average value, $\langle E^2 \rangle$, of E^2 arises from the presence of time dependent dipole moments in neighbouring electron groups. These time dependent moments give rise to the van der Waals' forces between non-bonded atoms, hence their effect on σ_x is known as the van der Waals shift [10, 11]. The value of $\langle E^2 \rangle$, the non-zero time average field, can be obtained approximately from the equation [10] :

$$\langle E^2 \rangle = 3PI/r^6, \quad (7)$$

in which P is the polarizability of the electron group, I is the first ionization potential and r is the distance separating the fluorine atom from the electron group.

It is demonstrated in this paper that the ortho effects observed for fluorobenzenes can be accounted for satisfactorily using equation (6). The ^{19}F shifts in the complete series of fluorochlorobenzenes reported here show pronounced ortho effects : the fluorine atoms with ortho chlorine neighbours are shifted more to low fields than those with para chlorine neighbours. In addition, these compounds provide data which can be used to test the general validity of equation (5).

2. EXPERIMENTAL

2.1. Materials

All the samples were kindly provided by Professor W. K. R. Musgrave of Durham University.

The purity, in terms of the fluorine content, was checked using the fluorine magnetic resonance spectra. In the following cases complete separation of

isomers by either distillation or vapour phase chromatography proved to be difficult and mixtures were used in the present investigation :

$C_6F_2Cl_4$: a pure sample of the para isomer was available but the spectra of the meta and ortho compounds were obtained from a mixture containing 20 per cent ortho, 57 per cent meta and 23 per cent para. At infinite dilution in CCl_4 , the ^{19}F chemical shift of the para isomer measured from $CFCl_3$, was found to be 6266.0 ± 0.3 and 6265 ± 0.5 c sec $^{-1}$ for the pure sample and the mixture respectively, thus interaction between isomers is negligible at low solute concentrations.

$C_6F_3Cl_3$: 1,3,5-trifluoro-2,4,6-trichlorobenzene was a pure sample. Spectra of the remaining isomers were determined from a mixture of composition :

1, 2, 3-trifluoro-4, 5, 6-trichlorobenzene	14 per cent
1, 2, 4-trifluoro-3, 5, 6-trichlorobenzene	75 per cent
1, 3, 5-trifluoro-2, 4, 6-trichlorobenzene	2 per cent
fluorine-containing impurity	9 per cent

$C_6F_4Cl_2$: the sample examined contained all three isomers in the following percentages :

ortho	55 per cent
meta	22 per cent
para	22 per cent
fluorine-containing impurity	1 per cent

C_6F_5OH : the sample contained 50 per cent *t*-butanol.

2.2. N.M.R. measurements

^{19}F resonance spectra were recorded at $25 \pm 1^\circ C$ using a Varian V4300 B N.M.R. spectrometer operating at 56.4 Mc sec $^{-1}$. Spectra were calibrated with the aid of a Muirhead-Wigan decade oscillator type D 890 A. At least ten recordings were made of each spectrum. Errors quoted are mean dispersions.

Chemical shift measurements were made on solutions of the sample in carbon tetrachloride containing 5 mole per cent of trichlorofluoromethane. Reducing the $CFCl_3$ concentration did not affect the values obtained. Furthermore, there was no change in separation of the ^{19}F band of 5 mole per cent $CFCl_3$ in CCl_4 contained in a capillary and that from 5 mole per cent $CFCl_3$ in 5 mole per cent solutions of C_6FCl_5 , sym- $C_6F_3Cl_3$ or C_6F_5I dissolved in CCl_4 . The chemical shift data for the fluorochlorobenzenes given in table 4 have been extrapolated to infinite dilution and transferred to a hexafluorobenzene reference scale : the most dilute solutions had a sample concentration of 2 mole per cent. The remaining compounds (except C_6F_5OH) were examined as 5 mole per cent solutions in CCl_4 containing 5 mole per cent $CFCl_3$, again chemical shifts are referred to hexafluorobenzene. The dilution is great enough to give chemical shifts approximating to those at infinite dilution. The error is probably not greater than 3 c sec $^{-1}$ (at 56.4 Mc sec $^{-1}$).

Many of the compounds studied give simple first-order ^{19}F resonance spectra but others required detailed analysis in order to evaluate the coupling constants. The 1, 2, 4-trifluoro-3, 5, 6-trichlorobenzene isomer gives an ABX type spectrum ; the 1, 2, 3, 4-tetrafluoro-5, 6-dichlorobenzene ^{19}F spectrum is of the AA'XX' type ; the compounds of general formula C_6F_5X yield complex ^{19}F spectra which require analysis as AA'BXX' spin systems. To a first approxi-

mation, the spectra of the $\text{C}_6\text{F}_5\text{X}$ compounds can be treated as being of the $\text{AA}'\text{PXX}'$ type. This approximate treatment gives the results in good agreement (within experimental error) with those observed. The interaction of the hydrogen nucleus in pentafluorobenzene can be regarded as a first order perturbation and thus eliminated from the analysis. An exception to the foregoing is $\text{C}_6\text{F}_5\text{OME}$ whose ^{19}F spectrum has a complex region corresponding to overlapping of the meta and para fluorine signals. The chemical shift of the central band of this region was measured.

3. RESULTS AND DISCUSSION

The compounds examined and the ^{19}F chemical shifts and spin coupling constants obtained from them are listed in tables 4, 7, 8, 9 and 10.

3.1. Fluorochlorobenzenes

Equation (5) will now be applied to the case of the fluorochlorobenzenes. Replacement of a fluorine atom in C_6F_6 by a chlorine atom changes the π -electronic charge distribution at each of the remaining atoms. The shift of the para-fluorine nucleus in $\text{C}_6\text{F}_5\text{Cl}$ measured from C_6F_6 should be described almost entirely by equation (5) because the para-fluorine nucleus is remote from the substituent. Values of $q(\text{C}_z)$, $q(\text{F}_z)$ and $p(\text{C}_z\text{F}_z)$ may be calculated by means of the Hückel L.C.A.O. molecular orbital method. Both C_6F_6 and $\text{C}_6\text{F}_5\text{Cl}$ have been treated as 12 orbital, 18 electron problems and the appropriate secular equations have been solved with the aid of a Ferranti Pegasus digital computer. The main difficulty in applying the H.M.O. method is in the choice of suitable values for the Coulomb (α) and the exchange (β) integrals for the fluorine and the chlorine atoms. Using values of α and β recommended by Streitwieser [12] ($\alpha_{\text{F}} = 3\beta$, $\alpha_{\text{Cl}} = 2\beta$, $\beta_{\text{F}} = 0.7\beta$ and $\beta_{\text{Cl}} = 0.4\beta$), the π -electron charge densities for $\text{C}_6\text{F}_5\text{Cl}$ have been calculated and the differences between these values and the corresponding values in C_6F_6 have been substituted into equation (5). This gives rise to a negative value of the product of δ and ΔE , ($\delta\Delta E$) for the para-fluorine nucleus. The observed positive chemical shift for this nucleus requires a negative value for the average excitation energy ΔE which is absurd. These values of α and β were rejected and better ones sought using the necessary criterion that the selected functions should produce electron densities which together with a positive ΔE value give shifts in the observed direction. If the assumption of an equal value of ΔE for both C_6F_6 and $\text{C}_6\text{F}_5\text{Cl}$ is valid then a satisfactory set of parameters is $\alpha_{\text{F}} = 2\beta$, $\alpha_{\text{Cl}} = \beta$, $\beta_{\text{F}} = \beta$ and $\beta_{\text{Cl}} = 0.4\beta$. The selected values of α are consistent with those estimated using orbital electronegativities [13] ($\alpha_{\text{F}} = 2\beta$ to 2.5β and $\alpha_{\text{Cl}} = 1\beta$ to 1.5β). These values have been used for the calculations on all the fluorochlorobenzenes and some justification for their use is found in that they give rise to ΔE values in good agreement with those found by Taft and co-workers [5] for fluorobenzenes using equation (5).

The next step in the calculation is to combine the values of $\delta\Delta E$ for $\text{C}_6\text{F}_5\text{Cl}$ with the chemical shift contributions from the electric fields at the fluorine atoms using equations (6) and (7). Replacement of a fluorine atom in C_6F_6 by a chlorine atom changes the values of E_z , E^2 and $\langle E^2 \rangle$ at each of the remaining atoms. E_z and E^2 were obtained as the vector sum of the fields arising from point dipoles situated at the mid-points of the C-F and the C-Cl bonds. The molecules were

assumed to have the carbon atoms at the corners of a regular hexagon with inter-nuclear distances of $r_{\text{CC}} = 1.39 \text{ \AA}$, $r_{\text{CF}} = 1.30 \text{ \AA}$ and $r_{\text{CCl}} = 1.70 \text{ \AA}$ [14]. The bond moments of the C-F and the C-Cl bonds in aromatic compounds have been taken to be 1.6 D and 1.7 D respectively, hence replacing F by Cl does not lead to an appreciable change in E_z or E^2 . A further contribution to the B term is made by the non-zero time-averaged field $\langle E^2 \rangle$ which was estimated using equation (7). Replacement of a fluorine by a chlorine atom is accompanied by a large change in $\langle E^2 \rangle$ because of the appreciable difference in the bond polarizabilities of the C-F and the C-Cl bonds which were taken to be [15, 16]:

$$P_{\text{C-F}} = 0.633 \times 10^{-24} \text{ cm}^3,$$

$$P_{\text{C-Cl}} = 2.604 \times 10^{-24} \text{ cm}^3.$$

The values of the ionization potentials of the fluorine and the chlorine atoms are [17]:

$$I_{\text{F}} = 28.5 \times 10^{-12} \text{ ergs},$$

$$I_{\text{Cl}} = 20.8 \times 10^{-12} \text{ ergs}.$$

Although these values are probably poor approximations to bond excitation energies, they were used in equation (7) as the only data available. Substitution into equation (7) gives:

$$\left. \begin{aligned} \langle E^2 \rangle_{\text{F}} &= \frac{53.98}{r^6} \times 10^{-36} \text{ e.s.u.}, \\ \langle E^2 \rangle_{\text{Cl}} &= \frac{162.71}{r^6} \times 10^{-36} \text{ e.s.u.} \end{aligned} \right\} \quad (8)$$

The results for E_z , E^2 and $\langle E^2 \rangle$ for C_6F_6 and $\text{C}_6\text{F}_5\text{Cl}$ are given in table 3. Only very small changes were observed for the case of E_z (this was also true for all the fluorochlorobenzenes) and this together with the relatively small value expected for the constant A ($\sim -10 \times 10^{-12} \text{ e.s.u.}$) make it desirable to neglect the AE_z term from the calculations.

By carrying out the appropriate subtractions of the parameters given in tables 1 and 2 and using the ^{19}F chemical shifts between C_6F_6 and the ortho-, meta- and para-fluorine nuclei of $\text{C}_6\text{F}_5\text{Cl}$ it is possible to set up three equations in the unknowns B and ΔE :

$$\sigma_{\text{ortho}} = 21.693 \times 10^{-6} = +0.4162 \times 10^{12} B + 3.184 \times 10^{-6} (\Delta E)^{-1}, \quad (9)$$

$$\sigma_{\text{meta}} = 0.819 \times 10^{-6} = +0.0148 \times 10^{12} B - 0.147 \times 10^{-6} (\Delta E)^{-1}, \quad (10)$$

$$\sigma_{\text{para}} = 6.216 \times 10^{-6} = +0.0089 \times 10^{12} B - 4.527 \times 10^{-6} (\Delta E)^{-1}. \quad (11)$$

Values for B and ΔE can then be obtained from equations (9) and (11) (the effect at the meta position is less exactly described by equation (10)):

$$\Delta E = 0.7752 \text{ eV},$$

$$B = 42.26 \times 10^{-18} \text{ e.s.u.}$$

A least squares solution at equations (9), (10) and (11) gives similar values. The values of ΔE and B predict a value for σ_{meta} in $\text{C}_6\text{F}_5\text{Cl}$ of $+0.436 \times 10^{-6}$ in good agreement with the observed value. The value of $B = 42.26 \times 10^{-18} \text{ e.s.u.}$ is

similar in magnitude to that found for SiF_4 (43.5×10^{-18} e.s.u.) and is not unreasonable in view of the suggested 25 per cent double-bond character in the C–F bonds in fluoro-aromatics [8, 9]. The value of ΔE of 0.7752 eV is of the same order of magnitude as that found by Taft *et al.* [5] for fluorobenzenes ($\Delta E \sim 1.0$ eV).

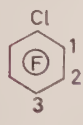
		$q(\text{C}_z)$	$q(\text{F}_z)$	$\rho(\text{C}_z\text{F}_z)$	$\delta\Delta E$ p.p.m. eV
C_6F_6		1.07352	1.92640	0.25942	
	1	1.03306	1.92142	0.27398	+3.184
	2	1.07601	1.92666	0.25864	–0.147
	3	1.04690	1.92238	0.26999	+4.527

Table 1. Electron densities and bond orders in C_6F_6 and $\text{C}_6\text{F}_5\text{Cl}$.

$$\alpha_{\text{F}} = 2\beta, \alpha_{\text{Cl}} = \beta, \beta_{\text{F}} = \beta, \beta_{\text{Cl}} = 0.4\beta.$$

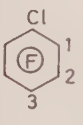
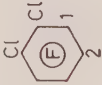
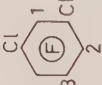

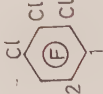
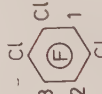
		$E_z \times 10^{-6}$ (e.s.u.)	$E^2 \times 10^{-12}$ (e.s.u.)	$\langle E^2 \rangle \times 10^{-12}$ (e.s.u.)	$(E^2 + \langle E^2 \rangle) \times 10^{-12}$ (e.s.u.)
C_6F_6		0.3642	0.1327	0.5474	0.6801
	1	0.3639	0.1356	0.9607	1.0963
	2	0.3634	0.1321	0.5628	0.6949
	3	0.3676	0.1351	0.5539	0.6890

Table 2. Values of E_z , E^2 and $\langle E^2 \rangle$ at the fluorine atoms in C_6F_6 and $\text{C}_6\text{F}_5\text{Cl}$.

The values of B and ΔE thus obtained were used to calculate the chemical shifts of all the fluorochlorobenzenes measured relative to C_6F_6 . Table 3 shows the calculated values of the π -electron charge densities and bond orders and of the electric field parameters. Table 4 shows the observed and calculated chemical shifts: there is no obviously discernible pattern in the value of $(\delta_{\text{obs}} - \delta_{\text{calc}})$ except that these values tend to increase with increasing chlorine substitution. The differences for the dichloro derivatives are small except for the ortho-compound suggesting that steric hindrance of chlorine atoms might be important. However, this does not fit in with the good agreement between observed and calculated shifts for 1, 2, 3, 4-tetrachloro-5, 6-difluorobenzene. We cannot account for the large value of $(\delta_{\text{obs}} - \delta_{\text{calc}})$ for the symmetrical 1, 3, 5-trichloro compound.

3.2. Perfluorophenyl compounds

The moderate success achieved in relating the ^{19}F chemical shifts in fluoro-chlorobenzenes to charge densities and electric fields led us to apply the theory to $\text{C}_6\text{F}_5\text{X}$ compounds in which the atomic substituent X is H, Br or I.

	$q(C_z)$	$q(F_z)$	$p(C_z F_z)$	$E_z \times 10^{-6}$ (e.s.u.)	$(\langle E^2 \rangle + E^2) \times 10^{-12}$ (e.s.u.)
 { 1 2 }	1.03526	1.92170	0.27314	0.3630	1.1079
	1.04873	1.92243	0.26956	0.3616	0.7001
 { 1 2 3 }	0.99288	1.91657	0.28827	0.3636	1.5063
	1.00624	1.91727	0.28470	0.3621	1.0983
	1.07840	1.92685	0.25788	0.3628	0.7098
 { 1 2 }	1.03939	1.92149	0.27355	0.3630	1.1080
 { 1 2 3 }	1.00885	1.91754	0.28380	0.3615	1.1180
	1.05047	1.92246	0.26918	0.3609	0.7149
 { 1 2 3 }	0.99549	1.91683	0.28735	0.3635	1.5216
	1.00654	1.91698	0.28498	0.3614	1.11
	1.03699	1.92172	0.27274	0.3625	1.1230

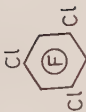
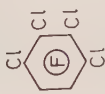
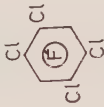
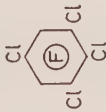
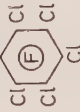
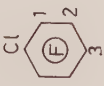
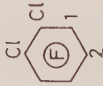
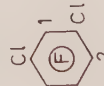


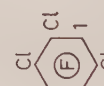
	0.96591	1.91027	0.29859	0.3618	1.5114
	1.00907	1.91723	0.28413	0.3607	1.1281
	0.99800	1.91708	0.28650	0.3622	1.5361
	0.96804	1.91242	0.29855	0.3611	1.5263
	0.97010	1.91250	0.29800	0.3604	1.5412

Table 3. Electron densities, bond orders and electric fields in fluorochlorobenzenes.

	δ_{electric}	$\delta_{\text{electronic}}$	total δ_{calc}	$\delta_{\text{obs}}^{\dagger}$	$\delta_{\text{obs}} - \delta_{\text{calc}}$
 { 1 2 3 }	17.589	4.107	21.693	21.693	0.000
	0.6254	-0.1895	0.436	1.028	0.592
	0.3761	5.840	6.216	6.216	0.000
 { 1 2 }	18.079	3.933	22.012	26.172	4.160
	0.8452	6.406	7.251	6.650	-0.601
 { 1 2 3 }	34.915	7.885	42.800	43.885	1.085
	17.673	10.565	28.238	27.739	-0.499
	1.255	0.1026	1.358	1.638	0.280
	18.083	4.240	22.323	22.280	-0.043
 { 1 2 }	18.506	10.588	29.094	31.709	2.615
	1.471	7.005	8.475	6.509	-1.967
 { 1 2 3 }	35.562	8.032	43.594	47.884	4.290
	18.307	12.031	30.338	27.693	-2.645
	18.717	4.657	23.374	26.140	2.766

	35.131	31.441	66.572	49.588	16.984
	18.932	12.086	31.018	31.349	0.331
	36.175	8.088	44.263	51.182	6.919
	35.760	15.299	51.059	53.271	2.212
	36.390	15.920	52.310	56.830	4.520

† Shifts were measured from CFC1₃ internal reference and converted to C₆F₆ reference using the relationship:

$$\delta_{C_6F_6} = 162.28 + \delta_{CFC1_3}$$

Table 4. Calculated and observed chemical shifts (relative to C₆F₆) in fluorochlorobenzenes.

X	r_{C-X} [14] (Å)	μ_{C-X} [18] (Debye)	ρ_{C-X} [15] ($\times 10^{24}$ cm ³)	I_{C-X} [17] ($\times 10^{12}$ ergs)
Br	1.85	-1.77	3.754	18.8
I	2.05	-1.42	5.752	16.7
H	1.09	+0.5	0.645	20.8

Table 5. Molecular parameters for C₆F₅X compounds.

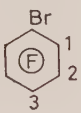
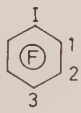
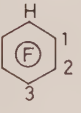
		$q(C_z)$	$q(F_z)$	$\rho(C_z F_z)$	$E_z \times 10^{-6}$ (e.s.u.)	$\langle E^2 + \langle E^2 \rangle \rangle \times 10^{-12}$ (e.s.u.)
	1	1.02855	1.92086	0.27562	0.3674	1.2428
	2	1.07629	1.92669	0.25855	0.3640	0.7012
	3	1.04395	1.92193	0.27119	0.3580	0.6805
	1	1.02365	1.92025	0.27738	0.3384	1.4178
	2	1.07656	1.92672	0.25847	0.3549	0.7014
	3	1.04046	1.92139	0.27254	0.3512	0.6766
	1	1.01920	1.91970	0.27897	-0.1982	0.5354
	2	1.07680	1.92673	0.25839	-0.3130	0.6441
	3	1.03724	1.92093	0.27379	-0.3231	0.6517

Table 6. Charge densities, bond orders and electric fields in C₆F₅X compounds.

A calculation similar to that for $\text{C}_6\text{F}_5\text{Cl}$ was carried out using the molecular parameters for the monosubstituted perfluorobenzenes listed in table 5. The Coulomb and exchange integrals were taken to be :

$$\begin{aligned}\alpha_{\text{F}} &= 2\beta, & \beta_{\text{F}} &= \beta \\ \alpha_{\text{Br}} &= 0.7\beta, & \beta_{\text{Br}} &= 0.3\beta \\ \alpha_{\text{I}} &= 0.6\beta, & \beta_{\text{I}} &= 0.2\beta \\ \alpha_{\text{H}} &= 0\beta, & \beta_{\text{H}} &= 0\beta\end{aligned}$$

and the π -electron charge densities are shown in table 6.

When X is Br or I, the method of calculation is identical with that already described for $\text{C}_6\text{F}_5\text{Cl}$ because $\mu_{\text{C-X}}$ is little different from $\mu_{\text{C-F}}$ and the E_z term may be omitted from the calculations. By carrying out the appropriate subtractions of the values in table 6 and substituting these into equations (5) and (6) gives :

$\text{C}_6\text{F}_5\text{Br}$:

$$\begin{aligned}\sigma_{\text{ortho}} &= 29.740 \times 10^{-6} = 0.5627 \times 10^{12}B + 3.535 \times 10^{-6}(\Delta E)^{-1}, \\ \sigma_{\text{meta}} &= 1.680 \times 10^{-6} = 0.0211 \times 10^{12}B - 0.163 \times 10^{-6}(\Delta E)^{-1}, \\ \sigma_{\text{para}} &= 7.630 \times 10^{-6} = 0.0004 \times 10^{12}B - 5.001 \times 10^{-6}(\Delta E)^{-1};\end{aligned}$$

hence $\Delta E = 0.6568 \text{ eV}$ and $B = 43.29 \times 10^{-18} \text{ e.s.u.}$

$\text{C}_6\text{F}_5\text{I}$:

$$\begin{aligned}\sigma_{\text{ortho}} &= 43.100 \times 10^{-6} = 0.7377 \times 10^{12}B + 3.966 \times 10^{-6}(\Delta E)^{-1}, \\ \sigma_{\text{meta}} &= 2.630 \times 10^{-6} = 0.0213 \times 10^{12}B - 0.199 \times 10^{-6}(\Delta E)^{-1}, \\ \sigma_{\text{para}} &= 9.750 \times 10^{-6} = -0.0035 \times 10^{12}B + 5.689 \times 10^{-6}(\Delta E)^{-1};\end{aligned}$$

hence $\Delta E = 0.5734 \text{ eV}$ and $B = 49.05 \times 10^{-18} \text{ e.s.u.}$

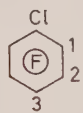
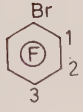
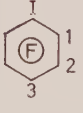
The values of ΔE and B were obtained by solving the above equations involving σ_{ortho} and σ_{para} and the values are seen to be in fair agreement with the corresponding values for $\text{C}_6\text{F}_5\text{Cl}$: again a least squares solution of all three equations gives similar values. The rather high value of B for $\text{C}_6\text{F}_5\text{I}$ may arise from an inaccurate estimate of $P_{\text{C-I}}$. Using these values of ΔE and B the following σ_{meta} shielding constants were calculated :

$$\begin{aligned}\text{C}_6\text{F}_5\text{Br}, \sigma_{\text{meta}} &= 0.665 \times 10^{-6}, \\ \text{C}_6\text{F}_5\text{I}, \sigma_{\text{meta}} &= 0.698 \times 10^{-6}.\end{aligned}$$

The above treatment when applied to $\text{C}_6\text{F}_5\text{H}$ proved to be incapable of predicting the observed chemical shifts ($\delta_{\text{ortho}} = 23.39$, $\delta_{\text{meta}} = 0.22$ and $\delta_{\text{para}} = 8.78 \text{ p.p.m.}$). In this case the change in E_z is important and because the direction of the C-H bond moment ($\sim 0.5 \text{ D}$) is uncertain, the chemical shift calculation is fraught with many difficulties. However, neither sign of the C-H bond moment leads to correct chemical shift predictions: ($\delta_{\text{calc}} - \delta_{\text{obs}}$) values for the ortho-fluorine nuclei of as large as -23 p.p.m. were found. Part of this discrepancy could arise from the many approximations of the theory and the uncertainty in the values of μ , P and I for the system.

The ^{19}F resonance spectra of some of $\text{C}_6\text{F}_5\text{X}$ compounds have been investigated in which X is not a single atom but a group (see tables 8 and 9). In these cases no detailed calculations were attempted because of the difficulty of estimating values of Coulomb and exchange integrals and other necessary parameters. However, an estimate of the ortho effect can be obtained by a comparison of the ortho- and the para-fluorine chemical shifts for each compound. For the

compounds $\text{C}_6\text{F}_5\text{NHCH}_3$, $\text{C}_6\text{F}_5\text{OCH}_3$ and $\text{C}_6\text{F}_5\text{OH}$, the AE_z term will be unimportant and the $(\delta_{\text{para}} - \delta_{\text{ortho}})$ values will reflect the influence of the $B(E^2 + \langle E^2 \rangle)$ term. In fact, the bond polarizabilities and dipole moments [19] of these molecules ($P_{\text{C-N}} = 1.0 \times 10^{-24} \text{ cm}^3$, $P_{\text{C-O}} = 1.3 \times 10^{-24} \text{ cm}^3$, $\mu_{\text{C-N}} = 1.52 \text{ D}$ and $\mu_{\text{C-O}} = 1.3 \text{ D}$) give predicted ortho shifts in the right direction. In the cases of $\text{C}_6\text{F}_5\text{Sn}(\text{CH}_3)_3$ and $\text{C}_6\text{F}_5\text{HgCH}_3$ the values^a of $\mu_{\text{C-Sn}} (= 2.5 \text{ D})$ [20] and $\mu_{\text{C-Hg}} (= 2.8 \text{ D})$ are probably in the opposite direction to $\mu_{\text{C-F}}$ [21], hence there will be a large change in the values of E_z which could account for the large observed ortho shifts. Thus although the polarizabilities of the C-Hg and C-Cl bonds

		$B \times 10^{18}(\text{e.s.u.})$	$\Delta E(\text{ev})$	$\delta_{\text{calc}}(\text{p.p.m.})$	$\delta_{\text{obs}}(\text{p.p.m.})$
	1	42.26	0.7752	21.693†	21.693
	2			0.436	1.028
	3			6.216†	6.216
	1	+43.29	0.6568	29.739†	29.74
	2			0.665	1.68
	3			7.629†	7.63
	1	+49.05	0.5734	43.101†	43.10
	2			0.698	2.63
	3			9.750†	9.75

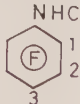
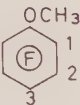
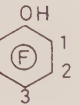
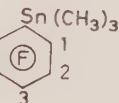
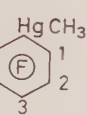
† The perfect agreement between calculated and observed δ values for the ortho and para fluorine nuclei is bound to occur because of the method of calculation of B and ΔE .

Table 7. Values of B and ΔE for monohalopentafluorobenzenes, and observed and calculated chemical shifts.

are almost equal, the values of $(\delta_{\text{para}} - \delta_{\text{ortho}})$ for $\text{C}_6\text{F}_5\text{HgCH}_3$ and $\text{C}_6\text{F}_5\text{Cl}$ are very different. A further possible cause of the large ortho shifts in the tin and mercury derivatives could arise from large changes in ΔE values for the C-F bonds ortho to the substituent since both metal atoms possess low lying excited states. An additional complication arises if a polyatomic substituent places atoms close to an ortho-fluorine atom.

3.3. F-F coupling constants

Table 10 shows the values of the F-F coupling constants in a number of pentafluorophenyl compounds. The values of the coupling constants between nuclei ortho and meta to each other (J_{34} , J_{24} , J_{35} and J_{26}) will have significant contributions from both σ and π - σ interaction mechanisms [22] but in the case of para coupling constants (J_{25}), the five-bond coupling, the value of J_{FF} is dominated by the σ - π mechanism.

		$\delta(\text{p.p.m.})^\dagger$ (± 0.08 p.p.m.)	$\delta_{\text{para}} - \delta_{\text{ortho}}(\text{p.p.m.})$
	$\left\{ \begin{array}{l} 1 \\ 2 \\ 3 \end{array} \right.$	$\begin{array}{l} 0.39 \\ -2.93 \\ -10.79 \end{array}$	-11.18
	$\left\{ \begin{array}{l} 1 \\ 2 \\ 3 \end{array} \right.$	$\begin{array}{l} -3.94 \\ -2.1^\ddagger \\ -2.1^\ddagger \end{array}$	-6.0
	$\left\{ \begin{array}{l} 1 \\ 2 \\ 3 \end{array} \right.$	$\begin{array}{l} -1.41 \\ -2.86 \\ -8.22 \end{array}$	-6.81
	$\left\{ \begin{array}{l} 1 \\ 2 \\ 3 \end{array} \right.$	$\begin{array}{l} 39.98 \\ 1.61 \\ 9.53 \end{array}$	-30.45
	$\left\{ \begin{array}{l} 1 \\ 2 \\ 3 \end{array} \right.$	$\begin{array}{l} 40.37 \\ 2.23 \\ 8.76 \end{array}$	-31.61

† Shifts were measured from CFC1₃ internal reference and converted to C₆F₆ reference using the relationship

$$\delta_{\text{C}_6\text{F}_6} = 162.28 + \delta_{\text{CFC1}_3}.$$

‡ The error in this value is uncertain because of the complex nature of the spectrum.

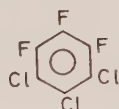
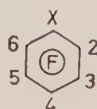
Table 8. ¹⁹F chemical shifts of C₆F₅X compounds relative to C₆F₆.

X	$\pm J_{34}$	$ J_{24} $	$\pm J_{23}^\dagger$	$\mp J_{25}^\dagger$	$ J_{26} ^\dagger$	$ J_{35} ^\dagger$
H	18.7	1.3	21.0	8.9	1.2	2.2
Cl	19.5	< 0.5	20.4	6.1	2.0	5.2
Br	19.9	1.1	21.8	6.4	1.7	5.4
I	19.8	1.92	23.0	7.1	1.2	5.0
NHCH ₃	21.6	6.9	21.1	4.5	2.3	3.9
Sn(CH ₃) ₃	19.1	1.9	26.7	12.0	1.5	6.5
OH	21.1	6.1	21.0	4.4	2.8	3.4
HgCH ₃	19.5	1.1	28.3	11.6	1.6	6.6

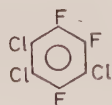
† The assignment is tentative being based upon the likelihood that $|J_{35}| > |J_{26}|$ for the compounds C₆F₅Cl, C₆F₅Br and C₆F₅I.

‡ From the analysis J_{23} is opposite in sign to J_{25} . If it is assumed that there are no sign changes in going from C₆F₄X₂ to C₆F₅X compounds then J_{ortho} is opposite in sign to J_{meta} and J_{para} for fluorobenzenes generally.

Table 9. Values of J_{FF} in c sec⁻¹ (± 0.2) in some pentafluorophenyl compounds



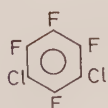
$$|J_{ortho}| = 20.1 \pm 0.1$$



$$|J_{ortho}| = 20.6 \pm 0.1$$

$$|J_{meta}| = 0.75 \pm 0.05$$

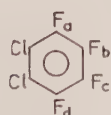
$$|J_{para}| = 9.05 \pm 0.1$$



$$|J_{ortho}| = 20.1 \pm 0.1$$

$$|J_{meta}| = 2.22 \pm 0.05$$

$$|J_{para}| = 7.77 \pm 0.05$$



$$|J_{F_a F_c}| = 19.9 \pm 0.2$$

$$J_{F_a F_b} = \pm 20.8 \pm 0.2$$

$$J_{F_a F_c} = J_{F_b F_d} = \mp 1.7 \pm 0.2$$

$$|J_{F_a F_d}| = 7.8 \pm 0.2$$

Coupling constants were assigned by comparison with values obtained for the other fluorochlorobenzenes

Table 10. J_{FF} values (c sec⁻¹) in fluorochlorobenzenes.

The treatment of McConnell [23] and of Karplus [24] gives the value of the σ - π interaction as :

$$J(\sigma-\pi) = \frac{K}{\Delta\pi} a_F^2,$$

where K is a constant, a_F is the isotropic interaction constant and $\Delta\pi$ is an average singlet-triplet excitation energy. The value of $\Delta\pi$ is not equal to that of ΔE in equation (3), but both excitation energies will depend upon the presence of low-lying excited states in much the same way. Examination of table 10 shows that J_{25} does increase slightly going from $X = \text{Cl}$ to $X = \text{I}$, but that a large increase occurs when $X = \text{SnCH}_3$. This suggests that $\Delta\pi$ and ΔE are exceptionally small for this compound and could explain the excess ortho shift in this compound.

We are indebted to Dr. J. Eve of Newcastle University for assistance with the computations.

REFERENCES

- [1] RAMSEY, N. F., 1951, *Phys. Rev.*, **78**, 699.
- [2] SAIKA, A., and SLICHTER, C. P., 1954, *J. chem. Phys.*, **22**, 26.
- [3] KARPLUS, M., and DAS, T. P., 1961, *J. chem. Phys.*, **34**, 1683.
- [4] PROSSER, F., and GOODMAN, L., 1963, *J. chem. Phys.*, **38**, 374.
- [5] TAFT, R. W., PROSSER, F., GOODMAN, L., and DAVIS, G. T., 1963, *J. chem. Phys.*, **38**, 380.
- [6] BUCKINGHAM, A. D., PITCHER, E., and STONE, F. G. A., 1962, *J. chem. Phys.*, **36**, 124.
- [7] BUCKINGHAM, A. D., 1960, *Canad. J. Chem.*, **38**, 300.
- [8] PETRAKIS, L., and BERNSTEIN, H. J., 1962, *J. chem. Phys.*, **37**, 2731.
- [9] PETRAKIS, L., and BERNSTEIN, H. J., 1963, *J. chem. Phys.*, **38**, 1562.
- [10] BUCKINGHAM, A. D., BERNSTEIN, H. J., and RAYNES, W. T., 1963, *J. chem. Phys.*, **36**, 3481.
- [11] HOWERD, B. B., LINDER, B., and EMERSON, M. T., 1962, *J. chem. Phys.*, **36**, 485.
- [12] STREITWIESER, A., 1961, *Molecular Orbital Theory for Organic Chemists* (New York : Wiley).
- [13] HINZE, J., and JAFFÉ, H. H., 1962, *J. Amer. chem. Soc.*, **84**, 540.
- [14] *Tables of Interatomic Distances and Configuration in Molecules and Ions*, 1958, Ed. L. E. Sutton (London : The Chemical Society).
- [15] SMYTH, C. P., 1931, *Dielectric Constant and Molecular Structure* (New York : The Chemical Catalogue Company).
- [16] LE FÈVRE, R. J. W., and LE FÈVRE, C. G., 1959, *J. chem. Soc.*, p. 2670.
- [17] LANDOLT, H. H., and BORNSTEIN, R., 1950, *Zahlenwerte und Functionen* (Berlin Julius Springer-Verlag), I Band, I Teil.
- [18] SUTTON, L. E., 1931, *Proc. roy. Soc. A*, **133**, 668.
- [19] ARONEY, M., and LE FÈVRE, R. J. W., 1960, *J. chem. Soc.*, p. 3600.
- [20] CHAMBERS, R. D., and CHIVERS, T., 1963 (private communication).
- [21] CHAMBERS, R. D., COATES, G. E., LIVINGSTONE, J. G., and MUSGRAVE, W. K. R., 1963, *J. chem. Soc.*, p. 4367.
- [22] GUTOWSKY, H. S., and WILLIAMS, G. A., 1959, *J. chem. Phys.*, **30**, 717.
- [23] MCCONNELL, H. M., 1959, *J. chem. Phys.*, **30**, 126.
- [24] KARPLUS, M., 1960, *J. chem. Phys.*, **33**, 1842.

Alternant molecular orbital treatment of the allyl cation, radical and anion

by D. P. CHONG and J. W. LINNETT

Inorganic Chemistry Laboratory, Oxford

(Received 29 January 1964)

Calculations have been made using the alternant molecular orbitals (AMO) proposed by Löwdin, which are designed to make some allowance for correlation effects arising from interelectron repulsion, for the electrons in the π -systems of the allyl radical and ions. Calculations have also been carried out at the same general level of approximation using a full configuration interaction (CI) treatment and the non-paired spatial orbitals first used by Hirst and Linnett. It is found that the function using non-paired spatial orbitals resembles the full CI one more closely than does the AMO function. This conclusion is based on the calculation of energies and overlap integrals.

1. INTRODUCTION

One problem in devising electronic wave functions for polyatomic molecules is to make satisfactory allowance for the tendency of electrons having opposed spins to keep apart because of electrostatic repulsion. Two methods have recently been proposed which aim to allow for this. The first of these makes use of so-called alternant molecular orbitals (AMO) and was proposed by Löwdin [1]; the second was first used by Hirst and Linnett [2] and called by them non-pairing (NP) to indicate that every electron is placed in a different spatial orbital. In order to stress that this procedure implies only an absence of spatial-pairing, it is proposed to call this the method of non-paired spatial orbitals (NPSO), meaning that a pair of electrons is never assigned to the same spatial-orbital, (i.e. no two electrons are given the same spatial function). This paper describes the application of these two methods to the π -systems of the allyl cation, radical and anion containing 2, 3 and 4 electrons respectively. A corresponding full configuration interaction (CI) treatment has been carried out so that a more satisfactory assessment of the two methods can be made.

The calculations have been carried out using the same molecular dimensions as those used by Hirst and Linnett. The core approximation due to Goepfert-Mayer and Sklar [3] was again used. The values of some of the three-centre integrals were improved but the changes were small. However the C.I. and NPSO calculations were repeated so that a strict comparison with the AMO calculations would be possible. Slater-type $2p\pi$ atomic orbitals were used with $Z' = 3.18$.

2. CALCULATIONS AND RESULTS

The following symbols are used: a , b and c for the normalized Slater-type $2p\pi$ atomic orbitals on the three atoms taken in order; χ , orthonormal LCAO molecular orbitals; Φ , anti-symmetrized wave functions based on orthonormal molecular orbitals (ASMO); ϕ , orthonormal AMOs; Ψ , anti-symmetrized alternant molecular orbitals (ASAMO). In addition, calculations were made using

the alternant molecular orbitals derived using orthogonalized atomic orbitals (OAO). These are symbolized by a^0 , b^0 and c^0 and the other functions based on them by χ^0 , Φ^0 , ϕ^0 and Ψ^0 .

In general, the LCAO molecular orbitals are:

$$\chi_1 = C_1(a + kb + c),$$

$$\chi_2 = C_2(a - c),$$

$$\chi_3 = C_3(a - lb + c),$$

where $l = 2(1 + kS_{ab} + S_{ac})/(k + 2S_{ab})$ for orthogonality, and C_1 , C_2 and C_3 are the normalization constants. There remains, therefore, an undetermined parameter k , for which several choices are possible, such as setting l and k equal, or using the best k for the anti-symmetrized MO function for each of the three species. For the single-configuration ASMO treatment (see Results), this parameter k is varied to minimize the energy of each species, and the values of best k for the cation, radical, and anion are 1.5712, 1.5143 and 1.4608 respectively. However, for the basic set of LCAO molecular orbitals from which the AMOs are to be constructed, k has been chosen to be $\sqrt{2}$, the value one would obtain from a Hückel- or Wheland-type approximation, so that the present results can be directly compared with those of Dearman and Lefebvre [4], who carried out an AMO treatment of the radical. (This simple approximation neglects electron correlation, which is precisely what the AMO method sets out to take into account.) The orthonormal LCAO molecular orbitals, then, are:

$$\chi_1 = 0.424543(a + c) + 0.600395b,$$

$$\chi_2 = 0.721263(a - c),$$

$$\chi_3 = 0.610764(a + c) - 0.888299b,$$

which are almost identical with those employed by Dearman and Lefebvre [4]. The transformation of the χ functions into AMO's (ϕ) is given by:

$$\begin{bmatrix} \phi_1 \\ \phi_2 \\ \phi_3 \end{bmatrix} = \begin{bmatrix} \cos \theta & 0 & \sin \theta \\ 0 & 1 & 0 \\ \cos \theta & 0 & -\sin \theta \end{bmatrix} \begin{bmatrix} \chi_1 \\ \chi_2 \\ \chi_3 \end{bmatrix},$$

or more conveniently by

$$\phi_1 = (1 + \lambda^2)^{-1/2}(\chi_1 + \lambda \chi_3),$$

$$\phi_2 = \chi_2,$$

$$\phi_3 = (1 + \lambda^2)^{-1/2}(\chi_1 - \lambda \chi_3),$$

where $\lambda = \tan \theta$.

2.1. Cation

The four ASMO configurations having the symmetry of the ground state (1A_1) may be represented by:

$$\Phi_1^+ = (\chi_1, \chi_1), \quad \Phi_2^+ = \frac{1}{\sqrt{2}}\{(\chi_1, \chi_3) + (\chi_3, \chi_1)\},$$

$$\Phi_3^+ = (\chi_2, \chi_2), \quad \Phi_4^+ = (\chi_3, \chi_3),$$

where (χ_1, χ_1) represents the determinant for two electrons both occupying the orbital χ_1 . In all cases the spin orbitals are associated with the space orbitals in the order $\alpha\beta$. The alternant molecular orbital function can be developed by

application of the symmetry and spin projection operators to the function $\phi_1(1)\alpha(1)\phi_3(2)\beta(2)$. This gives

$$\frac{1}{2}\{(\phi_1, \phi_3) + (\phi_3, \phi_1)\} = \frac{1}{1+\lambda^2}\{\Phi_1^+ - \lambda^2\Phi_4^+\}.$$

Since this function is not normalized,

$$\Psi^+ = \Phi_1^+ - \lambda^2\Phi_4^+$$

may equally well be used.

2.2. Radical

The four ASMO configurations having the symmetry of the ground state (2A_2) may be represented by:

$$\Phi_1 = (\chi_1, \chi_1, \chi_2), \quad \Phi_2 = -\frac{1}{\sqrt{6}}\{2(\chi_1, \chi_2, \chi_3) + (\chi_2, \chi_1, \chi_3) + (\chi_1, \chi_3, \chi_2)\},$$

$$\Phi_3 = \frac{1}{\sqrt{2}}\{(\chi_2, \chi_1, \chi_3) - (\chi_1, \chi_3, \chi_2)\},$$

$$\Phi_4 = (\chi_3, \chi_3, \chi_2);$$

the order of the associated spin functions is $\alpha\beta\alpha$. The alternant molecular orbital function has been developed by Dearman and Lefebvre [4] by applying the symmetry and spin projection operators to the function

$$\phi_1(1)\alpha(1)\phi_3(2)\beta(2)\phi_2(3)\alpha(3).$$

This gives

$$\frac{1}{3}\{2(\phi_1, \phi_3, \phi_2) + (\phi_3, \phi_1, \phi_2) + (\phi_1, \phi_2, \phi_3)\}$$

and

$$\Psi = \Phi_1 + \sqrt{\frac{2}{3}}\lambda\Phi_2 - \lambda^2\Phi_4.$$

2.3. Anion

The four ASMO configurations having the symmetry of the ground state (1A_1) may be represented by

$$\Phi_1^- = (\chi_1, \chi_1, \chi_2, \chi_2),$$

$$\Phi_2^- = (\chi_1, \chi_1, \chi_3, \chi_3);$$

$$\Phi_3^- = \frac{1}{\sqrt{2}}\{(\chi_1, \chi_3, \chi_2, \chi_2) + (\chi_3, \chi_1, \chi_2, \chi_2)\},$$

$$\Phi_4^- = (\chi_2, \chi_2, \chi_3, \chi_3);$$

the order of the associated spin functions being $\alpha\beta\alpha\beta$. The alternant molecular orbital function can be developed by applying the symmetry and spin projection operators to the function

$$\phi_1(1)\alpha(1)\phi_3(2)\beta(2)\phi_2(3)\alpha(3)\phi_2(4)\beta(4).$$

This gives

$$\frac{1}{2}\{(\phi_1, \phi_3, \phi_2, \phi_2) + (\phi_3, \phi_1, \phi_2, \phi_2)\}$$

and

$$\Psi^- = \Phi_1^- - \lambda^2\Phi_4^-.$$

2.4. *Orthogonalized atomic orbitals*

The AMO calculation has also been carried out using orthogonalized atomic orbitals (OAO) which are related to the atomic orbitals by:

$$a^0 = 1.02687a - 0.13776b + 0.00685c,$$

$$b^0 = -0.13776a + 1.05432b - 0.13776c,$$

$$c^0 = 0.00685a - 0.13776b + 1.02687c.$$

The molecular orbitals are then:

$$\chi_1^0 = \frac{1}{2} (a^0 + \sqrt{2}b^0 + c^0)$$

$$\chi_2^0 = \frac{1}{\sqrt{2}} (a^0 - c^0)$$

$$\chi_3^0 = \frac{1}{2} (a^0 - \sqrt{2}b^0 + c^0).$$

These are combined together to give alternant molecular orbitals in a manner identical with that already described. Calculations carried out along these lines will be called OAO AMO.

2.5. *Results*

The results of these calculations are shown in the table which lists the energies obtained using (a) a single configuration antisymmetrized MO function with a variable parameter k in place of $\sqrt{2}$ in χ_1 ; (b) a valence-bond function of the

Function	Present calculations			Hirst-Linnett [2]		
Cation	E (k or λ)	$E - E_{CI}$	$1 - S$	E (k or λ)	$E - E_{CI}$	$1 - S$
MO	-2.16156 (1.5712)	0.07263	0.0351	-2.1635 (1.563)	0.0707	0.034
VB	-2.15349 (0.1208)	0.08070	0.0615	-2.1538 (0.1222)	0.0804	0.068
AMO	-2.19512 (0.4159)	0.03907	0.0253	—	—	—
OAO AMO	-2.19615 (0.4157)	0.03804	0.0257	—	—	—
NPSO	-2.21980 (0.2512)	0.01439	0.0116	-2.2199 (0.252)	0.0143	0.012
CI	-2.23419	—	—	-2.2342	—	—
Radical						
MO	-1.99382 (1.5143)	0.13238	0.0717	-1.9937 (1.511)	0.1316	0.055
VB	-2.12122 (0.2164)	0.00498	0.0275	-2.1205 (0.2212)	0.0048	0.002
AMO	-2.12378 (0.4516)	0.00242	0.0011	—	—	—
OAO AMO	-2.12434 (0.4513)	0.00186	0.0008	—	—	—
NPSO	-2.12540 (0.2769)	0.00080	0.0004	-2.1245 (0.2790)	0.0008	0.0004
CI	-2.12620	—	—	-2.1253	—	—
Anion						
MO	-0.98622 (1.4608)	0.07923	0.0381	-0.9877 (1.4767)	0.0785	0.038
VB	-0.97212 (0.1183)	0.09333	0.0747	-0.9707 (0.1195)	0.0955	0.076
AMO	-1.02070 (0.4077)	0.04475	0.0337	—	—	—
OAO AMO	-1.02096 (0.4079)	0.04449	0.0325	—	—	—
NPSO	-1.03612 (1.5891)	0.02933	0.0152	-1.0362 (1.5991)	0.0300	0.016
CI	-1.06545	—	—	-1.0662	—	—

Calculated energies in Rydbergs using various functions. The values of λ or k necessary for energy minimization are given in parenthesis. The parameters k for the various functions are defined in the paper by Hirst and Linnett. Values of the difference from unity of the overlap integral (S) with the CI function are also included.

Coulson–Fischer [5] type; (c) an AMO function; (d) an AMO function based on OAO; (e) a non-pairing function; and (f) a full CI function. The table also gives the results obtained by Hirst and Linnett [2] for comparison. It also includes the values of the adjustable parameters (λ for the AMO functions, otherwise k). From Dearman and Lefebvre's calculations for the radical, the energy calculated using an AMO function was 0.00153 Rydbergs above the CI energy, (with $\lambda = 0.4500$). Our corresponding figures are 0.00242 with $\lambda = 0.4516$. The present results agree in essentials with those of Hirst and Linnett [2]. The changes resulting from changes in the values of some of the integrals are small.

3. DISCUSSION

The results in the table show that, for the two ions, the two AMO functions roughly halve the values of $(E - E_{\text{CI}})$ relative to that obtained using a single configuration MO function with variable k †. For the radical the improvement is much greater. For the ions the performance of the MO and VB functions is similar, but, for the radical, the VB function gives an energy much closer to the CI value. For all three species the NPSO functions allow more successfully for the effects of electron repulsion than do the AMO functions. The value of $E - E_{\text{CI}}$ for the NPSO functions is about half that for the AMO functions. The result of using the overlap integral as a means of testing the functions would be similar.

The NPSO function will, of course, suffer from the same faults as the CI function (e.g. lack of allowance for σ – π interaction) but it is reasonable to presume that when it becomes possible to correct for these faults in the CI function it will also be possible to correct for them in the NPSO functions.

One of us (D.P.C.) wishes to thank N.A.T.O. for a post-doctoral Fellowship.

† The values of $(E - E_{\text{CI}})$ for Φ_1^+ , Φ_1 , and Φ_1^- are 0.07520, 0.13348 and 0.07948 Rydbergs respectively.

REFERENCES

- [1] LÖWDIN, P.-O., 1953, *Symposium on Molecular Physics* (Tokyo: Maruzen), p. 13.
- [2] HIRST, D. M., and LINNETT, J. W., 1962, *J. chem. Soc.*, pp. 1035, 3844.
- [3] GOEPPERT-MAYER, M., and SKLAR, A. L., 1938, *J. chem. Phys.*, **6**, 645.
- [4] DEARMAN, H. H., and LEFEBVRE, R., 1961, *J. chem. Phys.*, **34**, 72.
- [5] COULSON, C. A., and FISCHER, I., 1949, *Phil. Mag.*, **40**, 386.

Ein neues Programm zur quantentheoretischen Berechnung von Molekülen und Atomsystemen

I. Grundlagen

von H. PREUSS

Max-Planck-Institut für Physik und Astrophysik, München, Germany

(Received 15 July 1963)

Bei allen Verfahren der Quantenchemie, in denen die Wellenfunktion als Summe von Determinanten dargestellt wird, treten bei Verwendung von Slater- oder slaterähnlichen Funktionen grosse Intergrationsschwierigkeiten auf. Diese können praktisch beseitigt werden, wenn sogenannte reine Gaußfunktionen verwendet werden. Es handelt sich dabei um Funktionen vom Typ

$$\phi_{\lambda}(\mathbf{r}) = \exp -\alpha_{\lambda}(\mathbf{r} - \mathbf{r}_{\lambda})^2,$$

bei denen der Vektor \mathbf{r}_{λ} beliebig im Raum verschoben sein kann, also α_{λ} und \mathbf{r}_{λ} als Variationsparameter verwendet werden können. Das auf diese Weise modifizierte Verfahren erlaubt eine neue Interpretation der Ψ -Funktionen-Darstellung, die sehr anschaulich ist.

Nach einer Diskussion der Determinantenentwicklung bezüglich reiner Ψ -Zustände, wird anhand von einigen Testrechnungen die Brauchbarkeit dieser reinen Gaußfunktionen untersucht. Es zeigt sich, dass diese unbedenklich zu Molekülberechnungen herangezogen werden können.

1. EINFÜHRUNG

In den letzten Jahren sind einige Verfahren und Programme vorgeschlagen und angewendet worden, die eine rein theoretische Berechnung von Moleküleigenschaften zum Ziele haben. Es handelt sich dabei um Verfahren, die ohne empirische Anleihe, also sozusagen *ab initio*, die Wellenfunktionen und die dazugehörigen Energieeigenwerte beliebig genau zu berechnen gestatten [1-3].

Solche Programme, die eine abgewandelte und erweiterte Form der Methode der Konfigurationenwechselwirkung darstellen, sind nur mit großen Rechenmaschinen zu bewältigen und sehen ihre Stärke darin, daß allein nach Vorgabe der Elektronenanzahl n und eines bestimmten Funktionsansatzes χ_j ($j=1\dots$), sowie der Lage \mathcal{R}_{λ} ($\lambda=1\dots N$) der N Atomkerne mit den Ladungen Z_{λ} ($\lambda=1\dots N$), die Rechnungen begonnen werden können, und danach keinerlei Informationen mehr notwendig sind.

Dieses Vorgehen kann prinzipiell auf jede chemische Verbindung angewendet werden, wobei die Genauigkeit der Resultate hauptsächlich von der Anzahl M der verwendeten Funktionen ψ_K abhängt

$$\Psi = \sum_{K=1}^M C_K \psi_K, \quad (1)$$

und von den χ_j , mit denen die ψ_K aufgebaut werden. Bisher hat man für die ψ_K fast ausschließlich Determinanten verwendet

$$\psi_K = \frac{1}{\sqrt{n!}} \det \{ \bar{\chi}_j(i) \}, \quad (1a)$$

$$\bar{\chi}_j = \chi_j^{\alpha\beta} \quad (\alpha, \beta, \text{ Spinfunktionen}), \quad (1b)$$

Über die Bedeutung solcher Methoden in der Quantenchemie ist schon des

öfteren diskutiert worden [3, 4]. Handelt es sich doch hier letzten Endes um eine mit Hilfe von Rechenmaschinen vollautomatische Integration der Schrödingergleichung (in at. E .)

$$\mathcal{H}\Psi = \mathcal{E}\Psi; \quad \int \Psi^* \Psi d\tau = 1 \quad (2)$$

mit

$$\mathcal{H} = \sum_{i=1}^n H(i) + \sum_{i=1}^{n-1} \sum_{j=i+1}^n \frac{1}{r_{ij}} \quad (2a)$$

und

$$H(i) = \frac{1}{2}\Delta_i - \sum_{\lambda=1}^N \frac{Z_{\lambda}}{r_{\lambda i}}, \quad (2b)$$

sodaß sich die Frage erhebt, welches Verständnis bezüglich der Natur der chemischen Bindung in dem jeweils vorliegenden Molekül damit erreicht worden ist. Ohne Zweifel nämlich kann das Ziel solcher Methoden letztlich nur darin bestehen, die Automation so weit zu treiben, daß nur noch die Vorgabe von n , Z_{λ} und \mathcal{R}_{λ} ausreicht, um Ψ_s und die dazugehörigen Energieeigenwerte \mathcal{E}_s des Systems mit beliebiger Genauigkeit zu bestimmen, wobei die Größe der zu behandelnden Moleküle, bei vorgegebener Genauigkeit und Rechenzeit, allein von der Kapazität der elektronischen Rechenmaschine abhängt. Dabei dürfte dann der Funktionensatz ψ_K (bzw. χ_j) von vornherein fixiert sein, oder wird von der Maschine selbst, je nach Problem, aufgebaut. Wenn eine Interpretation der ψ_K möglich ist, so besteht eine wesentliche Information des Verfahrens in der Angabe der C_K in (1). Die obige Frage läßt sich daher so beantworten, daß allein die Interpretation von ψ_K , soweit überhaupt möglich ein gewisses Verständnis der chemischen Bindung im Rahmen dieser Verfahren ermöglicht, indem $|C_K|^2$ ein Maß dafür ist, wie stark, ψ_K an der Beschreibung des Moleküls beteiligt ist. Mit anderen Worten: Der Ansatz (1) erlaubt eine Analyse der Ψ -Funktion in dem Sinne, daß nach der Beteiligung der einzelnen ψ_K am Zustandekommen von Ψ gefragt wird. Der Ansatz (1) setzt also schon eine gewisse Kenntnis voraus, wobei sehr viele ψ_K , entsprechend ihrer Bedeutung, von vornherein weggelassen werden, was sich in einem endlichen M ausdrückt.

In der Methode der Konfigurationen-Wechselwirkung (CI-Verfahren) [3, 4] bedeuten die ψ_K Elektronenkonfigurationen, wobei in der Regel für χ_j Slaterfunktionen Verwendung finden, die zu einem recht komplizierten Integrationsproblem führen, wenn mit Ψ die Energie des Systems berechnet werden soll. In vielen Fällen sind aber die in Frage kommenden Konfigurationen nicht bekannt, sodaß zuweilen recht willkürlich eine Auswahl aus den angeregten Zuständen vorgenommen wird, um M nicht zu groß werden zu lassen. Aus diesem Grunde wurde in Erweiterung dieses Vorgehens das sogenannte Verfahren der 'co-detors' entwickelt [2], welches den Begriff der Konfiguration nicht mehr in dem obigen engen Sinne kennt. Es handelt sich zwar immer noch um reine Zustände ('pure state wave-function'), doch ist man in den Eielektronenfunktionen nicht mehr ausschließlich auf Slaterfunktionen angewiesen. Damit geht freilich ein Teil der 'Anschaulichkeit' der ψ_K verloren, besonders dann, wenn für χ_j Funktionen Verwendung finden, die bestimmte Charakteristika der Slaterfunktionen nicht mehr besitzen, wie etwa [4].

$$\chi_j^{(nlm)}(\mathbf{r}) = X^n Y^l Z^m \exp[-\alpha(\mathbf{r} - \mathbf{r}_{\lambda})^2] \quad (3)$$

wo \mathbf{r}_λ den Ort eines im Molekül vorkommenden Atoms bedeutet und die kartesischen Koordinaten von einem weitgehend beliebig im Molekül liegenden Koordinatenursprung zählen [20]. In ähnlicher Weise wurde mit

$$\chi_j^{(nlm)}(\mathbf{r}) = P_l^{(m)}(\cos \vartheta) \exp(im\phi) \exp[-\alpha(\mathbf{r} - \mathbf{r}_\lambda)^2] \quad (3a)$$

gerechnet [5], worin die Polarkoordinaten ϑ und ϕ entweder wieder von einem bestimmten Punkt im Molekül aus definiert waren, oder, wieder mehr an die Slaterfunktionen angelehnt, vom Atom λ aus gezählt wurden.

Verzichtet man auf eine physikalische (oder chemische) Interpretation der ψ_K , so laufen die Verfahren mit (1) auf eine Entwicklung der Ψ -Funktion nach einem vollständigen Funktionensystem ψ_K ($k=1, 2, \dots$) hinaus, wobei, wegen (1a), die Vollständigkeit schon von den χ_j erfüllt werden muß [2].

Ein Beispiel für solche Ansätze sind die Ansätze für das H_2^- - und HeH^+ -Molekül [6, 7],

$$\Psi = \exp[-(\delta_1\mu_1 + \delta_2\mu_2)] \sum C_{mnjkp} \{\mu_1^m \mu_2^n r_1^j r_2^k + \mu_1^n \mu_2^m r_1^k r_2^j\} r_{12}^p \quad (4)$$

die Entwicklungen in elliptischen Koordinaten darstellen und sogar in diesem einzigen Falle auf die Determinantendarstellung (1a) verzichten. Dadurch wird allerdings auch auf eine allgemeine Konstruktionsvorschrift für ψ_K , die im Prinzip bei den anderen Verfahren auf alle Moleküle anwendbar bleibt, verzichtet.

Eine Mittelstellung nimmt der Ansatz (5) ein, der am Li_2 -Molekül ausprobiert wurde [8]:

$$\Psi = \sum_{m,n,j,k} C_{mnjk} \{\psi_{mnjk} + \psi_{nmkj}\}$$

$$\psi_{mnjk} = \begin{vmatrix} \phi_a(1s/1)\alpha(1) & \phi_a(1s/2)\alpha(2) \dots & \phi_a(1s/6)\alpha(6) \\ \phi_a(1s/1)\beta(1) \dots & & \cdot \\ f_{mj}(1)\alpha(1) \dots & & \cdot \\ \phi_b(1s/1)\alpha(1) \dots & & \cdot \\ \phi_b(1s/1)\beta(1) \dots & & \cdot \\ f_{nk}(1)\beta(1) \dots & & f_{nk}(6)\beta(6) \end{vmatrix} \quad (5)$$

$$f_{mj}(i) = \mu_i^m v_{ij} \exp(-\lambda\mu_i) \quad f_{nk}(i) = \mu_i^n v_{ik} \exp(-\lambda\mu_i)$$

$$\mu_i = \frac{1}{R}(r_{ai} + r_{bi}) \quad r_i = \frac{1}{R}(r_{ai} - r_{bi})$$

2. MATHEMATISCHE ASPEKTE

Allen Verfahren dieser Art ist gemeinsam, daß die Variation der C_K auf Energieminimum auf ein Säkulargleichungssystem führt

$$\sum_{K=1}^M C_K \{H_{KL} - S_{KL}\tilde{\mathcal{E}}\} = 0; \quad (L=1 \dots M), \quad (6)$$

aus dessen Determinante

$$\det \{H_{KL} - S_{KL}\tilde{\mathcal{E}}\} = 0 \quad (6a)$$

die Näherungswerte $\tilde{\mathcal{E}}_s$ für die Energie in (2) erhalten werden, für die die folgenden Ungleichungen gelten

$$\tilde{\mathcal{E}}_s \geq \mathcal{E}_s; \quad (s=1 \dots M). \quad (7)$$

Die obigen Matrixelemente H_{KL} und S_{KL} ergeben sich im einzelnen zu

$$H_{KL} = \int \psi_K^* \mathcal{H} \psi_L d\tau, \quad S_{KL} = \int \psi_K^* \psi_L d\tau. \quad (8)$$

Hier beginnt nun das oben erwähnte Integrationsproblem. Bezeichnen wir die

χ_j die zur K -ten Determinante gehören mit $\chi_j^{(K)}$ oder kürzer mit K_j , so läßt sich (1 b) schreiben

$$\bar{K}_j = K_j \sigma_j^K; \quad \sigma_j^K = \begin{Bmatrix} \alpha \\ \beta \end{Bmatrix}, \quad (1c)$$

und die H_{KL} und S_{KL} ergeben sich mit (1 a) zu [9]

$$H_{KL} = \sum_i^n \sum_j^n [\bar{K}_i | H | \bar{L}_j] B_{KL}(i/j) + \sum_{\substack{k \\ (k \neq l)}}^n \sum_{\substack{l \\ i=1}}^{n-1} \sum_{j=i+1}^n [\bar{K}_k L_i | \bar{K}_l \bar{L}_j] B_{KL}(kl/ij), \quad (9)$$

$$S_{KL} = \begin{vmatrix} [\bar{K}_1 | L_1] [\bar{K}_1 | L_2] \dots [\bar{K}_1 | L_n] \\ \vdots \\ [\bar{K}_n | L_1] \dots [\bar{K}_n | L_n] \end{vmatrix} \equiv B_{KLj} (K, L = 1 \dots M). \quad (10)$$

Dabei bedeuten die Abkürzungen in (9) und (10) die folgenden Integrale

$$[\bar{K}_k \bar{L}_i | \bar{K}_l \bar{L}_j] = [\sigma_k^K | \sigma_i^L] [\sigma_l^K | \sigma_j^L] [K_k L_i | K_l L_j], \quad (11a)$$

$$[\bar{K}_i | H | \bar{L}_j] = [\sigma_i^K | \sigma_j^L] \left\{ -\frac{1}{2} [\Delta | K_i L_j] - \sum_{\mu=1}^N Z_\mu [r_\mu^{-1} | K_i L_j] \right\}, \quad (11b)$$

$$[\bar{K}_j | \bar{L}_i] = [\sigma_j^K | \sigma_i^L] [K_j | L_i], \quad (11c)$$

und weiter

$$[K_k L_i | K_l L_j] = \int \int \chi_k^{(K)*}(1) \chi_i^{(L)}(1) \frac{1}{r_{12}} \chi_l^{(K)*}(2) \chi_j^{(L)}(2) d\tau_1 d\tau_2, \quad (12a)$$

$$-\frac{1}{2} [\Delta | K_i L_j] = -\frac{1}{2} \int \chi_i^{(K)*} \Delta \chi_j^{(L)} d\tau, \quad (12b)$$

$$[r_\mu^{-1} | K_i L_j] = \int \chi_i^{(K)*} \frac{1}{r_\mu} \chi_j^{(L)} d\tau = [\mu^{-1} | K_i L_j], \quad (12c)$$

$$[K_i | L_j] = \int \chi_i^{(K)*} \chi_j^{(L)} d\tau. \quad (12d)$$

Ferner ist $B_{KL}(i/j)$ die Unterdeterminante von B_{KL} , die dadurch erhalten wird, daß in B_{KL} die i -te Spalte und die j -te Zeile gestrichen werden und das Ergebnis mit $(-1)^{i+j}$ multipliziert wird. Entsprechend ist $B_{KL}(kl/ij)$ als Unterdeterminante zweiter Ordnung von B_{KL} zu bilden.

Wir sehen daraus, daß es nicht nur eine große Anzahl von Integralen zu berechnen gilt, die daher sehr genau sein müssen, sondern daß auch die Integrale selbst zu heute noch nicht befriedigend gelösten Problemen führen. Während nämlich das Überlappungsintegral (12 d) und das Integral der kinetischen Energie (12 b) maximal zwei Zentren enthalten können, die von den beiden χ -Funktionen herrühren, kann schon das Kernwechselwirkungsintegral maximal dreizentrig sein. Im Zweielektronen-Wechselwirkungsintegral (12 a) schließlich, können alle vier Funktionen um verschiedene Zentren definiert sein.

Wir sind heute noch nicht in der Lage, Drei- und Vierzentrenintegrale ausreichend genau zu berechnen [10], sodaß bisher mit dieser Methode fast nur zweiatomige Systeme berechnet worden sind. In allen anderen wenigen Fällen sind eine große Anzahl von Integralapproximationen notwendig, sodaß diese Ergebnisse mit ziemlichen Fehlern behaftet sind.

Besonders diese Schwierigkeiten sind es, die ein solches Verfahren heute noch recht umständlich und langwierig machen. Das Lösen der Säkulargleichungen (6), (6 a) dagegen, ist mit größeren Rechenmaschinen noch vergleichsweise bequem

durchzuführen. Es ist bisher bei größeren Molekülen noch nicht möglich gewesen das gesamte Verfahren in einem Schritt (ohne Herausgabe von Zwischenergebnissen zur Weiterrechnung) zu bewältigen, wenn χ -Funktionen nach (3), (3 a) oder Slaterfunktionen Verwendung fanden.

3. DIE Ψ -FUNKTIONEN REINER ZUSTÄNDE

Ein weiteres Problem tritt auf (besonders wenn es sich um die Berechnung von angeregten Zuständen handelt), wenn es gilt, die Ψ -Funktion, die ja keine Eigenfunktion zu \mathcal{H} ist, zumindestens als Eigenfunktion zu bestimmten Operatoren \mathcal{O} anzusetzen, die mit \mathcal{H} vertauschbar sind

$$\mathcal{H}\mathcal{O} - \mathcal{O}\mathcal{H} \equiv 0. \quad (13)$$

Solche Ψ -Funktionen, die reine Zustände repräsentieren, werden durch die Eigenwerte dieser Operatoren klassifiziert. Die Variationsfunktion Ψ^\dagger hat somit schon bestimmte Eigenschaften der exakten Lösung, was für die zu erwartenden Ergebnisse von Vorteil ist. Auch rechnerisch ist ein solcher Ansatz von Vorteil, denn sind ϕ und ϕ' zwei Eigenfunktionen von \mathcal{O} zu verschiedenen Eigenwerten \mathcal{O} und \mathcal{O}' , so gilt

$$\int \phi^* \phi' d\tau = 0 \quad (14)$$

und

$$\int \phi^* \mathcal{H} \phi' d\tau = 0. \quad (15)$$

Wird daher eine endliche Anzahl von ϕ_K -Funktionen zu einem linearen Ansatz zusammengefaßt, so zerfällt, wegen (14), die Matrix der Faktoren von C_K in (6) in eine Reihe von Blöcken, die den einzelnen Eigenwerten \mathcal{O} zugeordnet werden können. Das Säkularproblem kann daher auf diese Weise in seinem Grad reduziert werden.

Für \mathcal{O} kommen im allgemeinen die Operatoren des Spins \mathcal{S}^2 und \mathcal{S}_z in Frage, die mit \mathcal{H} nach (2 a) vertauschbar sind, sowie gewisse Symmetriepoperatoren, wenn das Molekül in den jeweiligen Kernlagen Symmetrien besitzt. Die Determinanten nach (1 a) sind immer Eigenfunktionen zu \mathcal{S}_z . Die Eigenfunktionen zu \mathcal{S}^2 lassen sich durch Linearkombinationen der Eigenfunktionen zu einem bestimmten Eigenwert von \mathcal{S}_z darstellen [11]. Bei linearen Molekülen ist noch der Operator \mathcal{L}_z des Drehimpulses in Richtung der Molekülachse mit \mathcal{H} vertauschbar. Die zu den Eigenwerten $L_z = 0, \pm 1, \pm 2 \dots$ gehörenden Eigenfunktionen oder Zustände werden bekanntlich mit den Symbolen $\Sigma, \Pi^\pm, \Delta^\pm \dots$ bezeichnet.

Liegen keine Symmetrien vor und handelt es sich auch um kein lineares Atomsystem, so kann nur mit Hilfe von \mathcal{S}_z und \mathcal{S}^2 das Säkularproblem reduziert werden.

4. DIE VERWENDUNG VON REINEN GAUSSFUNKTIONEN [12, 19]

Wie wir oben gesehen hatten, tritt besonders das Integralproblem bei der Berechnung der Matrixelemente H_{KL} und S_{KL} in den Vordergrund. Aus diesem Grunde sind in den letzten Jahren eine Reihe von sehr umfangreichen Integraltabellen veröffentlicht worden [10, 13]. Nur mit sehr großen Rechenmaschinen darf man hoffen, auch die Integrationen bei diesen Verfahren in einem

† Im Vergleich zur Lösung Ψ mit $\tilde{\Psi}$ bezeichnet.

Arbeitsgang zu erledigen. Es bleibt auch dann noch die Berechnung der H_{KL} und S_{KL} die Hauptarbeit.

Es gibt nun einen Funktionssatz χ_j mit dem die Integrale in (12) eine sehr einfache Form annehmen. Es handelt sich dabei um die sogenannten reinen Gaußfunktionen.

$$\chi_\lambda(\mathbf{r}) = \left(\frac{2\alpha_\lambda}{\pi}\right)^{3/4} \exp[-\alpha_\lambda(\mathbf{r} - \mathbf{r}_\lambda)^2], \quad (16)$$

mit denen sich die Integrale von (12) in der folgenden Form ergeben [2, 4]

$$[\lambda\mu | \nu\sigma] = B_{\nu\sigma}^{\lambda\mu} K(B_{\nu\sigma}^{\lambda\mu} | \mathbf{r}_{\lambda\mu} - \mathbf{r}_{\nu\sigma}) [\lambda\mu] [\nu\sigma], \quad (17a)$$

$$-\frac{1}{2}[\Delta | \lambda\mu] = \frac{1}{2}A_{\lambda\mu} \{3 - (\mathbf{r}_\lambda - \mathbf{r}_\mu)^2 A_{\lambda\mu}\} [\lambda\mu], \quad (17b)$$

$$[\sigma^{-1} | \lambda\mu] = C_{\lambda\mu} K(C_{\lambda\mu} | \mathbf{r}_\sigma - \mathbf{r}_{\lambda\mu}) [\lambda\mu], \quad (17c)$$

$$[\lambda\mu] = (\alpha_\lambda \alpha_\mu)^{-3/4} A_{\lambda\mu}^{3/2} \exp[-\frac{1}{2}(\mathbf{r}_\lambda - \mathbf{r}_\mu)^2 A_{\lambda\mu}], \quad (17d)$$

wobei die χ_λ -Funktionen mit λ abgekürzt wurden. Die Abkürzungen in (17) bedeuten im einzelnen

$$A_{\lambda\mu} = \frac{2\alpha_\lambda \alpha_\mu}{\alpha_\lambda + \alpha_\mu}, \quad (18a)$$

$$B_{\nu\sigma}^{\lambda\mu} = \left[\frac{(\alpha_\lambda + \alpha_\mu)(\alpha_\nu + \alpha_\sigma)}{\alpha_\lambda + \alpha_\mu + \alpha_\nu + \alpha_\sigma} \right]^{1/2}, \quad (18b)$$

$$C_{\lambda\mu} = (\alpha_\lambda + \alpha_\mu)^{1/2}, \quad (18c)$$

$$\mathbf{r}_{\lambda\mu} = \frac{\alpha_\lambda \mathbf{r}_\lambda + \alpha_\mu \mathbf{r}_\mu}{\alpha_\lambda + \alpha_\mu}, \quad (18d)$$

und es ist

$$K(\tilde{u}) = \frac{2}{\tilde{u}\sqrt{\pi}} \int_0^{\tilde{u}} \exp(-t^2) dt. \quad (19)$$

Die Funktion (19) kann mit Hilfe der Potenzreihe [10]

$$K(\tilde{u}) \approx \tilde{K}(\tilde{u}) = \begin{cases} \sum_{i=0}^{10} a_i X^i & \tilde{u} \leq 3,093 \\ \frac{1}{\tilde{u}} & \tilde{u} \geq 3,093 \end{cases} \quad (19a)$$

wobei

$$X = \frac{3(1 - \hat{u})}{3 + \tilde{u}}, \quad (19b)$$

bis auf einen Fehler

$$|K(\tilde{u}) - \tilde{K}(\tilde{u})| \leq 4,0 \times 10^{-6} \quad (0 \leq \tilde{u} < \infty) \quad (19c)$$

abgeschätzt werden, der für fast alle Rechnungen klein genug ist. Die Koeffizienten in (19a) ergeben sich zu

$$\begin{aligned} a_0 &= +0,84270001 & a_5 &= +0,10125920 \\ a_1 &= +0,57015786 & a_6 &= -0,07848160 \\ a_2 &= -0,16778274 & a_7 &= -0,02565184 \\ a_3 &= -0,25060352 & a_8 &= +0,03788288 \\ a_4 &= +0,10478112 & a_9 &= +0,00236288 \\ & & a_{10} &= -0,00824832. \end{aligned} \quad (19d)$$

Im Hinblick auf die sonst mit Atomfunktionen erhaltenen Integralasdrücke, sind diese bei Verwendung von (16) so einfach, daß es nicht mehr notwendig ist, die auftretenden Integrale zu tabellieren. Sie können leicht im Rahmen des Programms von Fall zu Fall berechnet werden.

Es ist jetzt im Einzelnen zu prüfen, wie gut diese einfachen Funktionen (16) die bisher gebrauchten Ansätze approximieren und wie brauchbar sie sich bei Variationsrechnungen erweisen.

5. TESTRECHNUNGEN MIT REINEN GAUSSFUNKTIONEN

Als einfachste Rechnung wurden die ns -Zustände des H -atoms mit Hilfe eines linearen Ansatzes [10]

$$\Psi = \sum_{\lambda=1}^M C_{\lambda} \left(\frac{2\alpha_{\lambda}}{\pi} \right)^{3/4} \exp(-\alpha_{\lambda} r^2) \quad (20)$$

berechnet, wobei die Variationsparameter α_{λ} nach

$$\alpha_{\lambda} = \alpha_1 (1,5)^{\lambda-1} \quad (20 a)$$

auf einen einzigen (α_1) zurückgeführt wurden (Skalenfaktor). Alle Gaußfunktionen sind im Atommittelpunkt ($r_{\lambda}=0$) lokalisiert.

In der folgenden Tabelle 1 sind die Ergebnisse wiedergegeben worden, wobei die \tilde{E}_n die aus (6 a) erhaltenen Näherungswerte für die Energieeigenwerte† darstellen (in atomaren Einheiten: at. E : a.u.)

M	\tilde{E}_1	\tilde{E}_2	\tilde{E}_3	\tilde{E}_4	\tilde{E}_5	α_1
2	-0,4307	-0,0887				0,1544 0,0579
3	-0,4757	-0,0922	-0,0351			0,1664 0,0543 0,0274
4	-0,4795	-0,1093	-0,0374	-0,0186		0,1537 0,0621 0,0264 0,0157
5	-0,4907	-0,1119	-0,0451	-0,0202	-0,0114	0,1543 0,0584 0,0309 0,0154 0,0099
∞	-0,5000	-0,1250	-0,0556	-0,0312	-0,0200	—

Tabelle 1.

Es ist bemerkenswert, daß für den $1s$ -Zustand (für $M=1$ ergibt sich $-0,424$) die erhaltenen Energiewerte für $M=1$ und 2 bzw. für $M=3$ und 4 ziemlich ähnlich sind. Dies ist so zu verstehen, daß der Ansatz für $M=1$ schon den größten Teil der Dichteverteilung erfaßt, und daß eine kleine Verbesserung nur durch zwei

† Da sich die Gesamtenergien von Atomen und Molekülen durch einen Term der Kernwechselwirkungsenergie unterscheiden, sollen Atomenergien mit E , Molekülenenergien mit \mathcal{E} , bezeichnet werden.

weitere Gaußfunktionen erreicht werden kann, damit sich diese teilweise kompensieren können. Ebenso können erst für $M=5$ je zwei der vier weiteren Funktionen sich partiell gegenseitig aufheben. Die erhaltenen C_λ bestätigen diese Auffassung, wie Tabelle 2 zeigt.

M	C_1	C_2	C_3	C_4	C_5
2	+1,0	+0,8433			
	+1,0	-0,8892			
3	+1,0	-1,1613	+0,6649		
	+1,0	-0,0528	-0,7445		
	+1,0	-1,7368	+0,7777		
4	+1,0	-0,3284	-0,3476	+0,5591	
	+1,0	-1,7301	+1,3919	-0,5765	
	+1,0	-0,9179	-0,6489	+0,6397	
	+1,0	-2,5106	+2,2043	-0,6772	
5	+1,0	-1,7948	+2,0355	-1,2273	+0,4362
	+1,0	-0,9427	-0,0729	+0,6368	-0,4777
	+1,0	-2,2087	+2,2124	-1,4554	+0,4939
	+1,0	-1,7175	+0,2939	+1,0969	-0,5451
	+1,0	-3,1835	+4,0547	-2,4550	+0,5948

Tabelle 2.

Dieselben Verhältnisse liegen bei den Zuständen $2s$ und $3s$ vor, bei denen zwei bzw. drei Funktionen schon die Dichteverteilung zum größten Teil erfassen.

Für $M=6$ ergeben sich die vier tiefsten \tilde{E}_n zu $-0,493$, $-0,118$, $-0,047$ und $-0,024$.

In Anbetracht der willkürlichen Annahme (20 a) stimmen die \tilde{E}_n -Werte schon recht gut mit den exakten Werten überein. Setzt man

$$\exp(-\gamma r) \approx A \exp(-ar^2) + B \exp(-br^2) \quad (21)$$

und bestimmt A , B , a und b , bei vorgegebenem γ aus dem Minimum des Fehlerquadrates

$$\int_0^\infty [\exp(-\gamma r) - (A \exp(-ar^2) + B \exp(-br^2))]^2 dr = \mu^2, \quad (22)$$

so wird dieses etwa bei den Werten

$$\begin{aligned} a &= 0,1526\gamma^2 & b &= 0,8573\gamma^2 \\ A &= 0,20988 & B &= 0,47998 \end{aligned} \quad (22a)$$

erhalten und beträgt

$$\mu^2 = \frac{1}{\gamma^3} 0,00079. \quad (22b)$$

Aus diesem Beispiel ersieht man, daß zwei Gaußfunktionen schon sehr gut eine $1s$ -Funktion annähern können [10].

Es liegt nun nahe, für eine $2p_z$ -Funktion den folgenden Näherungsansatz zu machen [12, 19]:

$$\phi(2p_z) \approx \exp[-\alpha(\mathbf{r} - \mathbf{r}_\lambda)^2] - \exp[-\alpha(\mathbf{r} - \mathbf{r}_\mu)^2] \quad (23)$$

wobei die beiden Gaußfunktionen, um $2|z_0|$ auf der z -Achse gegeneinander verschoben, auf zwei gegenüberliegenden Punkten zum Atommittelpunkt liegen.

($\mathbf{r}_\lambda = \{0, 0, z_0\}$; $\mathbf{r}_\mu = \{0, 0, -z_0\}$). Wird mit (23) die Energie des H -Atoms in α und z_0 zum Minimum gemacht, so erhält man $\tilde{E} = -0,1132$ at. E . (exakt $-0,125$ at. E .) und die Parameterwerte betragen

$$\alpha = 0,045 \quad z_0 = 0,332. \quad (23 a)$$

Anstelle einer $2s$ -Funktion kann zum Beispiel mit

$$\exp(-\alpha_2 r^2) - \gamma_2 \exp(-\beta_2 r^2) \quad (24)$$

gerechnet werden, wobei (24) auf einer Näherung der $1s$ -Funktion

$$\exp(-\alpha_1 r^2) + \gamma_1 \exp(-\beta_1 r^2) \quad (25)$$

orthogonal ist. Dies führt zu

$$\gamma_2 = \frac{\left[\frac{1}{\alpha_1 + \alpha_2} \right]^{3/2} + \gamma_1 \left[\frac{1}{\beta_1 + \alpha_2} \right]^{3/2}}{\left[\frac{1}{\alpha_1 + \beta_2} \right]^{3/2} + \gamma_1 \left[\frac{1}{\beta_1 + \beta_2} \right]^{3/2}}. \quad (25 a)$$

Wird wieder mit (24) und (25) am H -Atom der Erwartungswert der Energie minimiert, so erhält man für

$$\alpha_1 = 0,2014 \quad \beta_1 = 1,332 \quad \gamma_1 = +1,378 \quad (26 a)$$

und

$$\alpha_2 = 0,017 \quad \beta_2 = 0,3064 \quad \gamma_2 = +3,113 \quad (26 b)$$

die Energiewerte (in at. E .)

$$\tilde{E}(1s) = -0,4858 \quad (\text{exakt } -0,5000) \quad (26 c)$$

$$\tilde{E}(2s) = -0,1206 \quad (\text{exakt } -0,125). \quad (26 d)$$

Am H_2^+ -Molekül wurde bisher mit dem Ansatz [16]

$$\Psi = \left(\frac{2\alpha}{\pi} \right)^{3/4} \{ \exp[-\alpha(\mathbf{r} - \mathbf{r}_\lambda)^2] + \exp[-\alpha(\mathbf{r} - \mathbf{r}_\mu)^2] \} \quad (27)$$

gerechnet, wobei α und die beiden Vektoren variiert wurden. Die Punkte λ und μ wurden dabei symmetrisch von den beiden Protonen a und b nach innen auf der Kernverbindungsachse verschoben. Für $\alpha = 0,282$ wurden die folgenden Ergebnisse für $R_{ab} = 2,0$ (Bindungsabstand) erhalten.

$ \mathbf{r}_\lambda - \mathbf{r}_\mu =$	R_{ab}	$0,667R_{ab}$	$0,333R_{ab}$	0
Energie = (in at. E .)	$-0,499$	$-0,510$	$-0,505$	$-0,501$

Tabelle 3.

Es ergab sich also schon in dieser einfachen Näherung, bei der α für alle Abstände $|\mathbf{r}_\lambda - \mathbf{r}_\mu|$ gleich ist, eine Bindungsenergie, die allerdings mit $-0,010$ at. E . noch ziemlich stark von exakten Wert $-0,100$ at. E . abweicht. Wurde envier Gaußfunktionen verwendet, von denen zwei in a und b , die anderen beiden im Abstand $0,667R_{ab}$ lokalisiert waren, so resultierte eine Bindungsenergie von $-0,052$. Die Differenz gegenüber dem Wert der Energie mit diesem Ansatz für $R_{ab} \rightarrow \infty$, ergab sich allerdings schon zu $-0,081$ at. E .

Schließlich wurde mit der Funktion [16]

$$\Psi = \left(\frac{2\alpha}{\pi}\right)^{3/4} \{ \exp [-\alpha\{(\mathbf{r}_1 - \mathbf{r}_a)^2 + (\mathbf{r}_2 - \mathbf{r}_b)^2\}] + \exp [-\alpha\{(\mathbf{r}_1 - \mathbf{r}_b)^2 + (\mathbf{r}_2 - \mathbf{r}_a)^2\}] \} \quad (28)$$

das H_2 -Molekül berechnet. Man erhielt hier im Gleichgewichtsabstand und bei $\alpha = 0,283$ eine Bindungsenergie von $-0,101$ at. E ., während der exakte Wert $-0,174$ at. E . beträgt.

6. DIE INTERPRETATION EINES VERALLGEMEINERTEN CI-VERFAHRENS MIT REINEN GAUßFUNKTIONEN†

Aus den bisher bekannten Testrechnungen mit Gaußfunktionen vom Typ (16) läßt sich schon sagen, daß dieser Funktionstyp ebenfalls zu Molekülrechnungen herangezogen werden kann. Die Tatsache, daß die notwendigen Integrationen in H_{KL} und S_{KL} nach (17) auf ein beachtenswertes Minimum reduziert werden, dürfte für den Anwendungsbereich von Ansätzen nach (1), (1a) von großer Bedeutung sein. Aber nicht nur die bequemen Integrationen, die gegebenenfalls mit einer größeren Anzahl von Gaußfunktionen im Aufbau des linearen Ansatzes (1), (1a) erkaufte werden müssten (was allerdings im Rahmen der automatisierten Rechnungen das wesentlich kleinere Übel darstellt), lassen die Gaußfunktionen für Rechnungen der hier diskutierten Art günstig erscheinen, auch eine neuartige Interpretation des Ansatzes (1), (1a), die sich in diesem Falle anbietet, ermöglicht auf eine ganz andere Weise als bisher Informationen über die Elektronenverteilungen in Molekülen zu erhalten.

Bilden wir mit den Gaußfunktionen nach (16) die Determinanten ψ_K in (1), (1a), wobei gegebenenfalls Linearkombinationen von ψ_K zu bestimmten Eigenwerten von \mathcal{S}^2 auftreten können, die dann wieder anstelle von ψ_K in (1) geschrieben werden, so wird ein solches ψ_K , von den α_λ ($\lambda = 1 \dots n$) vorerst abgesehen, allein durch die Angabe der n Vektoren \mathbf{r}_λ festgelegt sein. Die Gesamtheit aller n \mathbf{r}_λ -Vektoren, die zu einem ψ_K gehören, wollen wir die K -te Elektronenkonstellation \mathbf{r}_K nennen. ψ_K stellt nämlich das antisymmetrische Produkt von n Gaußfunktionen nach (16) dar, wobei jedes Elektron eine bestimmte Gaußfunktion besetzt. Da wir annehmen dürfen, daß diese Funktionen beliebig im Raum lokalisiert sein können, stellen sie ein vollständiges Funktionssystem dar [2], und wir können vorerst alle α_λ gleich Eins setzen.

In diesem Sinne ist $|C_K|^2$ ein Maß dafür, wie stark die K -te Elektronenkonstellation an der Beschreibung der Gesamtwellenfunktion beteiligt ist. Die Entwicklung nach Elektronenkonstellationen ψ_K , entsprechend (1), (1a) und (16), stellt somit eine Analyse von $\tilde{\Psi}$ nach den ψ_K dar. Betrachten wir etwa die 3-parametrische Näherung $\tilde{\Psi}$ für die Ψ -Funktion des Heliums [17]

$$\tilde{\Psi} = \exp [-1,815(r_1 + r_2)][1 + 0,29r_{12} + 0,132(r_1 - r_2)^2], \quad (29)$$

so sehen wir in (29), daß $|\tilde{\Psi}|^2$ auf einer Kugeloberfläche ($r_1 = r_2 = r_0$) in

$$|\tilde{\Psi}|^2_{r_1=r_2=r_0} \exp(-7,260r_0)(1 + 0,29r_{12})^2. \quad (29a)$$

übergeht, und daß $|\tilde{\Psi}|^2_{r_1=r_2=r_0}$ am größten ist, wenn sich die beiden Elektronen

† Wir wollen ein solches Vorgehen das Verfahren der Gauss-Konstellationen nennen (Konstellationen mit Gaussorbitalen, KGO-Verfahren).

an zwei diametral gegenüberliegenden Punkten befinden, da dann $r_{12} = 2r_0$ ist. Im Sinne unserer Vorstellung der Elektronenkonstellationen darf man daher erwarten, daß $|C_K|^2 > |C_L|^2$ sein wird, wenn die K -te Konstellation gerade dem obigen Fall entspricht, während sich in ψ_L die beiden Gaußfunktionen an irgendwelchen zwei Punkten auf der Kugel (Radius r_0) befinden, für die $r_{12} < 2r_0$ ist.

Die $|C_K|^2$ haben damit eine 'anschauliche' Bedeutung gewonnen. Der Übergang von einer Elektronenkonstellation zu einer anderen kann stetig vorgenommen werden, sodaß darin eine Möglichkeit besteht, die Gesamtenergie des Systems auf diese Weise zu minimisieren. Es werden auf diesem Wege die Konstellationen mit den größten Gewichten herausgesucht! Werden daneben bei fixierten Konstellationen die α_λ variiert, so kann aus deren Größenordnungen zueinander geschlossen werden, an welchen Stellen \mathbf{r}_λ einer bestimmten Konstellation, die einzelnen Elektronen schwach oder stark lokalisiert sind. Ein großes α_λ zeigt, daß die betreffende Gaußfunktion nur in einem kleinen Raumbereich von Null verschieden ist. Das Elektron, welches diesen 'Gauß-Zustand' besetzt, besitzt also eine hohe kinetische Energie, wie es im allgemeinen in Kernnähe der Fall ist.

Gehen wir in (1), (1a) unter Verwendung von Elektronenkonstellationen mit reinen Gaußfunktionen zur kontinuierlichen Darstellung über, so erhalten wir eine Form der Gauß'schen Integraltransformation [18]

$$\Psi(\mathbf{r}) = \int \det\{\chi_j(\mathbf{r}, \mathbf{f})\} C(\mathbf{f}) d\mathbf{f}; \quad (\alpha_\lambda = 1) \quad (30)$$

in der über die Konstellationen \mathbf{f} integriert wird. $C(\mathbf{f})$ ist dann die Gewichtsfunktion der zu \mathbf{f} gehörenden Elektronenkonstellation.—Das hier beschriebene Verfahren soll in Zukunft an einer Reihe von Molekülen erprobt werden, wobei daran gedacht ist, nach Vorgabe der einzelnen Elektronenkonstellationen und der α_λ , die Bestimmung der C_K und \tilde{E} nach (6), (6a) durchzuführen. Da die Integration dabei einfach ist und die Bereitstellung der \mathbf{f}_k und α_λ , besonders wenn viele Konstellationen Berücksichtigung finden, nicht mehr so stark vom Molekültyp abhängt und bequem gehandhabt werden kann, ist gerade bei diesem Verfahren eine besonders weitgehende Automatisierung des Rechenprogramms möglich.

LITERATUR

- [1] ARAI, T., 1961, Preprint, Carnegie Institute of Technology, Pittsburgh.
- [2] BOYS, S. F., 1959, *Proc. roy. Soc. A*, **200**, 542 ; 1960, *Ibid.*, **259**, 402.
- [3] COOLEY, J. W., 1961, Report of the AEC Computing and Applied Mathematics Center, Institute of Mathematical Sciences, New York University, May.
- [4] BOYS, S. F., 1950, *Proc. roy. Soc. A*, **201**, 125 ; 1952, *Phil. Trans.*, **245**, 139. McWEENY, R., 1950, *Nature, Lond.*, **166**, 21 ; 1953, *Acta Cryst.*, **6**, 631.
- [5] TIEN-CHI-CHEN, und SPONER, H., 1955, Molecular Quantum Mechanics Conference, Texas.
- [6] JAMES, H. M., und COOLIDGE, A. S., 1933, *J. chem. Phys.*, **1**, 825.
- [7] COULSON, C. A., und DUNCANSON, W. E., 1938, *Proc. roy. Soc. A*, **165**, 90.
- [8] JAMES, H. M., 1934, *J. chem. Phys.*, **2**, 794.
- [9] LÖWDIN, P. O., 1955, *Phys. Rev.*, **97**, 1474.
- [10] PREUSS, H., 1956–1960, *Integraltafeln zur Quantenchemie*, Band I–IV (Berlin : Springer).
- [11] LÖWDIN, P. O., 1958, Technical note 12, Quantum Chemistry Group, Uppsala. FIESCHI, R., und LÖWDIN, P. O., 1957, Technical note, Quantum Chemistry Group, Uppsala.
- [12] PREUSS, H., 1956, *Z. Naturf. A*, **11**, 823.

- [13] KOTANI, M., AMEMIYA, A., ISHIGURO, E., und KIMURA, T., 1955, *Tables of Molecular Integrals* (Tokyo : Maruzen). MILLER, J., GERHAUSER, J. M., und MATSEN, F. A., 1959, *Quantum Chemistry Integrals and Tables* (Texas Press). SAHNI, R. C., und COOLEY, J. W., 1959, Technical note D-146, NASA. LOFTHUS, A., 1961, *Mol. Phys.*, **4**, 17 ; 1962, *Ibid.*, **5**, 105. Roothaan, C. C. J., 1955, Special Technical Report, University of Chicago.
- [14] HEITLER, W., und RUMER, R., 1930, *Göttinger Nachr.*, S. 277 ; 1931, *Z. Phys.*, **68**, 12. WEYL, H., 1930, *Göttinger Nachr.*, S. 286. HELLMANN, H., 1937, *Einführung in die Quantenchemie*, Kap. VI (Wien : Deuticke).
- [15] MCWEENY, R., 1955, *Proc. roy. Soc. A*, **232**, 114. NESBET, R., 1955, *Proc. roy. Soc. A*, **230**, 312.
- [16] MÜLLER, C. R., und CAHILL, J. M., 1955, Molecular Quantum Mechanics Conference, Texas.
- [17] HELLMANN, H., 1937, *Einführung in die Quantenchemie* (Wien : Deuticke), S. 109.
- [18] HOFACKER, L., und PREUSS, H., 1961, *Z. Naturf. A*, **16**, 513.
- [19] Neuerdings hat WHITTEN, F. L., 1963, *J. chem. Phys.*, **39**, 349, diese idee wieder aufgegriffen.
- [20] MECKLER, A., 1953, *J. chem. Phys.*, **21**, 1750. KIMBALL, G. E., und NEUMARK, G. F., 1957, *J. chem. Phys.*, **26**, 1285. NESBET, R. K., 1960, *J. chem. Phys.*, **32**, 1114. BOYS, S. F., und COOK, G. B., 1960, *Rev. mod. Phys.*, **32**, 285. ALLEN, L. C., 1962, *J. chem. Phys.*, **37**, 200. HARRISON, M. L., 1963, *MIT, QPR*, **49**, 82, 78, 74, 70.

Transient nuclear magnetic resonance signals for liquids with exchanging nuclei

by J. G. POWLES and J. H. STRANGE

Physics Department, Queen Mary College (University of London),
Mile End Road, London, E.1

(Received 26 November 1963)

Experimental results are given for both the steady-state proton magnetic resonance line shape and for the echo amplitude modulation pattern for liquid methyl alcohol over a temperature range which includes the collapse of the J multiplet due to increasingly rapid hydroxyl proton exchange.

A theory is given for the modulation of the echo amplitude in the presence of exchange by a generalization of Anderson and Weiss's method [9] and also by use of McConnell's equations [10]. An approximate theory is also given which gives considerable insight into the physical meaning of the more complex exact solutions. The value of the approximate method is also illustrated by applying it to the analysis of the collapse of the complex methyl multiplet in NN dimethyl formamide.

It is shown that, generally speaking, the echo amplitude modulation measurement, while giving similar results as for the steady-state measurements, have certain advantages both in the determination of coupling constants and exchange correlation times.

It is shown that, for the exchange model used, the echo amplitude modulation ought to be independent of pulse spacing for J coupling but not for the chemical shift case. The fact that the observed modulation is dependent to some extent on pulse spacing in methyl alcohol may be indicative that a more elaborate model of the exchange process is necessary.

1. INTRODUCTION

The indirect spin-spin coupling between magnetic nuclei (J coupling) in magnetic resonance is usually measured from the steady-state absorption spectrum. The simplest case is for two spins $\frac{1}{2}$ with an effective coupling Hamiltonian for the spins A and B in a molecule in a liquid given by $hJ\mathbf{I}_A \cdot \mathbf{I}_B$ and a chemical shift between A and B given by δ , where J and δ are expressed in c.p.s. For $J \ll \delta$ this is called AX. The signals from A and X spins are separate and each is split into a doublet with separation J c.p.s. On the other hand, the value of J may also be determined by a transient experiment due to Hahn and Maxwell [1]. An improved version of this echo method was recently discussed [2, 3]. In this method a series of pulses of intense radio frequency field at the resonance frequency are applied and echo nuclear signals appear at certain times (for details see § 3.1). In the presence of J coupling the *amplitude* of the echoes is modulated. In the simplest AX case the modulation is given by $|\cos \pi J t|$, where t is the time of the echo and so J can be determined.

It is well known [4-6] that when one of the nuclei which is involved in the J coupling is exchanged, the coupling tends to be removed when the rate of exchange

is comparable with or greater than J and the multiplets mentioned above in the steady-state experiment 'collapse', so that the J value is no longer measurable. However, from a study of the line shape as a function of temperature, together with a theory of the exchange process, the correlation time for the exchange process, τ_c , can be determined as a function of temperature under certain conditions. The corresponding effect in the echo experiment is a tendency to lose the echo amplitude modulation and also a variation of the overall attenuation of the modulated signal. As we have pointed out elsewhere [3], the transient experiment has certain advantages over the steady-state one. There is an additional variable at our disposal, the pulse spacing. The effect of J can be seen to temperatures typically some 10°C higher than in the steady-state experiment. Finally the echo experiment is possibly more sensitive to the actual details of the exchange process.

If the steady-state signal is split because of chemical shift only, the simplest case being two lines of equal intensity with separation δ , the echo amplitude in the absence of exchange is independent of δ . In the presence of exchange the echo amplitude is attenuated and this case will be investigated theoretically although no experiments are reported here.

In this paper we investigate the effect on the echo amplitude modulation of proton exchange of the hydroxyl proton in liquid methyl alcohol containing a trace of water and compare with the results found from the corresponding steady-state experiment. We also present various theoretical analyses of the effect.

2. EXPERIMENTAL

The equipment for the pulse experiments has been described elsewhere [7] as well as the special procedures valuable for observing J modulation of echoes [2, 3].

The steady-state measurements were made using a Varian HR60 high resolution spectrometer. Thus these spectra are for a resonance frequency of 56.4 Mcps, when for methyl alcohol $J/\delta \simeq 0.05$. The transient experiments were for a resonance frequency of 20.8 Mcps when for methyl alcohol $J/\delta \simeq 0.15$. For this J/δ value the simple theory of AX_3 is not really applicable, since second-order effects can be seen and the theory for AB_3 (i.e. J/δ not $\ll 1$) ought to be used. However, we have shown [3, 8] that by choosing the pulse spacing

(1) Tempera- ture in $^\circ\text{C}$	(2) True J value in c.p.s.	(3) Apparent J from steady- state spectrum	(4) Apparent J from transient experiment		(5) τ_c in seconds from steady state	(6) Decay constant of transient	
			$\tau = (J^2 + \delta^2)^{-1/2}$ (i.e. τ short)	$\tau = 2(J^2 + \delta^2)^{-1/2}$ (i.e. τ long)		τ short	τ long
-60	4.95	5.0	4.95	4.95	—	—	—
-33	5.03	4.6	5.00	4.8	0.20	0.25	0.25
-20	5.05	3.8	4.9	4.65	0.13	0.18	0.14
-11	5.08	2.8	4.85	4.5	0.10	0.12	0.12
+4	5.10	—	4.5	3.9	0.06	0.08	0.07
23	5.13	—	—	—	0.03	0.14	0.12

Table 1.

$\tau = n(J^2 + \delta^2)^{-1/2}$, where n is an integer, these second-order effects can be largely eliminated and the AX theory is then sufficiently good, at least in this particular case. We find it convenient in these experiments to use $n=1$ and $n=2$ (see table 1).

Some examples of the experimental results for the sample of methyl alcohol at various temperatures are given in figure 1. The steady-state signals are for the methyl 'doublet' only. The transient signals are for both groups of protons but, as we have shown elsewhere [3], this signal is little different from the signal that would be obtained from the methyl group protons alone, since an echo modulation from an AX_3 system is very similar to that for the corresponding AX system particularly if the interpretation is based on the zeros of the echo amplitude modulation as ours is. The detector is such that one observes the modulus of the echo amplitude, e.g. $|\cos \pi Jt|$ rather than $\cos \pi Jt$.

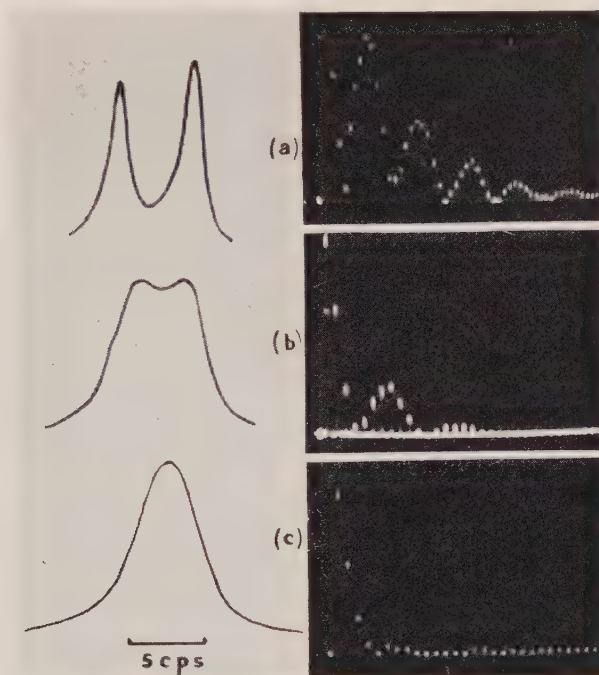


Figure 1. Comparison of the steady state on the left and the transient signals on the right for a sample of methyl alcohol at various temperatures : (a) -60°C , (b) -11°C , (c) $+4^{\circ}\text{C}$.

3. THEORY AND INTERPRETATION

We give first an outline of the theory of the echo modulation for the AX case and then for AB_3 , as in methyl alcohol. We then consider the developments required in Anderson and Weiss's [9] theory of the steady-state line shape with exchange, for both J and δ splitting. We also show that similar results are obtained, less elegantly, using McConnell's [10] formulae. Finally we give a rather different approach to the study of the effects of exchange on both transient and steady-state signals. This has the advantages of giving a clearer physical picture of the behaviour of the spin system and leads to approximations of known accuracy which can be used for interpreting the experimental results.

3.1. *Echo modulation without exchange*

After the initial 90° pulse the equilibrium longitudinal nuclear magnetization is turned into the transverse plane. In the following we consider its motion relative to a system of coordinates rotating at the mean frequency of resonance, so that we calculate the modulation of the r.f. signal directly. We take the 90° pulse with its magnetic field in the rotating y axis. It is easily shown [11] that for the AX case, i.e. $J \ll \delta$, the freely precessing transverse magnetization may be regarded as four separate precessing classical magnetizations at the frequencies $(\pm \frac{1}{2}\delta \pm \frac{1}{2}J)$ c.p.s. corresponding to the four lines of the steady-state AX spectrum and the four types of protons, A_+ which are A protons coupled to X protons with spin up (or down) and similarly for A_- , X_+ and X_- . Thus at a time τ after the 90° pulse the four magnetizations have accumulated phase shifts, ϕ , as indicated in figure 2(b). The effect of a 180° pulse about the rotating x axis

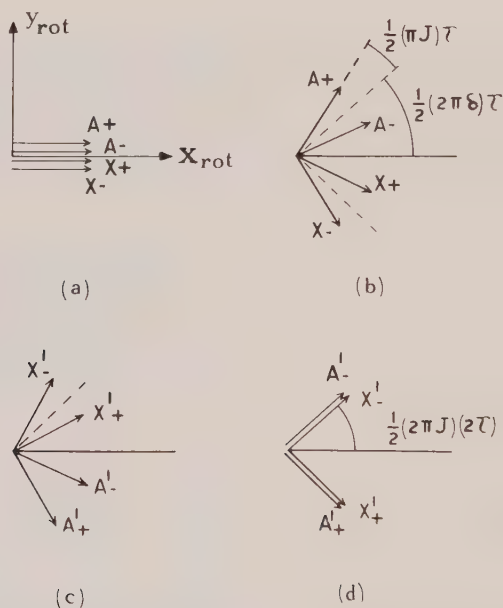


Figure 2. Illustrating echo modulation due to J coupling in the AX system : (a) Just after the 90° pulse, (b) τ after the 90° pulse, (c) just after a 180° pulse at τ , (d) τ after the 180° pulse.

at time τ is not simply to rotate the magnetization 180° about this axis, since we have to deal with a non-classical system not describable in general by magnetic fields. It is significant that the A and X nuclei are effectively identical during pulses but not between them. A 180° pulse effectively changes the sign of J associated with each magnetization, so that, for example, the magnetization A_-' which was associated with A_- before the 180° pulse now has a frequency $(\frac{1}{2}\delta - \frac{1}{2}J)$ rather than $(\frac{1}{2}\delta + \frac{1}{2}J)$. This 90° , 180° pulse sequence is the Carr-Purcell [12] sequence as modified by Meiboom and Gill [13]. Actually the relative phase of the 90° and 180° pulses is not important in our experiments. At a further time τ later the magnetizations are as in figure 2(d). Thus dephasing due to δ has disappeared. Similarly any phase shifts, ϕ , due to inhomogeneities of the

main field disappear at the time 2τ only. This is the basis of echo formation [14] and justifies our ignoring field inhomogeneities if we study only the *amplitude* of the echo. The effective rotating magnetization at time 2τ is $\cos \pi J(2\tau)$. If one applies a series of 180° pulses at the times $\tau, 3\tau, 5\tau$ echoes appear at the times $2\tau, 4\tau, \dots$, and the amplitude will be $\cos \pi Jt$, where t is the time at which the echo occurs. This is the echo amplitude modulation. As far as the echo amplitude is concerned we need only consider the behaviour of any one of the sets of nuclei A or X. In addition we need not bother any further about δ . The effect of a 180° pulse for J splitting is expressed mathematically as simply changing the values ϕ and $\dot{\phi}$ before the pulse into $-\phi$ and $-\dot{\phi}$ after the pulse, a fact which we shall use below.

For the AX_3 case the X signal is a strong doublet and in the transient experiment it is again sufficient to consider only the X magnetization if we are concerned with zeros of the modulation although this is not quite as obvious as for AX. Further, this is also true for special pulse spacings for AB_3 if J/δ is not too large [3] and in particular it is so for the proton signal of methyl alcohol at 20.8 Mc/s.

If we have an AX system with a chemical shift δ c.p.s. and no J coupling it is clear that the echo amplitude is not modulated. We shall also consider the effect of exchange on this system.

In so far as we can consider the system as described by precessing classical magnetizations, except during the pulses, we can in general consider the transient signal $G(t)$ due to one or more magnetizations with a frequency difference from resonance of $\phi(t')$ at time t' so that :

$$G(t) = \cos \int_0^t \dot{\phi}(t') dt', \quad (1)$$

or a sum of such terms.

We are interested in the echo amplitude at t which we will call $E(t)$. For AX with $\phi(t') = \pi J$ independent of t' , equation (1) leads to $E(t) = \cos \pi Jt$ as before.

For liquid methyl alcohol we are interested in observing the transient signal associated with the methyl doublet as the hydroxyl proton exchanges between different molecules. This process is presumably catalysed by the trace of water present. When a new proton replaces the original one it may have the same or opposite spin with equal probability, ignoring the small Boltzmann factor. For a given CH_3 group, $J(t)$ either continues to have the same sign or changes sign, so we now write $\phi(t') = \pi J(t')$ and

$$G(t) = \left\langle \cos \int_0^t \pi J(t') dt' \right\rangle \text{ or } \text{Re} \left\langle \exp i \int_0^t \pi J(t') dt' \right\rangle, \quad (2)$$

where the average sign is an ensemble average for the set of spins. The evaluation of $G(t)$ now of course depends on the statistical properties assumed for $J(t')$. Similarly for the chemical shift.

3.2. Exact theory of echo modulation with exchange

The model we use for the exchange is the well-known one that $J(t)$ changes sign instantaneously and that the probability of a change of sign in dt is dt/τ_c , which is statistically a Markov process. Since the exchange to a new proton has equal chance of changing the sign of $J(t)$ or not, the probability of proton

exchange rather than sign exchange in dt is $2dt/\tau_c$. Consequently, in investigating the exchange mechanism, say as a rate process or reaction rate, the quantity $\tau_c/2$ is more directly relevant.

We adapt Anderson and Weiss's theory [9] of the line shape under exchange (see Abragam [15]) to our particular case and extend it to the echo amplitude problem. This is essentially a classical calculation. It will not prove necessary to use the correct quantum mechanical treatment [6] which is required for exchange rates comparable to or greater than the Larmor frequency.

Suppose the absorption without exchange has sharp lines at ω_γ from the mean position (we introduce the natural line width due to other effects later). In our case ω_γ is $\pm\pi J$. Then we can write:

$$G(t) = \sum_{\gamma} G_{\gamma}(t), \quad (3)$$

where $G_{\gamma}(t)$ is the term in $G(t)$ which corresponds to nuclei with $\phi = \omega_{\gamma}$ at time t . It can be shown [9, 15] that for any particular term G_{β} :

$$\frac{dG_{\beta}}{dt} = i\omega_{\beta}G_{\beta} + \sum_{\gamma} \pi(\omega_{\gamma}, \omega_{\beta})G_{\gamma}(t), \quad (4)$$

where π depends on the nature of the exchange process and is given explicitly below. If π is a matrix with elements $\pi_{\alpha\beta}$ equal to $\pi(\omega_{\alpha}, \omega_{\beta})$, \mathbf{G} a row vector with components G_{α} and ω a matrix with elements $\omega_{\alpha\beta}$ equal to $\omega_{\alpha}\delta_{\alpha\beta}$, we can write (4) as:

$$\frac{d\mathbf{G}}{dt} = \mathbf{G}(i\omega + \pi), \quad (5)$$

so that

$$\mathbf{G}(t) = \mathbf{G}(0) \exp(i\omega + \pi)t, \quad (6)$$

where $\mathbf{G}(0)$ is a row vector given by the distribution of the spins among the frequencies ω_{γ} at $t=0$.

If $G(t)$ is the signal after a 90° pulse applied to a spin system in equilibrium it is called the Bloch decay. In this case we put $\mathbf{G}(0) = \mathbf{W}$ where the components of the vector \mathbf{W} are the equilibrium probabilities of the spins corresponding to the various ω_{γ} . Thus the Bloch decay is given by

$$G(t) = \mathbf{W} \exp(i\omega + \pi)t \cdot \mathbf{1} \quad (7)$$

where $\mathbf{1}$ is the unit column vector.

Since the line shape, $I(\omega)$, is the Fourier transform of the Bloch decay we have:

$$I(\omega) = \text{re} \int_0^\infty G(t) \exp(-i\omega t) dt = \text{re}[\mathbf{W} \cdot \mathbf{A}^{-1}\mathbf{1}], \quad (8)$$

where \mathbf{A}^{-1} is the inverse of the matrix $\mathbf{A} = i(\omega - \omega\mathbf{E}) + \pi$, \mathbf{E} being the unit matrix [9, 15].

In our case we have:

$$\omega = \begin{bmatrix} \pi J & 0 \\ 0 & -\pi J \end{bmatrix}, \quad \pi = \begin{bmatrix} -1/\tau_c & 1/\tau_c \\ 1/\tau_c & -1/\tau_c \end{bmatrix} \quad \text{and} \quad \mathbf{W} = [\tfrac{1}{2}, \tfrac{1}{2}], \quad (9)$$

so that the line shape given by equation (8) is:

$$I(\omega) = 4\pi^2 J^2 \tau_c^{-1} / [\omega^4 + 2\omega^2(2\tau_c^{-2} - \pi^2 J^2) + (\pi J)^4]. \quad (10)$$

When τ_c is such that $\pi J \tau_c \gg 1$, we expect the exchange to have little effect and equation (10) reduces to:

$$I(\omega) \simeq \tau_c / [1 + (\omega - \pi J)^2 \tau_c^2] + \tau_c / [1 + (\omega + \pi J)^2 \tau_c^2], \quad (10')$$

i.e. two Lorentzian lines centred at $\pm \pi J$ with widths corresponding to τ_c^{-1} . The distance between the peaks is $2\pi J$, i.e. J c.p.s. The line width can therefore be used to measure τ_c .

In the next approximation the maxima of the two peaks move together to a separation which we call J_A c.p.s. given approximately by:

$$J_A = J [1 - (\pi J \tau_c)^{-2}]. \quad (11)$$

Thus an estimate of τ_c can also be obtained, for slow exchange, from the apparent splitting. An example of this effect for methyl alcohol is given in column 3 of table 1 where increasing temperature corresponds to decreasing τ_c . The true value of J (column 2) was obtained for specially dry samples. The true variation of J with temperature has been discussed elsewhere [3, 20].

At the other extreme of very rapid exchange, i.e. $\pi J \tau_c \ll 1$ the steady-state signal collapses to one central Lorentzian line given by:

$$I(\omega) = 2 \cdot (2/\pi^2 J^2 \tau_c) / [1 + \omega^2 (2/\pi^2 J^2 \tau_c)^2], \quad (10'')$$

with a width corresponding to $\pi^2 J^2 \tau_c / 2$, i.e. again a sharp line from whose width τ_c can be obtained when J is known. In principle τ_c can be found from the exact line shape formula (10) for any value of $\pi J \tau_c$. In practice it is quite difficult to do much more than fit the extreme cases which we have discussed above because of the sensitiveness of the line shape to additional influences. One of these is the spin-spin relaxation (T_2) which is always present and is itself temperature dependent. This in particular will usually be a more important source of line broadening at the two extremes where $\pi J \tau_c \gg 1$ or $\ll 1$. The intermediate shapes are also very sensitive to the slight main field inhomogeneity.

Since we have ignored δ and field inhomogeneity in our particular application $G(t)$, given by equation (7), is not the experimental decay after a 90° pulse but only an auxiliary quantity, which will lead eventually to a prediction of the echo amplitude. Similarly for $G_a(t)$, etc. Nevertheless, we give an explicit evaluation of $G(t)$, since it is of interest in the discussion of the echo given below. $G(t)$ in equation (7) cannot be evaluated immediately because the matrix $i\omega + \pi$ given explicitly by equation (9) is not diagonal. Put $Y_+ = (i\omega + \pi)t$. Suppose Y_+ is diagonalized by the matrix D_+ to give the diagonal matrix X , i.e.

$$D_+ Y_+ D_+^{-1} = X. \quad (12)$$

We require $\exp Y_+$ but

$$\exp Y_+ = \exp (D_+^{-1} X D_+) = D_+^{-1} (\exp X) D_+ \quad (13)$$

and $\exp X$ can be written down immediately since X is diagonal.

For ω and π given by equation (9) we find:

$$D_+ = (1 - \exp(2\theta))^{-1/2} \begin{bmatrix} 1 & -i \exp(i\theta) \\ i \exp(i\theta) & 1 \end{bmatrix}$$

and

$$X = -\frac{t}{\tau_c} \begin{bmatrix} 1 + i \sinh \theta & 0 \\ 0 & 1 - i \sinh \theta \end{bmatrix}, \quad (14)$$

where $\cosh \theta = \pi J \tau_c$.

Therefore:

$$\begin{aligned} \exp X &= \begin{bmatrix} \exp - (1 + i \sinh \theta) \frac{t}{\tau_c} & 0 \\ 0 & \exp - (1 - i \sinh \theta) \frac{t}{\tau_c} \end{bmatrix} \\ &= \exp \left(-\frac{t}{\tau_c} \right) \begin{bmatrix} \exp \left(-i \sinh \theta \cdot \frac{t}{\tau_c} \right) & 0 \\ 0 & \exp \left(i \sinh \theta \cdot \frac{t}{\tau_c} \right) \end{bmatrix}. \quad (15) \end{aligned}$$

Using (13), (14) and (15) in (7) we find:

$$\begin{aligned} G(t) &= \mathbf{W} \cdot D_+^{-1} \cdot \exp X \cdot D_+ \mathbf{1} \\ &= \exp(-t/\tau_c) \{ \cosh(1 - \pi^2 J^2 \tau_c^2)^{1/2} t / \tau_c + (1 - \pi^2 J^2 \tau_c^2)^{-1/2} \\ &\quad \times \sinh(1 - \pi^2 J^2 \tau_c^2)^{1/2} t / \tau_c \}. \quad (16) \end{aligned}$$

We defer discussion of this formula until we have found the echo amplitude.

The *same* formula is valid for a pair of chemically shifted lines on replacing J by δ .

At time τ after the 90° pulse we have:

$$G_\alpha(\tau_-) = \sum_\gamma W_\gamma [\exp(i\omega + \pi)\tau]_{\gamma\alpha}, \text{ where } \gamma = \alpha \text{ or } \beta. \quad (17)$$

The effect of the 180° pulse at τ is (a) to change the sign of phases and (b) to exchange the roles of magnetizations as explained in §3.1. The effect of (a) is to change the sign of all the ω 's in (17) and of (b) to exchange α and β . Thus just after the pulse we have:

$$G_\beta(\tau_+) = \sum_\gamma W_\gamma [\exp(-i\omega + \pi)\tau]_{\gamma\alpha}$$

and similarly for $G_\alpha(\tau_+)$. These are the new initial values at time τ_+ which correspond to the initial condition $\mathbf{G}(0) = \mathbf{W}$ at $t=0$. In fact

$$\mathbf{G}(\tau_+) = \mathbf{W} \cdot \exp(-i\omega + \pi)\tau \mathbf{P}, \quad (18)$$

where \mathbf{P} is the matrix

$$\begin{bmatrix} 0 & 1 \\ 1 & 0 \end{bmatrix}$$

which changes a vector $[a, b]$ into $[b, a]$. This $\mathbf{G}(\tau_+)$ is the new initial condition for times $t > \tau$, i.e.

$$\mathbf{G}(\tau + t') = \mathbf{W} \cdot \exp\{(-i\omega + \pi)\tau\} \cdot \mathbf{P} \cdot \exp\{(i\omega + \pi)t'\} \cdot \mathbf{1},$$

i.e. the first echo amplitude at $t=2\tau$ or $t'=\tau$ is:

$$E_{1J}(2\tau) = \mathbf{W} \exp\{(-i\omega + \pi)\tau\} \cdot \mathbf{P} \cdot \exp\{(i\omega + \pi)\tau\} \cdot \mathbf{1}. \quad (19)$$

This is readily generalized to the n th echo appearing at $2n\tau$ which is given by:

$$\begin{aligned} E_{nJ}(2n\tau) &= \mathbf{W} \exp\{((-1)^n i\omega + \pi)\tau\} \\ &\quad \cdot \underbrace{\mathbf{P} \cdot \exp\{((-1)^{n-1} i\omega + \pi)2\tau\} \cdot \mathbf{P} \cdot \exp\{((-1)^{n-2} i\omega + \pi)2\tau\} \cdot \mathbf{P} \dots}_{n-1 \text{ terms}} \\ &\quad \times \exp\{(i\omega + \pi)\tau\} \cdot \mathbf{1}; \quad (20) \end{aligned}$$

ω , π and \mathbf{W} are given in equation (9).

In equation (19) $\exp(-i\omega + \pi)\tau$ can be evaluated as was $\exp(i\omega + \pi)\tau$ by changing the sign of J . This does not affect X . D_+ becomes D_- , etc., where

$$D_- = [1 - \exp(-2\theta)]^{-1/2} \begin{bmatrix} 1 & i \exp(-i\theta) \\ -i \exp(-i\theta) & 1 \end{bmatrix}.$$

Equation (19) becomes:

$$E_1(2\tau) = \mathbf{W} D_-^{-1} \exp(X) D_- P D_+^{-1} \exp(X) D_+ \mathbf{1}.$$

After some algebra this simplifies considerably, e.g.

$$D_- P D_+^{-1} = \begin{bmatrix} -1 & 0 \\ 0 & 1 \end{bmatrix}$$

and we obtain finally:

$$E_{1J}(2\tau) = \exp(-2\tau/\tau_c) \{ \cosh(1 - \pi^2 J^2 \tau_c^2)^{1/2} (2\tau)/\tau_c + (1 - \pi^2 J^2 \tau_c^2)^{-1/2} \sinh(1 - \pi^2 J^2 \tau_c^2)^{1/2} (2\tau)/\tau_c \}. \quad (21J)$$

This result is remarkable in that $E_1(2\tau)$ is the same as $G(2\tau)$, i.e. the 180° pulse has had no effect on the amplitude of the signal at 2τ . We have also shown explicitly using equation (20), that the n th echo at time t is given by equation (21J) with 2τ replaced by t . This means that in fact $G(t)$ can be measured by the echo amplitude and that the amplitude of any echo is independent of the number of pulses preceding it. Explicitly $E_n(t) = G(t)$. This result will be explained in § 3.4.

It should be noted that this is *not* true for the chemical shift case with exchange. As already stated (cf. equation (16)):

$$G_\delta(t) = \exp(-t/\tau_c) \{ \cosh(1 - \pi^2 \delta^2 \tau_c^2)^{1/2} t/\tau_c + (1 - \pi^2 \delta^2 \tau_c^2)^{-1/2} \sinh(1 - \pi^2 \delta^2 \tau_c^2)^{1/2} t/\tau_c \}. \quad (22)$$

The 180° pulse at τ in this case only changes the phases and *not* the identity of the magnetizations. This means that \mathbf{P} is now just the unit matrix and equation (19) becomes

$$E_{1\delta}(2\tau) = \mathbf{W} \exp(-i\omega + \pi)\tau \exp(i\omega + \pi)\tau \mathbf{1}. \quad (19\delta)$$

Similarly for equation (20). In ω , δ replaces J .

After evaluation as above we find:

$$E_{1\delta}(2\tau) = \exp(-2\tau/\tau_c) \{ [1 - (\pi\delta\tau_c)^2]^{-1} \cosh[1 - (\pi\delta\tau_c)^2]^{-1/2} (2\tau)/\tau_c + [1 - (\pi\delta\tau_c)^2]^{1/2} \sinh[1 - (\pi\delta\tau_c)^2]^{1/2} 2\tau/\tau_c - (\pi\delta\tau_c)^2 [1 - (\pi\delta\tau_c)^2]^{-1} \}. \quad (21\delta)$$

This is not of the same form as $G(t)$ and so the echo amplitude in general *depends* on the pulse spacing. This is discussed further below and a physical explanation is given later. An approximate expression for $E_{n\delta}(t)$ for certain special conditions has been given by Luz and Meiboom [16]†.

For no exchange, i.e. $\tau_c \rightarrow \infty$, we find $E_{1J}(t) \rightarrow \cos \pi J t$ and $E_{1\delta}(t) \rightarrow 1$ as expected. It is also evident that the same expressions are obtained for $E_{nJ}(t)$ and $E_{n\delta}(t)$.

† Actually the interaction in [16] is of J type, but to a non-resonant nucleus (^{17}O). This is equivalent to a δ interaction for resonant nuclei and so explains their observed dependence on pulse spacing and is not inconsistent with (21J) and (21δ).

For slow exchange, i.e. $\pi J \tau_c \gg 1$ equation (21J) becomes:

$$E_J(t) \simeq \exp(-t/\tau_c) \cos\{\pi J[1 - (2\pi^2 J^2 \tau_c^2)^{-1}]t - (\pi J \tau_c)^{-1}\}. \quad (21J')$$

This predicts (1) an apparent coupling constant $J[1 - (2\pi^2 J^2 \tau_c^2)^{-1}]$ c.p.s., (2) a phase shift $(\pi J \tau_c)^{-1}$ radians (the trivial error that $E_J(0) \neq 1$ is a result of the approximation) and (3) an exponential overall decay with time constant τ_c . All these features have been observed in our echo experiments.

(1) The apparent J from the echo is nearer the true J than to J_A deduced from the separation of the steady-state doublets for given τ_c because the 2 in equation (21J') is absent in equation (11). This is seen to be confirmed by experiment by comparing columns (3) and (4) of table 1 apart from the difficulty that the apparent J depends on pulse spacing, n . This is not to say that the Bloch decay equation (16) (or the echo amplitude equation (21J)) is inconsistent with the line shape equation (10) which is its Fourier transform. The apparent J value from the distance between the maxima of the absorption curve is not exactly the same quantity as the frequency of the echo amplitude modulation. This difference also helps to explain why we see modulation of the echo amplitude even at temperatures such that the steady-state doublet has collapsed (see figure 1(c) and table 1). Dr. Loewenstein has pointed out that some of the difference also comes from the fact that the echo amplitude is entirely unaffected by field inhomogeneity to which the absorption line in the intermediate situation is extremely sensitive.

	$t_0 = \frac{1}{2}\tau_c$		$t_0 = \tau_c$		$t_0 = 2\tau_c$	
n	$p(n)$	$\Sigma p(n)$	$p(n)$	$\Sigma p(n)$	$p(n)$	$\Sigma p(n)$
0	0.606	0.606	0.367	0.367	0.135	0.135
1	0.303	0.909	0.367	0.734	0.270	0.405
2	0.076	0.985	0.183	0.917	0.270	0.675
3	0.013	0.998	0.061	0.978	0.180	0.855
4	0.001	0.999	0.015	0.993	0.090	0.945

Table 2.

(2) The phase shift of the echo modulation for the experimental result illustrated in figure 1(b) is 0.14 radians. Since at this temperature of -11°C $\tau_c = 0.11$ sec as given in table 1, columns 5 and 6, we have $(\pi J \tau_c)^{-1} = 0.58$ radians. The difference between these two numbers is possibly due to the fact that we measure an AB_3 rather than an AB case. It might also be indicative of a different exchange mechanism from that adopted.

(3) τ_c obtained using the line shape equation (10) is given in table 1, column 5. The decay constant of the echo signal is given in column 6. According to equation (21J') this should be the same as τ_c so long as $\pi J \tau_c \gg 1$. The two estimates of τ_c indeed agree up to a temperature of 4°C . At this temperature we estimate that $\pi J \tau_c = 1.1$. A more precise comparison of both τ_c and apparent J by the two methods is made difficult by the dependence on pulse spacing.

For rapid exchange, i.e. $\pi J \tau_c \ll 1$ equation (21J) reduces to:

$$E_{1J} \simeq \exp - \frac{1}{2} \pi^2 J^2 \tau_c t. \quad (21J'')$$

The collapsed steady-state line for $\pi J \tau_c \ll 1$, equation (10''), is a Lorentzian width $\frac{1}{2} \pi^2 J^2 \tau_c$ which corresponds to equation (21J'').

We have throughout neglected all other relaxation of the transverse magnetization. In echo experiments this is usually adequately accounted for by multiplying the echo amplitude at time t by a factor $\exp[-t/T_2(T)]$ which corresponds to an additional line broadening $T_2^{-1}(T)$ in the steady-state spectrum. Clearly in the two extremes the broadening due to exchange can only be measured (a) for $\pi J\tau_c \gg 1$ if $T_2 \gg \tau_c$ and (b) for $\pi J\tau_c \ll 1$ if $T_2 \gg 2/\pi^2 J^2 \tau_c$. In practice T_2 values are usually such that the exchange broadening dominates only in the collapse region where $\pi J\tau_c \simeq 1$. This is illustrated for methyl alcohol in figure 1 (a) for -60°C , where $T_2 \simeq 0.5$ sec and the decay is mostly due to T_2 rather than τ_c which is estimated from the higher temperature measurements to have the value 1 sec at -60°C for our sample. We are unable to illustrate this effect at the high temperature end (when $\pi J\tau_c \ll 1$) because our decay was then controlled by self-diffusion attenuation [12] which could however have been removed by more elaborate experimental procedures [13]. In any case a more precise theory is required for very rapid exchange [6]. This theory could be extended to other than doublet cases.

For the chemically shifted multiplet the echo is given by equation (21 δ). For slow exchange, i.e. $\pi\delta\tau_c \gg 1$, equation (21 δ) becomes:

$$E_{1\delta}(t) \simeq \exp(-t/\tau_c) \{1 + (\pi\delta\tau_c)^{-1} \sin \pi\delta t - (\pi\delta\tau_c)^{-2} \cos \pi\delta t + \dots\}. \quad (21\delta')$$

This shows that for slow exchange the correlation time τ_c can be obtained from the attenuation of the echo and that this is practically independent of pulse spacing. It is also interesting that for moderately slow exchange the echo is modulated so that δ can be measured, whereas δ is not observable when no exchange occurs. This is all explained physically in § 3.4.

For fast exchange, i.e. $\pi\delta\tau_c \ll 1$, equation (21 δ) becomes:

$$E_\delta(t) \simeq \exp - \frac{1}{2} \pi^2 \delta^2 \tau_c t, \quad (21\delta'')$$

which is of the same form as (21 J''). It shows that for very rapid exchange the echo amplitude is independent of pulse spacing. This result is in agreement with Piette and Anderson [17] and with the limiting case of the approximate formula of Luz and Meiboom [16]. Thus τ_c can be determined if T_2 is favourable and the exchange is slow enough to justify the use of the classical theory.

3.3. The McConnell theory

McConnell [10] has proposed a set of equations for exchanging systems which correspond to an earlier more involved theory [18]. It is not clear whether this theory corresponds exactly to the Anderson and Weiss theory [19] which we have used here. It does however lead to the same expressions for the line shape, e.g. equation (10). The equations have been used by Luz and Meiboom [16] but are only solved approximately and in the case of fast exchange. We have therefore used the equations to calculate the J and δ echo amplitudes and we show them to be valid also for transient signals.

For our case of only two lines of equal intensity without exchange, the equations for the rotating complex transverse magnetizations associated with the A and X nuclei are:

$$\left. \begin{aligned} \frac{dG_A}{dt} - i\frac{\Delta}{2} G_A + \frac{1}{\tau_c} (G_A - G_X) &= 0, \\ \frac{dG_X}{dt} + i\frac{\Delta}{2} G_X + \frac{1}{\tau_c} (G_X - G_A) &= 0, \end{aligned} \right\} \quad (23)$$

where $\Delta/2\pi$ is δ or J . $G_A = M_{xA} + iM_{yA}$, i.e. the complex rotating magnetization due to the A nuclei, etc.

We can solve these equations in terms of $G_{\pm} = G_A \pm G_X$ and obtain:

$$G_+(t) = A \exp(x_1 t) + B \exp(x_2 t),$$

$$G_-(t) = \frac{2}{i\Delta} [Ax_1 \exp(x_1 t) + Bx_2 \exp(x_2 t)],$$

G_+ is the observed signal $G(t)$ of the previous section and

$$x_{1/2} = -\frac{1}{\tau_c} \left\{ 1 \mp \left[1 - \left(\frac{\Delta\tau_c}{2} \right)^2 \right]^{1/2} \right\}.$$

After a 90° y pulse at $t=0$, $G_+(0)=1$ and $G_-(0)=0$ and we find for the Bloch decay:

$$G_+(t) = (x_2 - x_1)^{-1} [x_2 \exp(x_1 t) - x_1 \exp(x_2 t)]. \quad (24)$$

Substitution of x_1 and x_2 in (24) gives equation (16) or (22) and consequently the line shape equation (10).

The effect of a 180° x pulse at time τ is to give $M_x \rightarrow M_x$, $M_y \rightarrow -M_y$ for the δ case and for J to give in addition the change in identity. Thus the effect of the pulse is $G_+ \rightarrow G_+^*$ for both δ and J and $G_- \rightarrow \pm G_-^*$ for δ or J respectively. In taking the complex conjugate the effect of x_1 and x_2 can be shown to be as if one simply ignored this operation on them whatever the value of $(\Delta\tau_c/2)$. By using the conditions above to match the magnetizations the constants A and B in G_+ and G_- after the 180° pulse can be determined from G_{\pm} before the pulse and the echo amplitude expressions are found. The echo for the J case is:

$$E_{1J}(2\tau) = (x_1 - x_2)^{-1} [x_2 \exp[x_1(2\tau)] - x_1 \exp[x_2(2\tau)]], \quad (25)$$

which has the same form as equation (24) and so again shows that the pulses have no effect for J . Equation (25) reduces to equation (21J) on substituting for x_1 and x_2 .

For the δ case we find:

$$E_{1\delta}(2\tau) = (x_1 - x_2)^{-2} \{ x_2(x_1 + x_2) \exp[x_1(2\tau)] - 4x_1x_2 \exp[(x_1 + x_2)\tau] + x_1(x_1 + x_2) \exp[x_2(2\tau)] \}, \quad (26)$$

which again shows that this echo is affected by pulse spacing.

Equation (26) reduces to equation (21 δ) on substituting for x_1 and x_2 .

It seems very probable therefore that McConnell's equations also give the same answer as Anderson and Weiss's for transients. Which set of equations one uses is therefore a matter of mathematical convenience.

3.4. Approximation theory of echo modulation with exchange

In view of the mathematical nature of the previous sections we feel it is of interest to present a rather different approach to the problem. This has the advantage of making clearer both the nature of the physical processes actually occurring and the significance of the several special cases which we have discussed. It may also be more adaptable to generalization than the exact treatment.

We first study the distribution in phase of the nuclei associated with one of the transverse magnetizations. We assume first that this is initially A_+ , i.e. $\phi(0) = +\pi J$. The following theory also applies to the chemical shift case and

more complex combined ones. The phase shift accumulated in time t is:

$$\phi(t) = \int_0^t \dot{\phi}(t') dt' = \int_0^t \pi J(t') dt'. \quad (27)$$

When exchange takes place there is a distribution over ϕ at time t . Let $P_+(\phi) d\phi$ be the probability of finding ϕ in $d\phi$. $P_+(\phi)$ is normalized so that:

$$\int_{-\infty}^{\infty} P_+(\phi) d\phi = \int_{-\pi Jt}^{\pi Jt} P_+(\phi) d\phi = 1.$$

The limits of ϕ are reduced to $\pm \pi Jt$ since clearly $|\phi| \leq \pi Jt$. The resultant magnetization and hence the amplitude of the transient signal, which we call $G(t)$, although it is not necessarily the decay signal after a 90° pulse, is given by:

$$G(t) = \int_{-\pi Jt}^{\pi Jt} P_+(\phi) \cos \phi d\phi. \quad (28)$$

We first study $P_+(\phi)$ since this in fact determines the echo amplitude as well as $G(t)$. The distribution of the magnetization for which $\dot{\phi}(0) = -\pi J$ is given by $P_-(\phi) = P_+(-\phi)$ but in view of $\cos \phi$ in equation (28) it will give an identical contribution to $G(t)$. We therefore ignore it in the following. Indeed we can also ignore the magnetization associated with the X nuclei.

We develop expressions for $P_+(\phi)$ using the same stochastic assumptions for $J(t')$ as in the previous section. We then evaluate $G(t)$ and compare the results with the ones obtained there.

For no exchange, i.e. $\pi J \tau_c \rightarrow \infty$, $J(t') = J$ for $\dot{\phi}(0) = +\pi J$. Hence

$$P_+(\phi) = \delta(\phi - \pi Jt)$$

and

$$G(t) = \int_{-\pi Jt}^{\pi Jt} \delta(\phi - \pi Jt) \cos \phi d\phi = \cos \pi Jt,$$

as in §3.1.

We now allow exchanges and consider the changes of sign of $J(t')$ during the interval up to t . The changes in sign have a Poisson distribution, i.e. $p(n)$, the probability of n changes of sign in t , is given by:

$$p(n) = \frac{1}{n!} (t/\tau_c)^n \exp(-t/\tau_c). \quad (29)$$

We therefore consider the probability distributions of ϕ when exactly n changes of sign of J occur and call these $P_{+n}(\phi)$, so that:

$$P_+(\phi) = \sum_{n=0}^{\infty} p(n) P_{+n}(\phi), \quad (30)$$

where

$$\int_{-\pi Jt}^{\pi Jt} P_{+n}(\phi) d\phi = 1.$$

Clearly

$$G(t) = \sum_{n=0}^{\infty} G_n(t), \quad (31)$$

where

$$G_n(t) = p(n) \int_{-\pi Jt}^{\pi Jt} P_{+n}(\phi) \cos \phi d\phi. \quad (32)$$

It is from now on assumed that $P_{+n}(\phi)$ is the distribution evaluated at time t unless otherwise stated.

Since the $p(n)$ are known it is possible to find the values of the signal $G(t)$ up to any given time t_0 , which accounts for any chosen proportion of all the nuclei provided the corresponding functions $P_{+n}(\phi)$ up to the corresponding value of n are known. This is of particular interest for times up to about τ_c . For instance, up to the time τ_c only 8 per cent of the nuclei (see table 2) have suffered more than two changes of sign. It may be expected therefore that

$$\sum_0^2 G_n(t)$$

gives 92 per cent of the signal correctly at $t = \tau_c$ and correspondingly better for $t < \tau_c$. It may well be possible to make a plausible guess for $G(t)$ for later times and we give one expression below for $t \gg \tau_c$.

Before obtaining the $P_{+n}(\phi)$ we find the first two means of the distribution $P_+(\theta)$. For this we need the probabilities P_{\pm} that $J(t')$ is $\pm J$ at time t' if $J(t')$ was $+J$ at $t' = 0$. For our model, which corresponds to the random telegraph signal [19] for $J(t)$, we have:

$$P_{\pm} = \frac{1}{2} [1 \pm \exp(-2t/\tau_c)], \quad (33)$$

since

$$P_+ = p(0) + p(2) + p(4) + \dots$$

The mean value $\bar{\phi}$ of ϕ is:

$$\begin{aligned} \bar{\phi} &= \pi \int_0^t J(t') dt' = \pi J \int_0^t [P_+(t') - P_-(t')] dt' \\ &= \frac{1}{2} \pi J \tau_c [1 - \exp(-2t/\tau_c)] \end{aligned} \quad (34)$$

and so

$$\frac{\bar{\phi}}{\pi J t} = 1 - t/\tau_c + \frac{2}{3}(t/\tau_c)^2 - \frac{1}{3}(t/\tau_c)^3 + \frac{2}{15}(t/\tau_c)^4 - \frac{2}{45}(t/\tau_c)^5 + \dots, \quad (34')$$

and for

$$t \gg \tau_c \quad \bar{\phi} \rightarrow \frac{1}{2} \pi J \tau_c. \quad (34'')$$

Again,

$$\begin{aligned} \bar{\phi}^2 &= \pi^2 \overline{\int_0^t J(t') dt' \int_0^t J(t'') dt''} \\ &= \pi^2 \int_0^t dt' \int_{-t'}^{t-t'} \overline{J(t') J(t' + \tau)} d\tau. \end{aligned}$$

For our $J(t')$,

$$\overline{J(t') J(t' + \tau)} = J^2 \exp(-2|\tau|/\tau_c).$$

$$\therefore \bar{\phi}^2 = \frac{1}{2} \pi^2 J^2 \tau_c^2 [2t/\tau_c - 1 + \exp(-2t/\tau_c)]; \quad (35)$$

and so:

$$\frac{\bar{\phi}^2}{(\pi J t)^2} = 1 - \frac{2}{3}(t/\tau_c) + \frac{1}{3}(t/\tau_c)^2 - \frac{2}{15}(t/\tau_c)^3 + \frac{2}{45}(t/\tau_c)^4. \quad (35')$$

The coefficients are similar to those of $\bar{\phi}$. For

$$t \gg \tau_c \quad \bar{\phi}^2 \rightarrow \pi^2 J^2 \tau_c t. \quad (35'')$$

The distribution $P_{+n}(\phi)$ is sharp for $t \ll \tau_c$ and it spreads as illustrated in figure 3 until for $t \gg \tau_c$ it becomes Gaussian. Just as successive terms $G_n(t)$ contribute to $G(t)$ and $P_{+n}(\phi)$ to $P_+(\phi)$, the subsidiary means $\bar{\phi}_n^m$ contribute to $\bar{\phi}^m$, where

$$\bar{\phi}_n^m = \int_{-\pi J t}^{\pi J t} \phi^m P_{+n}(\phi) d\phi = (\pi J t)^m a_{nm},$$

and the a_{nm} are time independent. In fact it is easy to show that

$$\bar{\phi}^m = \bar{\phi}_0^m - (\bar{\phi}_0^m - \bar{\phi}_1^m)(t/\tau_c) + (\frac{1}{2}\bar{\phi}_0^m - \bar{\phi}_1^m + \frac{1}{2}\bar{\phi}_2^m)(t/\tau_c)^2 + \dots \quad (36)$$

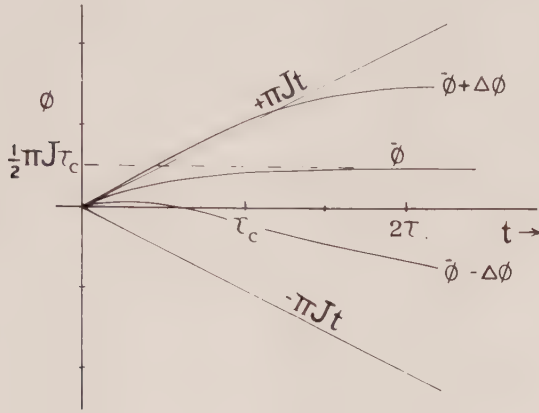


Figure 3. Showing the time variation of $\bar{\phi}$ and $\bar{\phi} \pm (\bar{\phi}^2 - \bar{\phi}_0^2)^{1/2}$ when $\dot{\phi}(0) = +\pi J$, for the exchange model discussed in the text.

so that the subsidiary means $\bar{\phi}_n^m$ can be obtained from the expansion of $\bar{\phi}^m$ as a power series in (t/τ_c) . For example, we find using (34') and (36) that:

$$\bar{\phi}_0/\pi J t = a_{01} = 1, \quad \bar{\phi}_1/\pi J t = 0, \quad \bar{\phi}_2/\pi J t = \frac{1}{3}, \quad \text{etc.} \quad \dots$$

Similarly for $\bar{\phi}^2$ we find, using equation (35') that:

$$\bar{\phi}_0^2/(\pi J t)^2 = a_{02} = 1, \quad \bar{\phi}_1^2/(\pi J t)^2 = \frac{1}{3}, \quad \bar{\phi}_2^2/(\pi J t)^2 = \frac{1}{3}, \quad \text{etc.}$$

This independent evaluation of the means is a useful check on the expressions for $P_{+n}(\phi)$ deduced below.

For the nuclei which do not exchange, $\dot{\phi}$ remains $+\pi J$ in the whole interval $(0, t)$, as in figure 4(a), so that:

$$P_{+0}(\phi) = \delta(\phi - \pi J t) \quad (37)$$

with total probability $p_0 = \exp(-t/\tau_c)$ and so $\bar{\phi}_0/\pi J t = \bar{\phi}_0^2/(\pi J t)^2 = 1$ as found above:

$$G_0(t) = P_0 \int P_{+0}(\phi) \cos \phi d\phi = \exp(-t/\tau_c) \cos \pi J t. \quad (38)$$

This is a good approximation to $G(t)$ for $t \ll \tau_c$. Then $\pi J t \ll \pi J \tau_c$, so that it is a *useful* approximation when $\pi J \tau_c \gg 1$. In fact it is the Bloch decay corresponding to the steady-state signal equation (10') for $\pi J \tau_c \gg 1$. This is already a useful formula for interpretation of the slow exchange results since even if $t \ll \tau_c$ one can observe at least the initial part of the decay $\exp(-t/\tau_c)$ and so determine τ_c .

If exactly *one* change of sign of $\dot{\phi}$ occurs during the interval $(0, t)$ we have one typical realization in figure 4(b) for which $\phi(t) = \pi J (2t' - t)$. The probability of the change in sign occurring in dt' at t' in the interval $(0, t)$ is dt'/τ_c , which is

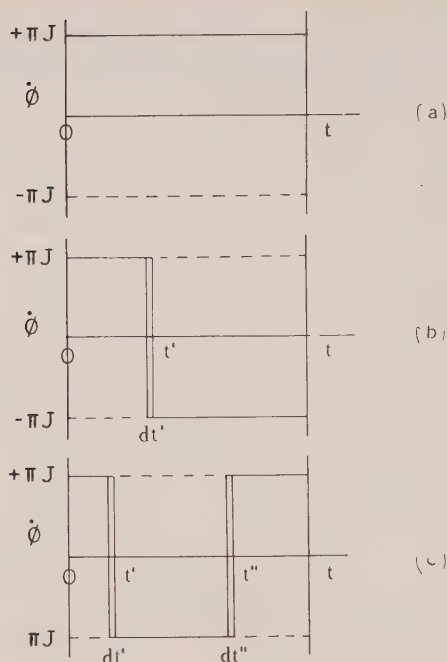


Figure 4. Illustrating the behaviour of the quantity $\dot{\phi}(t)$ for the stochastic model used in the text : (a) no change during $(0, t)$, (b) one change in sign of $\dot{\phi}$ during $(0, t)$, (c) two changes in $\dot{\phi}$ during $(0, t)$.

independent of t' . Therefore $P_{+1}(\phi)$ is a uniform distribution between $\phi = \pi J t$ (when $t' = t$) and $\phi = \pi J t$ (when $t' = 0$), i.e.

$$P_{+1}(\phi) = \frac{1}{2\pi J t}, \quad (39)$$

so that $\bar{\phi}_1/\pi J t = 0$ and $\bar{\phi}_1^2/(\pi J t)^2 = \frac{1}{3}$, as already found above. The next approximation for $G(t)$, using (31) and (32), is therefore:

$$\begin{aligned} G(t) &= G_0 + G_1 = \exp(-t/\tau_c) \left[\cos \pi J t + \frac{1}{\pi J \tau_c} \sin \pi J t \right] \\ &\simeq \exp(-t/\tau_c) \cos \{ \pi J t - (\pi J \tau_c)^{-1} \} \quad \text{if } \pi J \tau_c \gg 1. \end{aligned} \quad (40)$$

The latter expression is clearly related to the expression $(21J')$ for E_1 , which is the same as $G(t)$ when $\pi J t \tau_c \gg 1$. It is not however directly comparable since (40) is an approximation to $G(t)$ for $t < \tau_c$, a different condition. This difference is further emphasized by calculating the line shape corresponding to (40) which is:

$$I(\omega) \simeq I_0(\omega) + I_1(\omega) = \sum_{\pm} \left[\frac{\tau_c}{1 + (\omega \pm \pi J)^2 \tau_c^2} + \frac{\tau_c (\omega \pm \pi J)/\pi J}{1 + (\omega \pm \pi J)^2 \tau_c^2} \right]. \quad (41)$$

This corresponds to two non-Lorentzian peaks separated so that the apparent coupling constant is $J[1 - (2\pi^2 J^2 \tau_c^2)^{-1}]$ which differs from the correct peak separation for $\pi J \tau_c > 1$ given by equation (11) but does correspond to the modulation frequency of equation $(21J')$.

For two changes of sign in the interval $(0, t)$ as in figure 4(c) we have $\phi(t) = \pi J(t + 2t' - 2t'')$. The probability of the second change at t'' is independent

of t'' but of course $t' < t'' < t$, i.e. $\pi J(2t' - t) < \phi < \pi Jt$ for given t' and the distribution of ϕ is uniform in this range. Again all values of t' are equally probable so the resultant distribution for ϕ is assymetric and it is easily shown that:

$$P_{+2} = \frac{1}{2\pi Jt} (1 + \phi/\pi Jt), \quad (42)$$

for which $\bar{\phi}_2/\pi Jt = \frac{1}{3}$ and $\bar{\phi}_2^2/(\pi Jt)^2 = \frac{1}{3}$, as already shown above. It is worth remarking at this point that the assymetry in P_{+2} (and in fact in P_{+0} , P_{+4} , etc.) are not observable because we always observe not only the nuclei which at $t=0$ contribute to A_+ (i.e. $\dot{\phi}(0) = +\pi J$) but also those for A_- where $\dot{\phi}(0) = -\pi J$. Consequently the total distribution is really $\frac{1}{2}(P_{+2} + P_{-2}) = 1/2\pi Jt$, etc. Similarly $\bar{\phi} = \frac{1}{2}(\bar{\phi}_+ + \bar{\phi}_-) = 0$. However, the observable $G(t)$ has zero contribution for odd powers of ϕ so we still need not bother with $P_-(\phi)$, etc. for the moment.

We now have:

$$G(t) \simeq G_0 + G_1 + G_2 = \exp(-t/\tau_c) \left[\cos \pi Jt + \frac{1}{\pi J\tau_c} \left(1 + \frac{1}{2} \frac{t}{\tau_c} \right) \sin \pi J\tau_c \right] \quad (43)$$

$$\simeq \exp(-t/\tau_c) \left[\cos \pi Jt \left\{ \left(1 - \frac{1}{2(\pi J\tau_c)^2} \right) - \frac{1}{\pi J\tau_c} \right\} \right], \quad (43')$$

when $\pi J\tau_c > 1$ and $t < \tau_c$. This expression is identical with the one for E_1 given in equation (21J') for $\pi J\tau_c > 1$ which we know to be the same as $G(t)$.

We know that this $G(t)$ in (43) corresponds to at least 92 per cent of the signal for times up to $t = \tau_c$ for *any value* of $\pi J\tau_c$, whereas it would be quite difficult to estimate the accuracy of the approximation to E_1 in equation (21J) for any $\pi J\tau_c$ value.

The evaluation of subsequent terms $P_{+n}(\phi)$ and $G_n(t)$ is straightforward but increasingly tedious. We give the result up to $n=4$:

$$\begin{aligned} \sum_{n=0}^4 p(n)P_{+n}(\phi) = \exp(-t/\tau_c) & \left[\delta(\phi - \pi Jt) \right. \\ & + \frac{1}{2\pi J\tau_c} \left\{ 1 + \frac{1}{2}(1 + \phi/\pi Jt) \left(\frac{t}{\tau_c} \right) + \frac{1}{4}(1 + \phi/\pi Jt)(1 - \phi/\pi Jt) \left(\frac{t}{\tau_c} \right)^2 \right. \\ & \left. \left. + \frac{1}{16}(1 + \phi/\pi Jt)(1 - \phi/\pi Jt)(1 + \phi/\pi Jt)(t/\tau_c)^3 \right\} \right], \quad (44) \end{aligned}$$

$$\begin{aligned} \sum_{n=0}^4 G_n(t) = \exp(-t/\tau_c) & \left[\cos \pi Jt + \frac{1}{\pi J\tau_c} \left(1 + \frac{1}{2} \frac{t}{\tau_c} \right) \sin \pi Jt \right. \\ & \left. - \frac{1}{2(\pi J\tau_c)^2} \left(\frac{t}{\tau_c} \right) \left(1 - \frac{1}{4} \frac{t}{\tau_c} \right) \cos \pi Jt + \frac{1}{2(\pi J\tau_c)^3} \left(1 + \frac{1}{4} \frac{t}{\tau_c} \right) \sin \pi Jt \right]. \quad (45) \end{aligned}$$

This result shows that equation (43) contains all terms of order $1/\pi J\tau_c$ and this is clearly why it agrees with E_1 from the exact theory. It may be remarked that this approximation to $G(t)$ is the signal for at least 95 per cent of the nuclei up to $t = 2\tau_c$, and so practically all of the modulation is revealed by it.

In the other extreme of $t \gg \tau_c$ any particular value of ϕ (except very near $\pm \pi Jt$) is the result of a large number of small contributions so that the distribution

$P_+(\phi)$ is Gaussian with mean value $\bar{\phi}$ and mean square $\bar{\phi}^2$ given by equations (34'') and (35'').

$$\begin{aligned} \therefore P_+(\phi) &= 2\pi[\bar{\phi}^2 - (\bar{\phi})^2]^{-1/2} \exp -(\phi - \bar{\phi})^2/2(\bar{\phi}^2 - (\bar{\phi})^2) \\ &= 2\pi(\pi J \tau_c)^2 (t/\tau_c)^{-1/2} \exp -(\phi - \frac{1}{2}\pi J \tau_c)^2/2(\pi J \tau_c)^2 (t/\tau_c), \end{aligned} \quad (46)$$

and using this in equation (28) leads to:

$$G(t) = \exp(-\frac{1}{2}\pi^2 J^2 \tau_c t) \cos \frac{1}{2}(\pi J \tau_c) \text{ for } t \gg \tau_c. \quad (47)$$

This function can be used as a 'tail' for $G(t)$ given by equation (44) for $t \gg \tau_c$. It is also of importance in its own right when $\pi J \tau_c \ll 1$, i.e. for fast exchange, since then it constitutes almost all the observable decay and then:

$$G(t) \simeq \exp(-\frac{1}{2}\pi^2 J^2 \tau_c t). \quad (47')$$

This corresponds to E_{1J} in equation (21J'') and the line shape equation (10'').

We are now in a position to calculate the echo amplitude. At time τ after the 90° pulse we have a distribution $P_+(\phi)_\tau = \sum p(n)_\tau P_{+n}(\phi)$ which is the magnetization for the nuclei which had $\dot{\phi} = +\pi J$ initially and similarly for $P_-(\phi)$ and we have emphasized that the distribution is to be evaluated at time τ . Consider the effect of a 180° pulse on the nuclei in $d\phi$ at ϕ . These nuclei have their phase reversed and also their $\dot{\phi}$'s reversed. But the part of $P_+(\phi)_\tau$ which has $\dot{\phi} = +\pi J$ is:

$$P_{++}(\phi)_\tau = [p(0)_\tau P_{+0}(\phi) + p(2)_\tau P_{+2}(\phi) + \dots]$$

and the part of $P_+(\phi)_\tau$ which has $\dot{\phi} = -\pi J$ is

$$P_{+-}(\phi)_\tau = [p(1)_\tau P_{+1}(\phi) + p(3)_\tau P_{+3}(\phi) \dots].$$

Hence after the 180° pulse we have a new distribution composed of

$$P_{++}(-\phi)_\tau = [(p(0)_\tau P_{+0}(-\phi) + \dots) \dots]$$

which has $\dot{\phi} = -\pi J$ together with

$$P_{+-}(-\phi)_\tau = [p(1)_\tau P_{-1}(-\phi) + \dots]$$

which has $\dot{\phi} = +\pi J$. But it is easy to show that $P_{+0}(-\phi) = P_{-0}(\phi)$, $P_{+2}(-\phi) = P_{-2}(\phi)$, etc. Hence after the 180° pulse the distribution associated with nuclei with $\dot{\phi} = -\pi J$ at $t = \tau +$ is $[p(0)_\tau P_{-0}(\phi) + p(2)_\tau P_{-2}(\phi) + \dots]$. Similarly one can show that $P_{+1}(-\phi) = P_{-1}(\phi)$, $P_{+3}(-\phi) = P_{-3}(\phi)$, etc., so that the nuclei with $\dot{\phi} = +\pi J$ at $t = \tau +$ have a distribution

$$[p(1)_\tau P_{-1}(\phi) + p(3)_\tau P_{-3}(\phi) + \dots],$$

i.e. the total distribution $P_+(\phi)_\tau$ before the pulse has become

$$[p(0)_\tau P_{-0}(\phi) + p(1)_\tau P_{-1}(\phi) + \dots] = P_-(\phi)_\tau$$

after the pulse. In the same way $P_-(\phi)_\tau$ before the pulse becomes $P_+(\phi)_\tau$ after the pulse. Hence the 180° pulse has *no effect* on the distribution for *all* nuclei which is $\frac{1}{2}[P_+(\phi) + P_-(\phi)]$. This is shown diagrammatically in figure 5 (a). It is clear therefore that the distribution at $t = 2\tau$ is just $\frac{1}{2}[P_+(\phi)_{2\tau} + P_-(\phi)_{2\tau}]$, i.e. the echo $E_{1J}(2\tau)$ has the same form as the Bloch decay. This explains the identical form of equations (16) and (21J). Clearly the echo does not depend on the number of pulses used, i.e. on the pulse spacing. Explicitly $E_n(t) = E_1(t)$ for all n .

It can be seen that this result is largely independent of the exchange model. If there is at time τ a number N of nuclei whose phase is in $d\phi$ at ϕ and it is possible to say that αN of these have $\dot{\phi} = +\pi J$ and $(1 - \alpha N)$ have $\dot{\phi} = -\pi J$ at that moment the 180° pulse puts these nuclei in $d\phi$ at $-\phi$ with αN of them having $\dot{\phi} = -\pi J$ and $(1 - \alpha N)$ with $\dot{\phi} = +\pi J$. This has no effect on the observable signal. Thus the pulse only affects the distribution if it can affect the nuclei while they are actually exchanging.

We now show that the chemical shift case is quite different. In this case the pulse causes no change in ϕ (or identity) and so as illustrated in figure 6(b) the distribution just after the 180° pulse is quite different from that before. Obviously one gets for distribution $P_+(\phi)$ before the pulse that the nuclei with $\dot{\phi} = +\pi\delta$ after the pulse have a distribution $[p(0)_\tau P_{-0}(\phi) + p(2)_\tau P_{-2}(\phi) + \dots]$ and those with $\dot{\phi} = -\pi\delta$ the distribution $[p(1)_\tau P_{-1}(\phi) + p(3)_\tau P_{-3}(\phi) + \dots]$. Similarly for the effect of the pulse on $P_-(\phi)$ before the pulse. Hence the distribution at time τ after the 180° pulse is:

$$P\delta(\psi) = \int_{-\pi\delta\tau}^{\pi\delta\tau} \{ [p(0)_\tau P_{-0}(\phi) + p(2)_\tau P_{-2}(\phi) + \dots] P_+(\psi - \phi)_\tau + [p(1)_\tau P_{-1}(\phi) + \dots] P_-(\psi - \phi)_\tau \} d\phi. \quad (48)$$

Consequently the echo at 2τ is:

$$E_{1\delta}(2\tau) = \int_{-\pi\delta(2\tau)}^{\pi\delta(2\tau)} P_\delta(\psi) \cos \psi d\psi, \quad (49)$$

which must be equivalent to equation (21 δ).

When $t \ll \tau_c$:

$$\begin{aligned} P_\delta(\psi) &\simeq \int_{-\pi\delta\tau}^{\pi\delta\tau} \left\{ [\exp(-\tau/\tau_c)\delta(\phi + \pi\delta\tau)][\exp(-\tau/\tau_c)\delta(\psi - \phi - \pi\delta\tau)] \right. \\ &\quad \left. + \left[\frac{\tau}{\tau_c} \exp(-\tau/\tau_c) \frac{1}{2\pi\delta\tau} \right] [\exp(-\tau/\tau_c)2\delta(\psi - \phi + \pi\delta\tau)] \right\} d\phi \\ &= \exp(-2\tau/\tau_c) [\delta(\psi) + (\pi\delta\tau_c)^{-1} F(\psi)], \end{aligned} \quad (48')$$

where $F(\psi) = 1$ for $\psi < 0$ and 0 for $\psi > 0$. Therefore

$$E_{1\delta}(2\tau) = \exp(-2\tau/\tau_c) [1 + (\pi\delta\tau_c)^{-1} \sin \pi\delta(2\tau)], \quad (49')$$

which corresponds to equation (21 δ').

When $t \gg \tau_c$ $P_+(\phi)_\tau$ is given by equation (46) with δ in place of J . Since practically all nuclei have suffered a large number of exchanges the nuclei with $\dot{\phi} = \pm\pi\delta$ at τ will make equal contributions to $P_+(\phi)_\tau$ for all ϕ (except those with ϕ near $\pm\pi\delta\tau$). Consequently the 180° pulse does not affect the (Gaussian) distribution and so $P_\delta(\psi)$ is as equation (46) with t , ϕ and J replaced by 2τ , ψ and δ respectively. Consequently corresponding to (47') we have:

$$E_{1\delta}(2\tau) = \exp -\frac{1}{2}\pi^2\delta^2\tau_c(2\tau) \text{ for } \tau \gg \tau_c \text{ and } \pi\delta\tau_c \ll 1.$$

This is the same as equation (21 δ'') but it is clear that the same expression will be obtained whatever the number of pulses, i.e. this decay is independent of pulse spacing provided the pulses are not closer than τ_c , a condition which is unlikely to be violated for fast exchange.

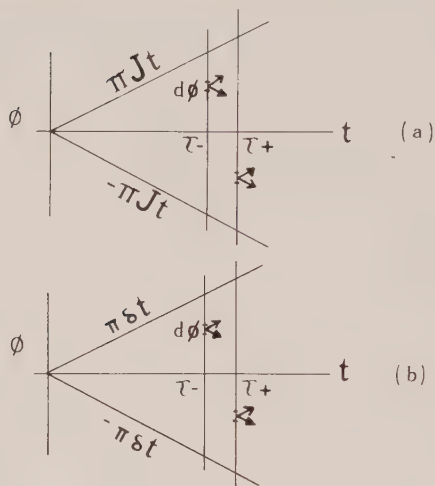


Figure 5. The effect of a 180° pulse on the distribution in ϕ . The nuclei in $d\phi$ at ϕ before the pulse ($\tau-$) are composed of two groups with $\phi = \pi J$ (or $\pm \pi \delta$) represented by the open or closed arrow heads respectively. After pulse ($\tau+$) the new situation of these nuclei are shown for (a) J coupling and (b) δ splitting. This illustrates the different effect of a 180° pulse in each case.

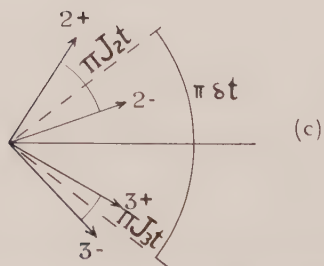
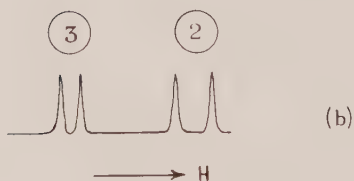
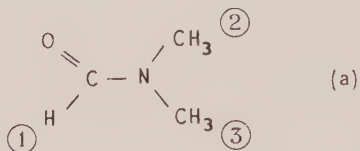


Figure 6. (a) The molecular structure of N,N-dimethyl formamide, (b) the methyl spectrum shown diagrammatically, (c) the phase picture for no exchange.

3.5. Internal flexibility in dimethyl formamide

As another illustration of the usefulness of the approximate treatment we consider a rather more complicated case. The methyl proton signal in dimethyl formamide $\text{H} \cdot \text{CO} \cdot \text{N}(\text{CH}_3)_2$ consists of two doublets one of which corresponds to one set of methyl protons and the other to the other group of methyl protons being split by $J_2 = 0.8$ c.p.s. and $J_3 = 0.4$ c.p.s. respectively by J interaction with the single formamide proton. As the temperature of the liquid is raised the multiplet collapses to a doublet [21]. This is presumed to be due to an internal re-orientation process in which the two methyl groups exchange places. When this occurs both the shielding (δ) and the J coupling for each set of methyl protons changes. Fraenkel and Franconi suppose that the collapsed doublet has a splitting $\frac{1}{2}(J_2 + J_3)$ which agrees fairly well with the measured splitting. While we agree with their result we find the justification for it rather weak. The ϕ diagram for this case, for no exchange and J_2 and J_3 having the same sign, is given in figure 6(c). The \pm signs distinguish the methyl protons in molecules with the two different states of the (1) proton. For rapid exchange we expect to have for times longer than τ_c a Gaussian distribution of ϕ about some mean value. It is obvious that the one set of molecules gives signals corresponding to jumps between $2+$ and $3+$ so that the mean value of ϕ is $\bar{\phi} = \pi \frac{1}{2}(J_2 + J_3)t$ and the limits of ϕ are $\pi(\delta + J_2)t$ and $-\pi(\delta - J_3)t$. This is instead of 0, and $\pm \pi Jt$ respectively for the simple case. These limits are $\pm \pi[\delta + \frac{1}{2}(J_2 - J_3)]t$ relative to $\pi \frac{1}{2}(J_2 + J_3)t$. Using the theory of § 3.4 we see that the total distribution for $t \gg \tau_c$ is Gaussian with a mean of $\pm \pi \frac{1}{2}(J_2 + J_3)t$ and a mean square *relative to the mean* of $\Delta^2 t \tau_c$ where $\Delta = \pi[\delta \pm \frac{1}{2}(J_2 - J_3)]$. The alternative sign is for the nuclei in molecules corresponding to $2-$ and $3-$. It is easy to show that:

$$G(t) = \exp(-t/T) \cos \pi \frac{1}{2}(J_2 + J_3)t$$

where

$$T = 2/\pi^2[\delta \pm \frac{1}{2}(J_2 - J_3)]^2 \tau_c.$$

This corresponds to a pair of steady-state doublets both with a splitting of $\frac{1}{2}|J_2 + J_3|$ c.p.s. and widths corresponding to $\frac{1}{2}\pi^2[\delta \pm \frac{1}{2}(J_2 - J_3)]^2 \tau_c$. If we now assume that the two J couplings have opposite signs the resultant splitting is found to be $\frac{1}{2}|J_2 - J_3|$ with widths corresponding to $\frac{1}{2}\pi^2[\delta \pm \frac{1}{2}(J_2 + J_3)]^2 \tau_c$. Hence in general the splitting is $\frac{1}{2}[|J_2| + |J_3|]$ as assumed in reference [21], but there are two pairs of lines superposed with widths $\pi^2[\delta \pm \frac{1}{2}(|J_2| - |J_3|)]^2 \tau_c$ respectively. It is therefore impossible to determine the relative signs of J_2 and J_3 from this experiment.

We have previously reported multiple echo experiments on dimethyl formamide [3]. The spin echo amplitude modulation is predicted to be

$$E_n(t) = \frac{1}{7} |6 \cos \pi \frac{1}{2}(J_2 + J_3)t \cos \pi \frac{1}{2}(J_2 - J_3)t + \cos^3 \pi J_2 t \cos^3 \pi J_3 t|$$

for no internal reorientation and $J_{23} = 0$. Since J_2 and J_3 are small and $|J_2| - |J_3|$ is even smaller, we were only able to observe the term $\cos \pi \frac{1}{2}(|J_2| + |J_3|)t$, which as we see now above is independent of the internal re-orientation. Effects due to re-orientation in this molecule are therefore very difficult to detect at all by the spin echo technique.

4. THE MODEL FOR THE EXCHANGE PROCESS

The model we have used here is popular because of its mathematical tractability and its physical reasonableness. It is difficult to test the validity of the model since this usually involves fitting the experimental results to a theoretical formula which contains at least one adjustable parameter. One general result which we have which is unusual in this type of investigation is that for the J coupling case and for the usual model the signal should be independent of pulse spacing. Indeed, as we have already pointed out, this should be true for any model in which the value of ϕ can be other than $\pm \pi J$ for a finite time. In other words it should be possible to investigate the time taken in the exchange process itself, an obvious first correction to make to the random telegraph type of model. Although we have in fact observed some dependence of the signal on pulse spacing in methyl alcohol it is not possible to be sure that this indicates that the effectively instantaneous exchange model is not adequate in this case. It could well be that the pulse spacing dependence arises from the fact that we have an AB_3 case not AX and not even AX_3 so that the corrections we have made and the special procedures used to allow for this have been inadequate. We therefore merely point out that if a suitable example could be found, the dependence of the echoes on pulse spacing would constitute a simple and direct check on the validity of the stochastic model for the exchange process. No such simple check is possible for the δ case with exchange where different models merely give slightly different complex situations and always involve disposable parameters.

REFERENCES

- [1] HAHN, E. L., and MAXWELL, D. E., 1951, *Phys. Rev.*, **84**, 1246; 1952, *Ibid.*, **88**, 1070.
- [2] POWLES, J. G., and HARTLAND, A., 1961, *Proc. phys. Soc., Lond.*, **77**, 273.
- [3] POWLES, J. G., and STRANGE, J. H., 1962, *Disc. Faraday Soc.*, No. 34, p. 30.
- [4] GUTOWSKY, H. S., MCCALL, D. W., and SLICHTER, C. P., 1953, *J. chem. Phys.*, **21**, 279.
- [5] ARNOLD, J. T., 1956, *Phys. Rev.*, **102**, 136.
- [6] KAPLAN, J. I., 1958, *J. chem. Phys.*, **28**, 278.
- [7] POWLES, J. G., and LUSZCZYNSKI, K., 1959, *J. sci. Instrum.*, **36**, 57.
- [8] Equation (4) of reference [3] has now been proved to be correct for AB.
- [9] ANDERSON, P. W., and WEISS, P. R., 1953, *Rev. mod. Phys.*, **25**, 269. ANDERSON, P. W., 1954, *J. phys. Soc., Japan*, **9**, 316.
- [10] MCCONNELL, H. M., 1958, *J. chem. Phys.*, **28**, 430.
- [11] POWLES, J. G., 1959, *Rep. Prog. Phys.*, **22**, 433.
- [12] CARR, H. Y., and PURCELL, E. M., 1952, *Phys. Rev.*, **88**, 415; 1954, *Ibid.*, **94**, 630.
- [13] MEIBOOM, S., and GILL, P., 1958, *Rev. sci. Instrum.*, **29**, 688.
- [14] HAHN, E. L., 1950, *Phys. Rev.*, **80**, 580.
- [15] ABRAGAM, A., 1961, *The Principles of Nuclear Magnetism* (Oxford: Clarendon Press), p. 448 *et seq.*
- [16] LUZ, Z., and MEIBOOM, S., 1963, *J. chem. Phys.*, **39**, 366.
- [17] PIETTE, L. H., and ANDERSON, W. A., 1959, *J. chem. Phys.*, **30**, 899.
- [18] GUTOWSKY, H. S., MCCALL, D. W., and SLICHTER, C. P., 1953, *J. chem. Phys.*, **21**, 279.
- [19] RICE, S. O., 1954, *Selected Papers on Noise and Stochastic Processes*, edited by N. Wax (New York: Dover).
- [20] POWLES, J. G., and STRANGE, J. H., 1961, *Mol. Phys.*, **5**, 329.
- [21] FRAENKEL, G., and FRANCONI, C., 1960, *J. Amer. chem. Soc.*, **82**, 4478.

RESEARCH NOTES

An heuristic estimate of correlation energies in many-electron atoms

by CHR. KLIXBÜLL JØRGENSEN

Cyanamid European Research Institute, Cologne (Geneva), Switzerland

(Received 20 January 1964 ; revision received 4 February 1964)

It is now well known that the correlation energy in the isoelectronic series He, Li^+ , Be^{++} , is remarkably constant and has an asymptotic value close to 0.46–0.47 Hartree (≈ 2 Rydberg units) [1]. Since the interelectronic repulsion energy in a two-electron system with Slater radial functions corresponding to a definite effective charge η (the kinetic energy of the system being $+\eta^2$ Hartree and the nuclear attraction energy for the two electrons $-2Z\eta$) is $J(1s, 1s) = \frac{5}{8}\eta$ Hartree, one might consider that the correlation between the two electrons decreases this quantity to an apparent value $\frac{5}{8}(\eta - \eta_0)$. The constant

$$\eta_0 = 0.0747 - 0.0752 \quad (1)$$

is close to the reciprocal hyperfine structure constant divided by the ratio between the protonic and electronic masses :

$$137.03/1836.6 = 0.074612, \quad (2)$$

though it is not certain whether this is an accident or has a profound electrodynamic reason.

Clementi calculated the correlation energy in series containing 3, 4, 5, . . . , 10 electrons [1] and 11, 12, . . . , 18 electrons [2]. The results were rather unexpected, showing a large variation in the constants a_0 and a_1 in the linear functions (see figure) :

$$-E_{\text{corr}} = a_0 + a_1 Z \quad (3)$$

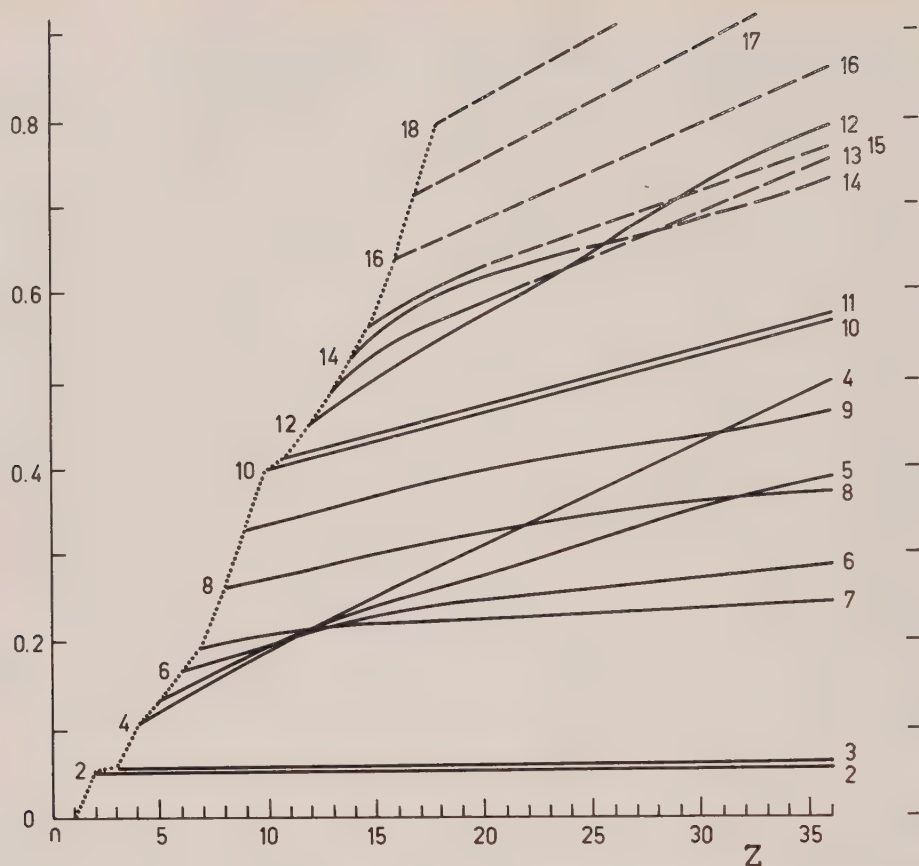
as a function of the number N of electrons. The most unexpected result was perhaps that for $N = 10$, the parameter $a_1 = 0.0136$ Hartree is quite different from zero, whereas a_0 equals 0.326 Hartree. From the point of view of perturbation theory, one would expect the closed-shell $1s^2 2s^2 2p^6$ to show no η -dependent correlation energy [3].

We propose the following empirical rules for a first-order approximation to the η -independent part of the correlation energy in a many-electron atom :

I. The repulsion between electrons in two shells having different principal quantum number n does not contribute to the correlation energy.

II. The $F^0(nl, n'l')$ and $F^0(nl, nl)$ integrals for electrons having the same n are diminished by the correlation energy as if Z was $\eta_0 = 0.0747$ smaller.

III. The $F^k(nl, nl)$ integrals for positive k (or at least those contributing to deviations of the term energies from the baricentres of the configurations [3]) are affected by the correlation as if Z (or perhaps rather η) was one unit smaller.



The correlation energy in units of 1 Hartree = 2 Rydberg units according to Clementi [1, 2] as function of atomic number Z . Each curve represents a definite number N of electrons.

Using the explicit formula for hydrogenic integrals given by Linderberg and Shull [4], one finds according to rule II the total decrease of the expression for $N=10$:

$$F^0(1s, 1s) + F^0(2s, 2s) + 12 F^0(2s, 2p) + 15 F^0(2p, 2p) \quad (4)$$

to be 0.406 Hartree, comparing reasonably well with Clementi's result 0.392. In the series of neutral atoms going from lithium to neon (and subtracting the supposedly constant effect of the helium core) one obtains :

	$N=$	rule II	rules II + III	Clementi [2]	(5)
Li	3	0	0	0.002	
Be	4	0.011	0.011	0.050	
B	5	0.035	0.035	0.080	
C	6	0.073	0.062	0.113	
N	7	0.124	0.092	0.143	
O	8	0.189	0.179	0.212	
F	9	0.268	0.268	0.278	
Ne	10	0.360	0.360	0.347	

These results obviously are affected by the phenomenon of near-orbital degeneracy in Be though the two last columns run rather parallel. It is possible to have interactions between the configurations $1s^2 2s^2 2p^q$ and $1s^2 2p^{q+2}$ for the ground terms ${}^2P(N=5)$ and ${}^3P(N=6)$ but not for the subsequent ${}^4S(7)$, ${}^3P(8)$ and ${}^2P(9)$. Correspondingly, the Z -dependence becomes much weaker [2] in the series $N=6$ and 7 but reappears weakly for $N=8$ and 9, imitating the unexplained behaviour for $N=10$ discussed above.

Quite generally, if the F^0 integrals are approximately proportional to n^{-2} , and if rule II holds, the ratio of correlation energy in the systems He, Ne, Cu^+ and the 60-electron system $1s^2 2s^2 2p^6 3s^2 3p^6 3d^{10} 4s^2 4p^6 4d^{10} 4f^{14}$ (only expected to be realized for high ionic charges such as Hg^{+20}) would be $1 : 8 : 25 : 56$, the number of appropriate F^0 quantities for each value of n being $n^2(2n^2 - 1)$. Though this result is not very different from a direct proportionality to the electron number $2 : 10 : 28 : 60$, the increase in each shell is rather parabolic as function of N in agreement with the neutral atoms indicated in the figure.

I would like to thank my friend, the late Dr. R. E. Trees, and also Dr. R. E. Watson and Professor André Julg, Marseille, and my colleague, Dr. E. A. C. Lucken, for many stimulating discussions.

REFERENCES

- [1] CLEMENTI, E., 1963, *J. chem. Phys.*, **38**, 2248.
- [2] CLEMENTI, E., 1963, *J. chem. Phys.*, **39**, 175.
- [3] JØRGENSEN, C. K., 1962, *Orbitals in Atoms and Molecules* (London: Academic Press).
- [4] LINDERBERG, J., and SHULL, H., 1960, *J. mol. Spectrosc.*, **5**, 1.

Electron spin resonance of the SeO_2^- radical ion

by R. J. COOK, J. R. ROWLANDS and D. H. WHIFFEN

Basic Physics Division, National Physical Laboratory, Teddington,
Middlesex

(Received 19 March 1964)

Electron spin resonance studies have been made on a number of inorganic free radicals and an interesting series is the pyramidal XO_3 species of which

NO_3^- [1, 2], PO_3^- [3, 4, 5], AsO_3^- [6], SO_3^- [7] and ClO_3^- [8]

are already known. In an attempt to prepare the further member, SeO_3^- , a single crystal of sodium hydrogen selenite, NaHSeO_3 , was irradiated with high energy γ -rays when a strong resonance signal was developed. The details, given below, are not in accord with the expectation for the radical SeO_3^- , in particular the g -tensor does not have cylindrical symmetry, but they are in accord with the expectations for the radical SeO_2^- , which could be formed by loss of an $-\text{OH}$ fragment from the HSeO_3^- ion. Since the radical was not in fact the desired SeO_3^- , since some overlapping of lines occurs, since the lines varied rapidly with crystal orientation, since the relative signs of the hyperfine tensor elements could not be determined and since the crystal structure is not known, a precise study of the problem did not seem warranted. However the g - and the hyperfine coupling tensors were obtained and the radical identity established and this information is briefly presented in this note.

For a general crystal orientation there are four strong narrow resonance lines and these coalesce to only two lines in a manner consistent with two pairs of radical sites the members of each pair being related by a twofold axis in monoclinic symmetry. The principle g -factors for one pair of sites were 2.0267, 2.0057 and 1.9969 and for the other pair 2.0269, 2.0063 and 1.9965. These were determined by examination of three sets of spectra at 9000 Mc/s corresponding to rotation of the crystal about three orthogonal axes. The exact klystron frequency was measured with a calibrated wavemeter and the magnetic field was measured from the proton resonance frequency and the g -factors are believed to be accurate to ± 0.0010 . The g -factors of the radicals in the two pairs of sites are very close to each other and it is suggested that the same chemical species can be trapped in two inequivalent sites. The yields of radicals in the two sites were about equal. Although 92.4 per cent of selenium nuclei in natural abundance are isotopes of zero spin, the remaining 7.6 per cent are ^{77}Se with a spin of $1/2$. It was clearly demonstrated that the radical contained selenium by the existence of two weak companions to each main line, spaced almost equally on each side of it and with 4 per cent of the intensity of the main line. These are consistent with the ^{77}Se containing radicals, when the slight correction to the centre due to second order terms is considered [3]. The principal hyperfine coupling elements for the first pair of sites were 670, 270 and 230 Mc/s, and for the second pair 670, 270 and 250 Mc/s. The errors might be as much as ± 20 Mc/s for the smaller values so that the conclusion that the two pairs of sites each contain the same chemical species is confirmed. The large

Radical	Ref.					Mc/s				XO ₂ Spin population (valence shell)					
		g_{xx}	g_{yy}	g_{zz}	g_{av}	a_{xx}	a_{yy}	a_{zz}	a_{av}	if $a_{yy}, a_{zz} + ve$			if $a_{yy}, a_{zz} - ve$		
										Xs	Xp	O	Xs	Xp	O
¹⁴ NNO ₂ ⁻ O ₃ ⁻ SO ₂ ⁻ ³⁵ ClO ₂ ⁷⁷ SeO ₂ ⁻	[1]	2.0038	2.0099	2.0070	2.0069	86	±20	±14		0.026	0.54	0.23	0.011	0.77	0.11
	[12]	2.0025	2.0174	2.0113	2.0104										
	[10, 13]				2.005										
	[14] †	2.0036 1.9967	2.0183 2.0268	2.0088 2.0062	2.0107 2.0132	189† 670	-44 ±270	-32 ±240	38				0.008 0.004	0.58 0.86	0.21 0.07

† This paper; average of the two sites. x is perpendicular to radical plane, z is twofold symmetry axis and y the O...O direction in each case.

‡ Reference [14] has 204 Mc/s but T. Cole (personal communication) states that 189 Mc/s is the correct value.

coupling of 670 Mc/s was parallel, within 5° , to the direction of the smallest g -factor for each of the sites.

In SO_3^- the g -factor is very close to 2.004 for all directions [6] and the average hyperfine coupling corresponds to a sulphur 3s orbital spin population of 0.13. The coupling for a 4s self-consistent field wave function in ^{77}Se would be 13,470 Mc/s and even a spin population of 0.10 would give hyperfine couplings greatly in excess of the observed values. This, and the lack of cylindrical symmetry to the g -tensor, makes attribution to the radical SeO_3^- most improbable. The radical SeO_2^- , which is the next most likely selenium containing species, would be in a 2B_1 state [9] with the unpaired electron in the π system. Other triatomic radicals in analogous 2B_1 states whose electron resonance has been studied are

NO_2^- [1, 2, 10], O_3^- [11, 12], SO_2^- [10, 13] and ClO_2 [14, 15].

The g -factors and hyperfine couplings are collected in the table. It can be seen that SeO_2^- falls into line with the other 2B_1 species, especially in having large but unequal values of g in the radical plane. The largest value is assigned to g_{yy} on theoretical grounds since this arises from admixture of the configuration in which one of the lone pair electrons is promoted to the half-filled shell which should lie at a low energy and give a large positive contribution. The spin-orbit coupling constant of the 4p shell in selenium is [16] about 1688 cm^{-1} compared to 586 cm^{-1} for 3p in chlorine and less for the other valence shells, so that large departures from the free spin value, 2.0023 are expected. The rather low values of g_{xx} for SeO_2^- is unexpected as simple considerations suggest g_{xx} to be almost the free spin value. Direct comparison of the hyperfine couplings is inappropriate since the nuclear moments and charges differ and it is common to quote the spin populations in valence s and p shells based on the SCF wave functions [16]. However, an extra difficulty arises since the relative signs of the principal hyperfine couplings have not been determined except for ClO_2 , where comparison can be made with solution spectra and the small values are found to be negative. In each case one may safely assume the largest element, a_{xx} to be positive and that a_{yy} and a_{zz} have the same sign as each other, since the spin population is largely in the selenium 4p orbital. The population assignments for both signs of a_{xx}/a_{yy} are given in the table. Since there is a doubly filled b_1 one electron molecular orbital, one would expect this to have the larger coefficients for the more electronegative central elements [7] and the central atom character of the spin population reduces with electronegativity since the second, half-filled b_1 orbital should be orthogonal to the filled b_1 orbital. Pauling's original electronegativity table [17] gives $\text{Se} < \text{Cl} = \text{N}$. On this basis a negative sign is to be preferred for the smaller couplings in SeO_2^- . Measurements in solution or ENDOR experiments would be needed to confirm this assignment.

This work forms part of the programme of the Basic Physics Division of the National Physical Laboratory and is published by permission of the Director.

REFERENCES

- [1] JACCARD, C., 1961, *Phys. Rev.*, **124**, 60.
- [2] ATKINS, P. W., and SYMONS, M. C. R., 1962, *J. chem. Soc.*, p. 4794.
- [3] HORSFIELD, A., MORTON, J. R., and WHIFFEN, D. H., 1961, *Mol. Phys.*, **4**, 473.

- [4] HANNA, M. W., and ALTMAN, L. J., 1962, *J. chem. Phys.*, **36**, 1788.
- [5] MORTON, J. R., 1963, *J. Phys. Chem. Solids*, **24**, 209.
- [6] LIN, W. C., and McDOWELL, C. A., 1963/4, *Mol. Phys.*, **7**, 223.
- [7] CHANTRY, G. W., HORSFIELD, A., MORTON, J. R., ROWLANDS, J. R., and WHIFFEN, D. H., 1962, *Mol. Phys.*, **5**, 233.
- [8] COLE, T., 1961, *J. chem. Phys.*, **35**, 1169.
- [9] WALSH, A. D., 1953, *J. chem. Soc.*, p. 2266.
- [10] CLARK, H. C., HORSFIELD, A., and SYMONS, M. C. R., 1961, *J. chem. Soc.*, p. 7.
- [11] McLACHLAN, A. D., SYMONS, M. C. R., and TOWNSEND, M. G., 1959, *J. chem. Soc.*, p. 952.
- [12] ATKINS, P. W., BRIVATI, J. A., KEEN, N., SYMONS, M. C. R., and TREVALION, P. A., 1962, *J. chem. Soc.*, p. 4785.
- [13] EAGER, R. L., and MAHADEVAPPA, D. S., 1963, *Canad. J. Chem.*, **41**, 2106.
- [14] COLE, T., 1960, *Proc. nat. Acad. Sci., Wash.*, **46**, 506.
- [15] BENNETT, J. E., and INGRAM, D. J. E., 1956, *Phil. Mag.*, **1**, 109.
- [16] MORTON, J. R., ROWLANDS, J. R., and WHIFFEN, D. H., 1961, Report BP. 13. Atomic properties for interpreting e.s.r. data. National Physical Laboratory.
- [17] PAULING, L., 1939, *Nature of the Chemical Bond* (Cornell University Press).

Effect of intramolecular Van der Waals forces on N.M.R. spectra

by V. M. S. GIL and W. A. GIBBONS

University of Sheffield, Chemistry Department

(Received 4 March 1964)

Although the effect of intermolecular Van der Waals forces on N.M.R. chemical shifts has been widely investigated [1-6] less attention has been paid possible intramolecular contributions. Reid [7] attributed the low-field shift of the 4 and 5 protons of phenanthrene to this effect whilst Schaefer *et al.* [8] found by a rough calculation that a proton intramolecular dispersion shift may amount to -1.5 p.p.m.

During a comparative study of steric effects in the corresponding derivatives of benzene, mesitylene and 1,3,5-tri-*t*-butylbenzene we found anomalous low-field shifts of the protons of the substituent group and of the ortho-alkyl groups, in the case of the tri-*t*-butylbenzene derivatives. Models of these compounds show that the substituent and the ortho groups interfere strongly with each other.

Substituent X	X-mesitylene			1-X-2,4,6-TTBB		
	X	<i>o</i>	<i>p</i>	X	<i>o</i>	<i>p</i>
CH ₃	+0.18	+0.02	+0.02	-0.27	-0.15	+0.01
NH ₂	+0.17	+0.22	+0.14	-0.49	-0.13	+0.05
OH	+0.44	+0.14	+0.14	-0.32	-0.10	+0.04

Chemical shifts (in p.p.m.) of the substituent protons relative to the corresponding benzene derivative and of the *o*- and *p*-alkyl groups relative to the parent hydrocarbons. Solutions 1 per cent in CCl₄. Internal standard : TMS. Negative sign indicates low-field shifts.

All the three substituents in the table are electron donating groups and so are the alkyl groups. Let us then consider the shift of the X protons in the tri-alkylbenzenes relative to the corresponding benzene derivative. Since the substituent X is attached to a ring having other electron releasing groups, the electron donating effect of X is expected to be smaller than in the benzene derivative. On the other hand, the steric effect due to the bulky ortho groups is also likely to reduce the electronic interaction of the planar groups with the ring. Both these effects mean an increase of the electron density on the substituent and give rise accordingly to a shift to high field. For the planar substituents this high-field shift is further enhanced by the twisting from the plane of the ring because the low field-shift due to the ring current effect is maximum for protons in the plane of the ring (puckering would similarly cause high-field shifts, but this seems to be absent when one considers the ring proton chemical shifts).

† On leave from the University of Coimbra, Portugal.

All these considerations apply to both types of compounds. On this basis, the results for the X-mesitylenes are not surprising but the X proton shifts for the tri-*t*-butylbenzene derivatives are in the opposite direction. We attribute this displacement of the X signal to low-field to Van der Waals interactions involving the substituent X and the *o-t*-butyl groups. Such interactions cause a distortion of the electron cloud around the protons, which is usually thought to be an expansion leading consequently to a reduction in shielding; on the other hand, the time dependent character of this distortion which arises from rotations or oscillations of the groups attached to the ring leads again to a negative shift [2, 5, 8].

The shifts observed for the methyl protons in the X-mesitylenes are consistent with a residual interaction of X with the ring. The same seems to occur in the tri-*t*-butylbenzene derivatives when one considers the para alkyl shifts. But again the ortho group shifts have the opposite sign. Since magnetic anisotropy effects are usually considered to be small for the present substituents and reaction field effects are not likely to be important for 1 per cent mole solutions in CCl₄ (in fact there is practically no shift of the *t*-butyl signals on passing from CCl₄ to acetone as solvent), the low-field shift displayed by the *o-t*-butyl signals is also likely to be due to Van der Waals forces.

The results for the halogen, nitro and carbonyl derivatives of mesitylene and 1,3,5-tri-*t*-butylbenzene plus a comparative study of the ring proton shifts will be published soon.

V. M. S. G. thanks the Comissão Coordenadora da Investigação para a NATO (Portugal) for the award of a postgraduate scholarship. W. A. G. thanks Professor G. Porter and the British Petroleum Company for the award of a fellowship.

REFERENCES

- [1] STEPHEN, M. J., 1958, *Mol. Phys.*, **1**, 223.
- [2] BUCKINGHAM, A. D., SCHAEFER, T., and SCHNEIDER, W. G., 1960, *J. chem. Phys.*, **32**, 1227.
- [3] BOTHNER-BY, A. A., 1960, *J. mol. Spectrosc.*, **5**, 52.
- [4] HOWARD, B. B., LINDER, B., and EMERSON, M. T., 1962, *J. chem. Phys.*, **36**, 485.
- [5] RAYNES, W. T., BUCKINGHAM, A. D., and BERNSTEIN, H. J., 1962, *J. chem. Phys.*, **36**, 3481.
- [6] LUMBROSO, N., WU, T. K., and DAILEY, B. P., 1963, *J. phys. Chem.*, **67**, 2469.
- [7] REID, C., 1957, *J. mol. Spectrosc.*, **1**, 18.
- [8] SCHAEFER, T., REYNOLDS, W. F., and YONEMOTO, T., 1963, *Canad. J. Chem.*, **41**, 2969.

Low-energy states of the CH₂ radical

by R. N. DIXON

Department of Chemistry, Sheffield University

(Received 6 December 1963)

This paper describes theoretical calculations of the energy of low-lying electronic states of CH₂ as functions of HCH angle. The method uses Hurley's modification of Moffitt's method of Atoms in Molecules to allow for intra-atomic electron correlation. The results are in agreement with experiment, giving a linear $^3\Sigma_g^-$ ground state. The first excited state is a bent 1A_1 state which lies no more than 0.6 eV above the ground state.

1. INTRODUCTION

The geometrical and electronic structure of the CH₂ radical is of interest both in spectroscopy and in free radical reaction kinetics. Herzberg [1] has recently observed two absorption spectra for the CH₂ radical. One of these near 1400 Å is assigned to a $^3\Sigma_u^- \leftarrow ^3\Sigma_g^-$ Rydberg transition from a lower state that is most probably linear, although a slight deviation from linearity cannot be ruled out. The second is a $^1B_1 \leftarrow ^1A_1$ transition in the red involving a lower state that has a valence angle of 103°. A further weak system near 3400 Å is probably a second singlet system. The variation with experimental conditions of the relative intensity of the triplet and singlet systems suggest that the $^3\Sigma_g^-$ state is the ground state. This deduction is supported by evidence from the reactions of CH₂ [2].

Theoretical calculations of the energies of the low-lying states of CH₂ have been made by Gallup [3], Foster and Boys [4] and Padgett and Krauss [5]. All these calculations predict a low-lying $^3\Sigma_g^- (^3B_1)$ state, but with an equilibrium angle of 160°, 130° and 130° respectively, and a near 90° 1A_1 state. The first two calculations make the 3B_1 state the ground state, and the third makes the 1A_1 state the ground state. All these calculations are therefore at variance with experiment.

In references [4] and [5] some allowance for electron correlation—apart from that due to anti-symmetrizing the wavefunction—is introduced by the method of configuration interaction. However, a very large set of configurational functions must be used even in atomic calculations to give good agreement with the experimental energy. Jordan and Longuet-Higgins have circumvented this problem [6] in a semi-empirical calculation in which the values of all the relevant energy contributions are deduced from experimental quantities involving C, CH, CH₃ and CH₄.

In this paper two theoretical calculations of the energies of low lying states of CH₂ are described. The first of these is an *ab initio* calculation using the valence-bond (v.b.) method. The second uses the intra-atomic correlation correction (i.c.c.) modification of Moffitt's [7] method of atoms in molecules, introduced

by Hurley and used by him with considerable success in the description of the electronic structure of the first row diatomic hydrides [8].

2. BASIC FUNCTIONS

The basic atomic orbitals are taken as orthonormal Slater functions centred on the carbon and hydrogen nuclei :

$$\begin{aligned} k &= \left(\frac{\zeta_1^3}{\pi}\right)^{1/2} \exp(-\zeta_1 r_c), \\ s &= N\{(\zeta_2^5/3\pi)^{1/2} r \exp(-\zeta_2 r_c) - \alpha k\}, \\ \begin{Bmatrix} x \\ y \\ z \end{Bmatrix} &= \begin{Bmatrix} x \\ y \\ z \end{Bmatrix} (\zeta_2^5/\pi)^{1/2} \exp(-\zeta_2 r_c), \\ h_1 &= \pi^{-1/2} \exp(-r_{h_1}), \\ h_2 &= \pi^{-1/2} \exp(-r_{h_2}). \end{aligned}$$

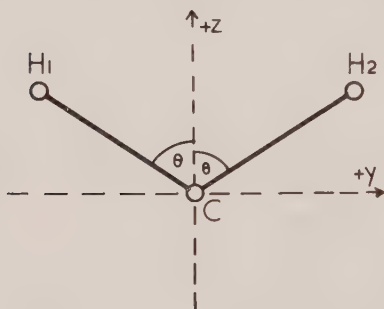


Figure 1. The coordinate system.

The orbital exponents have the Slater values, $\zeta_1=5.7$, $\zeta_2=1.625$, and the coordinate system is illustrated in figure 1. All the basic atomic integrals involving these orbitals have been evaluated by Padgett and Krauss [5] for the internuclear distance of the CH radical, $R=1.124 \text{ \AA}=2.124 \text{ A.U.}$, using exact methods for the two-centre integrals, and Mulliken's approximation [9] for the three-centre integrals. Their self-consistent field molecular orbital (s.c.f.m.o.) calculations are based on these integrals. The v.b. calculations were simplified by combining h_1 and h_2 to give two new orbitals which transform according to irreducible representations of the point group of linear or bent CH_2 :

$$\begin{aligned} p &= 2^{-1/2}(h_1 + h_2) ; \quad \sigma_g(D_{\infty h}) \text{ or } a_1(C_{2v}); \\ q &= 2^{-1/2}(h_2 - h_1) ; \quad \sigma_u(D_{\infty h}) \text{ or } b_2(C_{2v}). \end{aligned}$$

A basis of valence bond functions was chosen by expanding the s.c.f.m.o. wavefunctions of Padgett and Krauss in the terms of the orbitals k, s, x, y, z, p and q and discarding those functions which did not include two electrons in the k orbital. This gave nine functions for each of the three lowest states of linear CH_2 , 18 each for the two $^1\text{A}_1$ states and 24 each for the $^3\text{B}_1$ and $^1\text{B}_1$ states of bent CH_2 .

3. LINEAR CH_6

3.1. Valence bond-calculation

The three lowest states of linear CH_2 arise from the M.O. configuration :

$$(1\sigma_g)^2(2\sigma_g)^2(1\sigma_u)^2(1\pi_u)^2 ; \quad ^3\Sigma_g^-, ^1\Delta_g, ^1\Sigma_g^+,$$

giving v.b. wavefunctions :

$\psi_a = k\bar{k} s\bar{s} y\bar{y} \pi^2 $	Coefficient = 0.198
$\psi_b = k\bar{k} s\bar{p} y\bar{y} \pi^2 $	0.144
$\psi_c = k\bar{k} s\bar{s} y\bar{q} \pi^2 $	0.205
$\psi_d = k\bar{k} s\bar{p} y\bar{q} \pi^2 $	0.149
$\psi_e = k\bar{k} p\bar{p} y\bar{y} \pi^2 $	0.052
$\psi_f = k\bar{k} s\bar{s} q\bar{q} \pi^2 $	0.106
$\psi_g = k\bar{k} p\bar{p} y\bar{q} \pi^2 $	0.054
$\psi_h = k\bar{k} s\bar{p} q\bar{q} \pi^2 $	0.078
$\psi = k\bar{k} p\bar{p} q\bar{q} \pi^2 $	0.028

The symbol $|\dots|$ denotes a Slater determinant, or a combination of determinants, normalized for infinite nuclear separation ; \widehat{ab} denotes the v.b. pair function :

$$\widehat{ab} = 2^{-1/2}(|ab| - |\bar{a}\bar{b}|)$$

and for each electronic state π^2 takes one of the forms :

$$\begin{aligned} \psi_{a-i} |\pi^2| &= |zx| ; & {}^3\Sigma_g^-({}^3\text{B}_1), \\ \psi_{a'-i'} |\pi^2| &= 2^{-1/2}(|z\bar{x}| - |\bar{z}x|) ; & {}^1\Delta_g \quad ({}^1\text{B}_1), \\ \psi_{a''-i''} |\pi^2| &= 2^{-1/2}(|z\bar{z}| - |x\bar{x}|) ; & ({}^1\text{A}_1), \\ \psi_{a'''-i'''} |\pi^2| &= 2^{-1/2}(|z\bar{z}| + |x\bar{x}|) ; & {}^1\Sigma_g^+({}^1\text{A}_1). \end{aligned}$$

The electronic wavefunction Ω is expressed in the form $\Omega = \Psi\Gamma$, where Ψ is the row vector $(\psi_a \dots \psi_i)$ and Γ is the column vector of coefficients. The evaluation of the matrices of the Hamiltonian and other operators is greatly simplified by effecting a transformation to a set of Schmidt orthonormal orbitals in which p and q are replaced by two orbitals f and g . For the general case, with $\angle\text{HCH} = 2\theta$, these are :

$$\begin{aligned} f &= \frac{\{h_1 + h_2 - 2\langle h|s\rangle s - 2\langle h|k\rangle k - 2\langle h|\sigma\rangle \sin\theta z\}}{2\{1 - 2\langle h|s\rangle^2 - 2\langle h|k\rangle^2 - 2\langle h|\sigma\rangle^2 \sin^2\theta + \langle h_1|h_2\rangle\}^{1/2}} ; (a_1) \\ g &= \frac{\{h_2 - h_1 - 2\langle h|\sigma\rangle \cos\theta y\}}{2\{1 - 2\langle h|\sigma\rangle^2 \cos^2\theta - \langle h_1|h_2\rangle\}^{1/2}} ; (b_2) \end{aligned}$$

where $\langle h|\sigma\rangle$ is the overlap integral between a hydrogen orbital and a carbon 2p orbital directed at the hydrogen atom. The orthonormal set of functions Θ obtained by replacing p by f and q by g in the Ψ functions span the same function space as the Ψ functions, and are related to them by a matrix transformation (Hurley [7]):

$$\Psi = \Theta S, \quad S_{\alpha\beta} = \int \theta_\alpha \psi_\beta d\tau.$$

The overlap integrals $S_{\alpha\beta}$ were evaluated in terms of the atomic overlap integrals using the method of Löwdin [10]. The overlap matrix S and its inverse $T = S^{-1}$ are the key to Hurley's i.c.c. method.

The coefficients Γ in the Ψ and Θ bases are related by :

$$\Gamma(\psi) = T\Gamma(\theta) ; \quad \Gamma(\theta) = S\Gamma(\psi)$$

and the matrices representing an operator X in the two bases are related by :

$$X(\psi) = S^\dagger X(\theta) S, \quad X(\theta) = T^\dagger X(\psi) T.$$

The energy matrix $H(\theta)$ was evaluated by standard techniques after transforming the integrals over the orbitals k, s, x, y, z, h_1 and h_2 into those over $k, s,$

x, y, z, f and g . The v.b. matrices for the ${}^3\Sigma_g^-$, ${}^1\Delta_g$ and ${}^1\Sigma_g^+$ states differ only by a constant on the diagonal, and one matrix therefore suffices for all three states. The solutions to the secular equation;

$$H(\theta)\Gamma(\theta) = E\Gamma(\theta)$$

were evaluated using the Ferranti Mercury computer at Sheffield University, both for the complete set $\theta_a - \theta_i$, and for various selections of the basis functions. The selections were chosen in such a way that the reduced basis sets Θ still span the same function space as the corresponding Ψ sets.

3.2. The intra-atomic correlation correction

Hurley [8] has shown that the intra-atomic correlation correction may be introduced into the matrix energy by replacing H by :

$$H'(\psi) = H(\psi) + \frac{1}{2}\{S^\dagger S(W - \tilde{W}) + (W - \tilde{W})S^\dagger S\}$$

or

$$H'(\theta) = H(\theta) + \frac{1}{2}\{S(W - \tilde{W})T + T^\dagger(W - \tilde{W})S^\dagger\}.$$

State	Basis function	Dissociation products		
		Carbon	Hydrogen	$W - \tilde{W}$ (A.U.)
${}^3\Sigma_g^-$	ψ_a	$C^=(s^2p^4, {}^3P)$	$2H^+$	-0.653
	ψ_b	$C^-(sp^4, \frac{2}{3}{}^4P + \frac{1}{3}{}^2P)$	$H + H^+$	-0.439
	ψ_c	$C^-(s^2p^3, \frac{2}{3}{}^4S^0 + \frac{1}{3}{}^2D^0)$	$H + H^+$	-0.347
	ψ_d	$C(sp^3, \frac{5}{12}{}^5S^0 + \frac{1}{4}{}^3S^0 + \frac{1}{4}{}^3D^0 + \frac{1}{12}{}^1D^0)$	$\frac{3}{2}H + \frac{1}{4}H^+ + \frac{1}{4}H^-$	-0.269
	ψ_e	$C(p^4, {}^3P)$	$H + \frac{1}{2}H^+ + \frac{1}{2}H^-$	-0.386
	ψ_f	$C(s^2p^2, {}^3P)$	$H + \frac{1}{2}H^+ + \frac{1}{2}H^-$	-0.260
	ψ_g	$C^+(p^3, \frac{2}{3}{}^4S^0 + \frac{1}{3}{}^2D^0)$	$H + H^-$	-0.235
	ψ_h	$C^+(sp^2, \frac{2}{3}{}^4P + \frac{1}{3}{}^2P)$	$H + H^-$	-0.214
	ψ_i	$C^{++}(p^2, {}^3P)$	$2H^-$	-0.219
${}^1\Delta_g$	ψ_a	$C^=(s^2p^4, {}^1D)$	$2H^+$	-0.679
	ψ_b	$C^-(sp^4, {}^2D)$	$H + H^+$	-0.482
	ψ_c	$C^-(s^2p^3, {}^2D^0)$	$H + H^+$	-0.373
	ψ_d	$C(sp^3, \frac{3}{4}{}^3D^0 + \frac{1}{4}{}^1D^0)$	$\frac{3}{2}H + \frac{1}{4}H^+ + \frac{1}{4}H^-$	-0.301
	ψ_e	$C(p^4, {}^1D)$	$H + \frac{1}{2}H^+ + \frac{1}{2}H^-$	-0.452
	ψ_f	$C(s^2p^2, {}^1D)$	$H + \frac{1}{2}H^+ + \frac{1}{2}H^-$	-0.281
	ψ_g	$C^+(p^3, {}^2D^0)$	$H + H^-$	-0.282
	ψ_h	$C^+(sp^2, {}^2D)$	$H + H^-$	-0.245
	ψ_i	$C^{++}(p^2, {}^1D)$	$2H^-$	-0.261
${}^1\Sigma_g^+$	ψ_a	$C^=(s^2p^4, \frac{1}{3}{}^1D + \frac{2}{3}{}^1S)$	$2H^+$	-0.718
	ψ_b	$C^-(sp^4, \frac{1}{3}{}^3D + \frac{2}{3}{}^3S)$	$H + H^+$	-0.507
	ψ_c	$C^-(s^2p^3, {}^2P^0)$	$H + H^+$	-0.409
	ψ_d	$C(sp^3, \frac{3}{4}{}^3P^0 + \frac{1}{4}{}^1P^0)$	$\frac{3}{2}H + \frac{1}{4}H^+ + \frac{1}{4}H^-$	-0.303
	ψ_e	$C(p^4, \frac{1}{3}{}^1D + \frac{2}{3}{}^1S)$	$H + \frac{1}{2}H^+ + \frac{1}{2}H^-$	-0.453
	ψ_f	$C(s^2p^2, \frac{1}{3}{}^1D + \frac{2}{3}{}^1S)$	$H + \frac{1}{2}H^+ + \frac{1}{2}H^-$	-0.313
	ψ_g	$C^+(p^3, {}^2P^0)$	$H + H^-$	-0.272
	ψ_h	$C^+(sp^2, \frac{1}{3}{}^3D + \frac{2}{3}{}^3S)$	$H + H^-$	-0.252
	ψ_i	$C^{++}(p^2, \frac{1}{3}{}^1D + \frac{2}{3}{}^1S)$	$2H^-$	-0.230

Table 1. Basis functions for linear CH_2 .

$(W - \bar{W})$ is a diagonal matrix with elements which give the difference between the empirical energies (W) of the appropriate dissociation products and the corresponding values (\bar{W}) calculated using one-configuration Slater-type wavefunctions with optimum values of ζ_1 and ζ_2 for each stationary state. Most of the required values of $W_i - \bar{W}_i$ are given by Hurley [8]; the others are discussed in the appendix. The dissociation products and values of $(W_i - \bar{W}_i)$ are listed in table 1.

Table 2 compares the calculated energies of atomization for various selections of the basis functions. In the v.b. and s.c.f.m.o. calculations the atomization energies are referred to the calculated ground state energies of the products $\text{C}(s^2p^2, {}^3\text{P}) + 2\text{H}$, (-38.622 A.U.), and in the i.c.c. calculations to the corresponding empirical energy (-38.855 A.U.). Neither the v.b. nor s.c.f.m.o. calculations give more than a small fraction of the observed atomization energy (≥ 7.5 eV, Herzberg [11]). Introduction of the i.c.c. method increases the binding energy to about 75 per cent of the experimental value.

		Basis			
		$a-i$	$a-f$	$a-d$	$abcdfh$
${}^3\Sigma_g^-$	Valence bond	1.12	0.94	0.82	1.00
	i.c.c.	5.70	5.41	5.23	5.43
	s.c.f.m.o.†	0.0	—	—	—
${}^1\Delta_g$	Valence bond	-0.75	-0.92	-1.04	-0.86
	i.c.c.	4.70	4.43	4.22	4.39
	s.c.f.m.o.†	-1.8	—	—	—
${}^1\Sigma_g^+$	Valence bond	-2.61	-2.79	-2.88	-2.73
	i.c.c.	3.49	3.21	3.01	3.28
	s.c.f.m.o.†	-3.7	—	—	—

† Padgett and Krauss (5).

Table 2. Calculated energies of atomization for linear CH_2 (electron volts).

4. BENT CH_2

The total number of v.b. functions arising from the expansion of the self-consistent field molecular orbital wavefunctions for bent CH_2 is very large, and a criterion was sought upon which a reduced basis could be chosen. Table 2 shows that for linear CH_2 a reduction of the basis from nine to the six which have the largest coefficients in the expanded s.c.f.m.o. wavefunction leads to an increase of about 0.12 eV in the v.b. calculations and about 0.25 eV in the i.c.c. calculations. It was assumed that for all values of the HCH angle the use of a reduced basis of v.b. functions chosen in this same manner would lead to a similar accuracy in representation of the molecular energy. For each state of bent CH_2 the basis was therefore chosen to include the predominant six v.b. functions in the expansion of the 90° s.c.f.m.o. wavefunction, plus the predominant six functions for the corresponding 180° wavefunction, some of which were common to both angles.

4.1. B_1 states

The B_1 states of bent CH_2 arise from the molecular orbital configuration :

$$(1a_1)^2(2a_1)^2(1b_2)^2(3a_1)(1b_1) ; \quad {}^3B_1, {}^1B_1.$$

The predominant v.b. functions in the expansion for 90° are $\psi_k, \psi_c, \psi_j, \psi_a, \psi_l, \psi_f$ in order of decreasing coefficient. The basis was therefore chosen to include nine functions in all, of which three (ψ_j, ψ_k , and ψ_l) have Π_u symmetry for 180° . The additional functions for bent CH_2 are given in table 3.

3B_1 $\psi_a, \psi_b, \psi_c, \psi_d, \psi_f, \psi_h$, and :			$W - \tilde{W}$ (A.U.)
$\psi_j = k\bar{k} s\bar{s} y\bar{y} px $	$\text{C}^-(s^2p^3, \frac{1}{2}^2D^0 + \frac{1}{2}^2P^0) + \text{H} + \text{H}^+$		-0.391
$\psi_k = k\bar{k} s\bar{s} y\bar{q} px $	$\text{C}(s^2p^2, \frac{3}{4}^3P + \frac{1}{4}^1D) + \frac{3}{2}\text{H} + \frac{1}{4}\text{H}^+ + \frac{1}{4}\text{H}^-$		-0.252
$\psi_l = k\bar{k} s\bar{s} q\bar{q} px $	$\text{C}^+(s^2p, {}^2P^0) + \text{H} + \text{H}^-$		-0.244
1B_1 $\psi_{a'}, \psi_{b'}, \psi_{c'}, \psi_{d'}, \psi_{f'}, \psi_{h'}$ and :			
$\psi_{j'} = k\bar{k} s\bar{s} y\bar{y} p\bar{x} $	Dissociation products as for 3B_1		
$\psi_{k'} = k\bar{k} s\bar{s} y\bar{q} p\bar{x} $			
$\psi_{l'} = k\bar{k} s\bar{s} q\bar{q} p\bar{x} $			

Table 3. Basis functions for B_1 states of CH_2 .

4.2. 1A_1 states

For linear CH_2 the 1A_1 components of the ${}^1\Delta_g^+$ and ${}^1\Sigma_g^+$ functions include the terms $2^{-1/2}\{|z\bar{z}| - |x\bar{x}|\}$ and $2^{-1/2}\{|z\bar{z}| + |x\bar{x}|\}$ respectively. Much of the lowering in energy of the lowest 1A_1 state on bending arises from the removal of the degeneracy of the z and x orbitals. The basis set for bent 1A_1 states was therefore chosen from the expansion of both the lowest and second lowest 1A_1 s.c.f.m.o. wavefunctions :

$$(1a_1)^2(2a_1)^2(1b_2)^2(3a_1)^2 ; \quad {}^1A_1,$$

$$(1a_1)^2(2a_1)^2(1b_2)^2(1b_1)^2 ; \quad {}^1A_1,$$

giving 18 functions in all, nine from each state. The functions $\psi_{a''-h''}$ and $\psi_{a'''-h'''}$ are retained in this form, rather than in the simpler forms which include either $|z\bar{z}|$ or $|x\bar{x}|$, since the i.c.c. method requires that the basis functions be non-interacting for infinite internuclear separation. The functions additional to those for 180° are given in table 4.

$\psi_{a'}, \psi_{b'}, \psi_{c'}, \psi_{d'}, \psi_{f'}, \psi_{h'}, \psi_{a''}, \psi_{b''}, \psi_{c''}, \psi_{d''}, \psi_{f''}, \psi_{h''}$ and :			$W - \tilde{W}$ (A.U.)
$\psi_m = k\bar{k} s\bar{s} y\bar{y} \widehat{z}\widehat{p} $	$\text{C}^-(s^2p^3, \frac{1}{2}^2D^0 + \frac{1}{2}^2P^0) + \text{H} + \text{H}^+$		-0.391
$\psi_n = k\bar{k} s\bar{s} y\bar{q} \widehat{z}\widehat{p} $	$\text{C}(s^2p^2, \frac{3}{4}^3P + \frac{1}{4}^1D) + \frac{3}{2}\text{H} + \frac{1}{4}\text{H}^+ + \frac{1}{4}\text{H}^-$		-0.252
$\psi_o = k\bar{k} s\bar{s} q\bar{q} \widehat{z}\widehat{p} $	$\text{C}^+(s^2p, {}^2P^0) + \text{H} + \text{H}^-$		-0.244
$\psi_p = k\bar{k} s\bar{s} y\bar{y} x\bar{x} $	$\text{C}^-(sp^3, {}^1P^0) + 2\text{H}^+$		-0.780
$\psi_q = k\bar{k} s\bar{s} y\bar{q} x\bar{x} $	$\text{C}^-(sp^4, \frac{3}{4}^3P + \frac{1}{4}^2D) + \text{H} + \text{H}^+$		-0.509
$\psi_r = k\bar{k} s\bar{s} q\bar{q} x\bar{x} $	$\text{C}(sp^3, \frac{1}{2}^1D^0 + \frac{1}{2}^1P^0) + \text{H} + \frac{1}{2}\text{H}^+ + \frac{1}{2}\text{H}^-$		-0.363

Table 4. Basis functions for 1A_1 states of CH_2 .

5. Π_u STATES

Padgett and Krauss [5] found that the lowest excited states of CH₂ above those discussed in § 3 arise from the configuration :

$$(1\sigma_g)^2(2\sigma_g)^2(1\sigma_u)^2(1\pi_u)(3\sigma_g); \quad {}^1\Pi_u, {}^3\Pi_u$$

and have their minimum energy in the linear form. The states of bent CH₂ which correlate with these linear states are approximately described by higher solutions of the 1A_1 , 1B_1 and 3B_1 secular equations, confirming their linearity. More accurate calculations of the ${}^1\Pi_u$ and ${}^3\Pi_u$ energies for 180° were made using bases of six functions each, chosen from the expanded self-consistent field molecular orbital wavefunction (table 5).

${}^3\Pi_u \quad \psi_j, \psi_k, \psi_l \text{ and :}$			$W - \bar{W} \text{ (A.U.)}$
$\psi_s = k\bar{k} \ p\bar{p} \ y\bar{y} \ sx $	$C(sp^3, \frac{1}{2}{}^3D^0 + \frac{1}{2}{}^3P^0)$	$+H + \frac{1}{2}H^+ + \frac{1}{2}H^-$	-0.300
$\psi_t = k\bar{k} \ p\bar{p} \ y\bar{q} \ sx $	$C^+(sp^3, \frac{2}{3}{}^4P + \frac{1}{4}{}^3D + \frac{1}{12}{}^3P)$	$+H + H^-$	-0.207
$\psi_u = k\bar{k} \ p\bar{p} \ q\bar{q} \ sx $	$C^{++}(sp, {}^3P^0)$	$+2H^-$	-0.218
${}^1\Pi_u \quad \psi_{j'}, \psi_{k'}, \psi_{l'} \text{ and :}$			
$\psi_{s'} = k\bar{k} \ p\bar{p} \ y\bar{y} \ \widehat{sx} $	$C(sp^3, \frac{1}{2}{}^1D^0 + \frac{1}{2}{}^1P^0)$	$+H + \frac{1}{2}H^+ + \frac{1}{2}H^-$	-0.363
$\psi_{t'} = k\bar{k} \ p\bar{p} \ y\bar{q} \ \widehat{sx} $	$C^+(sp^3, \frac{3}{4}{}^3P + \frac{1}{4}{}^3D)$	$+H + H^-$	-0.266
$\psi_{u'} = k\bar{k} \ p\bar{p} \ q\bar{q} \ \widehat{sx} $	$C^{++}(sp, {}^1P^0)$	$+2H^-$	-0.273

Table 5. Basis functions for Π_u states of CH₂.

6. POPULATION ANALYSES

Two analyses of each wavefunction were carried out. Hurley [8] has shown that a rigorous definition of the relative weights of valence-bond structures may be given by occupation numbers ν_α defined as :

$$\nu_\alpha = \sum_\beta \Gamma_\alpha(\psi) M_{\alpha\beta} \Gamma_\beta(\psi);$$

$M = S^\dagger S$ is the overlap matrix of the ψ functions. The values of ν_α were more easily determined from the coefficients $\Gamma(\theta)$:

$$\nu_\alpha = \sum_\beta \Gamma_\alpha(\psi) S_{\beta\alpha} \Gamma_\beta(\theta) = \sum_{\beta\gamma} T_{\alpha\gamma} \Gamma_\gamma(\theta) S_{\beta\alpha} \Gamma_\beta(\theta).$$

Gross atomic populations (Mulliken [12]) $N(\rho)$ for each orbital (ρ) were then evaluated for each wavefunction using :

$$N(\rho) = \sum_\alpha n(\rho) \nu_\alpha,$$

where $n(\rho)$ is the number of electrons in the orbital ρ (or $\bar{\rho}$) in the v.b. function ψ_α . The sum of these gross atomic populations over the carbon orbitals, N_c , represents the total electron density on the carbon atom. This last analysis requires that if ψ_α is a sum of elementary Slater determinants, as is the case for many functions, then these determinants may only differ in the arrangement of electron spins and must contain the same atomic orbitals. The 1A_1 functions containing $|z\bar{z}| \pm |x\bar{x}|$ do not satisfy this condition. The coefficients Γ and the matrices S and T for the 1A_1 states were therefore transformed to correspond to π_u^2 in the form $|x\bar{x}| (\psi_a^{iv} - \bar{h}^{iv})$ or $|z\bar{z}| (\psi_a^v - \bar{h}^v)$.

7. NUMERICAL RESULTS

The calculated atomization energies for the various electronic states and angles of CH_2 are illustrated in figure 2. The corresponding electron densities, N_e , are shown in figure 3, in which comparison is made with values calculated from the one-configuration s.c.f.m.o. wavefunctions of Padgett and Krauss [5].

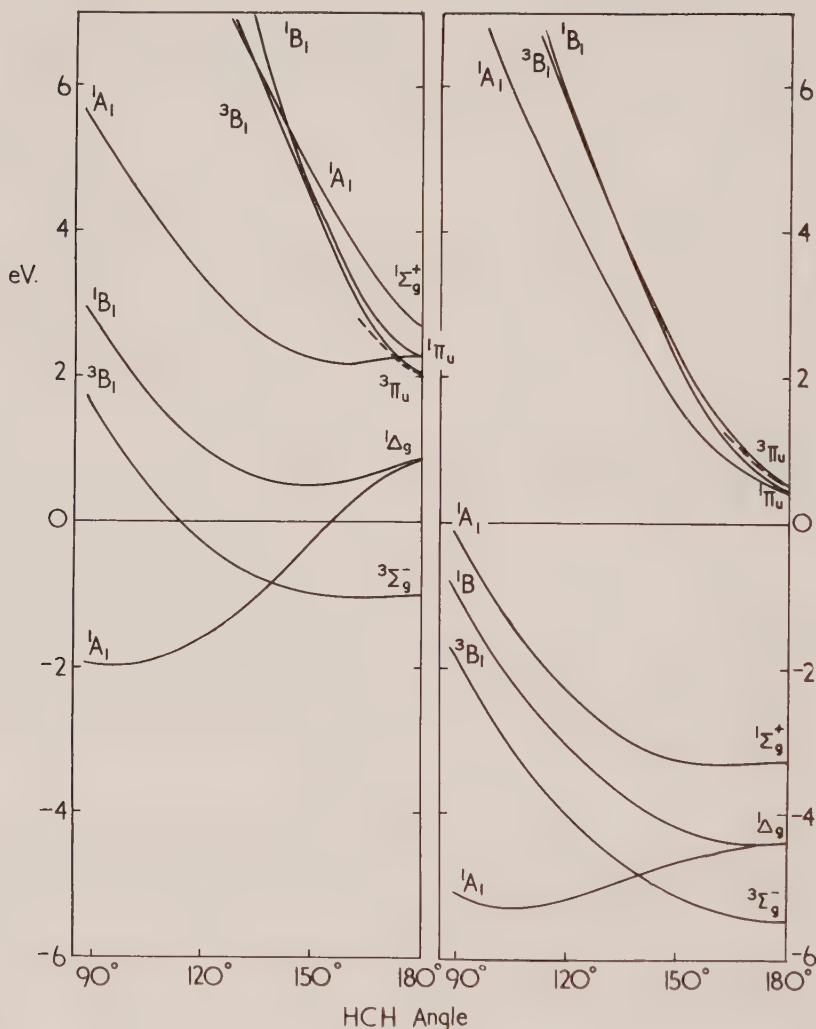


Figure 2. The calculated electronic energies of CH_2 with respect to atomization. (a) v.b. calculation; energy with reference to the calculated energy of $\text{C}(s^2p^2, {}^3\text{P}) + 2\text{H}$. (b) i.c.c. calculation; energy with reference to the observed energy of $\text{C} + 2\text{H}$.

The results of the v.b. calculations are very similar to those for the s.c.f.m.o. calculations: however, the v.b. energy of each state at 180° is significantly lower than the s.c.f.m.o. energy, but there is a smaller lowering of energy in the bent molecule. Thus the curve for the ${}^3\Sigma_g^-({}^3\text{B}_1)$ state shows a flat-bottomed minimum at 180° in the v.b. calculations, whereas the s.c.f.m.o. curve has a minimum at 140° . This difference may be associated with the greater flexibility

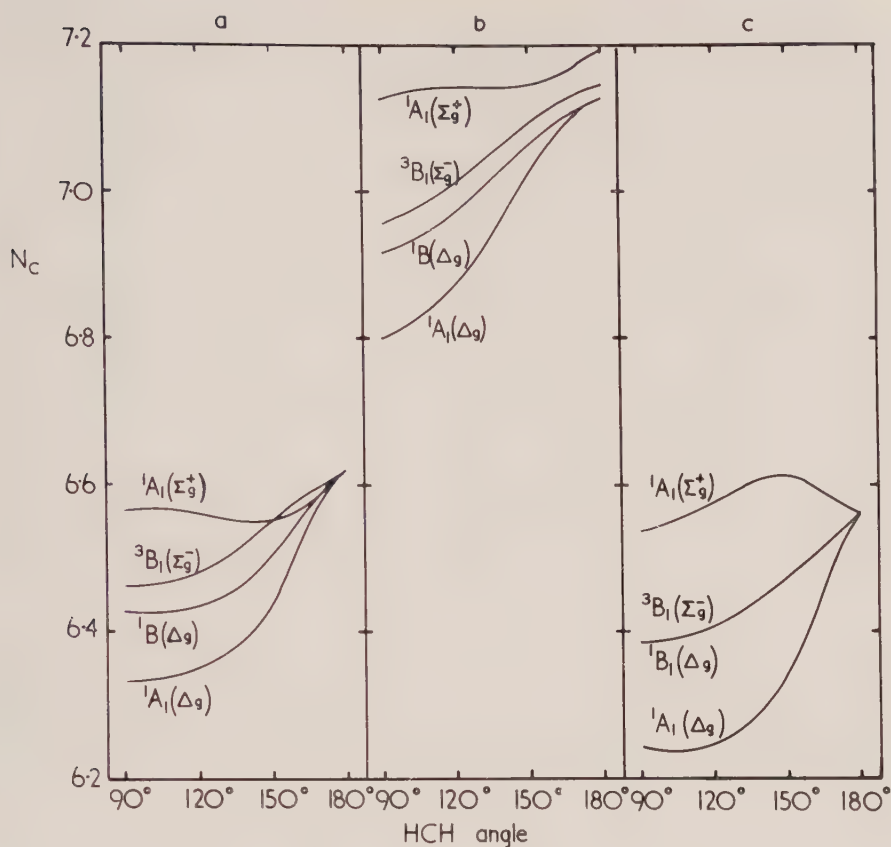


Figure 3. The calculated electron density on the carbon atom, N_c , for states of CH_2 (a) v.b. calculation; (b) i.c.c. calculation; (c) s.c.f.m.o. calculation (Padgett and Krauss [5]).

Transition	HCH angle	Wavefunction		
		s.c.f.m.o.	v.b.	i.c.c.
${}^3\Pi_u \leftarrow {}^3\Sigma_g^-$	180°	1.3×10^{-2}	1.3×10^{-2}	1.3×10^{-2}
${}^1B_1 \leftarrow {}^1A_1$	180°	0	0	0
	150°	1.9×10^{-3}	1.0×10^{-5}	4.4×10^{-5}
	120°	9.2×10^{-3}	8.0×10^{-5}	4.2×10^{-5}
	90°	1.7×10^{-2}	1.4×10^{-4}	1.9×10^{-5}
${}^1A_1 \leftarrow {}^1A_1$	180°	0	0	0
	150°	0	8.4×10^{-4}	1.7×10^{-3}
	120°	0	7.7×10^{-5}	1.2×10^{-3}
	90°	0	2.6×10^{-7}	6.8×10^{-4}

Table 6. f -values for the spin-allowed transitions of CH_2 .

State	W exp. (A.U.)	\tilde{W} calc. (A.U.)	$W - \tilde{W}$ (A.U.)
$C^{++}(p^2, {}^3P)$	-35.921	-35.812	-0.109
1D	-35.882	-35.731	-0.151
1S	-35.715	-35.610	-0.105
$C^{++}(sp, {}^3P^0)$	-36.308	-36.200	-0.108
${}^1P^0$	-36.080	-35.917	-0.163
$C^+(p^3, {}^4S^0)$	-36.796	-36.640	-0.156
${}^2D^0$	-36.757	-36.530	-0.227
${}^2P^0$	-36.674	-36.457	-0.217
$C(p^4, {}^3P)$	—	—	-0.359†
1D	—	—	-0.425†
1S	—	—	-0.426†
$C=(s^2p^4, {}^3P)$	—	—	-0.653†
1D	—	—	-0.679†
1S	—	—	-0.737†
$C=(sp^5, {}^1P^0)$	—	—	-0.780†

† See text.

Table 7. Energies of atomic stationary states.

of the v.b. wavefunctions compared with the s.c.f.m.o. wavefunctions. If the slight delocalization of the $1\sigma_g$ or $1a_1$ orbital is ignored the s.c.f.m.o. wavefunctions for the three lowest states at 180° have only two adjustable parameters, and the bent states have either three or five: the v.b. wavefunctions have six adjustable coefficients at 180° and either eight or seventeen when bent.

The i.c.c. method leads to a very considerable further lowering in energy of the $(\pi_u)^2$ states, but a much smaller lowering of the Π_u states. The greater electronegativity of the linear sp hybridized C atom compared with the unhybridized C atom is evident in the greater lowering in energy for linear CH_2 than for bent CH_2 . The i.c.c. results of figure 2(b) are very similar to the semiempirical results of Jordan and Longuet-Higgins [6].

In the i.c.c. theory the energy differences between the ${}^3\Sigma_g^-$, ${}^1\Delta_g$ and ${}^1\Sigma_g^+$ states for 180° are about 60 per cent of those for the v.b. and s.c.f.m.o. calculations. In the latter two methods this difference is given by the $\pi\pi'$ exchange integral. Orbital calculations also overestimate the separation of the three lowest states (s^2p^2 , 3P , 1D , 1S) of the C atom by about the same factor. These differences between the i.c.c. energies are not very sensitive to changes in the values of the basic integrals or in the estimated correlation error for $C=$ states, and should therefore be accurate to about 10 per cent. The i.c.c. calculations also give a minimum in the energy curve for the lowest 1A_1 state at an HCH angle of 105° , compared with the experimental value of 103° [1]. Thus it would seem that the shape of this curve cannot be seriously in error. The calculated minimum energy of the 1A_1 state is 0.11 eV above that for the linear ${}^3\Sigma_g^-$ state. This energy difference is for a constant bond length of 1.12_1 \AA . Herzberg has shown that the bond length is 1.03_6 \AA in the ${}^3\Sigma_g^-$ state and 1.12 \AA in the bent 1A_1 state. The known force constants of CH bonds lead to an estimate of $\sim 0.29 \text{ eV}$ for the lowering in energy of the ${}^3\Sigma_g^-$ state upon contraction of the bonds from 1.12 \AA to 1.04 \AA .

There are two main sources of error in the i.c.c. calculations : the approximation of the values of the three-centre integrals and the estimation of the correlation error for $\text{C}^=$ states. Some exact values of three-centre integrals have been evaluated for the linear molecule, showing that in some instances the approximation was very poor [13]. However, it is probable that the errors involved do not vary rapidly with angle. The correlation errors for $\text{C}^=$ states are discussed in the appendix, and it is concluded that in the i.c.c. calculations values have been used that are too great, possibly by as much as 0.1 A.U. This conclusion is supported by examination of the gross atomic populations. Simple v.b. theory would describe the $^1\text{A}_1$ state at 90° as having two pure p bonds, and the ground state of the CH radical as having one pure p bond. For CH_2 , $^1\text{A}_1$ 90° , the i.c.c. gross populations show a net excess charge of $-0.80e$ on the carbon atom, compared with $-0.33e$ in the v.b. calculations and $-0.39e$ in the s.c.f.m.o. calculations. The corresponding figures for CH, $X(^2\Pi)$ are i.c.c. $-0.16e$, v.b. $-0.01e$, s.c.f.m.o. $-0.01e$ [8]. The shift of $-0.47e$ in CH_2 in passing from the v.b. to the i.c.c. method is thus considerably greater than twice that for CH ($-0.15e$), indicating that in CH_2 the i.c.c. method places too great an emphasis on $\text{C}^=$ structures. To a first approximation an error ΔE in the correlation error for all $\text{C}^=$ states is reflected in an error of ($\nu=\Delta E$) in the molecular energy. For $\Delta E=0.1$ A.U. the values of $\nu^=$ would increase the energy of the $^3\Sigma_g^-$ state at 180° by 0.35 eV more than the $^1\text{A}_1$ state at 105° . We therefore conclude that $0.6 \text{ eV} \geq E(^1\text{A}_1, 105^\circ) - E(^3\Sigma_g^-, 180^\circ) \geq 0$.

The calculations are therefore in agreement with the experimental identity of the ground state of CH_2 as the $^3\Sigma_g^-$ state, and the estimate of the excitation energy of the $^1\text{A}_1$ state is very similar to the value of 0.45 eV calculated by Jordan and Longuet-Higgins [6].

8. TRANSITION INTENSITIES

The oscillator strengths of the lower spin-allowed transitions for absorption from the lowest $^1\text{A}_1$ and $^3\Sigma_g^-$ states were obtained from the formulae [14] :

$$f = \frac{2\Delta E}{3} |\mathbf{R}|^2,$$

$$\mathbf{R}_{kl} = \int \Omega_k \left(\sum_i \mathbf{r}_i \right) \Omega_l d\tau = \Gamma_k^\dagger(\theta) \mathbf{R}(\theta) \Gamma_l(\theta),$$

where the transition energy ΔE and the vector coordinates \mathbf{r}_i are in atomic units. For degenerate states \mathbf{R} is evaluated over all possible final component states that can combine with one initial component state. Numerical values are given in table 6. The various estimates of the intensity of the $^3\Pi_u \leftarrow ^3\Sigma_g^-$ transition are in good agreement with one another. However, for the singlet states there is a wide variation in calculated f -value for different types of wavefunction. For the simple m.o. theory the $^1\text{A}_1 \leftarrow ^1\text{A}_1$ transition is a double electron jump, and therefore forbidden. Configuration interaction between the two $^1\text{A}_1$ configurations discussed in § 4.2 would considerably modify this conclusion, so that both the $^1\text{B}_1 \leftarrow ^1\text{A}_1$ and $^1\text{A}_1 \leftarrow ^1\text{A}_1$ transitions might be observed. In view of the restricted bases for the v.b. and i.c.c. calculations no reliable estimate can be given for the relative intensity of these two transitions, since an analysis of the transition moment matrix shows that additional functions that have a negligible effect on the molecular energy may have a large effect on the intensities.

The author is indebted to Dr. M. Krauss for supplying a copy of the basic integrals for CH_2 , and to Dr. J. N. Murrell for stimulating discussions.

APPENDIX

Correlation errors were calculated for a number of states of C, C^+ , C^{++} and C^- not available in the literature and are given in table 7. The calculated energies were minimized for each state with respect to the two parameters ζ_1 and ζ_2 of the orbitals given in § 2. The experimental energies of known states were taken from the spectroscopic tables of Moore [15]. The values of $(W - \bar{W})$ for C^- states were obtained by quadratic extrapolation from corresponding states of F^+ , O and N^- . However, comparison of the values of $(W - \bar{W})$ along the series O^- , O^- , O, O^+ [8, 16] with the series C^- , C^- , C, C^+ , C^{++} suggests that this extrapolation has resulted in an overestimate of ~ 0.05 A.U. in the values of $(W - \bar{W})$ for C^- . An iso-electronic extrapolation was not possible for the $\text{C}(\text{p}^4)$ states. A comparison was therefore made of the values of $(W - \bar{W})$ for states of $\text{C}^{++}(\text{p}^2)$ and $\text{C}^+(\text{p}^3)$, and the corresponding states of $\text{C}^+(\text{sp}^2)$ and $\text{C}(\text{sp}^3)$ respectively, in each case where the spin of the added s electron increases the multiplicity of the state by one but with no change in L . With calculated term values using single configuration wavefunction the correspondence was not very good. However, when configuration interaction was allowed between the p^2 , ^1S and s^2 , ^1S states of C^{++} , and the p^3 , $^2\text{P}^0$ and s^2p , $^2\text{P}^0$ states of C^+ the increase in correlation error in going from the lowest state of $\text{C}^{++}(\text{p}^2)$ to the lowest state of $\text{C}^+(\text{sp}^2)$ was equal within 0.003 A.U. to the increase in going from the lowest state of $\text{C}^+(\text{p}^3)$ to the lowest state of $\text{C}(\text{sp}^3)$, with similar agreement for higher pairs of differences. The mean of these values was then used to obtain values of $(W - \bar{W})$ for $\text{C}(\text{p}^4)$ states from corresponding states of $\text{C}^-(\text{sp}^4)$. The values in table 7 are corrected to refer to one configuration calculations, and are probably reliable to ± 0.005 A.U.

REFERENCES

- [1] HERZBERG, G., 1961, *Proc. roy. Soc. A*, **262**, 291.
- [2] FREY, H. M., 1960, *J. Amer. chem. Soc.*, **82**, 5947.
- [3] GALLUP, G. A., 1957, *J. chem. Phys.*, **26**, 716.
- [4] FOSTER, J. M., and BOYS, S. F., 1960, *Rev. mod. Phys.*, **32**, 305.
- [5] PADGETT, A., and KRAUSS, M., 1960, *J. chem. Phys.*, **32**, 189.
- [6] JORDAN, P. C. H., and LONGUET-HIGGINS, H. C., 1962, *Mol. Phys.*, **5**, 121.
- [7] MOFFITT, W., 1951, *Proc. roy. Soc. A*, **210**, 245.
- [8] HURLEY, A. C., 1958, *Proc. roy. Soc. A*, **248**, 119 ; 1959, *Ibid.*, **A**, **249**, 402.
- [9] MULLIKEN, R. S., 1944, *J. Chim. phys.*, **46**, 497.
- [10] LÖWDIN P. O., 1955, *Phys. Rev.*, **97**, 1474.
- [11] HERZBERG, G., 1961, *Canad. J. Phys.*, **39**, 1511.
- [12] MULLIKEN, R. S., 1955, *J. chem. Phys.*, **23**, 1833.
- [13] KRAUSS, M. (private communication).
- [14] MULLIKEN, R. S., and RIEKE, C. A., 1941, *Rep. Progr. Phys.*, **8**, 231.
- [15] MOORE, C. E., 1949, Atomic energy levels. N.B.S. Circular 467.
- [16] HURLEY, A. C., 1960, *Rev. mod. Phys.*, **32**, 400.

Theory of the isotropic g value of 4.27 found for some high-spin ferric ions

by J. S. GRIFFITH

Department of Mathematics, Manchester College of Science and Technology,
Manchester, 1

(Received 22 January 1964)

It has been suggested [4] that an isotropic g value of 4.27 given by the high-spin ferric ion occurs because $D=0$, $E \neq 0$ in a quadratic fine-structure spin-Hamiltonian. The plausibility of this interpretation is discussed and defended in the present paper. However, it is shown that $D=0$, $E \neq 0$ does not follow in any simple way from the symmetry of the environment, but probably arises through the effect of a ligand field on one of the excited 4T_1 terms of the ferric ion. This is possible, providing the ligand field has a rather curious mixed symmetry. g values are given for the four doublets of $S=7/2$ when $D=0$, $E \neq 0$; they do not even possess axial symmetry.

1. THE HIGH-SPIN FERRIC ION

It has been observed that in certain environments the high-spin ferric ion does not give its usual resonance behaviour with g near 2. This has been ascribed to the presence of terms in the fine-structure part of the spin-Hamiltonian which give energies large compared with the quantum of energy corresponding to the frequency of the resonance measurement [1-7].

The ground term of the free ferric ion is 6S and so the high-spin ferric ion has $S=\frac{7}{2}$ and no orbital degeneracy in its ground manifold. It has been shown that the second-order modification to the energies of the ground manifold by the spin-orbit coupling interaction can always be represented in a spin-Hamiltonian by an expression quadratic in the components of the spin vector [8]. Therefore, when there is a large splitting of the ground manifold, it is to be expected that the great majority of this splitting comes from a quadratic fine-structure spin-Hamiltonian $\mathcal{H}(S)$. If we choose our axes to be the principal axes of this quadratic form, then

$$\mathcal{H}(S) = aS_x^2 + bS_y^2 + cS_z^2, \quad (1)$$

with a, b, c real. The part $\frac{1}{3}(a+b+c)S^2$ of $\mathcal{H}(S)$ represents only the position of the centre of gravity of the six states and if we subtract this out we are left with :

$$\mathcal{H}(S) = D(S_z^2 - \frac{1}{3}S(S+1)) + E(S_x^2 - S_y^2), \quad (2)$$

where $D = c - \frac{1}{2}a - \frac{1}{2}b$, $E = \frac{1}{2}(a-b)$, $S = \frac{7}{2}$. Including the interaction with an external magnetic field and expressing the result in terms of S_z and shift operators $S^\pm = S_x \pm iS_y$ gives :

$$\begin{aligned} \mathcal{H}(S) = & D(S_z^2 - \frac{1}{3}S(S+1)) + \frac{1}{2}E((S^+)^2 + (S^-)^2) \\ & + g\beta(H_zS_z + \frac{1}{2}H^+S^- + \frac{1}{2}H^-S^+), \end{aligned} \quad (3)$$

where $H^\pm = H_x \pm iH_y$ and g is the free electron g value. We take $g=2$. The matrix of $\mathcal{H}(S)$ may be written down at once.

In the two limiting cases $D \neq 0, E = 0$ and $D = 0, E \neq 0$, the energies and eigenfunctions of $\mathcal{H}(S)$ for zero magnetic fields are easily and explicitly obtainable. In the first case one doublet has $g_{\parallel} = 2, g_{\perp} = 6$ and this has been observed in various haemoglobin and myoglobin derivatives and in glasses [1-5]. In the second case the three doublets have energies $0, \pm 2E\sqrt{7}$. The one with zero energy gives an isotropic g value of $30/7$. Castner *et al.* [4] (following Sands [2]) observed this in glasses as a sharp resonance and have interpreted it as being the case $D = 0, E \neq 0$. It has also been observed in biological materials [9]. We investigate this case in greater detail.

Castner *et al.* worked with a frequency of $\frac{1}{3} \text{ cm}^{-1}$ and found $2E\sqrt{7} \approx 1.7 \text{ cm}^{-1}$. There are matrix elements of the magnetic field between the zero energy doublet and the other two and if these were too large, a field-dependent modification of the g value would occur. The theoretical treatment of this is essentially straightforward, although no simple explicit formulae can be given. A rough numerical estimate indicates the field-dependence to be very small at this frequency. Such a modification would, in any case, only occur to second-order in the field H as the first-order term cancels out. A field-dependence of the g value would be essentially equivalent to a breakdown of the assumption that we may correctly consider the interaction with the external magnetic field to first order after having taken the spin-orbit coupling to second order. It is possible that such a breakdown might be observed if the measurement were performed at Q band (1.25 cm^{-1}).

Castner *et al.* did not discuss the origin of the splitting in detail. However, they argued that an environment which was an octahedron distorted so as to produce, in my terminology [10], a component $C_z^{T_{2g}}$ in the ligand field would give $E \neq 0$ and $D = 0$. This is because $S_x^2 - S_y^2$ is the z component of a T_{2g} representation of the octahedral group if we take x and y axes bisecting the usual octahedral axes. For similar reasons they argued that a regular tetrahedral coordination FeA_2B_2 could do the same if A and B were different. We shall show that they were wrong in supposing that in such an environment D is necessarily zero but that it does happen that D should be small relative to E . The reasons for this are given in the next section and are somewhat fortuitous.

Another natural question about the isotropic g value is this: take the spin-Hamiltonian of equation (3) with $D = 0$ and general S , then does one usually get an isotropic g value or is the case $S = \frac{5}{2}$ (and $S = \frac{1}{2}$) an exception? $S = \frac{7}{2}$ occurs for $Gd^{3+}4f^7$ and for this case there is no isotropic, nor even an axially symmetric g value (see §3 and reference [9]). For spins $S = 2n + \frac{1}{2}$, with n integral, there is always just one doublet with energy zero. The next example is $S = \frac{9}{2}$ and here this doublet has an isotropic g value of $70/11$.

2. ORIGIN OF SPLITTING OF THE GROUND TERM

Presumably we have here a situation in which the dominant component of the ligand field has octahedral or tetrahedral symmetry. Then the ground 6S gets split under second-order perturbation theory by the split components of the lowest 4T_1 term. This situation has been discussed elsewhere [7] for a dominantly octahedral situation, but a tetrahedral field produces formally similar effects. It was found that

$$\left. \begin{aligned} D &= \frac{1}{10} S^2 (2E_z^{-1} - E_x^{-1} - E_y^{-1}), \\ E &= \frac{1}{10} S^2 (E_x^{-1} - E_y^{-1}), \end{aligned} \right\} \quad (4)$$

where ζ is the spin-orbit coupling parameter for a single d electron and E_x, E_y, E_z are the energies of the three component ${}^4X, {}^4Y, {}^4Z$ of the 4T_1 relative to 6S . Equation (4) was calculated for the strong-field coupling case.

Our problem is now : how can we get $D=0, E \neq 0$. Because the $g=30/7$ resonance appears in several situations it is extremely unlikely that it occurs because of some accidental cancellation to give $D=0$, but must surely have some rather general reason for its origin. General reasons are usually group-theoretic ones connected with degeneracies. There are three essentially different possibilities namely $E_x=E_y=E_z$; $E_x=E_y \neq E_z$; E_x, E_y, E_z all different. The first forces $D=E=0$, and the second $E=0$. The third could give $D=0, E \neq 0$, but, at least at first sight, only by some accident.

The apparent paradox is resolved by observing that both the environments considered by Castner *et al.* have a rather curious kind of symmetry which is more symmetric than the overall symmetry group of the site. These environments are the regular tetrahedral arrangement MA_2B_2 and the distorted octahedral arrangement MA_6 having the four equatorial A ligands at the vertices of a rectangle. Then the ligand field due to these environments, when broken up into components transforming according to irreducible representations of the group T_d (for MA_2B_2) or O_h (for the distorted MA_6), turns out to have a specially simple form. Apart from its totally symmetric part, there is only a piece transforming according to the z component of a T_2 representation. It will be shown in the following paper [10] that such a symmetry splits a 4T_1 term into three equally spaced components. We shall also find there that an octahedral coordination of the type MA_3B_3 having symmetry C_{2v} would do the same. Choosing the axes suitably, the 4T_1 splits into ${}^4X, {}^4Y, {}^4Z$ with energies $m+a, m-a, m$ respectively. We then have :

$$D = -\frac{a^2\zeta^2}{5m(m^2-a^2)}, \quad E = -\frac{a\zeta^2}{5(m^2-a^2)}. \quad (5)$$

D is not zero, which indicates the danger of supposing that the form of the fine-structure Hamiltonian necessarily matches that of the environment in detail (as appears to have been assumed by Castner *et al.* [4]).

It is difficult to know the values of the parameters in equation (5). However the consequent values of D and E are at least of the right order of magnitude. Castner *et al.* find $D/E \leq 0.05, E \approx \frac{1}{3} \text{ cm}^{-1}$. If we put $\zeta = 400 \text{ cm}^{-1}, a = 10^3 \text{ cm}^{-1}, m = 10^4 \text{ cm}^{-1}$ we get $D/E = 0.1, E = \frac{1}{3} \text{ cm}^{-1}$. Clearly by juggling with the parameters we could satisfy both conditions if we wished. We have demonstrated, then, that the two environments considered by Castner *et al.*, and also one new one, could give the observed isotropic g value. We have not, of course, completely excluded the possibility that some entirely different kind of environment might do so too.

3. OTHER PROBLEMS

For gadolinium, which is $4f^7 {}^8S$, we would again expect $E \neq 0, D$ small for the three environments which gave this situation for ferric iron. Solution of the secular equations for $D=0$ gives energies $\pm xE\sqrt{3}$, where $x^2 = 21 \pm 4\sqrt{21}$ for the four doublets. The g values, however, have not even axial symmetry, being for one pair of doublets $g_z^1 = 0.26, g_x^1 = 0.18$ or 13.78 , $g_y^1 = 13.78$ or 0.18 and for the other $g_z^2 = 3.74, g_x^2 = 2.79$ or $8.40, g_y^2 = 8.40$ or 2.79 . $g_z^1 + g_z^2 = 4$ exactly.

Walsh *et al.* [9] observed $g = 5.90$ for gadolinium bound to DNA and the present calculation agrees with their final view that this g value is not due to an environment having $E \neq 0$, D small.

REFERENCES

- [1] BENNETT, J. E., INGRAM, D. J. E., GEORGE, P., and GRIFFITH, J. S., 1955, *Nature, Lond.*, **170**, 394.
- [2] SANDS, R. H., 1955, *Phys. Rev.*, **99**, 1222.
- [3] GRIFFITH, J. S., 1956, *Proc. roy. Soc. A*, **235**, 23.
- [4] CASTNER, T., NEWELL, G. S., HOLTON, W. C., and SLICHTER, C. P., 1960, *J. chem. Phys.*, **32**, 668.
- [5] BENNETT, J. E., GIBSON, J. F., INGRAM, D. J. E., HAUGHTON, T. M., KERKUIT, G. A., and MUNDAY, K. A., 1961, *Proc. roy. Soc. A*, **262**, 395.
- [6] GRIFFITH, J. S., 1961, *The Theory of Transition-metal Ions* (Cambridge University Press).
- [7] GRIFFITH, J. S., 1964, *Proceedings of Symposium on Quantum Aspects of Polypeptides and Polynucleotides*, Stanford, 1963, Biopolymers, Symposia No. 1, Interscience.
- [8] GRIFFITH, J. S., 1960, *Mol. Phys.*, **3**, 79.
- [9] WALSH, W. M., RUPP, L. W., and WYLUDA, B. J., 1963, *Proceedings of the First International Conference on Paramagnetic Resonance*, Jerusalem 1962 (Academic Press).
- [10] GRIFFITH, J. S., 1964, *Mol. Phys.*, **8**, 217.

Intermediate symmetry

by J. S. GRIFFITH

Department of Mathematics, Manchester College of Science
and Technology, Manchester 1

(Received 22 January 1964)

In quantum mechanical situations possessing symmetry, information may be obtained about degeneracies of states by considering the symmetry group H concerned. In the present paper it is shown that in certain cases extra information about matrix elements may be deduced by working in a suitably chosen larger group G containing H . The situation is then said to possess a symmetry intermediate between H and G . Applications are made to ligand fields arising from octahedral and tetrahedral coordination, when the attached ligands are not necessarily all the same.

1. INTRODUCTION

In the previous paper we based the interpretation of fine-structure splitting of the spin-Hamiltonian for the ferric ion on considering the effect of a ligand field upon an excited 4T_1 term. It was remarked that for certain ligand fields this 4T_1 term split into three equally separated, spatially non-degenerate parts. It was said that this was because the ligand field had a simpler behaviour than might have been expected by merely examining the overall symmetry group of the environment. We intend, in this paper, to examine this type of situation more deeply, to show this is a special case of a more general situation, and to justify the assertion made in the previous paper about the splitting of the 4T_1 term.

Before starting, let us examine one particular environment discussed in the last paper in more detail. That is the situation where one has a complex MA_2B_2 and both A and B are envisaged as producing axially symmetric effects upon the metal ion M . We take the Z axis to bisect the BMB angle. The complex has symmetry C_{2v} and therefore if we classify this field under the tetrahedral group we expect to get three kinds of component occurring, a fully symmetric component transforming as A_1 and two other components transforming respectively as T_{2z} and $E\theta$. (This is because each of these three transform according to the unit representation of C_{2v} .) However, in fact we only get the first two of these, as may be seen quite readily by the following geometrical argument. Let us consider formally that A is split into the two parts $\frac{1}{2}(A+B)$ and $\frac{1}{2}(A-B)$, added together equally. Similarly let B be split into the two parts $\frac{1}{2}(A+B)$ and $\frac{1}{2}(B-A)$, again added together equally. Evidently the first of the two parts gives rise to something transforming according to the fully symmetric representation A_1 , whilst the second part gives rise to something transforming as a z component of T_2 . Obviously there is nothing transforming according to $E\theta$. It is this lack of an $E\theta$ component which will enable us to deduce that the T_1 term splits into three equally spaced components.

The situation we are discussing here is a slightly unusual one. We may see this as follows. In problems involving crystal fields or ligand fields it is usual to take the symmetry group H to be that of the environment of the ion concerned. It is then supposed that the only information which can be obtained by purely symmetry arguments must arise from operating within that symmetry group. As far as the energies of the states of the ion are concerned, the only direct deduction is that it must be possible to arrange them in sets forming bases for irreducible representations. Any two functions belonging to the same set then have necessarily the same energy. However, nothing can be said about the relative energies of different sets.

Before continuing, let us emphasize that we are talking 'strictly'. In practice, of course, much more information may be obtained from largely group-theoretic arguments, assuming certain other things to be approximately true. For example, that the environment has a higher symmetry than that represented by H , that the ion may be correctly represented by giving an electron configuration such as $3d^n$, that terms such as the spin-orbit coupling are totally symmetric under the full rotation group rather than merely under the symmetry group of the ion, etc. In this paper, however, we show that quite apart from such considerations, one may sometimes obtain more information than the group H can offer. Further, this information includes numerical relationships among the energy separations of different irreducible representations.

In an abstract sense, this could occur as follows. Take a group G having a sub-group H which is the actual environmental symmetry group. The irreducible representations $\Gamma_1 \dots \Gamma_n$ of G then give representations of H . Any arbitrary function V may be expanded as a sum of components $V(\Gamma_i M_i)$ by using the irreducible idempotents [2] (or projection operators) of the group algebra to give :

$$V = \sum_{\Gamma_i M_i} a(\Gamma_i M_i) V(\Gamma_i M_i). \quad (1)$$

Here $V(\Gamma_i M_i)$ is the M_i component of a set of functions transforming according to the irreducible representation Γ_i . $a(\Gamma_i M_i)$ are constants. V may also be expanded in terms of the irreducible representations γ_i of H to give :

$$V = \sum_{\gamma_i M_i} b(\gamma_i M_i) V_1(\gamma_i M_i); \quad (2)$$

combining (1) and (2) shows that an arbitrary V belonging to the unit representation of H may be written in an expansion like equation (1) but with a number p of arbitrary constants equal to the number of times the unit representation of H occurs among the irreducible representations of G .

As an illustration, suppose G to be the octahedral group O and $H = D_4$. Then, in the notation of Griffith [3], the components A_1' and $E\theta$ of the group O give rise to the unit representation of D_4 . So $p=2$, and equation (1) becomes :

$$V = a(A_1') V(A_1') + a(E\theta) V(E\theta). \quad (3)$$

We shall shortly use the irreducible tensor operator formalism of Griffith [3], whereupon equation (3) becomes :

$$V = a(A_1') V_i^{A_1} + a(E\theta) V_\theta^E. \quad (4)$$

We have shown that the most general function having symmetry D_4 satisfies equation (4) and obviously the converse is true. Therefore the symmetry of

an environment may be specified by stating a group G and stating the form of tensor operator under G , necessary to specify the most general environment of that symmetry.

However, we have already seen that there can be an environment with symmetry group H such that there is a group G containing H with respect to which the most general tensor operator of equation (2) possible for the environment is not the most general possible for a function fully symmetric under H . This always occurs if the number p defined above is greater than 2 and the tensor operator contains only q independent constants, where $1 < q < p$. In such a case, the environment has less symmetry than G , but more than H . We shall say it has an intermediate symmetry.

An example of a function having intermediate symmetry under the octahedral group is the electrostatic potential V due to four positive and four negative charges arranged at the vertices of a cube. If these are taken to have equal magnitude and arranged alternately, the potential V transforms according to A_{2u} of the octahedral group O_h . The symmetry group of the arrangement is T_d , however, and a function transforming according to A_1 of T_d would normally have components transforming according to both A_{1g} and A_{2u} of O_h . Thus if we classify our states according to O_h we have the selection rule :

$$\langle \Gamma_1 M_1 | V | \Gamma_2 M_2 \rangle = 0 \text{ for } \Gamma_1 \neq \Gamma_2,$$

which would not be true for a general V symmetric under T_d .

So far we have only considered examples with $p=2$. In these, the intermediate symmetry is only interesting if the environment contains no component belonging to the unit representation of the larger group G at all. However, this is not so when $p \geq 3$. Suppose for example, there is a representation of degree three of O , or O_h , which breaks up into three representations of degree one under H . If the environment has merely symmetry H , there is no reason for these three states to have their energies related in any way. But if $p \geq 3$ and V contains only the unit representation of G and a component of one other, there is necessarily one equation connecting the energies of these three states. For they depend on a matrix containing only two arbitrary constants. Examples of this are given in the last section of the paper.

2. REGULAR ARRANGEMENTS OF LIGANDS

The example of intermediate symmetry for which we shall find a useful application is that of a ligand field generated by a regular arrangement of ligands. The field due to different ligands, $A, B, C \dots$ attached to the same metal ion M is assumed to be additive, while that from a single ligand is assumed axially symmetric about the axis joining the metal ion to the nearest atom of the ligand. This latter requirement means that the field $V(A)$ due to a ligand A along the axis is left invariant by all elements of the symmetry group $C_{\infty v}(l)$ about that axis. The first requirement means that the field due to a set of ligands, $A, B \dots$ is the sum :

$$V = V(A) + V(B) + \dots \quad (5)$$

of the V for each ligand separately. No assumption that the metal electrons are in d or f orbitals, rather than general molecular orbitals is necessary. With

ligands such as H_2O or pyridine, our assumption of axial symmetry can only be maintained if we believe unsymmetrical π -bonding to be energetically unimportant, which is presumably acceptable for F^- , Cl^- , Br^- , I^- , CO , N^- and even NH_3 (possibly also H_2O , see Sugano and Shulman [4]).

We shall now investigate the symmetry properties of V and see that it normally has a symmetry intermediate between G , that of the arrangement of ligands assuming them to be all identical, and H , the true symmetry group of the ligands. Consider first the field $V(A)$ of a single ligand A along an axis l and decompose it into a sum of irreducible tensor operators under G . Write K for the intersection of the two groups G and $C_{\infty v}(l)$. Then only those components of tensor operators under G which transform as the unit representation of K can occur with non-zero coefficients in $V(A)$. Conversely a linear combination of such tensor operators with an arbitrary set of reduced matrix elements with respect to any orbitals of interest gives the most general possible field $V(A)$.

Consider now ligands in regular octahedral or tetrahedral arrangements. The symmetry group G becomes respectively O_h or T_d . However, unless all ligands are identical, the group H will be a proper sub-group of G . For one of the ligands, A say, the group K will be the intersection :

$$\left. \begin{aligned} K_{\text{oct}} &= O_h \wedge C_{\infty v}(l) = C_{4v}(l), \\ K_{\text{tet}} &= T_d \wedge C_{\infty v}(l) = C_{3v}(l), \end{aligned} \right\} \quad (6)$$

in the two cases. For the octahedral arrangement we have six different tensor operator representations of $V(A)$ depending on which axis A lies. They may be written :

$$\left. \begin{aligned} \text{OZ} : V(A) &= A_{\epsilon}^{A_{1g}} + A_{\theta}^{Eg} + A_z^{T_{1u}}, \\ -\text{OZ} : V(A) &= A_{\epsilon}^{A_{1g}} + A_{\theta}^{Eg} - A_z^{T_{1u}}, \\ \text{OX} : V(A) &= A_{\epsilon}^{A_{1g}} - \frac{1}{2}A_{\theta}^{Eg} + \frac{1}{2}\sqrt{3}A_{\epsilon}^{Eg} + A_x^{T_{1u}}, \\ -\text{OX} : V(A) &= A_{\epsilon}^{A_{1g}} - \frac{1}{2}A_{\theta}^{Eg} + \frac{1}{2}\sqrt{3}A_{\epsilon}^{Eg} - A_x^{T_{1u}}, \\ \text{OY} : V(A) &= A_{\epsilon}^{A_{1g}} - \frac{1}{2}A_{\theta}^{Eg} - \frac{1}{2}\sqrt{3}A_{\epsilon}^{Eg} + A_y^{T_{1u}}, \\ -\text{OY} : V(A) &= A_{\epsilon}^{A_{1g}} - \frac{1}{2}A_{\theta}^{Eg} - \frac{1}{2}\sqrt{3}A_{\epsilon}^{Eg} - A_y^{T_{1u}}. \end{aligned} \right\} \quad (7)$$

Here each of the A_{β}^b is an irreducible tensor operator belonging to the component β of the irreducible representation b of the group O_h . For any pair of orbitals, or n -particle states, $|\alpha\alpha\rangle$ and $|c\gamma\rangle$ there are just three separate reduced matrix elements of the A_{β}^b of equations (7). These are defined as in Griffith [3] by the equation :

$$\langle \alpha\alpha | A_{\beta}^b | c\gamma \rangle = \langle \alpha || A^b || c \rangle V \begin{pmatrix} a & c & b \\ \alpha & \gamma & \beta \end{pmatrix} \quad (8)$$

and the V symbol is the product of a V symbol for the octahedral group with a V symbol for the group of order two containing the inversion.

For another ligand, B say, we shall have a similar set of equations but with B replacing A . The transformation properties of B_{β}^b under the group O_h are, of course, the same as those of A_{β}^b but the reduced matrix elements will generally be different. In accordance with our assumption about additivity, the tensor operator corresponding to all six ligands is just the sum of those for each one separately. They are given in table 1(a), together with the actual symmetry of the complex, for a set of representative arrangements of complexes $A_n B_{6-n}$.

Complex	Axes for B	Symmetry Group	Tensor operator	p	q
MA_6	—	O_h	$6A_{1g}$	1	1
MA_3B	OZ	C_{4v}	$5A_{1g} + B_{1g} + B_{2g} + B_{3g} + B_{4g}$	3	3
MA_4B_2	OZ, — OZ	D_{4h}	$4A_{1g} + 2B_{1g} + 2B_{2g} + 2A_{2g}$	2	2
MA_4B_2	OX, OY	C_{2v}	$4A_{1g} + 2B_{1g} + A_{2g} + B_{2g} + B_{3g} + B_{4g} + B_{5g} + B_{6g}$	5	3
MA_3B_3	OX, OY, OZ	C_{3v}	$3A_{1g} + 3B_{1g} + B_{2g} + B_{3g} + B_{4g} + B_{5g} + B_{6g}$	4	2
MA_3B_3	OX, — OX, OZ	C_{2v}	$3A_{1g} + 3B_{1g} + \sqrt{3}B_{2g} - \sqrt{3}A_{3g} + B_{4g} + B_{5g} + B_{6g}$	6	3

(a)

Complex	Axes for B	Symmetry Group	Tensor operator	p	q
MA_4	—	T_d	$4A_i A_1$	1	1
MA_3B	a	C_{3v}	$3A_i A_1 + B_i A_1 + \sqrt{3} B_\tau T_\tau - \sqrt{3} A_\tau T_\tau$	2	2
MA_2B_2	a, b	C_{2v}	$2A_i A_1 + B_i A_1 + 2B_g T_g - 2A_g T_g$	3	2

(9)

Table 1. Tensor operators for fields in regularly coordinated complexes of the general formula MA_mB_n . (a) Octahedral coordination. (b) Tetrahedral coordination. $a = (111)$ axis, $b = (-1, -1, 1)$ axis.

Note that by using the trigonal system of quantization for the octahedral group, the tensor operator having C_{3v} symmetry becomes :

$$V = 3A_{\epsilon}^{A_{1g}} + 3B_{\epsilon}^{A_{1g}} + \sqrt{3}B_{\tau}^{T_{1u}} - \sqrt{3}A_{\tau}^{T_{1u}}.$$

For the tetrahedral group, T_d , the tensor operators for a single ligand are :

$$\left. \begin{aligned} (111) \text{ axis : } V(A) &= A_{\epsilon}^{A_1} + A_x^{T_2} + A_y^{T_2} + A_z^{T_2}, \\ (-1, -1, 1) \text{ axis : } V(A) &= A_{\epsilon}^{A_1} - A_x^{T_2} - A_y^{T_2} + A_z^{T_2}, \\ (1, -1, -1) \text{ axis : } V(A) &= A_{\epsilon}^{A_1} + A_x^{T_2} - A_y^{T_2} - A_z^{T_2}, \\ (-1, 1, -1) \text{ axis : } V(A) &= A_{\epsilon}^{A_1} - A_x^{T_2} + A_y^{T_2} - A_z^{T_2}. \end{aligned} \right\} \quad (9)$$

The corresponding operators for MA_nB_{4-n} are given in table 1(b), trigonal quantization being used for the complex MA_3B .

In table 1 is also given p , the number of distinct times the unit representation of the symmetry group of the complex occurs among the irreducible representations of the larger group (O_h or T_d). So is q , the number of independent kinds of tensor operator occurring in the tensor operator representation of the ligand field. Note that in an expression such as :

$$f = B_x^{T_{1u}} - A_x^{T_{1u}} + B_y^{T_{1u}} - A_y^{T_{1u}},$$

there is really only one independent operator

$$C_{\beta}^{T_{1u}} = B_{\beta}^{T_{1u}} - A_{\beta}^{T_{1u}},$$

and the matrix elements of f between a pair of orbitals $|a\alpha\rangle$ and $|c\gamma\rangle$ depend on the V coefficients and just one reduced matrix element, as in equation (8). For those complexes for which $p = q$, no additional information is obtained by working in the higher symmetry group (although of course it may still be more convenient for other reasons). In the four cases in table 1 where $p \neq q$, we have non-trivial cases of intermediate symmetry.

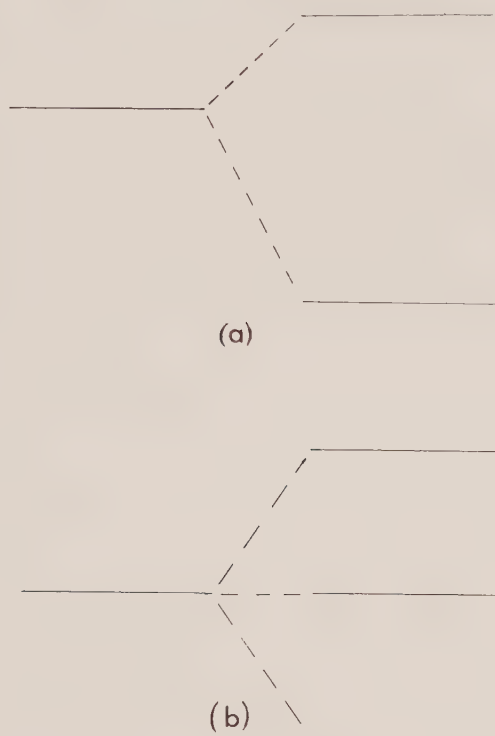
For complexes with three or more kinds of ligands, we can easily write down the corresponding operators from equations (7) and (9). Even in the most general octahedrally coordinated complexes we only get operators transforming according to A_{1g} , E_g and T_{1u} . Similarly only A_1 and T_2 appear in tetrahedral complexes. However, if all the ligands are different, the actual symmetry group of the complex is just the trivial group containing a single element.

3. MATRIX ELEMENTS

The most interesting and curious general consequence of the restricted forms of tensor operators derived above is that the field due to any octahedrally coordinated complex $MABCDEF$, with the given assumption, has zero matrix elements between t_2 and e orbitals. This is because the tensor operators occurring in equations (7) belong to the three representations A_{1g} , E_g and T_{1u} , none of which occur in the direct product $E_g T_{2g}$. Hence the division into t_2 and e orbitals remains exact, even though the complex may have no non-trivial element in its symmetry group. For tetrahedral coordination, T_2 is contained in ET_2 , so the corresponding result is not true in general.

Next we consider the splitting of a set of states $|a\alpha\rangle$ transforming according to a one-valued representation a of O_h or T_d . Here the states may be orbitals

of n -particle states $|SaM_s\alpha\rangle$. The tensor operators transforming as A_1 only shift the centre of gravity, while under O_h those transforming as T_{1u} are zero within any single set of states because of parity. Hence, in table 1, the complexes MA_6 , MA_4 , and MA_3B_3 with C_{3v} symmetry cause no splitting. For the remainder the parts of the tensor operators which cause splitting fall into four categories,



Schematic splitting of T_1 and T_2 states under tensor operators.

written succinctly as C_θ^E , C_ϵ^E , $C_\tau^{T_2}$ and $C_z^{T_2}$. We have dropped the suffix g because we may clearly work in the group O rather than O_h . Then $C_\tau^{T_2}$ and $C_z^{T_2}$ do not split E states, while C_θ^E and C_ϵ^E have as their only non-vanishing elements :

$$\begin{aligned}\langle E\theta|C_\theta^E|E\theta\rangle &= -\frac{1}{2}R; & \langle E\theta|C_\epsilon^E|E\epsilon\rangle &= \frac{1}{2}R; \\ \langle E\epsilon|C_\theta^E|E\epsilon\rangle &= \frac{1}{2}R; & \langle E\epsilon|C_\epsilon^E|E\theta\rangle &= \frac{1}{2}R,\end{aligned}$$

where we used equation (8) and table C2.1 of Griffith [3]. R is a reduced matrix element. The energies are $\pm \frac{1}{2}R$ in each case.

Much more valuable information can be derived for states of T_1 and T_2 symmetry. Since the V coefficients satisfy :

$$V\begin{pmatrix} T_1 & T_1 & c \\ \alpha & \beta & \gamma \end{pmatrix} = V\begin{pmatrix} T_2 & T_2 & c \\ \alpha & \beta & \gamma \end{pmatrix}$$

for all c, α, β, γ it follows that the general form of the splitting is the same for T_1 and T_2 . The actual matrices are given in table 2. It readily follows that

for C_θ^E and $C_\tau^{T_2}$, a T state splits into a degenerate doublet and a singlet. However, for C_ϵ^E and $C_z^{T_2}$ it splits into three equally spaced singlets. This is illustrated schematically in the figure, which is drawn for positive R . The fields represented by C_ϵ^E and $C_z^{T_2}$ afford examples of the intermediate symmetry implying relationships between matrix elements which do not follow from the properties of the symmetry group of the site. Application of this result to the theory of the ferric ion E.S.R. spectrum was given in the previous paper.

C_θ^E	x	y	z
x	R	0	0
y	0	R	0
z	0	0	$-2R$

C_ϵ^E	x	y	z
x	$-\frac{1}{2}R$	0	0
y	0	$\frac{1}{2}R$	0
z	0	0	0

$C_\tau^{T_2}$	x	y	z
x	$R/3\sqrt{2}$	0	0
y	0	$R/3\sqrt{2}$	0
z	0	0	$-R\sqrt{2/3}$

$C_z^{T_2}$	x	y	z
x	0	$-R/\sqrt{6}$	0
y	$-R/\sqrt{6}$	0	0
z	0	0	0

Table 2. The matrices of the four distinct non-trivial types of tensor operator within a set of T_1 or T_2 states. R is a reduced matrix element.

It has been noted elsewhere that $^{2S+1}T_1$ or $^{2S+1}T_2$ terms have much analogy with ^{2S+1}P atomic terms [5, 6]. Because of this one may write operators consisting of combinations of S and L which are equivalent with ^{2S+1}P to any true operator within $^{2S+1}T_i$. Our four tensor operators may clearly be represented by :

$$\left. \begin{aligned} C_\theta^E &\sim R(3L_z^2 - 2), \\ C_\epsilon^E &\sim R(L_x^2 - L_y^2), \\ C_\tau^{T_2} &\sim (R/3\sqrt{2})(3L_z^2 - 2), \\ C_z^{T_2} &\sim (R/\sqrt{6})(L_x L_y + L_y L_x). \end{aligned} \right\} \quad (10)$$

REFERENCES

- [1] GRIFFITH, J. S., 1964, *Mol. Phys.*, preceding paper.
- [2] WEYL, H., 1946, *The Classical Groups* (Princeton, New Jersey), p. 117.
- [3] GRIFFITH, J. S., 1962, *The Irreducible Tensor Method for Molecular Symmetry Groups* (New Jersey : Prentice-Hall, Inc.).
- [4] SUGANO, S., and SHULMAN, R. G., 1963, *Phys. Rev.*, **130**, 517.
- [5] ABRAGAM, A., and PRYCE, M. H. L., 1951, *Proc. roy. Soc. A*, **205**, 135.
- [6] GRIFFITH, J. S., 1961, *The Theory of Transition-metal Ions* (Cambridge University Press), §§ 9.5, 10.2 and Chap. 12.

Electron spin resonance absorption spectrum of CO_2^- molecule-ions in single crystal calcite†

by S. A. MARSHALL, A. R. REINBERG‡, R. A. SERWAY
and J. A. HODGES

Physics Division, IIT Research Institute, Chicago, Illinois

(Received 16 December 1963)

An electron spin resonance absorption spectrum due to CO_2^- molecule-ions has been observed at 3 cm wavelength in single crystals of optical grade calcite. The spectrum exhibits orthorhombic symmetry with both the ^{12}C and ^{13}C isotopically substituted CO_2^- molecule-ions having the same g -tensor components given by $g_{zz}=2.00161$, $g_{xx}=2.00320$ and $g_{yy}=1.99727$, where z refers to the carbonate-ion C–O bond direction, x the crystal [111] direction and y the direction perpendicular to these two. The CO_2^- molecule-ions are located at carbonate-ion sites with their planes parallel to those of carbonate-ions and with their two-fold symmetry axes parallel to the z direction. The hyperfine structure tensor components associated with the ^{13}C isotope are $A_{zz}=177.28$ oe, $A_{xx}=134.62$ oe, and $A_{yy}=131.69$ oe.

1. INTRODUCTION

The molecule-ion CO_2^- like NO_2 is a triatomic species having 17 valence electrons and has a bent configuration with a bond angle of approximately 134° . Its paramagnetic character makes its study of interest not only for its own sake but also from the point of view of being a molecular species whose properties can be compared with those of the isoelectronic NO_2 molecule. The electron spin resonance absorption spectrum of the CO_2^- molecule-ion in γ -irradiated alkali-metal formate single crystals has been reported by Ovenall and Whiffen [1,2] by Brivati *et al.* [3] and by Atkins *et al.* [4]. In neutron irradiated single crystals of calcite, Kemp observed a similar spectrum but did not positively identify it as being due to CO_2^- molecule-ions [5–7]. In addition, he failed to report the hyperfine structure spectrum due to the 1.1 per cent naturally abundant ^{13}C ($I=\frac{1}{2}$) isotopically substituted CO_2^- molecule-ions, probably because of the over abundance of radiation produced paramagnetic species which tend to obscure the weak hyperfine doublet pattern which is only one two-hundredth the intensity of the main CO_2^- spectrum. Ovenall and Whiffen have, however, identified such a hyperfine structure spectrum in γ -irradiated sodium formate [2]. In this system, the hyperfine structure spectrum seems well resolved with signals well above background noise.

In the present report, the results of an investigation on the spectrum of CO_2^- molecule-ions in calcite are presented. The g and A tensor components of the spin Hamiltonian for this molecule-ion in calcite are found to be substantially the same as those reported by Ovenall and Whiffen for this molecule-ion in γ -irradiated sodium formate. In addition to these results, a careful analysis of

† This work supported by the U.S. Air Force, Rome, New York.

‡ Present address : Texas Instruments Research Laboratories, Dallas, Texas.

the experimental data indicates that the g -tensor components for the ^{13}C substituted CO_2^- molecule-ions are, to within experimental error, the same as those for ^{12}C .

2. EXPERIMENT

Calcite single crystals of optical quality used in this investigation were obtained from the Crystal Optics Company of Chicago, Illinois and from the Chicago Natural History Museum through the courtesy of Dr. E. Olsen. Specimens were cut from large single crystals into rectangular parallelepipeds of dimensions $\frac{3}{16}$ by $\frac{3}{16}$ by $\frac{3}{4}$ in. Preliminary orientation of the specimens was achieved by referencing the cuts with crystal cleavage planes. Final orientation was achieved by x-ray diffraction and optical interference procedures. The oriented specimens were mounted along the axis of a cylindrical cavity resonator operating in the TE_{011} mode whose loaded Q was of the order of 5000. A 3 cm wavelength spectrometer with 30 Mc/sec superheterodyne detection was used in this investigation. The signal oscillator frequency was measured directly by heterodyning a sample of the oscillator output with harmonics from a 10 Mc/sec quartz crystal controlled oscillator. Magnetic fields were measured with a nuclear magnetic resonance magnetometer using an electronic counter for read-out.

3. RESULTS

Optical grade calcite single crystals containing less than ten parts per million of iron group ion impurities were used in this electron spin resonance absorption investigation. A complex spectrum has been observed covering a Zeeman field region from 400 oe to 8000 oe. Of the numerous resonance absorptions in this field region, one set of three lines was found to have orthorhombic symmetry. Since this three-line spectrum exhibits three-fold symmetry about the crystal [111] direction, see figure 1, and since it collapses into a single resonance absorption when the Zeeman field is parallel to the crystal [111] direction, it is concluded that the paramagnetic species responsible for this spectrum are located at carbonate-ion sites, are coplanar with the carbonate-ions and have two-fold symmetry axes parallel to the C-O bond direction of the carbonate ions, there being three such equivalent directions in calcite. From this spectral behaviour, it is concluded that the paramagnetic species are CO_2^- molecule-ions. Figure 2 graphically represents the orientation of these molecule-ions in calcite.

The spin Hamiltonian used in interpreting this spectrum takes the simple form :

$$\mathcal{H} = g\beta HS_{z'}, \quad (1)$$

where z' is the Zeeman field direction, g is given by :

$$g = [g_{xx}^2 \sin^2 \theta \cos^2 \phi + g_{yy}^2 \sin^2 \theta \sin^2 \phi + g_{zz}^2 \cos^2 \theta]^{1/2} \quad (2)$$

and β is the Bohr magneton. At 77°K the components of the spectroscopic splitting tensor were measured to be $g_{zz} = 2.00161$, $g_{x,x} = 2.00320$ and $g_{yy} = 1.99727$, where this coordinate system is referenced to the CO_2^- molecule-ion as shown in figure 2. At this temperature, for clear calcite single crystals of optical quality having low iron group ion impurity content, the CO_2^- molecule-ion resonance absorption lines have total widths between points of half intensity of the order of 30 milli-oersteds. At room temperature the widths increase

to such an extent that complete resolution of the three lines is not possible even at the most favourable Zeeman field orientation. Below 77°K , the widths of the resonance lines are not noticeably narrowed even in the clearest crystals investigated. As a consequence of the narrowness of these resonance absorption lines, the peak field positions could be determined to within an uncertainty of 20 millioersts.

In so-called butterscotch calcite, which is naturally occurring calcite having a golden coloration, the CO_2^- molecule-ion electron spin resonance absorption

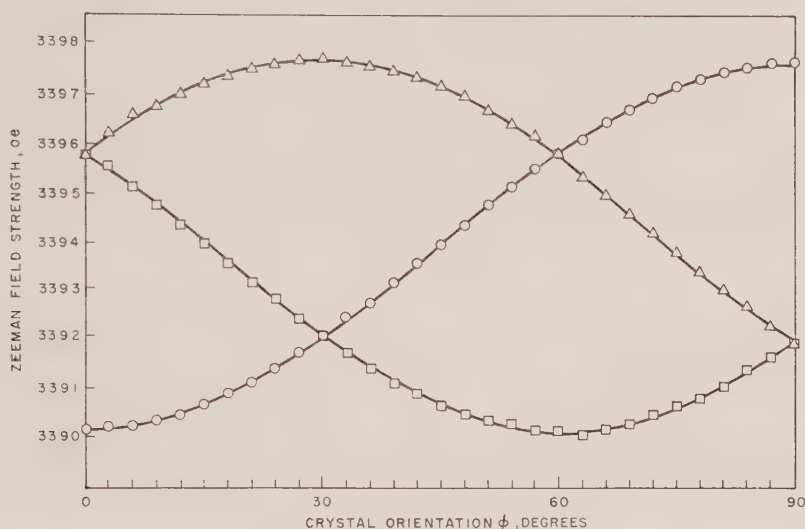


Figure 1. Angular dependence of the CO_2^- molecule-ion resonance absorption field strengths taken in the plane of the carbonate ions.

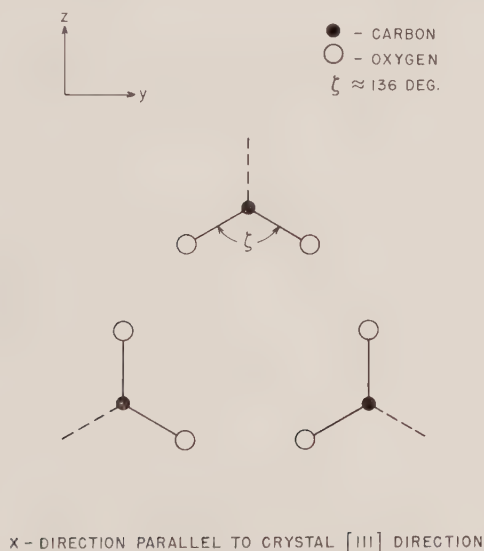


Figure 2. Graphical representation of the three distinct CO_2^- molecule-ion orientations.

spectrum appears strengthened by one to two orders of magnitude depending upon the density of coloration. For such crystals, the widths of the CO_2^- resonance absorption lines are found to be roughly two to three times the widths of the resonance absorption lines in clear calcite. Calcite single crystals subjected to neutron irradiation exhibit a golden to brownish coloration and the CO_2^- molecule-ion resonance absorption line intensities increase in a manner commensurate with the irradiation dosage. Clear calcite crystals were irradiated with neutrons having a mean energy of 1 meV for 13.4 hours in a flux of 10^{12} neutrons/cm²/sec. These crystals exhibited CO_2^- molecule-ion resonance absorption lines of sufficient strength to be displayed on an oscilloscope screen at signal oscillator power levels of 10^{-8} W. For calcite crystals so irradiated as well as for butterscotch calcite, a companion spectrum has been observed corresponding to $S = \frac{1}{2}$, $I = \frac{1}{2}$ and having symmetry properties identical to those of the spectrum identified as CO_2^- . This companion spectrum is interpreted as being due to ^{13}C isotopically substituted CO_2^- molecule-ions. The spin Hamiltonian used to interpret this companion spectrum is the same as that given by equation (1) with the addition of the hyperfine interaction term :

$$\mathcal{H} = I \cdot \vec{A} \cdot \vec{S}. \quad (3)$$

The hyperfine structure tensor for this spectrum is found to be diagonal in the same coordinate system as that which diagonalizes the spectroscopic splitting tensor. Its components are given by $A_{zz} = 177.28$ oe, $A_{xx} = 134.62$ oe and $A_{yy} = 131.69$ oe, where $A_{ii} = \tilde{A}_{ii}/g_{ii}\beta$. Figure 3 shows the isofrequency plot for this spectrum taken in the same plane as that for the plot shown in figure 1.

Each component of the hyperfine tensor can be written in the form :

$$A_{ii} = K + T_{ii} \quad (i = x, y, z), \quad (4)$$

where K is the strength of the Fermi contact interaction and T_{ii} are the principal components of the traceless dipole-dipole interaction. In solving for K and T_{ii} , four of the eight possible sign combinations for the principal components of the hyperfine structure tensor yield negative values for the Fermi contact interaction and are therefore rejected [8]. In addition, the two combinations with A_{xx} and A_{yy} of opposite signs are rejected since for a linear combination of s and p functions the hyperfine structure spectrum should be isotropic, or nearly so, in the x - y plane. Of the remaining possible sign combinations, the choice of all $A_{ii} > 0$ seems more acceptable than $A_{zz} < 0$, $A_{xx}, A_{yy} > 0$ because of the similarity in structure between CO_2^- and NO_2 . For the case of NO_2 in a crystalline solid the choice of all $A_{ii} > 0$ is found to be necessary in order to obtain a Fermi contact interaction term comparable to that observed for gaseous NO_2 [4, 9]. As a consequence of the traceless character of T and upon making the choice of all $A_{ii} > 0$ the value of the Fermi contact interaction term for CO_2^- in calcite is given by $K = 147.86$ oe. Upon having solved for K , the three components of the anisotropic dipole-dipole interaction tensor are found to be $T_{zz} = 29.42$ oe, $T_{xx} = -13.24$ oe and $T_{yy} = -16.17$ oe. In the table a comparison is made between the spectral parameters quoted here and in ref. [2] with those for $\text{CO}_2(\text{H})$ in γ -irradiated potassium bicarbonate [10]. Such a comparison provides confirmation that the spectra reported here and in ref. [2] are due to the same paramagnetic species and that these species are CO_2^- molecule-ions. Following the procedure used in ref. [2], the foregoing results for the strength of the

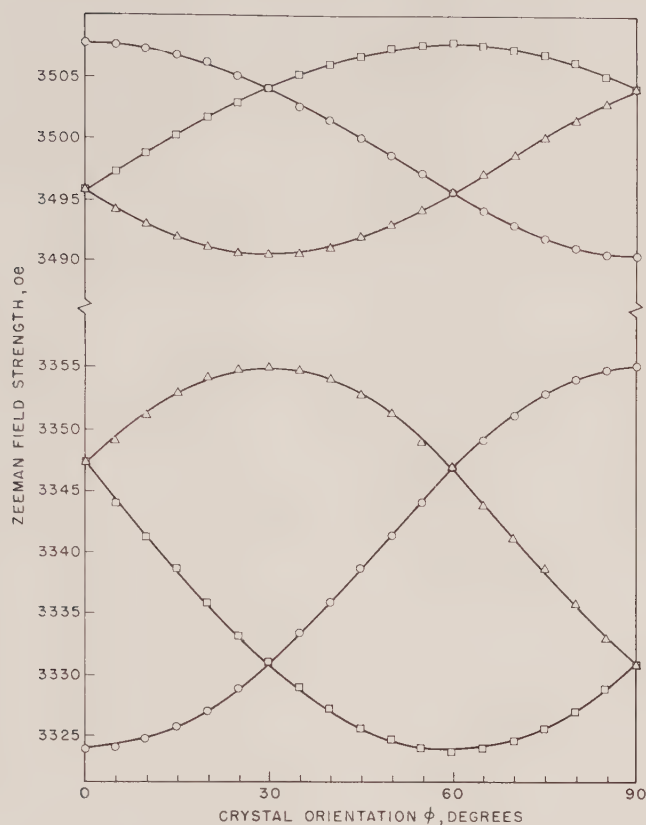


Figure 3. Angular dependence of the ^{13}C isotopically substituted CO_2^- molecule-ion resonance absorption field strengths taken in the plane of the carbonate ions.

	Calcite	γ -irradiated sodium formate†	$\text{CO}_2(\text{H})$ in γ -irradiated potassium bicarbonate‡
g_{zz}	2.00161 ± 0.00005	2.0014	2.0014
g_{xx}	2.00320 ± 0.00005	2.0032	2.0031
g_{yy}	1.99727 ± 0.00005	1.9975	1.9971
A_{zz}	$(177.28 \pm 0.05) \text{ oe}$	195 oe	179 oe
A_{xx}	$(134.62 \pm 0.05) \text{ oe}$	156 oe	142 oe
A_{yy}	$(131.69 \pm 0.05) \text{ oe}$	151 oe	133 oe

†See reference [2].

‡See reference [10].

Comparison of the CO_2^- molecule-ion spectral parameters in calcite and γ -irradiated sodium formate with those of $\text{CO}_2(\text{H})$ in γ -irradiated potassium bicarbonate.

Fermi contact interaction and the components of T can be used to estimate the bond angle for the CO_2^- molecule-ion. The results of such a calculation yield an angle of 136° which is to be compared with 134° for the NO_2 molecule [3, 11, 12] and for the CO_2^- molecule-ion in γ -irradiated sodium formate [2].

Because of the precision with which the Zeeman field strengths of the very narrow CO_2^- molecule-ion absorption lines could be determined, simultaneous measurements of the g -tensor components for the ^{12}C and the ^{13}C isotopically substituted CO_2^- molecule-ions were made. While making these measurements, special experimental precautions were taken in obtaining the required data. For example, the signal oscillator frequency was constantly monitored during a data taking run which consisted of taking the resonance absorption field positions of the two ^{13}C hyperfine structure components and the associated central ^{12}C resonance absorption field position. No runs were accepted for which the signal oscillator frequency changed by more than the equivalent of ± 0.01 oe during the data taking process. Zeeman field strengths were obtained by placing the probe of a nuclear magnetic resonance absorption magnetometer as close to the calcite specimen as possible. Due to the finite dimensions of the cavity resonator and dewar system, this separation could not be made less than 1 in. Thus, the g -tensor components could not be measured to within a precision commensurate with the magnetometer readings and the microwave signal oscillator frequency determinations. However, by not altering the configuration of the magnetometer probe and calcite specimen during a run, the g -tensor differences between the ^{13}C and ^{12}C species could be determined to within a precision corresponding to g -value uncertainties of one part in 10^5 . In analysing the obtained data, the full four by four eigenvalue determinant was expanded and solved for so that errors due to perturbation approximations would not be introduced. The result of this expansion is given by the following formula :

$$H_{\pm} = \frac{1}{2} H_2 \left\{ \left[1 + \frac{1}{4} \frac{(A_{jj} - A_{kk})^2}{H_2^2} \right]^{1/2} + \left[1 + \frac{1}{4} \frac{(A_{jj} + A_{kk})^2}{H_2^2} \right]^{1/2} \right\} \\ \pm \frac{1}{2} H_1 \left\{ \left[1 + \frac{1}{4} \frac{(A_{jj} - A_{kk})^2}{H_1^2} \right]^{1/2} + \left[1 + \frac{1}{4} \frac{(A_{jj} + A_{kk})^2}{H_1^2} \right]^{1/2} \right\}, \quad (5)$$

where H_2 and H_1 are the high and low resonance absorption field values of the ^{13}C hyperfine structure components, $H_+ = 2H_0$, $H_- = A_{ii}$ and where H_0 is the central field position associated with ^{13}C . Beginning with the values of A_{zz} , A_{xx} and A_{yy} obtained from second-order perturbation calculations, the foregoing expression was used to obtain the components of the hyperfine structure tensor by applying iterations which were found to rapidly converge. In addition, the values of g_{ii} given by $h\nu/\beta H_0$ for the ^{13}C isotopically substituted CO_2^- molecule-ions were obtained from this expression and were found, within experimental error, to be the same as those for the more abundant ^{12}C species.

REFERENCES

- [1] OVENALL, D. W., and WHIFFEN, D. H., 1960, *Proc. chem. Soc.*, p. 420.
- [2] OVENALL, D. W., and WHIFFEN, D. H., 1961, *Mol. Phys.*, **4**, 135.
- [3] BRIVATI, J. A., KEEN, N., SYMONS, M. C. R., and TREVALIAN, P. A., 1961, *Proc. chem. Soc.*, p. 66.
- [4] ATKINS, P. W., KEEN, N., and SYMONS, M. C. R., 1962, *J. chem. Soc.*, p. 2873.
- [5] KEMP, J. C., 1960, AFOSR Report No. TN-60-509.

- [6] KEMP, J. C., 1960, *J. chem. Phys.*, **33**, 1269.
- [7] KEMP, J. C., 1961, *J. chem. Phys.*, **35**, 377.
- [8] COHEN, M. H., KANZIG, W., and WOODRUFF, T. O., 1957, *Phys. Rev.*, **108**, 1096.
- [9] CASTLE, J. G., and BERINGER, R., 1950, *Phys. Rev.*, **80**, 114.
- [10] CHANTRY, G. W., HORSFIELD, A., MORTON, J. R., and WHIFFEN, D. H., 1962, *Mol. Phys.*, **5**, 589.
- [11] BIRD, G. R., 1956, *J. chem. Phys.*, **25**, 1040.
- [12] MOORE, G. E., 1943, *J. opt. Soc. Amer.*, **43**, 1045.

Die $^1\Sigma$ - und $^3\Sigma$ -Energiekurven von zweiatomigen Systemen mit zwei Elektronen

von H. PREUSS

Max-Planck-Institut für Physik und Astrophysik, München

(Received 2 September 1963)

Mit einem einzigen Variationsansatz werden die Energiekurven der Verbindungen H_2 , HeH^+ , He_2^{++} und LiH^{++} für die Zustände $^1\Sigma$ und $^3\Sigma$ berechnet, sowie die der Eielektronenmoleküle H_2^+ und HeH^+ . Die Ergebnisse werden in Form von Kurven angegeben, wobei auch der Zusammenhang zwischen den Parametern des Variationsansatzes und dem Kernabstand graphisch dargestellt wird.

In der Einleitung wird auf die Bedeutung von Potentialkurven zweiatomiger Systeme für die Bestimmung von Energiehyperflächen drei- und vieratomiger Systeme eingegangen, die zur wellenmechanischen Behandlung der chemischen Reaktionsvorgänge notwendig sind.

1. EINLEITUNG

Fast alle chemischen Reaktionen, die in der Natur beobachtet werden, setzen sich aus einer Reihe von sogenannten Elementarreaktionen (elementary processes, reaction steps) zusammen (komplexe Reaktionen). Nur in wenigen Fällen tritt eine Elementarreaktion allein auf. Andererseits ist es zuweilen schwierig, im Verlaufe einer komplexen Reaktion die einzelnen Reaktionsschritte nachzuweisen und die dabei auftretenden Reaktionspartner zu fixieren.

Erst die Kenntnis der einzelnen Elementarreaktionen und ihrer Geschwindigkeitskoeffizienten (rate constants, specific reaction rates) erlaubt, nach Lösung eindimensionaler Differentialgleichungen, die von verschiedener Ordnung sein können, den Verlauf einer komplexen Reaktion vorsauzusagen. Beim Zustandekommen einer chemischen Reaktion wirken somit die verschiedenen Reaktionsschritte als elementare Folge-, Neben- und Gegenreaktion zusammen [1, 2].

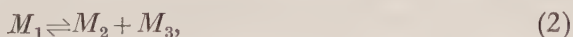
Es sind zur Zeit nur wenige Gasreaktionen bekannt, bei denen eine Aufklärung der Struktur möglich gewesen war. Chemische Reaktionen in Lösungen oder festen Körpern konnten bisher noch nicht eindeutig auf die Elementarreaktionen zurückgeführt werden.

Es besteht also die Notwendigkeit, die Elementarreaktionen experimentell und theoretisch zu erfassen, damit ein Einblick in den Mechanismus komplexer Reaktionen möglich ist [3].

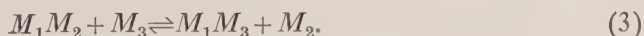
Als verschiedene Typen von Reaktionsschritten sind u.a. zu nennen, die Umwandlung



wie sie etwa zwischen bestimmten Isomeren beobachtet werden kann, der Zerfall



sowie die Austauschreaktion



Dabei bezeichnen M_1 , M_2 und M_3 bestimmte Moleküle oder Atome. Zuweilen können die Vorgänge (1) bis (3) noch in einzelne Schritte zerlegt werden, wenn Anregungen stattfinden. Etwa nach



oder



Auch der Einfluß von Katalysatoren auf die Reaktionsvorgänge läßt sich in diesem Rahmen behandeln [4, 5].

Die Frage, ob eine Reaktion ablaufen *kann*, wird mit der Berechnung des thermodynamischen Gleichgewichts beantwortet. Ein solches Gleichgewicht wird durch das Bestreben nach Verringerung der Gesamtenergie des Systems und durch das Bestreben nach Vermehrung der Unordnung (Erhöhung der Entropie) bestimmt.

Eine weitere Frage ist, mit welcher Geschwindigkeit sich das Gleichgewicht einstellt, oder, mit anderen Worten, mit welchen Geschwindigkeiten die verschiedenen Umsetzungen bei den Reaktionen verlaufen. Damit wird man auf die Bestimmung der Geschwindigkeitskoeffizienten k geführt.

Während also die chemische Thermodynamik nur Aussagen über die Gleichgewichtszustände zu liefern vermag, ist es mit Hilfe der Kinetik möglich den, zeitlichen Ablauf von Reaktionen zu bestimmen.

Nun zeigt die Erfahrung, daß nicht jeder 'Stoß' zwischen Reaktionspartnern zur Reaktion führt. Nach der kinetischen Theorie nimmt die Zahl der Stöße (bei Gasreaktionen) mit \sqrt{T} zu, während nach einer von Arrhenius empirisch gefundenen Beziehung

$$k = A \exp(-E_a/RT) \quad (6)$$

die Reaktionsgeschwindigkeit proportional einer e-Funktion ist.

Allen Reaktionen ist gemeinsam, daß eine bestimmte Energie notwendig ist, damit die Reaktion eingeleitet werden kann. Diese Energieschwelle wird im allgemeinen 'Aktivierungsenergie' genannt und spiegelt sich in der GröÙ E_a in (6) wider. Diese Interpretation ist klassisch nicht mehr verständlich zu machen, sondern verlangt zu ihrer Behandlung die Quantentheorie.

Die Beziehung (6) ist nicht in allen Fällen erfüllt. Es werden bei manchen Reaktionen T -Abhängigkeiten von k gemessen, die sich nur schwer über weite Temperaturbereiche mit Gleichung (6) darstellen lassen [1]. Es hat sich gezeigt, daß man mit

$$k = BT^n \exp(-E_b/RT) \quad (7)$$

die Verhältnisse im großen und ganzen befriedigend beschreiben kann. Man sieht daraus, daß die GröÙen E_a bzw. E_b in (6) bzw. (7) nicht so ohne weiteres mit der Vorstellung einer weitgehend temperaturunabhängigen Aktivierungsenergie verbunden werden können.

Aufgabe der quantentheoretischen Chemie ist es nun, Wege zur Berechnung der Geschwindigkeitskoeffizienten aufzuzeigen. Neben die Aktivierungsenergie, als BestimmungsgröÙe für die Reaktionsgeschwindigkeit, tritt nach (6) oder (7) noch ein sogenannter 'Wahrscheinlichkeitsfaktor' A bzw. B , der unter anderen berücksichtigt, daß nur bestimmte Stellen der Moleküle reaktionsfähig sind. Daneben geht in diesen Faktor auch die Entropieänderung ein, die bei der Reaktion stattfindet.

Jedenfalls kann aus der Tatsache, daß eine Reaktion in der Energiebilanz (Bindungsenergien, Schwingungs- und Rotationsenergien) sich als exotherm oder endotherm ergibt, nicht geschlossen werden, daß die Reaktion bei jedem Stoß in der angegebenen Richtung verläuft [2].

2. DIE ENERGIEHYPERFLÄCHEN

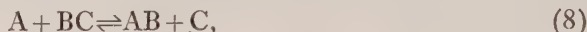
In der Quantenchemie kennen wir, neben einer Reihe von halbtheoretischen Verfahren [6], zur Berechnung von 'Aktivierungsenergien' und 'Wahrscheinlichkeitsfaktoren', also von k , hauptsächlich zwei theoretische Verfahren: Die sogenannte 'transition-state'-Theorie [7] und die zeitabhängige Störungsrechnung bewegter Atome und Moleküle in ihren verschiedenen Modifikationen [8]. Während die erste eine Abschätzung der Größen A (bzw. B) in (6) und (7) erlaubt, sowie einen Zusammenhang herstellt zwischen E_a (bzw. E_b) und den verschiedenen Energiezuständen, gestattet die zweite Methode eine Absolutberechnung von Übergangswahrscheinlichkeiten während des Reaktionsvorganges, sodaß damit jedenfalls im Prinzip die Bestimmung von Reaktionsgeschwindigkeiten möglich wird. Alle Verfahren aber, auch die halbtheoretischen, setzen die Kenntnis der Energiefunktionen von Atomsystemen voraus. Es handelt sich dabei um die Abhängigkeit der Gesamtenergie von der Lage der Atomkerne im Raum (Adiabatenflächen), deren Darstellung man Energiehyperflächen nennt [9]. Die Berechnung von Energiehyperflächen steht also im Mittelpunkt, wenn Aussagen über chemische Reaktionsvorgänge im Rahmen der Quantenchemie gewonnen werden sollen. Mit ihrer Hilfe läßt sich auch das optische Verhalten von Molekülen studieren, sowie deren geometrische Struktur in den jeweiligen Energiezuständen.

Die verschiedenen Verfahren der quantentheoretischen Chemie haben daher fast immer die Bestimmung von Energiefunktionen zum Ziel. Entweder die Lage der verschiedenen Energiehyperflächen bei nahezu festgehaltenen Atomkernen, wie etwa in der LCAO-MO-Methode [10] für aromatische und ungesättigte Verbindungen, sowie im LCBO-Verfahren [11] für Moleküle mit lokalisierten Bindungen, oder, mehr auf den Grundzustand bezogen, im Rahmen der Methode der Spinzustände [12] und im Valenzstrukturverfahren [13]. Verbesserte Energiefunktionen lassen sich, wenn auch unter größerem Rechenaufwand, aus den selbstkonsistenten Verfahren erhalten (SCF-Verfahren) [14]. Daneben gibt es noch eine Reihe weiterer Methoden, die auf verschiedenen Wegen versuchen, die Energiehyperflächen zu berechnen [15]. Die jeweiligen Verfahren legen ihr Schwergewicht entweder auf eine möglichst gute Energie als Funktion der Kernabstände, oder auf eine Berechnung der angeregten Zustände in einem kleinen Kernabstandebereich. Die zu den genäherten Energiewerten erhaltenen Dichteverteilungen lassen daneben Schlüsse zu, an welchen Positionen im Molekül die Reaktionen zu erwarten sind. Auf diese Weise ist es möglich, die Wahrscheinlichkeiten von Parallelreaktionen abzuschätzen und die während der Reaktion auftretenden oft sehr kurzlebigen Zwischenprodukte zu untersuchen.

Die Form der Energiehyperflächen kann sehr verschieden sein. Bisher ist eine einfache analytische Approximation nur im einfachsten Falle einer eindimensionalen Energiefunktion (Energiekurve) gelungen [16], wie sie bei zweiatomigen Systemen vorliegt. In allen anderen Fällen ist der Verlauf der Energie nur in der Umgebung des absoluten Minimums bestimmt worden. Zur Zeit fehlen noch

Berechnungen von Energiefunktionen, wenn die Anzahl der Atome größer als drei ist*.

Zur Behandlung einer Reaktion vom Typus



dessen Energiehyperflächen im Grundzustand $\mathcal{E}(R_{ab}, R_{bc})$ galitativ etwa das in Abb. 1 angegebene Aussehen hat, wenn lineare Anordnung der drei Atome, A, B, C, angenommen wird und kein stabiler dreiatomiger Zustand existiert,

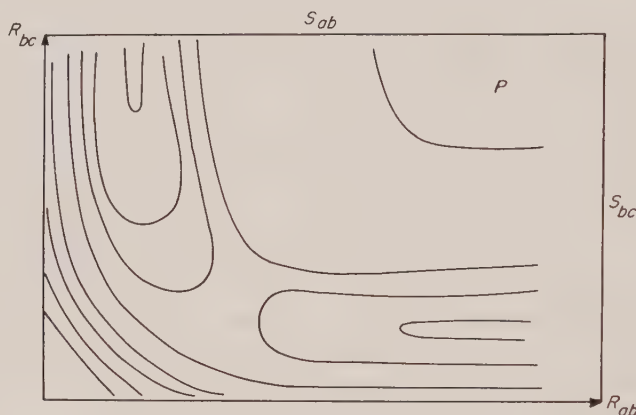


Abb. 1

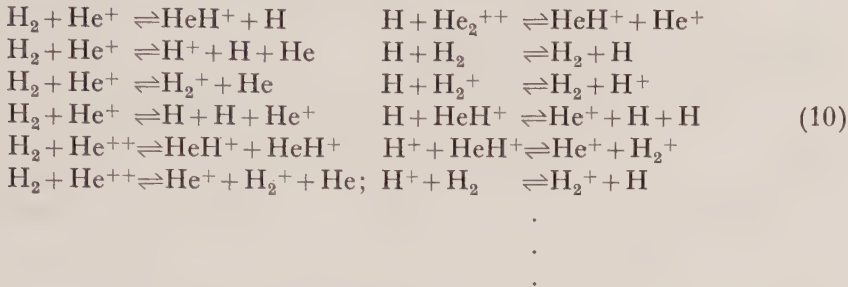
dürfte die Kenntnis der Energiefunktion zu mindestens das 'Tal' entlang notwendig sein, damit die oben angegebenen Verfahren angewendet werden können. Die senkrechten Schnitte S_{ab} und S_{bc} zeigen in der Seitensicht die Energiekurven der stabilen Gebilde BC und AB in (8). Es ist daher möglich, eine sinnvolle Interpolation der Fläche der Abb. 1 zu erhalten, wenn die Energiekurven von AB und BC als bekannt vorausgesetzt werden, sowie die Höhe der Energieebene, wo alle drei Atome unendlich weit entfernt sind [17]. Zieht man von $\mathcal{E}(R_{ab}, R_{bc})$ noch die Kernabstoßung AB,

$$E(R_{ab}, R_{bc}) = \mathcal{E}(R_{ab}, R_{bc}) - \left\{ \frac{Z_a Z_b}{R_{ab}} + \frac{Z_a Z_c}{R_{ac}} + \frac{Z_c Z_b}{R_{cb}} \right\}, \quad (9)$$

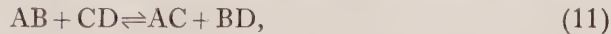
so erhält man die reine Elektronenenergie des dreiatomigen Systems, die sich für $R_{ab} \rightarrow 0, R_{bc} \rightarrow \infty$; $R_{ab} \rightarrow \infty, R_{bc} \rightarrow 0$ sowie für $R_{ab} \rightarrow 0, R_{bc} \rightarrow 0$ als Summe von Atomenergien ergibt. Auch diese Werte können zur approximativen Bestimmung von $E(R_{ab}, R_{bc})$ herangezogen werden [18]. Im Rahmen eines solchen Vorgehens gewinnt, besonders für Reaktionen, die Berechnung von Energiekurven zweiatomiger Systeme an Wert. Aus diesem Grunde sind in der vorliegenden Arbeit eine Reihe von Energiekurven mit Hilfe des Variationsverfahrens näherungsweise bestimmt worden. Es handelt sich dabei vorerst um Systeme, die zwei Elektronen enthalten, also um H_2 , HeH^+ , He_2^{++} , sowie um LiH^{++} . Daneben sind zur Vollständigkeit noch die Eielektronenmoleküle H_2^+ und HeH^{++} aufgenommen worden.

* Bezüglich Energieflächen mehratomiger Systeme verge. H. Preuss: *Theoret. chim. Acta* (im Druck).

Mit diesen Rechnungen ist dann der erste Schritt getan, um danach Approximationen für die (adiabatischen) Energiehyperflächen etwa der folgenden Reaktionen zu erhalten



Die oben angegebenen Interpolationsverfahren [17, 18] erlauben auch eine näherungsweise Bestimmung der Energiefunktionen von Reaktionen der Art



wie sie schon in den Beispielen (10) aufgenommen worden sind. In einer folgenden Arbeit soll daher unter Zugrundelegung der zweiatomigen Potentialkurven auf diese Möglichkeiten eingegangen werden.

3. DER VARIATIONSANSATZ

Der Hamiltonoperator eines zwei- bzw. einelektronischen Systems mit zwei Zentren der Ladungen Z_a und Z_b lautet in atomaren Einheiten (at. E.).

$$\mathcal{H} = -\frac{1}{2}\Delta_1 - \frac{1}{2}\Delta_2 - \left\{ \frac{Z_a}{r_{a1}} + \frac{Z_b}{r_{b1}} + \frac{Z_a}{r_{a2}} + \frac{Z_b}{r_{b2}} \right\} + \frac{1}{r_{12}}, \quad (12)$$

$$\mathcal{H} = -\frac{1}{2}\Delta - \left\{ \frac{Z_a}{r_a} + \frac{Z_b}{r_b} \right\}. \quad (13)$$

Der Variationsansatz für (12) hat hier die Form

$$\Psi = (\alpha\beta\gamma\delta) + \mu(\gamma\delta\alpha\beta) + \lambda(\beta\alpha\delta\gamma) + \lambda\mu(\delta\gamma\beta\alpha), \quad (14)$$

wobei

$$(\alpha\beta\gamma\delta) = N \exp - (\alpha r_{a1} + \beta r_{b1} + \gamma r_{a2} + \delta r_{b2}) \quad (N = \text{Normierungskonstante}). \quad (14a)$$

$\alpha, \beta, \gamma, \delta$ sowie λ und μ sind die Variationsparameter; dabei ist zu beachten, daß Ψ (neben dem Pauliprinzip) gewisse Symmetriebedingungen erfüllen muß, wenn es sich um ein gleichatomiges Molekül handelt ($Z_a = Z_b$). Bedeuten P_{ab} und P_{12} Vertauschungsoperatoren für $a \leftrightarrow b$ und $1 \leftrightarrow 2$, so gelten für (14) die folgenden Beziehungen der Tabelle 1.

Funktion	λ	μ	Symmetrien	
Ψ_1	-1	-1	$P_{ab}\Psi_1 = -\Psi_1$	$P_{12}\Psi_1 = -\Psi_1$
Ψ_2	+1	-1	$P_{ab}\Psi_2 = +\Psi_2$	$P_{12}\Psi_2 = -\Psi_2$
Ψ_3	-1	+1	$P_{ab}\Psi_3 = -\Psi_3$	$P_{12}\Psi_3 = +\Psi_3$
Ψ_4	+1	+1	$P_{ab}\Psi_4 = +\Psi_4$	$P_{12}\Psi_4 = +\Psi_4$

Tab. 1

Man erkennt daraus, daß μ die Symmetrie der Ψ -Funktion bezüglich der Elektronenvertauschung bestimmt. Ψ_1 und Ψ_2 gehören daher zu Triplett-Zuständen, während Ψ_3 und Ψ_4 Singulett-Zustände beschreiben. Es zeigt sich weiter [19], daß Ψ_4 und Ψ_1 die tiefsten Singulett- und Triplett-Zustände darstellen. Wir haben somit allgemein:

$$^1\Sigma: \Psi_4 \equiv \Psi_S = \{(\alpha\beta\gamma\delta) + (\gamma\delta\alpha\beta)\} + \lambda\{(\beta\alpha\delta\gamma) + (\delta\gamma\beta\alpha)\} \quad (15a)$$

$$^3\Sigma: \Psi_1 \equiv \Psi_A = \{(\alpha\beta\gamma\delta) - (\gamma\delta\alpha\beta)\} + \lambda\{(\beta\alpha\delta\gamma) - (\delta\gamma\beta\alpha)\}, \quad (15b)$$

wobei für gleichatomige Systeme ($Z_a = Z_b$) der Wert von $\lambda = +1$ in (15a) sein muß, dagegen ist in (15b) $\lambda = -1$ zu setzen. Ist dagegen $Z_a \neq Z_b$, so kann λ noch als Variationsparameter verwendet werden.

Die Variation der Parameter α , β , γ und δ kann nicht in beliebigen Bereichen durchgeführt werden. Bei der Ausführung der Normierung von (15) zeigt sich, daß diese nur für

$$\alpha + \beta > 0 \quad \gamma + \delta > 0 \quad (16)$$

möglich ist. Daneben ergibt sich, daß für bestimmte Parameterwerte die Variationsfunktion identisch verschwindet. Die folgende Tabelle 2 gibt diese Werte als Funktion von λ und μ wieder. Bei der Variation dürfen daher diese Gebiete im $\alpha\beta\gamma\delta$ -Raum nicht benutzt werden.

$\mu \backslash \lambda$	-1	0	+1
-1	$\alpha = \gamma \neq \beta = \delta$ $\alpha = \beta = \gamma = \delta$ $\alpha = \beta \neq \gamma = \delta$	$\alpha = \gamma \neq \beta = \delta$ $\alpha = \beta = \gamma = \delta$	$\alpha = \delta \neq \beta = \gamma$ $\alpha = \beta = \gamma = \delta$ $\alpha = \gamma \neq \beta = \delta$
+1	$\alpha = \delta \neq \beta = \gamma$ $\alpha = \beta = \gamma = \delta$ $\alpha = \beta \neq \gamma = \delta$	—	—

Tab. 2

Die Ansätze (15) sind sehr variabel und gehen für bestimmte Parameterwerte in schon früher bekannte über. So liefert zum Beispiel

$$\begin{aligned} \alpha &= Z_a & \gamma &= 0 \\ \beta &= 0 & \delta &= Z_b, \end{aligned} \quad (17)$$

bis auf eine Konstante, die bekannten Heitler-London-Funktionen [20]

$$\Psi_{\text{HL}} = \left\{ \begin{aligned} &(Z_a 00 Z_b) + (0 Z_a Z_b 0) \quad ^1\Sigma, \\ &(Z_a 00 Z_b) - (0 Z_a Z_b 0) \quad ^3\Sigma, \end{aligned} \right\} \quad (18)$$

die für $R \rightarrow \infty$ exakte Lösungen des Problems (12) darstellen. Wird dagegen

$$\left. \begin{aligned} \alpha &= \delta = p \\ \beta &= \gamma = 0 \end{aligned} \quad \text{oder} \quad \begin{aligned} \beta &= \gamma = p \\ \alpha &= \delta = 0 \end{aligned} \right\} \quad (19)$$

gesetzt, so erhält man einen Ansatz von Wang [21], in welchem p als Variationsparameter auftritt

$$\Psi_w = \left\{ \begin{aligned} &(p 00 p) + (0 p p 0) \quad ^1\Sigma \\ &(p 00 p) - (0 p p 0) \quad ^3\Sigma \end{aligned} \right\} \quad (20)$$

(18) sowie (20) stellen die sogenannten kovalenten Anteile der Zweielektronenbindung dar. Für

$$\alpha = \gamma = p \quad \text{oder} \quad \beta = \delta = p \quad (21 a)$$

$$\beta = \delta = 0 \quad \text{oder} \quad \alpha = \gamma = 0 \quad (21 b)$$

wenn $\lambda = \mu = 1$, geht (15 a) dagegen in einen reinen Ionenterm über, denn wir erhalten, wieder bis auf eine Konstante,

$$\Psi_I = (p0p0) + (0p0p). \quad (22)$$

Wird dabei λ noch frei gehalten, so ist λ in

$$\Psi_{I\lambda} = \begin{cases} (p0p0) + \lambda(0p0p) & \text{(nach (21 a))} \\ (0p0p) + \lambda(p0p0) & \text{(nach (21 b))} \end{cases} \quad (23)$$

ein Maß für das Verhältnis der Strukturen, bei denen die beiden Elektronen entweder bei a oder b sind. Schließlich folgt für $\alpha = \beta = \gamma = \delta = p$ und $\lambda = 0$, $\mu = 1$ der Ansatz

$$\Psi_{JCP} = (pppp), \quad (24)$$

der in einer Rechnung von James, Coolidge und Present [22] als nullte Näherung für den $^1\Sigma$ -Zustand verwendet wurde.

Für $R \rightarrow 0$ gehen die Gleichungen (15) bis auf eine Konstante über in

$$\Psi_{\Lambda S}(R=0) = \begin{cases} (\alpha + \beta 00\gamma + \delta) + (\gamma + \delta 00\alpha + \beta) \, ^1S, \\ (\alpha + \beta 00\gamma + \delta) - (\gamma + \delta 00\alpha + \beta) \, ^3S, \end{cases} \quad (25)$$

wobei in den Ausdrücken (14 a) $a=b$ gesetzt werden muß. Diese Ansätze sind bei der Berechnung von Helium und der heliumähnlichen Ionen als sogenannte 'open-shell'-Funktionen bekannt [23].

In den letzten Jahren sind einige Spezialfälle von (15 a) als Variationsansätze für H_2 verwendet worden. So zum Beispiel [24]

$$\Psi' = (\alpha\beta\beta\alpha) + (\beta\alpha\alpha\beta), \quad (26)$$

oder [25].

$$\Psi'' = (\alpha\beta\alpha\beta) + (\beta\alpha\beta\alpha). \quad (27)$$

Von Harris [26] wurde mit dem Ansatz

$$\Psi''' = (\alpha 0 \beta \gamma) + (\beta \gamma \alpha 0) \quad (28)$$

gerechnet und schließlich wurde angesetzt [27]

$$\Psi''' = c_A \{ \alpha 0 0 \alpha \} + (0 \alpha \alpha 0) + c_B \{ (\beta \beta \gamma \gamma) + (\gamma \gamma \beta \beta) \}, \quad (29)$$

und die Energie von H_2 in α , β und γ sowie c_A/c_B minimisiert. Die tiefsten Energien der Ansätze Ψ' bis Ψ''' betragen $-0,1493$ at. E ; $-0,1544$ at. E ; $-0,1529$ at. E und $-0,1553$ at. E , wenn die Energie der getrennten Atome abgezogen wurde. Die wirkliche Bindungsenergie ist $-0,1764$ at. E ($-4,74$ eV). Die berechneten Bindungsabstände nach (26) bis (29) betrugen alle $1,41$ at. E und stimmen mit dem exakten Wert überein.

Die Ergebnisse lassen erkennen, daß mit den Ansätzen ein Teil der Bindungsenergie nicht erfaßt wird. Man kann dies auf folgende Weise zeigen. Führen wir für jedes Elektron elliptische Koordinaten ein [19]

$$r_a + r_b = R\mu, \quad r_a - r_b = R\nu, \quad \phi, \quad (30)$$

wobei der Winkel ϕ um die Verbindungsachse der beiden Atome zählt, so

läßt sich die exakte Lösung des Operators (12) in eine Fourierreihe nach $\cos [m(\phi_1 - \phi_2)]$ bzw. $\sin [m(\phi_1 - \phi_2)]$ entwickeln.

$$\Psi_{\text{exakt}} = \sum_{m=0}^{\infty} \chi_m(\mu_1 \mu_2 \nu_1 \nu_2) \left\{ \begin{array}{l} \cos [m(\phi_1 - \phi_2)], \\ \sin [m(\phi_1 - \phi_2)]. \end{array} \right\} \quad (31)$$

Betrachtet man den Ausdruck (14) und führt in diesen elliptische Koordinaten ein, so sieht man, daß alle bisher diskutierten Ansätze nicht von ϕ_1 und ϕ_2 abhängen. Mit den Variationsansätzen wird daher die 'beste' Funktion in $\mu_1 \mu_2 \nu_1$ und ν_2 gesucht. Man berücksichtigt damit nicht die 'Winkelkorrelation' der Elektronen [28]. χ_0 liefert also die tiefste Energie, wenn nur die Radialkoordinaten der Elektronen verwendet werden [29]. Man bezeichnet diesen Grenzwert der Energie, der von den oben angegebenen Variationsansätzen im besten Falle erreicht werden kann, als σ -Grenze der Energie, da für diese Funktionen die Projektion des Drehimpulses auf die Kernverbindungsachse verschwindet.

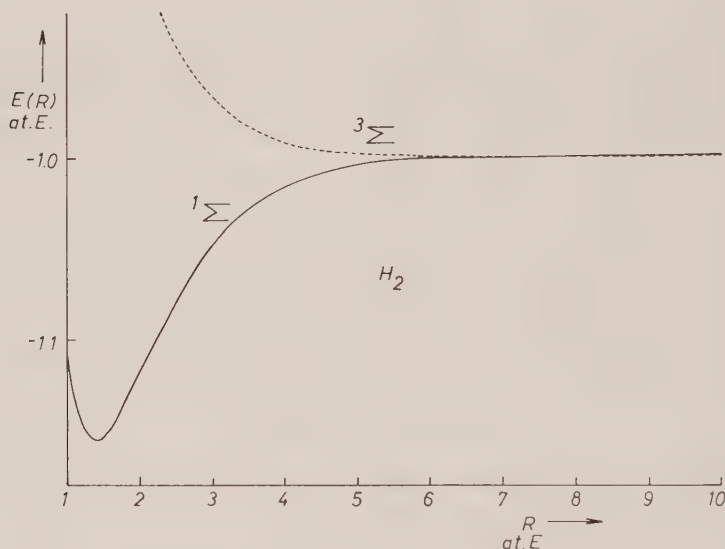


Abb. 2

Mit dem Ansatz (14) wird daher eine gute Approximation der σ -Grenze von zweielektronischen Zweizentren-Systemen zu erwarten sein. Für die meisten Fälle dürfte eine solche Näherung ausreichen. Im Falle des H_2 -Moleküls scheint diese Abweichung nach den bisherigen Rechnungen etwa 0,5 eV zu betragen.

Für das Einelektronensystem (12 a) wurde, entsprechend (14), mit dem Ansatz

$$\Psi = \begin{cases} (\alpha\beta) + \lambda(\beta\alpha) & \sigma \text{ 1s bzw. } z\sigma \\ (\alpha\beta) - \lambda(\beta\alpha) & \sigma^* \text{ 1s bzw. } y\sigma \end{cases} \quad (32a)$$

$$(32b)$$

die Energie zum Minimum gemacht. Die Funktion (32 a) für $\lambda = 1$ stimmt mit dem Ansatz von Guillemin und Zener [30] überein, der für H_2^+ verwendet wurde und dort praktisch die exakte Energie von $-0,602$ at. E bei $R_{\min} = 1,99$ at. E lieferte.

Fast alle bisher durchgeführten Variationsrechnungen bestimmen nur die tiefste Energie und den dazugehörigen Bindungsabstand. Für die in der Einleitung genannten Gründe ist es notwendig, die Potentialkurven für einen größeren

R -Bereich zu kennen, sowie die für jedes R vorliegende Näherungsfunktion. Aus diesem Grunde werden hier die Parameter in (14) auch als Funktionen von R berechnet.

4. DIE ENERGIEVARIATION UND IHRE ERGEBNISSE

Die Energie $E(R)$ ergibt sich mit (14) und (14a) in der Form

$$E = \frac{A'}{R} + \frac{B'}{R^2} \quad (33)$$

wobei A' und B' Funktionen von Z_a , Z_b , sowie von $\alpha R = \bar{\alpha}$, $\beta R = \bar{\beta}$, $\gamma R = \bar{\gamma}$, $\delta R = \bar{\delta}$ und λ sind. Für (32a, b) kommen in A' und B' neben Z_a , Z_b nur $\bar{\alpha}$ und $\bar{\beta}$ vor. Die Rechnungen wurden so vorgenommen, daß bei fixiertem R , E in α , β , γ , und δ minimiert wurde. Die Ergebnisse sind in den Figuren 2 bis 5 für die Systeme H_2 , He_2^{++} , HeH^+ und LiH^{++} graphisch dargestellt. Die Figuren 6 und 7 enthalten die entsprechenden Kurven für HeH^{++} und H_2^+ . Einige davon enthalten Energieminima E_{\min} ; diese sind, zusammen mit den entsprechenden Gleichgewichtsabständen R_{\min} , in der Tabelle 3 zusammengefaßt worden. Tabelle 3 enthält darüberhinaus noch die Energien, die sich nach (14), (14a) für $R \rightarrow \infty$ ergeben, sowie die Angaben der getrennten Atome für die jeweilige Kurve.

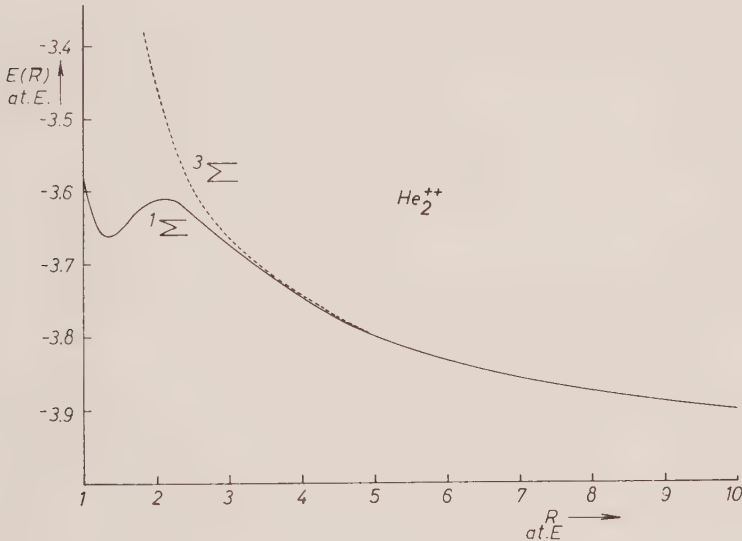


Abb. 3

Schließlich sind in den Figuren 8 bis 11 die Parameter λ , $\bar{\alpha}$, $\bar{\beta}$, $\bar{\gamma}$ und $\bar{\delta}$ als Funktion des Kernabstandes angegeben worden. Die gestrichelten Kurven gehören zum $^3\Sigma$ -Zustand.

Die Rechnungen wurden mit der elektronischen Rechenmaschine G3 durchgeführt. Die auftretenden Integrale in A' und B' von (33) sind nach bekannten Standardmethoden bestimmt worden [31], wobei die vorliegenden Integraltabellen von großem Nutzen waren [32].

5. DISKUSSION DER ERGEBNISSE

5.1. H_2 -Molekül

Einige vergleichbare Rechnungen sind schon im Abschnitt 3 besprochen worden. Mit dem Wert $-0,1554$ at. E bei $R_{\min}=1,411$ at. E (Tab. 3) dürfte wohl etwa die σ -Grenze erreicht sein. Das Ergebnis der Tab. 3 für H_2 liegt nur wenig tiefer als das des Ansatzes (29). Tiefere Energiewerte sind bisher mit einem Ansatz, der keine Winkelkorrelation enthält, noch nicht erhalten worden.

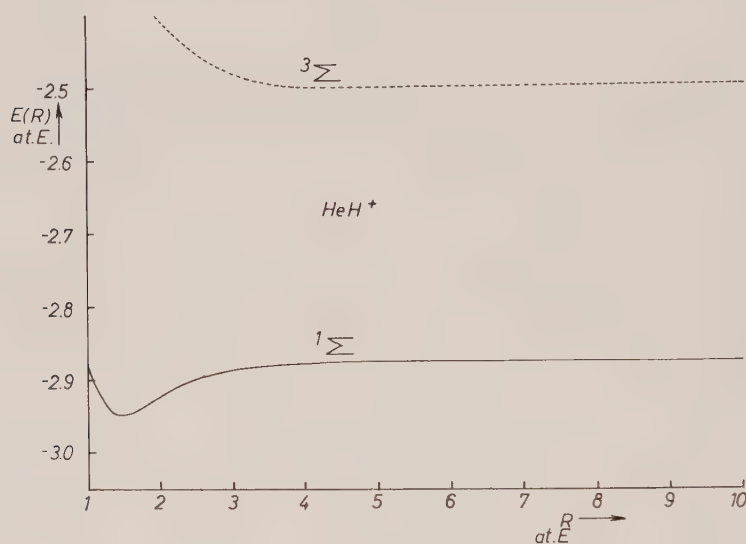


Abb. 4

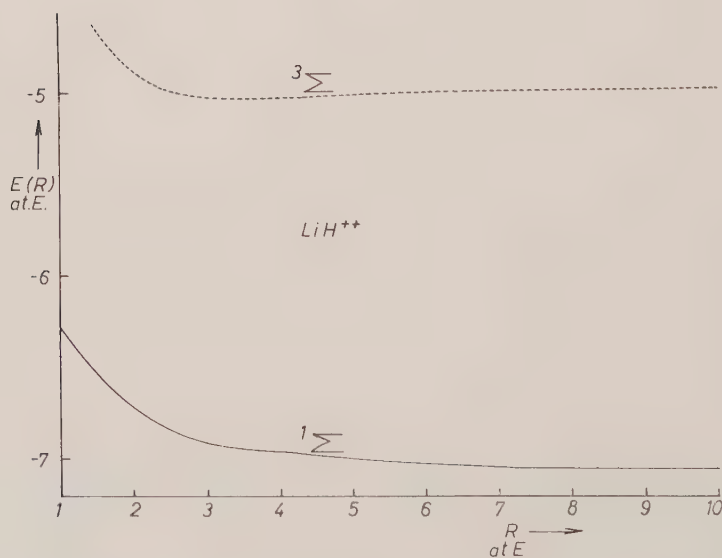


Abb. 5

Der Wert $-0,1554$ at. E , der hier berechnet wurde, entspricht $-4,22$ ev. Es ist bemerkenswert, daß mit Ansätzen, die den Abstand r_{12} der Elektronen enthalten, [34] wie etwa

$$\Psi = \{(\alpha 0 \alpha 0) + (0 \alpha 0 \alpha) + (\alpha 0 0 \alpha) + (0 \alpha \alpha 0)\}(1 + p r_{12}) \quad (34)$$

oder [35]

$$\Psi = \{(\alpha 0 \alpha 0) + (0 \alpha 0 \alpha) + \beta[(\alpha 0 0 \alpha) + (0 \alpha \alpha 0)]\}(1 + p r_{12}) \quad (35)$$

auch nur $-4,11$ ev bzw. $-4,14$ ev berechnet worden sind. Dagegen lieferte eine Variationsfunktion, die die gegenseitige Polarisierung der H-Atome berücksichtigte [35] $-4,24$ ev. Der Ansatz enthielt unter anderen auch die kartesischen Koordinaten x, y der beiden Elektronen als Faktoren zu Exponentialausdrücken. Alleinige Berücksichtigung der Polarisierung in der Form [36]

$$\Psi = (\alpha 0 \alpha 0)\{1 + p z_{a1}\}\{1 + p z_{b2}\} + (0 \alpha \alpha 0)\{1 + p z_{a2}\}\{1 + p z_{b1}\} \quad (36)$$

ergibt im Minimum nur eine Bindungsenergie von $-4,02$ ev. Der Ansatz (36) enthält nach (31) keine Winkelkorrelation. Interessant ist noch die Funktion

$$\Psi = \exp[-\alpha(r_{c1} + r_{d2})] + \exp[-\alpha(r_{c2} + r_{d1})], \quad (37)$$

bei der die Zentren c und d symmetrisch und variabel von a und b nach innen verschoben angenommen wurden [37]. Dieser Ansatz, der ebenfalls keine Winkelkorrelation enthält, liefert den erstaunlich guten Wert von $-4,15$ ev.

Molekül	$^1\Sigma$			$^3\Sigma$		
	R_{\min}	E_{\min}	$\frac{A+B}{E(A)+E(B)}$	R_{\min}	E_{\min}	$\frac{A+B}{E(A)+E(B)}$
H_2	1,411	$-1,15540$	$\frac{H+H}{-1,0}$	—	—	$\frac{H+H}{-1,0}$
HeH^+	1,442	$-2,94920$	$\frac{He+H^+}{-2,8757}$	4,51	$-2,50260$	$\frac{He^++H}{-2,5}$
He_2^{++}	1,332	$-3,66301$	$\frac{He^++He^+}{-4,0}$	—	—	$\frac{He^++He^+}{-4,0}$
LiH^{++}	—	—	$\frac{Li^++H^+}{-7,249}$	3,488	$-5,03874$	$\frac{Li^{++}+H}{-5,0}$
H_2^+	1,998	$-0,60244$	$\frac{H+H^+}{-0,5}$	—	—	$\frac{H+H^+}{-0,5}$
HeH^{++}	—	—	$\frac{He^++H^+}{-2,0}$			

Tab. 3

In Abb. 8 sind die Parameter als Funktion von R für H_2 nach (15) angegeben worden. Charakteristisch ist, daß sich $\bar{\alpha}$ und $\bar{\delta}$ wesentlich größer als $\bar{\gamma}$ und $\bar{\beta}$ ergeben, wobei die beiden letzteren nahezu gleich sind. Das deutet daraufhin, daß der erweiterte Heitler-London-Ansatz (20) schon eine gute Näherung ist und das wesentliche Verhalten der Ψ -Funktion erfaßt. Das gilt auch für den Triplett-Zustand. Das lineare Ansteigen von $\bar{\alpha}$ und $\bar{\delta}$ zeigt darüber hinaus, daß schon ab $R > 5$ at. E die Beziehungen (19) erfüllt sind. Der Parameter p

in (19) ergibt sich aus Abb. 8 ab $R > 5$ at. E zu nahezu 1, sodaß der Ansatz (18) mit $Z_a = Z_b = 1$ schon ab diesen R -Werten im wesentlichen die Lösung beschreibt. Bezüglich weiterer Rechnungen am H_2 sei auf die Arbeit [47] hingewiesen.

Für $R \rightarrow 0$ werden dann, in Übereinstimmung mit anderen Rechnungen, nach (25) die Werte $\alpha + \beta = 2,1832$ und $\gamma + \delta = 1,1886$ erhalten. Die Energie des Heliums ergibt sich mit dem Ansatz (25) zu $-2,8757$ at, während $-2,9037$ at. E der exakte Wert ist [23].

Für sehr große Kernabstände durchläuft die Triplett-Kurve ein sehr schwaches Minimum [38, 35]. Die Rechnungen mit dem Ansatz (15 b) lieferten keine weitere Vertiefung dieses Minimums.

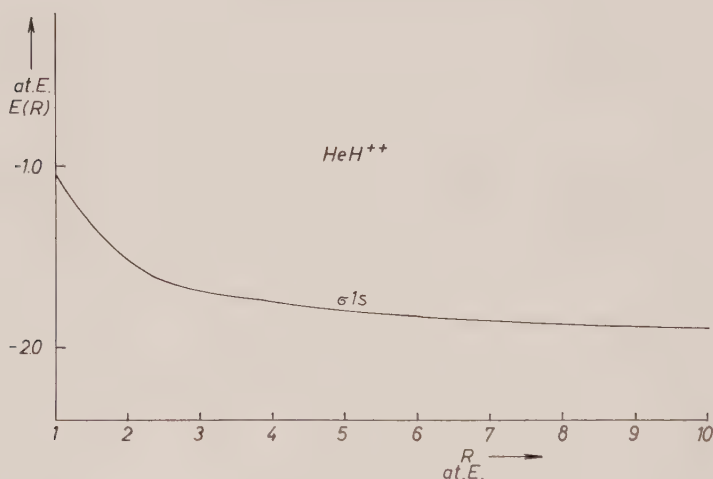


Abb. 6

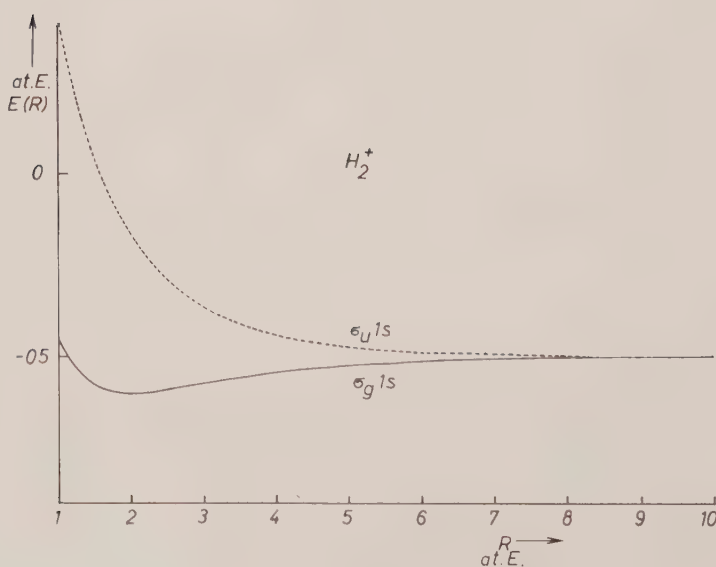


Abb. 7

5.2. HeH⁺-Molekül

Diese Verbindung, die massenspektroskopisch nachgewiesen ist [39, 49], wurde das erste Mal von Beach berechnet [40] (man vergl. auch [50]). Er fand bei einem Bindungsabstand von $R_{\min} = 1,57$ at. E eine tiefste Energie von $-2,922$ at. E ($^1\Sigma$ -Zustand). Bezogen auf die exakte Energie des Heliums liefert dieser Wert eine obere Schranke für die Bindungsenergie von $-0,49$ ev. Leider sind

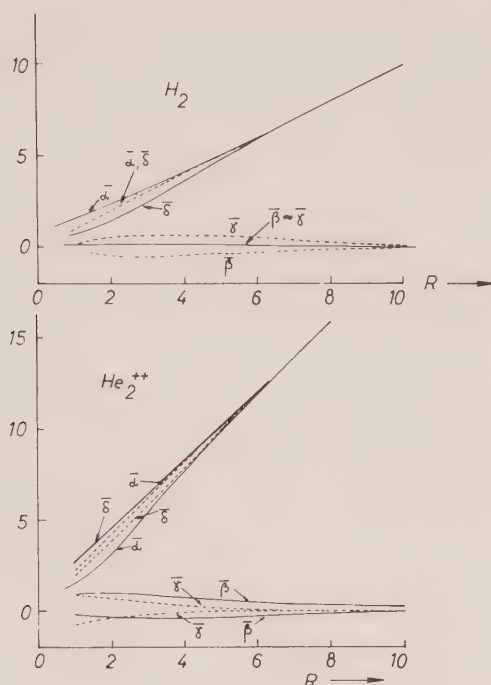


Abb. 8

bisher keine Daten über Bindungsabstand und Energie dieser Verbindung bekannt. Der in der Rechnung [40] verwendete Variationsansatz hatte die Form

$$\Psi = (\alpha 0 \alpha 0) + p_1 \{(\alpha' 0 \alpha 0) + (\alpha 0 \alpha' 0)\} + p_2 \{(\alpha 0 0 \alpha) + (0 \alpha \alpha 0)\} \quad (38)$$

in welchem α , p_1 und p_2 variiert wurden. α' bedeutet, daß im Ausdruck (14 a) an Stelle der $1s$ -Funktion eine $2p\sigma$ -Funktion eingesetzt ist.

$$(\alpha' 0 \alpha 0) = z_{a1} \exp[-\alpha(r_{a1} + r_{a2}^p)]. \quad (38a)$$

Wenn die effektive Abschirmzahl in der $2p\sigma$ -Funktion gesondert variiert wurde [41], so resultierte eine Energie von $-2,9327$ at. E . Der Bindungsabstand betrug dabei $1,446$ at. E . Dagegen lieferte eine Rechnung [41] mit dem Ansatz

$$\Psi = \exp[-\delta(\mu_1 + \mu_2)] \sum_{n,m,j,k} c_{mnjkp} (\mu_1^m \mu_2^n \nu_1^j \nu_2^k + \mu_1^n \mu_2^m \nu_1^k \nu_2^j) r_{12}^p \quad (39)$$

wobei die elliptischen Koordinaten μ und ν in (30) erklärt sind, nur den Wert $-2,9161$ at. E , obwohl die folgenden Terme berücksichtigt worden waren

$$r_1 + r_2, r_1^2 + r_2^2, r_1 r_2, r_{12}. \quad (39a)$$

Wurde an Stelle von r_{12} der Ausdruck $\mu_1 + \mu_2$ in (39) verwendet, so resultierte sogar nur $-2,9072$ at. E , ein Wert, der nur um $-0,0032$ at. E tiefer als der des Heliums liegt. Erst nach Verwendung von 12 Termen in (39), wobei zwei davon

r_{12} enthielten, konnte Toh [42] den bisher besten Energiewert von $-2,9506$ at. E erhalten. Der Bindungsabstand ergab sich dabei zu $1,346$ at. E . Die Bindungsenergie beträgt hier $-1,275$ ev.

Der Ansatz (15 a) liefert schon fast die gleiche Energie im Minimum, nämlich $-2,9492$ at. E (Tab. 3), was einer Bindungsenergie von $-1,237$ ev entspricht. Dagegen wird ein Bindungsabstand von $1,442$ at. E erhalten, der den Ergebnissen der früheren Rechnungen [41] sehr nahe liegt. Diese Anweichung ist unverstündlich.

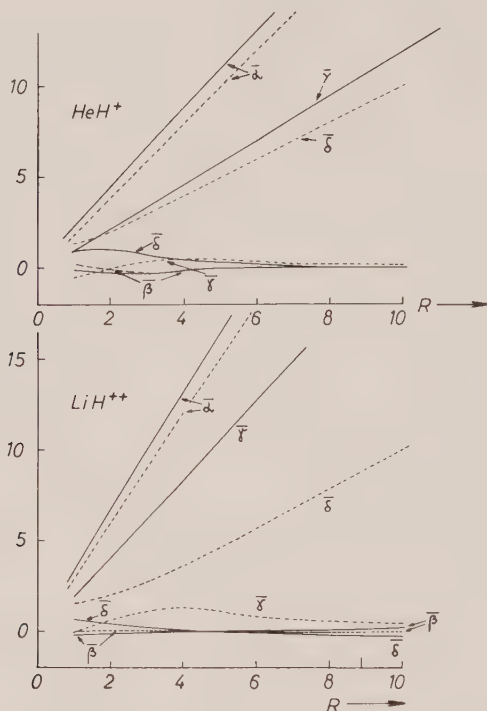


Abb. 9

Der Verlauf der Parameter $\bar{\alpha}$, $\bar{\beta}$, $\bar{\gamma}$ und $\bar{\delta}$ für $^1\Sigma$ in Abb. 9 zeigt, daß sich, im Gegensatz zu den Verhältnissen in H_2 , $\bar{\alpha}$, und $\bar{\gamma}$ wesentlich größer als $\bar{\beta}$ und $\bar{\delta}$ ergeben. Der nahezu lineare Verlauf von $\bar{\alpha}$ und $\bar{\gamma}$, wobei für große R , $\bar{\beta}$ und $\bar{\delta}$ verschwinden, und die Kleinheit von λ (Abb. 11) zeigen, daß nur der Ionenzustand $\text{He} + \text{H}^+$, der auch als erster Term in (38) vorkommt, den wesentlichen Anteil an der Darstellung der Eigenfunktion hat; ein Hinweis darauf, daß für große R das Molekül in ein Heliumatom und ein Proton zerfällt. Aus Abb. 9 folgt weiter, daß für $R > 5,0$ at. E . der Ionenzustand, bei dem beide Elektronen beim Helium sind, schon fast vollständig zur Beschreibung des Systems ausreicht.

Alle Rechnungen zeigen eindeutig, daß der $^1\Sigma$ -Zustand für $R \rightarrow \infty$ in die beiden Gebilde He und H^+ zerfällt, so daß ein Zerfall in He^+ und H , wie kürzlich vermutet wurde [43], ausgeschlossen ist.

Für kleine R ($R < 2$ at. E) kommt $\bar{\delta}$ in die Größenordnung von $\bar{\gamma}$, was bedeutet, daß in diesen Bereichen, neben dem Ionenzustand $\text{He} - \text{H}^+$, auch kovalente Anteile eine wesentliche Rolle spielen. Die Elektronenenergie geht für $R \rightarrow 0$ in

die des Li^+ über. Der Variationsansatz (15 a), der dann die Form (25) annimmt, liefert für $\alpha + \beta = 3,2949$ und $\gamma + \delta = 2,0789$ einen Energiewert von $-7,2490$ at. E [23]. Der exakte Wert für Li^+ beträgt $-7,2799$ at. E .

Die Tatsache, daß auch Ansätze mit r_{12} keine wesentliche Energieminderung gegenüber unserem Wert erbrachten (s. (39)), kann bedeuten, daß in Bereich des Bindungsabstandes die Winkelkorrelation im HeH^+ geringer als im H_2 -Molekül ist.

Der Triplett-Zustand von HeH^+ ist bisher noch nicht berechnet worden. Neu ist daher, daß in diesem Falle für $R_{\min} = 4,51$ at. E ein schwaches Energieminimum von $-2,5026$ at. E vorliegt, was einer 'Bindungsenergie' von $-0,07$ ev entspricht. Ob in dieser flachen Energiemulde ein stabiler Zustand existiert,

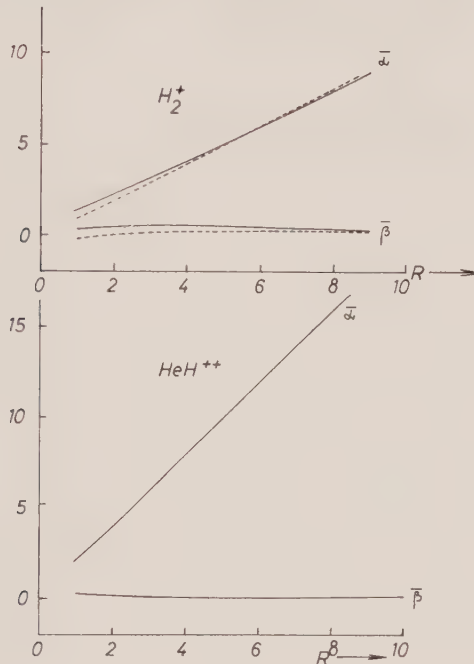


Abb. 10

müßte noch genauer untersucht werden. Interessant ist der Verlauf der Parameter im $^3\Sigma$ -Zustand (Abb. 9). Es handelt sich hier um eine vorwiegend kovalente Bindung, da jetzt $\bar{\alpha}$ und $\bar{\delta}$ die beiden größten Parameter sind. Im Einklang damit steht, daß der $^3\Sigma$ -Zustand für $R \rightarrow \infty$ in die Atome He^+ und H übergeht. Trotzdem ist im Bereich $3,0 \leq R \leq 5,0$ auch ein Ionenzustand merklich an der Bindung beteiligt, da $\bar{\gamma}$ in diesem Bereich ein schwaches Maximum durchläuft (Abb. 9). Das Zusammenwirken beider Bindungsformen dürfte die Ursache des Minimums sein.

Aus Abb. 11 folgt noch, daß der Wert von λ , welcher hier ebenfalls Variationsparameter ist, für $R \geq 1,0$ at. E . nahe Null erhalten wird. Das gilt für beide Zustände $^1\Sigma$ und $^3\Sigma$ und bedeutet, daß im Falle der Ionenbindung des $^1\Sigma$ -Zustandes nach (23) nur die Struktur, wo beide Elektronen beim Helium sind, eine Rolle spielt. Im Triplett-Zustand durchläuft λ bei $R \approx 2,5$ at. E . noch ein

ganz schwaches Maximum; die wesentlich kovalente Bindung nach (15 b) kann also schon mit $\lambda=0$ beschrieben werden.

5.3. He_2^{++} -Molekül

Die berechnete Energie der $^1\Sigma$ -Kurve ist in Abb. 3 dargestellt. Sie kann als Überlagerung einer kovalenten Bindung mit der Abstoßungskurve der beiden Ionen $\text{He}^+ - \text{He}^+$ verstanden werden [45], worauf auch das lineare Anwachsen von $\bar{\alpha}$ und $\bar{\delta}$ (Abb. 8) mit R und die kleinen Werte von $\bar{\beta}$ und $\bar{\gamma}$ hinweisen. Im $^3\Sigma$ -Zustand wird daher, bei gleichem Verhalten der Parameter, nur die Abstoßungskurve $1/R$ erhalten. Für $R \rightarrow 0$ liefert unser Ansatz eine Elektronenenergie des Be^{++} von $-13,6230$ at. E (exakter Wert: $-13,6558$ at. E).

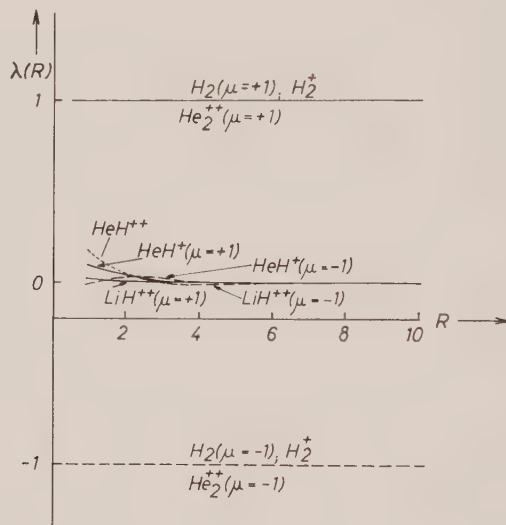


Abb. 11

Das He_2^{++} -Molekül ist auf Grund seiner Potentialkurve eine sogenannte metastabile Verbindung [48]. Leider fehlen noch Messungen über Gleichgewichtsabstand und Bindungsenergie. Pauling [44], der den $^1\Sigma$ -Grundzustand mit einer Linearkombination von kovalenten und ionischen Anteilen nach (20) und (22) als Variationsfunktion berechnete, erhielt bei 1,420 at. E . ein Energieminimum von etwa $-3,63$ at. E . Das Maximum wurde bei dieser Rechnung im Abstand $R=2,03$ at. E . gefunden. Die Energiedifferenz der beiden Werte von Minimum und Maximum ergab sich dabei zu $-0,0514$ at. E . $= -1,4$ ev und muß als die Bindungsenergie des He_2^{++} -Moleküls betrachtet werden.

Die bisher genaueste Rechnung wurde mit 40 Termen des Ansatzes (39) durchgeführt [46]. Sie lieferte ein Minimum von $-3,6798$ at. E . bei $R_{\min}=1,32$ at. E . Leider wurden Lage und Größe des Energiemaximums nicht numerisch angegeben.

Im Vergleich zu diesen Rechnungen liegt unser Ergebnis im Minimum ($R_{\min}=1,33$ at. E) nur um $0,0168$ at. E . höher (Tab. 3). Daraus muß der Schluß

gezogen werden, daß die Winkelkorrelation in diesen R -Bereichen des He_2^{++} -Moleküls sehr klein ist.

Man sieht daraus, daß schon mit einer 4-parametrischen Näherungsfunktion eine gute Approximation der Energiekurve erhalten werden kann.

Die $^3\Sigma$ -Kurve wurde bisher noch nicht berechnet.

5.4. Das System $(\text{LiH})^{++}$

Die Potentialkurven von (LiH^{++}) wurden bisher noch nicht quantentheoretisch bestimmt. Die $^1\Sigma$ -Kurve des Grundzustandes liefert Abstoßung für alle R -werte und ergibt für $R \rightarrow \infty$, Li^+ und ein Proton (Abb. 5). In Einklang damit zeigt der Verlauf der Parameter als Funktion des Kernabstandes, daß vorwiegend eine starke Ionenwechselwirkung vorliegt (Abb. 9). Die Elektronenenergie ergibt sich für $R \rightarrow 0$ zu der des Be^{++} , wie dies schon beim He_2^{++} der Fall gewesen ist.

Überraschend zeigt die Kurve des Triplett-Zustandes bei $R_{\min} = 3,488$ at. E . ein Energieminimum von $-5,03874$ at. E . Da die $^3\Sigma$ -Kurve für große R die Dissoziationsprodukte Li^{++} und H liefert, deren Gesamtenergie exakt $-5,0$ at. E . beträgt, so ist damit eine obere Grenze für die Bindungsenergie des LiH^{++} -Moleküls im Triplettzustand von $-1,06$ ev gefunden. Dieser Wert ist rund 15 mal größer als die 'Bindungsenergie' des HeH^+ -Triplett-Zustandes (Tab. 3). Die Größenverhältnisse der Parameter $\tilde{\alpha}$, $\tilde{\beta}$, $\tilde{\gamma}$ und $\tilde{\delta}$ (Abb. 9) weisen auf das Vorliegen einer vorwiegend kovalenten Bindung hin, da $\tilde{\alpha}$, $\tilde{\delta} \gg \tilde{\gamma}$, $\tilde{\beta}$. Im R -Bereich des Minimums überlagert sich dann noch eine ionische Bindungsform, wie das schwache Maximum von $\tilde{\gamma}$ beweist. Das gleiche Ergebnis war, wenn auch schwächer, im HeH^+ (Triplett) erhalten worden. Man wird daher das größere Energieminimum im LiH^{++} gegenüber HeH^+ so zu verstehen haben, daß sich im Ersteren durch die größere Verschiedenheit der Kernladungen neben der kovalenten Bindung eine stärkere Ionenbindung ausbilden kann. Die große Verschiedenheit der Kernladung führt dagegen im Grundzustand des LiH^{++} zur Abstoßung, während diese im HeH^+ noch nicht so stark ist, sodaß sich im $^1\Sigma$ -Zustand noch, ein im Vergleich zum H_2 -Molekül schwaches, Minimum ausbilden kann. Die höher ionisierten Systeme BeH^{+++} oder LiHe^{+++} dürften nicht mehr stabil sein.

Wie in der anderen heteroatomaren Verbindung HeH^+ ist auch hier der λ -Wert klein. (Abb. 11), was wieder auf das Vorliegen einer Ionenstruktur hinweist.

5.5. Das HeH^{++} -System und das Molekül H_2^+

Die Einelektronensysteme HeH^{++} und H_2^+ sind schon vor längerer Zeit praktisch exakt berechnet worden [51–56]. Vergleicht man die hier erhaltenen Kurven (Abb. 6) mit den genauen Rechnungen, so zeigt sich, daß die Abweichungen gering sind und im mittleren R -Bereich in die Zeichengenauigkeit fallen. Das mag zum größten Teil daran liegen, daß der Ansatz (32 a) für beide Fälle, $R \rightarrow 0$, und $R \rightarrow \infty$, die exakte Lösung von (12 a) darstellt. Für H_2^+ muß dann gelten

$$\alpha + \beta = 2, \quad R \rightarrow 0$$

$$\left. \begin{array}{l} \alpha = 1 \\ \beta = 0 \end{array} \right\} \lambda = 0 \quad \text{b.z.w.} \quad \left. \begin{array}{l} \beta = 1 \\ \alpha = 0 \end{array} \right\} \lambda = 0, \quad R \rightarrow \infty, \quad (40)$$

während im Falle des HeH^{++} die folgenden α - und β -Werte in (32 a) die exakten Lösungen liefern

$$\alpha + \beta = 3, \quad R \rightarrow \infty$$

$$\left. \begin{array}{l} \alpha = 2 \\ \beta = 0 \end{array} \right\} \lambda = 0 + \text{b.z.w.} \quad \left. \begin{array}{l} \alpha = 0 \\ \beta = 2 \end{array} \right\} \lambda = 0, \quad R \rightarrow \infty. \quad (40 a)$$

Auch der Ansatz (32 b) geht auf dieselbe Weise für $R \rightarrow \infty$ in die Lösung der Schrödingergleichung über.

Aus Abb. 10 erkennt man, daß sich im HeH^{++} für alle $R > 1,0$ at. E . das Elektron bevorzugt am Helium aufhält. Auch im H_2^+ wird schon ab $R > 5,0$ at. E . das Elektron fast nur bei einem der beiden Zentren vorgefunden. Bei kleineren Kernabständen in H_2^+ werden dann α und β vergleichbar in der Größe.

Für die hierzu durchgeführte Rechnung möchte ich Frau I. Funke meinen besten Dank sagen. Dem Verband der Chemischen Industrie danke ich für die Unterstützung bei der Ausführung dieser und der damit im Zusammenhang stehenden Untersuchungen.

LITERATUR

- [1] FROST, A. A., und PEARSON, R. G., 1953, *Kinetics and Mechanism* (New York: Wiley).
- [2] CREMER, E., und PAHL, M., 1961, *Kinetik der Gasreaktionen* (Berlin: De Gruyter).
- [3] CRAVE, D. J., HAMMOND, S., und LWOSKI, W., 1962, *Die Reaktionsmechanismen in der organischen Chemie* (Stuttgart: Hirzel); SLATER, N. B., 1959, *Theory of Unimolecular Reactions* (London: Methuen); FRANZEN, V., 1958, *Reaktionsmechanismen* (Heidelberg: Hüthig). SEMJONOW, N. N., 1961, *Einige Probleme der chemischen Kinetik und Reaktionsfähigkeit* (Berlin: Akademie-Verlag); *Investigations of Rates and Mechanisms of Reactions*, Vol. I, edited by A. Weissberger (London: Interscience); HINE, J., 1960, *Reaktivität und Mechanismus* (Stuttgart: Thieme); LAIDLER, K. J., 1955, *The Chemical Kinetics of Excited States* (Oxford: Clarendon Press); BARNETT, E. B., 1956, *Mechanism of Organic Chemical Reactions* (London: Blackie); HAMMETT, L. P., 1944, *The Theory of Rate Processes* (New York: McGraw-Hill); SCHUMACHER, H. J., 1938, *Chemische Gasreaktionen* (Darmstadt: Steinkopf); HINSHELWOOD, C. N., 1945, *The Kinetics of Chemical Change* (Oxford: Clarendon Press); SZABO, Z. G., 1960, *Fortschritte in der Kinetik der homogenen Gasreaktionen* (Darmstadt: Steinkopf).
- [4] SCHWAB, G. M., 1940, *Handbuch der Katalyse* (Berlin: Springer).
- [5] LANGENBECK, W., 1949, *Die organischen Katalysatoren* (Berlin: Springer).
- [6] EVANS, M. G., und POLYANI, M., 1935, *Trans. Faraday Soc.*, **31**, 875; OGG, R. A., und POLYANI, M., 1935, *Trans. Faraday Soc.*, **31**, 604.
- [7] PELZER, H., und WIGNER, E., 1931, *Z. phys. Chem.*, B, **15**, 445; EYRING, H., 1935, *J. chem. Phys.*, **3**, 107; WYNNE-JONES, W. F. K., und EYRING, H., 1935, *J. chem. Phys.*, **3**, 492; EYRING, H., 1935, *Chem. Rev.*, **17**, 65; EVANS, M. G., und POLYANI, M., 1935, *Trans. Faraday Soc.*, **31**, 875; EYRING, H., und POLYANI, M., 1931, *Z. phys. Chem.* B, **12**, 279.; EYRING, H., 1932, *Chem. Rev.*, **10**, 103.
- [8] BORN, M., und OPPENHEIMER, R., 1927, *Ann. Phys., Lpz.*, **84**, 457; MORSE, P. M., und STÜCKELBERG, E. W. G., 1931, *Ann. Phys., Lpz.*, **9**, 579.; LONDON, F., 1931, *Z. Phys.*, **74**, 143; ROSENKEWITSCH, L., 1933, *Phys. Z. Sowjet.*, **3**, 236; HELLMANN, H., und SYRKIN, J. K., 1935, *Acta phys.-chim. URSS*, **2**, 505; HELLMANN, H., 1937, *Einführung in die Quantenchemie* (Wien: Deuticke), S. 320.
- [9] HIRSCHFELDER, J., EYRING, H., und ROSEN, N., 1936, *J. chem. Phys.*, **4**, 121.; HIRSCHFELDER, J., 1938, *J. chem. Phys.*, **6**, 794; SHAVITT, J., 1959, *J. chem. Phys.*, **31**, 1359; LAIDLER, K. J., und SHULER, K. E., 1951, *Chem. Rev.*, **48**, 153.
- [10] HUND, F., 1928, *Z. Phys.*, **51**, 739; HÜCKEL, E., 1931, *Z. Phys.*, **70**, 204; 1932, *Ibid.*, **76**, 628; MULLIKEN, R. S., 1932, *Phys. Rev.*, **41**, 49; 1949, *J. chem. Phys.*, **46**, 497, 675.

- [11] HALL, G. G., 1950, *Proc. roy. Soc. A*, **205**, 541. BROWN, R. D., und MATSEN, F. A., 1953, *J. chem. Phys.*, **21**, 1298.
- [12] HEITLER, W., und LONDON, F., 1927, *Z. Phys.*, **44**, 455. SLATER, J. C., 1931, *Phys. Rev.*, **38**, 1109; 1953, *Rev. mod. Phys.*, **25**, 199.
- [13] PAULING, L., 1931, *J. Amer. chem. Soc.*, **53**, 1367. RUMER, A., 1932, *Göttinger Nachr.* S. 377. PAULING, L., 1933, *J. chem. Phys.*, **1**, 280. WHELAND, G., 1955, *Resonance in Organic Chemistry* (New York: Wiley).
- [14] ROTHAAAN, C. C. J., 1951, *Rev. mod. Phys.*, **23**, 69.
- [15] MATSEN, F. A., 1953, *J. chem. Phys.*, **21**, 928. BINGEL, W., 1956, *Z. Naturf. A*, **12**, 59. MOFFITT, W., 1951, *Proc. roy. Soc. A*, **210**, 245. PREUSS, H., 1958, *Z. Naturf. A*, **13**, 364; 1960, *Naturwissenschaften*, **11**, 241.
- [16] MORSE, P. M., 1929, *Phys. Rev.*, **34**, 57.
- [17] PREUSS, H., 1962, *Theor. chim. Acta.*, **1**, 42.
- [18] PREUSS, H., 1957, *Z. Naturf. A*, **12**, 599; 1958, *Ibid.*, **13**, 364.
- [19] HELLMANN, H., 1937, *Einführung in die Quantenchemie* (Wien: Deuticke), S. 124.
- [20] HEITLER, W., und LONDON, F., 1957, *Z. Phys.*, **44**, 455.
- [21] WANG, S. C., 1928, *Phys. Rev.*, **31**, 579.
- [22] JAMES, H. M., COOLIDGE, R., und PRESENT, R., 1936, *J. chem. Phys.*, **4**, 187.
- [23] SHULL, H., und LÖWDIN, P. O., 1956, *J. chem. Phys.*, **25**, 1035.
- [24] NORDSIECK, A., 1940, *Phys. Rev.*, **58**, 310.
- [25] MÜLLER, C. R., und EYRING, H., 1951, *J. chem. Phys.*, **19**, 1495.
- [26] HARRIS, F. E., 1957, *J. chem. Phys.*, **27**, 812.
- [27] ELLISON, F. O., und COMPANION, A. L., 1959, *J. chem. Phys.*, **31**, 285.
- [28] GREEN, L. C., MULDER, M. M., und MILNER, P. C., 1953, *Phys. Rev.*, **91**, 35.
- [29] SHULL, H., 1958, Technical Note 17, University of Uppsala.
- [30] GUILLEMIN, V., und ZENER, C., 1929, *Proc. nat. Acad. Sci., Wash.*, **14**, 314.
- [31] KOTANI, M., AMEMIYA, A., ISHIGURO, E., und KIMURA, T., 1955, *Tables of Molecular Integrals* (Tokyo: Maruzen).
- [32] PREUSS, H., 1956–61, *Integraltafeln zur Quantenchemie*, Band I–IV (Berlin: Springer). MILLER, J., GERHAUSER, J. M., und MATSEN, F. A., 1959, *Quantum Chemistry Integrals and Tables* (Austria: Texas Press).
- [33] FROST, A., und BRAUNSTEIN, J., 1951, *J. chem. Phys.*, **19**, 1133.
- [34] BERENCZ, F., 1954, *Acta physica Hung.*, **4**, 149.
- [35] HIRSCHFELDER, J. O., und LINNET, J. W., 1950, *J. chem. Phys.*, **18**, 130.
- [36] ROSEN, N., 1931, *Phys. Rev.*, **38**, 255, 2099.
- [37] GURNEE, E. F., und MAGEE, J. C., 1950, *J. chem. Phys.*, **18**, 142.
- [38] BINGEL, W. A., PREUSS, H., und SCHMIDTKE, H. H., 1961, *Z. Naturf. A*, **16**, 434.
- [39] M'EWEN, S., und ARNOT, T., 1939, *Proc. roy. Soc. A*, **172**, 107.
- [40] BEACH, J. Y., 1936, *J. chem. Phys.*, **4**, 353.
- [41] COULSON, C. A., und DUNCANSON, W. E., 1938, *Proc. roy. Soc. A*, **165**, 90.
- [42] TOH, S., 1940, *Proc. phys. math. Soc., Japan*, **22**, 119.
- [43] BHATTACHARYA, R., 1961, *Proc. nat. Inst. Sci., India*, **27**, 185.
- [44] PAULING, L., 1933, *J. chem. Phys.*, **1**, 56.
- [45] HURLEY, A. S., und MATSEN, V. W., 1961, *J. chem. Phys.*, **34**, 1919.
- [46] KOLOS, W., und ROTHAAAN, C. C. J., 1960, *Rev. mod. Phys.*, **32**, 219.
- [47] MCLEAN, A. D., WEISS, A., und YOSHIMINE, M., 1960, *Rev. mod. Phys.*, **32**, 211.
- [48] HERZBERG, G., 1950, *Molecular Spectra and Molecular Structure*, I (New York: Van Nostrand).
- [49] BAINBRIDGE, K. T., 1933, *Phys. Rev.*, **44**, 57. GLOCKLER, G., FULLER, D. L., und ROE, C. P., 1933, *J. chem. Phys.*, **1**, 703.
- [50] GLOCKLER, G., und FULLER, D. L., 1933, *J. chem. Phys.*, **1**, 886.
- [51] TELLER, E., 1930, *Z. Phys.*, **61**, 458.
- [52] BATES, D. R., und CARSON, T. R., 1956, *Proc. Camb. phil. Soc.*, **234**, 207.
- [53] HYLLERAAS, E., 1931, *Z. Phys.*, **71**, 729.
- [54] BURRAU, O., 1927, *K. danske vidensk. Selsk.*, **7**, 1.
- [55] BABER, W. G., und HASSE, H., 1935, *Proc. Camb. phil. Soc.*, **31**, 564.
- [56] JAFFE, G., 1934, *Z. Phys.*, **87**, 535.

The electron spin resonance spectrum of the NF_2 radical trapped in inert matrices at 4.2°K

J. B. FARMER, M. C. L. GERRY† and C. A. McDOWELL‡

Department of Chemistry, University of British Columbia,
Vancouver 8, B.C., Canada

(Received 2 December 1963)

The electron spin resonance spectrum of the NF_2 radical, trapped in argon and krypton matrices at 4.2°K , has been analysed to yield the isotropic contributions of the hyperfine interactions of both nitrogen and fluorine atoms. Effects due to anisotropy of the g -tensor have been observed from which we have calculated the principal values of the g -tensor. Theoretical estimates of the expected magnitudes of the principal values of the g -tensor have been made. These lead most readily to the interpretation of our experimental results for the radical trapped in an argon matrix with a matrix ratio of $M/R=300$, as indicating that at 4.2°K the NF_2 radical is evidently rotating sufficiently freely about an axis perpendicular to the molecular plane to give a g -tensor which is apparently axially symmetrical.

1. INTRODUCTION

The study of free radicals by the inert matrix isolation method [1] has been extremely fruitful. Using this technique many workers have been able to determine the structures of several free radicals which would have proved extremely difficult to handle by any other method. Most of the studies have utilized optical spectroscopic methods and a considerable amount of valuable detailed information has been obtained from the study of both the ultra-violet and infra-red spectra of the trapped radicals. Electron spin resonance methods [2-5] have also been applied with considerable success to study the magnetic resonance behaviour of atoms and radicals trapped in inert non-magnetic matrices at low temperatures. The experimental techniques utilized in this latter type of work are extremely difficult, particularly in those studies carried out at the temperature of liquid helium, 4.2°K ; but the method does frequently lead to the identification of radicals when optical spectroscopy may not lead to an unequivocal interpretation. In addition it is frequently possible to deduce important information about the nature of the electronic structure of the radical from its electron spin resonance spectrum when other spectroscopic methods may not at the time be adequate. The present paper reports the results of our study of the electron spin resonance spectrum of the NF_2 radical. The experiments were carried out with the NF_2 radical trapped in several inert

† Present address: Department of Physical Chemistry, University Chemical Laboratory, Lensfield Road, Cambridge, England.

‡ Present address: Department of Theoretical Chemistry, University Chemical Laboratory, Lensfield Road, Cambridge, England.

matrices at 4.2°K. This radical is of particular interest because few radicals containing fluorine have been studied, and furthermore it was thought to be desirable to compare the electron spin resonance spectrum of the NF_2 radical with those observed for NO_2 [3, 5] and NH_2 [2], when trapped in inert matrices at 4.2°K.

Nitrogen difluoride exists in equilibrium with tetrafluorohydrazine at room temperature. Electron spin resonance studies on this gaseous mixture by Piette *et al.* [6] led to the observation of a broad resonance 104 gauss wide, and centred at about $g=2.01$. No hyperfine splitting was observed, though, of course, a nine-line spectrum would be expected if one neglects effects due to coupling of the electronic and molecular rotational angular momentum. This latter coupling would lead to a very complex spectrum such as has been observed for nitrogen dioxide in the gas phase [7]. Presumably all fine structure in the electron spin resonance spectrum of NF_2 in the gas phase has been smeared out by collisional broadening.

2. EXPERIMENTAL

The tetrafluorohydrazine, 99.1 per cent pure, was obtained from Air Products and Chemicals Inc., Allentown, Pa., and as the reported impurities were not paramagnetic it was used without further treatment. This compound is toxic and explosive and care is therefore required in its handling.

Argon and krypton which were used as inert gas matrices, were Matheson Research Grade products. Fisher Spectroanalysed carbon tetrachloride was also used as a matrix material. Experiments were carried out at mole ratios of matrix to radical precursor (M/R) of 300 and 1200 in both argon and krypton, and 1200 in carbon tetrachloride. The trapping of the nitrogen difluoride was achieved by depositing the room temperature equilibrium mixture of N_2F_4 , NF_2 and matrix gas on the liquid helium cooled sapphire rod in the microwave resonance cavity (see below). This procedure prevented the recombination of the NF_2 radicals which would otherwise have occurred on cooling the mixture down to 4.2°K. Deposition was continued until a very high signal-to-noise ratio was observed on the electron spin resonance spectrometer. The spectra were mostly taken at 4.2°K but observations were continued during the warm-up period after all the liquid helium had evaporated, until the electron spin resonance signal disappeared. No appreciable saturation of the resonance was observed at a microwave power level of 1 mw, which was used in all our experiments.

Our apparatus was based on the design used by Jen *et al.* [3], but differed from it in some important respects. Figure 1 gives a diagrammatic sketch showing a cross section of the essential details of the liquid helium dewar attached to the microwave cavity. The liquid helium dewar is based on the design of Duerig and Mador [8]. The central container holds the liquid helium and is shielded by another dewar containing liquid nitrogen; the vacuum envelope is pumped down to about 10^{-7} mm Hg with an oil diffusion pump and a rotatory oil pump; an ionization gauge being used to measure the pressure.

The microwave cavity is attached directly to the liquid helium container, and centred in it is a 0.15 in. diameter sapphire rod on which the gaseous samples are condensed. As mentioned above, the sapphire rod is attached to the bottom of the liquid helium container. To minimize the evaporation of the liquid

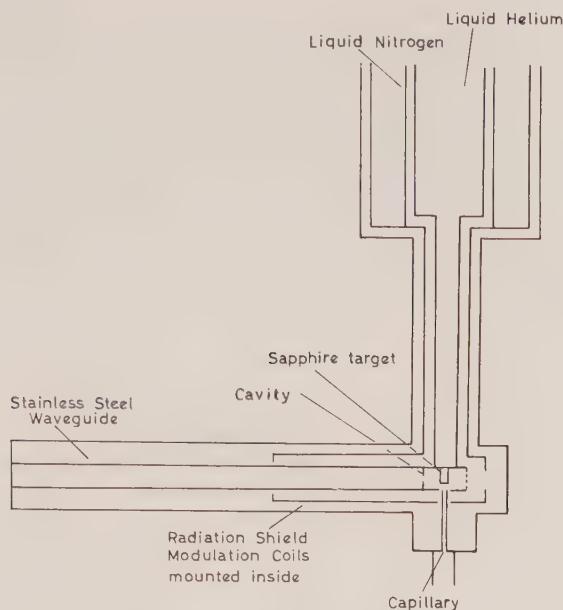


Figure 1. Diagrammatic view of the low temperature apparatus for E.S.R. studies.

helium due to the entry of heat from external sources the cavity was connected to the external microwave circuitry by a length of type 304 stainless steel waveguide having a wall thickness of 0.01 in. In the bottom of the cavity there was a hole through which penetrated a stainless steel capillary $\frac{1}{16}$ in. diameter, 0.005 in. wall thickness, and this acted as the orifice through which the gaseous samples entered before they condensed on the liquid-helium-cooled sapphire rod which was positioned immediately above.

The electron spin resonance spectrometer operating in the X band was frequently stabilized. The microwave cavity was rectangular in cross section and operated in the TE_{012} mode. A Hewlett Packard 524/525/540 frequency counter was used to measure the microwave frequency and the magnetic field, which was supplied by a 6 in. Varian magnet fitted with ring shim pole caps, was measured with a proton magnetic resonance magnetometer. The magnetic field was modulated at a frequency of 400 c/sec.

3. RESULTS

The electron spin resonance spectra observed for NF_2 radical trapped in the different inert matrices at 4.2°K all showed rather similar features. In general all the spectra had three major peaks with the centre one of greater amplitude but narrower than the other two. The low field peak was greater in amplitude than the higher field one. Figures 2 and 3 show two slightly different spectra observed for the NF_2 radical trapped in an argon matrix, at different M/R ratios. Both show features which are clearly ascribed to anisotropies in the g -factors for the radical as well as to anisotropy of the hyperfine

interaction tensors. These phenomena have been previously observed in the E.S.R. spectra of randomly oriented radicals trapped in polycrystalline matrices [2-5].

Since the spectrum (figure 6) consists of a triplet due to the nitrogen hyperfine interaction superimposed on the fluorine triplet, the outer lines will be influenced by the anisotropies of both the hyperfine interaction tensors. This is evidently why the outer lines are nearly twice as broad as the central line (see figures 2 and 3). The central line will be influenced only by anisotropy in the nitrogen hyperfine interaction tensor, and as this is generally small it may be ignored in estimating the components of the g -tensor.

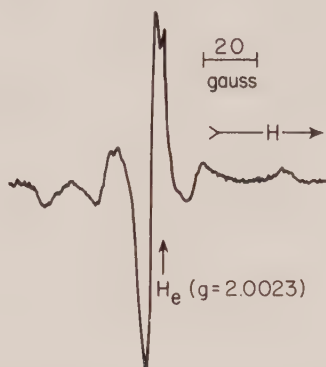


Figure 2. Electron spin resonance spectrum of the NF_2 radical in an argon matrix ($M/R=300$) at 4.2°K .

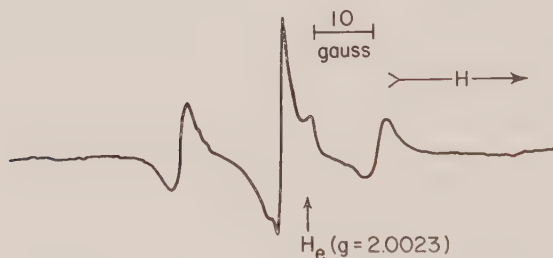


Figure 3. Electron spin resonance spectrum of the NF_2 radical in an argon matrix ($M/R=1200$) at 4.2°K .

From the spectrum shown in figure 3 it would seem that at the higher M/R ratio used in that particular experiment, the rotation of the NF_2 radical is less free than in the experiment to which figure 2 refers even though in the latter case the M/R ratio was four times smaller. Figure 4 shows the E.S.R. spectrum of NF_2 in a krypton matrix ($M/R=300$) at 4.2°K . This spectrum shows little detailed structure and it is apparent that here there has been an averaging of the anisotropic portions of both the hyperfine interaction tensor and the g -tensor. The krypton matrix thus seems to permit the NF_2 radical to rotate more freely than does the argon at the same temperature and the same M/R ratio.

When carbon tetrachloride is used as a matrix the E.S.R. spectrum observed for the trapped NF_2 radical at 4.2°K is somewhat distorted as compared with those found with inert gas matrices (see figure 5). The two outer peaks of the triplet were very weak as compared with the centre peak. They were also much wider than the corresponding peaks observed in argon and krypton matrices. The apparent g -factor calculated at the point where the centre peak crossed the baseline was 2.0049 ± 0.0004 , the same value as calculated from the experimental results for argon and krypton as matrices.



Figure 4. Electron spin resonance spectrum of the NF_2 radical in a krypton matrix ($M/R=300$) at 4.2°K .

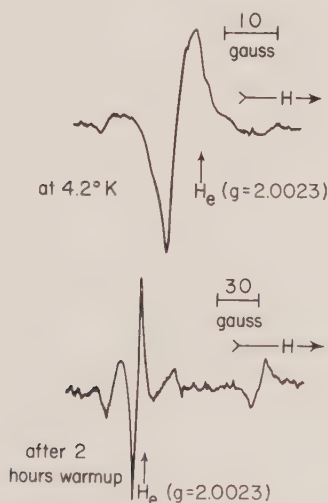


Figure 5. Electron spin resonance spectra observed for the NF_2 radical at 4.2°K and during warming-up in a carbon tetrachloride matrix ($M/R=1200$).

When the temperature of the matrices in which the radicals were trapped was changed the observed E.S.R. spectrum for the NF_2 radical changed considerably. This change in temperature was brought about by allowing the liquid helium to evaporate and permitting the matrix to be heated by radiation from the surrounding liquid nitrogen dewar. Essentially the same changes were observed during warm-up for both the argon and krypton matrices (see figure 6). The

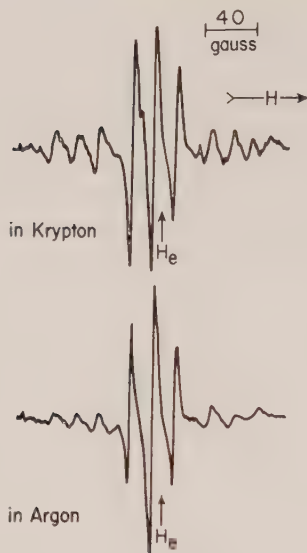


Figure 6. Electron spin resonance spectra observed for the NF_2 radical during the warming-up of the argon and krypton matrices.

peak-to-peak widths of the two outer lines in the E.S.R. spectrum of the NF_2 radical decreased, their amplitudes increased and the asymmetrical nature of the central peak was considerably reduced. The most striking features observed as the result of taking several spectra during the warming-up period was the resolution of the original three peaks into a fairly symmetrical spectrum consisting of nine lines, as would be anticipated for the NF_2 radical. The same results were observed in both argon and krypton matrices and undoubtedly this nine-line spectrum is due to the NF_2 radical rotating almost freely in the matrices at the temperature at which the observations were made. The main triplet separation was 60 ± 2 gauss and this must be ascribed to the hyperfine coupling constant of the fluorine atoms because of the observed intensity ratios. The smaller triplet splitting was 17 ± 2 gauss and as this has three lines of almost equal intensity it obviously must be attributed to splitting caused by the hyperfine interaction of the nitrogen atom. Measurement of the g -factor for the NF_2 radical rotating more or less freely in the inert gas matrices (figure 6) gave a value of 2.0053 ± 0.0006 .

In the case of carbon tetrachloride no corresponding resolution of the hyperfine structure was found at any temperature during the warm-up period. The lower part of figure 5 shows the E.S.R. spectrum observed for the trapped NF_2 some two hours after warm-up. The intensities of the two outer peaks are much greater relative to the central one. This is the only new feature observed with this set of experiments using carbon tetrachloride as a matrix material.

4. DISCUSSION

4.1. Electronic structure of the NF_2 radical

The NF_2 radical belongs to the symmetry group C_{2v} and the possible L.C.A.O. molecular orbital can readily be established. In labelling the orbitals we assume that the NF_2 radical is in the yz plane with the z axis being the C_2 rotational axis

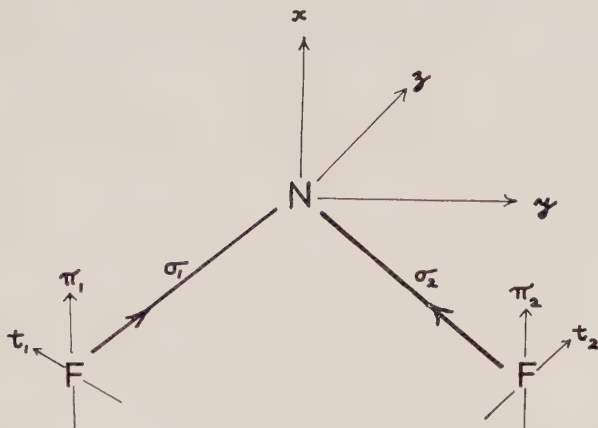


Figure 7. Geometry and coordinate system for the NF_2 radical. The radical is lying in the yz plane, i.e. z is the C_2 symmetry axis.

bisecting the NF_2 bond angle. The x axis is taken as being perpendicular to the molecular yz plane (see figure 7). In constructing the molecular orbitals, we make use of atomic orbitals formed from the $2s$ and $2p$ atomic orbitals of the nitrogen atom and the $2s$ and $2p$ orbitals of the fluorine atoms. It is assumed that the $2s$ orbitals of the fluorine atoms do not take part in bond formation. The bonding molecular orbitals are formed from $2p_\sigma$ orbitals directed along the NF bonds, and there are $2p_t$ fluorine orbitals in the molecular plane perpendicular to the NF bonds. The symmetries of the resulting molecular orbitals are given in the table. We have denoted the various orbitals as $(1a_1)^2(1b_2)^2$ in the assumed order of increasing energy. Though there are no detailed calculations to justify the ordering of the orbitals, it is likely that they are mostly in the correct order [9, 10].

Symmetry class	Nitrogen atomic orbitals	Fluorine atomic orbitals
A_1	s, p_z	$\frac{1}{2}(\sigma_1 + \sigma_2); \frac{1}{2}(t_1 + t_2); \frac{1}{2}(s_1 + s_2)$
A_2	—	$\frac{1}{2}(\pi_1 - \pi_2)$
B_2	p_y	$\frac{1}{2}(\sigma_1 - \sigma_2); \frac{1}{2}(t_1 - t_2); \frac{1}{2}(s_1 - s_2)$
B_1	p_x	$\frac{1}{2}(\pi_1 + \pi_2)$

The nineteen valency electrons are most likely distributed to give the electronic configuration $(1a_1)^2(1b_2)^2(2a_1)^2(2b_2)^2(3a_1)^2(1b_1)^3(3b_2)^2(4a_1)^2(1a_2)^2(2b_1)^1$. The ground state of the NF_2 radical is, therefore, 2B_1 .

Electronic structure of the NF_2 radical with symmetry C_{2v} .

The odd electron in the NF_2 radical has according to our ordering of the molecular orbitals given in the table to go into an orbital which has symmetry b_1 , hence the ground electronic state of the radical is 2B_1 . It may be noted that the isoelectronic radical ClO_2 also has a 2B_1 ground state [11]; the same being true of the isoelectronic radical anion SO_2^- [12]. The $(2b_1)$ orbital is

built up from a p_x orbital on the N atom overlapping out of phase with each of the two p_x orbitals on the fluorine atoms. It is largely N-F anti-bonding and F-F bonding.

Unfortunately the spectra are not sufficiently detailed to permit reasonably accurate estimates to be made of the anisotropic hyperfine interactions for either the nitrogen or fluorine atoms. We are, therefore, unable to calculate the p-character of the odd electron molecular orbital.

The isotropic hyperfine interaction due to an electron with s character is given by the equation :

$$A_{\text{iso}} = \frac{8\pi}{3h} g_e g_N \beta_e \beta_N |\Psi_s(0)|^2, \quad (1)$$

where g_e is the free electron g -factor, β_e the electron Bohr magneton, g_N is the nuclear g -factor for the nucleus causing the hyperfine interaction ($g_N = \mu_N/I$), β_N is the nuclear Bohr magneton, h is Planck's constant, and $|\Psi_s(0)|^2$ is the square of the s-wave function evaluated at the nucleus. For nitrogen we have $|\Psi_{N_{2s}}(0)|^2 = 34.0 \times 10^{24} \text{ cm}^{-3}$ [12], thus our value of 17 gauss or 47.6 Mc/s for the isotropic nitrogen hyperfine interaction in NF_2 gives a value of 0.03 for the square of the contribution of the 2s orbital of nitrogen to the odd-electron molecular orbital. Similarly from the observed value of 168 Mc/s for the isotropic hyperfine interaction for the fluorine atom we calculate from the theorem value [13] for $|\Psi_{F_{2s}}(0)|^2$, a contribution of 0.004 from the 2s orbital of each fluorine atom in NF_2 to the wave function describing the orbital occupied by the unpaired electron. It is interesting to note that in the NH_2 radical the contribution of the 2s nitrogen orbital to the wave function for the orbital occupied by the odd electron in that radical is 0.02 and in this case also the odd electron is in an orbital with symmetry b_1 . Another interesting comparison is provided by the ClO_2 radical where again the odd electron is in an orbital with symmetry b_1 and the s-character of that orbital has been found to be 0.01 [11]. According to our description of the electronic structure of the NF_2 radical the orbital occupied by the odd electron having symmetry b_1 would require the electron to be in a pure p orbital. The fact that the wave function is found to have a small amount of s-character must surely arise from configurational interaction involving the 2s and 2p electrons on the nitrogen and fluorine atoms. In the other similar radicals namely, NO_2 and CO_2^- , no data are available concerning the s-character of the odd electron molecular orbital due to configuration interaction from the 2s electrons of the oxygen atoms because of course the nuclear spin of ^{16}O is zero and so no isotropic hyperfine interaction can be observed for the oxygen atoms.

4.2. Calculation of components of the g -tensor

The NF_2 radical undoubtedly has symmetry C_{2v} and we shall assume that this symmetry is, in general, maintained in the polycrystalline inert gas matrices in which we have studied its electron spin resonance spectrum. This would certainly seem to be a reasonable assumption, for the crystalline field effects in solid argon or krypton are unlikely to be so great as to cause distortion of the NF_2 geometry so that the C_{2v} symmetry is destroyed. The shapes of the observed

peaks in the electron spin resonance of NF_2 trapped in argon ($M/R=300$) at 4.2°K (see figure 2) are also in agreement with this viewpoint.

Many theoretical treatments [15–19] of the line shapes to be expected for polycrystalline substances with g -tensor anisotropies show that for an axially symmetrical paramagnetic species a line shape of the same kind as that shown in the central peak of figure 2 is to be expected. The sharp minimum occurs at g_\perp and the shoulder at g_\parallel . From our data we calculate the following values for the components of the g -tensor, $g_\parallel = 2.0022$, $g_\perp = 2.0059$.

The spectrum shown in figure 3 closely resembles what would be expected for a randomly oriented radical in a polycrystalline matrix when there are three different principal values for the g -tensor. From the positions at which the inflections occur in the central line we calculate the three principal values of the g -tensor as $g_1 = 2.0022 \pm 0.0004$, $g_2 = 2.0051 \pm 0.0004$, and $g_3 = 2.0066 \pm 0.0004$. Why there should be exhibited in this case the three different principal values for the g -tensor is not clear. It might have been expected that the higher M/R ratio of the argon matrix would have permitted at least the same freedom of rotation of the NF_2 radical as is observed for the experiment at the lower M/R ratio. On the other hand, it could certainly be the case that at the higher M/R ratio there is a stronger crystalline field effect from the argon matrix and/or the NF_2 radicals are preferentially trapped at lattice sites which do not permit as much freedom of rotation as is the case for the matrix with a lower M/R ratio. It may also just be possible that the lines in the experiment carried out at a M/R ratio of 300 (see figure 2) are slightly broadened so that the difference between g_2 and g_3 is obscured. We shall, however, adopt the viewpoint that the experimental results shown in figure 2 are indeed those for the case of an axially symmetrical radical with $g_\parallel = 2.0022 \pm 0.0004$ and $g_\perp = 2.0059 \pm 0.0004$.

In calculating the components of the g -tensor from the usual equation obtained from second-order perturbation theory difficulties arise for radicals containing several centres, e.g. NF_2 each with contributions to the overall spin-orbit coupling. These difficulties arise because the angular momentum is usually measured about a particular point in the radical, e.g. the nitrogen atom, and the evaluation of matrix elements such as $\langle \psi_i | L | \psi_j \rangle$, where ψ_i and ψ_j are the fluorine atomic orbitals on the same atom leads to difficulties arising from the fact that the usual formula for the calculation of g -values is not gauge-invariant [20]. For the NF_2 radical it is, however, permissible to use an approximate formula which is adequate for our present purposes. This required equation [20, 21] is :

$$g_z = g_e + \frac{1}{8} \sum_p \sum_n \sum_k \frac{\langle \psi_p | I_{zk} | \psi_n \rangle \langle \psi_n | \xi_k(r_k) I_{zk} | \psi_p \rangle}{\epsilon_p - \epsilon_n}, \quad (2)$$

where ψ_p is any orbital which contains an odd electron, ψ_n is any orbital either full or empty and ϵ_p and ϵ_n are the energies of the orbitals ψ_p and ψ_n . $\xi_k(r_k)$ is a function which decreases rapidly with r ; therefore the only term which contributes appreciably is the one for which $k'' = k' = k$ and we can replace it by ζ_k , the appropriate spin-orbit function for the k th atom.

We write the molecular orbitals as a linear combination of atomic orbitals :

$$\psi_p = \sum_i a_i \phi_{\text{N}_i} + \sum_i b_i \phi_{\text{F}_i}, \quad (3)$$

where ϕ_{N_i} is a nitrogen atomic orbital and ϕ_{F_j} represents the fluorine atomic orbitals. A similar equation can be written for ψ_n . Substituting from (3) into (2) we get :

$$g_z = g_e + 2 \sum_{p(\neq p)} \sum_{i,j} \frac{\zeta_N a_i^{(p)} a_j^{(n)} \langle \phi_{N_i} | l_{zN} | \phi_{N_j} \rangle \langle \phi_{N_j} | l_{zN} | \phi_{N_i} \rangle}{\epsilon_p - \epsilon_n} + 2 \sum_{n(\neq p)} \sum_{i,j} \frac{2 \zeta_F b_i^{(p)} b_j^{(n)} \langle \phi_{F_i} | l_{zF} | \phi_{F_j} \rangle \langle \phi_{F_j} | l_{zF} | \phi_{F_i} \rangle}{\epsilon_p - \epsilon_n} \quad (4)$$

Analogous equations may be written for g_y and g_x .

The l_z component of the angular momentum transforms according to the A_2 representation of group C_{2v} , so that the matrix element $\langle \psi_p | l_z | \psi_n \rangle$ is zero unless ψ_n is of species B_2 . This follows because ψ_p is of species B_1 . There are several of the molecular orbitals of NF_2 which belong to the representation B_2 but it is highly probable that the most important one is $(3b_2)$ which is a bonding orbital. There is also, of course, the anti-bonding orbital lying above the $(2b_1)$ orbital containing the odd electron. Both of these two (b_2) orbitals affect the g -value in opposite ways. The spin-orbit coupling of the $(2b_1)$ and $(3b_2)$ orbitals will lead to a value of $g_z > g_e$, whereas the effect of spin-orbit coupling of $(2b_1)$ and $(4b_2)$ leads to $g_z < g_e$. It is difficult to assess what may be the result of these two opposing contributions as the spacings of the various energy levels in the NF_2 radicals are not known. It may, however, be safely assumed that the net result will be to make $g_z \geq g_e$.

In a like manner we may now estimate the magnitudes of the two components g_x and g_y . The l_x component of the angular momentum transforms according to the B_2 representation and so the states which may couple with B_1 must belong to the representation A_2 if the matrix element $\langle \psi_p | l_x | \psi_n \rangle$ is to be finite. No one-electron orbitals are known for the NF_2 radical (see table) which do not yield the result $\langle \psi_p | l_x | \psi_n \rangle = 0$. We have therefore the result that $g_x = g_e$. The remaining component of the angular momentum l_y transforms according to the representation B_1 and thus if the matrix element $\langle \psi_p | l_y | \psi_n \rangle$ is to be finite ψ_n must be of symmetry A_1 . Since

$$l_y |p_{zN}\rangle = -ip_{xN} \quad \text{and} \quad l_y \left| \frac{1}{\sqrt{2}} (t_1 + t_2) \right\rangle = i \cos(\theta/2) (\pi_1 + \pi_2) / \sqrt{2}$$

it follows that g_y will exceed g_e approximately by the amount :

$$\frac{2\{\zeta_N a_i^{(p)} a_j^{(n)} + \zeta_F b_i^{(p)} b_j^{(n)} \cos^2(\theta/2)\}}{\Delta} \quad (5)$$

where $\Delta = \{\epsilon(2b_1) - \epsilon(4a_1)\}$ and θ is the complement of the FNF angle. A contribution in the opposite direction is possible if there is spin-orbital coupling to the empty $5a_1$ anti-bonding orbital. It is, however, more than likely that the overall effect is to make (5) the predominant contribution, in which case we have $g_y > g_e$.

These estimated magnitudes taken with our experimental results shown in figure 2 indicate that $g_x = g_{||}$. It follows that $g_{\perp} = \frac{1}{2}(g_z + g_y)$ leading to the conclusion that $g_{\perp} > g_e$. Both of these conclusions are in agreement with our experimental results that $g_{||} = 2.0022$ and $g_{\perp} = 2.0058$. Consequently we

conclude that in the case of the argon matrix at $M/R=300$ and 4.2°K the NF_2 radical is rotating freely about the x axis, i.e. the axis perpendicular to the molecular plane. Rotations about the other two axes are somewhat restricted.

It is of interest to compare the electron spin resonance spectra of NO_2 and NF_2 . The spectrum of NO_2 trapped in solid argon at 4.2°K shows structure which has been interpreted as arising from anisotropies in both the g -tensor and the hyperfine interaction tensor [5, 22]. Adrian [22] has shown that values of the components of the g -tensor imply that the NO_2 radical is rotating freely about the y axis (see figure 6). This can readily be understood, for the O-N-O angle is $134^\circ 15'$, so this radical can be expected to rotate more freely about the y axis than any other one. With NF_2 , however, the valency angle is 104.2° [23] and it becomes possible for a radical with this geometry to rotate more freely about the x axis which is perpendicular to the molecular plane in agreement with our results. We may here note that infra-red studies on the NF_2 radical trapped in a nitrogen matrix at 20°K show that the absorption bands for this radical are very sharp and clearly resolved from those of the parent N_2F_4 . Clearly this is what one would expect were the NF_2 radical to rotate in the nitrogen matrix.

We may perhaps in conclusion mention that the molecular geometry of the NF_2 radical does not require the g -tensor to exhibit the apparent axial symmetry which is implied by our interpretation of the spectrum shown in figure 2. The theoretical evaluation of the magnitudes of the principal values of the g -tensor given above shows that $g_x=2.0023$ and g_y and g_z are both likely to exceed the free electron value. As we have mentioned earlier in this paper, the spectrum shown in figure 3 is most readily interpreted as showing that the g -tensor of the radical has three different principal values, i.e. $g=2.0022$, $g_2=2.0051$ and $g_3=2.0066$. This is in agreement with the theoretical predictions. Furthermore, it is at once apparent that by rotation about the x axis the NF_2 radical would readily appear to have an axially symmetric g -tensor because the values of g_2 and g_3 are so nearly equal.

We wish to thank the National Research Council and the Defence Research Board of Canada for grants in support of this work. M. C. L. G. wishes to thank the National Research Council of Canada for a Bursary and a Studentship during the years 1960-62. C. A. McD. thanks the same body for the award of a Senior Research Fellowship during the tenure of which this paper was completed.

REFERENCES

- [1] PIMENTEL, G. C., 1960, *Formation and Trapping of Free Radicals*, Ed. A. M. Bass and H. P. Broida (New York: Academic Press Inc.), Chap. 4.
- [2] FONER, S. N., 1958, *Phys. Rev. Letters*, **1**, 91.
- [3] JEN, C. K., FONER, S. N., COCHRAN, E. L., and BOWERS, V. A., 1959, *Phys. Rev.*, **112**, 1160.
- [4] COCHRAN, E. L., ADRIAN, F. J., and BOWERS, V. A., 1961, *J. chem. Phys.*, **34**, 1161; 1962, *Ibid.*, **36**, 1661, 1938.
- [5] FARMER, J. B., HUTCHISON, D. A., and McDOWELL, C. A. (unpublished work).
- [6] PIETTE, L. H., JOHNSON, F. A., BOOMAN, K. A., and COLBURN, C. B., 1961, *J. chem. Phys.*, **35**, 1481.
- [7] FARMER, J. B., and McDOWELL, C. A. (to be published).

- [8] DUERIG, W. H., and MADOR, I. L., 1952, *Rev. sci. Instrum.*, **23**, 421.
- [9] WALSH, A. D., 1953, *J. chem. Soc.*, p. 2266.
- [10] MULLIKEN, R. S., 1958, *Canad. J. Chem.*, **36**, 10.
- [11] CURL, R. F., Jr., 1962, *J. chem. Phys.*, **37**, 779.
- [12] DUNITZ, J. D., 1956, *Acta Cryst.*, **9**, 579.
- [13] DOUSMANIS, G. C., 1955, *Phys. Rev.*, **97**, 967.
- [14] CLEMENTI, E., ROTHMAN, C. C. J., and YOSHIMINE, M., 1962, *Phys. Rev.*, **127**, 1618.
- [15] BLEANEY, B., 1950, *Proc. phys. Soc., Lond. A*, **63**, 407; 1951, *Phil. Mag.*, **42**, 441; 1960, *Proc. Phys. Soc., Lond. A*, **75**, 621.
- [16] SANDS, R. H., 1955, *Phys. Rev.*, **99**, 1222.
- [17] KNEUBÜHL, F. K., 1960, *J. chem. Phys.*, **33**, 1074.
- [18] SEARL, J. W., SMITH, R. C., and WYARD, S. J., 1961, *Proc. phys. Soc., Lond. A*, **78**, 1174.
- [19] COCHRAN, E. L., ADRIAN, F. J., and BOWERS, V. A., 1961, *J. chem. Phys.*, **34**, 1161.
- [20] STONE, A. J., 1963, *Proc. roy. Soc. A*, **271**, 433.
- [21] LONGUET-HIGGINS, H. C., and STONE, A. J., 1962, *Mol. Phys.*, **5**, 417.
- [22] ADRIAN, F. J., 1962, *J. chem. Phys.*, **36**, 1692.
- [23] HARMONY, M. D., MYERS, R. J., SCHOEN, L. J., LIDE, D. R., Jr., and MANN, D. E., 1961, *J. chem. Phys.*, **35**, 1129.

Electronic spectra of *p*-benzosemiquinone ions

by YOSHIYA HARADA and HIROO INOKUCHI

The Institute for Solid State Physics, The University of Tokyo

(Received 8 August 1963)

The absorption spectra of non-substituted, 2,5-dimethyl-, 2,5-di-*tert*-butyl-, trimethyl-, tetramethyl-*p*-benzosemiquinone ions have been measured. In alkaline ethylene glycol fairly stable semiquinone ions were prepared by an oxidation of hydroquinones or by a reduction of quinones at room temperature.

It is found that in visible or near ultra-violet region *p*-benzosemiquinone ions have three intense absorption bands due to $\pi \rightarrow \pi^*$ allowed transitions in addition to a weak absorption in the region $450 \sim 550 \text{ m}\mu$ presumably due to $n \rightarrow \pi^*$ transition.

1. INTRODUCTION

Semiquinones are interesting compounds which are formed as intermediate species of an organic redox system of the type, quinone-hydroquinone. It is known that the semiquinone in solution with a value of appropriate pH exists in two forms, namely the semiquinone radical ($\text{QH}\cdot$) and the semiquinone ion ($\text{Q}^{\cdot-}$) which are present in ionic equilibrium [1, 2] (figure 1).

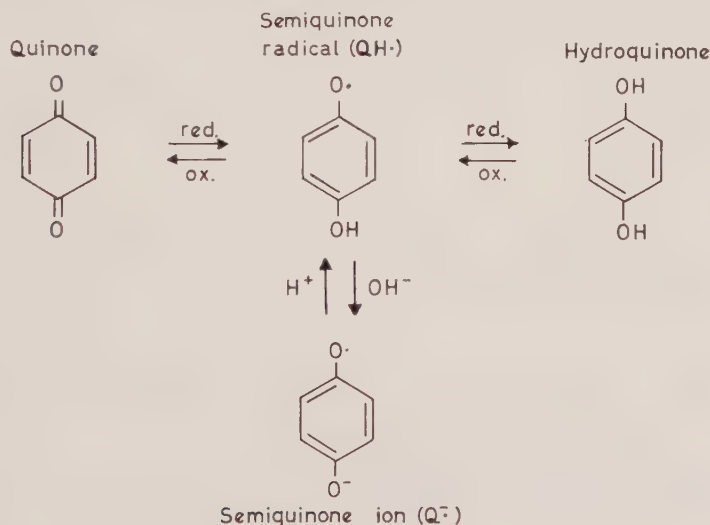


Figure 1. The semiquinone radical and the semiquinone ion.

In a previous paper [3], semiquinone ions were prepared by an oxidation of hydroquinones or by a reduction of quinones in alkaline ethylene glycol. In the viscous medium, the free radical was kept stable for a fairly long period because it was prevented from rapid side reactions and we succeeded in extending the wavelength region of the spectral response of several semiquinone ions to $230 \text{ m}\mu$

at room temperature. By applying these techniques for the case of di-*tert*-butyl-*p*-benzosemiquinone ion, two new absorption bands having maxima at 373 and 323.5 $m\mu$ were found in addition to the band with a peak at 436 $m\mu$ (with a subsidiary peak at 411 $m\mu$) which had been obtained by earlier workers for *p*-benzosemiquinone ion [4] or its derivatives [1, 2].

In the present work the absorption spectra of *p*-benzosemiquinone ion and its derivatives are studied further in the same way as was carried out in a previous paper [3].

2. EXPERIMENTAL

Semiquinone ions were prepared in a mixture of ethylene glycol (three parts) and aqueous potassium hydroxide (one part), either by reduction of the quinone with sodium dithionite or by oxidation of the hydroquinone with atmospheric oxygen. The methods have been described elsewhere [3]. Since the concentration of potassium hydroxide is adjusted to 0.1~0.25 M in the solutions used for the reactions, it may be considered that semiquinones exist in the ionized form for ($Q^{\cdot-}$) and the presence of the radical (QH^{\cdot}) can be actually neglected†.

The structural formulae of the semiquinone ions studied in the present work are collected in figure 2.

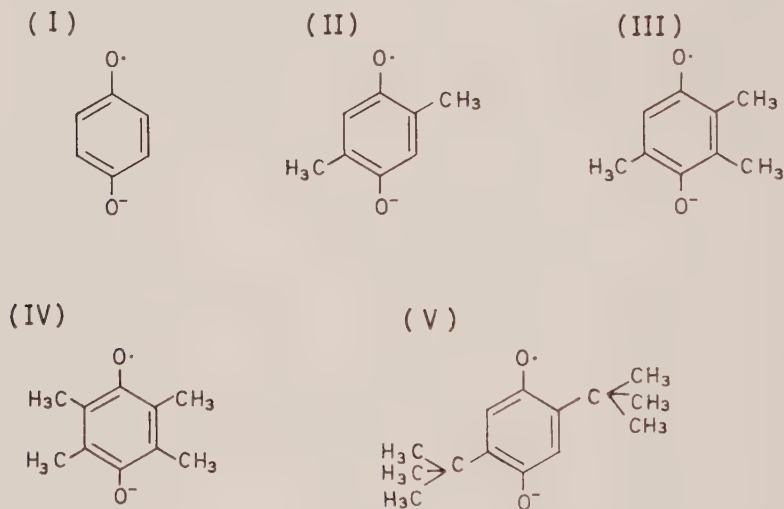


Figure 2. The structural formulae of the semiquinone ions studied.

- (I) *p*-benzosemiquinone ion.
- (II) 2,5-dimethyl-*p*-benzosemiquinone ion.
- (III) Trimethyl-*p*-benzosemiquinone ion.
- (IV) Tetramethyl-*p*-benzosemiquinone (durosemiquinone) ion.
- (V) 2,5-di-*tert*-butyl-*p*-benzosemiquinone ion.

2.1. The formation of the semiquinone ions by reduction of the quinone solutions

2,5-dimethyl- (II in figure 2) and tetramethyl-*p*-benzosemiquinone (durosemiquinone; IV in figure 2) ions were prepared by reduction of the corresponding quinones. Since the quinones are easily attacked by alkali, potassium

† For instance, the equilibrium constant in 50 per cent EtOH/H₂O for the reaction $Q^{\cdot-} + H^+ \rightleftharpoons QH^{\cdot}$ of durosemiquinone is 1.2×10^{-6} l./mol [1]. Therefore, the concentration ratio of $[QH^{\cdot}]/[Q^{\cdot-}]$ in the solutions is less than 10^{-7} .

hydroxide aqueous solutions should be added to the ethylene glycol solutions of quinones immediately before reduction. The quinone solution (10^{-4} mol/l.) thus obtained was poured into a cylindrical cell ($l=1$ cm) with a stopper and was reduced by an addition of sodium dithionite. After the excess dithionite, if present, was oxidized with atmospheric oxygen, the absorption spectrum of the hydroquinone ion was measured with a Cary recording spectrophotometer, model-14 at $25^{\circ}\text{C}\dagger$. By further oxidation the spectra in various reducing steps of the quinone could be observed.

2.2. The formation of the semiquinone ions by oxidation of the hydroquinone solutions

Non-substituted (I in figure 2), trimethyl- (III in figure 2) and 2,5-di-*tert*-butyl-*p*-benzosemiquinone ions (V in figure 2) were prepared by oxidation of the corresponding hydroquinones. The potassium hydroxide aqueous solution (1 mol/l.) was added to the hydroquinone dissolved in ethylene glycol (10^{-4} mol/l.) and the mixture was homogenized in a glass vessel. The change of its colour from colourless to yellow showing the formation of the semiquinone ion occurred immediately after mixing. With combination of oxidizing reagent, atmospheric oxygen, and reducing one, sodium dithionite, the equilibrium between the hydroquinone and quinone was controlled to obtain suitable steps of the redox system.

The measurements of their absorption spectra were also carried out using a Cary recording spectrophotometer, model-14 at 25°C . One scanning from 550 to $220\text{ m}\mu$ was made within two minutes. Four absorption bands, which are assumed to be due to the semiquinone ion as discussed in the following section, were observed in the same ratio of intensities in various steps of the redox reaction and simultaneously disappeared in both the final steps, the quinone and the hydroquinone. Moreover, the process of $\text{quinone} \rightleftharpoons \text{hydroquinone}$ via the intermediate semiquinone ion can be carried out several times without the appearance of foreign bands. Hence, none of these four bands may be due to products of secondary reactions.

3. RESULTS AND DISCUSSION

3.1. Di-*tert*-butyl-*p*-benzosemiquinone ion

Owing to the bulky substituents this semiquinone ion is the most stable one of those studied in the present experiment. The absorption spectra of the solutions obtained by oxidation of the hydroquinone are given in figure 3. Curve 1 of figure 3 shows the spectrum of the original hydroquinone in ethylene glycol. On an addition of potassium hydroxide aqueous solution, the hydroquinone was oxidized to the quinone (curve 4) through the intermediate steps of oxidation (curves 2 and 3) \ddagger . Curve 2 is the mixture of the absorption spectra of the hydroquinone and the semiquinone ions while curve 3 which corresponds to a further

\dagger While the absorption spectrum of sodium dithionite has a broad band with a maximum at $315\text{ m}\mu$, its oxidized species does not absorb appreciably above $230\text{ m}\mu$. Hence, the presence of the latter does not obstruct the measurement of the optical densities of the semiquinone ion to this wavelength.

\ddagger Curves 2 and 3 were obtained by the following procedure. One part of the potassium hydroxide aqueous solution, 1 mol/l., was added to three parts of the sample solution. When both solutions were homogenized in a glass vessel, the hydroquinone was oxidized to the quinone. This quinone solution was put into a cylindrical cell and reduced back with an addition of sodium dithionite obtaining the spectrum given by curve 2 or 3.

oxidation step than curve 2 shows the co-existence of the semiquinone ion and the quinone, the peak of the original hydroquinone no longer appearing†. As is easily seen from curve 2 or 3, in the visible and near ultra-violet regions the absorption spectrum of the semiquinone ion is composed of three intense bands; one band of those has two peaks at 436 and 411 $m\mu$ ‡ and the others having maxima at 373 and 323.5 $m\mu$, respectively. The consideration of the intensities shows that these three absorption bands may be due to the $\pi \rightarrow \pi^*$ allowed transition. This assignment is supported by the results of the ASMO calculation which will be reported in the following paper [5]. In addition to the above bands, there is a weak absorption in the 450~550 $m\mu$ region, which might be due to an $n \rightarrow \pi^*$ transition, namely, the transition from the non-bonding electron orbital of the oxygen atom to an excited π -electron orbital.

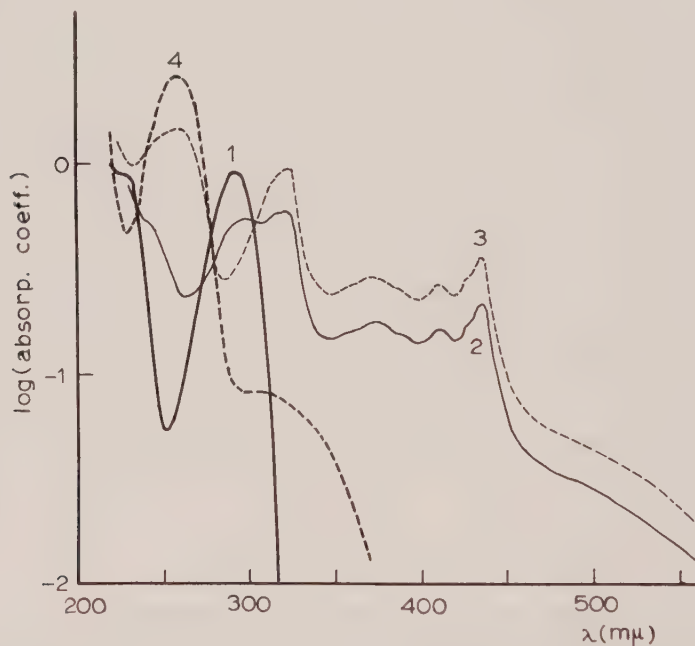


Figure 3. The absorption spectra of the solutions obtained by oxidation of di-tert-butylhydroquinone.

- | | |
|---|---|
| 1. Hydroquinone (2.06×10^{-4} mol/l.) in ethylene glycol. | } in
alkaline
ethylene
glycol. |
| 2. Semiquinone ion (ca. 26 per cent) + hydroquinone (ca. 74 per cent) | |
| 3. Semiquinone ion (ca. 43 per cent) + quinone (ca. 57 per cent) | |
| 4. Quinone (1.55×10^{-4} mol/l.) | |
- The total concentration of curve 2 or 3 is 1.55×10^{-4} mol/l.

The concentration of the quinone in curve 3 is obtained from the values of the extinction coefficient, ϵ_q , and the optical density at 257.5 $m\mu$, where ϵ_q is determined from curve 4 to be 1.66×10^4 l. mol $^{-1}$ cm $^{-1}$. Knowing the concentration of the semiquinone ion which is assumed to be the difference between the

† In the case of a lower OH^- concentration, e.g. $[\text{OH}^-] = 0.025$ mol/l., the formation of the semiquinone ion is scarce and with the formation of the semiquinone ion three species, the quinone, the semiquinone ion and the hydroquinone ion, exist together.

‡ The frequency difference of about 1400 cm^{-1} between these two peaks may presumably correspond to the C-O stretching frequency in the excited state.

total concentration and that of the quinone enables us to estimate the extinction coefficients of the absorption maxima of the semiquinone ion (curve 3). The results are given in the table. In the case of curve 3 the concentration of the semiquinone ion is 0.67×10^{-4} mol/l., while the total concentration being 1.55×10^{-4} mol/l. Thus the quantity of the semiquinone ion amounts to 43 per cent of that of the original hydroquinone.

3.2. Tetramethyl-*p*-benzosemiquinone (durosemiquinone) ion

This semiquinone ion was prepared by reduction of duroquinone with sodium dithionite.

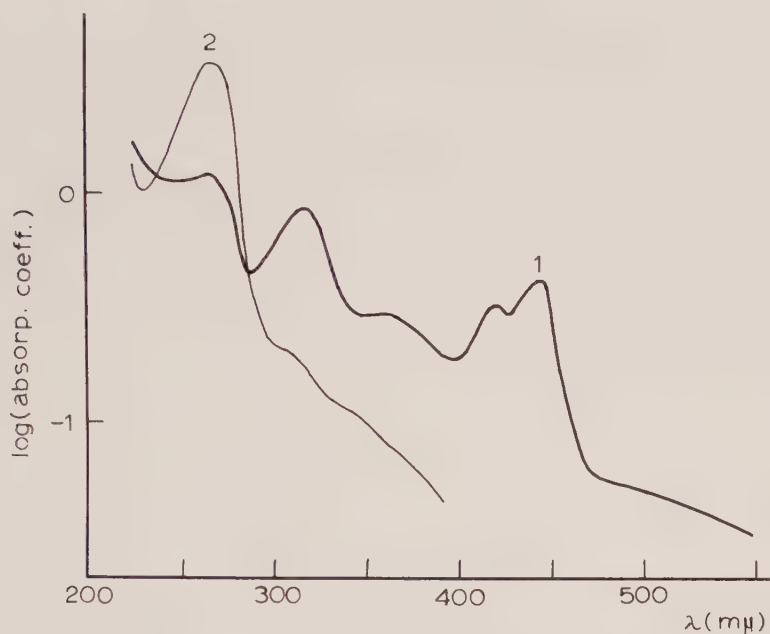


Figure 4. The absorption spectrum of the solution by reduction of duroquinone.

- | | |
|--|-------------------------------------|
| 1. Semiquinone ion with some amount of the quinone | } in alkaline
ethylene
glycol |
| 2. Quinone (1.88×10^{-4} mol/l.) | |

The absorption spectrum of the semiquinone ion including some amount of the quinone is given in figure 4. Four bands which were found in the spectral response of di-*tert*-butyl-*p*-benzosemiquinone ion appeared also for the durosemiquinone ion as shown in figure 4. In spite of its stability due to the full substitution of methyl group, the semiquinone was not stable enough to allow the determination of the exact value of the molar extinction coefficient. Especially its quinone is easily attacked by alkali. For instance, when one part of potassium hydroxide solution (1 mol/l.) was added to three parts of the quinone solution (1.16×10^{-4} mol/l.), the intensity of the peak at $264\text{ m}\mu$ of the quinone was diminished to 75 per cent of the initial value within ten minutes. From the time dependence of the peak intensity it was found that the rate of the decomposition of the quinone, at least within one hour, was proportional to the square of the

concentration of the quinone, the second order rate coefficient being $2.95 \times 10^2 \text{ l./mol min.}$ This behaviour shows that the combination of two molecules occurs at the initial stage of the decomposition following a bi-molecular reaction. In the case of di-tert-butyl-*p*-benzoquinone (or its semiquinone ion), on the contrary, the chemical change caused by alkali was negligibly small within several minutes and we could obtain the absorption spectrum of the semiquinone ion. This suggests that the attack by alkali takes place on the oxygen atoms.

3.3. Other semiquinone ions

Although trimethyl- and dimethyl-*p*-benzosemiquinone ions were much more unstable than the durosemiquinone ion and the absorption spectra changed considerably within a few minutes, the positions of the three intense bands due to the $\pi \rightarrow \pi^*$ transitions could still be determined in a fairly strong alkaline solution of ethylene glycol. However, in the case of non-substituted *p*-benzosemiquinone ion, a weak alkaline medium should be used for detecting the semiquinone ion, since the ion caused chemical reaction immediately in such strong alkaline solutions as those used for the formation of other semiquinone ions. Since, as was previously stated, the concentration of semiquinone ions is very low in weak alkaline media, a concentrated hydroquinone solution must be used for obtaining the spectral response curve of the semiquinone ion. In this case, only the longest wavelength band $432 \text{ m}\mu$ (with a subsidiary peak at $408 \text{ m}\mu$) could be observed, while the shorter wavelength bands were masked by the tail of the absorption band of hydroquinone itself.

	$\lambda \text{ (m}\mu\text{)}$			
Benzo-	432	408	—	—
	430 ($\epsilon_{\text{max}} = 7.4 \times 10^3$)	404†	—	—
2,5-dimethyl-	436	412	370 (s)	318
Trimethyl-	437	413	365	317
Tetramethyl-	442	418	360 (s)	313
	440 ($\epsilon_{\text{max}} = 10 \times 10^3$)	416‡	—	—
	438	415§	—	—
2,5-di-tert-butyl- ϵ_{max}	436 5.3×10^3	411 4.0×10^3	373 4.2×10^3	323.5 14.0×10^3

† Ref. [4]; solvent, NaOH aq. solution.

‡ Ref. [2]; solvent, NaOH aq. solution.

§ Ref. [1]; solvent, 50 per cent EtOH/H₂O + 0.02N-NaOH.

|| (s) designates a shoulder.

The absorption maxima of *p*-benzosemiquinone ions.

The absorption maxima of various *p*-benzosemiquinone ions studied in the present work are collected in the table, together with the results of other investigators.

Finally, it remains to be reported that the semiquinone ion can be prepared from the quinone in alkaline ethylene glycol only by expelling oxygen dissolved in it. For instance, the alkaline ethylene glycol solution of duroquinone developed gradually a yellow colour having the spectrum of the semiquinone ion as nitrogen is bubbled through the solution†. This showed that oxygen dissolved in the solution participates in the equilibrium between the quinone and the hydroquinone. It has been shown in the oxidation of di-*tert*-butyl-hydroquinone with atmospheric oxygen that one can control the equilibrium of the reaction to some extent and can obtain the appropriate intermediate steps (curve 2 or 3 of figure 3). This probably corresponds to shifts of the equilibrium resulting from the change of the concentration of dissolved oxygen.

The authors wish to thank Professor S. Nagakura for his valuable suggestions. Their thanks also are due to Dr. Y. Matsunaga for his helpful discussion.

REFERENCES

- [1] BRIDGE, N. K., and PORTER, G., 1958, *Proc. roy. Soc. A*, **244**, 259, 276.
- [2] BAXENDALE, J. H., and HARDY, H. R., 1953, *Trans. Faraday Soc.*, **49**, 1433.
- [3] HARADA, Y., and MATSUNAGA, Y., 1961, *Bull. chem. Soc., Japan*, **34**, 585.
- [4] DIEBLER, H., EIGEN, M., and MATTHIES, P., 1961, *Z. Elektrochem.*, **65**, 634.
- [5] HARADA, Y., 1964, *Mol. Phys.*, **8**, 273.

† In this case, ethylene glycol seems to act as a reducing reagent.

Electronic structure of *p*-benzosemiquinone ion

by YOSHIYA HARADA

The Institute for Solid State Physics, The University of Tokyo

(Received 8 August 1963)

The electronic structure of *p*-benzosemiquinone ion is studied with the aid of the semi-empirical ASMO treatment including configuration interaction.

Firstly, the simple MO's of this ion are obtained using the iterative method. According to the simple MO calculation the lack of uniformity of π -electron densities due to the existence of heteroatoms is found to be notable in the *p*-benzosemiquinone ion. It is shown that the calculated excitation energies can explain the peak wavelengths in the observed absorption spectra, if the effect of this lack of uniformity in π -electron densities is reflected in the atomic integrals.

1. INTRODUCTION

While the electronic structures of hydrocarbon mono-negative ions have been studied considerably [1], the theoretical investigations of those of semiquinone ions have scarcely ever been made [2] because of the deficient knowledge concerning the optical absorption spectra and also of the difficulty in carrying out a reliable calculation with systems containing heteroatoms. In previous papers [3] we have studied the absorption spectra of some semiquinone ions in a viscous solvent and found that substituted *p*-benzosemiquinone ions have three intense absorption bands in visible or near ultraviolet region; their absorption peaks are around 440 m μ , 370 m μ and also 320 m μ †.

In this article the electronic structure of *p*-benzosemiquinone ion is studied with the aid of the semi-empirical ASMO treatment including configuration interaction to interpret these absorption bands.

2. THEORY AND CALCULATIONS

2.1. Formulation

The theoretical method to calculate the electronic structure of *p*-benzosemiquinone ion is based on the framework of the semi-empirical ASMO CI method due to Pariser and Parr [4], with only the π -electrons considered explicitly.

The Hamiltonian operator, \mathcal{H} is expressed in the form

$$\mathcal{H} = \sum_i \mathcal{H}_{\text{core}}(i) + \sum_{i>j} \frac{e^2}{r_{ij}}, \quad (1)$$

where $\mathcal{H}_{\text{core}}(i)$ possesses the kinetic energy operator for π -electron i and also its potential energy operator in the field of the core :

$$\mathcal{H}_{\text{core}}(i) = \mathcal{T}(i) + \mathcal{U}_{\text{core}}(i). \quad (2)$$

† In addition to these bands there is a weak absorption in the region 450~550 m μ , which might be due to an n - π^* transition.

The ortho-normal molecular orbitals (simple MO), ϕ_i , are given by:

$$\phi_i = \sum_{\mu} C_{i\mu} \chi_{\mu}, \quad (3)$$

where χ_{μ} is the μ th $2p\pi$ atomic orbital of carbon or oxygen.

In the ground state of mono-negative ions such as semiquinone ions, the lowest anti-bonding orbital, ϕ_{n+1} , is occupied by one electron, so that the ground state is doublet. For this configuration the anti-symmetrized molecular orbital (ASMO), ${}^2\Psi_g$ is described by:

$${}^2\Psi_g = (N!)^{-1/2} |\phi_1 \bar{\phi}_1 \phi_2 \bar{\phi}_2 \dots \phi_n \bar{\phi}_n \phi_{n+1}|, \quad (4)$$

where $N(=2n+1)$ is the number of π -electrons. If we confine ourselves to the singly excited configurations, the excited wave functions fall into the following five classes[†]:

$${}^2\Psi_{n+1, k'} = (N!)^{-1/2} |\phi_1 \bar{\phi}_1 \phi_2 \bar{\phi}_2 \dots \phi_n \bar{\phi}_n \phi_{k'}|, \quad (5)$$

$${}^2\Psi_{i, n+1} = (N!)^{-1/2} |\phi_1 \bar{\phi}_1 \phi_2 \bar{\phi}_2 \dots \phi_i \dots \phi_n \bar{\phi}_n \phi_{n+1} \bar{\phi}_{n+1}|, \quad (6)$$

$$\Psi_{ik'}(A) = (N!)^{-1/2} |\phi_1 \bar{\phi}_1 \phi_2 \bar{\phi}_2 \dots \phi_i \dots \phi_n \bar{\phi}_n \phi_{n+1} \bar{\phi}_{k'}|, \quad (7)$$

$$\Psi_{ik'}(B) = (N!)^{-1/2} |\phi_1 \bar{\phi}_1 \phi_2 \bar{\phi}_2 \dots \phi_i \dots \phi_n \bar{\phi}_n \phi_{n+1} \phi_{k'}|, \quad (8)$$

$$\Psi_{ik'}(C) = (N!)^{-1/2} |\phi_1 \bar{\phi}_1 \phi_2 \bar{\phi}_2 \dots \bar{\phi}_i \dots \phi_n \bar{\phi}_n \phi_{n+1} \phi_{k'}|, \quad (9)$$

where $\Psi_{ik'}$ describes the configuration due to the one-electron excitation from some orbital, ϕ_1 filled in ${}^2\Psi_g$, to a higher unfilled orbital, $\phi_{k'}$. Since these functions, $\Psi_{ik'}(A)$, $\Psi_{ik'}(B)$ and $\Psi_{ik'}(C)$ are not the eigen functions of the spin operator, \mathcal{S}^2 , the following linearly independent configurations are taken [1]:

$${}^2\Psi_{ik'}(\text{I}) = 6^{-1/2} [\Psi_{ik'}(A) + \Psi_{ik'}(B) - 2\Psi_{ik'}(C)], \quad (10)$$

$${}^2\Psi_{ik'}(\text{II}) = 2^{-1/2} [\Psi_{ik'}(A) - \Psi_{ik'}(B)], \quad (11)$$

$${}^4\Psi_{ik'} = 3^{-1/2} [\Psi_{ik'}(A) + \Psi_{ik'}(B) + \Psi_{ik'}(C)]. \quad (12)$$

Here, ${}^2\Psi_{ik'}(\text{I})$ and ${}^2\Psi_{ik'}(\text{II})$ both correspond to doublet states, $S_z = \hbar/2$, $S^2 = (3/4)\hbar^2$, whereas ${}^4\Psi_{ik'}$ to a quartet state, $S_z = \hbar/2$, $S^2 = (15/4)\hbar^2$. Since doublet-quartet transitions are spin-forbidden ones, a given electronic state function, ${}^2\Phi_{\omega}$, is approximated by a linear combination of doublet functions:

$${}^2\Phi_{\omega} = \sum_i A_{\omega i} {}^2\Psi_i, \quad (13)$$

where ${}^2\Psi_i$ stands for one of the wave functions given by equations (4), (5), (6), (10) and (11).

By applying the above mentioned configuration interaction process, the energy levels and wave functions of the *p*-benzosemiquinone ion can be evaluated with satisfactory results. Further, the oscillator strength, f , is calculated by the method described by Mulliken and Rieke [5]:

$$f = 1.085 \times 10^{11} \omega_{ab} \sum_{i=x,y,z} |(\Phi_a | M_i | \Phi_b)|^2, \quad (14)$$

where ω_{ab} is the frequency of the transition in cm^{-1} .

[†] Since the configuration corresponding to $S_z = \hbar/2$ (not $S_z = -\hbar/2$) has been chosen as the ground state, we may take only these configurations corresponding to $S_z = \hbar/2$ as the excited states.

2.2. Simple MO for *p*-benzosemiquinone ion

In order to apply the present method to a particular molecule, firstly we must obtain MO's which are expressed linearly in terms of AO's. The calculation of these orbitals is made using the iterative method described by Nagakura [6].

In the present investigation, calculations† are repeated five times, until the evaluated values of the π -electron densities and the bond orders become self-consistent. The final results are shown in figure 1. Further, the final orbital energies and the corresponding MO's are given in table 1.

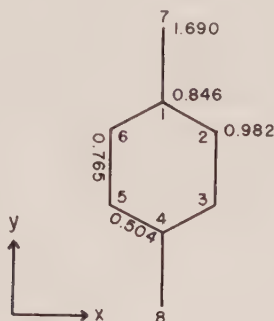


Figure 1. Electron densities and bond orders of *p*-benzosemiquinone ion.

Symmetry	$\frac{E - \alpha}{\beta}$	Molecular orbital
b_{1u}	2.276	$\phi_1 = 0.4164(\chi_1 + \chi_4) + 0.3150(\chi_2 + \chi_3 + \chi_5 + \chi_6) + 0.3581(\chi_7 + \chi_8)$
b_{3g}	1.898	$\phi_2 = 0.4066(\chi_1 - \chi_4) + 0.1312(\chi_2 - \chi_3 - \chi_5 + \chi_6) + 0.5479(\chi_7 - \chi_8)$
b_{1u}	1.166	$\phi_3 = 0.0416(\chi_1 + \chi_4) + 0.2957(\chi_2 + \chi_3 + \chi_5 + \chi_6) - 0.5686(\chi_7 + \chi_8)$
b_{2g}	1.034	$\phi_4 = 0.5000(\chi_2 + \chi_3 - \chi_5 - \chi_6)$
b_{3g}	0.387	$\phi_5 = 0.4062(\chi_1 - \chi_4) + 0.2724(\chi_2 - \chi_3 - \chi_5 + \chi_6) - 0.4319(\chi_7 - \chi_8)$
a_u	-1.014	$\phi_6 = 0.5000(\chi_2 - \chi_3 + \chi_5 - \chi_6)$
b_{1u}	-1.094	$\phi_7 = 0.5600(\chi_1 + \chi_4) - 0.2517(\chi_2 + \chi_3 + \chi_5 + \chi_6) - 0.2200(\chi_7 + \chi_8)$
b_{3g}	-1.986	$\phi_8 = 0.4118(\chi_1 - \chi_4) - 0.3982(\chi_2 - \chi_3 - \chi_5 + \chi_6) - 0.1150(\chi_7 - \chi_8)$

Table 1. Molecular orbitals and orbital energies of *p*-benzosemiquinone ion.

2.3. Semi-empirical evaluation of integrals

Molecular integrals, $[ij|kl]$ and I_{ij} , are expanded in terms of atomic integrals which are divided into two types of atomic integrals, namely Coulomb repulsion integrals‡ and core integrals. These integrals are evaluated by the semi-empirical procedure analogous to that of Pariser and Parr [4].

† On the first step of this iterative calculation the bond distances are necessary for the evaluation of the overlap integrals. As the bond distances of *p*-benzosemiquinone ion have not yet been determined, the values of *p*-benzoquinone (Robertson, J. M., 1935, *Proc. roy. Soc. A*, **150**, 106); $r_{c_1o} = 1.14$ Å, $r_{c_1c_2} = 1.50$ Å, $r_{c_2c_3} = 1.32$ Å) were used. These values being gradually corrected in the course of the iteration, the final ones are $r_{c_1o} = 1.20$ Å, $r_{c_1c_2} = 1.43$ Å and $r_{c_2c_3} = 1.38$ Å.

‡ From the assumption of zero differential overlap, all integrals except those of the Coulomb type are neglected.

2.3.1. *Coulomb repulsion integrals*

The Coulomb repulsion integrals are given by:

$$(\mu\mu|\nu\nu) = \int \chi_\mu^*(1) x_\nu^*(2) \frac{e^2}{r_{12}} \chi_\mu(1) \chi_\nu(2) d\tau. \quad (15)$$

The one centre-Coulomb repulsion integral, $(\mu\mu|\mu\mu)$ is obtained by:

$$(\mu\mu|\nu\nu) = W_\mu - A_\mu, \quad (16)$$

where W_μ and A_μ are the valence state ionization potential and the electron affinity of atom μ , respectively. Since W_μ and A_μ must be regarded as varying with the π -electron density, $P_{\mu\mu}$, and also its lack of uniformity is notable in *p*-benzosemiquinone ion (cf. figure 1), W_μ and A_μ are determined by the following method [7] so as to allow for this variation. Firstly, for atoms in the first row of the periodic table the effective nuclear charge, Z_μ is varied according to the electron density around the corresponding nucleus:

$$Z_\mu = N_\mu - 1.35 - 0.35(\sigma_\mu + P_{\mu\mu}), \quad (17)$$

where N_μ and σ_μ are the atomic number and the number of σ -electrons contributed to the molecular framework by atom μ , respectively. If W_μ 's are plotted against Z_μ 's for the (sp^3 , V_4) valence state of the iso-electronic series, B^- , C, N^+ , the curve is parabolic†:

$$W_\mu(sp^3, V_4) = 3.52Z_\mu^2 - 8.96Z_\mu + 3.36. \quad (18)$$

Further, for the valence states, (sp^4 , V_3), (s^2p^4 , V_2) and (s^2p^5 , V_1) of the isoelectronic series, C^- , N, O^+ ; N^- , O, F^+ ; and O^- , P, Ne^+ :

$$W_\mu(sp^4, V_3) = A_\mu(sp^3, V_4) = 3.715Z_\mu^2 - 16.183Z_\mu + 13.933, \quad (19)$$

$$W_\mu(s^2p^4, V_2) = 3.855Z_\mu^2 - 16.586Z_\mu + 12.936, \quad (20)$$

$$W_\mu(s^2p^5, V_1) = A_\mu(s^2p^4, V_2) = 4.125Z_\mu^2 - 27.212Z_\mu + 39.251, \quad (21)$$

are obtained. Then, substitution of equations (18) and (19) into (16) gives for the (sp^3 , V_4) valence state:

$$(\mu\mu|\mu\mu) = -0.195Z_\mu^2 + 7.223Z_\mu - 10.573. \quad (22)$$

Similarly, equations (16), (20) and (21) yield for the (s^2p^4 , V_2) valence state:

$$(\mu\mu|\mu\mu) = -0.360Z_\mu^2 + 10.626Z_\mu - 26.315. \quad (23)$$

Thus, one-centre Coulomb integrals of carbon and oxygen atoms in the semiquinone ions are obtained from equations (22) and (23), respectively.

The two-centre Coulomb integrals were calculated for $r_{\mu\nu} \geq 2.8 \text{ \AA}$ from the uniformly charged sphere model formula [8] using the effective nuclear charges given by equation (17). For $r_{\mu\nu} < 2.80 \text{ \AA}$ they were obtained from the extrapolation formulae of the type:

$$ar + br^2 = \frac{1}{2}[(\mu\mu|\mu\mu) + (\nu\nu|\nu\nu)] - (\mu\mu|\nu\nu), \quad (24)$$

in which the constants a and b are obtained by fitting values calculated from the uniformly charged sphere model formula for $r_{\mu\nu} = 2.80 \text{ \AA}$ and 3.70 \AA .

† Various valence-state ionization potentials have been calculated from atomic spectroscopic data (Pritchard, H. O., and Skinner, H. A., 1955, *Chem. Rev.*, **55**, 745; Moore, C. E., 1949, *Atomic Energy Levels*, Vol. I, Circular of the National Bureau of Standards).

2.3.2. Core integrals

The core integrals are given by:

$$H_{\mu\nu}^{\text{core}} = \int \chi_{\mu}^*(1) \mathcal{H}^{\text{core}}(1) \chi_{\nu}(1) d\tau \equiv \begin{cases} \alpha_{\mu} & (\mu = \nu), \\ \beta_{\mu\nu} & (\mu \neq \nu). \end{cases} \quad (25)$$

Neglecting the penetration integrals, α_{μ} is calculated from the formula:

$$\alpha_{\mu} = -W_{\mu} - \sum_{\nu \neq \mu} (\mu\mu|\nu\nu), \quad (26)$$

	$r_{\mu\nu}$	$P\mu\mu \neq 1\dagger$	$P\mu\mu = 1\dagger$
(CC CC); (11 11)	0 Å	11.16 eV	10.84 eV
(22 22)	0	10.88	10.84
(22 33)	1.38	7.43	7.41
(11 22)	1.43	7.37	7.31
(11 33)	2.43	5.45	5.43
(OO OO); (77 77)	0	12.78	14.58
(77 88)	5.21	2.73	2.74
(CC OO); (11 77)	1.20	8.29	8.58
(22 77)	2.28	5.81	5.88
α_{C} ; α_1	—	—54.48	—53.84
α_2	—	—51.70	—51.57
α_{O} ; α_7	—	—47.13	—51.81
β_{CC} ; β_{12}	1.43	—2.04	—2.04
β_{23}	1.38	—2.53	—2.53
β_{CO} ; β_{17}	1.20	—2.95	—2.95
W_{C} ; W_1	—	12.18	11.42
W_2	—	11.51	11.42
W_{O} ; W_7	—	13.04	17.38

† The values in which the lack of uniformity in π -electron densities is reflected.

‡ The values calculated assuming that each atom of the molecule is neutral.

Table 2. The values of some of the atomic integrals and the valence state ionization potentials of *p*-benzosemiquinone ion.

where W_{μ} is determined from equation (18) or (20). $\beta_{\mu\nu}$ is neglected except in the case where μ refers to the nearest neighbour with ν . When μ and ν refer to the nearest neighbours with each other, $\beta_{\mu\nu}$ is calculated from the Kon's equations [9]:

$$\beta_{cc} = -\frac{17.464}{r_{cc}^6} \text{ eV}, \quad \beta_{co} = -\frac{8.8086}{r_{co}^6} \text{ eV}, \quad (27)$$

where r is the internuclear distance in angstroms. The proportionality constants of equation (37) were so chosen as to reproduce the observed first transition energies of ethylene and formaldehyde. These equations were applied to the assignment of the absorption bands of various compounds and gave fairly good results.

In the actual calculation $P_{\mu\mu}$ and $r_{\mu\nu}$, which have been obtained as the final results of the iterative procedure, are used, whereas the bond angles of the benzene ring are assumed to be 120° . Some of the atomic integrals of *p*-benzosemiquinone ion calculated by the present method are given in the third column of table 2, together with the values of W_μ . The fourth column of this table shows the corresponding values calculated assuming that each atom is neutral ($P_{\mu\mu} = 1$).

3. RESULTS AND DISCUSSION

In the calculation with configuration interaction, the ground and the singly excited doublet configurations were mixed. Seven configurations were considered for ${}^2B_{3g}$ states, nine for ${}^2B_{2u}$ states, five for 2A_u states and also seven for ${}^2B_{2g}$ states.

Symmetry	Energy (ev)†	ASMO with CI
B_{3g}	-2.389	${}^2\Phi_1 = 0.8601{}^2\Psi_{25} - 0.1976{}^2\Psi_{25} - 0.1267{}^2\Psi_{58} + 0.2772{}^2\Psi_{37}(\text{I})$ $+ 0.3393{}^2\Psi_{37}(\text{II}) - 0.0972{}^2\Psi_{28}(\text{I}) - 0.0612{}^2\Psi_{28}(\text{II})$
B_{1u}	0.571	${}^2\Phi_2 = 0.6261{}^2\Psi_{57} + 0.6887{}^2\Psi_{35} - 0.1933{}^2\Psi_{15} - 0.0315{}^2\Psi_{46}(\text{I})$ $+ 0.0384{}^2\Psi_{46}(\text{II}) - 0.1498{}^2\Psi_{38}(\text{I}) - 0.0645{}^2\Psi_{38}(\text{II})$ $+ 0.1737{}^2\Psi_{27}(\text{I}) - 0.1927{}^2\Psi_{27}(\text{II})$
A_u	1.090	${}^2\Phi_3 = 0.9700{}^2\Psi_{56} - 0.0577{}^2\Psi_{47}(\text{I}) - 0.0615{}^2\Psi_{47}(\text{II})$ $+ 0.2234{}^2\Psi_{26}(\text{I}) - 0.0459{}^2\Psi_{26}(\text{II})$
B_{1u}	2.069	${}^2\Phi_4 = 0.6534{}^2\Psi_{57} - 0.5754{}^2\Psi_{35} + 0.1085{}^2\Psi_{15} + 0.2747{}^2\Psi_{46}(\text{I})$ $- 0.1308{}^2\Psi_{46}(\text{II}) - 0.1247{}^2\Psi_{38}(\text{I}) + 0.2836{}^2\Psi_{38}(\text{II})$ $+ 0.1939{}^2\Psi_{27}(\text{I}) + 0.0637{}^2\Psi_{27}(\text{II})$
B_{2g}	2.719	${}^2\Phi_5 = 0.4412{}^2\Psi_{45} + 0.3964{}^2\Psi_{36}(\text{I}) + 0.7571{}^2\Psi_{36}(\text{II})$ $+ 0.0513{}^2\Psi_{48}(\text{I}) - 0.2312{}^2\Psi_{48}(\text{II}) - 0.1368{}^2\Psi_{16}(\text{I})$ $- 0.0157{}^2\Psi_{16}(\text{II})$

† The energy of B_{3g} ground state without CI (the ground state energy of figure 2 (1)) is taken to be zero.

Table 3. ASMO'S and MO energies of *p*-benzosemiquinone ion (those of higher electronic states are neglected.)

The wave functions of the ground state and of the lower excited ones, together with the excitation energies are shown in figure 3. For the purpose of comparison with these values excitation energies were also evaluated using the parameters of the fourth column in table 2 (parameters obtained assuming that each atom in the molecule is neutral). The calculated excitation energies with and without CI are collected in figure 2 in comparison with the observed values. As is seen in figure 2, the theoretical results obtained by considering configuration interaction can explain the peak wavelengths in the observed absorption spectra, if the effect of the lack of uniformity in π -electron densities is reflected in the atomic integrals (figure 2 (2)).

On the other hand, when one has no regard for this effect, the agreement between the calculated and the observed results is poor, in spite of mixing of the

† In the CI calculation of figure 2 (4), the same configurations as those of figure 2 (2) were considered.

rather many configurations† (figure 2 (4)). This behaviour may conceivably be common to molecules containing heteroatoms in their π -electronic systems, since the existence of heteroatoms bring about the lack of uniformity of π -electron densities.

It is clear from the results given in figure 2 that the configuration interaction plays an important role for the assignment of the optical absorption spectra. This situation may be introduced from the incompleteness of the simple MO's employed to this calculation. Although the present procedure to obtain the simple MO's is a self-consistent one, the application of incompletely defined one-electron Hamiltonian is unsatisfactory. When one proceeds to the ASMO CI calculation for larger semiquinone ions, it may well be necessary to establish the procedure of obtaining better simple MO's in order to keep away from the laborious work of invoking the extensive configuration interaction.

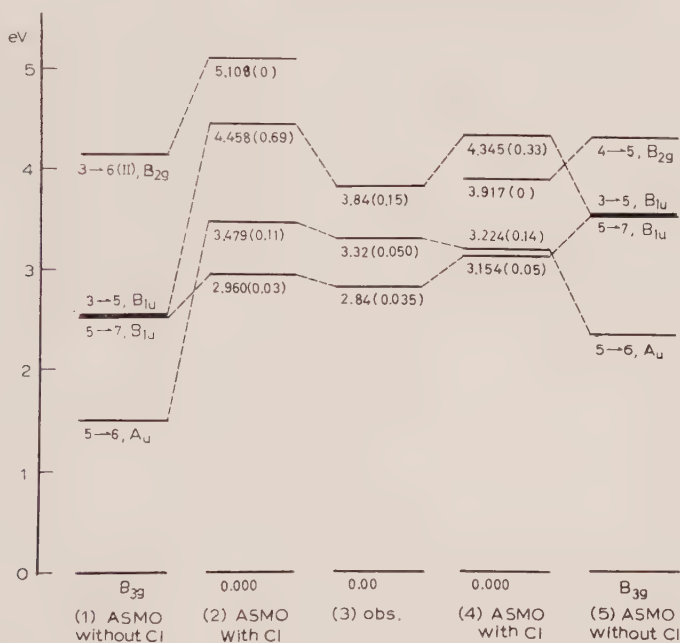


Figure 2. The observed and calculated energy levels (oscillator strengths are given in parentheses). In the case of (1) or (2) the effect of the lack of uniformity in π -electron densities is reflected in the atomic integrals. For (4) or (5) the effect of the lack of uniformity in π -electron densities is not reflected in the atomic integrals. Observed values are those of di-tert-butyl-*p*-benzosemiquinone ion in an alkaline ethylene glycol [3]. The first π - π^* transition for non-substituted *p*-benzosemiquinone ion has been observed at 432 m μ , i.e. 2.87 eV. In each case the energy of B_{3g} ground state is taken to be zero.

The author wishes to thank Professor S. Nagakura and Professor H. Inokuchi for their kind direction throughout the course of this work. His thanks are also due to Dr. A. Kuboyama and Professor H. Thubomura for their helpful discussion.

REFERENCES

- [1] BALK, P., DE BRUIJN, S., and HOIJTINK, G., J. 1957, *Rec. trav. chim. Pays-Bas*, **76**, 907. HOIJTINK, G. J., 1959, *Mol. Phys.*, **2**, 85.
- [2] MATSUNAGA, Y., 1960, *Bull. chem. Soc., Japan*, **33**, 1436. VINCOW, G., and FRAENKEL, G. K., 1961, *J. chem. Phys.*, **34**, 1333. For the purpose of analysing hfs of E.S.R. spectra of semiquinone ions, these authors only calculated unpaired π -electron densities by the simple MO method.
- [3] HARADA, Y., and MATSUNAGA, Y., 1961, *Bull. chem. Soc., Japan*, **34**, 585. HARADA, Y., and INOKUCHI, H., 1964, *Mol. Phys.*, **8**, 265.
- [4] PARISER, R., and PARR, R. G., 1953, *J. chem. Phys.*, **21**, 466, 767. PARISER, R., 1956, *J. chem. Phys.*, **24**, 250.
- [5] MULLIKEN, R. S., and RIEKE, C. A., 1941, *Rep. Progr. Phys.*, **8**, 231.
- [6] NAGAKURA, S., 1952, *Bull. chem. Soc., Japan*, **25**, 164. NAGAKURA, S., and KUBOYAMA, A., 1954, *J. Amer. chem. Soc.*, **76**, 1003.
- [7] BROWN, R. D., and HEFFERNAN, M. L., 1958, *Trans. Faraday Soc.*, **54**, 757. MATAGA, S., and MATAGA, N., 1959, *Z. Phys. Chem.*, **19**, 231.
- [8] PARR, R. G., 1952, *J. chem. Phys.*, **20**, 1499.
- [9] KON, H., 1955, *Bull. chem. Soc., Japan*, **28**, 275.

Hypersensitive pseudoquadrupole transitions in lanthanides

by CHR. KLIXBÜLL JØRGENSEN

Cyanamid European Research Institute,
Cologne (Geneva), Switzerland

and B. R. JUDD

Laboratoires de Bellevue, C.N.R.S., Bellevue,
Seine et Oise, France

(Received 15 January 1964; revision received 4 February 1964)

It is pointed out that the absorption lines of the lanthanides that are peculiarly sensitive to changes in the ligands are consistent with the selection rules for quadrupole radiation within the 4f shell. A number of sources for this sensitivity are examined, and it is concluded that it owes its origin to the inhomogeneity of the dielectric. According to this mechanism, there is an asymmetrical distribution of the dipoles induced by the electromagnetic field in the medium surrounding a lanthanide ion. The variation across the lanthanide ion of the electric vector is very much greater than for the case of a homogeneous dielectric, and the intensities of quadrupole transitions are enormously enhanced.

1. INTRODUCTION

For a given lanthanide ion, it often happens that one or more of the narrow absorption bands caused by internal transitions in the partly filled 4f shell become more intense, frequently by an order of magnitude, when the water molecules of the aquo ions are replaced by other ligands, whereas the other narrow bands show almost no change in intensity. Acetylacetonates have been studied by Moeller and Ulrich [1], acetates by Sonesson [2], phenanthroline complexes by Kononenko and Poluektov [3], while Carnall *et al.* [4–6] and Abrahamer and Marcus [7] have extensively investigated molten nitrates and concentrated solutions of nitrates in organic solvents. If we examine the *SLJ* designations [8, 9] of the excited levels of these hypersensitive transitions, a striking regularity at once appears: The selection rule $\Delta J = \pm 2$ is rigorously obeyed; the excited levels almost always have a value of *J* two units lower than that of the corresponding ground level, the single exception being the hypersensitive transition ${}^7F_0 \rightarrow {}^5D_2$ in Eu(III); and, in so far as Russell–Saunders coupling obtains, the value of *L* is also two units lower than that of the corresponding ground multiplet. Furthermore, the converse is true; all the known transitions satisfying these conditions are hypersensitive. The excited levels (indicating the most important *LS* component; due to intermediate coupling effects, *S* is frequently

mixed) of the known hypersensitive transitions are as follows (1 kK = 1000 cm⁻¹) :

$^4\text{I}_{9/2} \rightarrow ^4\text{G}_{5/2}$	at 17.3 kK of $4f^3$	Nd(III)
$^6\text{H}_{5/2} \rightarrow ^6\text{F}_{1/2}$	at 6.2 kK of $4f^5$	Sm(III) [4]
$^7\text{F}_0 \rightarrow ^5\text{D}_2$	at 21.5 kK of $4f^6$	Eu(III) [10-12]
$^6\text{H}_{15/2} \rightarrow ^6\text{F}_{11/2}$	at 7.7 kK of $4f^9$	Dy(III) [6]
$^5\text{I}_8 \rightarrow ^3\text{K}_6$	at 22.2 kK of $4f^{10}$	Ho(III)
$^5\text{I}_8 \rightarrow ^5\text{G}_6(?)$	at 26.2 kK of $4f^{10}$	Ho(III) [7]
$^4\text{I}_{15/2} \rightarrow ^2\text{H}_{11/2}$	at 19.2 kK of $4f^{11}$	Er(III)
$^4\text{I}_{15/2} \rightarrow ^4\text{G}_{11/2}$	at 26.5 kK of $4f^{11}$	Er(III)
$^3\text{H}_6 \rightarrow ^3\text{F}_4$	at 12.6 kK of $4f^{12}$	Tm(III) [7]

It is well known [13] that the selection rules for electric quadrupole transitions are $\Delta J \leq 2$, and, if Russell-Saunders coupling obtains, $\Delta L \leq 2$, $\Delta S = 0$. In spite of the similarity between these rules and the conditions satisfied by the hypersensitive transitions, we cannot immediately infer that the absorption is actually quadrupole in character. Instances where the effect of one kind of perturbation mimics that of another kind occur frequently in atomic spectroscopy (for example, second-order spin-orbit interaction perturbs the levels of a multiplet in an identical way to first-order spin-spin interaction [14]). In fact, the hypersensitivity can easily be embraced in the formal theory that has already been developed for line intensities of solutions of lanthanide ions. According to this theory, which was constructed on the hypothesis that all transitions are forced electric dipole in origin, the oscillator strength P for an absorption transition from the level Ψ_J to the level $\Psi'_{J'}$ is given by :

$$P = \sum_{\lambda=2,4,6} \nu T_{\lambda} (\Psi_J \| U^{(\lambda)} \| \Psi'_{J'})^2, \quad (1)$$

where ν is the corresponding frequency, and $\mathbf{U}^{(\lambda)}$ is the unit tensor operator whose single-particle components $\mathbf{u}^{(\lambda)}$ have amplitudes defined by :

$$(f \| \mathbf{u}^{(\lambda)} \| f) = 1.$$

To account in a formal way for the hypersensitivity, we need only suppose that of the three parameters T_{λ} ($\lambda = 2, 4$, or 6), T_2 is peculiarly sensitive to the environment of the lanthanide ions.

To see this, we proceed as follows. For the matrix element of $\mathbf{U}^{(2)}$ not to vanish, we must have $|J - J'| \leq 2$: and, in the limit of Russell-Saunders coupling, where Ψ and Ψ' correspond to definite values SL and $S'L'$ of the total spin and total orbital angular momentum quantum numbers, the dependence on J and J' of this contribution to P is contained in the expression :

$$A(J, J') = \delta(S, S')(2J+1)(2J'+1) \left\{ \begin{matrix} L & L' & 2 \\ J' & J & S \end{matrix} \right\}^2.$$

Particular cases of the 6- j symbol can be found from the tables of Rotenberg *et al.* [16], though it is not difficult to exhibit the dependence of $A(J, J')$ on J' . We first note that for $A(J, J')$ not to vanish, $S' = S$. A glance at a table of the permitted terms of the configurations f^n at once reveals that, as a consequence of the Pauli Exclusion Principle and the fact that S and L are determined by Hund's Rule, L' never exceeds $L - 2$. Owing to the triangular condition on the three numbers forming the upper row of the 6- j symbol, L' must in fact be

equal to its maximum value $L-2$ for the 6- j symbol not to vanish. There are now two cases to consider: either the lanthanide ion corresponds to a 4f shell that is more than half-full, or to one that is less than half-full. (The ion Gd(III), corresponding to an exactly half-filled shell, is of no immediate interest to us.) In the former case, $J=L+S$, and, with $S'=S$ and $L'=L-2$, all 6- j symbols vanish except those for which $J'=J-2$. If, on the other hand, the shell is less than half-full, we have $J=L-S$, and the 6- j symbol is non-vanishing for several values of J' . However, on using the detailed algebraic expression for the 6- j symbol [16], we readily find that in this case:

$$\frac{A(J, J'-1)}{A(J, J')} = \frac{(2J'-1)(L-S+3+J')(L-1+S+J')}{(2J'+1)(L-S+3-J')(L-1+S-J')}.$$

This expression is typically of the order of 5 or 10. This means that, of the five transitions $J \rightarrow J-2, J-1, J, J+1, J+2$, the influence of the parameter T_2 should invariably be felt most strongly by the first, namely $J \rightarrow J-2$. Since terms associated with the other parameters T_4 and T_6 usually make substantial contributions to any transition, we should not be surprised if a variation of intensity proves difficult to detect in those cases where $J' \neq J-2$.

We can therefore relate all the observed selection rules for the hypersensitive lines, unusual though they are, to the variation of a single parameter, T_2 . The central question, that of the origin of the variation, remains. In treating this below, we examine a number of possible mechanisms. For each one we introduce a parameter $T_2^{(i)}$ representing the contribution to the observed T_2 . Owing to the concomitant effects of T_4 and T_6 , it is difficult to extract an accurate value of T_2 from experiment without a lengthy and detailed analysis for every ion-solvent combination. Since our aim is to discover the source of the hypersensitivity, we need not consider in detail all the hypersensitive transitions mentioned above. It is convenient to limit ourselves to Nd(III) and Er(III), particularly the former. A special study of the line intensities for just these two cases has already been performed for aqueous solutions [15], thereby making available a number of matrix elements of $\mathbf{U}^{(2)}$ that would otherwise have to be calculated.

2. PURE QUADRUPOLE RADIATION

We should first inquire whether it is conceivable that the hypersensitive transitions could be electric quadrupole in character. Take the nucleus of a lanthanide ion as the origin of coordinates. The purely electric (as opposed to magnetic) energy of a 4f electron in the electromagnetic radiation field is $-eV$, where the electric potential V is a function of x, y, z and t . Expanding this product in a power series in r , and neglecting an additive constant, we obtain:

$$\mathcal{H} = e(\mathbf{r} \cdot \mathbf{E}) + er^2(2/3)^{1/2}(\mathbf{C}^{(2)} \cdot (\nabla \mathbf{E})^{(2)}) \quad (2)$$

for the first two terms. The notation of Edmonds [17] is used for the tensor products. The electric intensity \mathbf{E} and its derivatives are to be evaluated at the origin. For f electrons, the tensors $\mathbf{C}^{(2)}$ and $\mathbf{U}^{(2)}$ are related by the equivalence:

$$\mathbf{C}^{(2)} \equiv -(28/15)^{1/2} \mathbf{U}^{(2)}.$$

It is, of course, the second term in equation (2) that gives rise to electric quadrupole transitions. For the moment, we make the usual assumption that the lanthanide ion is embedded in a perfectly homogeneous dielectric of refractive index n .

Treating \mathcal{H} as a perturbation, and averaging over all possible orientations for \mathbf{E} , we obtain :

$$P' = \nu T_2^{(1)} (\Psi_J \| U^{(2)} \| \Psi'_{J'})^2 \quad (3)$$

for the contribution to the total oscillator strength of a transition $\Psi_J \rightarrow \Psi'_{J'}$, where:

$$T_2^{(1)} = \frac{112}{225(2J+1)} \left(\frac{\pi^3}{\alpha} \right) \left(\frac{a_0}{\lambda} \right)^2 \left(\frac{a_0}{c} \right) \chi(f | (r^2/a_0^2) | f)^2. \quad (4)$$

In this expression, a_0 is the Bohr radius, α is the fine structure constant, λ is the wavelength of a particular band and $\chi = n(n^2 + 2)^2/9$. As far as possible, the component factors of $T_2^{(1)}$ have been constructed to be dimensionless. We note that the right-hand side of equation (3) is of the same form as regards its dependence on J and J' as the first term in the summation of equation (1). Thus, for a small range of λ , the relative intensities of electric quadrupole transitions will be identical to those of forced electric dipole transitions for which T_2 is the dominant parameter.

According to Hoogschagen and Gorter [18], $P = 1.05 \times 10^{-5}$ for the line at 17.3 kK in aqueous solutions of Nd(III). An increase by a factor of four, which is by no means uncommon for hypersensitive lines, gives $P = 4.1 \times 10^{-5}$. Putting in the value [15] of the appropriate reduced matrix element, we find that this corresponds to $T_2 = 8.8 \times 10^{-20}$ sec. We now calculate $T_2^{(1)}$ from equation (4), taking $\lambda = 5800 \text{ \AA}$, $1/\alpha = 137$, $a_0 = 0.53 \text{ \AA}$, $J = 9/2$, $\chi = 2.10$ (appropriate to water), $(4f | (r^2/a_0^2) | 4f) = 1.0$ (from Freeman and Watson's calculation for Nd^{3+} [19]), and $a_0/c = 1.76 \times 10^{-19}$ sec. The result is :

$$T_2^{(1)} = 6.5 \times 10^{-25} \text{ sec},$$

which falls short of the observed figure by a factor of 10^5 .

As it stands, this calculation would give variations in $T_2^{(1)}$ only through variations in χ , which are much too small to account for the difference. Recently however, evidence for weak σ -anti-bonding effects involving the 4f electrons of lanthanide ions has become apparent [20]. In the L.C.A.O. approximation, pure 4f orbitals are replaced by combinations of the type:

$$\psi_{\text{M.O.}} = a\psi_{4f} - b\psi_{\sigma},$$

where, in a symbolic notation, ψ_{σ} represents a combination of σ -orbitals of the ligand atoms having the same symmetry type as the corresponding 4f orbital ψ_{4f} . It is known from the nephelauxetic effect [21-23] that the order of magnitude of b is 0.1 for most lanthanide complexes. Under exceptional circumstances, corresponding to strongly conjugated ligands, it would not be surprising if b were as large as 0.2. In such cases, we may make the replacement :

$$(4f | (r/a_0)^2 | 4f) \rightarrow (\sigma | (r/a_0)^2 | \sigma)/25$$

in equation (4) if the radical extension of ψ_{σ} is sufficiently large. But even if the orbitals ψ_{σ} extend as far as 5 \AA from the nucleus of the lanthanide ion, corresponding to $(\sigma | (r/a_0)^2 | \sigma) \sim 100$, we gain at most a factor of the order of 20 in the calculation of $T_2^{(1)}$. Since $T_2^{(1)}$ now depends critically on the orbitals ψ_{σ} and the constant b , we could understand qualitatively the hypersensitivity of the lines in question ; but the discrepancy by a factor of over 10^3 that remains forces us to discard this mechanism, at any rate in the simple form presented here.

3. FORCED ELECTRIC DIPOLE RADIATION

It is natural to speculate on whether the variation of T_2 could be accommodated within the framework of the theory of forced electric dipole radiation that led up to equation (1). The chief difficulty here is that almost any reasonable mechanism for producing a change in T_2 would produce equally or more important changes in T_4 and T_6 . Thus hypersensitivity would be a characteristic of all absorption lines, in disagreement with experiment. For example, a change in the radial extension of the 4f, 5d, or 5g orbitals would affect all those radical integrals such as $\langle 4f|r^k|5d \rangle$ which, for k odd, are responsible for the coupling of configurations of opposite parity [15]. However, such a change influences two parameters, T_{k-1} and T_{k+1} , and hence by varying the integrals for $k=3$, it would be impossible to obtain a variation in T_2 without a simultaneous change in T_4 .

This argument is not valid for $k=1$, since all matrix elements of $\mathbf{U}^{(0)}$ that accompany T_0 vanish. In fact, it would suggest a possible source for the variation of T_2 were it not for the fact that there are no terms of the type involving single powers of r in the usual expression for the contribution to the Hamiltonian for the interaction of a lanthanide ion with its neighbours. The reason for excluding such terms is that their presence would imply an electric field at the nucleus of the lanthanide ion, which could therefore not be in equilibrium. This argument is undoubtedly correct for crystals, but a moment's thought shows that it certainly cannot be applied with equal force to solutions. After all, the lanthanide ions do not occupy fixed points in the liquid; and if one of them is to move, an electric field must be present at its nucleus, since virtually all the mass of the ion is located there.

To get an idea of the electric fields required to account for the observed hypersensitivity, we suppose that the motion in the liquid has suddenly given rise to a charge $\pm e$ a distance ρ from the nucleus of the lanthanide ion. The contribution $T_2^{(2)}$ to T_2 produced by the electric field at the nucleus is found to be given by

$$T_2^{(2)} = \chi' \left(\frac{a_0}{c} \right) \left(\frac{4\pi}{3\alpha} \right) \left(\frac{a_0}{\rho} \right)^4 \frac{8}{945(2J+1)} \\ \times \left[9 \sum_{n'} \frac{|(4f|(r/a_0)|n'd)|^2}{\Delta(n'd)/\Delta_0} + 5 \sum_{n'} \frac{|(4f|(r/a_0)|n'g)|^2}{\Delta(n'g)/\Delta_0} \right]^2,$$

where $\Delta_0 = 219 \text{ kK}$, $\chi' = 1.19$ [13], and $\Delta(n'd)$ denotes the energy required to excite a 4f electron into the orbital $n'l$. For Nd(III), we take $\Delta(5d)/\Delta_0 = 0.26$, and ignore other orbitals for simplicity. We use $\langle 4f|(r/a_0)|5d \rangle = 0.87$ [15] and arrive at the result:

$$T_2^{(2)} = 7(a_0/\rho)^4 \times 10^{-17} \text{ sec.} \quad (5)$$

To obtain the required value of $8.8 \times 10^{-20} \text{ sec}$ for T_2 , it is necessary that $\rho \simeq 3 \text{ \AA}$. This is of the same order of magnitude as the distance to the nearest neighbours of the lanthanide ion, and it implies that they are ejected from their positions sufficiently frequently for the lanthanide ion never to come into static equilibrium with its nearest neighbours. Apart from the difficulty of understanding how only T_2 of the three parameters T_λ could be sensitive to this mechanism, there is strong experimental evidence against it. Sayre *et al.* [24] have found that

in fluorescence the line ${}^5D_0 \rightarrow {}^7F_2$ of Eu(III) is very much enhanced if alcohol instead of water is used as a solvent. (We might, of course, have expected such a line to be hypersensitive.) Nevertheless, the fine structure of 7F_2 is clearly discernible, pointing to a rigid structure for each europium ion and at least its nearest neighbours. Moreover, there is no marked intensity change in passing from room temperature down to 4°K , where the alcohol forms a glass. Such a drop in temperature would produce an enormous decrease in the random motion of the atoms and ions; and yet no significant decrease in the intensity is observed. For these reasons, we reject the above mechanism.

4. VIBRATIONAL EFFECTS

Before going on to discuss what we feel to be the true explanation for the hypersensitivity, we consider briefly the possibility that the transitions are not purely electronic, but correspond to the simultaneous excitation of a vibrational mode in the structure comprising the lanthanide ion and its immediate surroundings. These vibrational motions produce electric fields at the nucleus, and, just as in §3 above, they give rise to a contribution $T_2^{(3)}$ to T_2 . Similar radial integrals appear in the calculations, and we find:

$$T_2^{(3)} \simeq (N(\rho'')^2 \rho^4 / (\rho')^6) T_2^{(2)},$$

where ρ' is the radius of the oscillating complex comprising the lanthanide ion and its immediate neighbours, ρ'' the amplitude of the oscillation and N is a dimensionless factor depending on the geometry of the vibrating complex and on the charges on the ligands. With the aid of equation (5), we find:

$$T_2^{(3)} \simeq 7(N(\rho'')^2 a_0^4 / (\rho')^6) \times 10^{-17} \text{ sec.} \quad (6)$$

In order for the experimentally observed increase of T_2 not to be accompanied by simultaneous increases in T_4 , and T_6 , we can restrict our attention to those modes of oscillation in which the lanthanide ion and at least its nearest neighbours vibrate as an almost rigid unit. This is because T_4 and T_6 depend on the higher harmonics in the electric potential produced by the surroundings of the lanthanide ion, and these in turn depend on higher inverse powers of the radial distance than that part of the potential responsible for contributions to T_2 only. An added reason for selecting such modes for study is that in alcoholic solutions of Eu(III), the pure electronic transitions from 5D_0 to the five components of 7F_2 and from 7F_0 to the five components of 5D_2 appear to be enhanced; hence, if the increase is due to vibronic transitions, the vibrations must have an exceptionally low frequency. Thus ρ' should be at least 4 \AA , or roughly $10a_0$. Simple models suggest N should be of the order of 10. As for ρ'' , it can scarcely be larger than $a_0/5$, for otherwise the oscillations of the lanthanide ion and its immediate neighbours would carry the ions of the surrounding medium with them. This is not to rule out the possibility of oscillations of larger amplitude; but if they occur we should have to take into account the consequent distribution of charge in the medium at distances ρ' very much larger than $10a_0$; and, in view of the dependence of $T_2^{(3)}$ on $(\rho')^{-6}$, we anticipate that their contributions to $T_2^{(3)}$ would be negligible. Putting in equation (6) the values of the parameters, we find $T_2^{(3)} \sim 10^{-22} \text{ sec}$. This is too small by a factor of roughly 10^3 . We conclude that the hypersensitive transitions cannot arise from vibrational effects.

5. INHOMOGENEOUS DIELECTRIC

In deriving the intensity of pure quadrupole radiation in § 2, it was assumed that the lanthanide ion is embedded in a homogeneous dielectric of refractive index n . In this approximation, the amplitude of the tensor $(\nabla \mathbf{E})^{(2)}$ depends on that fact that, at any given instant, there is a spatial variation of the electric intensity vector \mathbf{E} . Since the wavelength of visible radiation is very much greater than the dimension of the lanthanide ion, there will be only a slight change of \mathbf{E} from one side of the ion to the other. However, a very large contribution to \mathbf{E} comes from dipoles induced in the medium by the electromagnetic radiation; and if they are not distributed in a perfectly homogeneous manner, the variation of \mathbf{E} across the ion can be profoundly altered.

To obtain an estimate of this effect, we first write:

$$\mathbf{E} = \mathbf{E}_0 \exp(i\boldsymbol{\kappa} \cdot \mathbf{r}),$$

thereby separating out the spatial variation of \mathbf{E} that is characteristic of an electromagnetic wave propagated in the direction of a vector $\boldsymbol{\kappa}$. For a homogeneous medium of refractive index n , the magnitude of $\boldsymbol{\kappa}$ is related to the frequency ν by the equation $|\boldsymbol{\kappa}| = 2\pi\nu n/c$, and \mathbf{E}_0 is a function solely of the time. In this case,

$$(\nabla \mathbf{E})^{(2)} = (i\boldsymbol{\kappa} \mathbf{E})^{(2)},$$

and so

$$|(\nabla \mathbf{E})^{(2)}|/|\mathbf{E}| \simeq |\boldsymbol{\kappa}| = 2\pi n/\lambda. \quad (7)$$

We now consider the situation in an inhomogeneous medium. As a simple model, we suppose, to begin with, that ions of equal polarizability α extend in a cubic array from the lanthanide ion with the exception of the ion at the position \mathbf{R} which has a polarizability 2α . We may relate the local electric field at the lanthanide ion to the dipoles induced by the electromagnetic radiation in the ions of the cubic lattice by the Lorentz-Lorenz formula [25]. If the ion at \mathbf{R} were unexceptional, we would have $(\nabla \mathbf{E}_0)^{(2)} = 0$ at the nucleus of the lanthanide ion, as in the case of a homogeneous dielectric; but with an additional induced moment of μ , the amplitude of $(\nabla \mathbf{E})^{(2)}$ is roughly equal to $5|\mu|/R^4$, where $R = |\mathbf{R}|$. The exact value of the numerical coefficient, taken here to be 5, depends on the relative orientation of \mathbf{R} and μ . The ratio ξ of this amplitude to that in the case of pure quadrupole radiation can be calculated from equation (7). The result is:

$$\xi \simeq \frac{15}{4\pi^2} \frac{n^2 - 1}{n(n^2 + 2)} \left(\frac{a}{R}\right)^3 \left(\frac{\lambda}{R}\right), \quad (8)$$

where a is the lattice constant. To get a numerical result, we put $n = 1.5$, $\lambda = 5000 \text{ \AA}$, and $a = 2.5 \text{ \AA}$. The ratio ξ is very sensitive to R ; if we set $R = a$, for which the exceptional ion is a nearest neighbour of the lanthanide ion, we find $\xi \simeq 75$. The intensity for pure quadrupole radiation depends on the square of $(\nabla \mathbf{E})^{(2)}$; hence the mechanism considered here will enhance $T_2^{(1)}$ by a factor of about 5000. In other words,

$$T_2^{(4)} \simeq \xi^2 T_2^{(1)} \simeq 3 \times 10^{-21} \text{ sec.}$$

This result is still smaller than the required value of $8.8 \times 10^{-20} \text{ sec}$; but only by a factor of 30. One might be tempted to apply the covalency argument of § 2 to account for the difference; but apart from the theoretical inconsistency in having to rely on those parts of the 4f electron eigenfunctions that lie at larger

radial distances than R , the experimental data [24] on the level splittings of 5D_2 and 7F_2 of Eu(III), which are very similar in both alcoholic and aqueous solutions, strongly suggest that no very striking change in $\langle r^2 \rangle$ is associated with the hypersensitivity.

A better way of accounting for the discrepancy is to improve the point-dipole model. The polarization produced by the electromagnetic field on an ion can be more realistically represented by an atomic orbital that has been slightly displaced from its normal position, or by a superposition of such orbitals. For a nearest neighbour, this resultant orbital, having a finite extension, approaches and penetrates the outer shells of the lanthanide ion, thereby leading to a greatly increased interaction with the 4f electrons. For example, if the electron of this orbital spends half its time at a distance $R/2$ from the lanthanide nucleus, and the other half at a distance $3R/2$ (instead of all of its time at a distance R), then ξ is increased by a factor of a little over 8. Since $T_2^{(4)}$ depends on ξ^2 , this is more than enough to remove the discrepancy. Moreover, the value of $\frac{1}{2}R$ implied in this calculation, namely $\frac{1}{2}R = 1.25 \text{ \AA}$, is considerably greater than the radius of the 4f electrons; hence there is no reduction to be made because of the penetration of the orbital inside the 4f shell. For once, the internal nature of the 4f electrons works to our advantage.

6. DISCUSSION

From the arguments given above, we conclude that the hypersensitivity of certain lines in the spectra of lanthanide ions has its origin in the inhomogeneity of the solvent. This greatly increases the spatial variation of the electric vector \mathbf{E} of the electromagnetic field, thereby enhancing permitted quadrupole transitions by a large factor. The most striking effects would be expected for highly polarizable solvent molecules, clustered in an asymmetric fashion around the lanthanide ions. We know virtually nothing about the structures of the solutions that exhibit strongly enhanced lines, but there definitely appears to be a connection between hypersensitivity and the polarizability of the solvent molecules, to judge from the refractive indices of the solutions.

It should be pointed out that the enhanced lines, although following the quadrupole selection rules, are, in principle, experimentally distinguishable from pure quadrupole transitions; for $T_2^{(1)}$ depends on λ^{-2} (see equation (4)), whereas $T_2^{(4)}$, like $T_2^{(2)}$ and $T_2^{(3)}$, is independent of λ . This distinction can be checked. According to Carnall [5], the ratio of the extinction coefficients for the two hypersensitive lines of Er(III) (at 26.5 kK and 19.2 kK) is 20.0/11.1, which is equal to 1.80. The relevant reduced matrix elements of $\mathbf{U}^{(2)}$ have already been given as 0.9533 and 0.8456 respectively [15]; with the aid of equations (3) and (4) we find that this ratio should be:

$$(26.5/19.2)^3(0.9533/0.8456)^2 = 3.34$$

for pure quadrupole radiation, and only

$$(26.5/19.2)(0.9533/0.8456)^2 = 1.76$$

for the radiation deriving from the inhomogeneity of the dielectric. The latter is certainly in better agreement with the experimental figure; however, the accord is probably in part fortuitous, since ξ^2 depends on $(n^2 - 1)^2$, and small changes in n , such as could easily occur over a range of λ as large as that considered here, might lead to significant corrections to the calculated figures.

If the hypersensitive lines, in their enhanced form, are ever observed in a single crystal, it will be possible to compare the polarizations of their components with what would be expected from pure quadrupole radiation. Theoretically, we would expect agreement only if the five components of $(\nabla \mathbf{E})^{(2)}$ are proportional to the five components of $(\nabla \mathbf{E}_0)^{(2)}$ at the nucleus of a lanthanide ion. There seems to be no reason to suppose that such a proportionality should be the rule rather than the exception. Because of these differences, if for no others, we refer to the hypersensitive transitions as *pseudoquadrupole*.

The different dependence on λ of quadrupole and pseudoquadrupole transitions has already been noted. The effect of an inhomogeneous dielectric is to offset the factors $(a_0/\lambda)^m$ that normally make higher terms in the expansion of \mathcal{H} given in equation (2) utterly negligible. This means that, from the theoretical point of view, we cannot discount out of hand the possibility that transitions of a higher multipole character than quadrupole can arise; though, since lines for which $\Delta J > 2$ are not hypersensitive, we can be reasonably sure that higher multipole radiation is unimportant. A possible reason for this is that the electrons of the neighbours of a lanthanide ion prefer to occupy s or p orbitals of the lanthanide ion when they approach it. A p orbital, pulsating in step with the electromagnetic field, would create an electric field that is of precisely the right symmetry to excite only quadrupole transitions; the s orbital, being spherically symmetric, would not play a role.

Having established that the hypersensitive transitions are pseudoquadrupole in those cases where they dominate the spectrum, we must consider the possibility that these transitions are at least in part pseudoquadrupole even when, as for aqueous solutions of lanthanide ions, their intensities are not abnormally large. In fact, it has already been noticed that of the three parameters T_2 , T_4 and T_6 , the first is rather larger than would be anticipated on the basis of forced electric dipole calculations in which d orbitals alone are admixed into the 4f orbitals [15]. The same conclusion was arrived at by Axe [26], who examined fluorescence in single crystals of europium ethylsulphate. In both instances, it was inferred that g orbitals were responsible for the discrepancy. However, the closure argument [15] that was used in an attempt to justify this result seems in retrospect unsatisfactory because it places the g orbitals of the continuum at too low an energy. We feel now that it would be more reasonable to ascribe the rather high value of T_2 to the presence of a contribution from pseudoquadrupole radiation, though further work is needed to put the matter beyond question.

7. CONCLUSION

The intensities of the pseudoquadrupole transitions depend on the squares and higher powers of many of the quantities that appear in the calculations, and this sensitivity makes our approximations and especially the models that we have used more susceptible to criticism. In the absence at present of detailed knowledge of the surroundings of the lanthanide ions, it seems virtually impossible to do accurate work. In spite of the fact that our calculations are order-of-magnitude estimates, we feel convinced that the origin of the hypersensitivity lies in the inhomogeneity of the dielectric, as reflected in the unequal distribution of the electromagnetically induced dipoles in the medium surrounding a lanthanide ion.

REFERENCES

- [1] MOELLER, T., and ULRICH, W. F., 1956, *J. inorg. nucl. Chem.*, **2**, 164.
- [2] SONESSON, A., 1958, *Acta chem. scand.*, **12**, 1937.
- [3] KONONENKO, L. I., and POLUEKTOV, N. S., 1962, *Russ. J. inorg. Chem.* (Engl. trans.), **7**, 965.
- [4] CARNALL, W. T., GRUEN, D. M., and MCBETH, R. L., 1962, *J. phys. Chem.*, **66**, 2159.
- [5] CARNALL, W. T., 1962, *Analyt. Chem.*, **34**, 786.
- [6] CARNALL, W. T., 1963, *J. phys. Chem.*, **67**, 1206.
- [7] ABRAHAMER, I., and MARCUS, Y., 1963, *Israel Atomic Energy Commission Report*, IA-809.
- [8] VAN UITERT, L. G., and JIDA, S., 1962, *J. chem. Phys.*, **37**, 986.
- [9] JØRGENSEN, C. K., 1962, *Orbitals in Atoms and Molecules* (London : Academic Press).
- [10] FREED, S., 1942, *Rev. mod. Phys.*, **14**, 105.
- [11] BAYER-HELMS, F., 1958, *Z. Naturf. A*, **13**, 161.
- [12] MILLER, D. G., SAYRE, E. V., and FREED, S., 1958, *J. chem. Phys.*, **29**, 454.
- [13] BROER, L. J. F., GORTER, C. J., and HOOGSCHAGEN, J., 1945, *Physica*, **11**, 231.
- [14] TREES, R. E., 1951, *Phys. Rev.*, **82**, 683.
- [15] JUDD, B. R., 1962, *Phys. Rev.*, **127**, 750.
- [16] ROTENBERG, M., BIVINS, R., METROPOLIS, N., and WOOTON, J. K., 1959, *The 3-j and 6-j Symbols* (Cambridge, Massachusetts : Massachusetts Institute of Technology Press).
- [17] EDMONDS, A. R., 1960, *Angular Momentum in Quantum Mechanics* (Princeton, New Jersey : Princeton University Press).
- [18] HOOGSCHAGEN, J., and GORTER, C. J., 1948, *Physica*, **14**, 197.
- [19] FREEMAN, A. J., and WATSON, R. E., 1962, *Phys. Rev.*, **127**, 2058.
- [20] JØRGENSEN, C. K., PAPPALARDO, R., and SCHMIDTKE, H.H., 1963, *J. chem. Phys.*, **39**, 1422.
- [21] JØRGENSEN, C. K., 1956, *Math.fys. Medd.*, **30**, No. 22.
- [22] JØRGENSEN, C. K., 1962, *Progress inorg. Chem.*, **4**, 33.
- [23] JØRGENSEN, C. K., PAPPALARDO, R., and RITTERSHAUS, E., 1964, *Z. Naturf. A*, **19**, 424.
- [24] SAYRE, E. V., MILLER, D. G., and FREED, S., 1957, *J. chem. Phys.*, **26**, 109.
- [25] MOTT, N. F., and GURNEY, R. W., 1940, *Electronic Processes in Ionic Crystals* (Oxford : University Press).
- [26] AXE, J. D., 1963, *J. chem. Phys.*, **39**, 1154.

RESEARCH NOTES

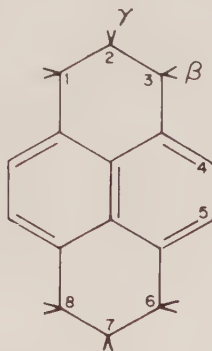
Conformational interconversion in the monovalent ions of 1,2,3,6,7,8-hexahydropyrene

by E. DE BOER and A. P. PRAAT

Koninklijke/Shell-Laboratorium, Amsterdam
(Shell Research N.V.)

(Received 24 February 1964)

The electron spin resonance spectra of the ions of 1,2,3,6,7,8-hexahydropyrene have been investigated.



The monopositive ion was produced either by dissolving the parent compound in concentrated sulphuric acid or in SO_2 , to which a small amount of BF_3 had been added. The mononegative ion was prepared by reduction with sodium in 1,2-dimethoxyethane.

The spectrum of the positive ion in SO_2 at -95°C consists of a superposition of two resonances of identical g values, which we attribute to the boat and chair conformations of the ion, present in equal amounts. With two sets of four splitting constants (see table) the observed hyperfine pattern can be matched completely. In agreement with expectations the equatorially (β') and axially (β) oriented protons have quite different splitting constants. The assignment given in the table is based on theoretical considerations [1]. From the observed second-order splitting of the central line we calculate for a_β a value of 14.8 ± 0.3 , in perfect agreement with the listed values.

One would also expect two different γ splitting constants. However, at temperatures several degrees below the freezing points of the solvents we still observe a single γ splitting constant, giving rise to a quintuplet splitting of each line.

The interpretation of the low-temperature spectrum of the negative ion required one set of four splitting constants only. Apparently the difference between the splitting constants of the two isomers is too small to make the resonances separately observable.

Drastic changes occur in the spectra when the temperature of the solutions is raised. This is illustrated in figure 1 for the mononegative ion. At a temperature of $+23^{\circ}\text{C}$ the observed lines represent only 36/256 of the total intensity of the hexahydropyrene ion spectrum. The other hyperfine components are

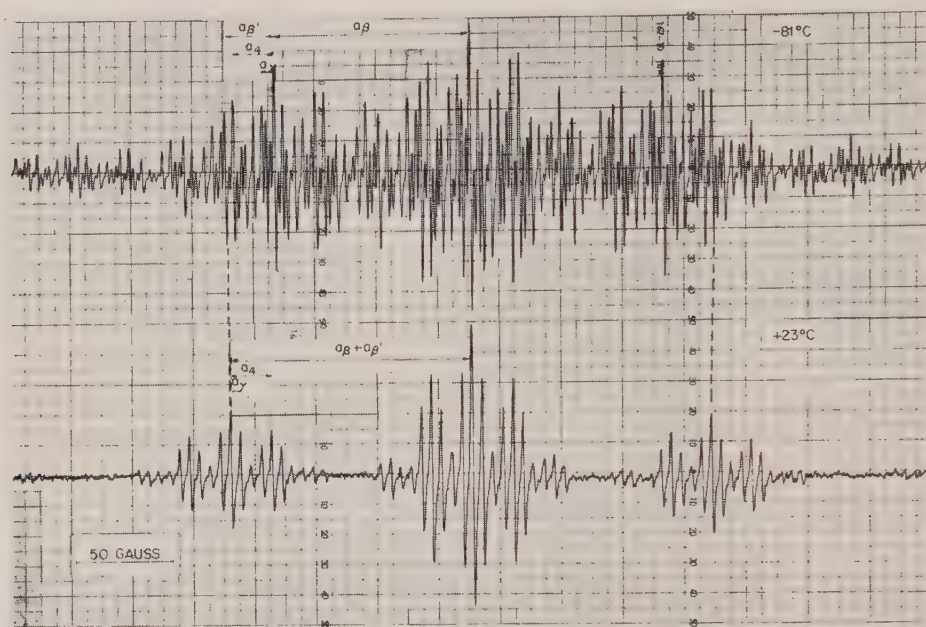


Figure 1. Central part of the first derivative curve of the E.S.R. spectrum of the mononegative ion of 1,2,3,6,7,8-hexahydropyrene in 1,2-dimethoxyethane at -81°C and $+23^{\circ}\text{C}$ with Na^+ as counter-ion. The dotted lines mark the unshifted components at $\pm(a_{\beta} + a_{\beta'})$. Modulation 100 kc/s, 0.03 gauss. Apparatus used: Varian V-4502-01. Varian magnet V-4012 A.

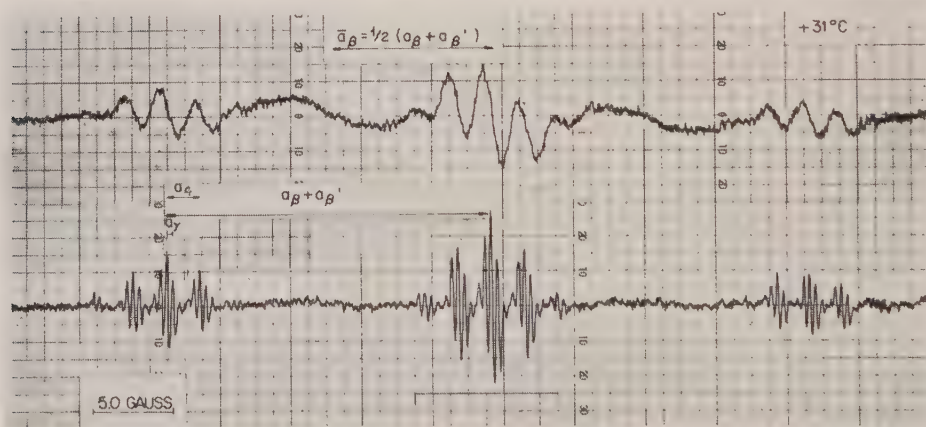


Figure 2. The three central groups of the first derivative curve of the E.S.R. spectrum of the monpositive ion of 1,2,3,6,7,8-hexahydropyrene in concentrated sulphuric acid at $+31^{\circ}\text{C}$. Upper curve modulation amplitude 1 gauss, lower curve modulation amplitude 0.120 gauss.

broadened and are unobservable with a field modulation adjusted to give proper recording of the narrow lines. Figure 2 gives the spectrum of the monopositive ion; the upper curve using high field modulation amplitude clearly shows the presence of broad lines.

In analogy with the interpretation given by Dixon and Norman [2] for the E.S.R. spectrum of the dioxane radical and by Fessenden and Schuler [3] for the E.S.R. spectrum of the cyclohexyl radical, the variations in the spectra of the ions of hexahydropyrene can be explained by dynamical equilibria between the boat and chair forms of the ions. This causes modulations in the isotropic aliphatic splitting factors, which in the limit of rapid interconversion give rise to a pronounced line-width alternation effect [4]. If the correlation diagram is drawn for the fine structure due to the eight β protons assuming that a_β and a_β' have the same sign it is clearly noted that a boat-chair transformation does not affect the positions of the outer lines, eight of the 16 components of the lines at a distance $\pm(a_\beta + a_\beta')$ from the central line and 18 of the 36 components of the central line. Therefore, these five lines remain narrow at all rates.

	Hexahydropyrene ⁺ SO ₂ H₂SO₄			Hexahydropyrene ⁻ 1,2-dimethoxyethane, Na ⁺	
	- 95°C		+ 31°C	- 81°C	+ 23°C
<i>a_γ</i>	0.40	0.40	0.36	0.50	0.42
<i>a_β</i> ₁	14.70	14.63	—	8.03	—
<i>a_β</i>	3.64	3.90	—	2.02	—
<i>a_β</i> + <i>a_β</i> ₁	—	—	18.3	—	9.86
<i>a₄</i>	1.90	1.90	1.90	1.69	1.69

Splitting constants in 1,2,3,6,7,8-hexahydropyrene ions in gauss.

If the rate becomes comparable to the hyperfine frequency one will observe only these five lines with an intensity ratio 1:8:18:8:1 and separated by $a_\beta + a_{\beta'}$. These lines are further split by the four aromatic protons and the four equivalent γ protons, resulting in a hyperfine pattern of five groups, consisting of 25 lines each. The observed high-temperature spectra correspond to this (see figures), which proves that a_β and $a_{\beta'}$ have indeed the same sign. If the signs were different the five groups would be separated by $|a_\beta| - |a_{\beta'}|$. The experimental intensity distribution of the five unshifted lines is in agreement with the ratio 1:8:18:8:1, predicted on the basis that the two sets of three CH₂ groups move independently of each other. If they moved in conjunction the intensity ratio should be 1:16:36:16:1.

A more detailed kinetic study is in progress.

REFERENCES

- [1] COLPA, J. P., and DE BOER, E., 1964, *Mol. Phys.*, **7**, 333.
- [2] DIXON, W. T., and NORMAN, R. O. C., 1963, Sixth International Symposium on Free Radicals, Cambridge, July.
- [3] FESSENDEN, R. W., and SCHULER, R. H., 1963, *J. chem. Phys.*, **39**, 2147.
- [4] CARRINGTON, A., 1962, *Mol. Phys.*, **5**, 425. FREED, J. H., and FRAENKEL, G. K., 1963, *J. chem. Phys.*, **39**, 326. DE BOER, E., and MACKOR, E. L., 1964, *J. Amer. chem. Soc.*, **86**, 1513.

Scheibe's rule and the SCF theory

by U. H. KOLLAARD and J. P. COLPA

Department of Theoretical Chemistry, Laboratory for Physical Chemistry,
University of Amsterdam, The Netherlands

(Received 1 April 1964)

1. INTRODUCTION

Some years ago Scheibe pointed out that in many atoms and molecules the energy difference between the lowest excited singlet state and the lowest state of ionization (in which one electron of the highest occupied orbital has been removed) is approximately constant and also approximately equal to the corresponding difference in the hydrogen atom [1] (see table 1). This regularity has been known since in the German literature as 'das Scheibesche Phänomen' or as the hydrogen rule. In the following we shall refer to it as Scheibe's rule. (We prefer to call it a rule rather than a phenomenon.)

	I (a)	Δ	$C = I - \Delta$
Biphenyl	8.3 (b)	4.8 (c)	3.5
Naphthalene	8.2 (f)	4.4 (c)	3.8
Phenanthrene	8.1 (g)	4.3 (d)	3.8
Anthracene	7.4 (g)	3.5 (d)	3.9
Pyrene	7.6 (g)	3.7 (c)	3.9
Perylene	7.1 (g)	2.8 (e)	4.3
Tetracene	7.0 (g)	2.9 (d)	4.1

(a) All these values are rounded off to 0.1 ev.

(b) Streitwieser, A., and Nair, P. M., 1959, *Tetrahedron*, **5**, 149.

(c) Watson, A. T., and Matsen, F. A., 1950, *J. chem. Phys.*, **18**, 1305.

(d) Ham, N. S., and Ruedenberg, K., 1955, Technical Report, Laboratory of Molecular Structure and Spectra, University of Chicago.

(e) Streitwieser, A., 1961, *MO Theory for Organic Chemistry*, p. 218.

(f) Matsen, F. A., 1956, *J. chem. Phys.*, **24**, 602.

(g) Riegler, G. B., and Czekalla, J., 1959, *Z. Elektrochem.*, **63**, 6.

Table 1. Experimental values for 'Scheibe's constant' C expressed in electron volts.

Hartmann tried to explain Scheibe's rule for the case of conjugated and aromatic hydrocarbons. He explicitly states [2] that the usual LCAO-SCF theory, with a $2p_z\pi$ atomic orbital basis and an explicit consideration of electron repulsion, fails to account for the observed regularity. This statement has recently been repeated by Hohlneicher and Scheibe [3]. Hartmann and co-workers indicate as the way out an extension of the theory of Hückel with the use of np_z orbitals ($n=3, 4$, etc.). Electron repulsion is neglected in this theory

[2-4]; overlap can be taken into account, but appears to have little influence [5]. It has been possible, however, to interpret the spectra and the ionization potentials of many organic molecules and ions with the SCF theory using $2p_z$ orbitals only. Therefore it appears incomprehensible why the use of higher p_z orbitals should be necessary to understand Scheibe's rule. In the following we will show that for a series of aromatic molecules the usual LCAO-SCF method (using $2p_z$ orbitals only) gives results which are in agreement with Scheibe's rule.

2. THEORY AND CALCULATIONS

The energy difference considered by Scheibe is the ionization energy of the first excited singlet state, which we shall denote by C . This quantity equals the difference between the ionization energy I and the excitation energy Δ of the first singlet state:

$$C = I - \Delta.$$

We now express C in terms of the MO theory. The highest occupied molecular orbital is denoted by m , the lowest unoccupied orbital by $m+1$. According to Koopmans' theorem we may write: $I = -\epsilon_m$, when ϵ_m is the eigenvalue which belongs to the m th eigenfunction (orbital) of the Hartree-Fock operator of the molecule. For Δ we have the expression [6]:

$$\Delta = \epsilon_{m+1} - \epsilon_m - J_{m, m+1} + 2K_{m, m+1}.$$

So for C we get:

$$C = I - \Delta = -\epsilon_{m+1} + J_{m, m+1} - 2K_{m, m+1}. \quad (1)$$

We have calculated the Coulomb integrals $J_{m, m+1}$ and the exchange integrals $K_{m, m+1}$ for a group of hydrocarbons in a LCAO approximation using the SCF orbitals and the repulsion parameters γ_{rp} . The values of these parameters were taken from Pariser [7]. The ϵ 's and the orbitals were calculated with Pople's modification of Roothaan's method [6, 8]. The Coulomb parameter α (U_{11} in Pople's notation), which only gives a constant shift in the values of the ϵ 's, was left undetermined. We can now check the constancy of C without knowing α . As many experimental values of I and Δ of aromatic hydrocarbons are known we can further get an empirical value of α by comparing the theoretical and experimental values of C . The results of the calculations are summarized in table 2.

	$\epsilon_{m+1} - \alpha$	$J_{m, m+1}$	$K_{m, m+1}$	$C + \alpha$	C_{theor} $\alpha = -9.72$	C_{exp}
Biphenyl	10.010	5.4751	0.6952	-5.9253	3.79	3.5
Naphthalene	9.764	5.7633	0.9451	-5.8909	3.83	3.8
Phenanthrene	9.645	5.2058	0.7685	-5.9762	3.74	3.8
Anthracene	9.058	5.1708	0.9062	-5.6996	4.02	3.9
Pyrene	9.007	4.7898	0.8941	-6.0054	3.71	3.9
Perylene	8.704	4.4454	0.6854	-5.6294	4.09	4.3
Tetracene	8.618	4.7579	0.8717	-5.6035	4.12	4.1

Table 2. Results of the calculations of 'Scheibe's constant' C expressed in electron volts.

3. DISCUSSION

From table 1 we see that the experimental values of C are fairly constant in a series of aromatic hydrocarbons: the average value is $C_{\text{exp}} = 3.9 + 0.17 \text{ ev}$. If we calculate C with formula (1) we also find approximately constant values the average of which is $C_{\text{theor}} = -5.82 \pm 0.15 - \alpha \text{ ev}$. Comparing these two values we find: $\alpha = -9.72 \pm 0.32 \text{ ev}$ which is a very acceptable value. In the last but one column of table 2 we give the values of C calculated with $\alpha = -9.72 \text{ ev}$. Comparison of the calculated and experimental values (which are not very accurate) shows that for the molecules we considered the usual LCAO-SCF theory gives results which are in fair agreement with Scheibe's rule. Our results are in conflict with Hartmann's statement that the results of an LCAO-SCF calculation with a $2p_z$ atomic orbital basis do not agree with Scheibe's rule.

REFERENCES

- [1] SCHEIBE, G., and BRÜCK, D., 1959, *Z. Elektrochem.*, **54**, 403; 1962, *Berichte*, **85**, 867.
SCHEIBE, G., KERN, I., and DÖRR, F., 1959, *Z. Elektrochem.*, **63**, 117.
SCHEIBE, G., 1961, *Chimia*, **15**, 10.
- [2] HARTMANN, H., 1960, *Z. Naturf. A*, **15**, 993; 1962, *Pure appl. Chem.*, **4**, 15.
- [3] HOHLNEICHER, G., and SCHEIBE, G., 1963, *Tetrahedron*, **19** (suppl. 2), 189.
- [4] RUCH, E., 1961, *Z. Naturf. A*, **16**, 808.
- [5] BINGEL, W. A., PREUSS, H., and SCHMIDTKE, H. H., 1961, *Z. Naturf. A*, **16**, 1328.
- [6] ROOTHAAN, C. C. J., 1951, *Rev. mod. Phys.*, **23**, 69.
- [7] PARISER, R., 1956, *J. chem. Phys.*, **24**, 250.
- [8] POPL, J. A., 1953, *Trans. Faraday Soc.*, **49**, 1375.

Restricted rotation of alkyl groups in alkyl cyclooctatetraene anions

by A. CARRINGTON and P. F. TODD

Department of Theoretical Chemistry, University Chemical Laboratory,
Lensfield Road, Cambridge

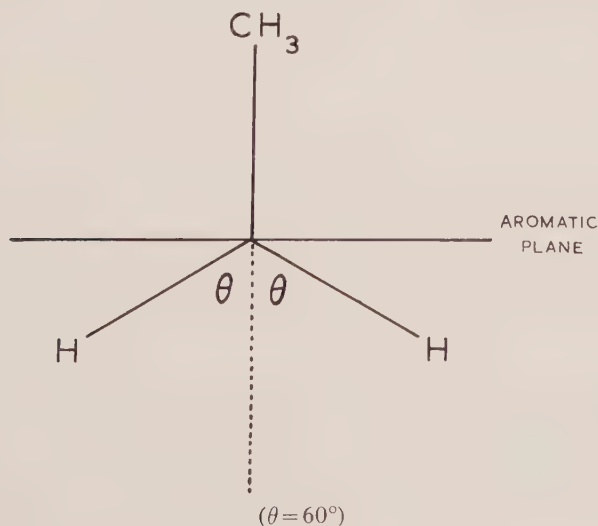
(Received 18 March 1964)

In a recent paper [1] we described the electron spin resonance spectra of the anions of methyl, ethyl and *n*-propyl cyclooctatetraene. We drew attention to anomalies in the hyperfine splitting from the alkyl protons but did not provide a quantitative explanation. We now do so in this note.

In the methyl cyclooctatetraene anion the methyl proton splitting is 5.1 gauss but in the ethyl and *n*-propyl cyclooctatetraene anions the —CH_2 splitting is only 2.5 gauss. This large difference is surprising since we know from the ring proton splittings that the spin density on the ring carbon atom to which the alkyl group is bonded decreases only very slightly.

We believe that this effect is due to restricted rotation of the ethyl group. Single crystal studies [2] of radicals containing the $\cdot\text{C—CH}_3$ unit show that, if the methyl group is not rotating, the splitting due to each methyl proton is $\rho B \cos^2 \theta$, where B is a constant, ρ is the carbon $2p_\pi$ spin population and θ is the angle between the C—H bond and an axis on the methyl carbon atom parallel to the axis of the p_π orbital containing the unpaired electron. In the methylcyclooctatetraene anion we assume essentially free rotation of the methyl group; the hyperfine splitting is therefore the average value of $\rho B \cos^2 \theta$, equal to $\rho B/2$.

In ethyl cyclooctatetraene we expect the configurations of lowest energy to be the two in which the C—CH₃ bond is perpendicular to (above or below) the



plane of the ring (figure 2). Hence the splitting due to each $-\text{CH}_2$ proton will be $\rho B \cos^2 \theta = \rho B/4$. This result holds irrespective of the rate of interconversion, provided other configurations are unimportant.

Restricted rotation is expected to be particularly pronounced in cyclooctatetraene derivatives if the ring is planar when the molecule possesses an extra electron, as we and others [3] have proposed. The smaller ring bond angle in alkyl benzene derivatives leads to decreased steric hindrance between ring and alkyl group protons. However, we might still expect to observe a difference between methyl and ethyl splittings and results on *p*-alkyl nitrobenzene anions point to such an effect. Ayscough *et al.* [4] show that in *p*-methyl and *p*-ethyl nitrobenzene anions the nitrogen and ring proton splittings are the same in both radicals but the alkyl proton splitting decreases from 3.7 to 2.8 gauss. We suggest that the ethyl group rotates faster than 8 Mc/sec but that, here too, the configurations indicated above are favoured; the splitting observed is not therefore the result of an *isotropic* time average over values of $\cos^2 \theta$. One might well expect the splitting to be temperature dependent, as has been discussed in a similar context by Stone and Maki [5].

P.F.T. thanks I.C.I. Ltd., Petrochemical and Polymer Laboratory, for leave of absence.

REFERENCES

- [1] CARRINGTON, A., and TODD, P. F., 1964, *Mol. Phys.*, **7**, 533.
- [2] HORSFIELD, A., MORTON, J. R., and WHIFFEN, D. H., 1961, *Mol. Phys.*, **4**, 425.
- [3] KATZ, T. J., and STRAUSS, H. L., 1960, *J. chem. Phys.*, **32**, 1873.
- [4] AYSCOUGH, P. B., SARGENT, F. P., and WILSON, R., 1963, *J. chem. Soc.*, p. 5418.
- [5] STONE, E. W., and MAKI, A. H., 1962, *J. chem. Phys.*, **27**, 1326.

Zero-field splitting of the lowest triplet state of some aromatic hydrocarbons: Calculation and comparison with experiment

by J. H. VAN DER WAALS and G. TER MATEN

Koninklijke/Shell-Laboratorium, Amsterdam (Shell Research N.V.)

(Received 14 February 1964)

It is investigated how far the zero-field splitting of the lowest triplet state of aromatic hydrocarbons can quantitatively be accounted for with a π -electron representation of the wave function. The calculations are based on triplet SCF-MO's, as obtained from an extension by Colpa of Pariser's formalism to open-shell systems. Interaction with all π -electron configurations that are either singly or doubly excited relative to the lowest triplet configuration is included. The pertinent integrals over $2p_z$ Slater AO's have been evaluated by numerical integration, with a result almost identical to that obtained by Gouterman and Moffitt for Gaussian AO's.

When the calculated values of the parameters D and E in the spin Hamiltonian for naphthalene, anthracene and phenanthrene are compared with experiment, those of D are found to be 15–20 per cent too high, whereas those of E —though lying in the right order—are considerably too large. The contribution to the splitting parameters due to spin polarization of the σ -electrons in the C–C and C–H bonds by the π -electrons is then estimated. It is found that the effect is of the right order of magnitude to bring the calculated and observed values of D to agreement.

Finally, a semi-empirical method of calculation is suggested to take account of σ – π polarization and the uncertainty in the precise values of the dipole–dipole integrals between two electrons on neighbouring atoms. Calculations for naphthalene, anthracene, phenanthrene and triphenylene with this modified method yield values of D which are in perfect agreement with experiment, but those of $|E|$ —which are very sensitive to changes in the configurational mixing—are less reliably predicted. The value of D for the (trigonal) phenalenylium ion is also calculated; it is of the right order of magnitude.

1. INTRODUCTION

The first successful electron resonance experiment on the lowest triplet (phosphorescent) state of an aromatic hydrocarbon was carried out by Hutchison and Mangum on a dilute solution of naphthalene in a durene single crystal [1]. They described their results in terms of a spin Hamiltonian which, on addition of a constant shift $-\frac{1}{3}DS^2$ following from theory, can be written as:

$$\mathcal{H} = g|\beta|\mathbf{H} \cdot \mathbf{S} + D(S_z^2 - \frac{1}{3}\mathbf{S}^2) + E(S_x^2 - S_y^2). \quad (1)$$

The parameters D and E account for the fact, predicted by Weissman, that in the absence of an external field the degeneracy of the triplet state of the naphthalene molecule is removed through dipolar interaction between the electron spins. In subsequent work it has been shown that these zero-field splitting (ZFS)

parameters can also be obtained from spectra of solutions of randomly oriented molecules in a rigid glass [2-4].

The first calculations of ZFS patterns in aromatic hydrocarbons were made by Gouterman and Moffitt [6] and by Hamerka [7]; later more general formulations have been published by McWeeny [8] and McLachlan [9]. From their work it follows that a calculation of the dipolar interaction between the electron spins on the basis of a simple LCAO-MO π -electron model leads to a splitting of the right order of magnitude. When we made our first electron resonance experiments on phosphorescent molecules in rigid glasses [2] we tried to give a quantitative interpretation of the variation of zero-field splitting with molecular structure on the basis of a theoretical calculation very similar to that of Gouterman. All two-centre integrals were retained in the expansion of the matrix elements, but the agreement was decidedly unsatisfactory for wave functions obtained by minimizing the energy through interaction of the three lowest π -electron configurations, and the attempts were abandoned [5].

In general, spin densities calculated according to LCAO-MO models for aromatic free radicals have been found to be in surprisingly good agreement with observed hyperfine coupling constants. However, by this achievement one should not be led to expect an equally simple and successful interpretation of spin-spin coupling, for the following reason. In order to get a satisfactory representation of the spin distribution in an LCAO-MO treatment, configuration interaction (CI) has to be considered [9]. That is, the many-electron wave function is to be represented by:

$$\Phi_0 + \sum c_k \Phi_k,$$

where Φ_0 is an anti-symmetrized product representing the lowest configuration of a given multiplicity and the Φ_k are similar products for configurations of the same multiplicity that are singly or doubly excited relative to Φ_0 . Now the spin density operator, being a sum of one-electron operators, can only give contributions linear in c_k for those Φ_k that are *singly* excited relative to Φ_0 . But in the spin-spin interaction which involves two-electron operators, *all* Φ_k , whether singly or doubly excited, may give contributions linear in the c_k . Hence, a large number of non-diagonal matrix elements between configurations differing in the occupation of two orbitals, has to be included in the calculation of spin-spin coupling, the analogues of which would vanish in the calculation of spin densities [9].

Since our earlier work on spin-spin interaction, Dr. Colpa of this laboratory has extended the Roothaan-Pople SCF-LCAO-MO method to open-shell systems [11]. In particular he has developed a computer programme for finding the lowest SCF triplet-state wave function of aromatic systems which is then subsequently improved by configuration interaction; his numerical procedure is a generalization of that used by Pariser [12]. With the aid of the wave functions obtained from this programme we have now recalculated the zero-field splittings of a few aromatic molecules and compared them with experimental values†.

† After completion of the present work two studies have been published by Boorstein and Gouterman [30] and by Ying-Nan Chiu [31] in which several of our results have been anticipated. However, they consider interaction with a few configurations only and so have to use wave functions that are quite different from those which minimize the energy in order to achieve agreement between theory and experiment.

2. CALCULATION

2.1. The wave function

The procedure used may be illustrated for naphthalene. In table 1 the triplet SCF-MO's and their symmetries are given. The precise significance of these MO's will be discussed below; for the time being one may think in terms of simple Hückel MO's, which lie in the same order. The lowest triplet state is SA (i.e. ${}^3B_{2u}$) and has $(e; e')$ as the leading configuration. This notation expresses that, relative to the ground configuration in which the MO's $a \dots e$ are all doubly occupied, one electron is excited from each of the bonding MO's preceding the semicolon into one of the anti-bonding MO's after the semicolon. Hence, a triplet-state wave function of $(e; e')$ is represented by:

$$\Phi_0 = {}^3(e; e')^{(\nu)} = \mathcal{A} a(1)a(2)b(3)b(4)c(5)c(6)d(7)d(8)e(9)e'(10) \times S(1,2)S(3,4)S(5,6)S(7,8)T^{(\nu)}(9,10). \quad (2)$$

Here \mathcal{A} is the anti-symmetrizing and renormalizing operator, $S(i,j)$ a singlet spin function of the electron pair i, j and $T^{(\nu)}(k,l)$ one of the three triplet spin eigenfunctions in zero-field, formerly denoted as T_x, T_y, T_z [16, 2]. Unless marked to the contrary, we shall henceforth omit the superscript labels 3 and ν and assume that we deal with that component $T^{(z)}$ which has its spin angular momentum in the plane $z=0$.

MO	Symmetry		Energy (ev)	LCAO coefficients		
	$x=0$	$y=0$		Atom 1	Atom 2	Atom 10
a'	S	A	14.681	0.3025	-0.2340	-0.4555
b'	A	A	12.748	0.2509	-0.4325	0
c'	S	S	11.614	0.3979	-0.1658	-0.3582
d'	S	A	10.975	0.0117	0.4096	-0.4053
e'	A	S	7.288	0.4325	-0.2509	0
e	A	A	3.671	0.4325	0.2509	0
d	S	S	-0.016	0.0117	-0.4096	0.4053
c	S	A	-0.655	0.3979	0.1658	0.3582
b	A	S	-1.789	0.2509	0.4325	0
a	S	S	-3.722	0.3025	0.2340	0.4555

The labels in the second column denote symmetry of the MO relative to the plane $x=0, y=0$; e.g. AS is anti-symmetric for reflection in $x=0$ and symmetric in $y=0$.

Table 1. SCF-MO's for lowest triplet state of naphthalene.

In his procedure for determining the MO's to be used in (2) Colpa prescribes that the SCF-MO's sought by iteration should be those for the state of lowest energy which, moreover, is an eigenstate of \mathbf{S}^2 with eigenvalue 2. To illustrate what this means in practice we have collected in table 2 all π -electron MO configurations for naphthalene of SA symmetry that can contribute to the zero-field splitting through first-order interaction with $(e; e')$; cf. [9] and below. Pairs of degenerate configurations have been combined into the appropriate linear combinations (*plus* or *minus* states [12, 13]).

From those orbital configurations in which just two MO's are singly occupied only one triplet arises, but when four MO's are singly occupied three different triplets can be constructed which have been labelled A, B, C by analogy with McLachlan's notation. When for brevity omitting all doubly occupied orbitals and taking the first such configuration of table 2 as an example, these are defined as:

$$(de; e'c') \begin{Bmatrix} A \\ B \\ C \end{Bmatrix} = \mathcal{A} \dots d(7)c'(8)e(9)e'(10) \begin{Bmatrix} S(7,8)T(9,10) \\ T(7,8)S(9,10) \\ 2^{-1/2} \{S(7,10)T(8,9) + S(8,9)T(7,10)\} \end{Bmatrix}. \quad (3)$$

Type	Configuration	Energy relative to ($e; e'$) (ev)	Contribution to ZFS	
			$D/hc \text{ cm}^{-1}$	$E/hc \text{ cm}^{-1}$
I (a)	$(ee; e'b'), (be; e'e')$	9.076	0	0
I (a) I (b) I (b)	$\{(de; e'c') \mp (ce; e'd')\} \begin{Bmatrix} A \\ B(-) \\ C(+) \end{Bmatrix}$	11.629	0 0.0029 -0.0032	0 -0.0005 0.0014
I (a) I (b) I (b)	$\{(ce; e'a') \mp (ae; e'c')\} \begin{Bmatrix} A \\ B(-) \\ C(+) \end{Bmatrix}$	15.336	0 0.0000 -0.0033	0 0.0000 0.0006
II (a) II (a) II (a) II (a) II (a)	$(d; d')$ $(c; c')$ $(b; b')$ $(a; a')$ $\{(d; a') + (a; d')\}$	7.374 8.652 10.920 14.787 11.080	Sub-totals of CI calculation (cf. table 5) 0.1155 -0.0291	
II (b) II (b)	$\{(ee; d'c') - (dc; e'e')\}$ $\{(ee; c'a') - (ac; e'e')\}$	11.629 15.336	-0.0058 0.0000	0.0010 0.0000
II (c)	$(dee; e'e'd')$ and other analogues of II (a)	14.607 > 15.8	} 0.0048	-0.0011
Total contributions of π -configurations to ZFS			0.1109	-0.0277

Table 2. Excited π -electron triplet configurations of naphthalene which by configuration interaction with $(e; e')$ contribute to spin-spin coupling.

For the purpose of the present calculation the entries in the table have been classified into five types.

I. Orbital configuration singly excited relative to $(e; e')$:

- (a) spin pairing identical to that in $(e; e')$;
- (b) spin pairing different from that in $(e; e')$, as in B, C.

II. Orbital configuration doubly excited relative to $(e; e')$ and

- (a) singly excited relative to the (singlet) ground state ('Pariser type');
- (b) doubly excited relative to the ground state;
- (c) triply excited relative to the ground state;

only those configurations having two half-filled MO's can here contribute in first order.

The configurations of type I (a) need not further be considered. Interaction with them is included in Colpa's triplet state SCF procedure: the orbitals $a \dots a'$ are made self-consistent in the sense that the matrix elements for CI between $(e; e')$ and all π -electron configurations of type I (a) are identically zero.

The interaction between $(e; e')$ and the four other types was accounted for in either of two ways. For the molecules investigated, by far the strongest interaction was found to occur with the type II (a) configurations, which are just those to which Pariser limited himself in his calculations on electronic spectra [12]. Accordingly, a CI calculation was made in which the electron repulsion energy was minimized, using $(e; e')$ plus all type II (a) configurations as a basis in the variational procedure. For naphthalene the lowest triplet state is then found to be:

$$\Psi_{T,0} = 0.9275(e; e') + 0.1875(d; d') + 0.2656(c; c') + 0.1613(b; b') \\ + 0.0848(a; a') - 0.0201\{(a; d') + (d; a')\}. \quad (4)$$

The contribution to ZFS arising from interaction with the types I (b), II (b) and (c) configurations of table 2 was approximated by first-order perturbation theory, in the manner discussed by McLachlan [9]. Since the contribution from these configurations—which are doubly or triply excited relative to the *singlet* ground state—proved to be very small, two simplifying assumptions were introduced in the perturbation treatment, namely

- (i) the leading term $(e; e')$ was taken as zero-order wave function Φ_0 , instead of the full expression (4);
- (ii) the energy denominators were taken equal to the difference $\Delta\epsilon$ of the sums of the orbital energies.

In other words, a 'corrected' Ψ_T is constructed from $\Psi_{T,0}$, which is approximated by:

$$\Psi_T = \Psi_{T,0} - \sum_k \frac{\langle \Phi_k | \sum_{\mu < \nu} e^2 / r_{\mu\nu} | \Phi_0 \rangle}{\Delta\epsilon_k} \Phi_k, \quad (5)$$

where the wave functions Φ_k represent those of the type I (b), II (b) and (c) configurations of table 2. The pertinent CI matrix elements are given in table 3 [9]; these were then evaluated numerically in the manner used by Pariser [12].

2.2. Matrix elements for spin-spin interaction

The Hamiltonian for dipolar interaction between the electron spins is given by:

$$\mathcal{H}_{ss} = (g\beta)^2 \sum_{\mu < \nu} \left\{ \frac{\mathbf{s}_\mu \cdot \mathbf{s}_\nu}{r_{\mu\nu}^3} - \frac{3(\mathbf{s}_\mu \cdot \mathbf{r}_{\mu\nu})(\mathbf{s}_\nu \cdot \mathbf{r}_{\mu\nu})}{r_{\mu\nu}^5} \right\}. \quad (6)$$

	Element between (e ; e') and	Configuration interaction	\mathcal{H}_{ss}
I (b_B)	$\sqrt{\frac{1}{2}}\{(de; e'c')_B - (ce; e'd')_B\}$	$\{\langle ec' 1/r_{\mu\nu} de\rangle - \langle e'c' 1/r_{\mu\nu} de'\rangle\}$	$\left\{ -\left\langle [e, c'] \left \frac{\mathcal{D}}{\mathcal{E}} \right [d, e] \right\rangle + \left\langle [e', c'] \left \frac{\mathcal{D}}{\mathcal{E}} \right [d, e'] \right\rangle \right\}$
I (b_C)	$\sqrt{\frac{1}{2}}\{(de; e'c')_C + (ce; e'd')_C\}$	$-\sqrt{2}\{\langle ec' 1/r_{\mu\nu} de\rangle + \langle e'c' 1/r_{\mu\nu} de'\rangle\}$	$-\sqrt{\frac{1}{2}}\left\{ \left\langle [e, c'] \left \frac{\mathcal{D}}{\mathcal{E}} \right [d, e] \right\rangle + \left\langle [e', c'] \left \frac{\mathcal{D}}{\mathcal{E}} \right [d, e'] \right\rangle \right\}$
II (a)	(d ; d')	$-\langle de' 1/r_{\mu\nu} ed'\rangle$	$\left\langle [d, e'] \left \frac{\mathcal{D}}{\mathcal{E}} \right [e, d'] \right\rangle$
II (b)	$\sqrt{\frac{1}{2}}\{(ee; d'c') - (dc; e'e')\}$	$\sqrt{2}\langle [d', c'] 1/r_{\mu\nu} [e, e']\rangle$	$\sqrt{2}\left\langle [d', c'] \left \frac{\mathcal{D}}{\mathcal{E}} \right [e, e'] \right\rangle$
II (c)	(dee ; $e'e'd'$)	$-\langle de 1/r_{\mu\nu} e'd'\rangle$	$\left\langle [d, e] \left \frac{\mathcal{D}}{\mathcal{E}} \right [e', d'] \right\rangle$

$$\begin{pmatrix} \mathcal{D} \\ \mathcal{E} \end{pmatrix} = \frac{3}{4}(g\beta)^2 r_{\mu\nu}^{-5} \begin{pmatrix} r_{\mu\nu}^2 - 3x_{\mu\nu}^2 \\ y_{\mu\nu}^2 - x_{\mu\nu}^2 \end{pmatrix}; \quad [d, e] = 2^{-1/2}\{d(\mu)e(\nu) - d(\nu)e(\mu)\}.$$

Within the present approximation the contribution to ZFS of the type II (b) configurations is minus twice that of type I (b_B).

Table 3. Expansion of matrix elements in integrals over MO's.

The equivalence for a non-degenerate electronic state of \mathcal{H}_{ss} with the field-independent part of (1) was demonstrated by Van Vleck [14] and very recently discussed in detail by McLachlan [15].

For every pair μ, ν the terms in (6) can be grouped so that their spin-dependent parts—and consequently also their orbital parts—transform like the spherical harmonics of the second degree, i.e.

$$\begin{aligned} \mathcal{H}_{ss} = & - (g\beta)^2 \sum_{\mu < \nu} r_{\mu\nu}^{-5} \left\{ (s_{\mu z} s_{\nu z} - \frac{1}{3} \mathbf{s}_{\mu} \cdot \mathbf{s}_{\nu}) \frac{3}{2} (3z_{\mu\nu}^2 - r_{\mu\nu}^2) \right. \\ & + (s_{\mu x} s_{\nu x} - s_{\mu y} s_{\nu y}) \frac{3}{2} (x_{\mu\nu}^2 - y_{\mu\nu}^2) \\ & \left. + \sum_{\substack{p \neq q \\ x, y, z}} (s_{\mu p} s_{\nu q} + s_{\mu q} s_{\nu p}) 3p_{\mu\nu} q_{\mu\nu} \right\}. \end{aligned} \quad (7)$$

Now Van Vleck has pointed out that *within a given multiplet* the matrix elements of the individual terms $(s_{\mu z} s_{\nu z} - \frac{1}{3} \mathbf{s}_{\mu} \cdot \mathbf{s}_{\nu})$, $(s_{\mu x} s_{\nu x} - s_{\mu y} s_{\nu y})$, etc. are proportional to those of the corresponding expressions for the total spin, $(S_z^2 - \frac{1}{3} \mathbf{S}^2)$, $(S_x^2 - S_y^2)$, etc. For a molecule like naphthalene the coordinate axes may be taken to coincide with the symmetry axes so that the matrix elements of the last sum in (7), which contain cross-products such as $x_{\mu\nu} y_{\mu\nu}$, vanish. Because of the above proportionality the remaining terms of (7) then are identical with the field-independent part of (1). For a molecule of low symmetry the orientation of the principal axes relative to the molecular frame is not known *a priori*; it is that for which the matrix elements of the three cross-products in (7) again vanish and the equivalence of \mathcal{H}_{ss} with (1) is preserved.

From (1) it follows that in the absence of a magnetic field the component $T^{(z)}$ of the triplet has an energy $Z = -\frac{3}{2}D$. On the other hand, when writing down the corresponding matrix element of (7) one obtains for the first parameter in (1):

$$D = -\frac{3}{2}Z = -\frac{3}{4}(g\beta)^2 \langle \Psi_T^{(z)} | \sum_{\mu < \nu} (3s_{\mu z} s_{\nu z} - \mathbf{s}_{\mu} \cdot \mathbf{s}_{\nu}) (r_{\mu\nu}^2 - 3z_{\mu\nu}^2) r_{\mu\nu}^{-5} | \Psi_T^{(z)} \rangle. \quad (8)$$

Since the triplet spin eigenfunctions for zero-field, $T^{(x)}$, $T^{(y)}$, $T^{(z)}$ transform into one another by changing the labels of the axes, the spin-dependent part of (8) does not depend on the labelling. For instance,

$$\langle T(\mu, \nu)^{(z)} | 3s_{\mu z} s_{\nu z} - \mathbf{s}_{\mu} \cdot \mathbf{s}_{\nu} | T(\mu, \nu)^{(z)} \rangle = \langle T(\mu, \nu)^{(x)} | 3s_{\mu x} s_{\nu x} - \mathbf{s}_{\mu} \cdot \mathbf{s}_{\nu} | T(\mu, \nu)^{(x)} \rangle,$$

etc. for y . Thus, if we calculate the eigenenergies X and Y of the x and y components of the triplet, subtract them and change axes in the spin-dependent parts we obtain for the second parameter:

$$E = \frac{1}{2}(Y - X) = -\frac{3}{4}(g\beta)^2 \langle \Psi_T^{(z)} | \sum_{\mu < \nu} (3s_{\mu z} s_{\nu z} - \mathbf{s}_{\mu} \cdot \mathbf{s}_{\nu}) (y_{\mu\nu}^2 - x_{\mu\nu}^2) r_{\mu\nu}^{-5} | \Psi_T^{(z)} \rangle. \quad (9)$$

These results, of course, are identical to those derived by McWeeny [8] and subsequently by McLachlan [9] from density matrices. (An apparent difference between, e.g., (8) and (9) above and McLachlan's equations (27)–(29) [9] by a factor $-\frac{1}{2}$ arises because the present elements are those for the eigenstate $T^{(z)}$ with $m_z=0$, instead of a 'standard state' with $m_z=1$.) The integration over the spin coordinates is a relatively simple matter as in the integrals $\langle {}^3\Phi_m | \mathcal{H}_{ss} | {}^3\Phi_n \rangle$ all electrons which are in closed shells in both the configurations

${}^3\Phi_m$ and ${}^3\Phi_n$ may be disregarded [8]. The resulting expressions for these matrix elements, most of which have already been given by McLachlan [9], are collected in the last column of table 3.

2.3. Numerical evaluation of the spin-spin integrals

Let d_i denote the LCAO coefficient with which the AO p_i on carbon atom i appears in the MO d . Because of the pairing properties [10, 12] one then has for a numbering of the atoms as in table 1:

$$d'_i = (-1)^{i+1} d_i. \quad (10)$$

Expanding the elements of the last column of table 3 in integrals over AO's one obtains, for instance:

$$\begin{aligned} \langle [d, e'] | \mathcal{D} | [e, d'] \rangle &= \sum_{j>i} (d_i e'_j - d_j e'_i) (e_i d'_j - e_j d'_i) \langle [p_i, p_j] | \mathcal{D} | [p_i, p_j] \rangle \\ &\quad + 3\text{- and 4-centre integrals} \end{aligned} \quad (11)$$

$$\begin{aligned} &= \sum_{j-i=u} (d_i e_j + d_j e_i)^2 \langle [p_i, p_j] | \mathcal{D} | [p_i, p_j] \rangle \\ &\quad - \sum_{j-i=g} (d_i e_j - d_j e_i)^2 \langle [p_i, p_j] | \mathcal{D} | [p_i, p_j] \rangle + \dots \end{aligned} \quad (12)$$

where u stands for odd and g for even integers. The corresponding expression for E is identical except that in the atomic integrals \mathcal{E} is to be replaced by $\mathcal{E}' \cos 2\gamma_{ij}$ [6]. Here \mathcal{E}' is expressed in a primed coordinate system which has the line joining nuclei i and j as y' axis, and which is obtained by rotating the unprimed (molecular) coordinate system over an angle γ_{ij} around the z axis.

On substituting $d=e$ in (12) this expression becomes that for the diagonal element of the lowest triplet configuration ($e; e'$) and the second sum cancels out because of the pairing properties. Apparently, only integrals between atoms separated by an odd number of bonds occur in the diagonal elements when restricting oneself to two-centre integrals. The two most important of these integrals of \mathcal{D} and \mathcal{E} over atomic orbitals, i.e. those between ortho and para pairs, were evaluated by brute force through six-dimensional numerical integration on our former Mark I* Ferranti computer. (For a potentially superior method of calculation cf. footnote at the end of § 3.3.)

As wave functions $2p_z$ Slater orbitals were used:

$$[p_i, p_j] = 2^{-1/2} \{ p(\mathbf{r}_{i\mu}) p(\mathbf{r}_{j\nu}) - p(\mathbf{r}_{j\mu}) p(\mathbf{r}_{i\nu}) \}, \quad (13)$$

with

$$p(\mathbf{r}_{i\mu}) = (\tfrac{1}{2}Z)^{5/2} \pi^{-1/2} z_{i\mu} \exp(-Zr_{i\mu}), \quad (14)$$

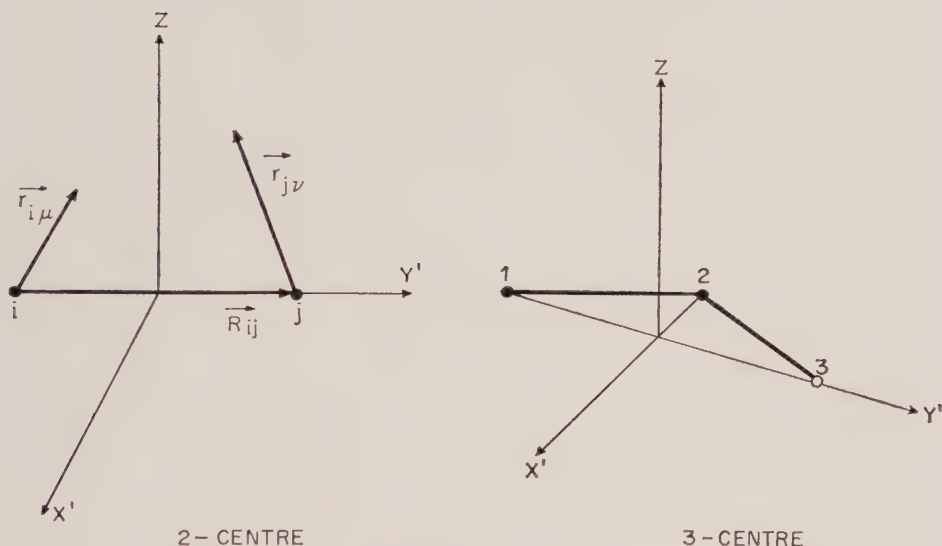
where $\mathbf{r}_{i\mu}$ denotes the position of electron μ relative to nucleus i and $Z=3.18$. The integrals over atomic orbitals can then be written as, for instance for an ortho pair:

$$\begin{aligned} \left(\frac{D_{12}}{E_{12'}} \right) &= \langle [p_1, p_2] \left| \left(\frac{\mathcal{D}}{\mathcal{E}'} \right) \right| [p_1, p_2] \rangle \\ &= \frac{1}{2} \int \int \{ p(\mathbf{r}_{1\mu}) p(\mathbf{r}_{2\nu}) - p(\mathbf{r}_{1\mu} - \mathbf{R}_{12}) p(\mathbf{r}_{2\nu} + \mathbf{R}_{12}) \}^2 \left(\frac{\mathcal{D}}{\mathcal{E}'} \right) d\mathbf{r}_{1\mu} d\mathbf{r}_{2\nu}. \end{aligned} \quad (15)$$

The vector \mathbf{R}_{12} , which points from nucleus 1 to nucleus 2, was assumed to have a length $R_{12}=1.39 \text{ \AA}$ (cf. figure).

In the six-dimensional space spanned by the components of $\mathbf{r}_{1\mu}$, $\mathbf{r}_{2\nu}$ the integrals (15) are symmetrical with respect to reflection in the hyperplanes $x_{1\mu}=0$, $y_{1\mu}=\frac{1}{2}R_{12}$, $z_{1\mu}=0$, and hence the actual numerical integration could be restricted to one octant of $\mathbf{r}_{1\mu}$ space. Because of the limited memory capacity of our computer, integration space was divided into two regions, namely

	$0 \leq x_{1\mu} \leq 4$	$-4 \leq x_{2\nu} \leq 4$
inner region	$-2 \leq y_{1\mu} \leq 4$	$-10 \leq y_{2\nu} \leq 0$
units $\delta = \frac{1}{8}R_{12}$	$0 \leq z_{1\mu} \leq 6$	$-6 \leq z_{2\nu} \leq 6$
	$0 \leq x_{1\mu} \leq 10$	$-8 \leq x_{2\nu} \leq 8$
total region	$-8 \leq y_{1\mu} \leq 4$	$-12 \leq y_{2\nu} \leq 8$
units $\delta = \frac{1}{8}R_{12}$	$0 \leq z_{1\mu} \leq 10$	$-10 \leq z_{2\nu} \leq 10$



Orientation of axes in integrals over AO's.

The integration over the inner region was carried out with a cubical mesh of size $\delta = \frac{1}{8}R_{12}$ and that over the remainder with a mesh of 2δ . By numerical analysis it was estimated that neglected 'outer space' would contribute less than 2 per cent. Parallel with D and E' the value of the normalization integral, i.e. (15) *without* the operators \mathcal{D} or \mathcal{E}' was evaluated; its total amounted to 0.904 instead of $(1 - S^2) = 0.932$. This corroborates the above estimate: \mathcal{D} and \mathcal{E}' are proportional to $r_{\mu\nu}^{-3}$ and the large majority of electron configurations lying in the neglected region has large $r_{\mu\nu}$ values and so contributes far less to D and E' than to the normalization.

Whenever $\mathbf{r}_{1\mu} = \mathbf{r}_{2\nu} + \mathbf{R}_{12}$ one has $r_{\mu\nu} = 0$, i.e. coincidence of the two electrons. The operators \mathcal{D} and \mathcal{E}' then go to infinity, but because of the anti-symmetric character of the triplet wave functions the contribution to the integral remains finite. In the numerical procedure the contributions of the volume elements around the points with $r_{\mu\nu} = 0$ were assessed by integration of a series expansions of the integrals. In accordance with McConnell's analysis [17] the contribution of these volume elements to the total was found to be small.

Results of the numerical integrations are given in table 4, for the two-centre integrals between ortho and para pairs and also, as a check on the approximation, for the three-centre integrals:

$$\left(\begin{matrix} D_{123} \\ E'_{123} \end{matrix} \right) = \langle [p_1, p_2] \left(\begin{matrix} \mathcal{D} \\ \mathcal{E}' \end{matrix} \right) [p_2, p_3] \rangle, \quad (16)$$

which are the most important of those neglected in the expansion (11)†. The procedure used for the latter types was in essence similar to that described in detail for the ortho integrals.

	D/hc cm^{-1}		E'/hc cm^{-1}	
	Slater AO's	Gaussian AO's [6]	Slater AO's	Gaussian AO's [6]
Two-centre (15): 1, 2	0.176	0.184	0.225	0.234
average		0.180		0.229
semi-empirical (cf. § 3.4)		0.155		0.200
1, 3		0.061		0.077
1, 4	0.042	0.043	0.048	0.052
1, 6		0.021		0.024
1, 7		0.015		0.017
2, 8		0.010		0.011
2, 7		0.009		0.010
Three-centre (16): 1, 2, 3	0.006		0.013	

$$\left(\begin{matrix} \mathcal{D} \\ \mathcal{E}' \end{matrix} \right) = \frac{3}{4}(g\beta)^2 r_{\mu\nu}^{-5} \left(\begin{matrix} r_{\mu\nu}^2 - 3x_{\mu\nu}^2 \\ y_{\mu\nu}'^2 - x_{\mu\nu}'^2 \end{matrix} \right).$$

For numbering of nuclei see table 1; for coordinate systems see figure. The values in bold type are those used in further numerical calculations.

Table 4. Integrals of \mathcal{D} and \mathcal{E}' over AO's.

The second set of entries in table 4 are for Gaussian AO's as used by Gouterman and Moffitt in their calculations of zero-field splittings [6]. In order to make the two sets strictly comparable the exponent in the Gaussians was changed from $\alpha=0.403$ [6] to $\alpha=0.399$ so as to maintain maximum overlap with our Slater AO's with $Z=3.18$, and R_{12} was reduced from 1.40 to 1.39 Å. There is a most remarkable agreement between the values of the ortho and para integrals for the two types of atomic wave functions. Probably, this is because the largest contribution to the ZFS integrals arises from the interaction between the regions

† Actually, the numerical values of the three-centre integrals

$$\langle [p_1, p_2] \left(\begin{matrix} \mathcal{D} \\ \mathcal{E}' \end{matrix} \right) [p_1, p_3] \rangle$$

will probably be larger than those of (16), but because of the pairing properties their coefficient in the expansion (12) for diagonal matrix elements will vanish, just as for the two-centre integrals between *meta* atoms.

with highest electron density above and below nucleus i with the analogous regions near nucleus j . As the exponentials in the Gaussian and Slater orbitals are so adapted that maximum overlap between them occurs, the regions of highest density are roughly coincident for both types of AO's. Because of this close agreement no further numerical integrations were carried out and in our further work the values printed in bold type in table 4 have been used.

3. RESULTS

3.1. Detailed calculations for π -electrons

The results of the calculations on naphthalene have been included in table 2, whilst the individual matrix elements occurring in the CI calculation are specified in table 5. Precisely similar calculations were made for anthracene and phenanthrene; cf. table 6. Interactions between spins located on atoms further apart than those occurring in the naphthalene molecule were neglected. The symmetries of the lowest triplet states of these molecules following from the SCF-CI calculations conform with the commonly accepted 3p assignment [12, 13] (Clar's notation) of the phosphorescence transition; i.e. the leading configurations again correspond to excitation between bonding and anti-bonding MO's that are paired.

For all three molecules, naphthalene, anthracene and phenanthrene, it was found that the values of D and E in the 3p states are almost completely determined by the interaction amongst the lowest triplet and those type II (a) configurations which arise from excitation between paired orbitals. As far as D is concerned these configurations only yield positive contributions, since all two-centre integrals over u pairs in the expansion (12) and its analogue for non-diagonal elements come in with a positive sign because of the pairing properties (cf. also table 5). Hence, highly excited configurations of this type, even if they have a relatively small coefficient in a wave function such as (4), still may not be omitted: their non-diagonal elements of D with $(e; e')$ all have the same sign and so accumulate with the number of configurations included. Thus, with the present model, and especially for large molecules, it is quite inadequate to consider the three or four lowest configurations only; as apparent from table 5 a calculation based on a single Hückel configuration is less warranted still [5].

The effect of interaction with configurations other than those of type II (a), as assessed by perturbation theory, was found to be small. This is because, except for the highly energetic type II (c) configurations, the contributions of the different bonds to each of the sums analogous to that in (12) (or its equivalent in the expression for the CI matrix element) may now be negative as well as positive; since a great number of terms are involved the values of the matrix elements for CI and ZFS are thereby greatly reduced. As, moreover, types I (b_c) and II (b) always give a negative, and types I (b_B) and II (c) a positive spin correlation [9], the relatively small contributions of the individual configurations further tend to cancel each other out in the total (cf. table 2). When considering the approximate nature of calculations of the present kind it would thus seem reasonable to follow Pariser and to neglect these configurations altogether, at least for (stable) polynuclear aromatic hydrocarbons.

The error introduced by systematically neglecting all three- and four-centre integrals, likewise, must be small. In the expansion (12) every specific type of

$D/hc \text{ cm}^{-1}$		$E/hc \text{ cm}^{-1}$						
		$(e; e')$	$(d; d')$	$(c; c')$	$(b; b')$	$(a; a')$	$(d; a') + (a; d')$	
$(e; e')$	0.0618	-0.0034	-0.0371	0.0080	-0.0420	-0.0296	0.0012	$(e; e')$
$(d; d')$	0.0290	0.0811	0.0629	-0.0250	0.0532	0.0513	-0.0100	$(d; d')$
$(c; c')$	0.0282	0.0227	0.1008	-0.0209	-0.0227	-0.0654	-0.0288	$(c; c')$
$(b; b')$	0.0312	0.0498	0.0210	0.0928	0.0378	0.0088	-0.0566	$(b; b')$
$(a; a')$	0.0270	0.0359	0.0502	0.0394	0.1184	-0.0022	0.0424	$(a; a')$
$(d; a') + (a; d')$	0.0012	0.0092	0.0228	-0.0696	0.0560	0.2360	0.1304	$(d; a') + (a; d')$
$(e; e')$		$(d; d')$	$(c; c')$	$(b; b')$	$(a; a')$	$(d; a') + (a; d')$		

The matrix elements listed occur in the interaction of configurations such as $(e; e')$ and $(d; d')$ and thus are equal to

$$\langle [d, e'] \left| \frac{\mathcal{D}}{\mathcal{C}} \right| [e, d'] \rangle \quad (\text{cf. table 3}).$$

Table 5. ZFS matrix elements between 'Pariser configurations' of naphthalene.

	Naphthalene			Anthracene			Phenanthrene			Triphenylene			Phenalenylium		
		$D/\hbar c$	$E/\hbar c$		$D/\hbar c$	$E/\hbar c$		$D/\hbar c$	$E/\hbar c$		$D/\hbar c$			$D/\hbar c$	
Observed	[18]	+0.099	-0.015	[28]	0.072 (0.049 (0.027)	± 0.007 ± 0.033 ± 0.040	[18]	0.100	-0.047	[2]	0.134	[28]		0.053†	
Detailed calculation CI with II (a) PT† for I (b) ; II (b), (c)	B_{2u}	0.116	-0.029	B_{2u}	0.083	-0.013	B_2	0.118	-0.056						
		-0.005	+0.001		-0.007	+0.001		-0.003							
		0.111	-0.028		0.076	-0.012		0.115	-0.056						
Total π -electrons		0.101	-0.028		0.070	-0.012		0.105	-0.057						
Total with σ - π correction (20)															
Semi-empirical calculation (§ 3.4)	B_{2u}	0.099	-0.024	B_{2u}	0.071	-0.009	B_2	0.100	-0.048	A_1'	0.134	E_1		0.064	
	B_{1g}	0.118	-0.043	B_{1g}	0.100	-0.029	A_1	0.095	-0.013						

In assigning signs to the observed parameters, it has been assumed that D is positive ; this has only been proved for naphthalene [29].
 x -axis along long axis, z -axis perpendicular to molecular plane.

† Value uncertain because of Jahn-Teller instability.

Table 6. Observed and calculated zero-field splittings cm^{-1} .

them, unlike the two-centre integrals, in general occurs with both positive and negative coefficients; hence these integrals—which are small anyway—will cancel each other out to a considerable extent. This is borne out by the following example: when the most important three-centre integrals (16) are retained the values of the ZFS parameters following from the CI calculation on naphthalene are only changed by $+0.0012 \text{ cm}^{-1}$ (D) and $+0.0017 \text{ cm}^{-1}$ (E).

3.2. Comparison with experiment

The experimental results quoted in table 6 for naphthalene and phenanthrene are those determined by Brandon, Gerkin and Hutchison in a biphenyl host crystal, the others have been derived from experiments on glasses. The latter type of experiment permits of an unambiguous determination of the ZFS *pattern*, but not of the assignment of the individual levels to the molecular axes. In the case of anthracene an ambiguity thus arises. The physically most plausible combination of D and E values is that first reported in the table, but mathematically the two alternative entries in brackets are equally acceptable.

When considering the great oversimplification introduced with wave functions of the present kind it is gratifying to find that the calculated values of D are only 15–20 per cent too high for the three molecules concerned. The values of E , which are more sensitive to the precise electron distribution, are exaggerated but their relative order is correct. That the results for D are in better agreement with experiment than that of the more sophisticated calculation of Tinkham and Strandberg [19] on the ground state of O_2 is thought to be due to the extensiveness of our molecular systems: in an aromatic molecule the electrons with parallel spin will on average be rather far apart, and so the overall spin distribution may be more important than the detailed form of the wave function.

However, as has also been noted by McConnell, there is one source of potential error in the present π -electron model which needs investigation: to what extent does interaction between σ - and π -electrons affect the dipolar interaction between the electrons? We have made an analysis of the consequences of this interaction for spin-orbit and electron spin-spin coupling, and in the next section the conclusions of this analysis, as far as relevant to the present problem, are summarized briefly. For all details we refer to a future publication [20].

3.3. The effect of interaction between π - and σ -electrons

Within a pure π -electron model the two electrons with parallel spin can never be on the same carbon atom, and thus no one-centre integral appeared in the calculations thus far. But, for instance from the occurrence of hyperfine splitting in the ESR spectra of aromatic radicals in solution, it is clear that interaction between π - and σ -electrons may not be neglected [21, 22]. This entails that configurations have to be considered in which, apart from any excitation within the π -system, an electron is excited from a bonding (σ) to an anti-bonding (σ') MO of a C–C or C–H bond†. Different types of such configurations occur; they are the analogues of those given in table 2 for pure π -excitation. As in these configurations the two triplet electrons may simultaneously be on the same nucleus, a small amount of interaction with them should have a pronounced effect on spin-spin and (spin-orbit) coupling.

† We tacitly neglect the admixture of Rydberg states which will have a similar but probably smaller influence.

For C-H bonds the contribution due to interaction with the different types of configurations involving excitation of σ -electrons cancel each other out to a first approximation; e.g. for naphthalene their total contribution to D is estimated at -0.0009 cm^{-1} . For C-C bonds, however, the situation is different. If the lowest triplet configuration is non-degenerate, say $(m; k')$, then interaction of it with the σ -electrons in the bond between atoms i and j can be shown to give a contribution to ZFS approximately equal to [20]:

$$4\xi(m_i k_j + m_j k_i)^2 \left\{ \left\langle [p_i, t_i] \left| \frac{\mathcal{D}}{\mathcal{E}'} \right| [p_i, t_i] \right\rangle - \left\langle [p_i, t_j] \left| \frac{\mathcal{D}}{\mathcal{E}'} \right| [p_i, t_j] \right\rangle \right\}. \quad (17)$$

Here t_i, t_j stand for the trigonal hybrids on atoms i and j that are directed at each other. The quantity ξ expresses the degree to which states with an electron in the anti-bonding orbital σ'_{ij} are admixed; in the simple model due to McConnell [21] it corresponds to:

$$\xi = - \left\langle \sigma'_{ij} p_i \left| \frac{e^2}{r_{12}} \right| p_i \sigma_{ij} \right\rangle \Delta E^{-1}_{\sigma \rightarrow \sigma'}. \quad (18)$$

Fortunately, the value of ξ cannot only be obtained from this formula, but it also manifests itself in the ^{13}C splitting of the ESR spectra of aromatic radicals; according to the work of Karplus and Fraenkel [23] a plausible value is $\xi = 0.0225$.

The one-centre integral in (17) was determined by partial integration[†] with a result identical to that recently published by Higuchi [24]; the two-centre integral was again evaluated by six-dimensional numerical integration. Since the present type of integrals might be sensitive to the precise form of the atomic wave functions, the expansion by Löwdin [25] of the 1D SCF orbitals of carbon in Slater functions was used, as recommended by Higuchi. One thus obtains for (17) in cm^{-1} :

$$4\xi(m_i k_j + m_j k_i)^2 \left\{ \begin{pmatrix} -0.622 \\ +0.302 \end{pmatrix} - \begin{pmatrix} -0.134 \\ +0.230 \end{pmatrix} \right\}. \quad (19)$$

On substituting the value of ξ into this equation and summing over all bonds

[†] This procedure was suggested by Oosterhoff. As the operator for dipolar interaction can also be written as

$$\mathcal{H}_{ss} = (g\beta)^2 \sum_{\mu < \nu} (\mathbf{s}_\mu \cdot \nabla_\mu)(\mathbf{s}_\nu \cdot \nabla_\nu) \frac{1}{r_{\mu\nu}}$$

one has, for instance,

$$\begin{aligned} & \langle [p_i, t_i] | \mathcal{D} | [p_i, t_i] \rangle \\ &= \frac{3}{4}(g\beta)^2 \iint \{p_i(1)t_i(2) - p_i(2)t_i(1)\}^2 \frac{\partial}{\partial z_1} \frac{\partial}{\partial z_2} \frac{1}{r_{12}} \mathbf{dr}_1 \mathbf{dr}_2 \end{aligned}$$

and thence through integration by parts

$$= \frac{3}{4}(g\beta)^2 \iint \frac{1}{r_{12}} \frac{\partial}{\partial z_1} \frac{\partial}{\partial z_2} \{p_i(1)t_i(2) - p_i(2)t_i(1)\}^2 \mathbf{dr}_1 \mathbf{dr}_2.$$

The latter integral is analogous to an electron repulsion integral and can be solved by standard techniques. Because of the antisymmetry of the triplet wave function $[p_i, t_i]$ with respect to interchange of electrons, the integrands in the matrix elements remain finite when $r_{12} \rightarrow 0$ although \mathcal{H}_{ss} alone does not [2]; hence no singularities need be considered. Although we have not yet used the above procedure for the reduction of the two-centre dipolar integrals it should certainly facilitate their analytical evaluation.

the total contribution to ZFS due to interaction with the σ -electrons is found to be:

$$\sum_{i < j} (m_i k_j + m_j k_i)^2 \left(\frac{-0.044}{+0.006} \right) \text{ cm}^{-1}. \quad (20)$$

The corrections to ZFS calculated from (20) indeed reduce the values of D appreciably and bring them to within a few per cent of the observed ones. Of course, this remarkable agreement, which has been obtained without fitting any parameters other than those chosen by Pariser, may be partly fortuitous. Physically, the reduction in D is due to a small admixture of configurations in which two triplet electrons are near the same carbon nucleus: one in a $2p_z$ orbital and the other in a σ -hybrid. For this situation $\langle 3z_{12}^2 \rangle^2 > \langle r_{12}^2 \rangle$, so that a negative contribution to D results.

The values of $|E|$ are practically unaffected by the correction and remain too large, especially for naphthalene. We shall return to this point in the next section.

3.4. *Semi-empirical calculation*

The complexity of the preceding calculations stands in contrast to the crudity of the basic model. It should be remembered that our knowledge of wave functions in molecules is insufficient to rely on the precise values derived for the dipolar interaction integrals over atomic orbitals, especially those between nearest neighbours which are the most sensitive to the precise form of the wave function. In fact, the close agreement found between Gauss and Slater orbitals may be misleading. True atomic wave functions fall off more slowly at large distances than either of these, and their use in the calculation of the integrals would almost certainly have led to somewhat lower values (cf. [24] for a specific example concerning the first integral in (17)). A further uncertainty is related to the effective nuclear charge: there is no sound reason why the value of Z that is best for calculating the energies of an atom, should be the most suitable average for calculating dipolar interaction in molecules [26, 27].

When considering these uncertainties, it may be more realistic to take a semi-empirical approach and to fit the dipolar integrals between nearest neighbours to the experimental data on ZFS, and to see whether the variation of ZFS with molecular structure is then predicted correctly. Such a procedure would have the further advantage of automatically including σ - π interaction, because the correction (20) depends in the same way on the MO coefficients as does the contribution of the nearest neighbour pairs in the pure π -electron model; cf. first term of (12). After all, the expression (20) provides only a crude estimate for the decrease of D due to σ - π interaction, whilst its prediction regarding E is questionable. For the latter the two integrals in (19) nearly cancel each other out and thus the result should be sensitive to minor changes in the wave function.

In line with the above idea we repeated the calculations in a simplified manner by restricting ourselves like Pariser [12] to the CI calculation with all type II (a) configurations, but neglecting the types I (b), II (b) and (c). The integrals of table 4 were again used, after reducing those for ortho pairs by about 15 per cent. The results for the three molecules previously considered, as well as for triphenylene and the odd alternant phenalenylium ion are given at the bottom of table 6. (For the latter two systems it was verified that the contribution from the configurations that are now neglected is again small.)

As far as D is concerned there is a surprising agreement between calculation and experiment. The values of E for the few molecules here considered lie in the right order, although for naphthalene the absolute value remains too large.

How relatively good the agreement in fact is, becomes apparent when calculating the ZFS of the higher triplet of the first three molecules by the same procedure. As is already apparent from Gouterman's early calculations [6], the ZFS pattern of these molecules proves to vary considerably with the orbital symmetry of the electronic state. In this respect an essential difference between D and E should be noted: whereas the value of D is primarily determined by the overall symmetry of the state, that of E is very sensitive to the precise configurational mixing. This is well illustrated by the diagonal elements of table 5: those of D are of comparable magnitude, but those of E alternate in sign. Thus, a slight increase in the weight with which $(d; d')$ enters into the function (4), at the expense of $(e; e')$ and $(c; c')$ would leave D almost invariant, but would make E much less negative.

The conclusion of the present work would seem to be that, although the calculation of the ZFS of the triplet states of aromatic molecules is more involved than that of spin densities, yet the results of such calculations appear to be reasonably realistic and may be used with some confidence in the symmetry assignment of the lowest triplet states. It is imperative, however, to allow for configuration interaction with the type II (a) configurations—i.e. those considered by Pariser in his energy calculations [12]—and to take account of σ - π interaction in some form.

The authors are much indebted to Professor J. P. Colpa for putting the triplet SCF computer programme which he developed at their disposal and to Mr. P. M. van Kempen and Miss M. J. Wiggers de Vries for programming the numerical integrations. The stimulating cooperation with Dr. M. S. de Groot and a number of discussions with Professor L. J. Oosterhoff and Professor P. W. Kasteleyn are gratefully acknowledged.

REFERENCES

- [1] HUTCHISON, C. A., and MANGUM, B. W., 1958, *J. chem. Phys.*, **29**, 952; 1961, *Ibid.*, **34**, 908.
- [2] VAN DER WAALS, J. H., and DE GROOT, M. S., 1959, *Mol. Phys.*, **2**, 333. DE GROOT, M. S., and VAN DER WAALS, J. H., 1960, *Mol. Phys.*, **3**, 190.
- [3] YAGER, W. A., WASSERMAN, E., and CRAMER, R. M. R., 1962, *J. chem. Phys.*, **37**, 1148.
- [4] KOTTIS, PH., and LEFEBVRE, R., 1963, *J. chem. Phys.*, **39**, 393.
- [5] VAN DER WAALS, J. H., 1961, unpublished results presented at the Quantum Chemistry Conference, Oxford.
- [6] GOUTERMAN, M., and MOFFITT, W., 1959, *J. chem. Phys.*, **30**, 1107. GOUTERMAN, M., 1959, *J. chem. Phys.*, **30**, 1369.
- [7] HAMEKA, H. F., 1959, *J. chem. Phys.*, **31**, 315. PITZER, R. M., and HAMEKA, H. F., 1962, *J. chem. Phys.*, **37**, 2725.
- [8] MCWEENY, R., 1961, *J. chem. Phys.*, **34**, 399, 1065. MCWEENY, R., and MIZUNO, Y., 1961, *Proc. roy. Soc. A*, **259**, 554.
- [9] McLACHLAN, A. D., 1962, *Mol. Phys.*, **5**, 51.
- [10] POPLE, J. A., 1953, *Trans. Faraday Soc.*, **49**, 1375, with further references.
- [11] COLPA, J. P. (to be published).
- [12] PARISER, R., and PARR, R. G., 1953, *J. chem. Phys.*, **21**, 446, 767. PARISER, R., 1956, *J. chem. Phys.*, **24**, 250.

- [13] POPLÉ, J. A., 1955, *Proc. phys. Soc., Lond.*, **68**, 81. MURRELL, J. N., and LONGUET-HIGGINS, H. C., 1955, *Proc. phys. Soc., Lond.*, **68**, 329.
- [14] VAN VLECK, J. H., 1951, *Rev. mod. Phys.*, **23**, 213.
- [15] McLACHLAN, A. D., 1963, *Mol. Phys.*, **6**, 441.
- [16] HAMEKA, H. F., and OOSTERHOFF, L. J., 1958, *Mol. Phys.*, **1**, 358.
- [17] McCONNELL, H. M., 1959, *Proc. nat. Acad. Sci., Wash.*, **45**, 172.
- [18] BRANDON, R. N., GERKIN, R. E., and HUTCHISON, C. A., 1962, *J. chem. Phys.*, **37**, 447.
- [19] TINKHAM, M., and STRANDBERG, M. W. P., 1955, *Phys. Rev.*, **97**, 937.
- [20] VAN DER WAALS, J. H., *Mol. Phys.* (to be published).
- [21] McCONNELL, H. M., 1956, *J. chem. Phys.*, **24**, 764. McCONNELL, H. M., and CHESNUT, D. B., 1958, *J. chem. Phys.*, **28**, 107.
- [22] WEISSMAN, S. I., 1956, *J. chem. Phys.*, **25**, 890.
- [23] KARPLUS, M., and FRAENKEL, G. K., 1961, *J. chem. Phys.*, **35**, 1312.
- [24] HIGUCHI, J., 1963, *J. chem. Phys.*, **38**, 1237.
- [25] LÖWDIN, P. O., 1953, *Phys. Rev.*, **90**, 120.
- [26] SLATER, J. C., 1960, *Quantum Theory of Molecular Structure*, Vol. I (McGraw-Hill), p. 227.
- [27] DUNCANSON, W. E., and COULSON, C. A., 1944, *Proc. roy. Soc., Edinb.*, **62**, 37.
- [28] DE GROOT, M. S., and VAN DER WAALS, J. H., *Mol. Phys.*, (to be published).
- [29] KLEIN, M. P., unpublished results. HORNIG, A. W., and HYDE, J. S., 1963, *Mol. Phys.*, **6**, 33.
- [30] BOORSTEIN, S. A., and GOUTERMAN, M., 1963, *J. chem. Phys.*, **39**, 2443.
- [31] YING-NAN CHIU, 1963, *J. chem. Phys.*, **39**, 2736, 2749.

Theory of optical rotatory power

by W. J. A. MAASKANT† and L. J. OOSTERHOFF

Department of Theoretical Organic Chemistry,
Leiden University, Holland

(Received 14 February 1964)

A general theory of natural optical rotatory power is given, applicable to dense media. The statistical mechanical treatment includes the effect of correlations between molecules. The molecules are characterized by classically defined polarizability tensors which are explained quantum mechanically. A generalized wave equation is derived which holds for a medium which may be anisotropic as well as optically active. A new demonstration of the extinction theorem is given. The theory is applied to isotropic media.

NOTATION AND SYMBOLS.

1. INTRODUCTION.

2. RESPONSE OF AN ISOLATED MOLECULE TO A LIGHT WAVE.

- 2.1. Classical radiation formulae.
- 2.2. Introduction of molecular polarizability tensors.
- 2.3. Quantum mechanical derivation of the polarizability tensors.
- 2.4. General remarks.

3. THE AVERAGE QUANTITIES.

- 3.1. Fundamental equations.
- 3.2. Molecular distribution functions.
- 3.3. Long-range and short-range interactions.
- 3.4. The macroscopic polarization densities.

4. THE GENERAL WAVE EQUATION AND THE EXTINCTION THEOREM.

- 4.1. The differential equation for an arbitrary wave in an anisotropic optically active medium.
- 4.2. Extinction theorem.

5. ISOTROPIC MEDIA.

- 5.1. Wave equation for an isotropic medium.
- 5.2. Calculation of the rotatory power. Method I.
- 5.3. Calculation of the rotatory power. Method II.
- 5.4. Limitations.
- 5.5. Illustrations.

APPENDIX.

REFERENCES.

† This work forms also part of a thesis (Maaskant, Thesis, Leiden, 1963). During the preparation of the manuscript we learned that a similar investigation had been carried out at the Department of Theoretical Physics. This will be published as R. H. Terwiel, Thesis, Leiden, 1964, and as P. Mazur and R. H. Terwiel, *Physica*, **30**, 1964.

NOTATION AND SYMBOLS

The description of the optical rotatory power requires scalar quantities and cartesian tensors of the first, second and third rank. In some equations the tensors are written in components. As much as possible the first five characters of the Greek alphabet are used as suffixes. The summation convention is applied which means that one has to sum over the three values of an index if it appears twice (contraction).

We also use a shorthand notation where all vector and tensor quantities are in bold type. The dyadic product of two tensors of arbitrary rank is denoted by writing one next to the other without a connecting sign in between. A dot between two tensors indicates a contraction, a colon a double contraction. For example, $\nabla \mathbf{E}^e$ in equation (3.7) is a second-order tensor and $\nabla \cdot \mathbf{E}^e = \text{div } \mathbf{E}^e$ is a scalar. This notation, however, is not unambiguous as it does not show which indices are contracted. To avoid confusion some of the equations are given in both notations.

List of symbols

A	second-order polarizability tensor density	M	macroscopic magnetic dipole density
$A_{\alpha\beta}^{kl}$	interaction tensor between particles k and l	N	total number of molecules in the system
A_0	scalar polarizability density	P	macroscopic electric dipole density
B, B'	third-order polarizability tensor densities	\mathbf{P}_{nm}	electric dipole transition moment
B_0, B'_0	scalar polarizability densities	Q	macroscopic higher moment density
B	macroscopic magnetic induction	R, R', R_k	position vectors
D_{kl}	auxiliary function	R_{12}	$ \mathbf{R}' - \mathbf{R} $
D	dielectric displacement	R_{AC}	distance of A to molecular centre C
E, E^e	macroscopic, external electric field strength	S_{kl}	auxiliary function
$(\mathbf{E})^L$	internal electric field	$S^{(\cdot, \cdot)}$	surface integral over the outer boundary
$(\nabla \mathbf{E})^L$	internal derivative of the electric field	dS	surface element
E_m, E_n	energy levels	T_{kl}	static dipole-dipole tensor
F	dynamic dipole-dipole interaction tensor	U	second-order unit tensor
G	dynamic interaction tensor	V	volume of the medium
H	macroscopic magnetic field strength	W, W'	auxiliary vectors
I	auxiliary integrals	$Y(\mathbf{R}, \mathbf{R}')$	Green's function
a	radius of a sphere	$g(R_{12})$	distribution function
a	vector potential	$h(R_{12})$	distribution function
b	unit vector	$2\pi\hbar$	Planck's constant
c	velocity of light <i>in vacuo</i>	h	microscopic magnetic field strength
e_i	charge of particle i	i	$\sqrt{-1}$
e	microscopic electric field strength	k	$2\pi/\lambda = \omega/c$

\mathbf{k}	quadrupole moment	$0(R)$	volume of a small sphere at \mathbf{R}
m_i	mass of particle i	\mathbf{p}_k	dipole moment of particle k
\mathbf{m}	magnetic dipole moment	$(\mathbf{p}_i)_{\text{op}}$	momentum operator of particle i
i, j, k, l	particle indices	\mathbf{q}_k	higher moment of particle k
m, s		$\mathbf{r}_B, \mathbf{r}, \mathbf{r}'$	position vectors in the molecular space
n, \bar{n}	refractive indices	$s(R)$	surface of a small sphere at \mathbf{R}
\mathbf{n}	n times unit vector in direction of the wave	t	time
$n \dots$	distribution functions	\mathbf{u}	unit vector
(\mathbf{R}, \dots)		\mathbf{v}	charge velocity
m, n	numbering of wave functions	\mathbf{z}	Hertz potential
α, β, γ	coordinate indices	ρ	charge density
δ, ϵ, μ		\sum	macroscopic surface
α_0	scalar polarizability	σ_k	scalar polarizability constant
α	second-order polarizability tensor	$\sigma(\mathbf{r}, \mathbf{r}')$	polarizability tensor density
$[\alpha\beta\gamma]$	permutation tensor	φ_n, φ_m	wave functions
β, β'	third-order polarizabilities	ϕ	scalar potential
β_0, β'_0	scalar polarizabilities	χ	rotation angle
γ	angle	ψ	phase angle
$\delta(\mathbf{R}_i - \mathbf{R})$	Dirac δ -function	ω	circular frequency
$\delta_{\alpha\beta}$	Weierstrass symbol	∇	Nabla operator
ζ, ζ_{nn}	auxiliary functions	Δ	Laplace operator
$d\eta$	line element of a normal vector	$*$	complex conjugate
$\eta(\mathbf{r}, \mathbf{r}')$	polarizability tensor density		
θ	orientation parameters of a molecule	\mathfrak{P}	function of \mathbf{P}
λ	wavelength	\mathfrak{E}	function of \mathbf{E}^e
ν	number density	\mathfrak{S}	function of surface integrals
		\mathfrak{p}_B	dipole moment density at B

1. INTRODUCTION

In the theory of optical rotatory power—as in theories of other phenomena of light refraction—two fundamental problems have to be dealt with:

- How does a single molecule respond to an oscillating electromagnetic field?
- How does the cooperation of the individual molecules lead to the phenomenon of optical activity?

The first problem belongs essentially to the domain of quantum mechanics. At least the motions of electrons and nuclei as induced by the electromagnetic field have to be derived by the methods of quantum mechanics. For the field, which acts on the molecule, as well as for the field produced by the molecule (Rayleigh scattering) a classical description suffices (semi-classical method; Kramers† [1], chapter 8).

The second problem involves the application of classical statistical mechanics to a system of molecules with radiation interactions.

† Abbreviated in this paper by Kr.

It may seem that both problems have been discussed profusely so that a further study would be superfluous. A closer inspection, however, reveals that this is not at all the case. In the first place it is unsatisfactory that the classical description of the response of a molecule to an oscillating field has not been formulated sufficiently generally so that it encompasses the model of linearly coupled oscillators [2-5] as well as the one-electron model [6], which both are contained in the quantum mechanical formulae [7]. Furthermore, the statistical mechanics has never been developed further than the so-called Lorentz-approximation, which means that in calculating the field acting on an individual molecule the effect of correlations with surrounding molecules has been neglected (internal field problem).

In the present paper the polarization of a molecule by an oscillating electromagnetic field is first formulated by classically defined polarizabilities which then are explained in quantum mechanical formulation. The statistical mechanics of an aggregate of molecules under the action of a light wave coming from external sources is developed, including correlation effects. We have used the ideas introduced by Yvon in the theory of normal refraction but with important differences. Whereas Yvon tacitly assumes the applicability of Maxwell's equations for continuous matter, thus avoiding the proof of the extinction theorem (the elimination of the incident wave inside matter), no such assumption is used by us. Instead we derive a generalized wave equation which governs the propagation of polarization through matter that may be anisotropic as well as optically active. Thereupon a general proof of the extinction theorem can be given. For an isotropic medium the general wave equation takes a simple form which enables one to calculate the rotation of the plane of polarization of a linearly polarized beam of light without the artifice of splitting it into two circularly polarized beams.

2. RESPONSE OF AN ISOLATED MOLECULE TO A LIGHT WAVE

2.1. *Classical radiation formulae*[†]

The microscopic Maxwell-Lorentz equations, which describe the electromagnetic fields and their dependences on the charge and current distribution are:

$$c\nabla \times \mathbf{e} + \mathbf{h} = 0, \quad (2.1)$$

$$c\nabla \times \mathbf{h} - \dot{\mathbf{e}} = \rho \mathbf{v}, \quad (2.2)$$

$$\nabla \cdot \mathbf{h} = 0, \quad (2.3)$$

$$\nabla \cdot \mathbf{e} = \rho, \quad (2.4)$$

\mathbf{e} and \mathbf{h} are the microscopic electric and magnetic field strengths respectively, ρ is the charge density and \mathbf{v} is the charge velocity, consequently $\rho \mathbf{v}$ is the current density. The equation of continuity follows from (2.2) and (2.4):

$$\nabla \cdot (\rho \mathbf{v}) + \dot{\rho} = 0. \quad (2.5)$$

The field strengths can be derived from a scalar potential ϕ and a vector potential \mathbf{a} :

$$\mathbf{e} = -\nabla\phi - \frac{1}{c}\dot{\mathbf{a}}, \quad (2.6)$$

$$\mathbf{h} = \nabla \times \mathbf{a}, \quad (2.7)$$

ϕ and \mathbf{a} are not completely defined by these equations. Their choice can be restricted by the so-called Lorentz gauge:

$$\nabla \cdot \mathbf{a} + \frac{1}{c}\dot{\phi} = 0. \quad (2.8)$$

[†] Rationalized gaussian units are used.

Consequently ϕ and \mathbf{a} satisfy the wave equations:

$$\Delta\phi - \frac{1}{c^2}\ddot{\phi} = -\rho, \quad (2.9)$$

$$\Delta\mathbf{a} - \frac{1}{c^2}\ddot{\mathbf{a}} = -\frac{(\rho\mathbf{v})}{c}. \quad (2.10)$$

Solutions of these equations are:

$$\phi_A = \int_V \frac{\{\rho\}_B}{4\pi R_{AB}} dV_B, \quad (2.11)$$

$$\mathbf{a}_A = \frac{1}{c} \int_V \frac{\{\rho\mathbf{v}\}_B}{4\pi R_{AB}} dV_B, \quad (2.12)$$

to which solutions of the homogeneous equations can be added. R_{AB} is the distance between two points A and B and the braces mean that ρ and $\rho\mathbf{v}$ have to be taken at the retarded time $(t - R_{AB}/c)$. For normal refraction and optical rotation only those components of ρ and $\rho\mathbf{v}$ are of importance, which are induced by the light wave and which have the same time dependency. The same applies to other field quantities and they can therefore be written as the product of a time independent part and a factor $\exp(i\omega t)$, where ω is the circular vibration frequency of the light.

By virtue of (2.5) it is possible to derive the charge and current density from a single vector:

$$\rho\mathbf{v} = \dot{\mathbf{p}}, \quad \rho = -\nabla \cdot \mathbf{p}; \quad (2.13)$$

$\mathbf{p} = (1/i\omega)\rho\mathbf{v}$ is the dipole moment density of the—microscopic—true charge distribution.

Similarly ϕ and \mathbf{a} can be derived from a Hertz potential \mathbf{z} :

$$\mathbf{a} = \frac{1}{c}\dot{\mathbf{z}}, \quad \phi = -\nabla \cdot \mathbf{z}; \quad (2.14)$$

$\mathbf{z} = (c/i\omega)\mathbf{a}$ satisfies the wave equation:

$$\Delta\mathbf{z} - \frac{1}{c^2}\ddot{\mathbf{z}} = -\mathbf{p}. \quad (2.15)$$

The solution of this equation is:

$$\mathbf{z}_A = \int_V \frac{\{\mathbf{p}\}_B}{4\pi R_{AB}} dV_B \quad \text{or} \quad \mathbf{z}_A = \int_V \mathbf{p}_B \frac{\exp(-ikR_{AB})}{4\pi R_{AB}} dV_B, \quad (2.16)$$

to which solutions of the homogeneous equation can be added and where \mathbf{e} and \mathbf{h} can be derived from \mathbf{z} by:

$$\mathbf{e} = \nabla\nabla \cdot \mathbf{z} - \frac{1}{c^2}\ddot{\mathbf{z}}, \quad (2.17)$$

$$\mathbf{h} = \frac{1}{c}\nabla \times \dot{\mathbf{z}}. \quad (2.18)$$

Since all quantities depend on time by a factor $\exp(i\omega t)$, we can simplify these equations to:

$$\mathbf{e} = \nabla\nabla \cdot \mathbf{z} + k^2\mathbf{z}, \quad (2.19)$$

$$\mathbf{h} = ik\nabla \times \mathbf{z}. \quad (2.20)$$

When the dipole moment distribution of a scattering molecule is known, the Hertz potential can be determined by equation (2.16). If the molecules are

spherical or nearly spherical it is useful to enclose the entire source by the smallest possible sphere and to develop the dipole distribution with respect to the centre of this sphere. The Hertz vector outside this sphere can then be developed in a series consisting of products of spherical Bessel- and Hankelfunctions, and Legendre polynomials [8, 9] or in terms of so-called 'irreducible tensors' (cf. [10]).

Darwin [11] and Hoek [12, 13] use a Taylor series development which can be written as:

$$\mathbf{z}_A = \int_V \mathbf{p}_B \exp(\mathbf{r}_B \cdot \nabla) \frac{\exp(-ikR_{AC})}{4\pi R_{AC}} dV_B; \quad (2.21)$$

R_{AC} is the distance of A to the molecular centre C . \mathbf{r}_B is the vector from this origin to some point B in the molecule. The nabla operator differentiates the function of R_{AC} at the molecular centre. The integration is over the molecular volume.

When we take only the first two terms of the series and in addition assume that the wavelength of light is much larger than the radius of the molecular sphere, both developments are identical. The result is:

$$\mathbf{z}_A = \mathbf{p} \frac{\exp(-ikR_{AC})}{4\pi R_{AC}} + \mathbf{q} \cdot \nabla \frac{\exp(-ikR_{AC})}{4\pi R_{AC}}, \quad (2.22)$$

where

$$\mathbf{p} = \int_V \mathbf{p}_B dV_B \quad \text{and} \quad \mathbf{q} = \int_V \mathbf{p}_B \mathbf{r}_B dV_B. \quad (2.23)$$

In index notation:

$$(z_A)_\alpha = p_\alpha \frac{\exp(-ikR_{AC})}{4\pi R_{AC}} + q_{\alpha\beta} \nabla_\beta \frac{\exp(-ikR_{AC})}{4\pi R_{AC}}. \quad (2.24)$$

For later use we give the formula of the electric field, arising from equations (2.19) and (2.22):

$$\mathbf{e} = (\nabla \nabla + k^2 \mathbf{U}) \cdot \left\{ \mathbf{p} \frac{\exp(-ikR_{AC})}{4\pi R_{AC}} + \mathbf{q} \cdot \nabla \frac{\exp(-ikR_{AC})}{4\pi R_{AC}} \right\} \quad (2.25)$$

or

$$e_\alpha = (\nabla_\alpha \nabla_\beta + k^2 U_{\alpha\beta}) \left\{ p_\beta \frac{\exp(-ikR_{AC})}{4\pi R_{AC}} + q_{\beta\gamma} \nabla_\gamma \frac{\exp(-ikR_{AC})}{4\pi R_{AC}} \right\}. \quad (2.26)$$

Here \mathbf{U} or $U_{\alpha\beta}$ is the second-order unit tensor. The first term between the braces gives the electric dipole radiation. The second term is responsible for magnetic dipole and quadrupole radiation (see, e.g., Jeffreys and Jeffreys [14], § 24.23).

Not all redundancy is avoided in these formulae since the Hertz vector may contain a part which corresponds to a zero electric field (see § 2.4.2).

2.2. Introduction of molecular polarizability tensors

The dipole moment distribution \mathbf{p} which according to the previous section determines the radiation field, depends itself on the electric field distribution inside the molecule originating from outside the molecule:

$$\mathbf{p}(\mathbf{r}) = \int_{\text{mol}} \boldsymbol{\sigma}(\mathbf{r}, \mathbf{r}') \cdot \mathbf{e}(\mathbf{r}') d\mathbf{r}'. \quad (2.27)$$

The polarizability $\sigma(\mathbf{r}, \mathbf{r}')$ is a second-order tensor density, which relates the field strength at the point \mathbf{r}' to the polarization at \mathbf{r} . The quantity $\sigma(\mathbf{r}, \mathbf{r}')$ is a generalization of the tensors \mathbf{A}^{kl} introduced by Born in his theory of optical rotatory power ([3], p. 406). Born considers a molecule consisting of a number of coupled anisotropic harmonic oscillators. \mathbf{A}^{kl} gives the dependence of the polarization of oscillator k on the electric field strength at oscillator l . In Born's theory the fundamental relation

$$A_{\alpha\beta}^{kl} = A_{\beta\alpha}^{lk} \quad (2.28)$$

was derived on the assumption that the coupled oscillators form a conservative system. It will be shown in the next section that a similar relation exists for the tensor density $\sigma(\mathbf{r}, \mathbf{r}')$:

$$\sigma_{\alpha\beta}(\mathbf{r}, \mathbf{r}') = \sigma_{\beta\alpha}(\mathbf{r}', \mathbf{r}) \quad (2.29)$$

$\sigma(\mathbf{r}, \mathbf{r}')$ is not only a generalization of Born's model in the sense that a continuous distribution of oscillators is considered, but also encompasses the one-electron model introduced by Condon *et al.* [6]. It then describes how the induced motion of the electron at point \mathbf{r} depends on the field strength everywhere inside the molecule.

It is advantageous to characterize the state of polarization of a molecule with the moments of the continuous dipole distribution since for our purpose a few moments suffice (see, e.g., equation (2.25)). On the other hand, for the dependence of these moments on the electric field distribution it will be sufficient to develop the electric field by a Taylor expansion with respect to the origin and to restrict ourselves to the first two terms. We write:

$$\mathbf{e}(\mathbf{r}') = \exp[(\mathbf{r}' \cdot \nabla)] \mathbf{e}, \quad (2.30)$$

where the differentiations are to be taken at the centre of the molecule.

The total dipole moment of the molecule is:

$$\mathbf{p} = \int \mathbf{p}(\mathbf{r}) d\mathbf{r} = \mathbf{p}^{(1)} + \mathbf{p}^{(2)} + \dots, \quad (2.31)$$

where

$$\mathbf{p}^{(1)} = \iint \sigma(\mathbf{r}, \mathbf{r}') d\mathbf{r} d\mathbf{r}' \cdot \mathbf{e} = \alpha \cdot \mathbf{e} \quad (2.32)$$

and

$$\mathbf{p}^{(2)} = \iint \sigma(\mathbf{r}, \mathbf{r}') \mathbf{r}' d\mathbf{r} d\mathbf{r}' : (\nabla \mathbf{e}) = \beta : (\nabla \mathbf{e}). \quad (2.33)$$

The second moment is defined by:

$$\mathbf{q} = \int \mathbf{p}(\mathbf{r}) \mathbf{r} d\mathbf{r} = \iint \sigma(\mathbf{r}, \mathbf{r}') \mathbf{r} d\mathbf{r} d\mathbf{r}' \cdot \mathbf{e} = \beta' \cdot \mathbf{e}. \quad (2.34)$$

In the case of the second moment we will retain the first term of the expansion. For the sake of clarity we will describe the equations (2.32), (2.33) and (2.34) also in index notation:

$$p_{\alpha}^{(1)} = \iint \sigma_{\alpha\beta}(\mathbf{r}, \mathbf{r}') d\mathbf{r} d\mathbf{r}' e_{\beta} = \alpha_{\alpha\beta} e_{\beta}, \quad (2.35)$$

$$p_{\alpha}^{(2)} = \iint \sigma_{\alpha\beta}(\mathbf{r}, \mathbf{r}') r'_{\gamma} d\mathbf{r} d\mathbf{r}' (\nabla_{\gamma} e_{\beta}) = \beta_{\alpha\beta\gamma} (\nabla_{\gamma} e_{\beta}), \quad (2.36)$$

$$q_{\alpha\gamma} = \iint \sigma_{\alpha\beta}(\mathbf{r}, \mathbf{r}') r_{\gamma} d\mathbf{r} d\mathbf{r}' e_{\beta} = \beta'_{\alpha\beta\gamma} e_{\beta}. \quad (2.37)$$

2.3. Quantum mechanical derivation of the polarizability tensors

As mentioned in the introduction to this section calculation of the current density distribution which determines the Rayleigh scattering of a molecule in a stationary state n is essentially a quantum mechanical problem. The solution is (Kr, equation (8-223)†):

$$[\rho \mathbf{v}]_{nn} = \frac{1}{c} \mathbf{W}, \quad (2.38)$$

where:

$$\mathbf{W} = \sum'_m \left\{ \frac{\{\rho \mathbf{v}^0\}_{nm} \int \mathbf{a} \cdot \{\rho \mathbf{v}^0\}_{mn} dV}{\hbar(-\omega + \omega_{mn})} + \frac{\left(\int \mathbf{a} \cdot \{\rho \mathbf{v}^0\}_{nm} dV \right) \{\rho \mathbf{v}^0\}_{mn}}{\hbar(\omega + \omega_{mn})} - \mathbf{a} \zeta_{nn} \right\}. \quad (2.39)$$

The dash beside the summation sign denotes that $m \neq n$. \mathbf{a} is the microscopic vector potential inside the molecular volume, coming from outside the molecule. ω and ω_{mn} are the circular frequency of the incident light and the circular transition frequency from $m \rightarrow n$ ($\hbar \omega_{mn} = E_m - E_n$). $\{\rho \mathbf{v}^0\}_{mn}$ is the matrix element of the unperturbed current density operator, which is given by (cf. Kr, equation (8-9)):

$$\{\rho \mathbf{v}^0\}_{nm} = \sum_i \left[\int \frac{1}{2} (\varphi_n^* e_i \mathbf{v}_i^0 \varphi_m + \varphi_m e_i \mathbf{v}_i^{0*} \varphi_n^*) \prod_{j \neq i} d\mathbf{r}_j \right]_{\mathbf{r}_i = \mathbf{r}} \quad (2.40)$$

φ_n and φ_m are time independent wave functions.

The unperturbed velocity operator is:

$$\mathbf{v}_i^0 = \frac{1}{m_i} (\mathbf{p}_i)_{\text{op}} \quad (\text{Kr, equation (8-4)}). \quad (2.41)$$

Here $(\mathbf{p}_i)_{\text{op}}$ is the momentum operator of particle i , m_i is its mass:

$$\zeta_{nn} = \sum_i \frac{e_i^2}{m_i} \left[\int \varphi_n^* \varphi_n \prod_{j \neq i} d\mathbf{r}_j \right]_{\mathbf{r}_i = \mathbf{r}} \quad (\text{Kr, equation (8-221)}). \quad (2.42)$$

The current distribution $[\rho \mathbf{v}]_{nn}$ depends on time through \mathbf{a} which contains the time factor $\exp(i\omega t)$; therefore

$$\mathbf{p} = \frac{1}{i\omega c} \mathbf{W}. \quad (2.43)$$

Since \mathbf{a} is the vector potential of the field which has its origin outside the molecule it behaves as a field *in vacuo*. This implies that it is possible to choose the gauge of the potentials ϕ and \mathbf{a} such that $\phi = 0$.

Consequently:

$$\nabla \cdot \mathbf{a} = 0 \quad (2.44)$$

and

$$\mathbf{e} = -\frac{1}{c} \dot{\mathbf{a}}. \quad (2.45)$$

Combining (2.39), (2.43) and (2.45):

$$\mathbf{p} = \frac{1}{\omega^2} \mathbf{W}', \quad (2.46)$$

† Kramers explicitly indicates that the real part of the right-hand side has to be taken. In the present considerations it will not be confusing to omit this indication.

where

$$\mathbf{W}' = \sum_m' \left\{ \frac{\{\rho \mathbf{v}^0\}_{nm} \int \mathbf{e} \cdot \{\rho \mathbf{v}^0\}_{mn} dV}{\hbar(-\omega + \omega_{mn})} + \frac{\left(\int \mathbf{e} \cdot \{\rho \mathbf{v}^0\}_{nm} dV \right) \{\rho \mathbf{v}^0\}_{mn}}{\hbar(\omega + \omega_{mn})} - \zeta_{nn} \mathbf{e} \right\}. \quad (2.47)$$

This can be written as:

$$\mathbf{p}(\mathbf{r}) = \int \boldsymbol{\eta}(\mathbf{r}, \mathbf{r}') \cdot \mathbf{e}(\mathbf{r}') d\mathbf{r}' + \zeta(\mathbf{r}) \mathbf{e}(\mathbf{r}), \quad (2.48)$$

where \mathbf{r} and \mathbf{r}' are the coordinates of two points within the molecule:

$$\eta_{\alpha\beta}(\mathbf{r}, \mathbf{r}') = \frac{1}{\omega^2} \sum_m' \left\{ \frac{\{\rho v_{\alpha}^0(\mathbf{r})\}_{nm} \{\rho v_{\beta}^0(\mathbf{r}')\}_{mn}}{\hbar(-\omega + \omega_{mn})} + \frac{\{\rho v_{\beta}^0(\mathbf{r}')\}_{nm} \{\rho v_{\alpha}^0(\mathbf{r})\}_{mn}}{\hbar(\omega + \omega_{mn})} \right\}, \quad (2.49)$$

$$\zeta(\mathbf{r}) = -\frac{1}{\omega^2} \zeta_{nn}; \quad (2.50)$$

Comparing (2.48) with (2.27) it appears that $\boldsymbol{\eta}$ and ζ together are equivalent to $\boldsymbol{\sigma}(\mathbf{r}, \mathbf{r}')$:

$$\boldsymbol{\sigma}(\mathbf{r}, \mathbf{r}') = \boldsymbol{\eta}(\mathbf{r}, \mathbf{r}') + \zeta(\mathbf{r}) \delta(\mathbf{r} - \mathbf{r}') \mathbf{U}; \quad (2.51)$$

$\delta(\mathbf{r} - \mathbf{r}')$ is the Dirac δ -function. \mathbf{U} is the second-order unit tensor. $\boldsymbol{\eta}(\mathbf{r}, \mathbf{r}')$ as well as $\zeta(\mathbf{r})$ are real quantities. This can easily be shown by choosing all the wave functions φ_n , φ_m real, which is always possible if the Hamilton operator, having φ_n and φ_m as eigenfunctions, does not contain an imaginary part. $\{\rho \mathbf{v}^0\}_{nm}$ is then an imaginary operator and from (2.40) it is clear that:

$$\{\rho \mathbf{v}^0\}_{nm} = -\{\rho \mathbf{v}^0\}_{nm}^* = -\{\rho \mathbf{v}^0\}_{mn}. \quad (2.52)$$

Equation (2.49) can be simplified now to:

$$\eta_{\alpha\beta}(\mathbf{r}, \mathbf{r}') = \frac{2}{\omega^2} \sum_m' \omega_{mn} \frac{\{\rho v_{\alpha}^0(\mathbf{r})\}_{nm} \{\rho v_{\beta}^0(\mathbf{r}')\}_{mn}}{\hbar(\omega_{mn}^2 - \omega^2)}. \quad (2.53)$$

It follows from this equation that:

$$\eta_{\alpha\beta}(\mathbf{r}, \mathbf{r}') = \eta_{\beta\alpha}(\mathbf{r}', \mathbf{r}). \quad (2.54)$$

Since $\zeta \mathbf{U}$ is isotropic a similar formula applies to $\boldsymbol{\sigma}(\mathbf{r}, \mathbf{r}')$:

$$\sigma_{\alpha\beta}(\mathbf{r}, \mathbf{r}') = \sigma_{\beta\alpha}(\mathbf{r}', \mathbf{r}), \quad (2.55)$$

which was already mentioned before.

For the general formulae for α , β and β' we have to substitute in (2.32), (2.33) and (2.34) the expression for $\boldsymbol{\sigma}(\mathbf{r}, \mathbf{r}')$. The results are:

$$\alpha_{\alpha\beta} = \frac{2}{\hbar} \sum_m' \frac{\omega_{mn}}{\omega_{mn}^2 - \omega^2} (P_{nm})_{\alpha} (P_{mn})_{\beta}, \quad (2.56)$$

$$\beta_{\alpha\beta\gamma} = \frac{2}{\hbar} \sum_m' \frac{1}{\omega_{mn}^2 - \omega^2} \frac{1}{\omega_{mn}} \int \{\rho v_{\alpha}^0(\mathbf{r})\}_{nm} d\mathbf{r} \int \{\rho v_{\beta}^0(\mathbf{r}')\}_{mn} r'_{\gamma} d\mathbf{r}' \quad (2.57)$$

$$\beta'_{\alpha\beta\gamma} = \frac{2}{\hbar} \sum_m' \frac{1}{\omega_{mn}^2 - \omega^2} \frac{1}{\omega_{mn}} \int \{\rho v_{\alpha}^0(\mathbf{r})\}_{nm} r_{\gamma} d\mathbf{r} \int \{\rho v_{\beta}^0(\mathbf{r}')\}_{mn} d\mathbf{r}'. \quad (2.58)$$

Here

$$\mathbf{P}_{nm} = \frac{1}{i\omega_{nm}} \dot{\mathbf{P}}_{nm} = \frac{1}{i\omega_{nm}} \int \{\rho \mathbf{v}^0(\mathbf{r})\}_{nm} d\mathbf{r} \quad (\text{Kr, equation (8-24)}). \quad (2.59)$$

For the derivation of the well-known formula (2.56) use is made of:

$$\frac{1}{i\hbar} \sum_m [(P_{nm})_\alpha (\dot{P}_{mn})_\beta - (\dot{P}_{nm})_\beta (P_{mn})_\alpha] = \sum_i \frac{e_i^2}{m_i} U_{\alpha\beta}, \quad (2.60)$$

which are the commutation relations of \mathbf{P}_{nm} and $\dot{\mathbf{P}}_{nm}$ (Kr, equation (8-204)). Similarly for the derivation of β and β' use is made of the analogous relations:

$$\frac{1}{i\hbar} \sum_m \left[(P_{nm})_\alpha \int \{\rho v_\beta^0(\mathbf{r}')\}_{mn} r'_\gamma d\mathbf{r}' - \int \{\rho v_\beta^0(\mathbf{r}')\}_{nm} r'_\gamma d\mathbf{r}' (P_{mn})_\alpha \right] = \sum_i \frac{e_i^2}{m_i} (r_\gamma)_{nn} U_{\alpha\beta}. \quad (2.61)$$

2.4. General remarks

2.4.1. Magnetic dipole and electric quadrupole moment

A number of authors prefer to formulate the response of a single molecule to an electromagnetic perturbation in terms of electric and magnetic moments. This formulation is inviting if one assumes that the equations:

$$\mathbf{D} = \mathbf{E} + \mathbf{P}, \quad (2.62)$$

$$\mathbf{B} = \mathbf{H} + \mathbf{M}, \quad (2.63)$$

have a well-defined meaning and that the phenomenological quantities \mathbf{P} and \mathbf{M} depend on the molecular moments in a well-known way, so that this relation offers no problem (e.g. Rosenfeld [7], Condon *et al.* [6], Eyring *et al.* [15]). In our treatment the validity of these equations is immaterial and therefore it is not necessary to introduce magnetic dipole moments and electric quadrupole moments as such.

For the sake of comparison, however, we will give the relation between the second-order moment \mathbf{q} and the usual definitions of magnetic and quadrupole moments.

The magnetic moment is defined by:

$$\mathbf{m} = \frac{1}{2c} \int_V \mathbf{r} \times (\rho \mathbf{v}) d\mathbf{r} \quad (2.64)$$

(Heitler [16], p. 24, equation (23 b)) with (2.13), (2.34) and (2.37):

$$m_\alpha = \frac{1}{2c} [\alpha\beta\gamma] \dot{q}_{\gamma\beta} = \frac{1}{2c} [\alpha\beta\gamma] \beta'_{\gamma\epsilon\beta} \dot{e}_\epsilon, \quad (2.65)$$

where

$$\begin{aligned} [\alpha\beta\gamma] &\text{ is the permutation tensor,} \\ [\alpha\beta\gamma] &= 1 \quad \text{for } \alpha=1, \beta=2, \gamma=3 \text{ or cycl.,} \\ [\alpha\beta\gamma] &= -1 \quad \text{for } \alpha=2, \beta=1, \gamma=3 \text{ or cycl.,} \\ [\alpha\beta\gamma] &= 0 \quad \text{for } \alpha=\beta, \beta=\gamma \text{ or } \gamma=\alpha. \end{aligned}$$

The quadrupole moment can be defined by the equation:

$$k_{\alpha\gamma} = \int_V p_\alpha r_\gamma d\mathbf{r} + \int_V p_\gamma r_\alpha d\mathbf{r} \quad (2.66)$$

(Stratton [8], p. 433, equation (17)).

Consequently:

$$k_{\alpha\gamma} = q_{\alpha\gamma} + q_{\gamma\alpha} \quad (2.67)$$

Generally the quadrupole moment is neglected in considerations about optical rotatory power, as its influence vanishes for an isotropic liquid if the

molecules have no specific interaction (see §5, equation (5.4)). Vol'kenshtein [17] showed that for anisotropic media the quadrupole moment cannot be neglected because of the conservation of energy. In the case of an isotropic liquid where the molecules can have a strong interaction we cannot neglect them either.

2.4.2. Duplicate rule

Since $\nabla \cdot \mathbf{e} = 0$ we can add to $\beta_{\alpha 11}$, $\beta_{\alpha 22}$ and $\beta_{\alpha 33}$ an arbitrary vector component σ_α , without changing the dipole moment. A similar relation holds for the tensor β' . Here the reason is that the Hertz vector may contain a part which corresponds to zero electric field (see the end of §2.1). This implies that:

$$\beta'_{1\beta 1} + \beta'_{2\beta 2} + \beta'_{3\beta 3} = \text{arbitrary} \quad (2.68)$$

(cf. Hoek [12], p. 52). Similar relations also apply to higher order polarizability tensors (Darwin's duplicate rule, Darwin [11]).

3. THE AVERAGE QUANTITIES

Introduction

The response of a single molecule to a monochromatic light wave, which was discussed in the former section, forms the basis of the study of a system of many molecules. The first task is to set up equations which give the polarization of an arbitrarily selected molecule due to the external field and the secondary fields of all the other molecules. These equations have to be averaged in order to obtain macroscopic quantities (§3.1). In the reduction of these equations we make use of molecular distribution functions (§3.2) and the closely related distinction between short-range and long-range interactions (§3.3). In §3.4 the macroscopic polarizability densities are derived.

3.1. Fundamental equations

We consider a medium consisting of N equivalent molecules in statistical equilibrium. These molecules are supposed to be sufficiently spherical so that the series development of the Hertz vector discussed in the preceding chapter (equation (2.21)) can be applied. The position of a molecule is specified by the coordinates of its centre and by its orientation, both with respect to a space-fixed coordinate system. The polarizabilities α , β and β' , which were introduced in §2.2, are so defined that the determination of the polarization of a molecule requires only the knowledge of the effective electric field and its derivative at the molecular centre.

The electric field to which a molecule k is subjected consists of the external field \mathbf{E}^e coming from outside the medium and the secondary fields scattered by all the other molecules. This is expressed in the formula:

$$\mathbf{e}(\mathbf{R}) = \mathbf{E}^e(\mathbf{R}) - \sum_l' \mathbf{F}(\mathbf{R}, \mathbf{R}_l) \cdot \mathbf{p}_l - \sum_l' \mathbf{G}(\mathbf{R}, \mathbf{R}_l) : \mathbf{q}_l \quad (3.1)$$

or

$$e_\alpha(\mathbf{R}) = E_\alpha^e(\mathbf{R}) - \sum_l' F_{\alpha\beta}(\mathbf{R}, \mathbf{R}_l) p_\beta^{(l)} - \sum_l' G_{\alpha\beta\gamma}(\mathbf{R}, \mathbf{R}_l) q_{\beta\gamma}^{(l)} \quad (3.2)$$

The dash at the \sum sign means that $l=k$ has to be omitted:

$$F_{\alpha\beta}(\mathbf{R}, \mathbf{R}_l) = -(\nabla_\alpha \nabla_\beta + k^2 U_{\alpha\beta}) \frac{\exp(-ik|\mathbf{R}_l - \mathbf{R}|)}{4\pi|\mathbf{R}_l - \mathbf{R}|}, \quad (3.3)$$

$$G_{\alpha\beta\gamma}(\mathbf{R}, \mathbf{R}_l) = -(\nabla_\alpha \nabla_\beta + k^2 U_{\alpha\beta}) \nabla_\gamma \frac{\exp(-ik|\mathbf{R}_l - \mathbf{R}|)}{4\pi|\mathbf{R}_l - \mathbf{R}|}; \quad (3.4)$$

\mathbf{R} is the position vector in a space-fixed coordinate system of a point inside molecule k ; \mathbf{R}_l denotes the centre of the molecule l . The differentiations are applied at \mathbf{R}_l . These formulae follow immediately from (2.25).

The polarization moments of molecule k can be calculated from the electric field and its derivative by:

$$\mathbf{p} = \mathbf{p}^{(1)} + \mathbf{p}^{(2)} = \boldsymbol{\alpha} \cdot \mathbf{e}(\mathbf{R}_k) + \boldsymbol{\beta} : (\nabla \mathbf{e})_{\mathbf{R}=\mathbf{R}_k}, \quad (3.5)$$

$$\mathbf{q} = \boldsymbol{\beta}' \cdot \mathbf{e}(\mathbf{R}_k), \quad (3.6)$$

From these equations it follows that:

$$\begin{aligned} \mathbf{p}_k = & \boldsymbol{\alpha}_k \cdot \mathbf{E}_k^e - \sum_l' \boldsymbol{\alpha}_k \cdot \mathbf{F}_{kl} \cdot \mathbf{p}_l - \sum_l' \boldsymbol{\alpha}_k \cdot \mathbf{G}_{kl} : \mathbf{q}_l \\ & + \boldsymbol{\beta}_k \cdot \{(\nabla \mathbf{E}^e)_k - \sum_l' (\nabla_k \mathbf{F}_{kl}) \cdot \mathbf{p}_l\}, \end{aligned} \quad (3.7)$$

$$\mathbf{q}_k = \boldsymbol{\beta}_k' \cdot \mathbf{E}_k^e - \sum_l' \boldsymbol{\beta}_k' \cdot \mathbf{F}_{kl} \cdot \mathbf{p}_l. \quad (3.8)$$

Products of third-order polarizabilities are neglected, since their contribution to the dipole moment of k is small with respect to other terms. Therefore the moments \mathbf{q}_l do not appear in the expression for the derivative of the electric field (equation (3.7)). Similarly the moments \mathbf{q}_l are neglected in equation (3.8).

It is from these equations that expressions for the macroscopic moment densities as statistical averages have to be derived. These macroscopic moment densities determine the propagation of light through the medium.

The averaging procedure may be formulated in different ways. Kirkwood [18], Yvon [19] and also Mazur and Jansen [20], Mazur and Mandel [21], Mazur and Postma [22], use ensemble averages, whereas Hoek [12, 13] and Rosenfeld [23], following Lorentz [24], think in terms of space averages. This approach has the advantage of a certain visualization, especially if the liquid for which the laws of light refraction are derived is actually a rigid glass. We prefer, following Kramers ([1], § 95), to consider our averages as "averages over planes of constant light phase". Since in the theory of optical rotatory power the dimensions of a molecule can no longer be neglected with respect to the wavelength of light, the volume over which an average has to be taken should be small compared to a molecular diameter, at least in the direction of the light wave. Therefore the volume element has to be enclosed by two planes of constant light phase, a small distance apart, but of such extension that a large number of molecules have their centres inside the volume element. For the rest the averaging procedure is identical to that described by Hoek ([12], p. 25) and Rosenfeld ([23], chapter VI, § 1).

Indicating average values by a bar, equation (3.7) becomes:

$$\overline{\mathbf{p}_k} = \overline{\boldsymbol{\alpha}_k} \cdot \overline{\mathbf{E}_k^e} - \sum_l' \overline{\boldsymbol{\alpha}_k \cdot \mathbf{F}_{kl} \cdot \mathbf{p}_l} - \sum_l' \overline{\boldsymbol{\alpha}_k \cdot \mathbf{G}_{kl} : \mathbf{q}_l} + \overline{\boldsymbol{\beta}_k} \cdot (\overline{\nabla \mathbf{E}^e})_k - \sum_l' \overline{\boldsymbol{\beta}_k \cdot \nabla_k \mathbf{F}_{kl} \cdot \mathbf{p}_l}. \quad (3.9)$$

The bar means that the average is extended over the positions of the centres and orientations of all the molecules, except over the position of the centre of molecule k . $\overline{\mathbf{p}_k}, \overline{\alpha_k}$ thus become functions of \mathbf{R}_k . The averaging is actually performed by integration of equation (3.7) after multiplication by an appropriate distribution function. This function gives the relative frequency density of finding all the molecules with their centres at specified points and with given orientations. In the neighbourhood of molecule k the distribution of the centres and orientations of molecules l will strongly depend on the position and orientation of k . At greater distances this correlation gradually disappears. There it is allowed to average over the positions and orientations of molecules l disregarding the position and orientation of k . Henceforth we denote these molecules by the suffix s .

If then as an example we consider the second term of equation (3.9), it becomes:

$$-\sum_l' \overline{\alpha_k \cdot \mathbf{F}_{kl} \cdot \mathbf{p}_l} - \sum_s \overline{\alpha_k \cdot \mathbf{F}_{ks} \cdot \mathbf{p}_s} \quad (3.10)$$

The bar over \mathbf{F}_{ks} has to be continued as a second bar over $\overline{\mathbf{p}_s}$, because $\overline{\mathbf{p}_s}$ still depends on the position of the centre of s .

This expression suggests the introduction of a field and of a field-derivative, which we will call the internal field:

$$\mathbf{E}_k^L = \mathbf{E}_k^e - \sum_s' \overline{\mathbf{F}_{ks} \cdot \mathbf{p}_s} - \sum_s \overline{\mathbf{G}_{ks} \cdot \mathbf{q}_s} \quad (3.11)$$

and the internal derivative of the field:

$$(\nabla \mathbf{E})_k^L = (\nabla \mathbf{E})_k^e - \sum_s \overline{(\nabla_k \mathbf{F}_{ks}) \cdot \mathbf{p}_s} \quad (3.12)$$

In (3.12) a term with \mathbf{q} could be omitted. With these expressions (3.9) can be written as:

$$\overline{\mathbf{p}_k} = \overline{\alpha_k} \cdot \mathbf{E}_k^L + \overline{\beta_k} : (\nabla \mathbf{E})_k^L - \sum_l' \overline{\alpha_k \cdot \mathbf{F}_{kl} \cdot \mathbf{p}_l} - \sum_l' \overline{\alpha_k \cdot \mathbf{G}_{kl} \cdot \mathbf{q}_l} - \sum_l' \overline{\beta_k : \nabla_k \mathbf{F}_{kl} \cdot \mathbf{p}_l} \quad (3.13)$$

In the same way we find for (3.8):

$$\overline{\mathbf{q}_k} = \overline{\beta_k'} \cdot \mathbf{E}_k^L - \sum_l' \overline{\beta_k' \cdot \mathbf{F}_{kl} \cdot \mathbf{p}_l} \quad (3.14)$$

When all correlations are neglected $\overline{\mathbf{p}_k}$ becomes:

$$\overline{\mathbf{p}_k} = \overline{\alpha_k} \cdot \mathbf{E}_k^L + \overline{\beta_k} : (\nabla \mathbf{E})_k^L \quad (3.15)$$

and

$$\overline{\mathbf{q}_k} = \overline{\beta_k'} \cdot \mathbf{E}_k^L, \quad (3.16)$$

since in this case, as shown by Lorentz, the sum over l does not contribute to the field at k . (3.15) and (3.16) form together the simplest approximations for the moments of an optically active molecule.

3.2. Molecular distribution functions

A further reduction of the equations (3.13) and (3.14) can be obtained with the molecular distribution functions introduced by Kirkwood [18] and Yvon [19] and generalized to include orientations by Mazur and Postma [22]. We summarize the definitions and properties of the simplest molecular distribution functions.

The number density at \mathbf{R} is written as $\nu(\mathbf{R})$. Similarly $n_1(\mathbf{R}, \theta)$ is defined as the density of molecules with position \mathbf{R} and orientation θ . In a homogeneous medium both $\nu(\mathbf{R})$ and $n_1(\mathbf{R}, \theta)$ are uniform—except close to the boundary of the

system—and therefore in fact independent of \mathbf{R} . The molecular distribution functions pertaining simultaneously to pairs of molecules are $n_2(\mathbf{R}, \mathbf{R}')$ and $n_2(\mathbf{R}, \mathbf{R}', \theta, \theta')$. In a homogeneous and isotropic medium $n_2(\mathbf{R}, \mathbf{R}')$ and $n_2(\mathbf{R}, \mathbf{R}', \theta, \theta')$ depend on \mathbf{R} and \mathbf{R}' only through the distance $R_{12} = |\mathbf{R}' - \mathbf{R}|$. For $n_2(\mathbf{R}, \mathbf{R}')$, Yvon derived a power series in $1/N$:

$$n_2(\mathbf{R}, \mathbf{R}') = \nu^2 \left\{ g(R_{12}) + \frac{1}{N} h(R_{12}) + \dots \right\}. \quad (3.17)$$

For increasing R_{12} :

$$g(R_{12}) \rightarrow 1 \quad \text{and} \quad h(R_{12}) \rightarrow h_0(R_{12}) \quad (3.18)$$

(cf. Yvon [19], I, p. 25, equation (67), Brown [25], pp. 65, 66).

Like $n_2(\mathbf{R}, \mathbf{R}')$, $n_2(\mathbf{R}, \mathbf{R}', \theta, \theta')$ and similar distribution functions for three or more particles tend to products of distribution functions of a smaller number of molecules when the intermolecular distances increase. Yvon showed that in liquids and gases consisting of molecules which are small with respect to the wavelength of light, the influence of the correlation between molecules is restricted to an area, which is also small compared to the wavelength. In addition Yvon proved that the reaction field which still would exist if mechanical correlations could be disregarded, apart from the impenetrability of molecules, is due to interactions which are also restricted to a region of the same extension. We assume with Mazur and Postma [22] that these results also apply for the orientational part of the correlations.

In view of these considerations it is expedient to introduce the concept of a 'correlation sphere' with a radius of the same order of magnitude as the 'correlation length'. The idea is that the molecule which is at the centre of this sphere feels the influence of the molecules outside the sphere as if they form a continuum. The molecules inside the sphere, however, have to be considered as particles.

3.3. Long-range and short-range interactions

With the aid of the molecular distribution functions the formulae for the internal field and the internal derivative of the field can be written as:

$$\begin{aligned} \mathbf{E}^L(\mathbf{R}) = & \mathbf{E}^e(\mathbf{R}) - \nu^{-2} \int \mathbf{F}(\mathbf{R}, \mathbf{R}') n_2(\mathbf{R}, \mathbf{R}') \cdot \mathbf{P}(\mathbf{R}') d\mathbf{R}' \\ & - \nu^{-2} \int \mathbf{G}(\mathbf{R}, \mathbf{R}') n_2(\mathbf{R}, \mathbf{R}') : \mathbf{Q}(\mathbf{R}') d\mathbf{R}', \end{aligned} \quad (3.19)$$

$$(\nabla \mathbf{E})^L(\mathbf{R}) = (\nabla \mathbf{E}^e)(\mathbf{R}) - \nu^{-2} \int \nabla_{\mathbf{R}} \mathbf{F}(\mathbf{R}, \mathbf{R}') n_2(\mathbf{R}, \mathbf{R}') \cdot \mathbf{P}(\mathbf{R}') d\mathbf{R}', \quad (3.20)$$

where the macroscopic polarization densities are defined by:

$$\mathbf{P}(\mathbf{R}) = \nu \mathbf{p}_k, \quad (3.21)$$

$$\mathbf{Q}(\mathbf{R}) = \nu \mathbf{q}_k. \quad (3.22)$$

The integrals over \mathbf{R}' can be applied to the whole medium, since the distribution function $n_2(\mathbf{R}, \mathbf{R}')$ becomes zero for distances $|\mathbf{R}' - \mathbf{R}|$ smaller than a molecular diameter and therefore singularities do not occur. Actually, however, a sphere with its centre at \mathbf{R} can be excluded from the integral without changing its value as long as its radius is small with respect to the wavelength of light. This result, which was already known in the theory of the normal refraction, also

applies to optically active systems, as is shown in the Appendix. The derivation depends essentially on the properties of $\mathbf{F}(\mathbf{R}, \mathbf{R}')$ for small values of the argument $|\mathbf{R}' - \mathbf{R}|$ and the assumption that the variations of \mathbf{P} over a region of the order of magnitude of the correlation sphere are comparable to the variations of the external field.

We will choose the correlation sphere as the volume to be excluded from the integrations since outside this sphere $n_2(\mathbf{R}, \mathbf{R}') = \nu^2$ (except to terms proportional to $1/N$, which will be neglected). (3.19) and (3.20) become:

$$\mathbf{E}^L(\mathbf{R}) = \mathbf{E}^e(\mathbf{R}) - \int_{0(R)}^V \mathbf{F}(\mathbf{R}, \mathbf{R}') \cdot \mathbf{P}(\mathbf{R}') d\mathbf{R}' - \int_{0(R)}^V \mathbf{G}(\mathbf{R}, \mathbf{R}') : \mathbf{Q}(\mathbf{R}') d\mathbf{R}', \quad (3.23)$$

$$(\nabla \mathbf{E})^L(\mathbf{R}) = (\nabla \mathbf{E}^e)(\mathbf{R}) - \int_{0(R)}^V \nabla_{\mathbf{R}}(\mathbf{R}, \mathbf{R}') \cdot \mathbf{P}(\mathbf{R}') d\mathbf{R}'. \quad (3.24)$$

The assumption that the correlation radius is small with respect to the wavelength implies that the \mathbf{F}_{kl} -operator for the particles inside the correlation sphere can be replaced by the static dipole-dipole tensor \mathbf{T}_{kl} .

$$\mathbf{T}_{kl} = -\nabla \nabla \frac{1}{4\pi R_{lk}}. \quad (3.25)$$

Yvon showed this approximation to be valid in the theory of normal refraction. In the case of optical activity it cannot be adopted without further inquiry. However, the validity still holds since the terms in the series development of \mathbf{F}_{kl} after \mathbf{T}_{kl} contain k to the second and higher powers. For similar reasons $\mathbf{G}_{kl} \rightarrow \nabla_l \mathbf{T}_{kl}$ (see Appendix). Thus we reach the results:

$$\begin{aligned} \overline{\mathbf{p}_k} = & \overline{\alpha_k} \cdot \overline{\mathbf{E}_k^L} + \overline{\beta_k} : (\nabla \mathbf{E})_k^L - \sum_l' \overline{\alpha_k \cdot \mathbf{T}_{kl} \cdot \mathbf{p}_l} \\ & - \sum_l' \overline{\alpha_k \cdot \nabla_l \mathbf{T}_{kl} : \mathbf{q}_l} - \sum_l' \overline{\beta_k : \nabla_k \mathbf{T}_{kl} \cdot \mathbf{p}_l} \end{aligned} \quad (3.26)$$

and

$$\overline{\mathbf{q}_k} = \overline{\beta'_k} \cdot \overline{\mathbf{E}_k^L} - \sum_l' \overline{\beta'_k \cdot \mathbf{T}_{kl} \cdot \mathbf{p}_l}. \quad (3.27)$$

Apparently the electric field at particle k is composed of three contributions:

- The external field \mathbf{E}^e .
- The field due to the polarization outside the correlation sphere, which can be calculated as arising from a continuum.
- The short-range contribution due to the granular structure of the medium inside the correlation sphere.

The derivative of the field can be divided similarly.

As will be shown in the next section, the field arising from the continuum can be written as the sum of two surface integrals: one over the surface of the correlation sphere, the other over the external surface. This last integral cancels the external field (extinction theorem). A consequence of this situation is that the electric field at molecule k can be calculated from contributions arising from the immediate neighbourhood of molecule k only.

3.4. The macroscopic polarization densities

In order to evaluate (3.26) and (3.27), which after multiplication with ν give the macroscopic polarization densities \mathbf{P} and \mathbf{Q} , we have to substitute expressions for \mathbf{p}_l and \mathbf{q}_l . For the moments of a molecule l we will not use expressions similar

to (3.26) and (3.27), but instead we will try to write the polarizing field at l in terms of \mathbf{E}_k^L and $(\nabla \mathbf{E})_k^L$. In a certain sense we could say that the field coming into the correlation sphere from outside is regarded as an 'external' field for all molecules which are inside this sphere. This 'external' field is supposed to be described sufficiently accurately by:

$$\mathbf{E}_k^L + \mathbf{R}_{lk} \cdot (\nabla \mathbf{E})_k^L, \quad (3.28)$$

where \mathbf{R}_{lk} is the vector pointing from the centre of k to the centre of l . This field differs from the field which actually polarizes molecule l according to equations similar to (3.26) and (3.27). The difference is due to the neglect of correlations between molecules l inside the correlation sphere and outside. But the idea of the correlation sphere is that these correlations are not perceivable at molecule k and thus are of no importance for the calculation of $\overline{\mathbf{p}}_k$.

Up to terms quadratic in the polarizabilities (3.26) becomes :

$$\begin{aligned} \overline{\mathbf{p}}_k = & \overline{\alpha}_k \cdot \mathbf{E}_k^L + \overline{\beta}_k : (\nabla \mathbf{E})_k^L - \sum_l' \overline{\alpha}_k \cdot \mathbf{T}_{kl} \cdot \overline{\alpha}_l \cdot \mathbf{E}_k^L \\ & - \sum_l' \overline{\alpha}_k \cdot \nabla_l \mathbf{T}_{kl} : \overline{\beta}_l' \cdot \mathbf{E}_k^L - \sum_l' \overline{\beta}_k : \nabla_k \mathbf{T}_{kl} \cdot \overline{\alpha}_l \cdot \mathbf{E}_k^L \\ & - \sum_l' (\overline{\alpha}_k \cdot \mathbf{T}_{kl} \mathbf{R}_{lk} \cdot \overline{\alpha}_l) : (\nabla \mathbf{E})_k^L - \sum_l' (\overline{\alpha}_k \cdot \nabla_l \mathbf{T}_{kl} \mathbf{R}_{lk} : \overline{\beta}_l') : (\nabla \mathbf{E})_k^L \\ & - \sum_l' (\overline{\beta}_k : \nabla_k \mathbf{T}_{kl} \mathbf{R}_{lk} \cdot \overline{\alpha}_l) : (\nabla \mathbf{E})_k^L - \sum_l' \overline{\alpha}_k \cdot \mathbf{T}_{kl} \cdot \overline{\beta}_l : (\nabla \mathbf{E})_k^L \\ & + \sum_{l,m}' \overline{\alpha}_k \cdot \mathbf{T}_{kl} \cdot \overline{\alpha}_l \cdot \mathbf{T}_{lm} \cdot \mathbf{p}_m + \sum_{l,m}' \overline{\alpha}_k \cdot \nabla_l \mathbf{T}_{kl} : \overline{\beta}_l' \cdot \mathbf{T}_{lm} \cdot \mathbf{p}_m \\ & + \sum_{l,m}' \overline{\beta}_k : \nabla_k \mathbf{T}_{kl} \cdot \overline{\alpha}_l \cdot \mathbf{T}_{lm} \cdot \mathbf{p}_m + \sum_{l,m}' \overline{\alpha}_k \cdot \mathbf{T}_{kl} \cdot \overline{\beta}_l : \nabla_l \mathbf{T}_{lm} \cdot \mathbf{p}_m \\ & + \sum_{l,m}' \overline{\alpha}_k \cdot \mathbf{T}_{kl} \cdot \overline{\alpha}_l \cdot \nabla_m \mathbf{T}_{lm} : \mathbf{q}_m. \end{aligned} \quad (3.29)$$

This series can be continued to any desired accuracy. In the last five terms we have omitted for the sake of brevity to substitute the appropriate expressions for \mathbf{p}_m and \mathbf{q}_m . We will need these terms later in a discussion of the reaction field. The success of this development depends on how many terms have to be taken into account.

The terms quadratic in the polarizability will be discussed in some detail. The terms $-\sum_l' \overline{\alpha}_k \cdot \nabla_l \mathbf{T}_{kl} : \overline{\beta}_l' \cdot \mathbf{E}_k^L$ and $-\sum_l' \overline{\beta}_k : \nabla_k \mathbf{T}_{kl} \cdot \overline{\alpha}_l \cdot \mathbf{E}_k^L$ are corrections to the term $-\sum_l' \overline{\alpha}_k \cdot \mathbf{T}_{kl} \cdot \overline{\alpha}_l \cdot \mathbf{E}_k^L$. These corrections arise if it is deemed worthwhile to account for third-order polarizabilities. The ratio of these correction terms to the principal term is about equal to a molecular radius divided by the intermolecular distance. They are as important in the theory of the static dielectric constant as in the theory of refraction. Nevertheless they are almost always neglected. The terms proportional to the internal derivative of the field, are responsible for optical activity. The term $-\sum_l' (\overline{\alpha}_k \cdot \mathbf{T}_{kl} \mathbf{R}_{lk} \cdot \overline{\alpha}_l) : (\nabla \mathbf{E})_k^L$ is the counterpart of a molecular model of coupled oscillators as are encountered in the theories of Born [3], Kuhn and Freudenberg [2], Kooy [4] and Kirkwood [5]. The following three are again correction terms, which are smaller by the same previously mentioned ratio. Since for dense media this factor is not very small (it can amount to 0.3) it may be worthwhile to investigate numerically the influence of the contributions of polarizabilities, of higher order than the third.

Similar remarks apply to the expression for the moment $\overline{\mathbf{q}}_k$ which follows from (3.27):

$$\overline{\mathbf{q}}_k = \overline{\beta'_k} \cdot \mathbf{E}_k^L - \sum_l \overline{\beta'_k \cdot \mathbf{T}_{kl} \cdot \alpha_l} \cdot \mathbf{E}_k^L - \sum_l \overline{(\beta'_k \cdot \mathbf{T}_{kl} \mathbf{R}_{lk} \cdot \alpha_l)} : (\nabla \mathbf{E})_k^L + \sum_{l,m} \overline{\beta'_k \cdot \mathbf{T}_{kl} \cdot \alpha_l \cdot \mathbf{T}_{lm} \cdot \mathbf{p}_m}. \quad (3.30)$$

We will neglect the third term as it is a factor R_{lk}/λ smaller than the second one. We mention that the second term is the counterpart of the last quadratic term of (3.29).

The macroscopic moment densities $\mathbf{P}(\mathbf{R})$ and $\mathbf{Q}(\mathbf{R})$ can now be written as:

$$\mathbf{P}(\mathbf{R}) = \overline{\mathbf{A}} \cdot \mathbf{E}^L(\mathbf{R}) + \overline{\mathbf{B}} : (\nabla \mathbf{E})^L(\mathbf{R}), \quad (3.31)$$

$$\mathbf{Q}(\mathbf{R}) = \overline{\mathbf{B}'} \cdot \mathbf{E}^L(\mathbf{R}); \quad (3.32)$$

$\overline{\mathbf{A}}$, $\overline{\mathbf{B}}$ and $\overline{\mathbf{B}'}$ are averaged polarizability densities corresponding to α , β and β' :

$$\begin{aligned} \overline{\mathbf{A}} = \nu \left[\overline{\alpha_k} - \sum_l \overline{\alpha_k \cdot \mathbf{T}_{kl} \cdot \alpha_l} - \sum_l \overline{\alpha_k \cdot \nabla_l \mathbf{T}_{kl} : \beta'_l} - \sum_l \overline{\beta_k : \nabla_l \mathbf{T}_{kl} \cdot \alpha_l} \right. \\ + \sum_l \overline{\alpha_k \cdot \mathbf{T}_{kl} \cdot \alpha_l \cdot \mathbf{T}_{lk} \cdot \alpha_k} + \sum_l \overline{\alpha_k \cdot \nabla_l \mathbf{T}_{kl} : \beta'_l \cdot \mathbf{T}_{lk} \cdot \alpha_k} \\ + \sum_l \overline{\beta_k : \nabla_l \mathbf{T}_{kl} \cdot \alpha_l \cdot \mathbf{T}_{lk} \cdot \alpha_k} + \sum_l \overline{\alpha_k \cdot \mathbf{T}_{kl} \cdot \beta'_l : \nabla_l \mathbf{T}_{lk} \cdot \alpha_k} \\ \left. + \sum_l \overline{\alpha_k \cdot \mathbf{T}_{kl} \cdot \alpha_l \cdot \nabla_k \mathbf{T}_{lk} : \beta'_k} \right], \quad (3.33) \end{aligned}$$

$$\begin{aligned} \overline{\mathbf{B}} = \nu \left[\overline{\beta_k} - \sum_l \overline{\alpha_k \cdot \mathbf{T}_{kl} \mathbf{R}_{lk} \cdot \alpha_l} - \sum_l \overline{\alpha_k \cdot (\nabla_l \mathbf{T}_{kl}) \mathbf{R}_{lk} : \beta'_l} \right. \\ - \sum_l \overline{\beta_k : (\nabla_k \mathbf{T}_{kl}) \mathbf{R}_{lk} \cdot \alpha_l} - \sum_l \overline{\alpha_k \cdot \mathbf{T}_{kl} \cdot \beta_l} \\ \left. + \sum_l \overline{\alpha_k \cdot \mathbf{T}_{kl} \cdot \alpha_l \cdot \mathbf{T}_{lk} \cdot \beta_k} \right], \quad (3.34) \end{aligned}$$

$$\overline{\mathbf{B}'} = \nu \left[\overline{\beta'_k} - \sum_l \overline{\beta'_k \cdot \mathbf{T}_{kl} \cdot \alpha_l} + \sum_l \overline{\beta'_k \cdot \mathbf{T}_{kl} \cdot \alpha_l \cdot \mathbf{T}_{lk} \cdot \alpha_k} \right]. \quad (3.35)$$

We have included all terms involving pair distribution functions up to the third order in the polarizabilities. Explicitly a term like $\nu \sum_l \overline{\alpha_k \cdot \mathbf{T}_{kl} \cdot \alpha_l}$ reads as:

$$\int \alpha(\theta) \cdot \mathbf{T}(\mathbf{R}, \mathbf{R}') \alpha(\theta') n_2(\mathbf{R}, \mathbf{R}', \theta, \theta') d\mathbf{R}' d\theta d\theta'.$$

4. THE GENERAL WAVE EQUATION AND THE EXTINCTION THEOREM

Introduction

In the equations:

$$\mathbf{P}(\mathbf{R}) = \mathbf{A} \cdot \mathbf{E}^L(\mathbf{R}) + \mathbf{B} : (\nabla \mathbf{E})^L(\mathbf{R}), \quad (4.1)$$

$$\mathbf{Q}(\mathbf{R}) = \mathbf{B}' \cdot \mathbf{E}^L(\mathbf{R}), \quad (4.2)$$

\mathbf{E}^L and $(\nabla \mathbf{E})^L$ depend on the external field and the polarizations everywhere in the medium. Thus they are relations between macroscopic quantities which have the form of integro-differential equations. It appears to be possible, however, to derive a differential equation for the moment densities \mathbf{P} and \mathbf{Q} .

The usual procedure to effectuate this (e.g. Rosenfield [23]) consists in assuming for \mathbf{P} a plane wave with constant amplitude and then to show that the internal field propagates in a similar way. An essential step in the derivation is the

elimination of the external field \mathbf{E}^e which is annihilated by an integral over the outer surface of the medium (extinction theorem).

Hoek [12], however, showed that for an isotropic medium without optical activity a more fundamental treatment is possible, which consists in first deriving the wave equation and then proving the extinction theorem without specifying the wave motion.

For optically active media Hoek returns again to the first-mentioned procedure, which is also followed by authors dealing with anisotropic media (Darwin [11], Mazur *et al.* [21–22]).

We will show that Hoek's method can be generalized for an anisotropic as well as optically active medium. Without specifying the type of wave motion we will derive a differential equation for the polarization density \mathbf{P} . With the aid of this equation the extinction theorem, which is no longer necessary for deriving the wave equation, follows.

4.1. The differential equation for an arbitrary wave in an anisotropic optically active medium

In the equations (4.1) and (4.2):

$$E_{\alpha}^L(\mathbf{R}) = E_{\alpha}^e(\mathbf{R}) + \int_{0(R)}^V \{(\nabla_{\alpha} \nabla_{\beta} + k^2 U_{\alpha\beta}) Y(\mathbf{R}, \mathbf{R}')\} P_{\beta}(\mathbf{R}') d\mathbf{R}' + \int_{0(R)}^V \{(\nabla_{\alpha} \nabla_{\beta} + k^2 U_{\alpha\beta}) \nabla'_{\gamma} Y(\mathbf{R}, \mathbf{R}')\} Q_{\beta\gamma}(\mathbf{R}') d\mathbf{R}', \quad (4.3)$$

$$(\nabla_{\gamma} E_{\beta})^L(\mathbf{R}) = \nabla_{\gamma} E_{\beta}^e(\mathbf{R}) + \int_{0(R)}^V \{(\nabla_{\beta} \nabla_{\delta} + k^2 U_{\beta\delta}) \nabla_{\gamma} Y(\mathbf{R}, \mathbf{R}')\} P_{\delta}(\mathbf{R}') d\mathbf{R}'; \quad (4.4)$$

∇'_{γ} means a differentiation at \mathbf{R}' , and ∇_{γ} at \mathbf{R} . V denotes the volume of the medium, from which $0(R)$, a small sphere centred at \mathbf{R} , is excluded. After the integrations the radius of this small sphere is reduced to zero.

$$Y(\mathbf{R}, \mathbf{R}') = \frac{1}{4\pi} \frac{\exp(-ik|\mathbf{R}' - \mathbf{R}|)}{|\mathbf{R}' - \mathbf{R}|}. \quad (4.5)$$

As products of third-order polarizabilities are always neglected we can combine (4.2) with (4.1):

$$\mathbf{Q}(\mathbf{R}) = \mathbf{B}' \cdot \mathbf{A}^{-1} \cdot \mathbf{P}(\mathbf{R}). \quad (4.6)$$

We need a number of formulae which are obtained through integration by parts:

$$\int_{0(R)}^V \{\nabla'_{\gamma} Y(\mathbf{R}, \mathbf{R}')\} P_{\delta}(\mathbf{R}') d\mathbf{R}' = S_{\gamma\delta}^{(1)} - \int_{0(R)}^V Y(\mathbf{R}, \mathbf{R}') \nabla'_{\gamma} P_{\delta}(\mathbf{R}') d\mathbf{R}', \quad (4.7)$$

$$\int_{0(R)}^V \{\nabla'_{\beta} \nabla'_{\gamma} Y(\mathbf{R}, \mathbf{R}')\} P_{\delta}(\mathbf{R}') d\mathbf{R}' = S_{\beta\gamma\delta}^{(2)} + \frac{1}{3} \delta_{\beta\gamma} P_{\delta}(\mathbf{R}) + \int_{0(R)}^V Y(\mathbf{R}, \mathbf{R}') \nabla'_{\beta} \nabla'_{\gamma} P_{\delta}(\mathbf{R}') d\mathbf{R}', \quad (4.8)$$

$$\int_{0(R)}^V \{\nabla'_{\alpha} \nabla'_{\beta} \nabla'_{\gamma} Y(\mathbf{R}, \mathbf{R}')\} P_{\delta}(\mathbf{R}') d\mathbf{R}' = S_{\alpha\beta\gamma\delta}^{(3)} - \frac{1}{5} (\delta_{\beta\gamma} \nabla_{\alpha} + \text{cycl.}) P_{\delta}(\mathbf{R}) - \int_{0(R)}^V Y(\mathbf{R}, \mathbf{R}') \nabla'_{\alpha} \nabla'_{\beta} \nabla'_{\gamma} P_{\delta}(\mathbf{R}') d\mathbf{R}'. \quad (4.9)$$

The surface integrals over the outer boundary Σ with normal unit vectors \mathbf{u} are:

$$S_{\gamma\delta}^{(1)} = \int_{\Sigma} Y(\mathbf{R}, \mathbf{R}') u_{\gamma} P_{\delta}(\mathbf{R}') dS, \quad (4.10)$$

$$S_{\beta\gamma\delta}^{(2)} = \int_{\Sigma} \{\nabla'_{\beta} Y(\mathbf{R}, \mathbf{R}')\} u_{\gamma} P_{\delta}(\mathbf{R}') dS - \int_{\Sigma} Y(\mathbf{R}, \mathbf{R}') u_{\beta} \nabla'_{\gamma} P_{\delta}(\mathbf{R}') dS, \quad (4.11)$$

$$S_{\alpha\beta\gamma\delta}^{(3)} = \int_{\Sigma} \{\nabla'_{\alpha} \nabla'_{\beta} Y(\mathbf{R}, \mathbf{R}')\} u_{\gamma} P_{\delta}(\mathbf{R}') dS - \int_{\Sigma} \{\nabla'_{\alpha} Y(\mathbf{R}, \mathbf{R}')\} u_{\beta} \nabla'_{\gamma} P_{\delta}(\mathbf{R}') dS \\ + \int_{\Sigma} Y(\mathbf{R}, \mathbf{R}') u_{\alpha} \nabla'_{\beta} \nabla'_{\gamma} P_{\delta}(\mathbf{R}') dS. \quad (4.12)$$

With these equations (4.1) can be reduced to:

$$\mathfrak{P}_1(\mathbf{R}) + \mathfrak{C}(\mathbf{R}) + \mathfrak{S}_1(\mathbf{R}) + \int_{0(R)}^V Y(\mathbf{R}, \mathbf{R}') \mathfrak{P}_2(\mathbf{R}') d\mathbf{R}' = 0. \quad (4.13)$$

The following abbreviations are used:

$$\mathfrak{P}_1(\mathbf{R}) = P_{\alpha}(\mathbf{R}) - \frac{1}{3} A_{\alpha\beta} P_{\beta}(\mathbf{R}) + \frac{1}{5} A_{\alpha\beta} B'_{\gamma\epsilon\delta} (A^{-1})_{\epsilon\mu} (\delta_{\beta\gamma} \nabla_{\delta} + \text{cycl.}) P_{\mu}(\mathbf{R}) \\ - \frac{1}{5} B_{\alpha\beta\delta} (\delta_{\beta\gamma} \nabla_{\delta} + \text{cycl.}) P_{\gamma}(\mathbf{R}), \quad (4.14)$$

$$\mathfrak{C}(\mathbf{R}) = -A_{\alpha\beta} E_{\beta}^e(\mathbf{R}) - B_{\alpha\beta\gamma} \nabla_{\gamma} E_{\beta}^e(\mathbf{R}), \quad (4.15)$$

$$\mathfrak{S}_1(\mathbf{R}) = -A_{\alpha\beta} S_{\beta\gamma\gamma}^{(2)} - A_{\alpha\beta} B'_{\gamma\epsilon\delta} (A^{-1})_{\epsilon\mu} \{S_{\beta\gamma\delta\mu}^{(3)} + k^2 \delta_{\beta\gamma} S_{\delta\mu}^{(1)}\} \\ + B_{\alpha\beta\delta} \{S_{\beta\gamma\delta\gamma}^{(3)} + k^2 \delta_{\beta\gamma} S_{\delta\gamma}^{(1)}\}, \quad (4.16)$$

$$\mathfrak{P}_2(\mathbf{R}') = -A_{\alpha\beta} \{\nabla'_{\beta} \nabla'_{\gamma} + k^2 U_{\beta\gamma}\} P_{\gamma}(\mathbf{R}') \\ + A_{\alpha\beta} B'_{\gamma\epsilon\delta} (A^{-1})_{\epsilon\mu} \{\nabla'_{\beta} \nabla'_{\gamma} + k^2 U_{\beta\gamma}\} \nabla'_{\delta} P_{\mu}(\mathbf{R}') \\ - B_{\alpha\beta\delta} \{\nabla'_{\beta} \nabla'_{\gamma} + k^2 U_{\beta\gamma}\} \nabla'_{\delta} P_{\gamma}(\mathbf{R}'). \quad (4.17)$$

Applying to equation (4.13) the operator $(\Delta + k^2)$ leads to:

$$(\Delta + k^2) \mathfrak{P}_1(\mathbf{R}) - \mathfrak{P}_2(\mathbf{R}) = 0, \quad (4.18)$$

since this operator annihilates the external field and its derivatives and also the integrals over the outer surface of the medium. At the same time use is made of:

$$(\Delta + k^2) \int_{0(R)}^V Y(\mathbf{R}, \mathbf{R}') \mathfrak{P}_2(\mathbf{R}') d\mathbf{R}' = -\mathfrak{P}_2(\mathbf{R}) \quad (4.19)$$

(see Hoek [12], Appendix).

Substituting the expressions for \mathfrak{P}_1 and \mathfrak{P}_2 , the wave equation can be written as:

$$(\Delta + k^2) \{P_{\alpha}(\mathbf{R}) - \frac{1}{3} A_{\alpha\beta} P_{\beta}(\mathbf{R}) + \frac{1}{5} A_{\alpha\beta} B'_{\gamma\epsilon\delta} (A^{-1})_{\epsilon\mu} (\delta_{\beta\gamma} \nabla_{\delta} + \text{cycl.}) P_{\mu}(\mathbf{R}) \\ - \frac{1}{5} B_{\alpha\beta\delta} (\delta_{\beta\gamma} \nabla_{\delta} + \text{cycl.}) P_{\gamma}(\mathbf{R})\} \\ + A_{\alpha\beta} \{\nabla_{\beta} \nabla_{\gamma} + k^2 U_{\beta\gamma}\} P_{\gamma}(\mathbf{R}) \\ - A_{\alpha\beta} B'_{\gamma\epsilon\delta} (A^{-1})_{\epsilon\mu} \{\nabla_{\beta} \nabla_{\gamma} + k^2 U_{\beta\gamma}\} \nabla_{\delta} P_{\mu}(\mathbf{R}) \\ + B_{\alpha\beta\delta} \{\nabla_{\beta} \nabla_{\gamma} + k^2 U_{\beta\gamma}\} \nabla_{\delta} P_{\gamma}(\mathbf{R}) = 0. \quad (4.20)$$

For the general case of an anisotropic and optically active medium this is a rather intricate equation. In § 5 this equation will be applied to the case of an isotropic optically active medium.

4.2. Extinction theorem

The extinction theorem can be proved by substituting $(\Delta + k^2) \mathfrak{P}_1(\mathbf{R}')$ for $\mathfrak{P}_2(\mathbf{R}')$ under the integral sign of equation (4.13). By application of Green's

theorem, the integral can be reduced according to:

$$\begin{aligned}
 & \int_{0(R)}^V Y(\mathbf{R}, \mathbf{R}') (\Delta + k^2) \mathfrak{P}_1(\mathbf{R}') \\
 &= \int_{0(R)}^V [Y(\mathbf{R}, \mathbf{R}') \Delta \mathfrak{P}_1(\mathbf{R}') - \{\Delta Y(\mathbf{R}, \mathbf{R}')\} \mathfrak{P}_1(\mathbf{R}')] d\mathbf{R}' \\
 &= \int_{\Sigma} \left[Y(\mathbf{R}, \mathbf{R}') \frac{\partial \mathfrak{P}_1(\mathbf{R}')}{\partial \eta} - \left\{ \frac{\partial Y(\mathbf{R}, \mathbf{R}')}{\partial \eta} \right\} \mathfrak{P}_1(\mathbf{R}') \right] dS \\
 &\quad - \int_{s(R)} \left[Y(\mathbf{R}, \mathbf{R}') \frac{\partial \mathfrak{P}_1(\mathbf{R}')}{\partial \eta} - \left\{ \frac{\partial Y(\mathbf{R}, \mathbf{R}')}{\partial \eta} \right\} \mathfrak{P}_1(\mathbf{R}') \right] dS. \quad (4.21)
 \end{aligned}$$

The surface integral over the small sphere is equal to $\mathfrak{P}_1(\mathbf{R})$. The integral over the outer surface is abbreviated by $\mathfrak{S}_2(\mathbf{R})$. $d\eta$ is a line element of the outward normal in a point of the surface in \mathbf{R}' -space (\mathbf{R} is to be regarded as constant).

Substituting this result in equation (4.13) leads to:

$$\mathfrak{C}(\mathbf{R}) + \mathfrak{S}_1(\mathbf{R}) + \mathfrak{S}_2(\mathbf{R}) = 0, \quad (4.22)$$

which is the mathematical formulation of the extinction theorem.

5. ISOTROPIC MEDIA

5.1. Wave equation for an isotropic medium

In the case of isotropy the tensor \mathbf{A} becomes the unit tensor multiplied by a scalar A_0 ; \mathbf{B} and \mathbf{B}' are reduced to the permutation tensor multiplied by constants B_0 and B'_0 .

$$\bar{A}_{\alpha\beta} = A_0 U_{\alpha\beta}, \quad (5.1)$$

$$\bar{B}_{\alpha\beta\gamma} = B_0 [\alpha\beta\gamma], \quad (5.2)$$

$$\bar{B}'_{\alpha\beta\gamma} = B'_0 [\alpha\beta\gamma]. \quad (5.3)$$

If (5.3) is substituted in (4.2) it follows that:

$$Q_{\alpha\gamma} = -Q_{\gamma\alpha} \text{ and } Q_{\alpha\alpha} = 0. \quad (5.4)$$

This means that in an isotropic medium the quadrupole moment, which depends on the symmetric part of \mathbf{Q} , vanishes (§2.4).

Substitution of (5.1), (5.2) and (5.3) in (4.20) yields:

$$(1 - \frac{1}{3}A_0)(\Delta + k^2)P_\alpha + A_0\{\nabla_\alpha \nabla_\beta + k^2 U_{\alpha\beta}\}P_\beta + (B_0 - B'_0)k^2[\alpha\beta\gamma]\nabla_\gamma P_\beta = 0. \quad (5.5)$$

Multiplying (5.5) with ∇_α and summing over α gives:

$$(1 + \frac{2}{3}A_0)(\Delta + k^2)\nabla_\alpha P_\alpha = 0. \quad (5.6)$$

As \mathbf{P} does not satisfy the same wave equation as \mathbf{E}^c equation (5.6) implies that

$$\nabla_\alpha P_\alpha = 0, \quad (5.7)$$

if the assumption $A_0 \neq -\frac{3}{2}$ holds.

Equation (5.7) simplifies (5.5) to:

$$\Delta P_\alpha + k^2 \frac{1 + \frac{2}{3}A_0}{1 - \frac{1}{3}A_0} P_\alpha + k^2 \frac{B_0 - B'_0}{1 - \frac{1}{3}A_0} [\alpha\beta\gamma]\nabla_\gamma P_\beta = 0. \quad (5.8)$$

5.2. Calculation of the rotatory power. Method I

The conventional way of deriving a formula for the rotatory power is to split up the linearly polarized beam of light in two circularly polarized waves. This point of view is arrived at by looking for solutions of (5.8) which at the same time satisfy:

$$(\Delta + n^2 k^2)\mathbf{P} = 0. \quad (5.9)$$

Substituted in (5.8) it follows that :

$$\left(n^2 - \frac{1 + \frac{2}{3}A_0}{1 - \frac{1}{3}A_0}\right) \mathbf{P} + \frac{B_0 - B'_0}{1 - \frac{1}{3}A_0} \nabla \times \mathbf{P} = 0. \quad (5.10)$$

Applying the operator $\nabla \times$ to this equation and using :

$$\nabla \times \nabla \times \mathbf{P} = \nabla \nabla \cdot \mathbf{P} - \Delta \mathbf{P} = -\Delta \mathbf{P} = n^2 k^2 \mathbf{P}, \quad (5.11)$$

it follows :

$$\left(n^2 - \frac{1 + \frac{2}{3}A_0}{1 - \frac{1}{3}A_0}\right) \nabla \times \mathbf{P} + n^2 k^2 \frac{B_0 - B'_0}{1 - \frac{1}{3}A_0} \mathbf{P} = 0. \quad (5.12)$$

From the equations (5.10) and (5.12) it follows that :

$$\left(n^2 - \frac{1 + \frac{2}{3}A_0}{1 - \frac{1}{3}A_0}\right) = \pm \frac{B_0 - B'_0}{1 - \frac{1}{3}A_0} nk, \quad (5.13)$$

with the corresponding solutions :

$$\mathbf{P} \pm \frac{1}{nk} \nabla \times \mathbf{P} = 0. \quad (5.14)$$

The meaning of this result can perhaps best be illustrated by considering a plane wave travelling in the 3-direction :

$$\mathbf{P} = \mathbf{P}_0 \exp(-inkr_3). \quad (5.15)$$

In components (5.14) yields :

$$P_1 \pm iP_2 = 0. \quad (5.16)$$

With a right-handed choice of axes the + sign refers to a right-handed, the - sign to a left-handed circularly polarized wave. Calling the roots of (5.13) corresponding to the upper or lower sign n_+ , n_- :

$$n_+ - n_- = \frac{B_0 - B'_0}{1 - \frac{1}{3}A_0} k. \quad (5.17)$$

The rotation of the plane of polarization follows from Fresnel's formula :

$$\chi = \frac{\pi}{\lambda_{\text{vac}}} (n_- - n_+) \quad (5.18)$$

which becomes :

$$\chi = \frac{k^2}{2} \frac{B'_0 - B_0}{1 - \frac{1}{3}A_0}. \quad (5.19)$$

The right-hand side of (5.13) is very small with respect to the other terms in the equation. For example, a rotation of 1 radian/cm implies that

$$(n_- - n_+) \quad \text{or} \quad \frac{B'_0 - B_0}{1 - \frac{1}{3}A_0} k$$

is of the order of magnitude of 10^{-5} , whereas n^2 is about 2. Therefore to a good approximation :

$$n^2 = \frac{1 + \frac{2}{3}A_0}{1 - \frac{1}{3}A_0} \quad \text{or} \quad \frac{1}{1 - \frac{1}{3}A_0} = \frac{n^2 + 2}{3}. \quad (5.20)$$

Substitution in (5.19) yields :

$$\chi = \frac{k^2}{2} \left(\frac{n^2 + 2}{3} \right) (B'_0 - B_0). \quad (5.21)$$

This equation has the same appearance as Hoek's final formula. It also contains the factor $(n^2 + 2)/3$ to the first power. The difference is that our constants B_0 and B'_0 incorporate the reaction field and correlation effects. Given our model equation (5.21) is in principle exact, since B_0 and B'_0 can be calculated to any desired accuracy.

Although we have not explicitly dealt with mixtures it will be obvious how the present treatment can be extended to systems containing different molecules.

5.3. Calculation of the rotatory power. Method II

It may be of some interest to consider also other solutions of equation (5.8) which more closely correspond to what happens in actual polarimetry. We introduce as a trial solution a plane wave, again travelling in the 3-direction but having a real amplitude which may also depend on r_3 ('linearly' polarized light with rotating plane of polarization):

$$\mathbf{P}(r_3) = \mathbf{P}_0(r_3) \exp(-iknr_3). \quad (5.22)$$

Writing \mathbf{u} for the unit vector in the 3-direction, the equation $\nabla \cdot \mathbf{P} = 0$, yields:

$$\mathbf{u} \cdot \mathbf{P}'_0 - ikn\mathbf{u} \cdot \mathbf{P}_0 = 0. \quad (5.23)$$

Since \mathbf{P}_0 and \mathbf{P}'_0 are real it follows that $\mathbf{u} \cdot \mathbf{P}_0 = 0$, which implies that we have a transverse wave.

With the abbreviations:

$$\bar{n}^2 = \frac{1 + \frac{2}{3}A_0}{1 - \frac{1}{3}A_0} \quad \text{and} \quad \gamma = \frac{1}{2} \frac{B_0 - B'_0}{1 - \frac{1}{3}A_0} k^2, \quad (5.24)$$

the wave equation becomes:

$$(\Delta + k^2\bar{n}^2)\mathbf{P} - 2\gamma\nabla \times \mathbf{P} = 0. \quad (5.25)$$

Substituting (5.22) in (5.25) yields:

$$\mathbf{P}_0'' - 2ikn\mathbf{P}'_0 + k^2(\bar{n}^2 - n^2)\mathbf{P}_0 + 2ikn\gamma\mathbf{u} \times \mathbf{P}_0 - 2\gamma\mathbf{u} \times \mathbf{P}'_0 = 0. \quad (5.26)$$

Writing the real and imaginary parts of this equation gives:

$$\mathbf{P}_0'' + k^2(\bar{n}^2 - n^2)\mathbf{P}_0 - 2\gamma\mathbf{u} \times \mathbf{P}'_0 = 0, \quad (5.27)$$

$$\mathbf{P}_0 - \gamma\mathbf{u} \times \mathbf{P}_0 = 0. \quad (5.28)$$

From these two equations \mathbf{P}_0 and the value of n can be derived. Scalar multiplication of (5.28) with \mathbf{P}_0 gives:

$$\mathbf{P}_0 \cdot \mathbf{P}'_0 = 0, \quad (5.29)$$

which implies that the absolute length of the vector \mathbf{P}_0 is constant. It is easily shown that the solution of (5.28) and (5.29) is:

$$(P_0)_1 = |P_0| \cos(\gamma r_3 + \psi), \quad (5.30)$$

$$(P_0)_2 = |P_0| \sin(\gamma r_3 + \psi), \quad (5.31)$$

This means that the angle χ (in radians/cm) over which the vector \mathbf{P}_0 ('plane of polarization') has rotated to the right is:

$$\chi = -\gamma, \quad (5.32)$$

which is the same result as (5.19), as it should be of course.

Differentiation of equation (5.28) together with this equation yields:

$$\mathbf{P}_0'' + \gamma^2\mathbf{P}_0 = 0. \quad (5.33)$$

On the other hand, the differentiated equation (5.28) together with (5.27) give :

$$\mathbf{P}_0'' + k^2(n^2 - \bar{n}^2)\mathbf{P}_0 = 0. \quad (5.34)$$

These two equations imply that :

$$n^2 = \bar{n}^2 + \frac{1}{k^2} \gamma^2. \quad (5.35)$$

For all practical purposes $n = \bar{n}$.

5.4. Limitations

It may be useful to recapitulate at this point the main characteristics of our model and to discuss its limitations. We consider the medium as an assembly of identical almost spherical molecules each of which is characterized by polarizability tensors α , β and β' . An arbitrarily selected molecule has a position and orientation which are correlated with positions and orientations of other molecules within a sphere, the correlation sphere, about the selected molecule. With molecules outside this sphere no correlations have to be taken account of. This model of course is only of limited applicability.

A first limitation consists in the neglect of the dependence of polarizability terms on the density of the medium (Jansen-Mazur effect). The influence of this effect on the polarizability densities \mathbf{B} and \mathbf{B}' has not yet been studied. In a classical picture of the polarizability this effect is due to anharmonically bound electrons. Anharmonicity, however, is important in the one-electron model for optically active molecules (Condon *et al.* [6]). It consists of an anisotropic harmonic oscillator with an added cubic term in the potential energy.

Perhaps more serious is the deviation from the spherical shape. Here too, it is difficult to estimate the error introduced by our assumptions without explicit calculations. This point could be very important in the case of macromolecules, but on the other hand, phenomenologically the optical properties of systems with large molecules do not deviate essentially from systems with small molecules.

A drawback of our model is that in the final formula \mathbf{B} and \mathbf{B}' occur in the combination $B_0 - B'_0$, which in our derivation of this formula is more or less fortuitous. In other derivations based on simpler models (Born [3], Kooy [4]) or in some macroscopic derivations (Ramachandran and Ramaseshan [26]) optical activity is described by one second-order pseudo tensor (gyration tensor), which is not necessarily built up from two third-order tensors.

Although the transition to an isotropic medium has not been made until § 5, the general formulae which have been given before should not be applied to an anisotropic medium without caution. For the molecular distribution functions were supposed to depend on the distance between the molecules and not on the direction of the line connecting their centres.

5.5. Illustrations

As a first illustration we will derive the expression for the optical activity of a molecule represented by coupled anisotropic polarizabilities. This model has been studied extensively by Born [3], Kuhn and Freudenberg [2], Kooy [4] and Kirkwood [5]. To this model we can apply equation (3.34) neglecting all β and β' -tensors and considering a molecule as an assembly of almost spherical units with anisotropic polarizabilities α , interacting through dipole-dipole forces. The fact that the units constitute an optically active molecule shows up in a strong

correlation between positions and orientations of the units. In this description the molecule may be rigid as well as flexible. Neglecting correlations between molecules, equation (3.34) applied to the present model yields:

$$B_0 = -\nu \sum_{k,l=1}^j \overline{\alpha_k \cdot \mathbf{T}_{kl} \mathbf{R}_{lk} \cdot \alpha_l}, \quad (5.36)$$

where j is the number of units in a molecule and ν is the number of molecules in 1 cm^3 . This equation can be simplified by assuming that the polarizabilities are linear along the unit vectors \mathbf{b}_k and \mathbf{b}_l :

$$\alpha_k = \sigma_k \mathbf{b}_k \mathbf{b}_k, \quad (5.37)$$

$$\alpha_l = \sigma_l \mathbf{b}_l \mathbf{b}_l. \quad (5.38)$$

Introducing (cf. Looyenga [27]):

$$S_{kl} = \frac{1}{4\pi r_{lk}^5} \{3(\mathbf{b}_k \cdot \mathbf{R}_{lk})(\mathbf{b}_l \cdot \mathbf{R}_{lk}) - R_{lk}^2(\mathbf{b}_l \cdot \mathbf{b}_k)\}, \quad (5.39)$$

$$D_{kl} = \overline{\mathbf{b}_k \mathbf{b}_l \mathbf{R}_{lk}} = \frac{1}{6}[\mathbf{b}_k \times \mathbf{b}_l] \cdot \mathbf{R}_{lk}, \quad (5.40)$$

we find:

$$B_0 = -\nu \sum_{k,l=1}^j \sigma_k \sigma_l S_{kl} D_{kl}. \quad (5.41)$$

In molecules where all groups attached to an asymmetric carbon atom have axial symmetry about the bond joining them to the asymmetric centre, these pairwise interactions contribute nothing to the optical activity (Kauzmann and Eyring [28], Kauzmann *et al.* [29]). In that case higher approximations of equation (3.34) should be used.

As a second illustration we will for a simple case derive an approximation to the reaction field. Let us omit the correlation between the particles except that they can be approximated as hard spheres which cannot approach more closely than a molecular diameter. In addition we will assume that the α polarizabilities are isotropic. From equation (3.34) it follows:

$$\begin{aligned} \bar{B}_{\alpha\beta\gamma} = & \nu\beta_0[\alpha\beta\gamma] - \nu \sum_l \alpha_0^2 \overline{T_{\alpha\beta}^{(kl)} R_{\gamma}^{(lk)}} \\ & - \nu \sum_l \alpha_0 \overline{\nabla_{\epsilon}^{(l)} T_{\alpha\delta}^{(kl)} R_{\gamma}^{(lk)}} [\delta\beta\epsilon] \beta_0' \\ & - \nu \sum_l \beta_0 [\alpha\delta\epsilon] \overline{\nabla_{\epsilon}^{(k)} T_{\delta\beta}^{(kl)} R_{\gamma}^{(lk)}} \alpha_0 - \nu \sum_l \alpha_0 \overline{T_{\alpha\delta}^{(kl)}} [\delta\beta\gamma] \beta_0 \\ & + \nu \sum_l \alpha_0^2 \overline{T_{\alpha\delta}^{(kl)} T_{\delta\epsilon}^{(lk)}} [\epsilon\beta\gamma] \beta_0. \end{aligned} \quad (5.42)$$

The second and fifth term can easily be shown to vanish (see Appendix). The third is zero because the averaged fourth-order tensor is symmetric in the indices δ and ϵ , while the permutation tensor is antisymmetric in these indices. For similar reasons the fourth term is zero. The sixth term, which represents the first approximation to the reaction field does not vanish:

$$\overline{T_{\alpha\delta}^{(kl)} T_{\delta\epsilon}^{(lk)}} = \frac{1}{48\pi V} \frac{1}{a^3} \delta_{\alpha\epsilon}, \quad (5.43)$$

where V is the volume of the medium and a is the radius of a molecule (see Kirkwood [18]; Kirkwood's \mathbf{T} is 4π times the tensor \mathbf{T} used by us). Summing (5.43) over all particles and substituting in (5.42) yields:

$$\bar{B}_{\alpha\beta\gamma} = \nu\beta_0 \left\{ 1 + \frac{\alpha_0^2 \nu}{48\pi a^3} \right\} [\alpha\beta\gamma]. \quad (5.44)$$

Similarly (3.35) yields:

$$\bar{B}'_{\alpha\beta\gamma} = \nu\beta'_0 \left\{ 1 + \frac{\alpha_0^2\nu}{48\pi a^3} \right\} [\alpha\beta\gamma]. \quad (5.45)$$

Aslanian and Vol'kenshtein [30] also calculate the reaction field in order to study theoretically the influence of solvent on optical activity. They use a more specialized model than we do. This results in a correction term which has the same shape, but is less simple than ours.

APPENDIX

In § 3.3 it has been stated without proof that in a number of integrals a spherical region does not contribute to the value of these integrals. The integrals are:

$$I_1 = \nu^{-2} \int^V \mathbf{F}(\mathbf{R}, \mathbf{R}') n_2(\mathbf{R}, \mathbf{R}') \cdot \mathbf{P}(\mathbf{R}') d\mathbf{R}', \quad (A1)$$

$$I_2 = \nu^{-2} \int^V \mathbf{G}(\mathbf{R}, \mathbf{R}') n_2(\mathbf{R}, \mathbf{R}') : \mathbf{Q}(\mathbf{R}') d\mathbf{R}', \quad (A2)$$

$$I_3 = \nu^{-2} \int^V \nabla_R \mathbf{F}(\mathbf{R}, \mathbf{R}') \cdot \mathbf{P}(\mathbf{R}') d\mathbf{R}'. \quad (A3)$$

The radius of the sphere which has its centre at \mathbf{R} should be small with respect to the wavelength of light. Small means that if the integral over the spherical region is expanded in powers of k , terms with powers > 1 can be neglected.

In order to simplify the proof we assume that \mathbf{P} and \mathbf{Q} can be represented by plane waves:

$$\mathbf{P}(\mathbf{R}') = \mathbf{P}(\mathbf{R}) \exp \{ik\mathbf{n}(\mathbf{R} - \mathbf{R}')\}, \quad (A4)$$

$$\mathbf{Q}(\mathbf{R}') = \mathbf{Q}(\mathbf{R}) \exp \{ik\mathbf{n}(\mathbf{R} - \mathbf{R}')\}, \quad (A5)$$

where \mathbf{n} is n times the unit vector in the direction of the wave. n is the refractive index.

Expanding $\mathbf{F}(\mathbf{R}, \mathbf{R}') \cdot \mathbf{P}(\mathbf{R}')$ to the first power in k , yields:

$$F_{\alpha\beta}(0, r) P_\beta(r) = \frac{1}{4\pi} \left[\frac{1}{r^3} (3b_\alpha b_\beta - \delta_{\alpha\beta}) - ik \frac{n_\gamma}{r^2} (3b_\alpha b_\beta b_\gamma - \delta_{\alpha\beta} b_\gamma) \right] P_\beta(0), \quad (A6)$$

where \mathbf{b} is a unit vector pointing from \mathbf{R} to \mathbf{R}' and $r = |\mathbf{R}' - \mathbf{R}|$. If now we integrate over the polar angles θ and ϕ , the term independent of k and the term proportional to k vanish. The higher-order terms may be neglected according to our assumption.

Similarly for I_2 we develop $\mathbf{G}(\mathbf{R}, \mathbf{R}') : \mathbf{Q}(\mathbf{R}')$ which becomes:

$$G_{\alpha\beta\gamma}(0, r) Q_{\beta\gamma}(r) = \frac{1}{4\pi} \left[\frac{1}{r^4} \{ -15b_\alpha b_\beta b_\gamma + 3(b_\gamma \delta_{\alpha\beta} + b_\beta \delta_{\alpha\gamma} + b_\alpha \delta_{\beta\gamma}) \} \right. \\ \left. + \frac{ikn_\delta}{r^3} \{ 15b_\alpha b_\beta b_\gamma b_\delta - 3(b_\delta b_\gamma \delta_{\alpha\beta} + b_\delta b_\beta \delta_{\alpha\gamma} + b_\delta b_\alpha \delta_{\beta\gamma}) \} \right] Q_{\beta\gamma}(0). \quad (A7)$$

Again terms independent of k and proportional to k disappear after integration over a spherical shell. This result applies immediately to I_3 as:

$$\nabla_R \mathbf{F}(\mathbf{R}, \mathbf{R}') = -\mathbf{G}(\mathbf{R}, \mathbf{R}'). \quad (A8)$$

REFERENCES

- [1] KRAMERS, H. A., 1938, *Quantentheorie des Elektrons und der Strahlung* (Leipzig: Akad. Verlag) (German edition). 1957, *Quantum Mechanics* (Amsterdam: North-Holland Publishing Company) (English edition).
- [2] KUHN, W., and FREUDENBERG, K., 1936, *Hand- und Jahrbuch der chemischen Physik*, 8 III Leipzig (published before in 1932).
- [3] BORN, M., 1933, *Optik* (Berlin: Julius Springer Verlag); 1918, *Ann. Phys., Lpz.*, **55**, 177.
- [4] KOOY, J. M. J., 1936, Thesis, Leiden.
- [5] KIRKWOOD, J. G., 1937, *J. chem. Phys.*, **5**, 479.
- [6] CONDON, E. U., ALTAR, W., and EYRING, H., 1937, *J. chem. Phys.*, **5**, 753.
- [7] ROSENFELD, L., 1928, *Z. Phys.*, **52**, 161.
- [8] STRATTON, J. A., 1941, *Electromagnetic Theory* (New York: McGraw-Hill).
- [9] PHILLIPS, M., 1962, *Handbuch der Physik*, IV (Berlin: Springer Verlag).
- [10] ROSE, M. E., 1957, *Elementary Theory of Angular Momentum* (New York: Wiley).
- [11] DARWIN, C. G., 1924, *Trans. Camb. phil. Soc.*, **23**, 137.
- [12] HOEK, H., 1941, *Physica*, **8**, 209.
- [13] HOEK, H., 1939, Thesis, Leiden.
- [14] JEFFREYS, H., and JEFFREYS, B. S., 1956, *Methods of Mathematical Physics* (Cambridge University Press).
- [15] EYRING, H., WALTER, J., and KIMBALL, G. E., 1949, *Quantum Chemistry* (New York: Wiley).
- [16] HEITLER, W., 1954, *Quantum Theory of Radiation* (Oxford: Clarendon Press).
- [17] VOL'KENSHTEIN, M. V., 1950, *J. exp. theor. Phys.*, **20**, 342.
- [18] KIRKWOOD, J. G., 1936, *J. chem. Phys.*, **4**, 592.
- [19] YVON, J., 1937, *Act. Scient. Ind.*, No. 542, Fluctuations en Densité (I) (Paris: Hermann et Cie); 1937, *Ibid.*, No. 543, La Propagation et la Diffusion de la Lumière (II) (Paris: Hermann et Cie).
- [20] MAZUR, P., and JANSEN, L., 1955, *Physica*, **21**, 208; JANSEN, L., and MAZUR, P., 1955, *Physica*, **21**, 193.
- [21] MAZUR, P., and MANDEL, M., 1956, *Physica*, **22**, 289, 299.
- [22] MAZUR, P., and POSTMA, B. J., 1959, *Physica*, **25**, 251.
- [23] ROSENFELD, L., 1951, *Theory of Electrons* (Amsterdam: North-Holland Publishing Company).
- [24] LORENTZ, H. A., 1902, *Proc. Acad. Sci., Amst.*, 254; *Enc. math. Wiss.*, II, No. 1, 200; 1952, *Theory of Electrons* (New York: Dover Publications) (originally 1915).
- [25] BROWN, W. F., 1956, *Handbuch der Physik*, XVII (Berlin: Springer Verlag).
- [26] RAMACHANDRAN, G. N., and RAMASESHAN, S., 1961, *Handbuch der Physik*, XXV/1 (Berlin: Springer Verlag), Section 36.
- [27] LOOYENGA, H., 1955, Thesis, Leiden.
- [28] KAUFMANN, W., and EYRING, H., 1941, *J. chem. Phys.*, **9**, 41.
- [29] KAUFMANN, W., CLOUGH, F. B., and TOBIAS, I., 1961, *Tetrahedron*, **13**, 57.
- [30] ASLANIAN, V. M., and VOL'KENSHTEIN, M. V., 1959, *Opt. Spectry*, **7**, 132 (English translation).

Intermolecular vibrations of solid carbon dioxide

by S. H. WALMSLEY

William Ramsay and Ralph Forster Laboratories,
University College, University of London

and J. A. POPLE†

Basic Physics Division, National Physical Laboratory,
Teddington, Middlesex

(Received 25 February 1964)

The low-frequency lattice vibrations of solid carbon dioxide are calculated using an intermolecular force law between pairs of molecules based on a Lennard-Jones 6-12 potential and electric quadrupole interactions. For zero wave-vector, it is possible to separate motions into pseudo-translational and pseudo-rotational types. Results are compared with available data from infra-red and Raman spectroscopy, and the nature of the normal modes is described.

1. INTRODUCTION

The vibrations of molecular crystals may be broadly divided into an intramolecular class, closely related to the internal vibrations of individual molecules, and an intermolecular class consisting mainly of motions of molecules relative to each other. Some coupling between these two types occurs, but as the intermolecular kind are usually at lower frequencies (at least for small molecules), the motions may be separated as a first approximation. In such an approximation, intermolecular vibrations can be treated as motions of 'rigid' molecules interacting according to some prescribed force law as is common in statistical mechanical theories of liquids and gases. As some of the low-frequency crystal vibrations are amenable to study by infra-red and Raman spectroscopy, they are a potential source of information about intermolecular forces. The aim of this paper is to indicate how these frequencies may be calculated using a given force field (possibly derived from independent gaseous measurements) and general lattice dynamics of the type described by Born and Huang [1]. The theory is developed in terms of the carbon dioxide crystal as an example using a force field including the interaction of the electric quadrupole moments of the molecules [2, 3]. However, many features are easily extended to other crystals of symmetrical linear molecules. In the final section, the theory is used in a discussion of the experimental infra-red and Raman spectra of solid carbon dioxide.

† Present address : Department of Chemistry, Carnegie Institute of Technology, Pittsburgh 13, Pa., U.S.A.

2. THE INTERMOLECULAR POTENTIAL

In order to connect the crystal properties as closely as possible with molecular interactions in gases, we shall use the pair interaction hypothesis, according to which the total potential energy of an assembly of molecules in one particular configuration may be written as a sum of interaction energies between pairs,

$$U = \sum_{i < j} u_{ij}, \quad (2.1)$$

where u_{ij} depends only on the relative coordinates and directions of molecules i and j .

For axially symmetrical molecules, the pair interaction energy u_{12} can be expanded [2] in surface harmonics of the angles giving the molecular directions relative to the line joining the centres (figure 1). Thus if R is the distance between centres,

$$u(R, \theta_1, \phi_1, \theta_2, \phi_2) = \sum_{l_1=0}^{\infty} \sum_{l_2=0}^{\infty} \sum_m \zeta^{(l_1 l_2 : m)}(R) S_{l_1 m}(\theta_1, \phi_1) S_{l_2 m}(\theta_2, \phi_2), \quad (2.2)$$

where S_{lm} are surface harmonics:

$$S_{lm}(\theta, \phi) = \left[(2l+1) \frac{(l-|m|)!}{(l+|m|)!} \right]^{1/2} P_l^{|m|}(\cos \theta) \exp(im\phi) \quad (2.3)$$

and $\zeta^{(l_1 l_2 : m)}(R)$ are radial functions (zero if $|m| > l_1$ or $|m| > l_2$) specifying the various components. For molecules with a centre of symmetry such as carbon dioxide, only even values of l_1 and l_2 appear in (2.2).

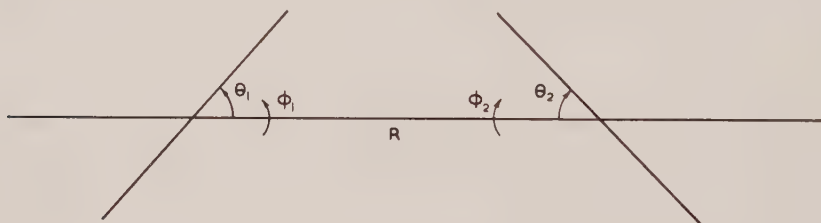


Figure 1. Angular coordinates of interacting axial molecules.

The leading term in the expansion (2.2) is $\zeta^{(00:0)}(R)$ and is independent of $\theta_1, \phi_1, \theta_2$ and ϕ_2 . It is the central force component of the total potential and can be approximated by a Lennard-Jones 6-12 potential of the form:

$$\zeta^{(00:0)}(R) = 4\epsilon \{ (R_0/R)^{12} - (R_0/R)^6 \}. \quad (2.4)$$

Higher terms in the expansion measure various kinds of orientational intermolecular effects. The terms involving $\zeta^{(20:0)}(R)$ specify certain features of the steric forces which determine molecular shape. They also include part of the directional dependence of the dispersive attractive forces.

The interaction between permanent electric quadrupole moments is particularly important for carbon dioxide molecules. This is described by the terms with $l_1 = l_2 = 2$ in the general expansion. If the quadrupole moment† is Θ , the ζ -functions are given by:

$$\frac{1}{6} \zeta^{(22:0)} = \frac{1}{4} \zeta^{(22:1)} = \zeta^{(22:2)} = \frac{1}{6} \Theta^2 R^{-5}. \quad (2.5)$$

† The quadrupole moment is defined by $\Theta = \sum_i e_i (z_i^2 - x_i^2)$ when z_i is measured along the molecular axis.

In the later sections of this paper, we shall use a total intermolecular potential consisting of a 6–12 central force part (equation (2.4)) together with the quadrupole interaction (2.5). Although other components are undoubtedly present, this type of potential does give a reasonably satisfactory description of the second virial data on gases and the dimensions and overall energy of the crystal (2.3). The methods used, however, can be easily applied to other potentials if further information becomes available.

The form in which the potential is expressed in (2.4) involves relative coordinates and is not suitable for calculations on crystals where a fixed coordinate system (related to crystal axes) is preferable. The surface harmonics may easily be expressed in terms of the vector components R_α of the intermolecular line and the direction cosines $\Lambda_\alpha^{(1)}$ and $\Lambda_\alpha^{(2)}$ of the two molecular axes. Tensor analysis gives (using the convention of implied summation over repeated suffixes):

$$\begin{aligned}
 S_{20}(\theta_1, \phi_1) &= \frac{1}{2}\sqrt{5}\Lambda_\alpha^{(1)}\Lambda_\gamma^{(1)}[3R_\alpha R_\gamma - R^2\delta_{\alpha\gamma}]R^{-2}, \\
 S_{20}(\theta_1, \phi_1)S_{20}(\theta_2, \phi_2) &= \frac{5}{4}\Lambda_\alpha^{(1)}\Lambda_\beta^{(2)}\Lambda_\gamma^{(1)}\Lambda_\delta^{(2)}[9R_\alpha R_\beta R_\gamma R_\delta - 3R^2R_\alpha R_\gamma \delta_{\beta\delta} \\
 &\quad - 3R^2R_\beta R_\delta \delta_{\alpha\gamma} + R^4\delta_{\alpha\gamma}\delta_{\beta\delta}]R^{-4}, \\
 S_{21}(\theta_1, \phi_1)S_{21}(\theta_2, \phi_2) + S_{2-1}(\theta_1, \phi_1)S_{2-1}(\theta_2, \phi_2) \\
 &= \frac{15}{2}\Lambda_\alpha^{(1)}\Lambda_\beta^{(2)}\Lambda_\gamma^{(1)}\Lambda_\delta^{(2)}[2R_\alpha R_\beta R_\gamma R_\delta - R^2R_\gamma R_\delta \delta_{\alpha\beta} - R^2R_\alpha R_\beta \delta_{\gamma\delta}]R^{-4}, \\
 S_{22}(\theta_1, \phi_1)S_{22}(\theta_2, \phi_2) + S_{2-2}(\theta_1, \phi_1)S_{2-2}(\theta_2, \phi_2) \\
 &= \frac{15}{4}\Lambda_\alpha^{(1)}\Lambda_\beta^{(2)}\Lambda_\gamma^{(1)}\Lambda_\delta^{(2)}[R_\alpha R_\beta R_\gamma R_\delta - 2R^2R_\gamma R_\delta \delta_{\alpha\beta} \\
 &\quad - 2R^2R_\alpha R_\beta \delta_{\gamma\delta} + R^2R_\alpha R_\gamma \delta_{\beta\delta} + R^2R_\beta R_\delta \delta_{\alpha\gamma} - R^4\delta_{\alpha\gamma}\delta_{\beta\delta} \\
 &\quad + 2R^4\delta_{\alpha\beta}\delta_{\gamma\delta}]R^{-4}. \tag{2.6}
 \end{aligned}$$

Substitution in the general expansion (2.2) with the ζ -functions (2.5) gives the full quadrupole–quadrupole interaction energy:

$$\begin{aligned}
 u_{\text{quadrupole}} &= (\Theta^2/4R^9)\Lambda_\alpha^{(1)}\Lambda_\beta^{(2)}\Lambda_\gamma^{(1)}\Lambda_\delta^{(2)}\left[105R_\alpha R_\beta R_\gamma R_\delta \right. \\
 &\quad \left. - 15 \sum_6 R^2R_\alpha R_\beta \delta_{\gamma\delta} + 3 \sum_3 R^4\delta_{\alpha\beta}\delta_{\gamma\delta} \right], \tag{2.7}
 \end{aligned}$$

where \sum_6 and \sum_3 indicate summation over six and three similar terms. This equation could be obtained more directly, but the derivation through (2.6) could be applied to other types of $\zeta^{(l_1 l_2; m)}(R)$ functions.

3. CRYSTAL STRUCTURE AND SYMMETRY ELEMENTS

Carbon dioxide crystals are cubic, belonging to the space group T_h^6 , with four molecules per unit cell [4–6]. They are centred at $(0, 0, 0)$, $(\frac{1}{2}, \frac{1}{2}, 0)$, $(0, \frac{1}{2}, \frac{1}{2})$ and $(\frac{1}{2}, 0, \frac{1}{2})$. The sets of translationally equivalent molecules associated with these positions will be labelled 1, 2, 3, 4 respectively. The orientations of the molecular axes in the unit cell are towards the body centres as illustrated in figure 2.

The symmetry elements that will be important are those of the space group which leaves the unit cell invariant, in this case T_h . There are four three-fold axes C_3 along the molecular directions, three two-fold screw axes C_2 parallel to the cubic axes together with the inversion operator i four S_6 axes and three glide planes σ . The character table for this group is given in table 1.

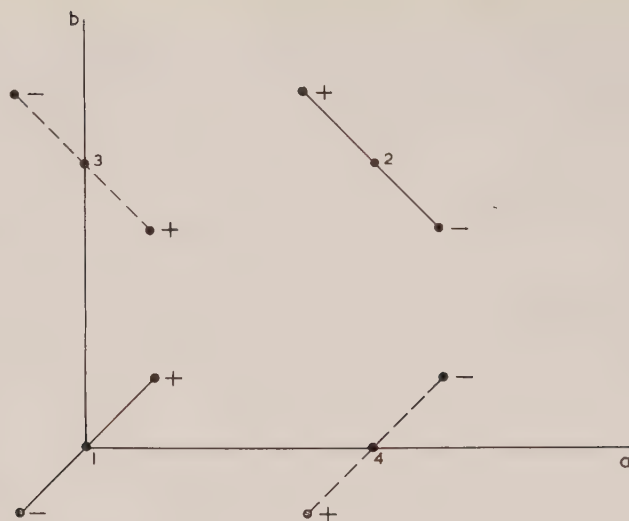


Figure 2. Geometry of CO_2 crystals (the centres of the molecules denoted by dotted lines lie half a cell dimension above the ab plane).

	E	$3C_2$	$4C_3$	$4C_3^2$	i	3σ	$4S_6^5$	$4S_6$
A_g	1	1	1	1	1	1	1	1
A_u	1	1	1	1	-1	-1	-1	-1
E_g	$\begin{Bmatrix} 1 \\ 1 \end{Bmatrix}$	$\begin{Bmatrix} 1 \\ 1 \end{Bmatrix}$	$\begin{Bmatrix} \omega \\ \omega^2 \end{Bmatrix}$	$\begin{Bmatrix} \omega^2 \\ \omega \end{Bmatrix}$	$\begin{Bmatrix} 1 \\ 1 \end{Bmatrix}$	$\begin{Bmatrix} 1 \\ 1 \end{Bmatrix}$	$\begin{Bmatrix} \omega \\ \omega^2 \end{Bmatrix}$	$\begin{Bmatrix} \omega^2 \\ \omega \end{Bmatrix}$
E_u	$\begin{Bmatrix} 1 \\ 1 \end{Bmatrix}$	$\begin{Bmatrix} 1 \\ 1 \end{Bmatrix}$	$\begin{Bmatrix} \omega \\ \omega^2 \end{Bmatrix}$	$\begin{Bmatrix} \omega^2 \\ \omega \end{Bmatrix}$	$\begin{Bmatrix} -1 \\ -1 \end{Bmatrix}$	$\begin{Bmatrix} -1 \\ -1 \end{Bmatrix}$	$\begin{Bmatrix} -\omega \\ -\omega^2 \end{Bmatrix}$	$\begin{Bmatrix} -\omega^2 \\ -\omega \end{Bmatrix}$
T_g	3	-1	0	0	3	-1	0	0
T_u	3	-1	0	0	-3	1	0	0

Table 1. Character table for T_h group

$$\left[\omega = \exp \left(\frac{2\pi i}{3} \right) \right].$$

The two-fold screw axes are chosen so that molecule 1 is carried into molecule 2 by a C_2 axis parallel to a , that is C_2^a . Similarly $1 \rightarrow 3$ under C_2^b and $1 \rightarrow 4$ under C_2^c .

4. DISPLACEMENT AND SYMMETRY COORDINATES

The positions of molecules in the crystal may be specified by the cartesian coordinates of their centres and the direction cosines of the molecular axes. In the vibration problem, we are only concerned with the dynamics of small displacements from equilibrium and appropriate incremental coordinates are convenient.

For the molecular centres, the displacement of the q th molecule in the p th cell will be denoted by $r_\alpha(p/q)$, ($\alpha = x, y, z$). The unit vector specifying the direction of this molecule will be denoted by:

$$\Lambda_\alpha\left(\frac{p}{q}\right) = \Lambda_\alpha^0\left(\frac{p}{q}\right) + \lambda_\alpha\left(\frac{p}{q}\right), \quad (4.1)$$

where Λ_α^0 is the equilibrium value and $\lambda_\alpha(p/q)$ is the displacement coordinate. Each molecule has only two orientation degrees of freedom because of the redundancy conditions:

$$\sum_\alpha \left[\Lambda_\alpha\left(\frac{p}{q}\right) \right]^2 = \sum_\alpha \left[\Lambda_\alpha^0\left(\frac{p}{q}\right) \right]^2 = 1. \quad (4.2)$$

It is convenient to transform these molecular coordinates to symmetry coordinates for the crystal space group. The first step is to form a set having irreducible symmetry with respect to lattice translations. These are given by expressions of the type:

$$\left. \begin{aligned} N^{-1/2} \sum_p \exp\{2\pi i \mathbf{k} \cdot \mathbf{R}(p)\} r_\alpha\left(\frac{p}{q}\right), \\ N^{-1/2} \sum_p \exp\{2\pi i \mathbf{k} \cdot \mathbf{R}(p)\} \lambda_\alpha\left(\frac{p}{q}\right), \end{aligned} \right\} \quad (4.3)$$

where N is the number of unit cells in the crystal, \mathbf{k} is a wave vector and $\mathbf{R}(p)$ the position vector of the centre of the p th cell.

Symmetry		Coordinate
S_1	A_u	$[(x_1 + x_2 - x_3 - x_4) + (y_1 - y_2 + y_3 - y_4) + (z_1 - z_2 - z_3 + z_4)]/\sqrt{12},$
S_2, S_3	E_u	$\left\{ \begin{aligned} &[-(x_1 + x_2 - x_3 - x_4) - (y_1 - y_2 + y_3 - y_4) + 2(z_1 - z_2 - z_3 + z_4)]/\sqrt{24}, \\ &[(x_1 + x_2 - x_3 - x_4) - (y_1 - y_2 + y_3 - y_4)]/\sqrt{8}, \end{aligned} \right.$
S_4, S_5, S_6	T_u	$\frac{1}{2}(x_1 - x_2 + x_3 - x_4), \frac{1}{2}(y_1 - y_2 - y_3 + y_4), \frac{1}{2}(z_1 + z_2 - z_3 - z_4),$
S_7, S_8, S_9	T_u	$\frac{1}{2}(x_1 - x_2 - x_3 + x_4), \frac{1}{2}(y_1 + y_2 - y_3 - y_4), \frac{1}{2}(z_1 - z_2 + z_3 - z_4),$
S_{10}, S_{11}, S_{12}	T_u	$\frac{1}{2}(x_1 + x_2 + x_3 + x_4), \frac{1}{2}(y_1 + y_2 + y_3 + y_4), \frac{1}{2}(z_1 + z_2 + z_3 + z_4),$
S_{13}, S_{14}	E_g	$\left\{ \begin{aligned} &[-(l_1 + l_2 - l_3 - l_4) - (m_1 - m_2 + m_3 - m_4) + 2(n_1 - n_2 - n_3 + n_4)]/\sqrt{24}, \\ &[(l_1 + l_2 - l_3 - l_4) - (m_1 - m_2 + m_3 - m_4)]/\sqrt{8}, \end{aligned} \right.$
S_{15}, S_{16}, S_{17}	T_g	$\left\{ \begin{aligned} &[-(l_1 - l_2 + l_3 - l_4) - (m_1 + m_2 - m_3 - m_4) + 2(n_1 + n_2 + n_3 + n_4)]/\sqrt{24}, \\ &[-(l_1 - l_2 - l_3 + l_4) + 2(m_1 + m_2 + m_3 + m_4) - (n_1 + n_2 - n_3 - n_4)]/\sqrt{24}, \\ &[2(l_1 + l_2 + l_3 + l_4) - (m_1 - m_2 - m_3 + m_4) - (n_1 - n_2 + n_3 - n_4)]/\sqrt{24}, \end{aligned} \right.$
S_{18}, S_{19}, S_{20}	T_g	$\left\{ \begin{aligned} &[(l_1 - l_2 + l_3 - l_4) - (m_1 + m_2 - m_3 - m_4)]/\sqrt{8}, \\ &[-(l_1 - l_2 - l_3 + l_4) + (n_1 + n_2 - n_3 - n_4)]/\sqrt{8}, \\ &[(m_1 - m_2 - m_3 + m_4) - (n_1 - n_2 + n_3 - n_4)]/\sqrt{8}, \end{aligned} \right.$
S_{21}, S_{22}, S_{23}	T_g^\dagger	$\left\{ \begin{aligned} &[(l_1 - l_2 + l_3 - l_4) + (m_1 + m_2 - m_3 - m_4) + (n_1 + n_2 + n_3 + n_4)]/\sqrt{12}, \\ &[(l_1 - l_2 - l_3 + l_4) + (m_1 + m_2 + m_3 + m_4) + (n_1 + n_2 - n_3 - n_4)]/\sqrt{12}, \\ &[(l_1 + l_2 + l_3 + l_4) + (m_1 - m_2 - m_3 + m_4) + (n_1 - n_2 + n_3 - n_4)]/\sqrt{12}, \end{aligned} \right.$
S_{24}	A_g^\dagger	$[(l_1 + l_2 - l_3 - l_4) + (m_1 - m_2 + m_3 - m_4) + (n_1 - n_2 - n_3 + n_4)]/\sqrt{12}.$

† Redundant coordinates.

Table 2. Symmetry coordinates for zero wave vector.

In this paper we are primarily concerned with those crystal vibrations which interact with long wavelength radiation in infra-red and Raman spectroscopy. These correspond to small values of \mathbf{k} . At $\mathbf{k} = 0$ the displacements in each cell

are identical and it then becomes possible to use the other elements of crystal symmetry to construct symmetry coordinates. In the following sections only the zero wave vector condition will be examined in detail. We therefore define the coordinates (4.3) with $\mathbf{k}=0$ as

$$\left. \begin{aligned} r_{\alpha}(q) &= N^{-1/2} \sum_p r_{\alpha} \left(\frac{p}{q} \right), \\ \lambda_{\alpha}(q) &= N^{-1/2} \sum_p \lambda_{\alpha} \left(\frac{p}{q} \right). \end{aligned} \right\} \quad (4.4)$$

The symmetry coordinates obtained by standard group theoretical methods [7] with the T_h character table are listed in table 2. Here symbols $x_1, y_1, \dots, l_1, m_1, \dots$ are used as shortened forms of $r_x(1), r_y(1), \dots, \lambda_x(1), \lambda_y(1), \dots$. It is evident that for $\mathbf{k}=0$, there is complete separation of pseudo-translational and pseudo-rotational motions into different symmetries. The transformation shown in the table will be written in the general form:

$$\left. \begin{aligned} S_i &= \sum_{\alpha, q} T'_{i, \alpha q} r_{\alpha}(q), \quad (i=1, \dots, 12), \\ S_i &= \sum_{\alpha, p} T''_{i, \alpha p} \lambda_{\alpha}(p), \quad (i=13, \dots, 24), \end{aligned} \right\} \quad (4.5)$$

where T' and T'' are 12×12 matrices.

Of the translational symmetry coordinates, the T_u set S_{10}, S_{11}, S_{12} represent uniform motion of the whole crystal and may be ignored. For the rotational coordinates, the redundancy conditions (4.2) become:

$$\left. \begin{aligned} 2(l_1 + m_1 + n_1) + (3/N)^{1/2}(l_1^2 + m_1^2 + n_1^2) &= 0, \\ 2(l_2 - m_2 - n_2) + (3/N)^{1/2}(l_2^2 + m_2^2 + n_2^2) &= 0, \\ 2(-l_3 + m_3 - n_3) + (3/N)^{1/2}(l_3^2 + m_3^2 + n_3^2) &= 0, \\ 2(-l_4 - m_4 + n_4) + (3/N)^{1/2}(l_4^2 + m_4^2 + n_4^2) &= 0. \end{aligned} \right\} \quad (4.6)$$

Clearly redundant coordinates are $(l_1 + m_1 + n_1)$, $(l_2 - m_2 - n_2)$, $(-l_3 + m_3 - n_3)$ and $(-l_4 - m_4 + n_4)$ which must be zero to first order. They span irreducible representations $A_g + T_g$ and give rise to the symmetry coordinates $S_{21}, S_{22}, S_{23}, S_{24}$ (table 2).

5. CRYSTAL DYNAMICS OF PSEUDO-TRANSLATIONAL MODES WITH ZERO WAVE VECTOR

The frequencies of pseudo-translational modes at $\mathbf{k}=0$ can be calculated from the dynamical equations for the symmetry coordinates $S_i (i=1, \dots, 9)$. These are not coupled to the rotational coordinates because of the different symmetries. If the potential energy U for small displacements with $\mathbf{k}=0$ is written:

$$2U = \sum_{ij=1}^{12} F_{ij} S_i S_j, \quad (5.1)$$

the angular frequencies ω are given by the roots of the 12×12 secular equation:

$$|F_{ij} - M\omega^2 \delta_{ij}| = 0, \quad (5.2)$$

where M is the mass of a molecule. This determinant will break into smaller blocks according to the symmetries listed in table 2. The three roots of (5.2)

arising from S_{10}, S_{11}, S_{12} will be zero corresponding to uniform translations of the whole lattice.

The force constants F_{ij} have to be related to derivatives of U with respect to the basic displacement coordinates $r_\alpha(p/q)$. Using (4.4) and (4.5) and noting that $T'_{i, \alpha q}$ is an orthogonal matrix, we obtain:

$$F_{ij} = \partial^2 U / \partial s_i \partial s_j = \sum_{\alpha \beta} \sum_{qq'} T'_{i, \alpha q} T'_{j, \beta q'} \sum_{p'} \left[\partial^2 U / \partial r_\alpha \left(\frac{p}{q} \right) \partial r_\beta \left(\frac{p'}{q'} \right) \right], \quad (5.3)$$

all derivatives being taken at the equilibrium configuration.

We next make the nearest neighbour approximation, according to which the derivatives in (5.3) are neglected unless $(p/q), (p'/q')$ are either identical or correspond to immediately adjacent molecules. For given p and q , this means that the sum over p' and q' contains only thirteen terms. Further, since the potential energy is unaffected by uniform translation of the lattice, the self force constants are given in terms of the interaction constants by:

$$\left[\partial^2 U / \partial r_\alpha \left(\frac{p}{q} \right) \partial r_\beta \left(\frac{p}{q} \right) \right] = - \sum_{p'q'}^* \left[\partial^2 U / \partial r_\alpha \left(\frac{p}{q} \right) \partial r_\beta \left(\frac{p'}{q'} \right) \right], \quad (5.4)$$

where \sum^* indicates that the term $p'=p, q'=q$ is omitted. (5.4) implies that $F_{ij}=0$ if i or j takes one of the values 10, 11, 12.

Each term on the right-hand side of (5.4) can be directed from the single pair interaction function u between molecules (p/q) and (p'/q') .

The various nearest neighbour force constants are themselves related by the symmetry of the lattice and can all be expressed in terms of the constants for one particular pair. We shall choose this pair as molecules 1 and 2 of figure 2 and write:

$$u_{xy} = \partial^2 u_{12} / \partial r_x \left(\frac{p}{1} \right) \partial r_y \left(\frac{p}{1} \right) \quad (5.5)$$

and similar expressions. Using (5.3), table 2 and lattice symmetry, we obtain:

$$\begin{aligned} F_{11} &= 8(u_{yy} + u_{zz} + 2u_{yz}), \\ F_{22} &= F_{33} = 8(u_{yy} + u_{zz} - u_{yz}), \\ F_{44} &= F_{55} = F_{66} = 8(u_{xx} + u_{yy}), \\ F_{77} &= F_{88} = F_{99} = 8(u_{xx} + u_{zz}), \\ F_{48} &= F_{67} = F_{59} = 8u_{yz}. \end{aligned} \quad (5.6)$$

All other F_{ij} ($i, j=1, \dots, 12$) vanish.

The derivatives of the potential u_{12} can now be evaluated using the combined 6-12 and quadrupole potentials given in equations (2.4) and (2.7). Writing (X, Y, Z) for the position vector of molecule 2, relative to molecule 1, and substituting appropriate direction cosines in (2.7) (from figure 2), we obtain,

$$\begin{aligned} u_{12} &= 4\epsilon[(R_0/R)^{12} - (R_0/R)^6] \\ &\quad + (\Theta^2/3R^9)[9X^4 - (Y^4 + Z^4) - 27X^2(Y^2 + Z^2) + 33Y^2Z^2 \\ &\quad \quad \quad + 10YZ(Y^2 + Z^2) - 60X^2YZ]. \end{aligned} \quad (5.7)$$

Differentiating twice and noting that $(X, Y, Z) = (\frac{1}{2}, \frac{1}{2}, 0)a_0$, it follows that:

$$\begin{aligned} u_{xx} &= (48\epsilon/a_0^2)[12(2R_0^2/a_0^2)^6 - 3(2R_0^2/a_0^2)^3] - 225\sqrt{2}(\Theta^2/a_0^7), \\ u_{yy} &= (48\epsilon/a_0^2)[12(2R_0^2/a_0^2)^6 - 3(2R_0^2/a_0^2)^3] + 95\sqrt{2}(\Theta^2/a_0^7), \\ u_{zz} &= (48\epsilon/a_0^2)[-2(2R_0^2/a_0^2)^6 + (2R_0^2/a_0^2)^3] + 130\sqrt{2}(\Theta^2/a_0^7), \\ u_{yz} &= 260\sqrt{2}(\Theta^2/a_0^7). \end{aligned} \quad (5.8)$$

Substitution in (5.6) gives the complete F_{ij} matrix. a_0 is the lattice constant.

6. CRYSTAL DYNAMICS OF PSEUDO-ROTATIONAL MODES WITH ZERO WAVE VECTOR

The frequencies of the pseudo-rotational modes with $\mathbf{k} = 0$ have to be obtained from derivatives of the potential energy U with respect to the angular coordinates $S_{13}, S_{14}, \dots, S_{24}$ listed in table 2. However, as mentioned earlier, these are not all independent and the general analysis must be modified to take this into account.

If we consider *unrestricted* variation of U for all values of l_1, \dots, n_4 , using a potential of the type (2.7) a small displacement expansion has the form:

$$U = \frac{1}{2} \sum_{i,j=13}^{24} F_{ij} S_i S_j + \sum_{i=21}^{24} D_i S_i. \quad (6.1)$$

There is no reason why the first derivatives D_i ($i = 21, \dots, 24$) should be zero in the equilibrium configuration, since the coordinates $S_{21}, S_{22}, S_{23}, S_{24}$ have to vanish to first order in real displacements.

Now we really require the expansion of U for restricted variation in which the coordinates S_{21}, \dots, S_{24} are determined by the redundancy conditions (4.6) which may be rewritten:

$$S_k = \sum_{pq=13}^{24} a_{kpq} S_p S_q = \sum_{pq=13}^{20} a_{kpq} S_p S_q + 0(S^4) \quad (k = 21, 22, 23, 24). \quad (6.2)$$

If these four relations are substituted in (6.1), the potential energy expansion can be written:

$$U = \frac{1}{2} \sum_{ij=13}^{20} G_{ij} S_i S_j, \quad (6.3)$$

where, by double differentiation of (6.1) and use of (6.2):

$$\begin{aligned} G_{ij} &= F_{ij} + \sum_k (\partial U / \partial S_k) (\partial^2 S_k / \partial S_i \partial S_j) \\ &= F_{ij} + 2 \sum_k D_k a_{ktij}. \end{aligned} \quad (6.4)$$

The calculation of the normal frequencies is now straight-forward. If I is the moment of inertia of a molecule about a line through the centre and perpendicular to the molecular axis, the angular frequencies ω are given by the roots of the 8×8 secular equation:

$$|G_{ij} - I\omega^2 \delta_{ij}| = 0. \quad (6.5)$$

Again this breaks up into smaller blocks corresponding to symmetries $E_g + 2T_g$.

The constants F_{ij} and D_k can be related to derivatives of U with respect to the basic angular displacement coordinates $\lambda_\alpha(p/q)$. From (4.4), (4.5) and (6.1),

we obtain :

$$\begin{aligned}
 D_k &= 2\partial U/\partial S_k = N^{1/2} \sum_{\alpha} \sum_q T''_{k, \alpha q} \left[\partial U/\partial \lambda_{\alpha} \left(\frac{p}{q} \right) \right], \\
 F_{ij} &= (\partial^2 U/\partial S_i \partial S_j) \text{ unrestricted} \\
 &= \sum_{\alpha\beta} \sum_{qq'} T''_{i, \alpha q} T''_{j, \beta q'} \sum_{p'} \left[\partial^2 U/\partial \lambda_{\alpha} \left(\frac{p}{q} \right) \partial \lambda_{\beta} \left(\frac{p'}{q'} \right) \right], \quad (6.6)
 \end{aligned}$$

all derivatives being taken at the equilibrium configuration.

As in the previous section, F_{ij} and D_k can be related (using the lattice symmetry) to potential energy derivatives for the molecular pair 1 and 2 in a particular cell. Using the quadrupole potential given by (2.4) and (2.7), the final results for the G_{ij} matrix elements are :

$$\begin{aligned}
 G_{13, 13} &= 68\sqrt{2}(\Theta^2/a_0^5), \\
 G_{15, 15} &= (548/3)\sqrt{2}(\Theta^2/a_0^5), \\
 G_{18, 18} &= 380\sqrt{2}(\Theta^2/a_0^5), \\
 G_{15, 18} &= 200\sqrt{(2/3)}(\Theta^2/a_0^5). \quad (6.7)
 \end{aligned}$$

Vibrational frequencies can then be evaluated from the secular equation (6.5).

7. DISCUSSION

In the previous sections we have dealt with the dynamics of zero wave vector vibrations using the Lennard-Jones potential function together with a quadrupole-quadrupole interaction. The three parameters involved, ϵ , r_0 and Θ now have to be given numerical values so that actual vibration frequencies can be calculated. The values chosen are :

$$\left. \begin{aligned}
 \Theta &= -4.1 \times 10^{-26} \text{ e.s.u.}, \\
 \epsilon &= 3.18 \times 10^{-14} \text{ ergs}, \\
 r_0 &= 3.72 \times 10^{-8} \text{ cm.}
 \end{aligned} \right\} \quad (7.1)$$

The quadrupole moment Θ is the value for the free molecule recently measured by Buckingham and Disch [8]. ϵ and r_0 are then obtained (using this Θ) from the observed heat of sublimation at 0°K and the corresponding lattice constant a_0 [2]. Calculated frequencies are listed in table 3 and compared with observations by infra-red and Raman spectroscopy.

Pseudo-translational modes			Pseudo-rotational modes		
Symmetry	Calculated	Observed	Symmetry	Calculated	Observed
T_u	74	68	E_g	35	64
E_u	77	—	T_g^g	48	77
A_u	94	—	T_g	88	112
T_u	113	114			

Table 3. Calculated and observed frequencies (in cm^{-1}) for carbon dioxide lattice vibrations.

Anderson [9] has measured the far infra-red spectrum of solid CO_2 and has found two bands at 114 and 68 cm^{-1} . As only transitions involving T_u vibrations are dipole-allowed in infra-red spectra, these are assigned to the two calculated T_u frequencies at 74 and 113 cm^{-1} . The agreement is good, but it should be noted that this part of the calculation is not very sensitive to the quadrupole interaction term. If the quadrupole moments are neglected completely and ϵ and r_0 re-chosen to fit the heat of sublimation and the lattice constant, the calculated infra-red frequencies are 77 and 112 cm^{-1} .

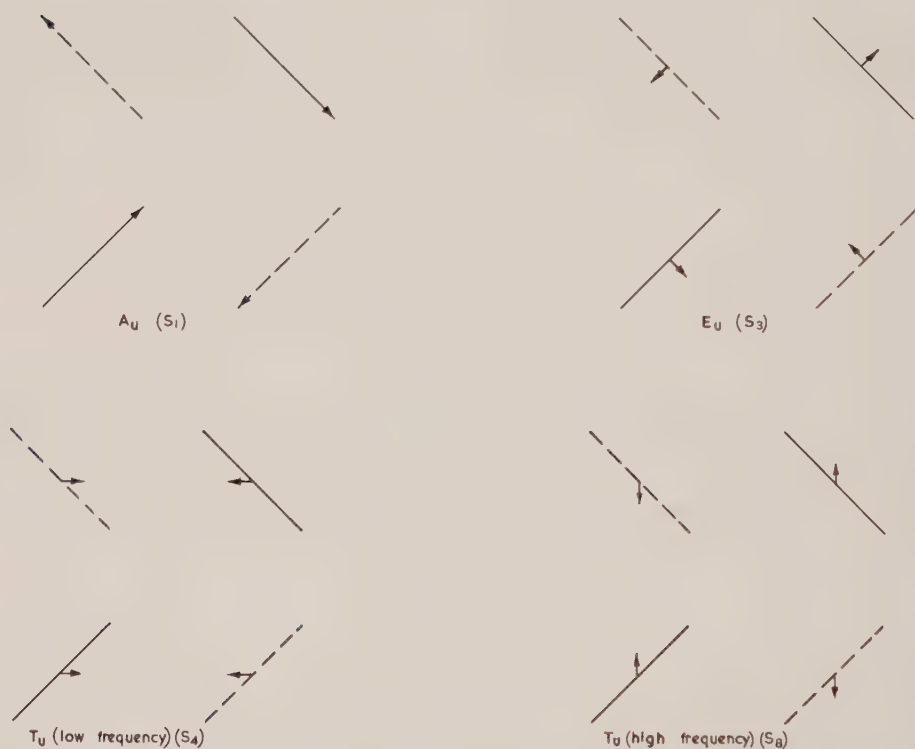


Figure 3. Form of pseudo-translational modes for the unit cell molecules illustrated in figure 2. (Arrows for the S_1 coordinate represent displacements along the molecular axes; elsewhere they are displacements in the ab plane.)

Although the excitation of T_u vibrations are formally allowed, the model used cannot explain the absorption intensity since no dipole moment is developed when rigid non-polarizable molecules are displaced. However, the inclusion of a term involving the dipole induced by the neighbouring quadrupole could lead to an overall dipole moment in the distorted configuration and hence to non-zero absorption. Anderson's experiments do not give a quantitative estimate of the intensity of the bands but it is clear that they are very weak.

Gaizauskas [10] has found three lines at 112 , 77 and 64 cm^{-1} in the Raman spectrum. These presumably correspond to the three zero wave-vector pseudo-rotational vibrations, all of which should be Raman active. Dows [11] has summarized the available information on this type of lattice vibration.

All three frequencies occur in combination bands involving internal molecular vibrations. The calculated frequencies are about two-thirds of the observed values. Only the quadrupole part of the potential contributes to the pseudo-rotational frequencies, so the results emphasize the approximate nature of the potential function used.

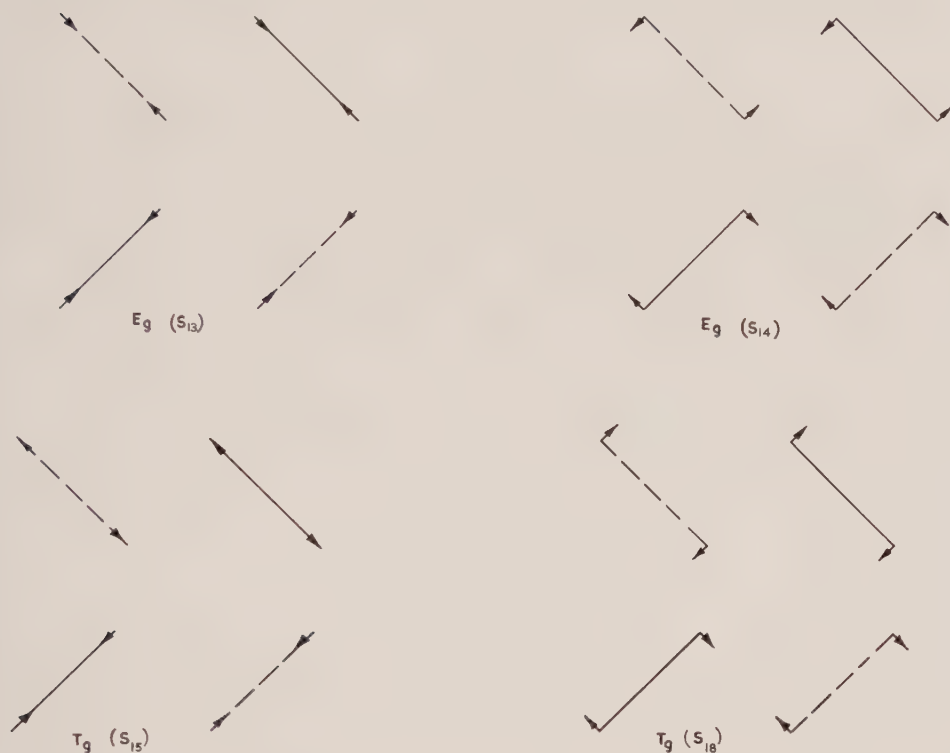


Figure 4. Form of pseudo-rotational modes for the unit cell molecules illustrated in figure 2. (Arrows for S_{13} and S_{15} represent rotational motions in the plane containing the molecule and the c -axis; elsewhere they are displacements in the ab plane.)

It is possible to describe the qualitative form of the various vibrations if the appropriate normal coordinates are examined in detail. The form of pseudo-translational modes is illustrated in figure 3. For the two T_u vibrations, the symmetry coordinates illustrated (S_4 and S_8) are normal coordinates if the quadrupole moment is zero, S_4 having the lower frequency. The quadrupole interaction mixes the two vibrations, but only slightly, and the description shown in figure 3 is approximately correct. The actual normal coordinates are $0.99S_4 - 0.16S_8$ for the low frequency vibration (68 cm^{-1}) and $0.16S_4 + 0.99S_8$ for the high frequency one (114 cm^{-1}).

The form of the pseudo-rotational modes is shown in figure 4. Both components of the E_g vibration are illustrated. One of these involves changes in the polar angles θ (if the c -direction is the polar axis) and the other changes in the polar angles ϕ . One component of each of the two T_g symmetry coordinates is

illustrated. These motions are mixed in the actual normal modes. The normal coordinates, which are independent of the magnitudes of the parameters ϵ , r_0 and Θ , are $0.91S_{15} - 0.32S_{18}$ for the low frequency vibration and $0.32S_{15} + 0.91S_{18}$ for the high frequency.

This work forms part of the programme of the Basic Physics Division of the National Physical Laboratory and is published by permission of the Director.

REFERENCES

- [1] BORN, M., and HUANG, K., 1954, *Dynamical Theory of Crystal Lattices* (Oxford University Press).
- [2] POPLÉ, J. A., 1954, *Proc. roy. Soc. A*, **221**, 498, 508.
- [3] BUCKINGHAM, A. D., 1959, *Quart. Rev. chem. Soc., Lond.*, **13**, 183.
- [4] DE SMEDT, J., and KEESOM, W. H., 1924, *Proc. Acad. Sci. Amst.*, **27**, 839; 1926, *Z. Krist-allogr.*, **62**, 312.
- [5] MARK, H., and POHLAND, E., 1925, *Z. Kristallogr.*, **61**, 293; 1926, *Ibid.*, **64**, 113.
- [6] McLENNAN, J. C., and WILHELM, J. O., 1925, *Trans. roy. Soc. Can.*, **19**, 51.
- [7] WILSON, E. B., DECUIS, J. C., and CROSS, P. C., 1955, *Molecular Vibrations* (McGraw-Hill).
- [8] BUCKINGHAM, A. D., and DISCH, R. L., 1963, *Proc. roy. Soc. A*, **273**, 275.
- [9] ANDERSON, A., and WALMSLEY, S. H., 1964, *Mol. Phys.*, **7**, 583.
- [10] GAIZAUSKAS, V., 1955, Ph.D. Thesis Toronto, quoted in reference [11].
- [11] DOWS, D. A., 1959, *Spectrochim. Acta.*, **13**, 308.

The electron spin resonance spectrum of the radical anion of 1,3,5—trinitrobenzene

by P. H. H. FISCHER† and C. A. McDOWELL‡

Department of Chemistry, University of British Columbia, Vancouver 8, B.C., Canada

(Received 13 January 1964; revision received 12 March 1964)

The radical anion of 1,3,5-trinitrobenzene has been prepared by electrolysis in a solution of acetonitrile and its electron spin resonance spectrum measured. A well-resolved spectrum consisting of 28 lines is observed and it can be interpreted on the assumption that the radical is planar with symmetry D_{3h} , and that the odd electron is in a degenerate orbital. The hyperfine coupling constants given by the above analysis of the spectrum are,

$$a^N = 2.48 \text{ gauss} \quad \text{and} \quad a^H = 4.14 \text{ gauss.}$$

These are larger than the values predicted by the molecular orbital spin densities. The g -factor has been found to be 2.0036 ± 0.0002 and apart from this being larger than the free electron value, nothing has been found which can be attributed to Jahn–Teller effects which might have been expected to have been important in this radical anion which according to our Hückel type L.C.A.O. molecular orbital calculations has the odd electron in a degenerate orbital.

1. INTRODUCTION

The reduction of *s*-trinitrobenzene by alkali metals in solution in dimethoxyethane and tetrahydrofuran has been found by Ward [1] to produce free radicals. An electron spin resonance spectrum was observed consisting of 14 lines which was explained in terms of the interaction of the spin of the free electron with only one nitrogen nucleus and three equivalent hydrogen nuclei. A similar explanation was also offered to account for the electron spin resonance spectra observed for a series of dinitro-compounds from which radicals were produced by the same method. Since the above method of producing radicals from nitro-compounds leads to anomalous results we have used an electrochemical reduction method which yields the radical anions free from any interfering cations. Others [2–6] have also used this method for nitrogen-containing compounds with success. We have obtained the completely resolved spectra for the radical anions of all the dinitrobenzenes, and wish now to report complete resolution of the spectrum of the *s*-trinitrobenzene radical anion.

The E.S.R. spectrum of this anion is of contemporary interest for several reasons. The *s*-trinitrobenzene radical anion, if planar, would have symmetry D_{3h} , and its E.S.R. spectrum may, therefore, be expected to exhibit some of the peculiarities previously observed for anions with orbitally degenerate ground states and which have been attributed to Jahn–Teller effects. Again it would also be reasonably expected that the anomalous line-widths and line-intensities

† Present address: Max-Planck Institut für Mediz. Forschung Institut für Chemie Laboratory, Heidelberg/Baden, Germany.

‡ Present address: Department of Theoretical Chemistry, University Chemical Laboratory, Lensfield Road, Cambridge, England.

recently observed [7, 8, 18] for the *m*-dinitrobenzene radical anion would here again be encountered, and perhaps in a somewhat enhanced manner. Furthermore, our completely resolved spectrum of the *s*-trinitrobenzene radical anion is of added interest because of Ward's [1] recent observation that the E.S.R. spectrum of the radical produced by the reduction of this compound by sodium dissolved in dimethoxyethane does not exhibit the expected hyperfine interaction pattern. In this connection we may also mention the somewhat similar observation that the E.S.R. spectra for the photo-induced paramagnetic species from *s*-trinitrobenzene and nitrobenzene in donor solvents exhibited hyperfine interaction due to only one nitrogen nucleus [11, 12].

2. EXPERIMENTAL

Eastman Kodak 1,3,5-trinitrobenzene was recrystallized three times from chloroform and twice sublimed under high vacuum. A beautifully crystalline almost colourless substance was obtained which had a m.p. of 120.5–121.5°C. Spectroscopic grade acetonitrile, b.p. 81.5°C, was thoroughly degassed by repeated freezing, pumping and melting. It was then distilled directly into the electron spin resonance electrolysis cell. Tetra-*n*-propyl ammonium perchlorate was used as the supporting electrolyte. The compound was recrystallized twice before use.

The electrochemical E.S.R. cell was an improved design of the type introduced by Hausser *et al.* [10]. It consisted essentially of two parts. The lower part, made entirely of quartz, ended in a piece of 2 mm internal diameter Vitrosil when the cell was used with non-polar solvents, but for more polar solvents like acetonitrile, a quartz end-tube of only 1 mm internal diameter was used. The upper part of the cell had a stop-cock to permit the cell to be filled and evacuated. Two tungsten leads for the electrolysis current were sealed into the top of the cell. The anode consisted of either a piece of platinum foil spot-welded to a tungsten rod, or of a pool of mercury in which the tungsten rod was immersed. To prevent contamination of the resonant cavity which might have occurred by the accidental breaking of the cell during an experiment, a platinum wire cathode was welded to a tungsten rod and covered with a very fine Teflon sleeve with the exception of a 3 cm length inside the resonant cavity.

Electrolysis of a solution of 1,3,5-trinitrobenzene (TNB) in acetonitrile at a potential of -0.48 volts with respect to a saturated calomel electrode showed that several different paramagnetic species were produced. At the beginning of the electrolysis a narrow resonance spectrum, about 10.25 gauss in width was observed which was attributed to a $\text{TNB}^- \rightarrow \text{TNB}$ electron donor-acceptor (EDA) complex. This was followed by a well-resolved spectrum which was clearly identified as being that of the TNB^- radical anion.

The E.S.R. spectra were determined using a Varian spectrometer with 100 kc/s modulation and a 12 in. magnet. The magnetic field was measured using a proton resonance magnetometer.

3. RESULTS AND DISCUSSION

The well-resolved 28 line spectrum which we attribute to the radical anion of *s*-trinitrobenzene is shown in figure 1. This spectrum is certainly the expected one resulting from the interaction of the spin of one electron with the nuclear spins of three equivalent nitrogen nuclei and three equivalent protons. It is

obviously quite different from the spectra reported by Lagercrantz and Yhland [11], and Ward [12], who observed, respectively, photo-induced paramagnetic spectra in solutions of *s*-trinitrobenzene and nitrobenzene in donor solvents. In these spectra the hyperfine structure observed was that caused by one dominant nitrogen nucleus. Ward [12] has shown that photo-excitation of the nitrobenzene-tetrahydrofuran charge transfer complex caused one of the protons of the tetrahydrofuran to be transferred to the nitrobenzene molecule, thus leading to the observed additional hyperfine splitting.

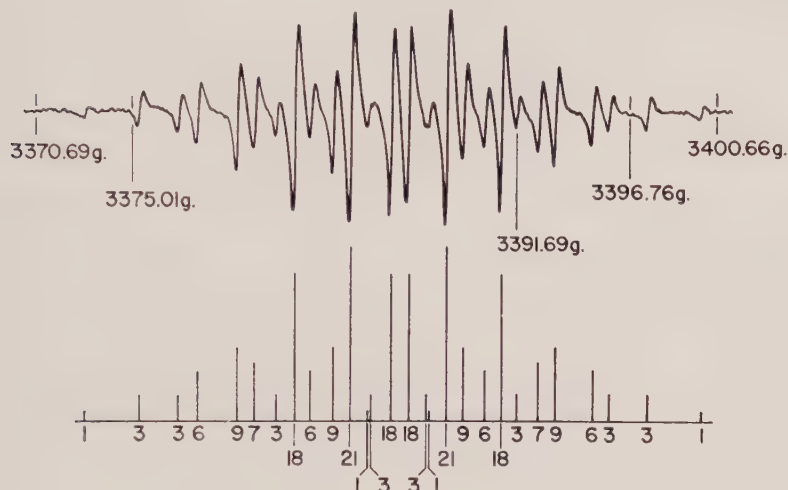


Figure 1. The electron spin resonance spectrum of the *s*-trinitrobenzene radical anion in acetonitrile solution. Beneath the experimentally observed spectrum the theoretically predicted spectrum is shown. The numbers along the abscissa are the predicted theoretical line intensities.

Our analysis of the E.S.R. spectrum of the *s*-trinitrobenzene radical anion leads to the assignment of the following hyperfine interaction constants: $a^N = 2.48$ gauss and $a^H = 4.14$ gauss. The theoretical spectrum given by this set of hyperfine coupling constants is shown in figure 1 and it is at once apparent that there is excellent agreement between the theoretically predicted spectrum and the experimentally observed hyperfine interaction pattern. Our estimates of the values for the hyperfine coupling constants a^N and a^H lead to an overall predicted spectrum width of 27.3 gauss and the experimentally observed spectrum width is 27.13 gauss.

When the three NO_2 groups in *s*-trinitrobenzene radical anion are co-planar with the benzene ring the radical belongs to the symmetry group D_{3h} . We shall label the atoms in the radical with this symmetry as indicated in figure 2. A simple Hückel L.C.A.O. molecular orbital treatment involving 19 π -electrons on 15 centres leads to the result that the odd electron in the radical must be accommodated in an orbital possessing the symmetry of the representations A_1'' , A_2'' or E'' of group D_{3h} . Solution of the appropriate secular equations shows that the odd electron must go into one of the degenerate E'' orbitals to form the radical in its ground state. In solving the secular equations the coulombic and resonance integrals were written in the usual form $\alpha_x = \alpha_c + h_x \beta_{cc}$ and $\beta_{xy} = k_{xy} \beta_{cc}$, where α_c

and β_{cc} are the coulombic and resonance integrals for the carbon atoms in benzene. The values used for h_x and k_{xy} were those given by Rieger and Fraenkel [7] based on their study of a large number of aromatic nitro-substituted radical anions, i.e. $k_N=2.2$, $h_0=1.4$, $k_{Nm}=1.67$ and $k_{CN}=1.2$.

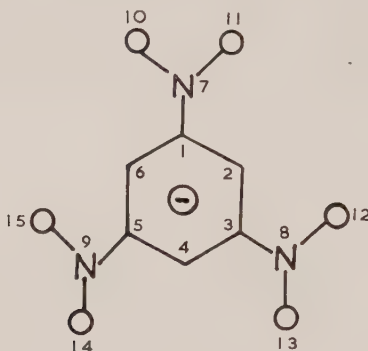


Figure 2. Numbering system for the *s*-trinitrobenzene radical anion, symmetry D_{3h} .

The following values for the spin densities thus result; atoms 2,4,6, $\rho_c=0.12844$; atoms 7,8,9, $\rho_N=0.06726$. From the equation $a=Q\rho_c$ we calculate, from our experimental value for a using $Q=-23.7$ gauss [7], that for atoms 2, 4 and 6, $\rho_c(\text{expt})=0.1746$. As mentioned above, the Hückel type calculations which we have made predict that the ground state of the anion with symmetry D_{3h} is orbitally degenerate. If this prediction of the Hückel theory that the anion is in an orbitally degenerate state is correct, then our experiments show that the D_{3h} symmetry is preserved in the anion. Had the radical anion lower symmetry the calculated spin densities would no longer be equal for the three nitrogen or hydrogen atoms. The orbital with symmetry A_2'' lies 0.152β above the degenerate E'' orbitals. Were the odd electron to be in this orbital with symmetry A_2'' the anion would also be predicted to have three equivalent hydrogen and nitrogen atoms. It would, however, be necessary to postulate some form of perturbation to cause an inversion of the order of the orbitals if the odd electron were to go into the A_2'' orbital rather than into one of the degenerate E'' orbitals.

As will be seen the molecular orbital L.C.A.O. calculations for spin densities in the *s*-trinitrobenzene radical anion are not in good agreement with the experimentally observed ring-proton hyperfine splittings. Rieger and Fraenkel [7] likewise found very poor agreement between the calculated and experimental values for ring-proton spin densities for the related *m*-dinitrobenzene radical anion. Our calculations of spin densities by the McLachlan [13] method for introducing what is an approximation to configuration interaction likewise led to poor agreement between the theoretical spin densities and the experimental results. In these calculations a value of $\lambda=1.2$ was used, as that has been found to lead to satisfactory results for aromatic anions, including heterocyclic ones [13, 7, 6, 14]. It must be pointed out, however, that it is clearly not satisfactory to apply the McLachlan method to π -electron systems which have an odd electron in a degenerate orbital. The necessity to make linear combinations of the wavefunctions of the degenerate pair makes it difficult in these cases to justify calculations of spin densities for orbitals with configuration interaction included by the McLachlan method.

It is, of course, well known that the Hückel L.C.A.O. molecular orbital theory predicts that the ground states of radical anions with symmetries D_{xh} with $x=3, 6, 8$, etc. will be orbitally degenerate. Such orbitally degenerate ions are subject to molecular distortions because of Jahn-Teller effects. Radical anions with orbitally degenerate ground states which have been studied by electron spin resonance include the anions of benzene (B^-), triphenylene (Tp^-), coronene (C^-), cyclooctatetraene (O^-), as well as the cation of coronene (C^+). Townsend and Weisman (15) observed that the proton hyperfine structure in the E.S.R. spectra of B^- , Tp^- , and C^- was unusually broad. Less broad lines were, however, observed for the cyclooctatetraene anion [22]. Several authors have attempted to account for the anomalous line-widths observed for these anions on the basis of the theory of the dynamical Jahn-Teller effect [15, 16].

The line-widths which we have observed in the E.S.R. spectrum of the radical anion of *s*-trinitrobenzene (figure 1) are very much narrower than those found for the B^- , Tp^- and C^- anions. They correspond more nearly to those observed for the cyclooctatetraene radical anion. Now our Hückel calculations predict that the unpaired electron in the *s*-trinitrobenzene radical anion occupies an orbital with symmetry E'' of group D_{3h} . According to the Jahn-Teller theorem, vibrations with symmetry E'' will for this anion be able to cause a first-order splitting of the electronic degeneracy. This case is, therefore, rather similar to that of the B^- type anions. For this reason it is all the more surprising that we find such a well resolved spectrum for the radical anion of *s*-trinitrobenzene. Our experimental observations are closely similar to those of Strauss, Katz and Fraenkel [22] who found no large effects in the E.S.R. spectrum of the cyclooctatetraene anion could be attributed to Jahn-Teller effects.

Another somewhat surprising feature of the spectrum of the *s*-trinitrobenzene radical anion is that one does not observe the same type of anomalous line-widths and line intensities as found in the E.S.R. spectrum of the *m*-dinitrobenzene radical anion. In the spectrum of this latter species the hyperfine line arising from the $I(N) = \pm 2$ transitions are normal in line-width and intensity, whereas those lines due to the $I(N) = \pm 1, 0$ transitions show anomalous broadening and are less intense than would have been expected. These anomalous line-widths in the E.S.R. spectrum of the *m*-dinitrobenzene radical anion can be explained [7, 8, 18] by time-dependent fluctuations of the nitrogen hyperfine coupling constants. The nitrogen hyperfine coupling constants a^N can be assumed to be a function of the angle ϕ , which the nitrogroups make with the plane of the benzene ring, i.e. we may write for the nitrogen hyperfine coupling constant the symbol $a^N(\phi)$. The rotational modulation of $a^N(\phi)$ causes line-width variations by inducing secular and non-secular relaxation processes [19]. Similar processes would naturally be expected to be operative in the *s*-trinitrobenzene radical anion also, but our spectrum shows no anomalies in the line-widths nor in the intensities of the hyperfine components. It would, therefore, seem that the nitrogroups in the *s*-trinitrobenzene radical anion can all rotate freely so that the matrix elements of $[a^{N1}(\phi_1)\mathbf{I}_1 + a^{N2}(\phi_2)\mathbf{I}_2 + a^{N3}(\phi_3)\mathbf{I}_3] \cdot \mathbf{S}$ do not deviate from the average value $\langle a^N(\phi) \rangle [\mathbf{I}_1 + \mathbf{I}_2 + \mathbf{I}_3] \cdot \mathbf{S}$.

Finally we may perhaps comment on the magnitude of the experimental *g*-value which we have determined to be $g = 2.0036 \pm 0.0002$. McConnell [20] has pointed out that the *g*-values for symmetrical radicals with vibronic degenerate ground states may be somewhat larger than free electron *g*-value because of the

special importance of the spin-orbit interactions in these cases. Our result for the g -factor of the s -trinitrobenzene radical anion is in agreement with this expectation, as is the work of Blois *et al.* [20]. These authors found that the g -value of C^- and possibly also of B^- were slightly higher than those of other aromatic radicals. It must, however, be pointed out that Strauss *et al.* [22] have recently reported that the g -value for the cyclooctatetraene radical anion is 2.0025 ± 0.0001 , which is almost the free electron value.

We wish to thank the National Research Council of Canada for generous grants in support of this work. P.H.H.F. thanks the same body for the award of a Bursary and a Studentship during the period 1959–1963. C.A.Mc.D. is also much indebted to the same body for the award of a Senior Research Fellowship during the 1963/64 academic year.

REFERENCES

- [1] WARD, R. L., 1961, *J. Amer. chem. Soc.*, **83**, 1296.
- [2] GESKE, D. H., and MAKI, A. H., 1960, *J. Amer. chem. Soc.*, **82**, 2671.
- [3] MAKI, A. H., and GESKE, D. H., 1960, *J. chem. Phys.*, **33**, 825.
- [4] FREED, J. H., and FRAENKEL, G. K., 1962, *J. chem. Phys.*, **37**, 1156.
- [5] RIEGER, P. H., BERNAL, I., WEINMUTH, W. H., and FRAENKEL, G. K., 1963, *J. Amer. chem. Soc.*, **85**, 683.
- [6] FISCHER, P. H. H., and McDOWELL, C. A., 1963, *J. Amer. chem. Soc.*, **85**, 2694.
- [7] RIEGER, P. H., and FRAENKEL, G. K., 1963, *J. chem. Phys.*, **39**, 609.
- [8] FISCHER, P. H. H., 1963, Thesis, University of British Columbia.
- [9] WARD, R. H., 1963, *J. chem. Phys.*, **36**, 1405.
- [10] HAUSSER, K. H., HÄBICH, A., and FRANZEN, V., 1961, *Z. Naturf. A*, **16**, 836.
- [11] LAGERCRANTZ, C., and YHLAND, M., 1962, *Acta chem. scand.*, **16**, 1799.
- [12] WARD, R. L., 1963, *J. chem. Phys.*, **38**, 2588.
- [13] McLACHLAN, A. D., 1960, *Mol. Phys.*, **3**, 233.
- [14] RIEGER, P. H., and FRAENKEL, G. K., 1962, *J. chem. Phys.*, **37**, 2795.
- [15] TOWNSEND, M. G., and WEISSMAN, S. I., 1960, *J. chem. Phys.*, **32**, 309.
- [16] McCONNELL, H. M., and McLACHLAN, A. D., 1961, *J. chem. Phys.*, **34**, 1.
- [17] SNYDER, L. C., and McLACHLAN, A. D., 1962, *J. chem. Phys.*, **36**, 1159.
- [18] McDOWELL, C. A., 1963, *Rev. mod. Phys.*, **35**, 525.
- [19] FREED, J. H., and FRAENKEL, G. K., 1963, *J. chem. Phys.*, **39**, 326.
- [20] McCONNELL, H. M., 1961, *J. chem. Phys.*, **34**, 13.
- [21] BLOIS, Jr., M. S., BROWN, H. W., and MALING, J. E., 1960, B. L. Report No. 12, U.S. Air Force Contract AF 18(600)–1511, Project No. 9777, October.
- [22] STRAUSS, H. L., KATZ, T. J., and FRAENKEL, G. K., 1963, *J. Amer. chem. Soc.*, **85**, 2360.

Raman selection rules for vibration-rotation transitions in symmetric top molecules

by IAN M. MILLS†

Spectroscopy Laboratory, Massachusetts Institute of Technology

(Received 18 March 1964)

Symmetry restrictions on Raman selection rules can be obtained, quite generally, by considering a Raman allowed transition as the result of two successive dipole allowed transitions, and imposing the usual symmetry restrictions on the dipole transitions. This leads to the same results as the more familiar polarizability theory, but the vibration-rotation selection rules are easier to obtain by this argument.

The selection rules for symmetric top molecules involving the $(+l)$ and $(-l)$ components of a degenerate vibrational level with first-order Coriolis splitting are derived in this paper. It is shown that these selection rules depend on the order of the highest-fold symmetry axis C_n , being different for molecules with $n=3$, $n=4$, or $n \geq 5$; moreover the selection rules are different again for molecules belonging to the point groups D_{nd} with n even, and S_m with $\frac{1}{2}m$ even, for which the highest-fold symmetry axes C_n and S_m are related by $m=2n$.

Finally it is shown that an apparent anomaly between the observed Raman and infra-red vibration-rotation spectra of the allene molecule is resolved when the correct selection rules are used, and a value for the A rotational constant of allene is derived without making use of the zeta sum rule.

1. INTRODUCTION

In a recent paper [1] I discussed the dipole selection rules in symmetric top molecules involving the $(+l)$ and $(-l)$ components of a degenerate vibronic level with first-order Coriolis splittings. The selection rules relate the $(+l)$ or $(-l)$ components to the sign of ΔK , where K is the modulus of the component of the total angular momentum about the figure axis, and a simple rule was given for determining this relationship for any transition in any symmetric top molecule. In this paper the equivalent selection rules for Raman transitions are discussed. These results have been previously discussed by Placzek and Teller [2], and by Placzek [3], and by Teller [4], and for certain point groups the selection rules are quoted by Herzberg [5]; however, none of these authors give the $(+l)$ and $(-l)$ selection rules with generality, and Herzberg—who is the only author to give the results in the modern notation—actually quotes the correct selection rules only for molecules whose highest-fold symmetry axis is C_3 or C_4 . In particular, the selection rules for the point group D_{2d} (which are necessary, for example, to interpret the vibration-rotation Raman spectrum of the allene molecule) do not appear to have been previously derived.

It is possible to derive vibration-rotation selection rules from the usual polarizability theory of Raman spectra, by considering the matrix elements of the components of the polarizability tensor relative to axes fixed in space. This is the

† Permanent address: Department of Chemistry, University of Reading, England.

method adopted by Placzek and Teller [2]. However, an intrinsically simpler method of deriving symmetry restrictions on the selection rules is provided by the 'third common level rule', which was used in the early discussions of Raman spectra, before the polarizability theory was developed. This states that a Raman transition from an initial state i to a final state k can take place only if there exists some third state j such that both of the transitions $i \rightarrow j$ and $j \rightarrow k$ are dipole allowed. If the correct symmetry restrictions are imposed on the dipole transitions $i \rightarrow j$ and $j \rightarrow k$, then the correct restrictions on the Raman transitions $i \rightarrow k$ will be obtained.

The physical significance of the third common level rule is as follows. A Raman transition may be thought of as taking place in two stages; first the molecule absorbs a quantum of the exciting radiation $h\nu$, making a transition to a virtual state v such that $(\bar{E}_v - E_i)/h = \nu_{vi} = \nu$, the frequency of the exciting radiation; second, the molecule emits a quantum of radiation $h\nu_{vk} = (\bar{E}_v - E_k)$, thus making a transition to the final state k . Both the absorption and the emission may be thought of as taking place by the usual dipole mechanism, so that they must obey dipole selection rules. However, the virtual state is not a stationary state of the molecule; the wavefunction in this state is a superposition of contributions from all stationary states j of the appropriate symmetry, but of various energy values E_j —not generally equal to the expectation value of the energy \bar{E}_v in the virtual state. The existence of the virtual state is thus dependent on the existence of some stationary states j such that the dipole transitions $i \rightarrow j$ and $j \rightarrow k$ are both allowed. If the symmetry species of i and k are such that there are no states j for which $i \rightarrow j$ and $j \rightarrow k$ are dipole allowed, then the Raman transition $i \rightarrow k$ is forbidden.

Quantum mechanically these results are expressed in the general formula for the induced transition moment of the molecule between the states i and k of the Raman transition. Following Placzek [3], we find that the intensity of the scattered radiation is proportional to:

$$I = \frac{64\pi^4(\nu + \nu_{ik})^4}{3c^3} |C_{ik}|^2,$$

where the induced transition moment C_{ik} is given by:

$$C_{ik} = \sum_j \left[\frac{(UM_{ij})\mathbf{M}_{jk}}{h(\nu_{ji} - \nu)} + \frac{\mathbf{M}_{ij}(UM_{jk})}{h(\nu_{jk} + \nu)} \right]. \quad (1)$$

In this equation \mathbf{U} defines the amplitude of the electric vector of the incident radiation of frequency ν according to:

$$\epsilon = \mathbf{U}^* \exp(2\pi i \nu t) + \mathbf{U} \exp(-2\pi i \nu t);$$

also $h\nu_{ji} = E_j - E_i$, $h\nu_{jk} = E_j - E_k$, and \mathbf{M}_{ij} and \mathbf{M}_{jk} are the dipole transition moments $\langle i|\boldsymbol{\mu}|j\rangle$ and $\langle j|\boldsymbol{\mu}|k\rangle$. Writing $[C_\rho]_{ik}$ and U_σ for components of the vectors \mathbf{C} and \mathbf{U} ($\sigma, \rho = x, y$ or z), and writing:

$$[C_\rho]_{ik} = \sum_\sigma [c_{\rho\sigma}]_{ik} U_\sigma,$$

we obtain from (1):

$$[c_{\rho\sigma}]_{ik} = \sum_j \left[\frac{[M_{\sigma ij}][M_\rho]_{jk}}{h(\nu_{ji} - \nu)} + \frac{[M_\rho]_{ij}[M_\sigma]_{jk}}{h(\nu_{jk} + \nu)} \right]. \quad (2)$$

Quite generally, for the Raman transition $i \rightarrow k$ to be allowed, one of the components of the tensor $[\mathbf{C}]_{jk}$ must be non-zero, and we see that this will happen as long as there exists some other state j such that both of the transition moments $[\mathbf{M}]_{ij}$ and

$[\mathbf{M}]_{jk}$ are non-zero. The usual polarizability theory of Raman spectra is obtained by making the Born–Oppenheimer approximation and assuming that the transition moments are independent of the nuclear coordinates, and further assuming that $v \ll v_{ji}$ for the lowest excited electronic level j ; then, if i and k refer to different vibrational states of the ground electronic state, equation (2) reduces to a vibrational matrix element of the static electronic polarizability α .

After this brief discussion of the third common level rule, we shall use it to derive Raman selection rules for vibration–rotation transitions. This makes the problem simple, because once we know the dipole selection rules, the Raman selection rules follow directly. If we impose only the restrictions implied by molecular symmetry on the selection rules, we could proceed by classifying all of the vibration–rotation states of the molecule according to the symmetry species of the full symmetry group of the molecule, following Hougen [6], and then applying Hougen’s general dipole selection rule to two successive transitions. In the discussion in this paper, however, I shall assume that the rotational wavefunction can be factorized from the vibronic wavefunction, and derive the more restrictive selection rules which are obtained when the rotational wavefunctions are those appropriate to a rigid symmetric top. Although the method is applied in this paper only to vibration–rotation selection rules in symmetric top molecules, it is easy to derive Raman selection rules for all types of transition in any molecule by the third common level rule.

There is one difference between the symmetry restrictions on Raman selection rules imposed by the usual polarizability theory, and those imposed by the third common level rule, and I am indebted to Drs. J. K. G. Watson and J. T. Hougen for drawing my attention to this point. The third common level rule may allow certain Raman transitions which are forbidden in the polarizability theory: for example, an $A_1 \leftrightarrow A_2$ transition in a C_{3v} molecule is forbidden by the polarizability theory, but is allowed by the third common level rule, since $A_1 \leftrightarrow E \leftrightarrow A_2$ are both dipole allowed. More generally, the Raman scattering tensor \mathbf{c} in equation (2) transforms like the nine components of the complete square of the dipole moment operator, whereas the polarizability tensor α transforms like the six components of the symmetrized square of the dipole moment operator; thus the representation of \mathbf{c} may contain symmetry species which do not occur in the representation of α , leading to a relaxation of the selection rules. The further restrictions obtained from the polarizability theory result from the approximation involved in reducing \mathbf{c} to α . The question of which selection rules are correct obviously depends on the errors involved in this approximation; since almost all observed Raman spectra to this date obey the more restrictive selection rules of the polarizability theory, it would seem that the approximation is generally a good one.

Fortunately the results obtained in the remaining sections of this paper are not affected by this difference: they can be derived by either the polarizability theory or the third common level rule, and the latter method is used only because the results are easier to derive and visualize by this method.

2. SYMMETRIC TOP MOLECULES

The electric dipole selection rules for rovibronic transitions in symmetric top molecules are discussed in my earlier paper [1]. The results give a simple relation between the value of ΔK for the transition and the vibrational species of

the two combining states. The species of the wave functions under the operation of the highest-fold axis of symmetry are characterized by an angle θ , $(+l)$ and $(-l)$ levels of degenerate states being distinguished by positive and negative values of θ in the range $-\pi < \theta < +\pi$; it is then found that dipole transitions obey the following selection rules†:

- (i) For most point groups, in which the highest-fold symmetry axes C_n and S_m are related by $m \leq n$, the transitions are given by:

$$\left. \begin{aligned} \Delta K &= +1 \text{ with } \Delta\theta = +2\pi/n, \\ \Delta K &= 0 \text{ with } \Delta\theta = 0 \\ \text{or} \quad \Delta K &= -1 \text{ with } \Delta\theta = -2\pi/n. \end{aligned} \right\} \quad (3)$$

- (ii) For the exceptional point groups D_{nd} with n even, and S_m with $\frac{1}{2}m$ even, in which the highest-fold symmetry axes C_n and S_m are related by $m = 2n$, the transitions are given by:

$$\left. \begin{aligned} \Delta K &= +1 \text{ with } \Delta\theta = +2\pi/m, \\ \Delta K &= 0 \text{ with } \Delta\theta = \pi, \\ \text{or} \quad \Delta K &= -1 \text{ with } \Delta\theta = -2\pi/m. \end{aligned} \right\} \quad (4)$$

These selection rules can be conveniently related to the symmetry species of the combining states by ' θ circle diagrams' [1], in which values of θ are plotted clock-wise around the circumference of a circle, such that all the A species are represented by a point at the top of the circle ($\theta = 0$), all the B species by a point at the bottom ($\theta = \pi$), and all $E(+l)$ and $E(-l)$ species by points around the right-hand and left-hand sides respectively ($0 < \theta < \pi$ and $-\pi < \theta < 0$). The allowed dipole transitions connect points on the circumference of the circle according to the rules (3) or (4). The species of the combining states with respect to σ_h , i , σ_v , and dihedral C_2 , are not given by this procedure, but these further restrictions are easy to determine, and they do not affect the $(+l)$ and $(-l)$ selection rules.

The allowed Raman transitions are obtained by considering all possible combinations of two successive dipole transitions. First we note that since $\Delta J = 0, \pm 1$ is always allowed in dipole transitions (except that $\Delta J = 0$ is forbidden if $K = 0$ and $\Delta K = 0$), we shall evidently find $\Delta J = 0, \pm 1$ and ± 2 to be allowed in Raman transitions. This result is essentially independent of the selection rules for ΔK , and the vibrational species of the combining states‡.

We now consider the Raman selection rules for ΔK . As in electric dipole spectra we find that these are correlated to the vibrational symmetry species of the combining states, and we find that we must consider the point groups D_{nd} with n even and S_m with $\frac{1}{2}m$ even to constitute a special case.

† Throughout this paper K is the modulus of the component of total angular momentum about the top axis, and θ is essentially the exponent in the factor $\exp(-i\theta)$ which multiplies the wavefunction under the symmetry operation C_n or S_m ; however, see reference [1] for a precise definition of θ and of $(+l)$ and $(-l)$ levels. ΔK is to be interpreted as K (upper)– K (lower) for Raman transitions, and similarly for $\Delta\theta$.

‡ Actually the selection rules for J and K do become correlated for transitions involving levels with $J = K$, through the general restriction on the quantum numbers that $J \geq K$.

(i) Point groups C_3 (C_3 , C_{3v} , C_{3h} , D_3 , D_{3d} , S_6)

$$\left. \begin{array}{l} \Delta K = +1: E(+l) \leftarrow A \\ \Delta K = -1: E(-l) \leftarrow A \end{array} \right\} \Delta \nu_{\text{sub}} = 2[A(1 - \xi) - B]$$

$$\left. \begin{array}{l} \Delta K = +2: E(-l) \leftarrow A \\ \Delta K = -2: E(+l) \leftarrow A \end{array} \right\} \Delta \nu_{\text{sub}} = 4[A(1 + \frac{1}{2}\xi) - B]$$

(ii) Point groups C_4 (C_4 , C_{4v} , C_{4h} , D_4 , D_{4h})

$$\left. \begin{array}{l} \Delta K = +1: E(+l) \leftarrow A \\ \Delta K = -1: E(-l) \leftarrow A \end{array} \right\} \Delta \nu_{\text{sub}} = 2[A(1 - \zeta) - B]$$

$$\Delta K = \pm 2: B \leftarrow A \quad \Delta \nu_{\text{sub}} = 4[A - B]$$

(iii) Point groups C_n with $n \geq 5$ (C_n , C_{nv} , C_{nh} , D_n , D_{nh})
 D_{nd} with n odd, and S_m with $\frac{1}{2}m$ odd)

$$\left. \begin{array}{l} \Delta K = +1: E_1(+l) \leftarrow A \\ \Delta K = -1: E_1(-l) \leftarrow A \end{array} \right\} \Delta \nu_{\text{sub}} = 2[A(1 - \zeta) - B]$$

$$\left. \begin{array}{l} \Delta K = +2: E_2(+l) \leftarrow A \\ \Delta K = -2: E_2(-l) \leftarrow A \end{array} \right\} \Delta \nu_{\text{sub}} = 4[A(1 - \frac{1}{2}\zeta) - B]$$

(iv) Point groups D_{nd} with n even, and S_m with $\frac{1}{2}m$ even

(a) Point groups D_{2d} and S_4 :

$$\left. \begin{array}{l} \Delta K = +1: E(-l) \leftarrow A \\ \Delta K = -1: E(+l) \leftarrow A \end{array} \right\} \Delta \nu_{\text{sub}} = 2[A(1 + \zeta) - B]$$

$$\Delta K = \pm 2: B \leftarrow A \quad \Delta \nu_{\text{sub}} = 4[A - B]$$

(b) Point groups D_{4d} and S_8 :

$$\left. \begin{array}{l} \Delta K = +1: E_3(-l) \leftarrow A \\ \Delta K = -1: E_3(+l) \leftarrow A \end{array} \right\} \Delta \nu_{\text{sub}} = 2[A(1 + \zeta) - B]$$

$$\left. \begin{array}{l} \Delta K = +2: E_2(+l) \leftarrow A \\ \Delta K = -2: E_2(-l) \leftarrow A \end{array} \right\} \Delta \nu_{\text{sub}} = 4[A(1 - \frac{1}{2}\zeta) - B]$$

Raman selection rules for $(+l)$ and $(-l)$ components in transitions from a totally symmetric ground state to a degenerate excited state. The states are characterized by their symmetry species under the operation C_n (or S_m) only; see text. $\Delta \nu_{\text{sub}}$ is the coefficient of K in the expression for the sub-band origins. $\Delta K = K$ (upper) $- K$ (lower) in the sense of the arrow.

If we exclude these point groups, and apply the selection rules (1) to two successive dipole transitions, it is evident that the Raman transitions $\Delta K=0$, ± 1 , ± 2 will all be allowed according to the following rules:

$$\left. \begin{aligned} \Delta K &= +2 \text{ with } \Delta\theta = +4\pi/n, \\ \Delta K &= +1 \text{ with } \Delta\theta = +2\pi/n, \\ \Delta K &= 0 \text{ with } \Delta\theta = 0, \\ \Delta K &= -1 \text{ with } \Delta\theta = -2\pi/n, \\ \Delta K &= -2 \text{ with } \Delta\theta = -4\pi/n. \end{aligned} \right\} \quad (5)$$

or

Applying the results (5) to a θ circle diagram gives the symmetry species (under the operation C_n) of the vibrational states which combine for any specified value of ΔK . For transitions from a totally symmetric initial state with $\Delta K = \pm 1$ or ± 2 the results are summarized under (i), (ii) and (iii) of the table, and some of the allowed transitions are illustrated on θ circle diagrams in figures 1 and 2.

Figure 1 applies to molecules with the highest-fold axis C_3 , and we note that these form a special case, since there is only one kind of E species in the molecule — E_2 being equivalent to E_1 with the $(+l)$ and $(-l)$ levels interchanged. The results are given in the table. This peculiar property of C_3 molecules was also noted by Placzek and Teller (p. 230 of reference [2]). Molecules with the highest-fold axis C_4 are also a somewhat special case, since in this case E_2 species are equivalent to B species, for which there is usually no vibrational degeneracy, and in consequence no distinction between $(+l)$ and $(-l)$ levels. The results are given

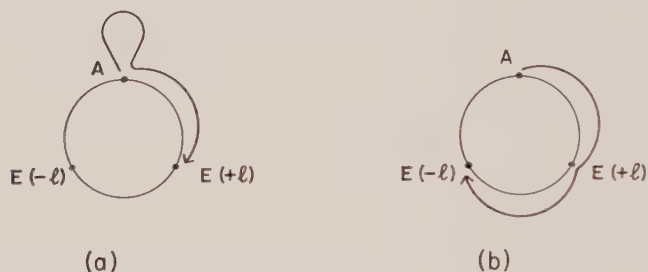


Figure 1. Raman transitions in a C_3 molecule, interpreted as two successive dipole transitions: (a) $\Delta K = +1$, $E(+l) \leftarrow A$; (b) $\Delta K = +2$, $E(-l) \leftarrow A$.

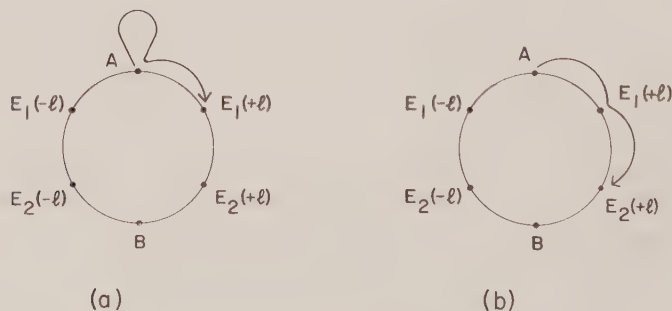


Figure 2. Raman transitions in a C_6 molecule, interpreted as two successive dipole transitions: (a) $\Delta K = +1$, $E_1(+l) \leftarrow A$; (b) $\Delta K = +2$, $E_2(+l) \leftarrow A$.

in the table (ii). Finally, for molecules with the highest-fold axis C_n where $n \geq 5$, the transitions are illustrated in figure 2; in this case E_1 and E_2 species are always both present, and we obtain what should really be regarded as the general result, given in the table (iii).

It should be noted that the different selection rules for $\Delta K = \pm 2$ for $n=3$, $n=4$ and $n \geq 5$, give rise to different formulae for the sub-band origins in each case. The linear term in K which is primarily responsible for the spacing of the sub-band origins, is given in the table for each situation. If, for example, the rotational structure of the E_{2g} Raman vibrations of benzene vapour should ever be resolved, the sub-band origins should be interpreted according to the formulae:

$$\nu_{\text{sub}} = \nu_0 + 4[A'(1 - \zeta_i) - B'] \pm 4[A'(1 - \tfrac{1}{2}\zeta_i) - B']K + [(A' - B') - (A'' - B'')]K^2. \quad (6)$$

The formula (IV, 75) in Herzberg [5] is only correct for molecules with the highest-fold axis C_n , where $n=3$, and it should be replaced by equation (6) for the cases where $n \geq 5$ †.

We now return to the exceptional point groups D_{nd} with n even, and S_m with $\frac{1}{2}m$ even, for which the dipole selection rules are given by (4). From two successive dipole transitions we can, again, achieve $\Delta K=0$, ± 1 , or ± 2 , but in this case the correlation with $\Delta\theta$ will be as follows:

$$\begin{aligned} \Delta K &= +2 \text{ with } \Delta\theta = +4\pi/m, \\ \Delta K &= +1 \text{ with } \Delta\theta = \pi + 2\pi/m, \\ \Delta K &= 0 \text{ with } \Delta\theta = 0, \\ \Delta K &= -1 \text{ with } \Delta\theta = \pi - 2\pi/m, \\ \Delta K &= -2 \text{ with } \Delta\theta = -4\pi/m. \end{aligned} \quad (7)$$

or

By applying (7) to the θ circle diagram for the appropriate point group we obtain

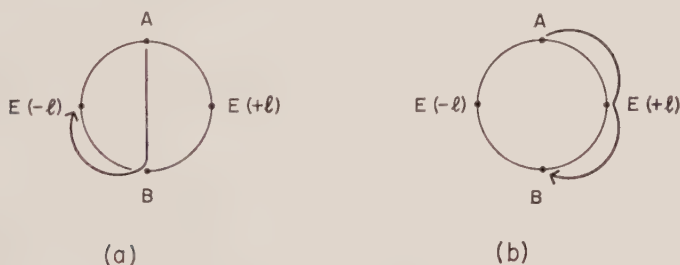


Figure 3. Raman transitions in a D_{2d} or S_4 molecule, interpreted as two successive dipole transitions: (a) $\Delta K = +1$, $E(-l) \leftarrow A$; (b) $\Delta K = +2$, $B \leftarrow A$.

the symmetry species (under the operation S_m) of the vibrational states which combine for any specified value of ΔK . For transitions from a totally symmetric initial state with $\Delta K = \pm 1$ or ± 2 the results are summarized in the table (iv), and for the most important point groups of this category, D_{2d} and S_4 , the allowed transitions are illustrated in figure 3.

† These selection rules are correctly stated by Placzek and Teller [2] (p. 233) and by Placzek [3] (p. 341); however, Teller [4] (p. 133), like Herzberg [5], appears to give the correct selection rules only for the case of C_3 molecules.

The important change is the introduction of an extra term π into the expression for $\Delta\theta$ for the transitions $\Delta K = \pm 1$, which has the effect of reversing the $(+l)$ and $(-l)$ selection rule for these transitions. Thus for $\Delta K = \pm 1$ transitions in D_{2d} molecules we obtain the following formula for the sub-band origins:

$$\nu_{\text{sub}} = \nu_0 + A'(1 + 2\zeta_i) - B' \pm 2[A'(1 + \zeta_i) - B']K + [(A' - A'') - (B' - B'')]K^2. \quad (8)$$

This result does not appear to have been previously derived†. Transitions with $\Delta K = 0$ or ± 2 are not affected by these changes. For D_{2d} and S_4 molecules $\Delta K \pm 2$ gives rise to $B \leftarrow A$ transitions for which there are no $(+l)$ and $(-l)$ components, but for D_{4d} and S_8 molecules $\Delta K = \pm 2$ gives the same formulae as we would obtain for C_8 molecules.

In conclusion it should be repeated that there will often be further restrictions on the selection rules due to the presence of i , σ_h , σ_v or dihedral C_2 , in the symmetry operations of the point group, which have not been discussed in this section. These may be obtained either from the conventional polarizability theory, or from the third common level rule, by interpreting a Raman transition as the result of two successive dipole transitions. In general, of course, the results will be identical. The discrepancy referred to at the end of the preceding section can arise only for transitions with $\Delta K = 0$ between $A_1 \leftrightarrow A_2$ and $B_1 \leftrightarrow B_2$ pairs of levels, and does not arise for Raman transitions involving a degenerate vibrational state.

3. VIBRATION-ROTATION SPECTRA OF ALLENE

The rotational structure of the degenerate CH stretching vibration of the allene molecule, at 3090 cm^{-1} , has been studied in both the infra-red and the Raman spectra [7, 8]. Although neither spectrum was observed with sufficient resolving power to show the J structure, both showed a regular series of sharp Q branches, which are interpreted as being due to the sub-bands arising from the different transitions in K .

Allene is known to belong to the point group D_{2d} , and the band in question is the ν_8 fundamental, the vibrational symmetry of the transition being $E \leftarrow A_1$. From the considerations of the last section we observe that the infra-red and Raman spectra of this band should obey different selection rules: in the infra-red spectrum we should observe $\Delta K = \pm 1$ with $E(+l) \leftarrow A_1$, and in the Raman spectrum $\Delta K = \pm 1$ with $E(\mp l) \leftarrow A_1$. The resulting formula for the sub-band origins in the Raman spectrum is given in equation (8), whereas the equivalent formula for the infra-red spectrum is the more familiar one obtained by reversing the sign of ζ_i in (8), given in Herzberg [5] as equation (IV, 60). Thus we should not expect the Q branches of the sub-bands to appear at the same frequencies in the two spectra, unless it happens that $\zeta_8 = 0$.

† If the selection rules are derived by the method of Placzek and Teller [2], the change in the selection rule appears in the following way. Because the defining symmetry operation for these molecules is a rotation reflection, and not a pure rotation, the α_{xz} and α_{yz} components of the polarizability tensor *change sign* under S_m , although all the other components transform under S_m in the same way as they would under C_m . In consequence equation (20 b) on p. 217 of Placzek and Teller's paper should read:

$$M' - M = \lambda + \mu + m/2,$$

where the extra term $m/2$ appear *only* when $|\lambda + \mu| = 1$, i.e. where $\Delta M (= \Delta K$ in our notation) $= \pm 1$. This change gives the correct selection rules for the point groups in question.

In fact, over most of the band, the observed wavenumbers of the Q branches in the two spectra are nearly, but not quite, the same. This is reasonable, because the two modes of this degenerate vibration should be largely localized in opposite ends of the molecule, so that ζ_8 may be expected to be very close to zero. In the high frequency wing of the band, however, a rotational perturbation is observed, and it is an interesting fact that it appears in different sub-bands in the infra-red and Raman spectra. Brodersen and Richardson [8], who show a graph comparing the observed Q branches in the two spectra, remark that "... it is very surprising that the perturbation appears at higher K values in the Raman spectrum than in the infrared spectrum". I believe that this is simply an experimental confirmation of the fact that the two bands are obeying different selection rules, and that the perturbation (which is discussed in more detail below) appears at different values of K in the $(+l)$ and $(-l)$ levels.

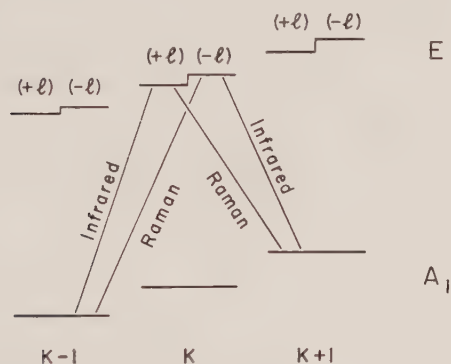


Figure 4. Allowed transitions in an $E \leftarrow A_1$ vibrational band in a D_{2d} molecule. Energy levels are shown for a single value of J and for three different values of K .

Once we recognise the correct selection rules, it is in principle possible to form combinations of infra-red and Raman transitions that give the quantities $A'' - B''$, $2A'\zeta_8$, and $(A' - B')$ independently. Some typical transitions are illustrated in figure 4, and we observe, for example, that

$${}^R Q_{K-1}(J), \text{ infra-red} - {}^P Q_{K+1}(J), \text{ Raman} \\ = F''(J, K+1) - F''(J, K-1) = 4K(A'' - B''). \quad (9)$$

However, the application of combinations like (9) involves the assumption that there are no systematic errors of calibration between infra-red and Raman observations. This difficulty may be avoided in the following way. Overend and Thompson [7] fitted the observed Q branches in the infra-red to a quadratic formula in K to obtain the following result:

$$\nu_8 + A'(1 - 2\zeta_8) - B' = 3090.02 \text{ cm}^{-1}, \quad (10 a)$$

$$A'(1 - \zeta_8) - B' = 4.525 \text{ cm}^{-1}, \quad (10 b)$$

$$(A' - A'') - (B' - B'') = -0.013 \text{ cm}^{-1}. \quad (10 c)$$

Brodersen and Richardson [8] also fitted the observed Q branches in the Raman spectrum to a quadratic formula in K , and found slightly different coefficients; if we interpret their results according to equation (8) we obtain:

$$\nu_8 + A'(1 + 2\zeta_8) - B' = 3090.18 \text{ cm}^{-1}, \quad (11 a)$$

$$A'(1 + \zeta_8) - B' = 4.477 \text{ cm}^{-1}, \quad (11 b)$$

$$(A' - A'') - (B' - B'') = -0.0256 \text{ cm}^{-1}. \quad (11 c)$$

By solving (10 *b*) and (11 *b*) we obtain:

$$A'\zeta_8 = -0.024 \text{ cm}^{-1}. \quad (12)$$

and

$$(A' - B') = 4.501 \text{ cm}^{-1}. \quad (13)$$

A value of $A'\zeta_8$ can also be obtained by solving (10 *a*) and (11 *a*); however, this suffers from the objection mentioned above that it is very sensitive to systematic errors between the Raman and infra-red calibrations; indeed, by comparing (10 *a*) and (11 *a*) with (12) we observe that there is just such a systematic error of the order 0.3 cm^{-1} . If we average the results (10 *c*) and (11 *c*), and make use of (13), we can solve for $(A'' - B'')$. Finally, by making use of the pure rotational Raman observation [9] of the value of B'' , and by further assuming that $(B' - B'')$ in small compared to $(A' - A'')$, we obtain the following vibrational and rotational constants for the ν_8 fundamental of allene:

$$\left. \begin{aligned} \nu_8 &= 3085.6 \pm 0.1 \text{ cm}^{-1}, \\ B'' &= 0.2965 \pm 0.0001 \text{ cm}^{-1} \text{ (ref. [9])}, \\ A'' &= 4.816 \pm 0.005 \text{ cm}^{-1}, \\ A' &= 4.797 \pm 0.005 \text{ cm}^{-1}, \\ \zeta_8 &= -0.0005 \pm 0.001. \end{aligned} \right\} \quad (14)$$

Except for B'' , the estimates of error on the above results are my own estimates based on the authors' original estimates of error, the consistency of the data, and the analysis presented here. It should be emphasised that the zeta sum rule has not been used in this analysis.

The value of A' obtained in (14) is almost exactly equal to the corresponding value for ethylene, implying that the geometry of the CH_2 groups in the two molecules is identical to within the accuracy of the experimental data. This value of A'' is in good agreement with Eaton and Thompson's results on allene— $1.1-d_2$ [10], but is in rather poor agreement with almost all the previous determinations of A for allene from a study of the infra-red perpendicular bands. There are two reasons for this. The first is that most of the earlier workers made use of the zeta sum rule in their analysis, and in fact used the wrong value of the zeta sum, as shown by Mills and Duncan [11]. The second reason is that all of the earlier analyses have been based on an incorrect assignment of the Q branches in the ν_9 fundamental band. In a paper to be published shortly [12] it will be shown that the RQ_0 sub-band of the ν_9 fundamental should be associated with the Q branch at 1002 cm^{-1} ; if all of the perpendicular bands are re-analysed using this assignment, and using the correct zeta sum rule, the results give a value of the A rotational constant in excellent agreement with the result (14). Thus it seems that the results in (14) may be taken to be quite reliable.

By combining the value of A'' in (14) with the values of B'' determined by Stoicheff [9], the molecular geometry is found to be:

$$\angle \text{HCH} = 118.2 \pm 0.5^\circ, \text{ CH} = 1.084 \pm 0.005 \text{ \AA}, \text{ and CC} = 1.309 \text{ \AA}.$$

To complete this discussion we offer a tentative explanation of the rotational perturbation which is observed in the high RQ_K sub-bands in both the infra-red and Raman spectra of ν_8 . The effect is to shift the apparent Q branch maxima to high frequencies; in the infra-red this perturbation appears around $K=7$ or 8, and in the Raman spectrum around $K=9$ or 10. A possible explanation lies in Coriolis perturbation about the X and Y axes between $\nu_8(E \leftarrow A_1)$ and the fundamentals of $\nu_1(A_1 \leftarrow A_1)$ and $\nu_5(B_2 \leftarrow A_1)$. An examination of the matrix elements the perturbation operator $(-p_x P_x - p_y P_y)/I_B$ shows that the perturbation connects the pair of levels $|v_1=1; J, K+1\rangle$ and $|v_8=1, (+l); J, K\rangle$, and also the pair of levels $|v_5=1; J, K+1\rangle$ and $|v_8=1, (-l); J, K\rangle$. The first perturbation should show a resonance when $\nu_1 + F'(J, K+1) = \nu_8 + F'(J, K(+l))$, and the second when $\nu_5 + F'(J, K+1) = \nu_8 + F'(J, K(-l))$. Thus such perturbations can appear at different positions in the $(+l)$ and $(-l)$ levels of ν_8 . Since the band origins of ν_1 , ν_5 and ν_8 are all accurately known it is possible to estimate where the resonance should occur and hence where the perturbation should appear in the spectrum; such estimates suggest that this could be an explanation of the observed perturbation, but more detailed observations of the spectra are required to verify this interpretation.

I am indebted to Dr. B. P. Stoicheff for a critical reading of the manuscript of this paper, and to several colleagues for assistance in translating references [2] and [3] from the German.

REFERENCES

- [1] MILLS, I. M., 1964, *Mol. Phys.*, **7**, 549.
- [2] PLACZEK, G., and TELLER, E., 1933, *Z. Phys.*, **81**, 209.
- [3] PLACZEK, G., 1934, *Handb. Radiol.*, **6**, 205.
- [4] TELLER, E., 1943, *Handb. Jb. Chem. Phys.*, **9**, 43.
- [5] HERZBERG, G., 1945, *Infrared and Raman Spectra* (D. van Nostrand Co. Inc.).
- [6] HOUGEN, J. T., 1962, *J. chem. Phys.*, **37**, 1433; 1963, *Ibid.*, **39**, 358.
- [7] OVEREND, J., and THOMPSON, H. W., 1956, *Trans. Faraday Soc.*, **52**, 1295.
- [8] BRODERSEN, S., and RICHARDSON, E. H., 1960, *J. mol. Spectrosc.*, **4**, 439.
- [9] STOICHEFF, B. P., 1955, *Canad. J. Phys.*, **33**, 811.
- [10] EATON, D. R., and THOMPSON, H. W., 1959, *Proc. roy. Soc., A*, **250**, 39.
- [11] MILLS, I. M., and DUNCAN, J. L., 1962, *J. mol. Spectrosc.*, **9**, 244.
- [12] SMITH, W. L., DUNCAN, J. L., and MILLS, I. M., (to be published).

Excitons in molecular crystals

by G. N. FOWLER

University of Newcastle upon Tyne

(Received 27 January 1964)

A discussion is given of excitons in molecular crystals using the analogy of the electron gas and the results are compared with those of Hall and Hopfield. Physical processes in which excitons are likely to be important are briefly reviewed.

1. INTRODUCTION

In a recent paper by Hall [1], referred to in the following as A, a new approach to the theory of excitation waves in a molecular crystal has been proposed. It is the purpose of the present paper to discuss this in detail in order to demonstrate the connection with previous work on excitations in solids. It will be shown that Hall's theory fails to satisfy an important restriction on the functional dependence of dielectric constant on frequency and the appropriate corrections are derived.

We begin by summarizing the theory presented in A. It is concerned with the interaction of optically excited molecules in a molecular crystal and represents this interaction as an interaction between electric dipoles situated at lattice sites in the crystal. Given the translational symmetry of the crystal this interaction gives rise in a familiar way to a contribution to the total energy of the crystal which has the form of an energy band. It is shown that techniques well known in handling dipolar sums make it possible to write this contribution in the form:

$$W(\mathbf{k}) = U - \mathbf{T} \cdot \mathbf{E}_i + \frac{4\pi}{v} \frac{(\mathbf{T} \cdot \mathbf{k})^2}{k^2} - \frac{4\pi}{3v} (\mathbf{T} \cdot \mathbf{T}). \quad (1)$$

Here U is the excitation energy of one molecule, \mathbf{T} is the transition dipole moment of a molecule, \mathbf{E}_i is the effective field produced by the dipoles inside a large sphere drawn round an arbitrary point in the crystal (as in the Lorenz-Lorentz treatment of dipolar sums), \mathbf{k} is the crystal momentum and v the volume of the unit cell. Hall proceeds to show that retardation is important in this problem so that Maxwell's equations are to be satisfied in the medium. Since the fields are now time dependent the perturbation is also time dependent and this introduces a further time dependence into the crystal wave functions. The various conditions arising in this way give rise to a dispersion relation connecting frequency with wave number when it is assumed that all the physical quantities introduced have a space time dependence of the form:

$$\mathbf{T} = \mathbf{T}_0 \exp(i\mathbf{k} \cdot \mathbf{x} - i\omega t). \quad (2)$$

This dispersion relation has three types of solution, one longitudinal and two transverse. We shall be most concerned with the transverse solutions of which

one corresponds to an electromagnetic wave travelling through the crystal and is independent of \mathbf{T} . The other is the one which is of real physical interest because it is produced by the dipole interactions and has a transverse character so that it corresponds to an excitation wave which can be directly produced by incident electromagnetic radiation. It is the demonstration of the existence of this particular excitation mode which is the essentially new and important result of A. Further examination of the dispersion relation for this mode reveals that it has the form of a cubic equation for ω with one negative and two positive roots of which the negative root is discarded as having no physical significance.

It is at this point that we recall that such excitation modes must correspond to zeros of a generalized wave number and frequency dependent dielectric constant $\epsilon(\mathbf{k}, \omega)$ [2, 3] because they refer to the possibility of non-vanishing electric fields in the medium in the absence of external sources.

Now the fact that the electric and magnetic fields must be real implies that:

$$\epsilon(\mathbf{k}, \omega) = \epsilon^*(-\mathbf{k}, -\omega)$$

or

$$\left. \begin{aligned} \operatorname{Re} \epsilon(\mathbf{k}, \omega) &= \operatorname{Re} \epsilon(-\mathbf{k}, -\omega), \\ \operatorname{Im} \epsilon(\mathbf{k}, \omega) &= -\operatorname{Im} \epsilon(-\mathbf{k}, -\omega). \end{aligned} \right\} \quad (3)$$

These are the appropriate crossing relations familiar in Kramers-Kronig dispersion theory. Together with arguments based on Lorentz invariance they imply that if ϵ is taken to be real, then the roots of $\epsilon(\mathbf{k}, \omega) = 0$ will be symmetric about $\omega = 0$, a feature which is not reproduced by the solutions corresponding to the interesting mode found in A. Indeed the asymmetry of the latter may be traced back to the use of (2) in both Maxwell's equations and the time dependent Schroedinger equation. Solutions of the former may be chosen to be real or complex at will, solutions of the latter may not.

After the work reported in the present paper was completed the author's attention was called to the work of Hopfield [2] and Agranovitch [3] on the same problem. These authors give a treatment, using the methods of second quantization, which parallels very closely that given by Hall. The results, however, are different and agree with those given in the following. In view of this discrepancy and because the presentation is, in some respects, different from the other authors referred to we feel that it is worth while to present a further discussion of the problem.

We begin by discussing it from the electromagnetic field point of view.

2. ELECTROMAGNETIC FIELD POINT OF VIEW†

We shall restrict ourselves to the transverse modes only, so that the propagation modes in the crystal are given by the poles of the photon propagator. This is defined as:

$$D(x-x') = 2\delta_{\mu\nu} \langle 0 | T(A_\mu(x), A_\nu(x')) | 0 \rangle,$$

where $|0\rangle$ represents the photon vacuum state, the A_μ are the exact electromagnetic field variables and T is the time ordering operator. We may express D in terms of D_0 , the corresponding quantity to D for non-interacting photons and \mathcal{P} a quantity representing the polarization of the system which is defined by:

$$\mathcal{P} = \delta_{\mu\nu} \prod_{\mu\nu},$$

† We use units in which $\hbar = c = 1$.

where $\prod_{\mu\nu}^{-1}$ is related to A_μ and the induced current by:

$$j_\mu = \int \prod_{\mu\nu}(x-x') A_\nu(x') dx',$$

and we take the transverse part only of $\prod_{\mu\nu}$.

The resulting formal expression for D is:

$$D = \frac{D_0}{1 - D_0 \mathcal{P}}$$

and in Fourier space:

$$D_0 = \frac{1}{k^2 - \omega^2}.$$

For \mathcal{P} we may use the usual Kramers-Heisenberg formula for the case of a single excited state chosen to be the particular dipole excited state which is of interest. This gives:

$$D = \frac{D_0}{1 + D_0 \frac{8\pi e^2 |\mathbf{T}|^2 \omega^2 \Delta}{v(\omega^2 - \Delta^2)}}, \quad (4)$$

where \mathbf{T} is the dipole matrix element, $\Delta = E_{l_D} - E_{l_0}$ is the dipole excitation energy in the free molecule, v is the volume of the unit cell and we assume one molecule per unit cell. Hence $D^{-1} = 0$ is the required condition.

It is also useful to introduce a two-electron Green's function K defined by:

$$K = \delta_{\mu\nu}(i)^2 \langle 0 | T(j_\mu(x) j_\nu(x')) | 0 \rangle,$$

where $j_\mu(x)$ is the electron current expressed in terms of electron field variables $\psi(x)$, T the time ordering operator and $|0\rangle$ represents the ground state of the electron system. This may be related to the quantities D and \mathcal{P} following Tyablikov and Bonch-Bruевич [5] so that

$$D = D_0 + D_0 K D_0$$

or formally

$$K = \frac{\mathcal{P}}{1 - D_0 \mathcal{P}} \quad \text{and} \quad D = D_0 + D_0 \mathcal{P} D.$$

This demonstrates that the excitation modes of the system correspond to the photon propagation modes in that a pole of D corresponds to a pole of K .

We take up the question of the response of the system in the next section.

3. DIPOLE SYSTEM POINT OF VIEW

A convenient approach to the problem from the point of view of the system may be found by a slight adaptation of Wentzel's [6] discussion of the diamagnetism of a dense electron gas. The electron field variables are replaced by scalar meson pair variables according to the following prescription.

We first introduce electron annihilation and creation operators by

$$\psi(\mathbf{x}) = \sum_{\mathbf{p}, l} a_{\mathbf{p}, l} u_{\mathbf{p}, l}(\mathbf{x}). \quad (5)$$

The states $u_{\mathbf{p}, l}(\mathbf{x})$ are Bloch states of momentum \mathbf{p} and angular momentum band l . When this is done the Hamiltonian for the electron field system will

consist of products of annihilation and creation operators. We next single out pairs of such operators:

$$c_{\mathbf{p}, \mathbf{q}} = a_{\mathbf{p}, l_0}^\dagger a_{\mathbf{p}+\mathbf{q}, l_D}.$$

Where $a_{\mathbf{p}, l_0}^\dagger$ is the creation operator of an electron of momentum in band l_0 , the ground state band, and $a_{\mathbf{p}+\mathbf{q}, l_D}$ is the annihilation operator of an electron of momentum $\mathbf{p} + \mathbf{q}$ in band l_D , the excited dipole band. We now introduce canonical meson pair variables by the substitution:

$$\left(\frac{1}{2\omega_{\mathbf{p}, \mathbf{q}}}\right)^{1/2} (c_{\mathbf{p}, \mathbf{q}} + c_{-\mathbf{p}, -\mathbf{q}}^\dagger) = \phi_{\mathbf{p}, \mathbf{q}} \equiv \phi_{-\mathbf{p}, -\mathbf{q}}^\dagger, \quad (6)$$

$$i\left(\frac{\omega_{\mathbf{p}, \mathbf{q}}}{2}\right)^{1/2} (c_{\mathbf{p}, \mathbf{q}}^\dagger - c_{-\mathbf{p}, -\mathbf{q}}) = \Pi_{\mathbf{p}, \mathbf{q}} \equiv \Pi_{-\mathbf{p}, -\mathbf{q}}^\dagger, \quad (6')$$

with

$$\omega_{\mathbf{p}, \mathbf{q}} = E_{\mathbf{p}+\mathbf{q}, l_D} - E_{\mathbf{p}, l_0}.$$

The free Hamiltonian of the electron field then becomes:

$$H_0 = \frac{1}{2} \left(\sum_{\mathbf{p}, \mathbf{q}} \Pi_{\mathbf{p}, \mathbf{q}}^\dagger \Pi_{\mathbf{p}, \mathbf{q}} + \omega_{\mathbf{p}, \mathbf{q}}^2 \phi_{\mathbf{p}, \mathbf{q}}^\dagger \phi_{\mathbf{p}, \mathbf{q}} - \omega_{\mathbf{p}, \mathbf{q}} \right). \quad (7)$$

With regard to the interactions of the electron field we note that the positive background, usually considered uniform, is in our case sufficient to screen out the purely Coulomb interaction by definition. The interactions which remain are the Coulomb interactions of the transition dipoles, which we shall include in a simple way at a later stage, and the interaction of the electron field with the transverse quantized electromagnetic field. This latter may be written in the form:

$$H_I = i \sum_{\mathbf{k}} \Phi_{\mathbf{k}}^{(r)} (4\pi)^{1/2} \frac{e}{2m} \sum_{\mathbf{p}} |\langle \mathbf{p} \cdot \mathbf{e} \rangle| \Pi_{\mathbf{p}, \mathbf{k}} \left(\frac{2}{\omega_{\mathbf{p}, \mathbf{k}}} \right)^{1/2} + \text{h.c.}, \quad (8)$$

where $\langle \mathbf{p} \cdot \mathbf{e} \rangle$ is given by:

$$\langle \mathbf{p} \cdot \mathbf{e} \rangle = \int u_{\mathbf{p}+\mathbf{k}, l_D}(\mathbf{x}) \nabla \cdot \mathbf{e} \exp(i\mathbf{k} \cdot \mathbf{x}) u_{\mathbf{p}, l_0}(\mathbf{x}) d\mathbf{x}. \quad (8')$$

Here \mathbf{e} is the radiation polarization vector and we use the Coulomb gauge. Strictly speaking (8) and (8') are correct only in the nearly free approximation, and we should use (6) and (6') with a phase difference between the two terms of the left-hand sides but this does not introduce anything new.

The free radiation field is:

$$H_{\text{rad}} = \frac{1}{2} \sum_{\mathbf{q}} \Pi_{\mathbf{q}}^{(r)\dagger} \Pi_{\mathbf{q}}^{(r)} + \nu_{\mathbf{q}}^2 \Phi_{\mathbf{q}}^{(r)\dagger} \Phi_{\mathbf{q}}^{(r)},$$

where

$$\nu_{\mathbf{q}}^2 = \mathbf{q}^2,$$

and the additional quadratic term in the Hamiltonian is of the form:

$$H_I^{(2)} = \sum_{\mathbf{k}} \Phi_{\mathbf{k}}^{(r)\dagger} \Phi_{\mathbf{k}}^{(r)} 4\pi \frac{e^2}{m^2} \sum_{\mathbf{p}} \frac{|\langle \mathbf{p} \cdot \mathbf{e} \rangle|^2}{\omega_{\mathbf{p}, \mathbf{k}}}, \quad (9)$$

using the oscillator strength sum rule.

If we now replace $\prod_{\mathbf{p}, \mathbf{k}}$ according to:

$$\prod_{\mathbf{p}, \mathbf{k}} \rightarrow -i\omega_{\mathbf{p}, \mathbf{k}} \phi_{\mathbf{p}, \mathbf{k}}$$

(essentially a semi-classical approximation), we find that:

$$H_I = \sum_{\mathbf{k}} \Phi_{\mathbf{k}}^{(r)} \frac{e}{2m} \sum_{\mathbf{p}} |\langle \mathbf{p} \cdot \mathbf{e} \rangle| (2\omega_{\mathbf{p}, \mathbf{k}})^{1/2} \phi_{\mathbf{p}, \mathbf{k}} + \text{h.c.} \quad (10)$$

The problem is now soluble by a normal mode transformation and we find that the equation for the eigenfrequencies, including $H_I^{(2)}$, is:

$$1 - \frac{8\pi\omega^2 e^2}{(\omega^2 - \nu_{\mathbf{k}}^2)m^2} \sum_{\mathbf{p}} \frac{|\langle \mathbf{p} \cdot \mathbf{e} \rangle|^2}{(\omega^2 - \omega_{\mathbf{p}, \mathbf{k}}^2)\omega_{\mathbf{p}, \mathbf{k}}} = 0 \quad (11)$$

This is the same as the previous result with $\Delta = \omega_{\mathbf{p}, \mathbf{k}}$.

Two comments are appropriate at this point. The first is that in common with the corresponding treatment of the electron gas our result involves the random phase approximation. This will be discussed further below. The second is that in contrast with the case of the electron gas the particle hole pairs are partially correlated in the present case. This is implied by the fact that \mathbf{p} dependent matrix elements appear in the interaction terms.

4. RESULTS

Before comparing these results with those given in A we must consider in more detail the physical significance of the random phase approximation applied to the present case. In the first place it is well known that the R.P.A. does not include the local field corrections [7]† which need to be included in calculating the dielectric constant. These local field corrections are the contributions from the surface charges at the surface of the large sphere drawn round the point at which the field is to be found and the contribution from the polarized matter inside the sphere. These contributions are only to be found when we go beyond the R.P.A., since in that approximation different Fourier components of the density fluctuation do not combine and we cannot describe localized charge fluctuations. Since it is to be expected that corrections to the R.P.A. should be important in the present case because the particles and holes are correlated, significant deviations from the R.P.A. may arise. However, for the moment we shall compare the results given by (11) directly with those of A and we shall then see what changes need to be made to allow for local field corrections.

If we make the tight binding approximation we find that the eigenfrequencies are given by:

$$\omega_{\mathbf{k}}^2 = \frac{1}{2}(\Delta^2 + \mathbf{k}^2) + \frac{4\pi e^2 |\mathbf{T}|^2 \Delta}{v} \pm \frac{1}{2} \left\{ \left(\Delta^2 + \mathbf{k}^2 + \frac{8\pi \Delta e^2 |\mathbf{T}|^2}{v} \right)^2 - 4\Delta^2 \mathbf{k}^2 \right\}^{1/2}, \quad (12)$$

taking one dipole in the unit cell.

The transverse frequency dependent dielectric constant is given by:

$$\epsilon_T(\omega_{\mathbf{k}}) = \frac{\mathbf{k}^2}{\omega_{\mathbf{k}}^2} = 1 + \frac{8\pi e^2 |\mathbf{T}|^2 \Delta}{v(\Delta^2 - \omega_{\mathbf{k}}^2)}, \quad (13)$$

which is of course the usual result.

† This is also implied by the omission of Umklapp processes.

If we retain only the positive frequency part of \mathcal{P} we recover Hall's result, provided we allow for the local field corrections by making a change in the interaction terms of (8), namely:

$$-\frac{\omega_{\mathbf{k}}^2}{\mathbf{k}^2 - \omega_{\mathbf{k}}^2} \rightarrow -\frac{\omega_{\mathbf{k}}^2(1 + \bar{e})}{\mathbf{k}^2 - \omega_{\mathbf{k}}^2} - \frac{1}{3}. \quad (14)$$

The quantity \bar{e} appears when we allow for the polarizing effect of the field inside the sphere by assuming that it is proportional to the field outside with proportionality constant \bar{e} .

In making this change we are including the dipole-dipole interactions which we have so far omitted. The second term on the right-hand side of (14) corresponds to the transverse instantaneous interaction, the term proportional to \bar{e} is not included by Hopfield.

With this modification the dispersion relation for $\omega_{\mathbf{k}}$ becomes:

$$\begin{aligned} \omega_{\mathbf{k}}^2 = & \frac{1}{2}(\Delta^2 + \mathbf{k}^2) + \frac{4(2 + 3\bar{e})\pi e^2 |\mathbf{T}|^2 \Delta}{3v} \\ & \pm \frac{1}{2} \left\{ \left(\Delta^2 + \mathbf{k}^2 + \frac{8}{3v} (2 + 3\bar{e})\pi e^2 |\mathbf{T}|^2 \Delta \right)^2 - 4\mathbf{k}^2 \Delta \left(\Delta - \frac{4}{3} \frac{(2 + 3\bar{e})}{v} \pi e^2 |\mathbf{T}|^2 \right) \right\}^{1/2} \end{aligned} \quad (15)$$

and ϵ_T is now given by:

$$\epsilon_T = 1 + \frac{4\pi(2 + 3\bar{e})\Delta e^2 |\mathbf{T}|^2}{v \left(\Delta^2 - \omega_{\mathbf{k}}^2 - \frac{4\pi\Delta e^2 |\mathbf{T}|^2 (2 + 3\bar{e})}{3v} \right)}.$$

This gives, for example, a pole of ϵ_T at:

$$\omega_{\mathbf{k}} = \left(\Delta^2 - \frac{4\pi e^2 |\mathbf{T}|^2 \Delta (2 + 3\bar{e})}{3v} \right)^{1/2}.$$

This agrees with Hopfield's result if we take $\bar{e} = 0$. If we expand in $e^2 |\mathbf{T}|^2 / \Delta$ we find the approximate result:

$$\omega_{\mathbf{k}} = \Delta - \frac{2\pi e^2}{3v} |\mathbf{T}|^2 (2 + 3\bar{e}),$$

in agreement with Hall as we would expect since for small $e^2 |\mathbf{T}|^2 / \Delta$, \mathcal{P} is given by its positive frequency part to a good approximation. Corrections for finite band width can be incorporated in an obvious way.

5. DISCUSSION

The physical nature of the excitation modes follows directly from the nature of the normal mode transformation which we have used. The excitation modes are particle hole plus photon modes. From the point of view of the field they are photons with a cloud of virtual particle hole pairs. At this stage and for frequencies between Δ and ω_1 such that $\epsilon(\omega_1) = 0$ there are no photon eigenvalues for real k . However, if we allow for absorption processes such as phonon production which absorb the particle hole pairs (excitons) or photons, then by allowing Δ to become complex we find that in certain circumstances there are

then three roots of the real part of (11), two of which correspond to the eigenmodes described above, while the third has a value close to Δ .

In order to understand the physical origin of this new mode we first of all disregard absorption and compare the present case with the rather similar problem of the Lee model [13] and it is then convenient to include a finite exciton width by allowing for the ground state and excited state band widths. When this is done we may infer that although there is no root of (11) for frequencies ω within the exciton band there will be a root of the analytic continuation of (11) on the first unphysical sheet reached through the cut in the ω plane arising from the possibility of real photon exciton transitions. This pole of D corresponds to the now unstable photon, unstable because it can 'decay' into a particle hole pair. When we include absorption by allowing the exciton energies to become complex this in effect exposes part of the unphysical sheet so that the unstable pole is visible. Thus for some real values of k we encounter three poles and for other values one only. This implies that in that case the other two poles have moved on to a different unphysical sheet. The third mode is therefore essentially the photon decay mode into excitons. Since the absorption occurs mainly through excitons it is this mode which is chiefly responsible for the absorption of radiation. The position of the main absorption band would then be identical with that found in the free molecule were it not for the local field corrections. These tend to shift the absorption band towards lower frequencies to an extent which depends very much on the magnitude of the local field corrections.

For a further discussion of the physical questions involved in the absorption of light by molecular crystals the reader is referred to Hopfield's paper.

The conclusion which we may draw at this point from a comparison of the work of Hall and Hopfield with the foregoing is that whereas Hall considers the problem from the point of view of the retarded interaction between the dipoles, Hopfield and the author treat the radiation field and the dipole system on a equal footing. This maintains the correct crossing property and provides a more satisfactory physical interpretation of the phenomena.

If we turn to the interpretation of experiments we find, apart from Hopfield's work on CdS [8] two possible areas where the foregoing considerations may be particularly relevant. The first is the phenomenon of hypochromism, which is discussed in a separate paper by the author [9], but the general conclusion is that the dynamic exciton modes give a contribution to the oscillator strength in addition to that coming from the main absorption band. Hence the reduction in absorption of molecules when in crystalline aggregates, i.e. hypochromism.

The second concerns the origin of photoconductivity in molecular crystals and in particular the fact that large photo-currents can be generated by light which is not energetic enough to produce photo-electrons directly. This has been attributed to exciton-exciton interactions by Northrop and Simpson [10] and this mechanism has been further discussed by Choi and Rice [11]. The latter authors consider the exciton-exciton (or particle hole-particle hole in our terminology) interaction arising from the transition dipole-dipole interaction and find reasonable agreement with experiment. However it should be clear from the foregoing that the interactions of the transverse excitons are already taken into account as local field corrections and the longitudinal excitons are not excited hence this explanation fails. An alternative in terms of dynamic excitons immediately suggests itself. This could be the coupling of dynamic

excitons of the ω_- mode, due to particle hole phonon interactions, to give a ω_+ dynamic exciton. This could then produce a photo-electron in exactly the same way as a photon of the appropriate frequency since the ω_+ (and ω_-) modes are essentially combinations of photon and particle hole states. This would give an increase in photo-current with temperature and a non-linear dependence on intensity as observed by Silver *et al.* quoted by Choi and Rice [12].

Thanks are due to Professor Hall for a stimulating seminar in which the author's interest on this problem originated and to Dr. I. D. C. Gurney for discussions.

The author is also indebted to the referee for calling the work of Agranovitch [3] to his attention.

REFERENCES

- [1] HALL, G. G., 1962, *Proc. roy. Soc. A*, **270**, 285.
- [2] HOPFIELD, J. J., 1958, *Phys. Rev.*, **112**, 1555.
- [3] AGRANOVITCH, V. M., 1960, *Soviet Physics, J.E.T.P.*, **10**, 307.
- [4] PINES, D., 1961, *The Many-body Problem* (New York : W. A. Benjamin Inc.).
- [5] TYABLIKOV, S. V., and BONCH-BRUEVICH, V. L., 1962, *Advanc. Phys.*, **11**, 317.
- [6] WENTZEL, G., 1957, *Phys. Rev.*, **108**, 1593.
- [7] NOZIERES, P., and PINES, D., 1958, *Nuovo Cim.*, **9**, 470.
- [8] HOPFIELD, J. J., and THOMAS, D. G., 1959, *Phys. Rev.*, **116**, 573.
- [9] FOWLER, G. N., 1964, *Mol. Phys.*, **8**, 383.
- [10] NORTHROP, D. C., and SIMPSON, O., 1958, *Proc. roy. Soc. A*, **244**, 377.
- [11] CHOI, S. I., and RICE, S. A., 1962, *Phys. Rev. Letters*, **8**, 410.
- [12] CHOI, S. I., and RICE, S. A., 1963, *J. chem. Phys.*, **38**, 366.
- [13] LEVY, M., 1959, *Nuovo Cim.*, **13**, 115.

On the theory of hypochromism

by G. N. FOWLER

University of Newcastle upon Tyne

(Received 27 January 1964)

The response of a molecular crystal to electromagnetic radiation is discussed in terms of a response function using the analogy of the electron gas and the results of the previous paper. A qualitative explanation of the phenomenon of hypochromism is suggested according to which the 'missing' oscillator strength goes into the photon-exciton modes found by Hopfield.

1. INTRODUCTION

A characteristic feature of the absorption of electromagnetic radiation by polymers is the sharp decrease in absorption compared with that of the corresponding monomer. An explanation of this phenomena, the so-called hypochromic effect, has recently been put forward by Bolton and Weiss [1] which takes into account the role of the imaginary part of the polarization in reducing the effective radiation field amplitude at the actual lattice sites, thus reducing the absorption. This approach has been further discussed by Nesbet [2] who gives a detailed microscopic account of the induced field. There are however ambiguities in the treatment of the latter author and in any case none of these authors attempt to account for the 'missing' oscillator strength.

In the following the absorption of radiation is discussed using the quantum field techniques of an earlier paper [3] (referred to as A in the following). It is shown that the dynamic excitons first introduced by Hall [4] and further discussed in A could indeed account for the hypochromic effect. The 'missing' oscillator strength is to be found in the excitation of particle hole plus photon modes of the polymer system, discussed in A. These are transverse excitation modes of both lower and higher frequency than the absorption band and they can be understood as arising through the interaction of the transition dipoles of the system with the electromagnetic field in the medium. It should be mentioned that these modes are not strongly absorbed and this is true in particular of the higher frequency mode so that they may be not readily observable in the absorption spectrum at higher frequencies. The formal parallel between this system and the electron gas is close and is discussed in more detail in A.

2. THE RESPONSE OF THE SYSTEM

The transition amplitude for the absorption of radiation by the system is given in terms of the matrix element†:

$$M_{0n} = \langle \Psi_n | \int d^4x \mathbf{j}(x) \cdot \mathbf{A}(x) | \Psi_0 \rangle \quad (1)$$

† We use units in which $\hbar = c = 1$.

with

$$\mathbf{j}(x) = \frac{e}{m} \psi^\dagger(x) \mathbf{p} \psi(x)$$

and $|\Psi_0\rangle$ and $|\Psi_n\rangle$ are exact eigenstates of the system.

We write for the radiation field vector potential:

$$\mathbf{A}(x) = \sum_{\lambda=1,2} \mathbf{e}^\lambda \sum_{\mathbf{k}, \omega} a_{\mathbf{k}}^\lambda \exp(i\mathbf{k} \cdot \mathbf{x} - i\omega t) + \text{h.c.},$$

where λ denotes the polarization and we work in the Coulomb gauge so that

$$\text{div } \mathbf{A} = 0.$$

The current in second quantized form may be written in Heisenberg picture:

$$\mathbf{j}(\mathbf{x}, t) = \exp(-iHt) \mathbf{j}(\mathbf{x}) \exp(iHt),$$

where H is the total Hamiltonian of the system.

The time integration in (1) may now be carried out to give:

$$M_{0n} = 2\pi \langle \Psi_n | \int \mathbf{j}(\mathbf{x}) \cdot \mathbf{A}(\mathbf{x}) d\mathbf{x} | \Psi_0 \rangle (\delta(\omega - E_n + E_0) + \delta(\omega + E_n - E_0)). \quad (2)$$

The transition probability per unit time is therefore

$$P = 2\pi |\langle \Psi_n | \int \mathbf{j}(\mathbf{x}) \cdot \mathbf{A}(\mathbf{x}) d\mathbf{x} | \Psi_0 \rangle|^2 (\delta(\omega - E_n + E_0) + \delta(\omega + E_n - E_0)). \quad (3)$$

In Fourier space this may be written for the \mathbf{k} component of \mathbf{A} :

$$P_{\mathbf{k}} = 2\pi \sum_{\lambda} |a_{\mathbf{k}}^\lambda \langle \Psi_n | \mathbf{e}^\lambda \cdot \mathbf{j}(\mathbf{k}) | \Psi_0 \rangle|^2 \delta(\omega - E_n + E_0), \quad (4)$$

taking into account only absorption processes and unpolarized radiation.

We can now discuss the response of the system in terms of a response function [5]

$$R(\mathbf{k}, \omega) = \sum_n |\langle \Psi_n | \mathbf{e}^\lambda \cdot \mathbf{j}(\mathbf{k}) | \Psi_0 \rangle|^2 \delta(\omega - E_n + E_0), \quad (5)$$

and if $\mathbf{j}(\mathbf{k})$ is identified with

$$\frac{ie}{m} \sum_{\mathbf{p}} \hat{p} \prod_{\mathbf{p}, \mathbf{k}} \left(\frac{\omega_{\mathbf{p}, \mathbf{k}}}{2} \right)^{-1/2} + \text{h.c.}, \quad (5')$$

using the notation of A, then R is the imaginary part of the positive frequency part of a particle hole propagator which we have denoted by K in A.

In fact [5]:

$$R(\mathbf{k}, \omega) = \frac{1}{2\pi^2} \text{Im} \int_0^\infty ds \int_{-\infty}^\infty d\omega' \exp[i(\omega - \omega')s] \frac{\mathcal{P}(\mathbf{k}, \omega')}{1 - D_0 \mathcal{P}(\mathbf{k}, \omega')}, \quad (6)$$

where \mathcal{P} is the polarization of the system, D_0 the free photon propagator and V the volume of the unit cell.

In order to evaluate (6) we can complete the contour of integration over ω' in the lower half plane of a particular Riemann sheet (see A) of the complex variable ω' and find a sum of contributions from the zero of the denominator plus a background term arising from the deformation of the contour of integration.

After integrating over s we can see that the main contribution will come from the values of ω given by the poles of D , the photon propagator defined in A. As has been discussed in A, there are three such poles for a certain range of k , and of the three, one corresponds to the absorption line of the free molecule. The other two correspond to the dynamic excitons discussed in A and references [4] and [6] (if we calculate \mathcal{P} using $\Pi_{\mathbf{p},\mathbf{q}} \rightarrow i\omega_{\mathbf{p},\mathbf{q}}\phi_{\mathbf{p},\mathbf{q}}$). (Alternatively since we are only concerned with the imaginary part of the integral in (6) we may find this directly from the definition of K and the fact that R is the imaginary part of the positive frequency part of K .) If we disregard the denominator in (6) we find just the usual absorption line characteristic of the free molecule.

It may now readily be shown using the Hamiltonian of A including absorption processes and the usual canonical commutation relations of A that:

$$\begin{aligned} \sum_{i=1}^3 [j_i^\dagger(\mathbf{k}), [j_i(\mathbf{k}), H]] &= \int_{-\infty}^{\infty} \omega(R(\mathbf{k}, \omega) + R(-\mathbf{k}, \omega)) d\omega \\ &= \frac{e^2}{m^2} \sum_{\mathbf{p}'} \left(\omega_{\mathbf{p}'} - \frac{8\pi e^2 |\mathbf{T}|^2}{3v} \right) \left| \int u_{\mathbf{p}'+\mathbf{k}, l_D}(\mathbf{x}) \nabla \exp(i\mathbf{k} \cdot \mathbf{x}) u_{\mathbf{p}', l_0}(\mathbf{x}) d\mathbf{x} \right|^2, \quad (7) \end{aligned}$$

where the second term in the bracket arises from local field corrections if (5') holds.

If we make the usual approximation of neglecting the k dependence of the right-hand side of this equation we find, for our two-band model, that (7) is closely related to the total oscillator strength of the electrons concerned in the transition. Since the latter quantity satisfies a sum rule we may infer that a reduction in oscillator strength for absorption will occur which is compensated by the oscillator strength going mainly into the higher frequency exciton mode (since higher frequencies are favoured in (9)). This could clearly account for the hypochromic effect.

3. DISCUSSION

The explanation given by Bolton and Weiss may be recovered by taking the longitudinal terms in the dipole-dipole interaction only. The denominator of (6) then reduces to the usual dielectric constant. If one now performs the integration as before the numerator pole gives the Bolton-Weiss result and the denominator zero now corresponds to a longitudinal plasma type excitation which would not be excited by incident radiation. After this work was completed the author's attention was drawn to a paper by Hopfield [6] in which the importance of the dynamic exciton modes discussed in A in the absorption of light by crystals is also discussed in a similar way. The circumstances in which these modes are expected to be important depend upon the particle hole interactions neglected in A, that is interactions with phonons, impurities and lattice defects. Thus, provided the rate of energy transfer between particle hole and photon is large compared with all other particle hole transition probabilities, the analysis presented in the foregoing is applicable. Furthermore the techniques used in A require that the number of excitations be small compared with the total number of molecules in the crystal. Hence, even for quite small polymer aggregates, the effect may be noticeable and has indeed been observed. Also it is known that in the case of the nucleic acids when the polymer exists in the

rod form the hypochromic effect is observed and when it is in the form of a coil the effect largely disappears. This may be due to the fact that the phonon spectrum and the exciton phonon coupling should be very different in the two cases, and it may be that the conditions for the existence of dynamic excitons are not satisfied in the second case.

Thanks are due to Professor J. J. Weiss for drawing the author's attention to this problem and to Professor R. E. Peierls and Dr. E. J. Squires for discussions.

REFERENCES

- [1] BOLTON, H. C., and WEISS, J. J., 1962, *Nature, Lond.*, **195**, 666.
- [2] NESBET, R. K., 1962, preprint.
- [3] FOWLER, G. N., 1964, *Mol. Phys.*, **8**, 375. Referred to as A.
- [4] HALL, G. G., 1962, *Proc. roy. Soc.*, **270**, 285.
- [5] GLICK, A. J., 1961, *Ann. Phys.*, **17**, 61.
- [6] HOPFIELD, J. J., 1958, *Phys. Rev.*, **112**, 1555.

Dye sensitized photo-response in organic semiconductors

by V. MYLNIKOV and A. TERENIN

Physics Department, Leningrad University, U.S.S.R.

(Received 9 March 1964)

It has been shown that the organic photo-semiconductor, copper-phenyl-acetylide (PAC) can be spectrally sensitized outside the range of its proper photo-response by several cationic, anionic and neutral organic dyes (methylene blue, pinacyanol, chlorophyll *a*, erythrosin, the phthalocyanines, hematin). Not only monomolecularly adsorbed dyes are efficient, but also dye dimers and its more aggregated forms.

The proper photo-sensitivity of PAC is also changed by dye adsorption, either diminished, or enhanced. The results are discussed considering the signs of the photo-carriers, and a mechanism of the phenomenon suggested.

1. INTRODUCTION

The spectral sensitization of the inner photo-effect by adsorbed dyes is well known for the inorganic semiconductors (ZnO, AgHal, TlHal, CdS) [1-8] and has found technical applications, e.g. in xerography [9-10].

Some years ago we attacked the same problem for the organic semiconductors, without much success, owing to the small photo-carrier concentration and their low mobility in them, as compared with those in the inorganic semiconductors. The introduction of some dyes, e.g. phthalocyanine-Mg, into films of organic polymers (polyvinyl-carbazole, polyvinylbutyral, etc.) seemed to confer to them a photo-sensitivity in the spectral range absorbed by the dye. However, it soon became clear that the effect was due to the aggregated dye particles in the film, exhibiting their own photo-response, as was proved measuring the action spectrum of the photo-e.m.f. of such a film by the condenser method, widely used in this laboratory [3-7]. The effect of spectral sensitization observed by Greig *et al.* [11, 12] in dyed polymer films had possibly the same origin, since the sensitized photo-current was directly proportional to the dye concentration, without an optimum.

Only recently we succeeded in obtaining a real spectral sensitization of some acetylenic polymers, which photoconductive properties have been previously established and investigated by us [13-15], but the highest sensitization effect has been observed not with these polymers, but with copper-phenyl-acetylide,



shortly PAC, [16] the inner photo-effect in which has been revealed and studied by us earlier [17].

† A polymer with coordination between Cu and acetylene groups [31, 32].

2. EXPERIMENTAL

PAC is a yellow powder poorly soluble in all the ordinary solvents. The dyes used for sensitization are indicated below. The dying of the PAC powder was carried out by bathing it in ethanol dye solutions at different concentrations (10^{-6} to 10^{-2} M), or by adding a few drops of the solution to the powder†. In some cases the dyed powder has been immersed into the solvent to remove the excess of the dye. This did not produce a marked elution, which indicates that the dye is strongly held by the adsorbent. All these procedures were performed in open air, and the desiccation of the sample has proved to be unimportant. Absorption spectra of the dye solutions have been measured with a UNICAM SP-700 spectrophotometer.

The photo-semiconductivity in the dyed PAC sample has been investigated with two methods: the usual one of the transversal d.c. photo-conductivity and that of the a.c. photo-e.m.f.

This latter is used in this laboratory [3-6, 13, 16] for the detection and study of the photo-induced charge liberation in inorganic and organic semiconductors. In it a thin layer (0.5 mm thick) of the semiconductor is placed between the conducting plates of a condenser, being prevented from contact with them by inserted silica laminae (0.1 mm thick). The layer is illuminated through the semi-transparent platinum coating, forming the front plate of the condensers, with intermittent light (300 c.p.s.). The a.c. of the released charge carrier, diffusing along the path of the light, owing to the concentration gradient, induces an alternating e.m.f. on the condenser, which after amplification (gain 100 000) and rectification is measured as function of the wavelength of the incident monochromatic light. The addition of a phase detector [4, 5] to the set up allowed the sign of the front electrode, and therefore the sign of the diffusing predominant charge carriers, to be determined. For measurements of the d.c. transversal photo-conductivity, the powder, in the form of a paste in ethanol, was deposited on the 5 mm wide gap between sputtered platinum electrodes on a polished silica plate, the applied d.c. potential being varied between 30 and 100 v. The photo-current under constant illumination was measured by a standard d.c. amplifier. The action spectrum in the range from 300 to 900 m μ has been measured with a grating monochromator ($f/5$), the spectral slit-width being mostly 1 m μ mm. An incandescent 70 w lamp was used for the visible and a 120 w high pressure xenon lamp in the ultra-violet range. The incident flux E , measured with a calibrated thermocouple, was from 10^{12} to 10^{15} photons/cm² sec. The spectral response curves (action spectra) are given in relative units, I_{ph}/E for the photo-e.m.f. (V_{ph}), and i_{ph}/E for the photo-conductivity current (i_{ph}). Both are thus reduced to equal incident photon numbers. With the help of neutral light-filters it has been found that the photo-response was linear versus the incident light intensity, within 15-20 per cent.

The spectral curves of the photo-e.m.f. are plotted under the abscissa axis when the sign of the photo-carriers is negative and above it when positive.

3. RESULTS

3.1. Methylene blue (MB)

3.1.1. Photo-e.m.f.

MB is most suitable for sensitization experiment since it does not exhibit in the aggregated form neither photo-conductivity nor photo-e.m.f. at the sensitivity

† Figures 2-6 relate to results obtained by the last procedure.

level of our set-ups. According to [4], MB photo-sensitizes the p-semiconductors TiHal and AgHal very efficiently, but does not sensitize the n-semiconductor ZnO . On figure 1 the spectral response curve for the photo-e.m.f. of PAC itself is shown (curve 1). In agreement with our previous paper [17] the spectral threshold of the proper photo-conductivity and the photo-e.m.f. of PAC is situated at $520 \text{ m}\mu$ (2.4 eV). After PAC has been immersed in an ethanol solution of MB (10^{-3} M) and dried its spectral response is represented by curves

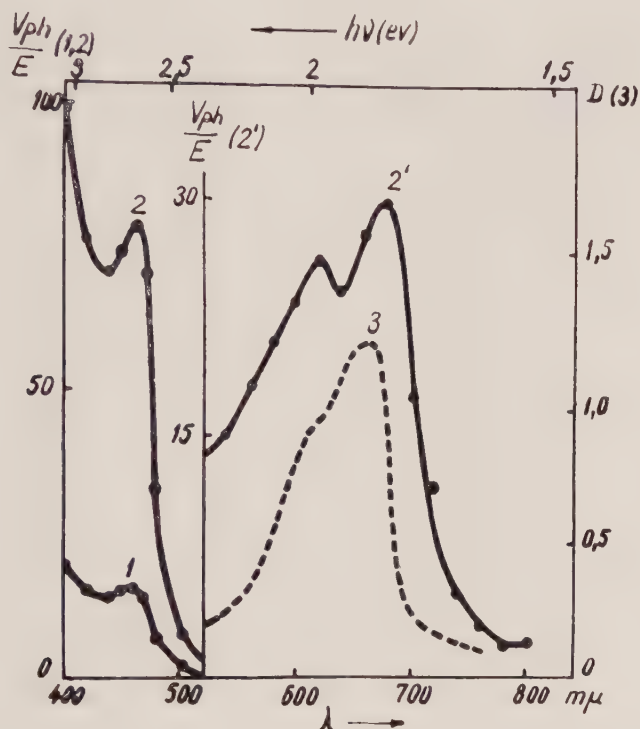


Figure 1. Spectra for the PAC photo-e.m.f.: Curve (1) before, and curves (2) and (2') after immersing in a $1.0 \times 10^{-3} \text{ M}$ ethanol solution of MB; curve (3) absorption spectrum of the solution (optical density D).

2 and 2'. It will be seen that a photo-response appears in the range of the absorption maximum of MB at $680 \text{ m}\mu$ characteristic of the monomolecular form of the dye in the dilute initial solution (curve 3). The observed (on curve 2') enhancement of the second maximum at $620 \text{ m}\mu$ in comparison to the solution spectrum is obviously connected with the presence of dye dimers on the surface of PAC†. The shift of the maximum photo-response to the longer wavelength by *ca.* $15 \text{ m}\mu$ relatively to the solution is usually the case for the adsorbed state.

It has been found that the sign of the charge carriers both in the proper and sensitized spectra ranges is *positive*.

† The surface concentration of the dye has not been measured, but judging from spectral evidence there is a direct correspondence between it and the concentration in the dye bath. As mentioned below the surface favours an aggregation of the dye on it, as is also known for dyes, adsorbed on AgBr .

As seen in figure 1, the adsorption of MB markedly changes also the proper photo-sensitivity of PAC. When the monomolecular form of the adsorbed dye dominates the positive proper photo-e.m.f. is increased by a factor of 5 to 10 without a change in the spectral distribution (curve 2).

As a rule this increase takes place regularly, when adsorption is carried out by immersing the PAC powder into the dye solution. When the dying is accomplished by drops of the dye solution soaking the PAC powder, the spectral response

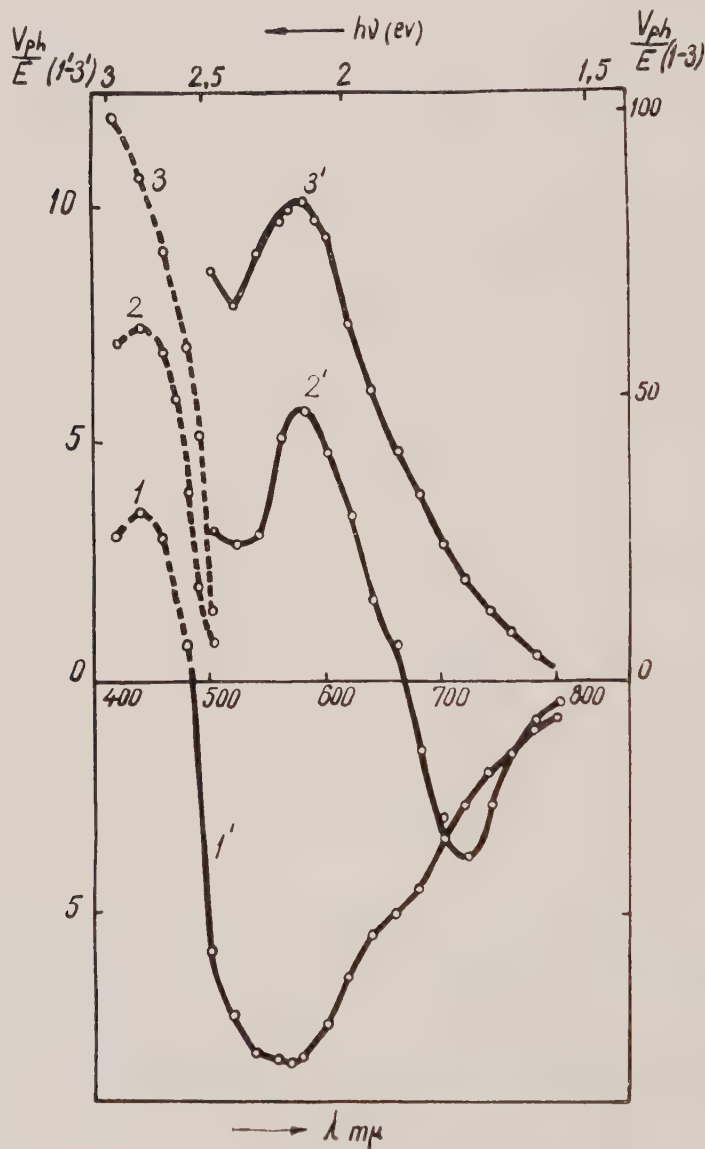


Figure 2. Spectra for the PAC photo-e.m.f. sensitized by a MB ethanol solution of 1×10^{-3} M concentration. Curves (1) and (1') after 10 min stay in air; curves (2) and (2') the same sample after 24 hours' stay; curves (3) and (3') the same after five days' stay.

curve and the sign of the photo-e.m.f. essentially depend on the time elapsing after the dyeing. Curves 1 and 1' in figure 2 represent measurements made 10 min after the dyeing. In that case the photo-response spectrum in the sensitized range is different from that of a dilute solution, but similar to that of a solid dye layer [18, 19]. It is remarkable that the sign of the dominant photo-carriers in the sensitized spectral range is under these conditions *negative* (curve 1').

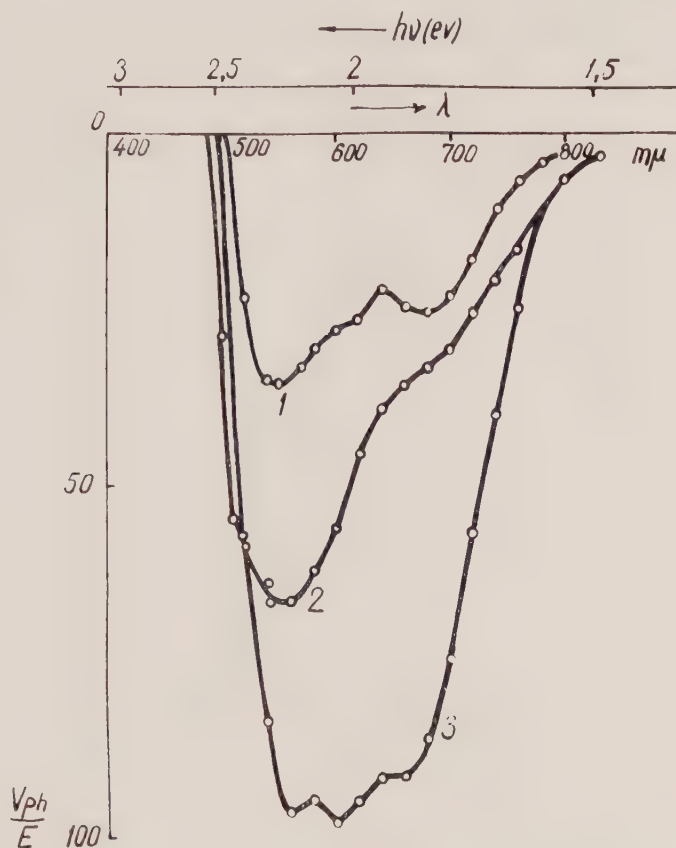


Figure 3. Spectra of the photo-e.m.f. of PAC, measured 10 min after sensitization by MB at the following concentrations of the ethanol solutions. Curve (1) 1.0×10^{-4} M; curve (2) 1.0×10^{-2} M; curve (3) 1.0×10^{-3} M.

Moreover, the proper positive photo-e.m.f. of PAC is now decreased comparatively to the undyed initial sample. On staying in open air the sensitized photo-e.m.f. reverses its sign, becoming *positive*. Thus the spectral curves 2 and 2' are for the same sample after 24 hours' stay in open air. Positive charge carriers appear in the short wavelength range of the sensitized spectrum, whereas in the long wavelength region they are still negative. On prolonged stay (4 days) the sensitized photo-e.m.f. becomes positive on the entire spectral range (curves 3 and 3'). At the same time there is observed an enhancement of the positive photo-e.m.f. in the proper spectral range (figure 2, curves 1, 2 and 3). After a sample possessing a positive photo-e.m.f. on the entire spectral range has been

immersed into pure ethanol and then dried, the sensitized photo-e.m.f. assumes a negative sign. Simultaneously the proper positive photo-e.m.f. of PAC is decreased. Upon staying in open air the spectrum reverts to that in figure 2. Such a reversible cycle can be performed several times without remaining changes.

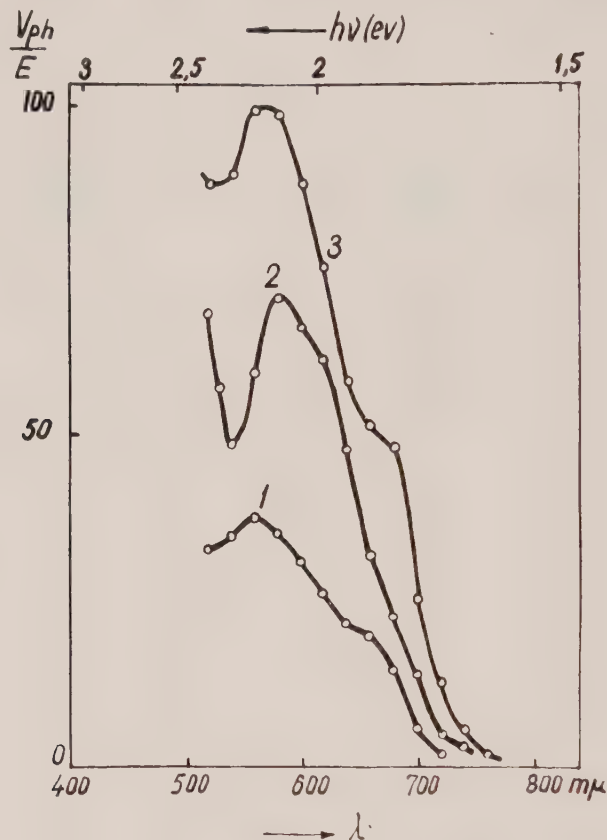


Figure 4. Spectra of the photo-e.m.f. of PAC eight days after sensitization by MB in ethanol at the following concentrations: curve (1) 1.0×10^{-4} M; curve (2) 1.0×10^{-2} M; curve (3) 1.0×10^{-3} M.

3.1.2. Dependence of the efficiency of sensitization on MB concentration

Measurements have been carried out 10 min after the dyeing with different concentrations of the dye solution (from 10^{-6} to 10^{-2} M). It follows from figure 3 that the optimum sensitization efficiency is observed at a concentrations of *ca.* 10^{-3} M (curve 3). It may be remarked that an increase of the concentration tends to enhance the short wavelength maxima, as compared with that at $680 \text{ m}\mu$, as should be expected if dimers and more aggregated forms of the dye also produced a photo-sensitization. The sign of the photo-carriers is in these cases *negative*.

However, as pointed out above, the photo-e.m.f. reverses its sign on staying for some time after dyeing. The spectral response curves for the same sensitized samples are as shown on figure 3, but after 8 days' staying, are represented on

figure 4 for different concentrations of the dye bath. As in the case of the negative photo-e.m.f. the sensitization efficiency has its maximum at about 10^{-3} M (curve 3).

If the magnitude of the proper photo-e.m.f. at $400\text{ m}\mu$ is taken as 100 per cent, then under optimum conditions the sensitized photo-e.m.f. reaches from 30 to 40 per cent, similarly for the sensitization efficiency of the inorganic semiconductors [3-7, 20].

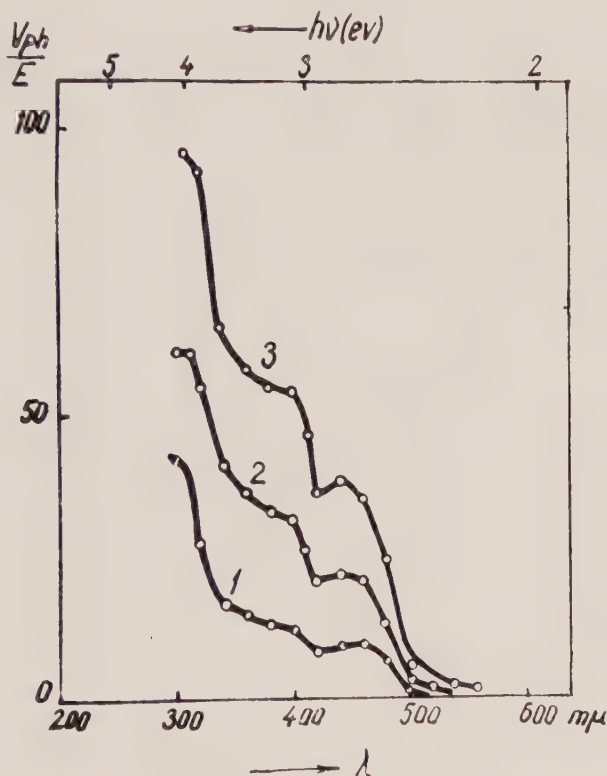


Figure 5. Spectra of the proper photo-e.m.f. of PAC, curve (1) before; curve (2) after sensitization with a MB ethanol solution (1.0×10^{-3} M); curve (3) with a 1.0×10^{-5} M ethanol solution.

It may be seen from figure 4 that the concentration increase is accompanied by an increase of the intensity ratio of the $580\text{ m}\mu$ band to the $680\text{ m}\mu$ one. This means that more highly aggregated dye forms prevail under these conditions. It must be stressed that the time necessary for the conversion of the negative photo-e.m.f. into a positive one rises with increased dye concentration. The lower the concentration, the more rapidly this conversion takes place. When the dye concentration is of the order of 10^{-6} M it takes only a few minutes after the dyeing for the appearance of a positive photo-e.m.f. in the sensitized spectral range. When the concentration is about 10^{-2} M it takes five days of staying in open air for such a conversion.

The proper photo-e.m.f. of PAC in the spectral regions in which the dye does not absorb also depends on the dye concentration. Curve 1 in figure 5 represents the spectral response for the photo-e.m.f. of the undyed PAC, whereas curves 2 and 3 correspond to PAC with MB adsorbed from solutions of 10^{-3} and 10^{-5} M respectively. These spectral curves have been measured after such a lapse of time, when in the sensitized spectral ranges the photo-e.m.f. has become positive. Repeated experiments showed that, at variance to the sensitized photo-e.m.f. for which the optimum sensitivity is reached at a concentration of 10^{-3} M, the proper photo-e.m.f. is the highest at dye concentrations of 10^{-5} to 10^{-6} M.

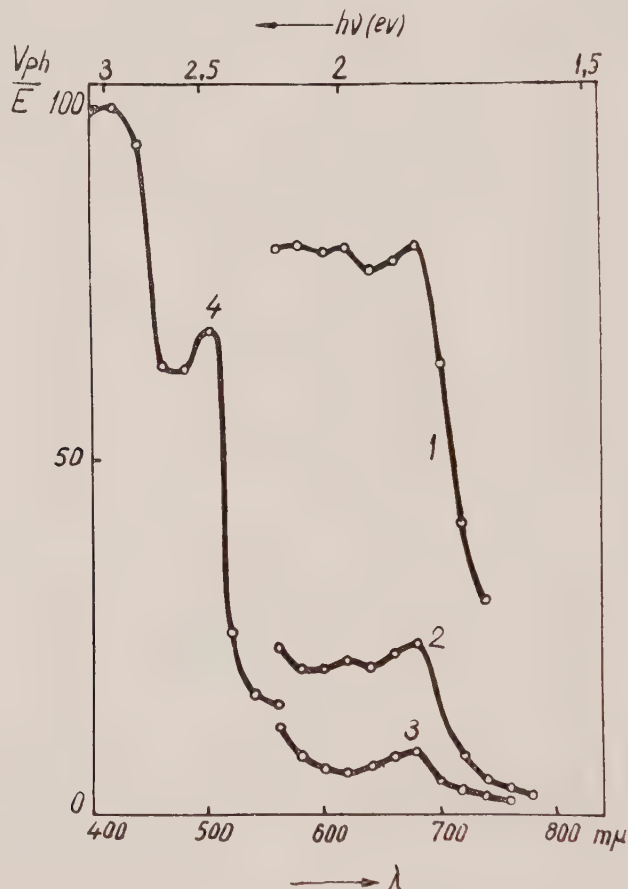


Figure 6. Spectra of the PAC photo-conductivity sensitized with MB ethanol solutions of the following concentrations. Curve (1) 1.0×10^{-3} M; curve (2) 1.0×10^{-4} M; curve (3) 1.0×10^{-5} M; curve (4) photo-conductivity in the proper photo-sensitivity range of PAC.

3.1.3. Photo-conductivity

The photo-conductivity of PAC can also be photo-sensitized in the absorption range of MB (figure 6). As in the case of the photo-e.m.f. the largest response is observed at a bath concentration of about 10^{-3} M (curve 1). If the concentration reaches *ca.* 10^{-2} M the sensitized photo-conductivity is small. It is significant

that a decrease in the dye concentration is accompanied by an increase of the long wavelength maximum at $680 \text{ m}\mu$, the sensitization spectrum approaching that of a dilute dye solution. The participation of dimers and more aggregated dye forms in the sensitization appears on increasing the dye concentration. The dark conductivity of PAC does not practically change after MB absorption, but the latter produces a striking decrease, 2 to 10 times, of the PAC proper photo-conductivity, the decrease becoming larger at higher concentration of the dye. This effect is just the reverse to that observed for the photo-e.m.f. (§ 3.1.1).

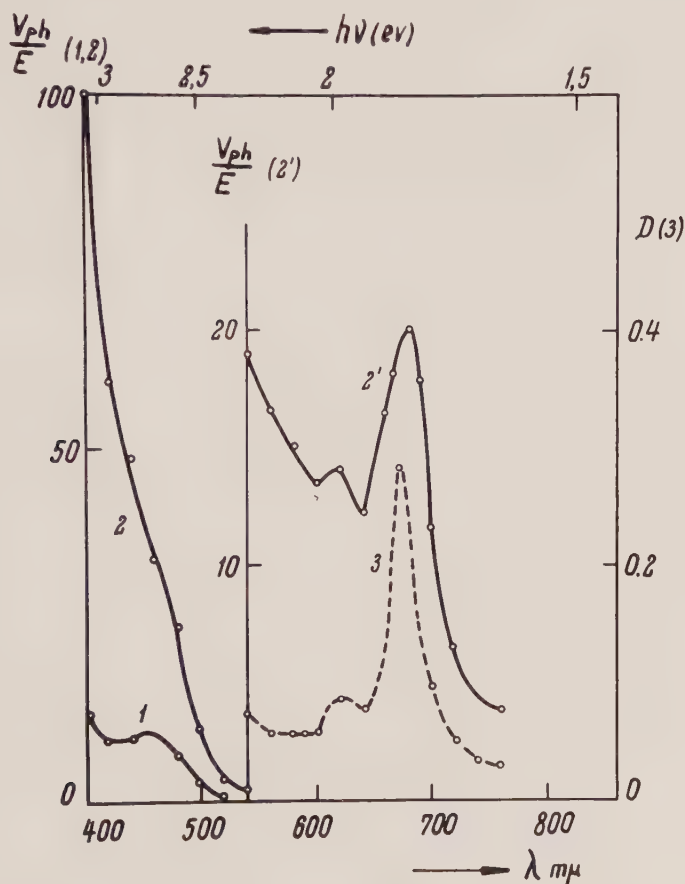


Figure 7. Spectra of the PAC photo-e.m.f. Curve (1) before; curves (2) and (2') after sensitization with a chlorophyll *a* ethanol solution ($1.0 \times 10^{-3} \text{ M}$); curve (3) absorption spectrum of the solution.

3.2. Chlorophyll *a*

As shown before in this laboratory chlorophyll is a good spectral sensitizer of the photo-conductivity and photo-e.m.f. of ZnO [4-6, 21]. A similar sensitization has been found by us for the photo-conductivity and photo-e.m.f. of PAC (figure 7). After chlorophyll adsorption an increase in the proper

photo-e.m.f. (curve 2) and in the range of the chlorophyll *a* absorption spectrum are clearly manifested, the main maximum at 680 m μ and a subsidiary one at 620 m μ appearing (curve 2').

The sensitization spectrum corresponds very closely to the chlorophyll *a* absorption spectrum in ethanol (10^{-3} M) (curve 3), but is shifted to the longer wavelengths by *ca.* 10 m μ as is expected for the adsorbed state. The photo-e.m.f. is positive in all the spectral ranges. Similar results have been obtained for the photo-conductivity, but the proper photo-conductivity increases less than the proper photo-e.m.f. on chlorophyll absorption. As in the previous case of MB the dark conductivity does not practically change on pigment adsorption.

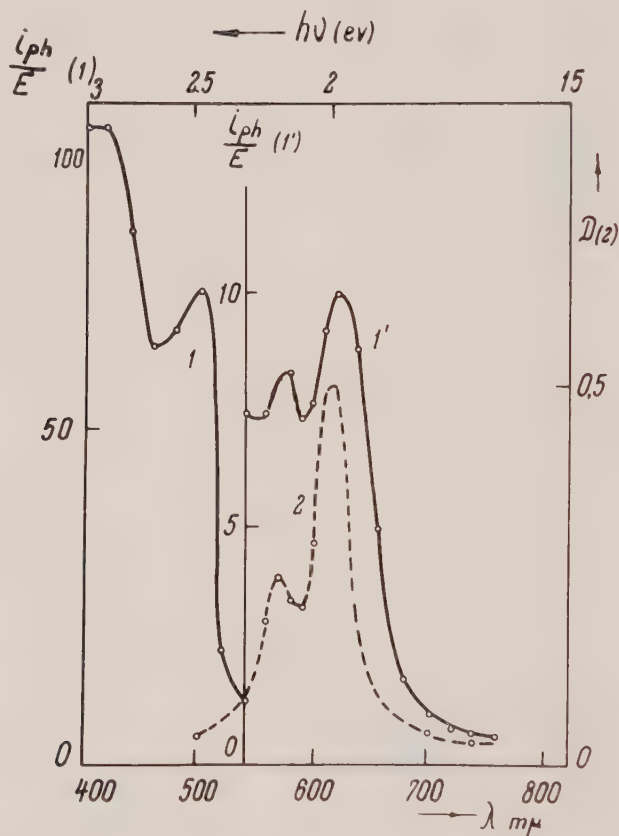


Figure 8. Spectra of the PAC photo-conductivity sensitized with pinacyanol. Curve (1) and (1') after immersing in a ethanol solution of the dye (1.0×10^{-3} M); curve (2) absorption spectrum of the solution.

3.3. Pinacyanol

The photo-conductivity spectral curves of PAC with adsorbed pinacyanol are given in figure 8 (curves 1 and 1'). As in the cases of MB and chlorophyll there is observed a small shift of the maxima in respect to the solution spectrum (curve 2). The relative enhancement of the maximum at 570 m μ as compared with the monomolecular one at 620 m μ in the photo-conductivity spectrum

clearly shows that the aggregated forms of pinacyanol takes part also in the sensitization. Similarly to MB, but in contrast to chlorophyll the proper photo-conductivity of PAC is always decreased 5–10 times by pinacyanol adsorption. As with the other adsorbates, the dark conductivity is not practically changed by the dye adsorption. For pinacyanol the behaviour of the sensitized photo-e.m.f. was similar to that of the photo-conductivity. The proper photo-e.m.f. is decreased 2–3 times. The photo-e.m.f. is *positive* in the proper and the sensitized ranges.

Spectral sensitization of the photo-e.m.f. and the photo-conductivity of PAC has been established also for erythrosin (anionic dye), the phthalocyanines with Mg and Cu and hematin (neutral pigments) and with a series of various dyes [16]. The increase of the proper PAC photo-e.m.f. after the dye adsorption is the most pronounced for erythrosin (30-fold).

Recently Steketee and Jonge [22] reported on the spectral sensitization of the photo-conductivity of an anthracene monocrystal flake, inserted between liquid electrolytic electrodes, in which dyes, rhodamine B, MB and proflavin, have been dissolved. It is not clear whether this effect has a counterpart in the photo-voltaic effect of CuHal sensitized by dyes in an electrolyte solution, discovered by Rigollot in 1893 [23, 24].

4. DISCUSSION

The fundamental mechanism of the spectral sensitization by dyes of photo-semiconductors is not as yet clear [7]. There are two alternative view-points on the process by which the charge carriers do get into the conduction band under the action of photons absorbed by the dye, which are inferior in magnitude to the gap in the semiconductor. Some authors favour an electron 'injection' from the adsorbed excited dye molecule [8, 25–27]. Others prefer to assume that the excitation energy of the dye molecule is handed over to charge carriers kept in local traps in the forbidden zone [3–7, 28–30]. It is clear that both alternatives are equivalent if the electron interchange between the dye molecule and the semiconductor levels is brought to completion in a time of 10^{-9} sec.

The results described above demonstrate that dyes of very different classes, viz. strong electron acceptors, like MB and easily oxidizable, like chlorophyll can sensitize the organic photo-semiconductors, similarly for the case of the inorganic ones. The sensitizers belong to different dye classes, viz. cationic (MB, pinacyanol), anionic (erythrosin), uncharged (chlorophyll *a*, the phthalocyanines, hematin). The dyes used are likewise sensitizers of photographic emulsions (pinacyanol), or desensitizers (MB). As in the case of the inorganic semiconductors, the sensitization is optimally produced by separate adsorbed dye molecules, but dimers and more aggregated forms are also efficient.

As mentioned above for MB adsorbed on PAC, the sign of the photo-current carriers in the sensitized spectral range was negative in the initial stage, being opposite to that of the semiconductor itself (figure 2). This fact might be considered as an argument for an electron transfer from MB molecules and their aggregates to PAC, thus confirming the alternative of an electron injection into the semiconductor [8, 25–27]. MB, however, does not show as a solid by itself; neither photoconductivity, nor photo-e.m.f. as the sensitivity level of our set-ups. It can equally be assumed that the semiconductor (PAC)

possesses under stationary conditions two sets of traps, viz. filled and empty ones. The photo-excited dye molecule gives up its energy to filled traps and raises the trapped electrons to the conduction band, producing temporarily a negative photo-e.m.f. These traps on prolonged stay of the sample in air are emptied by adsorbed O_2 molecules. Then excited dye molecules transfer their energy to electrons in the valency band, displacing them to the vacant traps and thus sensitizing a transport of holes in the former. In distinction to the electron transfer mechanism from the excited sensitizer, the energy transfer mechanism does not require a definite height of the dye excited level relatively to the height of the semiconductor conduction band [7].

This view-point is further confirmed by the fact, that in the case of pinacyanol the sign of the sensitized photo-current carriers in the spectral range of the aggregated dye (λ_{\max} 570 m μ) is positive, i.e. coincides with that of the semiconductor itself (PAC), whereas aggregated pinacyanol possesses only negative photo-carriers as shown by the photo-e.m.f. [4]. It may be remarked that for inorganic semiconductors the sign of the sensitized photo-carriers has generally been found identical to that of the proper photo-effect of the semiconductor, independently of the semiconducting type of the sensitizer itself as a solid [3-7].

Another phenomenon not frequently observed for the inorganic semiconductors is the marked change on the proper photo-sensitivity in PAC produced by dye adsorption. If the adsorbed dye creates on the surface of the semiconductor sites capable of capturing the predominant photo-carriers (holes) the photo-e.m.f. in the proper spectral range should decrease, as observed (figure 2). But if these sites can capture only the accessory carriers, the photo-e.m.f. should increase. Evidently the dye can prevent or help the separation of carriers of different sign. From this view-point it can be explained why the photo-conductivity decreases in both cases, since it responds to both carriers of the photo-current which alike are trapped.

The abnormal increase of the proper photo-conductivity of PAC in the case of sensitization by chlorophyll may be ascribed to the fact that the dye has a strong second absorption band in the same spectral range and therefore can act there as a sensitizer.

We are indebted to Dr. A. M. Sladkov for the samples of the acetylenic monomers and polymers, and for helpful discussions.

REFERENCES

- [1] KAMEYAMA, N., and FUKAMOTO, T., 1939, *J. Soc. chem. Ind. Japan*, **42**, 244.
- [2] KAMEYAMA, N., and FUKAMOTO, T., 1939, *J. Soc. chem. Ind. Japan*, **42**, 426.
- [3] PUTZEIKO, E., and TERENIN, A., 1949, *J. phys. Chem., Moscow*, **23**, 676.
- [4] TERENIN, A., PUTZEIKO, E., and AKIMOV, I., 1957, *J. Chim. phys.*, **54**, 716.
- [5] TERENIN, A., and PUTZEIKO, E., 1958, *J. Chim. phys.*, **55**, 681.
- [6] TERENIN, A., PUTZEIKO, E., and AKIMOV, I., 1959, *Trans. Faraday Soc.*, **27**, 83.
- [7] TERENIN, A., and AKIMOV, I., 1961, *Z. phys. Chem.*, **217**, 307.
- [8] NELSON, R. C., 1956, *J. opt. Soc. Amer.*, **46**, 13.
- [9] GILEVICH, I., and NEMIROVSKY, E. L., 1961, *Electrography* (Moscow).
- [10] GIAIMO, E. G., 1962, *R.C.A. Rev.*, **23**, 96.
- [11] GREIG, H. G., 1962, *R.C.A. Rev.*, **23**, 413.
- [12] MEHL, W., GREIG, H. G., and WOLF, N. F., 1962, *Organic Crystal Symposium*, Ottawa, Program Abstracts, p. 204.

- [13] MYLNIKOV, V. S., SLADKOV, A. M., KUDRJAVTSEV, U. P., LUNEVA, L. K., KORSHAK, V. V., and TEREININ, A. N., 1962, *C.R. Acad. Sci. U.R.S.S.*, **144**, 840.
- [14] MYLNIKOV, V. S., 1963, *C.R. Acad. Sci. U.R.S.S.*, **148**, 620.
- [15] MYLNIKOV, V. S., PUTZEIKO, E., and TEREININ, A. N., 1963, *C.R. Acad. Sci. U.R.S.S.*, **149**, 897.
- [16] MYLNIKOV, V. S., and TEREININ, A. N., 1964, *C.R. Acad. Sci. U.R.S.S.*, **155**, 1167.
- [17] MYLNIKOV, V. S., and TEREININ, A. N., 1963, *C.R., Acad. Sci. U.R.S.S.*, **153**, 1381.
- [18] VARTANJAN, A., 1956, *J. phys. Chem., Moscow*, **30**, 424.
- [19] VARTANJAN, A., 1956, *J. phys. Chem., Moscow*, **30**, 1028.
- [20] MARKEVICH, N., and PUTZEIKO, E., 1962, *J. phys. Chem., Moscou*, **36**, 2393.
- [21] PUTZEIKO, E., and TEREININ, A., 1953, *C.R. Acad. Sci. U.R.S.S.*, **90**, 105.
- [22] STEKETEE, J. W., and J. DE JONGE, 1963, *Proc. Koninkl. Nederl. Academie van Wetenschappen*, **66**, 76.
- [23] RIGOLLOT, M. H., 1893, *C.R., Acad. Sci., Paris*, **116**, 878.
- [24] RIGOLLOT, M. H., 1897, *J. de Physique*, **6**, 520.
- [25] NODDACK, W., ECKERT, G., and MEIER, H., 1952, *Z. Elektrochem*, **56**, 739.
- [26] SHEIBE, G., and DÖRR, F., 1950, *Z. Elektrochem.*, **54**, 403.
- [27] SHEIBE, G., and DÖRR, F., 1959, *Z. Elektrochem.*, **63**, 117.
- [28] MOTT, N. F., 1948, *Photogr. J.*, B **88**, 1948.
- [29] MITCHELL, J. W., and MOTT, N. F., 1957, *Phil. Mag.*, **2**, 1149.
- [30] MITCHELL, J. W., 1958, *J. photogr. Sci.*, **6**, 57.
- [31] KORSHAK, V. V., SLADKOV, A. M., and KUDRJAVTSEV, U. P., 1960, *Vissokomolekularnye Soedineniya*, **2**, 1824.
- [32] BLAKE, D., CALVIN, G., and COATES, G. E., 1959, *Proc. chem. Soc.*, p. 396.

RESEARCH NOTES

The electron resonance spectra of free radicals dissolved in liquid crystals

by A. CARRINGTON and G. R. LUCKHURST

Department of Theoretical Chemistry, University Chemical Laboratory,
Lensfield Road, Cambridge

(Received 13 April 1964)

Determination of the absolute signs of isotropic nuclear spin-spin couplings in nuclear resonance, and electron-nuclear hyperfine couplings in electron resonance is rather difficult. In a recent series of papers, Buckingham [1] has drawn attention to an ingenious method of solving the problem in nuclear resonance. Application of a strong electric field across a solution of the molecule of interest (which must possess a permanent electric dipole moment) results in partial orientation. The dipole-dipole contribution to the nuclear spin-spin coupling, which can be calculated rather accurately, is thus no longer averaged to zero. By observing whether the coupling constant increases or decreases in the presence of the electric field, the absolute sign of the isotropic interaction may be determined.

It seems possible that one might achieve the same objective by using a liquid crystal as solvent in order to effect partial alignment. After our work had been commenced, Saupe and Englert [2] described the nuclear resonance spectrum of benzene dissolved in *p*-azoxyanisole and showed that the dipole-dipole couplings, which average to zero in isotropic fluids, result in the observation of a complex eighteen line spectrum, as might be expected.

We have examined the electron spin resonance spectrum of diphenylpicrylhydrazyl (DPPH) and the tetracyanoethylene anion (TCNE⁻) using *p*-azoxyanisole as solvent. Above 135°C *p*-azoxyanisole is an isotropic liquid and the usual hyperfine patterns [3, 4] are obtained. DPPH shows a five-line spectrum arising from interaction involving two almost equivalent nitrogen atoms, with a coupling constant of 9.2 gauss. TCNE⁻ shows the characteristic nine-line pattern with splitting 1.58 gauss. These hyperfine patterns change abruptly below the nematic-isotropic transition temperature [5] (135°C) and at 119°C, just above the melting point, the nitrogen splitting constants in DPPH and TCNE⁻ are 7.8 and 0.62 gauss respectively. These splittings increase slightly with increase in temperature through the nematic range (118° to 135°C) and just below the transition temperature the coupling constants are 8.0 and 0.94 gauss.

In the presence of a magnetic field, clusters of solvent molecules in the bulk fluid are known to be aligned with the long axis parallel to the field [6]. TCNE⁻ is a planar radical and we therefore conclude that the preferred orientation will be that in which the magnetic field is parallel to the radical plane. As a result of this, assuming axial symmetry of the hyperfine interaction, there will be a non-vanishing contribution from the parallel component of the nitrogen anisotropic hyperfine tensor. The spin density in the nitrogen 2p_π orbital is

estimated [7] to be 0.0745 and the contribution to the anisotropic tensor will be axially symmetric, with calculated approximate in-plane values of -1.06 gauss and a perpendicular component of $+2.12$ gauss. The contribution from spin density on the adjacent carbon atom, which would destroy the axial symmetry, is calculated to be negligibly small. Hence if the TCNE radicals are accurately aligned, the nitrogen splitting constant would be either 2.64 or 0.52 gauss, depending on whether the isotropic coupling constant is negative or positive. We conclude that the coupling must be positive, as expected on theoretical grounds, and that the radicals are indeed almost completely aligned in the manner suggested.

Similar calculations for DPPH suggest that the nitrogen coupling constant would decrease from 9.2 gauss to approximately 3 gauss, if the radical was completely aligned with the $N=N$ bond parallel to the magnetic field. However, the radical is far from being planar and we would not expect accurate alignment. Slight preferential orientation is sufficient to account for the observed 1.4 gauss decrease in the coupling constant.

Assuming one can always deduce the preferred orientation, we see no reason why this method should not be used to determine the signs of other isotropic coupling constants, notably for aromatic C-H protons and ^{13}C nuclei. Furthermore, it should be possible to demonstrate directly positions of negative spin density in aromatic radicals. The only limitation is that of finding radicals which are soluble and stable in a liquid crystal solvent.

We thank the D.S.I.R. for a maintenance grant to G.R.L. and for the purchase of a Varian E.P.R. spectrometer used in this work.

REFERENCES

- [1] BUCKINGHAM, A. D., and LOVERING, E. G., 1962, *Trans. Faraday Soc.*, **58**, 2077.
BUCKINGHAM, A. D., and McLAUCHLAN, K. A., 1963, *Proc. chem. Soc.*, p. 144.
BUCKINGHAM, A. D., and POPL, J. A., 1963, *Trans. Faraday Soc.*, **59**, 2421.
- [2] SAUPE, E., and ENGLERT, G., 1963, *Phys. Rev. Letters*, **11**, 462.
- [3] LORD, N. W., and BLINDER, S. M., 1961, *J. chem. Phys.*, **34**, 1693.
- [4] PHILLIPS, W. D., ROWELL, J. C., and WEISSMAN, S. I., 1960, *J. chem. Phys.*, **33**, 626.
- [5] McLAUGHLIN, E., SHAKESPEARE, M. A., and UBBELOHDE, A. R., 1964, *Trans. Faraday Soc.*, **60**, 25.
- [6] MAIER, W., 1947, *Z. Naturf. A*, **2**, 458.
- [7] REIGER, P. H., and FRAENKEL, G. K., 1962, *J. chem. Phys.*, **37**, 2795.

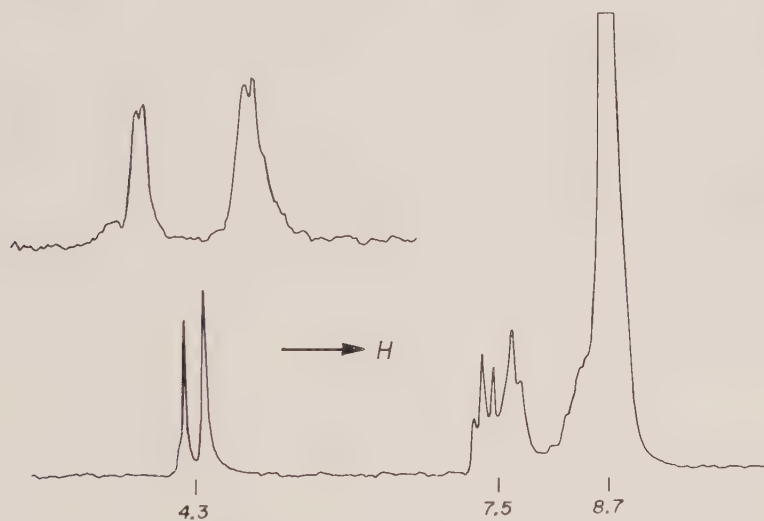
Conformation of the *EXO*-methylene ketone group in α -methylene cycloketones

by R. KAISER and D. L. HOOPER

Departments of Physics and Chemistry, University of New Brunswick,
Fredericton, N.B., Canada

(Received 14 May 1964)

Proton magnetic resonance data for α -methylene cycloketones have recently been reported in this journal [1], and their interpretation led to the conclusion that the *exo*-methylene group exists in the conformation *cis* to the keto group for ring sizes $n=5, 6, 7$ and 8 ; in the *trans* conformation for $n=9$ and 10 ; and is in partial free rotation for $n=16$. Certain difficulties with the interpretation of the spectrum of α -methylenecyclohexadecanone ($n=16$) have led us to a re-examination of this system.



Room temperature proton magnetic resonance spectrum of 79 per cent pure α -methylenecyclohexadecanone in CCl_4 solution at 56.4 Mc/sec.

The room temperature spectrum of a dilute solution of 79 per cent pure α -methylenecyclohexadecanone in carbon tetrachloride is shown in the figure. This sample is similar in composition to that used by Klose [2]. The two signals near $\tau=4.3$, magnified in the insert, are assigned to the two hydrogen nuclei of the methylene group. The signals near $\tau=7.5$ having an area approximately twice that of both methylene signals, are assigned to ring CH_2 groups α to the *exo*-methylene ketone group. A comparison with the spectrum of cyclohexadecanone (not shown) indicates that the signal to the right of $\tau=7.5$ arises

from the ring CH_2 group α to the keto group, and the signal to the left of $\tau = 7.5$ is therefore assigned to the ring CH_2 group α to the methylene group. These signals were not resolved by Klose [1] but confirmation of their assignment may be derived from his figure 5 which shows the signal from the ring CH_2 groups α to the methylene groups in $\alpha\alpha'$ -dimethylene cyclodecanone occurring at lower field than the unresolved signal in α -methylenecyclodecanone, which in turn occurs at lower field than the corresponding signal in cycloketones. The large signal at $\tau = 8.7$ is assigned to the remaining ring CH_2 groups.

Of particular interest is the methylene group signal shown at higher resolution in the insert. The two peaks are separated by 13 c.p.s. corresponding to 0.23 p.p.m. Since a similar splitting is not observed in other parts of the spectrum nor expected to be caused by spin coupling in this molecule, the two methylene hydrogens must be non-equivalent with a chemical shift difference $\Delta\tau = 0.23$ p.p.m. apparently caused mainly by the magnetic anisotropy of the keto group. Each peak is split into a doublet of 0.9 c.p.s. separation, probably caused by spin coupling between the two methylene protons. Averaging over several spectra of the same sample we find the high field peak to have 1.7 times the intensity of the low field one. The parameters $\Delta\tau = 0.23$ p.p.m., intensity ratio 1.7, were found unchanged over the temperature range from -52°C (in deuterated chloroform solution) to $+101^\circ\text{C}$ (in tetrachloroethylene solution). The instrumental resolving power was insufficient to monitor the 0.9 c.p.s. splitting over this temperature range.

The observations seem to be compatible with any one of three assumptions: The methylene group may be (i) fixed *cis* to the keto group, (ii) fixed *trans* to the keto group, (iii) frequently changing at random time intervals between the *cis* and *trans* conformations (free rotation). The resolution of a 0.9 c.p.s. spin coupling requires that in cases (i) and (ii) the lifetime of the *cis* or *trans* state respectively is at least 0.5 sec at room temperature. Similarly, in case (iii) the lifetime of either state must be less than 3×10^{-4} sec at room temperature if a chemical shift difference of 0.5 p.p.m. between the *cis* and *trans* signal for either methylene hydrogen is assumed.

ϕ	0°	20°	40°	60°	80°	90°	100°	120°	140°	160°	180°
$\Delta\tau$	0.64	0.31	-0.31	-0.53	-0.47	-0.36	-0.28	-0.10	+0.04	0.12	0.15 p.p.m.

Calculated chemical shift differences for the methylene hydrogen nuclei in the *exo*-methylene ketone group for several values of the dihedral angle ϕ .

Table 1.

A decision may be reached with the help of the data presented in table 1. Shown there are the calculated chemical shift differences between the two methylene proton signals for several values of the dihedral angle ϕ between the keto and *exo*-methylene groups. The calculation is based on the bond susceptibilities:

$\chi_{xx}^{\text{C}=0} = -33.4$, $\chi_{yy}^{\text{C}=0} = +2.8$, $\chi_{zz}^{\text{C}=0} = +15.6$, $\Delta\chi^{\text{C}-\text{C}} = 4.0 \times 10^{-6} \text{cm}^3/\text{mole}$ derived from a study of the proton magnetic resonance spectra of substituted amides [3]. It is seen that case (i) should give $\Delta\tau_{\text{calc}} = 0.64$ p.p.m., contrary to

the value $\Delta\tau=0.23$ p.p.m. measured for ring size $n=16$ but in agreement with Klose's results for $n=5, 6, 7$ and 8 . Case (ii) should give $\Delta\tau_{\text{calc}}=0.15$ p.p.m. in reasonable agreement with the observed value, and case (iii) should give

$$\int_0^\pi \Delta\tau_{\text{calc}} d\phi/\pi = -0.07 \text{ p.p.m.}$$

in disagreement with the observed value. It thus appears that assumption (ii), i.e. the methylene group is fixed *trans* to the keto group, is the correct one.

Klose's results for other ring sizes then indicate that for small rings the *cis* conformation is enforced by the skeleton structure, and that with increasing ring size the *trans* conformation becomes more and more favoured until at $n=16$ it is considerably more stable than the *cis* conformation. The collapse of the two methylene signals for ring sizes $n=9$ and 10 would thus indicate frequent transitions between the *cis* and *trans* conformations (free rotation) in the rings of intermediate size.

Our observed intensity ratio of 1.7 cannot be explained on this basis. The line shape of the high field methylene peak suggests that this signal is superimposed on another peak which may result from the 21 per cent impurity in the sample. Klose's attempt to explain his $1:3$ intensity ratio by postulating partial free rotation of the methylene group does not appear convincing, especially when an apparent error in his value for $\overline{\Delta\delta}$ is corrected ($\overline{\Delta\delta}=0.15$ p.p.m. should read $\overline{\Delta\delta}=0.015$ p.p.m.).

We wish to thank Professor M. Mühlstädt of the University of Leipzig, Germany, for the samples and analysis of cyclohexadecanone and α -methylene-cyclohexadecanone. The assistance of the National Research Council of Canada in the form of a grant in aid of research and the award of a studentship to one of us (D.L.H.) is gratefully acknowledged.

REFERENCES

- [1] KLOSE, G., 1963, *Mol. Phys.*, **6**, 585.
- [2] MÜHLSTÄDT, M. (private communication).
- [3] HOOPER, D. L., 1964, Thesis, University of New Brunswick.

Hyperfine coupling in $\dot{\text{C}}\text{OH}$ containing radicals

by D. E. HENN and D. H. WHIFFEN

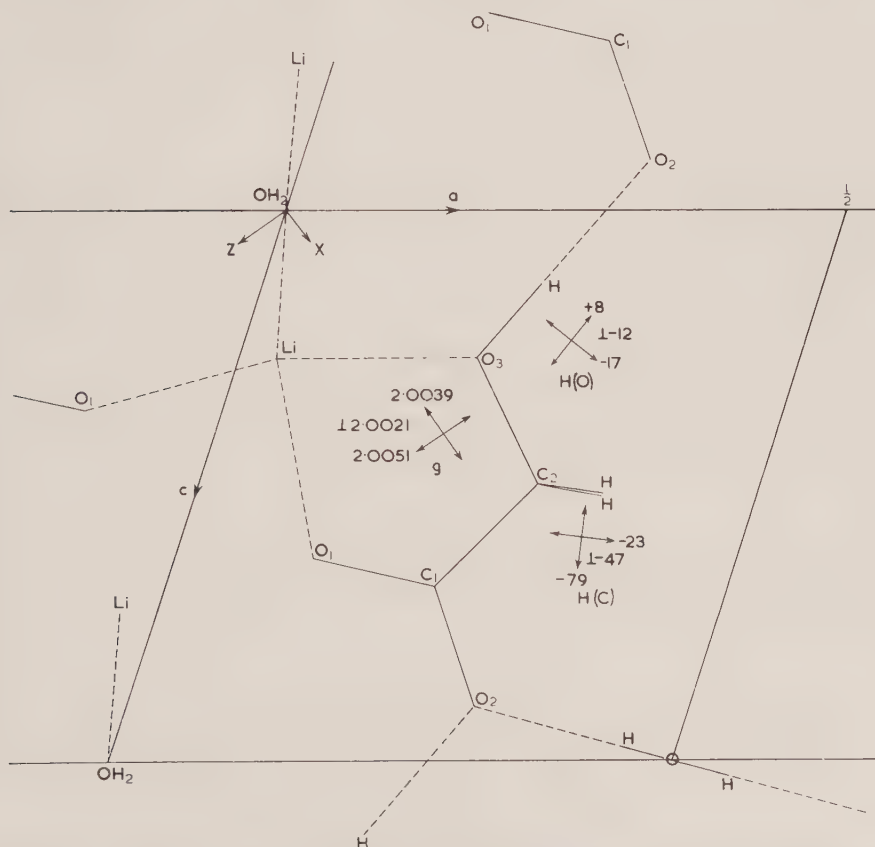
Basic Physics Division, National Physical Laboratory, Teddington, Middlesex

(Received 26 May 1964)

The hydrogen hyperfine coupling in the electron spin resonance Hamiltonian of radicals containing the $\dot{\text{C}}\text{-CHX}_2$ structure is well established to depend on the angle of twist about the C-C bond [1-4] and the formula for the coupling a ,

$$a = B_0 + B_2 \cos^2 \theta,$$

has been suggested, where θ is the dihedral angle between the C-CH plane and the plane containing the p orbital of the unpaired electron and the C-C bond. The particular values $B_0 = +9$ Mc/s and $B_2 = +122$ Mc/s have been suggested on experimental grounds [3], although these may be effective values if averaged over



Part of the structure of lithium glycollate monohydrate projected on the ac plane showing the principal direction of the electron spin resonance tensors [7]. X and Z refer to the chosen directions of reference [7].

zero-point and thermal motions [5,6]. The corresponding problem for a $\text{>}\dot{\text{C}}\text{-OH}$ structure is less clear and even the sign of B_0 has been uncertain. However, in the radical $(\text{COO}-)\text{H}\dot{\text{C}}\text{-OH}$ derived by irradiation from lithium glycollate monohydrate there is reason [7] to think that $\theta = \pi/2$. The isotropic coupling is then equal to B_0 and was found to be ± 7 Mc/s, but the sign was indeterminate. Derbyshire [8] has suggested that the negative sign is correct on the basis of the numerical values of the anisotropy and the present note presents confirmation of this sign from the crystal structure [9] determined by x-ray diffraction. The monoclinic crystal, space group C_{2h}^3 ($C2/m$), has four molecules per unit cell. The structure is in full agreement with the earlier resonance measurements and in particular there is a plane of symmetry of the glycollate ion, $\text{CH}_2(\text{OH})\text{CO}_2^-$, perpendicular to b and all its atoms except the two hydrogens lie in this plane as does the lithium ion (figure). The water of crystallization lies on the two-fold axes above and below the plane. The top face of figure 1 of reference [7] was identified as $\{20\bar{1}\}$ and the end triangles as $\{001\}$. This enables the spin resonance information [7] to be laid on the plan as in our figure. The smallest numerical principal value of the $\text{H}(\text{C})$ hyperfine tensor of -23 Mc/s occurs, as expected, parallel to the external bisector of the $\text{C}_1\text{C}_2\text{O}_3$ angle. More interesting, the smallest numerical coupling of ± 8 Mc/s of the $\text{H}(\text{O})$ tensor is nearly parallel to the $\text{O}_3\text{-H}$ bond: this hydrogen is located by a short interionic $\text{O}_3\text{-H}\cdots\text{O}_2$ dimension indicating hydrogen bonding between adjacent glycollate ions. This follows in direction the prediction of Derbyshire [8] assuming a negative isotropic coupling of -7 Mc/s and principal values of $+8$, -12 and -17 Mc/s.

The mechanism leading to a negative sign of the isotropic coupling is presumably some delocalization of the unpaired electron density in the π system from the carbon to the hydroxyl oxygen and then there is the normal sign reversal associated with hydrogen atoms in the nodal plane of a π system. Such delocalization can not occur in the $\text{>}\dot{\text{C}}\text{-CHX}_2$ system as the carbon p orbital is fully involved in bonding to the X groups.

B_2 is expected to be positive for $\text{>}\dot{\text{C}}\text{-OH}$ and if there is some zero point averaging in the present case the static value of B_0 might be even more negative. At least its negative sign seems established.

This work forms part of the Research programme of the Basic Physics Division, National Physical Laboratory and is published by permission of the Director. We should like to acknowledge the assistance of Miss R. H. Colton with the x-ray analysis.

REFERENCES

- [1] HELLER, C., and MCCONNELL, H. M., 1960, *J. chem. Phys.*, **32**, 1535.
- [2] POOLEY, D., and WHIFFEN, D. H., 1961, *Mol. Phys.*, **4**, 81.
- [3] HORSFIELD, A., MORTON, J. R., and WHIFFEN, D. H., *Mol. Phys.*, **4**, 425.
- [4] MIYAGAWA, I., and ITOH, K., 1963, *J. chem. Phys.*, **36**, 2157.
- [5] STONE, E. W., and MAKI, A. H., 1962, *J. chem. Phys.*, **37**, 1326.
- [6] KASHIWAGI, M., and KURITA, Y., 1963, *J. chem. Phys.*, **39**, 3165.
- [7] POOLEY, D., and WHIFFEN, D. H., 1961, *Trans. Faraday Soc.*, **57**, 1445.
- [8] DEBRYSHIRE, W., 1962, *Mol. Phys.*, **5**, 225.
- [9] COLTON, R. H., and HENN, D. E. (to be published).

Resonance transfer of molecular excitation energy

by A. D. McLACHLAN

Department of Theoretical Chemistry, University Chemical Laboratory,
Lensfield Road, Cambridge

(Received 26 February 1964; revision received 23 April 1964)

The rate of energy transfer between two identical molecules in empty space is calculated, assuming that initially one molecule is excited and the other is in its ground state, and that electric dipole interactions are responsible for the coupling. The time-dependent Schrödinger equation for molecules and radiation is solved by Van Hove's resolvent operator. The probability that the second molecule is excited oscillates with time at close distances and decays exponentially at long distances. This calculation leads to the apparent contradiction that the excitation energy travels faster than light. The difficulty disappears if one looks at the behaviour of observables rather than wave functions. Calculations are made for the situation where the molecules start in their ground state and then the first one is excited by an external source of radiation. The dipole moment of the second behaves in almost the same way as if the two molecules were a pair of coupled damped harmonic oscillators.

1. INTRODUCTION

When a molecule is in an optically excited state it can pass on its energy to other molecules in several ways [1]. Some of these, such as electron transfer and inelastic collisions require a contact between the two molecules. In other cases, however, transfer of energy takes place between two well-separated molecules at distances of up to 100 Å. The simplest example is that of two identical molecules in empty space, where electronic excitation migrates from one to the other by a resonance process. In a gas this causes sensitized fluorescence from molecules which cannot absorb the incident radiation directly [2]. A similar process can occur with dye molecules in solution and leads to a depolarization of the fluorescence radiation in concentrated solutions, especially when the solvent is a viscous one [3, 4]. Resonance transfer can also occur over long distances between impurity atoms in crystals.

In this paper we shall calculate the transfer of excitation energy between two identical molecules, A and B, in empty space, assuming that they are too far apart for their electron clouds to overlap. There are two limiting cases, which are well known. At distances R much smaller than the wavelength of the light the pair of molecules behaves like a single electronic system [5-7]. If one calls the ground state of the pair $|0\rangle$, and if the states where just one molecule A or B is excited are called $|a\rangle$ and $|b\rangle$, the approximate stationary states of the coupled system are the sum and difference $|+\rangle$ and $|-\rangle$:

$$|\pm\rangle = \frac{1}{\sqrt{2}}\{|a\rangle \pm |b\rangle\} \quad (1.1)$$

and their energies are raised or lowered by a first-order splitting $\hbar\Delta$:

$$W_{\pm} = \hbar(\omega_0 \pm \Delta). \quad (1.2)$$

If molecule A is excited initially then its energy is completely transferred to the other after a time $\tau = \pi/2\Delta$ and continues to oscillate back and forth with period 2τ until a light quantum is given off and the whole system returns to its ground state. Δ is the Coulomb interaction energy between the transition dipole moments \mathbf{p}_a and \mathbf{p}_b to the excited states of the two molecules:

$$\hbar\Delta = \left\{ \frac{\mathbf{p}_a \cdot \mathbf{p}_b}{R^3} - \frac{3(\mathbf{p}_a \cdot \mathbf{R})(\mathbf{p}_b \cdot \mathbf{R})}{R^5} \right\}. \quad (1.3)$$

The transition dipole moments between $|+\rangle$ or $|-\rangle$ and the ground state $|0\rangle$ are therefore

$$\frac{1}{\sqrt{2}}(\mathbf{p}_a \pm \mathbf{p}_b); \quad (1.4)$$

so if the molecules lie parallel the transition from $|+\rangle$ to $|0\rangle$ is electric dipole allowed, but that from $|-\rangle$ is forbidden, and part of the excitation energy can be trapped for a relatively long time in this state. At long distances the situation is rather different. If one molecule is excited at first, then a time R/c must pass before the radiation from it can reach the second, and the Coulomb field, being proportional to $1/R^3$, will be much smaller than the radiation field of the emitted photons, which varies as $1/R$. Thus the transfer process is simply the emission of a photon which is reabsorbed by the second molecule. Retardation effects become important, and so does radiation damping; for the initial excitation may have decayed away completely before the second molecule becomes excited.

Clearly a quantum treatment of the radiation is necessary to investigate the situation properly at all distances, and several discussions based on second order time-dependent perturbation theory [8–10] have appeared. These authors have generally contented themselves with demonstrating that the second molecule does not become excited until the light wave from the first reaches it, and these perturbation theories cannot describe the oscillatory behaviour of the excitation at closer distances.

The most thorough discussion is by Hamilton [11]. He gives an exact solution of the time-dependent Schrödinger equation for two molecules and a photon which is valid at all distances. Also, after the present work was completed, Stephen [12] published a similar treatment of the resonance process at close distances.

All these theories lead to an apparent paradox, since the second molecule seems to become excited before the photon can reach it. Although Heitler [13–15] suggests that these difficulties can be overcome by a canonical transformation of the wave functions, his approach has been criticized [16, 17] and is rather difficult to use. The difficulty appears to come from a conflict between two ideas. Firstly, the requirement that in the quantum theory of radiation sources must emit outgoing waves of purely positive frequency and sinks absorb ingoing waves of negative frequencies [18, 19]. Secondly the classical idea that it is possible to prepare the first molecule in its excited state at the instant $t=0$ and then switch on the interaction with the radiation.

In this paper the aim is to give a consistent causal description of the excitation transfer, which holds at both large and small distances. Instead of discussing what happens to the wave functions when the molecules and photons start from some specified initial state, we look at observables like the dipole moment of one of

the molecules or the electric field at some point in space. Furthermore, since the only true stationary state of the molecules is their ground state, we restrict ourselves to situations where the whole system starts in its ground state and is then excited by an external force which acts on one molecule. The energy transfer is then traced through the time dependence of the physical observables.

We attack the problem in three stages. Section 2 gives the method, in principle, for describing the response to the external force. This is applied to a classical harmonic oscillator model of the molecules. In §3 Van Hove's resolvent operator method [20-24] is used to solve the time dependent Schrödinger equation for two molecules and a photon. Then Van Hove's method is used in §4 to calculate the response to an external force. Finally the two approaches are compared in §5.

2. RESPONSE TO AN EXTERNAL FORCE

Let us suppose that a small classical electromagnetic field, of potential $a_\nu(\mathbf{r}, t)$, acts on the first molecule; the whole system of molecules and radiation being initially in its coupled ground state $|\Psi_0\rangle$. The perturbing Hamiltonian is

$$F = - \int \hat{J}_{a\mu}(\mathbf{r}) a_\mu(\mathbf{r}, t) d\mathbf{r}, \quad (2.1)$$

where $\hat{J}_{a\mu}(\mathbf{r})$ is the charge and current operator for the first molecule, and the four-vector notation

$$J_\mu a_\mu = \mathbf{J} \cdot \mathbf{a} - \rho\phi \quad (2.2)$$

is used. Transfer of excitation to the second molecule is shown by changes in the mean value $\bar{J}_{b\mu}(\mathbf{r}, t)$ of its currents and charges. According to Kubo and Tomita's theory [25] this mean value is

$$\bar{J}_{b\mu}(\mathbf{r}, t) = \frac{i}{\hbar} \int_0^\infty d\tau \int d\mathbf{r}' \langle [\hat{J}_{b\mu}(\mathbf{r}, \tau), \hat{J}_{a\nu}(\mathbf{r}', 0)] \rangle a_\nu(\mathbf{r}', t - \tau). \quad (2.3)$$

Formula (2.3) only applies for fields so weak that the response can be considered linear. $\hat{J}_a(\mathbf{r}, t)$ and $\hat{J}_b(\mathbf{r}, t)$ are the Heisenberg current operators in the coupled system, and the brackets $\langle \rangle$ stand for the average value of the commutator in $|\Psi_0\rangle$. Alternatively the disturbance might be an external classical current distribution $j(\mathbf{r}, t)$ which excites the quantized radiation field. The radiation will reach molecule A and then B. In this experiment $\hat{J}_b(\mathbf{r}, t)$ depends on $j(\mathbf{r}', t - \tau)$ through the response function

$$\frac{i}{\hbar} \langle [\hat{J}_b(\mathbf{r}, \tau), \hat{A}(\mathbf{r}', 0)] \rangle, \quad (2.4)$$

in which $\hat{A}(\mathbf{r}, t)$ is the electromagnetic potential operator of the quantized radiation. A third experiment is to excite the system by an external current at \mathbf{r}' and then measure the scattered radiation from molecule B at some other point \mathbf{r} . The scattered potential depends on

$$\frac{i}{\hbar} \langle [\hat{A}(\mathbf{r}, \tau), \hat{A}(\mathbf{r}', 0)] \rangle. \quad (2.6)$$

To calculate the commutators of the coupled system in its ground state, a general method [25, 26] is to switch on the interaction:

$$V = - \int [\hat{J}_{a\mu}(\mathbf{r}) + \hat{J}_{b\mu}(\mathbf{r})] \hat{A}_\mu(\mathbf{r}) d\mathbf{r}, \quad (2.7)$$

adiabatically, with a time factor $\exp(\alpha t)$ from time $t = -\infty$ to $t = 0$. Then one finds [27] the power series expansion

$$\langle [\hat{J}_b(\mathbf{r}, 0), \hat{J}_a(\mathbf{r}', -\tau)] \rangle = \sum_{n,s} \left(\frac{-i}{\hbar} \right)^n \int dt_1 \dots dt_n \exp[(\alpha(t_1 + t_2 + \dots t_n))] \\ \times \langle [[J_b(\mathbf{r}, 0), V(t_1)], \dots V(t_s)], J_a(\mathbf{r}', -\tau), V(t_{s+1}), \dots V(t_n)] \rangle. \quad (2.8)$$

Here $V(t)$ and $J(t)$ are operators in the interaction representation

$$V(t) = \exp(iH_0 t) V \exp(-iH_0 t); \quad (2.9)$$

the times are restricted to $0 > t_1 > \dots t_s > -\tau > t_{s+1} \dots > t_n$, and the limit is taken as α tends to zero. To evaluate the terms of the series it is important to notice that the commutator of the free fields is a pure number:

$$\frac{i}{\hbar} [A_\mu(\mathbf{r}, \tau), A_\nu(\mathbf{r}', 0)] = \delta_{\mu\nu} \Delta(\mathbf{r}, \mathbf{r}'; \tau); \quad (2.10)$$

$$\Delta(\mathbf{r}, \mathbf{r}'; \tau) = \frac{c}{R} \{ \delta(R - c\tau) - \delta(R + c\tau) \}, \quad (2.11)$$

where $R = |\mathbf{r} - \mathbf{r}'|$. It is equal to the classical retarded potential when $\tau > 0$. An expansion of the multiple commutators in (2.8) shows that each term contains at least one commutator $\Delta(\mathbf{r}, \mathbf{r}'; t - t')$ with times $0 > t > t' > -\tau$, which must therefore vanish unless $(t - t') > R/c$, or $\tau > R/c$. Thus the currents on the two molecules commute exactly for time intervals less than R/c and excitation travels with the velocity of light. Two further results can easily be proved. Firstly the formula

$$\langle [\hat{J}_b(\mathbf{r}, 0), \hat{A}(\mathbf{r}', -\tau)] \rangle = \int_0^\tau dt_1 \int d\mathbf{r}_1 \\ \times \langle [\hat{J}_b(\mathbf{r}, 0), \hat{J}_a(\mathbf{r}_1, -t_1) + \hat{J}_b(\mathbf{r}_1, -t_1)] \rangle \Delta(\mathbf{r}_1, \mathbf{r}'; \tau - t_1), \quad (2.12)$$

which proves that the excitation of molecule B by an external current source can be split into two stages; the arrival of retarded fields at the molecules, and the response of the two molecules to these fields. Secondly

$$\langle [\hat{A}(\mathbf{r}, 0), \hat{A}(\mathbf{r}', -\tau)] \rangle = \Delta(\mathbf{r}, \mathbf{r}'; \tau) \\ + \int_0^\tau dt_1 \int_0^{t_1} dt_2 \Delta(\mathbf{r}, \mathbf{r}_1; t_1) \langle [\hat{J}(\mathbf{r}_1, 0), \hat{J}(\mathbf{r}_2, t_1 - t_2)] \rangle \Delta(\mathbf{r}_2, \mathbf{r}'; t_2). \quad (2.13)$$

This means that the electromagnetic field arriving at \mathbf{r} is the sum of the direct field from the source and the classical retarded fields of the excited molecules. The commutator $\langle [\hat{J}_b(\tau), \hat{J}_a(0)] \rangle$ therefore enters into the description of each of our experiments on the pair of molecules.

In the electric dipole approximation [27] the interaction of the molecules with radiation is written

$$V = -\hat{\mathbf{p}}_a \cdot \hat{\mathbf{E}}(\mathbf{a}) - \hat{\mathbf{p}}_b \cdot \hat{\mathbf{E}}(\mathbf{b}), \quad (2.14)$$

and the response to an external electric field depends on commutators like

$$\frac{i}{\hbar} \langle [\hat{\mathbf{p}}_b(\tau), \hat{\mathbf{p}}_a(0)] \rangle. \quad (2.15)$$

Since the molecules are supposed to be identical it is simpler to work with the sum and difference $\hat{\mathbf{p}}_\pm$. Also, instead of the response functions we consider their

Fourier transforms, the symmetric and anti-symmetric polarizabilities

$$\alpha_{\pm}(\omega) = \frac{i}{\hbar} \int_0^{\infty} \langle [\hat{\mathbf{p}}_{\pm}(\tau), \hat{\mathbf{p}}_{\pm}(0)] \rangle \exp(i\omega\tau) dt, \quad (2.16)$$

Before starting a quantum-mechanical calculation it is useful to work out the polarizability of the molecules in a classical way. The molecules are treated as two classical linear harmonic oscillators of frequency ω_0 and oscillator strength f at a distance R apart along the z axis. The two transition dipole moments are supposed to be parallel, making an angle θ with the z axis, and to be of magnitude p , so that $f = 2m\omega_0 p^2 / \hbar e^2$. Since the radiation field and the molecules behave as an assembly of coupled oscillators, and since the normal modes and the polarizabilities are the same for quantum as for classical oscillators, the results should be relevant.

Suppose that a light wave which produces a small oscillating electric field $E_0 \exp(-i\omega t)$ along the molecular axes acts on both molecules simultaneously with the same phase at each. Each oscillator performs a damped forced oscillation in the combined electric fields from the light wave, the other oscillator, and itself. The electric field depends on the response function

$$\frac{i}{\hbar} [E_i(\mathbf{r}, \tau), E_k(\mathbf{r}', 0)] = T_{ik}(\mathbf{r}, \mathbf{r}'; \tau), \quad (2.17)$$

where the indices i, k stand for x, y, z ; and the Fourier transform of the tensor T_{ik}

$$T_{ik}(\mathbf{r}, \mathbf{r}'; \omega) = [\nabla_i \nabla_k - \delta_{ik} \nabla^2] \frac{\exp(i\omega R/c)}{R} \quad (2.18)$$

gives the retarded electric field of a classical dipole oscillator. Thus if the dipole moment of the first molecule has amplitude P , then it produces an electric field along the axis of the second equal to

$$(T' + iT'')P \exp(-i\omega t), \quad (2.19)$$

with in-phase and out-of-phase parts given by

$$\left. \begin{aligned} T'(R, \omega) &= \frac{1}{R^3} \{ (3 \cos^2 \theta - 1) [\cos kR + kR \sin kR] + \sin^2 \theta k^2 R^2 \cos kR \}, \\ T''(R, \omega) &= \frac{1}{R^3} \{ (3 \cos^2 \theta - 1) [\sin kR - kR \cos kR] - \sin^2 \theta k^2 R^2 \sin kR \}, \end{aligned} \right\} \quad (2.20)$$

where $k = \omega/c$. The molecule also produces a reaction field on itself, which comes from radiation damping, and has the form

$$iT''_0(\omega)P \exp(-i\omega t), \quad (2.21)$$

where $T''_0(\omega)$ is the limit of $T''(R, \omega)$ as R tends to zero, and has the value

$$T''_0(\omega) = 2\omega^2/3c^3. \quad (2.22)$$

Adding these fields together, one finds a pair of simultaneous equations for the amplitudes x_a and x_b of the oscillations at frequency ω :

$$\left. \begin{aligned} m(\omega_0^2 - \omega^2)x_a &= fe^2 [iT''_0 x_a + (T' + iT'')x_b] - feE_0, \\ m(\omega_0^2 - \omega^2)x_b &= fe^2 [iT''_0 x_b + (T' + iT'')x_a] - feE_0. \end{aligned} \right\} \quad (2.23)$$

The solution has both molecules oscillating in phase, each with a dipole moment $\alpha_+(\omega)E_0$. If the external fields are out of phase there is a similar anti-symmetric

solution. The two polarizabilities

$$\alpha_{\pm}(\omega) = \frac{fe^2}{m(\omega_0^2 - \omega^2) - fe^2[iT''_0 \pm (T' + iT'')]} \quad (2.24)$$

look like the polarizabilities of a damped classical oscillator, except that the factors T depend on the frequency. The result can be rewritten in the form

$$\alpha_{\pm}(\omega) = \frac{fe^2/m}{\omega_{\pm}^2 - \omega^2 - i\omega\gamma_{\pm}}, \quad (2.25)$$

which implies that the two modes of the coupled oscillators have different frequencies ω_{\pm} and damping factors γ_{\pm} . Since T is small at most distances, one finds

$$\omega_{\pm} = \omega_0 \pm \Delta(\omega_0); \quad \gamma_{\pm} = \gamma_0 \pm \gamma_{AB}. \quad (2.26)$$

Here $\Delta(\omega_0)$ is an effective energy splitting, which reduces to (1.3) at close distances but oscillates at long distances:

$$\Delta(\omega_0) = -(P^2/\hbar)T'(R, \omega_0). \quad (2.27)$$

γ_0 is the usual damping factor for the separate molecules, $\gamma_0 = (4p^2\omega_0^3/3\hbar c^3)$, and γ_{AB} represents the effect of their interaction:

$$\gamma_{AB} = \frac{2p^2}{\hbar} T''(R, \omega_0). \quad (2.28)$$

At very close distances γ_{AB} and γ_0 are equal. This means that $\gamma_+ = 2\gamma_0$ and $\gamma_- = 0$, in accordance with the usual electric dipole selection rules (1.4). At long distances γ_{AB} becomes very small, and each excited state decays independently with its ordinary radiative lifetime $\tau_0 = 1/\gamma_0$.

To link up these results with the question of energy transfer, let us give the first oscillator a displacement x at $t=0$ and then calculate the subsequent displacement of the second. The initial displacement is obtained by superposing the two normal modes with equal amplitudes. Then the value of x_b is the real part of

$$x_b = \frac{1}{2}x\{\exp[-(\frac{1}{2}\gamma_+ + i\omega_+)t] - \exp[-(\frac{1}{2}\gamma_- + i\omega_-)t]\}. \quad (2.29)$$

It oscillates back and forth with a frequency $2\Delta(\omega_0)$ and an average decay rate γ_0 . Efficient energy transfer will occur between two molecules if the transfer time τ is not greater than the decay time τ_0 . This condition is only met if $R < \lambda/2\pi$, for according to (1.1) and (2.22)

$$\tau/\tau_0 = (2\pi R/\lambda)^3 [2\pi/3(3\cos^2\theta - 1)]. \quad (2.30)$$

Thus energy transfer to a single molecule over longer distances is not very probable. If, however, the excited molecule is surrounded by a large number of acceptor molecules the total probability of a resonant transfer to one of them falls off much more slowly. All the retardation effects are included in the frequency dependence of $T'(\omega)$ and $T''(\omega)$.

3. THE RESOLVENT METHOD

In this section we consider how the wave function $|\Psi(t)\rangle$ of the molecules and radiation develops from an arbitrary initial state $|\Psi(0)\rangle$ when the coupling with the photons is included. For simplicity we shall assume that each molecule has only one excited state, of energy $\hbar\omega_a$ or $\hbar\omega_b$, and restrict the wave function

to be a linear combination of the following unperturbed excited states :

- $|a\rangle$ A excited, but not B, no photons.
- $|b\rangle$ B excited, but not A, no photons.
- $|r\rangle$ photon in state r , no molecules excited.
- $|r'\rangle$ photon in state r , both molecules excited.

We use the scheme of quantization in which longitudinal and scalar photons are used [13] to replace the usual Coulomb interaction between charges. Also, in the electric dipole approximation the interaction Hamiltonian takes the form

$$-\hat{\mathbf{p}} \cdot \mathbf{E}(\mathbf{r}) \quad (3.1)$$

for each molecule. If $\hbar H$ is the total Hamiltonian its off-diagonal matrix elements all vanish, except for

$$\left. \begin{aligned} A_r &= \langle a|H|r\rangle = \langle b|H|r'\rangle = -(p_a/\hbar)E(\mathbf{a})^{0r}, \\ B_r &= \langle b|H|r\rangle = \langle a|H|r'\rangle = -(p_b/\hbar)E(\mathbf{b})^{0r}, \end{aligned} \right\} \quad (3.2)$$

and their complex conjugates. $E(\mathbf{a})^{0r}$ stands for the matrix element of the electric field along the molecular axis of A between the states with and without the photon r . The first few rows of the energy matrix H therefore have the form :

$$\begin{array}{c} 2' \\ 1' \\ a \\ b \\ 1 \\ 2 \end{array} \left[\begin{array}{cc|cc|cc} \omega_a + \omega_b + \omega_2 & 0 & B_2^* & A_2^* & 0 & 0 \\ 0 & \omega_a + \omega_b + \omega_1 & B_1^* & A_1^* & 0 & 0 \\ \hline B_2 & B_1 & \omega_a & 0 & A_1 & A_2 \\ A_2 & A_1 & 0 & \omega_b & B_1 & B_2 \\ \hline 0 & 0 & A_1^* & B_1^* & \omega_1 & 0 \\ 0 & 0 & A_2^* & B_2^* & 0 & \omega_2 \end{array} \right] \quad (3.3)$$

We do not yet assume that the molecules are identical. The connection between $|\Psi(t)\rangle$ and $|\Psi(0)\rangle$ is

$$|\Psi(t)\rangle = U(t)|\Psi(0)\rangle; \quad U(t) = \exp(-iHt). \quad (3.4)$$

Following Van Hove [20, 21] we first form the resolvent operator

$$R(z) = (H - z)^{-1}, \quad (3.5)$$

with z an arbitrary complex number, and then find $U(t)$ as a contour integral

$$U(t) = -\frac{1}{2\pi i} \oint R(z) \exp(-izt) dz \quad (3.6)$$

round a contour which encircles the poles of $R(z)$ on the real axis of z . The matrix elements of R are found very easily using determinants [28], for if $D(z)$ is the determinant of the matrix $(H - z)$, and $D_{mn}(z)$ is its m, n signed minor, one has

$$R_{mn}(z) = D_{nm}(z)/D(z), \quad (3.7)$$

$$U_{mn}(t)(-1) = -\frac{1}{2\pi i} \oint \frac{D_{nm}(z)}{D(z)} \exp(-izt) dz. \quad (3.8)$$

The determinants of the matrix (3.3) are simple to work out, and allow an exact calculation of $U(t)$. The matrix of U between the molecular states $|a\rangle$ and $|b\rangle$ is particularly interesting because $U_{ba}(t)$ and $U_{aa}(t)$ are the probability amplitudes that the initial state with molecule A excited has either excited the second molecule

or remained unaltered after a time interval t . It turns out that this 2×2 section \mathcal{R} of the resolvent matrix is itself the inverse of a new matrix

$$\mathcal{R} = [\mathcal{H}(z) - z]^{-1} = \begin{bmatrix} \omega_a + g_{aa}(z) - z & g_{ab}(z) \\ g_{ba}(z) & \omega_b + g_{bb}(z) - z \end{bmatrix}^{-1} \quad (3.9)$$

in which $g_{ab}(z)$ is the function

$$g_{ab}(z) = \sum_r \frac{A_r B_r^*}{z - \omega_r} + \sum_r \frac{B_r A_r^*}{z - \omega_a - \omega_b - \omega_r} = k_{ab}(z) + k_{ba}(z - \omega_a - \omega_b) \quad (3.10)$$

and g_{aa} , g_{bb} are defined similarly. According to (3.3) and (3.6), if $\mathcal{U}(t)$ is the sub-matrix of $U(t)$ which refers to the states a and b , then

$$\mathcal{U}(t) = -\frac{1}{2\pi i} \oint \frac{\exp(-izt)}{\mathcal{H}(z) - z} dz. \quad (3.11)$$

This may be interpreted as if $\mathcal{H}(z)$ were a frequency-dependent effective Hamiltonian coupling the unperturbed molecular states, in which the coupling with the photons gives effective energy matrix elements like $g_{ab}(z)$.

It is now important to look into the analytic behaviour of the matrices $g(z)$ and $k(z)$. The sum in (3.10) is really an integral, because the photons form a continuous spectrum of states. For this reason $k_{ab}(z)$ does not have discrete poles on the real axis, but a finite discontinuity [20]. The matrix elements A_r and B_r are found by standard methods, and one finds

$$\frac{\pi}{\hbar} \sum_r E(\mathbf{a})^{0r} E(\mathbf{b})^{r0} \delta(\omega_r - \omega) = T''(R, \omega), \quad (3.12)$$

where $T''(R, \omega)$ is given in (2.20). The sum in (3.10) now becomes

$$k_{ab}(z) = (p_a p_b / \pi \hbar) \int_0^\infty \frac{T''(R, \omega)}{z - \omega} d\omega \quad (3.13)$$

with $k_{ab} = k_{ba}$. This is a regular function of z except across the real axis, where it tends to different limits

$$k_{ab}(\omega \pm i\epsilon) = K_{ab}(\omega) \mp iJ_{ab}(\omega) \quad (3.14)$$

on the two sides as $\epsilon \rightarrow 0$. $K_{ab}(\omega)$ and $J_{ab}(\omega)$ are both real functions of ω . The integral for $k_{aa}(z)$ corresponding to (3.13) actually diverges on the real axis, and $K_{aa}(\omega)$ is infinite. This is a self-energy effect, and we shall remove it by arbitrarily setting $K_{aa} = 0$. On the other hand, the imaginary part J_{aa} is finite and leads to damping of the state $|a\rangle$. Its value is

$$J_{aa}(\omega) = (p_a^2 / \hbar) T''_0(\omega). \quad (3.15)$$

In the same way, the matrix elements of $g(z)$ have a finite discontinuity:

$$g_{ab}(\omega \mp i\epsilon) = E_{ab}(\omega) \mp i\Gamma_{ab}(\omega), \quad (3.16)$$

where $\Gamma_{ab}(\omega) = J_{ab}(\omega) + J_{ab}(\omega - \omega_a - \omega_b)$ because of (3.10).

To avoid complications let us now assume that the two molecules are identical with $p_a = p_b = p$, and $\omega_a = \omega_b = \omega_0$. In this case it is easiest to work with the new states $|\pm\rangle$ of (1.1) because then $\mathcal{U}(t)$ is a diagonal matrix with two elements $\mathcal{U}_{++}(t)$ and $\mathcal{U}_{--}(t)$. Transforming (3.9) and (3.11) into the new form gives

$$\mathcal{U}_{++}(t) = -\frac{1}{2\pi i} \oint \frac{\exp(-izt)}{[\omega_0 + g_{\pm}(z) - z]} dz, \quad (3.17)$$

with a similar expression for $\mathcal{U}_{--}(t)$. Here

$$g_{\pm}(z) = g_{aa}(z) \pm g_{ab}(z). \quad (3.18)$$

Taking the contour to be the pair of lines $z = \omega \pm i\epsilon$ for $\omega > 0$, one obtains the integral

$$\mathcal{U}_{++}(t) = \frac{1}{\pi} \int_0^{\infty} \frac{\Gamma_+(\omega) \exp(-i\omega t)}{[\omega_0 + E_+(\omega) - \omega]^2 + [\Gamma_+(\omega)]^2} d\omega. \quad (3.19)$$

In this integral two different time scales enter. When t is small the frequency variation of $E(\omega)$ and $\Gamma(\omega)$ is dominant, and this is due to the finite velocity of light. After a longer time ($t \gg R/c$) the largest contribution comes from frequencies close to ω_0 , or rather to the displaced frequencies ω_{\pm} which satisfy the relation

$$\omega_{\pm} = \omega_0 + E_{\pm}(\omega_{\pm}) \approx \omega_0 + E_{\pm}(\omega_0). \quad (3.20)$$

In this range of times the probability amplitude varies as

$$\mathcal{U}_{++}(t) = \exp(-i\omega_+ t) \exp(-\frac{1}{2}\gamma_+ t) \quad (3.21)$$

with a damping factor $\gamma_+ = 2\Gamma_+(\omega_0)$. This result looks very like the one we found in §2 and agrees with the usual theory of radiation damping [29–31]. Indeed the states turn out to have the same energy shifts and lifetimes as the equivalent classical harmonic oscillators. The value of $g_{ab}(\omega_0)$ can be found by standard methods. It is

$$\begin{aligned} g_{ab}(\omega_0 + i\epsilon) &= -\frac{p^2}{\hbar^2} \sum_r \left\{ \frac{E(\mathbf{a})^{0r} E(\mathbf{b})^{r0}}{\omega_r - \omega_0 - i\epsilon} + \frac{E(\mathbf{b})^{0r} E(\mathbf{a})^{r0}}{\omega_r + \omega_0 + i\epsilon} \right\} \\ &= \frac{-p^2}{\hbar} [T'(R, \omega) + iT''(R, \omega)]. \end{aligned} \quad (3.22)$$

The real part of $g_{aa}(\omega_0 + i\epsilon)$ diverges and has been set equal to zero, but the imaginary part, according to (3.15) is

$$\Gamma_{aa}(\omega_0) = (p^2/\hbar) T''_0(\omega_0) = \frac{1}{2}\gamma_0. \quad (3.23)$$

Collecting these results together we find that

$$g_{\pm}(\omega_0 + i\epsilon) = \pm \Delta(\omega_0) - \frac{1}{2}i(\gamma_0 \pm \gamma_{AB}), \quad (3.24)$$

so that the frequencies and damping factors in (3.20) and (3.21) are identical with those found before in (2.26).

It is now time to examine the probability, after a very short time, that a transition has taken place from $|a\rangle$ to $|b\rangle$. This is

$$|\bar{U}_{ba}(t)|^2, \quad (3.25)$$

where

$$\bar{U}_{ba}(t) = U_{ba}(t) \exp(i\omega_0 t) = -\frac{1}{2\pi i} \oint R_{ba}(z + \omega_0) \exp(-izt). \quad (3.26)$$

We shall show that it differs from zero at times $t < R/c$ before light can have passed between the molecules. Although this does not conflict with modern ideas of causality [18, 19] it is a surprising fact which does not seem to have been noticed before [8–11].

To prove this we shall approximate the matrix elements of $R(z)$ by treating $g_{ba}(z)$ as a small quantity. (This does not affect the validity of the result.) Thus

$$\left. \begin{aligned} R_{aa}(z) &= R_{bb}(z) \approx [\omega_0 + g_{aa}(z) - z]^{-1}, \\ R_{ba}(z) &\approx R_{bb}(z) g_{ba}(z) R_{aa}(z). \end{aligned} \right\} \quad (3.27)$$

In this approximation the probability amplitude that $|a\rangle$ remains $|a\rangle$ is

$$\bar{U}_{aa}(t) \approx \exp(-\gamma_0 t). \quad (3.28)$$

To calculate $\bar{U}_{ba}(t)$ we use Hugenholtz's convolution theorem [22], which is like the convolution theorem for ordinary Fourier transforms. Then (3.27) gives

$$\begin{aligned} \bar{U}_{ba}(t) &= \int_0^t dt_1 \int_0^{t_1} dt_2 \bar{U}_{bb}(t-t_1) \bar{G}_{ba}(t_2) \bar{U}_{aa}(t_1-t_2) \\ &= \int_0^t dt_1 \int_0^{t_1} dt_2 \bar{G}_{ba}(t_2) \exp[-\gamma_0(t-t_2)]; \end{aligned} \quad (3.29)$$

where

$$\begin{aligned} \bar{G}_{ba}(t) &= -\frac{1}{2\pi i} \oint g_{ba}(\omega_0 + z) \exp(-izt) dz \\ &= -(2p^2/\pi\hbar) \cos \omega_0 t \int_0^\infty T''(R, \omega) \exp(-i\omega t) d\omega \end{aligned} \quad (3.30)$$

because of (3.13). If the frequency range of the integral (3.30) is extended to $-\infty$ we obtain the retarded electric field (2.17) resolved along the axes of the two dipoles:

$$T(R, t) = \frac{i}{\pi} \int_{-\infty}^\infty T''(R, \omega) \exp(i\omega t) d\omega. \quad (3.31)$$

At long distances its value, from (2.20) is

$$\begin{aligned} &-\frac{\sin^2 \theta}{\pi R} \int_{-\infty}^\infty i \frac{\omega^2}{c^2} \sin \frac{\omega R}{c} \exp(-i\omega t) d\omega \\ &= \frac{\sin^2 \theta}{Rc} \frac{\partial^2}{\partial t^2} [\delta(ct-R) - \delta(ct+R)]. \end{aligned} \quad (3.32)$$

The quantity which appears in (3.30) is the positive frequency part of $T(R, t)$, and the truncated Fourier integral is

$$\frac{\sin^2 \theta}{2Rc} \frac{\partial^2}{\partial t^2} [\delta_+(ct-R) - \delta_+(ct+R)], \quad (3.33)$$

where $\delta_+(x)$ is the function

$$\delta_+(x) = \delta(x) - \frac{i}{\pi} P\left(\frac{1}{x}\right), \quad (3.34)$$

and P stands for the principal part of the function.

Since the function $\bar{G}_{ba}(t)$, and hence $\bar{U}_{ba}(t)$, differs from zero outside the light cone $t < R/c$ it might seem that the second molecule could become excited before a light ray from the first could reach it. Mathematically this is due to the occurrence of the $\delta_+(ct-R)$ function in the integral (3.30), which appears because the frequency ω of the emitted photon must be positive. However, there is no physical paradox, because it is not the wave functions but the values of physical observables, which are measured in any experiment, and the observables as we showed in §2, do not change until the light reaches the second molecule. One might also argue that the unperturbed states $|a\rangle$ and $|b\rangle$ are not real states, and have no direct physical meaning, so that it is not possible to prepare the system at time $t=0$ in one of these states. However, it appears from the discussion in §5 that this point is not important.

4. CALCULATION OF THE POLARIZABILITY

To calculate the symmetric or anti-symmetric polarizability from equation (2.16) we first consider the simpler quantity

$$\langle p_+(t)p_+(0) \rangle = \sum_n \langle \Psi_0 | p_+ | \Psi_n \rangle \langle \Psi_n | p_+ | \Psi_0 \rangle \exp[-i(\epsilon_n - \epsilon_0)t], \quad (4.1)$$

where $|\Psi_0\rangle$ and $|\Psi_n\rangle$ are the true ground and excited states of the system, with energies $\hbar\epsilon_0$, $\hbar\epsilon_n$. The resolvent operator

$$R(z) = \sum_{n=0}^{\infty} \frac{|\Psi_n\rangle \langle \Psi_n|}{\epsilon_n - z} \quad (4.2)$$

has a discrete pole at ϵ_0 , and its residue is the projection operator for the ground state:

$$Q = |\Psi_0\rangle \langle \Psi_0| = \lim_{z \rightarrow \epsilon_0} [(\epsilon_0 - z)R(z)]. \quad (4.3)$$

One therefore obtains (4.1) as a contour integral:

$$\langle p_+(t)p_+(0) \rangle = -\frac{1}{2\pi i} \oint \Phi_+(z) \exp(-izt) dz, \quad (4.4)$$

$$\Phi_+(z) = \text{Tr} \{ Q p_+ R(z + \epsilon_0) p_+ \},$$

and the polarizability is the limit as $\epsilon \rightarrow 0$ of

$$\alpha_+(\omega) = \frac{1}{\hbar} [\Phi_+(\omega + i\epsilon) + \Phi_+(-\omega - i\epsilon)]. \quad (4.5)$$

Since the molecules are identical every state of the system is even or odd on reflection in a plane midway between them. The ground state is even, p_+ is an even operator, and so all the intermediate states $|\Psi_n\rangle$ are even too. Also the phases of the photons may be chosen so that they are each even or odd, with $A_r = \pm B_r$ in the energy matrix. The resolvent matrix will be constructed from a smaller set of states than before, since otherwise the calculation leads to some very heavy algebra. The states will be formed from the following set

Ground state components	{	0>	Molecules in ground state. No photons
	{	m+>	Molecules in +> state. One even photon m(+).
	{	m->	Molecules in -> state. One odd photon m(-).

Upper state components (even)	{	+>	Molecules in +> state. No photons.
	{	r+>	Molecules in ground state. Even photon r(+).

There are also similar components for the odd upper state.

The off-diagonal elements of the energy matrix are now

$$\langle 0 | H | m \pm \rangle = \hbar C_{m \pm}, \quad \langle \pm | H | r \pm \rangle = \hbar C_{r \pm}, \quad (4.6)$$

$$C_{r \pm} = \frac{1}{\sqrt{2}} (A_r \pm B_r). \quad (4.7)$$

The elements of the upper state part of the resolvent matrix are then found:

$$R_{++} = \frac{1}{(\omega_0 - z) + k_+(z)}; \quad R_{r+,+} = -\frac{C_{r+}^*}{(\omega_r - z)} R_{++}; \quad (4.8)$$

$$R_{r+,s+} = \frac{\delta_{rs}}{(\omega_r - z)} + \frac{C_{r+}^* C_{s+}}{(\omega_r - z)(\omega_s - z)} R_{++};$$

where

$$k_{\pm}(z) = k_{aa} \pm k_{ab} = \sum_r \frac{|C_{r\pm}|^2}{z - \omega_r}, \quad (4.9)$$

and the functions $k(z)$ are defined in (3.10). Similarly the ground-state part gives

$$R_{00}(z) = \frac{1}{k_0(z) - z}, \quad (4.10)$$

with $k_0 = (k_+ + k_-)$, and has a pole at ϵ_0 , fixed by the condition $\epsilon_0 = k_0(\epsilon_0)$. The residue at the pole gives the projection

$$Q_{00} = \frac{1}{1 - k'_0(\epsilon_0)}. \quad (4.11)$$

and the other components of Q are

$$\left. \begin{aligned} Q_{m\pm,0} &= \frac{-C_{m\pm}^*}{(\omega_0 + \omega_m - \epsilon_0)} Q_{00}, \\ Q_{m\pm,n\pm} &= \frac{C_{m\pm}^* C_{n\pm}}{(\omega_0 + \omega_m - \epsilon_0)(\omega_0 + \omega_n - \epsilon_0)} Q_{00}. \end{aligned} \right\} \quad (4.12)$$

After some algebra the trace (4.4) gives

$$\Phi_+(z) = \frac{2p^2 Q_{00}}{[(z + \omega_0)R_{++}(\epsilon_0 - \omega_0)]^2} \{R_{++}(\epsilon_0 + z) - (z + \omega_0)R'_{++}(\epsilon_0 - \omega_0) - R_{++}(\epsilon_0 - \omega_0)\}. \quad (4.13)$$

Before considering the behaviour of this function we note that ϵ_0 and $k'(\epsilon_0)$ are divergent quantities because of self-energy effects, but since ϵ_0 is actually the dispersion energy of the atoms it is very small, and can here be taken as zero. So will $k'_0(\epsilon_0)$. The constant $R_{++}(\epsilon_0 - \omega_0)$ is almost equal to $(2\omega_0)^{-1}$.

$\Phi_+(z)$ has a finite discontinuity across the positive real axis, but it is finite elsewhere, including the point $z = -\omega_0$. According to (4.5) the imaginary part of $\alpha_+(\omega)$ for $\omega > 0$ is proportional to the imaginary part of $\Phi_+(z)$:

$$\alpha''_{+}(\omega) = \frac{2p^2}{\hbar} \left(\frac{2\omega_0}{\omega_0 + \omega} \right)^2 \frac{J_+(\omega)}{[\omega_0 + K_+(\omega) - \omega]^2 + [J_+(\omega)]^2}. \quad (4.14)$$

Here $K_+(\omega) \pm iJ_+(\omega)$ are the limits of $k_{\pm}(z)$ on the real axis. In the neighbourhood of ω_0 the factor $(2\omega_0/\omega_0 + \omega)$ is close to one, and the complete polarizability has the approximate value

$$\alpha_+(\omega) = \frac{2p^2}{\hbar} \frac{1}{\omega_0 + K_+(\omega) - iJ_+(\omega)}. \quad (4.15)$$

This is like the polarizability of a molecular state with excitation frequency $[\omega_0 + K_+(\omega_0)]$ and damping $J_+(\omega_0)$. In fact (3.13) gives

$$J_+(\omega_0) = \frac{p^2}{\hbar} [T''(R, \omega_0) + T''_0(\omega_0)] = \frac{1}{2}(\gamma_0 + \gamma_{AB}), \quad (4.16)$$

$$K_+(\omega_0) = (p^2/\hbar\pi)P \int_0^\infty \frac{T''(R, x)}{\omega_0 - x} dx \approx \Delta(\omega_0), \quad (4.17)$$

and the results agree almost exactly with those of §§2 and 3. Precisely similar results can also be obtained for the anti-symmetric polarizability.

The response of the quantized system is almost the same as for the classical oscillators. The differences between (2.26) and (4.14) arise because each molecule has only been allowed one excited state, and because the resolvent matrix only includes a small basic set of states. The description of the system by commutation relations rather than wave functions automatically ensures that all interactions travel with the speed of light.

5. THE DESCRIPTION BY WAVE FUNCTIONS

It is interesting to examine more closely the relation between the two descriptions of energy transfer, by linear response theory in §2, and by time-dependent wave functions in §3. To do this let us first look at the precise form of the stationary state wave functions. The ground state $|\Psi_0\rangle$ is found by applying the projection operator Q (4.3) to the unperturbed state $|0\rangle$.

$$Q|0\rangle = |\Psi_0\rangle \langle \Psi_0|0\rangle. \quad (5.1)$$

Using (4.11) and (4.12) one then finds the normalized ground state:

$$|\Psi_0\rangle = N_0 \left\{ |0\rangle - \sum_{m\pm} \frac{C_{m\pm}^*}{\omega_0 + \omega_m - \epsilon_0} |m\pm\rangle \right\}, \quad (5.2)$$

where $N_0^2 = Q_{00}$. The excited states can be found in the same way. We define the projection operator $Q(\omega)$ for the continuum states:

$$Q(\omega) = |\omega\rangle \langle \omega| = \frac{1}{2\pi i} [R(\omega + i\epsilon) - R(\omega - i\epsilon)], \quad (5.3)$$

and then there are a series of symmetrical stationary states $|\omega+\rangle$ derived by projecting onto the unperturbed state $|+\rangle$.

$$|\omega+\rangle = \frac{Q(\omega)|+\rangle}{N_+(\omega)}, \quad (5.4)$$

where $N_+(\omega)$ is the normalizing factor

$$N_+^2(\omega) = Q_{++}(\omega) = \frac{1}{\pi} \frac{J_+(\omega)}{[(\omega_0 - \omega) + K_+(\omega)]^2 + [J_+(\omega)]^2}. \quad (5.5)$$

Substitution of (4.8) into (5.3) leads at once to the result

$$|\omega+\rangle = N_+(\omega) \left(|+\rangle - \sum_r \left[\frac{P}{\omega_r - \omega} + \pi \delta(\omega_r - \omega) \left\{ \frac{\omega_0 - \omega + K_+(\omega)}{J_+(\omega)} \right\} \right] C_{r+}^* |r+\rangle \right) \quad (5.6)$$

There will also be a similar set of odd excited states $|\omega-\rangle$ obtained by projection from $|-\rangle$.

In §3 we calculated the time variation of the state which started with the wave function $|+\rangle$ at $t=0$. In terms of the stationary states we have the expansion

$$|+\rangle = \int_0^\infty |\omega+\rangle \langle\omega+|+\rangle d\omega = \int_0^\infty N_+(\omega) |\omega+\rangle d\omega \quad (5.7)$$

and the time variation is now obvious because each stationary state develops with a phase factor $\exp(-i\omega t)$. To see the relation with the linear response theory let us suppose that a small perturbation in the form of a pulse

$$V = -\lambda(p_a + p_b)\delta(t) \quad (5.8)$$

is applied to the system in its ground state. Immediately after the pulse the wave function is

$$|\Psi\rangle = |\Psi_0\rangle + \lambda|\Psi_+\rangle, \quad (5.9)$$

where the function $|\Psi_+\rangle$ is a certain combination of excited states:

$$|\Psi_+\rangle = \frac{i}{\hbar} \int_0^\infty P_+(\omega) |\omega+\rangle d\omega, \quad (5.10)$$

and $P_+(\omega)$ is defined to be the matrix element:

$$P_+(\omega) = \langle\omega+|P_a + P_b|\Psi_0\rangle. \quad (5.11)$$

Since we know the stationary states it is easy to calculate this quantity exactly (within our restricted basic set of states). The result is

$$P_+(\omega) = N_0 N_+(\omega) p \sqrt{2} [(\omega_0 + \omega - \epsilon_0) R_{++}(\epsilon_0 - \omega_0)]^{-1} \quad (5.12)$$

$$\approx N_0 N_+(\omega) p \sqrt{2} \left(\frac{2\omega_0}{\omega_0 + \omega} \right). \quad (5.13)$$

This agrees nicely with our calculation of the polarizability in (4.14) and also shows that $|\Psi_+\rangle$ is practically the same state as $|+\rangle$. Thus the two descriptions in §2 and §3 are almost equivalent.

The change in the average value of the dipole moment after the pulse is

$$\bar{p}_+(t) = \langle\Psi_0|p_+|\Psi_+(t)\rangle + \langle\Psi_+(t)|p_+|\Psi_0\rangle, \quad (5.14)$$

and contains both positive and negative frequency parts. The time variation of the wave function only contains positive frequency parts. This explains the apparent paradox mentioned at the end of §3. $|\Psi_+\rangle$ and $\langle\Psi_+|$ contain parts which vary like the functions $\delta_\pm(ct-R)$, but in the average value (5.14) they combine to give the complete $\delta(ct-R)$ function.

I am most grateful to Dr. G. N. Fowler for a long discussion in which he pointed out how the results obtained in this paper should be interpreted, in the light of modern concepts of causality.

REFERENCES

- [1] CARIO, G., and FRANCK, J., 1923, *Z. Phys.*, **17**, 202.
- [2] FORSTER, T., 1959, *Disc. Faraday Soc.*, **27**, 7.
- [3] FORSTER, T., 1948, *Ann. Phys.*, **2**, 55.
- [4] FORSTER, T., 1946, *Naturwissenschaften*, **33**, 166.
- [5] KALLMANN, H., and LONDON, F., 1928, *Z. phys. Chem. B*, **2**, 207.

- [6] PERRIN, J., 1932, *Ann. Chim. (Phys.)*, **17**, 283.
- [7] KASHA, M., 1959, *Rev. mod. Phys.*, **31**, 162.
- [8] KIKUCHI, S., 1930, *Z. Phys.*, **66**, 58.
- [9] FERMI, E., 1932, *Rev. mod. Phys.*, **4**, 87.
- [10] HEITLER, W., and MA, S. T., 1949, *Proc. R. Inst. Acad.*, **52**, 109.
- [11] HAMILTON, J., 1949, *Proc. phys. Soc., Lond. A*, **62**, 12.
- [12] STEPHEN, M. J., 1964, *J. chem. Phys.*, **40**, 669.
- [13] HEITLER, W., 1957, *The Quantum Theory of Radiation*, 3rd edition (Oxford University Press).
- [14] HEITLER, W., and MA, S. T., 1949, *Phil. Mag.*, **40**, 651.
- [15] ARNOUS, E., and HEITLER, W., 1953, *Proc. roy. Soc., A*, **220**, 290.
- [16] FERRETTI, B., and PEIERLS, R. E., 1947, *Nature, Lond.*, **160**, 531.
- [17] WENTZEL, G., 1948, *Helv. phys. acta*, **21**, 49.
- [18] HILGEVOORD, J., 1960, *Dispersion Relations and Causal Description* (Amsterdam: North-Holland Publishing Co.).
- [19] MA, S. T., 1958, *Nuclear Phys.*, **7**, 163.
- [20] VAN HOVE, L., 1955, *Physica*, **21**, 901.
- [21] VAN HOVE, L., 1956, *Physica*, **22**, 343.
- [22] HUGENHOLTZ, N. M., 1957, *Physica*, **23**, 481.
- [23] HARRIS, R. A., 1963, *J. chem. Phys.*, **39**, 978.
- [24] VAN HOVE, L., HUGENHOLTZ, N. M., and HOWLAND, L. P., 1961, *Quantum Theory of Many-Particle Systems* (New York: W. A. Benjamin).
- [25] KUBO, R., and TOMITA, K., 1954, *J. phys. Soc., Japan*, **9**, 888.
- [26] GELL-MANN, M., and LOW, F., 1951, *Phys. Rev.*, **84**, 350.
- [27] McLACHLAN, A. D., 1963, *Proc. roy. Soc. A*, **271**, 387.
- [28] COULSON, C. A., and LONGUET-HIGGINS, H. C., 1947, *Proc. roy. Soc. A*, **191**, 39; **192**, 16.
- [29] WEISSKOPF, V., and WIGNER, E., 1930, *Z. Phys.*, **63**, 54.
- [30] WEISSKOPF, V., and WIGNER, E., 1930, *Z. Phys.*, **65**, 18.
- [31] WEISSKOPF, V., 1933, *Z. Phys.*, **85**, 541.

Proton magnetic resonance of symmetrical molecules

II. The analysis of A_2B_2 spectra by perturbation methods : the A_2X_2 and the $(AX)_2$ approximations†

by BO GESTBLOM, RAGNAR A. HOFFMAN and SÖREN RODMAR

Institute of Physics, University of Uppsala, Uppsala, Sweden

(Received 21 January 1964; revision received 19 May 1964)

Methods have been developed for the analysis of large-shift A_2B_2 spectra by perturbation techniques.

Modified first-order expressions for the A_2X_2 transition frequencies are given and two alternative types of second-order correction terms are added. For the first kind of expression the somewhat restrictive conditions pertain that all the coupling constants are to be small as compared to the relative chemical shift, whereas the second kind of expression was derived on the more general assumption that only the coupling constants between chemically shifted nuclei are small.

The expressions for the relative intensities have been supplemented with first-order correction terms (i.e. terms on the order of $L/(\nu_A - \nu_B)$ and $N/(\nu_A - \nu_B)$).

As a useful alternative, the very simple expressions obtained in the $(AX)_2$ approximation may be used whenever one of the coupling constants between the chemically shifted nuclei is large in comparison with the other couplings in the spin system. Expressions for the transition frequencies are given to first and second order and for the intensities to first order.

The analysis of the proton resonance spectra for a few disubstituted benzenes serve to illustrate the applicability of these perturbation methods.

1. INTRODUCTION

The problem of the analysis of N.M.R. spectra is greatly simplified if the molecules have symmetry properties. The simplest example is the AB_2 case where closed expressions for all transition frequencies and the intensities can be derived [2].

In the A_2B_2 case the use of basis functions with correct symmetry properties also greatly reduces the problem, i.e. the Hamiltonian matrix is to a large extent factorized [3, 4]. However, a complete factorization is not obtainable, and one is left with a 4×4 sub-matrix belonging to the symmetrical spin zero states, which in general cannot be further reduced. Thus, expressions for the transition frequencies and intensities can be given in closed form only for those lines that do not involve this 4×4 matrix. If an assignment of experimental lines to these theoretical transitions can be made in the analysis, several of the theoretical parameters can immediately be calculated. To get the complete solution, however, transitions involving the 4×4 matrix must be treated, the conventional method is a numerical diagonalization of this matrix and a comparison with the experimental spectrum. The study of several typical cases which has already been made may be of great help in the analysis [4-7].

† Paper I, see reference [1].

Several methods have been developed by which the diagonalization of the 4×4 matrix may be circumvented if a more extensive assignment of experimental lines to theoretical transitions can be made. Rao and Venkateswarlu [8] and Cox [9] have reduced the parameter problem involving the sub-matrix to the solution of an equation system derived from the secular equation. If a complete assignment can be made, simple algebraic expressions derived by Dischler and Maier [10] may be used to extract the N.M.R. parameters from the observed spectral line separations. Whitman [11] has programmed the search for such an assignment for a computer. To make an assignment in advance may be difficult in the general case, especially if there is overlapping of lines.

However, the ultimate test of an analysis must always be the complete calculation of the theoretical spectrum and its comparison with the experimental one. To calculate a general A_2B_2 spectrum is tedious and it is therefore valuable if approximative methods can be used to circumvent the diagonalization of the 4×4 matrix. In some cases the A_2B_2 spectrum closely resembles that of a simpler system, which indicates that an approximative method may be applied [1]. In the present paper we shall discuss A_2B_2 systems with a large relative shift where perturbation methods are conveniently applied in the analysis.

2. THEORY

In the A_2B_2 case the coupling constant notations and the quantities K , etc., are usually given as follows [3, 4, 12]:

$$\begin{array}{ccc}
 A(1) \xleftarrow{J_A} A(2) & & K = J_A + J_B \\
 \downarrow J & \nearrow J' & L = J - J' \\
 B(4) \xleftarrow{J_B} B(3) & & M = J_A - J_B \\
 & & N = J + J'
 \end{array}$$

The Hamiltonian matrix can always be factorized according to the total spin F_z of the basis functions. In the A_2B_2 system further factorization of the matrix can be achieved by choosing the basis functions symmetrical or anti-symmetrical with respect to reflection in the plane of symmetry. The energy matrix is then factorized into two 1×1 sub-matrices, five 2×2 sub-matrices and one 4×4 sub-matrix which belongs to the symmetrical spin zero states. The basis functions are usually chosen as products of the eigenfunctions for the A_2 and B_2 systems respectively with correct symmetry properties. In table 1 we have reproduced these basis functions and the corresponding matrix elements as given by Pople *et al.* [4, 12]. The spin products are arranged in order $\alpha(1)\beta(2)\alpha(3)\beta(4)$, etc. The 2×2 sub-matrices can readily be diagonalized by Jacobian transformations leaving the energy matrix diagonal except for the 4×4 matrix. The selection rules give a theoretical spectrum of 28 lines, four of which can generally be neglected as combination lines. The spectrum is symmetrically centred upon $(\nu_A + \nu_B)/2$, therefore only the half-spectrum of 12 lines need be handled. From the diagonalized part of the matrix six of these transitions can in general be accounted for, while the other six involve the spin zero symmetrical states.

2.1. A_2X_2 approximation

If the relative chemical shift $\nu_A - \nu_B$ is very large compared to the AB coupling constants, the factorization can be carried further as first discussed by McConnell *et al.* [3]. Then to a first approximation the A_2 and B_2 systems can be regarded

as independent, i.e. N and L are neglected, and the basis functions for the Hamiltonian are taken as products of the eigenfunctions of the A_2 and B_2 systems respectively as given in table 1. Terms containing the AB coupling constants in the Hamiltonian can then be introduced as perturbations. This should lead to the approximate diagonalization of the energy matrix, i.e. the off-diagonal elements become small compared to the corresponding differences between the diagonal elements.

Function notation	Function	Diagonal matrix element	Off-diagonal matrix elements
s_2	$\alpha\alpha\alpha\alpha$	$\nu_A + \nu_B + \frac{1}{2}N + \frac{1}{4}K$	
$1s_1$	$\frac{1}{\sqrt{2}}(\alpha\beta + \beta\alpha)\alpha\alpha$	$\nu_B + \frac{1}{4}K$	$\langle 1s_1 H 2s_1 \rangle = \frac{1}{2}N$
$2s_1$	$\frac{1}{\sqrt{2}}\alpha\alpha(\alpha\beta + \beta\alpha)$	$\nu_A + \frac{1}{4}K$	
$1s_0$	$\beta\beta\alpha\alpha$	$-\nu_A + \nu_B - \frac{1}{2}N + \frac{1}{4}K$	$\langle 1s_0 H 2s_0 \rangle = 0$
$2s_0$	$\alpha\alpha\beta\beta$	$\nu_A - \nu_B - \frac{1}{2}N + \frac{1}{4}K$	$\langle 1s_0 H 3s_0 \rangle = \langle 2s_0 H 3s_0 \rangle = \frac{1}{2}L$
$3s_0$	$\frac{1}{2}(\alpha\beta - \beta\alpha)(\alpha\beta - \beta\alpha)$	$-\frac{3}{4}K$	$\langle 1s_0 H 4s_0 \rangle = \langle 2s_0 H 4s_0 \rangle = \frac{1}{2}N$
$4s_0$	$\frac{1}{2}(\alpha\beta + \beta\alpha)(\alpha\beta + \beta\alpha)$	$\frac{1}{4}K$	$\langle 3s_0 H 4s_0 \rangle = -\frac{1}{2}L$
$1s_{-1}$	$\frac{1}{\sqrt{2}}(\alpha\beta + \beta\alpha)\beta\beta$	$-\nu_B + \frac{1}{4}K$	$\langle 1s_{-1} H 2s_{-1} \rangle = \frac{1}{2}N$
$2s_{-1}$	$\frac{1}{\sqrt{2}}\beta\beta(\alpha\beta + \beta\alpha)$	$-\nu_A + \frac{1}{4}K$	
s_{-2}	$\beta\beta\beta\beta$	$-\nu_A - \nu_B + \frac{1}{2}N + \frac{1}{4}K$	
$1a_1$	$\frac{1}{\sqrt{2}}(\alpha\beta - \beta\alpha)\alpha\alpha$	$\nu_B - \frac{1}{2}M - \frac{1}{4}K$	$\langle 1a_1 H 2a_1 \rangle = -\frac{1}{2}L$
$2a_1$	$\frac{1}{\sqrt{2}}\alpha\alpha(\alpha\beta - \beta\alpha)$	$\nu_A + \frac{1}{2}M - \frac{1}{4}K$	
$1a_0$	$\frac{1}{2}(\alpha\beta + \beta\alpha)(\alpha\beta - \beta\alpha)$	$\frac{1}{2}M - \frac{1}{4}K$	$\langle 1a_0 H 2a_0 \rangle = -\frac{1}{2}L$
$2a_0$	$\frac{1}{2}(\alpha\beta - \beta\alpha)(\alpha\beta + \beta\alpha)$	$-\frac{1}{2}M - \frac{1}{4}K$	
$1a_{-1}$	$\frac{1}{\sqrt{2}}(\alpha\beta - \beta\alpha)\beta\beta$	$-\nu_B - \frac{1}{2}M - \frac{1}{4}K$	$\langle 1a_{-1} H 2a_{-1} \rangle = -\frac{1}{2}L$
$2a_{-1}$	$\frac{1}{\sqrt{2}}\beta\beta(\alpha\beta - \beta\alpha)$	$-\nu_A + \frac{1}{2}M - \frac{1}{4}K$	

Table 1. Basis functions for an A_2B_2 system chosen as products of A_2 and B_2 eigenfunctions and corresponding matrix elements.

Let us assume in the further discussion that $\nu_A - \nu_B > 0$; this convention implies no limitation, since ν_A and ν_B cannot be distinguished by the analysis of the experimental spectrum. If we further assume that K and M are smaller in magnitude than $\nu_A - \nu_B$ and that $\nu_A - \nu_B - |K|$ and $\nu_A - \nu_B - |M|$ are much larger than $|L|$, and that $\nu_A - \nu_B$ is much larger† than $|N|$, we see that the only states that may still mix are $3s_0$ with $4s_0$ and $1a_0$ with $2a_0$. The corresponding sub-matrices may then easily be transformed to give a better choice of zeroth-order basis functions.

If $|K|$ or $|M|$ are close to $\nu_A - \nu_B$ other states will come close to degeneracy, e.g. if K is close to $\nu_A - \nu_B$ the states $1s_0$ and $3s_0$ will mix. The second-order corrections to the transition frequencies caused by such mixing are given below,

† This latter assumption is actually made at the outset in the A_2X_2 (large-shift) approximation, cf. above.

but to a first approximation we shall disregard mixing of states other than those having identical (i.e. vanishing) energy of interaction between the spins and the external field.

For the diagonalization of a general 2×2 matrix (H_{ik}) of the orthogonal states ϕ_1 and ϕ_2 we define the new orthogonal states:

$$\phi_1' = \phi_1 \cos \xi + \phi_2 \sin \xi, \quad (1)$$

$$\phi_2' = -\phi_1 \sin \xi + \phi_2 \cos \xi, \quad (2)$$

where the angle ξ is defined by:

$$\tan 2\xi = 2H_{12}/(H_{11} - H_{22}) \quad (3)$$

and is on the main branch $-\pi/4 \leq \xi \leq \pi/4$.

The transformed states will then have the energy eigenvalues:

$$E_1 = H_{11} + H_{12} \tan \xi, \quad (4)$$

$$E_2 = H_{22} - H_{12} \tan \xi, \quad (5)$$

where the states $\phi_1' \rightarrow \phi_1$ strictly as $H_{12} \rightarrow 0$ irrespective of signs and relative magnitudes of the matrix elements H_{ik} .

These expressions can now be applied in the transformation of the 2×2 submatrices to diagonal form. In table 2 the definitions of the transformed states and corresponding eigenvalues are given. The angles θ_s and θ_a are defined by:

$$\tan 2\theta_s = L/K, \quad (6)$$

$$\tan 2\theta_a = L/M, \quad (7)$$

and are on the main branch†.

Function notation	Function	Diagonal matrix element
$3s_0'$	$3s_0 \cos \theta_s + 4s_0 \sin \theta_s$	$-\frac{3}{4}K - \frac{1}{2}L \tan \theta_s$
$4s_0'$	$-3s_0 \sin \theta_s + 4s_0 \cos \theta_s$	$\frac{1}{4}K + \frac{1}{2}L \tan \theta_s$
$1a_0'$	$1a_0 \cos \theta_a - 2a_0 \sin \theta_a$	$\frac{1}{2}M - \frac{1}{4}K + \frac{1}{2}L \tan \theta_a$
$2a_0'$	$1a_0 \sin \theta_a + 2a_0 \cos \theta_a$	$-\frac{1}{2}M - \frac{1}{4}K - \frac{1}{2}L \tan \theta_a$

Table 2. Transformed states and matrix elements in the A_2X_2 approximation.

The notations for the diagonal matrix elements in table 2 differ from those commonly used [3, 4, 12]. The intention of using these alternative expressions for the energies is to get a strict correspondence between states and transitions regardless of the signs of the coupling constants.

The diagonal elements of the energy matrix in table 1, excluding those of the mixed states $3s_0$, $4s_0$ and $1a_0$, $2a_0$, and those of the transformed states of table 2 provide the first-order approximations of the energies. Thus, closed expressions for the transition frequencies and intensities to first order can readily be given. These are given in the third and sixth columns respectively of table 3.

† Obviously a changed notation (such as that implied by the transformation $\xi \rightarrow -\xi$ in the equations (1)–(5)) cannot produce any change in the physical properties or asymptotic behaviour of the transformed states: hence θ_s and θ_a may arbitrarily be defined so as to carry the same sign when K and M are of the same sign. We adhere to this practice [12].

If the conditions underlying the first-order approximation are no longer strictly fulfilled, the off-diagonal elements can be accounted for by extending the perturbation treatment to second order. Generally the parameters K and M cannot be assumed negligible compared to the relative chemical shift. In such cases the second-order terms are obtained by application of generalized [13] perturbation methods. The second-order corrections for this more general case are given in the fifth column of table 3 and are there denoted as 'general second-order corrections'.

The general second-order corrections are somewhat unwieldy; in many cases, however, not only N and L but also K and M are very small as compared to $\nu_A - \nu_B$. In such cases one may introduce all the couplings as perturbations and obtain an *alternative* set of second-order correction terms. These simplified corrections, which are applicable to a more restricted class of spectra, were derived by use of ordinary second-order perturbation theory, and are included in table 3 under the heading 'restricted second-order corrections'.

When transition frequencies are calculated up to second-order terms, the perturbational calculation of intensities should be extended at least to second order to provide the same relative accuracy for intensities as that achieved for the frequencies. However, only the first-order intensities are given in table 3, since the higher-order terms get too complex to be of value. Moreover, it should be kept in mind that—as yet—relative intensities cannot be measured very accurately.

2.2. $(AX)_2$ approximation

In A_2B_2 systems where the relative chemical shift is much larger than the coupling constants and where furthermore one of AB coupling constants, say J , is much larger than the remaining couplings, an even simpler approximation can be made. Thus, if the conditions

$$\nu_A - \nu_B \gg |J| \gg |J'|, \quad |J_A|, \quad |J_B| \quad (8)$$

are fulfilled we can treat the molecule as two almost independent AX systems where the coupling constants are introduced as perturbations. This approach will be denoted the $(AX)_2$ approximation. Thus we should choose the basis functions of the Hamiltonian as the products of AX eigenfunctions with the appropriate spin and symmetry properties. When this basis is used, we shall obtain an approximately diagonal energy matrix.

When the inequalities (8) are satisfied, we shall have:

$$L \approx N \quad \text{and} \quad |L/K| \gg 1, \quad |L/M| \gg 1.$$

From equations (6) and (7) we then infer that, in the $(AX)_2$ approximation, the basis functions $3s_0$, $4s_0$ and $1a_0$, $2a_0$ of table 1 should be replaced by functions of table 2 with $\theta_s = \theta_a = 45^\circ$, while the other basis functions are retained unchanged.

In table 4 we have listed the spin zero basis functions appropriate to the $(AX)_2$ case. The spin products are written in sequential order such that

$$\alpha\beta\alpha\beta = \alpha(1)\beta(2)\alpha(3)\beta(4), \text{ etc.}$$

The matrix elements of the total Hamiltonian for the spin zero states are also given in table 4, and it is seen that these sub-matrices are approximately diagonal, in that the off-diagonal elements are small as compared to the corresponding diagonal element differences. The diagonal elements of table 4, and of the non-zero spin states of table 1 then give the energies to first order, and the

Transition		Transition frequencies relative to ν_A			Relative intensity. First order
Serial no.	Assign-ment	First order	Restricted second-order corrections	General second-order corrections	
1	$1s_1 \rightarrow s_2$	$\frac{1}{2}N$	$+\frac{1}{4} \cdot \frac{N^2}{\nu_A - \nu_B} \nu$	$+\frac{1}{4} \cdot \frac{N^2}{\nu_A - \nu_B}$	$1 - \frac{N}{\nu_A - \nu_B}$
2	$1s_0 \rightarrow 1s_1$	$\frac{1}{2}N$	$+\frac{1}{4} \cdot \frac{L^2}{\nu_A - \nu_B}$	$-\frac{1}{4} \cdot \frac{N^2}{\nu_A - \nu_B} + \frac{1}{2} \left(\frac{(L \sin \theta_s - N \cos \theta_s)^2}{2(\nu_A - \nu_B) + N + L \tan \theta_s} + \frac{(L \cos \theta_s + N \sin \theta_s)^2}{2(\nu_A - \nu_B) + N - L \tan \theta_s - 2K} \right)$	$1 - \frac{N}{\nu_A - \nu_B}$
3	$s_{-2} \rightarrow 1s_{-1}$	$-\frac{1}{2}N$	$+\frac{1}{4} \cdot \frac{N^2}{\nu_A - \nu_B}$	$+\frac{1}{4} \cdot \frac{N^2}{\nu_A - \nu_B}$	$1 + \frac{N}{\nu_A - \nu_B}$
4	$1s_{-1} \rightarrow 2s_0$	$-\frac{1}{2}N$	$+\frac{1}{4} \cdot \frac{L^2}{\nu_A - \nu_B}$	$-\frac{1}{4} \cdot \frac{N^2}{\nu_A - \nu_B} + \frac{1}{2} \left(\frac{(L \cos \theta_s + N \sin \theta_s)^2}{2(\nu_A - \nu_B) - N + L \tan \theta_s + 2K} + \frac{(L \sin \theta_s - N \cos \theta_s)^2}{2(\nu_A - \nu_B) - N - L \tan \theta_s} \right)$	$1 + \frac{N}{\nu_A - \nu_B}$
5	$3s_0' \rightarrow 2s_1$	$K + \frac{1}{2}L \tan \theta_s$	$+\frac{1}{4} \cdot \frac{N^2}{\nu_A - \nu_B}$	$+\frac{1}{4} \cdot \frac{N^2}{\nu_A - \nu_B} - \frac{1}{2}(L \cos \theta_s + N \sin \theta_s)^2$ $\times \left(\frac{1}{2(\nu_A - \nu_B) + N - L \tan \theta_s - 2K} - \frac{1}{2(\nu_A - \nu_B) - N + L \tan \theta_s + 2K} \right)$	$\sin^2 \theta_s$ $\frac{L \sin 2\theta_s}{2(\nu_A - \nu_B)}$
6	$2s_{-1} \rightarrow 4s_0'$	$\frac{1}{2}L \tan \theta_s$	$+\frac{1}{4} \cdot \frac{N^2}{\nu_A - \nu_B}$	$+\frac{1}{4} \cdot \frac{N^2}{\nu_A - \nu_B} + \frac{1}{2}(L \sin \theta_s - N \cos \theta_s)^2$ $\times \left(\frac{1}{2(\nu_A - \nu_B) + N + L \tan \theta_s} - \frac{1}{2(\nu_A - \nu_B) - N - L \tan \theta_s} \right)$	$\cos^2 \theta_s$ $\frac{L \sin 2\theta_s}{2(\nu_A - \nu_B)}$

7	$4s_0' \rightarrow 2s_1$	$-\frac{1}{2} L \tan \theta_s$	$+\frac{1}{4} \cdot \frac{N^2}{\nu_A - \nu_B}$	$+\frac{1}{4} \cdot \frac{N^2}{\nu_A - \nu_B} - \frac{1}{2} (L \sin \theta_s - N \cos \theta_s)^2$ $\times \left(\frac{1}{2(\nu_A - \nu_B) + N + L \tan \theta_s} - \frac{1}{2(\nu_A - \nu_B) - N - L \tan \theta_s} \right)$	$\cos^2 \theta_s$ $+\frac{L \sin 2\theta_s}{2(\nu_A - \nu_B)}$
8	$2s_{-1} \rightarrow 3s_0'$	$-K - \frac{1}{2} L \tan \theta_s$	$+\frac{1}{4} \cdot \frac{N^2}{\nu_A - \nu_B}$	$+\frac{1}{4} \cdot \frac{N^2}{\nu_A - \nu_B} + \frac{1}{2} (L \cos \theta_s + N \sin \theta_s)^2$ $\times \left(\frac{1}{2(\nu_A - \nu_B) + N - L \tan \theta_s - 2K} - \frac{1}{2(\nu_A - \nu_B) - N + L \tan \theta_s + 2K} \right)$	$\sin^2 \theta_s$ $+\frac{L \sin 2\theta_s}{2(\nu_A - \nu_B)}$
9	$2a_0' \rightarrow 2a_1$	$M + \frac{1}{2} L \tan \theta_a$	$+\frac{1}{4} \cdot \frac{L^2}{\nu_A - \nu_B}$	$+\frac{1}{4} \cdot \frac{L^2}{\nu_A - \nu_B + M}$	$\sin^2 \theta_a$ $-\frac{L \sin 2\theta_a}{2(\nu_A - \nu_B)}$
10	$2a_{-1} \rightarrow 1a_0'$	$\frac{1}{2} L \tan \theta_a$	$+\frac{1}{4} \cdot \frac{L^2}{\nu_A - \nu_B}$	$+\frac{1}{4} \cdot \frac{L^2}{\nu_A - \nu_B - M}$	$\cos^2 \theta_a$ $-\frac{L \sin 2\theta_a}{2(\nu_A - \nu_B)}$
11	$1a_0' \rightarrow 2a_1$	$-\frac{1}{2} L \tan \theta_a$	$+\frac{1}{4} \cdot \frac{L^2}{\nu_A - \nu_B}$	$+\frac{1}{4} \cdot \frac{L^2}{\nu_A - \nu_B + M}$	$\cos^2 \theta_a$ $+\frac{L \sin 2\theta_a}{2(\nu_A - \nu_B)}$
12	$2a_{-1} \rightarrow 2a_0'$	$-M - \frac{1}{2} L \tan \theta_a$	$+\frac{1}{4} \cdot \frac{L^2}{\nu_A - \nu_B}$	$+\frac{1}{4} \cdot \frac{L^2}{\nu_A - \nu_B - M}$	$\sin^2 \theta_a$ $+\frac{L \sin 2\theta_a}{2(\nu_A - \nu_B)}$

Table 3. Transition frequencies for the A transitions in the A_2X_2 approximation to first and second order and the intensities to first order.

Notation	Function	Diagonal matrix element	Off-diagonal matrix elements
$1s_0$	$\beta\beta\alpha\alpha$	$-\nu_A + \nu_B - \frac{1}{2}N + \frac{1}{4}K$	$\langle 1s_0 H 2s_0 \rangle = 0$
$2s_0$	$\alpha\alpha\beta\beta$	$\nu_A - \nu_B - \frac{1}{2}N + \frac{1}{4}K$	$\langle 1s_0 H 3s_0 \rangle = \langle 2s_0 H 3s_0 \rangle = \frac{1}{2\sqrt{2}}(N+L)$
$3s_0$	$\frac{1}{\sqrt{2}}(\alpha\beta\alpha\beta + \beta\alpha\beta\alpha)$	$-\frac{1}{2}L - \frac{1}{4}K$	$\langle 1s_0 H 4s_0 \rangle = \langle 2s_0 H 4s_0 \rangle = \frac{1}{2\sqrt{2}}(N-L)$
$4s_0$	$\frac{1}{\sqrt{2}}(\alpha\beta\beta\alpha + \beta\alpha\alpha\beta)$	$\frac{1}{2}L - \frac{1}{4}K$	$\langle 3s_0 H 4s_0 \rangle = \frac{1}{2}K$
$1a_0$	$\frac{1}{\sqrt{2}}(\beta\alpha\alpha\beta - \alpha\beta\beta\alpha)$	$\frac{1}{2}L - \frac{1}{4}K$	$\langle 1a_0 H 2a_0 \rangle = \frac{1}{2}M$
$2a_0$	$\frac{1}{\sqrt{2}}(\alpha\beta\alpha\beta - \beta\alpha\beta\alpha)$	$-\frac{1}{2}L - \frac{1}{4}K$	

Table 4. Spin zero basis functions for an A_2B_2 system chosen as products of AX eigenfunctions and corresponding matrix elements.

Transition		Transition frequencies relative to ν_A		Relative intensities
Serial no.	Assignment	First order	Second-order corrections	First order
1	$1s_1 \rightarrow s_2$	$\frac{1}{2}N$	$+\frac{1}{4} \cdot \frac{N^2}{\nu_A - \nu_B}$	$1 - \frac{N}{\nu_A - \nu_B}$
2	$1s_0 \rightarrow 1s_1$	$\frac{1}{2}N$	$+\frac{1}{4} \cdot \frac{N^2}{\nu_A - \nu_B}$	$1 - \frac{N}{\nu_A - \nu_B}$
3	$s_{-2} \rightarrow 1s_{-1}$	$-\frac{1}{2}N$	$+\frac{1}{4} \cdot \frac{N^2}{\nu_A - \nu_B}$	$1 + \frac{N}{\nu_A - \nu_B}$
4	$1s_{-1} \rightarrow 2s_0$	$-\frac{1}{2}N$	$+\frac{1}{4} \cdot \frac{N^2}{\nu_A - \nu_B}$	$1 + \frac{N}{\nu_A - \nu_B}$
5	$3s_0 \rightarrow 2s_1$	$\frac{1}{2}(L+K)$	$+\frac{1}{4} \cdot \frac{N^2}{\nu_A - \nu_B} + \frac{1}{4} \cdot \frac{K^2}{L}$	$\frac{1}{2} - \frac{1}{2} \left(\frac{K}{L} + \frac{L}{\nu_A - \nu_B} \right)$
6	$2s_{-1} \rightarrow 4s_0$	$\frac{1}{2}(L-K)$	$+\frac{1}{4} \cdot \frac{N^2}{\nu_A - \nu_B} + \frac{1}{4} \cdot \frac{K^2}{L}$	$\frac{1}{2} + \frac{1}{2} \left(\frac{K}{L} - \frac{L}{\nu_A - \nu_B} \right)$
7	$4s_0 \rightarrow 2s_1$	$-\frac{1}{2}(L-K)$	$+\frac{1}{4} \cdot \frac{N^2}{\nu_A - \nu_B} - \frac{1}{4} \cdot \frac{K^2}{L}$	$\frac{1}{2} + \frac{1}{2} \left(\frac{K}{L} + \frac{L}{\nu_A - \nu_B} \right)$
8	$2s_{-1} \rightarrow 3s_0$	$-\frac{1}{2}(L+K)$	$+\frac{1}{4} \cdot \frac{N^2}{\nu_A - \nu_B} - \frac{1}{4} \cdot \frac{K^2}{L}$	$\frac{1}{2} - \frac{1}{2} \left(\frac{K}{L} - \frac{L}{\nu_A - \nu_B} \right)$
9	$2a_0 \rightarrow 2a_1$	$\frac{1}{2}(L+M)$	$+\frac{1}{4} \cdot \frac{L^2}{\nu_A - \nu_B} + \frac{1}{4} \cdot \frac{M^2}{L}$	$\frac{1}{2} - \frac{1}{2} \left(\frac{M}{L} + \frac{L}{\nu_A - \nu_B} \right)$
10	$2a_{-1} \rightarrow 1a_0$	$\frac{1}{2}(L-M)$	$+\frac{1}{4} \cdot \frac{L^2}{\nu_A - \nu_B} + \frac{1}{4} \cdot \frac{M^2}{L}$	$\frac{1}{2} + \frac{1}{2} \left(\frac{M}{L} - \frac{L}{\nu_A - \nu_B} \right)$
11	$1a_{-1} \rightarrow 2a_1$	$-\frac{1}{2}(L-M)$	$+\frac{1}{4} \cdot \frac{L^2}{\nu_A - \nu_B} - \frac{1}{4} \cdot \frac{M^2}{L}$	$\frac{1}{2} + \frac{1}{2} \left(\frac{M}{L} + \frac{L}{\nu_A - \nu_B} \right)$
12	$2a_{-1} \rightarrow 2a_0$	$-\frac{1}{2}(L+M)$	$+\frac{1}{4} \cdot \frac{L^2}{\nu_A - \nu_B} - \frac{1}{4} \cdot \frac{M^2}{L}$	$\frac{1}{2} - \frac{1}{2} \left(\frac{M}{L} - \frac{L}{\nu_A - \nu_B} \right)$

Table 5. Transition frequencies for the A transitions in the $(AX)_2$ approximation to first and second order and the intensities to first order.

transition frequencies and intensities to first order can be obtained directly in closed form. The extremely simple expressions obtained are listed in the third and fifth columns of table 5.

Actually, the first-order expressions for transition frequencies and intensities in the $(AX)_2$ case can be obtained directly from those of the A_2X_2 case by retaining terms up to first order (K/L and M/L) only, in the series expansions of the trigonometric functions. Thus :

$$\begin{array}{ll} \tan \theta_s = 1 - K/L & \tan \theta_a = 1 - M/L \\ \sin^2 \theta_s = \frac{1}{2}(1 - K/L) & \sin^2 \theta_a = \frac{1}{2}(1 - M/L) \\ \cos^2 \theta_s = \frac{1}{2}(1 + K/L) & \cos^2 \theta_a = \frac{1}{2}(1 + M/L) \\ \sin 2\theta_s = 1 & \sin 2\theta_a = 1 \end{array}$$

If the requirements underlying the approximation are no longer strictly fulfilled the perturbation treatment can easily be extended to second order. In table 5 the second-order corrections to the transition frequencies are included. Here generalized perturbation expressions have been applied [13], whereafter terms of a magnitude less than $J^2/(\nu_A - \nu_B)$ or K^2/J have been omitted, which is justified from the assumptions made.

In this case also the intensities are only given to first order.

3. ILLUSTRATIVE APPLICATIONS

In the present study we have applied the foregoing perturbation methods in the analysis of the spectra of three disubstituted benzenes: *o*-dibromobenzene, *p*-bromonitrobenzene and *p*-iodoaniline. The spectra of these compounds have earlier been studied by others [5, 16], and therefore the emphasis here is on the analysis.

To facilitate a systematic comparison of the various approximation methods a programme was set up for the IBM 1620 computer of this university to adjust the parameter set to a least squares fit of the theoretical and experimental transition frequencies. In this programme different approximations for the theoretical transition frequencies could be used, including the exact treatment by numerical diagonalization.

3.1. Experimental details

The compounds used were commercial products of highest purity. To remove dissolved oxygen, argon was bubbled through the sample tubes before these were sealed off.

The spectra were recorded on a Varian A-60 spectrometer. The sweep was calibrated with the side-band technique in which the power line frequency of 50.00 ± 0.05 c.p.s. was used as modulation frequency.

At least five recordings were made of each sample, and the uncertainty in the experimental line position is estimated to be less than 0.10 c.p.s.

3.2. Spectra

The proton magnetic resonance spectra of the three compounds studied are displayed in figures 1 and 2. The spectrum of *p*-iodoaniline (figure 1 *b*) might be called a normal A_2X_2 spectrum: the width of each of the two distinct A_2 and X_2 bands is very much less than that of the whole spectrum. In the case of *p*-bromonitrobenzene (figure 2), on the other hand, it is rather doubtful whether a large-shift approximation is feasible.

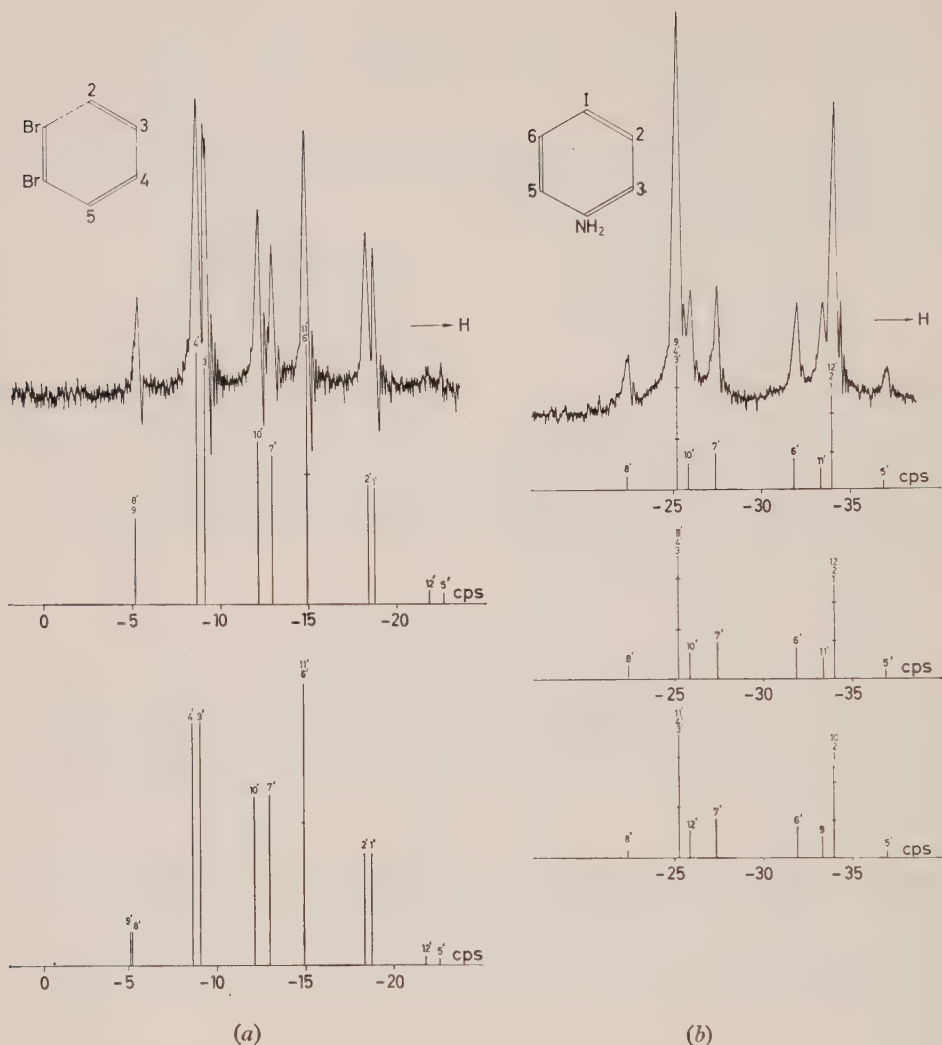


Figure 1. P.M.R.-spectra at 60 Mc/s of (a) *o*-dibromobenzene in a 26 per cent CS_2 solution and (b) *p*-iodoaniline in a 19 per cent CS_2 solution. Only the high field halves of the symmetrical multiplets are shown. In (a) two theoretical spectra are included; the upper one is that of the exact solution and the lower one is that of the generalized A_2X_2 treatment. In (b) the uppermost theoretical spectrum is that of the exact solution, the central one is that of the A_2X_2 treatment and the bottom one is that of the $(AX)_2$ treatment. In the approximate treatments the transition frequencies were calculated up to second order and the intensities to first order. In these calculations the parameter sets of tables 6 and 7 were used.

The band in each half-spectrum of the *para*-disubstituted benzenes may on inspection be further divided into two distinct parts, both of which display a prominent central peak of overlapping lines surrounded by weaker satellites. This additional simplification is caused by the preponderance of one of the A-B coupling constants (the *ortho* coupling) over the other coupling constants in deciding the gross structure in these spectra, and indicates that they may be analysed by use of the $(AX)_2$ approximation.

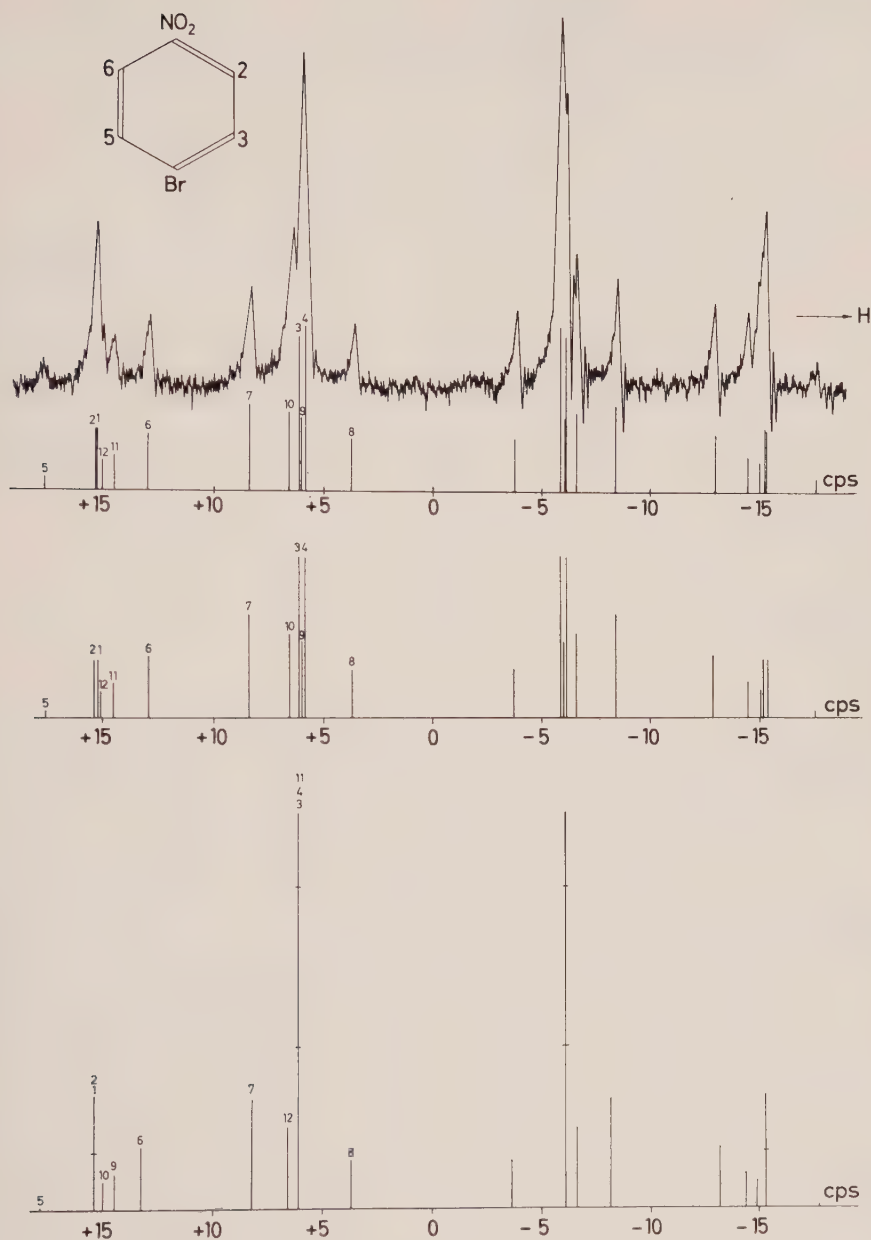


Figure 2. P.M.R.-spectrum of 60 Mc/s of *p*-bromonitrobenzene in a 16 per cent acetone solution. Three theoretical spectra are included in the figure; the uppermost is that of the exact solution, the central one is that of the A_2X_2 treatment and the one at the bottom is that of the $(AX)_2$ treatment. In the two approximate treatments the frequencies were calculated up to second-order terms and the intensities to first order. In the calculations the parameter sets of table 8 were used.

To obtain the correct assignments of experimental lines to theoretical transitions, and in order to estimate starting values of the N.M.R. parameters, trial spectra were calculated using the first-order A_2X_2 expressions or, for the *para*-disubstituted benzenes, the $(AX)_2$ expressions. The parameters were then

Parameter	Exact treatment	A_2X_2 approximation		
		First order	Restricted second order	General second order
$\nu_A - \nu_B$	26.10	27.40	26.10	26.05
J	8.10	8.00	8.00	8.10
J'	1.55	1.65	1.60	1.55
J_A	0.30	0.25	0.25	0.30
J_B	7.50	7.35	7.35	7.50
Root mean square deviation of transition frequencies†	0.02	0.22	0.12	0.03
Root mean square deviation of intensities‡		0.05		

† Deviation relative to the experimental transition frequencies.

‡ Deviation relative to the intensities of the exact treatment.

Table 6. Parameter sets (in c.p.s.) obtained for *o*-dibromobenzene using different A_2X_2 approximations in addition to the exact treatment.

Parameter	Exact treatment	A_2X_2 approximation			$(AX)_2$ approximation	
		First order	Restricted second order	General second order	First order	Second order
$\nu_A - \nu_B$	58.60	59.20	58.60	58.60	59.20	58.60
J	8.40	8.40	8.40	8.40	8.75	8.40
J'	0.30	0.35	0.35	0.30	0.00	0.35
J_A	2.20	2.20	2.20	2.20	2.20	2.20
J_B	2.85	2.85	2.85	2.85	2.85	2.80
Root mean square deviation of transition frequencies†	0.03	0.03	0.03	0.03	0.28	0.05
Root mean square deviation of intensities‡		0.01			0.03	

† Deviation relative to the experimental transition frequencies.

‡ Deviation relative to the intensities of the exact treatment.

Table 7. Parameter set (in c.p.s.) obtained for *p*-iodoaniline using different approximations in addition to the exact treatment.

Parameter	Exact treatment	A_2X_2 approximation			$(AX)_2$ approximation	
		First order	Restricted second order	General second order	First order	Second order
$\nu_A - \nu_B$	19.35	21.25	19.25	19.20	21.25	19.25
J	8.80	8.80	8.75	8.80	9.10	8.75
J'	0.35	0.50	0.45	0.30	0.20	0.45
J_A	2.20	2.00	2.00	2.25	2.10	2.00
J_B	2.80	2.60	2.60	2.90	2.65	2.55
Root mean square deviation of transition frequencies †	0.05	0.14	0.12	0.05	0.17	0.14
Root mean square deviation of intensities ‡		0.06			0.07	

† Deviation relative to the experimental transition frequencies.

‡ Deviation relative to the intensities of the exact treatment.

Table 8. Parameter set (in c.p.s.) obtained for *p*-bromonitrobenzene using different approximations in addition to the exact treatment.

adjusted to a least squares fit between calculated and observed line positions by use of the various approximations discussed in §2. The parameter sets so obtained are reported in tables 6, 7, and 8 where also the root mean square deviations as calculated from observed transition frequencies are given. In the tables, the parameter values have been rounded off to the nearest 0.05 c.p.s. which is more in agreement with the experimental accuracy.

A quantitative comparison between calculated and observed intensities is difficult to achieve, due to overlapping of lines among other things. Therefore the relative intensities calculated by the approximative A_2X_2 and $(AX)_2$ methods are compared only with those calculated by numerical diagonalization. The root mean square deviations so obtained are listed in tables 6, 7 and 8.

To estimate the uncertainty in the parameters of the exact solutions, the partial derivatives of the calculated line positions with respect to the parameters were determined. From the uncertainty of 0.10 c.p.s. in the experimental line positions, the parameters are estimated to be accurate within 0.10 c.p.s.

Of the five approximative methods described, the A_2X_2 treatment incorporating general second-order correction terms gives by far the best results, as may be seen from tables 6–8. In all three spectra the root mean square deviations are almost as small in the generalized A_2X_2 approximation as in the exact treatment. The coupling constants estimated by use of the generalized second-order A_2X_2 approximation agree with those of the exact solution within 0.05 c.p.s., but the relative shift values tend to be slightly too low when the relative shift becomes of an order of magnitude similar to that of the larger coupling constants.

When the relative chemical shift $\nu_A - \nu_B$ becomes much larger than the coupling constants, the two different second-order A_2X_2 treatments given become nearly equivalent (cf. table 3), and the simpler, restricted second-order correction terms will be sufficient, as exemplified by the case of *p*-iodoaniline (table 7).

In spectra where $L \approx N$ the restricted second-order correction terms for all transitions in one half-spectrum become nearly equal. Then only the relative chemical shift will be improved by inclusion of the restricted second-order terms; the coupling constants will be just the same as those estimated with only first-order A_2X_2 terms (cf. tables 3 and 6-8).

When using the first-order A_2X_2 treatment one will generally overestimate the relative chemical shift. The example of *p*-iodoaniline shows that care must be taken not to use this approximation too freely if accurate values of the shift are desired. The first-order estimates of the coupling constants are reasonably good, however, even in the case of *o*-dibromobenzene with a ratio of the largest coupling to the chemical shift as high as 0.3.

The first-order $(AX)_2$ treatment cannot be expected to give very satisfactory results when applied to *para*-disubstituted benzenes, because the condition that one A-B coupling constant should be very much larger than the other coupling constants in the molecule is not strictly fulfilled (actually $K/L \approx 0.6$ in *p*-iodoaniline). However, by inclusion of the second-order $(AX)_2$ terms very satisfactory results may be obtained, as exemplified by the case of *p*-iodoaniline, where the parameters of the second-order $(AX)_2$ analysis agree with those of the exact analysis well within the limits of error. In the limiting case of *p*-bromonitrobenzene (table 8), the $(AX)_2$ treatment can no longer be considered adequate, but it is noteworthy that the restricted second-order A_2X_2 corrections do not provide a better analysis of this spectrum than that obtained by the second-order $(AX)_2$ approximation.

A treatment analogous to the $(AX)_2$ approximation has been devised, which is applicable also in quite strongly coupled spectra. This so-called $(AB)_2$ approximation will be described and exemplified in a subsequent paper.

In the figures, calculated spectra in various approximations are indicated schematically below the observed ones; the frequencies are given with respect to the symmetry point of the spectrum as zero, and with decreasing frequency towards higher fields.

Structural assignments of the parameters found can be based on the well-known fact that $J_{ortho} > J_{meta} > J_{para}$ in benzenes and on the reasonably well-established regularities of substituent effects on chemical shifts [14, 16-25] and

Substituents	$\nu_2 - \nu_3$	J_{23}	J_{25}	J_{26}	J_{34}	J_{35}
1-Br, 6-Br	+26.10 †	8.10	0.30	—	7.50	1.55
1-I, 4-NH ₂	+58.60 ‡	8.40	0.30	2.20	—	2.85
1-NO ₂ , 4-Br	+19.35 §	8.80	0.35	2.20	—	2.80

† Measured in a 26 per cent CS₂ solution at 60 Mc/s.

‡ Measured in a 19 per cent CS₂ solution at 60 Mc/s.

§ Measured in a 16 per cent acetone solution at 60 Mc/s.

Table 9. N.M.R. parameters (in c.p.s.) and structural assignments for *o*-dibromobenzene, *p*-iodoaniline and *p*-bromonitrobenzene. The numbering of the ring positions are indicated in figures 1-2. The uncertainty in the parameters is 0.10 c.p.s. The sign convention for shifts is such that frequencies increase downfields. All coupling constants are positive [15].

coupling constants [23, 24, 26–30]. The results are summarized in table 9. The coupling constants found in the present study agree with those reported earlier by Dischler and Englert [5] and by Martin and Dailey [16] well within the combined limits of error.

4. CONCLUSION

The analysis of a general A_2B_2 spectrum is complicated and tedious and it is therefore expedient to use approximative simplified methods whenever applicable.

If the chemical shift is much larger than the coupling constants the ordinary first-order A_2X_2 approximation can be applied. Agreement within experimental error of calculated and observed spectra does not imply however that the N.M.R. parameters are correctly estimated by use of this approximation. This is illustrated by the case of *p*-iodoaniline (cf. the root mean square deviations in table 7).

When not negligible the restricted second-order A_2X_2 correction terms will always improve the chemical shift estimate but the coupling constants estimated by use of a restricted second-order treatment will be identical with those of the first-order analysis, whenever the parameters N and L are nearly equal. However, the general second-order correction terms will provide better estimates of the coupling constants also in this latter type of spectra. Only when the general second-order correction terms are used, can one expect an improvement of the estimated values for J_A and J_B (K and M) in any A_2B_2 spectrum.

Whenever applicable, the $(AX)_2$ approximation should be preferred, due to its simplicity. It is also the fastest method, for the calculation times on a computer are in the approximate ratios : exact diagonalization : A_2X_2 to second order, general expressions : A_2X_2 to second-order, restricted expressions : A_2X_2 to first order : $(AX)_2$ to second order : $(AX)_2$ to first order = 60 : 5 : 3 : 2 : 2 : 1.

The authors wish to express their sincere thanks to Professor Kai Siegbahn and Professor Arne Fredga for their interest in this work and for all facilities placed at their disposal.

REFERENCES

- [1] GESTBLOM, B., 1963, *Acta chem. scand.*, **17**, 280.
- [2] BERNSTEIN, H. J., POPL, J. A., and SCHNEIDER, W. G., 1957, *Canad. J. Chem.*, **35**, 65.
- [3] MCCONNELL, H. M., MCLEAN, A. D., and REILLY, C. A., 1955, *J. chem. Phys.*, **23**, 1152.
- [4] POPL, J. A., SCHNEIDER, W. G., and BERNSTEIN, H. J., 1957, *Canad. J. Chem.*, **35**, 1060.
- [5] DISCHLER, B., and ENGLERT, G., 1961, *Z. Naturf. A*, **16**, 1180.
- [6] WIBERG, K. B., and NIST, B. J., 1962, *The Interpretation of N.M.R. Spectra* (New York).
- [7] GRANT, D. M., HIRST, R. C., and GUTOWSKY, H. S., 1963, *J. chem. Phys.*, **38**, 470.
- [8] RAO, B. D., and VENKATESWARLU, P., 1961, *Proc. Indian Acad. Sci. A*, **54**, 1.
- [9] COX, P. F., 1963, *J. Amer. chem. Soc.*, **85**, 380.
- [10] DISCHLER, B., and MAIER, N., 1961, *Z. Naturf. A*, **16**, 318.
- [11] WHITMAN, D. R., 1962, *J. chem. Phys.*, **36**, 2085.
- [12] POPL, J. A., SCHNEIDER, W. G., and BERNSTEIN, H. J., 1959, *High-resolution Nuclear Magnetic Resonance* (New York).
- [13] PAULING, L., and WILSON, E. B., 1935, *Introduction to Quantum Mechanics* (New York) p. 195 ff.

- [14] SPIESECKE, H., and SCHNEIDER, W. G., 1961, *J. chem. Phys.*, **35**, 731.
- [15] BUCKINGHAM, A. D., and McLAUCHLAN, K. A., 1963, *Proc. chem. Soc.*, p. 144.
- [16] MARTIN, J., and DAILEY, B. P., 1962, *J. chem. Phys.*, **37**, 2594.
- [17] CORIO, P. L., and DAILEY, B. P., 1956, *J. Amer. chem. Soc.*, **78**, 3043.
- [18] BOTHNER-BY, A. A., and GLICK, R. E., 1956, *J. Amer. chem. Soc.*, **78**, 1071.
- [19] BOTHNER-BY, A. A., and GLICK, R. E., 1957, *J. chem. Phys.*, **26**, 1651.
- [20] FRASER, R. R., 1960, *Canad. J. Chem.*, **38**, 2226.
- [21] GRONOWITZ, S., and HOFFMAN, R. A., 1960, *Ark. Kemi*, **16**, 539.
- [22] DIEHL, P., 1961, *Helv. chim. acta*, **44**, 829.
- [23] ABRAHAM, R. J., and BERNSTEIN, H. J., 1961, *Canad. J. Chem.*, **39**, 905.
- [24] GRONOWITZ, S., SÖRLIN, G., GESTBLOM, B., and HOFFMAN, R. A., 1962, *Ark. Kemi*, **19**, 483.
- [25] GRONOWITZ, S., NORRMAN, B., GESTBLOM, B., MATHIASSEN, B., and HOFFMAN, R. A. 1964, *Ark. Kemi*, **22**, 65.
- [26] BANWELL, C. N., SHEPPARD, N., and TURNER, J. J., 1960, *Spectrochim. Acta*, **16**, 794.
- [27] BANWELL, C. N., and SHEPPARD, N., 1960, *Mol. Phys.*, **3**, 351.
- [28] WAUGH, J. S., and CASTELLANO, S., 1961, *J. chem. Phys.*, **35**, 1900.
- [29] SCHAEFER, T. P., 1962, *Canad. J. Chem.*, **40**, 1.
- [30] BANWELL, C. N., and SHEPPARD, N., 1962, *Disc. Faraday Soc.*, **34**, 115.

Die Berechnung der Potentialflächen von mehratomigen Systemen nach der Methode der Ladungsentwicklungen

von H. PREUSS

Max-Planck-Institut für Physik und Astrophysik, München

(Received 2 September 1963)

Die für die Diskussionen von Reaktionsvorgängen notwendigen Potentialflächen (Kurven) können sehr allgemein durch die Methode der Ladungsentwicklung erhalten werden. Es wird eine Formel angegeben, die für eine beliebige Anzahl von Elektronen und Atomkernen eine Näherung für die Potentialflächen bei kleinen Kernabständen darstellt. Das Vorgehen wird an Hand einiger Beispiele näher erläutert.

1. EINLEITUNG

Die stationären Zustände eines Systems, bestehend aus n Elektronen, die sich im Felde von N Atomkernen mit den Ladungen Z_μ ($\mu = 1 \dots N$) befinden, lassen sich aus der Schrödingergleichung

$$(\mathcal{H}' - \mathcal{E})\Psi = 0, \quad \langle \Psi | \Psi \rangle = 1 \quad (1)$$

bestimmen, wobei sich bei festgehaltenen Kernen der Hamiltonoperator \mathcal{H}' zu

$$\mathcal{H}' = T + \sum_{\mu=1}^N Z_\mu V_\mu + w + W \quad (2)$$

ergibt. Im einzelnen ist in atomaren Einheiten (at. E)

$$T = -\frac{1}{2} \sum_{i=1}^n \Delta_i, \quad (2a)$$

$$V_\mu = - \sum_{i=1}^n 1/r_{\mu i}, \quad (2b)$$

$$w = \sum_{i=1}^{n-1} \sum_{j=i+1}^n 1/r_{ij}, \quad (2c)$$

$$W = \sum_{\lambda=1}^{N-1} \sum_{\mu=\lambda+1}^N Z_\lambda Z_\mu / R_{\lambda\mu}, \quad (2d)$$

Die Kerne seien in den Raumpunkten $\mathbf{R}_\lambda = \{R_{\lambda x}, R_{\lambda y}, R_{\lambda z}\}$ festgehalten, die vom Koordinatenursprung 0 den Abstand $|\mathbf{R}_\lambda| = |\mathbf{R}_{\lambda 0}|$ haben. Damit ergibt sich $R_{\lambda\mu}$ in (2d) zu

$$R_{\lambda\mu} = |\mathbf{R}_{\lambda 0} - \mathbf{R}_{\mu 0}| = \sqrt{[(R_{\lambda x} - R_{\mu x})^2 + (R_{\lambda y} - R_{\mu y})^2 + (R_{\lambda z} - R_{\mu z})^2]}. \quad (3)$$

Die Gesamtheit aller Vektoren \mathbf{R}_λ ($\lambda = 1 \dots N$) wollen wir eine Kernkonstellation \mathbf{R} nennen.

Für das Folgende ist es günstiger, anstelle der Gesamtenergie \mathcal{E} die Elektronenenergie E zu betrachten, die sich aus \mathcal{E} durch Subtraktion der Kernwechselwirkungsenergie ergibt

$$E = \mathcal{E} - W. \quad (4)$$

Im Gegensatz zu \mathcal{E} und W ist E im ganzen \mathbf{R} -Raum stetig und beschränkt. Diese Eigenschaften machen E besonders geeignet für theoretische Untersuchungen und haben eine Reihe von Verfahren ermöglicht, wie etwa die Methode des 'vereinigten Atoms' [1, 3], oder das Verfahren der Atomassoziationen [2].

Aus (4) folgt, daß sich die Energiezustände E des Elektronensystems aus

$$(\mathcal{H} - E)\Psi = 0 \quad (5)$$

ergeben, wobei

$$\mathcal{H} = \mathcal{H}' - W = T + \sum_{\mu=1}^N Z_{\mu} V_{\mu} + w. \quad (5a)$$

2. DIE LADUNGSENTWICKLUNG

Wir wollen hier zuerst feststellen, daß E (wie auch \mathcal{E}), nach Vorgabe der N Zentren mit den Ladungen Z_{λ} , allein durch die jeweilige Kernkonstellation bestimmt ist.

Die einzelnen Energiezustände E_s sind also bei festem n Funktionen von Z_{λ} ($\lambda = 1 \dots N$) und \mathbf{R} :

$$E_s = E_s(n, Z_{\lambda}, \mathbf{R}); \quad s = 0, 1 \dots; \quad \lambda = 1 \dots N. \quad (6)$$

Dabei beschränken wir uns auf das diskrete Energiespektrum und wollen E_0 als den Grundzustand bezeichnen:

$$E_0 \leq E_1 \leq E_2 \leq \dots \quad (6a)$$

E_s als Funktion der \mathbf{R}_{λ} wird auch oft Energiehyperfläche genannt. Die an sich ziemlich triviale Feststellung der Gleichung (6) findet in den meisten konventionellen Verfahren der Quantenchemie immer noch viel zu wenig Beachtung. Dies zeigt sich im besonderen darin, daß viele Verfahren auf ein ganz bestimmtes Molekül zugeschnitten werden. Da aber der Wert einer Theorie darin gesehen werden muß, daß möglichst wenig Gleichungen einen möglichst großen Bereich unserer Erfahrung erfassen, so sollte versucht werden, im Rahmen einer 'ökonomischen Theorie' Methoden zu entwickeln, die eine Bestimmung der Funktionen $E_s(n, Z_{\lambda}, \mathbf{R})$ im Auge haben.

Die Möglichkeiten, wie solche Verfahren gefunden werden können, sollen hier untersucht werden.

Wenn man die Anzahl der Elektronen vorerst konstant hält, also eine Klasse von isoelektronischen Atomsystemen betrachtet, deren Zahl sehr stark mit n anwächst, so bestehen die beiden Möglichkeiten darin, entweder E_s in eine Reihe nach den Kernabständen oder nach den Kernladungen zu entwickeln. Dabei braucht es sich keineswegs um reine Potenzreihen zu handeln. Ganz allgemein kann man etwa beide Darstellungen in der Form

$$E_s = \sum_k \hat{\Omega}_k^{(s)}(\mathbf{R}_{\lambda}) \Gamma_k^{(s)}(Z_{\lambda}) \quad (7)$$

schreiben.

Die Entwicklung nach den $R_{\lambda\mu}$ (sogen. R -Entwicklung) ist bisher nur für

$$\hat{\Omega}_k^{(s)}(\mathbf{R}_{\lambda}) = \prod_{\lambda=1}^N |\mathbf{R}_{\lambda 0}|^{n_{\lambda}} \quad (k = k(n_{\lambda})) \quad (8)$$

untersucht worden [3], wobei die Entwicklungskoeffizienten $\Gamma(Z_{\lambda})$ durch die Zahlen n_{λ} ($\lambda = 1 \dots N$), die positiv vorausgesetzt waren, numeriert waren

$$0 \leq n_{\lambda} < \infty \quad (\lambda = 1 \dots N). \quad (8a)$$

Zur Zeit sind für $n=1; 2$ die Γ der Darstellung (7) mit (8) nur bis

$$0 \leq n_\lambda \leq 3 \quad (8b)$$

ausgerechnet worden, obwohl auch die weiteren Koeffizienten explizite bekannt sind [3]. Eine Hauptschwierigkeit besteht nämlich darin, daß wir dazu gewisse Kenntnisse über die exakte Lösung $\Psi^{(0)}$ des sogenannten 'vereinigten Atoms'

$$\mathcal{H}\Psi^{(0)} = \{T + ZV_0 + w\}\Psi^{(0)} = E(n, Z, 0)\Psi^{(0)} \quad (9)$$

haben müssen, wobei

$$Z = \sum_{\lambda=1}^N Z_\lambda \quad (9a)$$

und $E(n, Z, 0)$ die Energie des Atoms mit der Kernladung Z ist.

Dieses 'vereinigte Atom', welches aus dem ursprünglichen System durch den Übergang $R_{\lambda\mu} \rightarrow 0$ ($\lambda, \mu = 1 \dots N$) hervorgeht, wird als nullte Näherung aufgefaßt, wobei die $\Gamma(Z_\lambda)$ aus einer Störungsrechnung erhalten werden.

Eine Entwicklung nach den Z_λ ($\lambda = 1 \dots N$), als sogenannte Ladungs- oder Z_λ -Entwicklung bekannt, läßt sich ebenfalls mit Hilfe einer Störungsrechnung herleiten.

Als erster hat Hylleraas [4] eine solche Entwicklung mit

$$\Gamma_k^{(s)} = Z^k \quad (10)$$

für Zweielektronenatome ($n=2$) angegeben. Auch hier lassen sich die Koeffizienten Ω_k , die Konstanten sind, explizite angeben, wobei als nullte Näherung von einem Atom ohne Elektronenwechselwirkung w ausgegangen wird:

$$\mathcal{H}\Psi^{(0)} = (T + ZV_0)\Psi^{(0)} = \hat{E}(n, Z)\Psi^{(0)}. \quad (11)$$

Nach (2b) zerfällt \mathcal{H} in eine Summe von Einteilchen-Operatoren, die einem Eielektronenatom mit der Kernladung Z entsprechen

$$\mathcal{H} = \left(T - Z \sum_{i=1}^n 1/r_{0i} \right) = \sum_{i=1}^n \left(-\frac{1}{2}\Delta_i - (Z/r_{0i}) \right) = \sum_{i=1}^n h_i, \quad (11a)$$

so daß sich die exakte Lösung $\Psi^{(0)}$ von (11) als Determinante (oder als Summe von Determinanten) der wasserstoffähnlichen Funktionen Φ_j ergibt

$$\Psi^{(0)} = \det \{ \Phi_j(i) \}, \quad (12)$$

die Lösungen der Gleichung

$$h_i \Phi_j(i) = \left(-\frac{1}{2}\Delta_i - (Z/r_{0i}) \right) \Phi_j(i) = -(Z^2/2j^2) \Phi_j(i) \quad (13)$$

sind. $\hat{E}(n, Z)$ ergibt sich danach zu

$$\hat{E}(n, Z) = -\frac{1}{2}Z^2 \sum_{j=1}^{\infty} j^{-2} \hat{n}_j = Z^2 \hat{E}(n), \quad (14)$$

wobei die Eigenwerte von (13), mit dem tiefsten beginnend, aufsummiert werden, indem jeder Zustand j nur maximal $2j^2$ -fach besetzt sein darf (Pauliprinzip). Es ist

$$\sum_{j=1}^{\infty} \hat{n}_j = n. \quad (14a)$$

Man kann die Gleichungen (13) in eine Z -freie Form bringen, indem man die Transformationen

$$|\bar{\mathbf{r}}| = Z|\mathbf{r}|; \quad |\bar{\mathbf{R}}| = Z|\mathbf{R}|; \quad \mathbf{r} = \{x, y, z\} \quad (15)$$

eingührt. Damit erhält man für (13)

$$\bar{h}_i \Phi_j(i) = (-\frac{1}{2} \bar{\Delta}_i - (1/\bar{r}_{0i})) \Phi_j(i) = -(1/2j^2) \Phi_j(i), \quad (13 a)$$

und der Hamiltonoperator \mathcal{H}'' eines Atoms mit n Elektronen und der Kernladung Z am Ort 0 geht mit (15) über in

$$\mathcal{H}'' = Z^2 \bar{\mathcal{H}}'', \quad (16)$$

mit

$$\bar{\mathcal{H}}'' = \bar{T} + \bar{V}_0 + (1/Z) \bar{w} = \hat{\mathcal{H}} + (1/Z) \bar{w} = \sum_{i=1}^n \bar{h}_i + (1/Z) \bar{w} \quad (16 a)$$

$$= \sum_{i=1}^n (-\frac{1}{2} \bar{\Delta}_i - (1/\bar{r}_{0i})) + (1/Z) \sum_{i=1}^{n-1} \sum_{j=i+1}^n (1/\bar{r}_{ij}). \quad (16 b)$$

Die erste Summe in (16 b) stellt gerade die nullte Näherung nach (11) dar, sodaß $1/Z$ als Störparameter im Rahmen der Störungsrechnung aufgefaßt werden kann. Die Energie \bar{E} mit dem Operator $\bar{\mathcal{H}}''$ wird dann nach der Störungsrechnung als Potenzreihenentwicklung von $1/Z$ geschrieben

$$\bar{E} = \bar{\Omega}_0 + (1/Z) \bar{\Omega}_1 + (1/Z^2) \bar{\Omega}_2 + \dots \quad (17)$$

wobei

$$\bar{\Omega}_0 = \bar{E}(n) \quad (17 a)$$

ist. Wegen (16) ergibt sich schließlich die Elektronenenergie E zu

$$E = Z^2 \bar{E}(n) + \bar{\Omega}_0 Z + \bar{\Omega}_2 + (1/Z) \bar{\Omega}_3 + \dots, \quad (18)$$

sodaß für k in (10) die Einschränkung

$$k \leq 2 \quad (19)$$

gilt.

Mit der Entwicklung (18) ist somit eine spezielle Form von (7) gefunden worden, die für alle Atome mit n Elektronen gilt!

In den letzten Jahren ist begonnen worden, das Konvergenzverhalten solcher Reihen näher zu untersuchen [5]. Daneben wurden die ersten Koeffizienten $\bar{\Omega}_k$ auch für $4 \geq n > 2$ berechnet [6].

Mit dieser Methode lassen sich einige bemerkenswerte Beziehungen für die Integrale $\langle w \rangle$ und $\langle V_0 \rangle$ mit der exakten Wellenfunktion des Atoms finden [7], auf die wir kurz eingehen wollen.

Aus (9), (16) und (16 a) folgt

$$(\partial/\partial Z)(E/Z^2) = -(1/Z^2) \langle \bar{w} \rangle, \quad (20)$$

also

$$\langle w \rangle = 2E - Z(\partial E/\partial Z), \quad (21)$$

weil

$$\langle w \rangle = Z \langle \bar{w} \rangle. \quad (21 a)$$

Die Energiegleichung

$$\langle T \rangle + Z \langle V_0 \rangle + \langle w \rangle = E \quad (22)$$

nach Z differenziert liefert (Hellmann–Feynman-Theorem)

$$\frac{\partial E}{\partial Z} = \langle V_0 \rangle, \quad (22a)$$

sodaß sich $\langle T \rangle$ mit (21) in Übereinstimmung mit dem Virialsatz zu

$$\langle T \rangle = -E \quad (23)$$

ergibt.

Wir gehen jetzt dazu über, die Möglichkeiten von Ladungsentwicklungen für Moleküle zu besprechen.

3. Z_λ -ENTWICKLUNGEN FÜR MOLEKÜLE

Eine solche Entwicklung läßt sich ebenfalls angeben, wenn man annimmt, daß im Koordinatenursprung 0 das 'vereinigte Atom' liegt, dessen Kernladung durch (9a) gegeben ist. Führt man dann, mit dieser Bedeutung von Z nach (9a), die Transformationen (15) in (5a) aus, so ergibt sich

$$\mathcal{H} = Z^2 \bar{\mathcal{H}} \quad (24)$$

mit

$$\bar{\mathcal{H}} = T + (1/Z) \left\{ \sum_{\mu=1}^N Z_\mu \bar{V}_\mu + \bar{w} \right\}. \quad (24a)$$

Diesen Hamiltonoperator kann man in der folgenden Form

$$\bar{\mathcal{H}} = \{T + \bar{V}_0\} + (1/Z) \left\{ \sum_{\mu=1}^N Z_\mu (\bar{V}_\mu - \bar{V}_0) + \bar{w} \right\} = \hat{\mathcal{H}} + (1/Z) \bar{H} \quad (25)$$

schreiben. Damit ist wieder eine störungstheoretische Form gefunden, wenn $1/Z$ als Störparameter aufgefaßt wird. Es wird also von

$$\hat{\mathcal{H}} \hat{\Psi}_k = \{T + \bar{V}_0\} \hat{\Psi}_k = \bar{E}_k(n) \hat{\Psi}_k \quad (26)$$

als nullter Näherung ausgegangen, wie es auch in (16a), (16b) der Fall war. Es kann somit wieder eine Reihenentwicklung nach (17) angegeben werden, wobei die Ω , wegen der Form des Störoperators

$$\bar{H} = \sum_{\mu=1}^N Z_\mu (\bar{V}_\mu - \bar{V}_0) + \bar{w}, \quad (27)$$

noch Funktionen von Z_μ ($\mu = 1 \dots N$) sind. Um die Form der Funktionen $\Gamma(Z_\lambda)$ zu erhalten, muß man beachten, daß sich in der Störungsrechnung die $\bar{\Omega}$ als Potenzen der Matrixelemente mit \bar{H} ergeben, sodaß man für (7) schreiben kann [8]

$$E_s = \sum_{p=0}^{\infty} \sum_{m_\lambda} \Omega_p \left(a, b, \dots, \lambda, \dots, N \mid \bar{\mathbf{R}}_{\lambda 0} \right) \Gamma_p(m_\lambda, Z_\lambda) \quad (28)$$

mit

$$\Gamma_p(m_\lambda, Z_\lambda) = \frac{Z_a^{m_a} Z_b^{m_b} \dots Z_\lambda^{m_\lambda} \dots Z_N^{m_N}}{\left(\sum_{\lambda=1}^N Z_\lambda \right)^p}, \quad (28a)$$

wobei die Beziehung (24) noch verwendet worden ist. Da in (7) keine positiven

Potenzen von $Z = \sum_{\lambda=1}^N Z_{\lambda}$ vorkommen, gilt für die m_{λ} in Ω_p

$$0 \leq \sum_{\lambda=1}^N m_{\lambda} \leq p+2; \quad m_{\lambda} \geq 0. \quad (29)$$

In Erweiterung von (15) gilt hier

$$|\bar{\mathbf{R}}_{\lambda 0}| = \left(\sum_{\lambda=1}^N Z_{\lambda} \right) |\mathbf{R}_{\lambda 0}|, \quad (30)$$

beziehungsweise

$$\bar{R}_{\lambda i} = \left(\sum_{\lambda=1}^N Z_{\lambda} \right) R_{\lambda i}; \quad i = x; y; z. \quad (30a)$$

Damit ist die gewünschte Z_{λ} -Entwicklung für mehratomige Systeme gewonnen. Wir wollen darauf noch näher eingehen. Für $N=2$ (Zweizentrensystem) gibt es, nach p geordnet, folgende Ω_p -Funktionen

$$\Omega_p \begin{pmatrix} a & b \\ m_a & m_b \end{pmatrix} = \left\{ \begin{array}{ll} p=0 & \begin{array}{l} m_a: \quad 0 \ 0 \ 0 \ 1 \ 1 \ 2, \\ m_b: \quad 0 \ 1 \ 2 \ 0 \ 1 \ 0, \end{array} \\ p=1 & \begin{array}{l} m_a: \quad 0 \ 0 \ 0 \ 0 \ 1 \ 1 \ 1 \ 2 \ 2 \ 3, \\ m_b: \quad 0 \ 1 \ 2 \ 3 \ 0 \ 1 \ 2 \ 0 \ 1 \ 0, \end{array} \\ p=2 & \begin{array}{l} m_a: \quad 0 \ 0 \ 0 \ 0 \ 0 \ 1 \ 1 \ 1 \ 1 \ 2 \ 2 \ 2 \ 3 \ 3 \ 4, \\ m_b: \quad 0 \ 1 \ 2 \ 3 \ 4 \ 0 \ 1 \ 2 \ 3 \ 0 \ 1 \ 2 \ 0 \ 1 \ 0. \end{array} \\ \vdots & \vdots \end{array} \right\} \quad (31)$$

Liegen drei Zentren vor ($N=3$), so beginnt die Zählung der Ω_p in folgender Weise:

$$\Omega_p \begin{pmatrix} a & b & c \\ m_a & m_b & m_c \end{pmatrix} = \left\{ \begin{array}{ll} p=0 & \begin{array}{l} m_a: \quad 0 \ 0 \ 0 \ 0 \ 0 \ 0 \ 1 \ 1 \ 1 \ 2, \\ m_b: \quad 0 \ 0 \ 0 \ 1 \ 1 \ 2 \ 0 \ 0 \ 1 \ 0, \\ m_c: \quad 0 \ 1 \ 2 \ 0 \ 1 \ 0 \ 0 \ 1 \ 0 \ 0, \end{array} \\ p=1 & \begin{array}{l} m_a: \quad 0 \ 0 \ 0 \ 0 \ 0 \ 0 \ 0 \ 0 \ 0 \ 1 \ 1 \ 1 \ 1 \ 1 \ 1 \ 2 \ 2 \ 2 \ 3, \\ m_b: \quad 0 \ 0 \ 0 \ 0 \ 1 \ 1 \ 1 \ 2 \ 2 \ 3 \ 0 \ 0 \ 0 \ 1 \ 1 \ 2 \ 0 \ 0 \ 1 \ 0, \\ m_c: \quad 0 \ 1 \ 2 \ 3 \ 0 \ 1 \ 2 \ 0 \ 1 \ 0 \ 0 \ 1 \ 2 \ 0 \ 1 \ 0 \ 0 \ 1 \ 0 \ 0. \end{array} \\ \vdots & \vdots \end{array} \right\} \quad (32)$$

Für jedes p gibt es M Ω_p -Funktionen, wobei

$$M = \binom{p+N+2}{N}. \quad (33)$$

Die Abzählungen der Ω_p gelten für jedes fixierte n (isoelektronische Systeme). Der Übergang zu einer anderen Elektronenanzahl dürfte in allgemeinem die Funktionen Ω wesentlich verändern. $\Gamma(Z_{\lambda})$ bleibt unverändert, während der Übergang zu einer kleineren Anzahl von Zentren darin besteht, daß bestimmte $\bar{R}_{\lambda\mu}$ gleich Null gesetzt werden. Bei Kenntnis einer ausreichenden Anzahl von Ω_p -Funktionen für ein bestimmtes N ist somit die Energie als Funktion der Kernabstände für alle isoelektronischen Systeme mit einer Atomanzahl kleiner oder gleich N in der jeweiligen Näherungsstufe bekannt.

Wie im Falle der Z -Entwicklung bei Atomen (18), ist auch hier eine Untersuchung des Konvergenzverhaltens in Z_{λ} notwendig. Vorerst soll im folgenden die Form der Ω_p -Funktionen näher untersucht werden.

4. DIE Ω_p -FUNKTIONEN

Wir betrachten den Grundzustand, für den sich die ersten $\hat{\Omega}_k$ -Funktionen in (17) nach der Störungsrechnung [9] wie folgt ergeben

$$\hat{\Omega}_0 = \langle \hat{\Psi}_0 | T + \bar{V}_0 | \hat{\Psi}_0 \rangle = \hat{E}_0(n), \quad (34a)$$

$$\hat{\Omega}_1 = \langle \hat{\Psi}_0 | \bar{H} | \hat{\Psi}_0 \rangle, \quad (34b)$$

$$\hat{\Omega}_2 = \sum_{j=1}^{\infty} \frac{\langle \hat{\Psi}_0 | \bar{H} | \hat{\Psi}_j \rangle^2}{\hat{E}_0 - \hat{E}_j}, \quad (34c)$$

wobei als nullte Näherung von der Gleichung (26) ausgegangen wurde. Der Störoperator \bar{H} ist durch (27) definiert, und liefert, wenn er in (34b) und (34c) eingesetzt wird

$$\hat{\Omega}_1 = \sum_{\mu=1}^N Z_{\mu} \langle \hat{\Psi}_0 | \bar{V}_{\mu} - \bar{V}_0 | \hat{\Psi}_0 \rangle + \langle \hat{\Psi}_0 | \bar{w} | \hat{\Psi}_0 \rangle, \quad (35a)$$

$$\begin{aligned} \hat{\Omega}_2 = \sum_{j=1}^{\infty} \frac{1}{\hat{E}_0 - \hat{E}_j} \left\{ \sum_{\lambda=1}^N \sum_{\mu=1}^N Z_{\lambda} Z_{\mu} \langle \hat{\Psi}_0 | V_{\mu} - \bar{V}_0 | \hat{\Psi}_j \rangle \langle \hat{\Psi}_0 | \bar{V}_{\lambda} - \bar{V}_0 | \hat{\Psi}_j \rangle \right. \\ \left. + 2 \sum_{\mu=1}^N Z_{\mu} \langle \hat{\Psi}_0 | \bar{V}_{\mu} - \bar{V}_0 | \hat{\Psi}_j \rangle \langle \hat{\Psi}_0 | \bar{w} | \hat{\Psi}_j \rangle + \langle \hat{\Psi}_0 | \bar{w} | \hat{\Psi}_j \rangle^2 \right\}. \end{aligned} \quad (35b)$$

Für die Integrale von T und \bar{V}_0 mit $\hat{\Psi}_0$ gilt der Virialsatz

$$\langle \hat{\Psi}_0 | T | \hat{\Psi}_0 \rangle = -\hat{E}_0, \quad (36a)$$

$$\langle \hat{\Psi}_0 | \bar{V}_0 | \hat{\Psi}_0 \rangle = 2\hat{E}_0, \quad (36b)$$

sodaß mit (35b) einige Integrale auf \hat{E}_0 zurückgeführt werden können.

Wegen

$$E = \left(\sum_{\lambda=1}^N Z_{\lambda} \right)^2 \hat{\Omega}_0 + \left(\sum_{\lambda=1}^N Z_{\lambda} \right) \hat{\Omega}_1 + \hat{\Omega}_2 + \dots \quad (37)$$

lassen sich mit (35) die Ω -Funktionen in (28) bis zur Näherung zweiter Ordnung angeben. Man erhält im einzelnen

$$\Omega_0 \begin{pmatrix} \lambda & \mu & \nu & \sigma & \dots \\ 2 & 0 & 0 & 0 & \dots \end{pmatrix} = -\hat{E}_0 + \langle \bar{V}_{\lambda} \rangle + \sum_{j=1}^{\infty} \frac{\langle 0 | X_{\lambda} | j \rangle^2}{\hat{E}_0 - \hat{E}_j}, \quad (38a)$$

$$\Omega_0 \begin{pmatrix} \lambda & \mu & \nu & \sigma & \dots \\ 1 & 1 & 0 & 0 & \dots \end{pmatrix} = -2\hat{E}_0 + \langle \bar{V}_{\lambda} \rangle + \langle \bar{V}_{\mu} \rangle + 2 \sum_{j=1}^{\infty} \frac{\langle 0 | X_{\lambda} | j \rangle \langle 0 | X_{\mu} | j \rangle}{\hat{E}_0 - \hat{E}_j}, \quad (38b)$$

$$\Omega_0 \begin{pmatrix} \lambda & \mu & \nu & \sigma & \dots \\ 1 & 0 & 0 & 0 & \dots \end{pmatrix} = \langle \bar{w} \rangle + 2 \sum_{j=1}^{\infty} \frac{\langle 0 | X_{\lambda} | j \rangle \langle 0 | \bar{w} | j \rangle}{\hat{E}_0 - \hat{E}_j}, \quad (38c)$$

$$\Omega_0 \begin{pmatrix} \lambda & \mu & \nu & \sigma & \dots \\ 0 & 0 & 0 & 0 & \dots \end{pmatrix} = \sum_{j=1}^{\infty} \frac{\langle 0 | \bar{w} | j \rangle^2}{\hat{E}_0 - \hat{E}_j}, \quad (38d)$$

wobei die Abkürzungen

$$\left. \begin{aligned} \langle \bar{V}_{\lambda} \rangle &= \langle \hat{\Psi}_0 | \bar{V}_{\lambda} | \hat{\Psi}_0 \rangle; & \langle 0 | \bar{w} | j \rangle &= \langle \hat{\Psi}_0 | \bar{w} | \hat{\Psi}_j \rangle, \\ \langle \bar{w} \rangle &= \langle \hat{\Psi}_0 | \bar{w} | \hat{\Psi}_0 \rangle; & \langle 0 | X_{\lambda} | j \rangle &= \langle \hat{\Psi}_0 | \bar{V}_{\lambda} - \bar{V}_0 | \hat{\Psi}_j \rangle, \end{aligned} \right\} \quad (39)$$

eingeführt wurden. Die Näherung für E bis zur zweiten Ordnung wird daher

schon mit den Ω_p -Funktionen für $p=0$ erhalten. Sie verändert sich nicht mehr, wenn zu höheren Näherungen ($p>0$) übergegangen wird.

Die Z -Entwicklung, wie auch die oben besprochene R -Entwicklung, geht vom 'vereinigten Atom' als nullter Näherung aus, wobei im ersten Falle dieses ohne Elektronenwechselwirkung angenommen wird. Man darf daher erwarten, daß für große Kernabstände auch die Ω_p -Funktionen mit größerem p von Bedeutung sind. Es handelt sich hier darum, die exakte Wellenfunktion des Systems durch die Gesamtheit der Zustände (26) darzustellen.

Während aber in der R -Entwicklung bei endlicher Anzahl der Glieder für große Kernabstände die Energie unbeschränkt ansteigt, liefert die Z -Entwicklung dann schon endliche E -Werte, wenn die Atome getrennt werden.

Die Rechnungen werden durch die Mitnahme der angeregten Zustände Ψ_j sehr erschwert, zumal auch noch das Kontinuum von (26) in den Summen von (38) mit berücksichtigt werden muß!

Nur $\hat{\Psi}_0$ zu berücksichtigen, dürfte sicher eine schlechte Näherung ergeben, wie man aus der Approximation †

$$E \approx \hat{E}_0 \left(\sum_{\lambda=1}^N Z_{\lambda} \right)^2 + \langle \bar{v} \rangle \sum_{\lambda=1}^N Z_{\lambda} + \sum_{\lambda=1}^N Z_{\lambda}^2 \langle 0 | X_{\lambda} | 0 \rangle + \sum_{\lambda > \mu}^N \sum_{\mu}^N Z_{\lambda} Z_{\mu} \{ \langle 0 | X_{\lambda} | 0 \rangle + \langle 0 | X_{\mu} | 0 \rangle \} \quad (40)$$

erkennt, die selbst für alle $R_{\lambda\mu} \rightarrow 0$ wegen $X_{\lambda}, X_{\mu} \rightarrow 0$, für das vereinigte Atom die Energie

$$E \approx \hat{E}_0 Z^2 + \langle \bar{v} \rangle Z \quad (41)$$

ohne den absoluten Term liefert. Soweit wir Z -Entwicklung für Atome kennen, tritt in allen das absolute Glied negativ auf.

Eine bessere Näherung für (41) erhält man, wenn $\hat{\Psi}_0$ einen Skalenfaktor enthält, mit dem dann $\langle \mathcal{H} \rangle$ zum Minimum gemacht wird.

Es ergibt sich dann folgende Approximation [10]†

$$E \approx \hat{\Omega}_0 \left(\sum_{\lambda=1}^N Z_{\lambda} \right)^2 + \hat{\Omega}_1 \left(\sum_{\lambda=1}^N Z_{\lambda} \right) + \frac{\hat{\Omega}_n^2}{4\hat{\Omega}_0}. \quad (42)$$

Damit erhält man folgende Näherungen für die Ω_0 -Funktionen

$$\Omega_0 \begin{pmatrix} \lambda & \mu & \nu & \sigma & \dots \\ 2 & 0 & 0 & 0 & \dots \end{pmatrix} \approx \frac{\langle \bar{V}_{\lambda} \rangle^2}{4\hat{E}_0}, \quad (43 a)$$

$$\Omega_0 \begin{pmatrix} \lambda & \mu & \nu & \sigma & \dots \\ 1 & 1 & 0 & 0 & \dots \end{pmatrix} \approx \frac{\langle \bar{V}_{\lambda} \rangle \langle \bar{V}_{\mu} \rangle}{2\hat{E}_0}, \quad (43 b)$$

$$\Omega_0 \begin{pmatrix} \lambda & \mu & \nu & \sigma & \dots \\ 1 & 0 & 0 & 0 & \dots \end{pmatrix} \approx \frac{\langle \bar{V}_{\lambda} \rangle \langle \bar{v} \rangle}{2\hat{E}_0}, \quad (43 c)$$

$$\Omega_0 \begin{pmatrix} \lambda & \mu & \nu & \sigma & \dots \\ 0 & 0 & 0 & 0 & \dots \end{pmatrix} \approx \frac{\langle \bar{v} \rangle^2}{4\hat{E}_0}, \quad (43 d)$$

† Gl. (42) läßt sich verschärfen, worauf in einer anderen Arbeit eingegangen werden soll.

und für die Elektronenenergie des Systems gilt dann

$$E \approx \frac{1}{4\hat{E}_0} \left\{ \sum_{\lambda=1}^N Z_{\lambda} \langle V_{\lambda} \rangle + \langle \bar{w} \rangle \right\}^2 = \tilde{E}. \quad (44)$$

Läßt man in (44) alle $R_{\lambda\mu} \rightarrow 0$ gehen, so folgt daraus für die Energie des vereinigten Atoms

$$E(0) \approx \hat{E}_0 Z^2 + \langle \bar{w} \rangle Z + (\langle \bar{w} \rangle^2 / 4\hat{E}_0) = \tilde{E}(0). \quad (45)$$

Der letzte Term ist wegen $\hat{E}_0 < 0$ kleiner als Null. Die Energie ist gegenüber (41) um $|\langle \bar{w} \rangle^2 / 4\hat{E}_0|$ erniedrigt worden.

Wir hatten bisher noch keine Aussagen über den Ort \mathbf{R}_0 des vereinigten Atoms gemacht. Bei einer vollständigen Z_{λ} -Entwicklung ist die Energie von \mathbf{R}_0 unabhängig. Liegt dagegen nur eine beschränkte Anzahl von Funktionen vor, so ist die Lage von \mathbf{R}_0 ein freier Parameter, der durch Minimieren der Energie bestimmt werden kann.

Für $R_{\lambda\mu} \rightarrow 0$ muß \mathbf{R}_0 mit dem Ort der vereinigten Ladungen zusammenfallen, was wir beim Übergang von Gleichung (44) nach (45) schon berücksichtigt hatten; andernfalls liefert \mathbf{R}_0 nicht das Minimum der Energie.

Bei kleinen Kernabständen dürfte es noch günstig sein, \mathbf{R}_0 in den Schwerpunkt der Kernladungen Z_{λ} zu legen.

$$\mathbf{R}_0 \sum_{\lambda=1}^N Z_{\lambda} = \sum_{\lambda=1}^N Z_{\lambda} \mathbf{R}_{\lambda}. \quad (46)$$

Diese Annahme ist auch in der R -Entwicklung gemacht worden [1, 3]. Für den Übergang $R_{\lambda\mu} \rightarrow \infty$ dagegen erhält man aus (44)

$$E \approx \frac{\langle \bar{w} \rangle^2}{4\hat{E}_0} \leq 0; \quad \langle \bar{w} \rangle \geq 0 \quad (47a)$$

oder

$$E \approx \hat{E}_0 Z_{\lambda}^2 + \langle \bar{w} \rangle Z_{\lambda} + \frac{\langle \bar{w} \rangle^2}{4\hat{E}_0}, \quad (47b)$$

Je nachdem, ob (46) beibehalten wird, oder \mathbf{R}_0 mit \mathbf{R}_{λ} identifiziert wird. Für

$$Z_{\lambda} > - \frac{\langle \bar{w} \rangle}{\hat{E}_0} \quad (47c)$$

liegt die Energie nach (47b) tiefer als nach (47a). Man wird daher für $R_{\lambda\mu} \rightarrow \infty$ den Ort des vereinigten Atoms mit dem der größten Kernladung zusammenlegen.

Bei endlichen Kernabständen ist es notwendig, die Energie (44) in \mathbf{R}_0 zum Minimum zu machen. Man erhält dann ein $\mathbf{R}_{0,\min}$, welches eine Funktion der \mathbf{R}_{λ} ist

$$\mathbf{R}_{0,\min} = \mathbf{R}_0(\mathbf{R}_{\lambda}). \quad (48)$$

5. DIE BERECHNUNG DER INTEGRALE

Obwohl die Berechnung von \hat{E}_0 , $\langle \bar{V}_{\lambda} \rangle$ und $\langle \bar{w} \rangle$ im Prinzip nichts Neues enthält, soll zur Vollständigkeit kurz darauf eingegangen werden.

\hat{E}_0 setzt sich nach (26) aus einer Summe von Energien von Wasserstoffatomzuständen zusammen, wenn diese entsprechend dem Pauliprinzip besetzt werden.

Wir haben also

$$\hat{E}_0 = - \sum_{j=1}^{\infty} \frac{1}{2j^2} \hat{n}_j \quad (49)$$

wenn \hat{n}_j die Anzahl der Elektronen ist, die den Zustand mit der Hauptquantenzahl j besetzen. Es muß sein.

$$\sum_{j=1}^{\infty} \hat{n}_j = n. \quad (50)$$

Für H_2O ($n=10$) erhalten wir z.B. $n_1=2$ und $n_2=8$, also $\hat{E} = -2$ at. E . Der gleiche Wert ergibt sich auch für NH_3 , CH_4 oder $(\text{H}_2\text{-He-Li}_2)$. Der Operator $\hat{\mathcal{H}}$ in (26) setzt sich aus einer Summe von gleichen Teiloperationen \bar{h}_i nach (13 a) zusammen

$$\hat{\mathcal{H}} = \sum_{j=1}^n \bar{h}_j, \quad (51)$$

sodaß sich $\hat{\Psi}_0$ als Determinante (bzw. Determinanten, wenn keine abgeschlossenen Schalen vorliegen) der Lösungen Φ_j von (13 a) ergibt, die mit den Spinfunktionen α oder β multipliziert sind (vgl. (12))

$$\hat{\Psi}_0 = \frac{1}{\sqrt{n!}} \det \left\{ \Phi_j(i) \begin{Bmatrix} \alpha \\ \beta \end{Bmatrix} \right\}. \quad (52)$$

Die Φ_j sind Wasserstofffunktionen mit den Quantenzahlen j, l, m

$$\Phi_j \rightarrow \Phi(j, l, m) = N(j, l, m) \rho^l \exp(-\rho/2) L_{j+l}^{(2l+1)}(\rho) P_l^{(m)}(\cos \vartheta) \exp(im\phi); \quad \rho = \frac{2\bar{r}}{j}, \quad (53)$$

und der Normierungskonstanten

$$N^2(j, l, m) = \left(\frac{2}{j}\right)^3 \frac{(j-l-1)!(2l+1)(l-|m|)!}{2j[(j+l)!]^3 4\pi(l+|m|)!}. \quad (53 a)$$

Mit diesen Funktionen sind dann die Integrale $\langle \bar{V}_\lambda \rangle$ und $\langle \bar{w} \rangle$ zu berechnen. Die Polarkoordinate \bar{r} in (53) bedeutet, daß wir ursprünglich von der Gleichung (13) ausgegangen sind, und die Transformationen (15) eingeführt haben. Da für $Z=1$ die Gleichungen (15) in Identitäten übergehen, so handelt es sich bei den Funktionen (53), (53 a), wie oben schon angegeben, um Wellenfunktionen des H-Atoms, dessen Kernladung Eins beträgt.

Bei der Integration in $\langle \bar{V}_\lambda \rangle$ und $\langle \bar{w} \rangle$ kann daher so vorgegangen werden, daß in (53) $r = \bar{r}$ gesetzt wird, sowie $\bar{V}_\lambda = V_\lambda$, $\bar{w} = w$ in den Integralen, wobei das Volumenelement $d\bar{r}$ in $d\tau$ übergeht.

Die Integrale $\langle \bar{V}_\lambda \rangle$ und $\langle \bar{w} \rangle$ lassen sich durch zwei Basisintegrale ausdrücken

$$\int \Phi^*(1|j, l, m) \frac{1}{r_{\lambda 1}} \Phi(1|j', l', m') d\tau_1 = [\lambda^{-1}|j, l, m|j', l', m'], \quad (54)$$

$$\begin{aligned} \int \Phi^*(1|j, l, m) \Phi(1|j', l', m') \frac{1}{r_{12}} \Phi(2|j'', l'', m'') \Phi(2|j''', l''', m''') d\tau_1 d\tau_2 \\ = [j, l, m|j', l', m'|j'', l'', m''|j''', l''', m'''], \end{aligned} \quad (55)$$

in welchen die Φ -Funktionen in \mathbf{R}_0 zentriert sind. Das bedeutet, daß (54) eine Funktion von $\bar{\mathbf{R}}_0 - \bar{\mathbf{R}}_{\lambda 0}$ ist, während (55) ein abstandsunabhängiger Zahlenwert ist.

$\langle \bar{V}_\lambda \rangle$ und $\langle \bar{w} \rangle$ ergeben sich dann, wenn mehr als zwei Elektronen vorliegen als Linearkombinationen von Integralen (54), (55), bei denen die Quantenzahlen verschieden sind.

6. EINIGE BEISPIELE

6.1. $n=2$, $N=2$

Da nur ein Elektron vorliegt, so tritt $\langle \bar{w} \rangle$ in (44) nicht auf. \hat{E}_0 ergibt sich nach (49) zu $-0,5$ at. E., sodaß wir für (44) erhalten

$$\tilde{E} = -0,5 \{ Z_\lambda \langle \bar{V}_\lambda \rangle + Z_\mu \langle \bar{V}_\mu \rangle \}^2. \quad (56)$$

Das vereinigte Atom wollen wir auf die Verbindungsachse zwischen den Atomen λ und μ legen, sodaß $\langle \bar{V}_\lambda \rangle$ und $\langle \bar{V}_\mu \rangle$ Funktionen von $|\bar{\mathbf{R}}_0 - \bar{\mathbf{R}}_{\lambda 0}| = \bar{\mathbf{R}}_\lambda$ und $|\bar{\mathbf{R}}_0 - \bar{\mathbf{R}}_{\mu 0}| = \bar{\mathbf{R}}_\mu$ werden.

Im einzelnen erhalten wir

$$\hat{\Psi}_0 = \Phi_0(1, 0, 0) = \sqrt{(1/\pi)} \exp(-\bar{r}) \quad (57)$$

wobei \bar{r} von $\bar{\mathbf{R}}_0$ aus rechnet

$$\mathbf{r} = |\bar{\mathbf{r}} - \bar{\mathbf{R}}_0|. \quad (57a)$$

Mit (57) ergibt sich

$$\langle \bar{V}_\lambda \rangle = \langle \bar{V}_\lambda \rangle_1 = - \left[\frac{1}{\bar{R}_\lambda} - \frac{\exp(-2\bar{R}_\lambda)}{\bar{R}_\lambda} (1 + \bar{R}_\lambda) \right], \quad (58a)$$

$$\langle \bar{V}_\mu \rangle = \langle \bar{V}_\mu \rangle_1 = - \left[\frac{1}{\bar{R}_\mu} - \frac{\exp(-2\bar{R}_\mu)}{\bar{R}_\mu} (1 + \bar{R}_\mu) \right]. \quad (58b)$$

Wegen der gemachten Annahme über die Lage von \mathbf{R}_0 ist

$$\bar{R}_{\lambda\mu} = \bar{R}_\lambda + \bar{R}_\mu. \quad (59)$$

Hier tritt nun ein bemerkenswerter Effekt auf. Würde man \mathbf{R}_0 für $\mathbf{R}_{\lambda\mu} \rightarrow \infty$ immer zwischen die beiden Atome legen, so würde \tilde{E} wegen (47a) und (58) gegen Null gehen. Wird dagegen das vereinigte Atom in das Atom λ gelegt, so resultiert für $\mathbf{R}_{\lambda\mu} \rightarrow \infty$ der Wert $\tilde{E} = -Z_\lambda^2/2$, der mit dem exakten übereinstimmt, wenn $Z_\lambda \geq Z_\mu$; andernfalls ist $(Z_\lambda < Z_\mu)\lambda$ und μ zu vertauschen.

Geht dagegen $\mathbf{R}_{\lambda\mu} \rightarrow 0$, so ist, wegen $\langle \bar{V}_\lambda \rangle \rightarrow -1$; $\langle \bar{V}_\mu \rangle \rightarrow -1$, in jedem Falle

$$\lim_{R_{\lambda\mu} \rightarrow 0} \tilde{E} = -\frac{1}{2}(Z_\lambda + Z_\mu)^2, \quad (60)$$

was ebenfalls mit dem exakten Wert des vereinigten Atoms übereinstimmt.

Wir wollen noch daran erinnern, daß wir diese Übereinstimmung schon mit der Formel (56) erhalten haben, die wegen (43), (28) liefert

$$E = -\frac{1}{2} \langle \bar{V}_\lambda \rangle^2 Z_\lambda^2 - \frac{1}{2} \langle \bar{V}_\mu \rangle^2 Z_\mu^2 - \langle \bar{V}_\lambda \rangle \langle \bar{V}_\mu \rangle Z_\lambda Z_\mu + \dots \quad (61)$$

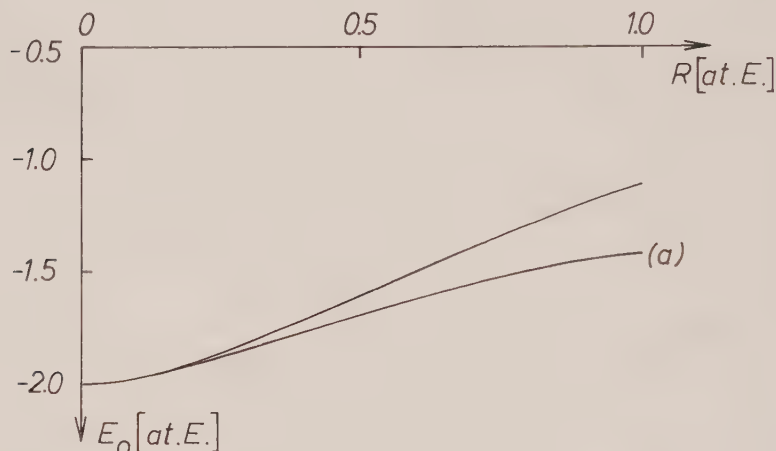
Die Figur 1 gibt die Kurve der Elektronenenergie für H_2^+ ($Z_\lambda = Z_\mu = 1$) nach (56) im Vergleich zur exakten wieder [11]. Im Hinblick auf die grobe Näherung nach (43) erhält man für kleine R -Werte schon eine gute Übereinstimmung.

Eine bessere Übereinstimmung wird zu erwarten sein, wenn die Ω_0 in (43) verbessert und die Ω_1 mitberücksichtigt werden, sodaß die Φ_j ($j > 1$) notwendig werden.

Es sei noch darauf hingewiesen, daß sich (56) bequem auf $N > 2$ erweitern läßt. Neben H_2^+ oder HeH^{++} ($N=2$) kann daher auch H_3^{++} oder das System $(\text{HeH}_2)^{3+}$ erfaßt werden, indem

$$\tilde{E} = -0,5 \left\{ \sum_{\lambda=1}^N Z_{\lambda} \langle \tilde{V}_{\lambda} \rangle \right\}^2 \quad (62)$$

geschrieben wird. Wir wollen auf diese Fragen in einer anderen Arbeit zurückkommen.



Figur 1. Elektronenergie des H_2^+ -Moleküls nach (56) im Vergleich zu den exakten Werten (Kurve a).

6.2. $n=2$, $N=2$.

Hier ist $\langle \tilde{w} \rangle \neq 0$ und kann wegen (45) aus den Z -Entwicklungen zweielektronischer Atome entnommen werden, die mit (45) in den ersten beiden Gliedern übereinstimmt [4]. Man erhält $\langle \tilde{w} \rangle = \frac{5}{8}$. Es ist bemerkenswert, daß sich das dritte Glied in (45) damit zu rund $-0,0977$ ergibt, während $-0,15765 \dots$ in der exakten Entwicklung auftritt. Wir haben also in dieser Näherung in Übereinstimmung mit der Ungleichung (45) rund 60% des absoluten Gliedes erfaßt. Für $n=2$ ist $\tilde{E}_0 = -1,0$, sodaß sich schreiben läßt:

$$\tilde{E} = -\frac{1}{4} \{ Z_{\lambda} \langle \tilde{V}_{\lambda} \rangle + Z_{\mu} \langle \tilde{V}_{\mu} \rangle + \frac{5}{8} \}^2, \quad (63)$$

oder nach (28) mit (43)

$$\begin{aligned} \tilde{E} = & -\frac{1}{4} \langle \tilde{V}_{\lambda} \rangle^2 Z_{\lambda}^2 - \frac{1}{4} \langle \tilde{V}_{\lambda} \rangle^2 + Z_{\mu}^2 - \frac{1}{2} \langle \tilde{V}_{\lambda} \rangle \langle \tilde{V}_{\mu} \rangle Z_{\lambda} Z_{\mu} \\ & - \frac{5}{16} \langle \tilde{V}_{\lambda} \rangle Z_{\lambda} - \frac{5}{16} \langle \tilde{V}_{\mu} \rangle Z_{\mu} - \frac{25}{256} + \dots \quad (63a) \end{aligned}$$

Im Grundzustand (Singulett) erhalten wir für $\tilde{\Psi}_0$ (normiert)

$$\tilde{\Psi}_0 = \Phi(1|1, 0, 0) \Phi(2|1, 0, 0), \quad (64)$$

wobei die Φ in (57) erklärt sind. Das 'vereinigte Atom' legen wir wieder wie in (59). Wegen (2b)

$$\tilde{V}_{\lambda} = -\frac{1}{\tilde{r}_{\lambda_1}} - \frac{2}{\tilde{r}_{\lambda_2}} \quad (65)$$

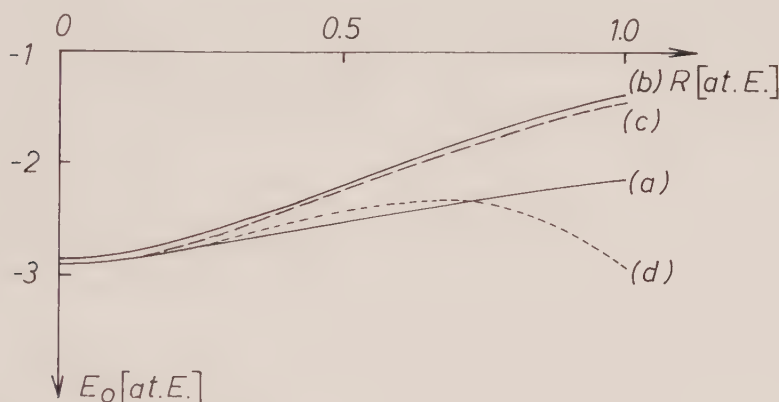
erhalten wir mit (64) und (58)

$$\langle \bar{V}_\lambda \rangle = 2\langle \bar{V}_\lambda \rangle_1; \quad \langle \bar{V}_\mu \rangle = 2\langle \bar{V}_\mu \rangle_1. \quad (66)$$

Die so erhaltene Kurve der Elektronenenergie (vgl. (4)) ist, worauf oben schon hingewiesen wurde, für große $R_{\lambda\mu}$ keine gute Näherung mehr. Immerhin geht sie, im Gegensatz zur R -Entwicklung, gegen einen endlichen Wert, der nach (63) $-\frac{25}{256}$ beträgt und unabhängig von Z_λ und Z_μ ist. Wird dagegen \mathbf{R}_0 nicht zwischen die beiden Atome gelegt, sondern fällt für $R_{\lambda\mu} \rightarrow \infty$ mit dem Atom λ zusammen, so resultiert $-\frac{1}{4}(\frac{5}{8} - 2Z_\lambda)^2$. Für $R_{\lambda\mu} \rightarrow 0$ wird nach (43), (66) und (58)

$$\tilde{E}(0) = -(Z_\lambda + Z_\mu)^2 + \frac{5}{8}(Z_\lambda + Z_\mu) - \frac{25}{256}. \quad (67)$$

In Figur 2 ist die Energiekurve des H_2 -Moleküls nach (63) für kleine Kernabstände im Vergleich zur bisher besten [1, 12] wiedergegeben.



Figur 2. Elektronenenergie des H_2 -Moleküls nach (63) (Kurve b) und (Kurve c) im Vergleich zu den besten berechneten Werten (Kurve a). Die Kurve d stellt die Energie nach der bisher besten R -Entwicklung dar [3]. (Abbruch nach R^3).

Auch hier müssen im nächsten Schritt die Ω_0 verbessert und die Ω_1 mitberücksichtigt werden.

Für H_2 ergibt sich nach (67) $\tilde{E}(0) = -2,8477$, während die Energie des He-Atoms $-2,9037$ beträgt.

Ist $N > 2$ so ist an Stelle von (63) zu schreiben

$$\tilde{E} = -\frac{1}{4} \left\{ \sum_{\lambda=1}^N \langle \bar{V}_\lambda \rangle + \frac{5}{8} \right\}^2. \quad (68)$$

Neben den Potentialkurven von H_2 , HeH^+ , LiH^{++} oder He_2^{++} können daher auch die von H_3^+ oder von dem System $(\text{HeH}_2)^{++}$ oder H_4^{++} im Rahmen dieser Näherung erhalten werden.

Wie oben schon bemerkt, folgt aus (68) stetig die Form (63), indem einige $\mathbf{R}_{\lambda\mu}$ gegen Null gehen.

Man kann die Darstellung (63 a) noch in der Weise verbessern, daß man darin einige Ω_p näherungsweise berücksichtigt, damit für $R_{\lambda\mu} \rightarrow 0$ die Z -Entwicklung für Zweielektronen-Atome erhalten wird, soweit diese heute bekannt ist [4]

$$E = -Z^2 + \frac{5}{8}Z - 0,15766 + \frac{0,00854}{Z} + \dots \quad (69)$$

Es dürfte daher eine bessere Näherung sein, wenn an Stelle von (63) geschrieben wird:

$$\begin{aligned} \tilde{E} = & -\frac{1}{4}\langle \tilde{V}_\lambda \rangle^2 Z_\lambda^2 - \frac{1}{4}\langle \tilde{V}_\mu \rangle^2 Z_\mu^2 - \frac{1}{2}\langle \tilde{V}_\lambda \rangle \langle \tilde{V}_\mu \rangle Z_\lambda Z_\mu \\ & - \frac{5}{16}\langle \tilde{V}_\lambda \rangle Z_\lambda - \frac{5}{16}\langle \tilde{V}_\mu \rangle Z_\mu - 0,15766 + \frac{0,00854}{Z_\lambda + Z_\mu}. \end{aligned} \quad (70)$$

Die Gleichung (69) liefert für $Z=2$ (He-Atom) $E = -2,90339$ at. E , was nur noch um rund 0,0003 vom exakten Wert nach oben abweicht.

In Figur 2 ist ebenfalls die Energiekurve nach (70) aufgenommen worden. Sie stimmt für kleine R -Werte schon recht gut mit der exakten Kurve überein. Zum Vergleich ist noch die Energiekurve nach der bisher besten R -Entwicklung aufgenommen worden [3], wobei dort nach R^3 abgebrochen würde.

Frau I. Funke sei für die hierzu durchgeführten Rechnungen herzlich gedankt.

REFERENCES

- [1] BINGEL, W. A., 1957, *Z. Naturf. A*, **12**, 59; 1959, *J. chem. Phys.*, **30**, 1250.
- [2] PREUSS, H., 1957, *Z. Naturf. A*, **12**, 599; 1958, *Ibid.*, **13**, 364; 1961, Habilitationsschrift, Universität Frankfurt; 1960, *Rev. mod. Phys.*, **35**, 646.
- [3] BINGEL, W. A., 1959, *J. chem. Phys.*, **30**, 1254.
- [4] HYLLERAAS, E. A., und MIDTDAL, J., 1930, *Z. Phys.*, **65**, 209; 1956, *Phys. Rev.*, **103**, 829.
- [5] KATO, T., 1951, *J. Fac. Sci. Tokyo Univ.*, **6**, 145. FRÖMAN, A., und HALL, G. G., 1960, Preprint 42, Quantum Chemistry Group, Uppsala.
- [6] LINDERBERG, J., 1960, Preprint 42, Quantum Chemistry Group, Uppsala; 1961, *Phys. Rev.*, **121**, 816. LINDERBERG, J., und SHULL, H., 1959, Preprint 32, Quantum Chemistry Group, Uppsala; 1961, *J. mol. Spectrosc.*, **3**, 1.
- [7] LÖWDIN, P. O., 1958, Preprint 6, Quantum Chemistry Group, Uppsala; 1959, *J. mol. Spectrosc.*, **3**, 46. FRÖMAN, A., 1958, Preprint 5, Quantum Chemistry Group, Uppsala; 1958, *Phys. Rev.*, **112**, 870.
- [8] PREUSS, H., 1960, *Naturwissenschaften*, **47**, 241.
- [9] Man vergl. z.B. Hellman; "Einführung in die Quantenchemie", S. 70, Paragraph 1, Deuticke (1937).
- [10] Man vergl. P. Gombas; "Theorie und Lösungsmethoden des Mehrteilchenproblems in der Wellenmechanik", Birkhauser (1950), S. 160.
- [11] BATES, D. R., LEDSHAM, A. G., und STEWART, A. G., 1953, *Phil. Trans. roy. Soc. A*, **246**, 215. KOTANI, M., OHNO, K., und KAYAMA, K., 1961, *Handb. Phys.*, Bd. XXXVII/2, Moleküle 2 (Berlin: Springer), S. 55.
- [12] KOLOS, W., und ROTHAAAN, C. C. J., 1960, *Rev. mod. Phys.*, **32**, 205. TOBIAS, I., und VANDERSLICE, J. T., 1961, *J. chem. Phys.*, **35**, 1852.

The electronic structure and spectrum of nitrobenzene

by O. MATSUOKA

Department of Chemistry, Tokyo University of Education,
Otsuka, Tokyo

and Y. I'HAYA

Department of Chemistry, The University of Electro-communication,
Chofu-shi, Tokyo, Japan

(Received 3 March 1964)

Calculations on the electronic spectrum of nitrobenzene are performed by the Pariser-Parr-Pople-Brown-Heffernan method employing five kinds of approximations for the core resonance integrals, penetration integrals and bond lengths. The calculated transition energies and intensities agree fairly well with experiment. It is confirmed that the calculation, using approximate bond lengths, may predict the transition energies well but not the intensities, and that penetration integrals are safely neglected when many configurations are mixed. It is suggested that adoption of fairly large values for core resonance integrals might be needed in the case that many doubly excited states are included in the configuration interaction procedure.

1. INTRODUCTION

During the past ten years several methods have been developed for calculating the electronic structures and spectra of conjugated hydrocarbons and their derivatives. Pariser and Parr [1] introduced the essential approximations in the method of anti-symmetric molecular orbitals, and their method has been applied to various molecules with remarkable success. With similar approximations Pople [2] developed a self-consistent field (SCF) procedure. Brown and Heffernan [3] took account of the fact that the variation of the electron density around a nucleus accompanies a change in the interaction integrals for the SCF calculation. Because of the complicated iteration procedure that has to be used in their method, only few molecules have been treated up to now. In this paper their method will be employed for calculating the electronic structure and spectrum of the nitrobenzene molecule.

Electronic aspects of nitrobenzene have been treated theoretically by many authors. Early investigators [4,5] studied, by the simple Hückel method, the chemical reactivity, dipole moment, bond lengths and transition energies of that molecule. Recent research [6-14] has been mainly concerned with the electronic spectrum, of which semi-quantitative predictions have been made. In most papers however use has been made of many empirical data for the choice of parameters necessary for the calculation. In this study a special attempt has been made to reduce the number of empirical parameters.

The purpose of the present paper is to calculate π - π^* transition energies and intensities. We examine also the effect of the variation of bond distances and core resonance integrals and the neglect of penetration integrals upon the transition energies.

2. METHOD OF CALCULATION

We shall here summarize the Pariser-Parr-Pople-Brown-Heffernan method by which the wave functions and energies of a given π -electron system may be obtained. In their method of calculation the Hamiltonian operator for the n π -electrons of a given molecule is assumed to be:

$$H = \sum_{i=1}^n H_{\text{core}}(i) + \frac{1}{2} \sum_{i=1}^n \sum_{j=1, j \neq i}^n \frac{e^2}{r_{ij}}. \quad (1)$$

Here the first term is the kinetic energy operator plus the potential energy operator for the electron i in the field of core, and the second term the electrostatic repulsion between π -electrons i and j .

If the molecule contains m atoms which contribute π -electrons to the system, the molecular orbitals may be expressed as:

$$\phi_i = \sum_{p=1}^m C_{ip} \chi_p, \quad (2)$$

χ_p being the $2p\pi$ atomic orbital centred on the atom p . Assuming some reasonable values for coefficients C_{ip}^0 , orbital energies ϵ and new coefficients C_{ip} are determined by the equations [15]:

$$\det |F_{pq} - \delta_{pq}\epsilon| = 0, \quad (3)$$

and

$$\sum_{p=1}^m C_{ip} (F_{pq} - \delta_{pq}\epsilon) = 0, \quad (4)$$

where F_{pq} are matrix elements of the Hartree-Fock operator. Processes (3) and (4) should be repeated until self-consistency is obtained.

Matrix elements in equations (3) and (4) may be calculated, zero differential overlap being assumed, from the formulae [2]:

$$F_{pp} = \alpha_p + \frac{1}{2} P_{pp} \gamma_{pp} + \sum_{q \neq p} P_{qq} \gamma_{pq} \quad (5)$$

and

$$F_{pq} = \beta_{pq} - \frac{1}{2} P_{pq} \gamma_{pq} \quad (p \neq q). \quad (6)$$

Here

$$P_{pq} = 2 \sum_i C_{ip} C_{iq}, \quad (7)$$

$$\alpha_p = \int \chi_p(1) H_{\text{core}}(1) \chi_p(1) dv(1), \quad (8)$$

$$\beta_{pq} = \int \chi_p(1) H_{\text{core}}(1) \chi_q(1) dv(1) \quad (9)$$

and

$$\gamma_{pq} = \int \chi_p(1) \chi_p(1) (e^2/r_{12}) \chi_q(2) \chi_q(2) dv(1, 2), \quad (10)$$

and the summation in equation (7) is over the occupied molecular orbitals in the closed-shell ground state.

Core coulomb integrals α_p in equation (8) are approximated by the expression [1]:

$$\alpha_p = -I_p - \sum_{s \neq p} (s : pp) - \sum_{q \neq p} n_q \gamma_{pq}, \quad (11)$$

where I_p is the appropriate valence state ionization energy, n_q the number of π -electrons contributed to the system by atom q , and $(s : pp)$ the penetration integral between neutral atoms and π -electrons in atom p . Core resonance integrals β_{pq} in equation (9) may be determined empirically or calculated by some formulae; they are supposed to be zero unless atoms p and q are adjacent.

Electronic repulsion integrals in equation (10) are obtained as follows:

(a) One-centre integrals γ_{pp} are calculated by the formula:

$$\gamma_{pp} = I_p - A_p, \quad (12)$$

where A_p is the appropriate valence state electron affinity of atom p . This formula is derived by the use of atoms-in-molecules idea and its advantage has been fully discussed by Pariser and Parr [1].

(b) Two-centre integrals γ_{pq} ($p \neq q$) are calculated for large distances from theoretical formulae (see equation (19)) and for small distances they are determined by use of a quadratic equation of the form [1]:

$$\gamma_{pq} = kr^2 + lr + \frac{1}{2}(\gamma_{pp} + \gamma_{qq}), \quad (13)$$

where r is the distance between atoms p and q , and the constants k and l are obtained by fitting values calculated theoretically for two large distances (see also § 3.2).

Here it should be noted that all integrals described above are functions of effective nuclear charge Z_p determined by [3]:

$$Z_p = N_p - 1.35 - 0.35(\sigma_p + P_{pp}), \quad (14)$$

where N_p stands for the atomic number of atom p , and σ_p is the number of $2s$ and $2p$ electrons contributed to the core by atom p .

Thus, forming various anti-symmetric products Φ_a from these molecular orbitals, the wave functions of the π -electron system may be expressed as:

$$\Psi = \sum_a A_a \Phi_a, \quad (15)$$

and the energies of the system E and coefficients A_a in equation (15) are determined by solution of:

$$\det |H_{ab} - \delta_{ab}E| = 0 \quad (16)$$

and

$$\sum_a A_a (H_{ab} - \delta_{ab}E) = 0, \quad (17)$$

where

$$H_{ab} = \int \Phi_a H \Phi_b dv. \quad (18)$$

3. DETAILS OF CALCULATION

3.1. Ionization energy and electron affinity

Appropriate valence state ionization energies and electron affinities that are necessary to the calculation of core integrals and electron repulsion integrals may be obtained from valence state energies. Table 1 shows these energies calculated by Moffitt's method [16–20] using atomic spectroscopic data [21]. In these

calculations the valence states are assumed to be $(sxyz, V_4)$ for carbon, $(sxyz^2, V_3)$ for nitrogen and (s^2x^2yz, V_2) for oxygen, and moreover carbon and nitrogen are supposed to be sp^2 hybridized.

The dependence of valence state ionization energies and electron affinities upon effective nuclear charges, being assumed to be parabolic [3, 20, 22], may be obtained from the values of these quantities of the isoelectronic series $C(Z=3.25)$, $N^+(Z=4.25)$, $O^{++}(Z=5.25)$ and $F^{+++}(Z=6.25)$ for carbon and nitrogen, and

Valence state			Energy (ev)
C^{+1} ,	$t_1t_2\sigma$;	V_3	19.684
C^0 ,	$t_1t_2\sigma\pi$;	V_4	8.263
C^{-1} ,	$t_1t_2\sigma\pi^2$;	V_3	7.68†
N^{+2} ,	$t_1t_2\sigma$;	V_3	54.946
N^{+1} ,	$t_1t_2\sigma\pi$;	V_4	(26.504)‡
N^0 ,	$t_1t_2\sigma\pi^2$;	V_3	14.23†
O^{+3} ,	$t_1t_2\sigma$;	V_3	(117.657)‡
O^{+2} ,	$t_1t_2\sigma\pi$;	V_4	64.168
O^{+1} ,	$t_1t_2\sigma\pi^2$;	V_3	32.780
O^{+1} ,	s^2y^2z ;	V_1	17.788
O^0 ,	s^2x^2yz ;	V_2	0.489
O^{-1} ,	$s^2x^2yz^2$;	V_1	-2.2†
F^{+4} ,	$t_1t_2\sigma$;	V_3	219.052
F^{+3} ,	$t_1t_2\sigma\pi$;	V_4	134.976
F^{+2} ,	$t_1t_2\sigma\pi^2$;	V_3	76.604
F^{+2} ,	s^2y^2z ;	V_1	57.719
F^{+1} ,	s^2x^2yz ;	V_2	18.072
F^0 ,	$s^2x^2yz^2$;	V_1	0.0
Ne^{+3} ,	s^2y^2z ;	V_1	(108.929)‡
Ne^{+2} ,	s^2x^2yz ;	V_2	41.880
Ne^{+1} ,	$s^2x^2yz^2$;	V_1	0.0
Na^{+4} ,	s^2y^2z ;	V_1	(178.004)‡
Na^{+3} ,	s^2x^2yz ;	V_2	(72.627)‡
Na^{+2} ,	$s^2x^2yz^2$;	V_1	0.0

Table 1. Valence state energy.

† From ref. (17).

‡ Brackets show that errors are involved.

Atom	a_0	a_1	a_2	b_0	b_1	b_2
Carbon } Nitrogen } Oxygen }	3.3897	-7.8986	1.1567	3.8223	-17.0631	15.6843
	3.9928	-19.1465	22.0388	3.8431	-23.1416	28.3563

Table 2. Dependence of ionization energy I_p and electron affinity A_p upon effective nuclear charge Z_p †.

$$\dagger I_p = a_0 Z_p^2 + a_1 Z_p + a_2, \quad A_p = b_0 Z_p^2 + b_1 Z_p + b_2.$$

Concerning why the same dependence upon Z holds for both carbon and nitrogen, see § 3.1 of the text.

O($Z=4.55$), F^+ ($Z=5.55$), Ne^{++} ($Z=6.55$) and Na^{+++} ($Z=7.55$) for oxygen [21]. Table 2 shows the quadratic dependence obtained from atomic data by least squares method. Because a preliminary calculation shows that nitrogen is charged almost singly positive in the molecule, the quadratic expressions for the ionization energy and electron affinity of nitrogen are taken to be the same as those of carbon.

3.2. Geometrical configuration and integrals over atomic orbitals

In the present calculation two geometrical configurations are adopted: one which has been found by x-ray crystal analysis of nitrobenzene [23], and another one obtained from an analysis of the Raman spectrum data of benzene

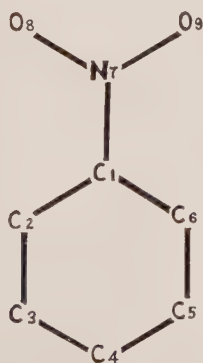
	From x-ray analysis†	Assumed§
C_1-C_2	1.367 Å	1.40 Å
C_2-C_3	1.426 Å	1.40 Å
C_3-C_4	1.363 Å	1.40 Å
C_1-N_7	1.486 Å	1.47 Å
N_7-O_8	1.208 Å	1.21 Å
$\angle C_2C_1C_6$	126°	120°
$\angle C_1C_2C_3$	116°	120°
$\angle C_2C_3C_4$	121°	120°
$\angle C_3C_4C_5$	120°	120°
$\angle C_2C_1N_7$	117°	120°
$\angle C_1N_7O_8$	118°	120°
$\angle O_8N_7O_9$	124°	120°

Table. 3 Geometrical structure of nitrobenzene†.

† The numbering of atoms is shown in the figure.

‡ Ref. [23].

§ From the Raman spectrum analysis of benzene [24] and the electron diffraction analysis of nitromethane [25].



Geometry of nitrobenzene.

[24] and the electron diffraction data of nitrobenzene [25]. Both are assumed to be planar and belong to symmetry group C_{2v} . The structures are given in table 3. The numbering of atoms is given in the figure.

For $r \geq 2.80 \text{ \AA}$, electronic repulsion integrals γ_{pq} are calculated theoretically by the multipole expansion formula [26]:

$$\gamma_{pq} = \frac{e^2}{a_0} \left\{ \frac{a_0}{r} - \frac{6a_0^3}{r^3} \left[\frac{1}{Z_p^2} + \frac{1}{Z_q^2} \right] + \frac{324}{Z_p^2 Z_q^2} \frac{a_0^5}{r^5} \right\}, \quad (19)$$

where $e^2/a_0 = 27.20976 \text{ eV}$ (1 A.U.) and $a_0 = 0.52917 \text{ \AA}$ (1 A.U.). For $r < 2.80 \text{ \AA}$ they are obtained from equation (13), constants k and l being determined by fitting values calculated from equation (19) for $r = 2.80 \text{ \AA}$ and $r = 3.70 \text{ \AA}$.

In this study three approximations are employed in evaluating core resonance integrals β_{pq} :

(a) They are assumed to be constant irrespective of the change of effective nuclear charges, and empirically determined values are used.

(b) They are calculated by the expression [27, 28]:

$$\beta_{pq} = -0.5 S_{pq} (I_p + I_q), \quad (20)$$

in which S_{pq} is the theoretically calculated overlap integral between $2p\pi$ orbitals on atoms p and q [29].

(c) They are obtained from the formula:

$$\beta_{pq} = -0.421197 S_{pq} (I_p + I_q). \quad (21)$$

The numerical constant in equation (21) is chosen so that the value of β_{pq} for benzene calculated by equation (20), using $r = 1.39 \text{ \AA}$ and $Z_p = Z_q = 3.25$, fits the empirical value -2.39 eV [1].

Assuming a Goeppert-Mayer and Sklar potential [30], penetration integrals are calculated purely theoretically by the use of Slater atomic orbitals [29, 31, 32]. They may be taken constant under the variation of effective nuclear charges as shown in table 4.

s	p	Z_p	($s : pp$) (eV)
1	2	3.10	0.646
		3.25	0.723
		3.40	0.644
1	7	4.20	0.400
		4.25	0.397
		4.30	0.395
7	1	3.20	0.429
		3.25	0.432
		3.30	0.435
7	8	4.30	1.140
		4.40	1.140
		4.50	1.145
8	7	4.20	0.835
		4.25	0.859
		4.30	0.932

Table 4. Variation of penetration integral ($s : pp$) with effective nuclear charge Z_p^\dagger .

† Following values for Z_s 's are employed: $Z_C = 3.25$, $Z_N = 3.90$ and $Z_O = 4.55$.

3.3. Classification of calculation

The present calculation may be divided into five classes according to the ways of approximating to core resonance integrals and penetration integrals and according to the geometrical structure adopted. The classification is given in table 5. Table 6 shows the values of penetration integrals used through calculations A, C, D, E.

	Calculation A	Calculation B	Calculation C	Calculation D	Calculation E
Core resonance integrals	Constant†	Constant†	Variable‡	Variable§ (adjusted)	Constant†
Penetration integrals	Included	Neglected	Included	Included	Included
Geometry	From x-ray crystal analysis data				Assumed¶

Table 5. Classification of calculation.

† See the second column of table 7.

‡ Varied with the change in the valence state ionization energy through equation (20). For their values, see the third column of table 7.

§ Varied by the use of equation (21); their values are listed in the fourth column of table 7.

|| Listed in the second column of table 3.

¶ Listed in the third column of table 3.

s^\dagger	p^\ddagger	$(s : pp) \text{ (ev)}^\S$
1	2	0.723
	3	0.010
	4	0.002
	7	0.397
	8	0.007
2	3	0.575
	4	0.008
	6	0.008
	7	0.004
3	8	0.001
	4	0.734
7	5	0.010
	1	0.432
	2	0.086
	3	0.027
8	8	1.140
	1	0.008
	7	0.859
	9	0.039

Table 6. Penetration integral ($s : pp$).

† Employed values for Z_s 's are the same as those listed in table 3.

‡ Following values for Z_p 's are used: $Z_C = 3.25$, $Z_N = 4.25$ and $Z_O = 4.40$.

§ Integral values less than 0.001 ev are not listed in the table (e.g. (2 : 99)).

3.4. Wave function and intensity of transition

All singlet configurations in which one electron is excited from an occupied molecular orbital to an unoccupied orbital in the ground state are mixed to determine the wave functions and energies of nitrobenzene. Therefore the secular equations to be solved are 11×11 for 1A_1 states and 9×9 for 1B_2 states.

The intensities of transition are expressed by oscillator strengths. They are obtained by the formula [33]:

$$f = 1.085 \times 10^{11} \omega_a Q_a^2, \quad (22)$$

where ω_a and Q_a are the transition energy in cm^{-1} and the transition moment in centimetres for the transition from the ground state to the excited state a , respectively. In calculating transition moments the zero differential overlap approximation is adopted.

4. RESULTS AND DISCUSSION

All numerical calculations were carried out in the HIPAC 103 digital computer at Tokyo University of Education. At each stage of the iteration process in the SCF routine, the integrals are modified by new Z_p 's in accordance with equations (11), (12), (13), (19) and (20) (or (21)), which in turn yield the new molecular orbitals for the next stage of the SCF routine. The molecular orbitals became self-consistent to five decimal places in seven iterations, on the average.

The calculated transition energies and intensities for the transition up to 10 eV are listed in table 8 together with the corresponding observed values. All methods except calculation C reproduce experimental values satisfactorily. In particular calculation A gives the best result, which is probably due to the adoption of proper core resonance integrals and bond lengths. From comparison of calculation A and calculation B, it is seen that the change of bond lengths is not very sensitive to the transition energies but quite sensitive to the intensities of transitions, specifically of higher transitions. The latter sensitiveness might not be reduced very much even by the inclusion of overlap integrals in the computation of transition moments. We may therefore conclude that the calculation using approximate bond lengths in general leads to a satisfactory result for transition energies but not for the values of oscillator strengths.

Calculation C yields rather high transition energies as a whole, and this is obviously due to the use of equation (20) which gives considerably large values for core resonance integrals, as shown in table 7. If the energy of each electronic

p	q	Calc. A, B, E	Calc. C†	Calc. D†
1	2	-2.39‡	-2.8934	-2.4360
1	7	-2.576‡	-2.7939	-2.3529
2	3	-2.39‡	-2.6512	-2.2342
3	4	-2.39‡	-2.9469	-2.4831
7	9	-3.0§	-3.7125	-3.1259

Table 7. Core resonance integral $\beta_{pq}(\text{eV})$.

† Values listed are those finally obtained in the SCF iterations.

‡ From ref. [1].

§ From ref. [8].

Calculation A		Calculation B		Calculation C			Calculation D		Calculation E		Observations†	
Energy	<i>f</i>	Energy	<i>f</i>	Energy	Energy adjusted	<i>f</i>	Energy	<i>f</i>	Energy	<i>f</i>	Energy	<i>f</i>
4·527	0·013	4·544	0·009	5·370	4·531	0·021	4·531	0·011	4·673	0·015	4·38	0·01
4·954	0·280	5·085	0·307	5·641	4·802	0·271	5·158	0·291	4·939*	0·111	} 5·11	0·17
5·170*	0·201	5·147*	0·208	6·210*	5·371*	0·048	5·345*	0·046	5·077	0·170		
6·470	0·078	6·549*	0·836	6·847*	6·008*	0·205	6·371*	0·460	6·379*	1·038	} 6·24	0·38
6·492*	0·297	6·629	0·006	7·324*	6·485*	1·356	6·491*	0·711	6·581	0·187		
6·632*	0·696	6·729*	0·138	7·373	6·534	0·104	6·539	0·085	6·983*	0·001	} 7·56	0·87
7·100	0·448	7·156	0·492	8·095	7·200	0·533	7·172	0·289	7·082	1·172		
7·493	0·726	7·500	0·714	8·631	7·774	0·846	7·410	0·890	7·554*	0·576	} 7·56	0·87
7·517*	0·206	7·514*	0·223	8·897*	8·085*	0·060	7·680*	0·098	7·842	0·212		
8·258*	0·002	8·274*	0·002	9·657	8·818	0·010	8·391	0·000	8·188*	0·045	} 7·56	0·87
8·531	0·004	8·560	0·002	9·770*	8·931*	0·000	8·461*	0·000	8·625	0·102		
8·999*	0·005	8·978*	0·005	10·430	9·591	0·000	9·076	0·000	8·923*	0·305	} 7·56	0·87
9·281	0·000	9·336	0·000	10·557*	9·718*	0·014	9·145*	0·009	9·174	0·023		

Table 8. Calculated and observed transition energies (ev) and oscillator strength†.

† States with asterisk are ¹A₁ and those without it are ¹B₂.

‡ From ref. [13].

state above the ground state is decreased in magnitude by 0.893 eV, however, good agreement with experiment is obtained, as seen by comparing the third and the sixth columns of table 8. This would suggest that the same extent of lowering in the state energies could be expected by the inclusion of doubly excited configurations. The same feature is seen in the recent work by Anno and Sado [34]. Including many doubly excited configurations in the usual Pariser-Parr method, they found that a rather large value of core resonance integral (-2.7217 eV) gave the best fit of the transition energies to experimental values. From these facts and from comparison of calculation C and calculation D, our conclusion is tentatively, that for an estimation of core resonance integral β equation (21) is satisfactory in the usual calculations while equation (20) is better for the more detailed calculation in which doubly excited configurations are included.

One may ask whether the penetration integrals can be neglected in the calculation of the spectrum. The SCF molecular orbitals obtained from calculation B in which all penetration integrals are neglected are not very close to those obtained from calculation A. Nevertheless calculation B gives almost the same transition energies and intensities as those predicted by calculation A. One may therefore conclude that penetration integrals are safely neglected if many configurations are included.

Finally, we make some remarks about the spectral assignment. The observed $288\text{ m}\mu$ (4.38 eV) band undoubtedly corresponds to the calculated 4.75 eV transition, from comparison of both predicted and observed values of transition energy and intensity. The direction of polarization is perpendicular to the molecular axis in accordance with experimental work by Labhart and Wagnière [14]. The band observed at $240\text{ m}\mu$ (5.11 eV) was previously interpreted to be the intramolecular charge transfer band by Nagakura and Tanaka [7], which has been confirmed recently by Nagakura *et al.* [13]. On the other hand Wentzel [35] interpreted the band to be the shifted $200\text{ m}\mu$ band of benzene ($B_{1u}-A_{1g}$). The charge transfer band of Nagakura *et al.* is a A_1-A_1 transition and the shifted benzene band is a B_2-A_1 in the notation of symmetry group C_{2v} , so that it is probable that both bands (one A_1-A_1 and one B_2-A_1) overlap in this region, as predicted by the present calculation. Further, our calculation shows that the observed $193\text{ m}\mu$ (6.42 eV) band consists of three transitions. At about 7.1 eV a band is calculated to have an oscillator strength $0.2-0.4$, but this has not been observed. At $164\text{ m}\mu$ (7.56 eV) a band is predicted to consist of two transitions. The bands of higher frequencies have not yet been found but, if observable, they seem to be very weak as table 8 shows.

One of the authors (O.M.) is indebted to Professor K. Suzuki of Tokyo University of Education and Mr. S. Cho of Gumma University for many helpful discussions during the course of this study.

REFERENCES

- [1] PARISER, R., and PARR, R. G., 1953, *J. chem. Phys.*, **21**, 466, 767.
- [2] POPLE, J. A., 1953, *Trans. Faraday Soc.*, **49**, 1375.
- [3] BROWN, R. D., and HEFFERNAN, M. L., 1958, *Trans. Faraday Soc.*, **54**, 757.
- [4] WHELAND, G. W., and PAULING, L., 1935, *J. Amer. chem. Soc.*, **57**, 2085.
- [5] FERNANDEZ, J., 1951, *C. R. Acad. Sci., Paris*, **233**, 403.
- [6] SIMONNETA, M., and VACIAGO, A., 1954, *Nuovo Cim.*, **11**, 596.

- [7] NAGAKURA, S., and TANAKA, J., 1954, *J. chem. Phys.*, **22**, 236.
- [8] TANAKA, J., 1958, *Nippon Kagaku Zasshi*, **79**, 1114.
- [9] TROTTER, J., 1959, *Canad. J. Chem.*, **37**, 351, 905; 1959, *Tetrahedron*, **8**, 13.
- [10] GODFREY, M., and MURRELL, J. N., 1961, *Proc. chem. Soc.*, p. 171.
- [11] PEACOCK, T. E., 1961, *Proc. phys. Soc., Lond.*, **78**, 460.
- [12] REKASHEVA, T. N., 1961, *Zhur. Fiz. Khim.*, **35**, 638.
- [13] NAGAKURA, S., KOJIMA, M., and MARUYAMA, Y., 1963, Technical Report of the Institute for Solid State Physics (The University of Tokyo), Series A, No. 74.
- [14] LABHART, H., and WAGNIÈRE, G., 1963, *Helv. chim. acta.*, **46**, 1314.
- [15] ROTHAAAN, C. C. J., *Rev. mod. Phys.*, **23**, 61.
- [16] MOFFITT, W., 1950, *Proc. roy. Soc. A*, **202**, 534; 1954, *Rep. Prog. Phys.*, **17**, 173.
- [17] SKINNER, H. A., and PRITCHARD, H. O., 1953, *Trans. Faraday Soc.*, **49**, 1254.
- [18] COMPANION, A., and ELLISON, F. O., 1958, *J. chem. Phys.*, **28**, 1.
- [19] PARKS, J. M., and PARR, R. G., 1960, *J. chem. Phys.*, **32**, 1657.
- [20] I'HAYA, Y., 1960, *Mol. Phys.*, **3**, 521.
- [21] MOORE, C. E., Atomic Energy Levels, Nat. Bur. Stand., 1949-1952, Circ., 467.
- [22] GLOCKER, G., 1934, *Phys. Rev.*, **46**, 111.
- [23] TROTTER, J., 1959, *Acta Cryst.*, **12**, 884.
- [24] STOICHEFF, B., 1954, *Canad. J. Phys.*, **32**, 339.
- [25] BROCKWAY, L. O., BEACH, J. Y., and PAULING, L., 1935, *J. Amer. chem. Soc.*, **57**, 2693.
- [26] PARR, R. G., 1960, *J. chem. Phys.*, **33**, 1184.
- [27] I'HAYA, Y., 1961, *Prog. Rep. on Electronic Process in Chem.*, No. 3, 1 (in Japanese); Preprint, International Symposium on Molecular Structure and Spectra, Tokyo, 1962, B110-4; *Advances in Quantum Chemistry* (Academic Press) (in the press).
- [28] BROWN, R. D., and HARCOURT, R. D., 1961, *Proc. chem. Soc.*, p. 216.
- [29] ROTHAAAN, C. C. J., 1951, *J. chem. Phys.*, **19**, 1445.
- [30] GOEPPERT-MAYER, M., and SKLAR, A. L., 1938, *J. chem. Phys.*, **6**, 645.
- [31] ANNO, T., MATSUBARA, I., and SADO, A., 1957, *Bull. chem. Soc., Japan*, **30**, 168.
- [32] RUEDENBERG, K., 1961, *J. chem. Phys.*, **34**, 1892.
- [33] MULLIKEN, R. S., and RIEKE, C. A., 1941, *Rep. Prog. Phys.*, **8**, 231.
- [34] ANNO, T., and SADO, A., 1963, *J. chem. Phys.*, **39**, 2293.
- [35] WENTZEL, A., 1954, *J. chem. Phys.*, **22**, 1623.

The N.M.R. spectrum and configuration of decafluorobiphenyl

by N. BODEN, J. W. EMSLEY†, J. FEENEY and L. H. SUTCLIFFE

Donnan Laboratories, The University, Liverpool

(Received 21 March 1964)

The ^{19}F ortho and para chemical shifts in decafluorobiphenyl have been calculated in terms of the π -electron charge distribution and the intramolecular electric fields as a function of the azimuthal angle. Comparison of the results with the observed chemical shifts shows that the angle in this molecule is 50° .

1. INTRODUCTION

In a previous paper [1] it was shown that the ^{19}F chemical shifts in substituted aromatic compounds can be predicted by taking into account both the π -electron charge distribution as calculated by L.C.A.O.-M.O. theory, and the resultant electric fields at the fluorine nuclei. The chemical shift can be written as a sum of two terms:

$$\left. \begin{aligned} \delta &= \delta_{\text{electronic}} + \delta_{\text{electric}}, \\ \delta &= (H_{\text{C}_6\text{F}_6} - H_{\text{sample}})/H_{\text{C}_6\text{F}_6} \times 10^6 \text{ p.p.m.} \end{aligned} \right\} \quad (1)$$

$$\text{where} \quad \delta_{\text{electronic}} = 488(\Delta E)^{-1} [11.9\Delta_q(F_z) + 0.1\Delta_q(C_z) + 3.9\Delta p(C_z F_z)], \quad (2)$$

$$\delta_{\text{electric}} = -B(\Delta E^2 + \Delta \langle E^2 \rangle). \quad (3)$$

In equation (2), $\Delta q(F_z)$, $\Delta q(C_z)$ and $\Delta p(C_z F_z)$ are the π -electron parameters relative to those in C_6F_6 and ΔE is an average excitation energy. In equation (3), E^2 is the square of the total electric field at the ^{19}F nucleus arising from point dipoles placed at the centre of any polar bonds in the molecule, and $\langle E^2 \rangle$ is the time-averaged square of the electric field produced by fluctuating dipoles in the bonds, again these are relative to C_6F_6 . $\langle E^2 \rangle$ is given approximately by:

$$\langle E^2 \rangle = \sum_i 3P_i I_i / r_i^6, \quad (4)$$

where P_i is the polarizability of the electron group, I_i is the first ionization potential and r_i is the distance separating the fluorine atom from the electron group. In reference [1] the values of r_i and P_i were taken to be those of electrons in chemical bonds, rather than atomic parameters, because this makes the calculation simpler. The values of r_i for the E^2 calculation are also computed in this way. Had we chosen to use atomic parameters then B would have had a different value but the results would not have been changed significantly.

† Now at Chemistry Department, The University, South Road, Durham City.

The purpose of the present paper is to extend these calculations to decafluorobiphenyl and to illustrate how the ^{19}F chemical shifts can be used to determine the stereochemistry of the molecule. Biphenyl itself is a planar molecule in the solid state [2]; however, electron diffraction studies on the vapour [3], ultra-violet [4] and nuclear magnetic resonance spectroscopic studies on solutions [5] indicate that the molecule is non-planar in both liquid and vapour states. Ortho-halogeno biphenyls [3, 4] are also non-planar in the solution and vapour states; in the case of 2,2'-difluorobiphenyl the azimuthal angle between the two aromatic rings is estimated to be 60° – 80° . The ^{19}F chemical shifts in decafluorobiphenyl provide an excellent method of verifying this non-planarity. The value of $\langle E^2 \rangle$ at the fluorine ortho to the ring junction will vary considerably in moving from a completely planar to an orthogonal ring configuration, hence the ^{19}F chemical shift should show a very sensitive dependence on the azimuthal angle, θ . Furthermore, the extent of conjugation between the two rings (and therefore the electronic contribution to the chemical shift) depends upon θ , the effect being most marked for the ortho and para shifts (see table 1).

2. RESULTS

Perfluorobiphenyl is an $\text{AA}'\text{A}''\text{A}''' \text{PP}'\text{P}''\text{P}''' \text{XX}'$ spin system and a full spectral analysis has not yet been attempted; however, the chemical shifts are large compared with the coupling constants and each group of peaks is

Azimuthal angle θ		$q(\text{F}_z)$	$q(\text{C}_z)$	$p(\text{C}_z\text{F}_z)$	$\delta_{\text{electronic}}$ (p.p.m.)
0°	ortho	1.91859	1.03389	0.27778	17.521
	para	1.92061	1.04464	0.27248	14.443
45°	ortho	1.91918	1.02708	0.27824	11.885
	para	1.92084	1.04118	0.27307	11.192
60°	ortho	1.91943	1.02342	0.27856	9.216
	para	1.92092	1.03934	0.27342	9.713
90°	ortho	1.91970	1.01920	0.27897	6.174
	para	1.92093	1.03724	0.27379	8.780
C_6F_6		1.92640	1.07352	0.25942	

Table 1. π -electron charge densities and bond orders in perfluorobiphenyl.

symmetrical about the mid-point, hence the chemical shifts can be measured from the geometric centres of the three multiplets. The spectrum was recorded at 56.4 Mc/s using a 5 mole per cent solution in CCl_4 containing 5 mole per cent CFCl_3 as internal reference. The results are:

	Observed shift from CFCl_3 (c/s)	Calculated shift from C_6F_6 (p.p.m.)
Ortho	7797.4	24.03
Meta	9067.0	1.52
Para	8475.3	12.01

The π -electron densities and bond orders were calculated by the Hückel molecular-orbital method. Decafluorobiphenyl was treated as a twenty-two orbital, 32 electron problem and the secular determinant was constructed using the Coulomb and exchange integrals:

$$\begin{aligned}\alpha_F &= 2\beta, \\ \beta_F^* &= \beta, \\ \beta_{11} &= \beta \cos \theta, \\ \alpha_C &= 0,\end{aligned}$$

where β is the exchange integral for normal C-C aromatic bonds. The exchange integral β_{11} , was chosen to have the form $\beta \cos \theta$, which means that it is zero when the two benzene rings are perpendicular to each other. For the latter configuration the situation is identical with that of pentafluorobenzene. The π -electron charge densities and bond orders for several selected values of θ are shown in table 1. In order to calculate a value of $\delta_{\text{electronic}}$ for perfluorobiphenyl from equation (2) a value for ΔE is required, and this has been obtained by using the shift of the fluorine para to hydrogen in pentafluorobenzene (see reference [1]). The shift was assumed to arise entirely from electronic effects, giving a value for ΔE of 0.70 e.v. Substitution of this value into equation (2) provides the values of $\delta_{\text{electronic}}$ for the ortho and para fluorines nuclei shown in table 1. The observed shift of the para fluorine is 12.01 p.p.m. and indicates that the two rings are at 45° to each other.

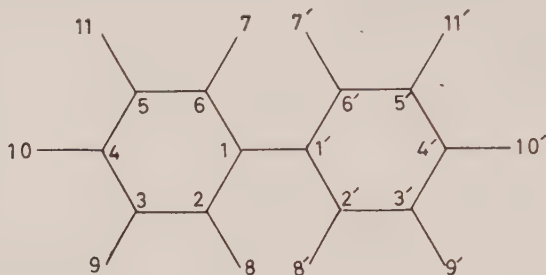
The shift of the ortho fluorines will be strongly influenced by the electric field effects, and it is this contribution to δ which is so sensitive to the value of θ . The values of E^2 , $\langle E^2 \rangle$ and E_z , the field component along the CF bond in the direction of the fluorine atom, were calculated using the molecular parameters:

$$\begin{aligned}r_{\text{C-F}} &= 1.30 \text{ \AA}, \\ r_{\text{C-C}}(\text{aromatic}) &= 1.39 \text{ \AA}, \\ r_{\text{C-C}} &= 1.52 \text{ \AA}, \\ \mu_{\text{C-F}} &= 1.6\text{D}, \\ P_{\text{C-F}} &= 0.633 \times 10^{-24} \text{ cm}^3, \\ I_F &= 28.5 \times 10^{12} \text{ ergs}, \\ P_{\text{C-C}} &= 1.013 \times 10^{-24} \text{ cm}^3, \\ I_C &= 18.03 \times 10^{-12} \text{ ergs}.\end{aligned}$$

All the bond angles were taken to be 120° .

E_z and E^2 arise from the static dipolar fields and values for these were calculated by placing point dipoles at the mid-point of the C-F bonds and finding the vector sum of the fields at the ortho fluorine nuclei. All the C-C bonds were assumed to be non-polar. $\langle E^2 \rangle$ was calculated by taking into account all the bonds in the same benzene ring (excluding the C-C bonds since these also appear in

the C_6F_6 molecule) and seven bonds in the other ring, C_2-C_1 , C_1-C_1' , C_1-C_6 , C_2-C_3 , C_6-C_5 , $C_2-F_{8'}$, $C_6-F_{7'}$.



The values of the seven bond-distances were calculated and used in equation (4) to calculate $\langle E^2 \rangle$. The values of E_z , E^2 and $\langle E^2 \rangle$ obtained for each value of θ are shown in table 2. In reference [1] it was shown that a value of B in equation (3) of between $(42 \text{ and } 49) \times 10^{-18}$ e.s.u. gives values of δ in agreement with experiment. The smallest value was 42.26×10^{-18} e.s.u. found from the shifts of the ortho and para ^{19}F nuclei in $C_6F_5\text{Cl}$ and it was decided to use this value in the present calculation since chlorine is nearly like fluorine. The values of δ_{electric} were then calculated from equation (3). The results of the above calculations are given in table 3, and the angular variations of δ , δ_{electric} and $\delta_{\text{electronic}}$ are shown in the figure.

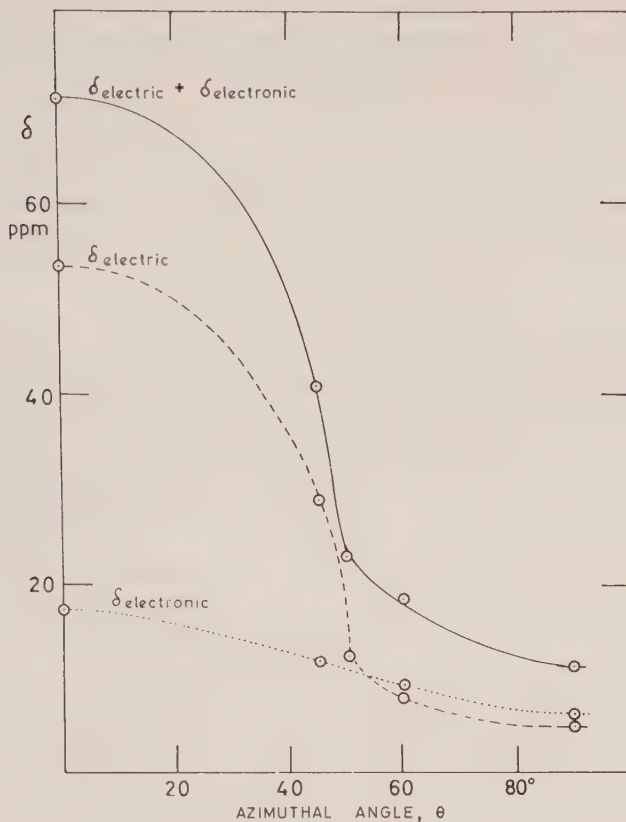
Because the changes in E_z are very small, the AE_z contribution [1] to the electric field effect can be safely ignored.

Azimuthal angle θ	$E_z \times 10^{-6}$ e.s.u.	$E^2 \times 10^{-12}$ e.s.u.	$\langle E^2 \rangle + 10^{-21}$ e.s.u.
0°	0.4336	0.2509	1.6940
45°	0.3204	0.1064	1.2609
50°	0.2735	0.0748	0.8989
60°	0.2615	0.0686	0.8253
90°	0.2191	0.0480	0.7485
C_6F_6	0.3642	0.1327	0.5474

Table 2. Values of the electric fields at the ortho fluorine nuclei in perfluorobiphenyl.

Azimuthal angle θ	δ_{electric} (p.p.m.)	δ (p.p.m.)
0°	53.447	70.968
45°	29.043	40.928
50°	12.408	22.9
60°	9.036	18.252
90°	4.922	11.096

Table 3. Values of δ_{electric} and total calculated δ (p.p.m.) for the ortho fluorine nucleus in perfluorobiphenyl.



The calculated variation of δ_{electric} , $\delta_{\text{electronic}}$ and δ ($=\delta_{\text{electronic}}+\delta_{\text{electric}}$) with θ , the azimuthal angle between the planes of the two benzene rings in perfluorobiphenyl.

3. CONCLUSIONS

The figure illustrates the very large changes in the value of δ for the ortho fluorine nuclei when the azimuthal angle θ is varied. For the values chosen for B and ΔE it is seen that almost exact agreement between observed and calculated values of δ is obtained when $\theta = 50^\circ$. This value of θ is in good agreement with the values found for 2,2', 2,2', 6,6'-fluorobiphenyls by other methods [3, 4, 6] and indicates that the values of B and ΔE are substantially correct. Because of the very large change in the calculated value of δ_{electric} between 40° and 50° , the value of θ obtained from this method is insensitive to changes in ΔE ; however, the good agreement between the observed shift of the para fluorine nucleus, 12.01 p.p.m., and the estimated value from table 1 for 50° , 10.5 p.p.m., shows that the value of ΔE used and the method of calculation are quite good approximations.

REFERENCES

- [1] BODEN, N., EMSLEY, J. W., FEENEY, J., and SUTCLIFFE, L. H., 1964, *Mol. Phys.*, **8**, 133.
- [2] TROTTER, J., 1961, *Acta Cryst.*, **14**, 1135.
- [3] BASTIANSEN, O., and SMEDVIK, L., 1954, *Acta chem. scand.*, **8**, 1593.
- [4] SUZUKI, H., 1959, *Bull. chem. Soc., Japan*, **32**, 1340.
- [5] HOFFMAN, R. A., KIKELL, P. O., and BERGSTRÖM, G., 1960, *Arkiv. Kemi*, **15**, 534.
- [6] LITTLEJOHN, A. C., and SMITH, J. W., 1953, *J. chem. Soc.*, p. 2456; 1954, *Ibid.*, p. 2552.

The compound-molecule model in the theory of chemical reactions

by E. E. NIKITIN

Institute of Chemical Physics, Academy of Sciences, Moscow, USSR

(Received 11 December 1963)

The model of a compound molecule is considered in connection with oscillator models of chemical reactions. It is shown that for non-adiabatic reactions the isolated level approximation is a reasonable one and that the transition-state theory may be used for calculating the rate constant for thermal reactions proceeding via the compound molecule. The intra-molecular energy exchange is discussed for Slater's and Kassel's models of activated molecules.

1. COMPOUND MOLECULE AND ACTIVATED COMPLEX

It is often suggested in calculations of the rate constants of chemical reactions that a reaction proceeds via an intermediate complex, the lifetime of which is essentially longer than the characteristic time of intramolecular motions.

In many cases there is no definite evidence yet for the existence of the complex. However, recent experimental data on reactions in molecular beams [1, 2] and on those involving a strongly non-equilibrium initial distribution [3, 4] seem to give some information about the possibility and conditions of intermediate complex formation. A reaction of this type would be described by the scheme:



where products A' and B' , for instance, may be identical to reactants A and B . In this case (1) and (2) will essentially describe a non-elastic scattering of A and B proceeding via a compound molecule AB^* . These processes seem to be important for vibrational relaxation in a mixture of gases reacting at high temperatures [5].

A compound molecule is very different from the transition complex of the Eyring theory [6]. The lifetime of the transition complex may be defined in various ways and it seems to have no well-established physical meaning [7]. But whatever the definition, it is important that the lifetime of the transition (or activated) complex does not exceed the time of transition through a region of configuration space that separates regions of relatively stable molecules, i.e. the time of the order of the vibrational period. The transition complex AB^\ddagger for reaction (1) may be defined as a state of a combined $A + B$ system that comes between A and B molecules on the one hand and the compound AB^* molecule on the other, on the potential-energy surface. For this definition to have a physical sense the configuration space volume corresponding to AB^\ddagger should be less than that of AB^* . This condition holds, e.g. for non-adiabatic, reactions proceeding with a change of the electronic state close to the point of quasi-crossing of terms. For

a one-dimensional case, the range Δq of the reaction coordinate q essential for non-adiabatic transition is approximately [8]:

$$\Delta q \sim (\hbar v / \Delta F)^{1/2}, \quad (3)$$

where v is a velocity close to the crossing point q^0 , $\Delta F = |\partial/\partial q [u_1(q) - u_2(q)]|_{q=q^0}$. For short-range forces of a characteristic length $1/\alpha$ one may put $F \sim \alpha D$, where D is the energy of molecular electronic excitation. On the other hand, a part of configurational space AB^* , corresponding to, e.g. a dissociation along the coordinate q , is $1/\alpha$. The product

$$\Delta q \alpha \sim (\hbar v \alpha / D)^{1/2} \quad (4)$$

is small for velocities, allowing adiabatic separation in most of the configuration space region. In what follows we shall consider only non-adiabatic reactions with a small $\hbar v \alpha / D$ parameter. The condition of a long lifetime for AB^* will then automatically be fulfilled because of the small probability of non-adiabatic transition.

The expansion of the cross section $\sigma(E)$ of reactions (1) and (2) in terms of partial cross sections $\sigma(E, l)$ would be of little use for calculating the rate constant k , since even at relatively low energies E of relative motion of A and B it would be necessary to include a great number of momenta l . Of course $\sigma(E, l)$ involves, besides E and l , other parameters describing the individual rotations of A and B and their internal state; these are left aside here only for the sake of simplicity. It would be more convenient to expand $\sigma(E)$ (or the rate constant $k(E) = \sigma(E)(2E/M_{AB})^{1/2}$) in terms of $\sigma(E, \epsilon)$ (or $k(E, \epsilon)$), each $\sigma(E, \epsilon)$ referring to a partial 'cross section' of a definite kinetic energy ϵ along the q -coordinate close to the q^0 point. Then

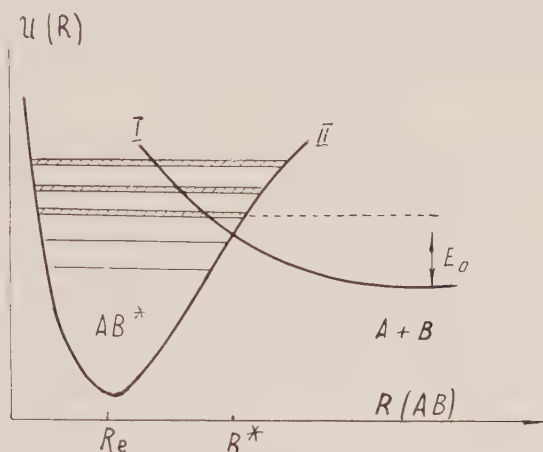
$$k(E) = \int \sigma(E, \epsilon) v f(E, \epsilon) d\epsilon, \quad (5)$$

where $f(E, \epsilon)$ is a normalized distribution function over the energy ϵ provided the kinetic energy of A and B at infinity has the prescribed E value. The form (5) is convenient when an average is taken over E : the distribution function then may be factorized into several terms, one of these being the Boltzmann factor $\exp(-\beta\epsilon)\epsilon^{-1/2}$, ($\beta = 1/kT$).

The three-dimensional problem of scattering may sometimes be reduced by such a factorization to a one-dimensional problem. This reduction may be made for adiabatic and non-adiabatic potential non-elastic scattering of atoms and diatomic molecules [9].

Following the general method of considering compound systems [10] let us introduce now the internal and external regions of the configuration space of AB , the former corresponding to all atoms being close together in a volume of molecular dimensions. These regions are separated by the hypersurface S , the various parts S_c of which correspond to possible A^* and B^* pairs (c denotes these pairs, i.e. the so-called reaction channels). The surface S_c refers to distances R_{AB} beyond which the polarization interaction vanishes (i.e. the interaction described by the virtual excitation of the internal states of A and B). A choice of such a definite surface must be made for model calculation of reaction rates, although this choice will not be unambiguous [11]. For non-adiabatic decomposition of AB^* in channel c with breaking of the q_c bond, the S_c surface may be defined by equation $q_c = q_c^0$, where q_c^0 is a coordinate of term crossing. Besides, it is necessary

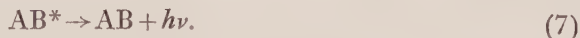
that the following condition be fulfilled: in the final electronic state of $A+B$ (term I, figure) the interaction of partners should be much weaker than in the initial state (term II) corresponding to the bound complex AB^* . Let us assume now that the levels of quasi-stationary states of AB^* overlap only slightly (the so-called 'isolated-level approximation' [10] discussed in § 3). This means, in particular, that all levels of AB^* are non-degenerate. The physical reason for this condition is the same as in the classical theory of vibrations in the system of harmonic oscillators, where degeneracy (i.e. equal frequencies) requires special consideration [12].



Under these conditions the amplitude $A_{c'}$ of the reaction in channel c' for the compound molecule AB^* formed in channel c is [10]:

$$A_{c'} = \sum_{\lambda} \frac{\Gamma_{c\lambda}^{1/2} \Gamma_{c'\lambda}^{1/2}}{E_{\lambda} - \epsilon - i\Gamma_{\lambda}}, \quad (6)$$

where E_{λ} is an energy level of AB^* , $\Gamma_{c\lambda}$ is its partial width corresponding to the decomposition in some channel c and $\Gamma_{\lambda} = \sum \Gamma_{c\lambda}$. Here Γ_{λ} may involve also the partial width $\Gamma_{\lambda}^{(d)}$ caused by deactivation (say by emission of light), and $\Gamma_{\lambda}^{(d)} = \frac{1}{2} \hbar k^{(d)}$, $k^{(d)}$ being the deactivation rate constant. This might be a process such as



2. REACTIONS OF POLYATOMIC MOLECULES

Rate constants for reactions of polyatomic molecules may be calculated from the basic formula of the transition-state theory [6], when averaging over the energy of a reaction coordinate involves the extra probability factor $|A_{c'}|^2$:

$$k(c, c') = \frac{Z^{\neq}}{Z(A)Z(B)} \int_0^{\infty} |A_{c'}|^2 v \exp(-\beta\epsilon) \frac{dp}{2\pi\hbar}, \quad (8)$$

where v and p are the velocity and momentum conjugate with the 'reaction'

coordinate, $Z(A)$ and $Z(B)$ are partition functions for A and B, and Z^\ddagger is the partition function for the transition complex AB^\ddagger .

The reaction model is supposed to be a molecule AB^* capable of predissociation along some bonds q_c . We consider the binding between A–B or A'–B' to be strong enough even without interaction between the bond in question and other bonds. This permits expressing the wave function of the c channel in the electronic state II (see figure) as a product $\psi_c = \psi_c'(q_c)\bar{\psi}_c(q_i)$, where $\psi_c'(q_c)$ is a vibrational function in the potential well of the type given in the figure, and $\bar{\psi}_c(q_i)$ the function of all other coordinates q_i . The dynamical interaction between q_c and q_i should be included, however, when calculating the wave functions $\varphi_\lambda(q_i \dots q_s)$ of the compound system AB^* . The level widths $\Gamma_{e\lambda}$ of AB^* are connected with the probability of predissociation, being proportional to the square of overlap integral for φ_λ and the function ϕ_c describing the system A + B in the electronic state I:

$$\Gamma_{e\lambda}^{1/2} \sim \langle \varphi_\lambda \phi_c \rangle. \quad (9)$$

The dependence of ϕ_c on q_i is identical to that for ψ_c . Then

$$\Gamma_{e\lambda}^{1/2} \sim \sum_c \langle \varphi_\lambda \psi_c' \rangle \langle \psi_c \phi_c \rangle = \sum_c \langle \varphi_\lambda \psi_c' \rangle \langle \psi_c' \phi_c' \rangle, \quad (10)$$

where ϕ_c' is a properly normalized function for one-dimensional motion along the reaction coordinate q_c in the electronic state I. Thus (6) and (8) make it possible to calculate the rate constant of a reaction proceeding via the compound molecule, under certain assumptions concerning the molecular vibrational function. Let us now consider the rate constant taking harmonic oscillator systems as models for molecules A, B and AB^* . This is an approximation widely used in chemical kinetics [13] in two forms—as a strictly harmonic system (the Slater model) and as a system with weak anharmonicity (the Kassel model).

2.1. The Slater model

For the sake of simplicity let us suppose that all vibrational levels of such a system are grouped within narrow energy intervals δE which are small compared to the mean vibrational quantum $\hbar\omega$ (a system of *almost* degenerate oscillators). This will mean that the φ_λ are connected with the ψ_c *almost* in the same way as for the system of degenerate oscillators. When the A–B bond in the compound molecule does not cause displacement of the equilibrium positions of nuclei, the infinite matrix $C_{\lambda c}$ connecting φ_λ and ψ_c can be factorized to blocks of dimensions

$$g_n = \frac{(n+s-1)!}{n!(s-1)!},$$

where n is the total number of vibrational quanta of AB^* and s is the number of oscillators. The matrix elements $C_{\lambda c}$ are completely defined by another matrix b_{ik} connecting the normal coordinate q_i in A and B with normal coordinates q_k^* in AB^* (evidently q_c is such a coordinate):

$$q_i = \sum_k b_{ik} q_k^*. \quad (11)$$

This assumption makes the problem less complex but still allows for energy exchange in AB^* due to change of the normal modes when passing from A + B to AB^* .

Let us consider now a channel c that refers to vibrationally unexcited fragments A and B trapped on the lowest predissociation level $n=n_0$ of the q_c oscillator. If channel c' refers to predissociation from a quasi-stationary state of AB^* corresponding to a multiplet of energy $E \sim \hbar\omega n_0$ and effective width δE , there will be only one term in (8), namely

$$\Gamma_{c\lambda} = \gamma_c \langle \varphi_\lambda \psi_c \rangle^2, \quad (12)$$

where γ_c is the level width of an *isolated* q_c oscillator and is connected with the probability of non-adiabatic transitions χ_c by equation $\gamma_c = \frac{1}{2}\hbar\nu\chi_c$. Here function φ_λ belongs to the same block as ψ_c , and the distribution of vibrational quantum numbers $n(j)$ in channel c (the A+B system) is $[0(1), 0(2) \dots n_0(c) \dots 0(s)]$; n_0 being the number of quanta, j the number of an oscillator. The distribution in channel c' is $[0(1), 0(2) \dots n_0(C') \dots 0(s)]$ (the A'+B' system), and that in the compound molecule is $[m_1(1), m_2(2) \dots m_c(c) \dots m_s(s)]$; the numbers m_k fulfil the condition $\sum m_k = n_0$.

In the approximation of a weak overlap of resonances the interfering terms in $|A_{c'}|$ should be neglected, so that

$$\sum_\lambda \frac{\Gamma_{c\lambda} \Gamma_{c'\lambda}}{(\epsilon - E_\lambda)^2 + \Gamma_\lambda^2} = \pi \sum_\lambda \frac{\Gamma_{c\lambda} \Gamma_{c'\lambda}}{\Gamma_\lambda} \delta(\epsilon - E_\lambda) \quad (13)$$

which may be considered as a good approximation for the condition $\Gamma_\lambda \ll kT$.

For calculation of the capture cross section $\Gamma_{c'\lambda}$ should be put as $\Gamma_\lambda^{(d)} \gg \Gamma_{c\lambda}$. Omitting the rather simple calculation, we obtain for the rate constant of capture k_{capt} via the multiple level $E \sim \hbar\omega n_0$.

$$k_{\text{capt}}(n_0) = \frac{kT}{2\pi\hbar} \cdot \frac{Z^\neq}{Z(A)Z(B)} \chi_c(n_0) \beta \hbar \omega \sum_\lambda \langle \varphi_\lambda \psi_c \rangle \exp(-\beta E_\lambda). \quad (14)$$

Taking [14]

$$\langle \varphi_\lambda \psi_c \rangle = \frac{b_{c1}^{2m_1}}{m_1!} \cdot \frac{b_{c2}^{2m_2}}{m_2!} \dots \frac{b_{cs}^{2m_s}}{m_s!} \cdot n_0! \quad (15)$$

and recalling that

$$E_\lambda = E_0 + \sum \hbar \Delta \omega_k m_k, \quad (16)$$

we find

$$\begin{aligned} \sum \langle \varphi_\lambda \psi_c \rangle^2 \exp[-\beta E_\lambda] &= [\sum b_{ck}^2 \exp(-\beta \hbar \Delta \omega_k)]^{n_0} \exp(-\beta E_0) \\ &\equiv x^{n_0} \exp[-\beta \hbar \omega n_0]. \end{aligned} \quad (17)$$

Inserting (17) into (14) we obtain:

$$k_{\text{capt}}(n_0) = \frac{kT}{2\pi\hbar} \frac{Z^\neq}{Z(A)Z(B)} \chi_c(n_0) \beta \hbar \omega x^{n_0} \exp(-\beta \hbar \omega n_0). \quad (18)$$

The coarse temperature dependence of k is due to the coarse vibrational structure of AB^* ('bands' with intervals $\hbar\omega$). The fine temperature dependence is determined by the importance of multiplet components of 'bands'.

For the association of two atoms we have:

$$\frac{kT}{2\pi\hbar} \frac{Z^\neq}{Z(A)Z(B)} = \pi (R^*)^2 \bar{v} \quad \text{and} \quad x=1; \bar{v} = \left(\frac{8kT}{\pi M_{AB}} \right)^{1/2}. \quad (19)$$

Moreover, in this case (12) holds not only for the lowest level n_0 but also for all $n \geq n_0$.

Thus, (18) becomes:

$$k_{\text{capt}}(n) = \pi(R^*)^2 \bar{v} \chi(n) \beta \hbar \omega \exp(-\beta \hbar \omega n). \quad (20)$$

The overall capture rate constant k_{capt} may be obtained from (20) by summing over vibrational levels $n \geq n_0$, supposed to be equidistant (for simplicity $\chi_c(n)$ is taken as constant):

$$k_{\text{capt}} = \pi(R^*)^2 \bar{v} \chi_c \frac{\beta \hbar \omega}{1 - \exp(-\beta \hbar \omega)} \exp(-\beta E_0). \quad (21)$$

For high temperatures ($\hbar \omega \ll kT$), equation (21) exhibits a temperature dependence that would be expected from classical considerations. For low temperatures ($\hbar \omega \gg kT$), when capture occurs essentially via one vibrational level n_0 , the overall temperature dependence $k_{\text{capt}}(n_0)$ will be as $T^{-1/2} \exp(-\beta E_0)$. According to Goldanskii [15] only one Breit-Wigner resonance results in the temperature dependence as $T^{-3/2} \exp(-\beta E_0)$ (valid, evidently, for s -capture). These two functions bracket the temperature dependence of the capture rate for any ratio of the gas kinetic radius R_0 to the Broglie wavelength of colliding molecules.

Turning now to the decomposition rate for channel c' , we put $\Gamma_{c\lambda}, \Gamma_{c'\lambda} \ll \Gamma_\lambda^{(d)}$, so that the general expression (6) will take the form:

$$k_{\text{dec}}^{cc'}(n_0) = \frac{kT}{2\pi\hbar} \frac{Z^\#}{Z(A)Z(B)} \chi_c \beta \hbar \omega \frac{\nu \chi_c}{k_{\text{deact}}} \sum_\lambda \langle \varphi_\lambda \psi_c \rangle^2 \langle \varphi_\lambda \psi_{c'} \rangle^2 \exp(-\beta E_\lambda). \quad (22)$$

It was not possible to calculate this sum over λ in a closed form. For $n \gg s$ an approximate evaluation may be carried out by the method of steepest descent, replacing the summation in (22) by integration. The main contribution is from terms corresponding to vibrational quantum number distribution such that

$$m_k^* = n |b_{ck} b_{c'k}| \exp(-\beta \hbar \Delta \omega_k). \quad (23)$$

Integration close to these maxima under the condition $\sum m_k = n_0$ results in

$$\begin{aligned} \sum_\lambda \langle \varphi_\lambda \psi_c \rangle^2 \langle \varphi_\lambda \psi_{c'} \rangle^2 \exp(-\beta E_\lambda) &= \exp(-\beta \hbar \omega n_0) \\ &\times \left[\sum_k b_{ck} b_{c'k} \exp(-\beta \hbar \Delta \omega_k) \right]^{n_0} \left[\prod_k |b_{ck} b_{c'k}| \exp(-\beta \hbar \Delta \omega_k) \right]^{-1/2} (4\pi n_0)^{-(s-1)/2}. \end{aligned} \quad (24)$$

This approximation is valid when $m_k^* \gg 1$. When some of the m_k^* are of the order of or lower than unity, the corresponding b_{ck} should be omitted and the number s should be decreased correspondingly. It follows that the lower the temperature the less the contribution of the 'upper' normal modes to the reaction rate.

Let us consider now the case $\beta \hbar \Delta \omega_k \ll 1$ and $c = c'$, which means reverse decomposition of AB^* :

$$\begin{aligned} k_{\text{dec}}^{cc}(n_0) &= \left[\frac{kT}{2\pi\hbar} \frac{Z^\#}{Z(A)Z(B)} \chi_c \beta \hbar \omega \exp(-\beta E_0) \right] \\ &\frac{\chi_c \nu \left[\prod_k b_{ck} \right]^{-1} (4\pi n_0)^{-(s-1)/2}}{k_{\text{deact}}}. \end{aligned} \quad (25)$$

The first factor here is the capture rate. Thus the numerator of the second factor should be identified with the reciprocal lifetime of AB^* relative to decomposition to $A + B$:

$$\tau = (\chi_c \nu)^{-1} \left(\prod_k b_{ck} \right) \left(4\pi \frac{E_0}{\hbar \omega} \right)^{\frac{1}{2}(s-1)}. \quad (26)$$

This is similar to the mean lifetime of the system of classical oscillators [12] τ_{cl} , which may be obtained from (26) replacing $\hbar\omega$ by kT . It is difficult to examine this transition more closely for (25) as the summation should be carried out over a great number of channels. Among these will be also the channel of inelastic scattering of $A+B$, when, e.g., an A atom is captured on the multiplet level $E \sim \hbar\omega(n+1)$ of a compound molecule AB^* and then redissociates leaving a quantum $\hbar\omega$ in the B molecule. However, it may be anticipated that the classical limit of (25) could be obtained if the factor $\beta\hbar\omega$ were omitted and τ were replaced by τ_{cl} . It must be mentioned that the mean lifetime (26) governs the rate of thermal decomposition of polyatomic molecules at low temperatures ($\hbar\omega \gg kT$) when tunnelling is not essential [16].

2.2. The Kassel model

The Kassel model assumes that the anharmonicity contribution to the nuclear potential is rather small, so that the coarse structure of the vibration spectrum is similar to that of a harmonic potential. However, anharmonicity is considered to be the cause of energy exchange between normal modes. Taking this into account, we suppose that the matrix elements of the anharmonic potential V_{anh} between the harmonic wave functions are larger than the splitting $\Delta\omega_k$ and that their variations in passing from $A+B$ to AB^* are also relatively great. It would be anticipated in this case that in the expansion of φ_λ all ψ_c of the same block should be present in approximately equal weights, so that $\langle \varphi_\lambda | \psi_c \rangle \sim (g_{nl})^{-1/2}$, where g_{nl} is the block dimensionality. Under the condition $\langle \varphi_\lambda^{harm} | V_{anh} | \varphi_\lambda^{harm} \rangle \ll \hbar\omega$ the maximum dimensionality of a block for n -quantum excitation is

$$G_n = (n+s-1)!/n!(s-1)!.$$

But because of the symmetry of a molecule such a block may happen to reduce to sub-blocks of a smaller dimensionality g_{nlb} and $\sum_e g_{nl} = g_n$. A similar reduction could take place for the harmonic model also. For the latter case the matrix $C_{\lambda c}$ is completely defined by the matrix c_{ci} the dimensionality of which is, in general, less than that of $C_{\lambda c}$. Thus, the number of sub-blocks for the harmonic model might be greater than for the anharmonic one. Let us take a three-atomic molecule. If the rotation-vibration interaction is neglected (the usual approximation of the transition state theory), its vibrational states may be classified according to the values of the vibrational angular momentum l (if $l \neq 0$), or to symmetry with respect to the plane containing the nuclei (Σ^+ and Σ^- terms). The dimensionality of a block g_{nl} is equal to the number of configurations $(\sigma_1^{n_1} \sigma_2^{n_2} \pi^{n_3})$ that lead to the term with a fixed total momentum l (σ_1 , σ_2 and π are functions of the stretching and bending modes, n_i are the corresponding phonon populations) under the condition $n_1 + n_2 + n_3 = n$. For the harmonic (Slater) model all configurations of different n_3 are independent. Thus it would be possible to classify vibrations as active or inactive with respect to their contribution to the rate of decomposition of AB^* . For the Kassel model this classification should be made on the basis of symmetry of the total vibrational function (terms), and not according to types of vibrations. Similar considerations for classical models have been treated in papers [17, 18].

As φ_λ functions always form a complete set the capture rate constant k_{capt} will be the same for both models (Slater's and Kassel's):

$$k_{\text{capt}}^c(n_0) = \frac{kT}{2\pi\hbar} \frac{Z^\neq}{Z(A)Z(B)} \chi_c(n_0) \beta \hbar \omega \exp(-\beta E_0). \quad (27)$$

When the symmetry of an initial channel c corresponds to a block g_{nl} of the compound molecule AB^* , we obtain for decomposition in channel c' (if $\Gamma_\lambda^d \gg \Gamma_\lambda^{\text{prediss}}$)

$$k_{\text{dec}}^{cc'} = k_{\text{capt}} \frac{\nu \chi_{c'}}{k_{\text{deact}}} \frac{B_c^{c'}}{g_{nl}}, \quad (28)$$

and $B_c^{c'}$ is either close to unity (if the symmetry of c and c' is the same) or zero (for different symmetry).

In the case of predissociation along one of the bonds of a linear three-atomic molecule, the coefficients b_{ck} corresponding to the bending modes will be zero. Then, according to (23), the total number of vibrational degrees of freedom $s = 4$ would be diminished to $s = 2$. The maximum value of τ is obtained with

$$b_{c1}^2 = b_{c2}^2 = \frac{1}{2}; \quad \tau_{\text{max}}^{\text{harm}} = (\chi\nu)^{-1} \sqrt{(\pi n_0)}. \quad (29)$$

This lifetime corresponds to decomposition of a compound molecule AB^* via the lowest energetically possible state of Σ^+ symmetry. To calculate τ for the Kassel model we note that $(n+s-1)/n!(s-1) \approx n^3/3$ levels are grouped into sets of $\sim \frac{1}{4}(n-l)^2$ levels differentiated by the value of the vibrational angular momentum l (with either sign). For the Σ^+ terms we have then:

$$\tau_{\text{max}}^{\text{anh}}(\Sigma^+) = (\chi\nu)^{-1} \frac{n_0^2}{4}. \quad (30)$$

When all states of energy $E_0 \sim n_0 \hbar \omega$ are mixed, τ will be:

$$\tau_{\text{max}}^{\text{anh}} = (\chi\nu)^{-1} \frac{n_0^3}{3!}. \quad (31)$$

The required intermixing of states with different l might be due to rotational-vibrational interaction only. Thus study of the lifetimes of simple molecules could give information on such interaction in highly vibrationally excited molecules.

3. VALIDITY OF THE COMPOUND MOLECULE MODEL

The expressions derived above are rather simple. This is due to the following assumptions.

1. A single incoming channel c (valid under the condition $\hbar\omega \gg kT$) and a quite simple structure of the vibrational spectrum of AB^* (the multiplet structure of bands spaced at intervals $\hbar\omega$). For the general case it would be necessary to average over all initial states.

2. Boltzmann distribution over states of external degrees of freedom. It gives the possibility of averaging motion over the reaction coordinate independently of other coordinates, and to avoid the lengthy procedure of calculating partial cross-sections. However, the activated-complex theory introduces an inevitable error in the rate constant, due to the impossibility of choosing *one* reaction coordinate and of exactly determining the activated complex configuration. This question is elaborated in detail for non-adiabatic scattering of two atoms (see Appendix).

3. Small overlapping of energy levels. The isolated-level approximation does not hold for adiabatic reactions. Rice [19] has shown that level width in an active molecule undergoing adiabatic decomposition is just that needed for smoothing peaked level distribution. For a non-adiabatic reaction this assumption is usually valid if the total level width $\Gamma = \sum_{\lambda} \Gamma_{\lambda}$ is small compared to $\hbar\omega$. Accidental or symmetry degeneracy in AB^* is an exception. The total predissociation width may be estimated according to the Landau-Zener formula [8]. The width would be maximum for levels above just the threshold. Using it as the upper boundary we should obtain:

$$\Gamma_{\text{prediss}} < \frac{V^2}{\hbar\omega N^{2/3}}, \quad (32)$$

where V is an electronic matrix element between states I and II and N is the number of vibrational quanta in the potential well of A-B. Taking $\omega \sim 1000-1500 \text{ cm}^{-1}$, $N \sim 30-100$ as characteristic values, and $V \sim 100-200 \text{ cm}^{-1}$ we find that the ratio $\Gamma/\hbar\omega$ will be between 10^{-2} and 10^{-4} . Thus the isolated-level approximation may be even valid for a certain number of such predissociation channels. Besides, it may happen that the total width Γ will be greater than kT , so that the resonance peak structure should be taken into account when averaging over ϵ .

It is worth while to mention that the capture and decomposition rates could be calculated by making use of the theory of non-stationary perturbation [20], but this method can only give quantities averaged over an energy interval δE which is large enough to construct a wave packet representing the localization of excitation in one of the molecular bonds. However, this method is valid for overlapping levels, when the lifetime of the compound molecule is comparable to the characteristic time $\hbar/(E_{\lambda} - E_{\lambda'})$, but, of course, is still much larger than $1/\omega$. For another extreme case, $\Gamma/\hbar\omega \gg 1$, one should use impact approximation [21]. This treatment of compound molecules is very similar to calculation of electron scattering via a virtually negative molecular ion [22]. In the latter case the total width Γ is that of the electronic term with respect to preionization, and the level spacing $E_{\lambda} - E_{\lambda'}$ is determined by the vibrational quantum $\hbar\omega$.

For non-adiabatic reactions which are of importance at low temperatures [12], the vibrational excitation of AB^* might not be very high. It means that both models—Slater's and Kassel's—could be useful in an interpretation of molecular decomposition. For adiabatic reactions the energy of vibrational excitation near the threshold is usually so high that neglect of energy transfer between normal modes would not be a reasonable approximation.

The author is greatly indebted to Professor N. D. Sokolov for helpful discussions.

APPENDIX

It would be instructive to verify the transition-state theory for a simple case of scattering of two atoms proceeding via an intermediate state of the compound molecule. The atoms move initially in the potential field I and then are held up in the potential well corresponding to II (figure). The level width of the vibrational state n of AB^* is [7]:

$$\Gamma_n = \frac{2}{\hbar} \nu_n \chi_n, \quad (A1)$$

where ν_n is the vibrational frequency, and χ_ν the non-adiabatic transition probability as given by the Landau-Zener formula (the threshold region may also be taken into account when necessary, but we shall not consider this question here). It will be noted that χ_n includes two 'pathways': $I(R > R^*) \rightarrow II(R < R^*)$ and $I(R > R^*) \rightarrow I(R < R^*) \rightarrow II(R > R^*) \rightarrow II(R < R^*)$. The partial resonance cross-section is [8]:

$$d\sigma_l = 4\pi \frac{2l+1}{k^2} \frac{\Gamma_n^2}{[E - E_n(l)]^2 + \Gamma^2}, \quad (\text{A } 2)$$

where Γ is the total width including, e.g., the radiative width.

To calculate $\sigma = \sum d\sigma_l$ we approximate AB^* by the oscillator-rigid rotator model, for which we have:

$$E_n(l) = E_n + \frac{\hbar^2 l(l+1)}{2M\tilde{R}^2}, \quad (\text{A } 3)$$

where the value of \tilde{R} lies somewhere between Re and R^* . Besides, we substitute integration for summation:

$$\frac{\pi}{k^2} \sum (2l+1) \rightarrow 2\pi \int \rho d\rho, \quad l = \frac{Mv\rho}{\hbar} \quad (\text{A } 4)$$

and approximate the last factor in (A 2) by $\pi(\Gamma_n^2/\Gamma)\delta[E - E_n(l)]$. Integration may then be performed easily and after averaging over E we obtain an expression for the mean scattering rate constant:

$$k_n = \langle \sigma v \rangle = \int \sum_l d\sigma_l f(E) dE = \pi \tilde{R}^2 \bar{v} \chi_n \frac{\nu_n \chi_n}{\nu_n \chi_n + k_{\text{rad}}} \hbar \beta \omega \exp(-\beta E_n). \quad (\text{A } 5)$$

This coincides with (20) except for the first factor. The difference (\tilde{R} in (A 5) and R^* in (20)) is due to the inherent approximation adopted by the transition-state theory: assumption of the existence of a separable reaction coordinate in the well-defined transition complex (which is essentially incorporated in the oscillator-rigid rotator approximation (A 3)). The physical parameter assumed to be small in this approximation is the ratio of the characteristic length of action of exchange forces to the gas-kinetic radius of a colliding pair. It is the same parameter that makes it possible to calculate the non-elastic molecular cross section in the so-called 'modified-wave-number' approximation [23].

REFERENCES

- [1] HERSCHBACH, D. R., 1962, *Trans. Faraday Soc.*, **33**, 149.
- [2] BECK, D. GREENE, E. F., and ROSS, J., 1962, *J. chem. Phys.*, **37**, 2895.
- [3] RABINOVITCH, B. S., KUBIN, R. F., and HARRINGTON, R. E., 1963, *J. chem. Phys.*, **38**, 405.
- [4] CURRENT, J. H., and RABINOVITCH, B. S., 1963, *J. chem. Phys.*, **38**, 783.
- [5] BAUER, S. H., and TSANG, S. C., 1963, *Phys. Fluids*, **6**, 183.
- [6] GLASSTONE, S., LAIDLER, K. J., and EYRING, H., 1941, *The Theory of Rate Processes* (London and New York).
- [7] TEMKIN, M. I., 1958, *In Certain Problems of Chemical Kinetics and Reactivity* by N. N. Semenov (Academy of Sciences, USSR), English translation (Pergamon Press, 1959), Appendix 1.
- [8] LANDAU, L. D., and LIFSHITZ, E. M., 1963, *Quantum Mechanics* Fizmatgiz (Russian).
- [9] NIKITIN, E. E., 1964, *Mol. Phys.*, **7**, 389.
- [10] LANE, A., and THOMAS, R., 1958, *Revs. mod. Phys.*, **30**, 257.

- [11] THIELE, E., 1963, *J. chem. Phys.*, **38**, 1959.
- [12] SLATER, N. B., 1959, *Theory of Unimolecular Reactions* (Cornell University Press).
- [13] KONDRATIEV, V. N., 1958, *Kinetics of Chemical Gas Reactions* (Academy of Sciences, USSR) (Russian).
- [14] ERDELYI, A., 1953, *Higher Transcendental Functions*, Vol. 2 (McGraw-Hill).
- [15] GOLDANSKII, V. I., 1959, *C.R. Acad. Sci., U.R.S.S.*, **127**, 1242.
- [16] NIKITIN, E. E., 1964, *Mol. Phys.* (in the press).
- [17] SLATER, N. B., 1962, *The Transition State* (Chemical Society Special Publication No. 16).
- [18] LAIDLER, K. J., and WOJCIECHOVSKI, B. W., cited in [17].
- [19] RICE, O. K., 1961, *J. phys. Chem.*, **65**, 1588.
- [20] NIKITIN, E. E., 1963, *C.R. Acad. Sci., U.R.S.S.*, **152**, 1395.
- [21] MATTHIZ, Z., and NEUDACHIN, V. G., 1963, *J. exp. theor. phys.*, **45**, 131.
- [22] HERZENBERG, A., and MANDL, F., 1962, *Proc. roy. Soc. A*, **270**, 48.
- [23] TAKAYANAGI, K., 1963, *Prog. theory. Phys.*, Suppl., **25**, 1.

The orbital penetration term in aromatic substituent effects

by D. P. CRAIG and G. DOGGETT†

William Ramsay and Ralph Forster Laboratories, University College London

(Received 6 April 1964)

The interaction of a substituent with a benzene ring is analysed as that of two weakly interacting independent systems. The analysis confirms that three distinct effects of substituents should be recognized, and that in addition to inductive and mesomeric effects the influence of interpenetration of π -electrons on the substituent and the aromatic system should be separately included. The effect of orbital penetration on the aromatic π -system is represented by a repulsive potential, and calculations made of the spectral intensity of the 2600 Å transition of substituted benzenes with one and two substituents. For F, Cl and CH₃ the experimental values are fairly well reproduced, one empirical parameter being needed to describe each substituent. The method of calculation is the same as that earlier used for the anilinium ion, avoiding the use of explicit forms of molecular wave functions.

1. INTRODUCTION

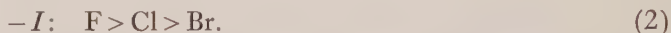
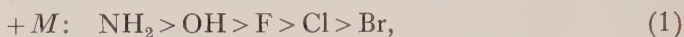
In the qualitative theory a substituent in an aromatic molecule acts in two ways. It has a mesomeric effect M and an inductive effect I , both of which can have the direction of electron donation ($+M$ and $+I$) or of electron withdrawal ($-M$ and $-I$) [1]. The mesomeric effect depends upon participation by structures corresponding to charge transfer, such as $\text{H}_2\text{N}^+=\text{C}_6\text{H}_5^-$ or $\text{O}_2\text{N}^-=\text{C}_6\text{H}_5^+$; the inductive effect depends on charge displacements in the aromatic system caused by the electrostatic induction of the substituent, according to its electrical character. The archetype is $-\text{NH}_3^+$, with the character of a positive charge.

In semi-quantitative descriptions by molecular orbital methods the induction is treated by assigning changed electronegativity parameters to the carbon atoms near the substituent, the change being graded to represent a fall-off with distance. The mesomeric effect is treated by combining the orbitals of the aromatic system with those of the substituent in new molecular orbitals, and calculating the properties of the π -electrons in the enlarged basis. Electron drifts into or out of the substituent then take place in the framework of the extended delocalized system.

In this paper we continue the development of an alternative treatment of substituent influences, already used [2] for the ammonio group $-\text{NH}_3^+$, the basis of which is to represent the effect of a substituent by a potential perturbing the states of the unsubstituted aromatic molecule, in a manner not calling for explicit molecular wave functions. This procedure we believe has certain advantages, and it leads in a natural way to quantitative values that can be attached to particular substituents, to describe the strength of their influence on aromatic

† Now at Department of Chemistry, University of Glasgow.

systems. A number of problems have suggested this re-examination of the basis of the treatment of substituent effects. For example there is the fact that the ammonio group $-\text{NH}_3^+$ makes no change in the electronic spectra of alternant hydrocarbons, despite its large influence on ground-state properties and altered reactivity. And there is also the disagreement recently discussed by Clark *et al.* [3] between the sequence of relative strengths of mesomeric substituents as judged on the one hand from ground-state properties and reactivity and on the other from electronic spectra. Thus Ingold [1] deduced the sequences (1) and (2) for the relative strengths in several common substituents:



Studies of the changes in electronic spectra lead to a different ordering [3, 4]; for example, in the halogens:



Theoretical studies have not been much concerned with these problems, though a number of molecular-orbital studies of both ground state properties and spectra have been published [5–10]. The recent work of Petruska [8] is of special interest.

2. GENERAL CONSIDERATION OF SUBSTITUENT EFFECTS

The common feature of most theoretical work is the treatment of substituted molecules in terms of properties of the aromatic residue and of the substituent separately. This approach is most suitable when the net drift of electrons between the substituent and aromatic residue is small. This basis being accepted, we expect to be able to analyse the interaction energy by treating the π -electrons of substituent and aromatic residue as weakly interacting independent systems, along conventional lines. We may then see whether this leads to a scheme that fits the qualitative categories of mesomeric and inductive effects in a convenient way.

In aniline, for example, the interacting systems of electrons are the lone pair electrons of nitrogen and the π -electrons of the benzene ring, the latter being in their ground state, in which they make up a closed shell, or in a spectroscopic excited state. In toluene the substituent electrons are the pseudo- π -electrons of the methyl group C-H bonds, and in $-\text{NO}_2$ they are the delocalized π -electrons including those of the N-O π -bond and an oxygen lone pair. In the ground state of aniline or nitrobenzene the situation may be compared with that of the interaction of two atoms with closed shells. In the excited state the analogy is with two dissimilar atoms, one in its lowest excited state: if the excitation energies are sufficiently different, the transfer of excitation between substituent and aromatic system is unimportant, and the interaction may be dealt with as in the ground state.

We now use the well-known result that, in a basis of orbitals localized on the interacting systems, the interaction energy may be analysed in the following scheme, always pre-supposing it to be smaller than the binding energies of the electrons in the separated systems. It will become apparent that the three sets of terms ought to be related to *distinct* substituent effects in the qualitative theory.

- (i) Electrostatic and dispersion-force interaction between π -electrons of substituent and aromatic residue.
- (ii) Repulsive orbital penetration terms from electron exchange between overlapping π -orbitals.
- (iii) Terms from participation by charge-transfer states of the type $\text{NH}_2^+-\text{Ph}^-$.

These do not exhaust the interactions, because there is no allowance for σ -electrons, inner-shell electrons or net charge on the substituent as in $-\text{NH}_3^+$. These are conveniently grouped with the other electrostatic terms in category (i).

Terms of type (iii) are at once recognizable as mesomeric because they depend upon charge migration. Both (i) and (ii) are inductive in the sense of the qualitative theory, because no charge transfer occurs, but they are very different in character. Penetration effects are of extremely short range because they depend on the overlap of substituent and ring orbitals, and overlap falls off quickly with distance. Interaction of type (i) may be of long or short range, depending on the substituent. The ammonio group NH_3^+ has a long-range effect, because of its net electrical charge, the influence of which drops as $1/r$. On the other hand, a group without net charge may have only dispersion force interactions with the π -electrons, falling off very rapidly with distance. Moreover categories (i) and (ii) differ a great deal in relative importance, (i) being relatively important in $-\text{NH}_3^+$ and much less so in Cl ; also they are often opposite in sign. For these reasons there are advantages in sub-dividing those effects of substituents that do not involve charge transfer into two classes, following the division into (i) and (ii) of the energy terms. We reserve the term 'inductive' for the first, and describe the second as the 'orbital penetration' effect.

The idea that three, and not two, independent characteristics are needed to specify the effect of a substituent is not new. Evans and de Heer [11] proposed it and Clark *et al.* [3] have recently developed it to deal with the anomalous behaviour of halogens as substituents by distinguishing, in the qualitative theory, the inductive effect I_σ on the σ -electrons of the ring system, from I_π , the inductive effect on the π -electrons. We now see that the sub-division follows from rather general features of weakly interacting electronic systems, confirming it as a suitable basis for theoretical treatments.

3. THE PENETRATION TERMS

In an earlier paper [2] a group that is primarily inductive in the strict sense, namely $-\text{NH}_3^+$, was treated in some detail; it has no mesomeric effect, and the penetration by the ring π -orbitals into the electron distribution of the N-H bonds can be included as a short-range potential added to modify the electrostatic effect of the unit charge. In this paper we deal with substituents in which the penetration terms are expected to outweigh or at least to be comparable with inductive and mesomeric terms: examples are the halogens and the methyl group in which the other effects are not too large. The amino and hydroxy substituents are included as groups with larger mesomeric effects for comparison purposes.

The penetration interaction is always repulsive; π -electron charge density is displaced from ring carbon atoms near the substituent and partitioned among the other atoms in the ring. This is simply a redistribution of π -electrons without net gain from the substituent: if the substituent also transfers charge into the ring (see

heading (iii) above) the two re-inforce; if the charge transfer is out of the ring, they are opposed. But we can look for evidence of the penetration effect only where charge transfer is small, or absent.

In the following sections a model is introduced to examine the electronic effects of penetration principally on the absorption spectrum. The results are compared with the spectra of the halobenzenes and toluene, to see to what extent penetration accounts for the changes in the benzene spectrum produced by substitution.

4. REPRESENTATION OF ORBITAL PENETRATION EFFECTS BY A POTENTIAL

A valuable discussion of the theory of orbital penetration has been given by McWeeny [12]. Charge-transfer states being assumed unimportant, he has shown that the interaction energy between two uncharged systems can be rigorously partitioned into Coulomb and penetration energies, the latter being repulsive. It follows from the analysis that if the electronic states of the two interacting systems are expressed in molecular orbitals, the penetration energy is proportional to the square of the overlap integral between the orbitals for the two systems. By expanding the benzene molecular orbitals in terms of atomic orbitals at the carbon centres, we readily see that the contributions by energy integrals over atomic orbitals vary with distance approximately as the square of the overlap of the substituent orbitals with the $2p\pi$ -orbitals at successive carbon centres round the ring. These contributions fall off very quickly with increasing distance; indeed if we take as a guide the square of the overlaps of carbon $2p\pi$ self-consistent field orbitals as a function of distance we find a variation over the important range that can be represented approximately as an inverse third or fourth power of the distance. No single inverse power fits very closely, as is not surprising, but for the larger substituent atoms such as Cl and Br the inverse cube law is the best. For very short distances an even steeper variation is found, arising from an increasing contribution by inner-shell penetration, but this is of no interest here. Thus if we are to represent the penetration as deriving from a potential with the substituent as its source an appropriate form is expression (5):

$$V_p(\rho) = \gamma/\rho^3; \quad (5)$$

γ is a constant to be evaluated empirically for each substituent, and ρ is the distance from the substituent in atomic units. As already shown [2], electrostatic effects are also readily described in a similar way by a potential with the substituent as source, and groups with both characteristics can be treated by addition of the appropriate potentials.

To evaluate the parameter γ for a substituent that has both inductive and penetration characteristics, it is desirable if possible to use results that depend only on the penetration. Now it is known that in the anilinium ion, in which the long-range electrostatic potential is the dominant term, the intensity of the 2600 Å ultra-violet absorption is unchanged from benzene. In uncharged groups like the halogens such long-range influences are smaller than in $-\text{NH}_3^+$ and can clearly be neglected in calculating the spectrum; and short-range electrostatic terms, such as the dispersion energy, are small compared with the penetration energy. The intensity change on substitution may therefore be taken to be independent of type (i) terms, i.e. independent of the inductive power of the substituent in the restricted sense used in this paper. This as will be seen allows the

constant γ to be evaluated, in all cases for which charge transfer can be neglected. Other experimental measures of the disturbance to the electronic system on substitution, such as the dipole moment and charge density, do not permit discrimination between inductive and other effects and are only of secondary importance for the present purpose. They will however be briefly referred to later.

5. THE MODEL FOR SINGLY SUBSTITUTED BENZENES

The substituent is treated as the source of a short-range repulsive potential (5). As in the treatment of the anilinium ion [2] the potential is studied as a perturbation on the states of free benzene. The ground and first excited states of the substituted molecule are expanded in wave functions for the π -states of benzene:

$$\phi(A) = a_1\varphi(A_{1g}) + a_2\varphi(B_{1u}) + a_3\varphi(E_{2g}) + a_4\varphi(E_{1u}), \quad (6)$$

$$\phi(B) = b_1\varphi(B_{2u}) + b_2\varphi(E_{2g}) + b_3\varphi(E_{1u}), \quad (7)$$

where $\phi(A)$ and $\phi(B)$ are symmetric and antisymmetric respectively under reflection in the mirror plane σ_v , containing the substituent, and normal to the benzene ring; the A and B species are non-interacting because the Hamiltonian is symmetric under σ_v . Equations to determine the coefficients a_i , b_i lead in the usual way to secular determinants of order four and three respectively.

6. EXPANSION OF THE PERTURBING POTENTIAL

We include in this section a recapitulation of the properties of the $1/\rho$ and $1/\rho^2$ potentials used earlier [2] as well as $1/\rho^3$ required here. The potential used to represent the inductive influence of the ammonium pole is given in expression (8). We can re-write this in the equivalent form (9), in which δ and β are two parameters to be determined. In (8) ϵ is the dielectric constant for electrostatic effects on the π -electrons, and α is the effective charge of the pole:

$$V_I = \epsilon^{-1}(-\alpha/\rho + 3/\rho^2) \quad (8)$$

$$= -(\delta/\rho - \beta/\rho^2); \quad (9)$$

ρ is the radial distance measured from the substituent as origin. This potential displays the long-range characteristics of the induction in contrast to the inverse cube potential (5) with its much larger strength at the nearest carbon than at any other, reflecting that the substituent π -electrons penetrate significantly only the π -orbital of the carbon atom to which it is attached.

V_I and V_p are now written in a more useful form by using the expansions of ρ^{-n} in Legendre polynomials [13]. The distance r is measured from an origin at the centre of the benzene ring, and σ is the fixed distance from the ring centre to the substituent. η the angle between the vectors \mathbf{r} and $\boldsymbol{\sigma}$ and P_n is a Legendre function of the first kind. We then have

$$\left. \begin{aligned} \rho^{-1} &= \sigma^{-1} \sum_n P_n(\cos \eta) h^n; \quad h = r/\sigma, \quad \sigma > r, \\ \rho^{-2} &= \sigma^{-2} \sum_n \{ (2n+1)/4h \} [-I_n(f) + P_n(f) \ln \{ (f+1)/(f-1) \}] P_n(\cos \eta), \\ \rho^{-3} &= \sigma^{-3} \sum_n \{ (2n+1)/(1-h^2) \} h^n P_n(\cos \eta), \end{aligned} \right\} \quad (10)$$

in which $2f = (h+1)/h$, and $I_n(f)$ is defined as follows:

$$I_n(f)/2 = P_{n-1}(f) \cdot (2n-1)/n + P_{n-3}(f) \cdot (2n-5)/(n-1) + \dots \\ + P_{n-2r+1}(f) \cdot (2n-4r+3)/(n-r+1) + \dots$$

The Legendre polynomials $P_n(\cos \eta)$ are now expressed in the angular coordinates of \mathbf{r} and $\boldsymbol{\sigma}$:

$$P_n(\cos \eta) = \sum_{m=-n}^n \frac{(n-|m|)!}{(n+|m|)!} P_n^{|m|}(\cos \Theta) P_n^{|m|}(\cos \theta) \exp[im(\varphi - \Phi)]. \quad (11)$$

Θ , Φ and θ , φ define the positions of the substituent and the current point respectively, e.g. for mono-substitution with the substituent on the z -axis, $\Theta = \pi/2$, $\Phi = 0$. V is written more compactly as (12) after substitution of (11) in (10):

$$V = V_p + V_I = (A_{IM} + A_{pM})\mathbf{M} + (A_{ID} + A_{pD})\mathbf{D} + \dots \\ = \mathcal{A}_M\mathbf{M} + \mathcal{A}_D\mathbf{D} + \mathcal{A}_Q\mathbf{Q} + \mathcal{A}_O\mathbf{O} + \mathcal{A}_S\mathbf{S} + \dots, \quad (12)$$

where, for the multipole operators we have:

$$\mathbf{M} = 1, \quad \mathbf{D} = z, \quad \mathbf{Q} = \frac{1}{2}(3z^2 - r^2), \quad \mathbf{O} = \frac{1}{2}(5z^3 - 3zr^2), \\ \mathbf{S} = \frac{1}{8}(35z^4 - 30z^2r^2 + 3r^4),$$

and

$$\mathcal{A}_M = \gamma\sigma^{-3}(1-h^2)^{-1} - \delta/\sigma + (\beta/4h\sigma^2) \ln\{(f+1)/(f-1)\},$$

$$\mathcal{A}_D = 3\gamma h\sigma^{-3}(1-h^2)^{-1} - \delta h/\sigma - (3\beta/2h\sigma^2) + (3\beta/4h\sigma^2)f \ln\{(f+1)/(f-1)\}, \text{ etc.}$$

It should be noted that the expansion of ρ^{-2} is different from equation (10) of reference [11], the sum over m having been replaced by the closed expression. The error in cutting off the expansion (12) increases the higher the inverse power of ρ , and is serious for ρ^{-3} , as may be illustrated by computing the potential at the carbon atoms C1 to C4, numbered away from the site of substitution, according to equation (10) and comparing with the exact values from equation (5). The following comparison refers to $\gamma = 1$ and $\sigma = 5.3 \text{ A.U.}$

	$V_p(\text{C1})$	$V_p(\text{C2})$	$V_p(\text{C3})$	$V_p(\text{C4})$
Equation (12)				
terminating at				
$\mathcal{A}_S\mathbf{S}$	0.0488 A.U.	0.0096	0.0025	0.00087
Equation (5)	0.0531 A.U.	0.0103	0.0029	0.00198

To avoid these errors it is essential to make expression (12) more flexible, so that the correct potentials are reproduced at each one of the carbon atoms. This is done as follows. Each component of V is defined by four parameters which are to be determined from the direct evaluation of ρ^{-n} at the carbon atoms C1, C2, C3 and C4, e.g. for ρ^{-3} equation (12) becomes:

$$V_p = \gamma[A_{pM}\mathbf{M} + aA_{pD}\mathbf{D} + bA_{pQ}\mathbf{Q} + cA_{pO}\mathbf{O} + dA_{pS}\mathbf{S}] \\ = \gamma\rho^{-3}.$$

a , b , c and d are found from the solution of the four equations:

$$[\gamma\rho^{-3}]_{\text{C1}} = [\gamma(A_{pM}\mathbf{M} + \dots)]_{\text{C1}}, \\ [\dots]_{\text{C2}} = [\dots]_{\text{C2}}, \\ \vdots \\ [\gamma\rho^{-3}]_{\text{C4}} = [\dots]_{\text{C4}}.$$

The following results are found for the potential $1/\rho^3$ with a C-X bond length of 1.41 Å.

$$a = 1.1901, \quad b = 1.6881, \quad c = 1.2503, \quad d = -0.0199.$$

Calculations with different C-X bond lengths show that as σ increases the values of a , b , c and d each tend to unity as in (12).

7. THE SECULAR EQUATIONS

The secular equations for the ground and first excited states reduce to the following simple forms identical with equations (13) and (14) given by Craig and Bishop [2]:

$$\begin{vmatrix} x & \mathcal{A}_D[A_{1g}|\mathbf{D}|E_{1u}] & \mathcal{A}_Q[A_{1g}|\mathbf{Q}|E_{2g}] & \mathcal{A}_O[A_{1g}|\mathbf{O}|B_{1u}] \\ + \mathcal{A}_O[A_{1g}|\mathbf{O}|E_{1u}] & + \mathcal{A}_S[A_{1g}|\mathbf{S}|E_{2g}] & & \\ x + \Delta W(E_{1u}) & \mathcal{A}_D[E_{1u}|\mathbf{D}|E_{2g}] & \mathcal{A}_Q[E_{1u}|\mathbf{Q}|B_{1u}] & \\ + \mathcal{A}_O[E_{1u}|\mathbf{O}|E_{2g}] & + \mathcal{A}_S[E_{1u}|\mathbf{S}|B_{1u}] & & \\ x + \Delta W(E_{2g}) & \mathcal{A}_D[E_{2g}|\mathbf{D}|B_{1u}] & & \\ & + \mathcal{A}_O[E_{2g}|\mathbf{O}|B_{1u}] & & \\ & x + \Delta W(B_{1u}) & & \end{vmatrix} = 0$$

$$\begin{vmatrix} x + \Delta W(B_{2u}) & \mathcal{A}_Q[B_{2u}|\mathbf{Q}|E_{1u}] & \mathcal{A}_D[B_{2u}|\mathbf{D}|E_{2g}] \\ + \mathcal{A}_S[B_{2u}|\mathbf{S}|E_{1u}] & + \mathcal{A}_O[B_{2u}|\mathbf{O}|E_{2g}] & \\ x + \Delta W(E_{1u}) & \mathcal{A}_D[E_{1u}|\mathbf{D}|E_{2g}] & \\ & + \mathcal{A}_O[E_{1u}|\mathbf{O}|E_{2g}] & \\ & x + \Delta W(E_{2g}) & \end{vmatrix} = 0$$

where the variable $x = W(A_{1g}) - W$ and $\Delta W(\Gamma) = W(\Gamma) - W(A_{1g})$. The diagonal quadrupole terms are omitted because they displace the energies of all states by approximately equal amounts, and so do not affect the results.

Finding the matrix elements of the multipole components of V is now reduced to a computation of multipole transition moments of the π -electron transitions in benzene. In principle, all of these are experimental quantities; but in practice only one transition moment is known:

$$[A_{1g}|\mathbf{D}|E_{1u}(A)] = [A_{1g}|\mathbf{D}|E_{1u}(B)] = 1.7 \text{ A.U.} = \lambda_{\text{exp.}}$$

The remaining matrix elements must at present be calculated. They can be obtained from molecular orbital theory and the results given in terms of a parameter $\lambda = kr_{\text{C-C}}$ equal to a constant times the C-C bond length [2]. λ is an effective ring radius for the benzene π -electrons. Craig and Bishop found that a value $\lambda = 0.65r_{\text{C-C}}$ fitted the anilinium ion results and, since k should be independent of substituent, the same value is used here. In the singly substituted benzenes the properties that may be most readily calculated on this basis are:

- (i) The contribution by the penetration term to the spectroscopic shift, S , of the lowest energy π -electron transition compared with benzene:

$$S = W(B) - W(A) - W(B_{2u}) + W(A_{1g})$$

- (ii) The contribution to the ground-state
- π
- electron dipole moment,
- D
- :

$$D = e[A|z|A] \\ = 0.5291 \times 4.8(2a_1a_4\lambda_{\text{exp}} - a_4a_3\lambda + a_3a_2\lambda) \text{ Debyes.}$$

- (iii) The oscillator strength,
- f
- , of the lowest
- π
- electron transition:

$$f = 1/3\{W(B) - W(A)\}Q^2.$$

The energy difference is here measured in Rydbergs and Q , the transition dipole length, in atomic units:

$$Q = a_1b_3\lambda_{\text{exp}} + a_4b_2\lambda/2 + a_3b_1\lambda/2 + a_2b_2\lambda/2 + a_3b_3\lambda/2.$$

- (iv) The ground-state charge distribution.

Of these only the intensities of the lowest transition (iii) can provide a test of the importance of the penetration mechanism: the calculations are concentrated on this point.

8. CALCULATION OF INTENSITIES IN THE SUBSTITUTED BENZENES

By assuming that the intensity of the lowest benzene π -transition is not changed by electrostatic interactions, we make the intensities depend only on γ , the substituent parameter in the potential (5) and on the quantities associated with benzene itself, namely the transition moments for transitions between its free molecule energy levels, and on the transition energy from the ground state to the E_{2g} state, which is not known from experiment. The results are not very sensitive to the energy and other characteristics of this transition and for the following the energy is taken to be 6.2 eV, i.e. the transition is taken to coincide with the $B_{1u} - A_{1g}$ system at 2000 Å in the spectrum.

Values of γ are first calculated for each substituent by fitting the purely electronic component of the observed intensity in the lowest ultra-violet absorption band, the potential being chosen to fit the $\gamma\rho^{-3}$ form at each carbon atom, as previously described. The results are shown in table 1.

Substituent	Oscillator strength (expt.) [8]	γ^\ddagger	Oscillator strength for chosen γ
-F	0.007	1.3	0.008
-Cl	0.0012	1.4	0.0013
-Br	0.0010	1.7	0.00095
-Me	0.0010	0.8	0.0011
-NH ₂	0.022	3.0†	0.022
-OH	0.016	2.5†	0.018

† See text.

‡ The value of γ is the best to the first decimal place.

Table 1. Values of the potential parameter γ .

The values of γ chosen in this way to fit the observed oscillator strengths provide a useful check of magnitudes. For fluorine the parameter $\gamma = 1.3$ gives $V = 1.3/r_{C-F}^3$ or 2.38 eV at the substituted carbon, for Cl the value is 1.23 eV, and for Br 0.94 eV.

The exchange integrals for the π -lone-pair orbitals with the adjacent carbon $2p\pi$ orbital are between 1–2 eV for fluorine, and probably about 1 eV for the others. The order-of-magnitude agreement between the orbital penetration measured by the exchange integral, and the potential required to fit the spectral intensities encourages the view that the mechanism of the spectral perturbation is correctly described; the additional effect of the short-range electrostatic terms must be very small. It is to be emphasized that the balance between penetration and inductive terms in ground-state properties, and in their influence on reactivity will be quite different from that in the determination of spectral properties, as already seen in the anilinium ion. The values of γ for $-\text{NH}_2$ and $-\text{OH}$ give unrealistically large potentials and arise from the attempt to assign to penetration what is really mesomeric spectral enhancement.

Substituent group	Orientation	Oscillator strengths	
		Calculated	Experimental [8]†
-F	<i>ortho</i>	0.010	
	<i>meta</i>	0.008	0.008
	<i>para</i>	0.026	0.021
-Cl	<i>o</i>	0.0016	0.002
	<i>m</i>	0.0011	0.002
	<i>p</i>	0.0046	0.005
-Br	<i>o</i>	0.0012	0.0013
	<i>m</i>	0.0008	0.0024
	<i>p</i>	0.0033	0.0032
-CH ₃	<i>o</i>	0.0012	0.0011
	<i>m</i>	0.0010	0.0012
	<i>p</i>	0.0037	0.0034
-NH ₂	<i>o</i>	0.026	0.054
	<i>m</i>	0.019	0.038
	<i>p</i>	0.052	0.046
-OH	<i>o</i>	0.022	0.024
	<i>m</i>	0.016	0.020
	<i>p</i>	0.0465	0.030

† Excluding vibronically induced component.

Table 2. Intensities in disubstituted benzenes.

The values of γ in table 1 are next used to calculate oscillator strengths for the disubstituted benzenes. The results are in table 2. In these results the substituents fall into two groups. For F, Cl, and CH₃ and to a lesser extent -Br there is fair agreement between calculated and experimental intensities and in most cases this could be improved by choosing γ values exactly to fit the reference molecules. Here the intensities for *o*- and *m*-disubstitution are close to that for single substitution, and all three are about one-third of that for *p*-disubstitution. This pattern of intensities is a characteristic of the short-range orbital penetration. In Br the *meta* intensity is high; this we believe shows the

greater importance of the mesomeric electron release from Br than from F, Cl or CH₃. The *para* intensity is however still further enhanced, suggesting that the full dominance of mesomeric over penetration term is not achieved as it is in -NH₂ and -OH, in which the characteristic pattern [8] of near equality in all three disubstituted molecules is strongly in evidence. This result may seem surprising for -CH₃ in view of the widely accepted mechanism of hyperconjugation for explaining the electronic properties of methyl substituted benzenes [14]. However, the pattern of the experimental oscillator strengths for the three xylenes suggests that the methyl group is behaving more like a substituent from which there is very little electron release. This observation supports our view that for the -CH₃ group, the penetration effect is more important than the mesomeric (hyperconjugative) effect.

From this analysis it may be concluded that the penetration contribution increases in the order CH₃ ~ Br < Cl < F; we cannot identify it in -NH₂ and -OH, in both of which mesomeric influences are so strong that the calculation of γ on the basis of orbital penetration is without real meaning. The order of effectiveness of the halogens is the same as the order of their inductive powers (i.e. the order of ionization potentials) but the sign is reversed, the penetration having the sense of electron repulsion while inductively the halogens have the sense of electron withdrawal. It is thus possible to reconcile the sequences (1)-(4) by noting that (4) is not a sequence of the $+I$ effect, but of $+P$, and that (1) is a sequence of charge displacement not only of $+M$ type, but of $+M$ combined with $+P$, the former predominantly in NH₂ and OH, and the latter in F, Cl and Br.

We may use the method to calculate the contribution made by the penetration term to other molecular properties. Thus the displacement of π -electron charge produced by the penetration repulsion gives a small contribution to the dipole moment in the sense X⁺-Ph⁻. Its magnitude in the monosubstituted compounds is, in Debyes: -F, 0.32; -Cl, 0.19; -Br, 0.19 and -CH₃, 0.14. Even in the largest of these, fluorobenzene, the charge displacements are extremely small and have the direction of an electron release: the *ortho* carbons have an electron excess of 0.003 electrons, the *meta* of 0.010 and the *para* carbon of 0.007 electrons. These charge displacements have to be compounded with those from the electrostatic influence of F, acting in the opposite sense, and are probably swamped by them. Also, the shift of the transition frequency is calculable from the displacements of the *A* and *B* states by the potential *V*. In the fluoride the major part of the observed displacements seem to have this origin. Thus we find a red shift in fluorobenzene of 190 cm⁻¹ (expt 270 cm⁻¹) in the *o*-difluorobenzene 200 cm⁻¹ (not recorded), in the *meta* 65 cm⁻¹ (180 cm⁻¹) and in *para* 850 cm⁻¹ (1246 cm⁻¹). With other substituents the penetration contribution is only a fraction of what is observed or, as in -OH and -NH₂ is only accidentally close to it.

Finally there is the relationship between the discussion hitherto and the qualitative theory of substituent effects given by Clark, Murrell and Tedder [3] who proposed a distinction between the inductive effect of a substituent acting on the σ -electron system (I_σ) and its inductive effect on the π -electron system (I_π). The latter is closely related to the penetration term, in that it arises from repulsion between the π -electrons of the substituent and the ring system. We have drawn attention to differences between the two viewpoints in relation to dependence on distance from the substituent et cetera. However, the important point is that, however described, three terms are needed to deal with the influence of a

substituent rather than two: the new one, either Clark, Murrell and Tedder's $I\pi$, or orbital penetration, is of importance especially in weakly mesomeric substituents. In such cases it causes electron displacements within the ring system with the same direction as that of mesomeric electron release from the substituent.

REFERENCES

- [1] INGOLD, C. K., 1953, *Structure and Mechanism in Organic Chemistry* (Ithaca, N.Y.: Cornell University Press) p. 67.
- [2] CRAIG, D. P., and BISHOP, D. M., 1963, *Mol. Phys.*, **6**, 139.
- [3] CLARK, D. T., MURRELL, J. N., and TEDDER, D. T., 1963, *J. chem. Soc.*, p. 1250.
- [4] FORBES, W. F., 1956, *Canad. J. Chem.*, **34**, 1447; 1961, *Ibid.*, **39**, 2295.
- [5] MATSEN, F. A., 1950, *J. Amer. chem. Soc.*, **72**, 5243.
- [6] MURRELL, J. N., 1955, *Proc. phys. Soc., Lond. A*, **68**, 969.
- [7] I'HAYA, Y., 1959, *J. Amer. chem. Soc.*, **81**, 6120, 6127.
- [8] PETRUSKA, J., 1961, *J. chem. Phys.*, **34**, 1111.
- [9] GOODMAN, L., and SHULL, H., 1957, *J. chem. Phys.*, **27**, 1388.
- [10] BABA, H., 1961, *Bull. chem. Soc., Japan*, **34**, 76.
- [11] EVANS, M. G., and DE HEER, J., 1950, *Quart. Rev.*, **4**, 94.
- [12] McWEENY, R., 1961, Preprint No. 59, Quantum Chemistry Group for Research in Atomic, Molecular and Solid State Theory, Uppsala, Sweden.
- [13] ROUTH, W., 1895, *Proc. Lond. math. Soc.*, p. 481.
- [14] COULSON, C. A., and CRAWFORD, V. A., 1953, *J. chem. Soc.*, p. 2052.

Regular models for solid hydrogen: III

by G. M. BELL

Mathematics Department, Chelsea College of Science and Technology,
and W. M. FAIRBAIRN†

Mathematics Department, Faculty of Technology, University of Manchester

(Received 1 April 1964)

A regular model for a hexagonal close-packed lattice of ortho-hydrogen molecules is treated by a first-order statistical approximation. With nearest-neighbour pair energies due mainly to the quadrupole-quadrupole interaction the model is unsymmetric and anisotropic but spatial ordering based on alternate layer sub-lattices occurs at low temperatures. To obtain correct ratios for the numbers of nearest-neighbour site links at different orientations to the crystal axis an octahedron of six sites is used as the basic group in the first-order approximation. It is found that a second-order transition to the layer sub-lattice distribution occurs at $T = 3.99^\circ\text{K}$.

1. INTRODUCTION

A regular model can be defined as one in which the configurational energy of an assembly depends linearly on the numbers of the various types of nearest-neighbour pair on a lattice; each coefficient is the interaction energy of the corresponding type of pair. In two previous papers [1, 2] the authors have discussed regular models relevant to pure solid ortho-hydrogen with a view to explaining the second-order or λ -type transition observed in solid hydrogen containing a high proportion of ortho-hydrogen [3–5]. We regard the ortho-hydrogen as composed of two species consisting respectively of molecules in the states $M=0$ and $M=\pm 1$ into which an axially symmetric molecular field splits the degenerate state $J=1$. The pair energies are due mainly to the quadrupole-quadrupole interaction but in the calculations corrections have been made to include the directional effects of the other forces, which are small. The model discussed differs from the well-known Ising model in that the degeneracies and the energies of pairs of like nearest neighbours are unequal for the two species. (Using the nomenclature of [1, 2] in which the $M=0$ species is labelled λ and the $M=\pm 1$ species is labelled μ this means that $g_\lambda \neq g_\mu$, $w_{\lambda\lambda} \neq w_{\mu\mu}$, $w_{\lambda\lambda}' \neq w_{\mu\mu}'$.) However, it was shown in [1] that the free energy of such an unsymmetric model is equal to that of an Ising model in a temperature-dependent external field, termed the 'effective field' and denoted by $H_e(T)$. Another interesting characteristic of these models is that the quadrupole-quadrupole interaction energy of a nearest-neighbour pair depends on the orientation to the crystal axis of the vector linking the two sites. Hence most lattices are 'anisotropic' and there are several interaction energies for pairs with similar members.

The close-packed lattice which is the most likely form for solid ortho-hydrogen is anisotropic in the above sense. We take the axis of quantization along the three-fold axis of greatest symmetry and then of the twelve vectors linking each site to its nearest neighbours six are at angle $\frac{1}{2}\pi$ and six at angle $\cos^{-1}(\pm\sqrt{\frac{2}{3}})$ to this axis. Henceforward, for brevity we shall term the vectors at angle $\frac{1}{2}\pi$ 'r-links' and

† Present address: Physics Department, The University, Lancaster.

those at $\cos^{-1}(\pm\sqrt{\frac{2}{3}})$'s-links'. It was shown in [2] that the free energy is considerably reduced by a sub-lattice ordering of the λ and μ species in alternate layers, each consisting of two adjacent parallel planes of sites parallel to the crystal axis. The corresponding second-order transition temperature T_c was found by applying the zeroth-order statistical approximation of taking the distribution on each sub-lattice as random. The existence of the second-order transition in this model is of considerable interest and the object of the present paper is to apply a better statistical approximation in which local ordering is not neglected.

2. THE BASIC GROUP OF SITES

We shall use a form of the first-order or quasi-chemical approximation where the system is regarded as an assembly of identical groups of sites occupied in various ways. A group consisting of six sites at the corners of an octahedron is chosen so as to give the correct ratio of r-links to s-links (see § 1) both inside each sub-lattice and between the sub-lattices. Figure 1 shows a projection of this group

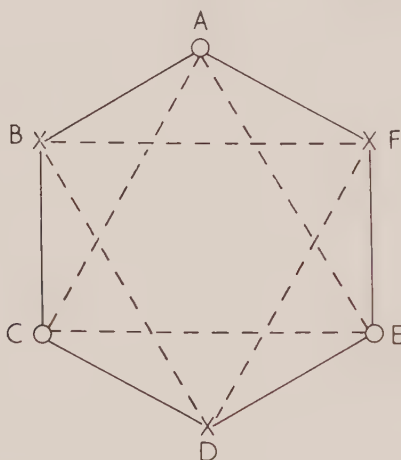


Figure 1. Projection of the basic group of sites. Dotted segments: site links at $\pi/2$ to the crystal axis (r-links). Full segments: site links at $\cos^{-1}(\pm\sqrt{\frac{2}{3}})$ to the crystal axis (s-links).

onto a plane perpendicular to the crystal axis; sites A, C and E lie in this plane while B, D and F are in an adjacent parallel plane. The dotted lines are r-links while full lines are s-links. (Figure 1 may be compared with [2], figure (a), p. 610).

Now, by [1], (4.4) we have for the quadrupole-quadrupole interaction:

$$w = w_{\lambda\mu} - \frac{1}{2}w_{\lambda\lambda} - \frac{1}{2}w_{\mu\mu} = -\frac{27\chi}{16}, \quad w' = w_{\lambda\mu}' - \frac{1}{2}w_{\lambda\lambda}' - \frac{1}{2}w_{\mu\mu}' = \frac{13\chi}{16}, \quad (2.1)$$

where the undashed and dashed quantities refer respectively to pairs with r- and s-links. The energy parameter χ , defined by [1] (4.4), is positive so that sub-lattice ordering is favoured if as many as possible of a given sites s-links are with sites in the same sub-lattice. Hence (see [2], p. 610, figure (b)) we postulated a division into equivalent sub-lattices, labelled (a) and (b), such that of the total number of nearest-neighbour pairs of sites, half are of the (a)-(a) or (b)-(b) types, with a ratio of one r-link to two s-links, while half are of the (a)-(b) type with two r-links to one s-link. Now for this structure A, B and F of our figure may be

regarded as (a) sites while C, D and E are (b) sites. Thus between the three (a)–(a) pairs in the group there are one r-link and two s-links (and similarly for the three (b)–(b) pairs) while between the six (a)–(b) pairs there are four r-links and two s-links. Thus, as stated above, the ratios of the different types of link in the group are the same as in the crystal as a whole.

There are 2^6 possible distributions of λ and μ molecules on the basic group of six sites. These are distinguished by the suffix i , and the symbols $n_i^{(a)}$, $n_i^{(b)}$, ν_i and ν_i' will denote respectively the numbers of μ on the three (a) and the three (b) sites and the numbers of r- and s-links between λ – μ nearest neighbour pairs. It will be found that distributions with the same values of $n_i^{(a)}$, $n_i^{(b)}$, ν_i and ν_i' have the same probability so that we attach the same label i to all such distributions and denote their number by w_i , termed the weight. With this convention number i goes from 0 to 27 and a table giving the five numbers $n_i^{(a)}$, $n_i^{(b)}$, ν_i , ν_i' and w_i for each value of i is given in the Appendix.

As an example figure 2 shows the possible distributions for $i=13$, when $n_{13}^{(a)}=1$, $n_{13}^{(b)}=2$, $\nu_{13}=\nu_{13}'=4$, $w_{13}=6$; the sites correspond to those in figure 1.



Figure 2. Distributions on the basic group of sites for $i=13$.

3. FIRST-ORDER EQUILIBRIUM RELATIONS

Regarding the lattice as an assembly of $\frac{1}{2}N$ six-site groups, so as to give the correct total number, $6N$, of nearest-neighbour pairs, we express the total number g of distributions on the lattice with given $N_\lambda^{(a)}$, $N_\mu^{(a)}$, $N_\lambda^{(b)}$ and $N_\mu^{(b)}$, the numbers of λ and μ on the sub-lattices, by

$$g = f(N_\lambda^{(a)}, N_\mu^{(a)}, N_\lambda^{(b)}, N_\mu^{(b)}) \left(\frac{1}{2}N \right)! / \prod_i \{ (\frac{1}{2}N \phi_i)! \}. \quad (3.1)$$

Here ϕ_i denotes the probability of a distribution of type i on the six-site group. Following the usual first-order approximation procedure, the first factor on the right-hand side of (3.1) is defined to yield the correct value:

$$g = \{ (\frac{1}{2}N)! \}^2 / \{ N_\lambda^{(a)}! N_\mu^{(a)}! N_\lambda^{(b)}! N_\mu^{(b)}! \}$$

for a random distribution of λ and μ on the lattice, when

$$\phi_i = (N_\mu^{(a)})^{n_i^{(a)}} (N_\lambda^{(a)})^{3-n_i^{(a)}} (N_\mu^{(b)})^{n_i^{(b)}} (N_\lambda^{(b)})^{3-n_i^{(b)}} / (\frac{1}{2}N)^6.$$

Hence, substituting in (3.1) and applying Stirling's theorem:

$$\ln f = 2 \{ N_\lambda^{(a)} \ln N_\lambda^{(a)} + N_\mu^{(a)} \ln N_\mu^{(a)} + N_\lambda^{(b)} \ln N_\lambda^{(b)} + N_\mu^{(b)} \ln N_\mu^{(b)} - N \ln (\frac{1}{2}N) \}. \quad (3.2)$$

The probabilities ϕ_i ($i=0, 1, 2, \dots, 27$) are not independent since they must satisfy the relation:

$$\sum_{i=0}^{27} w_i \phi_i = 1. \quad (3.3)$$

Since $N_\lambda^{(a)} + N_\mu^{(a)} = N_\lambda^{(b)} + N_\mu^{(b)} = \frac{1}{2}N$, only two of the four numbers $N_\lambda^{(a)}$, $N_\mu^{(a)}$, $N_\lambda^{(b)}$ and $N_\mu^{(b)}$ are independent and, as in [2], we express them in terms of the variables m and σ , the latter being the sub-lattice order parameter. These variables m and σ may be expressed in terms of the ϕ_i by:

$$N_\mu^{(a)}/\frac{1}{2}N = \frac{1}{2}(1 + m - \sigma) = \frac{1}{3} \sum_{i=0}^{27} n_i^{(a)} w_i \phi_i, \quad (3.4)$$

$$N_\mu^{(b)}/\frac{1}{2}N = \frac{1}{2}(1 + m + \sigma) = \frac{1}{3} \sum_{i=0}^{27} n_i^{(b)} w_i \phi_i. \quad (3.5)$$

Equations (3.4) and (3.5) give the numbers of μ on each sub-lattice in terms of the probabilities ϕ_i ; corresponding relations for species λ are obtained by subtracting these from (3.3) to give:

$$N_\lambda^{(a)}/\frac{1}{2}N = \frac{1}{2}(1 - m + \sigma) = \frac{1}{3} \sum_{i=0}^{27} (3 - n_i^{(a)}) w_i \phi_i, \quad (3.6)$$

$$N_\lambda^{(b)}/\frac{1}{2}N = \frac{1}{2}(1 - m - \sigma) = \frac{1}{3} \sum_{i=0}^{27} (3 - n_i^{(b)}) w_i \phi_i. \quad (3.7)$$

As we shall take m and σ as independent variables three of the ϕ_i must be regarded as dependent on m , σ and the other ϕ_i . We choose

$$\phi_0 (w_0 = 1, n_0^{(a)} = n_0^{(b)} = v_0 = v_0' = 0),$$

$$\phi_1 (w_1 = 3, n_1^{(a)} = 1, n_1^{(b)} = 0, v_1 = v_1' = 2),$$

and

$$\phi_2 (w_2 = 3, n_2^{(a)} = 0, n_2^{(b)} = 1, v_2 = v_2' = 2),$$

to be these dependent variables and then, from (3.3), (3.4) and (3.5):

$$\begin{aligned} \phi_1 &= \frac{1}{2}(1 + m - \sigma) - \frac{1}{3} \sum_{i=3}^{27} w_i n_i^{(a)} \phi_i, \\ \phi_2 &= \frac{1}{2}(1 + m + \sigma) - \frac{1}{3} \sum_{i=3}^{27} w_i n_i^{(b)} \phi_i \\ \phi_0 &= 1 - 3(1 + m) + \sum_{i=3}^{27} w_i (n_i^{(a)} + n_i^{(b)} - 1) \phi_i. \end{aligned} \quad (3.8)$$

Equilibrium conditions can now be obtained by equating to zero the derivatives of the configurational free energy F_c with respect to the 27 independent variables $m, \sigma, \phi_3, \dots, \phi_{27}$. By [1] (2.8):

$$\begin{aligned} F_c &= w N_{\lambda\mu} + w' N_{\lambda\mu}' - (N_\mu^{(a)} + N_\mu^{(b)} - N_\lambda^{(a)} - N_\lambda^{(b)}) H_e(T) d - kT \ln g \\ &= \frac{1}{2} N \sum_{i=0}^{27} w_i (v_i w + v_i' w') \phi_i - N m H_e(T) d - kT \ln g, \end{aligned} \quad (3.9)$$

where $H_e(T)d$ is an effective-field energy term (see [1]) and the distribution number g is given by (3.1) and (3.2). To simplify the equilibrium relations we introduce:

$$\begin{aligned} \eta &= \exp(-w/kT), \quad \eta' = \exp(-w'/kT), \\ \xi &= \frac{\phi_1}{\phi_0} \exp[2(w + w')/kT], \\ \zeta &= \frac{\phi_2}{\phi_0} \exp[2(w + w')/kT], \end{aligned} \quad (3.10)$$

and we then have the relations:

$$\phi_i = \eta^{\nu} \eta'^{\nu'} \xi^{n_i^{(a)}} \zeta^{n_i^{(b)}} \phi_0 \quad (i=0, 1, \dots, 27). \quad (3.11)$$

The first three of these are identities while the remaining 25 are the results of equating $\partial F_c / \partial \phi_i$ to zero for $i=3, \dots, 27$.

The two remaining equilibrium relations are obtained by equating $\partial F_c / \partial m$ and $\partial F_c / \partial \sigma$ to zero; these are, respectively:

$$\exp [4H_e(T) d/kT] \left\{ \frac{(1+m+\sigma)(1+m-\sigma)}{(1-m+\sigma)(1-m-\sigma)} \right\}^2 = \xi^3 \zeta^3, \quad (3.12)$$

$$\left\{ \frac{(1+m+\sigma)(1-m+\sigma)}{(1+m-\sigma)(1-m-\sigma)} \right\}^2 = \frac{\xi^3}{\zeta^3}. \quad (3.13)$$

From (3.4)–(3.7) and (3.11), $(1 \pm m \pm \sigma)$ may be expressed in terms of ξ , ζ and the temperature dependent quantities η and η' . Then (3.12) and (3.13) may be solved for ξ and ζ at any temperature and the μ – λ ratio and sub-lattice order deduced.

It should be noted that (3.13) is satisfied by $\sigma=0$, $\xi=\zeta$ at all temperatures; at high temperatures this disordered state solution is unique. When a solution exists for which $\sigma \neq 0$ then, from (3.12) and (3.13), the interchange of ξ and ζ gives another such solution with the sign of σ reversed. This is a consequence of the equivalence of the two sub-lattices. The lack of equivalence of the species λ and μ gives rise to the term in $H_e(T)$ due to which there is no similar symmetry with respect to the parameter m .

4. THE CRITICAL TEMPERATURE

If there is a second-order transition from the high-temperature disordered state ($\sigma=0$) to one in which there is a preferential distribution of λ and μ between the sub-lattices ($\sigma \neq 0$) it will occur at the temperature where other solutions of (3.13) appear in the neighbourhood of the solution $\xi=\zeta$. When σ is very small we may put $\zeta=\xi+\delta$, $\delta \ll 1$, and, retaining only first-order terms, (3.13) becomes:

$$4 \left\{ \frac{1}{1+m} + \frac{1}{1-m} \right\} \sigma = \frac{3\delta}{\xi}. \quad (4.1)$$

The distributions i on the basic group of sites listed in the Appendix fall into two sets. In one set $n_i^{(a)} = n_i^{(b)}$ and so, by (3.11), the probabilities ϕ_i are unaltered by interchange of ξ and ζ (i.e. by reversing the sign of σ). In the other set $n_i^{(a)} \neq n_i^{(b)}$ and the distributions are in pairs (bracketed together in the table) whose probabilities are interchanged by interchanging ξ and ζ . Denoting a summation over the first member of each of these latter pairs by \sum_i^* it follows from (3.4), (3.5) and (3.6) that:

$$\sigma = \frac{1}{3} \sum_i^* w_i (n_i^{(b)} - n_i^{(a)}) \eta^{\nu} \eta'^{\nu'} (\xi^{n_i^{(a)}} \zeta^{n_i^{(b)}} - \xi^{n_i^{(b)}} \zeta^{n_i^{(a)}}) \phi_0. \quad (4.2)$$

If, for $\sigma \ll 1$, $\xi = \zeta + \delta$, the first-order term only is retained in (4.2), if it is substituted into (4.1) and if δ is cancelled then we obtain a relation valid at the critical point:

$$\left(\frac{1}{1+m} + \frac{1}{1-m} \right) \phi_0 \sum_i^* w_i (n_i^{(b)} - n_i^{(a)})^2 \xi^{n_i^{(a)}} \zeta^{n_i^{(b)}} \eta^{\nu} \eta'^{\nu'} = 9/4 \quad (4.3)$$

At the critical point m may be obtained from (3.4)–(3.7) by putting $\sigma=0$ and $\xi=\zeta$ to give:

$$m = \frac{1}{3} \sum_{i=0}^{27} (n_i^{(a)} + n_i^{(b)} - 3) w_i \eta^{\nu_i} \eta'^{\nu_i'} \xi^{n_i^{(a)} + n_i^{(b)}} \phi_0. \quad (4.4)$$

Substitution of (4.4) and (3.3) into (4.3) gives a relation between T_c and ξ . To find T_c this must be solved in conjunction with (3.12) which for $\sigma=0$, $\xi=\zeta$, $T=T_c$ takes the form:

$$\exp [2H_e(T_c) d/kT_c] \left(\frac{1+m}{1-m} \right)^2 = \xi^3, \quad (4.5)$$

which, after substitution of (4.4) yields a second relation between T_c and ξ .

The variations of η and η' with temperature T depend on the values of w and w' (see 3.10). Expressions (2.1) for w and w' in terms of the energy parameter χ were obtained under the assumption that only quadrupole–quadrupole forces were acting between the molecules. However, although this interaction is predominant at the distances of molecular separation which exist in solid hydrogen ($r_0 \sim 4 \text{ \AA}$) there are also contributions from the valence and dispersion forces. Since these are much smaller they will not seriously affect any ordering produced by the quadrupole–quadrupole forces alone but they will contribute to the energies $w_{\lambda\mu}$, $w_{\lambda\mu}'$, $w_{\lambda\lambda}$, $w_{\lambda\lambda}'$, $w_{\mu\mu}$, $w_{\mu\mu}'$ of the nearest-neighbour pairs: hence they will alter w and w' .

These corrections were estimated using Nakamura's values [6] for the energy parameters in the valence and dispersion forces. The results are:

$$w = -4.423k, \quad w' = 1.975k.$$

For quadrupole–quadrupole forces alone the values are

$$w = -4.423k, \quad w' = 2.129k.$$

(Remarkably the corrections leave unaltered the value for the r-links which are at angle $\frac{1}{2}\pi$ to the axis of quantization.) The increase in the value of w' reinforces the arguments near the beginning of §2 about sub-lattice ordering.

On putting

$$\eta_c = \exp(4.423/T_c), \quad \eta_c' = \exp(-1.975/T_c)$$

in (4.3) and (4.5) and eliminating ξ numerically it is found:

$$T_c = 3.99^\circ\text{K}, \quad m_c = 0.239.$$

However, in order to be sure that a second-order transition does take place at this temperature T_c where the other solutions appear in the neighbourhood of the solution $\sigma=0$ it is necessary to eliminate the possibility of a first-order transition at some higher value of T . This was done by verifying numerically that at $T=T_c$ there are no solutions of (3.12) and (3.13) other than that giving $\sigma=0$, $m=0.239$, which corresponds to the second-order transition.

The value $T_c = 3.99^\circ\text{K}$ is, as expected, somewhat lower than the zeroth-order approximation result of 5.8°K : when account is taken of the valence and dispersion forces this drops to 5.69°K . The present calculation brings the theoretical value of T_c considerably nearer the value of 3.0°K for 100 per cent ortho-hydrogen which was obtained by extrapolation by Smith and Housley [5]. Since the first-order approximation still gives an overestimate of the true critical temperature

for a regular model it is probable that sub-lattice ordering due principally to quadrupole-quadrupole forces is the cause of the second-order transition in solid hydrogen. Further experimental measurements on ortho-rich hydrogen mixtures would be of great interest.

APPENDIX

Configuration number	zv_i	$n_i^{(a)}$	$n_i^{(b)}$	$n_i^{(a)} + n_i^{(b)}$	ν_i	ν_i'
0	1	0	0	0	0	0
1	3	1	0	1	2	2
2	3	0	1	1	2	2
3	3	1	1	2	4	4
4	2	1	1	2	4	2
5	2	2	0	2	4	2
6	2	0	2	2	4	2
7	4	1	1	2	2	4
8	1	2	0	2	2	4
9	1	0	2	2	2	4
10	1	2	1	3	0	6
11	1	1	2	3	0	6
12	6	2	1	3	4	4
13	6	1	2	3	4	4
14	2	2	1	3	4	2
15	2	1	2	3	4	2
16	1	3	0	3	4	2
17	1	0	3	3	4	2
18	1	3	1	4	2	4
19	1	1	3	4	2	4
20	4	2	2	4	2	4
21	2	3	1	4	4	2
22	2	1	3	4	4	2
23	2	2	2	4	4	2
24	3	2	2	4	4	4
25	3	3	2	5	2	2
26	3	2	3	5	2	2
27	1	3	3	6	0	0

Table of configurations on the basic group of sites

REFERENCES

- [1] BELL, G. M., and FAIRBAIRN, W. M., 1961, *Mol. Phys.*, **4**, 481.
- [2] BELL, G. M., and FAIRBAIRN, W. M., 1962, *Mol. Phys.*, **5**, 605.
- [3] REIF, F., and PURCELL, E. M., 1953, *Phys. Rev.*, **91**, 631.
- [4] HILL, R. W., and RICKETSON, B. W. A., 1954, *Phil. Mag.*, **45**, 277.
- [5] SMITH, G. W., and HOUSLEY, R. M., 1960, *Phys. Rev.*, **117**, 732.
- [6] NAKAMURA, T., 1955, *Prog. theor. Phys.*, **14**, 135.

The effect of relaxation on the symmetry of N.M.R. spectra

by JAY MARTIN ANDERSON

Department of Chemistry, Bryn Mawr College, Bryn Mawr,
Pennsylvania, 19010

(Received 23 March 1964; revision received 12 May 1964)

The effect of nuclear relaxation on the symmetry properties of N.M.R. spectra is examined in terms of the properties of the relaxation matrix elements R_{ijkl} . It is found that the symmetry relations $R_{ijkl} = R_{jilk} = R_{klij} = R_{lkij}$ obtain for one or more dominant relaxation mechanisms under 'extreme narrowing' conditions. Further, the symmetry relation $R_{ijkl} = R_{\lambda i, \lambda j, \lambda k, \lambda l}$ where λ is a spin inversion operator, is shown to obtain for (a) only one dominant relaxation mechanism or (b) two dominant relaxation mechanisms which have the same commutation properties with λ . This latter symmetry relation does not obtain for two dominant relaxation mechanisms with the same order of spatial dependence and different commutation properties with λ . The effect of nuclear relaxation can therefore yield unsymmetrical first-order spectra; the application of this analysis to the determination of the absolute sign of the spin-spin coupling constants is proposed.

1. THE RELAXATION MATRIX

The description of relaxation among nuclear spin energy levels has recently been discussed in terms of the equation of motion of a density matrix for the spin system [1]; this type of analysis has been successfully applied to nuclear magnetic double resonance [2, 3]. In this description, relaxation information may be contained in a four-subscripted array called the relaxation matrix [4], if certain assumptions about the spin system and its coupling with the lattice are valid [1-4]. When the approximation known as 'extreme narrowing' obtains (namely when the correlation time for molecular reorientation τ_c and the separation of the energy levels ω are in the relation $1 \gg \tau_c^2 \omega^2$), the formulae for the relaxation matrix elements [5] reduce to:

$$R_{aa'bb'} = J_{abab'} - 1/2 \delta_{c'b'} \sum_c J_{cbca} - 1/2 \delta_{ab} \sum_c J_{cb'ca'}, \quad (1)$$

$$J_{abab'} = 2\tau_c \overline{\langle a | \mathcal{H}' | b \rangle \langle a' | \mathcal{H}' | b' \rangle^*}, \quad (2)$$

where \mathcal{H}' is a stationary, random, Markovian operator connecting the spins and the lattice. Since the shape of an N.M.R. spectrum is governed by these quantities† it is appropriate to consider them in detail.

If one relaxation mechanism is dominant, \mathcal{H}' may be written as the product of spherical irreducible tensors:

$$\mathcal{H}'(t) = \mathbf{F}^{(Q)}(t) \cdot \mathbf{A}^{(Q)} = \sum_{q=-Q}^{+Q} F_q^{(Q)}(t) A_{-q}^{(Q)} (-1)^q, \quad (3)$$

where $\mathbf{F}^{(Q)}$ is a stationary, random, Markovian function of time and a function of

† See, for example, Baldeschwieler's definitions (*J. Chem. Phys.*, **40**, 459, (1964)) of T_1 and T_2 , equations (2.14), (2.17).

spatial coordinates, and $\mathbf{A}^{(Q)}$ is a spin operator. The expansion of equation (3) may be substituted into the defining equation for $J_{aba'b'}$, with the result that

$$\begin{aligned} J_{aba'b'} &= 2\tau_c \sum_q \overline{F_q \langle a | A_{-q} | b \rangle} \sum_{q'} \overline{F_{q'}^* \langle a' | A_{-q'} | b' \rangle}^* (-1)^{q+q'} \\ &= 2\tau_c \sum_{q,q'} \overline{F_q F_{q'}^*} \langle a | A_{-q} | b \rangle \langle a' | A_{-q'} | b' \rangle^* (-1)^{q+q'}, \end{aligned} \quad (4)$$

where Q is the rank of the tensor [3, 6, 7].

In this equation, the superscript (Q) indicating the rank of the tensors \mathbf{F} and \mathbf{A} has been dropped for simplicity, and the bar indicates an isotropic space average. Because F_q and $F_{q'}$ are elements of a spherical irreducible tensor \mathbf{F} , the average in equation (4) gives:

$$J_{aba'b'} = 2\tau_c \sum_q |F_q|^2 \langle a | A_{-q} | b \rangle \langle a' | A_{-q} | b' \rangle. \quad (5)$$

Since the matrix elements of $\mathbf{A}^{(Q)}$ are real, the complex conjugation has been dropped [3].

As given in equation (5), the spectral densities $J_{aba'b'}$ have two important symmetry properties. First, $J_{aba'b'} = J_{a'b'ab}$; furthermore, $J_{aba'b'} = J_{bab'a'}$, since $\langle b | A_{-q} | a \rangle \langle b' | A_{-q} | a' \rangle = \langle a | A_q | b \rangle \langle a' | A_q | b' \rangle$; the sum for $J_{bab'a'}$ includes the left term and the sum for $J_{aba'b'}$ includes the right term. This symmetry in $J_{aba'b'}$ is reflected in the relaxation matrix elements: $R_{aa'bb'} = R_{bb'aa'} = R_{a'ab'b} = R_{b'ba'a'}$.

Consider, however, a relaxation operator given by:

$$\mathcal{H}'(t) = \mathbf{F}^{(Q)} \mathbf{A}^{(Q)} + \mathbf{E}^{(P)} \mathbf{B}^{(P)}, \quad (6)$$

where there are two relaxation mechanisms of similar magnitude. For such an operator, a spectral density $J_{aba'b'}$ will be given by an equation analogous to equation (4):

$$\begin{aligned} J_{aba'b'} &= 2\tau_c \left\{ \sum_q \overline{F_q^{(Q)} F_q^{(Q)*}} \langle a | A_{-q}^{(Q)} | b \rangle \langle a' | A_{-q}^{(Q)} | b' \rangle^* \right. \\ &\quad + \sum_p \overline{E_p^{(P)} E_p^{(P)*}} \langle a | B_{-p}^{(P)} | b \rangle \langle a' | B_{-p}^{(P)} | b' \rangle^* \\ &\quad + \delta_{QP} \left[\sum_q \overline{F_q^{(Q)} E_q^{(P)*}} \langle a | A_{-q}^{(Q)} | b \rangle \langle a' | B_{-q}^{(P)} | b' \rangle^* \right. \\ &\quad \left. \left. + \overline{E_q^{(P)} F_q^{(Q)*}} \langle a | B_{-q}^{(P)} | b \rangle \langle a' | A_{-q}^{(Q)} | b' \rangle^* \right] \right\}. \end{aligned} \quad (7)$$

The presence of the term multiplied by δ_{QP} arises from the cross-product of the two parts of $\mathcal{H}'(t)$ shown in equation (6). This cross-term vanishes if $Q \neq P$ because $\mathbf{F}^{(Q)}$ and $\mathbf{E}^{(P)}$ are then spherical tensors of different rank. The terms in square brackets may be called 'cross-correlation terms', following Abragam's [8] definition of the cross-correlation function. When the cross-correlation terms are present ($Q = P$), the relations $J_{aba'b'} = J_{a'b'ab} = J_{bab'a'}$ are still valid; hence, $R_{aa'bb'} = R_{a'ab'b} = R_{bb'aa'} = R_{b'ba'a}$ as before. The symmetry relations which have been discussed so far enable us to write $T_2(ab) = T_2(ba)$ and $W_{ab} = W_{ba}$ for the more general case including cross-correlation. $T_2(ab)$ and W_{ab} are defined† by $T_2(ab) = -R_{abab}^{-1}$ and $W_{ab} = R_{aabb}$.

† See, for example, Baldeschwieler's definitions (*J. chem. Phys.*, **40**, 459, (1964)) of T_1 and T_2 , equations (2.14), (2.17).

2. THE SPIN INVERSION OPERATOR AND SYMMETRY OF SPECTRA

The symmetry properties of single and double resonance spectra have been explored with the use of spin inversion operators [9–12]. None of the previous treatments have taken the effect of relaxation into account. A known symmetry theorem [10] refers only to symmetry of position with equal intensity. This definition of symmetry [10] must be modified: A transition of nuclei of type A is said to be symmetric with another transition of nuclei of type A if the frequencies of these transitions lie at equal distances each side of the spectrum and have the same intensities and the same T_2 's. The previous theorem [10] stated that the spectrum would be symmetric if the transition $\psi_i \rightarrow \psi_j$ is symmetric to $\lambda_n \psi_i \rightarrow \lambda_n \psi_j$, and the set of all functions $\{\psi_i\}$ is the same as the set $\{\lambda_n \psi_i\}$; n refers to any nucleus except A . The tilde sign used in references [10–12] is here dropped for simplicity. The work of references [10] and [12] substantiates this theorem in the absence of relaxation. The present paper discusses the conditions for which $T_2(\psi_i, \psi_j) = T_2(\lambda_n \psi_i, \lambda_n \psi_j)$, which is the final criterion for spectral symmetry including relaxation effects.

The conditions for which $T_2(\psi_i, \psi_j) = T_2(\lambda_n \psi_i, \lambda_n \psi_j)$ are to be found by considering the conditions for which $R_{ijkl} = R_{\lambda i, \lambda j, \lambda k, \lambda l}$, where ψ_i has been replaced by i , etc., and λ_n by λ for convenience.

For one dominant relaxation mechanism,

$$\begin{aligned} J_{\lambda i, \lambda j, \lambda k, \lambda l} &= 2\tau_c \sum_q F_q F_q^* \langle \lambda i | A_{-q} | \lambda j \rangle \langle \lambda k | A_{-q} | \lambda l \rangle^* \\ &= 2\tau_c \sum_q F_q F_{-q} \langle i | \lambda A_{-q} | j \rangle^* \langle k | \lambda A_{-q} | l \rangle, \end{aligned} \quad (8)$$

since $\langle \lambda i | j \rangle = \langle i | \lambda j \rangle^* \dagger$. In order to further treat equation (8), it is necessary to know the commutation relations of λ with the elements A_{-q} .

The commutation relations of λ with \mathbf{I} are given in reference [10] as:

$$[\lambda, I_x]_+ = [\lambda, I_y]_+ = [\lambda, I_z]_+ = 0, \quad (9)$$

where λ and \mathbf{I} refer to the same nucleus. In the various relaxation mechanisms that have been proposed [3], the following \mathbf{A} tensors occur: magnetic dipole-dipole, $\mathbf{A} = \mathbf{I}(1)\mathbf{I}(2)$, rank two; nuclear quadrupole, $\mathbf{A} = \mathbf{II}$, rank two; spin-rotation, $\mathbf{A} = \mathbf{I}$, rank one; anisotropic shielding, $\mathbf{A} = \mathbf{HI}$, rank two; anisotropic spin-spin coupling, $\mathbf{A} = \mathbf{I}(1)\mathbf{I}(2)$, rank two; chemical exchange, $\mathbf{A} = \mathbf{I}$, rank one. From the anti-commutation relations of λ with \mathbf{I} , together with the antiunitary property of λ , these commutation rules follow:

$$\begin{aligned} \lambda I_z &= -I_z \lambda; \lambda I_+ = \lambda(I_x + iI_y) = -I_x \lambda + iI_y \lambda = -I_- \lambda = -I_+^\dagger \lambda; \\ \lambda I_- &= -I_+ \lambda = -I_+^\dagger \lambda. \end{aligned}$$

In the case of all the first-rank tensors, these commutation rules give $\lambda A_q = -A_{-q} \lambda$; for the quadrupole tensor, $\lambda A_q = A_{-q} \lambda$; therefore, for these tensors and the anisotropic shielding tensor:

$$J_{\lambda i, \lambda j, \lambda k, \lambda l} = 2\tau_c \sum_q F_q F_{-q} \langle i | A_{-q} \lambda^2 | j \rangle^* \langle k | A_{-q} \lambda^2 | l \rangle. \quad (10)$$

The eigenvalue of λ^2 is +1 if the spin is integral and -1 if the spin is half-integral [10]; hence:

$$\begin{aligned} J_{\lambda i, \lambda j, \lambda k, \lambda l} &= 2\tau_c \sum_q F_q F_{-q} \langle i | A_{-q} | j \rangle^* \langle k | A_{-q} | l \rangle \\ &= J_{ijkl}. \end{aligned} \quad (11)$$

† This property of λ is incorrectly given in reference [10], but corrected in reference [12].

It is therefore the case that, for these relaxation mechanisms, $R_{ijij} = R_{\lambda i, \lambda j, \lambda k, \lambda l}$ (using equation (1)), and that $T_2(\psi_i, \psi_j) = T_2(\lambda\psi_i, \lambda\psi_j)$.

On the other hand, for the dipole-dipole and anisotropic coupling tensors, which are of rank two, the commutation relations are not as simple. It is therefore not possible to write an equation such as equation (10) for dipole-dipole or anisotropic coupling. Systems for which either of these are the dominant relaxation mechanisms would not, therefore, be symmetric in the sense of this section even if they are first order. This effect is usually not observed since dipolar couplings increase rapidly with the number of nuclei in the molecule, which serves only to obscure the effect, and because such couplings are usually sufficiently small that the magnetic field inhomogeneity governs the line width. A two-spin-1/2 system with strong dipolar coupling (large magnetogyric ratio and small inter-nuclear distance) should show this effect.

Finally, if two relaxation mechanisms are dominant, the effect of spin inversion on the cross-correlation terms of equation (7) must be considered. For example, with an element J_{ijkl} defined as in equation (7), the first two terms may be invariant under spin inversion as outlined above; but:

$$\begin{aligned} & \sum_q F_q E_{-q} \langle \lambda i | A_{-q} | \lambda j \rangle \langle \lambda k | B_{-q} | \lambda l \rangle^* \\ &= \sum F_q E_{-q} \langle i | \lambda A_{-q} \lambda | j \rangle^* \langle k | \lambda B_{-q} \lambda | l \rangle \\ &= \sum_q F_q E_{-q} \langle i | A_{-q} \lambda^2 | j \rangle^* \langle k | B_{-q} \lambda^2 | l \rangle (\pm 1) \\ &= \pm \sum_q F_q E_{-q} \langle i | A_{-q} | j \rangle \langle k | B_{-q} | l \rangle. \end{aligned} \quad (12)$$

Here, only if **B** and **A** have the same commutation relations with λ is the sign positive, and does $J_{ijkl} = J_{\lambda i, \lambda j, \lambda k, \lambda l}$. It is apparent, of course, that situations for which **A** and **B** have different commutation relations with λ can arise only for rank two tensors. If these commutation rules are different, the $R_{ijkl} \neq R_{\lambda i, \lambda j, \lambda k, \lambda l}$; $T_2(\psi_i, \psi_j) \neq T_2(\lambda\psi_i, \lambda\psi_j)$; and the spectrum is not symmetric in that the relative widths of symmetrically placed and equally intense lines are different.

The results of the preceding theorem may be extended in the manner of reference [12] to yield a general theorem: The spectrum of transition frequencies of a Hermitian operator $\mathcal{H} = A + B$ consists of r symmetrical groupings about the r transition frequencies of B , if (a) A commutes with B and there exists some non-singular linear or non-linear operator P which (b) anticommutes with A , commutes with B , and (c) has the same commutation property (either commutes or anticommutes) with all dominant relaxation operators.

This result may finally be applied on the manner of reference [9] to yield a method for the determination of the absolute sign of spin-spin coupling constants. In that reference, it is shown that the Hamiltonian for a spin system has the same transition frequencies and intensities as the Hamiltonian with the sign of all coupling constants reversed. However, if there are two major relaxation mechanisms with different commutation relations with λ , these otherwise similar transitions have different widths (or equally well, different saturation factors [13]).

3. SAMPLE CALCULATIONS AND CONCLUSIONS

As an example, consider a spin system of two nuclei, A and X , which may relax through the coupling of the electric quadrupole moment of X with the field

gradient at the site of X , and through direct magnetic dipolar interaction. For simplicity, take A to be of spin $1/2$ and X of spin 1 .

The two relaxation operators are products each of rank two spherical tensors [3] whose factorization into spatial and spin parts in the notation of equation (3) and the preceding sections is not difficult if some statement is made about the symmetry of the environment of X . This information is necessary to evaluate the components of $\nabla \mathbf{E}$, the field-gradient tensor. As an example, in an environment of cylindrical symmetry, $\nabla \mathbf{E} = eq/2\mathbf{Y}^{(2)}$ [6, 14]. Table 1 shows the factors of the dipolar and quadrupole Hamiltonians.

Dipole-dipole		
q	Fq	Aq
2	$\frac{\hbar\gamma_i\gamma_j}{4r_{ij}^3} \sqrt{\left(\frac{15}{2\pi}\right)} \sin^2 \theta \exp(2i\phi)$	$-I_-(a)I_-(x) \sqrt{\left(\frac{3}{10\pi}\right)}$
1	$-\frac{\hbar\gamma_i\gamma_j}{2r_{ij}^3} \sqrt{\left(\frac{15}{2\pi}\right)} \sin \theta \cos \theta \exp(i\phi)$	$[I_-(a)I_z(x) + I_z(a)I_-(x)] \sqrt{\left(\frac{3}{10\pi}\right)}$
0	$\frac{\hbar\gamma_i\gamma_j}{4r_{ij}^3} \sqrt{\left(\frac{5}{\pi}\right)} (3 \cos^2 \theta - 1)$	$-\{I_z(a)I_z(x) - \frac{1}{4}[I_+(a)I_-(x) + I_-(a)I_+(x)]\} \frac{2}{\sqrt{(5\pi)}}$
-1	$-F_1^*$	$-A_1^\dagger$
-2	F_2^*	A_2^\dagger
Quadrupole		
q	Eq	Bq
2	$\frac{eq}{8} \sqrt{\left(\frac{15}{2\pi}\right)} \sin^2 \theta \exp(2i\phi)$	$\frac{eq}{A} \frac{\sqrt{6}}{4} I_+(x)^2$
1	$-\frac{eq}{4} \sqrt{\left(\frac{15}{2\pi}\right)} \sin \theta \cos \theta \exp(i\phi)$	$\frac{eQ}{A} \frac{\sqrt{6}}{4} [I_z(x)I_+(x) + I_+(x)I_z(x)]$
0	$\frac{eq}{8} \sqrt{\left(\frac{5}{\pi}\right)} (3 \cos^2 \theta - 1)$	$\frac{eQ}{A} \{[3I_z(x)^2 - I(x)[I(x) + 1]]\}$
-1	$-E_1^*$	$-B_1^\dagger$
-2	E_2^*	B_2^\dagger
$A = I(x)[2I(x) - 1]$		

Table 1. Components of the spherical tensors for dipole-dipole and quadrupole relaxation.

The relaxation matrix elements for the dipole-dipole and quadrupole relaxation mechanisms and the cross-correlation of these mechanisms were computed using equations (1) and (7) on an IBM 1620 computer. In a six-dimensional system, there are $6^4 = 1296$ such elements. A hypothetical case was chosen for which $\tau_c|E|^2 = \tau_c|F|^2 = \tau_c EF^* = \tau_c E^*F = 1$. The symmetry rules of the first section and the spin-inversion property of the second section were verified for these elements. The relative widths for the observed lines of the A - and X -spectrum are given in table 2. There is no asymmetry present in the A -spectrum, and hence no absolute sign is determinable from this spectrum. A potential asymmetry is present in the X -spectrum, however. Strictly speaking, this asymmetry would allow the determination of the sign of $\gamma_A\gamma_BqQ$ relative to J_{ax} . But, with the signs of γ_A, γ_X and qQ tabulated elsewhere (and here taken to be positive), the absolute sign of J_{ax} could be determined. Unfortunately, this determination cannot be made in the present case. The transition $1 \rightarrow 2$ has a different width than its symmetrical transition $4 \rightarrow 5$ and the transition $2 \rightarrow 3$ has a different width than its symmetrical transition $5 \rightarrow 6$. However, $1 \rightarrow 2$ and $2 \rightarrow 3$ are degenerate, as are $4 \rightarrow 5$ and $5 \rightarrow 6$. The overlapping lines will have the same shape. Each doubly degenerate line is a composite; the composition of each is the same, and the spectrum is symmetric and does not yield the absolute sign of J_{ax} .

Line $i \rightarrow j$	Position ν_{ij}	Relative Width $-R_{ijjj}$
$1 \rightarrow 4$	$\nu_a + J_{ax}$	8.766
$2 \rightarrow 5$	ν_a	6.555
$3 \rightarrow 6$	$\nu_a - J_{ax}$	8.766
$1 \rightarrow 2$	$\nu_x + J_{ax}/2$	10.005
$2 \rightarrow 3$	$\nu_x + J_{ax}/2$	9.105
$4 \rightarrow 5$	$\nu_x - J_{ax}/2$	9.105
$5 \rightarrow 6$	$\nu_x - J_{ax}/2$	10.005

Table 2. Positions and relative widths. A - and X -spectra of an AX system.

This problem was stimulated by members of the author's thesis examination committee at Harvard University. The author thanks a referee for pointing out an error in an earlier version of this paper; the referee wishes it to be acknowledged that he would not have detected this error had he not had the existence of the cross-term between dipole-dipole coupling and chemical shift anisotropy pointed out to him in a private communication from Professor Shimizu. Acknowledgment is made to the donors of the Petroleum Research Fund, administered by the American Chemical Society, for support of this research.

REFERENCES

- [1] ABRAGAM, A., 1961, *The Principles of Nuclear Magnetism* (New York: Oxford University Press), p. 264ff.
- [2] BALDESCHWIELER, J. D., 1964, *J. chem. Phys.*, **40**, 459.
- [3] ANDERSON, J. M., 1963, Thesis, Department of Chemistry, Harvard University.
- [4] REDFIELD, A. G., 1957, *IBM J. Res.*, **1**, 19.
- [5] BALDESCHWIELER, J. D., 1964, *J. chem. Phys.*, **40**, 459 (equations (2.9), (2.10), (2.11)).
- [6] ANDERSON, J. M., and BALDESCHWIELER, J. D., 1964, *J. chem. Phys.*, **40**, 3241.

- [7] ABRAGAM, A., 1961, *The Principles of Nuclear Magnetism* (New York: Oxford University Press), p. 289.
- [8] ABRAGAM, A., 1961, *The Principles of Nuclear Magnetism* (New York: Oxford University Press), p. 272.
- [9] FULTON, R. L., and BALDESCHWIELER, J. D., 1961, *J. chem. Phys.*, **34**, 1075.
- [10] ANDERSON, J. M., and BALDESCHWIELER, J. D., 1962, *J. chem. Phys.*, **37**, 39.
- [11] ANDERSON, J. M., and BALDESCHWIELER, J. D., 1963, *J. chem. Phys.*, **38**, 570.
- [12] ERNST, R., and ANDERSON, J. M., 1964, *J. chem. Phys.*, **40**, 3737.
- [13] POPL, J. A., SCHNEIDER, W. G., and BERNSTEIN, H. J., 1959, *High-resolution Nuclear Magnetic Resonance* (New York: McGraw-Hill), p. 31, equation (3-35).
- [14] POPL, J. A., 1958, *Mol. Phys.*, **1**, 168.

RESEARCH NOTES

On the proof of an identity

by G. DAS

Department of Physics, University of Chicago

(Received 8 April 1964)

In a recent article [1] the following identity was claimed to hold. However, no proof was given. (See equations (8·3) to (8·5) of Ref. [1].)

$$2 \frac{\Delta F}{kT} = \sum_{n=-\infty}^{+\infty} \log \frac{(\epsilon_1^2 + \xi_n^2)(\epsilon_2^2 + \xi_n^2)}{(\omega_1^2 + \xi_n^2)(\omega_2^2 + \xi_n^2)}, \quad (1)$$

where

$$\Delta F = F(\epsilon_1) + F(\epsilon_2) - F(\omega_1) - F(\omega_2) \quad (2)$$

with

$$F(\omega) = \frac{1}{2}\hbar\omega - kT \log \left[1 - \exp \left(-\frac{\hbar\omega}{kT} \right) \right] \quad (3)$$

and

$$\xi_n = \frac{2\pi n kT}{\hbar} = \alpha n, \quad \text{say.} \quad (4)$$

The equation (3), however, contains a small mistake. For, as is well-known, the partition function of a one-dimensional harmonic oscillator is given by:

$$z = \sum_{v=0}^{\infty} \exp \left[-\left(v + \frac{1}{2}\right) \frac{\hbar\omega}{kT} \right] = \frac{\exp \left(-\frac{\hbar\omega}{2kT} \right)}{1 - \exp \left(-\frac{\hbar\omega}{kT} \right)},$$

so that

$$F(\omega) = -kT \ln z = \frac{1}{2}\hbar\omega + kT \ln \left[1 - \exp \left(-\frac{\hbar\omega}{kT} \right) \right]. \quad (3')$$

With (3') in place of (3) the identity (1) will be established below:
Evaluation of the integral

$$\oint \pi f(z) \cot \pi z \, dz$$

over a contour at infinity containing the whole z -plane yields [2] the following formula:

$$\sum_{-\infty}^{+\infty} f(n) = -\sum \text{residues of } [\pi f(z) \cot \pi z] \text{ at all poles of } f(z). \quad (5)$$

Differentiating the right-hand side of (1) with respect to α as defined in (4), we have:

$$\frac{d}{d\alpha} \sum_{n=-\infty}^{+\infty} \log \frac{(\epsilon_1^2 + \alpha^2 n^2)(\epsilon_2^2 + \alpha^2 n^2)}{(\omega_1^2 + \alpha^2 n^2)(\omega_2^2 + \alpha^2 n^2)} = \sum_n \left[\frac{2\alpha n^2(\omega_1^2 - \epsilon_1^2)}{(\epsilon_1^2 + \alpha^2 n^2)(\omega_1^2 + \alpha^2 n^2)} + \frac{2\alpha n^2(\omega_2^2 - \epsilon_2^2)}{(\epsilon_2^2 + \alpha^2 n^2)(\omega_2^2 + \alpha^2 n^2)} \right]. \quad (6)$$

Now introducing the function:

$$f_1(z) = \frac{z^2}{(\epsilon_1^2 + \alpha^2 z^2)(\omega_1^2 + \alpha^2 z^2)}, \quad (7)$$

we have

$$\sum_{n=-\infty}^{\infty} \frac{n^2}{(\epsilon_1^2 + \alpha^2 n^2)(\omega_1^2 + \alpha^2 n^2)} = \sum \text{residues of } [\pi f_1(z) \cot \pi z] \text{ at poles of } f_1(z).$$

Residues at

$$\frac{i\epsilon_1}{\alpha}, \quad \frac{-i\epsilon_1}{\alpha}, \quad \frac{i\omega_1}{\alpha}, \quad \frac{-i\omega_1}{\alpha},$$

which are the only poles of $f_1(z)$, are, respectively:

$$\begin{aligned} \frac{\pi\epsilon_1}{2\alpha^3} \frac{\coth(\pi\epsilon_1/\alpha)}{\omega_1^2 - \epsilon_1^2}, \quad \frac{\pi\epsilon_1}{2\alpha^3} \frac{\coth(\pi\epsilon_1/\alpha)}{\omega_1^2 - \epsilon_1^2}, \\ \frac{\pi\omega_1}{2\alpha^3} \frac{\coth(\pi\omega_1/\alpha)}{\epsilon_1^2 - \omega_1^2}, \quad \frac{\pi\omega_1}{2\alpha^3} \frac{\coth(\pi\omega_1/\alpha)}{\epsilon_1^2 - \omega_1^2}, \end{aligned}$$

whence the series is evaluated. Evaluating the other series similarly the following expression for the derivative of (1) with respect to α is obtained:

$$\begin{aligned} -\frac{2\pi\epsilon_1}{\alpha^2} \coth \frac{\pi\epsilon_1}{\alpha} - \frac{2\pi\epsilon_2}{\alpha^2} \coth \frac{\pi\epsilon_2}{\alpha} \\ + \frac{2\pi\omega_1}{\alpha^2} \coth \frac{\pi\omega_1}{\alpha} + \frac{2\pi\omega_2}{\alpha^2} \coth \frac{\pi\omega_2}{\alpha}. \end{aligned}$$

Now directly differentiating $2(\Delta F/kT)$ with respect to α making use of the expression (3), we arrive obviously at the same expression as above. Hence the identity.

REFERENCES

- [1] McLACHLAN, A. D., GREGORY, R. D., and BALL, M. A., 1964, *Mol. Phys.*, **7**, 119.
- [2] MORSE, P. M., and FESHBACH, H., 1953, *Methods of Theoretical Physics*, Vol. I (McGraw-Hill Book Company Inc.), p. 413.

Note on the theory of dissociation pressures of gas hydrates

by ROBERT M. MAZO†

Institute of Theoretical Science and Department of Chemistry,
University of Oregon, Eugene, Oregon 97403

(Received 4 August 1964)

The cell theory of the gas hydrates [1] gives reasonably good results for the dissociation pressures of spherical and quasi-spherical solute molecules. For molecules which are not spherical, the calculated pressure is generally smaller than the observed pressure. The question arises: can this discrepancy be attributed, at least in part, to hindered rotation of a solute molecule in its cell? McKoy and Sinanoğlu [2] have argued that any such effect must be too small to matter. In this note we show that, regardless of the size of the effect, it is in the *wrong direction* to explain the discrepancy.

The theory gives [1]:

$$P = \frac{kT}{Q_1} \frac{y_1}{1-y_1} = \frac{kT}{Q_2} \frac{y_2}{1-y_2}, \quad (1)$$

$$\nu_1 \ln(1-y_1) + \nu_2 \ln(1-y_2) = -\Delta\mu/kT, \quad (2)$$

where P is the dissociation pressure of the solute, y_i is the fractional occupation of cells of type i , Q_i is the configurational partition function of a solute molecule in a cavity of type i , ν_i is the number of host molecules per cavity of type i . $\Delta\mu$, the chemical potential difference between the metastable and stable host lattices, is assumed independent of the occupation of the cells.

From (1) and (2) it follows that P decreases if Q_1 , say, increases. Let Q_1^a be the configurational partition function when the potential hindering rotation is taken into account, Q_1^s , the configurational partition function when the cell potential is taken to be the spherical average of the full aspherical potential. We show that $Q_1^a \geq Q_1^s$. Thus, taking hindered rotation into account can only lower the computed pressure.

The proof is remarkably simple. The potential energy of a solute molecule, $V(R, \Omega)$, can be written as a spherical part, $w(r)$, plus an aspherical deviation $v(R, \Omega)$:

$$V(R, \Omega) = w(R) + v(R, \Omega). \quad (3)$$

Here R denotes the distance of the centre of mass of the molecule from the centre of the cell, and Ω the orientational parameters of the molecule. The criterion for choosing w and v is that the average of v over all orientations should vanish, i.e. $w(R)$ is the orientational average of $V(R, \Omega)$ for fixed R . This is exactly the procedure used in [2].

Let $F_1^a = -kT \ln Q_1^a$ be the configurational free energy calculated from a Boltzmann factor with potential V , $F_1^s = -kT \ln Q_1^s$ that from a Boltzmann

† Alfred P. Sloan Fellow. This work was also supported by NSF grant GP 1951.

factor with potential w . It follows from a variational principle of statistical mechanics [3]† that

$$F_1^a \leq F_1^s + \langle v \rangle, \quad (4)$$

where $\langle v \rangle$ is the average of v weighted by $\exp(-w/kT)$. Hence:

$$Q_1^a \geq Q_1^s, \quad (5)$$

since, by construction, $\langle v \rangle$ vanishes.

Thus, explicit consideration of the aspherical part of an assumed potential can only lower the calculated pressure. However, as the calculations of McKoy and Sinanoğlu [2] show, the spherically averaged part of an aspherical potential may give a better representation of the field in the cavity than the simple Lennard-Jones-Devonshire average.

REFERENCES

- [1] VAN DER WAALS, J. H., 1959, *Advanc. chem. Phys.*, **2**, 1.
- [2] MCKOY, V., and SINANOĞLU, O., 1963, *J. chem. Phys.*, **38**, 2946.
- [3] GIRARDEAU, M., 1964, *J. chem. Phys.*, **40**, 899.

† W. Byers Brown has pointed out (*J. chem. Phys.*, to be published) that this variational principle can be found in the works of Gibbs.

Semi-classical analysis of weakly inelastic molecular collisions

by M. S. CHILD

Department of Chemistry, University of Glasgow, Scotland

(Received 12 May 1964)

Semi-classical analysis is applied to vibrationally and rotationally inelastic molecular collisions. The deflection angles for weak transitions are shown to be simply related to the classical deflection angles for elastic scattering under the initial and final conditions. The position of the crossing-point, at which the transition can occur without change of radial momentum, plays an important role in the discussion and expressions are derived for these points for systems undergoing rotational transitions. Finally it is shown that markedly inelastic behaviour recently observed in collisions between K and HBr is unlikely to arise from rotational transitions.

1. INTRODUCTION

This paper attempts to provide some physical insight into the mechanism which gives rise to inelastic behaviour during an intermolecular collision. Attention is confined to collisions between an atom A and a diatomic molecule BC; inelastic collisions, for the present argument, are those which involve a change in the vibrational or rotational state of BC. It will be further supposed that the collisions are sufficiently weakly inelastic to be treated by perturbation theory. With this restriction any quantum mechanical treatment of the problem is complicated by two factors. First, all translational waves are represented by infinite sums of partial waves and secondly one is required to evaluate radial integrals involving continuum wave functions. In a given case, of course, these difficulties can be surmounted with the help of high-speed computers, but this paper presents a more general algebraic treatment.

Following the established correspondence between the classical and quantum-mechanical theories of elastic scattering [1], we recognize that each partial wave in the infinite sum loosely represents the behaviour of a particle with a certain impact parameter. A limited number of outgoing partial waves therefore interfere constructively at any given scattering angle. Semi-classical arguments are used to approximate the radial integrals responsible for coupling the incident 'initial' partial waves to different 'final' waves. The most important integrals are those for which, at some classically accessible point R , the initial and final waves have the same de Broglie wavelength, and hence the same radial momentum. The Landau-Zener [2] formula can then be applied. The cases when R lies within the classically inaccessible region or too near to the classical turning points for semi-classical analysis are also investigated. In all cases the deflection angles for inelastic scattering may be simply obtained from the trajectories for elastic scattering under the initial and final conditions. Formulae for the various contributions to the differential scattering cross section are also derived.

The general theory is outlined in §2, where it is shown that the infinite sum which represents the scattering amplitude $f_i(\theta, \phi)$ into a given channel i may be composed of several distinct branches $f_i^{\Delta l}(\theta, \phi)$; each branch corresponds to a different change (Δl) in orbital angular momentum. The functions $f_i^{\Delta l}(\theta, \phi)$

are evaluated in § 3. Section 4 is devoted to the calculation of the crossing points R , which play an important part in the discussion, for rotational inelastic collisions. We note that when applied to the results of recent molecular beam experiments on the system $K + HBr$ [3], with some reservations this theory supports a remark by the authors to the effect that the apparently markedly inelastic behaviour at high scattering angles is unlikely to be due to rotational inelasticity; deviations of this type are expected to be small in this case, and they are probably most important between 15° and 35° . The appendices are devoted to mathematical considerations. Appendix A concerns the evaluation of semi-classical matrix elements and Appendix B the behaviour of the Airy function $Ai(t)$ near $t=0$.

2. GENERAL THEORY

Neglecting the motion of the centre of mass, the Hamiltonian for the system illustrated in figure 1 takes the form:

$$H = -\frac{\hbar^2}{2\mu} \nabla_\rho^2 - \frac{\hbar^2}{2m} \nabla_r^2 + V(r, \rho, \chi); \quad (1)$$

m and μ denote the reduced masses:

$$m = \frac{m_A(m_B + m_C)}{m_A + m_B + m_C} \quad \text{and} \quad \mu = \frac{m_B m_C}{m_B + m_C}. \quad (2)$$

The potential energy $V(r, \rho, \chi)$ may be conveniently expanded in Legendre polynomials:

$$V(r, \rho, \chi) = V_0(r, \rho) + V_1(r, \rho)P_1(\cos \chi) + \dots \quad (3)$$

Following the formal development of Bates's molecular wave function method for electronic transitions [4], at given r we find internal (vibrational-rotational) states $\phi_i(r, \rho)$ which satisfy:

$$\left[-\frac{\hbar^2}{2\mu} \nabla_\rho^2 + V_0(r, \rho) - W_i(r) \right] \phi_i(r, \rho) = 0, \quad (4)$$

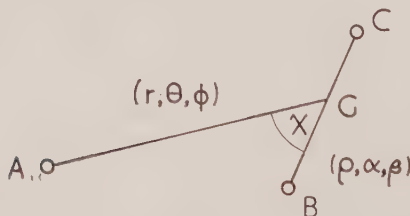


Figure 1. The coordinate system. G is the centre of mass of BC .

so that $W_i(r)$ denotes the instantaneous internal energy of BC . The total wave function is then taken in the form:

$$\Psi = \sum_i \psi_i(\mathbf{r}) \phi_i(r, \rho). \quad (5)$$

$\psi_i(\mathbf{r})$ therefore represents the relative motion of A and G when BC is in the internal state $\phi_i(r, \rho)$. The Schrödinger equation

$$(H - E)\Psi = 0 \quad (6)$$

then leads to the following set of coupled equations for the $\psi_i(\mathbf{r})$:

$$[\nabla_r^2 + k_i^2 - U_i(r)]\psi_i(\mathbf{r}) = \sum_j X_{ij}(\mathbf{r})\psi_j(\mathbf{r}), \quad (7)$$

where

$$k_i^2 = \frac{2m}{\hbar^2} [E - W_i(\infty)],$$

$$U_i(r) = \frac{2m}{\hbar^2} [W_i(r) - W_i(\infty)], \quad (8)$$

and

$$X_{ij}(\mathbf{r}) = \int \phi_i \left\{ \nabla_r^2 - \frac{2m}{\hbar^2} [V(r, \rho, \chi) - V_0(r, \rho)] \right\} \phi_j d^3\rho \\ + \int \phi_i \nabla_r \phi_j d^3\rho \cdot \nabla_r.$$

Allowance is therefore made for coupling induced by the variation with r of the internal wave functions $\phi_i(r, \rho)$. This may well be an important effect in potentially reactive systems. As for the form of $X_{ij}(\mathbf{r})$, which will be important later, if ϕ_i and ϕ_j differ by m in their azimuthal angular momentum quantum numbers, $X_{ij}(\mathbf{r})$ can be written in the form:

$$X_{ij}(\mathbf{r}) = \sum_{l=|m|}^L X_{ij}^l(r) P_l^m(\cos \theta) \exp(im\phi). \quad (9)$$

The upper limit L in equation (9) is the index of the last significant term in (3). In most practical problems this sum will therefore be quite short.

We now assume that the coupling terms X_{ij} are so small that equation (7) may be adequately solved by perturbation theory, using the method of distorted waves [1]. It is supposed that the system can be represented almost entirely by an elastically scattered wave with unit incident intensity,

$$\psi_0(\mathbf{r}) = \sum_{l_0=0}^{\infty} (2l_0+1) i^{l_0} \exp(i\eta_{l_0}) \frac{u_{l_0}(r)}{k_0 r} P_{l_0}^0(\cos \theta), \quad (10)$$

together with an appropriate initial internal state ϕ_0 . The functions $u_{l_0}(r)$ in equation (10) satisfy the following conditions:

$$\left\{ \frac{d^2}{dr^2} + k_0^2 - U_0(r) - \frac{l_0(l_0+1)}{r^2} \right\} u_{l_0}(r) = 0, \quad (11)$$

$$u_{l_0}(r) \sim \sin(k_0 r - l_0 \pi/2 + \eta_{l_0}).$$

$u_{l_0}(r)$ therefore clearly contains both incoming and outgoing waves. The remaining $\psi_i(\mathbf{r})$ must then satisfy:

$$\{\nabla_r^2 + k_i^2 - U_i(r)\} \psi_i(\mathbf{r}) = X_{0i}(\mathbf{r}) \psi_0(\mathbf{r}), \quad (12)$$

with boundary condition $\psi_i(\mathbf{r}) \sim \exp(ik_i r)$.

Equation (12) may be solved in terms of the corresponding Green's function [1]:

$$\begin{aligned} G_i(\mathbf{r}, \mathbf{r}') &= -\frac{1}{4\pi} \sum_{l_i=0}^{\infty} (2l_i+1) \frac{u_{l_i}(r) v_{l_i}(r')}{r r'} P_{l_i}(\cos \Theta) \quad \text{for } r' > r \\ &= -\frac{1}{4\pi} \sum_{l_i=0}^{\infty} (2l_i+1) \frac{v_{l_i}(r) u_{l_i}(r')}{r r'} P_{l_i}(\cos \Theta) \quad \text{for } r' < r, \end{aligned} \quad (13)$$

where

$$\cos \Theta = \cos \theta \cos \theta' + \sin \theta \sin \theta' \cos (\phi - \phi').$$

The functions $u_{l_i}(r)$ and $v_{l_i}(r)$ satisfy equations like (11), with the following boundary conditions:

$$\left. \begin{aligned} u_{l_i}(r) &\sim \sin(k_i r - l_i \pi/2 + \eta_{l_i}), \\ v_{l_i}(r) &\sim \frac{1}{k_i} \exp[i(k_i r - l_i \pi/2 + \eta_{l_i})]. \end{aligned} \right\} \quad (14)$$

$\psi_i(\mathbf{r})$ then takes the form:

$$\psi_i(\mathbf{r}) = \int_0^{\infty} G_i(\mathbf{r}, \mathbf{r}') X_{0i}(\mathbf{r}') \psi_0(\mathbf{r}') d^3 r'. \quad (15)$$

Consider first the angular part of the contribution to this integral from a single initial partial wave and a single term in the sum in (13). According to (9) the product $X_{0i}(\mathbf{r}') P_{l_0}^0(\cos \theta')$ must involve ϕ' only in the form $\exp(im\phi')$ and hence we can write:

$$\begin{aligned} &\int_0^{\pi} \int_0^{2\pi} \frac{(2l_0+1)(2l_i+1)}{4\pi k_0 k_i} P_{l_i}(\cos \Theta) X_{0i}(\mathbf{r}') P_{l_0}^0(\cos \theta') \sin \theta' d\theta' d\phi' \\ &= \sum_{\Delta l = -L}^L Y_{l_0 l_i}(\mathbf{r}') P_{l_i}^m(\cos \theta) \exp(im\phi), \end{aligned} \quad (16)$$

where $\Delta l = l_i - l_0$. Equation (16) provides the definition of the functions $Y_{l_0 l_i}(\mathbf{r}')$. The factors $(2l_0+1)/k_0 k_i$ are inserted for later convenience. It now only remains to define a corresponding set of radial integrals:

$$Z_{l_0 l_i} = \int_0^{\infty} u_{l_0}(r') Y_{l_0 l_i}(\mathbf{r}') u_{l_i}(r') dr', \quad (17)$$

and equation (15) takes the form:

$$\psi_i(\mathbf{r}) = \sum_{\Delta l = -L}^L f_i^{\Delta l}(\theta, \phi) \frac{\exp(ik_i r)}{r}, \quad (18)$$

where

$$f_i^{\Delta l}(\theta, \phi) = \sum_{l_i=0}^{\infty} i^{\Delta l} \exp[i(\eta_{l_0} + \eta_{l_i})] Z_{l_0 l_i} P_{l_i}^m(\cos \theta) \exp(im\phi). \quad (19)$$

Now in equation (19) $l_0 = l_i - \Delta l$ and hence $f_i^{\Delta l}(\theta, \phi)$ is the contribution to the scattering amplitude coming from processes which involve a change Δl in orbital

angular momentum. The total inelastic scattering amplitude in the channel i

$$f_i(\theta, \phi) = \sum_{\Delta l = -L}^L f_i^{\Delta l}(\theta, \phi), \quad (20)$$

and the corresponding differential scattering cross section $\sigma_i(\theta)$, is given by:

$$\sigma_i(\theta) = |f_i(\theta, \phi)|^2. \quad (21)$$

Note that ϕ enters equation (19) only as the common factor $\exp(im\phi)$ and hence $\sigma_i(\theta)$ is independent of ϕ .

In the following section expressions are derived for the $f_i^{\Delta l}(\theta, \phi)$ under various limiting conditions.

3. ANGULAR DISTRIBUTION

This section concerns the functions $f_i^{\Delta l}(\theta, \phi)$. Written as in (19) in the form of an infinite sum, $f_i^{\Delta l}(\theta, \phi)$ includes contributions from partial waves with all possible final orbital angular momenta (or in classical terms all possible impact parameters). We shall find however that at any given value of θ only a limited number of them make any significant contribution to the sum. Both $Z_{l_0 l_i}$ and $P_{l_i}^m(\cos \theta)$ in equation (19) are oscillating functions of l_i and hence $f_i^{\Delta l}(\theta, \phi)$ can be expressed as a combination of sub-branches of the form:

$$g(\theta, \phi) = \sum_{l_i=0}^{\infty} B(l_i, \theta, \phi) \exp[i\alpha(l_i, \theta)], \quad (22)$$

where $B(l_i, \theta, \phi)$ and $\alpha(l_i, \theta)$ are smoothly varying functions of l_i . Now at given θ , fluctuations in the second term in (22) lead to almost complete cancellations unless at some point $d\alpha/dl=0$ ($l_i=l_\theta$ say). If there is only one such point, by the method of stationary phase:

$$g(\theta, \phi) \simeq \sqrt{[2\pi/\alpha^{(2)}(l_\theta)]} B(l_\theta) \exp[i(\alpha(l_\theta) + \pi/4)]. \quad (23)$$

The stationary phase condition $d\alpha/dl=0$ can therefore be used to find that value of l_i at which the neighbouring outgoing partial waves contribute significantly to $g(\theta, \phi)$. Alternatively, one can fix l_i and ask in which directions the neighbouring partial waves interfere most constructively. The latter approach is more convenient at present. The fact that $\alpha(l, \theta)$ depends only on θ and not on ϕ and hence that the stationary phase condition determines only the scattering angle θ for given l_i , does not necessarily imply that the trajectories for inelastic scattering are restricted to the plane containing the 'incident' trajectory. This is true only when the azimuthal quantum number $m=0$. For $m \neq 0$, in order to conserve the azimuthal component of total angular momentum the scattered particle must spiral out around the incident direction; the shape of the spiral depends on θ .

In order to treat the $f_i^{\Delta l}(\theta, \phi)$ of equation (19) in this way, we now proceed to examine the variation with l_i of the Legendre functions $P_{l_i}^m(\cos \theta)$ and the radial integrals $Z_{l_0 l_i}$. Those $P_{l_i}^m(\cos \theta)$ for which $|l_i \sin \theta| \gg 0$ and $l_i \gg |m|$ may be expressed in asymptotic form:

$$P_{l_i}^m(\cos \theta) \simeq \sqrt{\left(\frac{2}{\pi \sin \theta}\right)} (l_i + \frac{1}{2})^{m-1/2} \cos \left[(l_i + \frac{1}{2})\theta + \frac{m\pi}{2} - \frac{\pi}{4} \right], \quad (24)$$

and we shall restrict attention to this range of l_i . Approximate expressions for the $Z_{l_0 l_i}$ are derived in Appendix A. These integrals vanish almost completely

unless at some point $r = R_{l_0 l_i}$ the radial wave functions $u_{l_0 l_i}(r)$ and $u_l(r)$ have the same de Broglie wavelength, in which case the transition can occur without change in radial momentum. The important range of integration lies immediately around this point (see § 51 of reference [6]) so $R_{l_0 l_i}$ may be meaningfully described as the transition point. The magnitude of the integral depends on the relation of $R_{l_0 l_i}$ to classical turning points a_{l_0} and a_{l_i} for $u_{l_0}(r)$ and $u_{l_i}(r)$ respectively. Three distinct cases are considered in Appendix A: (i) $R_{l_0 l_i} \gg a_{l_0}, a_{l_i}$, (ii) $R_{l_0 l_i} \simeq a_{l_0}, a_{l_i}$ and (iii) $R_{l_0 l_i} \ll a_{l_0}, a_{l_i}$. (The extent to which these cases cover the entire range $0 < R_{l_0 l_i} < \infty$ is also investigated.) Figure 2 applies to case (i) when $R_{l_0 l_i}$ is classically accessible. In this figure $E_i = k_i^2 \hbar^2 / 2m$ and $V_{l_i}(r) = V_i(r) + l_i(l_i + 1)\hbar^2 / 2mr^2$. The double-headed arrows measure the initial and final kinetic energies and these must be equal at the transition point $R_{l_0 l_i}$.

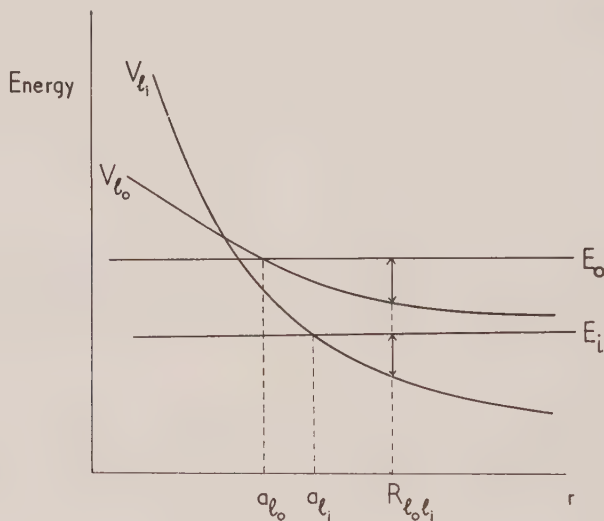


Figure 2. The dispositions of a_{l_0} , a_{l_i} and $R_{l_0 l_i}$ in case (i). V_{l_0} and V_{l_i} are the effective potential energy functions for the coupled initial and final partial waves; $R_{l_0 l_i}$ is the point at which the initial and final kinetic energies are equal.

3.1. Case (i) $R_{l_0 l_i} \gg a_{l_0}, a_{l_i}$

According to equations (19), (24) and (A 5), in this case the important part of the sum becomes:

$$f_i^{\Delta l}(\theta, \phi) = \sum_{l_i} B^{\Delta l}(l_i, \theta, \phi) \sqrt{p(R_{l_0 l_i})} \exp[i(\eta_{l_0} + \eta_{l_i})] \sin(\xi_{l_0} - \xi_{l_i} + \pi/4) \\ \times \cos\left[(l_i + \frac{1}{2})\theta + \frac{m\pi}{2} - \frac{\pi}{4}\right], \quad (25)$$

where

$$B^{\Delta l}(l_i, \theta, \phi) = \sqrt{\left(\frac{2}{\pi \sin \theta}\right)} (l_i + \frac{1}{2})^{m-1/2} T_{l_0 l_i}.$$

The functions $p(R_{l_0 l_i})$, $T_{l_0 l_i}$ and ξ_{l_i} are defined by equations (A 2) and (A 5).

$f_i^{\Delta l}(\theta, \phi)$ therefore contains four separate sub-branches, but barring rainbow-scattering only two of them include a point of stationary phase. For a repulsive potential for instance η_{l_0} and η_{l_i} increase with l_i ($l_0 = l_i - \Delta l$) and the stationary phase condition together with the demand that $\theta > 0$ lead to the following equations for θ :

$$\text{and } \left. \begin{aligned} \theta_+ &= \frac{\partial}{\partial l_i} (\eta_{l_0} + \eta_{l_i} + \xi_{l_0} - \xi_i) \\ \theta_- &= \frac{\partial}{\partial l_i} (\eta_{l_0} + \eta_{l_i} - \xi_{l_0} + \xi_{l_i}). \end{aligned} \right\} \quad (26)$$

θ_+ and θ_- therefore roughly represent the two possible scattering angles for particles with initial and final angular momenta l_0 and $l_i = l_0 + \Delta l$ respectively.

The existence of two significant sub-branches in $f_i^{\Delta l}(\theta, \phi)$ and two possible scattering angles has a simple physical explanation. There is a well-known connection between the semi-classical phase shift

$$\eta_{l_i} = \frac{1}{\hbar} \int_{a_{l_i}}^{\infty} p_{l_i}(r) dr - \int_{b_{l_i}}^{\infty} \sqrt{[k_i^2 - (l_i + \frac{1}{2})^2/r^2]} dr, \quad (27)$$

and the deflection angle for elastic scattering, namely:

$$\chi_{l_i}(-\infty, a_{l_i}) = \chi_{l_i}(a_{l_i}, \infty) = \partial \eta_{l_i} / \partial l_i. \quad (28)$$

In this notation $\chi_{l_i}(-x_1, x_2)$ and $\chi_{l_i}(x_1, x_2)$ are the angles between radii at $r = x_1$ and x_2 on the trajectories for incoming and outgoing motion respectively. Using the definition of the ξ_{l_i} in equation (A 5) and following similar arguments we find that

$$\left. \begin{aligned} \theta_+ &= \chi_{l_0}(-\infty, a_{l_0}) + \chi_{l_0}(a_{l_0}, R_{l_0 l_i}) + \chi_{l_i}(R_{l_0 l_i}, \infty), \\ \theta_- &= \chi_{l_0}(-\infty, -R_{l_0 l_i}) + \chi_{l_i}(-R_{l_0 l_i}, a_{l_i}) + \chi_{l_i}(a_{l_i}, \infty). \end{aligned} \right\} \quad (29)$$

In the present case the transition point $R_{l_0 l_i}$ is classically accessible and the particle must pass through it twice. The two branches correspond to the possibility that the transition may occur on either occasion. Equation (29) shows that the deflection angle may be found simply by following the classical trajectory for elastic scattering under the initial conditions and then changing to the appropriate 'final' trajectory. This situation is illustrated in figure 3 (a). It is interesting to find that the scattering angle θ is independent of m , although of course this is not necessarily true of the total scattering *amplitude*, which depends on the angular integrals $Y_{l_0 l_i}$ of equation (16).

As for the magnitude of $f_i^{\Delta l}(\theta, \phi)$, according to equations (23) and (25) it will contain the contributions:

$$\left[\frac{1}{4} \sqrt{\left(2\pi / \left| \frac{\partial \theta}{\partial l_i} \right| \right)} B^{\Delta l}(l_i, \theta_{\pm}, \phi) \sqrt{[p(R_{l_0 l_i})] \exp[i\alpha(l_i)]} \right]_{l_i = l_0 \pm} \quad (30)$$

from partial waves whose transition points lie in this region. In equation (30) the upper or lower signs are to be taken together and

$$\alpha(l_\theta) = [\eta_{l_0} + \eta_{l_i} - (l_\theta + \frac{1}{2})\theta]_{\pm} - (m-1)\pi/2 \pm (\xi_{l_0} - \xi_{l_i} - \pi/4)]_{l_i=l_\theta}. \quad (31)$$

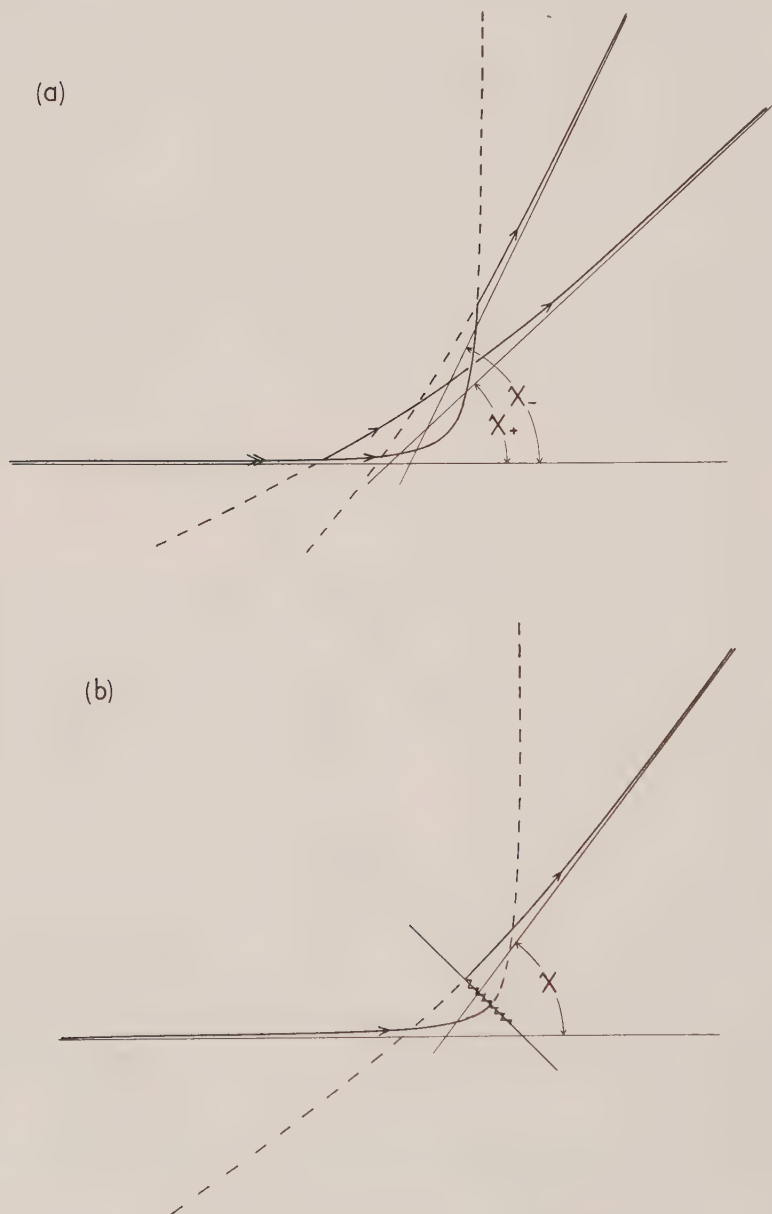


Figure 3. Inelastic scattering trajectories: (a) crossing point classically accessible; (b) crossing point classically inaccessible. The zig-zag line in (b) denotes quantum mechanical tunnelling to and from the crossing point.

For a given value of θ of course partial waves whose crossing points lie outside the present range may also contribute to $f_i^{\Delta}(\theta, \phi)$.

3.2. Case (ii) $R_{l_0 l_i} \simeq a_{l_0}, a_{l_i}$

In this case, according to equation (A 8), the integral $Z_{l_0 l_i}$ comes out in terms of an Airy function $\text{Ai}(t)$:

$$Z_{l_0 l_i} = \sqrt{\pi} T_{l_0 l_i} p_{0i}^{-1/2} \text{Ai}(t). \quad (32)$$

The origin of t corresponds to the critical value of l_i (l_* say) at which

$$R_{l_0 l_i} = a_{l_0} = a_{l_i} = a, \quad (33)$$

and it is therefore natural to expand the initial and final kinetic energies for neighbouring partial waves in the form:

$$\frac{1}{2m} [p_i(r)]^2 \simeq F_i(r-a) + G_i(l_* - l_i). \quad (34)$$

Direct substitution in (A 9) then leads to:

$$t = q(l_i - l_*), \quad (35)$$

where

$$q = \frac{1}{2m p_{0i}^2} \left(\frac{F_0 G_i - F_i G_0}{F_0 - F_i} \right). \quad (36)$$

t probably takes this simple form only for l_i very close to l_* ; but even for larger values of $|l_i - l_*|$, when t is a more complicated function of l_i , it is always true that t is positive when $R_{l_0 l_i} < a_{l_0}, a_{l_i}$ and negative when $R_{l_0 l_i} > a_{l_0}, a_{l_i}$. We should also note from equation (A 12) that

$$\frac{2}{3} |t|^{3/2} = \xi_{l_0} - \xi_{l_i}. \quad (37)$$

Now $\text{Ai}(t)$ can be written:

$$\text{Ai}(t) = F(t) \sin \lambda(t), \quad (38)$$

and this is the most convenient form for the present discussion. The auxiliary functions $F(t)$, $\lambda(t)$ and $\lambda'(t)$ are tabulated in Appendix B.

The significant part of $f_i^{\Delta l}(\theta, \phi)$ therefore becomes:

$$\begin{aligned} f_i^{\Delta l}(\theta, \phi) = \sum_{l_i} B^{\Delta l}(l_i, \theta, \phi) \sqrt{(\pi/p_{0i})} \exp[i(\eta_{l_0} + \eta_{l_i})] F(t) \sin \lambda(t) \\ \times \cos \left[(l_i + \frac{1}{2})\theta + \frac{m\pi}{2} - \frac{\pi}{4} \right]. \end{aligned} \quad (39)$$

Note that in the light of equations (A 9), (A 12) and (B 6) as $t \rightarrow -\infty$, equation (39) tends asymptotically to the form of (25), the corresponding equation for case (i). We see moreover from equation (39) that there are again four separate sub-branches, only two of which contain a point of stationary phase. For a repulsive potential the two stationary phase conditions are now:

$$\theta_{\pm} = \frac{\partial}{\partial l_i} (\eta_{l_0} + \eta_{l_i}) \pm \lambda'(t) \frac{\partial t}{\partial l_i}. \quad (40)$$

The separation between the two possible scattering angles for given l_i therefore depends on $\lambda'(t)$.

We see from (A 8) to (A 12) that for $t \ll 0$ the present case goes over exactly to case (i). As t increases however it is clear from the table in Appendix B that $\lambda'(t)$ decreases; in fact

$$\lambda'(t) \rightarrow -2t^{1/2} \text{sech}(\frac{4}{3}t^{3/2}) \quad \text{as } t \rightarrow \infty. \quad (41)$$

θ_+ and θ_- therefore tend to a common value as $R_{l_0 l_i}$ retreats deeper into the classically inaccessible region.

The two contributions to $f_i^{\Delta l}(\theta, \phi)$ have formally the same form as in (30), namely:

$$[\frac{1}{4}\sqrt{2\pi/|(\partial\theta_{\pm}/\partial l_i)|}]B^{\Delta l}(l_i, \theta, \phi)\sqrt{(\pi/p_{0i})}F(t)\exp[i\alpha(l_i)]_{l_i=l_{\theta\pm}} \quad (42)$$

where

$$\alpha(l_{\theta\pm}) = [\eta_{l_0} + \eta_{l_i} - (l_i + \frac{1}{2})\theta_{\pm} - (m-1)\pi/2 \pm (\lambda(t) - \pi/2)]_{l_i=l_{\theta\pm}}. \quad (43)$$

The behaviour of equation (42) for large values of t merits some consideration however. The table in Appendix B reveals that $F(t)$ increases quite sharply with t for $t > 0$, and in fact:

$$F(t) \sim \pi^{-1/2}t^{-1/4}[\cosh(\exp \frac{4}{3}t^{3/2})]^{-1/4}. \quad (44)$$

On the other hand, in view of the factors $\mp \pi/2$ in equation (43) the two contributions to $f_i^{\Delta l}(\theta, \phi)$ come in with opposite sign and will therefore tend to cancel. We have seen that $l_{\theta+}$ and $l_{\theta-}$ must tend towards each other and that $\lambda(t) \rightarrow 0$ as t increases so this cancellation becomes more and more complete. The net result of these two opposing factors is actually to reduce the overall value of $f_i^{\Delta l}(\theta, \phi)$ as $t \rightarrow \infty$. This follows from the cruder approximation:

$$\text{Ai}(t) \simeq \frac{1}{2}\pi^{-1/2}t^{-1/4}\exp(-\frac{2}{3}t^{3/2}) \quad (45)$$

for $t > 1$. In this form $\text{Ai}(t)$ contains no fluctuating term so there can be only one significant sub-branch in $f_i^{\Delta l}(\theta, \phi)$ and only one possible scattering angle, namely:

$$\theta = \frac{\partial}{\partial l}(\eta_{l_0} + \eta_{l_i}). \quad (46)$$

$f_i^{\Delta l}(\theta, \phi)$ must moreover contain the negative exponential term $\exp(-\frac{2}{3}t^{3/2})$, a physically acceptable result since for $t > 0$ $u_{l_0}(r)$ and $u_{l_i}(r)$ must tunnel into the classically inaccessible region to reach the transition point $R_{l_0 l_i}$. See figure 3 (b).

3.3. Case (iii) $R_{l_0 l_i} \ll a_{l_0}, a_{l_i}$

This case now offers no additional features. According to equation (A 14)

$$Z_{l_0 l_i} = \frac{1}{2}T_{l_0 l_i}[|p(R_{l_0 l_i})|]^{1/2}\exp(-|\xi_{l_0} - \xi_{l_i}|), \quad (47)$$

which has the same form as $\text{Ai}(t)$ in (45). The scattering angle, given by equation (46), is the mean deflection angle for classical elastic scattering under the initial and final conditions and the scattering amplitude $f_i^{\Delta l}(\theta, \phi)$ contains the contribution:

$$[\frac{1}{2}\sqrt{2\pi(\partial\theta/\partial l)}]\exp(-|\xi_{l_0} - \xi_{l_i}|)B^{\Delta l}(l_i, \theta, \phi)\sqrt{(|p(R_{l_0 l_i})|)\exp(i\alpha(l_{\theta}))}_{l_i=l_{\theta}},$$

where

$$\alpha(l_{\theta}) = [\eta_{l_0} + \eta_{l_i} - (l_i + \frac{1}{2})\theta]_{l_i=l_{\theta}}.$$

3.4. Summary

The most interesting conclusions from this section concern the trajectories of particles with different orbital angular momenta. For those partial waves whose transition points are classically accessible there are two possible scattering angles θ_+ and θ_- given by equation (29); they may be obtained quite simply from the 'initial' and 'final' trajectories for classical elastic scattering as shown in figure 3 (a). In passing through the critical region where $R_{l_0 l_i}$ lies near a_{l_0} and a_{l_i} ,

θ_+ and θ_- converge towards a common value until finally there is essentially only one possible scattering angle θ for those partial waves for which $R_{l_0 l_i}$ lies deep in the classically inaccessible region; θ is then the mean deflection angle for classical elastic scattering under the initial and final conditions. In this last situation the factor $\exp(-|\xi_{l_0} - \xi_{l_i}|)$ in the formula for the scattering amplitudes represents the difficulty of tunnelling beyond a_{l_0} , a_{l_i} to reach $R_{l_0 l_i}$.

4. CROSSING POINTS FOR ROTATIONAL TRANSITIONS

In view of the importance of the position of the crossing point (or transition point) $R_{l_0 l_i}$, it is interesting to investigate its relationship to the classical turning points a_{l_0} , a_{l_i} , as a function of l_i . We shall at present restrict attention to purely rotational excitations.

In this case $U_i(r) = U_0(r)$ in equations (7) and (8), and at the transition point

$$k_0^2 - l_0(l_0 + 1)/R_{l_0 l_i}^2 = k_i^2 - l_i(l_i + 1)/R_{l_0 l_i}^2, \quad (48)$$

where

$$k_i^2 = 2mE/\hbar^2 - j_i(j_i + 1)(m/\mu\rho_v^2). \quad (49)$$

$\mu\rho_v^2$ is the effective moment of inertia of BC in the given vibrational state. Hence

$$R_{l_0 l_i}^2 = - \frac{(l_i - l_0)(l_i + l_0 + 1)}{(j_i - j_0)(j_i + j_0 + 1)} \frac{\mu\rho_v^2}{m}. \quad (50)$$

Real values of $R_{l_0 l_i}$ therefore correspond to transitions for which $l_i > l_0$ and $j_i < j_0$ (or vice versa). Moreover, for given Δj the larger the magnitude of Δl , the more likely is it that $R_{l_0 l_i}$ is classically accessible. Now with a potential of the form given in (3) $|\Delta l|$ cannot exceed $|\Delta j|$ and hence equation (50) implies a weak angular momentum selection rule; transitions for which $\Delta l = -\Delta j$ are strongly preferred.

The question remains under what circumstances is $R_{l_0 l_i}$ classically accessible. Consider first the special case of a potential of the form:

$$U_0(r) = U_i(r) = A/r^2. \quad (51)$$

The formula for the classical turning point then becomes:

$$a_{l_i}^2 = \frac{l_i(l_i + 1) + A}{k_i^2}. \quad (52)$$

If l_m and δl are defined by the equations $l_m = l_0 - \delta l = l_i + \delta l$, $R_{l_0 l_i}$ coincides with a_{l_i} for the following values of l_m :

$$l_m = l_{\pm} = K\delta l - \frac{1}{2} \pm \frac{1}{2} \sqrt{[1 + 4(K^2 - 1)\delta l^2 - 4A]}, \quad (53)$$

where

$$K = (k_0^2 + k_i^2)/(k_0^2 - k_i^2).$$

(For a real transition point note that $K\delta l > 0$.) Provided therefore that the roots of equation (53) are real, provided that is that

$$1 + 4(K^2 - 1)\delta l^2 > 4A, \quad (54)$$

there will be a range of l_m values ($l_- < l_m < l_+$) for which $R_{l_0 l_i}$ is classically accessible and the corresponding partial waves will contribute most to the inelastic scattering amplitude. It may happen however that equation (53) has no real solutions in which case the inelastic scattering amplitude will probably be small. In this case

the most strongly coupled partial waves will be those for which $l_m = \mathcal{R}(l_{\pm}) = K\delta l - \frac{1}{2}$, because $R_{l_0 l_i}$ will then be most nearly classically accessible. Notice that equation (54) is most easily satisfied by large values K ; in other words the most likely collisions are those which involve small proportional changes in energy.

The qualitative conclusions from the above discussion are not limited to the chosen particularly convenient potential form. For any common potential function, steeply repulsive as $r \rightarrow 0$ and bounded at infinity, there will either be a range of l_m , $l_- < l_m < l_+$ (or possibly several ranges) for which $R_{l_0 l_i}$ is classically accessible or, if $R_{l_0 l_i}$ is always inaccessible, there will be one value of l_m for which it lies nearest to a_{l_0} and a_{l_i} . An attractive potential will tend to increase the range $l_- < l_m < l_+$ and a strongly repulsive one will reduce it. The l_m values, whose partial waves contribute most to the inelastic scattering cross section, are not necessarily small.

The Lennard-Jones (6-12) and Buckingham (exp 6) potentials are particularly convenient for this type of discussion because the form of a_l as a function of l may be extracted from published tables [8, 9]. In this context it is interesting to examine the results of a recent molecular beam investigation of collisions between K and HBr [3], which showed markedly inelastic behaviour at high scattering angles. The authors assume an exp-6 form for the spherical part of the scattering potential:

$$V(r) = \frac{\epsilon}{1 - (6\alpha)} \left[\frac{6}{\alpha} \exp \left[\alpha \left(1 - \frac{r}{r_m} \right) \right] - \left(\frac{r_m}{r} \right)^6 \right], \quad (55)$$

with the parameter values $\epsilon = 0.55$ kcal/mole, $\alpha = 12$ and $r_m = 4.5$ Å chosen to fit the low angle elastic scattering. The experiment was carried out over a range of values of relative kinetic energy (\bar{E}) from 1.49 kcal/mole to 4.49 kcal/mole and, at the temperature in the HBr beam (155°K), the most probable rotational state has $j = 2$. Examination of the published tables [9] shows that for the transition $\Delta j = 1 \leftarrow 2$ (for which $\Delta E \simeq 0.10$ kcal/mole) the crossing point always lies well within the classically inaccessible region. The tables do not permit exact comparison with the experimental values of \bar{E} , but for $\bar{E} = 5.5$ kcal/mole the least classically inaccessible transition point occurs at $l_0 \simeq 210$. For this partial wave $a_{l_0} \simeq 3.90$ Å, $R_{l_0 l_i} \simeq 2.60$ Å and the corresponding 'initial' scattering angle $\chi_{l_0} \simeq 35^\circ$. The corresponding figures for $\bar{E} = 2.75$ kcal/mole are $l_0 \simeq 160$, $a_{l_0} \simeq 3.92$ Å, $R_{l_0 l_i} \simeq 2.27$ Å and $\chi_{l_0} \simeq 30^\circ$. $R_{l_0 l_i}$ only becomes classically accessible when $\bar{E} < 20$ kcal/mole. The only rotational transition for which the situation is more favourable is $\Delta j = 0 \leftarrow 1$, but again $R_{l_0 l_i}$ is always classically inaccessible. In this case the figures for the most strongly coupled initial partial wave are as follows: at $\bar{E} = 5.5$ kcal/mol $l_0 \simeq 225$, $a_{l_0} \simeq 3.90$ Å, $R_{l_0 l_i} \simeq 3.78$ Å and $\chi_{l_0} \simeq 22.5^\circ$, and at $\bar{E} = 2.75$ kcal/mole $l_0 \simeq 175$, $a_{l_0} \simeq 4.04$ Å, $R_{l_0 l_i} \simeq 3.33$ Å and $\chi_{l_0} \simeq 15^\circ$.

On the basis of the chosen type of potential, these figures support the view of the authors [3] that the markedly inelastic behaviour at high scattering angles cannot be attributed to rotational transitions. The most important deviations due to rotational inelasticity are expected between 15° and 35° and in the present case even these are likely to be small. It is not clear however that the form of potential given in equation (55) is the only one which would cause the observed

low angle scattering [11] and this point cannot be definitely settled without more detailed information about the state of the system after collision.

The author is grateful to Professor D. R. Herschbach and Mr. R. J. Cross for interesting discussions on this subject. The work was partly carried out at the Lawrence Radiation Laboratory, University of California, Berkeley, under contract with the United States Atomic Energy Commission.

APPENDIX A

Semi-classical matrix elements

The integrals to be evaluated take the form

$$Z_{01} = \int_0^\infty u_0(r) Y(r) u_1(r) dr, \quad (\text{A } 1)$$

where $u_i(r)$ are radial wave functions for motion under total energy E_i and effective potential energy $V_i(r)$. The expressions which follow also involve the radial momenta $p_i(r)$, the forces $F_i(r)$ exerted by $V_i(r)$, the classical turning points a_i and the transition point R_{01} . These quantities are defined as follows:

$$\left. \begin{aligned} p_i(r) &= \sqrt{2m(E_i - V_i(r))}, \\ F_i(r) &= \partial V_i / \partial r, \\ E_i - V_i(a_i) &= 0, \\ E_0 - V_0(R_{01}) &= E_1 - V_1(R_{01}). \end{aligned} \right\} \quad (\text{A } 2)$$

It is assumed for the sake of argument that $F_0 > F_1$.

The effective range of integration is known to be restricted to the neighbourhood of R_{01} (see Landau and Lifshitz [6], § 51), so that

$$Z_{01} \simeq Y(R_{01}) \int_0^\infty u_0(r) u_1(r) dr, \quad (\text{A } 3)$$

and there are three distinct cases to be considered.

(i) $R_{01} \gg a_0, a_1$

Near R_{01} the wave functions are adequately represented by the W.K.B. approximations

$$u_i(r) = \sqrt{\left(\frac{\hbar k_i}{p_i(r)}\right)} \sin\left(\frac{1}{\hbar} \int_{a_i}^r p_i(r) dr + \pi/4\right). \quad (\text{A } 4)$$

Following Landau [2] directly we find that

$$\begin{aligned} Z_{01} &= \frac{1}{2} \left[\frac{2\pi\hbar^3 k_0 k_1 Y^2}{m p(F_0 - F_1)} \right]^{1/2} \sin(\xi_0 - \xi_1 + \pi/4) \\ &= T_{01} [p(R_{01})]^{-1/2} \sin(\xi_0 - \xi_1 + \pi/4) \quad \text{say,} \end{aligned} \quad (\text{A } 5)$$

where

$$\xi_i = \frac{1}{\hbar} \int_{a_i}^{R_{01}} p_i(r) dr.$$

(ii) $R_{01} \simeq a_0, a_1$

In this case the W.K.B. approximations break down near R_{01} , but the kinetic energy may be taken roughly proportional to r :

$$E_i - V_i(r) \simeq F_i(r - a_i). \quad (\text{A } 6)$$

With this approximation the $u_i(r)$ can be represented exactly by Airy functions (see (A 10)) involving $(r - a_i)$. The integral is more easily carried out however in terms of the momentum representatives (see p.72 of ref. [6])

$$\alpha_i(p) = \frac{1}{2} \sqrt{\left(\frac{\hbar k_i}{m F_i}\right)} \exp \left\{ -i \left(\frac{a_i p}{\hbar} + \frac{p^3}{6 m \hbar F_i} \right) \right\}. \quad (\text{A } 7)$$

Then

$$\begin{aligned} Z_{01} &= Y(R) \int_{-\infty}^{\infty} \alpha_0^*(p) \alpha_1(p) dp \\ &= \sqrt{\pi} T_{01} p_{01}^{-1/2} \text{Ai}(t), \end{aligned} \quad (\text{A } 8)$$

where

$$\begin{aligned} p_{01} &= \left(\frac{2 m \hbar F_0 F_1}{F_0 - F_1} \right)^{1/3}, \\ t &= -(p(R_{01})/p_{01})^2 \end{aligned} \quad (\text{A } 9)$$

and the Airy function

$$\text{Ai}(t) = \frac{1}{\pi} \int_0^{\infty} \cos \left(ut + \frac{1}{3} u^3 \right) du. \quad (\text{A } 10)$$

Consider now the asymptotic limit of (A 8) for large negative t ($t < 0$ corresponds to real $p(R_{01})$, i.e. $R_{01} > a_0, a_1$)

$$\text{Ai}(t) \simeq \pi^{-1/2} |t|^{-1/4} \sin \left(\frac{2}{3} |t|^{3/2} + \pi/4 \right), \quad (\text{A } 11)$$

and over the region where (A 6) applies:

$$\begin{aligned} \xi_0 - \xi_1 &= \frac{1}{\hbar} \left[\int_{a_0}^{R_{01}} p_0(r) dr - \int_{a_1}^{R_{01}} p_1(r) dr \right] \\ &= \frac{2}{3} t^{3/2}. \end{aligned} \quad (\text{A } 12)$$

Hence in the light of (A 9), within the limits of accuracy of (A 6) at $t = -1$, (A 5) is the exact asymptotic limit of (A 8).

(iii) $R_{01} \ll a_0, a_1$

This case may likewise be treated as the asymptotic limit of case (ii) for large positive t . It follows directly from the limiting expression for $t > 1$:

$$\text{Ai}(t) \sim \frac{1}{2} \pi^{-1/2} t^{-1/4} \exp \left(-\frac{2}{3} t^{3/2} \right) \quad (\text{A } 13)$$

that in this case

$$Z_{01} = \frac{1}{2} T_{01} [p(R_{01})]^{-1/2} \exp \left(-|\xi_0 - \xi_1| \right). \quad (\text{A } 14)$$

APPENDIX B

The behaviour of $\text{Ai}(t)$ near $t=0$.

A short table of auxiliary functions for the Airy integral

$$\text{Ai}(t) = F(t) \sin \lambda(t).$$

The values of $F(t)$ and $\lambda(t)$ are taken from published tables [10] and those of $\lambda'(t)$ calculated from the equation:

$$[F(t)]^2 \lambda'(t) = \text{Ai}'(t) \text{Bi}(t) - \text{Bi}'(t) \text{Ai}(t).$$

t	$F(t)$	$\lambda(t)$	$-\lambda'(t)$	$F(-t)$	$\lambda(-t)$	$-\lambda'(-t)$
0.0	0.7101	0.5236	0.6313	0.7101	0.5236	0.6313
0.1	0.7374	0.4628	0.5854	0.6855	0.5890	0.6773
0.2	0.7681	0.4065	0.5396	0.6635	0.6591	0.7231
0.3	0.8025	0.3548	0.4943	0.6435	0.7337	0.7686
0.4	0.8413	0.3076	0.4498	0.6255	0.8128	0.8136
0.5	0.8851	0.2648	0.4063	0.6091	0.8964	0.8580
0.6	0.9349	0.2263	0.3642	0.5941	0.9843	0.9014
0.7	0.9915	0.1920	0.3238	0.5804	1.0767	0.9448
0.8	1.0562	0.1615	0.2828	0.5679	1.1733	0.9871
0.9	1.1301	0.1348	0.2492	0.5563	1.2741	1.0287
1.0	1.2150	0.1116	0.2156	0.5456	1.3790	1.0694
1.2	1.4251	0.7454	0.1567	0.5264	1.6009	1.1486
1.4	1.7056	0.4812	0.1094	0.5098	1.8382	1.2246
1.6	2.0834	0.3002	0.0733	0.4953	2.0905	1.2977
1.8	2.5963	0.1812	0.0472	0.4824	2.3571	1.3680
2.0	3.2983	0.1059	0.0293	0.4709	2.6376	1.4357

The auxiliary functions $F(t)$, $\lambda(t)$ and $\lambda'(t)$.

REFERENCES

- [1] MOTT, N. F., and MASSEY, H. S. W., 1949, *The Theory of Atomic Collisions* (Oxford: Clarendon Press).
- [2] LANDAU, L. D., 1932, *Z. Phys. Sov. Un.*, **2**, 46.
- [3] BECK, D., GREENE, E. F., and ROSS, J., 1962, *J. chem. Phys.*, **37**, 2895.
- [4] BATES, D. R., MASSEY, H. S. W., and STEWART, A. L., 1953, *Proc. roy. Soc. A*, **216**, 437.
- [5] HOBSON, E. W., 1931, *The Theory of Spherical and Ellipsoidal Harmonics* (Cambridge).
- [6] LANDAU, L. D., and LIFSHITZ, E. M., 1958, *Quantum Mechanics* (Addison-Wesley).
- [7] FORD, K. W., and WHEELER, J. A., 1959, *Annals of Phys.*, **7**, 259.
- [8] HIRSCHFELDER, J. O., CURTISS, C. F., and BIRD, R. B., *Molecular Theory of Gases and Liquids* (New York).
- [9] MASON, E. A., 1957, *J. chem. Phys.*, **26**, 667.
- [10] MILLER, J. C. P., 1946, *B.A. Mathematical Tables*, pt. vol. B (Cambridge).
- [11] HERSCHBACH, D. R., and KWEI, G. H., 1963, *Lawrence Radiation Laboratory Report UCRL-11178* (Berkeley, California).

Integral equations in ionic solution theory

by A. R. ALLNATT

Department of Chemistry, University of Manchester, Manchester 13

(Received 27 July 1964)

An exact formal integral equation is derived for the solute radial distribution functions in a multi-component solution of ions interacting with a Coulomb potential plus a short-range potential. The equation resembles, in a certain sense defined by the use of a diagram formalism, the recent exact equation of the theory of fluids but involves the Debye-Hückel potential of average force (i.e. a shielded Coulomb potential plus the short-range potential) instead of the total direct potential. Well-defined approximations yield equations which are analogues of the hypernetted chain and Percus-Yevick equations. The possible usefulness of the equations for ionic solutions and defects in ionic crystals is indicated.

1. INTRODUCTION

One of the most successful theories of electrolyte solutions is that of Mayer [1] and is based on the cluster expansions of the McMillan-Mayer theory for thermodynamic functions [2] and radial distribution functions [3]. The problem of the divergence of individual cluster integrals for Coulomb forces was solved by a diagram classification and summation procedure which is now well known. Meeron [4, 5] has shown how the results can be written in a particularly simple form involving the familiar Debye-Hückel result plus an infinite series. This new series in powers of the concentration has coefficients which are convergent integrals involving the Debye-Hückel potential of average force rather than the unshielded Coulomb interaction. The two problems remaining are then to classify the terms in order of importance and to evaluate them. The progress made has been reviewed by Friedman [6].

Another approach to electrolyte theory is to derive integral equations for the radial distribution functions of the ions and to obtain approximate solutions of the equations, either numerically or analytically, at the concentrations of interest. This procedure has been used in particular by Falkenhagen and Kelbg [7] and by Kelbg [8], whose recent papers give references to other earlier work. In the theory of simple monatomic fluids much interest has been shown recently in the calculation of radial distribution functions from the hypernetted chain (HNC) and Percus-Yevick (PY) equations. These are particular well-defined approximations to an exact formal integral equation which can be derived from the virial expansion of the radial distribution function. The basis of the PY equation has been considered recently by Stell [9] and his paper contains references to the rather large number of recent papers on the exact equation and approximations to it. Solution of such integral equations by computer is more satisfactory at high densities than trying to work out successive terms in the virial expansion for the distribution functions. It would be interesting to have numerical studies of these equations for systems with Coulomb forces since the approximations made in

their derivation seem much better defined than those used previously. Carley [10] has recently studied these equations for a classical electron gas but so far no study for a two component system with Coulomb forces has been published although this is clearly of some interest.

It seems rather likely that the term by term evaluation of the Mayer ionic solution theory expansions will be impracticable at high concentrations and that, just as in the theory of fluids, one will have to work from an integral equation. The PY and HNC equations are possibilities. However, another possibility exists, namely, to put the Mayer ionic solution theory into the form of a set of integral equations for the radial distribution functions by starting from the series expansions for ionic solutions due to Meeron [5] noted above. One thus arrives at equations bearing the same relation to the Mayer ionic solution theory as the exact integral equations of fluid theory bear to the ordinary virial expansions for the radial distribution functions. However, these equations involve the Debye-Hückel potential of average force rather than the ordinary direct intermolecular attraction. This is unlikely to be any disadvantage since the shielded potential is much easier to handle both analytically and numerically than the corresponding direct Coulomb potential.

The derivation of such a set of integral equations is made in § 2, and a brief discussion of its use in § 3.

2. DERIVATION

The notation used by Meeron [3, 5, 11] will be used apart from minor changes. A bold-face letter \mathbf{n} denotes a set of n particles, n_s of kind s , $\mathbf{n} = n_1, n_2, \dots, n_\sigma$. The letter \mathbf{c} denotes the set of number densities $c_1, c_2, \dots, c_\sigma$ for the σ solute species, which are assumed to be all ions. The following conventions are used:

$$\mathbf{n}! = n_1! n_2! \dots n_\sigma!, \quad (2.1)$$

$$\mathbf{c}^{\mathbf{n}} = c_1^{n_1} c_2^{n_2} \dots c_\sigma^{n_\sigma}. \quad (2.2)$$

The pairwise potential of average force at infinite dilution for two solute particles of species i and j a distance R_{ij} apart will be written as the sum of an ideal Coulomb part and an unspecified short range part:

$$U_{ij} = U_{ij}^* + z_i z_j \epsilon^2 / D R_{ij}. \quad (2.3)$$

D is the macroscopic dielectric constant of pure solvent in the reference state, z_i and z_j are the algebraic charges on the ions of species i and j respectively, and ϵ is the magnitude of the electronic charge.

Meeron [5] has shown that the radial distribution function g_{ij} for a pair of ions of species i and j a distance R_{ij} apart can be written in the following form:

$$g_{ij} = \exp(k_{ij} - U_{ij}^* \beta + \alpha_{ij}). \quad (2.4)$$

Here β denotes $(kT)^{-1}$ and k_{ij} is the shielded potential defined by the equations:

$$k_{ij} = -z_i z_j \epsilon^2 \exp(-\kappa R_{ij}) / D R_{ij} kT, \quad (2.5)$$

$$\kappa^2 = 4\pi\epsilon^2 \left(\sum_{s=1}^{\sigma} c_s z_s^2 \right) / D kT. \quad (2.6)$$

The remaining term can be written in the form:

$$\alpha_{ij} = \sum_{\mathbf{m} \geq 1} \frac{\mathbf{c}^{\mathbf{m}}}{\mathbf{m}!} \int \theta(ij; \mathbf{m}) d\mathbf{m}. \quad (2.7)$$

The symbol $d\mathbf{m}$ denotes the product of the spatial coordinate elements of the solute particles in set \mathbf{m} and the single integration sign denotes an m -fold integration over these coordinates. The set \mathbf{m} does not contain the particles i and j . The $\theta(ij; \mathbf{m})$ are sums of products of k functions and ψ functions, the latter being defined by the equation:

$$\psi_{ij} = \exp(k_{ij} - U_{ij} * \beta) - 1 - k_{ij}. \quad (2.8)$$

Each product can be represented by a diagram in which each of the particles of the set $(i + j + \mathbf{m})$ is represented by a circle (node) and each function k_{rs} or ψ_{rs} involving particles r and s by a dotted or a full line respectively. The lines of a diagram are called bonds. Then $\theta(ij; \mathbf{m})$ is the sum of all products of k functions and ψ functions such that (i) every node of set \mathbf{m} is connected to both i and j either directly or by two or more independent paths, (ii) all nodes of set \mathbf{m} are connected among themselves independently of i and j , (iii) there is no direct bond between i and j , and (iv) only isolated k bonds appear. (An isolated k bond connects two nodes, each of which is directly connected to at least two other nodes or is connected to another node by a ψ bond. In other words there are no k bond chains in such diagrams. A chain is defined as a row of nodes each connected to the preceding one and to the following one by a single bond.) Examples of such diagrams are given in the figure.

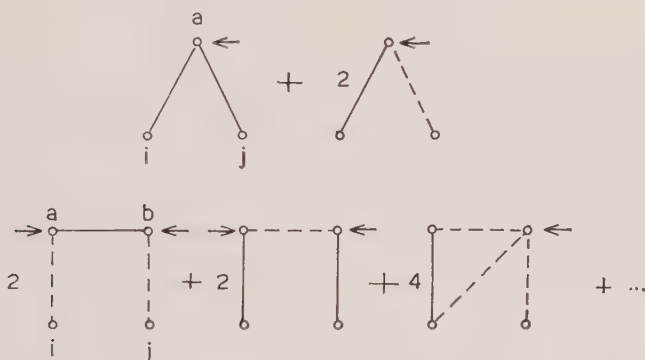


Diagram representation of some contributions to $Q(ij; a)$ and $Q(ij; ba)$.

The derivation of the preceding result assumes that the potential of average force at infinite dilution of the ions in the solution involves only pair interactions of the form of equation (2.3). The result can be generalized to include higher order interactions by following the method used by Friedman for the thermodynamic functions [6]. The final result of the argument which follows would then be slightly more complex but the method can still be carried through (see also § 3).

The argument that follows is very similar to that used by Meeron [11] to derive the exact integral equation for monatomic fluids but is complicated by the presence of two sorts of bond in the diagrams instead of one. If we cut a diagram at a node other than i and j and the diagram falls into two unconnected parts then the node is called a cutting point. Cutting points are indicated by arrows in the figure. We can thus write:

$$a_{ij} = \tau_{ij} + \zeta_{ij}, \quad (2.9)$$

where τ_{ij} is the sum of all contributions in which the corresponding diagrams

have cutting points and ζ_{ij} is the remainder. Among the diagrams of the τ_{ij} sum are many that contain pairs of adjacent cutting points. Adjacent cutting points are defined [11] to be such that there are no cutting points between two such adjacent cutting points (or such that there is no cutting point between a cutting point and i or j to which it is adjacent). Clearly in any diagram one can integrate over the coordinates of the subset of nodes in the sub-diagram connecting adjacent cutting points independently of all other nodes in the diagram and the integral is a function only of the relative coordinates of the adjacent cutting points. It is, therefore, possible to sum over all possible diagrams differing only in the sub-diagrams between a pair of adjacent cutting points. The sub-diagrams between adjacent cutting points, say k and l , can certainly be made up of either (a) diagrams of ζ_{kl} or their products, (b) products of τ_{kl} diagrams or of τ_{kl} and ζ_{kl} diagrams, (c) any of the diagrams in (a) and (b) to which has been added a bond k_{kl} or a bond ψ_{kl} , (d) a single bond ψ_{kl} . Let the sum of all such products defined in (a) to (d) be q_{kl} . We have the relation:

$$q_{kl} = \left(\sum_{s=1}^{\infty} \alpha_k^s / s! \right) (1 + k_{kl} + \psi_{kl}) - \tau_{kl} + \psi_{kl}, \quad (2.10)$$

and with the aid of (2.4) it is found that

$$q_{kl} = h_{kl} - \tau_{kl} - k_{kl}, \quad (2.11)$$

where

$$h_{kl} = g_{kl} - 1. \quad (2.12)$$

We note also that a bond k_{kl} is a possible joining sub-diagram between adjacent cutting points k and l provided that both k and l are also connected to a further sub-diagram which is topologically one of the types enumerated in (a) to (d) above (i.e. it must not form a k bond chain).

Consider next the set of chain diagrams in τ_{ij} composed of every possible chain of ψ bonds and isolated k bonds joining i and j . Every other diagram of τ_{ij} not in this set can be derived from a member of it by replacing a ψ bond by a suitable bond selected from those in (a) to (c) above.

Now, consider the terms in τ_{ij} which have composition $(i+j+\mathbf{M})$ and which have n cutting points of composition \mathbf{n} . The set $(\mathbf{M}-\mathbf{n})$ is divided into $(n+1)$ sub-sets of composition $\mathbf{l}_1, \mathbf{l}_2, \dots, \mathbf{l}_m, \dots, \mathbf{l}_{n+1}$. The set \mathbf{M} can be divided up into $(n+2)$ sub-sets in

$$\mathbf{M}! / \mathbf{n}! \mathbf{l}_1! \dots \mathbf{l}_{n+1}!$$

ways, and the integration over the coordinates of each sub-set \mathbf{l}_m can be done independently of all others. Bearing this result in mind let us sum over all terms in τ_{ij} which have the same set, \mathbf{n} , of cutting points. In τ_{ij} there will be just $\mathbf{n}!$ diagrams differing only in the order in which members of set \mathbf{n} which are of like species are encountered in passing from i to j via successive cutting points. Taking into account the result of the previous paragraph it is then clear that

$$\tau_{ij} = \sum_{\mathbf{n} \geq 1} \mathbf{c}^{\mathbf{n}} \int T(ij; \mathbf{n}) d\mathbf{n}, \quad (2.13)$$

where $T(ij; \mathbf{n})$ is the sum of all distinguishable chains of q bonds and isolated k bonds in which the intermediate nodes between i and j have composition \mathbf{n} and particles of the same species are counted as indistinguishable but particles of different species are distinguishable.

Let A_{ij} be the sum of all contributions to τ_{ij} in which the bond connected to i is a q bond, and let B_{ij} be the sum of all contributions in which the connection is a k bond, so that

$$\tau_{ij} = A_{ij} + B_{ij}. \quad (2.14)$$

It is readily seen from the expression for τ_{ij} in (2.13) that

$$A_{ij} = \sum_{k=1}^{\sigma} \int q_{ik} c_k (q_{kj} + k_{kj} + \tau_{kj}) d\mathbf{k}, \quad (2.15)$$

$$B_{ij} = \sum_{k=1}^{\sigma} \int k_{ik} c_k (q_{kj} + A_{kj}) d\mathbf{k}, \quad (2.16)$$

where $d\mathbf{k}$ denotes the coordinate element for the particle of species k . From the equations (2.14)–(2.16) and equation (2.11) an integral relation for the τ functions is obtained:

$$\begin{aligned} \tau_{ij} = & \sum_{k=1}^{\sigma} \int [(h_{ik} - \tau_{ik}) c_k h_{kj} - k_{ik} c_k (\tau_{kj} + k_{kj})] d\mathbf{k} \\ & + \sum_{k=1}^{\sigma} \sum_{l=1}^{\sigma} \int [k_{ik} c_k (h_{kl} - \tau_{kl} - k_{kl}) c_l h_{lj}] d\mathbf{k} d\mathbf{l}. \end{aligned} \quad (2.17)$$

The required integral relation for the radial distribution function is readily found by eliminating the τ from this equation using the relation:

$$\log g_{ij} + U_{ij}^* \beta - k_{ij} = \tau_{ij} + \zeta_{ij}. \quad (2.18)$$

It remains only to express ζ in terms of the radial distribution functions. A subgroup of the diagrams in ζ_{ij} have no bifocal points and are called prototype diagrams. (A pair of bifocal points is [11] a pair of nodes such that if cuts are made at both, the diagram separates into two or more diagrams of at least one node each, both cutting points being included in the same diagram.)

All the remaining ζ_{ij} diagrams can be derived from prototypes by substituting bonds by appropriate sub-diagrams, and for every given prototype diagram there is another in which a particular bond ψ has been replaced by k or vice versa. It is straightforward to see from these facts that

$$\zeta_{ij} = \sum_{n \geq 2} \frac{c^n}{n!} \int Z(ij; \mathbf{n}) d\mathbf{n}, \quad (2.19)$$

where $Z(ij; \mathbf{n})$ is the sum of all possible products of functions h connecting the nodes of set $(i+j+\mathbf{n})$ in prototype patterns. It is thus identical with the ζ sum of the fluid theory integral equation as derived by Meeron [11].

Another form of the relationship is to write:

$$g_{ij} = (1 + \tau_{ij} + \gamma_{ij}) \exp(k_{ij} - U_{ij}^* \beta), \quad (2.20)$$

which defines the functions γ_{ij} . The interpretation of γ_{ij} is as follows. Define a sum β_{ij} in exactly the same way as α_{ij} but omitting condition (ii) in the definition. Then γ_{ij} is the sum of all contributions to β_{ij} of graphs which contain no cutting points.

3. APPROXIMATE EQUATIONS

The approximation $\zeta = 0$ is exactly that required to obtain the HNC equation from the exact equation of fluids derived by Meeron [11] and others. With the same approximation the present equation would yield the same results if both were solved exactly. It differs from the HNC equation in involving the shielded

potential k_{ij} and the short range potential U_{ij}^* rather than total direct potential U_{ij} . An apparent disadvantage is that one needs an extra integration on each cycle of an iteration solution. However, if the solution is made using Fourier transform techniques via the convolution theorem then one merely has a function involving products both of three transforms and of two transforms instead of always products of two functions as in the HNC equations. The number of integrations per cycle and of unknown functions is the same for the two equations. The advantages of the present equation is that a relationship to the Mayer ionic solution theory is preserved, in the same sense that there is a relationship between solving the HNC equation and the ordinary virial expansion from which it is derived. For example, a simple iteration procedure is to eliminate h as $(\tau + q + k)$ on the right-hand side of (2.17) and solve the resultant equation for τ using Fourier transforms. The starting approximation is $\tau_{ij}^{(0)} = 0$, so that from equation (2.18)

$$g_{ij}^{(0)} = \exp(k_{ij} - \beta U_{ij}^*)$$

and hence $q_{ij}^{(0)} = \psi_{ij}$. $\tau_{ij}^{(1)}$ calculated from the equation for τ is equal to just the contribution of all chains of ψ bonds and isolated k bonds. Successive iterations add series and parallel combinations of such chains just as in iteration for the HNC equation [12]. This is of course not the only iteration scheme possible.

The method of the preceding paragraph is the analogue of the HNC method. Other approximation procedures corresponding to omission of different classes of diagrams are possible. For example the analogue of the Percus-Yevick procedure [9] would be to take $\gamma_{ij} = 0$ in equation (2.20), thus omitting from consideration all diagrams without cutting points. This class includes all the diagrams of the ζ sum and others which are taken into account in the HNC equation. In the fluid theory the PY approximation is an excellent procedure for short range forces since extensive cancellations occur in the diagrams of the omitted class. It is not obvious that it will be good Coulomb forces. Clearly only detailed calculations can settle this point whichever exact integral equation is used as the starting point for approximation.

The equation was derived retaining only pairwise contributions to the potential of average force whereas it is known that for ionic solutions an adequate theory must eventually include higher-order interactions. Both the integral equation of fluid theory and that derived from the Mayer ionic solution theory can be modified to include such contributions. The definition of the ζ sum must be modified. However, until the procedures for pairwise forces are better understood there is little point in writing down the more complex forms although this can be done.

Finally we may remark that the motivation for the preceding work originally stemmed from a study of ionic point defects in crystals. Here it is possible to construct a formalism which is essentially the analogue of the Mayer ionic solution theory in which the particles (defects) are restricted to discrete sites on a lattice [13]. However, the term by term evaluation of the analogue of the Mayer-Meeron type of expansion becomes very tedious since lattice summation must be done instead of integrations, and furthermore the convergence of the series is poor at temperatures and concentrations of practical interest (see for example [13]). It then becomes natural to seek an integral equation formulation which allows one to evaluate the contribution of the various classes of diagrams by making suitable approximations in the solution of the equation. We hope to give a further numerical study of the defect problem at a later date. In this particular

problem it seems that an integral equation form of the Mayer theory may have real advantages compared with the use of the equations derived from the exact equation involving the direct potential. The latter equations become very difficult to handle in numerical work for long-range forces between particles restricted to a lattice.

REFERENCES

- [1] MAYER, J. E., 1950, *J. chem. Phys.*, **18**, 1426.
- [2] McMILLAN, W. G., and MAYER, J. E., 1945, *J. chem. Phys.*, **13**, 276.
- [3] MEERON, E., 1957, *J. chem. Phys.*, **27**, 1238.
- [4] MEERON, E., 1957, *J. chem. Phys.*, **26**, 804.
- [5] MEERON, E., 1958, *J. chem. Phys.*, **28**, 630.
- [6] FRIEDMAN, H. L., 1962, *Ionic Solution Theory Based on Cluster Expansion Methods* (New York: Interscience Publishers).
- [7] FALKENHAGEN, E., and KELBG, G., 1957, *Disc. Faraday Soc.*, **24**, 20.
- [8] KELBG, G., 1960, *Z. phys. Chem.*, **214**, 8, 26, 141, 153.
- [9] STELL, G., 1963, *Physica*, **29**, 514.
- [10] CARLEY, D. D., 1963, *Phys. Rev.*, **131**, 1406.
- [11] MEERON, E., 1960, *J. math. Phys.*, **1**, 192.
- [12] VAN LEEUWEN, J. M. J., GROENEVELD, J., and DE BOER, J., 1959, *Physica*, **25**, 792.
- [13] ALLNATT, A. R., and COHEN, H. M., 1964, *J. chem. Phys.*, **40**, 1871.

Alternant molecular orbital treatment of trimethylenemethyl, $C(CH_2)_3$ and its ions

by D. P. CHONG and J. W. LINNETT

Inorganic Chemistry Laboratory, Oxford

(Received 25 June 1964)

Calculations have been carried out using alternant molecular orbitals (AMO) for the electrons in the π -system of planar $C(CH_2)_3^{++}$, $C(CH_2)_3^+$ and $C(CH_2)_3$. The results are compared with those that have been previously obtained using other approximation methods and the complete configuration interaction treatment. Because lower energies are obtained using improved AMO's, these improved AMO calculations have also been carried out for the allyl cation, radical and anion, which were treated in an earlier paper.

1. INTRODUCTION

In an effort to make allowance for the tendency of electrons of opposite spins to keep apart because of electrostatic repulsion, the method of different orbitals for different spins is sometimes used [1]. One of the methods of constructing different orbitals for different spins makes use of Coulson-Fischer type [2] wave functions within the framework of the valence bond (VB) method, with an adjustable parameter k which connects the Heitler-London treatment ($k=0$) with the bond-orbital treatment ($k=1$); another uses alternant molecular orbitals (AMO), as proposed by Löwdin [3]; a third method was recently devised by Hirst and Linnett [4], who constructed 'non-pairing' functions. This third procedure is now called the method of non-paired spatial orbitals (NPSO) to emphasize the implication of an absence of spatial pairing only [5-7].

While it would be desirable to assess the relative merits of these methods, not very many calculations have been carried out to provide a critical, direct comparison. In an earlier paper [5], the authors compared these three methods for the π -electron systems of allyl cation, radical and anion, showing that, for each of the three species, the NPSO treatment gives the lowest energy of the three, and the AMO treatment the second best. Recently, Empedocles and Linnett [6] showed that the NPSO function for benzene is again better than the AMO function. In this paper, we wish to report the results of AMO calculations for the electrons in the π -systems of trimethylenemethyl, $C(CH_2)_3$, and its ions, and compare them with those that have been reported earlier using the molecular orbital (MO) method, VB method, NPSO method, and the complete configuration interaction (CI) treatment [7]. In all three species, the nuclei were assumed to lie in one plane.

During the course of the present calculations, it was found that the energy of the AMO function can be improved by starting with an improved set of LCAO, molecular orbitals, especially for $C(CH_2)_3^{++}$. Consequently, a set of improved AMO energies have also been obtained for the allyl cation, radical, and anion, which were treated in one of our earlier papers [5].

2. CALCULATIONS

The assumptions and starting integrals are the same as in our earlier paper [7]. The AMO functions are constructed in a similar manner as previously described [5].

The general LCAO molecular orbitals for this system are:

$$\chi_1 = C_1(a + b + c + kx);$$

$$\chi_2 = C_2(2a - b - c);$$

$$\chi_3 = C_3(b - c);$$

$$\chi_4 = C_4(a + b + c - lx),$$

where a , b , c and x represent the $2p\pi$ -atomic orbitals on the carbon atoms, x referring to the central atom, and C_1 , C_2 , C_3 and C_4 are the normalization constants. The coefficients k and l are related by orthogonality:

$$l = 3(1 + kS_{ax} + 2S_{ab})(k + 3S_{ax})^{-1}.$$

For simplicity, k is chosen to be equal to l so that

$$k_1 = l_1 = (3 + 6S_{ab})^{-1/2} = 1.7981137.$$

This choice neglects the effect of electrostatic repulsion between the pair of electrons in each occupied MO, an effect which the AMO method is designed to take into account. The starting set of orthonormal LCAO molecular orbitals, then, are:

$$\chi_1 = 0.328426(a + b + c) + 0.590547x;$$

$$\chi_2 = 0.832843a - 0.416421(b + c);$$

$$\chi_3 = 0.721263(b - c);$$

$$\chi_4 = 0.522574(a + b + c) - 0.939647x.$$

The AMO functions constructed from this set of χ functions will be called the *simple* AMO functions.

Another perhaps more logical choice for the value of k is to use, for each species, the best k in the single-configuration anti-symmetrized MO wave function [7]. In this case, the coefficients k , l , C_1 and C_4 have a different set of values for each species.

The AMO functions constructed using this second choice of the improved orthonormal LCAO molecular orbitals will be called the *improved* AMO functions. For closed-shell configurations, the improved AMO's can be regarded as alternant LCAO-SCF-MO of a limited basis set.

What follows in the rest of this section on Calculations applies to both the simple and the improved AMOs.

The transformation of the χ functions into AMO's (ϕ) is given by:

$$\begin{bmatrix} \phi_1 \\ \phi_2 \\ \phi_3 \\ \phi_4 \end{bmatrix} = \begin{bmatrix} \cos \theta & 0 & 0 & \sin \theta \\ 0 & 1 & 0 & 0 \\ 0 & 0 & 1 & 0 \\ \cos \theta & 0 & 0 & -\sin \theta \end{bmatrix} \begin{bmatrix} \chi_1 \\ \chi_2 \\ \chi_3 \\ \chi_4 \end{bmatrix},$$

or more conveniently by :

$$\begin{aligned}\phi_1 &= (1 + \lambda^2)^{-1/2} (\chi_1 + \lambda\chi_4); \\ \phi_2 &= \chi_2; \quad \phi_3 = \chi_3; \\ \phi_4 &= (1 + \lambda^2)^{-1/2} (\chi_1 - \lambda\chi_4),\end{aligned}$$

where $\lambda = \tan \theta$, the mixing parameter to be varied.

2.1. $C(CH_2)_3^{++}$

The anti-symmetrized 1A_1 AMO function is obtained by applying the singlet spin projection operator $^1\mathbf{O}$ and the anti-symmetrizer \mathbf{A} to the function

$$\phi_1(1)\alpha(1)\phi_4(2)\beta(2).$$

This gives

$$\frac{1}{2}[(\phi_1, \phi_4) + (\phi_4, \phi_1)] = (1 + \lambda^2)^{-1}[\Phi_1^{++} - \lambda^2\Phi_2^{++}],$$

where

$$\Phi_1^{++} = (\chi_1, \chi_1);$$

$$\Phi_2^{++} = (\chi_4, \chi_4);$$

and

$$(m, n) = 1/\sqrt{2} \begin{vmatrix} m(1)\alpha(1) & n(1)\beta(1) \\ m(2)\alpha(2) & n(2)\beta(2) \end{vmatrix}.$$

Since this AMO function is not normalized, $\Psi_{\text{AMO}}^{++} = \Phi_1^{++} - \lambda^2\Phi_2^{++}$ may equally be used.

2.2. $C(CH_2)_3^+$

The ground state of this ion is a 2E state. One member of the degenerate pair of AMO function is obtained by application of the double spin projection operator $^2\mathbf{O}$ and the anti-symmetrizer \mathbf{A} to the function

$$\phi_1(1)\alpha(1)\phi_4(2)\beta(2)\phi_3(3)\alpha(3).$$

This yields

$$\frac{1}{3}[2(\phi_1, \phi_4, \phi_3) + (\phi_4, \phi_1, \phi_3) + (\phi_1, \phi_3, \phi_4)]$$

and

$$\Psi_{\text{AMO}}^+ = \Phi_1^+ + \sqrt{\frac{2}{3}}\lambda\Phi_2^+ - \lambda^2\Phi_3^+,$$

where

$$\Phi_1^+ = (\chi_1, \chi_1, \chi_3);$$

$$\Phi_2^+ = -\frac{1}{\sqrt{6}}[2(\chi_1, \chi_3, \chi_4) + (\chi_1, \chi_4, \chi_3) + (\chi_3, \chi_1, \chi_4)];$$

$$\Phi_3^+ = (\chi_4, \chi_4, \chi_3);$$

and

$$(l, m, n) = \frac{1}{\sqrt{(3!)}} \begin{vmatrix} l(1)\alpha(1) & m(1)\beta(1) & n(1)\alpha(1) \\ l(2)\alpha(2) & m(2)\beta(2) & n(2)\alpha(2) \\ l(3)\alpha(3) & m(3)\beta(3) & n(3)\alpha(3) \end{vmatrix}$$

2.3. $C(CH_2)_3$

The ground state of this species is a 3A_2 state. If the same procedure is followed in this case, i.e. applying the triplet spin projection operator $^3\mathbf{O}$ and the anti-symmetrizer \mathbf{A} to the function

$$\phi_1(1)\alpha(1)\phi_4(2)\beta(2)\phi_2(3)\alpha(3)\phi_3(4)\beta(4),$$

the resulting wave function is a mixture of 3A_2 and 3E states. In other words, the operations in this case fail to select a wave function of the proper symmetry. To remedy this, one makes use of the A_2 symmetry operator defined as:

$$\mathbf{S} = \frac{1}{6}(E + C_3^1 + C_3^2 - \sigma_a - \sigma_b - \sigma_c),$$

where the terms correspond to the elements of the C_{3v} symmetry group. Then, the anti-symmetrized 3A_2 AMO function can be obtained by applying these three operators in succession, i.e. $\mathbf{S}^3\mathbf{OA}$, to the above function, and one obtains:

$$\Psi_{\text{AMO}} = \Phi_1 - \lambda^2 \Phi_2,$$

where

$$\Phi_1 = \frac{1}{\sqrt{2}} [(\chi_1, \chi_1, \chi_2, \chi_3) - (\chi_1, \chi_1, \chi_3, \chi_2)];$$

$$\Phi_2 = \frac{1}{\sqrt{2}} [(\chi_4, \chi_4, \chi_2, \chi_3) - (\chi_4, \chi_4, \chi_3, \chi_2)];$$

and

$$(k, l, m, n) = \frac{1}{\sqrt{(4!)}} \begin{vmatrix} k(1)\alpha(1) & l(1)\beta(1) & m(1)\alpha(1) & n(1)\beta(1) \\ k(2)\alpha(2) & l(2)\beta(2) & m(2)\alpha(2) & n(2)\beta(2) \\ k(3)\alpha(3) & l(3)\beta(3) & m(3)\alpha(3) & n(3)\beta(3) \\ k(4)\alpha(4) & l(4)\beta(4) & m(4)\alpha(4) & n(4)\beta(4) \end{vmatrix}.$$

2.4. Allyl systems

The AMO functions for the allyl cation, radical, and anion have already been described [5]. Here, in the *improved* AMO treatment, the parameter k in the LCAO molecular orbital for the system has been set equal to the best values of the single-configuration antisymmetrized MO functions, namely 1.5712, 1.5143 and 1.4608 for the cation, radical and anion respectively, instead of $\sqrt{2}$.

2.5. Computational details

To show what kind of computations are involved, the calculations of the simplest example (simple AMO treatment of $\text{C}(\text{CH}_2)_3^{++}$) are described below:

Because the matrix elements s_{ij} and h_{ij} between the 1A_1 symmetry spinorbitals (ψ) of $\text{C}(\text{CH}_2)_3^{++}$ have already been calculated [7], the simplest way to proceed is to express Φ_1^{++} and Φ_2^{++} as linear combination of ψ_1 to ψ_4 , as defined in ref. [7]. That is, we need to find \mathbf{T} in:

$$\begin{bmatrix} \Phi_1^{++} \\ \Phi_2^{++} \end{bmatrix} = \mathbf{T} \begin{bmatrix} \psi_1 \\ \psi_2 \\ \psi_3 \\ \psi_4 \end{bmatrix}.$$

Then the matrix elements S_{ij} and H_{ij} between the orthonormal Φ^{++} 's are simply:

$$\left. \begin{aligned} \mathbf{S} &= \mathbf{T} \mathbf{s} \mathbf{T}^\dagger \\ \mathbf{H} &= \mathbf{T} \mathbf{h} \mathbf{T}^\dagger \end{aligned} \right\} \quad (1)$$

The overlap matrix serves as a check on orthonormality.

The \mathbf{T} matrix can be easily obtained for this species. The general unnormalized MO function is given in ref. [7] by:

$$\begin{aligned} \Psi_{\text{MO}}^{++}(k) &= (a + b + c + kx, a + b + c + kx) \\ &= \psi_1 + k\psi_2 + \psi_3 + k^2\psi_4. \end{aligned}$$

Therefore,

$$\Phi_1^{++} = C_1^2(\psi_1 + k\psi_2 + \psi_3 + k^2\psi_4);$$

$$\Phi_2^{++} = C_4^2(\psi_1 - k\psi_2 + \psi_3 + l^2\psi_4),$$

where $k=l=k_1$ in this example. Hence:

$$\mathbf{T} = \begin{bmatrix} 0.107864 & 0.193951 & 0.107864 & 0.348746 \\ 0.273083 & -0.491035 & 0.273083 & 0.882936 \end{bmatrix}.$$

Substituting this into equations (1), one gets a unit matrix for \mathbf{S} and

$$\begin{bmatrix} 2W_{2p} - 3.398907 & 0.177819 \\ 0.177819 & 2W_{2p} - 2.011539 \end{bmatrix}$$

in rydbergs for \mathbf{H} .

Now, the AMO function is $\Psi_{\text{AMO}}^{++} = \Phi_1^{++} - \lambda^2 \Phi_2^{++}$, which may be re-written as $\Phi_1^{++} + p\Phi_2^{++}$, where $p = -\lambda^2 \leq 0$. The energy expressed as a function of p is, therefore:

$$E(p) = (H_{11} + 2pH_{12} + p^2H_{22})(1 + p^2)^{-1}.$$

When this is minimized with respect to p , one obtains $2W_{2p} - 3.421335$ rydbergs for the energy.

All the computations were performed on a Mercury Ferranti computer at the Oxford University Computing Laboratory, using two or three more significant figures than is indicated here.

3. RESULTS AND DISCUSSION

The parameters and minimum energies of the simple and improved AMO functions are listed in table 1, together with the corresponding MO functions. It shows that for each species, the mixing parameter λ and the energy depression (with respect to the corresponding MO function) is roughly the same for both the simple and the improved AMO treatments.

The simple AMO results for the allyl system have been compared with the other approximate treatments [5]. It suffices to say, here, that the improvement in the AMO functions does not change the overall picture. Though given a better chance by the improvement, the AMO functions still do not yield energies better than the NPSO functions.

In table 2 the results for the trimethylenemethyl system are compared with those that have previously been obtained using other approximation methods [7]. In particular, we wish to see whether the AMO function or the NPSO function can approximate the CI function better. The energy difference, $E - E_{\text{CI}}$, is one of the measures of how well an approximate function approaches the best CI function; the overlap integral S (defined in table 2) is another. To put it more precisely, we may express the CI function as a linear combination of any complete set of orthonormal molecular wave functions u :

$$\Psi_{\text{CI}} = \sum_i C_i U_i,$$

where $C_i = \langle U_i | \Psi_{\text{CI}} \rangle$, from orthonormality of the U functions. If U_1 represents any of the approximate functions, then $C_1 = S$, by definition. Therefore, the overlap integral S measures how good the approximation

$$\Psi_{\text{CI}} = S U_1 + \dots$$

is by retaining only the first term.

Species	Function	k	λ	$E-E_{\text{CI}}$ rydbergs
$\text{C}(\text{CH}_2)_3^{++}$	MO	(k_1)	—	0.06857
	Simple AMO	(k_1)	0.3552	0.04614
	MO†	2.76412	—	0.03174
	Improved AMO	(2.76412)	0.3345	0.01296
$\text{C}(\text{CH}_2)_3^+$	MO	(k_1)	—	0.13470
	Simple AMO	(k_1)	0.3350	0.07453
	MO†	2.34547	—	0.12016
	Improved AMO	(2.34547)	0.3244	0.06343
$\text{C}(\text{CH}_2)_3$	MO	(k_1)	—	0.12863
	Simple AMO	(k_1)	0.3478	0.10711
	MO†	2.00365	—	0.12616
	Improved AMO	(2.00365)	0.3468	0.10481
$\text{CH}_2\text{CHCH}_2^+$	MO†	$(\sqrt{2})$	—	0.07520
	Simple AMO†	$(\sqrt{2})$	0.4159	0.03907
	MO†	1.5712	—	0.07263
	Improved AMO	(1.5712)	0.4146	0.03680
CH_2CHCH_2	MO†	$(\sqrt{2})$	—	0.13348
	Simple AMO†	$(\sqrt{2})$	0.4516	0.00242
	MO†	1.5143	—	0.13238
	Improved AMO	(1.5143)	0.4509	0.00169
$\text{CH}_2\text{CHCH}_2^-$	MO†	$(\sqrt{2})$	—	0.07948
	Simple AMO†	$(\sqrt{2})$	0.40477	0.04475
	MO†	1.4608	—	0.07923
	Improved AMO	(1.4608)	0.4078	0.04447

† Ref. [7]. ‡ Ref. [5].

Table 1. Results of ASMO and ASAMO calculations. A value of k in parentheses means that, for the calculation, k is not varied.

In table 2 we see that, in general, the NPSO method provides the best approximation to the CI treatment, both in energy and in the overlap integral. The only exception is $\text{C}(\text{CH}_2)_3^{++}$, for which the improved AMO function gives a lower energy than the NPSO function. However, as stated in ref. [7], the NPSO functions are not unique, and, if one starts with a second NPSO function for $\text{C}(\text{CH}_2)_3^{++}$:

$$\psi = (E + C_3^1 + C_3^2)[(a + kx, x + kb) + (x + kb, a + kx)],$$

instead of the more symmetric one used:

$$\Psi_{\text{NPSO}}^{++} = (E + C_3^1 + C_3^2)[(a + kx, b + kx) + (b + kx, a + kx)],$$

then the energy is only 0.00012 rydbergs above the best energy E_{CI} . This behaviour was also found for the allyl cation by Hirst and Linnett [4], who tried the two wave functions analogous to ψ and Ψ_{NPSO}^{++} above and obtained a lower energy for the asymmetric one.

In conclusion, we may state that the NPSO method allows for electron correlation better and can give a wave function more closely approximating the best

CI function than the other approximation methods, provided one has gained some experience in constructing NPSO functions.

Species	Function	$E-E$ rydbergs	$1-S$
$C(CH_2)_3^{++}$	VB†	0.07758	0.0301
	Simple AMO	0.04613	0.0187
	Improved AMO	0.01296	0.0058
	NPSO†	0.01491	0.0058
$C(CH_2)_3^+$	VB†	0.20827	0.2749
	Simple AMO	0.07453	0.0760
	Improved AMO	0.06343	0.0785
	NPSO†	0.03013	0.0238
$C(CH_2)_3$	VB†	0.01054	0.0045
	Simple AMO	0.10712	0.0545
	Improved AMO	0.10481	0.0538
	NPSO†	0.00295	0.0014

† Ref. [7].

Table 2. Comparison of various one-parameter approximations with the best CI function. The symbol S in the last column is defined as the overlap integral between the normalized approximate function with the normalized CI function.

We wish to thank Professor C. A. Coulson and our colleagues for helpful discussions, and the N.A.T.O. for a post-doctoral fellowship (to D.P.C.).

REFERENCES

- [1] LÖWDIN, P.-O., 1959, *Advanc. chem. Phys.*, **2**, 207.
- [2] COULSON, C. A., and FISCHER, I., 1949, *Phil. Mag.*, **40**, 386.
- [3] LÖWDIN, P.-O., 1953, *Symposium on Molecular Physics* (Tokyo: Maruzen), p. 13.
- [4] HIRST, D. M., and LINNETT, J. W., 1962, *J. chem. Soc.*, pp. 1035, 3844.
- [5] CHONG, D. P., and LINNETT, J. W., 1964, *Mol. Phys.*, **8**, 151.
- [6] EMPEDOCLES, P. B., and LINNETT, J. W., 1964, *Proc. roy. Soc. A*, **282**, 166.
- [7] CHONG, D. P., and LINNETT, J. W., paper submitted to *J. chem. Soc.*

A rigid sphere model for the melting of argon

by H. C. LONGUET-HIGGINS† and B. WIDOM

Department of Chemistry, Cornell University, Ithaca, N.Y., U.S.A.

(Received 25 April 1964)

A model is proposed for liquid and solid argon, in which the repulsive forces are represented by rigid cores and the attractive forces by a uniform background potential which depends on density but not on temperature. Thermodynamic consistency implies the equation of state:

$$p(n, T) = p^0(n, T) - an^2,$$

where p^0 is the pressure exerted by rigid spheres at the same number density n and temperature T , and a is independent of n and T . When p^0 is taken from the calculations of Alder and Wainwright it becomes possible to make an absolute calculation of the values of several dimensionless thermodynamic quantities characteristic of the triple point. All of these except certain second derivatives of the free energy agree very well with experiment, suggesting that the structure of liquids and solids near the triple point is mainly determined by the repulsive forces, the attractive forces serving merely to keep the molecules together.

1. INTRODUCTION

In 1957 Alder and Wainwright [1] reported a mechanical investigation of the equation of state of rigid spheres, and in the same year Wood and Jacobson [2] published the results of a Monte Carlo investigation leading to essentially the same conclusions. If one plots pV_0/NkT against V/V_0 , where V_0 is the close-packed volume, one obtains, for a finite number of spheres, two separate curves, one of which originates in the high density region and the other in the low density region. At values of V/V_0 near 1.6 the system oscillates back and forth between two alternate pressures; in the high pressure condition the spheres are distributed apparently at random, but in the low pressure condition they are more regularly arranged, and are approximately close-packed at the highest densities.

Various authors [3, 4] have suggested a connection between the phase transition which seems to occur in rigid spheres and the crystallization of a monatomic fluid. First of all, it is easy to see that the rigid sphere transition cannot possibly be related to the vaporization of a real liquid: the vapour pressure curve of a liquid terminates at the critical point, but in a rigid sphere assembly there is no characteristic energy to be identified with kT_c . Secondly, the rigid sphere transition occurs at values of V/V_0 comparable with those of solid and liquid argon at the triple point, and in both systems the more dense phase is ordered and the less dense phase disordered. Hence there is a *prima facie* case for regarding the rigid sphere transition as a crystallization rather than a condensation, and in this paper we shall show that a rigid sphere model, modified to allow for attractive forces, accounts well for the properties of argon at its triple point.

† Present address: Department of Theoretical Chemistry, University Chemical Laboratory, Cambridge, England.

2. THEORETICAL DEVELOPMENT

The basic physical idea underlying our model is that near the triple point the detailed structure of a liquid or solid is dominated by the repulsive part of the potential, the attractive forces serving merely to keep the molecules together. This idea has been successfully used by Reiss and his co-workers (see [5]) in their 'scaled particle' model of monatomic liquids, but in applying their theory to real liquids these authors found it necessary to invoke the experimental value of the density at given temperature and pressure. In this paper we shall develop a completely *a priori* theory of melting, in which the only required 'experimental' datum is the equation of state of rigid spheres as determined by Alder and Wainwright.

What we assume, in effect, is that near the triple point the repulsive forces between argon atoms are the same as for rigid spheres, but that the attractive forces merely provide a uniform negative potential, ψ , say. Because this is uniform it gives rise to no force on any molecule, so that at fixed density the system behaves exactly like an assembly of hard elastic spheres. If this assumption were strictly correct, the N -particle distribution function, and hence the cohesive energy, would depend only on the density and not on the temperature, so that ψ would have to be temperature-independent. But if this is so then thermodynamic consistency demands [6] that ψ be proportional to the density:

$$\psi = -2aN/V, \quad \text{say,} \quad (1)$$

and that the cohesive energy be of the form

$$U = -aN^2/V. \quad (2)$$

It then also follows [6] that the effect of ψ on the equation of state is to subtract aN^2/V^2 from the pressure of the hard sphere assembly, so that at given T and V

$$p = p^0 - aN^2/V^2, \quad (3)$$

where p^0 is the pressure that would be exerted by rigid spheres of diameter equal to the repulsive diameter of the molecules.

Equation (3) was also obtained by Kac *et al.* [4] in their discussion of systems with rigid cores and superimposed weak, long-range forces. We, however, are not assuming the attractive part of the potential to extend far beyond nearest neighbours; we are only supposing that the attractive *forces* due to the neighbours of a molecule largely cancel, though of course the potential *energy* of a molecule is the sum of contributions from all the molecules in its neighbourhood.

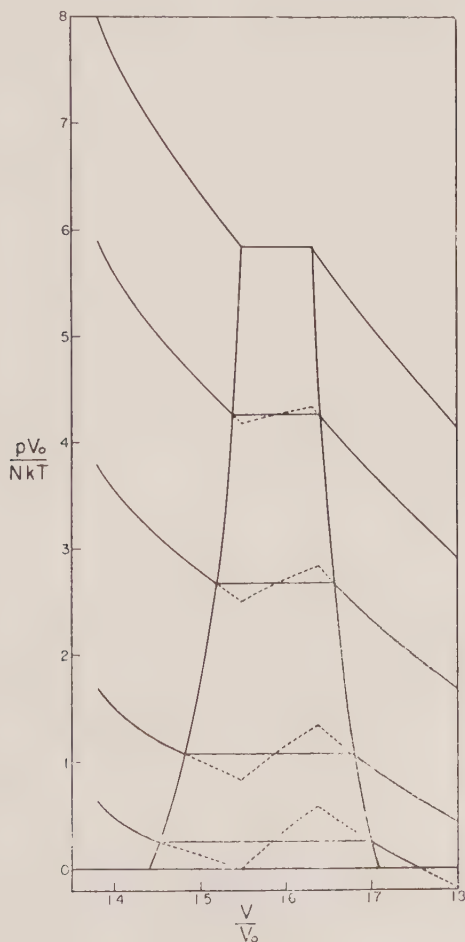
The theory based on equation (3), which is the starting point of our calculations, is essentially the van der Waals theory, but with p^0 taken to be the true 3-dimensional rigid-sphere pressure rather than being assigned the value $NkT/(V-b)$ as in the original van der Waals theory, this being the value of p^0 appropriate to one dimension. But the physical situations to which we are applying our theory are essentially different from those for which the van der Waals theory was originally designed; it would certainly be incorrect to suppose that at *low* densities ψ is a constant proportional to the density. With this limitation in mind we therefore confine our applications of equation (3) to the properties of argon at high densities, and are in effect using an old theory for quite a new purpose.

3. THE ISOTHERMS

It is convenient to write the equation of state of rigid spheres in the reduced form:

$$\frac{p^0 V_0}{NkT} = p_*^0 \left(\frac{V}{V_0} \right), \quad (4)$$

where V_0 is the close-packed volume, equal to $N\sigma^3/\sqrt{2}$, where σ is the hard-sphere diameter. This equation of state is represented by the top curve in the figure, which is based on the 1960 paper of Alder and Wainwright [7]. The reduced melting pressure is rather uncertain; we have drawn the horizontal segment in such a way that it meets the fluid curve at $V/V_0 = 1.63$, which is the estimated value of this ratio quoted in a recent paper by Ree and Hoover [8].



Uncorrected and equilibrium isotherms for an assembly with the reduced equation of state $pV_0/NkT = p^0 V_0/NkT - (aN/V_0kT)(V/V_0)^{-2}$, where p^0 is the pressure exerted by rigid spheres at temperature T and density N/V . For the five isotherms shown the parameter (aN/V_0kT) has the values 0, 4, 8, 12 and 14, reading down the figure.

The reduced equation of state of our model assembly is, according to equation (3):

$$\frac{pV_0}{NkT} = \frac{p^0V_0}{NkT} - \left(\frac{aN}{V_0kT} \right) \left(\frac{V}{V_0} \right)^{-2}. \quad (5)$$

The reduced equation of state therefore comprises a one-parameter family of isotherms, distinguished by their values of the parameter

$$\lambda = aN/V_0kT. \quad (6)$$

If no account is taken of thermodynamic stability, the above equation leads to isotherms which have a positive slope for values of V/V_0 between 1.55 and 1.63, which are the reduced volumes of the coexisting solid and fluid phases for rigid spheres. The figure shows four such isotherms, for values of λ equal to 4, 8, 12 and 14 respectively; the dotted portions represent thermodynamically unstable states, and the full horizontal segments have been obtained by the 'equal areas' construction of Maxwell. A word or two on this construction would seem to be called for.

It might be argued that one should apply the equal areas construction, not to the unstable isotherms shown in the figure, but to the isotherms which would have been obtained by subtracting the last term in equation (5) from the 'uncorrected' isotherm for rigid spheres, i.e. the isotherm which would be obtained by imposing the constraint of uniform density. In fact it can be shown without difficulty that the two procedures lead to precisely the same result, so that the objection is not a real one; but, to prove that the construction we have adopted leads to equal chemical potentials for the solid and liquid in equilibrium, we present the following elementary argument:

Let ABCD be the dotted part of one of the isotherms in the figure, B and C being the lowest and highest points, and let A'B'C'D' be the points lying immediately above ABCD on the rigid sphere isotherm, so that B'C' is the horizontal portion of that isotherm. Then the area under A'B'C'D' is, by definition:

$$\int_{V_A}^{V_D} p^0 dV = F_A^0 - F_D^0, \quad (7)$$

namely the difference in Helmholtz free energy between the rigid sphere assembly at A and at D. But at V_A and at V_D the Helmholtz free energies of the attracting and the non-attracting spheres are related by $F = F^0 - aN^2/V$, the second term being just the cohesive energy. Therefore, by equation (7):

$$\int_{V_A}^{V_D} \left(p^0 - \frac{aN^2}{V^2} \right) dV = F_A - F_D. \quad (8)$$

But the left-hand side of equation (8) is just the area under ABCD, which by our construction is also the area under the straight line AD, namely $p(V_D - V_A)$, where p is the pressure along this line. Hence:

$$p(V_D - V_A) = F_A - F_D, \quad (9)$$

from which it follows that the attracting sphere assembly has the same chemical potential at the points A and D,

It will be noted that the above proof of the equality of the chemical potentials at the ends of the horizontal segment AD does not depend, as Maxwell's original construction depended, upon the assumption that one can follow reversibly the unstable part of any isotherm. The possibility of finding such a direct proof arises from the fact that the true rigid sphere isotherm is everywhere thermodynamically stable, so that one can connect the free energies at A and at D without having to integrate the pressure along the unstable part of any isotherm.

4. IDENTIFICATION OF THE TRIPLE POINT

It might be doubted whether one could obtain theoretical information about the triple point without introducing experimental data in order to determine the parameter $\lambda = aN/V_0kT$. Fortunately, however, this necessity does not arise if one restricts attention to dimensionless quantities, such as the ratio of the solid and liquid volumes at the triple point. We shall now calculate a number of such dimensionless quantities from the information contained in the figure.

The first necessity is to identify the triple point itself. Here we make two assumptions, and justify the second by subsequent calculation. The first is that at the triple point temperature T_t the vapour is nearly enough ideal, and the second is that the reduced triple point pressure is very much smaller than unity. If the latter assumption is correct, then the triple point isotherm in the figure is that for which the horizontal portion essentially coincides with the axis of V/V_0 . The figure shows that for this isotherm λ is slightly greater than 14. A more precise value is 14.7, and the corresponding values of V_s and V_l are $1.43 V_0$ and $1.71 V_0$ respectively. The calculated ratio of liquid and solid volumes is therefore 1.19.

We next proceed to calculate the value of pV_l/NkT at the triple point. It has been shown by one of us [6] that the activity z of a fluid (normalized to the number density for very low pressures) is given by the equation:

$$\frac{n}{z} = \langle \exp(-\Psi/kT) \rangle, \quad (10)$$

where n is the number density, Ψ is the energy required to introduce a test molecule into the fluid *without* allowing for relaxation, and $\langle \rangle$ denotes a canonical average. For rigid spheres Ψ has one of the two values 0 or $+\infty$; for attracting rigid spheres, according to our model, it is either $-2an$ or $+\infty$. Hence if z^0 and z refer to non-attracting and attracting spheres respectively, then

$$\frac{n}{z} = \frac{n}{z^0} \exp(2an/kT), \quad (11)$$

so that

$$z = z^0 \exp(-2an/kT). \quad (12)$$

To find z^0 as a function of p we determine both these quantities as functions of number density. Using the thermodynamic relation:

$$kT \left(\frac{\partial \ln z^0}{\partial \ln n} \right)_T = \left(\frac{\partial p^0}{\partial n} \right)_T, \quad (13)$$

we deduce that

$$\ln z^0 = \frac{1}{kT} \int \frac{1}{n} \left(\frac{\partial p^0}{\partial n} \right)_T dn = \frac{p^0}{nkT} + \int \frac{p^0}{n^2 kT} dn. \quad (14)$$

To evaluate the second integral we employ the scaled-particle equation of state of Reiss *et al.* (see [5]), which is known to represent quite accurately the fluid branch of the rigid-sphere isotherm:

$$\frac{p^0}{nkT} = \frac{1 + vn + v^2 n^2}{(1 - vn)^3}, \quad (15)$$

where v is the volume of a sphere, related to V_0 by

$$v = \frac{\pi \sqrt{2} V_0}{6 N}. \quad (16)$$

Integrating, and adjusting the constant of integration so that z^0/n tends to unity at low densities, we obtain:

$$\ln z^0 = \frac{p^0}{nkT} - \ln \left(\frac{1 - vn}{n} \right) + \frac{3}{2(1 - vn)^2} - \frac{5}{2}. \quad (17)$$

Setting $z^0 = z \exp(2an/kT)$ and $p^0 = p + an^2$ we derive the relation:

$$\ln \left(\frac{z}{n} \right) = \frac{p}{nkT} - \frac{an}{kT} - \ln(1 - vn) + \frac{3}{2(1 - vn)^2} - \frac{5}{2} \quad (18)$$

between the activity, temperature, pressure and number density of our model liquid. But for the vapour, if it is assumed ideal:

$$z = \frac{p}{kT}. \quad (19)$$

Hence the following relation must be satisfied by the liquid at its vapour pressure:

$$\ln \left(\frac{p}{nkT} \right) = \frac{p}{nkT} - \frac{an}{kT} - \ln(1 - vn) + \frac{3}{2(1 - vn)^2} - \frac{5}{2}. \quad (20)$$

Assuming further as we did at the beginning of this section that p/nkT is much less than unity, we may set:

$$\frac{an}{kT} = \lambda \frac{V_0}{V_l} = \frac{14.7}{1.71} = 8.60 \quad (21)$$

and

$$1 - vn = 1 - \frac{\pi \sqrt{2} V_0}{6 V_l} = 0.567, \quad (22)$$

as obtained at the beginning of this section. Inserting these values into (20) we obtain:

$$\ln \left(\frac{p}{nkT} \right) = -5.86, \quad (23)$$

so that our second assumption is indeed justified.

5. OTHER PROPERTIES NEAR THE TRIPLE POINT

Having satisfied ourselves that the triple point isotherm is indeed that for which $\lambda = 14.7$, we can now calculate some other thermodynamic properties of the triple point. One of these is the entropy of fusion, in units of Nk , given by the Clapeyron-

Clausius equation:

$$\frac{\Delta S}{\Delta V} = \frac{dp_m}{dT}, \quad (24)$$

where p_m is the melting pressure. The figure shows that p_m is almost exactly linear in T according to the relation:

$$\frac{p_m V_0}{NkT} = 5.8 (1 - \lambda/14.7), \quad (25)$$

so that

$$\frac{dp_m}{dT} = 5.8 Nk/V_0. \quad (26)$$

Therefore at the triple point:

$$\Delta S = 5.8 Nk(V_l - V_s)/V_0, \quad (27)$$

so that

$$\left(\frac{\Delta S}{Nk}\right)_t = 1.64. \quad (28)$$

Another dimensionless quantity, independent of those already calculated, is the cohesive energy of the liquid, in units of NkT . According to equation (2):

$$U_l = -aN^2/V_l,$$

so that

$$\left(\frac{U_l}{NkT}\right)_t = -\lambda_t \left(\frac{V_l}{V_0}\right)^{-1} = -\frac{14.7}{1.71} = -8.6. \quad (29)$$

A more ambitious project for a theory of liquids is to predict second derivatives of the free energy, such as configurational specific heats, coefficients of thermal expansion and compressibilities. Such quantities are much more sensitive to errors in a theoretical model, but for what they are worth we give the values of C_V' , $(T\alpha_l)_t$ and $(NkT\beta_l/V_l)_t$ which are predicted by our theory. The first, which is defined as $(\partial U_l/\partial T)_V$ is necessarily zero in our model, since we have assumed ψ to be independent of T at constant density. The second and third are obtainable in a straightforward way from the isotherms in the figure, or from equations (3) and (15) if an analytic calculation is thought to be preferable. One finds:

$$(T\alpha_l)_t = 0.50, \quad (NkT\beta_l/V_l)_t = 0.058. \quad (24)$$

6. COMPARISON WITH EXPERIMENT

The table summarizes the predictions of our theory, as derived in the preceding sections, and the corresponding experimental values for argon [9]. (We have not thought it necessary to quote the available data on the other rare gases, since all these gases obey the principle of corresponding states to a good approximation.) For the first four quantities listed the agreement is remarkably good; for the next two it is considerably better than might have been expected. The last of the seven, the configurational specific heat at constant density, is incorrectly given as zero; but this is a necessary consequence of our physical assumptions.

Various conclusions suggest themselves. First, it is difficult to believe that such good quantitative agreement could arise from a physical picture which did not contain an important element of truth. If this is granted, it would appear that the rigid-sphere equation of state, on which our analysis is based, but which was obtained from calculations on a finite assembly, is probably a fairly accurate equation for the infinite assembly. It would be rash, of course, to conclude that the infinite hard-sphere assembly must show a first-order phase transition; but this hypothesis is at least consistent with the results which we have obtained.

A second point of interest is the possible existence of a critical melting temperature. If our model is to be taken seriously, a real liquid of spherical molecules should resemble more and more nearly an assembly of rigid spheres as the temperature is raised. So if rigid spheres show a first-order phase transition, argon should also exhibit one even at the highest temperatures. According to our model the melting pressure should be linear in the temperature, and though this simple law is not obeyed at high temperatures [10], it seems likely from our model that argon would freeze under sufficiently high pressures even at the highest temperatures attainable in the laboratory.

Finally, as to the model itself. Our basic assumption was that at high densities the structure of the liquid is mainly determined by the repulsive forces, and that the same is true for the solid. The quantitative success of our theory suggests that the crystal structures of other substances than the rare gases may also be largely determined by the repulsive rather than the attractive forces, provided that the latter are not too specific in their dependence on orientation.

	$(V_l/V_s)_t$	$\ln(pV_l/NkT)_t$	$(\Delta S/Nk)_t$	$(U_i/NkT)_t$
Theoretical value	1.19	-5.9	1.64	-8.6
Value for argon	1.114	-5.88	1.69	-8.53
	$(T\alpha)_t$	$(NkT\beta_l/V_l)_t$	(C_V'/Nk)	
Theoretical value	0.50	0.058	0	
Value for argon	0.366	0.0495	0.83	

REFERENCES

- [1] ALDER, B. J., and WAINWRIGHT, T. E., 1957, *J. chem. Phys.*, **27**, 1208.
- [2] WOOD, W. W., and JACOBSON, J. D., 1957, *J. chem. Phys.*, **27**, 1207.
- [3] WAINWRIGHT, T. E., ALDER, B. J., WOOD, W. W., PARKER, R. R., JACOBSON, J. D., and LONGUET-HIGGINS, H. C., 1958, *Nuovo Cim. Suppl.*, **9**, 116, 131, 133.
- [4] KAC, M., UHLENBECK, G. E., and HEMMER, P. C., 1963, *J. math. Phys.*, **4**, 216, 229.
- [5] FRISCH, H. L., 1964, *Advanc. chem. Phys.*, **6**, 229.
- [6] WIDOM, B., 1963, *J. chem. Phys.*, **39**, 2808.
- [7] ALDER, B. J., and WAINWRIGHT, T. E., 1960, *J. chem. Phys.*, **33**, 1439.
- [8] REE, F. H., and HOOVER, W. G., 1964, *J. chem. Phys.*, **40**, 939.
- [9] ROWLINSON, J. S., 1959, *Liquids and Liquid Mixtures* (London: Butterworths), and references therein.
- [10] ROWLINSON, J. S., 1964, *Mol. Phys.*, **8**, 107.

Nitroxydes [1]

IV. Le *t*-butyl isopropyl nitroxyde

par H. LEMAIRE, R. RAMASSEUL et A. RASSAT

Laboratoire de Chimie Organique Physique du Centre d'Etudes Nucléaires,
Chemin des Martyrs, Grenoble, Isère

(Received 24 March; revision received 25 May 1964)

Isopropyl-*t*-butyl nitroxide has been prepared by the reaction of *t*-butyl magnesium chloride on 2-nitropropane. Its E.P.R. spectrum is essentially a triplet of doublets (interaction with the nitrogen atom and the isopropyl proton). The hyperfine splittings are solvent dependent and, in water: $a_N = 16,83$ gauss, $a_H = 1,80$ gauss. A system of satellites is attributed to C_{13} in natural abundance. These data are discussed by comparison to the isoelectronic pentamethylacetone radical-ion.

In the stable conformation of both radicals, the isopropyl methyles are symmetrical relative to the nodal plane of the π system.

1. INTRODUCTION

Le *t*-butyl isopropyl nitroxyde peut être détecté par R.P.E. parmi les produits de la réaction du chlorure de *t*-butyl magnésium sur le nitro-2 propane. En solution, on observe (figure 1) un triplet de doublets ($g = 2,0055$):

$a_N = 16,83$ gauss, $a_H = 1,80$ gauss (dans l'eau),
 $a_N = 15,74$ gauss, $a_H = 1,68$ gauss (dans le diéthylèneglycol).



Figure 1.

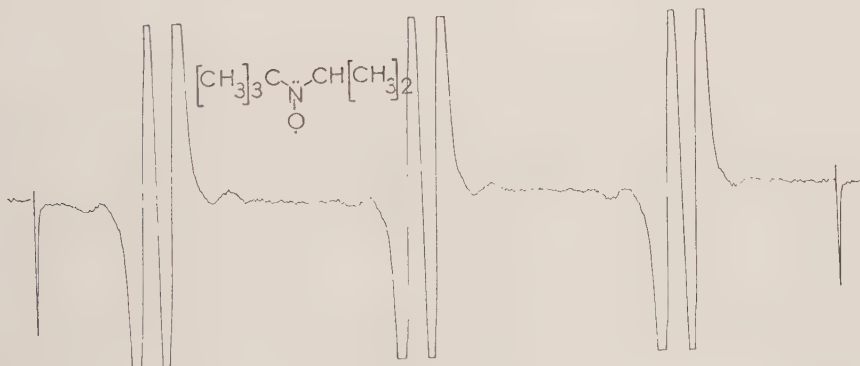


Figure 2.

Chaque composante des doublets se résout en 5 raies séparées de 0,3 gauss correspondant aux 6 protons de l'isopropyle (7 raies: 1-6-15-20-15-6-1, les deux raies extrêmes trop faibles n'apparaissant pas).

En outre, on observe deux raies satellites (figure 2) écartées de $6,80 \pm 0,3$ gauss (dans l'eau), attribuables au C_{13} en abondance naturelle en position isopropyle (puisque, pour le di *t*-butyl nitroxyde (DTBN), $a_{C_{13}} = 4,84 \pm 0,10$ gauss [1 a]).

La variation de a_N avec le solvant est caractéristique d'une liaison radical-solvant [2] et est corrélable au facteur Z de Kosower [3].

2. DISCUSSION

Théorie et expérience [4, 5] montrent que les écarts hyperfins de noyaux reliés par deux liaisons à un système π dépendent de leur position :

$$a_H \text{ ou } a_{C_{13}} = \beta \langle \cos^2 \theta \rangle \rho_N^\pi, \\ \beta_H \sim 50 \text{ gauss [6] et } \beta_{C_{13}} \sim 20 \text{ gauss [1 a]},$$

ρ_N^π est la densité de spin portée par l'atome non saturé auquel le groupe est lié, et θ est l'angle que font, en projection sur le plan perpendiculaire à la direction CN, l'axe de l'orbitale de l'azote et la direction CH ou C-C, la moyenne étant prise entre les positions extrêmes d'oscillation.

Pour le *t*-butyle, avec libre rotation $\langle \cos^2 \theta \rangle = \frac{1}{2}$.

Pour l'isopropyle, il existe deux positions d'équilibre correspondant à :

$$\theta = 0^\circ \text{ pour le proton et } \theta = 60^\circ \text{ pour les méthyles,}$$

ou bien

$$\theta = 90^\circ \text{ pour le proton et } \theta = 30^\circ \text{ pour les méthyles.}$$

La faible valeur (1,8 gauss dans l'eau) trouvée correspond à $\theta = 90^\circ$ pour le proton, donc à 30° pour les méthyles. Le rapport des $a_{C_{13}}$ entre le di-*t*-butyl nitroxyde et le *t*-butyl isopropyl nitroxyde doit alors être dans le rapport

$$\frac{\frac{1}{2}}{\cos^2(30^\circ)} = 1,50.$$

On trouve :

$$\frac{6,8}{4,8} = 1,41.$$

Par comparaison avec le diisopropyl nitroxyde, où $a_H = 4,7$ gauss, on voit que l'influence du deuxième substituant sur le a_H est importante : les oscillations autour de la position moyenne $\theta = 0$ sont plus fortes dans le diisopropyl nitroxyde que dans le *t*-butyl isopropyl nitroxyde, en rapport avec l'encombrement stérique du *t*-butyle supérieur à celui de l'isopropyle.

Par comparaison avec les cétyles isoélectroniques et isostères de l'hexaméthyl-acétone (HMA) ou de la pentaméthylacétone (PMA) [7, 8], on peut obtenir des renseignements sur l'allure des barrières de rotation autour des liaisons C-C et C-N.

Les écarts hyperfins mesurés sont donnés par le tableau.

	a_N ou $a_{C_{13}}$ (cétyle)	a_H	$a_{C_{13}}$
DTBN	17,22		4,84
HMA	49,6		7,60
TBIPN	16,93	1,8	6,80
PMA	49,8	2,38	13,0

Si le comportement rotationnel des groupes aliphatiques des nitroxydes et des cétyles était le même, on devrait avoir égalité des rapports des écarts hyperfins correspondants. On trouve :

$$\frac{1,8}{2,38} = 0,756 \quad \text{pour les } a_H,$$

$$\frac{4,84}{7,60} = 0,637 \quad \text{pour les } a_{C_{13}} \text{ des } t\text{-butyles},$$

$$\frac{6,80}{13,0} = 0,524 \quad \text{pour les } a_{C_{13}} \text{ des } isopropyles.$$

La variation constatée est nettement supérieure aux erreurs expérimentales. Le rapport des écarts hyperfins des C_{13} dans le cas du di-*t*-butyl nitroxyde et de l'hexaméthylacétone est toutefois indépendant des barrières de rotation, puisque dans les deux cas il y a libre rotation. D'ailleurs, les deux autres valeurs encadrent ce rapport, ce qui correspond à une barrière de rotation plus faible autour de la liaison C-N du nitroxyde que de la liaison C-C du cétyle, et donc à des oscillations plus grandes des liaisons C-H et C-CH₃ autour de leur position d'équilibre respective, $\theta = 90^\circ$ et $\theta = 30^\circ$. D'où l'augmentation du rapport des écarts hyperfins des protons et la diminution de celui des carbones en position méthyle.

De plus, les écarts hyperfins du C_{13} en position méthyle sont :

$$a_{C_{13}} = \frac{\beta_C}{2} \cdot \rho_C \pi \quad \text{pour l'hexaméthylacétone}$$

et :

$$a_{C_{13}} = \frac{\beta_N}{2} \cdot \rho_N \pi \quad \text{pour le di } t\text{-butyl nitroxyde}.$$

Les constantes β_C et β_N , calculables [1 *a*] par des intégrales de la méthode des liaisons de valence, étant peu différentes pour un carbone ou un azote, on est conduit à prendre :

$$\beta_C = \beta_N.$$

Dans ces conditions, la densité de spin portée par l'azote du nitroxyde est les 64/100e de la densité portée par le carbone du cétyle, diminution attendue en raison de la plus grande électronégativité de l'azote par rapport au carbone.

BIBLIOGRAPHIE

- [1] (a) Partie I: LEMAIRE, H., RASSAT, A., SERVOZ-GAVIN, P., et BERTHIER, G., 1962, *J. Chim. phys.*, 1247.
(b) Partie II: LEMAIRE, H., RASSAT, A., et RAVET, A. M., 1963, *Bull. Soc., chim. Fr.*, 1980.
(c) Partie III: BESSON, R., LEMAIRE, H., RASSAT, A., SALVI, A., et SERVOZ-GAVIN, P., *Colloque Amp. Bordeaux* 1963 (sous presse).
- [2] BRIERE, R., LEMAIRE, H., et RASSAT, A., 1964, *Tetrahedron Letters*, 1781.
- [3] KOSOWER, E. M., 1958, *J. Amer. chem. Soc.*, **80**, 3253.
- [4] HELLER, C., et McCONNELL, H. M., 1960, *J. chem. Phys.*, **32**, 1535.
- [5] STONE, E. W., et MAKI, A. H., 1962, *J. chem. Phys.*, **37**, 1326.
- [6] COPPINGER, G. M., et SWALEN, J. D., 1961, *J. Amer. chem. Soc.*, **83**, 4900.
- [7] HIROTA, N., et WEISSMAN, S. I., 1960, *J. Amer. chem. Soc.*, **82**, 4424.
- [8] SYMONS, M. C. R., 1962, *Tetrahedron*, **18**, 333.

The theory of the temperature dependence of N.M.R. spectra of paramagnetic octahedral complexes

by R. M. GOLDING

Chemistry Division, D.S.I.R., Wellington, New Zealand

(Received 11 May 1964)

The temperature dependence of the nuclear magnetic resonance, N.M.R., spectra of d^n octahedral complexes has been calculated for all the ground-state configurations. This function is similar to the comparable temperature dependent expression for the magnetic susceptibility of these molecules.

1. INTRODUCTION

N.M.R. spectroscopy has mainly been used to determine organic molecular structures by proton magnetic spectroscopy. As reported first by Bloembergen [1] N.M.R. results can be obtained from paramagnetic compounds, for example, Shulman and Jaccarino [2] have studied the ^{19}F resonance of crystalline manganous fluoride and Eaton *et al.* [3] have recorded the proton magnetic resonance of nickel chelates over a range of temperatures.

Bloembergen and Dickinson [4] suggested that the difference, ΔH , between the resonances for a paramagnetic complex in a dilute liquid solution and the related diamagnetic compound depends on the pseudo-contact term. However, McConnell and Chesnut [5] also took into consideration the Fermi contact term and showed by calculation for the $-\text{CH}$ fragment that under normal conditions of N.M.R. spectroscopy it is the main factor contributing to ΔH . They also derived the temperature dependent expression for ΔH when the molecule obeys the Curie law. In the general case however we must consider spin-orbit coupling in addition to the magnetic field interaction in evaluating the N.M.R. temperature dependence of paramagnetic complexes. In this paper we consider octahedral d^n complexes in order to illustrate the significance of this and other variables in predicting the N.M.R. results of these molecules.

2. THEORY

The energy separations of the Zeeman levels depend not only on the applied magnetic field, H , but also on the internal magnetic fields at the nuclei arising from the electronic configuration in the atom or molecule. These internal magnetic fields arising from unpaired electrons can be represented by the general n electron spin Hamiltonian which for d^n electronic configuration is:

$$\mathcal{H} = \frac{2g_N\beta\beta_N}{\langle r^3 \rangle} \left\{ \mathbf{L} \cdot \mathbf{I} + \frac{1}{7} \sum_i (4\mathbf{s}_i - (\mathbf{l}_i\mathbf{s}_i)\mathbf{l}_i - \mathbf{l}_i(\mathbf{l}_i\mathbf{s}_i))\mathbf{I} \right\} + \frac{16}{3} \pi g_N \beta \beta_N \sum \delta(r_{ik}) \mathbf{s}_i \mathbf{I} \quad (1)$$

in the usual notation (see reference [6]).

The first term, in curl brackets, arises from the dipolar interactions of the electron orbital angular momentum with the electron and nuclear spin momenta. The last term arises from the Fermi contact interaction. We concern ourselves here with the case when the molecule is in a dilute liquid solution and the g -tensor, is isotropic and thus we can write the spin Hamiltonian (1) as:

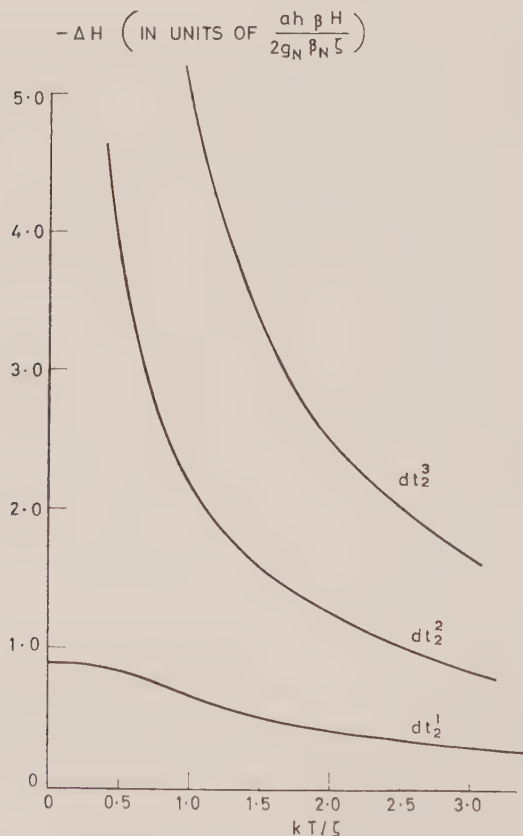
$$\mathcal{H} = \frac{16}{3} \pi g_N \beta \beta_N \sum \delta(r_{ik}) \mathbf{s}_i \cdot \mathbf{I}$$

$$= ha \mathbf{S} \cdot \mathbf{I},$$

where

$$a = \frac{16}{3h} \pi g_N \beta \beta_N \sum \delta(r_{ik}).$$

If the relaxation time is sufficiently short the average internal magnetic field at the nucleus is not zero and will be determined indirectly by the parameter a .



This figure illustrates the theoretical temperature dependence of the N.M.R. spectra for dt_2^1 , dt_2^2 and dt_2^3 complexes. $-\Delta H$ (gauss) is the change in the effective magnetic field at the nucleus due to the unpaired electrons in the molecule; T ; the absolute temperature; k : the Boltzmann's constant; ζ : the spin-orbit coupling constant in ergs; g_N : the nuclear Landé g -factor, and H : the applied magnetic field in gauss. The parameter a is in cycles per second.

Under these conditions the change in the effective magnetic field, ΔH , at the nucleus due to the unpaired electrons in the molecule is simply:

$$\Delta H = ah \langle S_z \rangle / g_N \beta_N, \quad (2)$$

where $\langle S_z \rangle$ is the time-averaged value of the z component of the electron spin. The problem now reduces to the evaluation of $\langle S_z \rangle$.

For the special case when the molecule obeys the Curie law

$$\langle S_z \rangle = -g\beta S(S+1)H/3kT.$$

We will now consider the evaluation of $\langle S_z \rangle$ for octahedral complexes by considering spin-orbit and magnetic field interactions within the ground term. In this case of octahedral site symmetry we need only consider the following possible types of term ${}^{2S+1}A_1$, ${}^{2S+1}A_2$, ${}^{2S+1}E$, ${}^{2S+1}T_1$ and ${}^{2S+1}T_2$. The first three terms each have zero spin-orbit matrix elements within themselves and consequently a molecule in such a ground state will obey the Curie law. However, since the last two terms have non-zero spin-orbit matrix elements within themselves we must consider spin-orbit and magnetic field interaction in evaluating the wavefunctions and the energy levels.

From the isomorphic property of the p and d electrons [6] we may consider the ${}^{2S+1}T_{iJ}$ terms as equivalent to ${}^{2S+1}P_J$, the spin-orbit interaction being given by $\nu \mathbf{L} \cdot \mathbf{S}$ and the magnetic field interaction by $\gamma \mathbf{L} + 2\mathbf{S}$ and $J = 1 + S$, S , $|S-1|$. Since the spin-orbit interaction is the greater interaction for the transition metal ions we shall diagonalize our matrices with respect to the spin-orbit interaction and treat the magnetic field interaction as a perturbation. Solving the appropriate matrices by perturbation theory yields the energy levels and wavefunctions as power series in H , namely:

$$E = W_0(JM) + g\beta MH + \dots$$

$$\psi = \psi(JM) - (\gamma - 2)\beta H \sum_{J'=J+1} \left\{ \frac{\langle J'M | L_z | JM \rangle}{E(J') - E(J)} \right\} \psi(J'M) + \dots,$$

where

$$W_0(JM) = \frac{\nu}{2} \{ J(J+1) - S(S+1) - 2 \}$$

and

$$g = \gamma + (2 - \gamma) \left\{ \frac{J(J+1) + S(S+1) - 2}{2J(J+1)} \right\},$$

except where $J=0$, in which case $g=4-\gamma$ [7].

Here

$$\psi(JM) = \sum_{M_L M_S} \langle 1S M_L M_S | 1S J M \rangle P_{M_L M_S}$$

where $\langle 1S M_L M_S | 1S J M \rangle$ are the usual Wigner coefficients and $P_{M_L M_S}$ represents the p -like atomic wavefunctions in the $M_L M_S$ notation.

Using these wavefunctions, ψ , in the $P_{M_L M_S}$ notation and the corresponding energy levels E , the time-averaged component of the electron spin $\langle S_z \rangle$ can be evaluated after some algebraic rearrangements as:

$$\langle S_z \rangle = \frac{\sum_J (2J+1) \langle S_z \rangle_J \exp [-W_0(JM)/kT]}{\sum_J (2J+1) \exp [-W_0(JM)/kT]}, \quad (3)$$

where

$$\langle S_z \rangle_J = -\frac{\beta H}{3kT} \left\{ \left(\frac{g-\gamma}{2-\gamma} \right) gJ(J+1) + 2 \frac{(g-\gamma)(g-2)}{(2-\gamma)} \frac{kT}{\nu} \right\}.$$

To determine γ and ν for a particular term we proceed as outlined by Griffith [6] by choosing a particular state in the $M_L M_S$ notation for the d electron wavefunction and evaluate the spin-orbit and magnetic interaction energies by comparing the coefficients with the results for the isomorphic $P_{M_L M_S}$ wavefunction. For d^n octahedral complexes the calculated $\langle S_z \rangle_J$ values required to evaluate $\langle S_z \rangle$ for the ground-state terms are tabulated in the table where the parameters A and B are defined by:

$$\langle S_z \rangle_J = -\frac{\beta H}{3kT} \left\{ \frac{A+BkT}{\zeta} \right\},$$

where ζ is the spin-orbit coupling constant of the transition metal ion.

In the case of the d^2 electronic configuration the high spin ground term is 3T_1 and the appropriate term depends on whether we consider weak, intermediate or strong field cases. In the table the term $d^2 t_2^2 {}^3T_1$ is the strong field term and the term $d^2 {}^3F {}^3T_1$ is the weak field term. For an intermediate field case $\langle S_z \rangle_J$ can be evaluated where $\nu = \frac{1}{2}\gamma\zeta$ and $-\frac{3}{2} \leq \gamma \leq -1$. Similarly, the high spin ground term for d^7 octahedral complexes is 4T_1 and $\langle S_z \rangle_J$ depends on whether we are considering a weak, intermediate or strong field. The term $d^7 t_2^5 e^2 {}^4T_1$ is the strong field term and the term $d^7 {}^4F {}^4T_1$ is the weak field term but for the intermediate field term $\nu = -\frac{1}{3}\gamma\zeta$ and $-\frac{3}{2} \leq \gamma \leq -1$.

The low spin ground terms for d^4 and d^5 are obtained from the $d^2 t_2^2 {}^3T_1$ and $d^4 t_2^1 {}^1T_2$ terms respectively by changing the sign of ζ throughout. The only other ground terms we have not considered have spin-only $\langle S_z \rangle$ values. Hence we have calculated the temperature dependence of the time-averaged electron spin value of all d^n octahedral paramagnetic complexes in their ground state.

Finally, substituting the calculated value for $\langle S_z \rangle$ in equation (2) yields the temperature dependence of the N.M.R. spectra of these complexes. We shall illustrate this temperature dependence for dt_2^1 , dt_2^2 and dt_2^3 complexes. From the table and equations (2) and (3):

$$\Delta H = -\frac{ah\beta H}{18\zeta g_N \beta_N} \left\{ \frac{3x-16+16 \exp(3x/2)}{1+2 \exp(3x/2)} \right\} \text{ for } dt_2^1,$$

$$\Delta H = -\frac{ah\beta H}{6\zeta g_N \beta_N} \left\{ \frac{5(3x+6) \exp(3x/2) + 3(x+6) \exp(x/2) - 48}{5 \exp(3x/2) + 3 \exp(x/2) + 1} \right\} \text{ for } dt_2^2$$

and

$$\Delta H = -\frac{ah\beta H}{2\zeta g_N \beta_N} \{5x\} \text{ for } dt_2^3,$$

where $x = \zeta/kT$. These functions are plotted in the figure.

3. COMPARISON OF χ AND ΔH

The magnetic susceptibility, χ [8] can be calculated from the summation of the magnetic moments weighted by the appropriate Boltzmann distribution factor over all the energy levels. On the other hand ΔH depends on the energy levels and their wavefunctions; both are expressed as power series in H , the applied magnetic field. The general expressions for χ and ΔH may now be compared. The magnetic susceptibility is [7]:

$$\chi = \frac{\sum_J (2J+1) \chi_J \exp[-W_0(JM)/kT]}{\sum_J (2J+1) \exp[-W_0(JM)/kT]}, \quad (4)$$

where

$$\chi_J = \frac{N\beta^2}{3kT} \left\{ g^2 J(J+1) + 2(g-\gamma)(g-2) \frac{kT}{\nu} \right\}.$$

χ and ΔH can be seen to have the same temperature dependence only when the molecule obeys the Curie law and in this special case:

$$\Delta H = - \frac{ah\chi}{2g_N\beta\beta_N N}.$$

Term	γ	ν	J	g	A	B
$d^1 t_2^{1/2} T_2$	-1	$-\zeta$	1/2	-2	1/2	-8/3
			3/2	0	0	4/3
$d^2 t_2^{2/3} T_1$	-1	$-\zeta/2$	0	5	0	-24
			1	1/2	1/2	3
			2	1/2	3/2	3
$d^2 {}^3F^3 T_1$	-3/2	$-3\zeta/4$	0	11/2	0	-56/3
			1	1/4	1/4	7/3
			2	1/4	3/4	7/3
$d^6 t_2^4 e^2 {}^5T_2$	-1	$\zeta/4$	1	7/2	21/2	18
			2	3/2	15/2	-10/3
			3	1	8	-16/3
$d^7 t_2^5 e^2 {}^4T_1$	-1	$\zeta/3$	1/2	4	5	20
			3/2	6/5	33/10	-88/25
			5/2	4/5	21/5	-108/25
$d^7 {}^4F^4 T_1$	-3/2	$\zeta/2$	1/2	13/3	65/12	140/9
			3/2	16/15	44/15	-616/225
			5/2	3/5	63/20	-84/20

The values of $\langle S_z \rangle_J$ are summarized for several terms where A and B are defined by the equation:

$$\langle S_z \rangle_J = - \frac{\beta H}{3kT} \left\{ A + \frac{BkT}{\zeta} \right\},$$

where ζ is the spin-orbit coupling constant. The parameters γ and ν are given for each term.

4. g ANISOTROPY

So far we have considered an isotropic g -tensor but a distortion from octahedral symmetry will produce g anisotropy. In this case the dipolar interaction term will not average to zero but is proportional to $g_{\parallel}^2 - g_{\perp}^2$ giving rise to the pseudo-contact term [4]. However, the calculated pseudo-contact term is an order of magnitude smaller than the experimental ΔH for the ^{14}N resonance in the $\text{Fe}(\text{CN})_6^{3-}$ ion [9], and is negligible for the planar CH_3 radical [5]. It appears that it is very small in most significant cases.

REFERENCES

- [1] BLOEMBERGEN, N., 1950, *Physica*, **16**, 95. BLOEMBERGEN, N., and POULIS, N. J., 1950, *Physica*, **16**, 915.
- [2] SHULMAN, R. G., and JACCARINO, V., 1957, *Phys. Rev.*, **108**, 1219.
- [3] EATON, D. R., JOSEY, A. D., PHILLIPS, W. D., and BENSON, R. E., 1962, *Disc. Faraday Soc.*, **34**, 77.
- [4] BLOEMBERGEN, N., and DICKINSON, W., C. 1950, *Phys. Rev.*, **79**, 179.
- [5] McCONNELL, H. M., and CHESNUT, D. B., 1958, *J. chem. Phys.*, **28**, 107.
- [6] GRIFFITH, J. S., 1961, *The Theory of Transition-Metal Ions* (Cambridge University Press).
- [7] GRIFFITH, J. S., 1958, *Trans. Faraday Soc.*, **54**, 1109.
- [8] VAN VLECK, J. H., 1932, *The Theory of Electric and Magnetic Susceptibilities* (Oxford University Press).
- [9] SHULMAN, R. G., 1958, *J. chem. Phys.*, **29**, 945.

Proton-proton double resonance studies of formamide- ^{15}N and N-methylformamide- ^{15}N

by A. J. R. BOURN and E. W. RANDALL

Queen Mary College, London University, Mile End Road,
London, E.1

(Received 3 July 1964)

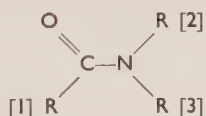
The magnitudes and some of the relative signs of the ^{15}N -H and H-H couplings in N-methylformamide- ^{15}N and formamide- ^{15}N have been determined. The ^{15}N -H couplings through one bond in these amides and in ammonia, ammonium ion and pyridinium ion are apparently dominated by the Fermi contact term, pyrrole being exceptional. Other couplings are quite successfully accounted for by the theory worked out for molecules with exclusively carbon frameworks.

Changes in the coupling constants of N-methylformamide with dilution in water can be partly explained by an increase in the C-N bond order by interaction with the water solvent.

1. INTRODUCTION

It is not usually possible to observe ^{14}N -H couplings because of electric quadrupole relaxation effects at the nitrogen-14 nucleus. Occasionally H-H couplings are obscured also. Whereas these latter couplings can sometimes be determined from ^{14}N - ^1H double irradiation experiments, observation of the N-H couplings is best done by substitution of the isotope ^{15}N , $I = \frac{1}{2}$, which results in sharp spin-multiplets. Amides which have been studied in this way are formamide- ^{15}N [1], N,N-dimethylformamide- ^{15}N [2] and N-phenylformamide- ^{15}N [3]. The single resonance work on formamide- ^{15}N has been repeated here as a preliminary to the proton-proton double resonance experiments.

The numbering of groups follows the numbering used previously [4]



as do the notations for configuration [3], coupling constants [3], and double resonance experiments [5, 6]. Other authors [7] use different conventions for the configurations.

2. EXPERIMENTAL

Spectra were initially taken on a Varian A-60 spectrometer (probe temperature $35^\circ\text{C} \pm 1^\circ\text{C}$). Calibration was by the audio sideband technique [8] using a Solartron audio oscillator (type CO 546) and a Venner transistorized counter (type TSA 3336).

N-methylformamide- ^{15}N and formamide- ^{15}N were supplied by Mercke, Sharp and Dohme of Canada, Ltd. with percentage enrichments of 99 per cent. N-methylformamide- ^{15}N was supplied in three solutions of 25.3 per cent, 48.9 per cent and 74.5 per cent by weight in distilled water and as one pure sample.

Formamide- ^{15}N was used as a 29.6 per cent solution, by weight, in acetone, which enabled all 24 lines in the spectrum to be resolved. In the pure liquid this is not possible [1].

The proton decouplings were all attempted on a Varian V4302 spectrometer at 60 Mc/s equipped with a flux stabilizer. Sample temperatures on this instrument were $25^\circ\text{C} \pm 1^\circ\text{C}$. Spectra were recalibrated (Hewlett Packard 300 CD audio oscillator) at this temperature, since the chemical shifts, particularly for formamide- ^{15}N , were temperature dependent. The 'field-sweep' method with double audio modulation and an audio phase-sensitive lock-in detector similar to that described by Freeman was used [9]. No attempt was made to measure the decoupling field strength, H_2 .

3. RESULTS AND ASSIGNMENTS

The protons of N-methylformamide- ^{14}N form an ABX_3 set [4, 10]. The AB features at low field are assigned to the CH and NH protons and are broadened by electric quadrupole relaxation of the ^{14}N nucleus to which they are coupled. The broadening was almost completely removed by $\text{H}-\{^{15}\text{N}\}$ double resonance [4].

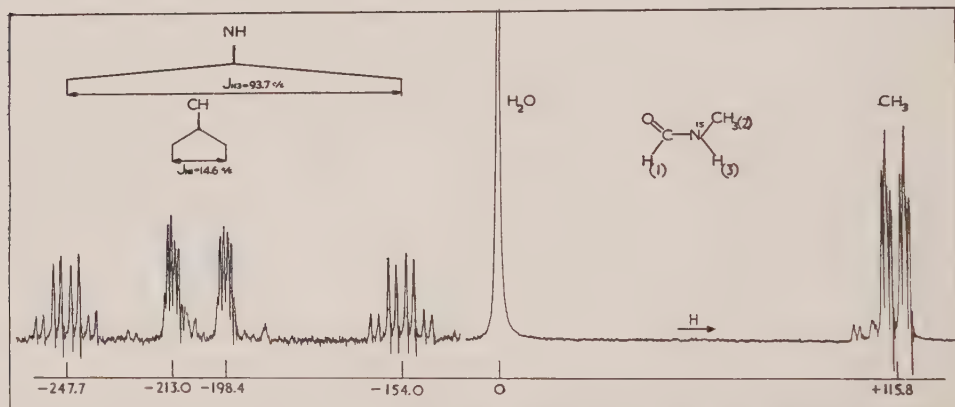


Figure 1. Proton spectrum of a 74.5 per cent solution by weight of N-methylformamide- ^{15}N in water at 60 Mc/s and 35° .

Substitution of the isotope ^{15}N produces sharp proton lines and additional doublet splittings (ABMX_3 case) as can be seen from figure 1, the proton spectrum of a 74.5 per cent solution by weight of N-methylformamide- ^{15}N in water.

The high field methyl feature is an octet. The largest and smallest splittings are 4.9 c/s and 0.8 c/s and are assigned to the couplings $J_{23}(\text{Me}-\text{H})$ and $J_{12}(\text{H}-\text{Me})$ [4, 10]. The additional doublet splitting of 1.1 c/s is assigned to $J_{\text{N}2}(\text{N}-\text{Me})$. This coupling is almost identical to the analogous coupling in N,N-dimethylformamide- ^{15}N [2].

The NH and CH resonances in N-methylformamide- ^{14}N would each be an octet of lines if they were not broadened by the ^{14}N quadrupole relaxation [4]. This is confirmed in the ^{15}N molecule where all eight lines are clearly visible in each multiplet (figure 2), which is split further into two distinct halves by the coupling $J_{\text{N}1}$ and $J_{\text{N}3}$ respectively and each half consists of two overlapping quartets.

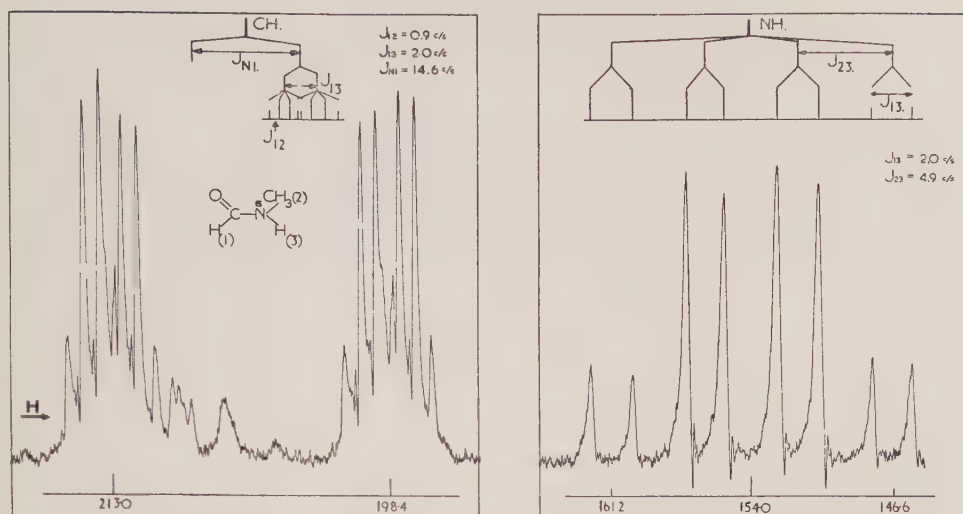


Figure 2. CH and part of the NH regions of the proton spectrum of N-methylformamide- ^{15}N at 60 Mc/s and 35°C . Shifts in c/s downfield from water.

The values of $J_{\text{N}3}$ and $J_{\text{N}1}$ correspond closely to the analogous couplings of 92.0 and 19.0 c/s respectively in formamide- ^{15}N , which are shown in table 1 together with the signs we have determined by double resonance.

The double resonance experiments in N-methylformamide- ^{15}N are clarified by reference to the nearest-neighbour spin-state diagram which has been drawn with all the coupling constants positive (see figure 3). The peaks are numbered there from low to high field.

The most feasible double resonance experiment is one involving the formyl and methylprotons. Irradiation at the centre of lines 17, 18, 19 and 21 caused 33 and 34 to collapse to a single line, as shown in figure 4(a). The value of $\nu_2 - \nu_1$, the difference between the modulation frequencies, for maximum decoupling was 311.0 c/s. This decoupling identified the $J_{\text{N}2}$ and $J_{\text{N}12}$ splittings and indicates that $J_{\text{N}1}$ and $J_{\text{N}2}$ have opposite signs and that J_{13} and J_{23} have the same sign.

	$J_{\text{N}1}$	$J_{\text{N}2}$ $J_{\text{N}2}(\text{N-Me})$	$J_{\text{N}3}$ $J_{\text{N}3}(\text{N-Me})$	Ref.
Formamide- ^{15}N pure	19.0	88.0	92.0	[1]
29.6 per cent acetone	± 16.4	± 86.4	± 89.7	†
N-methylformamide pure	15.6	1.2	92.6	†
75 per cent H_2O	± 14.6	∓ 1.4	± 93.7	
49 per cent	14.4	1.4	93.9	
25 per cent	14.1	1.4	93.6	
cis-N-phenylformamide	± 16.2	—	± 91.0	[3]
trans	± 15.0	± 88.3		
NN-dimethylformamide	± 15.6	∓ 1.2	∓ 1.1	[2]

† This paper.

Table 1. ^{15}N -H coupling constants in ^{15}N formamides (c/s ± 0.1 c/s).

Three further $\{H_1\}Me_2$ experiments confirm these signs. Irradiation of lines 20, 22, 23 and 24; 9, 10, 11 and 13; 12, 14, 15 and 16, causes lines 37 and 38, 35 and 36, 39 and 40 respectively to collapse. The decoupled spectra are shown in (b), (c) and (d) of figure 4, when the values of $\nu_2 - \nu_1$ correspond to 314.0 c/s, 327.2 c/s and 329.9 c/s respectively. The values of $\nu_2 - \nu_1$ for maximum decoupling calculated from the calibration were 311.9 c/s, 314.9 c/s, 327.9 c/s and 331.0 c/s. This discrepancy of almost 1.0 c/s between the experimental and calculated values may have been due to too high a value of H_2 necessitating a correction of the type proposed by Freeman and Anderson [11] or to a slight temperature dependence of the shifts.

To check the previous decouplings and the sign determinations the reverse double resonance experiments, $H_1\{Me_2\}$, were completed, in the same up-field sideband, by reversing the sign of $\nu_2 - \nu_1$. Irradiation of lines 33 and 34, 37 and

Origin of Transition		NH ₍₃₎	CH ₍₁₎	NH ₍₃₎	Me ₍₂₎
Numbering of Spectrum.		1 2 3 4 5 6 7 8	9 10 11 14 15 16 17 18 19 22 23 24	25 26 27 29 31 32	33 34 35 36 37 38 39 40
Neighbouring Spin	CH	$\alpha\beta\alpha\beta\alpha\beta\alpha\beta$		$\alpha\beta\alpha\beta\alpha\beta\alpha\beta$	$\alpha\beta\alpha\beta\alpha\beta\alpha\beta$
	NH		$\alpha\alpha\alpha\alpha\beta\beta\alpha\alpha\beta\beta$ $\beta\beta\beta\beta$		$\alpha\alpha\alpha\alpha\beta\beta\beta\beta$
	Me	a b c d a b c d	a c d c a c d c b a b d b a b d	a b c d a b c d	
	N	$\alpha\alpha\alpha\alpha\alpha\alpha\alpha\alpha$	$\alpha\alpha\alpha\alpha\beta\beta\beta\beta$ $\alpha\alpha\beta\beta$	$\beta\beta\beta\beta\beta\beta\beta\beta$	$\alpha\alpha\beta\beta\alpha\alpha\beta\beta$

Figure 3. Spin-state diagram for N-methylformamide- ^{15}N and diagrammatic proton spectrum for 60 Mc/s. $a = \alpha\alpha\alpha$; $b = \alpha\alpha\beta$; $c = \alpha\beta\beta$; $d = \beta\beta\beta$.

38, 35 and 36, and 39 and 40 causes coalescence of lines 17, 18, 19 and 21; 20, 22, 23 and 24; 9, 10, 11 and 13; and 12, 14, 15 and 16, as shown in figure 5 (b), (c), (d) and (e), respectively. The $\nu_1 - \nu_2$ values are again slightly smaller than the calibrated shift differences.

It is impossible to determine the relative sign of J_{12} and J_{23} by a $H_1\{H_3\}$ experiment, because of the impossibility of irradiating only two lines with the same methylproton spin state. The relative signs of J_{N1} and J_{N3} however can be determined by double resonance between these two groups. Irradiation of the high field half of the NH resonance, lines 25–32, coalesces the high field half of the CH resonance, lines 17–24, with maximum effect when $\nu_2 - \nu_1 = 45.9$ c/s. When the low field half of the NH resonance, lines 1–8, was irradiated no decoupling at

all was observed on lines 17–24. This indicated that $J_{\text{N}1}$ and $J_{\text{N}3}$ have the same sign. It is confirmed by irradiating lines 1–8 and collapsing lines 9–16 with maximum effect when $\nu_1 - \nu_2 = 35$ c/s. No decoupling was observed in this region of the CH resonance when the irradiating field H_2 was centred on lines 25–32.

The relative signs of $J_{\text{N}1}$ and $J_{\text{N}3}$ could also be found by inspection of the intensities in each half of the CH resonance. Thus lines 10 and 11 are stronger than lines 14 and 15, and lines 22 and 23 are stronger than lines 18 and 19 (figures 2 and 3). This behaviour is consistent only with $J_{\text{N}1}$ and $J_{\text{N}3}$ having the same sign, otherwise the above alternations in intensity would be reversed.

The relative signs and the magnitudes of the proton–proton couplings are given in table 2.

	J_{12}	$J_{12}(\text{H-Me})$	J_{13}	J_{23}	$J_{23}(\text{H-Me})$
Formamide- $^{15}\text{N}\dagger$	± 13.4	—	± 1.7	± 2.8	—
N-methylformamide- $^{15}\text{N}\ddagger$	—	∓ 0.8	± 1.9	—	± 4.9

\dagger 29.6 per cent by weight in acetone. \ddagger pure liquid.

Table 2. Magnitudes (c/s \pm 0.1 c/s) and relative signs of proton–proton couplings in formamide- ^{15}N and N-methylformamide- ^{15}N .

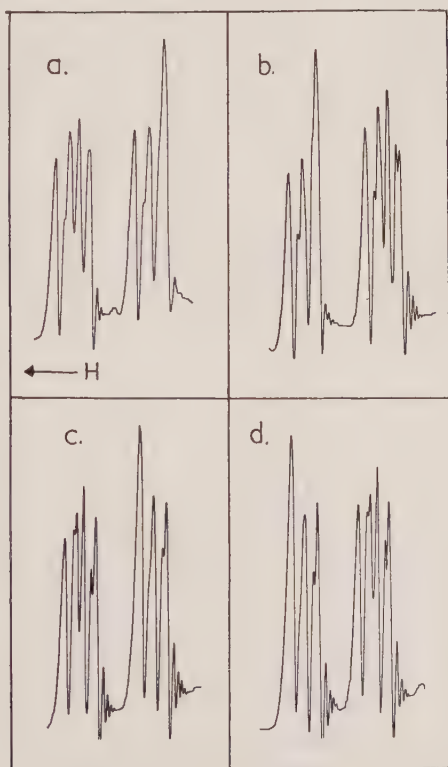


Figure 4. Proton–proton double irradiation, $\text{Me}_2\{\text{H}_1\}$, spectra for N-methylformamide- ^{15}N .

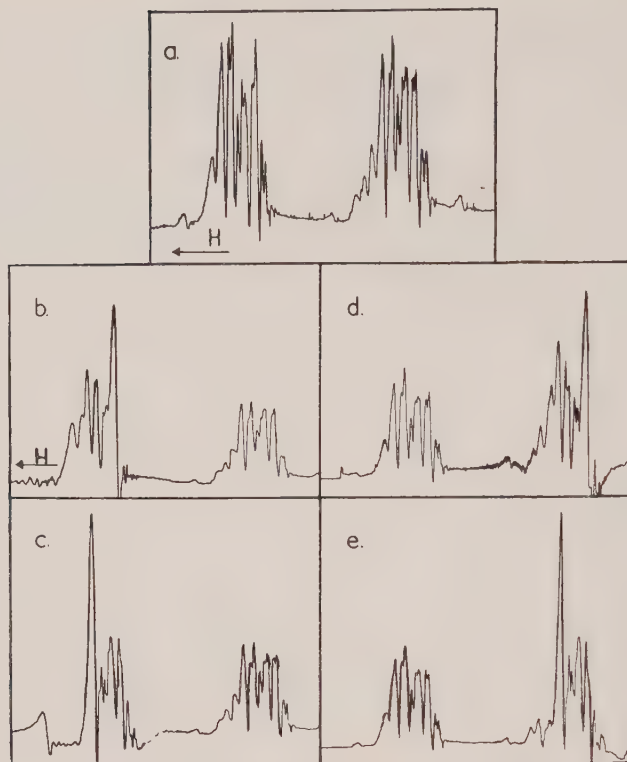


Figure 5. $H_1\{Me_2\}$ double irradiation spectra for N-methylformamide- ^{15}N : (a) undecoupled; (b), (c), (d), (e) decoupled.

Origin of Transition.		$CH_{(1)}$		$NH_{(3)}$		CH		$NH_{(2)}$				$NH_{(3)}$		$NH_{(2)}$											
Numbering of Spectrum.		1	2	3	4	5	6	7	8	9	10	11	12	13	14	15	16	17	18	19	20	21	22	23	24
Neighbouring Spin States.	CH							$\alpha\beta\alpha\beta$						$\alpha\alpha\beta\beta$					$\alpha\beta\alpha\beta$	$\alpha\alpha$	$\beta\beta$				
	$NH_{(3)}$	$\alpha\beta$		$\alpha\beta\alpha\beta$					$\alpha\beta$	$\alpha\beta$	$\alpha\beta$									$\alpha\beta$	$\alpha\beta$				
	$NH_{(2)}$	$\alpha\alpha$		$\beta\beta\alpha\alpha$		$\alpha\alpha\beta\beta$	$\beta\beta$												$\alpha\alpha\beta\beta$						
	N	$\alpha\alpha$		$\alpha\alpha\beta\beta$		$\alpha\alpha\alpha\alpha$	$\beta\beta$	$\alpha\alpha$	$\alpha\alpha$										$\beta\beta\beta\beta$	$\beta\beta$	$\beta\beta$				

Figure 6. Spin-state diagram for formamide- ^{15}N and diagrammatic assignment of the proton spectrum at 60 Mc/s.

The assignment of formamide- ^{15}N follows that given previously [1] and is shown in the spin state diagram (figure 6) for which all the couplings were assumed positive. The couplings are given in tables 1 and 2. The chemical shifts, δ , of a 29.6 per cent by weight solution in acetone ($\text{c/s} \pm 0.1 \text{ c/s}$) relative to the tetramethylsilane are $\delta_3 = -439.3$, $\delta_2 = -424.8$ and $\delta_1 = -490.2$.

The relative signs of the NH couplings in one set and of the H-H couplings in a second unrelated set were determined as before by proton-proton double resonance. Figure 7 shows the results of $\text{H}_1\{\text{H}_3\}$ and $\text{H}_3\{\text{H}_1\}$ experiments, which establish that $J_{\text{N}1}$ and $J_{\text{N}3}$ have the same sign, and that J_{12} and J_{23} also have the same sign. The remaining accessible signs were determined by an $\{\text{H}_2\}\text{H}_3$ experiment in which irradiation of lines 15 and 16 collapsed lines 8 and 10 indicating that $J_{\text{N}2}$ and $J_{\text{N}3}$ have the same sign, and that J_{12} and J_{13} have the same sign.

Other decouplings are described elsewhere [12].

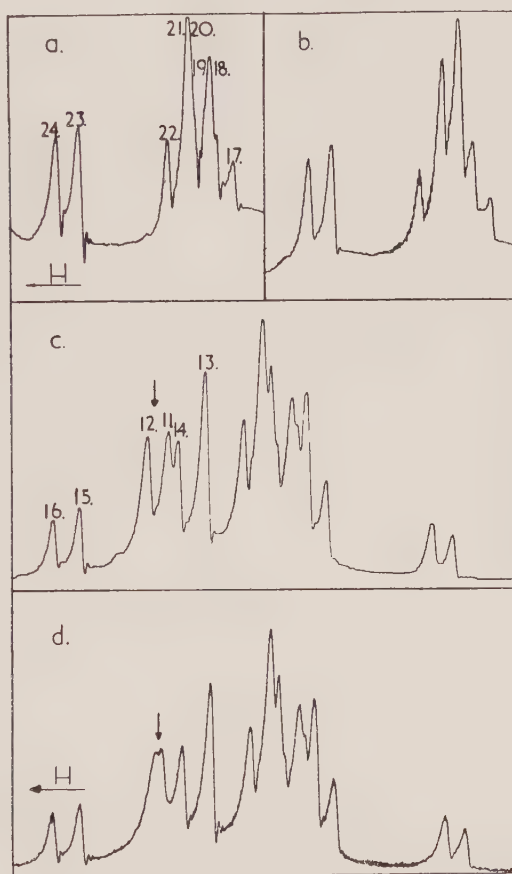


Figure 7. Proton resonance spectra of formamide- ^{15}N at 60 Mc/s.

(a) Part NH region of single resonance spectrum.

(b) Same region as in (a) with $\text{H}_3\{\text{H}_1\}$ double irradiation, $\nu_1 - \nu_2 = 80.4 \text{ c/s}$.

(c) Part CH region of single resonance spectrum.

(d) Same region as in (c) with $\text{H}_1\{\text{H}_3\}$ double irradiation, $\nu_2 - \nu_1 = 80.4 \text{ c/s}$.

4. DISCUSSION

4.1. *N-H coupling through one bond*

The one-bond couplings J_{N_2} and J_{N_3} should both be negative relative to an absolute positive sign for $J(^{13}\text{C-H})$ [13]. The reversal of sign should be due merely to the different signs of the magnetogyric ratios of ^{13}C and ^{15}N , and the most widely held definition for the signs of coupling constants, viz. a positive sign indicates that an antiparallel, as opposed to a parallel, arrangement of nuclear spins is the stable configuration. A determination of these absolute signs has not been made but we have established the necessary condition that the signs of J_{N_2} and J_{N_3} are the same.

Various accounts have been given of the values of directly bonded, generally $^{13}\text{C-H}$, couplings [13–18]. The hypothesis is that $J(^{13}\text{C-H})$ is determined mainly by the Fermi contact term and, since changes in excitation energy are rarely considered important, is therefore proportional to a^2 , the square of the coefficient of the carbon 2s wave function in the LCAO description of the hybrid orbital. Difficulties in the calculation of a^2 arise when the groups attached to carbon are different from each other, for then the s characters in the hybrid orbitals of any one carbon atom need not be equal. In cases where carbon has a coordination number of four, and the hybridization is close to sp^3 , sufficient compounds have been studied to enable empirical additivity relationships to be tested for these substituent effects upon $J(^{13}\text{C-H})$ [19, 20]. A rationalization of these empirical relationships on the basis of the Fermi contact term has been made by Juan and Gutowsky [21, 22].

The extension of the treatment to three and to two coordinate carbon involving hybridizations close to sp^2 and sp respectively is rather more difficult, and requires the introduction of π -contributions to J arising from the double bond adjacent to the C-H bond [21, 22].

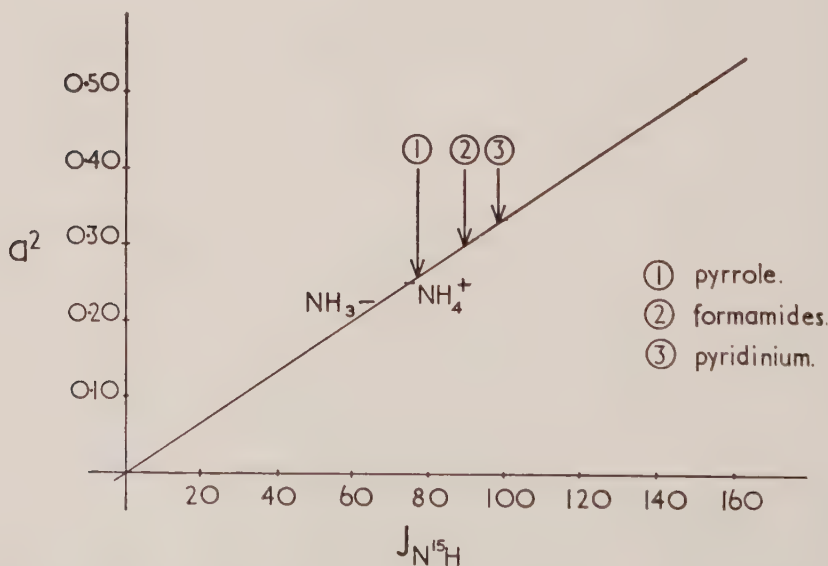


Figure 8. Hypothetical straight line plot of degree of s character, a^2 , against $J(^{15}\text{N-H})$ in c/s based on NH_3 , NH_4^+ and the origin. J values of other molecules shown.

Inconsistencies between the hypothesis and the s characters deduced by applying hybridization theory to structural data have been revealed [15, 21, 22].

In the case of NH bonds not only is the number of available accurate coupling constants small but structural data are also scant, and a rigorous test of the contact hypothesis is even harder to make than in the ^{13}C cases. Some discussion may be marginally useful even so, particularly since another method for investigating the structures at nitrogen atoms, e.g. in aniline, is very desirable.

Figure 8 shows a plot of a^2 against $J(^{15}\text{N}-\text{H})$. The straight line was set up using the symmetrical cases NH_4^+ and NH_3 , for which the $J(^{15}\text{N}-\text{H})$ couplings are 73.7 ± 0.1 c/s [18, 23] and 64.0 ± 2.0 c/s [24] respectively, and by assuming that $J=0$ when $a^2=0$. The appropriate values of a^2 are 0.25 and 0.224 for NH_4^+ and NH_3 respectively [18].

The range of J values in the formamides corresponds in this plot to

$$a^2 = 0.300 \pm 0.015.$$

If one neglects the unequal distribution of s character in the three nitrogen σ bonds in formamide, a^2 should be slightly less than 0.333 because the molecule is not quite planar [25]. The precise values for J depend upon the orientation of the N-H bond. It has already been pointed out that the shorter, N3, bond (having presumably the greater s character) has a larger coupling than the longer N2 bond [1].

Substituent effect on J_{N_2} and J_{N_3} are small at least for the three groups phenyl, methyl, and the hydrogen atom. We conclude that the N-H bonds are very similar in N-monosubstituted formamides and in formamide itself, and that the structure of the formamide framework does not vary greatly.

In the pyridinium ion $J(^{14}\text{N}-\text{H}) = 70$ c/s [26] from which $J(^{15}\text{N}-\text{H})$ is deduced to be 98.7. This corresponds in figure 8 to $a^2 = 0.33$, so that if the ion is planar the bond angles around the nitrogen atom should be approximately 120° .

For pyrrole $J(^{14}\text{N}-\text{H}) = 55 \pm 5$ c/s [27], hence $J(^{15}\text{N}-\text{H}) = 77 \pm 7$ c/s corresponding to a^2 being in the range 0.23 to 0.28. The value of a^2 deduced from the structural data (planar molecule [28], and $\widehat{\text{CNC}} = 105 \pm 4^\circ$ [29]) is 0.5 ± 0.1 [30]. This serious discrepancy points to a flaw in the excitation energy approximation, or in the hypothesis that the contributions to the coupling other than the contact term are negligible.

4.2. N-H coupling through two bonds

The values of the two-bond couplings $J_{\text{N}_2}(\text{N}-\text{Me})$ and $J_{\text{N}_3}(\text{N}-\text{Me})$ are small as are similar couplings involving ^{13}C [31]. These latter are apparently governed by the contact term [31], and we have similarly suggested (on scant evidence) that the contact term is important for J_{HCH} also [2].

The signs of the direct and two-bond $^{13}\text{C}-\text{H}$ couplings in approximately sp^3 situations are different for ethane [32] and ethyl iodide [33] (although not in 1,1,2,2 tetrabromoethane [34]). And, in a molecule where the ^{13}C atom is approximately sp hybridized, viz. propyne, the $^{13}\text{C}-\text{H}$ coupling across two bonds (neither of which is the multiple bond) is again negative relative to J_{CH} [35]. We may

therefore infer, on the contact hypothesis, that the relative signs of the one and two-bond ^{13}C -H couplings are also opposite for an sp^2 hybridized ^{13}C atom, provided again that the bonds involved are single bonds.

Substitution of a methyl group for a proton on the approximately sp^2 hybridized nitrogen atom of the amides studied here similarly reverses the sign of the ^{15}N -H coupling.

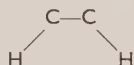
The magnitude of the second type of two-bond coupling in the ^{15}N amides, J_{N1} , is substantially higher than those just discussed and has the same sign as the direct coupling. It involves a bond with a bond order greater than one. The effect of an increase in bond order on the two-bond ^{13}C -H couplings is also to reverse the sign of this coupling relative to the direct coupling [32], although a higher bond order, > 2 , is apparently required than for the nitrogen case.

The large value of J_{N1} is, like the two-bond coupling $J(\text{C } ^{13}\text{C}-\text{H})$ in acetylene, apparently 'anomalous' [32].

4.3. H-H three-bond couplings

The signs of the proton-proton couplings have previously been discussed on the presumption that the Karplus treatment of ethylene can be extended to formamides [4]. In ethylene the cis and trans vicinal couplings are both positive (σ contribution of $+6.1$ c/s and $+11.9$ c/s respectively, plus a π bond contribution of $+1.5$ to both) relative to the positive direct coupling $J(^{13}\text{C}-\text{H})$ [36]. On this basis J_{12} and J_{13} in formamide should have the same sign. This is found to be so.

In a similar way one expects the couplings J_{13} and J_{23} (H-Me) in N-methylformamide to have the same sign because the theoretical σ contribution to a vicinal coupling



which is an average over all rotations is $+4.2$ c/s [36]. The measured value of J_{23} (H-Me) is 4.8 c/s. The positive sign for J_{23} (H-Me) relative to the positive cis vicinal coupling contradicts the sign inference made earlier [4] relative to an assumed positive sign for the four-bond coupling J_{12} (H-Me). This coupling is actually negative.

The values in c/s of the proton-proton couplings in formamide compared with those in ethylene are shown in table 3.

	J_{gem}	J_{cis}	J_{trans}	$\widehat{\text{HXH}}$
Ethylene, exptl.	$+2.5$	$+11.7$	$+19.4$	$117.4^\circ \dagger$
theo.	$?$	$6.1 + 1.5$	$11.9 + 1.5$	
Formamide	± 2.8	± 1.7	± 13.4	$118^\circ 53'$

\dagger See [37].

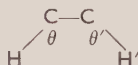
Table 3.

The vicinal couplings J_{cis} and J_{trans} in formamide might be expected to deviate only slightly from those in ethylene because, although the C-N bond order in formamide is less than one, the theoretical $J_{\text{vic}}(\pi)$ in ethylene which has a full double bond is only 1.7 c/s.

The actual values, however, are considerably reduced and the ratio $J_{\text{cis}}/J_{\text{trans}}$ is nowhere near either the theoretical or experimental value in ethylene. There is an embarrassment of factors which individually or collectively could account for these low vicinal couplings. These are

- (i) the effect of dihedral angle on J_{vic} [4, 36, 38],
- (ii) the effect of electronegative substituents [39–43], and
- (iii) the effects of variation in bond lengths [49].

Vicinal couplings are also expected to depend significantly on the angles $\theta = \widehat{\text{HCC}}$ and $\theta' = \widehat{\text{CCH}}$ [44],



and calculations show that $J_{\text{HH}}(\text{vic})$ should decrease as θ and θ' increase. The angle θ equals 113° in formamide and is smaller than the similar angle in ethylene so that the couplings ought to increase by comparison.

4.4. Long-range four-bond couplings

Karplus predicts theoretically [45] that the magnitude of long-range proton-proton couplings over four sigma bonds will be < 0.5 c/s. The few long-range couplings which have been observed in saturated systems have been < 0.8 c/s, negative in sign relative to positive vicinal couplings, and in some instances very stereo-specific. A σ -bond mechanism seems probable therefore. This negative sign for the four-bond couplings is predicted by the Dirac Vector Model [40].

The exact effect of the π electrons on J_{12} (H–Me) and J_{13} (H–Me) in N,N-dimethylformamide and J_{12} (H–Me) in N-methylformamide is open to speculation. Karplus' successful valence bond treatment of unsaturated systems [45] predicts that the π contribution to a coupling over four bonds will be -1.7 c/s for both cis and trans forms. It is unlikely that a partial π bond will make so large a contribution but the total effect of σ and π mechanisms should be a negative total J . In agreement with this, the long-range coupling J_{12} in N-methylformamide- ^{15}N was found to be negative, relative to a positive vicinal coupling, and not positive as suggested [4].

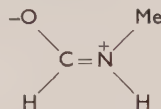
4.5. Geminal two-bond couplings, H–H

Several geminal proton couplings have been determined as negative, relative to absolute positive vicinal couplings, in contrast to early predictions [46, 47]. However, in ethylene, the geminal CH_2 coupling is positive $= +2.5$ c/s [32]. The corresponding geminal coupling $J_{23} = 2.8$ c/s in formamide is also positive. The parity of the actual magnitudes is probably fortuitous even though the two molecules have similar values of $\widehat{\text{HXH}}$. The presence of electronegative substituents X in vinyl compounds $\text{CH}_2=\text{CHX}$ has been observed to cause a decrease in the positive J_{gem} [39, 41] and Barfield and Grant [48] estimate that double bonds which are two bonds from geminal protons ($\text{H}_2\text{C}=\text{C}-\text{CH}_2\text{X}$) have an additive contribution to the geminal coupling.

4.6. Solvent effects on coupling constants

The effect of dilution of N-methylformamide- ^{15}N by water upon the coupling constants is given in table 1. It has already been postulated that the increase in

J_{13} in the ^{14}N compound, which is duplicated in the ^{15}N compound, on dilution is due to stabilization of the planar resonance form:



and the consequent reduction in the dihedral angle between the CH bond in the formyl group and the NH bond [4]. This hypothesis may be tested by applying it to other couplings in the molecule.

A more planar structure should produce a greater s character in the nitrogen σ bonds. We expect therefore an increase in the direct coupling $J_{\text{N}1}$ and the two-bond coupling $J_{\text{N}2}$ (N-Me), since the Fermi contact terms, postulated as the dominant terms in these couplings, increase with the percentage s character in the nitrogen bonds. The results are not at variance with these consequences.

The diminution of the coupling $J_{\text{N}1}$ is the largest change wrought by dilution. It was not predicted. The position here is complicated, as we have seen, by the partial double bond character of the C-N bond. If the σ -bond contribution to the coupling is largely unchanged by the solvent, i.e. the bond angle $\widehat{\text{HCN}}$ remains constant, the following argument holds. The major contribution to $J_{\text{N}1}$ is $J_{\text{N}1}(\sigma)$, i.e. $J_{\text{N}1}$ and $J_{\text{N}1}(\sigma)$ have the same sign, and therefore $J_{\text{N}1}(\sigma)$ and $J_{\text{N}1}(\pi)$ are of opposite sign. Since $J_{\text{N}1}$ has the same sign as the direct coupling $J_{\text{N}3}$, it follows that $J_{\text{N}1}(\pi)$, a two-bond coupling, is of opposite sign to the direct coupling. One may hence infer that the π contribution to a two-bond ^{13}C -H coupling has an opposite sign to the direct ^{13}C -H coupling, i.e. is negative.

We are grateful to the Director of the National Physical Laboratory, Teddington, for the use of the Varian HR.60 spectrometer and decoupler. We thank the Department of Scientific and Industrial Research for a Research Studentship (to A. J. R. B.), and Dr. D. H. Whiffen and Dr. K. A. McLauchlan for useful discussion.

REFERENCES

- [1] SUNNERS, B., PIETTE, L. H., and SCHNEIDER, W. G., 1960, *Canad. J. Chem.*, **38**, 681.
- [2] BOURN, A. J. R., and RANDALL, E. W., 1964, *J. mol. Spectrosc.*, **13**, 29.
- [3] BOURN, A. J. R., GILLIES, D. G., and RANDALL, E. W., 1964, *Tetrahedron* **20**, 1811.
- [4] RANDALL, E. W., and BALDESCHWIELER, J. D., 1962, *J. mol. Spectrosc.*, **8**, 365.
- [5] BALDESCHWIELER, J. D., and RANDALL, E. W., 1963, *Chem. Rev.*, **63**, 81.
- [6] RANDALL, E. W., 1962, *Disc. Faraday Soc.*, **34**, 156.
- [7] LA PLANCHE, L., and ROGERS, M. T., 1964, *J. Amer. chem. Soc.*, **86**, 337.
- [8] ARNOLD, J. T., and PACKARD, M. E., 1951, *J. chem. Phys.*, **24**, 468.
- [9] FREEMAN, R., 1960, *Mol. Phys.*, **3**, 435.
- [10] KOWALEWSKI, V. J., and DE KOWALEWSKI, D. G., 1960, *J. chem. Phys.*, **33**, 1794.
- [11] FREEMAN, R., and ANDERSON, W. A., 1962, *J. chem. Phys.*, **37**, 85.
- [12] BOURN, A. J. R., 1964, Ph.D. Thesis, London University.
- [13] POPLE, J. A., and SANTRY, D. P., 1964, *Mol. Phys.*, **8**, 1.
- [14] MULLER, N., and PRITCHARD, D. E., 1959, *J. chem. Phys.*, **31**, 768.
- [15] MULLER, N., and PRITCHARD, D. E., 1959, *J. chem. Phys.*, **31**, 1471.
- [16] MULLER, N., 1962, *J. chem. Phys.*, **36**, 359.
- [17] SHOOLERY, J. N., 1959, *J. chem. Phys.*, **31**, 1427.
- [18] KARPLUS, M., and GRANT, D. M., 1959, *Proc. nat. Acad. Sci., Wash.*, **45**, 1269.
- [19] MALINOWSKI, E. R., 1961, *J. Amer. chem. Soc.*, **83**, 4479.

- [20] MALINOWSKI, E. R., POLLARA, L. Z., and LARMANN, J. P., 1962, *J. Amer. chem. Soc.*, **84**, 2649.
- [21] GUTOWSKY, H. S., and JUAN, C., 1962, *Disc. Faraday Soc.*, **34**, 52.
- [22] JUAN, C., and GUTOWSKY, H. S., 1962, *J. chem. Phys.*, **37**, 2198.
- [23] BALDESCHWIELER, J. D., 1962, *J. chem. Phys.*, **36**, 152.
- [24] OGG, R. A., and RAY, J. D., 1957, *J. Chem. Phys.*, **26**, 1515.
- [25] COSTAIN, C. C., and DOWLING, J. M., 1960, *J. chem. Phys.*, **32**, 158.
- [26] SMITH, I. C., and SCHNEIDER, W. G., 1961, *Canad. J. Chem.*, **39**, 1158.
- [27] ROBERTS, J. D., 1956, *J. Amer. chem. Soc.*, **78**, 4495.
- [28] WILCOX, W. S., and GOLDSTEIN, J. H., 1952, *J. chem. Phys.*, **20**, 1656.
- [29] SCHOEMAKER, V., and PAULING, L., 1939, *J. Amer. chem. Soc.*, **61**, 1769.
- [30] SALES, K. D. (personal communication).
- [31] KARABATSOS, G. J., GRAHAM, J. D., and VANE, F., 1961, *J. phys. Chem.*, **65**, 1657.
- [32] LYNDEN BELL, R. M., and SHEPPARD, N., 1962, *Proc. roy. Soc. A*, **269**, 385.
- [33] DREESKAMP, H., and SACKMAN, E., 1962, *Z. phys. Chem.*, **34**, 261.
- [34] FREEMAN, R., and ANDERSON, W. A. (personal communication).
- [35] DREESKAMP, H., SACKMANN, E., and STEGMEIER, G., 1963, *Berichte der Bunsengesellschaft für physikalische Chemie*, **67**, 860.
- [36] KARPLUS, M., 1959, *J. chem. Phys.*, **30**, 11.
- [37] ALLEN, H. C., and PLYLER, E. K., 1958, *J. Amer. chem. Soc.*, **80**, 2673.
- [38] CONROY, H., 1960, *Advances in Organic Chemistry*, Vol. II (New York: Interscience).
- [39] SCHAEFER, T., 1962, *Canad. J. Chem.*, **40**, 1.
- [40] BANWELL, C. N., and SHEPPARD, N., 1962, *Disc. Faraday Soc.*, **34**, 115.
- [41] BANWELL, C. N., and SHEPPARD, N., 1960, *Mol. Phys.*, **3**, 351.
- [42] WAUGH, J. S., and CASTELLANO, S., 1961, *J. chem. Phys.*, **35**, 1900.
- [43] HUGGINS, M. L., 1953, *J. Amer. chem. Soc.*, **75**, 4123.
- [44] GUTOWSKY, H. S., and PORTE, A. L., 1961, *J. chem. Phys.*, **35**, 839.
- [45] KARPLUS, M., 1960, *J. chem. Phys.*, **33**, 1842.
- [46] KARPLUS, M., ANDERSON, D. H., FARRAR, T. C., and GUTOWSKY, H. S., 1957, *J. chem. Phys.*, **27**, 597.
- [47] GUTOWSKY, H. S., KARPLUS, M., and GRANT, D. M., 1959, *J. chem. Phys.*, **31**, 1278.
- [48] BARFIELD, M., and GRANT, D. M., 1963, *J. Amer. chem. Soc.*, **85**, 1899.
- [49] JONATHAN, N., GORDON, S., and DAILEY, B. P., 1963, *J. chem. Phys.*, **36**, 2443.

Hypochromism and optical rotation in helical polymers

by A. D. McLACHLAN and M. A. BALL

Department of Theoretical Chemistry, University Chemical Laboratory,
Lensfield Road, Cambridge

(Received 23 June 1964)

We show that the decreased light absorption and the anomalous optical rotatory dispersion in helical polynucleotides and polypeptides may be interpreted purely as a local field effect. The electric field of the incident light wave is screened off from each residue by the induced electric dipoles in the others. Quantum-mechanical calculations based on time-dependent Hartree theory and this local field picture correspond precisely with the formulae derived in Tinoco's, Rhodes's, and Moffitt's exciton theories, provided that the Coulomb interactions are small. The degenerate exciton waves in our theory correspond to normal modes of a set of coupled oscillators, and the rotational strengths and oscillator strengths are conserved. There is no conflict between Tinoco's theory of hypochromism and the ones proposed by Bolton and Weiss and by Nesbet. One new conclusion is that the energy shifts accompanying hypochromism should not vary much when the exciton coupling changes from the strong to the weak coupling limits.

1. OPTICAL PROPERTIES OF POLYMERS

The optical spectra of polypeptides and polynucleotides in solution alter markedly when the polymer chains change from a random to a helical structure. Two main effects are observed; hypochromism or hyperchromism—either a decrease or an increase of the optical absorption—and changes in the optical rotatory dispersion curves. In helical DNA for example, the light absorption in the 2600 Å π - π absorption band of the base pairs, which is polarized across the helix axis is only about 60 per cent of the absorption of its mononucleotides [1-3], yet the position and the shape of the absorption hardly change. The absorption rises to about 80-90 per cent of the monomer value when DNA goes into the random coil form, but some 10 per cent of the hypochromism still persists even in di- and tri-nucleotides, and their absorption peaks show a small blue shift of about 10 Å as compared with the monomers [4]. Polypeptides show a similar hypochromism in the 1900 Å π - π amide absorption when the chain forms the right-handed α -helix [5], but other electronic transitions can show hyperchromism: thus the weak n - π transition at 2800-3000 Å in the helical polynucleotide, which is polarized along the axis, is stronger than in the random coil [6] but the hyperchromism disappears on heating.

Hypochromism in the helical polymers is accompanied by anisotropy of the peaks in the electronic absorption. The spectra of oriented films of polypeptides show that the 1900 Å transition splits, with new peaks at 2060 and 1910 Å for light polarized parallel and perpendicular to the axis [7]. The change from a random coil to the right-handed helical structure in a polypeptide also causes a characteristic splitting [8-10] of the circular dichroism curve [θ], into a positive band centred at

1920 Å and a negative one at 2020 Å, with rotational strengths of $+3.6 \times 10^{-39}$ and -4.1×10^{-39} c.g.s. units. The molecular rotation curve $[\phi]$ is also complex. This contrasts with a single negative peak of strength -1.4×10^{-39} at 2160 Å in the circular dichroism of the random coil.

Hypochromism was first explained quantitatively by Tinoco [1, 11, 12] and independently by Rhodes [13]. They made the assumption that the individual residues in the polymer behave as separate non-overlapping electronic systems which are coupled by the Coulomb forces between the transition charge densities in each unit. These weak interactions have two effects. First each molecular excitation corresponds to a whole degenerate exciton band for a polymer; but the total oscillator strength in each band is unaltered even though the absorption maxima may shift. Secondly, the interaction causes a coupling between different bands so that one band may borrow oscillator strength from another. Tinoco and Rhodes calculated the exciton wave functions and oscillator strengths by first-order degenerate perturbation theory and concluded that hypochromism in polynucleotides was mainly due to the 2600 Å band ($f=0.31$) losing intensity to other higher π - π transitions, notably another perpendicular π - π base pair transition at 2000 Å ($f=0.61$). Although not enough is known about the directions and intensities of the transitions in the individual residues to do the calculation accurately, Tinoco's theory predicts a reduction of absorption in the 2600 Å band to about 70–90 per cent. He also explains how the effect should vary with the chain length [14].

Quite another kind of theory was proposed by Bolton and Weiss [15, 16]. In their model the polymer is taken to be a helical array of harmonic oscillators, each of which is excited by the total electric field of both the light wave and the other oscillators. Although their model does show hypochromism it is not clearly based on any quantum-mechanical theory, nor is their method of calculating the oscillator strength very satisfactory. For example it is not clear whether it is conserved in a polymer whose residues each only have one excited state. Later deVoe [17] developed the same idea more successfully. In his local field theory he calculated the induced electric dipole moment of each monomer unit in the average field of all the others by first-order perturbation theory, and obtained precisely the same result as Tinoco and Rhodes. However, there is still a good deal of argument about whether the local field theories and the exciton theory are compatible [15, 16, 18], and two further explanations have been put forward by Nesbet [18, 19]. The first, a treatment of the electronic interaction between a close pair of ethylene molecules, predicted a small hypochromism in all orientations, but Koutecky and Paldus [20] showed later that the hypochromic effect found by Nesbet is produced by the approximation method adopted by him. The second is a quantum-mechanical version of Bolton and Weiss's theory, which apparently violates the oscillator strength sum rule.

There is no controversy about the optical rotatory dispersion. The exciton theory for a polymer was originally developed by Kirkwood [21] and then improved by Moffitt [22, 23] and Moffitt *et al.* [24]. The rotational strength of a polymer transition is found to consist of two parts, one from the intrinsic strengths of the individual residues, and another which depends on the coupling between them and differs in the random-coil and helical structures. This last term causes the complex circular dichroism of polypeptides in the α helix form [10], and theoretical calculations by Moffitt and Yang [10], Fitts and Kirkwood [24] and Tinoco and

Woody [25] agree well with the observed dispersion curves. The theoretical formula given by the exciton theory is also the same as comes from the purely classical theories of Born, Oseen and Kuhn [26–28] and of Boys [29]. These authors treated a polymer as an assembly of coupled harmonic oscillators, rather in the manner of deVoe.

At present then it is generally agreed that the exciton theory explains the optical rotation of helical polymers, but there is still some disagreement and confusion about hypochromism. In this paper we hope to throw some light on the problem by using a different approach. This is the time-dependent self-consistent field theory [30–32]. The exciton theory begins by calculating the stationary states of the polymer and then allows optical transitions to take place between them; but the time-dependent method is a dynamical one, and describes the oscillatory motion of the electrons in the periodic electric field of the light wave. The wave function of the polymer is taken to be a simple product of residue wave functions, and each residue oscillates in the total field produced by the light wave and all the other induced electric dipoles. Thus the theory still assumes that the electrons of the different residues do not overlap, but are coupled by Coulomb forces. When the coupling is weak enough to be regarded as a perturbation the time-dependent method gives precisely the same results as the exciton theory for both the oscillator strengths and the optical rotation. An advantage of the dynamical theory is that it preserves the sum rules for oscillator strengths [33] and rotational strengths, so that none can be lost through careless approximations. Also the different contributions to the optical rotation have a simple physical meaning. The new method sets deVoe's ideas in a precise quantum-mechanical framework and confirms all his conclusions. It can also give a correct description of degenerate exciton bands and their complex rotatory dispersion. Finally it is possible to say a little more about the question of 'strong' and 'weak' coupling [34] within the exciton band.

We shall develop the method in several stages, starting with the simplest model first, in order to bring out the main features one by one.

2. OSCILLATOR STRENGTHS AND ROTATIONAL STRENGTHS

There are excellent review articles on the basic principles of optical rotation by Condon [35], Mason [36], Moscovitz [37] and Tinoco [38]. In this section we shall merely define some of the important quantities which are needed later.

An isotropic optically active medium has different values of the complex refractive index ($n - ik$) for left and right circular polarized light. These quantities determine the rotation ϕ and the ellipticity θ , which are measured in radians per centimetre:

$$\phi = \frac{\pi}{\lambda}(n_l - n_r), \quad \theta = \frac{\pi}{\lambda}(k_l - k_r), \quad (2.1)$$

ϕ is positive if the plane of polarization turns anti-clockwise on moving away from the light source. Experimental results are given in terms of molecular rotation $[\phi]$ and molecular ellipticity $[\theta]$, measured in degrees per mole per decimetre:

$$[\phi] = \left(\frac{18M}{\pi c}\right)\phi, \quad [\theta] = \left(\frac{18M}{\pi C}\right)\theta. \quad (2.2)$$

Here M is the molecular weight and C the concentration in gm/cm³. At a given angular frequency ω the rotation $[\phi]$ for a molecule in its ground state has contributions from the different electronic transitions with frequencies ω_n and rotational strengths R_n .

$$[\phi] = \frac{48N_0}{\hbar c} \left(\frac{n^2 + 2}{3} \right) \sum_n \frac{R_n \omega^2}{\omega_n^2 - \omega^2}, \quad (2.3)$$

where N_0 is Avogadro's number. $[\phi]$ and $[\theta]$ are connected with one another by a pair of dispersion relations [37, 39] so that the rotational strength of a transition can also be deduced from $[\theta]$, and hence from the different absorption indices (2.1). It is most convenient to use the molar extinction coefficients $\epsilon(\nu)$ and then the rotational strength (in c.g.s. units) is given by the formula

$$R_n = 22.9 \times 10^{-40} \int \frac{\epsilon_l - \epsilon_r}{\nu} d\nu. \quad (2.4)$$

The average intensity of absorption for unpolarized light is measured by the oscillator strength

$$f_n = 4.32 \times 10^{-9} \int \epsilon d\nu, \quad (2.5)$$

where ν is the frequency in cm⁻¹. In a molecule with n electrons the strengths obey the sum rules

$$\sum_n f_n = n, \quad \sum_n R_n = 0. \quad (2.6)$$

When an oscillating electric field \mathbf{E} acts on a single molecule it induces an electric dipole moment $\mathbf{P} = \alpha \mathbf{E}$, proportional to the polarizability α . An optically active molecule also acquires a magnetic moment

$$\mathbf{M} = \frac{1}{c} \beta \frac{\partial \mathbf{E}}{\partial t} \quad (2.7)$$

which has the correct phase relation with \mathbf{P} to cause optical rotation. The quantities α and β are expressed in terms of the oscillator strengths and rotational strengths by the formulae

$$\alpha(\omega) = \frac{e^2}{m} \sum_n \frac{f_n}{\omega_n^2 - \omega^2}, \quad \beta(\omega) = \frac{2c}{3\hbar} \sum_n \frac{R_n}{\omega_n^2 - \omega^2}. \quad (2.8)$$

Finally the quantum theory [40] gives the connection between f_n , R_n , and the matrix elements of the operators \mathbf{P} and \mathbf{M} for the transitions:

$$f_n = \frac{2m\omega_n}{3e^2\hbar} |(0|\mathbf{P}|n)|^2, \quad R_n = \text{Im} [(0|\mathbf{P}|n) \cdot (n|\mathbf{M}|0)]. \quad (2.9)$$

Here Im means the imaginary part. In a molecule with real wave functions the matrix elements of \mathbf{P} are real, and of \mathbf{M} are imaginary. If there is a reflection plane, or a centre of symmetry, no electronic transition can be simultaneously magnetic dipole and electric dipole allowed along the same direction.

α and β are scalar quantities obtained by averaging over all orientations; but for an oriented molecule the induced moments depend on tensor quantities α , β

$$\mathbf{P} = \alpha \cdot \mathbf{E}, \quad \mathbf{M} = \frac{1}{c} \beta \cdot \frac{\partial \mathbf{E}}{\partial t}. \quad (2.10)$$

Let \mathbf{e}_n and \mathbf{m}_n be unit vectors parallel to the electric and magnetic transition moments of each excited state. Then one can write

$$\alpha = \frac{3e^2}{m} \sum_n \frac{f_n(\mathbf{e}_n \cdot \mathbf{e}_n)}{\omega_n^2 - \omega^2}, \quad (2.11)$$

$$\beta = \frac{2c}{\hbar} \sum_n \frac{\rho_n(\mathbf{m}_n \cdot \mathbf{e}_n)}{\omega_n^2 - \omega^2}, \quad (2.12)$$

where the rotational strength is $R_n = \rho_n(\mathbf{m}_n \cdot \mathbf{e}_n)$.

In equation (2.7) the magnetic moment \mathbf{M} is taken about the centre of the molecule, but in a polymer the important quantity is the moment about the centre of the macromolecule, and so another effect must be included. The oscillating dipole \mathbf{P} is accompanied by a displacement current $(1/c)\partial\mathbf{P}/\partial t$ inside each residue, which has a magnetic moment

$$\mathbf{M}' = \frac{1}{2c} \left(\mathbf{r} \times \frac{\partial \mathbf{P}}{\partial t} \right) \quad (2.13)$$

about the centre. For a single molecule \mathbf{M}' is perpendicular to \mathbf{P} and does not contribute to the rotation, but this is not true in a polymer with many residues. We therefore introduce a tensor $\beta' = \frac{1}{2} \mathbf{r} \times \alpha$ such that $\mathbf{M}' = (1/c)\beta' \cdot \partial\mathbf{E}/\partial t$, of the form

$$\beta' = \frac{3e^2}{2m} \sum_n \frac{f_n([\mathbf{r} \times \mathbf{e}_n]\mathbf{e}_n)}{\omega_n^2 - \omega^2}. \quad (2.14)$$

Finally we shall need to introduce the Coulomb interaction V between the electronic transitions on pairs of neighbouring molecules a and b . The important quantities are the matrix elements

$$V_{ab}^{mn} = \langle \psi_{ma} \psi_{0b} | V | \psi_{0a} \psi_{nb} \rangle. \quad (2.15)$$

In the dipole approximation V_{ab}^{mn} is the interaction energy between the two transition electric dipole moments, and can be written

$$V_{ab}^{mn} = \left(\frac{3e^2\hbar}{2m} \right) \left(\frac{f_m f_n}{\omega_m \omega_n} \right)^{1/2} (\mathbf{e}_{am} \cdot \mathbf{T}_{ab} \cdot \mathbf{e}_{bn}). \quad (2.16)$$

Here \mathbf{T}_{ab} is the dipolar interaction tensor between the the pairs of molecules

$$\mathbf{T}_{ab} = \frac{1}{r^3} \left[\mathbf{I} - \frac{3(\mathbf{r} \mathbf{r})}{r^2} \right] \quad (2.17)$$

and r is the distance between them.

3. TIME-DEPENDENT WAVE FUNCTIONS

The time-dependent Hartree approximation has been described in detail elsewhere [30, 32, 41]. Here we shall outline the method as it is applied to a pair of interacting molecules. The wave function of the pair is assumed to be a product

$$\Psi(q_a, q_b, t) = \psi_a(q_a, t) \psi_b(q_b, t) \quad (3.1)$$

(apart from an unimportant phase factor) and then ψ_a and ψ_b satisfy the Schrödinger equations

$$\left. \begin{aligned} i\hbar \frac{\partial \psi_a}{\partial t} &= [H_a + \langle V_a \rangle] \psi_a, \\ i\hbar \frac{\partial \psi_b}{\partial t} &= [H_b + \langle V_b \rangle] \psi_b. \end{aligned} \right\} \quad (3.2)$$

H_a and H_b are the Hamiltonians of the separate molecules, $\langle V_a \rangle = \int \psi_b^* V \psi_b d\tau$ represents the average Coulomb field V produced by molecule b at a , $\langle V_b \rangle$ is a similar quantity. H_a and H_b are defined to be effective Hamiltonians. Thus H_a is the energy operator of molecule a in the average field of molecule b when b is in its ground state, and $\langle V_a \rangle$ vanishes if b is unexcited. The solutions of the equation $H_a \psi_a = E \psi_a$ give rise to a set of states $\psi_{0a}, \psi_{1a}, \dots$ for a in the average field of b , and the Hartree ground state of the pair is simply

$$\Psi_0 = \psi_{0a} \psi_{0b} \exp(-2iE_0 t/\hbar). \quad (3.3)$$

We now look for solutions of equations (3.2) when a small oscillating electric field \mathbf{E} acts on both molecules. It is clear from (3.2) that the total effective perturbing energy term for the first molecule is not simply $-\mathbf{E} \cdot \mathbf{P}_a$ but

$$H'_a = -\mathbf{E} \cdot \mathbf{P}_a + \langle V_a \rangle. \quad (3.4)$$

In the dipole approximation (2.16) one has $\langle V_a \rangle = \mathbf{P}_a \cdot \mathbf{T}_{ab} \cdot \langle \mathbf{P}_b \rangle$, so that H' takes the simple form

$$H'_a = -\mathbf{P}_a \cdot \mathbf{E}'_a \quad (3.5)$$

where \mathbf{E}'_a is the effective local field at molecule a and represents the combined effect of the external field and the field from the dipole moment induced in molecule b :

$$\mathbf{E}'_a = \mathbf{E} - \mathbf{T}_{ab} \cdot \langle \mathbf{P}_b \rangle. \quad (3.6)$$

This expression for the local field is almost the same as deVoe [17] derives by a classical argument. However, it is important to notice that \mathbf{P}_b is an expectation value, not an operator, and this comes about because the wave function (3.1) is restricted to be a simple product. The final assumption to make is that \mathbf{E}' is small enough to be considered a small perturbation. Then it is clear that the electric dipole moment induced in each molecule is equal to $\alpha \cdot \mathbf{E}'$. Thus one finds a pair of coupled equations for the average values of the induced dipole moments (omitting the $\langle \rangle$ brackets for simplicity)

$$\left. \begin{aligned} \mathbf{P}_a &= \alpha_a \cdot [\mathbf{E} - \mathbf{T}_{ab} \cdot \mathbf{P}_b], \\ \mathbf{P}_b &= \alpha_b \cdot [\mathbf{E} - \mathbf{T}_{ba} \cdot \mathbf{P}_a]. \end{aligned} \right\} \quad (3.7)$$

The magnetic moment induced in each molecule is also proportional to \mathbf{E}' rather than \mathbf{E} , with $\mathbf{M} = \beta \cdot \mathbf{E}'$, and so the Coulomb interaction also modifies the optical activity. Equation (3.7) is the basic equation of our method, and we shall now use it to investigate hypochromism and optical rotation.

4. A SIMPLE DIMER

Let us take a pair of identical rod-like molecules a, b stacked vertically above one another with their centres at the points $(0, 0, r)$ and $(0, 0, 0)$. The electric and magnetic transition moments are parallel in each molecule and lie in the xy plane, while the angle between the axes of the two molecules is 2δ , so that

$$\mathbf{e}_a = (\cos \delta, \sin \delta, 0)$$

and

$$\mathbf{e}_b = (\cos \delta, -\sin \delta, 0).$$

We shall begin by assuming that each molecule has only one electronic transition described by ω_n, f_n, R_n . Light polarized along the z -axis has no effect on the dimer, but in the xy plane the coupling produces important changes.

An electric field E along the x -axis makes both molecules oscillate in phase, each with an induced moment P , but since the total local field along each molecular axis is $(E \cos \delta - TP)$, with $T = \cos 2\delta/\tau^3$, the dipole moment is given by the relation

$$P = \frac{3e^2}{m} \frac{f_n}{\omega_n^2 - \omega^2} [E \cos \delta - TP]. \quad (4.1)$$

The dimer has a resultant dipole moment $P_x = 2P \cos \delta$, and one easily finds from (4.1) that

$$P_x = \frac{3e^2}{m} \left\{ \frac{2f_n \cos^2 \delta}{[\omega_n^2 + (3e^2 f_n T/m)] - \omega^2} \right\} E. \quad (4.2)$$

Thus the dimer has a transition of strength $2f_n \cos^2 \delta$ directed along the x -axis with a shifted frequency ω_x , defined so that

$$\omega_x^2 = \omega_n^2 + (3e^2 f_n T/m). \quad (4.3)$$

When T is small the approximate frequency shift is

$$\omega_x - \omega_n = 3e^2 f_n T / 2m\omega_n = V/\hbar, \quad (4.4)$$

where V , defined in (2.16), is the interaction energy between the two transition dipoles.

A field along the y -axis has precisely similar effects; except that now the molecules oscillate out of phase and so the local field is $(E \sin \delta + TP)$. The y transition of the dimer has strength $2f_n \sin^2 \delta$ and a lower frequency:

$$\omega_y^2 = \omega_n^2 - (3e^2 f_n T/m); \quad \omega_y - \omega_n = -V/\hbar. \quad (4.5)$$

The total oscillator strength of the dimer is still $2f_n$, so there is no hypochromism, and the pair of transitions has an exciton splitting $2V/\hbar$. This is all in complete agreement with Tinoco and Rhodes.

The optical rotation consists of two parts. The intrinsic rotation R_n of each unit gives

$$R_x = 2R_n \cos^2 \delta, \quad R_y = 2R_n \sin^2 \delta. \quad (4.6)$$

Then there is a contribution from the displacement currents. The x transition has a magnetic moment

$$M' = -\frac{1}{2c} r \sin \delta \frac{\partial P}{\partial t}, \quad (4.7)$$

and the corresponding rotational strength is

$$R = -\frac{1}{4} r \sin 2\delta (3e^2 f_n \hbar / 2m). \quad (4.8)$$

There is an equal and opposite strength for the y transition so that the total rotational strength is conserved. It can often happen that the intrinsic rotation R_n is very small for the given transition, so that all the strength comes from intermolecular coupling. In this case the rotatory power $[\phi]$ of the dimer is proportional to

$$\frac{2c}{3\hbar} R \left\{ \frac{\omega^2}{\omega_x^2 - \omega^2} - \frac{\omega^2}{\omega_y^2 - \omega^2} \right\}. \quad (4.9)$$

It reduces, for small exciton splitting, to a characteristic form first pointed out by Moffitt [22], with $[\phi]$ proportional to the fourth power of the frequency:

$$[\phi] = \frac{48N_0}{\hbar c} \left(\frac{n^2 + 2}{3} \right) \left(\frac{-4RV}{\hbar \omega_n} \right) \frac{\omega^2 \omega_n^2}{(\omega_n^2 - \omega^2)^2}. \quad (4.10)$$

This is the kind of complex dispersion seen in helical polypeptides [10]. Our one-state model of a dimer therefore accounts for some features of optical rotation but not for hypochromism, and so we must now consider the other excited states.

5. BORROWED INTENSITY

As a new model we take the pair of rod-like molecules with parallel axes, at an angle θ to the line joining them, and allow each molecule to have many excited states, so that α and β are given by (2.8). An electric field E along the common axis then excites the molecules in phase, and the anti-symmetric mode is forbidden. Now the local field at each dipole is $(E - TP)$ with

$$T = \frac{(1 - 3 \cos^2 \theta)}{r^3}, \quad (5.1)$$

whose sign depends on θ , and the total electric dipole moment is

$$2P = 2\alpha(\omega)[E - TP] = A(\omega)E. \quad (5.2)$$

Equation (5.2) defines a new polarizability for the dimer, of the form

$$A(\omega) = \frac{3e^2}{m} \sum_n \frac{F_n}{(\epsilon_n^2 - \omega^2)} \quad (5.3)$$

with shifted frequencies ϵ_n and strengths F_n , and elimination of P from (5.2) gives the relation

$$A(\omega) = \left[T + \frac{1}{\alpha(\omega)} \right]^{-1}. \quad (5.4)$$

Substituting (2.8) into (5.4), and treating T as a small quantity of the first order one finds the dimer has

$$\left. \begin{aligned} F_n &= 2f_n - \frac{6e^2 T}{m} \sum_m \frac{2f_m f_n}{(\omega_m^2 - \omega_n^2)}, \\ \epsilon_n &= \omega_n + V_{ab}^{nn}/\hbar. \end{aligned} \right\} \quad (5.5)$$

Thus the lowest transition loses intensity to all the higher ones and shows hypochromism if the molecules lie side by side ($\theta = 90^\circ$), but if they are head to tail $T < 0$ and there is hyperchromism. The f sum rule still holds and Tinoco's results are confirmed.

The displacement currents give no optical rotation because our model has a centre of symmetry, but there is still a contribution from the intrinsic rotation of each molecule. The equation for the total magnetic moment induced by the local field is

$$2M = 2\beta(\omega)[1 - TA(\omega)] \frac{1}{c} \frac{\partial E}{\partial t} = \frac{1}{c} B(\omega) \frac{\partial E}{\partial t}. \quad (5.6)$$

Using (5.4) one finds that

$$B = 2A\beta/\alpha \quad (5.7)$$

and the new rotational strength to first order is

$$R = R_n - \frac{3e^2 T}{m} \sum_m \frac{R_m f_n + f_m R_n}{\omega_m^2 - \omega_n^2}. \quad (5.8)$$

There is therefore a rotational borrowing effect quite analogous to the change of oscillator strength in (5.5).

The next stage in the theory is to allow for anisotropy and to have more than two molecules. For the present we shall ignore complications caused by the degeneracy of the exciton band. Then the borrowing can be derived in a very simple way.

To a first approximation $\mathbf{P} = \alpha \cdot \mathbf{E}$ for each molecule, so if \mathbf{T} is small the local field (3.6) is

$$\mathbf{E}_a' = \mathbf{E} - \sum_b \mathbf{T}_{ab} \cdot \alpha_b \cdot \mathbf{E}, \quad (5.9)$$

and the electric moment of molecule a is

$$\mathbf{P}_a = \{ \alpha_a - \sum_b \alpha_a \cdot \mathbf{T}_{ab} \cdot \alpha_b \} \cdot \mathbf{E}. \quad (5.10)$$

Clearly then, the total polarizability tensor of the polymer of N units is

$$\mathbf{A} = \sum_a \alpha_a - \sum_{a,b} \alpha_a \cdot \mathbf{T}_{ab} \cdot \alpha_b \quad (5.11)$$

(making the convention that $\mathbf{T}_{aa} = 0$). We now average over all orientations of the polymer, and find the scalar polarizability to first order

$$A(\omega) = \frac{3Ne^2}{m} \sum_n \frac{f_n}{(\omega_n^2 - \omega^2)} - \left(\frac{3e^2}{m} \right)^2 \sum_{m,n} \sum_{a,b} \frac{f_n f_m (\mathbf{e}_{an} \cdot \mathbf{e}_{bm})(\mathbf{e}_{an} \cdot \mathbf{T}_{ab} \cdot \mathbf{e}_{bm})}{(\omega_n^2 - \omega^2)(\omega_m^2 - \omega^2)}. \quad (5.12)$$

To find the oscillator strength we look at the behaviour of $A(\omega)$ near ω_n , ignoring the correction terms with $m = n$. The general result is that

$$F_n = Nf_n - \left(\frac{6e^2}{m} \right) \sum_m \sum_{a,b} \frac{f_n f_m (\mathbf{e}_{an} \cdot \mathbf{e}_{bm})(\mathbf{e}_{an} \cdot \mathbf{T}_{ab} \cdot \mathbf{e}_{bm})}{\omega_m^2 - \omega_n^2}. \quad (5.13)$$

The optical rotation comes out in the same way. Each molecule has an intrinsic magnetic moment

$$\mathbf{M}_a = \{ \beta_a - \sum_b \beta_a \cdot \mathbf{T}_{ab} \cdot \alpha_b \} \cdot \frac{1}{c} \frac{\partial \mathbf{E}}{\partial t} \quad (5.14)$$

and the displacement currents give an analogous contribution \mathbf{M}_a' , with β_a replaced by β_a' . The total rotation tensor \mathbf{B} therefore contains four contributions:

$$\mathbf{B} = \sum_a (\beta_a + \beta_a') - \sum_{a,b} (\beta_a \cdot \mathbf{T}_{ab} \cdot \alpha_b + \beta_a' \cdot \mathbf{T}_{ab} \cdot \alpha_b). \quad (5.15)$$

In the isotropic average β_a' gives nothing, and after substituting from (2.12) and (2.14) the new rotational strength is found:

$$\begin{aligned} R = NR_n - \frac{3e^2}{m} \sum_{a,b} \sum_m \frac{(\mathbf{e}_{an} \cdot \mathbf{T}_{ab} \cdot \mathbf{e}_{bm})}{\omega_m^2 - \omega_n^2} [\rho_m f_n (\mathbf{m}_{bm} \cdot \mathbf{e}_{an}) + \rho_n f_m (\mathbf{m}_{an} \cdot \mathbf{e}_{bm})] \\ - \frac{9e^4 \hbar}{4m^2 c} \sum_{a,b} \sum_m \frac{(\mathbf{e}_{an} \cdot \mathbf{T}_{ab} \cdot \mathbf{e}_{bm})}{\omega_m^2 - \omega_n^2} [\mathbf{r}_{ab} \times \mathbf{e}_{an} \cdot \mathbf{e}_{bm}] f_m f_n. \end{aligned} \quad (5.16)$$

Our result agrees exactly with Kirkwood's [21] and Moffitt's [22], so that we have been able to interpret the changed rotatory dispersion of a polymer purely as a local field effect.

One case of special interest is a polymer where β_a is very small for each transition and all the rotatory power arises from the last term of (5.15). Each degenerate exciton band then shows anomalous dispersion of the type (4.10). Provided that

$(\omega - \omega_n)$ is not too small one can still retain the resonant terms with $n = m$ in (5.15) and (5.16), and the magnetic moment is proportional to

$$B' = \frac{-3e^4}{4m^2} \sum_{a,b} \sum_{m,n} \frac{f_m f_n}{(\omega_m^2 - \omega^2)(\omega_n^2 - \omega^2)} (\mathbf{e}_{an} \cdot \mathbf{T}_{ab} \cdot \mathbf{e}_{bm}) [\mathbf{r}_{ab} \times \mathbf{e}_{an} \cdot \mathbf{e}_{bm}]. \quad (5.17)$$

The rotatory dispersion takes precisely the form described by Moffitt *et al.* [24]:

$$[\phi] = \frac{48N_0}{\hbar c} \left(\frac{n^2 + 2}{3} \right) \sum_{m,n} \frac{Q_{mn} \omega_m^2 \omega_n}{(\omega_m^2 - \omega^2)(\omega_n^2 - \omega^2)} \quad (5.18)$$

with the same amplitudes

$$Q_{mn} = \frac{-3e^2}{4mc} \left(\frac{f_m f_n}{\omega_m \omega_n} \right)^{1/2} \sum_{a,b} V_{ab}^{nm} [\mathbf{r}_{ab} \times \mathbf{e}_{an} \cdot \mathbf{e}_{bm}]. \quad (5.19)$$

Although (5.19) is the correct generalization of (4.10) the argument we have used is far from rigorous when the exciton band is degenerate, and it is therefore necessary to give a proper treatment of the individual degenerate transitions.

6. DEGENERATE EXCITON BANDS

For simplicity we shall begin by assuming only one excited state for each molecule. When an electric field E in the direction \mathbf{e} acts on the polymer the magnitudes P_a, P_b, \dots of the induced electric dipole moments are found from (3.7) to obey the equations

$$(\omega_n^2 - \omega^2)(m/3e^2 f_n) P_a + \sum_b (\mathbf{e}_{an} \cdot \mathbf{T}_{ab} \cdot \mathbf{e}_{bn}) P_b = E(\mathbf{e}_{an} \cdot \mathbf{e}). \quad (6.1)$$

They are of precisely the same form as the equations for the forced motion of a set of coupled harmonic oscillators, and the solution is found by introducing a set of weighted co-ordinates

$$q_a = \left(\frac{3e^2 f_n}{m} \right)^{1/2} P_a \quad (6.2)$$

and finding the orthogonal 'normal modes' and oscillation frequencies of the polymer when $E = 0$. In the i th mode $q_a = C_{ai}$, the frequency is ϵ_i , and (6.1) gives

$$(\omega_n^2 - \epsilon_i^2) C_{ai} + \sum_b \frac{3e^2 f_n}{m} (\mathbf{e}_{an} \cdot \mathbf{T}_{ab} \cdot \mathbf{e}_{bn}) C_{bi} = 0, \quad (6.3)$$

with the normalisation condition

$$\sum_a C_{ai} C_{aj} = \delta_{ij}. \quad (6.4)$$

Treating T as a small quantity and using (2.16) it is found that there is a small frequency shift for each mode, such that

$$\left. \begin{aligned} \hbar(\epsilon_i - \omega_n) &= \sum_{a,b} C_{ai} V_{ab}^{nn} C_{bi}, \\ \hbar(\epsilon_i - \omega_n) C_{ai} &= \sum_b V_{ab}^{nn} C_{bi}. \end{aligned} \right\} \quad (6.5)$$

In this approximation then, the normal modes and frequencies of the coupled oscillations correspond precisely with the degenerate exciton states found by Tinoco and Rhodes. By expressing the solution of (6.1) in terms of the normal modes the electric polarizability of the polymer is found:

$$\mathbf{A} = \frac{3e^2}{m} \sum_i \sum_{a,b} \frac{f_n (\mathbf{e}_{an} \mathbf{e}_{bn}) C_{ai} C_{bi}}{\epsilon_i^2 - \omega^2}, \quad (6.6)$$

and the oscillator strength comes out as

$$F_i = \sum_{a,b} C_{ai} C_{bi} (\mathbf{e}_{an} \cdot \mathbf{e}_{bn}) f_n. \quad (6.7)$$

The rotational strength is found similarly:

$$R_i = \sum_{a,b} C_{ai} C_{bi} (\mathbf{m}_{an} \cdot \mathbf{e}_{bn}) \rho_n + \frac{3e^2 \hbar f_n}{8mc} \sum_{a,b} C_{ai} C_{bi} [\mathbf{r}_{ab} \times \mathbf{e}_{an} \cdot \mathbf{e}_{bn}]. \quad (6.8)$$

Now that the degeneracy has been resolved, by forming normal modes, there is no Coulomb interaction between different modes within the same band, so that all the arguments of § 5 are valid for the borrowing of intensity by a mode in one band from all the modes in another. The borrowed oscillator strength F_i is obviously

$$- \frac{6e^2}{m} \sum_{a,b,c} \sum'_m \frac{f_m}{(\omega_m^2 - \omega_n^2)} C_{bi} C_{ci} (\mathbf{e}_{bn} \cdot \mathbf{e}_{am}) (\mathbf{e}_{am} \cdot \mathbf{T}_{ac} \cdot \mathbf{e}_{cn}), \quad (6.9)$$

and the borrowed rotational strength R_i has two parts:

$$- \frac{3e^2}{m} \sum_{a,b,c} \sum'_m \frac{1}{(\omega_m^2 - \omega_n^2)} C_{bi} C_{ci} (\mathbf{e}_{am} \cdot \mathbf{T}_{ac} \cdot \mathbf{e}_{cn}) \\ \times \left\{ [\rho_m f_n (\mathbf{m}_{am} \cdot \mathbf{e}_{bn}) + \rho_n f_m (\mathbf{m}_{bn} \cdot \mathbf{e}_{am})] + \frac{3e^2 \hbar f_m f_n}{4mc} [\mathbf{r}_{ab} \times \mathbf{e}_{am} \cdot \mathbf{e}_{bn}] \right\}. \quad (6.10)$$

The new strengths are the sums of (6.7) and (6.9) or (6.8) and (6.10). The total strengths of the entire band, obtained by adding all the orthogonal modes are still given correctly by (5.13) and (5.16).

Our self-consistent field theory of degenerate polymer bands agrees perfectly with Rhodes's theory of hypochromism [13] and Tinoco's treatment of optical rotation [38] up to first order in the Coulomb interaction. Our dynamical explanation of these effects in terms of the local field is therefore essentially equivalent to theirs.

One other interesting property of the band is the shifted centre of gravity of the absorption peak, which can be defined in terms of the average value of $F_i \epsilon_i$ for all the modes in the band. The result, using (6.3) and (6.4) to sum the terms, is a first-order shift

$$\Delta\omega = \frac{1}{N} \left(\frac{3e^2 f_n}{2m\omega_n} \right) \sum_{a,b} (\mathbf{e}_{an} \cdot \mathbf{e}_{bn}) (\mathbf{e}_{an} \cdot \mathbf{T}_{ab} \cdot \mathbf{e}_{bn}). \quad (6.11)$$

It is important to notice that the hypochromism depends on the angles between the transition moments with $m \neq n$, but the shift on the ones with $m = n$. Therefore there is no necessary general correlation between hypochromism and the direction of the shift.

7. A HELICAL POLYMER

We now consider the optical properties of a degenerate exciton band in a long right-handed helix of N identical residues as shown in the figure. It has radius d , step height Z and the angle of twist between adjacent residues is δ . Since we are interested in the effects of degeneracy each residue a will be considered to have only one excited state, whose transition moment vector \mathbf{e}_a has direction cosines $\cos r$, $\cos t$, $\cos v$ with the radial, tangential and vertical directions. The residues are numbered $\dots -2, -1, 0, 1, 2, \dots$ and axes are chosen so that \mathbf{e}_0 lies in the xz plane.

The wave-like normal modes of oscillation are fully determined by symmetry if we use periodic boundary conditions and ignore end effects; and only three are electric dipole allowed. Light polarized along the z -axis excites all the residues in phase with dipole moments P . The local field at residue 0, say, is

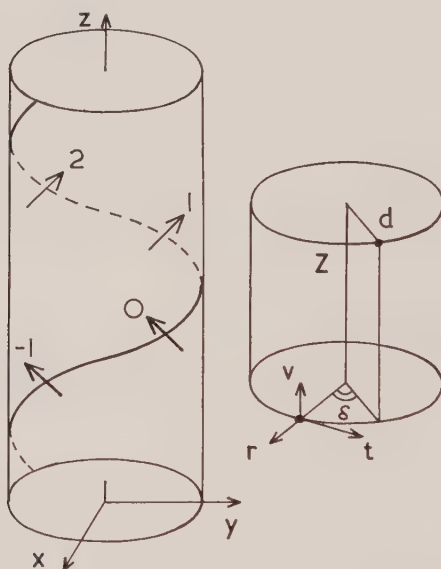
$$E_0' = E \cos v - \sum_a T_{0a} P_a, \quad (7.1)$$

so that the amplitude is given by a relation like (4.1):

$$P = \alpha(\omega)[E \cos v - T_{\parallel} P], \quad (7.2)$$

where T_{\parallel} is the sum of all the dipole fields. As in §4, the transition is shifted but there is no borrowing of intensity. The oscillator strength per residue is $f_n \cos^2 v$. For the rotational strength we take $\rho_n = 0$ in (6.8), and add up the displacement currents, using the formula

$$\begin{aligned} [\mathbf{r}_{ab} \times \mathbf{e}_a \cdot \mathbf{e}_b] &= 4d \cos v \cos t [\sin^2 \frac{1}{2}(a-b)\delta] \\ &\quad - Z \sin^2 v [(a-b) \sin(a-b)\delta]. \end{aligned} \quad (7.3)$$



A right-handed helical polymer of identical residues. The residues are numbered . . . $-2, -1, 0, 1, 2, \dots$ and the dimensions of the helix are: radius d ; step height Z ; angle of twist per residue, δ .

The first term in (7.3) is the one originally proposed by Moffitt [23] and gives a rotational strength per residue of

$$R_{\parallel} = \left(\frac{3e^2 \hbar}{4mc} \right) f_n d \cos v \cos t. \quad (7.4)$$

The sum of the second depends on the precise number of turns of the helix and needs a special discussion.

Light polarized along the x or y -axes excites a pair of modes where the electric moments P_a are respectively equal to $P \cos a\delta$ and $P \sin a\delta$. In the x mode the amplitude is given by

$$P = \alpha(\omega)[E \sin v - T_{\perp} P] \quad (7.5)$$

and $T_{\perp} = 2(T_{01} \cos \delta + T_{02} \cos 2\delta + \dots)$ is the sum of all the modulated dipole fields. The oscillator strength is $\frac{1}{2} f_{\parallel} \sin^2 v$ and the rotational strength again consists of two parts, the first being $-\frac{1}{2} R_{\parallel}$. The electronic spectrum therefore has two main absorption peaks of relative strengths $\cos^2 v$ and $\sin^2 v$ with a separation proportional to $(T_{\parallel} - T_{\perp})$:

$$\omega_{\parallel} - \omega_{\perp} = \sum_a V_{0a}(1 - \cos a\delta)/\hbar. \quad (7.6)$$

The rotational strengths R_{\parallel} and R_{\perp} are equal and opposite.

The second term of (7.3) is hard to deal with for an infinite helix, because it gives large contributions to R from pairs of residues which are at opposite ends of the helix. It is not really an end effect, because it contributes to the dispersion curve a term which is proportional to the number of residues; but for a *given mode* within the band the sum (6.8) is sensitive to the precise value of N . The overall contribution to the anomalous dispersion (5.18) is however independent of the precise value of N , because the terms in (7.3) are weighted with the factor V_{ab} which drops off rapidly with distance [24]. The Q value per residue is easily found:

$$Q = \frac{3e^2 f_n}{4mc\omega_n} \sum_a \{4d \cos v \cos t [V_{0a} \sin^2 \frac{1}{2} a\delta] - Z \sin^2 v [V_{0a} a \sin a\delta]\}. \quad (7.7)$$

The part proportional to Z tends to be small because the sum contains both positive and negative terms, so that (7.4) is not too bad an approximation [36].

8. CONCLUSION

It has been assumed throughout this paper that the exciton coupling is 'strong' compared with vibrational energies. This implies that one considers the whole polymer as a single electronic system and then applies the Born–Oppenheimer approximation afterwards to the entire helix. In 'weak coupling' theory the Coulomb interaction is much smaller than the vibrational energies and one uses the Born–Oppenheimer approximation inside each residue before coupling the vibronic levels of different residues together. It is well known that the total oscillator strength or rotational strength of a given electronic band is independent of the vibrational structure. Therefore the amount of hypochromism should not depend on whether coupling is strong or weak. However, the exciton band widths and first-order energy shifts must be affected, and Tinoco has argued [1, 38] that in weak coupling the first-order splittings of *vibronic* degenerate levels should be far too small to shift the absorption peak. Since the anomalous optical rotatory dispersion parameter Q_{nn} (5.18) also depends on these splittings it might also change.

Our dynamical theory leads to the conclusion that it does not make much difference whether the coupling is strong or weak. In weak coupling theory each electronic term f_n (2.8) in the polarizability of a residue is replaced by a sum

of contributions from a practically continuous band of vibrational structure, and the polarizability can often be represented quite well as a damped oscillator form:

$$\alpha(\omega) = \frac{3e^2}{m} \frac{f_n}{[(\omega_n^2 - \omega^2) - i\omega\gamma]}, \quad (8.1)$$

with the damping constant γ chosen to give the correct band width (This of course does not imply any actual radiation damping, but is just a convenient empirical fit to the band shape). Applying this form to a pair of parallel molecules with one *electronic* excited state, as in §5, and taking account of the local field, the new polarizability comes out as

$$A(\omega) = \frac{3e^2}{m} \frac{2f_n}{[(\epsilon_n^2 - \omega^2) - i\omega\gamma]}. \quad (8.2)$$

That is, the new vibronic band has the same damped shape as before, except for the first-order frequency shift of the peak from ω_n to ϵ_n where ϵ_n , is precisely the same frequency as in (5.5). The contradiction between this conclusion and Tinoco's argument is only apparent. The vibronic transition at the new band peak is *not the same one* as the old, so that it is quite possible for each unresolved vibronic line in the band to have only a tiny shift but for the band profile as a whole to move. What happens is that each vibronic transition on molecule *a* borrows from all the vibronic transitions of molecule *b* *within the same band* in a manner analogous to (5.5), so transitions near ϵ_n are enhanced by comparison with those near ω_n .

The validity of the time-dependent self-consistent field theory is restricted in several ways. The most important conditions are that the residues must not overlap, and that the coupling must be small enough to be regarded as a perturbation. If two very close electronic levels are strongly coupled it is better to use the exciton theory instead. This is because the Hartree product wave function (3.1) is no longer at all realistic. The Hartree method has two main virtues. It is easy to use and interpret, and it preserves the sum rules for f_n and R_n . We have not yet given a formal proof of this important property. In outline one procedure is to construct exact normal mode solutions of equation (3.7) in the manner of §6, including coupling between all the exciton bands. Each mode has coefficients C_{ani} from every band n , and the electronic spectrum has peaks at the frequencies ϵ_i , with strengths

$$F_i = \sum_{a,b} \sum_{m,n} C_{ani} C_{bmi} (f_n f_m)^{1/2} (\mathbf{e}_{an} \cdot \mathbf{e}_{bm}), \quad (8.3)$$

$$R_i = \sum_{a,b} \sum_{m,n} C_{ani} C_{bmi} \{ \rho_n (f_m / f_n)^{1/2} (\mathbf{m}_{an} \cdot \mathbf{e}_{bm}) + \frac{3e^2 \hbar}{8mc} (f_n f_m)^{1/2} \times [\mathbf{r}_{ab} \times \mathbf{e}_{an} \cdot \mathbf{e}_{bm}] \}. \quad (8.4)$$

The sum rules then follow directly from the orthogonality of the modes.

The local field interpretation of these optical effects has some interesting implications, because it allows one to imagine each residue in the polymer as surrounded by an oriented medium consisting of the other residues and the solvent. Clearly one ought to consider the effect of neighbouring polymers as well, and this suggests

that rather similar spectral changes might also follow alterations in the packing of the chains. For example one expects changes when a liquid crystal undergoes an order-disorder transition.

One of us, M.A.B., thanks the D.S.I.R. for a research grant, and we both thank Professor H. C. Longuet-Higgins, F.R.S., and Dr. R. Somorjai for their suggestions.

REFERENCES

- [1] TINOCO, I., 1960, *J. Amer. chem. Soc.*, **82**, 4785.
- [2] LAWLEY, P. D., 1956, *Biochim. biophys. Acta*, **21**, 481.
- [3] THOMAS, R., 1954, *Biochim. biophys. Acta*, **14**, 231.
- [4] MICHELSON, A. M., 1958, *Nature, Lond.*, **182**, 1502.
- [5] ROSENHECK, K., and DOTY, P., 1961, *Proc. nat. Acad. Sci., Wash.*, **47**, 1775.
- [6] RICH, A., and KASHA, M., 1960, *J. Amer. chem. Soc.*, **82**, 6197.
- [7] GRATZER, W. B., HOLZWARTH, G., and DOTY, P., 1961, *Proc. nat. Acad. Sci., Wash.*, **47**, 1785.
- [8] BLOUT, E. R., and IDELSON, M., 1956, *J. Amer. chem. Soc.*, **78**, 497.
- [9] HOLZWARTH, G., GRATZER, W. B., and DOTY, P., 1962, *J. Amer. chem. Soc.*, **84**, 3194.
- [10] MOFFITT, W., and YANG, J. T., 1956, *Proc. nat. Acad. Sci., Wash.*, **42**, 596.
- [11] TINOCO, I., 1961, *J. Amer. chem. Soc.*, **83**, 5047.
- [12] TINOCO, I., 1960, *J. chem. Phys.*, **33**, 1332.
- [13] RHODES, W., 1961, *J. Amer. chem. Soc.*, **83**, 3609.
- [14] TINOCO, I., and RICH, A., 1960, *J. Amer. chem. Soc.*, **82**, 6409.
- [15] BOLTON, H. C., and WEISS, J. J., 1962, *Nature, Lond.*, **195**, 666.
- [16] WEISS, J. J., 1963, *Nature, Lond.*, **197**, 1296.
- [17] DeVoe, H., 1963, *Nature, Lond.*, **197**, 1295.
- [18] NESBET, R. K., 1964, *Mol. Phys.*, **7**, 211.
- [19] NESBET, R. K., 1962, *Mol. Phys.*, **5**, 63.
- [20] KOUTECKY, J., and PALDUS, J., 1963, *Theor. chim. Acta*, **1**, 268.
- [21] KIRKWOOD, J. G., 1937, *J. chem. Phys.*, **5**, 479.
- [22] MOFFITT, W., 1956, *J. chem. Phys.*, **25**, 467.
- [23] MOFFITT, W., 1956, *Proc. nat. Acad. Sci., Wash.*, **42**, 736.
- [24] MOFFITT, W., FITTS, D. D., and KIRKWOOD, J. G., 1957, *Proc. nat. Acad. Sci., Wash.*, **43**, 723, 1046.
- [25] TINOCO, I., and WOODY, R. W., 1960, *J. chem. Phys.*, **32**, 461.
- [26] KUHN, W., 1932, *Handb. Jahrb. chem. Phys.*, **8**, (3), 47.
- [27] BORN, M., 1933, *Optik* (Berlin: J. Springer).
- [28] OSEEN, C. W., 1915, *Ann. Phys., Lpz.*, **48**, 1.
- [29] BOYS, S. F., 1934, *Proc. roy. Soc. A*, **144**, 655.
- [30] DIRAC, P. A. M., 1930, *Proc. Camb. phil. Soc.*, **26**, 376.
- [31] EHRENREICH, H., and COHEN, M. H., 1959, *Phys. Rev.*, **115**, 786.
- [32] McLACHLAN, A. D., and BALL, M. A., 1964, *Rev. mod. Phys.*, **36**, 844.
- [33] THOULESS, D. J., 1961, *Nucl. Phys.*, **22**, 78.
- [34] SIMPSON, W. T., and PETERSON, D. L., 1957, *J. chem. Phys.*, **26**, 588.
- [35] CONDON, E. U., 1937, *Rev. mod. Phys.*, **9**, 432.
- [36] MASON, S. F., 1963, *Quart. Rev.*, **17**, 20.
- [37] MOSCOWITZ, A., 1962, *Advances in Chemical Physics*, **4**, 67 (New York: Interscience).
- [38] TINOCO, I., 1963, *Advances in Chemical Physics*, **4**, 113 (New York: Interscience).
- [39] MOFFITT, W., and MOSCOWITZ, A., 1959, *J. chem. Phys.*, **30**, 648.
- [40] ROSENFELD, L., 1928, *Z. Phys.*, **52**, 161.
- [41] McLACHLAN, A. D., GREGORY, R. D., and BALL, M. A., 1963, *Mol. Phys.*, **7**, 119.

Fluorescence self-quenching in aromatic vapours

The effect of fluorescence reabsorption

by B. STEVENS and P. J. McCARTIN†

Department of Chemistry, The University, Sheffield 10, England

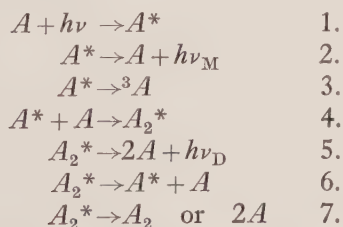
(Received 15 June 1964)

The quantum yields of naphthalene vapour fluorescence at 225°C and of phenanthrene vapour fluorescence at 365°C excited by the Hg 313 μ line are independent of concentration up to 0.014 and 0.007 moles/l. respectively; this is attributed to fast dissociation relaxation of the excimer at these temperatures.

The fluorescence of naphthalene vapour excited at temperatures of 355–435°C by the group of Hg lines at 365 μ decreases with increasing pressure at pressures below that at which absorption of the incident radiation is virtually complete, and is attributed to a combination of self-quenching and reabsorption of fluorescence. An analysis of the data for the limiting cases of complete and negligible fluorescence reabsorption provides upper and lower limits for self-quenching constant which are consistent with unit collisional quenching efficiency and a lifetime of $5.3 \pm 2.2 \times 10^{-9}$ sec at 355°C.

1. INTRODUCTION

Studies of fluorescence self-quenching provide information concerning the interaction of electronically excited and unexcited molecules of the same species. A review of the evidence available has led to the suggestion [1] that the photo-association of a planar aromatic hydrocarbon A (process 4) following electronic excitation (1) generally competes with fluorescence emission (2) and intersystem crossing (3), and is followed by the radiative relaxation (5), dissociation (6) or internal conversion (7) of the excimer A_2^* .



Thus the ultimate fate of the absorbed quantum at high concentrations is determined by the relative rates of processes 5, 6 and 7 which depend both on the molecular properties and on the conditions of observation.

Since the overall quantum yield of excimer fluorescence γ_D is given by

$$\frac{1}{\gamma_D} = \left\{ 1 + \frac{k_2 + k_3}{k_4 C} \right\} \left\{ 1 + \frac{k_6 + k_7}{k_5} \right\},$$

where C is the solute concentration, the observation of an excimer band for a large number of aromatic hydrocarbons and their derivatives in concentrated

† Present address: E. I. Dupont de Nemours, Wilmington, Delaware, U.S.A.

solution of low viscosity [2-4] or in the molten state [5, 6] indicates that

$$k_5 \ll (k_6 + k_7)$$

under the prevailing conditions. The failure to observe excimer fluorescence from phenanthrene, anthracene and naphthacene under conditions where

$$k_4 C \ll (k_2 + k_3)$$

indicates that either:

(a) dissociation relaxation (process 6) competes effectively with fluorescence emission (process 5) of A_2^* in which case the molecular fluorescence yield should be independent of concentration; the excimer band should appear at lower temperatures where the endothermic dissociation process 6 is suppressed as in the case of naphthalene [7]; or

(b) the probability of radiative relaxation k_5 is much less than that of internal conversion or photodimer formation k_7 which leads to an overall self-quenching of molecular fluorescence. Thus in the case of anthracene, self-quenching is accompanied by the production of the stable photodimer A_2 in solution [8], and has a negative temperature coefficient in the gas phase due to an increase in the rate of dissociation (process 6) at higher temperatures [9, 10].

This communication describes an investigation of fluorescence self-quenching for naphthalene, phenanthrene and naphthacene in the vapour phase where the collision frequency is some two orders of magnitude greater than the encounter frequency in solvents of low viscosity. The absence of self-quenching is to be expected for naphthalene if photo-association is an intermediate step since excimer dissociation is already dominant in solutions at room temperature, whilst the absence of self-quenching in phenanthrene would indicate that the failure to observe excimer fluorescence even at low temperatures is a consequence of the inequality $k_6 \gg k_5$ under the conditions of observation. Since naphthacene, on the other hand, undergoes photodimerisation in solution [11], the dominance of process 7 should be responsible for the absence of the excimer band as in the case of anthracene, and self-quenching might be expected to have a negative temperature coefficient.

2. EXPERIMENTAL

Measurements of relative fluorescence intensity as a function of vapour concentration were made using the apparatus previously described [10]; this utilizes the method of frontal observation, which minimizes geometrical effects due to optical density changes and allows the fraction of incident radiation absorbed to be measured simultaneously. The group of Hg lines at 365 mμ was isolated from a 125 watt stabilized high pressure arc (Mazda MBL/D) by 4 mm of chance 0X 1 filter together with 1 cm of aqueous $\text{CuSO}_4 \cdot 5\text{H}_2\text{O}$ (125 g/l.), and removed from the radiation intercepted by the detector by 1 cm of aqueous NaNO_2 (0.125 M). Naphthalene and phenanthrene were excited by the Hg lines at 313 mμ and 334 mμ transmitted from the same source by 2 cm of Bowen's solution L [12] combined with 4 mm of the Corning 9863 filter; in this case the radiation falling on the detector was intercepted by a Corning 7380 filter to remove the reflected incident beam.

The effects of added gases on the intensity of naphthacene vapour fluorescence were investigated using an apparatus previously constructed [13] for this purpose

in which the cell is connected to vacuum and storage lines by a metal valve. Since it was considered undesirable to subject this value to temperatures greater than 290°C , the vapour pressure of naphthacene was restricted to a value which produced an adequate intensity of fluorescence but which did not permit the measurement of any optical density changes at $365\text{ m}\mu$ produced by the addition of foreign gases [14].

Emission spectra of naphthacene vapour excited at different concentrations by the Hg $365\text{ m}\mu$ lines were photographed on a Hilger medium quartz spectrograph fitted with Ilford HP3 plates.

BDH (microanalytical) naphthalene, a sample of phenanthrene subjected to extensive zone melting by L. Light Ltd., and naphthacene donated by I.C.I. (Dyestuffs Division) were used without further purification other than a vacuum sublimation into the cell before sealing off.

3. RESULTS

Typical curves obtained for the concentration dependence of the ratio of fluorescence to reference signal F/R , and of the fraction of incident radiation absorbed I_A/I_0 , are shown for naphthacene, naphthalene and phenanthrene under the conditions stated in figures 1–3. The concentration of vapour in equilibrium with the solid or liquid hydrocarbon at each temperature was obtained from published vapour pressure data [15].

The microdensitometer traces of the naphthacene fluorescence spectrum shown in figure 4 provide evidence for strong reabsorption of the short-wave fluorescence (transmitted by the nitrite filter) at higher pressures. However,

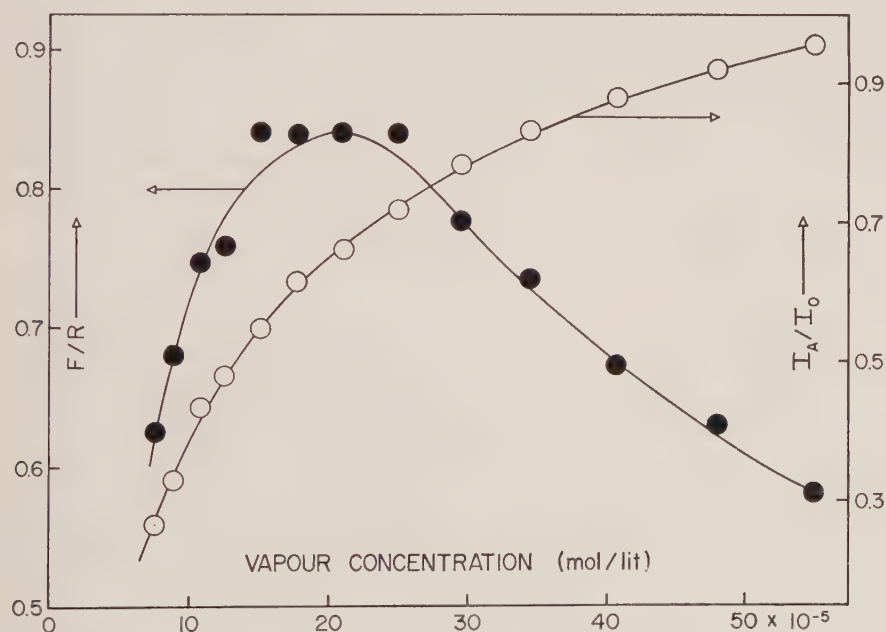


Figure 1. Variation of fluorescence/reference signal ratio F/R (filled circles) and fraction of incident light absorbed I_A/I_0 (open circles) with concentration of naphthacene vapour at 435°C . $\lambda = 365\text{ m}\mu$.

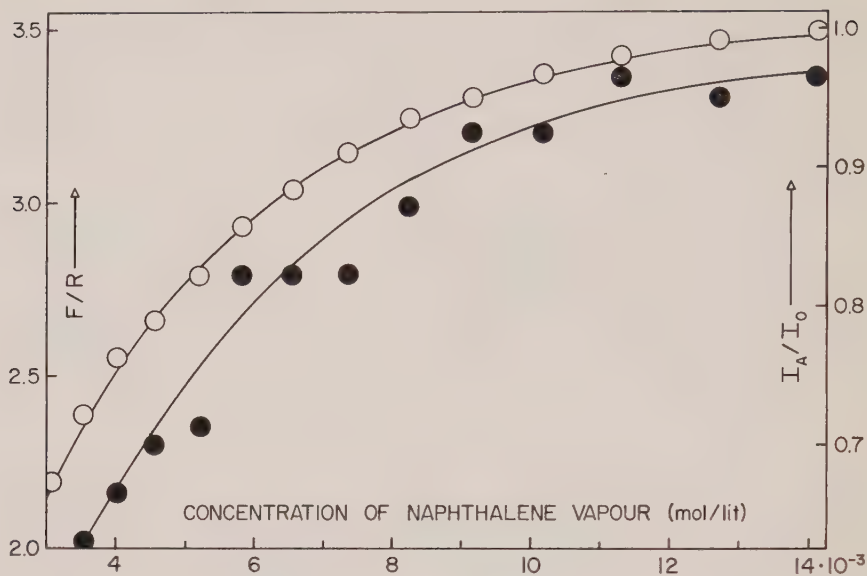


Figure 2. Variation of fluorescence/reference signal ratio F/R (filled circles) and fraction of incident light absorbed I_A/I_0 (open circles) with concentration of naphthalene vapour at 225°C. $\lambda = 313 \text{ m}\mu$.

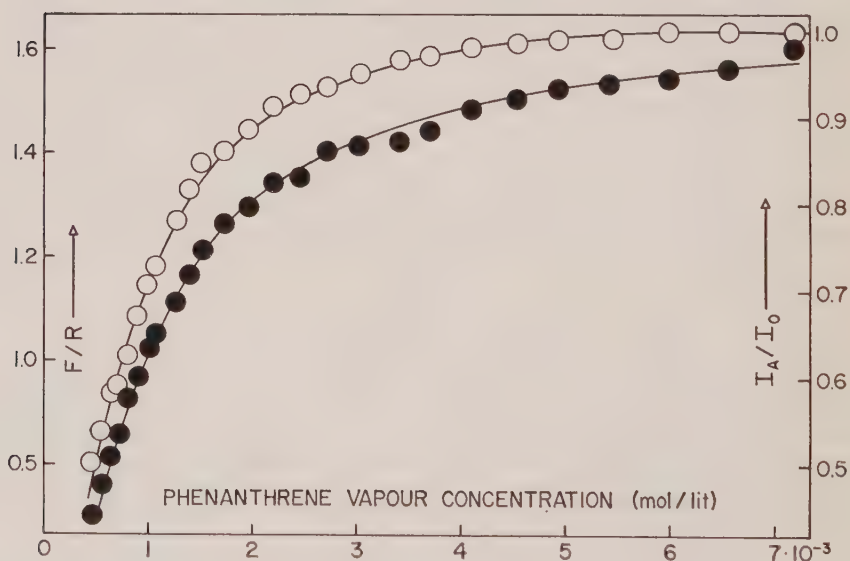


Figure 3. Variation of fluorescence/reference signal ratio F/R (filled circles) and fraction of incident light absorbed I_A/I_0 (open circles) with concentration of phenanthrene vapour at 365°C. $\lambda = 313 \text{ m}\mu$.

the use of a filter which transmitted only the unabsorbed long-wave fluorescence bands reduced the signal/noise ratio to the order of unity at low pressures and further restricted the already limited pressure range over which reliable measurements could be made.

Oxygen and nitric oxide were found to quench the fluorescence of naphthalene vapour to a similar extent, but since the effect of these gases on the extremely low optical density of the vapour could not be measured, these observations must remain qualitative.

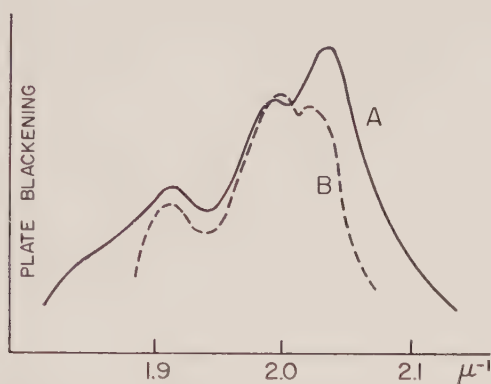


Figure 4. Microdensitometer traces of naphthalene vapour fluorescence at 350°C. $\lambda = 365 \text{ m}\mu$. A: at $7 \times 10^{-5} \text{ m/l.}$; B: at $4 \times 10^{-4} \text{ m/l.}$

4. DISCUSSION

4.1. Naphthalene

The maximum intensity of naphthalene vapour fluorescence is exhibited at a concentration well below that at which absorption of the incident radiation at $365 \text{ m}\mu$ is virtually complete (figure 1); this is attributed to reabsorption of the short-wave fluorescence bands at higher pressures shown in figure 4.

The appended treatment of fluorescence reabsorption for conditions of frontal illumination leads to the following expression for the measured ratio of detector signal F to reference signal R :

$$\frac{F}{R} = \frac{B\gamma_M I_0}{R} \sum_i \frac{S_i \phi_i \epsilon_\lambda}{\epsilon_\lambda + \epsilon_i} \{1 - \exp [-(\epsilon_\lambda + \epsilon_i)cd]\} \quad (1)$$

in terms of

the molecular fluorescence yield γ_M ,

an instrumental constant B ,

the intensity I_0 of incident radiation,

extinction coefficients ϵ_λ for the incident radiation and ϵ_i for the i th monochromatic component of fluorescence,

ϕ_i , the wavelength distribution function of the emission spectrum,

the detector sensitivity S_i for the i th fluorescence component,

the vapour concentration c and cell depth d .

In the absence of reabsorption equation (1) becomes:

$$\frac{F}{R} = \frac{B\gamma_M I_0}{R} \{1 - \exp (-\epsilon_\lambda cd)\} \sum_i S_i \phi_i, \quad (2)$$

which shows that, in so far as the exponential is the dominant concentration-dependent term at lower pressures, the effect of reabsorption is to increase the

apparent extinction coefficient for the incident light which would account for the effect observed. If this is the case, the assumption that light absorption is complete when the fluorescence intensity reaches its maximum value is not valid if the detector intercepts fluorescence radiation which is reabsorbed at higher concentrations.

It follows from equations (1) and (2) that, for frontal viewing, negative values of $d(F/R)/dc$ can only originate from negative coefficients of $d\gamma_M/dc$. Under photostationary conditions the quantum yield of molecular fluorescence γ_M is given by:

$$\gamma_M = \gamma_M^\circ / \left\{ 1 + \frac{k_4 c}{k_2 + k_3} \left[\frac{k_7}{k_5 + k_6 + k_7} \right] \right\}, \quad (3)$$

where $\gamma_M^\circ = k_2/(k_2 + k_3)$ is the quantum yield in the absence of collisional perturbation and the corresponding lifetime of the fluorescent state is $\tau = 1/(k_2 + k_3)$. Since no excimer band is observed, $k_5 \ll (k_6 + k_7)$ and (3) becomes:

$$\gamma_M = \gamma_M^\circ / (1 + Kc) \quad (4)$$

with

$$K = k_4 k_7 \tau / (k_6 + k_7). \quad (5)$$

Two limiting cases may be examined:

(a) the exponential term in (1) is negligible compared with unity at high pressures for each monochromatic fluorescence component in which case (I) may be rearranged with (4) to give:

$$\left(\frac{R}{F} \right) \approx (1 + Kc) \left\{ \frac{\gamma_M^\circ B I_0}{R} \sum_i \frac{S_i \phi_i \epsilon_\lambda}{\epsilon_\lambda + \epsilon_i} \right\}^{-1}, \quad c \rightarrow \infty$$

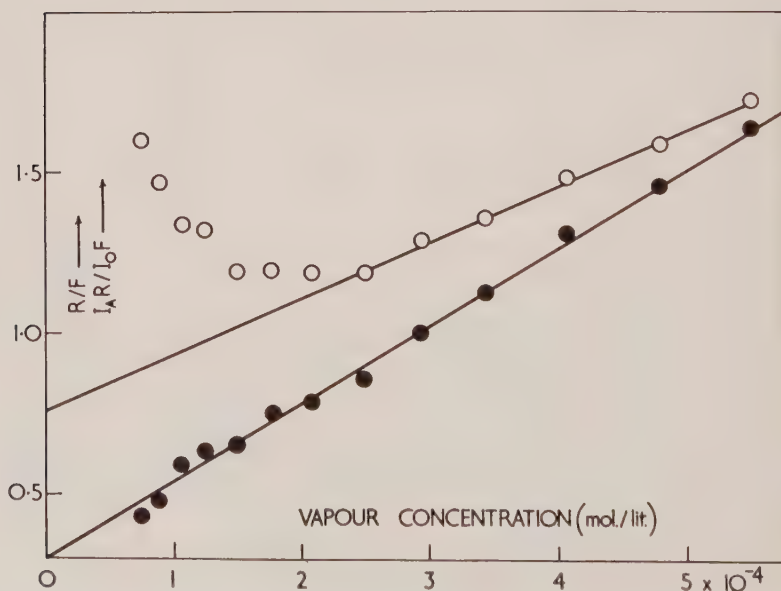


Figure 5. Plot of R/F (open circles) with $I_A R / I_0 F$ (filled circles) against naphthalene vapour concentration; conditions as for figure 1.

and a plot of R/F against c should be linear at high pressures as shown in figure 5 with

$$K_I = \text{slope/intercept.}$$

Since this approximation overestimates the effect due to reabsorption of fluorescence (particularly in the long-wave region where $\epsilon_i \simeq 0$), the values of K_I tabulated provide a lower limit to K .

(b) fluorescence reabsorption is negligible in which case (2) becomes:

$$I_A R/I_0 F = (1 + Kc) \left\{ \frac{\gamma_M^\circ B I_0}{R} \sum_i S_i \phi_i \right\}^{-1}.$$

As shown in figure 5, the quantity $I_A R/I_0 F$ is a linear function of c over the whole concentration range, and tabulated values of

$$K_{II} = \text{slope/intercept.}$$

provide an upper limit to K .

$T^\circ\text{C}$	355	386	409	435
$K > K_I$ (1. mole $^{-1}$)	= 2500	2500	2600	2300 ± 300
$K < K_{II}$ (1. mole $^{-1}$)	= 4700	5000	6500	8400 ± 500

Limiting values of self-quenching constant for naphthacene vapour fluorescence excited at 356 m μ .

An examination of the data tabulated shows that naphthacene vapour fluorescence is subject to efficient self-quenching and that fluorescence reabsorption contributes significantly to the concentration dependence of the experimental fluorescence yield. The marked increase in K_{II} with temperature reflects an increase in the extent of fluorescence reabsorption which is neglected in computing values of K_{II} from the experimental data.

Since there is no evidence for a decrease in K with increasing temperature as found for anthracene vapour, internal conversion of the excimer must be extremely efficient and $k_7 \gg k_6$; thus (5) may be written

$$\tau = K/k_4,$$

and on the assumption that process 4 operates with unit collisional efficiency at a collision diameter of 10 Å, the mean value

$$K = 3700 \pm 1500 \text{ l. mole}^{-1} \text{ at } 355^\circ\text{C}$$

provides an estimate of

$$\tau = 5.3 \pm 2.2 \times 10^{-9} \text{ sec at the same temperature.}$$

This may be compared with the value

$$\tau_0 = k_2^{-1} = 4.6 \times 10^{-8} \text{ sec}$$

computed from an oscillator strength of 0.08 [16], and is consistent with a quantum yield of molecular fluorescence in the range

$$\gamma_M^\circ = 0.11 \pm 0.05 \text{ at } 355^\circ\text{C.}$$

It has been suggested that the emitting sites in certain aromatic crystals are sandwich-like pairs of parallel molecules present in the unit cell [17] or at lattice or surface imperfection [18]. A relatively high concentration of such exciton

traps, which degrade electronic energy as efficiently as their vapour phase counterpart, A_2^* , could account for the extremely low fluorescence yield of crystalline naphthacene [19] in contrast to its behaviour in dilute liquid and solid solutions.

4.2. Naphthalene

It is evident from figure 2 that no decrease in the fluorescence intensity of naphthalene vapour is observed as its concentration is increased to 0.014 m/l. (433 mm Hg), although owing to the low extinction coefficient at 313 m μ it is only at this concentration that the light absorption approaches 100 per cent and it could be argued that $d(F/R)/dc$ may have negative values at higher pressures. However, since a self-quenching constant as small as

$$K = 201./\text{mole}$$

would reduce the value of F/R at the maximum recorded concentration to its value at 7×10^{-3} m./l., it is concluded that naphthalene does not exhibit self-quenching under the conditions described; thus

$$k_6 \gg (k_5 + k_7)$$

at 220°C, as anticipated on the grounds that the energy-dependent process 6 already competes favourably with processes 5 and 7 at room temperature.

4.3. Phenanthrene

Under the experimental conditions the incident radiation is completely absorbed at concentrations exceeding 4×10^{-3} m./l. over which range no decrease in fluorescence intensity is observed (figure 3); the absence of self-quenching under these conditions indicates that the dissociation process 6 is entirely responsible for excimer relaxation if photo-association is operative and suggests that excimer fluorescence may be observed in solution at very low temperatures if internal conversion is relatively slow. Evidence of such an emission under these conditions has recently been reported [20].

The authors are grateful to I.C.I. Ltd. (Dyestuffs Division) and L. Light Ltd., for gifts of hydrocarbons, to the Royal Society for a research grant, and to D.S.I.R. for the maintenance of P.J.M.

APPENDIX

The effect of fluorescence reabsorption on the fluorescence intensity measured (by a detector at A) at the front surface is examined with reference to figure 6, which shows a vertical cross section of the cell.

If I_0 is the intensity of light of wavelength λ (assumed monochromatic) incident on the front surface of the cell C, the intensity at the surface of the vapour layer of thickness dx is:

$$I = I_0 \exp(-\epsilon_\lambda cx),$$

where ϵ_λ and c are the extinction coefficient and concentration of vapour respectively. This layer absorbs an amount of light equal to:

$$\begin{aligned} dI &= I[1 - \exp(-\epsilon_\lambda c dx)] \\ &= I_0 \epsilon_\lambda c \exp(-\epsilon_\lambda cx) dx, \end{aligned}$$

if dx is infinitesimally small, and emits polychromatic fluorescence with a quantum yield of γ and intensity γdI over a solid angle of 4π . The intensity of polychromatic

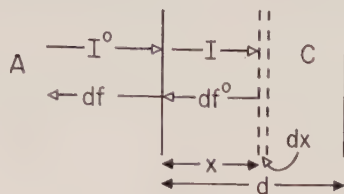


Figure 6

fluorescence emitted by the layer dx over the small solid angle α subtended by the detector surface is:

$$df^o = \alpha \gamma dI / 4\pi,$$

of which df_i^o is due to the i th monochromatic component, where

$$df_i^o = df^o \phi_i(\lambda)$$

and $\phi_i(\lambda)$, the distribution function of the fluorescence spectrum normalized such that

$$\int_0^\infty \phi_i(\lambda) d\lambda = 1$$

is assumed to be independent of concentration.

If ϵ_i is the extinction coefficient for reabsorption of the i th monochromatic fluorescence component and $\alpha/4\pi$ is sufficiently small for secondary emission to be neglected, the escaping intensity of this component at λ_i is:

$$df_i = df_i^o \exp(-\epsilon_i c x).$$

The signal registered by the detector due to this escaping component of fluorescence at λ_i from the vapour element dx will be:

$$dF_i = S_i df_i,$$

if S_i is the detector sensitivity at λ_i ; thus it follows that this fluorescence component at λ_i emitted by the whole vapour will produce a detector signal equal to:

$$\begin{aligned} F_i &= \frac{S_i \alpha \gamma}{4\pi} \phi_i(\lambda) I_0 \epsilon_\lambda c \int_0^d \exp[-(\epsilon_\lambda + \epsilon_i)cx] dx \\ &= \frac{S_i \alpha \gamma}{4\pi} \phi_i(\lambda) I_0 \frac{\epsilon_\lambda}{\epsilon_\lambda + \epsilon_i} \{1 - \exp[-(\epsilon_\lambda + \epsilon_i)cd]\}, \end{aligned}$$

if α may be assumed independent of x over the cell depth d . The total signal produced by all monochromatic components is, therefore:

$$F = \sum_i F_i = \frac{\alpha \gamma}{4\pi} I_0 \sum_i \frac{S_i \phi_i(\lambda) \epsilon_\lambda}{\epsilon_\lambda + \epsilon_i} \{1 - \exp[-(\epsilon_\lambda + \epsilon_i)cd]\}.$$

REFERENCES

- [1] STEVENS, B., 1961, *Nature, Lond.*, **192**, 725.
- [2] FORSTER, TH., and KASPER, K., 1955, *Z. Elektrochem.*, **59**, 977.
- [3] BERLMAN, I., 1961, *J. chem. Phys.*, **34**, 1083.
- [4] BIRKS, J. B., and CHRISTOPHOROU, L., 1964, *Proc. roy. Soc. A*, **277**, 571.

- [5] STEVENS, B., and DICKINSON, T., 1963, *J. chem. Soc.*, p. 5492.
- [6] BIRKS, J. B., and ALADEKOMO, J. B., 1964, *Spectrochim. Acta*, **20**, 15.
- [7] DOLLER, E., and FORSTER, TH., 1962, *Z. phys. Chem.*, **31**, 275.
- [8] BOWEN, E. J., and TANNER, D. W., 1955, *Trans. Faraday Soc.*, **51**, 475.
- [9] HARDTL, K. H., and SCHARMANN, A., 1957, *Z. Naturf. A*, **12**, 715.
- [10] STEVENS, B., and MCCARTIN, P. J., 1960, *Mol. Phys.*, **3**, 425.
- [11] BIRKS, J. B., APPLEYARD, J. H., and POPE, R., 1963, *Photochem. and Photobiol.*, **2**, 493.
- [12] BOWEN, E. J., 1946, *The Chemical Aspects of Light* (Oxford University Press), Appendix II.
- [13] STEVENS, B., 1959, *Disc. Faraday Soc.*, **27**, 34.
- [14] NEPORENT, B. S., 1947, *Zhur. Fiz. Khim.*, **21**, 1111.
- [15] INOKUCHI, H., SHIBA, S., HANDA, T., and AKAMATU, H., 1952, *Bull. chem. Soc., Japan*, **25**, 299. JORDON, T. E., 1954, *Vapour Pressures of Organic Compounds* (New York : Interscience).
- [16] KLEVENS, H. B., and PLATT, J. R., 1949, *J. chem. Phys.*, **17**, 470.
- [17] FERGUSON, J., 1958, *J. chem. Phys.*, **28**, 765.
- [18] STEVENS, B., 1962, *Spectrochim. Acta*, **18**, 439.
- [19] BOWEN, E. J., 1938, *Nature, Lond.*, **142**, 1081.
- [20] MCGLYN, S. P. (private communication).

Proton spin-lattice relaxation in aqueous ionic solutions

by G. T. JONES† and J. G. POWLES‡

Physics Department, Queen Mary College (University of London),
Mile End Road, London, E.1

(Received 21 July 1964)

The proton spin-lattice relaxation time, T_1 , has been measured for aqueous solutions of sodium, potassium, rubidium and magnesium chlorides up to a concentration of about $4N$ at 25°C . The sodium and the magnesium chloride solutions were also measured at 60°C and 100°C . The variation of $1/T_1$ is *not* linear with concentration, at least above about $\frac{1}{4}N$, in contrast with previous reports [1, 2]. The behaviour depends markedly on the nature of the salt and on the temperature. It is shown that almost the whole of the variation of T_1 as compared with that of water can be directly and simply related to the corresponding changes in the shear viscosity of the solutions. It is noted that the viscosity correction is better the higher the temperature of the solution.

1. INTRODUCTION

We have measured the proton spin lattice relaxation time, T_1 , for aqueous solutions of the chlorides of sodium, potassium, rubidium and magnesium at 25°C for concentrations up to $4N$ (N is the number of equivalents of the solute per litre of solution) and also at 60°C and 100°C for the sodium and magnesium chloride. The method of measurement was by a modified adiabatic fast passage technique using a Varian DP60 spectrometer, which is described elsewhere [3]. This method is capable of an accuracy of ± 2 per cent at room temperature and is rather less accurate at higher temperatures. The samples were prepared in sealed tubes from AnalaR grade chemicals and triple distilled water. The atmospheric oxygen was removed by the freeze, pump, thaw technique applied about six times, care being taken that the concentrations were not affected. The temperature of the solution was held constant to better than $\frac{1}{2}^\circ\text{C}$.

2. THE RESULTS

The observed values are given in the figures as plots of T_1^{-1} versus normality. In all cases the effect of the solute on the proton spin lattice relaxation time is certainly not linear with concentration for concentrations above about $\frac{1}{4}N$. We feel that the behaviour is likely to be non-linear for much lower concentrations than $\frac{1}{4}N$, although our measurements are not accurate enough to establish this clearly. This non-linearity is at variance with the conclusions of Hertz [1] and of Fabricand *et al.* [2] who claim that the variation of T_1^{-1} is linear with concentration up to about $2N$. We feel that our measurements are sufficiently accurate to

† Visiting from the Chemistry Department, University of Sheffield.

‡ Now at the University of Kent at Canterbury.

be quite sure that this is not so. Moreover a close inspection of the results of Fabricand *et al.* suggests that in several cases, particularly sodium chloride solutions, *their* results are also more properly to be interpreted as a non-linear variation. This is a matter of some importance because all the simple theoretical explanations of the effect, including in particular those in references [1] and [2] predict a linear variation of T_1^{-1} with N . We feel in fact that non-linear behaviour is much more likely for these quite concentrated solutions. Since the theory of concentrated ionic solutions is so notoriously complex we have not attempted any explanation of our results except for the rather empirical analysis given below.

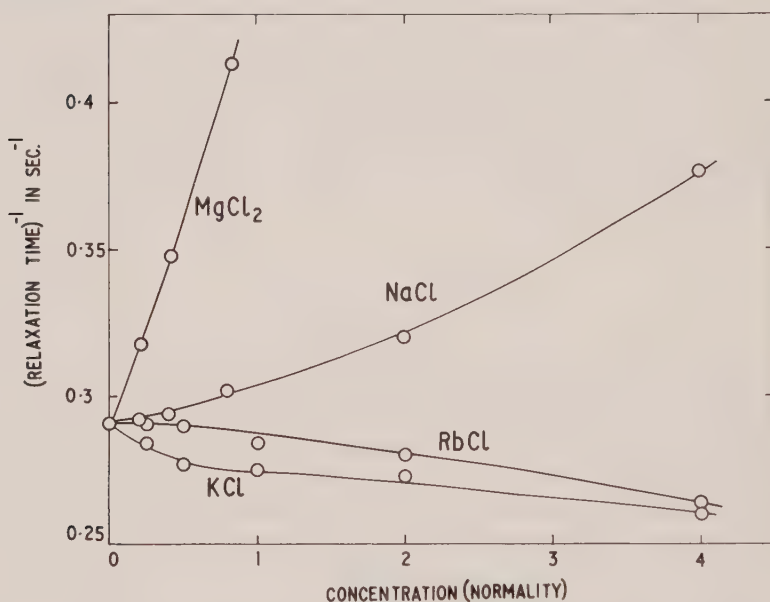


Figure 1. Effect of dissolved ionic chlorides on the proton spin lattice relaxation rate (T_1^{-1}) of water at 25°C (for higher concentrations of $MgCl_2$ see figure 3).

Apart from the important difference just discussed our results are in general agreement with those of Hertz and Fabricand *et al.* However, our measurements show that not only can different salts raise or lower T_1 but the detailed variation with concentration can be strikingly different. For example, we draw attention to the very different detailed dependence on concentration for sodium, potassium and rubidium chlorides in figure 1. In addition to this, both the magnitude of the effect and the detailed behaviour can change quite markedly with temperature as seen for sodium chloride solutions in figure 2 and for magnesium chloride solutions in figure 3. Magnesium chloride has a considerably greater effect on the proton T_1 than do the alkali halides. We suppose that this is associated with the well-known contention that the small doubly charged magnesium ion has a greater effect on the structure of water than the singly charged alkali metal ions.

The proton spin-lattice relaxation time in water is determined by the direct nuclear magnetic dipole-dipole interaction, for the temperature range considered here. These nuclear magnetic fields are fluctuating because of the reorientation of the water molecules, which varies the field at one proton in the molecule due to

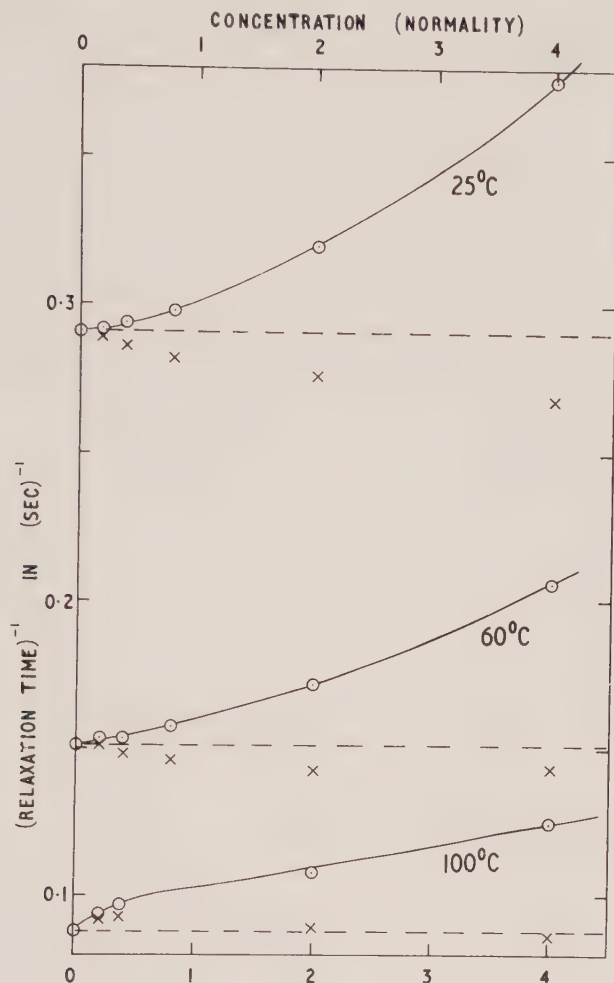


Figure 2. The proton spin-lattice relaxation rate (T_1^{-1}) as a function of concentration for solutions of sodium chloride at the temperatures indicated. The crosses are corrected values given by equation (4) as discussed in the text. The horizontal dashed lines indicate the pure water values.

the other. In addition the translational motion of the water molecules varies the field at a given proton due to protons in other molecules. We shall not discuss the effect in any detail but we shall adopt the well-known result [4] that

$$T_1^{-1} = (A + bN_0)\tau_c, \quad (1)$$

where A and b are constants, N_0 is the number of water molecules per cm^3 and τ_c is some correlation time which describes the random motion of the water molecules.

The value and dependence upon temperature of τ_c can be found approximately from the shear viscosity, η , of the liquid as originally suggested by Bloembergen *et al.* [4] and it is expected that

$$\tau_c \propto \eta/T. \quad (2)$$

This relation is moderately well obeyed as far as absolute value is concerned but is often found to be rather more accurate and useful in correcting for the effect of small *changes* in viscosity. Because of (1) and (2) we have:

$$T_1^{-1} \propto (A + bN_0)\eta/T. \quad (3)$$

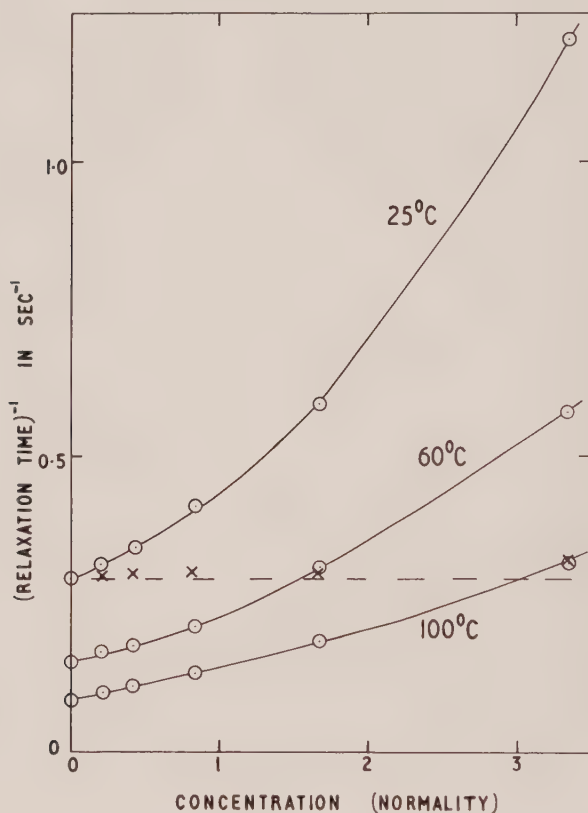


Figure 3. As in figure 2 but for magnesium chloride solutions. Note the changes in scale as compared with figure 2 owing to the large effect of this salt.

We have considered the possibility that the observed changes in T_1^{-1} in the ionic solutions as compared with pure water may be related to the well-known [5] corresponding changes of viscosity in these solutions. We also make the small correction due to changes in N_0 with concentration. We have, therefore, calculated a 'corrected' T_1^{-1} value given by:

$$T_1^{-1}{}_{\text{corrected}} = (T_1^{-1})_{\text{observed}} \times \left(\frac{A + bN_0 \text{ for water}}{A + bN_0 \text{ for solution}} \right) \times \left(\frac{\eta \text{ for water}}{\eta \text{ for solution}} \right). \quad (4)$$

These corrected values are shown for the sodium chloride solutions for the three temperatures 25, 60 and 100°C in figure 2. It is apparent that the greater part of the change in T_1^{-1} can be accounted for in this way. This can be understood when we note that T_1 is of the order of a few seconds and that in this time any particular proton will have been in all possible environments in the liquid including those both near and far removed from the ions. T_1 therefore reflects a mean environment, or molecular mobility, in the liquid. In the same way the viscosity reflects a mean molecular motion and so to some extent the two effects go together. In addition the correction is more satisfactory the higher the temperature. This result seems reasonable since the higher the temperature the less 'structure' there is in the liquid and micro (T_1) and macro (η) effects are more reasonably compared.

A similar calculation for the magnesium chloride solutions at 25°C shows (figure 3) that the change in T_1^{-1} in this case is even more satisfactorily accounted for by the change in viscosity even though the actual change in T_1^{-1} is very much greater than in the alkali halide solutions.

Corrections, as in equation (4) have also been applied in the case of the rubidium chloride and potassium chloride solutions where T_1^{-1} falls rather than rises on adding the salt. The correction is again in the correct direction, e.g. for KCl at 4*N* T_1^{-1} corrected is 0.266 and for RbCl at 1*N* it is 0.294. These results are not as satisfactory as for the other solutions, which is perhaps not surprising since the total changes in T_1^{-1} with concentration are quite small.

G. T. J. wishes to thank Dr. H. J. V. Tyrell for many helpful discussions and the D.S.I.R. for a grant.

REFERENCES

- [1] HERTZ, H. G., 1963, *Berichte der Bunsengesellschaft*, **67**, 311.
- [2] FABRICAND, B. P., GOLDBERG, S. S., LEIFER, R., and UNGER, S. G., 1964, *Mol. Phys.*, **7**, 425.
- [3] POWLES, J. G., 1963, *Berichte der Bunsengesellschaft*, **67**, 328.
- [4] BLOEMBERGEN, N., PURCELL, E. M., and POUND, R. V., 1948, *Phys. Rev.*, **73**, 679.
- [5] INTERNATIONAL CRITICAL TABLES, Vol. V, p. 12 *et seq.*

RESEARCH NOTE

The composition of the nematic mesophase of p-azoxyanisole

by H. C. LONGUET-HIGGINS and G. R. LUCKHURST

Department of Theoretical Chemistry, University Chemical Laboratory,
Lensfield Road, Cambridge

(Received 20 October 1964)

McLaughlin *et al.* [1] have measured the viscosity of p-azoxyanisole in the liquid crystal range and from this they have estimated the volume fraction of 'clusters' present in the nematic mesophase. They find that just above the melting point (118°C) the volume fraction of clusters is 0.18 and this decreases to 0.12 just below the nematic-isotropic transition point (135°C). We believe that these values are at least five times too small and we now discuss our reasons for this belief.

The electron resonance spectrum of the tetracyanoethylene anion (TCNE⁻) [2] has been measured using p-azoxyanisole as the solvent. In the nematic mesophase the radical-anions are partitioned between the clusters and the surrounding isotropic liquid. When the TCNE⁻ is in the isotropic liquid the anisotropic nitrogen hyperfine tensor is averaged to zero by the random motion of the radical leaving the isotropic nitrogen hyperfine splitting a^I . On the other hand, in a cluster TCNE⁻ is aligned so that the magnetic field is parallel to the plane of the molecule; hence there is a non-vanishing contribution from the parallel component of the anisotropic nitrogen hyperfine tensor giving a total hyperfine splitting a^A [2]. The observation of a single spectrum with fairly sharp lines implies that the radical-anions are exchanging rapidly between the clusters and the isotropic liquid so that the observed nitrogen hyperfine splitting $\langle a \rangle$ is simply a weighted average of a^A and a^I :

$$\langle a \rangle = \frac{n_2^A a^A + n_2^I a^I}{n_2^A + n_2^I}, \quad (1)$$

in which n_2^A is the number of solute molecules in the clusters and n_2^I is the number in the isotropic liquid.

Since a^A can be calculated fairly accurately [2] and a^I is known from experiment we can use the values of $\langle a \rangle$ together with McLaughlin *et al.*'s values for the volume fraction of clusters, which will not differ greatly from the mole fraction, x^A , to calculate the partition coefficient, K , of TCNE⁻ between the clusters and isotropic liquid:

$$K = \frac{n_2^A}{x^A} \frac{1 - x^A}{n_2^I}. \quad (2)$$

It turns out that just above the melting point the partition coefficient is 44 and just below the nematic-isotropic transition point it is 11. If the radicals in the clusters are not perfectly aligned these values of the partition coefficient must be

increased. These results are surprising, since they suggest that the clusters and isotropic liquid have markedly different solvent properties, at least for TCNE⁻. Fortunately elution gas liquid chromatography enables us to see if this is generally true.

If the comparatively small effects of the non-ideality of the gas phase and the pressure dependence of the activity coefficients are neglected the true retention volume, V_2^G , [3] of a volatile solute below the nematic-isotropic transition point is

$$V_2^G = \frac{n_1^L RT}{p_2^0} \left\{ \frac{x^A}{f_2^{A\infty}} + \frac{1-x^A}{f_2^{I\infty}} \right\}, \quad (3)$$

where n_1^L is the total number of moles of liquid crystal in the column, p_2^0 is the solute vapour pressure at column temperature T_K , $f_2^{A\infty}$ is the activity coefficient of the solute in the clusters, $f_2^{I\infty}$ is the activity coefficient of the solute in the isotropic liquid and the vanishingly small solute concentration is emphasized by the infinity superscript. Above the nematic-isotropic transition point the true retention volume is given by the usual expression:

$$V_2^G = \frac{n_1^L RT}{p_2^0 f_2^{I\infty}}. \quad (4)$$

It is reasonable to assume that the activity coefficients of the solute in the isotropic liquid are the same just above and just below the nematic-isotropic transition point. Then from equations (3) and (4) we can determine

$$f_2^{I\infty} \left\{ \frac{x^A}{f_2^{A\infty}} + \frac{1-x^A}{f_2^{I\infty}} \right\}$$

and from this we can obtain the partition coefficient since for dilute solutions this is simply $f_2^{I\infty} : f_2^{A\infty}$.

Kelker [4] has measured the true retention volumes of benzene, toluene, the isomeric xylenes and cyclohexane on p-azoxyanisole although he has not analysed his results using equations (3) and (4). His results show that for all these solutes

$$f_2^{I\infty} \left\{ \frac{x^A}{f_2^{A\infty}} + \frac{1-x^A}{f_2^{I\infty}} \right\} = 0.9 \quad (5)$$

near the nematic-isotropic transition point. Using McLaughlin *et al.*'s value of $x^A = 0.12$ we find that the partition coefficient for these solutes is 0.17 and again we have the surprising result that the solvent properties of the clusters and isotropic liquid are different but this time the situation is reversed.

We are presented with an apparent dilemma; why should the solvent properties of p-azoxyanisole be so different for benzene, say, and TCNE⁻? The most obvious answer to this is that we are dealing with different solutes. However, the fact that benzene and cyclohexane have approximately equal activity coefficients in p-azoxyanisole suggests that the electronic structure of the solute is not important. We have confirmed that the charge of the solute is also unimportant by studying the electron resonance spectra of neutral copper acetylacetonate and the copper catechol dianion dissolved in p-azoxyanisole. The spectra of both complexes above and below the nematic-isotropic transition point are practically identical. These facts lead us to believe that the partition coefficient, or $f_2^I : f_2^A$, for TCNE⁻ and benzene, say, should be similar,

The dilemma can be resolved if the value of x^A obtained from the viscosity of p-azoxyanisole is too small. Now it is apparent from the electron resonance measurements that the lifetime of TCNE \cdot in a cluster must be less than $|a^A - a^I|^{-1}$, i.e. less than 10^{-7} sec, in order to give a single spectrum. This implies that the lifetime of a cluster must itself be about 10^{-7} sec. However, the usual methods for the determination of viscosities employ low rates of shear so as to obtain Newtonian flow which means that the experiment is performed at essentially zero frequency. Since a particular cluster only exists for a short time the clusters do not behave as rigid ellipsoids [1] and so the Einstein formula cannot be used to estimate their volume fraction.

Assuming that McLaughlin *et al.*'s results are wrong let us use the electron resonance and elution gas liquid chromatography results to estimate the mole fraction of clusters in p-azoxyanisole. Equation (5) can be rearranged to:

$$x^A \left\{ 1 - \frac{f_2^{I\infty}}{f_2^{A\infty}} \right\} = 0.1, \quad (6)$$

so that the ratio $f_2^{I\infty} : f_2^{A\infty}$ or the partition coefficient must be less than unity. By using this result in equation (2) we see that

$$\frac{n_2^A}{n_2^I} < \frac{x^A}{1 - x^A} \quad (7)$$

and from the electron resonance measurements we find $n_2^A : n_2^I$ is 9.6 just above the melting point and 1.5 just below the transition point. Thus the mole fraction of clusters is greater than 0.9 just above the melting point and greater than 0.6 just below the transition point.

G. R. Luckhurst wishes to acknowledge a D.S.I.R. studentship.

REFERENCES

- [1] McLAUGHLIN, E., SHAKESPEARE, M. A., and UBBELOHDE, A. R., 1964, *Trans. Faraday Soc.*, **60**, 25.
- [2] CARRINGTON, A., and LUCKHURST, G. R., 1964, *Mol. Phys.*, **8**, 401.
- [3] PURNELL, H., 1962, *Gas Chromatography* (London and New York : Wiley), Chap. 10.
- [4] KELKER, H., 1963, *Z. Electrochem.*, **67**, 698.

INDEX OF AUTHORS (WITH THE TITLES OF PAPERS)

- ALLNATT, A. R.: Integral equations in ionic solution theory, 533
- ANDERSON, JAY MARTIN: The effect of relaxation on the symmetry of N.M.R. spectra, 505
- ATHERTON, N. M., and GOGGINS, A. E.: Association between pyrazine and sodium ions, 99
- BALL, M. A., *see* McLACHLAN, A. D.
- BELL, G. M., and FAIRBAIRN, W. M.: Regular models for solid hydrogen. III, 497
- BODEN, N., EMSLEY, J. W., FEENEY, J., and SUTCLIFFE, L. H.: The effects of π -electron distribution and intramolecular electric fields on the ^{19}F N.M.R. shielding in substituted perfluorobenzenes, 133
- BODEN, N., EMSLEY, J. W., FEENEY, J., and SUTCLIFFE, L. H.: The N.M.R. spectrum and configuration of decafluorobiphenyl, 467
- BOURN, A. J. R., and RANDALL, E. W.: Proton-proton double resonance studies of formamide- ^{15}N and N-methylformamide- ^{15}N , 567
- BUNKER, P. R.: The rotational-torsional wavefunctions of molecules that have two identical co-axial rotors, 81
- CARRINGTON, A., LONGUET-HIGGINS, H. C., and TODD, P. F.: The negative ions of tetraphenylene and 1, 2 : 5,6-dibenzcyclooctatetraene, 45
- CARRINGTON, A., and LUCKHURST, G. R.: Electron spin resonance line widths of transition metal ions in solution. Relaxation through zero-field splitting, 125
- CARRINGTON, A., and LUCKHURST, G. R.: The electron resonance spectra of free radicals dissolved in liquid crystals, 401
- CARRINGTON, A., and SMITH, I. C. P.: An electron spin resonance study of proton transfer equilibria involving the pyrogallol semiquinone radical, 101
- CARRINGTON, A., and TODD, P. F.: Restricted rotation of alkyl groups in alkyl cyclooctatetraene anions, 299
- CHILD, M. S.: Semi-classical analysis of weakly inelastic molecular collisions 517
- CHONG, D. P., and LINNETT, J. W.: Alternant molecular orbital treatment of the allyl cation, radical and anion, 151
- CHONG, D. P., and LINNETT, J. W.: Alternant molecular orbital treatment of trimethylene-methyl, $\text{C}(\text{CH}_2)_3$, and its ions, 541
- COLPA, J. P., *see* KOLLAARD, U. H.
- COOK, R. J., ROWLANDS, J. R., and WHIFFEN, D. H.: Electron spin resonance of the SeO_2^- radical ion, 195
- CRAIG, D. P., and DOGGETT, G.: The orbital penetration term in aromatic substituent effects, 485
- DAS, G.: On the proof of an identity, 513
- DE BOER, E., and PRAAT, A. P.: Conformational interconversion in the monovalent ions of 1,2,3,6,7,8-hexahdropyrene, 291
- DE KOWALEWSKI, DORA G., and KOWALEWSKI, VALDEMAR J.: Long-range coupling in the N.M.R. spectra of alkyl formates, 93
- DE KOWALEWSKI, VALDEMAR, J., *see* DE KOWALEWSKI, DORA G.
- DIXON, R. N.: Low-energy states of the CH_2 radical, 201
- DOGGETT, G., *see* CRAIG, D. P.
- EMSLEY, J. W., *see* BODEN, N.
- FAIRBAIRN, W. M., *see* BELL, G. M.
- FARMER, J. B., GERRY, M. C. L., and McDOWELL, C. A.: The electron spin resonance spectrum of the NF_2 radical trapped in inert matrices at 4.2°K, 253
- FEENEY, J., *see* BODEN, N.

- FISCHER, P. H. H., and McDOWELL, C. A.: The electron spin resonance spectrum of the radical anion of 1,3,5-trinitrobenzene, 357
- FOWLER, G. N.: Excitons in molecular crystals, 375
- FOWLER, G. N.: On the theory of hypochromism, 383
- GERRY, M. C. L., *see* FARMER, J. B.
- GESTBLOM, BO, HOFFMAN, RAGNAR, A., and RODMAR, SÖREN: Proton magnetic resonance of symmetrical molecules. II. The analysis of A_2B_2 spectra by perturbation methods: the A_2X_2 and $(AX)_2$ approximations, 425
- GIBBONS, W. A., *see* GIL, V. M. S.
- GIL, V. M. S., and GIBBONS, W. A.: Effect of intramolecular Van der Waals forces on N.M.R. spectra, 199
- GOGGINS, A. E., *see* ATHERTON, N. M.
- GOLDING, R. M.: The theory of the temperature dependence of N.M.R. spectra of paramagnetic octahedral complexes, 561
- GRIFFITH, J. S.: Theory of the isotropic g value of 4.27 found for some high-spin ferric ions, 213
- GRIFFITH, J. S.: Intermediate symmetry, 217
- HAARHOFF, P. C.: H-D isotope effects in the decomposition of acetylene by electron impact, 49
- HARADA, YOSHIYA: Electronic structure of *p*-benzosemiquinone ion, 273
- HARADA, YOSHIYA, and INOKUCHI, HIROO: Electronic spectra of *p*-benzosemiquinone ions, 265
- HEEN, D. E., and WHIFFEN, D. H.: Hyperfine coupling in $>\dot{C}OH$ containing radicals, 407
- HERBISON-EVANS, D., and RICHARDS, R. E.: ^{14}N chemical shifts in organic compounds, 19
- HODGES, J. A., *see* MARSHALL, S. A.
- HOFFMAN, RAGNAR A., *see* GESTBLOM, BO.
- HOOPER, D. L., *see* KAISER, R.
- I'HAYA, Y., *see* MATSUOKA, O.
- INOKUCHI, HIROO, *see* HARADA, YOSHIYA
- JONES, G. T., and POWLES, J. G.: Proton spin-lattice relaxation in aqueous ionic solutions, 607
- JØRGENSEN, CHR. KLIXBÜLL: An heuristic estimate of correlation energies in many-electron atoms, 191
- JØRGENSEN, CHR. KLIXBÜLL, and JUDD, B. R.: Hypersensitive pseudoquadrupole transitions in lanthanides, 281
- JUDD, B. R., *see* JØRGENSEN, CHR. KLIXBÜLL
- KAISER, R., and HOOPER, D. L.: Conformation of the *EXO*-methylene ketone group in α -methylene cycloketones, 403
- KAWAMORI, ASAKO, and SUZUKI, KEISUKE: Proton magnetic resonance of Würster's blue perchlorate, 95
- KOLLAARD, U. H., and COLPA, J. P.: Scheibe's rule and the SCF theory, 295
- LEHN, JEAN-MARIE, et RIEHL, JEAN-JACQUES: Interactions spin-spin nucléaires. II. Couplages spin-spin dans des époxydes substitués, 33
- LEMAIRE, H., RAMASSEUL, R., et RASSAT, A.: Nitroxydes. IV. Le *t*-butyl isopropyl nitroxyde, 557
- LINNETT, J. W., *see* CHONG, D.P.
- LONGUET-HIGGINS, H. C., *see* CARRINGTON, A
- LONGUET-HIGGINS, H. C., and LUCKHURST, G. R.: The composition of the nematic meso-phase of *p*-azoxyanisole, 613
- LONGUET-HIGGINS, H. C., and WIDOM, B.: A rigid sphere model for the melting of argon, 549

- LUCKHURST, G. R., *see* CARRINGTON, A.
- LUCKHURST, G. R., *see* LONGUET-HIGGINS, H. C.
- LUCKHURST, G. R., and ORGEL, L. E.: Solvent effects in the electron spin resonance spectrum of fluorenone ketyl, 117
- LYNDEN-BELL, RUTH M.: The line shapes of the E.S.R. spectrum of a system of interacting triplets, 71
- MAASKANT, W. J. A., and OOSTERHOFF, L. J.: Theory of optical rotatory power, 319
- MCCARTIN, P. J., *see* STEVENS, B.
- MCDOWELL, C. A., *see* FARMER, J. B.
- MCDOWELL, C. A., *see* FISCHER, P. H. H.
- McLACHLAN, A. D.: A variational solution of the time-dependent Schrödinger equation, 39
- McLACHLAN, A. D.: Resonance transfer of molecular excitation energy, 409
- McLACHLAN, A. D., and BALL, M. A.: Hypochromism and optical rotation in helical polymers, 581
- MARSHALL, S. A., REINBERG, A. R., SERWAY, R. A., and HODGES, J. A.: Electron spin resonance absorption spectrum of CO_2^- molecule-ions in single crystal calcite, 225
- MATSUOKA, O., and I'HAYA, Y.: The electronic structure and spectrum of nitrobenzene, 455
- MAZO, ROBERT M.: Note on the theory of dissociation pressures of gas hydrates, 515
- MILLS, IAN M.: Raman selection rules for vibration-rotation transitions in symmetric top molecules, 363
- MYLNIKOV, V., and TEREININ, A.: Dye sensitized photo-response in organic semiconductors, 387
- NIKITIN, E. E.: Mean lifetimes of active molecules and oscillator models of unimolecular reaction, 65
- NIKITIN, E. E.: The compound-molecule model in the theory of chemical reactions, 473
- ORGEL, L. E., *see* LUCKHURST, G. R.
- OOSTERHOFF, L. J., *see* MAASKANT, W. J. A.
- POPLE, J. A., and SANTRY, D. P.: Molecular orbital theory of nuclear spin coupling constants, 1
- POPLE, J. A., *see* WALMSLEY, S. H.
- POWLES, J. G., *see* JONES, G. T.
- POWLES, J. G., and STRANGE, J. H.: Transient nuclear magnetic resonance signals for liquids with exchanging nuclei, 169
- PRAAT, A. P., *see* DE BOER, E.
- PREUSS, H.: Ein neues Programm zur quantentheoretischen Berechnung von Molekülen und Atomsystemen. I. Grundlagen, 157
- PREUSS, H.: Die $^1\Sigma$ -und $^3\Sigma$ -Energiekurven von zweiatomigen Systemen mit zwei Elektronen, 233
- PREUSS, H.: Die Berechnung der Potentialflächen von mehratomigen Systemen nach der Methode der Ladungsentwicklungen, 441
- RAMASSEUL, R., *see* LEMAIRE, H.
- RANDALL, E. W., *see* BOURN, A. J. R.
- RASSAT, A., *see* LEMAIRE, H.
- REINBERG, A. R., *see* MARSHALL, S. A.
- RICHARDS, R. E., *see* HERBISON-EVANS, D.
- RIEHL, JEAN-JACQUES, *see* LEHN, JEAN-MARIE
- RODMAR, SÖREN, *see* GESTBLOM, BO
- ROWLANDS, J. R., *see* COOK, R. J.
- ROWLINSON, J. S.: The statistical mechanics of systems with steep intermolecular potentials, 107

- SANTRY, D. P., *see* POPLE, J. A.
SERWAY, R. A., *see* MARSHALL, S. A.
SMITH, I. C. P., *see* CARRINGTON, A.
STEVENS, B., and MCCARTIN, P. J.: Fluorescence self-quenching in aromatic vapours.
The effect of fluorescence reabsorption, 597
STRANGE, J. H., *see* POWLES, J. G.
SUTCLIFFE, L. H., *see* BODEN, N.
SUZUKI, KEISUKE, *see* KAWAMORI, ASAKO
- TERENIN, A., *see* MYLNIKOV, V.
TER MATEN, G., *see* VAN DER WAALS, J. H.
TODD, P. F., *see* CARRINGTON, A.
- VAN DER WAALS, J. H., and TER MATEN, G.: Zero-field splitting of the lowest triplet state
of some aromatic hydrocarbons: Calculation and comparison with experiment, 301
- WALMSLEY, S. H., and POPLE, J. A.: Intermolecular vibrations of solid carbon dioxide, 345
WHIFFEN, D. H., *see* COOK, R. J.
WHIFFEN, D. H., *see* HENN, D. E.
WIDOM, B., *see* LONGUET-HIGGINS, H. C.